NASA Conference Publication 3322

Fourth International Conference on Squeezed States and Uncertainty Relations

Edited by
D. Han
Goddard Space Flight Center
Greenbelt, Maryland

Kunchi Peng
Shanxi University
Taiyuan, Shanxi, P. R. China

Y. S. Kim
University of Maryland
College Park, Maryland

V. I. Man'ko
Lebedev Physical Institute
Moscow, Russia

Proceedings of a conference held at
the Shanxi University
Taiyuan, Shanxi, P. R. China
June 5 - 8, 1995

National Aeronautics and
Space Administration

Goddard Space Flight Center
Greenbelt, Maryland

1996

This publication is available from the NASA Center for AeroSpace Information,
800 Elkridge Landing Road, Linthicum Heights, MD 21090-2934, (301) 621-0390.

PRINCIPAL ORGANIZERS

K. C. Peng (Shanxi University)
Y. S. Kim (Univ. of Maryland)
V. I. Man'ko (Lebedev Physical Institute)

INTERNATIONAL ORGANIZING COMMITTEE

V. Buzek (Slovak Academy of Sciences)
G. C. Gou (Univ. of Science & Technology of China)
V. A. Isakov (Lebedev Institute)
C. Fabre (Pierre et Marie Curie University)
D. Han (NASA Goddard Space Flight Center)
K. Kakazu (Univ. of the Ryukyus, Okinawa)
M. S. Kim (Sogang University, Seoul)
J. Q. Liang (Shanxi University)
M. Man'ko (Lebedev Institute)
M. Rubin (Univ. of Maryland Baltimore County)
B. Sanders (MacQuarie University)
A. Sergienko (Univ. of Maryland Baltimore County)
Y. H. Shih (Univ. of Maryland Baltimore County)
W. H. Tan (Shanghai Institute of Optics & Fine Mechanics)
R. Tanas (Adam Mickiewicz University)
A. Vourdas (Univ. of Liverpool)
Y. Z. Wang (Shanghai Institute of Optics & Fine Mechanics)
L. A. Wu (Chinese Academy of Sciences)
M Xiao (Univ. of Arkansas)
G. Zhou (Shanxi University)

INTERNATIONAL ADVISORY COMMITTEE

G. S. Agarwal (Univ. of Hyderbad)
A. Albrecht (Imperial College)
C. O. Alley (Univ. of Maryland)
A Aspect (Univ. de Paris Sud)
A. O. Barut (Univ. of Colorado)
J. Birman (City College of CUNY)
C M Caves (Univ. of New Mexico)
C. Q. Cao (Peking University)
B. V. Chirikov (Novosibirsk)
A S. Chirkin (Moscow State University)
R Y. Chiao (Univ. of California, Berkeley)
F. DeMartini (Univ di Roma)
V Dodonov (Moscow Physical Technical University)

I. M. Dremin (Lebedev Physical Institute)
M. Fedorov (Inst. of General Physics, Moscow)
G. C. Ghirardi (ICTP and Univ. di Trieste)
L. Grishchuk (Washington University)
F. Haake (Univ. of Essen)
D. Han (NASA Goddard Space Flight Center)
O. Hirota (Tamagawa University, Tokyo)
S. Haroche (Lab. de Spectroscopie Hertzienne)
E. Jacobino (P. et M. Curie University)
J. Janszky (Research Lab. for Crystal Physics, Budapest)
C. K. Jen (Johns Hopkins University)
H. J. Kimble (California Inst. of Technology)
D. N Klysko (Moscow State Univeristy)
V. A. Kostelecky (Indiana University)
L. Lugiato (Univ. di Milano)
G. Milburn (Univ. of Queesland)
V. Mostepanenko (Univ. of St. Petersburg)
M. Namiki (Waseda University)
A. I. Nikishov (Lebedev Physical Institute)
J. Perina (Palacky University)
M. O. Scully (Texas A&M Univeristy)
J. H. Shapiro (Massachusetts Inst. of Tech.)
A. Shimony (Boston University)
A. I. Solomon (Open University)
E. C. G. Sudarshan (Univ. of Texas)
M. Teich (Columbia University)
P. Tombesi (Univ. di Camerino)
H. Umezawa (Univ. of Alberta)
A. Vinogradov (Lebedev Institute)
D. Walls (Univ. of Auckland)
D. H. Wang (Chinese Academy of Sciences)
Z. J. Wang (Shanghai Inst. of Optics & Fine Mechanics)
K. Wodkiewicz (Warsaw University)
K. B. Wolf (Univ. Nacional Auto. de Mexico)
Y. Yamamoto (Stanford University)
C. N. Yang (State Univ. of New York, Stony Brook)
G. Z. Yang (Chinese Academy of Sciences)
H. Yuen (Northwestern Univeristy)
F. Zaccaria (Univ. di Napoli)
A. Zeilinger (Univ. of Innsbruck)
W. Zurek (Los Alamos National Laboratory)

This Conference is supported in part by

International Union of Pure a... Applied Physics (IUPAP)
nternational Center for Theoretical Physics (ICTP)
Southeast Ocean Development Company
Committee of National Natural Science Foundation of China
The Commision of Planning of Shanxi Provincial Government
The Committee of Science and Technology of Shanxi Provincial Government
The Education Committee of Shanxi Provincial Government
Shanxi Traffic Information and Communication Company
The Institute of Physics of Academia Sinica University of Shangxi
Lebedev Physical Institute of the Russian Academy of Sciences
Goddard Space Flight Center of the U.S. National Aeronautics and Space Administration
University of Maryland Baltimore County
University of Maryland at College Park

PREFACE

The fourth International Conference on Squeezed States and Uncertainty Relations was held at Shanxi University, Taiyuan, Shanxi, China on June 5 - 8, 1995. This conference was jointly organized by Shanxi University, the University of Maryland (U.S.A), and the Lebedev Physical Institute (Russia). The first meeting of this series was called the Workshop on Squeezed States and Uncertainty Relations, and was held in 1991 at College Park, Maryland. The second and third meetings in this series were hosted in 1992 by the Lebedev Institute in Moscow and in 1993 by the University of Maryland Baltimore County, respectively.

The first three meetings in this series were called workshops, and the fourth meeting was an international conference sponsored by the International Union of Pure and Applied Physics (IUPAP) and by the International Center for Theoretical Physics (ICTP). At this meeting, there were a large number of Chinese and Japanese participants.

The scientific purpose of this series was initially to discuss squeezed states of light, but in recent years the scope is becoming broad enough to include studies of uncertainty relations and squeeze transformations in all branches of physics including of course quantum optics and foundations of quantum mechanics. Quantum optics will continue playing the pivotal role in the future, but the future meetings will include all branches of physics where squeeze transformations are basic transformation. This transition took place at the fourth meeting of this series held at Shanxi University in 1995

The fifth meeting in this series will be held in Budapest (Hungary) in 1997, and the principal organizer will be Jozsef Janszky of the Laboratory of Crystal Physics, P.O. Box 132, H-1052 Budapest, Hungary.

REGISTERED PARTICIPANTS AND AUTHORS

Adam, P., Lab. of Crystal Physics, P.O. Box 132, H-1052 Budapest, Hungary

Agarwal, Girish S. <gsa@prl.ernet.in>, Physical Research Laboratory, Navrangpura, Ahmedabad - 380 009, INDIA

Ba, Jianfen, Science Publishing House, Rm. 1, 16 North Street of East Huangchenggen, Beijing, China

Bachor, H. A. <hans@aerodec.anu.edu.au>, Dept. of Physics, The Australian National University, Canberra, ACT 0200, Australia

Bambah, Bindu A. <bbsp@uohyd.ernet.in>, School of Physics, Univ. of Hyderabad, Hyderabad 500 134, India

Ban, M., Research Div. of Quantum Communication Science , Tamagawa University, Tokyo 194, Japan

Barone, F., Inst. di Fisica Teorica, Mostra d'Oltremare, Pad. 19, I-80125 Napoli, Italy

Belenov, E. M., Lebedev Physical Institute, Leninsky Prospect 53, 117924 Moscow, Russia

Ben-Aryeh, Jacob <phr65yb@technion technion.ac.il>, Dept. of Physics, Technion, 32000 Haifa, Israel

Bramati, A., Universite P.et M.Curie, Case 74, 4 Place Jussieu, F-75252 Paris cedex 5, France

Cao, Chang-qi, Dept. of Physics, Pekiing University, Beijing 100871, China

Cao, H. , Ginzton Laboratory, Stanford University, Stanford, CA 94305, U.S.A.

Chen, J.,Dept. of Physics, Toyama University, Toyama 930, Japan

Chen, Wen-Yu <milburn@physics.uq.oz.au>, Dept. of Physics, Univ. of Queensland, St. Lucia 4072, Australia

Chen, Xuzong, Dept. of Radio-Electronics, Peking University, Beijing 100871, China

Chirkin, Anatoly S. <icono@comsim.phys.msu.su>, Dept. of Physics, Moscow State University, 119899 Moscow, Russia

Cui, Zhiyun, Dept. of Physics, Hebei University, Baoding 071002, China

D'Ariano, Mauro <dariano@pv.infn.it>, Dipto. di Fisica, Univ. di Pavia, 27100 Pavia, Italy

Daboul, Jamil <daboul@bguvms.bgu.ac.il>, Dept. of Physics, Ben Gurion University, 84105 Beer Sheva, Israel

Dattoli, G. <batisti@efr419.enea.it>, ENEA, INN-FIS, P.O. Box 65, I-00044 Frascati, Italy

De Martini Francesco <demartini@roma1.infn.it>, Dipto. di Fisica, Univ. Roma "La Sapeienza", I-00185 Roma, Italy

De Martino, Salvatore <demartino@vaxa.dia.unisa.it>, Dipto. di Fisica, Univ. di Salerno, 84081 Salerno, Italy

De Siena, Silvio <desiena@vaxsa.dia.unisa.it>, Dipto. di Fisica, Univ. di Salerno, 84081 Salerno, Italy

Di Giuseppe, G., Dipto. di Fisica, Univ. Roma "La Sapeienza", I-00185 Roma, Italy

Ding, Liang-En, Dept. of physics, East China Normal University, Shanghai 200062, China

Doktorov, Evgeny <doktorov%bas11.basnet.minsk.by@demos.su>, Institute of Physics, Belarus Academy of Sciences, 220602 Minsk, Belarus

Domokos, P., Lab. of Crystal Physics, P.O. Box 132, H-1052 Budapest, Hungary

Dong, Lifang, Institute of Physics, Academia Sinica, Beijing,100080, China

Dong, Zhengchao, Shandong Inst. of M and T, Jinan 250031, China

Duan, C. X., Institute of Scieence and Technology, Ocean University of Qingdao, Qingdao 266003, China

Duan, Lu-ming, Dept. of Physics, Univ. of Science and Technology of China, Hefei, Anhui 230026, China

Dubovik, V. M. <dubovik@theor.jinrc.dubna.su>, Bogoliubov Lab. of Theor Physics, Joint Inst. for Nuclear Research, 141980 Dubna, Russia

Dutta-Roy, Binayak <bnyk@tnp.saha.ernet.in>, Theory Group, Saha Institute of Nuclear Physics, Calcutta 700064, India

Edamatsu, Keiichi <eda@akiu.gw.tohoku.ac.jp>, Dept. of Physics, Tohoku University, Sendai 980, Japan

Edwards, P J., Advanced Telecommunications Eng. Centre, Faculty of Information Sciences and Engineering, Univ of Canberra, PO Box 1, Belconnen, ACT 2616, Australia

Fan, A., Dept. of Opto-electronics Science and Technology, Sichuan Univ., Chengdu, 610064, China

Fan, Hong-yi, Science and Technology Univ. of China, Hefei (Anhui), China

Fang, Mao Fa, Dept of Physics, Hunan Normal University, Changsha, Hunan 410081, China

Ferandez, David J. C. <david.fernandez@fis.cinvestav.mx>, Depto. de Fisica, CINVESTAV, AP14-740, 07000 Mexico, DF, Mexico

Fu, Guangsheng, Dept. of Physics, Hebei University, Baoding 071002, China

Fujikawa, Kazuo <fujikawa@danjuro.phys.s.u-tokyo.ac.jp>, Dept. of Physics, Univ. of Tokyo, Tokyo 113, Japan

Gagen, Michael J. <gagen@yukawa.kyoto-u.ac.jp>, Yukawa Inst. of Theor Physics, Kyoto University, Kyoto 606, Japan

Gao, Congshou, Dept. of Physics, Peking University, Beijing 100871, China

Gao, Jiangrui, Inst. of Opto-Electronic Research, Shanxi University, Taiyuan 030006, Shanxi, China

Georgiades, N., California Institute of Technology, Norman Bridge Lab of Physics 12-33, Pasadena, California 91125

Giacobino, E. <elg@spectro.jussieu.fr>, Universite P.et M.Curie, Case 74, 4 Place Jussieu, F-75252 Paris cedex 5, France

Grangier, P , Institut d'Optique, BP 147, 91403 Orsay, France

Grelu, P., Institut d'Optique, BP 147, 91403 Orsay, France

Gu, Qiao, Dept. of Physics, Northwest University, Xi'an 710069, China

Guo, Guang-can, Dept. of Physics, Univ. of Science and Technology of China , Hefei, Anhui 230026, China

Guo, Guang-can, Inst. of Opto-Electronic Research, Shanxi University, Taiyuan 030006, Shanxi, China

Gusev, A., Sternberg Astronomical Institute, Moscow State University, 103907 Moscow, Russia

Haake, Fritz, Fachbereich Physik, Univ. - GHS Essen, D-45117 Essen, Germany

Hamada, T., Dept. of Physics, Kanazawa Univ., Kakuma, Kanazawa 920-11, Japan

Han, Daesoo <han@trmm.gsfc.nasa.gov>, Goddard Space Flight Center, NASA, Code 910.1, Greenbelt, MD 20771, U.S.A.

He, Jinyu, Dept. of Physics, Dezhou Teacher's College, Shandong Provincs 253023, China

Hegerfeldt, Gerhard C. <hegerf@theo-phys.gwdg.de>, Inst. f. Theoretische Physik, Univ. Goettingen, D-3400 Goettingen, Germany

Hirayama, Minoru <hirayama@jpntyavm.bitnet>, Dept. of Physics, Toyama University, Toyama 930, Japan

Hirota, Osamu <hirota@lab.tamagawa.ac.jp>, Research Div. of Quantum Communication Science , Tamagawa University, Tokyo 194, Japan

Huang, Maoquan, Inst. of Opto-Electronic Research, Shanxi University, Taiyuan 030006, Shanxi, China

Huang, Q., Dept. of Physics, Southwest Jiaotong Univ Chengdu 610031, China

Huang, X., Advanced Telecommunications Engineering Centre, Faculty of Information Sciences and Engineering, Univ. of Canberra, PO Box 1, Belconnen, ACT 2616, Australia

Huang, Yijun, Dept. of Foundation, First Aeronautical College of Air Force, Xinyang 464000, China

Imoto, Nobuyuki, NTT Basic Research Lab., 3-1 Morinosato-Wakamiya, Atsugi-Shi, Kanagawa 243-01, Japan

Isakov, Vladimir I. <isakov@sci.lpi.ac.ru>, Lebedev Physical Institute, Leninsky Prospect 53, 117924 Moscow, Russia

Janszky, Jozsef <h1084jan@huella.bitnet>, Lab. of Crystal Physics, P.O. Box 132, H-1052 Budapest, Hungary

Jia, Suotang, Dept. of Phsics, East China Normal University, Shanghai 200062, China

Jiang, Hong-Ji, Dept. of physics, East China Normal University, Shanghai 200062, China

Jiang, Zhuo hong, Dept. of physics, Hailong Jiang University, Harbin 150080, China

Jost, V., Universite P.et M.Curie, Case 74, 4 Place Jussieu, F-75252 Paris cedex 5, France

Kakazu, Kiyotaka <kakazu@gen.u-ryukyu.ac.jp>, Dept. of Physics (Science College), Univ. of the Ryukyus, Okinawa 903-01, Japan

Kanavin, A. P., Lebedev Physical Institute, Leninsky Prospect 53, 117924 Moscow, Russia

Kanenaga, Masahiko <kanenaga@cfi.waseda.ac.jp>, Dept. of Physics, Waseda University, Tokyo 169, Japan

Key, F. Q. , Institute of Science and Technology, Ocean University of Qingdao, Qingdao 266003, China

Kilin, Sergey <kilin%bas08.basnet.minsk.by@demos.su>, Institute of Physics, Belarus Academy of Sciences, 220602 Minsk, Belarus

Kim, Myungshik <mshkim@ccs.sogang.ac.kr>, Dept. of Physics, Sogang Univ., POB 100-611, Seoul 100-611, S. Korea

Kim, Young Suh <kim@umdhep.umd.edu>, Dept. of Physics, Univ. of Maryland, College Park, MD 20742, U.S.A.

Kimble, H. J. <hjkimble@juliet.caltech.edu>, Dept. of Physics, California Institute of Technology, Pasadena, CA 91125, U.S.A.

King, Sun-Kun <g797302@phys.nthu.edu.tw>, Dept. of Physics, National Tsing-Hua University, Hsinchu 30043, Taiwan, ROC

Kis, Z., Lab. of Crystal Physics, P.O. Box 132, H-1052 Budapest, Hungary

Kobayashi, Tsunehiro <kobayash@het.ph.tsukuba.ac.jp>, Inst. of Physics, Univ. of Tsukuba, Tsukuba 305, Japan

Kon'kov, I. E., Pacific Oceanogical Institute, Lab. No. 3/5, 690041 Vladiovstock, Russia

Kong, X., Dept. of Physics, Qufu Normal Univ., Qufu, Shandong, China

Kosmachev, Oleg <komachev@hepi.academ.alma-ata.su>, Lab. of Theor. Physics, High Energy Institute, 480082 Almaty, Kazakhstan

Kozuka, Haruhisa <kozuka@lab.tamagawa.ac.jp>, Research Div. of Quantum Communication Science , Tamagawa University, Tokyo 194, Japan

Kulagin, Viktor <kul@sai.msk.su>, Sternberg Astronomical Institute, Moscow State University, 103907 Moscow, Russia

Leonski, W., Nonlinear Optics Division, Institute of Physics, Adam Mickiewicz Univ., Grunwakldzka 6, 60-780 Poznan, Poland

Levenson, M., Universite P.et M.Curie, Case 74, 4 Place Jussieu, F-75252 Paris cedex 5, France

Li, Fu-li , Dept. of Applied Physics, Xian Jiaotong University, Xian 710049, China

Li, Hui, Dept. of Physics, Yale University, New Haven, CT 06511, U.S.A.

Li, Qingning, Shanghai Institute of Optics and, Fine Mechanics,Academia Scinica, Shanghai 201800, China

Li, S., Dept. of Modern Applied Physics, Tsinghua Univ, Beijing 100084, China

Li, Shiqun, Dept. of Modern Applied Physics, Tsinghua Univ, Beijing 100084, China

Li, Xizeng, Dept. of Physics, Tianjin University, Tianjin 300072, China

Li, Yifeng, Acta Optics Sinica. P.O. Box 800211, Shanghai 201800, China

Li, Yimin, Dept. of Radio-Electronics, Peking University, Beijing 100871, China

Li, Zhonghao, Dept. Electronic and Informatin Technology, Shanxi University Taiyuan 030006, China

Lin, Qiong Gui, Dept. of Physics, Univ. of Zhongshan, Guangzhou 510276, China

Liu, Jinling, Dept. of Foudatiuon, First Aeronautical College of Air Force, Xingyang,Henan 464000, China

Liu, Tang Kun, Dept. of Physics, Hubei Teachers' College, Huangshi, Hubei, China

Liu, Xia-ji, Institute of Theoretical Physics, Northeast Normal University, Changchun,130024, China

Lu, Qiquang, Dept. of Physics, Harbin Teacher's College, Harbin 150080, China

Lu, Yajun, Dept. of Modern Applied Physics, Tsinghua Univ, Beijing 100084, China

Lui, Tang-Kun, Dept. of physics, Hubei Normal University, Huangshi 435002, China

Ma, Aiqun, Dept. of physics, Harbin college, Harbin 150020, China

Ma, L. Q., Institute of Scieence and Technology, Ocean University of Qingdao, Qingdao 266003, China

Ma, T., Dept. of Physics, Ning Xia University, Ren Chan 750021, China

Maddalena, P, Inst. di Fisica Teorica, Mostra d'Oltremare, Pad. 19, I-80125 Napoli, Italy

Man'ko, Margarita <manko@sci.fian.msk.su>, Lebedev Physical Institute, Leninsky Prospect 53, 117924 Moscow, Russia

Man'ko, Olga <manko@sci.fian.msk.su>, Lebedev Physical Institute, Leninsky Prospect 53, 117924 Moscow, Russia

Man'ko, Vladimir I. <manko@sci.fian.msk.su>, Lebedev Physical Institute, Leninsky Prospect 53, 117924 Moscow, Russia

Mao, Fa Fang, Dept. of Physics, Hunan Normal University, Changsha, Hunan 410081, China

Marin, F., Universite P.et M.Curie, Case 74, 4 Place Jussieu, F-75252 Paris cedex 5, France

Marrocco. M. Dipto. di Fisica, Univ. Roma "La Sapeienza", I-00185 Roma, Italy

Martin, F., Universite P.et M.Curie, Case 74, 4 Place Jussieu, F-75252 Paris cedex 5, France

Martin, Manuel <martin@sirio.ifuap.buap.mx>, Inst. de Fisica, Univ. Auto. de Puebla, Puebla, Pue. 72570, Mexico

Martsenuyk, M. A. <mvm@pgu.perm.su>, Dept. of Theoretical Physics, Perm State University, 614600 Perm, Russia

McClelland, D. E. , Dept. of Physics, Australian National University, Canberra, ACT 0200, Australia

Mielnik, Bogdan <bogdan@fis.cinvestav.mx>, Depto. de Fisica, CINVESTAV, AP14-740, 07000 Mexico, DF, Mexico

Milburn, G. J. <milburn@physics.uq.oz.au>, Dept. of Physics, Univ. of Queensland, St. Lucia 4072, Australia

Momose, Rei <momose@lab.tamagawa.ac.jp>, Research Div. of Quantum Communication Science , Tamagawa University, Tokyo 194, Japan

Morales-Guzman, J., Depto. de Fisica, CINVESTAV, AP 14-740, 07000 Mexico, DF, Mexico

Nafari, N. , Center for Theor. Phys.& Math.(AEOI), Dept. of Physics, Zanjan University , Zanjan, Iran

Namiki, Mikio <namiki@cfi.waseda.ac.jp>, Dept. of Physics, Waseda University, Tokyo 169, Japan

Nasiri, Sadolah <iasbsgz1@irearn.bitnet>, Center for Theor. Phys.& Math.(AEOI), Dept., of Physics, Zanjan University , Zanjan, Iran

Nayak, Nilankabtha <nayak@bose.ernet.in>, Bose National Centre for Basic Sciences, DB-17, Sector-1, Salt Lake City, Culcutta - 700064, India

Orszag, Miguel <morszag@lascar.puc.cl>, Facultad de Fisica, Pontifica Univ. Catolica, Casila 306, Santiago, Chile

Osaki, Masao <osaki@lab.tamagawa.ac.jp>, Research Div. of Quantum Communication Science , Tamagawa University, Tokyo 194, Japan

Oshiro, K., Dept. of Physics (Science College), Univ. of the Ryukyus, Okinawa 903-01, Japan

Ou, Z. Y. <zou@indyvax.iupui.edu>, Dept. of Physics, Indiana-Purdue University, Indianaplis, IN 46205, U.S.A.

Palma, Alejandro <palma@sirio.ifuap.buap.mx>, Inst. de Fisica, Univ. Auto. de Puebla, Puebla, Pue. 72570, Mexico

Pan, Jin-Fang, Dept. of Physics, Shanxi Teachers University, Linfen, Shanxi 041004, China

Parkins, A. S., Dept. of Physics, Univ. of Waikato, Hamilton, New Zealand

Pascazio, Saverio <pascazio@bari.infn.it>, Dipto. di Fisica, Univ. di Bari, I-70126 Bari, Italy

Pavicic, Mladen <mpavicic@olimp.irb.hr>, Dept. of Mathematics, Univ. of Zagreb, Zagreb, Croatia

Peng, Kunchi <pengkc@shanxi.ihep.ac.cn>, Inst. of Opto-Electronic Research, Shanxi University, Taiyuan 030006, Shanxi, China

Pittman, Todd B. <pittman@grumpy.umbc.edu>, Dept. of Physics, Univ. of Maryland Baltimore County, Baltimore, MD 21228, U.S.A.

Plastino, A., Dept. de Fisica, Univ. Nac. de La Plata, 1900 La Plata, Argentina

Poizat, J-Ph., Institut d'Optique, BP 147, 91403 Orsay, France

Polzik, E. S., Institute of Physics and Astronomy, Aarhus University, Aarhus C, DK-8000, Denmark

Portesi, Mariela <portesi@venus.fisica.unlp.edu.ar>, Dept. de Fisica, Univ. Nac. de La Plata, 1900 La Plata, Argentina

Prants, Sergei V. <poi@stv.iasnet.com>, Pacific Oceanogical Institute, Lab. No. 3/5, 690041 Vladiovstock, Russia

Qian, Zuliang, Dept. of Phsics, East China Normal University, Shanghai 200062, China

Qin, K., Dept. of Physics, Peking University, Beijing 100871, China

Qin, Lijuan, Dept. of Phsics, East China Normal University, Shanghai 200062, China

Quang, Nguyen Vinh <hanoi!bohr.ac.vn!nvquang@postbox.anu.edu.au>, Vietnam Physical Institute, Hanoi, Vietnam

Ralph, T. C. <timothy.ralph@anu.edu.au>, Dept. of Physics, Australian National University, Canberra, ACT 0200, Australia

Ren, Min, Dept. of physcs, Harbin college, Harbin 150020, China

Reyes, H. A., Depto. de Fisica, CINVESTAV, AP14-740, 07000 Mexico, DF, Mexico

Roch, J.-F. , Institut d'Optique, BP 147, 91403 Orsay, France

Romano, R., Inst. di Fisica Teorica, Mostra d'Oltremare, Pad. 19, I-80125 Napoli, Italy

Rubin, Morton H. <rubin@umbc3.umbc.edu>, Dept. of Physics, Univ. of Maryland Baltimore County, Baltimore, MD 21228, U.S.A.

Ryff, Luis Carlos , Inst. de Fisica, Univ. Fed. do Rio de Janeire, 21945-970 Rio de Janeiro, Brazil

Saha, Bijan <saha@theor.jinrc.dubna.su>, Bogoliubov Lab. of Theor. Physics, Joint Inst. for Nuclear Research, 141980 Dubna, Russia

Sasaki, M., Research Div. of Quantum Communication Science , Tamagawa University, Tokyo 194, Japan

Sergienko, Alexander V. <sasha@kelvin.umd.edu>, Dept. of Physics, Univ. of Maryland Baltimore County, Baltimore, MD 21228, U.S.A.

Shen, G. T. , Dept. of Physics, East China Normal University, Shanghai 200062, China

Shen, Y. , Dept. of Physics, East China Normal University, Shanghai 200062, China

Shen, Z. J. , Dept. of Physics, East China Normal University, Shanghai 200062, China

Shi, Deheng, Dept. of Foudatiuon, First Aeronautical College of Air Force, Xingyang,Henan 464000, China

Shi, Weichun, Dept. of Physics, Northeast Forsetry University, Harbin 150040, China

Shih, Yan-Hua <shih@umbc2.umbc.edu>, Dept. of Physics, Univ. of Maryland Baltimore County, Baltimore, MD 21228, U.S.A.

Smetanin, I. V. Lebedev Physical Institute, Leninsky Prospect 53, 117924 Moscow, Russia

Solimeno, S. <solimeno@napoli.infn.it>, Dipto. di Scienze Fisiche, Univ. di Napoli, I-80125 Naploli, Italy

Solomon, Allan I. <a.i.solomon@open.ac.uk>, Faculty of Mathematics, The Open University, Milton Keynes, MK7 6AA, United Kingdom

Strekalov, D. V., Dept. of Physics, Univ. of Maryland Baltimore County, Baltimore, MD 21228, U.S.A.

Su, Baoxia, Dept. of Physics, Tianjin University, Tianjin 300072, China

Su, Dachun, Dept. of Physics, Shanxi University, Taiyuan, Shanxi 030006, China

Sun, Chang-Pu, Institute of Theoretical Physics, Northeast Normal University, Changchun,130024, China

Sun, Hong, Dept. of Foundation, First Aeronautical College of Air Force, Xinyang 464000, China

Suzuki, Tomohiro <suzuki@eng.tamagawa.ac.jp>, Dept. of Inforomation and Communication Engineering, Tamagawa University Tokyo 194, Japan

Szabo, S., Lab. of Crystal Physics, P.O. Box 132, H-1052 Budapest, Hungary

Tan, Weihan, Joint Laboratory of Quantum Optics, Shanghai Institute of Optics and Fine Mechanics , Shanghai 201800, China

Tan, Weihan, Shanghai Institute of Optics and, Fine Mechanics,Academia Scinica, Shanghai 201800, China

Tanas, Ryszard <tanas@phys.amu.edu.pl>, Inst. of Physics, Adam Mickiewiez University, 60-780 Poznan, Poland

Tang, Zheng, Dept. of Modern Applied Physics, Tsinghua Univ, Beijing 100084, China

Taubman, M. S. <matt@aerodec.anu.edu.au>, Dept. of Physics, The Australian National University, Canberra, ACT 0200, Australia

Terazawa, Hidezumi, Inst. for Nuclear Study, Univ. of Tokyo, Tokyo 188, Japan

Tian, En-ke, Institute of Theoretical Physics, Northeast Normal University, Changchun,130024, China

Tian, Lai-ke, Dept. of Physics, Northwest University, Xi'an 710069, China

Tombesi, Paolo <tombesi@roma1.infn.it>, Dipto. di Matem. e Fisica, Univ. de Camerino, 62032 Camerino, Italy

Torres-Vega, Gabino <gabino.torres@fis.cinvestav.mx>, Depto. de Fisica, CINVESTAV, AP 14-740, 07000 Mexico, DF, Mexico

Vinogradov, Andrei V. <vinogran@quopt.fian.msk.su>, Lebedev Physical Institute, Leninsky Prospect 53, 117924 Moscow, Russia

Vitali, D., Dipto. di Matem. e Fisica, Univ. de Camerino, 62032 Camerino, Italy

Vourdas, A. <ee21@liverpool.ac.uk>, Dept. of Electrical Engineering, Univ. of Liverpool, Liverpool, L69 3BX, United Kingdom

Wan, Hai, Inst. of Opto-Electronic Research, Shanxi University, Taiyuan 030006, Shanxi, China

Wang, Chuankui, Institute of Optical Commnication, Liaocheng Teacher's College, Shandong Province 252059, China

Wang, Gang, Dept. of Electronics & Information Technoloy , Shanxi University, Taiyuan 030006,China

Wang, H., Inst. of Opto-Electronic Research, Shanxi University, Taiyuan 030006, Shanxi, China

Wang, Jisuo, Institute of Optical Commnication, Liaocheng Teacher's College, Shandong Province 252059, China

Wang, Qingji, Dept. of Radio-Electroncs, Peking University, Beijing 100871, China

Wang, Sheng Gui, Dept. of physics, Jiujiang Techer's college, Jiujiang 332000, China

Wang, W. S., Institute of Scieence and Technology, Ocean University of Qingdao, Qingdao 266003, China

Wang, Yiqiu, Dept. of Radio-Electroncs, Peking University, Beijing 100871, China

Wang, Zugeng, Dept. of Phsics, East China Normal University, Shanghai 200062, China

White, A. G. <agw654@cscgpo.anu.edu.au>, Dept. of Physics, Australian National University, Canberra, ACT 0200, Australia

Wu, Ling-An <wula@aphy01.iphy.ac.cn>, Institute of Physics, Academia Sinica, Beijing 100080, China

Wu, Meijuan, Dept. of Modern Applied Physics, Tsinghua Univ, Beijing 100084, China

Wunsche, Alfred <wuensche@photon.fta-berlin.de>, Arbeitsgruppe "Nichtklassische Stralung" , Humboldt Universitat zu Berlin, D-12489 Berlin, Germany

Xia, Hui-Rong, Dept. of physics, East China Normal University, Shanghai 200062, China

Xia, Yun Jie, Dept. of Physics, Qufu Normal Univ., Qufu, Shandong, China

Xiao, Min <mxiao@comp.uark.edu>, Dept. of Physics, Univ. of Arkansas, Fayettesville, AK 72701, U.S.A.

Xie, Changde <pengkc@shanxi.ihep.ac.cn>, Inst. of Opto-Electronic Research, Shanxi University, Taiyuan 030006, Shanxi, China

Xiong, Yongjia, Dept. of Physics, Xinyang Teacher's College, Xinyang, Henan 404000, China

Xu, Jian-Wen, Dept. of Physics, East China Normal University, Shanghai 200062, China

Xu, L., Institute of Nuclear Research, Academia Sinica, Shanghai, 201800, China

Xu, Lei, Dept. of Physics, Xi'an Jiaotong University, Xi'an 710049, China

Xu, Lei, Instutute of Nuclear Research, Academic Sinica, Shanghai 201800, China

Xu, W., Joint Laboratory of Quantum Optics, Shanghai Institute of Optics and Fine Mechanics , Shanghai 201800, China

Yamazaki, Kouichi <yamazaki@eng.tamagawa.ac.jp>, Dept. of Info. and Comm. Engineering, Tamagawa University, Tokyo 194, Japan

Yan, Chang Zhi, Dept. of physics, Harbin Institute of Electrical Technology , Harbin 150080, China

Yan, K., Dept. of Physics, Qufu Normal Univ., Qufu, Shandong, China

Yang, B. C., Dept. of Physics, East China Normal University, Shanghai 200062, China

Ye, Cen-Yun, Dept. of Physics, East China Normal University, Shanghai 200062, China

Yeong, K. C. , Dept. of Physics, Rensselaer Polytechnic Institute, Troy, NY 12180-3590

Yu, Guochen, Dept. of Foundation, First Aeronautical College of Air Force, Xinyang 464000, China

Yu, L., Institute of Scieence and Technology, Ocean University of Qingdao, Qingdao 266003, China

Yu, Shen, Dept. of Physics, East China Teachers's Univ., Shanghai 200062, China

Yuen, Horace P. <yuen@eecs.nwu.edu>, Dept. of Electrical Engineering, Northwestern University, Evanston, IL 60201, U.S.A.

Zaccaria, F., Inst. di Fisica Teorica, Mostra d'Oltremare, Pad. 19, I-80125 Napoli, Italy

Zhang, Ji-yue, Dept. of Physics, Northwest University, Xi'an 710069, China

Zhang, Junxiang, Institute of Opto-electeonics, Shanxi University, Taiyuan, Shanxi 030006, China

Zhang, Kaixi, Dept. of Physics, Hebei University, Baoding 071002, China

Zhang, Kuanshou, Institute of Opto-Electronics, Shanxi University, Taiyuan 030006, China

Zhang, Ping, Institute of Physics, Academia Sinica, Beijing, 100080, China

Zhang, T.-C. , Institut d'Optique, BP 147, 91403 Orsay , France

Zhang, Tiancai, Institute of Opto-Electronics , Shanxi University, Taiyuan 030006, China

Zhang, Xiao-yu, Dept. of Physics , Univ. of Science and Technology of China, Hefei, Anhui 230026, China

Zhang, Yong, Dept. of physics, East China Normal University, Shanghai 200062, China

Zhang, Zhi-Ming, Dept. of Physics, Xi'an Jiaotong University, Xi'an 710049, China

Zhao, Meicun, Laser Editor's Office of China, P.O. Box 800-211, Shanghai, China

Zhao, Qingxun, Dept. of Physics, Hebei University, Baoding 071002, China

Zhao, Y., Shandong Inst. of M and T, Jinan 250031, China

Zhou, Guosheng <zhougs@shanxi.ihep.ac.cn>, Dept. of Electronics and Information Technoloy , Shanxi University, Taiyuan 030006, China

Zhou, X., Dept. of Opto-electronics Science and Technology, Sichuan Univ., Chengdu, 610064, China

TABLE OF CONTENTS

SECTION I COHERENT AND SQUEEZE STATES 1

Squeezed States and Particle Production in
High Energy Collisions
B. Bambah 3

Coherent States for Kronecker Products of
Non Compact Groups: Formulation and Applications
B. Bambah and G. Agarwal 11

Higher-Order Squeezing in a Boson
Coupled Two-Mode System
A. Chizhov, J. Haus, and K. Yeong 19

New Interpretation of the Wigner Function
J. Daboul 25

Operatorial Approach to Generalized Coherent States
S. De Martino and S. De Siena 29

Two Different Squeeze Transformations
D. Han and Y. S. Kim 35

Antibunching Effect of k-Component q-Coherent States
J. He 41

Quantum State Engineering via
Coherent-State Superpositions
J. Janszky, P. Adam, S. Szabo, and P. Domokos 45

Generation of Higher-Order Squeezing in
Multiphoton Micromaser
F. Li and Q. Huang 51

Higher-Order Squeezing of Quantum Field and the
Generalized Uncertainty Relations in Non-Degenerate
Four-Wave Mixing
X. Li and B. Su 61

The Squeezing Operator and the Squeezing States of "Superspace"
A. Ma, C. Yan, Q. Lu, and W. Shi 67

The Total Gaussian Class of Quasiprobabilities and
Its Relation to Squeezed-State Excitations
A. Wünsche 73

Q(α) Function and Squeezing Effects
Y. Xia, X. Kong, K. Yan, and W. Chen 83

SECTION II FOUNDATIONS OF QUANTUM MECHANICS 87

Generalization of the Time-Energy Uncertainty
Relation of Anandan-Aharonov Type
M. Hirayama, T. Hamada, and J. Chen 89

Study of Nonclassical Fields in Phase-Sensitive Reservoirs
M. Kim and N. Imoto 95

Quantum Mechanical Noise in a Michelson
Interferometer with Nonclassical
Inputs-Nonperturbative Treatment
S. King 103

Vibrational Schroedinger Cats
Z. Kis, J. Janszky, A. Vinogradov, and T. Kobayashi 109

Correlated Light and Schrödinger Cats
V. Man'ko 115

Classical Trajectories and Quantum Spectra
B. Mielnik and M. Reyes 123

Quantum Zeno Effect in the Measurement Problem
M. Namiki and S. Pascazio 133

Multi-Particle Interferometry Based on
Double Entangled States
T. Pittman, Y. Shih, D. Strekalov,
A. Sergienko, and M. Rubin 139

Quantum Mechanics of a Two Photon State
M. Rubin 145

A Proposal for Testing Local Realism Without Using
Assumptions Related to Hidden Variable States
L. C. Ryff 151

Two-Photon Entanglement and EPR Experiments Using
Type-II Spontaneous Parametric Down Conversion
A. Sergienko, Y. Shih,
T. Pittman, and M. Rubin 159

The Contradiction Between the Measurement Theory of
Quantum Mechanics and the Theory That the Velocity of
Any Particle Can Not Be Larger Than the Velocity of Light
Y. Shen, Z. Shen, G. Shen, and B. Yang 165

Two-Photon "Ghost" Image and Interference-Diffraction
Y. Shih, A. Sergienko, T. Pittman,
D. Strekalov, and D. Klyshko 169

Squeezed States, Uncertainty Relations and the
Pauli Principle in Composite and Cosmological Models
H. Terazawa 179

Demonstration of Berry Phase in Optical Spectroscopy
H. Xia, Y. Zhang, H. Jiang, and L. Ding 193

SECTION III REPRESENTATIONS OF QUANTUM MECHANICS 201

Discrete Photodetection and Susskind-Glogower
Phase Operators
Y. Ben-Aryeh 203

A New Definition to the Phase Operator and Its Properties
L. Duan and G. Guo 209

There Aren't Non-Standard Solutions for the
Braid Group Representations of the QYBE
Associated with 10-D Representations of SU(4)
Y. Huang, G. Yu, and H. Sun 215

Solutions of the Quantum Yang-Baxter Equations
Associated with (1-3/2)-D Representations of SUq(2)
Y. Huang, G. Yu, and H. Sun 219

Quantization of Electromagnetic Fields in Cavities
K. Kakazu and K. Oshiro 223

On the Stochastic Quantization Method: Characteristics
and Applications to Singular Systems
M. Kanenaga and M. Namiki 229

Damped Oscillator With Delta-Kicked Frequency
O. Man'ko 235

Exponential Formulae and Effective Operations
B. Mielnik and D. Fernandez C. 241

The General Necessary Condition for the Validity of
Dirac's Transition Perturbation Theory
N. Quang 253

Nonclassical Properties of Q-Deformed
Superposition Light Field State
M. Ren, S. Wang, A. Ma, and Z. Jiang 259

Chiral Bozonization of Superconformal Ghosts
D. Shi, Y. Shen, J. Liu, and Y. Xiong 263

Number-Phase Uncertainty Relations for Optical Fields
R. Tanas 267

The Interference of the Dynamically Squeezed
Vibrational Wave Packets
A. Vinogradov, J. Janszky, and T. Kobayashi 273

Coherent States on Riemann Surfaces as m-Photon States
A. Vourdas 281

SECTION IV INFORMATION THEORY 287

Controlled Quantum Packets
S. De Martino and S. De Siena 289

A Secure Key Distribution System of Quantum Cryptography Based on the Coherent State
G. Guo and X. Zhang 297

Solvable Quantum Macroscopic Motions and Decoherence Mechanisms in Quantum Mechanics on Nonstandard Space
T. Kobayashi 301

On a Relation Between Quantum Interference and Standard Quantum Limit
R. Momose, M. Osaki, M. Ban, M. Sasaki, and O. Hirota 307

Physical Meaning of the Optimum Measurement Process in Quantum Detection Theory
M. Osaki, H. Kozuka, and O. Hirota 313

Decoherence and Exponential Law. A Solvable Model
S. Pascazio and M. Namiki 319

Preselected Sub-Poissonian Correlations
M. Pavicic 325

Generalized Entropic Uncertainty Relations with Tsallis' Entropy
M. Portesi and A. Plastino 331

Quantum Limits in Interferometric GW Antennas
R. Romano, F. Barone, P. Maddalena, S. Solimeno, F. Zaccaria, M. Man'ko, and V. Man'ko 337

Continuous Feedback and Macroscopic Coherence
P. Tombesi and D. Vitali 345

Classical-Quantum Correspondence by Means of Probability Densities
G. Torres Vega and J. Morales-Guzmán 353

On a New Detection Scheme for *M*-ary Orthogonal Coherent State Signal
K. Yamazaki 357

High-rate Strong-Signal Quantum Cryptography
H. Yuen 363

Theoretical Analysis About Quantum Noise Squeezing of Optical Fields From an Interactive Frequency-Doubled Laser
K. Zhang, C. Xie, and K. Peng 369

SECTION V QUANTUM OPTICS IN VACUUM 379

Experiments With Lasers and Frequency Doublers
H. Bachor, M. Taubman, A. White, T. Ralph, and D. McClelland 381

Amplitude and Transverse Quadrature Component Squeezing of Coherent Light in High Q Cavity by Injection of Atoms of Two-Photon Transition
C. Cao 389

Atomic Dipole Squeezing in the Correlated Two-Mode Two-Photon Jaynes-Cummings Model
Z. Dong and Y. Zhao 395

Observation of Two-Photon Excitation for Three-Level Atoms in a Squeezed Vacuum
K. Edamatsu, N. Ph. Georgiades, E. Polzik, H. Kimble, and A. Parkins 401

Effects of the Stark Shift on the Evolution of the Field Entropy and Entanglement in the Two-Photon Jaynes-Cummings Model
M. Fang 407

Experimental Observation of Thermal Self-Modulation in OPO
J. Gao, H. Wang, C. Xie, and K. Peng 419

Optimal Signal Filtration in Optical Sensors With Natural Squeezing of Vacuum Noises
A. Gusev and V Kulagin 427

Regular and Chaotic Quantum Dynamics of Two-Level Atoms in a Selfconsistent Radiation Field
L. Kon'kov and S. Prants 433

Motion of Cesium Atoms in the One-Dimensional Magneto-Optical Trap
Y. Li, X. Chen, Q. Wang, and Y. Wang 439

The Multiphoton Interaction of "Λ" Model Atom and Two-Mode Fields
T. Liu 451

Generation of Squeezed Light using Photorefractive Degenerate Two-Wave Mixing
Y. Lü, M. Wu, L. Wu, Z. Tang, and S. Li 457

Steady-State Squeezing in the Micromaser Cavity Field
N. Nayak 465

Cooperative Effects in a One Photon Micromaser
M. Orszag 471

Quantum Probability Cancellation Due to a Single-Photon State
Z. Ou 479

Reflection Spectrum of Two Level Atoms by an Evanescent Laser Wave
W. Tan and Q. Li 489

Quantum Interference Effects in Molecular Y- and Rhomb-Type Systems
H. Xia, C. Ye, J. Xu, and L. Ding 501

Application of Twin Beams in Mach-Zehnder Interferometer
J. Zhang, C. Xie, and K. Peng 507

Transient Sub-Poissonian Distribution for
Single-Mode Lasers
J. Zhang, Q. Gu, and L. Tian 517

Phase Noise Reduction of Laser Diode
T. Zhang, J. Poizat, P. Grelu, J. Roch,
P. Grangier, F. Marin, A. Bramati, V. Jost,
M. Levenson, and E. Giacobino 529

The Amplitude Nth-Power Squeezing of
Radiation Fields in the Degenerate Raman Process
Z. Zhang, J. Pan, and L. Xu 539

SECTION VI QUANTUM OPTICS IN NONVACUUM MEDIA 545

On the Theory of High-Power Ultrashort
Pulse Propagation in Raman-Active Media
E. Belenov, V. Isakov,
A. Kanavin, and I. Smetanin 547

Modification of Einstein A Coefficient in
Dissipative Gas Medium
C. Cao, H. Cao, and K. Qin 553

Multilevel Atomic Coherent States and
Atomic Holomorphic Representation
C. Cao and F. Haake 561

Generation of Antibunched Light by Excited
Molecules in a Microcavity Trap
F. De Martini, G. Di Giuseppe, and
M. Marrocco 565

Macroscopic Violation of Three Cauchy-Schwarz
Inequalities Using Correlated Light Beams from an
Infra-Red Emitting Semiconductor Diode Array
P. Edwards, X. Huang, Y. Li, and
Y. Wang 575

Photon Number-Phase Uncertainty Relation in the
Evolution of the Field in a Kerr-Like Medium
A. Fan and N. Sun 581

The Quantum Phase-Dynamical Properties of the Squeezed Vacuum State Intensity-Couple Interacting With the Atom
A. Fan, N. Sun, and X. Zhou 587

Quantum Noise in Laser Diodes
E. Giacobino, F. Marin, A. Bramati, V. Jost, J.-Ph. Poizat, J. Roch, P. Grangier, and T. Zhang 593

Competition Effect in Atomic-Molecular System
S. Jia, L. Qin, Z. Qian, Z. Wang, G. Wang, and G. Zhou 597

Fock State Generation From the Nonlinear Kerr Medium
W. Leonski and R. Tanas 607

The Dissipation in Lasers and in Coherent State
W. Tan and W. Xu 613

Mobility of Electron in DNA Crystals by Laser Radiation
K. Zhang, Q. Zhao, Z. Cui, P. Zhang, and L. Dong 623

Multiphoton Process and Anomalous Potential of Cell Membrane by Laser Radiation
K. Zhang, Q. Zhao, Z. Cui, P. Zhang, and L. Dong 627

Quantum Cohesion Oscillation of Electron Ground State in Low Temperature Laser Plasma
Q. Zhao, P. Zhang, L. Dong, and K. Zhang 631

Are There Optical Solitary Wave Solutions in Linear Media With Group Velocity Dispersion?
Z. Li and G. Zhou 635

SECTION I COHERENT AND SQUEEZE STATES

SQUEEZED STATES AND PARTICLE PRODUCTION IN HIGH ENERGY COLLISIONS

Bindu A. Bambah
School of Physics
Univ. Of Hyderabad Hyderabad-500134,India

Abstract

Using the 'quantum optical approach' we propose a model of multiplicity distributions in high energy collisions based on squeezed coherent states. We show that the k-mode squeezed coherent state is the most general one in describing hadronic mulitiplicity distributions in particle collision processes, describing not only $p\bar{p}$ collisions but e^+e^-, νp and diffractive collisions as well. The reason for this phenomenological fit has been gained by working out a microscopic theory in which the squeezed coherent sources arise naturally if one considers the Lorentz squeezing of hadrons and works in the covariant phase space formalism .

1 INTRODUCTION

Although Quantum Chromodynamics is widely believed to be the theory of Strong Interactions, very few experimental results support this claim. In particular the behaviour of QCD at small momentum transfer i.e low energies is not understood. This lack of understanding reflects itself in the fact that particle production in high energy collisions cannot be explained within QCD. Given the absence of a detailed dynamical theory of strong interactions , one can adopt a statistical outlook and try to forecast macroscopic behaviour of a strongly interacting system given only partial information about their internal states.Experimental information about hadronisation in high energy collisions comes from the observation of jets of hadrons and the distributions of the final state particles. By using analogies with quantum optical systems one can get information about the types of sources(Chaotic, coherent, etc) that are responsible for hadronic emission. Also, by using adapting another quantum optical effect such as the Hanbury-Brown Twiss effect one can study the size and lifetime of the emitting region. This information can then be used to put restrictions on the microscopic theory pursued from the quark-parton end [1].

The experimental quantities amenable to the quantum statistical approach are: the multiplicity Distribution of final state particles (PIONS)given by

$$P_n = \frac{\sigma_n}{\sigma_{inel}} \tag{1}$$

where σ_n n-pion cross-section, the number of particles produced per unit rapidity dN/dy , where $y = ln(\frac{E+p_L}{E-p_L})$ is the rapidity which plays the role of time in pion counting experiments, the moments of P_n and the two pion correlations which are analogous to Hanbury Brown Twiss effect for pions in rapidity space.

In particular, the quantum optical models are based on the assumption that multiparticle production takes place in two stages. In the initial stage formation of an excited system (fireball) which consists of a number of well defined phase space cells or 'sources' which then hadronize independently. In these models an ansatz is made about the statistical nature of these sources and the resulting multiplicity distributions are compared with data [2], [3]. Table 1. gives the comparison of various quantum optical models.

Table 1: Comparison of Quantum Optical Models of Multiplicity Distributions

Nature Of Source	Density matrix	Probability	Two pion
One Source	(Coherent State Rep)	Distribution	Correlations
$P(\alpha) = \frac{1}{\pi\bar{n}} exp^{(-\lvert\alpha\rvert^2/\bar{n})}$	$\rho_{nm} = \frac{\bar{n}^n}{(1+\bar{n})^{n+1}}\delta_{nm}$	Geometrical	$g^2(0) = 2$
$P(\alpha) = \delta^2(\alpha - \alpha')$	$\rho_{nn} = \frac{\lvert\alpha'\rvert^{2n} e^{-\lvert\alpha'\rvert^2}}{\Gamma(n+1)}$	Poissonian	$g^2(0) = 1$
$P(\alpha) = \frac{e^{\lvert\alpha-\alpha'\rvert^2/\bar{n}}}{\pi\bar{n}}$	$\rho_{nn} = \frac{\bar{n}^n}{(1+\bar{n})^{n+1}} e^{-\lvert\alpha'\rvert^2/(1+\bar{n})}$ $\times L_n(\frac{-\lvert\alpha'\rvert^2}{\bar{n}(1+\bar{n})})$	Glauber-Lachs	$1 \leq g^2(0) \leq 2.$
K sources			
Gaussian (Chaotic)	$\rho_{nn} = \frac{n+k-1)!}{n!(k+1)!}(\frac{\bar{n}/k}{1+\bar{n}/k})^n \frac{1}{(1+\bar{n}/k)^k}$	Negative Binomial	""
Coherent +Chaotic	$\rho_{nn} = \frac{(p\bar{n}/k)^n}{(1+p\bar{n}/k)^{n+k}}$ $\times e^{\left[\frac{-\gamma p\bar{n}}{1+p\bar{n}/k}\right]} L_n^{k-1}(\frac{-\gamma k}{(1+p\bar{n}/k)})$	Perina-McGill	""""

2 The Phenomenological model

Experimentally there exists a large class of data (νp) and low mass diffractive data that have mulplicity distributions with sub-Poissonian Statistics. Thus we seek a more general distribution than the ones given in table 1. A clue as to the appropriate distribution is that charged pions occur in pairs Furthermore the most general Gaussian source characterised by Gaussian Wigner Function . These facts point to the use of Squeezed Coherent states.
We find that the k-mode squeezed state $|\alpha, r>= |\alpha_1, r_1> |\alpha_2, r_2> \cdots |\alpha_k, r_k>$
characterised by the multiplicity distribution:

$$P_n{}^k = \Pi_i^k P_{n_i} \cdots \sum_i n_i = n \tag{2}$$

$$\begin{aligned} P_n{}^k &= e^{\left[-k\alpha^2(1+x)\right]}(1-x^2)^{k/2}(\frac{x}{2})^n \\ &\times \sum_{m=0}^{[\frac{n}{2}]} \frac{\gamma_m H_{n-2m}{}^2(\sqrt{k}y)2^{2m}}{m!(n-2m)!} \end{aligned}$$

$y = (\frac{\alpha^2(1+x)^2}{2x})^{\frac{1}{2}}$
$\gamma = \frac{k-1}{2}$; $\gamma_m = (\gamma+1)\cdots(\gamma+(m-1))$; $\gamma_0 = 1$

and the second order correlation function:

$$g_k^2(0) = 1 + \frac{2sinh^4(r) + (2\alpha^2 + 1)sinh^2(r) - sinh(2r)}{k(\alpha^2 + sinh^2(r))^2} \tag{3}$$

is the most general distribution that fits a wide range of data [4]. If $r > 0$ there are regions where $g_k^2(0) < 1$ and the distribution is narrower than Poissonian. If $r < 0$; $g_k^2(0)$ is always greater then 1 showing distributions which are broader than Poissonian.

Hadronic distributions in $p\bar{p}$ collisions show broader than Poisonnian multiplicity distributions with a long multiplicity tail, which gets broader and broader with the increase of energy. The $k = 3$ mode distribution for $\bar{n} = 13.6$, $x = -0.20$ and $\bar{n} = 26.1$, $x = -0.35$ respectively fit corresponding ISR ($62.2Gev$) and UA5 ($540Gev$) data, α for each of these is thus fixed.
To fit neutrino induced collisions in which the distribution is super-Poissonian ($(\frac{\Delta n}{\bar{n}}) < 1$), $k = 3, x = 0.5$ fit data well. e^+e^- collisions are fit by the k=2 squeezed coherent distribution with r close to zero . (nearly Poissonian.)

3 The Statistics confronts the Dynamics

We would now like to conjecture on the reason for this success and find an overlap with dyamical models. We search for incoming states of the hadronic fireball which will give rise to SQUEEZED COHERENT DISTRIBUTION. The candidate dynamical model of hadrons, which we find is appropriate is the covariant phase space model for hadrons which is a revival of Feynman et. al's relativistic harmonic oscillator model[5] Kim and Wigner pointed out that the covariant harmonic oscillator model is the natural language for a covariant description of phase-space [6], [7]. In this paper, we use the covariant phase space distribution description of relativistic extended particles to give a phenomenological description of multiplicity distributions in the high energy collisions of hadrons

Wave functions without time-like oscillations can be constructed by using the unitary representations of the Poincare group and imposing a covariant condition[8]. In this model two quarks bound together by a relativistic harmonic oscillator potential mapped onto O(3,1) invariant harmonic oscillator equation. The ground state wave function ψ_β^0 in the Lorentz boosted (primed) frame is

$$\psi_0^\beta(x') = [e^{-i\eta K_3}]\psi_0(x) \tag{4}$$

where K_3 boost generator along the z axis,

$$K_3 = i(z\frac{\partial}{\partial t} + t\frac{\partial}{\partial z}) \tag{5}$$

and $\eta = Tanh^{-1}(\beta)$

In 'Quantum Optical' language, using light- cone variables we have:

$$u = (t + z)/\sqrt{2} \quad v = (t - z)/\sqrt{2} \tag{6}$$

Then in the Lorentz-transformed frame:

$$\begin{aligned} q'_u &= e^{\eta}q_u \quad q'_v = e^{-\eta}q_v \\ u' &= e^{-\eta}u \quad v' = e^{\eta}v \end{aligned} \tag{7}$$

Introducing creation and annihilation operators

$$a_u = u + \frac{\partial}{\partial u} \ldots . a_v = v + \frac{\partial}{\partial v}$$
$$a_u^\dagger = u - \frac{\partial}{\partial u} \ldots \ldots a_v^\dagger = v - \frac{\partial}{\partial v}$$

we find that the wave function $\psi_n^\beta = \psi(u', v')$ is a two mode squeezed state.

$$\psi_0^\beta(u', v') = |0, \beta> = |0, \eta>_{u'} |0, -\eta>_{v'} \tag{8}$$

The excited state is given by:

$$|n, \beta> = (a_{u'}^\dagger)^n |0, \eta> (a_{v'}^\dagger)^n |0, -\eta> \tag{9}$$

The condition for absence of time-like oscillations in the hadronic rest-frame

$$(a_u' - a_v')|n, \beta> = 0. \tag{10}$$

The physical wave functions are

$$\psi_n^\beta(u', v') = |n, \beta> = \sum_{m=0}^{n} \left(\begin{array}{c} n \\ m \end{array} \right) |n - m, \eta>_{u'} |m, -\eta>_{v'} \tag{11}$$

in the Fock-space representation

$$\psi_n^\beta(u', v') = \sum_{n_1, n_2} \sum_{m=0}^{n} \left(\begin{array}{c} n \\ m \end{array} \right) G_{n_1, n-m}(\eta) G_{n_2, m}(-\eta) \psi_{n_1}^0(u) \psi_{n2}^0(v) \tag{12}$$

Where [9]:

$$G_{n,m} = (-1)^{\frac{m+n}{2}} \left(\frac{m!n!}{cosh(\eta)}\right) \left(\frac{tanh(\eta)}{2}\right)^{\frac{m+n}{2}} \times \sum_{\lambda}^{min[\frac{n}{2}, \frac{m}{2}]} \frac{\left(\frac{-4}{sinh^2(\eta)}\right)^\lambda}{(2\lambda)!(m/2 - \lambda)!(n/2 - \lambda)!} \tag{13}$$

for n,m even and

$$G_{n,m} = (-1)^{\frac{m+n}{2} - 3/2} \left(\frac{m!n!}{cosh(\eta)}\right) \left(\frac{tanh(\eta)}{2}\right)^{\frac{m+n}{2} - 1} \times \sum_{\lambda}^{min[\frac{n-1}{2}, \frac{m-1}{2}]} \frac{\left(\frac{-4}{sinh^2(\eta)}\right)^\lambda}{(2\lambda + 1)!(m - 1/2 - \lambda)!(n - 1/2 - \lambda)!} \tag{14}$$

for n,m odd. $G_{n,m}$ is non zero for both n,m even or both n,m odd , thus excitations of quarks occur in pairs. and the Lorentz squeezed vacuum is a many particle state . The above suggests

the identification of Hadronic sources in terms of squeezed states.
In the 'fireball picture ' the Wigner function of the source is , [10]

$$W^n(u,v,q_u,q_v) = (\frac{2}{\pi})^2 e^{-\frac{1}{2}(e^{\eta}u^2+e^{-\eta}q_u^2+e^{-\eta}v^2+e^{\eta}q_v^2)} \times \sum_{m=0}^{n}\left(\begin{array}{c} n \\ m \end{array}\right)(-1)^n L_{n-m}[e^{\eta}u^2 - e^{-\eta}q_u^2]L_m[e^{-\eta}v^2 - e^{\eta}q_v^2] \quad (15)$$

The number distribution for l particles in the n^{th} excited state.

$$P_l = \sum_{l_1+l_2=l}\sum_{m=0}^{n}\left(\begin{array}{c} n \\ m \end{array}\right)P_{l_1}^{n-m,sq}(\eta)P_{l_2}^{m,sq}(-\eta) \quad (16)$$

$$P_{l_2}^{m,sq} = \frac{(m)!l_2!}{(cosh(-\eta))^{2l_2+1}}(\frac{tanh(-\eta)}{2})^{m-l_2} \times F(-\eta,l_2,m)\cos^2(\frac{(m-l_2)\pi}{2}) \quad (17)$$

where:

$$F(-\eta,l_2,m) = \sum_{\lambda=0}^{min(l_2/2,(m-l_2)/2}\frac{(\frac{-4}{sinh^2(-\eta)})^{\lambda}}{(\lambda)!(l_2-2\lambda)!(m-l_2-2\lambda)!} \quad (18)$$

The cosine terms imply P_l vanishes when $|m-l_2|$ or $|n-m-l_1|$ is odd. so that the excited each of oscillator modes is excited in pairs.
If each pair is associated with a two quark bound state(pion), the excited state contains pair correlated pions!!!

4 Results and Conclusion

The picture emerging is as follows the distribution of the fireball results from the excitation of oscillator modes of the colliding hadrons. This excitation takes place in pairs. Modes de-excite statistically emitting 2 pairs of quarks which we identify as two pions The phase space distribution of the fireball:

$$|<n,\beta|n,-\beta'>|^2 = (2\pi)\int dudvW_{\beta}^n(u,v,q_u,q_v)W_{\beta'}^n(u,v,q_u,q_v) \quad (19)$$

Probability of emission of m particles from two independent populations 1 and 2 corresponding to each of the incident hadrons. forming an overlapping distributions is given as:

$$P_m = \sum_{m'=0}^{m}P_{m-m'}^1 P_{m'}^2 \quad (20)$$

Total probability distribution thus becomes a product of the probability distribution of four squeezed sources:

$$P_m = \sum_{m_1+-m_2+m_3+m_4=m}P_{m_1}^{sq}(\eta)P_{m_2}^{sq}(-\eta)P_{m_3}(\eta')P_{m_4}(-\eta')$$

For target Projectile collisions $\beta' = 0$ thus the probability of emitting n' particles is:

$$
\begin{aligned}
P_{n'} &= \sum_{p=0}^{n'} \sum_{m=0}^{n} \binom{n'}{p} \binom{n}{m} \\
&\times (-1)^{\frac{n'+n}{2}} (p!(n-m)!m!(n'-p)!)^{1/2} \frac{1}{cosh(\eta)} (\frac{tanh(\eta)}{2})^{\frac{n'+n}{2}} (-1)^{\frac{m+n'-p}{2}} \\
&\times \sum_{\mu\lambda}' \frac{(\frac{-4}{sinh^2(\eta)})^{\lambda+\mu}}{(2\mu)!(p/2-\mu)!(\frac{n'-p}{2}-\mu)!(m/2-\lambda)!(\frac{n-m}{2}-\lambda)!}
\end{aligned}
$$

As β increases the distribution gets broader .

For Central Collisions $\beta = \beta'$ and by plotting mP_m vs. $\frac{m}{<m>}$ for different values of β we see that the distributions become wider and skew symmetric as the value of β becomes larger. This is consistent with the variation seen in experimental data.

The total probability distribution for the two nucleon system for n pions is:

$$P_n^k = \sum_{\sum n_i = n} \prod_i^{k/2} P_{n_i}^{sq}(\eta) \sum_{\sum n_i = n} \prod_i^{k/2} P_{n_i}^{sq}(-\eta) \tag{21}$$

where k=6 for nucleon-nucleon collisions , k=4 for $\pi\pi$ collisions and k=3 for νp collisions (with η positive).

We include final state interactions in a simple fashion by assuming that the effect of interaction is to add coherence into the final state. This is consistent with the fact that in particle collisions experimental data shows some amount of coherence, especially in the low energy region , among the emitted particles. With the resulting density matrix we obtain the mutiplicity distribution for a variety of collisions and compare to data. The distribution we get is:

$$P_n^k = \sum_{\sum n_i = n} \prod_i^{k/2} P_{n_i}^{sq,coherent}(\alpha,\eta) \sum_{\sum n_i = n} \prod_i^{k/2} P_{n_i}^{sq,coherent}(\alpha,-\eta) \tag{22}$$

Where the average number of particles emitted by each mode is given by: $\overline{n}_i = \alpha^2 + Sinh^2(\eta)$ Above distribution fits the CERN ISR 62.2 GeV and UA5 540 GeV data. The k=3 distribution is compared with νp data. The data is well reproduced by the distribution. For e^+e^- collisions we take k=2 because the intermedeate state is the virtual $\bar{q}q$ state formed by the colliding electron and positron.

In terms of hadronic final states the LEP energy ($\sqrt{s}$ = 100 GeV) is equivalent to the SPS energy ($\sqrt{s}$ = 546 GeV) as far as total mutiplicitics are concerned, in so far as $\overline{n}^{e^+e^-}$(LEP) $\approx \overline{n}^{\bar{p}p}$(SPS) $\approx$26 .

For the same value of $\overline{n}$ much narrower distribution for e^+e^- distributions than the $\bar{p}p$ distributions. This is consistent with recent LEP data [11].

We can make some predictions for higher energies such as those observed at the LHC and SSC. Since widening of the distributions is related to the squeezing parameter η the lorentz boost of the hadronic fireball, at C.M.S. energies of 20 TeV and above we have a large β value and

higher modes will be excited. The multiplicity distribution for ultra-high energies is very broad and skew-symmetric. plot $\overline{n}P_n vs. \frac{n}{\overline{n}}$ for $\overline{p}p$ collisions for $\overline{n} = 50$

We can also calculate the Bose-Einstein Correlations of pions in this model by using the two mode state. Ongoing work is in progress to establish the connection of this model with QCD using the light cone formalism [12]. In this formalism it is also easy to incorporate temperature dependence by using Thermal Squeezed Coherent states. These would be of interest in heavy ion collisions.

5 Acknowledgements

I would like to thank Prof. Y.S. Kim and all the other organizers of ICSSUR '95 for their kind hospitality and support. I also acknowledge the support of the University Grants Commision,National Board of Higher Mathematics, INSA , DST and CSIR for their support.

References

[1] P.Carruthers and C.C.Shih, International Journal of Mod. Phys.**A2**(1987)1447.

[2] G.N. Fowler and R.M. Weiner in **'Hadronic Multipaticle Production'** Ed. P.Carruthers, (1988) 481.

[3] T.C. Meng in **Hadronic Multiparticle Production** Ed. P. Carruthers (1988), and references therein.

[4] B.Bambah and M.V.Satyanarayana Phys. Rev. D **38**(1988) 2202.

[5] R.P.Feynman,M.Kislinger and F.Ravndal Phys. Rev. D **3**(1971)2706.

[6] Y.S.Kim and E.P.Wigner, Phys. Rev. A **39**(1989)2829.

[7] Y.S.Kim and E.P.Wigner, Phys. Rev. D **49**(1990).

[8] Y.S. Kim and M.E.Noz.**'Theory and Applications of the Poincare Group'** (Reidel and Dortrecht,1986).

[9] M.V.Satyanarayana Phys. Rev. D **32** (1985) 400.

[10] S. Chaturvedi and V. Srinivasan Phys. Rev. A **40** (1989)6095.
; M.S.Kim, F.A.M. de Oliviera and P.L.Knight**"The Squeezing of Fock and Thermal States"** Imperial College Preprint,1991

[11] D. Decamp et. al. ALEPH COLLAB. , Phys. Lett. **B273** (1991)180.

[12] S.J.Brodsky in **Nuclear Chromodynamics** S.J. Brodsky and E.J. Moniz .eds. (World Scientific, 1986) and F.Lenz. ibid.

NEXT
DOCUMENT

COHERENT STATES FOR KRONECKER PRODUCTS OF NON COMPACT GROUPS: FORMULATION AND APPLICATIONS

Bindu A. Bambah
School of Physics
University Of Hyderabad Hyderabad-500134,India

G.S. Agarwal
Physical Research Labratory , Ahmedabad

Abstract

We introduce and study the properties of a class of coherent states for the group SU(1,1) X SU(1,1) and derive explicit expressions for these using the Clebsch-Gordan algebra for the SU(1,1) group. We restrict ourselves to the discrete series representations of SU(1,1). These are the generalization of the 'Barut Girardello' coherent states to the Kronecker Product of two non-compact groups. The resolution of the identity and the analytic phase space representation of these states is presented. This phase space representation is based on the basis of products of 'pair coherent states' rather than the standard number state canonical basis. We discuss the utility of the resulting 'bi-pair coherent states' in the context of four-mode interactions in quantum optics.

1 FORMULATION

1.1 Coupling of Pair coherent states in the fock state basis

For two mode systems the traditional SU(1,1) coherent states which have been extensively studied in the context of squeezing have been the Caves-Schumaker states [1], defined by the relation

$$|\zeta>=\exp(\zeta a^\dagger b^\dagger-\zeta^* ab)|0,0>, \tag{1}$$

In addition to these states many authours [2] [3] have considered the SU(1,1) coherent states of two mode systems or the 'pair coherent states' which were simultaneous eigenstates of ab and $a^\dagger a-b^\dagger b$

$$\begin{aligned} ab|\zeta,q> &= \zeta|\zeta,q>, \\ Q_1|\zeta,q> &= q_1|\zeta,q>. \end{aligned} \tag{2}$$

These can be mapped onto the SU(1,1) group by means of the two Boson realisation:

$$K_1^+=a^\dagger b^\dagger\ ,\ K_1^-=ab\ ,\ K_1^z=\frac{1}{2}(a^\dagger a+b^\dagger b+1)\ , \tag{3}$$

which form an SU(1,1) algebra with the commutation relations

$$\left[K_1^+, K_1^-\right] = -2K_1^z \,, \left[K_1^z, K_1^\pm\right] = \pm K_1^\pm. \tag{4}$$

The conservation law for Q_1 is related to the Casimir operator C for the SU(1,1) group; which can be written as

$$C = \frac{1}{4}(1 - (a^\dagger a - b^\dagger b)^2) = \frac{1}{4}(1 - Q_1^2). \tag{5}$$

Thus the eigenstate of Q_1 is also an eigenstate of C and the pair coherent state is related to the eigenstate of K_1^- by Barut and Girardello.

These generate a representation D^{q_1} that correspond to the positive discrete series representation of SU(1,1) [4]. In the number state basis, this corresponds to the basis states $|n_1 + q_1, n_1>$, where

$$|n_1 + q_1, n_1 >= \frac{(a^\dagger)^{n_1+q_1}(b^\dagger)^{n_1}}{((n_1!)(n_1+q_1)!)^{\frac{1}{2}}}|0,0>, \tag{6}$$

The pair coherent state in the number state basis labelled as $|\zeta_1, q_i>$ is

$$|\zeta_1, q_1 >= N_{q_1} \sum_{n_1=0}^{\infty} \frac{\zeta_1^{n_1}}{\sqrt{n_1!(n_1+q_1)!}}|n_1 + q_1, n_1>, \tag{7}$$

with

$$N_{q_1} = \left[(|\zeta_1|)^{-q_1} I_{q_1}(2|\zeta_1|)\right]^{-1/2} . \tag{8}$$

These states constitute a complete set in each sector q_i and the completeness relation is given by

$$\int d^2\zeta_1 \frac{2}{\pi} I_{q_1}(2|\zeta_1|) K_{q_1}(2|\zeta_1|)|\zeta_1, q_1 >< \zeta_1, q_1| \tag{9}$$

for the normalized states .

We now consider the group obtained by the addition of two SU(1,1) generators defined for four modes a,b,c,d.

$$\begin{aligned} K^+ &= a^\dagger b^\dagger + c^\dagger d^\dagger = K_1^+ + K_2^+ \,, \\ K^- &= ab + cd = K_1^- + K_2^- \,, \\ K^z &= \frac{1}{2}(a^\dagger a + b^\dagger b + c^\dagger c + d^\dagger d + 2) = K_1^z + K_2^z. \\ C &= \frac{(K^+K^- + K^-K^+)}{2} - K_z^2. \end{aligned} \tag{10}$$

The 'bi- pair coherent states' or the coherent states for the Kronecker Product are now the eigenstates of K^- ,C_1, C_2 and C . If we restrict ourselves to the positive discrete series representations of SU(1,1) then the Kronecker Product $D^{q_1} X D^{q_2}$ i.e the Clebsch Gordan series for SU(1,1) given by

$$D^{q_1} X D^{q_2} = \sum_{q \;\; q_1+q_2+1}^{\infty} D^q. \tag{11}$$

Thus a given representation in the Kronecker product is fixed by q, q_1, q_2

The eigenvalue problem that we wish to solve is

$$K^{-}|\zeta,q>=\zeta|\zeta,q> \quad ;C|\zeta,q>=(1/4-q^2/4)|\zeta,q> . \tag{12}$$

In terms of the product number state basis $|n_1+q_1,n_1>|n_2+q_2,n_2>$ we get:

$$\begin{aligned}|\zeta,n,q_1,q_2> &= N_n\sum_{k=0}^{\infty}\frac{(\zeta)^k}{[(k)!(k+2n+q_1+q_2+1)!]^{\frac{1}{2}}} \\ &\times \sum_{n_1,n_2} C^{q_1,q_2,n}_{n_1,n_2,n+k}\delta_{(n_1+n_2,n+k)}|n_1+q_1,n_1>|n_2+q_2,n_2> .\end{aligned} \tag{13}$$

we get an expression for the Kronecker Product states in terms of the CG coefficients in the photon number basis.

1.2 Clebsh Gordan Problem in the pair coherent state basis

Consider the four mode bases of the Hilbert space characterised by the product of two pair (SU(1,1) coherent states $|\zeta_1,q_1>|\zeta_2,q_2>$. Since these coherent states form an overcomplete set any vector in the four mode Hilbert space can be expanded in terms of these states. In particular the coherent state of the product SU(1,1) X SU(1,1) $|\zeta,q>$ can be expanded directly in terms of the unnormalized states

$$\begin{aligned}|\zeta_1,q_1>> &= \sum_{n=0}^{\infty}\frac{\zeta_1^n}{\sqrt{n!(n+q_1)!}}|n+q_1,n> , \\ |\zeta_2,q_2>> &= \sum_{m=0}^{\infty}\frac{\zeta_2^m}{\sqrt{m!(m+q_2)!}}|m+q_2,m> .\end{aligned} \tag{14}$$

The completeness relation for the unnormalised states $|\zeta_i,q_i>>$ can be deduced from (2.18) to be

$$\int d^2\zeta_i\frac{2}{\pi}|\zeta_i|^{q_i}K_{q_i}(2|\zeta_i|)|\zeta_i,q_i>><<\zeta_i,q_i| = 1. \tag{15}$$

The unnormalised states have th· ·dvantage that the operators $K_i^{\pm}$ and K_i^z can be expressed as differential operators. The completeness relation and resolution of the identity ensures that the product states $|\zeta_1,q_1>>|\zeta_2,q_2>>$ form the basis states for $D^{q_1}XD^{q_2}$ and any four mode state $|\psi>$ can be expanded as

$$|\psi>=\int <<\zeta_1,q_1<<\zeta_2,q_2|\psi>|\zeta_1q_1>>|\zeta_2,q_2>>d^2\sigma(\zeta_1)d^2\sigma(\zeta_2). \tag{16}$$

In this representation the quantity $<<\zeta_1,q_1,zeta_2,q_2|\psi>$ is an analytic function $\psi(\zeta_1^*,\zeta_2^*,q_1,q_2)$ and the operators K_1 and K_2 act as ifferential operators on this function. In particular the coherent state vector $|\zeta,q>$ in this four mode hilbert space can be written as:

$$|\zeta,q,q_1,q_2>=\int <<\zeta_1,q_1<<\zeta_2,q_2|\zeta,q>|\zeta_1q_1>>|\zeta_2,q_2>>d^2\sigma(\zeta_1)d^2\sigma(\zeta_2). \tag{17}$$

This becomes the equivalent of the Clebsch Gordon equation in the pair coherent state basis and the quantity The overlap function $<<\zeta_1,q_1|\zeta_2q_2|\zeta,q>=f(\zeta_1^*,\zeta_2^*,\zeta q_1,q_2)$ is the equivalent

of the Clebsch Godon coefiient for the SU(1,1) COHERENT STATE BASIS. The action of the generators of SU(1,1) X SU(1,1) on f is given by

$$\begin{aligned}(K_1^+ + K_2^+)f &= (\zeta_1^* + \zeta_2^*)f \\ (K_1^- + K_2^-)f &= [(\frac{\partial}{\partial\zeta_1^*}(q_1 + \zeta_1^*\frac{\partial}{\partial\zeta_1^*} + (\frac{\partial}{\partial\zeta_2^*}(q_2 + \zeta_2^*\frac{\partial}{\partial\zeta_2^*}]f \end{aligned} \tag{18}$$

On the other hand

$$K_f = \zeta f \quad ; Cf = [(1 - q^2)/4]f \tag{19}$$

Thus we get the following two differential equations for f:

$$\left[\frac{\partial}{\partial\zeta_1^*}(q_1 + \zeta_1^*\frac{\partial}{\partial\zeta_1^*}) + \frac{\partial}{\partial\zeta_2^*}(q_2 + \zeta_2^*\frac{\partial}{\partial\zeta_2^*})\right] f = \zeta f \,,$$

and

$$\begin{aligned}&\left[\zeta_1^*\zeta_2^*(\frac{\partial^2}{\partial\zeta_1^{*2}} - 2\frac{\partial}{\partial\zeta_1^*}\frac{\partial}{\partial\zeta_2^*} + \frac{\partial^2}{\partial\zeta_2^{*2}})\right] f \\ &+ \left[(q_1+1)\zeta_2^*(\frac{\partial}{\partial\zeta_1^*} - \frac{\partial}{\partial\zeta_2^*}) - (q_2+1)\zeta_1^*(\frac{\partial}{\partial\zeta_1^*} - \frac{\partial}{\partial\zeta_2^*})\right] f \\ &= -\left[\frac{q^2}{4} - \frac{(q_1+q_2+1)^2}{4}\right] f\end{aligned}$$

Solving these two equations we get [5]:

$$\begin{aligned} f &= << \zeta_1, q_1, \zeta_2, q_2 | \zeta, q >> \\ &= N(\zeta(\zeta_1^* + \zeta_2^*))^{-q/2} I_q(\sqrt{4\zeta(\zeta_1^* + \zeta_2^*)}(\zeta_1^* + \zeta_2^*)^n P_n^{q_2,q_1}(\frac{\zeta_1^* - \zeta_2^*}{\zeta_1^* + \zeta_2^*}) \end{aligned} \tag{20}$$

N is the normalisation . Thus the state $|\zeta, q>$ can be obtained from the relation:

$$|\zeta, q >= \frac{4N}{\pi^2}\int d^2\zeta_1 \int d^2\zeta_2 K_{q_1}(2|\zeta_1|)K_{q_2}(2|\zeta_2|) << \zeta_1, q_1, \zeta_2, q_2|\zeta, q >> |\zeta_1, q_1 >> |\zeta_2, q_2 >> \tag{21}$$

This is the Clebsch Gordon form for the product basis of Coherent states of SU(1,1) X SU(1,1).

It is interesting to note that by substituting the values of $|\zeta_1, q_1 >>$ and $|\zeta_2, q_2 >>$ given in equations (14) and using the expansion for the Jacobi Polynomial as well as the expansion of the Bessel function I_q and carrying out the various integrations we have:

$$\begin{aligned} |\zeta, q > &= N' \sum_{k=0}^{\infty} \frac{\zeta^k}{(k!(k+q)!)^{\frac{1}{2}}} \sum_{n_1,n_2} \delta_{(n_1+n_2,n+k)} \\ &\left[\frac{n_1!n_2!,(n_1+q_1)!(n_2+q_2)!k!}{(k+q)!}\right]^{\frac{1}{2}} ((n+q_1)!(n+q_2)!) \\ &\sum_l (-1)^l \frac{1}{l!(q_2+l)!(n-l)!(n_2-l)!(n_1-n-l)!(n+q_1-l)!}|n_1+q_1, n_1 > |n_2+q_2, n_2 \end{aligned} \tag{22}$$

By comparison with expression [13] in the previous section we have:

$$C^{q_1,q_2,n}_{n_1,n_2,n+k} = \left[\frac{n_1!n_2!,(n_1+q_1)!(n_2+q_2)!k!}{(k+2n+q_1+q_2+1)!}\right]^{\frac{1}{2}} ((n+q_1)!(n+q_2)!)^{1/2}$$
$$\sum_m (-1)^m \frac{1}{(q_2+m)!(n-m)!(n_2-m)!(n_1-n-m)!(n+q_1-m)!} \quad . \tag{23}$$

Which is the Clebsch Gordon coefficient for the canonical number state basis for SU(1,1)XSU(1,1)

2 SubPoissonian Properties of SU(1,1)XSU(1,1) coherent states

To give an idea of the Sub-Poissonian nature of these states let us consider a special case which is useful in physical applications. Consider the case $q_1 = q_2 = 0$; q=1 ; $\zeta \neq 0$
In this special case , we start with equal number of photons in the modes a and b and in c and d. Then

$$|\zeta,1,0,0>= N_1 \sum_k \frac{\zeta^k}{[(k+1)!(k)!]^{1/2}} \sum_{n_1,n_2} \frac{1}{(k+1)^{1/2}} \delta_{n_1+n_2,k} |n_1,n_1> |n_2,n_2> , \tag{24}$$

where

$$N_1 = \frac{(|\zeta|)^{1/2}}{[I_1(2|\zeta|)]^{1/2}} \quad . \tag{25}$$

The single mode probability distribution P_{n_1} and the mean number of photons $< n_1 >$ are given by

$$P_{n_1}(\zeta) = N_1^2 |\zeta|^{2n_1} \sum_{n_2} \frac{|\zeta|^{2n_2}}{(n_2+n_1+1)!^2} \quad , \tag{26}$$

and

$$< n_1 >= \frac{|\zeta| I_2(2|\zeta|)}{2I_1(2|\zeta|)} \tag{27}$$

A measure of the non-classical nature of the distribution is given by Mandel's Q parameter , which for the mode a is given by

$$Q = \frac{< n_1^2 > -(< n_1 >)^2 - < n_1 >}{< n_1 >} \tag{28}$$
$$= \frac{2|\zeta| I_3(2|\zeta|)}{3I_2(2|\zeta|)} - \frac{|\zeta| I_2(2|\zeta|)}{2I_1(2|\zeta|)}. \tag{29}$$

In fig. 1 we plot Q .vs. $|\zeta|$. For values of $|\zeta| < 2$, Q is negative showing the departure from the Poisonnian. The joint probability distribution $P_{n_1+n_2}$ can be calculated from P_{n_1,n_2} by the relation:

$$P_k = \sum_{n_1,n_2} \delta_{n_1+n_2,k} P_{n_1,n_2} = \frac{N_1^2 |\zeta|^{2k}}{k!(k+1)!} \tag{30}$$

The average value $< k >$ is given by:

$$\sum_k k P_k = \frac{|\zeta| I_2(2|\zeta|)}{I_1(2|\zeta|)} \tag{31}$$

In figure 2 we plot P_k.*vs.*k and compare it to the corresponding Poissonian with mean value $< k >$ and it is clear that the distribution is sub Poissonian.

3 Physical Applications

SU(1,1)XSU(1,1) states are useful states in dealing with physical systems involving four modes of the radiation fields. The physical problem could be the passage of two-beams of light each having two polarisation modes passing through a medium in which there is a competition between the non-linear gain due to an external pumping field and the non-linear absorption[7] [8],[9]. The states generated are precisely the states considered in this paper. Let each beam contain both left and right circularly polarised photons. Let a,b, a ,b denote the creation and annilation operators for RIGHT circularly polarised photons from beam 1 and beam 2 and $c, d, c^\dagger, d^\dagger$ denote the creation and annihilation operators for LEFT circularly polarised photons in beam 1 and beam 2. The master equation describing the dynamic behaviour of the fields resulting from the competition between two photon absorption and four wave mixing can be shown to be:

$$d\rho/dt = -K/2(O^\dagger O\rho - 2O\rho O^\dagger + \rho O^\dagger O) - i\left[G(O^\dagger + O), \rho\right] [3] \tag{32}$$

Where G denotes the four wave mixing susceptibility. Where K is related to the cross-section for two photon absorption and O = ab+cd. Defining an operator C=O+2iG/K We have:

$$d\rho/dt = -K/2(C^\dagger C\rho + \rho C^\dagger CC - 2C\rho C^\dagger) \tag{33}$$

Whose steady state solution: $C\rho = 0$ with $\rho = |\psi >< \psi|$ so that: $C|\psi >= 0$ implying that $O|\psi >= -2iG/K|\psi >$ or $(ab + cd)|\psi >= \lambda|\psi >$ Where $\lambda = -2iG/K$ Thus the steady state solutions of the master equations are eigenstates of the operator O. Furthermcre, if we now impose the condition that the initial state is one in which the difference in the in the the number of photons in the two polarisation modes of each beam is a constant, with q being the constant for the right circularly polarised photons and q being the constant for the left circularly polarised photon in beam 1 and beam 2, the states $|\psi >$ are just the SU(1,1) X SU(1,1) coherent states.

Another examples of processes where four modes of the radiation field are important involve phase conjugate resonators and the process of down conversion in the field of a standing pump wave[6] .In the latter case, the forward wave will produce the modes a and b and the backward pump will give the modes c and d. The Hamiltonian for such interactions will have the form

$$H = (\epsilon_f^* ab + \epsilon_b^* cd + c.c), \tag{34}$$

where ϵ_f and ϵ_b are the forward and backward fields. Again the relevant coherent states are the eigenstates of the operator

$$K^- = (ab + cd) = K_1^- + K_2^-. \tag{35}$$

Acknowledgments

I would like to thank the University Grants Commision, India, National Board of Higher Mathematics, India, Indian National Science Academy, DST and CSIR for financial support.

References

[1] C.M. Caves and B.L. Schumaker, Phys. Rev.A. **31**,3068 (1985);ibid, **A31** 3093, (1985) A.Perelomov, **'Generalized Coherent States'**(Springer-Verlag, 1985).

[2] A.O. Barut and L. Girardello, Communications in Math Physics **21**, 41, (1971) . B. Bhaumik, K. Bhaumik, and B Datta-Roy, J. Phys. Math A **9**, 1507 (1976) .

[3] G.S. Agarwal , J. Opt.,Soc.,Am. **B 5** , 1940 (1988).

[4] W. Holman and L. Biedenharn, Ann. of Phys. **39**, 1, (1966).

[5] M. Abramowitz and I. Stegun, **'Handbook of Mathematical Functions'** (Dover 1970)

[6] G.S. Agarwal, A.L. Gaeta and R. Boyd, Phys. Rev. **A47**, 597 (1993)

[7] G.S Agarwal, Phys. Rev. Lett. **59**, 827 (1986).

[8] T.J.Herzog, J.G.Rarity, H.Weinfurter, A. Zeilinger, Phys. Rev. Lett.**72**, 629 (1994) .

[9] D.Schauer, Phys. Rev. Lett. **70**, 2710 (1993) .

NEXT
DOCUMENT

HIGHER–ORDER SQUEEZING IN A BOSON COUPLED TWO–MODE SYSTEM

A. V. Chizhov
Bogoliubov Laboratory of Theoretical Physics
Joint Institute for Nuclear Research, 141980 Dubna, Russia

J. W. Haus and K. C. Yeong
Physics Dept., Rensselaer Polytechnic Institute, Troy, NY 12180–3590

Abstract

We consider a model for nondegenerate cavity fields interacting through an intervening Boson field. The quantum correlations introduced in this manner are manifest through their higher–order correlation functions where a type of squeezed state is identified.

1 Introduction

Squeezed state generation of electromagnetic fields provides a means of reducing uncertainty in one electric field quadrature at the expense of a larger uncertainty in its conjugate partner [1, 2]. It is one realization of nonclassical states (ideally, minimum uncertainty states) that has received wide attention. Ordinarily, in single or multi–mode squeezing, the fluctuations of linear combinations of the field operators are considered [1]; however, Hillery [3] introduced quadratic combinations of the field operators as a type of higher–order squeezing [4]. The higher–order combinations are examined to help elucidate the nature of the phase space occupied by the squeezed states.

We consider a two–mode model originally developed to study stimulated Raman scattering [5, 6]. In a cavity environment the model has features of amplifiers [7, 8] in which quantum states are rendered macroscopic and therefore, classically measurable, while at the same time the fields retain some quantum mechanical correlations. The introduction of both Stokes and anti–Stokes fields indirectly coupled through a Boson field, whose origin stems either from phonons or weak atomic excitation of the medium, is an interesting two–mode quantum system. It differs from several previous two–mode systems, eg. [1, 8, 9], because the two modes are coupled through the intermediate field that acts like a reservoir.

The emphasis of this paper is placed on higher–order squeezing found in the fields because squeezing of the linear combinations of the operators is not present in this model. A more complete discussion of the results can be found in [10]. The type of higher–order squeezing found is in the variance of the variables defined by Hillery, so–called sum or difference squeezing variables; they are used to infer that quantum correlations exist between the electromagnetic fields and the Boson fields.

2 Model

We investigate the model Hamiltonian for a stimulated Raman scattering process with undepleted laser field e_L, which can be treated classically. The fields in the interaction are the Stokes field. subscript S, and anti-Stokes field, subscript A, that are coupled through a Boson field with multiple modes [5, 6]:

$$\mathcal{H} = \hbar\omega_S a_S^\dagger a_S + \hbar\omega_A a_A^\dagger a_A + \sum_l \hbar\omega_{Bl} a_{Bl}^\dagger a_{Bl} - \sum_l (\hbar g_l e_L a_S^\dagger a_{Bl}^\dagger + \hbar\kappa^* e_L a_A^\dagger a_{Bl} + \text{h.c.}). \qquad (1)$$

This model has a bath of Bosons, eg., phonons that have excitation energies spread over a range of frequencies. In this model the Bosons are responsible for coupling the electromagnetic fields and for introducing damping, as well.

In order to calculate various moments we determine the characteristic function of the operators in normal-ordered form. The normal characteristic function after reducing the intermediate reservoir in the dynamical equations is expressed as an average over an initial distribution of complex amplitudes $\{\xi_S, \xi_A\}$, which is the coherent-state representation for the initial field operators,

$$C_N(\beta_S, \beta_A, t) = \left\langle e^{-B_S(t)|\beta_S|^2 - B_A(t)|\beta_A|^2 + [D_{SA}(t)\beta_S^*\beta_A^* + \text{c.c.}] + [\beta_S\xi_S^*(t) + \beta_A\xi_A^*(t) - \text{c.c.}]} \right\rangle, \qquad (2)$$

where we assume that the detuning parameter $\Delta = \omega_L - (\omega_S + \omega_A)/2$ is equal to zero and define

$$\xi_S(t) = u_S(t)\xi_S + v_S(t)\xi_A^*, \qquad \xi_A(t) = u_A(t)\xi_A + v_A(t)\xi_S^*.$$

The angular brackets denotes the average over the initial states of the Stokes and the anti-Stokes fields. The coefficients in the above expressions are obtained from solution of the Heisenberg equations of motion and the subsequent reduction of the Boson modes in the normal characteristic function using disentangling theorems. Letting $\Gamma = (\gamma_S - \gamma_A)|E_L|^2/2$, where the laser field is $E_L = e_L \exp(i\omega_L t)$ and the parameters

$$\gamma_S = 2\pi|g(\omega_B)|^2\rho(\omega_B), \qquad \gamma_A = 2\pi|\kappa(\omega_B)|^2\rho(\omega_B),$$

introduced from the Markoff approximation with the Boson excitation frequency $\omega_B = \omega_L - \omega_S$, the results are

$$\begin{aligned}
u_S(t) &= \frac{1}{\gamma_S - \gamma_A}(\gamma_S e^{\Gamma t} - \gamma_A); \qquad u_A(t) = \frac{1}{\gamma_S - \gamma_A}(\gamma_S - \gamma_A e^{\Gamma t}); \\
v_S(t) &= -v_A(t) = \frac{\sqrt{\gamma_S\gamma_A}}{\gamma_S - \gamma_A}(e^{\Gamma t} - 1)e^{i(2\phi_L + \psi_S - \psi_A)}; \\
B_S(t) &= \frac{1}{(\gamma_S - \gamma_A)^2}\left(\gamma_S^2(e^{2\Gamma t} - 1) + 2\gamma_S\gamma_A(1 - e^{\Gamma t})\right) + \frac{\gamma_A\bar{n}_V}{\gamma_S - \gamma_A}(e^{2\Gamma t} - 1); \\
B_A(t) &= \frac{\gamma_S\gamma_A}{(\gamma_S - \gamma_A)^2}(e^{\Gamma t} - 1)^2 + \frac{\gamma_A\bar{n}_V}{\gamma_S - \gamma_A}(1 - e^{2\Gamma t}); \\
D_{SA}(t) &= \frac{\sqrt{\gamma_S\gamma_A}}{\gamma_S - \gamma_A}\left(\frac{1}{\gamma_S - \gamma_A}(e^{\Gamma t} - 1)(\gamma_A - \gamma_S e^{\Gamma t}) + \bar{n}_V(e^{2\Gamma t} - 1)\right)e^{i(2\phi_L + \psi_S - \psi_A)}.
\end{aligned} \qquad (3)$$

The phases are defined by $E_L = |E_L|\exp(i\phi_L), g = |g|\exp(i\psi_S)$ and $\kappa = |\kappa|\exp(i\psi_A)$.

The usual definition of the two-mode operators is a linear combination of the creation and annihilation operators. However, we find that the model discussed here does not yield the usual squeezed state correlations between the Stokes and anti-Stokes fields. The coupling through the reservoir is aiso expected to degrade the coherence developed between the Stokes and the anti-Stokes fields during evolution. It is, therefore, surprizing that the fields do display quantum coherences in the higher-order correlations between the fields. To show this we adopt of the definitions of sum squeezing and difference squeezing used by Hillery [3].

2.1 Sum Squeezing

For sum squeezing we define the operators

$$V_1 = \frac{1}{2}(A_S^\dagger A_A^\dagger + A_S A_A), \qquad V_2 = \frac{i}{2}(A_S^\dagger A_A^\dagger - A_S A_A). \tag{4}$$

The product of their standard deviations, ΔV_i, satisfies the Heisenberg inequality

$$\Delta V_1 \Delta V_2 \geq \frac{1}{4}\langle N_A + N_S + 1\rangle . \tag{5}$$

The operators are in a quantum state, said to be sum squeezed in the V_1 direction when the variance of V_1 satisfies the inequality

$$(\Delta V_1)^2 < \frac{1}{4}\langle N_A + N_S + 1\rangle . \tag{6}$$

To determine whether the dynamics produces a higher-order squeezed state, we define the shifted variance

$$\delta V_1^2 = (\Delta V_1)^2 - \frac{1}{4}\langle N_A + N_S + 1\rangle ; \tag{7}$$

which is negative in the region of the quantum state.

The moments of these operators are calculated by using the characteristic function and the result for the sum squeezing shifted variance of V_1 is

$$\begin{aligned} \delta V_1^2 &= \frac{1}{4}\Big\langle \left[(\xi_S(t)\xi_A(t))^2 + 4D_{SA}(t)\xi_S(t)\xi_A(t) + 2(D_{SA})^2 + 2D_{SA}^*\xi_S(t)\xi_A(t) + \text{c.c.}\right] \\ &+ 2\left[|\xi_S(t)\xi_A(t)|^2 + B_S(t)|\xi_A(t)|^2 + B_A(t)|\xi_S(t)|^2 + |D_{SA}(t)|^2 + B_S(t)B_A(t)\right]\Big\rangle \\ &- \frac{1}{4}\langle \xi_S(t)\xi_A(t) + D_{SA}(t) + \text{c.c.}\rangle^2 . \end{aligned} \tag{8}$$

2.2 Difference Squeezing

For the definition of difference squeezing, define

$$W_1 = \frac{1}{2}(A_S A_A^\dagger + A_S^\dagger A_A), \qquad W_2 = \frac{i}{2}(A_S A_A^\dagger - A_S^\dagger A_A). \tag{9}$$

The state is difference squeezed in the W_1 operator when the variance of the operator satisfies the inequality ($\langle N_S\rangle > \langle N_A\rangle$)

$$(\Delta W_1)^2 < \frac{1}{4}\langle N_S - N_A\rangle . \tag{10}$$

The moments are calculated from the characteristic function, as discussed already in the previous subsection. We also define a shifted variance of W_1 in analogy with Eq. (7)

$$\delta W_1^2 = (\Delta W_1)^2 - \frac{1}{4}(N_A - N_S) \tag{11}$$

which is negative when the state is squeezed along the W_1 direction. For the difference squeezing variable W_1 we have the following expression

$$\begin{aligned} \delta W_1^2 &= \frac{1}{4}\Big\langle\Big[(\xi_S(t)\xi_A^*(t))^2 + 2D_{SA}^*(t)\xi_S(t)\xi_A(t) + \text{c.c.}\Big] + 2\Big[|\xi_S(t)\xi_A(t)|^2 + B_S(t)|\xi_A(t)|^2 \\ &+ B_A(t)|\xi_S(t)|^2 + |D_{SA}(t)|^2 + B_S(t)B_A(t) + |\xi_A(t)|^2 + B_A(t)\Big]\Big\rangle - \frac{1}{4}\langle\xi_S(t)\xi_A^*(t) + \text{c.c.}\rangle^2 . \end{aligned} \tag{12}$$

3 Results

There are several parameters occuring in the model and appearing in Section 2. The dynamical parameters, i.e. those appearing in the evolution equations have been previously defined. We note that the detuning is assumed to be small in our model and this parameter is set to zero. The initial states of the fields represent another set of important parameters. The choice of an initial state for the Stokes and anti-Stokes fields is dictated by experimental conditions. We restrict our discussion to combinations of two experimentally useful initial states: the coherent state and the chaotic state. Using one of the choices, we examine the quantum correlations developed betwwen the electromagnetic fields; of course, other situations, such as, a Fock state or a squeezed vacuum state could also be identified. The Boson field is considered to be in a chaotic state with an average number of excitations $\bar{n}_B$; when the Stokes and/or anti-Stokes fields are in a chaotic state, then their phases are randomized and their statistical properties are also represented by their average photon number $\bar{n}_S$ and $\bar{n}_A$, resp. When the Stokes and anti-Stokes fields are in coherent states, in addition to the average photon number, the phase of the fields, ϕ_S and ϕ_A, is also needed.

The plot of Figure 1 is a display of the shifted variance of the operator V_1 versus the interaction time t for the three different values of the phase $\phi = 2\phi_L - \psi_S - \psi_A$. The Stokes and anti-Stokes fields are both initially in a coherent state, $n_S = n_A = 2$, and the reservoir is in the vacuum state $\bar{n}_V = 0$. The time has been scaled to the product, $\gamma|E_L|^2$, where E_L is the laser field amplitude and in the results presented here we set $\gamma = \gamma_S = \gamma_A$, i.e. the damping constants are equal. The region of the curves with negative ordinate values corresponds to the case when light is V_1-sum squeezed. The phase value of $\phi = \pi/2$ continues to decrease as the interaction time increases which means that for large times squeezing occurs near the point $\phi = \pi/2$. As the average number of excitations is increased in the Boson reservoir, the region for squeezing deteriorates.

When both the Stokes and the anti-Stokes fields are initially in a chaotic state, the sum squeezing variable V_1 still shows squeezing and the phase $\phi = \pi/2$ is very robust to the values of the initial state (Figure 2). We note that the initial value of the shifted variance has been changed by the initial chaotic state of the variables.

No squeezing was found for the variable W_1, either with coherent or chaotic initial states.

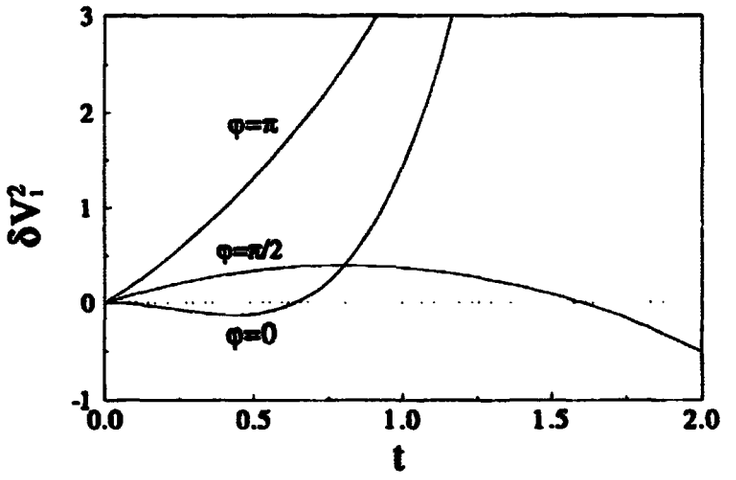

Figure 1: Plot of the sum squeezing shifted variance versus the interaction time for initially coherent Stokes and anti-Stokes fields. The phase $\phi = 2\phi_L + \psi_S - \psi_A$ has the values 0, $\pi/2$ and π.

4 Summary

In this paper we have examined a special model for the interaction between two modes in a cavity mediated by a Boson reservoir field [5, 6]. We find sum squeezing, a form of higher-order squeezing, over a range of interaction times and initial states. There are two salient features of our results; first, the intermediate field has a continuous spectrum of a reservoir, but still the two fields develop quantum mechanical correlations; and second, the quantum nature of the correlations is not manifest through the usual first order or even simple higher-order correlations among the operators, but through special combinations of the field operators.

There are other models where the fields are mediated by either electronic or acoustic fields, eg. a polariton or Brillouin scattering model [5, 6, 11]; these processes are analogous to the present model where the directly coupled fields are not detected in an experiment. In such cases experiments designed to measure higher-order correlations can reveal the underlying quantum correlations induced through the fields.

Acknowledgments

This work was supported by funds from the National Science Foundation Grant number PHY92-13449. from an NSF International Grant number INT 94-17628 and in part by Grant number RFD 300 from the International Science Foundation and Russian Government.

References

[1] R. Loudon and P. L. Knight, J. Mod. Optics **34**, 709 (1987).

[2] K. Zaheer and S. Zubairy, Adv. in Atomic, Molecular and Optical Physics **28**, 143 (1989).

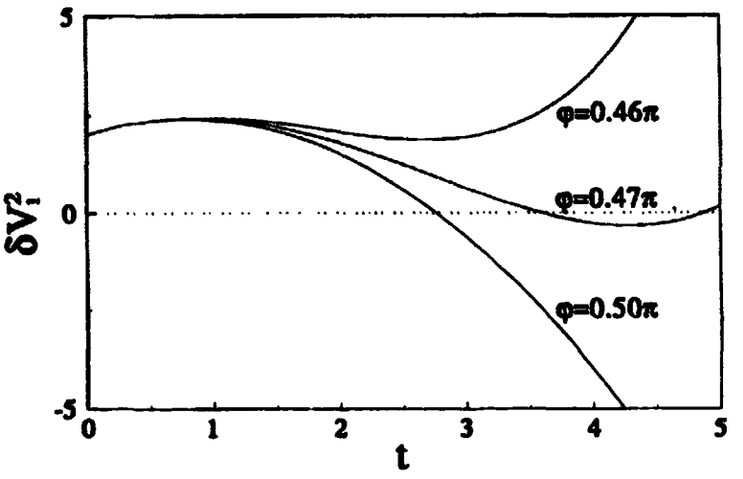

Figure 2: The sum squeezing shifted variance versus time for initially chaotic Stokes and anti-Stokes fields.

[3] M. Hillery, Opt. Commun. **62**, 135 (1987); Phys. Rev. A**36**, 3796 (1987); Phys. Rev. A**45**, 4944 (1992).

[4] C. K. Hong and L. Mandel, Phys. Rev. Lett. **54**, 323 (1985); Phys. Rev. A**32**, 974 (1985).

[5] D. F. Walls, J. Phys. A**6**,496 (1973).

[6] J. Peřina, Optica Acta **28**, 325 (1981); ibid. **28**, 1529 (1981).

[7] R. J. Glauber, in Proceedings of the VI International School on Coherent Optics, Ustron, Poland 1986, (Polish Academy of Sciences, Warsaw, 1987). Also in Group Theoretical Methods of Physics (Harwood Academic, NY, 1985), vol. I, p. 137.

[8] W. Wöger, H. King, R. J. Glauber and J. W. Haus, Phys. Rev. A**34**, 4859 (1986).

[9] J. W. Haus and H. J. Lee, Phys. Rev. A**43**, 4954 (1991); H. J. Lee and J. W. Haus, in Nonlinear Optics and Materials, eds. C. D. Cantrell and C. M. Bowden, Proc. of the SPIE **1497**, 228 (1991).

[10] A. V. Chizhov, J. W. Haus and K. C. Yeong, Phys. Rev. A**52**, 1698 (1995).

[11] A. V. Chizhov, B. B. Govorkov and A. S. Shumovsky, Mod. Phys. Lett. B**7**, 1233 (1993).

NEXT
DOCUMENT

New Interpretation Of The Wigner Function

Jamil Daboul

Physics Department, Ben Gurion University of the Negev
84105 Beer Sheva, Israel
(E-mail: daboul@bguvms.bgu.ac.il)

Abstract

I define a two-sided or forward-backward propagator for the pseudo-diffusion equation of the "squeezed" Q function. This propagator leads to squeezing in one of the phase-space variables and anti-squeezing in the other. By noting that the Q function is related to the Wigner function by a special case of the above propagator, I am led to a new interpretation of the Wigner function.

1 Introduction

The Wigner representation of any operator A is defined by

$$W(A;p,q) \equiv \int_{-\infty}^{\infty} (q-a \mid A \mid q+a)\, e^{2iap} da = Tr\,(A\,\mathbf{W}(p,q))\,, \tag{1}$$

where the rounded kets are eigenstates of the position operator, $\mathbf{Q}\,|x) = x\,|x)$, and $\mathbf{W}(p,q) \equiv \int_{-\infty}^{\infty} |q+a)(q-a|\,e^{2iap} da$ is a unitary and also a Hermitian operator, which can be interpreted as a displaced parity operator [2]. The Wigner representation yields functions of two variables, p and q, . ch may be looked upon as phase-space variables. These "Wigner functions" have interesting prope ies and are useful for various calculations [1]. The Wigner functions are often referred to as pseudo-probability functions, because they can take negative values, even when A is a positive operator, $A \geq 0$, such as the density operator ρ.

In contrast, the Husimi or Q representation [3] yield nonnegative functions for positive operators A: These functions are defined as follows

$$Q(A;p,q;\zeta) = \langle pq;\zeta \mid A \mid pq;\zeta\rangle = Tr\,(A\,\mathbf{\Pi}(pq;\zeta))\,, \quad \text{where} \quad \mathbf{\Pi}(p,q;\lambda) \equiv |\,pq;\zeta\rangle\langle pq;\zeta\,| \tag{2}$$

are projection operators on the squeezed states $|pq;\zeta\rangle$, which are defined by [4]

$$|pq;\zeta\rangle = \mathbf{D}(p,q)\mathbf{S}(\zeta)|0\rangle\,, \quad \text{where} \quad \zeta \equiv ye^{i\varphi} \quad (-\infty < y < \infty) \tag{3}$$

and $|0\rangle$ is the ground state of a specific harmonic oscillator, $\mathbf{a}|0\rangle = 0$. (i.e. $\mathbf{a}$ is the annihilation operator with a definite frequency ω_0; Henceforth, we set $\hbar = m = \omega_0 = 1$, for simplicity.) In (3)

$$\mathbf{D}(p,q) = \exp[-i(q\mathbf{P} - p\mathbf{Q})]\,, \tag{4}$$

is the displacement operator which generates the coherent states when applied to $|0\rangle$, and

$$\mathbf{S}(\zeta) = \exp\left[\frac{1}{2}\left(\zeta\mathbf{a}^{\dagger 2} - \zeta^{*}\mathbf{a}^{2}\right)\right]\,, \quad \left(\mathbf{a} \equiv \frac{\mathbf{Q}+i\mathbf{P}}{\sqrt{2}}\right) \tag{5}$$

is the squeezing operator, where the squeeze parameter y vanishes in the coherent-state limit.

If A is a density matrix ρ, then its Q function $Q(\rho;p,q;\zeta)$ can naturally be interpreted as a probability distribution. To emphasize this fact, the Q functions were denoted by P in [5, 6], instead of Q here.

For simplicity, I shall from now on discuss only squeezings which are pure boosts, without rotation, i.e. with $\varphi \equiv 0$ in (3), and use the squeezing parameter $\lambda := e^{2y}$ instead of y.

The Q and the Wigner functions are related as follows [1, 6]:

$$Q(A;p,q;\lambda) = \iint \frac{dp'dq'}{\pi} \exp[-\lambda^{-1}(p-p')^2 - \lambda(q-q')^2]\, W(A;p',q'). \tag{6}$$

In this paper, I shall first recall in Sec.2 that the Q functions (2) satisfy the partial differential equation (7). This equation describes how the Q functions $Q(p,q;\lambda)$ get changed in phase space (p,q) as the squeezing parameter λ is increased. In Sec.3 I define a forward-backward propagator for this equation. Finally, in Sec.4 I show that the Gaussian factor in the integral (6) is equal to a special case of the above propagator. This fact will yield the new interpretation of the Wigner function.

2 The Pseudo-Diffusion Equation

In previous papers [5, 6], it was shown that the Q functions, and other quantities, obey the following partial differential equation

$$\heartsuit(p,q;\lambda)\, Q(A;p,q;\lambda) \equiv \left[\frac{\partial}{\partial\lambda} - \frac{1}{4}\left(\frac{\partial^2}{\partial p^2} - \frac{1}{\lambda^2}\frac{\partial^2}{\partial q^2}\right)\right] Q(A;p,q;\lambda) = 0\,, \quad \text{where} \quad \lambda := e^{2y}\,, \tag{7}$$

where y is the squeezing parameter, as defined in (3). Eq. (7) was called [5, 6] *pseudo-diffusion equation*, because (a) it resembles the diffusion equation in 2 dimensions [7], where the parameter λ plays the role of time, and (b) the coefficients of $\frac{\partial^2}{\partial p^2}$ and $\frac{\partial^2}{\partial q^2}$ in (7) have opposite signs. Therefore, this equation describes a diffusive process in the p variable and an infusive one in the q variable *for all* λ. In this way a thin distribution along the q-axis get continuously deformed into a thin distribution along the p-axis, as λ is increased from 0 to ∞.

3 Solutions by Separation of Variables

The pseudo-diffusion equation (7) was solved by two methods [6]: by Fourier transform and by separation of variables. I shall now recall the latter method: Writing the solution as a product of two functions, $Q(p,q;\lambda) = \theta(p,\lambda)\psi(q,\lambda)$, where θ depends only on p and λ, and ψ depends only on q and λ, we get

$$\begin{aligned} 0 = \frac{1}{Q}\heartsuit Q \;&\equiv\; \frac{1}{\theta\psi}\left(\frac{\partial}{\partial\lambda} - \frac{1}{4}\left[\frac{\partial^2}{\partial p^2} - \frac{1}{\lambda^2}\frac{\partial^2}{\partial q^2}\right]\right)\theta\psi \\ &=\; \frac{1}{\theta}\left(\frac{\partial}{\partial\lambda} - \frac{1}{4}\frac{\partial^2}{\partial p^2}\right)\theta(p;\lambda) - \frac{1}{\psi}\left(-\frac{\partial}{\partial\lambda} - \frac{1}{4\lambda^2}\frac{\partial^2}{\partial q^2}\right)\psi(q;\lambda)\,. \end{aligned} \tag{8}$$

Since the first term in (8) depends only on p and λ, while the second term in (8) depends only on q and λ, we conclude that each of them must be equal to a function of λ only, which we denote

by $f(\lambda)$. In [6] the solutions for $f(\lambda) \neq 0$ were discussed. But for my purposes here, I shall only consider the case $f(\lambda) = 0$. For this case equation (8) yields the following two equations:

$$\left(\frac{\partial}{\partial\lambda} - \frac{1}{4}\frac{\partial^2}{\partial p^2}\right)\theta(p;\lambda) = 0 \qquad (9)$$

$$\left(-\frac{\partial}{\partial\lambda} - \frac{1}{4\lambda^2}\frac{\partial^2}{\partial q^2}\right)\psi(q;\lambda) = \frac{1}{\lambda^2}\left(\frac{\partial}{\partial\lambda^{-1}} - \frac{1}{4}\frac{\partial^2}{\partial q^2}\right)\psi(q;\lambda) = 0\,, \qquad (10)$$

where $\frac{\partial}{\partial\lambda} = -\frac{1}{\lambda^2}\frac{\partial}{\partial\lambda^{-1}}$ was used in (10). We see that θ obeys a 1-dimensional diffusion equation in p, where $\frac{1}{4}\lambda$ plays the role of time. Similarly, ψ obeys a diffusion equation in q, but with $\frac{1}{4}\lambda^{-1}$ playing the role of time. The solutions of the diffusion equation are well known [7]. In particular, the propagators of Eqs. (9) and (10) are specific solutions, given by

$$G_1(p-p',\lambda-\mu) = \frac{1}{\sqrt{\pi(\lambda-\mu)}}\exp\left[-\frac{(p-p')^2}{\lambda-\mu}\right], \qquad \text{for} \quad \lambda > \mu\,, \qquad (11)$$

$$G_1(q-q',\lambda^{-1}-\sigma^{-1}) = \frac{1}{\sqrt{\pi(\lambda^{-1}-\sigma^{-1})}}\exp\left[-\frac{(q-q')^2}{\lambda^{-1}-\sigma^{-1}}\right], \qquad \text{for} \quad \lambda < \sigma\,. \qquad (12)$$

Clearly, the products of the above two propagators yield a different solution of the pseudo-diffusion equation (7) for every 4-tupel (p', q', μ, σ):

$$G(p-p',q-q';\lambda,\mu,\sigma) \equiv G_1(p-p',\lambda-\mu)\,G_1(q-q',\lambda^{-1}-\sigma^{-1}) \qquad \text{for} \quad \mu < \lambda < \sigma\,,$$

$$= \frac{1}{\pi\sqrt{(\lambda-\mu)(\lambda^{-1}-\sigma^{-1})}}\exp\left[-\frac{(p-p')^2}{\lambda-\mu} - \frac{(q-q')^2}{\lambda^{-1}-\sigma^{-1}}\right]. \qquad (13)$$

I shall call these G functions *two-sided or forward-backward propagators* of the pseudo-diffusion equation (7), because they involve the two squeezing parameters, μ and σ, which are *on opposite sides of* λ. In particular, these G solutions have the proper limit when λ is approached from opposite directions:

$$\lim_{\mu\to\lambda-\epsilon\,,\;\sigma\to\lambda+\epsilon} G(p-p',q-q';\lambda,\mu,\sigma) = \delta(p-p')\delta(q-q')\,. \qquad (15)$$

Since the heart operator $\heartsuit$ is a linear, any superposition of the above 2-sided propagators will also be a solution of the pseudo-diffusion equation. In particular, if we fix the squeezing parameters μ and σ and integrate only over p' and q', we get solutions of the form

$$f(p,q;\lambda,\lambda) = \iint dp'dq'\,G(p-p',q-q';\lambda,\mu,\sigma)\,f(p',q';\mu,\sigma), \qquad \text{for} \quad \sigma > \lambda > \mu\,, \qquad (16)$$

for any given function $f(p,q;\mu,\sigma)$, provided that the integrals (16) exist.

4 The New Interpretation of the Wigner Function

An extreme case of the 2-sided propagators (14) is obtained by choosing $\mu = 0$ and $\sigma = \infty$. These squeezing parameters correspond to the values $-\infty$ and $+\infty$ of the $y = \frac{1}{2}\ln\lambda$ variable, respectively. For this choice of μ and σ, λ is free to take any positive value $\infty > \lambda > 0$. Moreover, the square-root factors in the two propagators cancel out. For this case, Eq. (16) becomes

$$f(p,q;\lambda,\lambda) = \iint \frac{dp'dq'}{\pi}\exp[-\lambda^{-1}(p-p')^2 - \lambda(q-q')^2]\,f(p',q';0,\infty), \qquad \text{for} \quad \lambda > 0\,. \qquad (17)$$

If we compare (17) with the well known relation (6) between the Q function and the Wigner function, we realize immediately that these two functions are simply related by the special 2-sided propagator $G(p-p', q-q'; \lambda, 0, \infty)$. Therefore, we are led in a natural way to the interpretation that *the Wigner function is a Q function, which is squeezed to* $y = +\infty$ *in the* q *variable and anti-squeezed to* $y = -\infty$ *in the* p *variable.*

Note that by applying the following relation

$$\int \frac{dp'}{\sqrt{\pi\lambda}} \exp[-\lambda^{-1}(p-p')^2]\, g(p') = \exp\left[\frac{\lambda}{4}\frac{d^2}{dp^2}\right] g(p)\,, \qquad \text{for} \quad \lambda > 0\,, \tag{18}$$

to (17), we obtain a formal solution $f(p, q; \lambda, \lambda)$ of the pseudo-diffusion equation (7), in terms of a differential operator applied to an arbitrary function $g(p, q) \equiv f(p, q; 0, \infty)$ of p and q:

$$f(p, q; \lambda, \lambda) = \exp\left[\frac{1}{4}\left(\lambda\frac{\partial^2}{\partial p^2} + \frac{1}{\lambda}\frac{\partial^2}{\partial q^2}\right)\right] f(p, q; 0, \infty)\,. \tag{19}$$

One can easily check, by simple differentiation with respect to λ, that this formal solution satisfies the pseudo-diffusion equation (7). In particular, if $g(p, q)$ is equal to the Wigner function of an operator A, then $f(p, q; \lambda, \lambda)$ is the corresponding Q function. This formal relatonship between these two functions was noted by Husimi [3].

As an application, we note that the relation (6) holds for every operator A, so that the corresponding two operators in Eqs. (1) and (2) are also related by the above special propagator:

$$\Pi(p, q; \lambda) = \iint \frac{dp'dq'}{\pi} \exp[-\lambda^{-1}(p-p')^2 - \lambda(q-q')^2]\, W(p', q')\,. \tag{20}$$

5 Conclusions

A one-sided propagator, which we would get for example from (14) by choosing $\mu, \sigma < \lambda$, is not suitable for the pseudo-diffusion equation (7), because one of the Gaussian factors in (14) will blow up at infinity. By showing that a special 2-sided propagator takes the Wigner function into a Q function, I concluded that the Wigner function can be regarded as a Q function, which is squeezed backwards ($\mu = 0$) in the p variable and forwards ($\sigma = \infty$) in q variable.

References

[1] Y. S. Kim and M. E. Noz, *Phase Space Picture of Quantum Mechanics*, World-Scientific, Singapore, 1991.

[2] R. F. Bishop and A. Vourdas, *Phys. Rev. A* **50**, 4488 (1994), and references therein.

[3] K. Husimi, *Prog. Theor. Phys.* **9**, 238 and 381 (1953).

[4] J. R. Klauder and B. S. Skagerstam, *Coherent States*, World-Scientific, Singapore, 1985. For a relatively recent review, see: M. M. Nieto, *What are squeezed states really like?* in: Frontiers in Nonequilibrium Statistical Physics, Eds. G. T. Moore and M. O. Scully, NATO ASI Series, vol. 135 (Plenum, New York, 1988).

[5] S. S. Mizrahi and J. Daboul. *Physica A* **189**, 635 (1992).

[6] J. Daboul, M. A. Marchiolli and S. S. Mizrahi, *J. of Physics A* **28**, 4623 (1995).

[7] D. V. Widder, *The Heat Equation*, Academic Press, London, 1975.

NEXT
DOCUMENT

OPERATORIAL APPROACH TO GENERALIZED COHERENT STATES

Salvatore De Martino
Silvio De Siena
Dipartimento di Fisica, Università di Salerno,
and INFN, Sezione di Napoli, Gruppo collegato di Salerno,
84081 Baronissi, Italy

Abstract

Generalized coherent states for general potentials, constructed through a controlling mechanism, can also be obtained applying on a reference state suitable operators. An explicit example is supplied.

1 Introduction

After the seminal works of Glauber, Klauder and Sudarshan [1], relevant generalizations and extensions of coherent states have been introduced, both in a group-theoretical framework [2], and in the direction of squeezing phenomena [3].

Moreover, a celebrated approach for general potentials was given in the case of classically integrable systems by Nieto and collaborators [4].

We have tackled the problem of building generalized coherent states from a point of view which can be useful also in a wider context [5]. In fact, if an interesting physical behaviour has been singled out for a quantum system, one can search for a controlling device which allows for its realization; we call this approach Controlled Quantum Mechanics (CQM) [6].

To this aim we use the methods of stochastic mechanics [7] [8]; however, we will show that these states can also be obtained in the standard operatorial approach.

2 The coherence constraint

We proceed now to apply the scheme of CQM to the problem of generalized coherent states. We will use in the following the notations $E(.)$ and $< . >$, respectively, for the stochastic mechanics and quantum mechanics mean values, sending back to [6] for the code of correspondence.

We search for states which are constrained to follow classical-like dynamics:

$$\frac{d}{dt} < \hat{p} >= F(< \hat{q} >, \Delta\hat{q}, t) \tag{1}$$

$$\frac{d^2}{dt^2}\Delta\hat{q} = G(<\hat{q}>, \Delta\hat{q}, t),$$

where F, G are known functions and $\Delta\hat{q}$ is the dispersion. A particular, but interesting, case is associated to constant dispersion.

If Φ denotes the potential associated to our states, the Ehrenfest equation

$$\frac{d}{dt} <\hat{p}> = - <\nabla\Phi> \tag{2}$$

always holds. Then we can write the above classical-like constraint in the more transparent form

$$<\nabla\Phi> = \nabla\Phi(x,t)|_{x=<\hat{q}>} + \delta F(<\hat{q}>, \Delta\hat{q}, t)$$

(3)

$$\frac{d^2}{dt^2}\Delta\hat{q} = G(<\hat{q}>, \Delta\hat{q}, t),$$

where δF is a known function. We note that for harmonic potentials this condition is always satisfied in the strict sense, that is with $\delta F = 0$.

However, for non-harmonic potentials the above condition becomes a true constraint. How this constraint can be imposed?

In the framework of stochastic mechanics the mean deterministic motion of the quantum process is ruled by the current velocity $v(x,t)$, while quantum fluctuations are associated to the osmotic velocity $u(x,t)$.

A given choice of $v(x,t)$ singles out a whole class of quantum states, all sharing a common mean motion. In our case, then, the constraint must be imposed through a suitable choice of the current velocity.

The natural choice is given by the following form of $v(x,t)$

$$v(x,t) = \frac{d}{dt}E(q) + \frac{(x - E(q))}{\Delta q}\frac{d}{dt}\Delta q \tag{4}$$

which is associated to the standard harmonic oscillator coherent and squeezed states [9]. We can expect, in fact, that these states are a sub-set of the whole class of states selected by the form (4), and that all these states exhibit mean classical-like motion in the sense of Eq.s (3).

Note that, in conventional quantum-mechanical formalism, choice (4) corresponds, through $mv = \nabla S$, to the well known quantum mechanical coherent phase

$$S = <\hat{p}> x + \frac{(<\{\hat{q},\hat{p}\}>/2) - <\hat{q}><\hat{p}>}{2(\Delta q)^2}(x - <\hat{q}>)^2 + S_0(t). \tag{5}$$

In order to find explicitely the form of the searched states, we must take into account the constitutive couple of equations

$$\partial_t\rho = -\nabla(\rho v),$$

(6)

$$\partial_t S + \frac{m}{2}v^2 - \frac{m}{2}u^2 - \frac{\hbar}{2}\nabla u = -\Phi,$$

that is the continuity equation and the Hamilton-Jacobi-Madelung (HJM) equation respectively.

Inserting expression (4) in the first of the Eq.s (6), the selected states result to be all the states with a (normalizable) probability density of the ("wave-like") form

$$\rho(x,t) = \frac{1}{\Delta q} exp\{2R(\xi)\} \quad , \quad \xi = \frac{x - E(q)}{\Delta q}, \tag{7}$$

with the corresponding form for the associated osmotic velocity

$$u \equiv (\frac{\hbar}{2m})\frac{\nabla \rho}{\rho} = \frac{1}{\Delta q} G(\xi). \tag{8}$$

¿From the expressions (5), (7) for S and ρ we obtain the wave functions of the generalized states

$$\Psi(x,t) = \frac{1}{\sqrt{\Delta q}} exp\{R(\xi)\} exp\{\frac{i}{\hbar} S\}. \tag{9}$$

Now, inserting Eq.s (4), (8) in the HJM equation (6), taking the gradient term by term, and computing the resulting identity in $x =< \hat{q} >$ (or in $x = 0$ if the potential is singular), we can simply verify that the classical-like constraint is fulfilled. Then, our aim is reached.

Finally, the HJM equation, with the inputs of Eq.s (4), (8), gives as output the controlling potential Φ.

It is immediately seen, however, that Φ must be in general a function $\Phi(x,t| < \hat{q} >, \Delta\hat{q})$ also of $< \hat{q} >$ and $\Delta\hat{q}$; namely, in order to control the coherence of the wave packet, it is needed a feed-back mechanism, which allows for readjusting the system at any time.

Let us now look with greater detail at the problem of spreading. Two choices are possible, that is constant or time-dependent dispersion.

a) *Constant dispersion*

If we require $\Delta\hat{q} = const.$, the general relation

$$\Delta q \frac{d}{dt} \Delta q = m\{E(qv) - E(q)E(v)\} \tag{10}$$

forces the current velocity to assume the "classical" value $v = dE(q)/dt \equiv E(v)$, which is exactly expression (4) when $d\Delta q/dt = 0$. Then our states in this case are the unique solution of the problem. Note that the right member of the last equation is connected to the quantum average of the position-momentum anticommutator [9].

b) *Squeezing*

If a time dependence is allowed for $\Delta\hat{q}$, one can ask the following question: are states (9) the natural generalization of the harmonic oscillator squeezed states? The answer is positive, due the following considerations.

First of all, a "stochastic squeezing condition" $\Delta q \Delta u = K\hbar/2m$ is satisfied, where $K^2 = (4m^2/\hbar^2)E(G^2(\xi))$.

Moreover, if we consider the whole quantum uncertainty product for our states, it is immediately proved [10], using Eq.s (4), (8), (10), that

$$(\Delta\hat{q})^2(\Delta\hat{p})^2 \equiv m^2(\Delta q)^2\{(\Delta u)^2 + (\Delta v)^2\} = K^2\frac{\hbar^2}{4} + \frac{m}{4}(\Delta\hat{q})^2(\frac{d}{dt}\Delta\hat{q})^2. \tag{11}$$

We see, then, that the uncertainty structure in this case has the same form as in the harmonic oscillator squeezing states, with the only difference of a rescaled Heisenberg part.

Finally, the dispersion satisfy the equation [10]

$$\frac{d^2}{dt^2}\Delta\hat{q} = \frac{K^2\hbar^2}{4m^2\Delta\hat{q}^3} - < \frac{\hat{q} - <\hat{q}>}{\Delta\hat{q}}\nabla\Phi >, \tag{12}$$

which is the natural generalization of that of the harmonic case [9].

Eq.s (11), (12) assure controlled squeezing.

3 Displacement and squeezing operators

One can now asks two questions:
-can we construct states (9) directly in the standard quantum mechanical formalism?
-how we can choice in the whole ciass of states (9) the physically interesting states?

We can answer both questions in the following way [10].

Consider a reference stationary state Ψ_0, for example the ground state of a physically relevant potential V.

Consider moreover the standard displacement and squeezing operators

$$\hat{D}_\alpha = exp\{\alpha a^\dagger - \alpha^* a\},$$

$$\hat{S}_{\Delta\hat{q}} = exp\{\frac{\zeta}{2}(a^2 - a^{\dagger 2})\}, \tag{13}$$

which are used to construct the harmonic oscillator coherent and squeezed states, and write them in terms of the position and momentum operators

$$\hat{D}_\alpha = exp\{\frac{i}{\hbar}S_0(t)\}exp\{\frac{i}{\hbar}P\hat{q}\}exp\{-\frac{i}{\hbar}Q\hat{p}\},$$

$$\hat{S}_{\Delta\hat{q}} = exp\{i[\frac{f(t)}{\hbar}\{\hat{q},\hat{p}\} + \frac{g(t)}{\Delta\hat{q}_0{}^2}\hat{q}^2]\}, \tag{14}$$

with

$$Q = <\hat{q}> - <\hat{q}>_0 \quad , \quad P = <\hat{p}>,$$

$$f(t) = -\frac{1}{2}ln\frac{\Delta\hat{q}}{\Delta\hat{q}_0} \quad , \quad g(t) = \frac{m}{\hbar}[1 - 2f(t)]^{-1}\frac{\frac{d}{dt}\Delta\hat{q}}{\Delta\hat{q}}. \tag{15}$$

Then it is simple to verify that the states

$$\Psi_G(x,t) = (\hat{D}_\alpha\Psi_0)(x,t) \tag{16}$$

and

$$(\hat{D}_a \hat{S}_{\Delta\hat{q}} \Psi_0)(x,t) \tag{17}$$

belong to our class (9) respectively in the case of constant dispersion and in the case of squeezing.

This answers not only the first question, obviously, but also the second one. In fact, we now have the following scheme, which will be clarified by the subsequent example.

Given a physical system described by a potential V, we can choice as reference state, for example, its ground state Ψ_0.

Applying on it operators (14), we obtain generalized coherent packets, whose centers follow the classical dynamics ruled by the potential V.

Inserting then the current and osmotic velocity associated to these states in the HJM equation (6), we obtain the controlling potential Φ which allows, through the feed-back mechanism, to retain states (9).

V and Φ must not be confused: the first (V), in fact, is the original potential, for example a molecular one, for which we want to construct generalized coherent states, while the second (Φ) simply describes the controlling device, that is it supplies the feed-back prescriptions needed to retain coherence.

4 Example

We develope now an explicit example.

Putting for simplicity $\hbar = m = 1$ in the following, let us consider the potential

$$V(x) = \frac{1}{2}\omega^2 x^2 + \frac{1}{x^2} \tag{18}$$

and choose as reference state its ground state

$$\Psi_0(x) = N_0 \frac{1}{2} x^2 exp\{-\frac{1}{2}\omega x^2\} \tag{19}$$

where N_0 is a normalization constant.

Applying on (19) the operators (14), we obtain the generalized coherent states

$$\Psi^{(g)}(x,t) \equiv (\hat{D}_a \hat{S}_{\Delta\hat{q}} \Psi_0)(x,t) = \frac{1}{\sqrt{\Delta\hat{q}}} exp\{R(\xi)\} exp\{iS\} \tag{20}$$

where S is the phase (5) and

$$R(\xi) = -a\xi^2 + 2\,ln(a\xi^2) + ln\,b, \tag{21}$$

with a, b suitable functions of ω.

Inserting in the HJM equation (6) expression (4), and the osmotic velocity associated to (20) through Eq. (8), we obtain for the center the classical equation

$$\frac{d}{dt} < \hat{p} >= -\omega^2(t) < \hat{q} > + \frac{\gamma(t)}{< \hat{q} >^3}, \tag{22}$$

and for the controlling potential the form

$$\Phi(x,t|<\hat{q}>,\Delta\hat{q}) = \frac{1}{2}\omega^2(t)x^2 + h(t)x + \frac{1}{2}\frac{\gamma(t)}{(x-<\hat{q}>)^2} + g(t), \tag{23}$$

where

$$\omega^2(t) = 2[a^2 - \Delta\hat{q}^{-1}\frac{d^2}{dt^2}\Delta\hat{q}] \ , \ \gamma(t) = 6(\Delta\hat{q})^4. \tag{24}$$

We see from Eq. (22) that the center follows just the classical motion associated to the potential V, Eq. (18), as previously claimed.

References

[1] R. J. Glauber, Phys. Rev. **130**, 2529 (1963); Phys. Rev. **131**, 2766 (1963); J. R. Klauder, J. Math. Phys. 1058 (1963); E. C. G. Sudarshan, Phys. Rev. Lett. **10**, 227 (1963).

[2] A. M. Perelomov, *Generalized Coherent States and Their Applications* (Springer-Verlag, Berlin, 1986).

[3] H. P. Yuen, Phys. Rev. A **13**, 2226 (1976).

[4] M. M. Nieto and L. M. Simmons, Jr., Phys. Rev. Lett. **41**, 207 (1978).

[5] S. De Martino, S. De Siena, and F. Illuminati, Mod. Phys. Lett. B **8**, 1823 (1994); S. De Martino, S. De Siena, F. Illuminati, Mod. Phys. Lett. B **9**, 823 (1995); S. De Martino, S. De Siena, F. Illuminati, *Dynamics of squeezing from generalized coherent states*, preprint 1995.

[6] S. De Martino and S. De Siena, *Controlled Quantum Packets*, in these proceedings.

[7] E. Nelson, *Dynamical Theories of Brownian Motion* (Princeton University Press, Princeton, 1967); *Quantum Fluctuations* (Princeton University Press, Princeton, 1985).

[8] F. Guerra, Phys. Rep. **77**, 263 (1981).

[9] S. De Martino, S. De Siena, F. Illuminati, and G. Vitiello, Mod. Phys. Lett. B **8**, 977 (1994).

[10] S. De Martino, S. De Siena, F. Illuminati, in preparation.

NEXT
DOCUMENT

TWO DIFFERENT SQUEEZE TRANSFORMATIONS

D. Han
National Aeronautics and Space Administration, Goddard Space Flight Center, Code 910.1, Greenbelt, Maryland 20771, U.S.A.

Y. S. Kim
Department of Physics, University of Maryland, College Park, Maryland 20742, U.S.A.

Abstract

Lorentz boosts are squeeze transformations. While these transformations are similar to those in squeezed states of light, they are fundamentally different from both physical and mathematical points of view. The difference is illustrated in terms of two coupled harmonic oscillators, and in terms of the covariant harmonic oscillator formalism.

The word "squeezed state" is relatively new and was developed in quantum optics, and was invented to describe a set of two photon coherent states [1]. However, the geometrical concept of squeeze or squeeze transformations has been with us for many years. As far as the present authors can see, the earliest paper on squeeze transformations was published by Dirac in 1949 [2], in which he showed that Lorentz boosts are squeeze transformations. In this report, we show that Dirac's Lorentz squeeze is different from the squeeze transformations in the squeezed state of light. The question then is how different they are. In order to answer this question, we shall use a system of two coupled harmonic oscillators.

Let us look at a phase-space description of one simple harmonic oscillator. Its orbit in phase space is an ellipse. This ellipse can be canonically transformed into a circle. The ellipse can also be rotated in phase space by canonical transformation. This combined operation is dictated by a three-parameter group $Sp(2)$ or the two- dimensional symplectic group. The group $Sp(2)$ is locally isomorphic to $SU(1,1), O(2,1)$, and $SL(2,r)$, and is applicable to many branches of physics. Its most recent application was to single- mode squeezed states of light [1, 3].

Let us next consider a system of two coupled oscillators. For this system, our prejudice is that the system can be decoupled by a coordinate rotation. This is not true, and the diagonalization requires a squeeze transformation in addition to the rotation applicable to two coordinate variables [3, 4]. This is also a transformation of the symplectic group $Sp(2)$.

If we combine the $Sp(2)$ symmetry of mode coupling and the $Sp(2)$ symmetry in phase space, the resulting symmetry is that of the (3 + 2)-dimensional Lorentz group [5]. Indeed, it has been shown that this is the symmetry of two-mode squeezed states [6, 7]. It is known that the (3 + 2)-dimensional Lorentz group is locally isomorphic to Sp(4) which is the group of linear canonical transformations in the four-dimensional phase space for two coupled oscillators. These canonical transformations can be translated into unitary transformations in quantum mechanics [7].

In addition, for the two-mode problem, there is another Sp(2) transformation resulting from the relative size of the two phase spaces. In classical mechanics, there are no restrictions on the area of phase space within the elliptic orbit in phase space of a single harmonic oscillator. In quantum mechanics, however, the minimum phase-space size is dictated by the uncertainty relation. For this reason, we have to adjust the size of phase space before making a transition to quantum mechanics. This adds another $Sp(2)$ symmetry to the coupled oscillator system [8]. However, the transformations of this $Sp(2)$ group are not necessarily canonical, and there does not appear to be a straightforward way to translate this symmetry group into the present formulation of quantum mechanics. We shall return to this problem later in this report.

If we combine this additional $Sp(2)$ group with the above- mentioned $O(3,2)$, the total symmetry of the two-oscillator system becomes that of the group $O(3,3)$, which is the Lorentz group with three spatial and three time coordinates. This was a rather unexpected result and its mathematical details have been published recently by the present authors [8]. This $O(3,3)$ group has fifteen parameters and is isomorphic to $SL(4,r)$. It has six $Sp(4)$-like subgroups and many $Sp(2)$ like subgroups.

Let us consider a system of two coupled harmonic oscillators. The Lagrangian for this system is

$$L = \frac{1}{2}\left\{m_1\dot{x}_1^2 + m_2\dot{x}_2^2 - A'x_1^2 + B'x_2^2 + C'x_1x_2\right\}, \tag{1}$$

with

$$A' > 0, \qquad B' > 0, \qquad 4A'B' - C'^2 > 0. \tag{2}$$

Then the traditional wisdom from textbooks on classical mechanics is to diagonalize the system by solving the eigenvalue equation

$$\begin{vmatrix} A' - m_1\omega^2 & C' \\ C' & B' - m_2\omega^2 \end{vmatrix} = 0. \tag{3}$$

There are two solutions for ω^2, and these solutions indeed give correct frequencies for the two normal modes. Unfortunately, this computation does not lead to a complete solution to the diagonalization problem. The above eigenvalue equation seems similar to that for the rotation, but it is not.

Let us go back to Eq.(1). This quadratic form cannot be diagonalized by rotation alone. Indeed, the potential energy portion of the Lagrangian can be diagonalized by one rotation, but this rotation will lead to a non-diagonal form for the kinetic energy. For this reason, we first have to replace x_1 and x_2 by y_1 and y_2 with the transformation matrix

$$\begin{pmatrix} x_1 \\ x_2 \end{pmatrix} = \begin{pmatrix} (m_2/m_1)^{1/4} & 0 \\ 0 & (m_1/m_2)^{1/4} \end{pmatrix} \begin{pmatrix} y_1 \\ y_2 \end{pmatrix}. \tag{4}$$

In terms of these new variables, the Lagrangian can be written as

$$L = \frac{\sqrt{m_1m_2}}{2}\left\{\dot{y}_1^2 + \dot{y}_2^2\right\} - \frac{1}{2}\left\{Ay_1^2 + By_2^2 + Cy_1y_2\right\}, \tag{5}$$

with

$$\begin{pmatrix} A \\ B \\ C \end{pmatrix} = \begin{pmatrix} \sqrt{m_2/m_1} & 0 & 0 \\ 0 & \sqrt{m_1/m_2} & 0 \\ 0 & 0 & 1 \end{pmatrix} \begin{pmatrix} A' \\ B' \\ C' \end{pmatrix}.$$

The Lagrangian of Eq.(5) can now be diagonalized by a simple coordinate rotation:

$$\begin{pmatrix} z_1 \\ z_2 \end{pmatrix} = \begin{pmatrix} \cos\alpha & \sin\alpha \\ -\sin\alpha & \cos\alpha \end{pmatrix} \begin{pmatrix} y_1 \\ y_2 \end{pmatrix}, \tag{6}$$

with

$$\tan(2\alpha) = \frac{C}{A-B}. \tag{7}$$

In this Lagrangian formalism, momenta are not independent variables. They are strictly proportional to their respective coordinate variables. When the coordinates are rotated by the matrix of Eq.(6), the momentum variables are transformed according to the same matrix. When the coordinates undergo the scale transformation of Eq.(4), the momentum variables are transformed by the same matrix. Thus, the phase-space volume is not preserved for each coordinate.

Let us approach the same problem using the Hamiltonian

$$H = \frac{1}{2}\left\{\frac{p_1^2}{m_1} + \frac{p_2^2}{m_2} + A'x_1^2 + B'x_2^2 + C'x_1x_2\right\}. \tag{8}$$

Here again, we have to rescale the coordinate variables. In this formalism, the central issue is the canonical transformation, and the phase-space volume should be preserved for each mode. If the coordinate variables are to be transformed according to Eq.(4), the transformation matrix for the momenta should be the inverse of the matrix given in Eq.(4). Indeed, if we adopt this transformation matrix, the new Hamiltonian becomes

$$H = \frac{1}{2\sqrt{m_1m_2}}\left\{p_1^2 + p_2^2\right\} + \frac{1}{2}\left\{Ax_1^2 + Bx_2^2 + Cx_1x_2\right\}. \tag{9}$$

As for the rotation, the rules of canonical transformations dictate that both the coordinate and momentum variables have the same rotation matrix. The above Hamiltonian can be diagonalized by the rotation matrix given in Eq.(6).

We can now consider the four-dimensional phase space consisting of variables in the following order.

$$(\chi_1, \chi_2, \chi_3, \chi_4) = (x_1, x_2, p_1, p_2). \tag{10}$$

For both the non-canonical Lagrangian system and the canonical Hamiltonian system, the mode-coupling rotation matrix is

$$R(\alpha) = \begin{pmatrix} \cos\alpha & \sin\alpha & 0 & 0 \\ -\sin\alpha & \cos\alpha & 0 & 0 \\ 0 & 0 & \cos\alpha & \sin\alpha \\ 0 & 0 & -\sin\alpha & \cos\alpha \end{pmatrix}. \tag{11}$$

On the other hand, they have different matrices for the scale transformation. For the canonical Hamiltonian system, the matrix takes the form.

$$S_-(\eta) = \begin{pmatrix} e^{\eta} & 0 & 0 & 0 \\ 0 & e^{-\eta} & 0 & 0 \\ 0 & 0 & e^{-\eta} & 0 \\ 0 & 0 & 0 & e^{\eta} \end{pmatrix}. \tag{12}$$

Here, t' s position and momentum variables undergo anti-parallel squeeze transformations. On the other hand, for non-canonical Lagrangian system, the squeeze matrix is written as

$$S_+(\eta) = \begin{pmatrix} e^{\eta} & 0 & 0 & 0 \\ 0 & e^{-\eta} & 0 & 0 \\ 0 & 0 & e^{\eta} & 0 \\ 0 & 0 & 0 & e^{-\eta} \end{pmatrix}. \tag{13}$$

We use the notation S_+ and S_- for the parallel and anti- parallel squeeze transformation respectively.

If we rotate the above squeeze matrices by 45° using the rotation matrix of Eq.(11), the anti-parallel squeeze matrix become

$$S_-(\eta) = \begin{pmatrix} \cosh\eta & \sinh\eta & 0 & 0 \\ \sinh\eta & \cosh\eta & 0 & 0 \\ 0 & 0 & \cosh\eta & -\sinh\eta \\ 0 & 0 & -\sinh\eta & \cosh\eta \end{pmatrix}, \tag{14}$$

and the parallel squeeze matrix takes the form

$$S_+(\eta) = \begin{pmatrix} \cosh\eta & \sinh\eta & 0 & 0 \\ \sinh\eta & \cosh\eta & 0 & 0 \\ 0 & 0 & \cosh\eta & \sinh\eta \\ 0 & 0 & \sinh\eta & \cosh\eta \end{pmatrix}. \tag{15}$$

Now the difference between these two matrices is quite clear. The squeeze matrix of Eq.(14) is applicable to two-mode squeezed states of light [7, 9, 10].

As for the squeeze matrix of Eq.(15), let us consider the Lorentz transformation of a particle along the z direction:

$$z' = (\cosh\eta)z + (\sinh\eta)t, \qquad t' = (\sinh\eta)z + (\cosh\eta)t. \tag{16}$$

Then the momentum and energy are transformed according to

$$P' = (\cosh\eta)P + (\sinh\eta)E, \qquad E' = (\sinh\eta)P + (\cosh\eta)E. \tag{17}$$

If we regard z and t as the two coordinate variables, the four- component vector of Eq.(10) takes the form

$$(\chi_1, \chi_2, \chi_3, \chi_4) = (z, t, P, E). \tag{18}$$

Thus, the parallel squeeze matrix performs a Lorentz boost. According to classical mechanics of coupled harmonic oscillators, this transformation appears like a non-canonical transformation. Then, is the Lorentz boost a non-canonical transformation? The answer is NO.

We would like to show that the Lorentz boost is an uncertainty- preserving transformation using the covariant oscillator formalism which has been shown to be effective in explaining the basic hadronic features observed in high energy laboratories [11]. According to this model, the ground-state wave function for the hadron takes the form

$$\psi_0(z,t) = \left(\frac{1}{\pi}\right)^{1/2} \exp\left\{-\frac{1}{2}\left(z^2 + t^2\right)\right\}, \tag{19}$$

where the hadron is assumed to be a bound state of two quarks, and z and t are space and time separations between the quarks. If the system is boosted, the wave function becomes [11]

$$\psi_\eta(z,t) = \left(\frac{1}{\pi}\right)^{1/2} \exp\left\{-\frac{1}{2}\left(e^{-2\eta}u^2 + e^{2\eta}v^2\right)\right\}, \tag{20}$$

where

$$u = (z+t)/\sqrt{2}, \qquad v = (z-t)/\sqrt{2}.$$

The u and v variables are called the light-cone variables [2]. The wave function of Eq.(19) is distributed within a circular region in the uv plane, and thus in the zt plane. On the other hand, the wave function of Eq.(20) is distributed in an elliptic region. This ellipse is a "squeezed" circle with the same area as the circle. The question then is how the momentum-energy wave function is squeezed.

The momentum wave function is obtained from the Fourier transformation of the expression given in Eq.(20):

$$\phi_\eta(q_z,q_0) = \left(\frac{1}{2\pi}\right)\int \psi_\eta(z,t)\exp\{-i(q_z z - q_0 t)\}dxdt. \tag{21}$$

If we use the variables:

$$q_u = (q_0 - q_z)/\sqrt{2}, \qquad q_v = (q_0 + q_z)/\sqrt{2}. \tag{22}$$

In terms of these variables, the above Fourier transform can be written as

$$\phi_\eta(q_z,q_0) = \left(\frac{1}{2\pi}\right)\int \psi_\eta(z,t)\exp\{-i(q_u u + q_v v)\}dudv. \tag{23}$$

The resulting momentum-energy wave function is

$$\phi_\eta(q_z,q_0) = \left(\frac{1}{\pi}\right)^{1/2} \exp\left\{-\frac{1}{2}\left(e^{-2\eta}q_u^2 + e^{2\eta}q_v^2\right)\right\}. \tag{24}$$

Because we are using here the harmonic oscillator, the mathematical form of the above momentum-energy wave function is identical with that of the space-time wave function given in Eq.(20). The Lorentz-squeeze properties of these wave functions are also the same. This certainly is consistent with the parallel squeeze matrix given in Eq.(15), and the Lorentz boosts appears like a non-canonical transformation.

However, we still have to examine how conjugate pairs are chosen from the space-time and momentum-energy wave functions. Let us go back to Eq.(21) and Eq.(23). It is quite clear that the light-cone variable u and v are conjugate to q_u and q_v respectively. It is also clear that the distribution along the q_u axis shrinks as the u-axis distribution expands. The exact calculation leads to

$$< u^2 >< q_u^2 >= 1/4, \qquad < v^2 >< q_v^2 >= 1/4. \tag{25}$$

Planck's constant is indeed a Lorentz-invariant quantity, and the Lorentz boost is a canonical transformation.

Because of the Minkowskian metric we used in the Fourier transformation of Eq.(21), the non-canonical squeeze transformation of Eq.(15) becomes a canonical transformation for the Lorentz boost. Otherwise, it remains non-canonical. Then, does this non-canonical transformation play

a role in physics? The answer is YES. The best known examples are thermally excited oscillator states [12] and coupled oscillator system where one of the oscillator is not observed [13, 14]. These systems serve as simple models for studying the role of entropy in quantum mechanics [15, 16].

These examples are for the cases where the phase space volume for each mode becomes larger than Planck's constant. In the classical mechanics of two coupled harmonic oscillators, the phase-space volume of each oscillator fluctuates. If one becomes larger, the other shrinks. In quantum mechanics, we do not have a theory of shrinking phase-space volumes. Without this, we cannot have a complete understanding of coupled oscillators in quantum mechanics.

References

[1] H. P. Yuen, Phys. Rev. A **13**, 2226 (1976).

[2] P. A. M. Dirac, Rev. Mod. Phys. **21**, 392 (1949).

[3] Y. S. Kim and M. E. Noz, *Phase Space Picture of Quantum Mechanics* (World Scientific, Singapore, 1991).

[4] H. Goldstein, *Classical Mechanics*, 2nd ed. (Addison-Wesley, Reading, MA, 1980).

[5] P. A. M. Dirac, J. Math. Phys. **4**, 901 (1963).

[6] R. F. Bishop and A. Vourdas, Z. Phyzik B **71**, 527 (1988).

[7] D. Han, Y. S. Kim, and M. E. Noz, Phys. Rev. A **41**, 6233 (1990).

[8] D. Han, Y. S. Kim, and M. E. Noz, J. Math. Phys. **36**, 3940 (1995).

[9] C. M. Caves and B. L. Schumaker, Phys. Rev. A **31**, 3068 (1985); B. L. Schumaker and C. M. Caves, Phys. Rev. A **31**, 3093 (1985). See also Fan, Hong-Yi and J. Vander Linder, Phys. Rev. A **39**, 2987 (1989).

[10] B. Yurke, S. McCall, and J. R. Klauder, Phys. Rev. A **33**, 4033 (1986).

[11] Y. S. Kim and M. E. Noz, *Theory and Applications of the Poincaré Group* (Reidel, Dordrecht, 1986).

[12] H. Umezawa, H. Matsumoto, and M. Tachiki, *Thermo Field Dynamics and Condensed States* (North-Holland, Amsterdam, 1982).

[13] B. Yurke and M. Potasek, Phys. Rev. A **36**, 3464 (1987).

[14] A. K. Ekert and P. L. Knight, Am. J. Phys. **57**, 692 (1989). For an earlier paper, see S. M. Barnett and P. L. Knight, J. Opt. Soc. Am. B **2** 467 (1985).

[15] J. von Neumann, *Die mathematische Grundlagen der Quanten- mechanik* (Springer, Berlin, 1932). See also J. von Neumann, *Mathematical Foundation of Quantum Mechanics* (Princeton University, Princeton, 1955).

[16] R. P. Feynman, *Statistical Mechanics* (Benjamin/Cummings, Reading, MA, 1972).

NEXT
DOCUMENT

Antibunching effect of k-component q-coherent states

Jinyu He
Dezhou Teacher's Colleye, Shandong Province 253023,P.R.China

Jisuo Wang, and Chuankui Wang
Department of Physics, Liaocheng Teacher's College
Shandong Province 252059,P.R.China

Abstract

We introduce the antibunching effect for the q-electromagnetic field, and study this kind nonclassical properties of k-component q-coherent states given by Kuang et al.[Phys.Lett.A173(1993)1]. The results show that all of them show antibunching effect.

Recently, coherent states of quatum algebras[1-3] (q-CSs) have attracted a lot of attention due to their maybe applications in many fields of physics and mathematical physics[4-5]. The Glauber-typed q-CSs[6-7] have been studies in great detail and applied widely to various concrete physical problems[8]. In the refrences[9-10], the even and odd q-CSs representations were constructed and the squeezing properties of them were discussed. The even and odd q-CSs are defined to be the eigenstates of the square (a_q^2) of the q-annihilation operator. More recently,k-component q-CSs were introduced and their properties were investigated by Kuang et al.[11]. On the basis of this work, in this paper, we study the antibunching effect of them, because of this effect has the typical nonclassical property. Squeezing properties of them were investigated by us[12].
The k-component (k is an integer and $k \geq 3$) $q-CSs$ were given by [11]

$$| z,k,i >_q = A_1^{-1/2}(| z |^2,k) \sum_{n=0}^{\infty} \frac{z^{kn+i}}{\sqrt{[kn+i]_q^!}} | kn+i >_q, (i = 0,1,\cdots,k-1), \tag{1}$$

$$A_i(| z |^2,k) = \sum_{n=0}^{\infty} \frac{| z |^{2(kn+i)}}{\sqrt{[kn+i]_q^!}}, (i = 0,1,2,\cdots,k-1) \tag{2}$$

where z is a complex number, the q-fractorial $[n]_q^! = [n]_q[n-1]_q \cdots [1]_q$ with the q-number $[X]_q = (q^X - q^{-X}/(q-q^{-1})$. Their actions on the basis vectors are

$$a_q^+ = \sqrt{[n+1]_q} \mid n+1 >_q, a_q \mid n >_q = \sqrt{[n]_q} \mid n-1 >_q . \tag{3}$$

It is easy to prove that the k states of (1) are all the eigenstates of the operator $a_q^k (k \geq 3)$ with the same eigenvalue z^k.
It is well known that, when the second-order correlation function of a light field[13] $g^{(2)}(0) < 1$, one says that the light field exhibits an antibunching effect. In a similar way, we introduce a second-

order q-correlation function for the q-light field,

$$g_q^{(2)} = \frac{{}_q<|\, a_q^{+2} a_q^2 \,|>_q}{{}_q<|\, a_q^{+} a_q \,|>_q^2}, \tag{4}$$

If the second-order q-correlation function of the q-light field $g_q^{(2)}(0) < 1$,we say that the q-light field exhibits the antibunching effect. Now, we study the antibunching effect of the k states given by (1).

Using the relations[11],

$$a_q^m \mid z,k,0>_q = z^m A_0^{-1/2} A_{k-m}^{1/2} \mid z,k,k-m>_q, (m=1,2,\cdots,k), \tag{5}$$

for the k states of (1), it is easy to prove that the relations hold:

$${}_q<z,k,0 \mid a_q^{+} a_q \mid z,k,0>_q = |\, z\,|^2 \, A_{k-1}/A_0, \tag{6}$$

$${}_q<z,k,m \mid a_q^{+} a_q \mid z,k,m>_q = |\, z\,|^2 \, A_{m-1}/A_m, (m=1,2,\cdots,k-1), \tag{7}$$

$${}_q<z,k,0 \mid a_q^{+2} a_q^2 \mid z,k,0>_q = |\, z\,|^4 \, A_{k-2}/A_0, \tag{8}$$

$${}_q<z,k,1 \mid a_q^{+2} a_q^2 \mid z,k,1>_q = |\, z\,|^4 \, A_{k-1}/A_1, \tag{9}$$

$${}_q<z,k,m \mid a_q^{+2} a_q^2 \mid z,k,m>_q = |\, z\,|^4 \, A_{m-2}/A_m, (m=2,3,\cdots,k-1). \tag{10}$$

By means of (6)-(10) the q-coherent degrees of the second order of the k states given by (1) can be obtained,respectively, they are

$$g_{q0}^{(2)}(0) = \frac{{}_q<z,k,0 \mid a_q^{+2} a_q^2 \mid z,k,0>_q}{{}_q<z,k,0 \mid a_q^{+} a_q \mid z,k,0>_q^2} = \frac{A_0 A_{k-2}}{A_{k-1}^2}, \tag{11}$$

$$g_{q1}^{(2)}(0) = \frac{{}_q<z,k,1 \mid a_q^{+2} a_q^2 \mid z,k,1>_q}{{}_q<z,k,1 \mid a_q^{+} a_q \mid z,k,1>_q^2} = \frac{A_1 A_{k-1}}{A_0^2} \tag{12}$$

$$g_{qm}^{(2)}(0) = \frac{{}_q<z,k,m \mid a_q^{+2} a_q^2 \mid z,k,m>_q}{{}_q<z,k,m \mid a_q^{+} a_q \mid z,k,m>_q^2} = \frac{A_{m-2} A_m}{A_{m-1}^2}, (m=2,3,\cdots,k-1). \tag{13}$$

Substituting (2) into (11), we obtain

$$g_{q0}^{(2)}(0) = \frac{\sum_{m=0}^{\infty} \left[\sum_{n=0}^{m} \frac{1}{[kn]_q![km-kn+k-2]_q!}\right] x^{km}}{x^k \sum_{m=0}^{\infty} \left[\sum_{n=0}^{m} \frac{1}{[kn+k-1]_q![km-kn+k-1]_q!}\right] x^{km}} = \frac{f_{q1}(x)}{x^k f_{q2}(x)}, \tag{14}$$

where $x = |\, z\,|^2$.Consider $k \geq 3$, while $[n]_q > [n-1]_q \geq 1$, therefore we have

$$\sum_{n=0}^{m} \frac{1}{[kn]_q![km-kn+k-2]_q!} > \sum_{n=0}^{m} \frac{1}{[kn+k-1]_q![km-kn+k-1]_q!}, \tag{15}$$

and hence $f_{q1}(x) > f_{q2}(x)$, so that $g_{q0}^{(2)} > 1$ when $x < 1$. However, when $x > 1$, there surely exist values of x (e.g.,$x^k > f_{q1}(x)/f_{q2}(x)$) for which the relation holds:

$$g_{q0}^{(2)}(0) = \frac{f_{q1}(x)}{x^k f_{q2}(x)} < 1. \tag{16}$$

Therfore, the state $| z,k,0 >_q$ may exhibis antibunching effect when $x > 1$. Substituting (2) into (12), we have

$$g_{q1}^{(2)}(0) = \frac{x^k \sum_{m=0}^{\infty} \left[\sum_{n=0}^{m} \frac{1}{[kn+1]_q![km-kn+k-1]_q!}\right] x^{km}}{\sum_{m=0}^{\infty} \left[\sum_{n=0}^{m} \frac{1}{[kn]_q![km-kn]_q!}\right] x^{km}} = \frac{x^k f_{q3}(x)}{f_{q4}(x)}, \tag{17}$$

Obviously,

$$\sum_{n=0}^{m} \frac{1}{[kn+1]_q![km-kn+k-1]_q!} < \sum_{n=0}^{m} \frac{1}{[kn]_q![km-kn]_q!}, \tag{18}$$

so that $f_{q3}(x) < f_{q4}(x)$. Therefore $g_{q1}^{(2)}(0) < x^k$,i.e., when $x \leq 1, g_{q1}^{(2)}(0) < 1$. From (2) and (13), we obtain

$$\begin{aligned} g_{qm}^{(2)}(0) &= \frac{\sum_{n'=0}^{\infty} \left[\sum_{n=0}^{n'} \frac{1}{[kn+m-2]_q![kn'-kn+1]_q!}\right] x^{kn'}}{\sum_{n'=0}^{\infty} \left[\sum_{n=0}^{n'} \frac{1}{[kn+m-1]_q![kn'-kn+m-1]_q!}\right] x^{kn'}} \\ &< \frac{\sum_{n=0}^{\infty} \frac{[n+1]_q}{[m-2]_q![m]_q!} x^{kn}}{\sum_{n=0}^{\infty} \frac{[n+1]_q}{\{[kn+m-1]_q!\}^2}} < \frac{\frac{1}{[m-2]_q![m]_q!} \sum_{n=0}^{\infty} [n+1]_q x^{kn}}{\frac{1}{\{[m-1]_q!\}^2}} = \frac{[m-1]_q \sum_{n=0}^{\infty} [n+1]_q x^{kn}}{[m]_q} \end{aligned} \tag{19}$$

Obviously,

$$\lim_{x \to 0} \sum_{n=0}^{\infty} [n+1]_q x^{kn} = [1]_q = 1, \tag{20}$$

¿From Eq.(19),we obtain

$$\lim_{x \to 0} g_{qm}^{(2)}(0) < \lim_{x \to 0} \frac{[m-1]_q \sum_{n=0}^{\infty} [n+1]_q x^{kn}}{[m]_q} = \frac{[m-1]_q}{[m]_q} < 1. \tag{2'}$$

Therefore, the states $| z,k,m >_q$ $(m = 2,3,\cdots,k-1)$ exhibit antibunching effect when $x \to 0$. We sum up the above results and obtain that all of the k states given by (1) show the antibunching effect, i.e., they are all nonclassical states.It had been proved[11] that the k states is the complete, therefore, they form a nonclassical cmplete representation. For example, in this picture,the q-coherent state $| z >_q$ may be expressed as:

$$| z >_q = exp(- | z |^2 /2) \sum_{i=0}^{k-1} A_i^{1/2}(| z |^2, k) | z,k,i >_q \tag{22}$$

It is interesting to note that when $q \to 1$, the eigenstates of the operator a_q^k become the states considered in our paper [11]. Therefore, this letter is a generalization of our paper[14] in the condition q-deformed.

References

[1] L.C.Biedenharn,J.phys.A.**22**.L873(1989).

[2] C.P.Sun and H.C.Fu,J.phys.A.**22**.L983(1989)

[3] R.Floreanini,V.P.Spiridon et al.,Phys.lett.B.**242**, 383(1991).

[4] G.L.Alvarez,C.Gomez et al.,Nucl.Phys.B. **330**,347(1991).

[5] J.R.Klauder and B.S.Skagerstam,Coherent states (Singapore, World Scientific,1989)

[6] P.P.Kulish and E.V.Damaskinsky,J.Phys.A. **23**,L415(1990).

[7] A.J.Bracken et al.,J.Phys.A.**24**,1379(1991).

[8] A.Solomon and J.Katriel,J.Phys.A.**24**,L1209(1990).

[9] L.M.Kuang and F.B.Wang,Phys.Lett.A.**173**,221(1993); **169**,225(1992).

[10] L.M.Kuang, F.B.Wang et al., Acta Opt.Sin.**13**,1008(1993)(in Chinese)

[11] L.M.Kuang,F.B.Wang and G.J.Zeng,Phys.Lett.A.**176**,1(1993).

[12] Wang Jisuo and Wang Chuankui,Acta Opt.Sin.**14**,1043(1994),(in Chinese).

[13] D.F.Walls,Nature.**306**,141(1983)

[14] Jinzuo Sun,Jisuo Wang and Chuankui Wang,Phys.Rev.A.**44**,3369(1991).

NEXT
DOCUMENT

QUANTUM STATE ENGINEERING VIA COHERENT-STATE SUPERPOSITIONS

J.Janszky, P.Adam, S.Szabo, P.Domokos
Research Laboratory for Crystal Physics
P.O. Box 132, H-1502 Budapest, Hungary

Abstract

The quantum interference between the two parts of the optical Schrödinger-cat state makes possible to construct a wide class of quantum states via discrete superpositions of coherent states. Even a small number of coherent states can approximate the given quantum states at a high accuracy when the distance between the coherent states is optimized, e. g. nearly perfect Fock state $|n\rangle$ can be constructed by discrete superpositions of $n+1$ coherent states lying in the vicinity of the vacuum state.

1 Introduction

Recently, much attention has been paid to the problem of generating quantum states of an electromagnetic field mode. In micromaser experiments various schemes have been proposed that allow us to create states with controllable number-state distribution [1, 2]. There are theoretical results presenting that certain quantum states can be arbitrarily well approximated by discrete superpositions of coherent states [3, 4]. The significance of applying a coherent-state expansion instead of the number-state one is to open new prospects in "quantum state engineering". Nonlinear interaction of the field, being initially in a coherent state, with a Kerr-like medium [5] or in degenerate parametric oscillator [6] leads to superpositions of finite number of coherent states. Back-action evading and quantum nondemolition measurements can also yield such superposition states [7, 8]. An atomic interference method has been developed, which can result in arbitrary superposition of coherent states on a circle in phase space [9]. Based on these promising schemes, implementation of experiments capable to produce required superpositions of coherent states can be anticipated.

In this paper we shall discuss the possibility to construct quantum states using coherent states superpositions. We find a simple set of superposition states which coincides with the Fock basis for any practical purpose.

2 Schrödinger-cat states

The superpositions of coherent states [10, 11],

$$|\alpha,\phi\rangle = c_\phi(|\alpha\rangle + e^{i\phi}|-\alpha\rangle), \tag{1}$$

referred to as Schrödinger-cat states, when the constituent coherent states are macroscopically distinguishable, have attracted much interest.

The two most typical superposition states are the even or "male" ($\phi = 0$) and odd or "female" ($\phi = \pi$) cat states. The case with small difference between the constituent states, by analogy, could be called Schrödinger-kitten states.

Although the coherent states are the most classical of all pure states of light, their simple superposition described by Eq. (1) shows remarkable nonclassical features as a consequence of the quantum interference [12, 13, 14]

The Wigner function of a Schrödinger-cat state with real $\alpha = x$

$$W(\beta) = \frac{c_+^2}{\pi}\left[\exp(-2|\beta - x|^2) + \exp(-2|\beta + x|^2) + 2\exp(-2|\beta|^2)\cos(4x\mathrm{Im}\beta + \phi)\right] \qquad (2)$$

leads us to better understanding the origin of the quantum interference. The first two terms in the Wigner function of Eq. (2) correspond to the Gaussian bells of the constituent coherent states while the third term describes an interference fringe pattern between the bells. We note that although two coherent states with strongly different arguments are almost orthogonal to each other, the maximal amplitude of the interference fringe remains two times larger than the amplitudes of the constituent coherent states, independently from the distance between them.

The wavelength of the fringe decreases with the increase of the distance between the coherent states, the phase of the fringe depends on the relative phase ϕ in Eq. (1) between the composite part of the cat state (Fig. 1).

The picture becomes more complicated if we superpose more than 2 coherent states. In this case multiple fringes can constructively or destructively interfere with each other and also with the original coherent state bells to produce different nonclassical states as we will show in the next Section.

3 State engineering

Let us consider a pure state given as a superposition of coherent states along the real axis in phase space [12, 3, 15]

$$|\psi\rangle = \int F(x)\,|\,x\rangle dx\,. \qquad (3)$$

Let us consider the following discrete superposition of coherent states along the real axis of the phase space

$$|\psi_N\rangle = \sum_{k=1}^{N} F_k\,|\,x_k\rangle\,. \qquad (4)$$

Here the coherent states $|\,x_k\rangle$ are chosen to be equally distributed at distances d along the real axis around the coherent state $|\,x_0\rangle$ that belongs to the center of the corresponding one-dimensional distribution function $F(x)$ (Eq. 3), i.e.

$$x_k = x_0 + \left(k - \frac{N+1}{2}\right)d\,, \quad k = 1, \ldots N\,. \qquad (5)$$

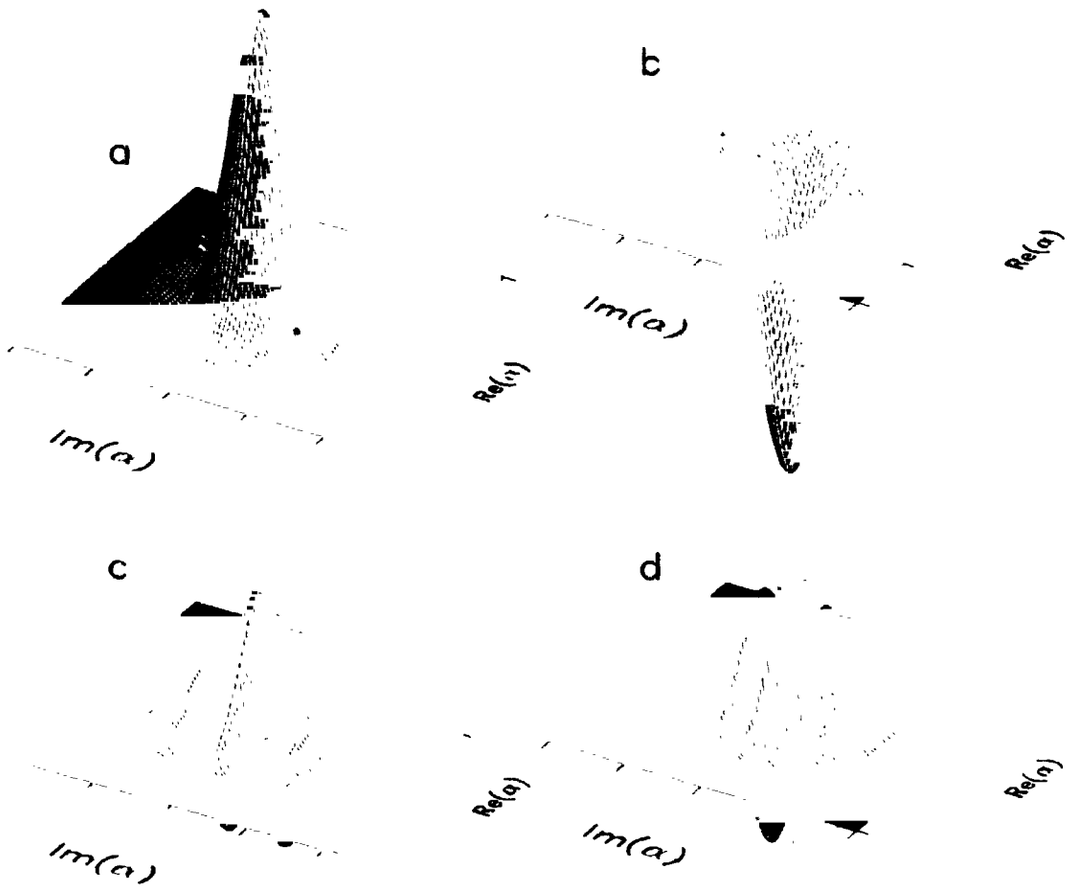

FIG. 1. The interference parts (fringes) of the Wigner functions of Schrödinger-cat states consisting of two coherent states put along the real axis of phase space. The phase difference between the coherent states changes the phase of the fringes, leading e. g. to the so-called male or female cat states (Fig.1a, $\phi = 0$ and Fig. 1b, $\phi = \pi$ respectively). Increasing the distance x of the coherent state from the origin of the phase space decreases the wave length of the fringes (Fig. 1a, $x = 0.6$; Fig. 1c, $x = 2$; Fig. 1d, $x = 4$).

The coefficients F_k are derived from the one-dimensional continuous distribution (Eq. 3)

$$F_k = cF(x_k)\,, \tag{6}$$

where c is a normalization constant.

As an example we consider displaced squeezed number states $|\, n, \zeta, Z\rangle$. Their interesting nonclassical properties were widely discussed in the literature [16]. The one-dimensional coherent-state representation of squeezed displaced number state along the real axis of phase space has the form [17]

$$F(x) = \tilde{c}_n H_n\left(\frac{x-Z}{\sqrt{2uv}}\right)\exp\left(-\frac{u-v}{2v}x^2 + \frac{(uZ - vZ^*)}{v}x\right)\,, \mathrm{Re}\left(\frac{u-v}{2v}\right) > 0\,. \tag{7}$$

The parameters u and v are connected to the complex squeezing parameter ζ in the usual way

$$u = \cosh r\,, \quad v = e^{i\theta}\sinh r\,. \tag{8}$$

We note that states $|\, 0, \zeta, Z\rangle$ are the well-known squeezed coherent states.

In Fig. 2. we show how a squeezed Fock state builds up as we use more and more coherent states in the superposition. Here $n = 1$, the squeezing parameter $r = 0.5$. The sampling distance d for each N was optimized, minimizing the mismatch between the desired and the approximating states. In Fig. 2a even at $N = 3$ coherent states the resulting state began to resemble the desired state. Fig. 2b shows state made of 4 coherent states. The emerging target state can be clearly seen. As we added more coherent states ($N = 5$ and $N = 6$ for Figs. 2c and 2d respectively) the approximation became more and more perfect. In fact, the picture of the Wigner function of the superposition of 6 coherent state is indistinguishable from that of the squeezed 1-photon state.

Another possibility for state construction is if we begin the discretization described in this section with a one-dimensional representation of the state on a circle in phase-space [3, 18].

The discrete superposition of $n + 1$ coherent states (a generalization of the female cat state) situated symmetrically on a circle with radius r in phase space

$$|\, n, r\rangle = c(r)\frac{\sqrt{n!}e^{\frac{r^2}{2}}}{(n+1)r^n}\sum_{k=0}^{n} e^{\frac{2\pi i}{n+1}k}\,|\, re^{\frac{2\pi i}{n+1}k}\rangle\,, \tag{9}$$

for small enough radius r leads to the n-photon Fock state $|\, n\rangle$ [19].

There are several experimental schemes which are appropriate to generate superposition states composed of coherent states lying on a circle in phase space. Making an initial coherent field interact with a sequence of two-level atoms detuned from the cavity resonance leads to such superpositions [8]. In the special case of their scheme, when the "phase-shift per photon" accumulated by the atomic dipoles crossing the cavity is a rational multiple of π, a symmetrical superposition of finite number of coherent states on a circle emerges. Required discrete superpositions on a circle, including the elements of the basis set given in Eq.(9), can be prepared in a single-atom interference method in a designed apparatus [9]. Superposition on a circle with small radius, that is essential in our case, can be generated in both of the above mentioned experimental schemes by starting with a field initially in coherent state with a small amplitude. The progress in quantum optics seems to enable us in the near future to create experimentally these superposition states.

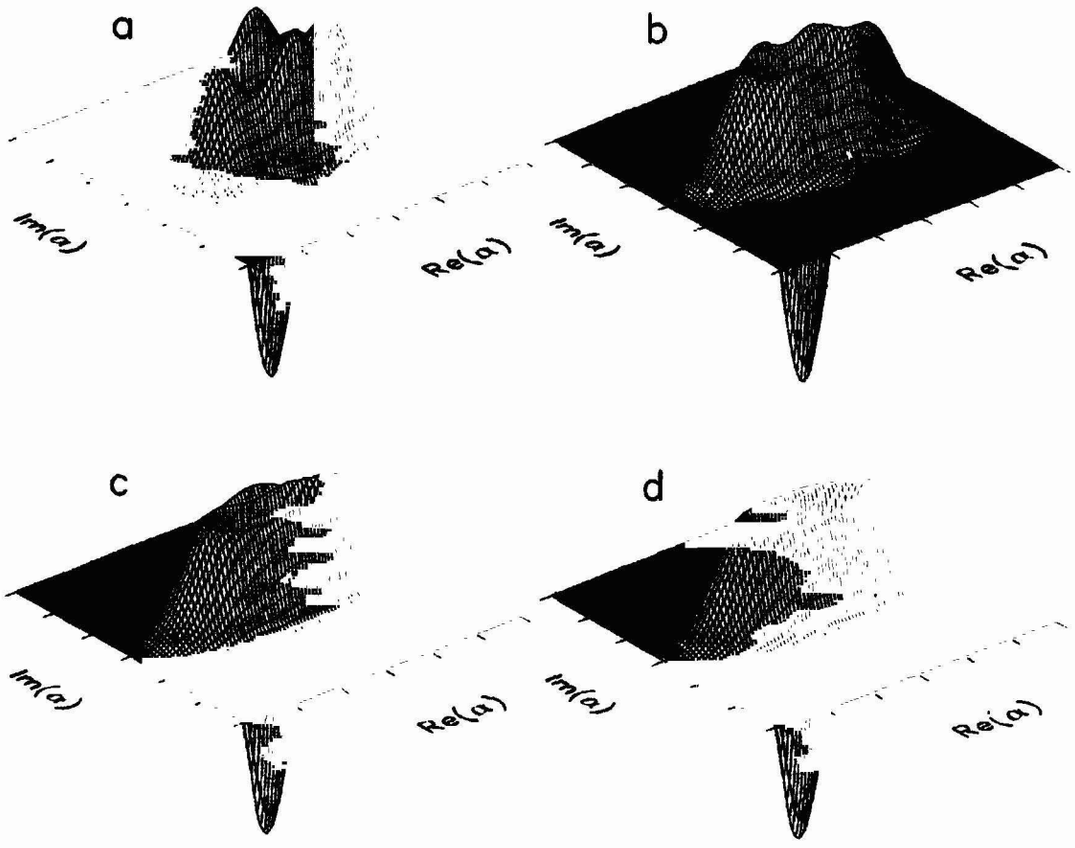

FIG. 2. Wigner functions of the coherent-state superpositions along the real axis approximating the squeezed number state $|\, n = 1, r = 0.5\rangle$. The numbers N of the constituent coherent states are equal to 3 (a), 4 (b), 5 (c), 6 (d) and the optimized distances d_{opt} of adjacent coherent states are equal to 1.27 (a), 1.13 (b), 1.03 (c) and 0.96 (d). Superposition of 6 coherent states gives surprisingly good approximation, while even that of 3 coherent states has features resembling the desired squeezed 1-photon state.

Acknowledgments

This work was supported by the National Research Scientific Fund (OTKA) of Hungary, under Contracts No. T14083, F17380.

References

[1] K. Vogel, V. M. Akulin, W. P. Schleich, Phys. Rev. Lett. **71**, 1816 (1993).

[2] B. M. Garraway, B. Sherman, H. Moya-Cessa, P. L. Knight, G. Kurizki, Phys. Rev. A **49**, 535 (1994).

[3] J. Janszky, P. Domokos, P. Adam, Phys. Rev. A **48**, 2213 (1993).

[4] P. Domokos, J. Janszky, P. Adam, T. Larsen, Quantum Opt. **6**, 187 (1994).

[5] B. Yurke, D. Stoler, Phys. Rev. Lett. **57**, 13 (1986).

[6] M. Wolinsky, H. J. Carmichael, Phys. Rev. Lett. **60**, 1836 (1988).

[7] B. Yurke, W. Schleich, D. F. Walls, Phys. Rev. A **42**, 1703 (1990).

[8] M. Brune, S. Haroche, J. M. Raimond, L. Davidovich, N. Zagury, Phys. Rev. A **45**, 5193 (1992).

[9] P. Domokos, J. Janszky, P. Adam, Phys. Rev. A **50**, 3340 (1994).

[10] V. V. Dodonov, I. A. Malkin, and V. I. Man'ko, Physica **72**, 597 (1974).

[11] M. Hillery, Phys. Rev. A **36**, 3796 (1987).

[12] J. Janszky, A.V. Vinogradov, Phys. Rev. Lett. **64**, 2771 (1990).

[13] V. Buzek, P. L. Knight, Opt. Commun. **81**, 331 (1991).

[14] W. Schleich, M. Pernigo, Fam Le Kien Phys. Rev. A, **44**, 2172 (1991).

[15] P. Adam, I. Foldesi, J. Janszky, Phys. Rev. A **49**, 1281 (1994).

[16] M. S. Kim, F. A. M. Oliviera, P. L. Knight, Phys. Rev. A **40**, 2494 (1989).

[17] I. Foldesi, P. Adam, J. Janszky, Phys. Lett. A, *in print* (1995).

[18] P. Domokos, J. Janszky, P. Adam, Phys. Rev. A **50**, 4293 (1994).

[19] J. Janszky, P. Domokos, S. Szabó, P. Adam, Phys. Rev. A **51**, 4191 (1995).

NEXT
DOCUMENT

Generation of higher-order squeezing in multiphoton micromaser

Fu-li Li
Department of Applied Physics, Xian Jiaotong University, Xian 710049, P. R. China

Qing Huang
Department of Physics, Southwest Jiaotong University, Chengdu 610031, People's Republic of China

Abstract

The generation of steady state higher-order squeezing in the sense of Hong and Mandel [Phys. Rev. Lett. 54, 323(1985); Phys. Rev. A32, 974(1985)] and also of Hillery [Phys. Rev. A36, 3796(1987)] in a multiphoton micromaser is studied. The results show that the cotangent state which is generated by the coherent trapping scheme in a multiphoton micromaser can exhibit not only second-order squeezing but also fourth-order and squared field amplitude squeezings. The influence of the cavity loss on the squeezings is investigated.

1 Introduction

The one-atom micromaser which has been developed in recent years[1-3] is an unique device in experimentally studying the interaction of a single atom with the quantized electromagnetic field in a cavity. It has theoretically or experimentally been shown that the field with nonclassical properties such as sub-poissonian photon distribution[4-5] and second quadrature squeezing[6-8] can be generated in a one-photon micromaser. The key physical process in the micromaser is the interaction of a two-level atom with a single-mode quantized electromagnetic field inside the cavity. As usual, the Jaynes- Cummings model[9] is employed to describe the process and the corresponding Hamiltonian is written as

$$\hat{E} = \hbar\omega_0\hat{S}_z + \hbar\omega\hat{a}^+\hat{a} + \hbar g(\hat{a}\hat{S}_- + \hat{a}^+\hat{S}_+) \tag{1}$$

where $\hat{S}_z = \frac{1}{2}(|e><e| - |g><g|)$, $\hat{S}_- = |e><g|$ and $\hat{S}_+ = |g><e|$. In the above, $|g>$ and $|e>$ denote the lower and upper states of the atom; $\pm\frac{1}{2}\hbar\omega_0$ are energies of the atomic levels; $\hat{a}^+$ and

$\hat{a}$ creation and annihilation operators of photons with frequency ω; $\hbar g$ is the atom-field coupling constant. It is seen in (1) that at a time only one photon is exchanged between the atom and the field while the transition of the atom from one level to another takes place. So, a micromaser which is built on the basis of (1) is called one-photon micromaser. The generalisation of (1) is

$$\hat{H} = \hbar\omega_0\hat{S}_z + \hbar\omega\hat{a}^+\hat{a} + \hbar g(\hat{a}^m\hat{S}_- + \hat{a}^{+m}\hat{S}_+) \tag{2}$$

where m is the photon multiple and other symbols have the same meanings as in (1). The difference of (2) from (1) is that m photons are allowed to be emitted or absorbed in the transition of the atom. A number of theoretical analyses have shown that time-dependent squeezing effects can be generated in the interaction described by (2)[10-13]. A micromaser which is built on the basis of (2) is called multiphoton micromaser($m \geq 2$). The purpose of this paper is to investigate higher order squeezing properties of cotangent state produced by the coherent trapping approach[14] in a multiphoton micromaser.

2 Higher-order squeezing properties of cotangent state

Suppose that at time t the state vector of the atom-field system is

$$|\Psi(t)>=\sum_{n=N_d}^{N_u} S_n|n>\otimes(\alpha|e>+\beta|g>) \tag{3}$$

in which the field is in the superposition $\sum_{n=N_d}^{N_u} S_n|n>$ and the atom in a coherent state $\alpha|e> +\beta|g>$. While the atom is flying inside the cavity, the state vector of the atom-field coupling system is evolving in time according to the time-dependent Schrödinger equation with (2). When the atom exits out of the cavity at time $t' = t + \tau$ the atom-field coupling system gets into the state

$$\begin{aligned}
|\Psi(t+\tau)> &= \exp[-i(\omega_0\hat{S}_z + \omega\hat{a}^+\hat{a})\tau] \\
&\times \{\sum_{n=N_d}^{N_u} S_n[\alpha\cos(\sqrt{(n+m)!/n!}g\tau)|n> \\
&- i\beta\sin(\sqrt{n!/(n-m)!}g\tau)|n-m>]|e> \\
&+ \sum_{n=N_d}^{N_u} S_n[\beta\cos(\sqrt{n!/(n-m)!}g\tau)|n> \\
&- i\alpha\sin(\sqrt{(n+m)!/n!}g\tau)|n+m>]|g>\}.
\end{aligned} \tag{4}$$

If requiring that except the exponential factor $\exp[-i(\omega_0\hat{S}_z+\omega\hat{a}^+\hat{a})\tau]$ induced by $\hbar\omega_0\hat{S}_z+\hbar\omega\hat{a}^+\hat{a}$ during the period τ the whole system completely returns to the initial state (3) after the atom left out of the cavity, i.e., $\exp[i(\omega_0\hat{S}_z+\omega\hat{a}^+\hat{a})\tau]|\Psi(t+\tau)>=|\Psi(t)>$, and making the interaction time τ fulfill the conditions

$$\sqrt{N_d!/(N_d-m)!}g\tau=q\pi,\qquad q=0,2,4,\cdots, \tag{5}$$

$$\sqrt{(N_u+m)!/N_u!}g\tau=p\pi,\qquad p=1,3,5,\cdots, \tag{6}$$

we can write (4) as

$$|\Psi(t+\tau)>=\exp[-i(\omega_0\hat{S}_z+\omega\hat{a}^+\hat{a})\tau]\sum_{n=N_d}^{N_u}S_n|n>\otimes(\beta|g>-\alpha|e>) \tag{7}$$

where S_n are determined by the recurrence relation

$$S_n=-i\frac{\alpha}{\beta}\cot(\frac{1}{2}\sqrt{n!/(n-m)!}g\tau)S_{n-m} \tag{8}$$

with $n=N_d+m, N_d+2m,\cdots,N_u$. In (7), except the phase factor $\exp(-i\omega\tau\hat{a}^+\hat{a})$, the field returns to the initial state $\sum_{n=N_d}^{N_u}S_n|n>$ and the magnitudes of the atomic level occupation probability amplitudes for the lower and upper states are same as in the initial state $\alpha|e>+\beta|g>$ but the relative phase of α to β changes π. Therefore, We can conclude that if the field is pumped into the state $\sum_{n=N_d}^{N_u}S_n|n>$ from an initial state it will no longer be affected by the succeeding atoms which are initially in the coherent state $\alpha|e>+\beta|g>$. In this sense, we say that the state $\sum_{n=N_d}^{N_u}S_n|n>$ is steady. Since the relation (8) is the cotangent function the corresponding state of the field is named the cotangent state[14].

To investigate squeezing properties of the cotangent state, we introduce the two slowly varying quadrature components of the field amplitude

$$\hat{d}_1=\frac{1}{2}(\hat{a}e^{i\omega t}+\hat{a}^+e^{-i\omega t});\qquad \hat{d}_2=\frac{1}{2i}(\hat{a}e^{i\omega t}-\hat{a}^+e^{-i\omega t}). \tag{9}$$

In an arbitrary state of the field, the N*th*-order moment of fluctuation of the field in $\hat{d}_i(i=1,2)$ is

$$\begin{aligned}<(\Delta\hat{d}_i)^N>=&<:(\Delta\hat{d}_i)^N:>+\frac{N!}{(N-2)!}\frac{1}{8}<:(\Delta\hat{d}_i)^{N-2}:>\\&+\frac{N!}{2!(N-4)!}\frac{1}{8^2}<:(\Delta\hat{d}_i)^{N-4}:>+\cdots+\frac{(N-1)!!}{2^N}\end{aligned} \tag{10}$$

where $\Delta\hat{d}_i = \hat{d}_i - < \hat{d}_i >$ and $<: (\Delta\hat{d}_i)^n :> (n = N, N-2, \cdots, 2)$ is the nth-order moment of the $\hat{d}_i$'s mean squared fluctuation in the normal order. For a coherent state of the field, one has $< (\Delta\hat{d}_i)^N >= (N-1)!!/2^N$. When the Nth-order moment of the mean squared fluctuation of $\hat{d}_i$ in a state is smaller than in a coherent state, that is, $< (\Delta\hat{d}_i)^N >< (N-1)!!/2^N$, we say that the state is a Nth-order squeezed state in the $\hat{d}_i$'s component. Hong and Mandel[15] have shown that the Nth-order squeezed state with an even N is nonclassical.

We may also define the two quadrature operators of the square of the field amplitude

$$\hat{Y}_1 = \frac{1}{2}(\hat{a}^2 e^{2i\omega t} + \hat{a}^{+2} e^{-2i\omega t}); \quad \hat{Y}_2 = \frac{1}{2i}(\hat{a}^2 e^{2i\omega t} - \hat{a}^{+2} e^{-2i\omega t}). \tag{11}$$

It is easily shown that $\hat{Y}_1$ and $\hat{Y}_2$ fulfill the commutator $[\hat{Y}_1, \hat{Y}_2] = i(2\hat{N}+1)$, where $\hat{N} = \hat{a}^+\hat{a}$. The uncertainty relation for their variances is $< (\Delta\hat{Y}_1)^2 >< (\Delta\hat{Y}_2)^2 >\geq< \hat{N} + \frac{1}{2} >^2$. For a coherent state of the field, the equality holds and we have $< (\Delta\hat{Y}_1)^2 >=< (\Delta\hat{Y}_2)^2 >=< \hat{N} + \frac{1}{2} >$. If either $< (\Delta\hat{Y}_1)^2 >$ or $< (\Delta\hat{Y}_2)^2 >$ is less than $< \hat{N} + \frac{1}{2} >$ in a state of the field, the state is called a squared amplitude squeezed state. Hillery[16] has shown that this squeezed state is also nonclassical.

For convenience, we will in the following discussions employ the two quantities

$$D_i^{(N)} = \frac{< (\Delta\hat{d}_i)^N >}{2^{-N}(N-1)!!} - 1, \quad ; \quad Q_i = \frac{< (\Delta\hat{Y}_i)^2 >}{< \hat{N} + \frac{1}{2} >} - 1, \quad (i = 1, 2) \tag{12}$$

to measure the squeezing degree. When $D_i^{(N)} < 0$ or $Q_i < 0$ the squeezings appear according to the above definition for squeezing.

Squeezing properties of the cotangent state with various photon multiples m have numerically been investigated. In our calculations the relative phase of the upper level probability amplitude α to the lower level one β is chosen $\pi/2$. We have found that the pronounced second- and fourth-order squeezings appear only for $m = 1$. In Figs. 1, $D_1^{(2)}$ and $D_1^{(4)}$ of the cotangent state with $m = 1$ are depicted against the ratio of α to β. It is observed in these figures that the strongest squeezing effect can be reached for a given N_a by a proper choice of α/β. For example, $D_1^{(4)} = -0.91$ can be acquired for $N_a = 40$ with $\alpha/\beta = 3.2$. This corresponds to the initial state of the atoms in which the occupation probabilities for the upper and lower levels are 0.91 and 0.09, respectively. We also notice that the fourth-order squeezing appears only in the regions of the second one. It means that the present fourth-order squeezing is not intrinsic[10] and is induced from the second one. In Figs. 2, Q_1 of the cotangent state with $m = 1$ and $m = 2$ versus α/β is shown. It is observed in these figures that for a given N_a there exists the value of α/β for the optimal squeezing. For example, Q_1 can reach -0.54 and -0.62 for $m = 1$ and $m = 2$, respectively, when $\alpha/\beta = 2.5$ and

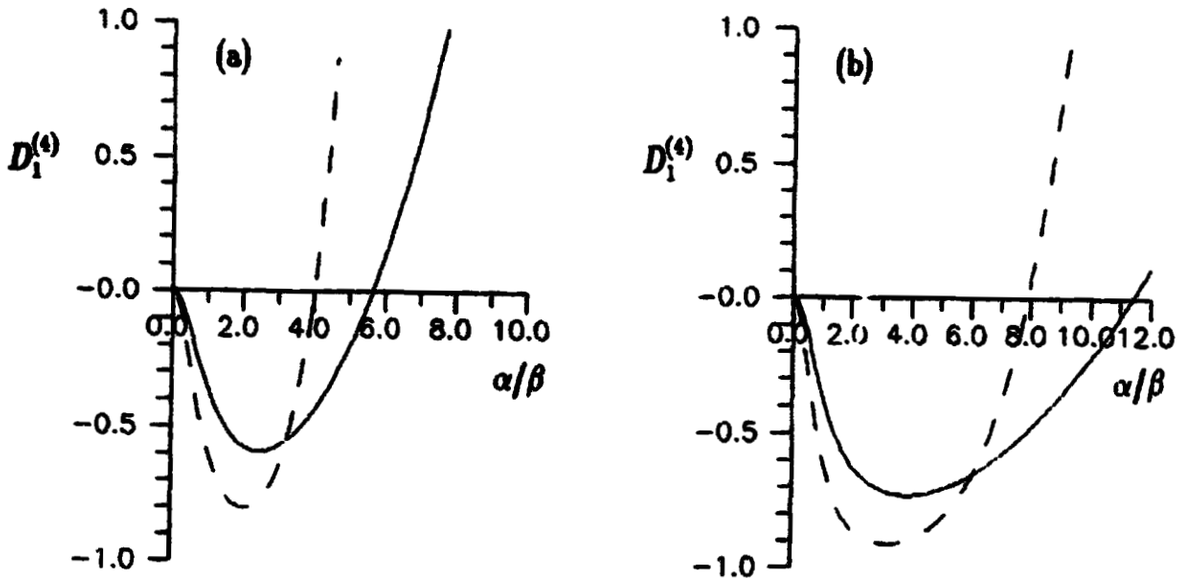

Figs. 1: $D_1^{(2)}$(solid line) and $D_1^{(4)}$ (dashed line) versus α/β with $N_d = 0$ and $m = 1$.
(a)$N_u = 10$;(b)$N_u = 40$.

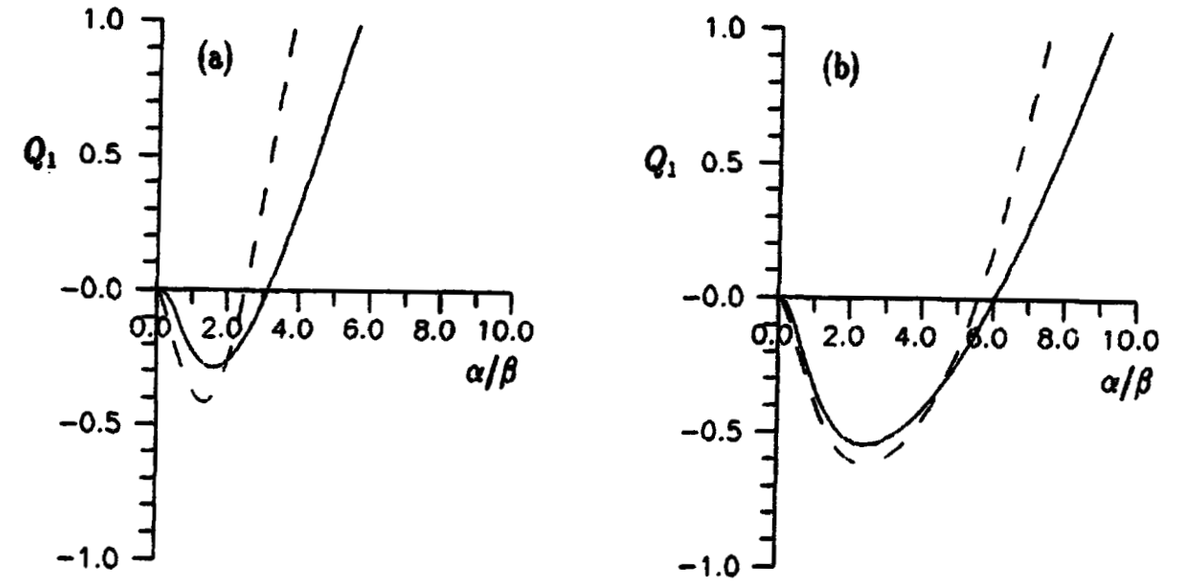

Figs. 2: Q_1 versus α/β with $N_d = 0$, $m = 1$(solid line) and $m = 2$(dashed line).
(a)$N_u = 10$;(b)$N_u = 40$.

$N_s = 40$. It means that these squeezing degrees can be acquired when the atoms are initially in the coherent state with the level occupation probabilities $\alpha^2 = 0.86$ and $\beta^2 = 0.14$. We also notice that the optimal squeezing in the two photon case is always stronger than in the one photon case for a given N_s. In our calculations we find that the squared amplitude squeezing disappears when $m > 2$. It means that this squeezing can be realized only in one-and two-photon micromasers by the coherent trapping approach.

3 Dynamic process of generation of steady state squeezing

We now turn our attention to dynamically generating the squeezing effects discussed above. Suppose that each of the atoms entering the cavity is initially in the coherent state $\alpha|e> + \beta|g>$, and the flight time of the atoms inside the cavity is τ. If at time t_i the density matrix of the field is $\hat{\rho}^{(f)}(t_i)$, at time $t_i + \tau$ the atom will leave out of the cavity and density matrix elements of the field can be written as

$$\begin{aligned}
&\hat{\rho}^{(f)}_{n'n}(t_i+\tau) = \exp[i(n-n')\omega\tau] \\
&\times\{[|\alpha|^2\cos(\sqrt{(n'+m)!/n'!}g\tau)\cos(\sqrt{(n+m)!/n!}g\tau) \\
&+|\beta|^2\cos(\sqrt{n'!/(n'-m)!}g\tau)\cos(\sqrt{n!/(n-m)!}g\tau)]\hat{\rho}^{(f)}_{n'n}(t_i) \\
&+|\beta|^2\sin(\sqrt{(n'+m)!/n'!}g\tau)\sin(\sqrt{(n+m)!/n!}g\tau)\hat{\rho}^{(f)}_{n'+mn+m}(t_i) \\
&+|\alpha|^2\sin(\sqrt{n'!/(n'-m)!}g\tau)\sin(\sqrt{n!/(n-m)!}g\tau)\hat{\rho}^{(f)}_{n'-mn-m}(t_i) \\
&+i\alpha\beta^*\cos(\sqrt{(n'+m)!/n'!}g\tau)\sin(\sqrt{(n+m)!/n!}g\tau)\hat{\rho}^{(f)}_{n'n+m}(t_i) \\
&-i\alpha^*\beta\sin(\sqrt{(n'+m)!/n'!}g\tau)\cos(\sqrt{(n+m)!/n!}g\tau)\hat{\rho}^{(f)}_{n'+mn}(t_i) \\
&+i\alpha^*\beta\cos(\sqrt{n'!/(n'-m)!}g\tau)\sin(\sqrt{n!/(n-m)!}g\tau)\hat{\rho}^{(f)}_{n'n-m}(t_i) \\
&-i\alpha\beta^*\sin(\sqrt{n'!/(n'-m)!}g\tau)\cos(\sqrt{n!/(n-m)!}g\tau)\hat{\rho}^{(f)}_{n'-mn}(t_i)\}. \qquad (13)
\end{aligned}$$

If the next atom enters the cavity at time t_{i+1}, there will be no atom inside the cavity within the time interval $t_i + \tau \le t \le t_{i+1}$. We suppose that during that interval the field relaxes at the rate γ to the thermal reservoir with the mean photon number n_b. This process is described by the master equation[5]

$$\begin{aligned}
&\frac{d\hat{\rho}^{(f)}(t)}{dt} = \frac{\gamma}{2}(n_b+1)(2\hat{a}\hat{\rho}^{(f)}(t)\hat{a}^+ - \hat{a}^+\hat{a}\hat{\rho}^{(f)}(t) - \hat{\rho}^{(f)}(t)\hat{a}^+\hat{a}) \\
&+\frac{\gamma}{2}n_b(2\hat{a}^+\hat{\rho}^{(f)}(t)\hat{a} - \hat{a}\hat{a}^+\hat{\rho}^{(f)}(t) - \hat{\rho}^{(f)}(t)\hat{a}\hat{a}^+), \quad t_i+\tau \le t \le t_{i+1}. \qquad (14)
\end{aligned}$$

On the basis of (13)-(14), we can study the dynamic evolution of the field while the atoms one by one pass through the cavity.

In the present calculations, we choose that the field is initially in the vacuum, and make the relative phase of α to β being $\pi/2$ and τ satisfying the conditions (5)-(6) with $q = 0$ and $p = 1$. Meanwhile, we take $\gamma = 5s^{-1}$, $g = 10kHz$ which are consistent with the parameters used in the current micromaser[4]. If the injection of the atoms is regular, i.e., the time distances between the adjacent atoms are same. In this case, the relaxation time of the field to the reservior is equal to $1/R - \tau$ where R is the atomic flux. In Figs.3-6. for the single photon case, the evolution of $D_1^{(4)}$ and Q_1 against the number of the atoms which have left out of the cavity is shown with various values of the atomic flux R. In these figures, the dashed line represents the result with $\gamma = 0$. According to the conditions for the present calcualtions, the steady state with $\gamma = 0$ must be the cotangent state. It is observed that when R is small the field has not the second- and fourth-order squeezing properties since the steady state resuts from the balance between the gain and the loss. As R increases, the gain brought by the atoms will overpass the cavity loss the steady state will arise from the coherent trapping because of the condition (6). Then the steady state exhibits the squeezing behaviour as shown in the figures. We also notice that when R is adequate large $D_1^{(4)}$ and Q_1 of the steady state are very close to the values of the cotangent state with the same parameters.

In Figs.7 and 8, for the two-photon case, the evolution of Q_1 against the number of the atoms is depicted. It is observed that the evolution behaviour is similar to shown in Figs. 5 and 6, and the squeezing becomes deeper than in the one photon case with the same value of R.

4 Conclusion

We have shown that the cotangent state produced by the coherent trapping scheme in a one-photon micromaser can exhibit steady state fourth-order as well as squared amplitude squeezings. The last squeezing can also appear in the cotangent state produced in a degenerate two-photon micromaser. The cotangent state of the field with these squeezing effects can be reached from the cavity vacuum by the atomic coherent pumping. The influence of the cavity loss on the squeezing effects has been investigated. The results show that when the flux of the atoms entering the cavity is moderately large the squeezings are not essentially affected by the cavity loss.

Acknowledgments

This work was supported by the National Natural Science Foundation of China.

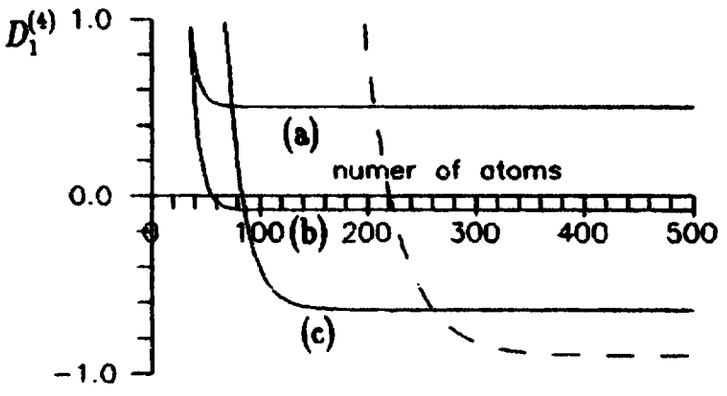

Fig.3: $D_1^{(4)}$ versus the number of atoms for one photon case with $N_a = 30$ and $\alpha/\beta = 2.9$. The values of the atomic flux for the lines are (a) $22s^{-1}$, (b) $30s^{-1}$ and (c) $50s^{-1}$.

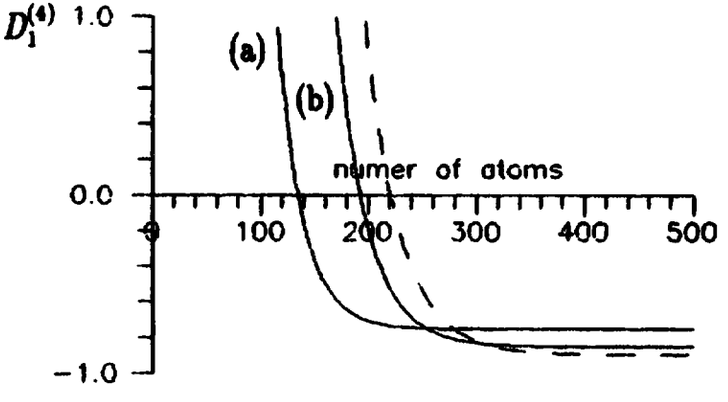

Fig.4: Same as Fig.3 but (a) $100s^{-1}$ and (b) $500s^{-1}$.

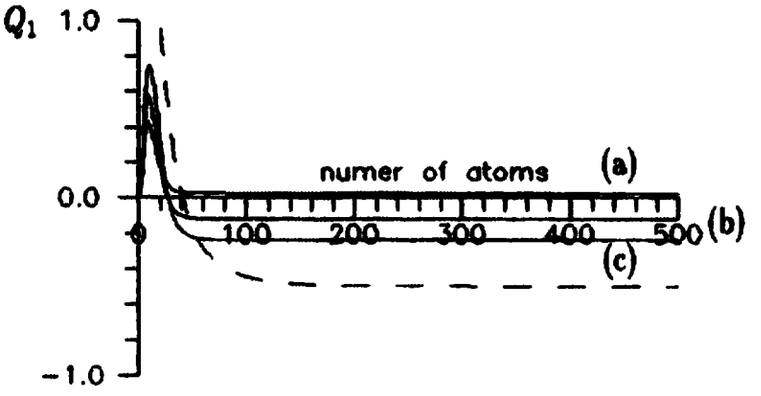

Fig.5: Q_1 versus the number of atoms for one photon case with $N_a = 30$ and $\alpha/\beta = 2.3$. (a)$20s^{-1}$;(b)$30s^{-1}$; (c)$50s^{-1}$.

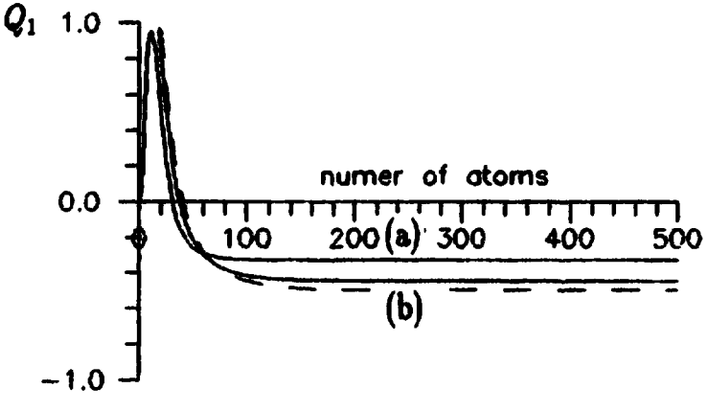

Fig.6: Same as Fig.5 but (a) $100s^{-1}$ and (b) $500s^{-1}$.

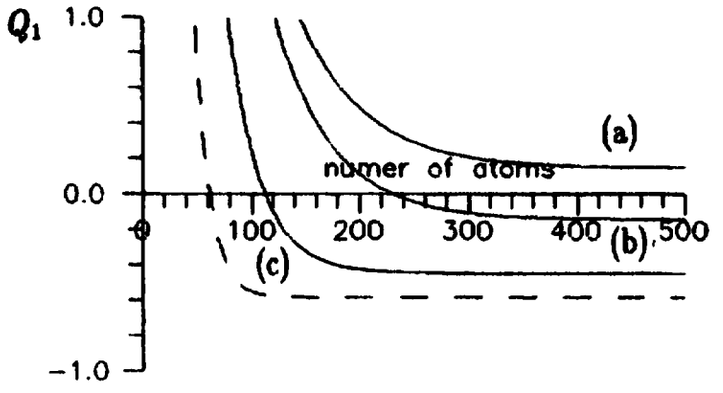

Fig.7: Q_1 versus the number of atoms for tow-photon case with $N_a = 30$ and $\alpha/\beta = 2.3$. (a)$33s^{-1}$;(b)$35s^{-1}$; (c)$50s^{-1}$.

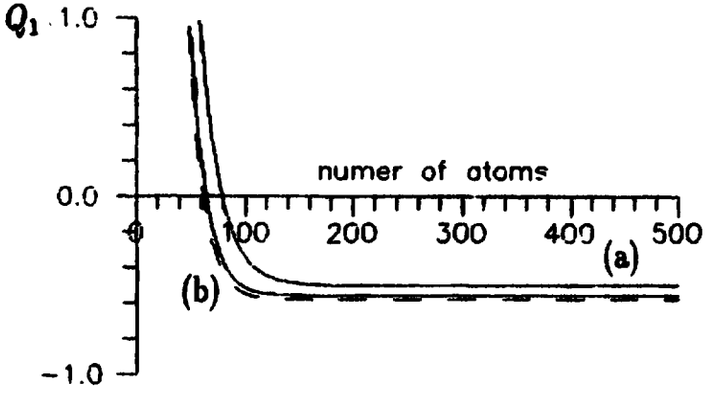

Fig.8: Same as Fig.7 but (a)$100s^{-1}$ and (b) $500s^{-1}$.

References

[1] G. Rempe, H. Walther and N. Klein, Phys. Rev. Lett. **58**, 353(1987).

[2] D. Meschede, H. Walther and G. Müller, Phys. Rev. Lett. **54**, 551(1985).

[3] M. Brune, J. M. Raimond, P. Goy, L. Davidovich, and S. Haroche, Phys. Rev. Lett. **59**, 1899(1987).

[4] G. Rempe, F. Schmidt-Kaler, and H. Walther, Phys. Rev. Lett. **64**, 2783(1990).

[5] P. Filipowicz, J. Javanainen and P. Meystre, Phys. Rev. **A34**, 3077(1986).

[6] S. Qamar and M. S. Zubairy, Phys. Rev. **A48**, (1993)1559.

[7] M. Orszag, R. Ramirez, J. C. Retamal, and L. Roa, Phys. Rev. **A45**, 6717(1992).

[8] Fu-li Li and Shun-jing Wang, Phys. Lett. **A148**, 320(1990).

[9] E. T. Jaynes and F. W. Cummings, Proc. IEEE **51**, 89(1963).

[10] Fam Le Kien, M. Kozierowski, and Tran Quang, Phys. Rev. **A38**, 263(1988).

[11] A. S. Shumovsky, Fam Le Kien and E. I. Aliskenderov, Phys. Lett. **A124**, 351(1987).

[12] C. C. Gerry and P. J. Moyer, Phys. Rev. **A38**, 5665(1988).

[13] Xiaoping Yang and Xiping Zheng, Phys. Lett. **A138**, 409(1989).

[14] J. J. Slosser and P. Meystre, Phys. Rev. **A41**, 3867(1990).

[15] C. K. Hong and L. Mandel, Phys. Rev. Lett. **54**, 323(1985); Phys. Rev. **A32**, 974(1985).

[16] M. Hillery, Phys. Rev. **A36**, 3796(1987).

NEXT
DOCUMENT

HIGHER-ORDER SQUEEZING OF QUANTUM FIELD AND THE GENERALIZED UNCERTAINTY RELATIONS IN NON-DEGENERATE FOUR-WAVE MIXING

Xi-zeng Li Bao-xia Su
Department of Physics, Tianjin University, Tianjin 300072, P.R.China

Abstract

It is found that the field of the combined mode of the probe wave and the phase-conjugate wave in the process of non-degenerate four-wave mixing exhibits higher-order squeezing to all even orders. And the generalized uncertainty relations in this process are also presented.

With the development of techniques for making higher-order correlation measurement in quantum optics, the new concept of higher-order squeezing of the single-mode quantum electromagnetic field was first introduced and applied to several processes by Hong and Mandel in 1985[1,2]. Lately Xi-zeng Li and Ying Shan have calculated the higher-order squeezing in the process of degenerate four-wave mixing[3] and presented the higher-order uncertainty relations of the fields in single-mode squeezed states[4]. As a natural generalization of Hong and Mandel's work, we introduced the theory of higher-order squeezing of the quantum fields in two-mode squeezed states in 1993. In this paper we study for the first time the higher-order squeezing of the quantum field and the generalized uncertainty relations in non-degenerate four-wave mixing (NDFWM) by means of the above theory.

1 Definition of higher-order squeezing of two mode quantum fields

The real two mode output field $\hat{E}$ can be decomposed into two quadrature components $\hat{E}_1$ and $\hat{E}_2$, which are canonical conjugates

$$\hat{E} = \hat{E}_1 cos(\Omega t - \phi) + \hat{E}_2 sin(\Omega t - \phi), \tag{1}$$

$$[\hat{E}_1, \hat{E}_2] = 2iC_0. \tag{2}$$

Then the field is squeezed to the Nth-order in $\hat{E}_1 (N = 1, 2, 3, \cdots)$ if there exists a phase angle ϕ such that $< (\Delta\hat{E}_1)^N >$ is smaller than its value in a completely two-mode coherent state of the field, viz.,

$$< (\Delta\hat{E}_1)^N > \quad < \quad < (\Delta\hat{E}_1)^N >_{two-mode\ \ coh.s.} \tag{3}$$

This is the definition of higher-order squeezing of two mode quantum fields.

2 Scheme for generation of higher−order squeezing via NDFWM

The scheme is shown in the following figure:

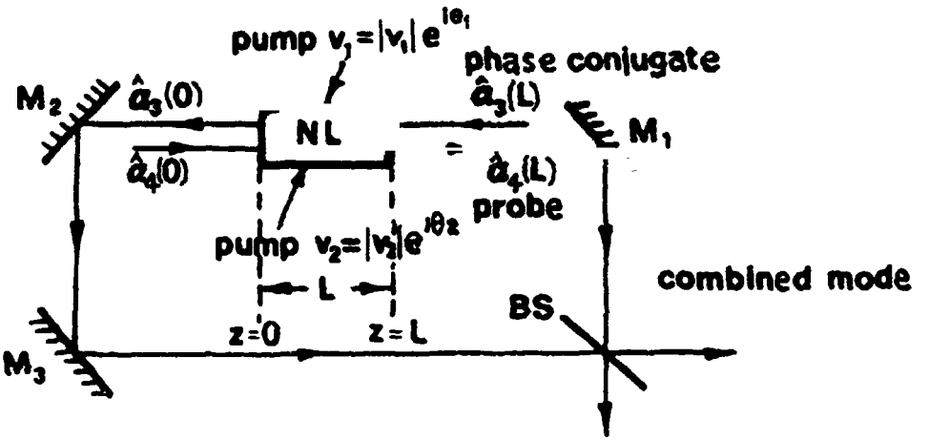

FIG. 1. Schematic for generation of higher−order squeezing via NDFWM. M_1, M_2, M_3 are mirrors, BS is the 50%−50% beam splitter

Where two strong, classical pump waves of complex amplitude ($v_1 = |v_1|e^{i\theta_1}$ and $v_2 = |v_2|e^{i\theta_2}$) with the same frequency Ω are incident on a nonlinear crystal possessing a third−order ($\chi^{(3)}$) nonlinearity. The length of the medium is L. $\hat{a}_4$ is the annihilation operator of the transmitted −probe wave with frequency ω_4, $\hat{a}_3$ is the annihilation operator of the phase−conjugate wave with frequency ω_3, and

$$\Omega = \frac{\omega_3 + \omega_4}{2} \tag{4}$$

The effective Hamiltonian of this interaction system has the form of

$$\hat{H} = \hbar\omega_3\hat{a}_3^+\hat{a}_3 + \hbar\omega_4\hat{a}_4^+\hat{a}_4 + \hbar g_0(v_1v_2\hat{a}_3^+\hat{a}_4^+e^{-2i\Omega t} + H.C) \tag{5}$$

where g_0 is the coupling const, t is the time propagation of light in NL crystal.

By solving the Heisenberg Equation of motion we get the output mode

$$\hat{a}_3(t) = [\mu\hat{a}_3(L) + \nu\hat{a}_4^+(0)]e^{-i\omega_3 t}, \quad (z = L - ct \quad \text{for} \quad \hat{a}_3) \tag{6}$$

$$\hat{a}_4(t) = [\mu\hat{a}_4(0) + \nu\hat{a}_3^+(L)]e^{-i\omega_4 t}, \quad (z = ct \quad \text{for} \quad \hat{a}_4) \tag{7}$$

where

$$\left.\begin{aligned} \mu &= sec|k|L, \\ \nu &= -ie^{i(\theta_1+\theta_2)}tan|k|L, \\ |k| &= \frac{g_0|v_1||v_2|}{c}. \end{aligned}\right\} \tag{8}$$

3 Combined mode and its quadrature components

It can be verified that the field of either $\hat{a}_3(0)$ or $\hat{a}_4(L)$ mode does not exhibit higher–order squeezing.

We consider the field of the combined mode of $\hat{a}_3(t)$ and $\hat{a}_4(t)$

$$\begin{aligned}\hat{E}(t) &= \sqrt{\frac{\omega_3}{2}}\hat{a}_3(t) - i\sqrt{\frac{\omega_4}{2}}\hat{a}_4(t) + (H.C) \\ &= \sqrt{\frac{\Omega}{2}}\lambda_3\hat{a}_3(t) - i\sqrt{\frac{\Omega}{2}}\lambda_4\hat{a}_4(t) + (H.C) \end{aligned} \tag{9}$$

where

$$\lambda_3 = \sqrt{\frac{\omega_3}{\Omega}}, \lambda_4 = \sqrt{\frac{\omega_4}{\Omega}} \tag{10}$$

and $-i$ denotes the phase delay. The units are chosen so that $\hbar = c = 1$.

$\hat{E}(t)$ can be decomposed into two quadrature components $\hat{E}_1$ and $\hat{E}_2$, which are canonical conjugates

$$\hat{E}(t) = \hat{E}_1 cos(\Omega t - \phi) + \hat{E}_2 sin(\Omega t - \phi), \tag{11}$$

where

$$\Omega = \frac{\omega_3 + \omega_4}{2}, \tag{12}$$

and ϕ is an arbitrary phase angle that may be chosen at will.

$\hat{E}_1$ can be expressed in term of initial modes $\hat{a}_3(L)$ and $\hat{a}_4(0)$,

$$\hat{E}_1 = g\hat{a}_3(L) + h\hat{a}_4(0) + g^*\hat{a}_3^\dagger(L) + h^*\hat{a}_4^\dagger(0), \tag{13}$$

where

$$g = \sqrt{\frac{\Omega}{2}}[\lambda_3\mu e^{-i\phi} + \lambda_4\nu^* e^{i(\phi+\pi/2)}]e^{i\epsilon t}, \tag{14}$$

$$h = \sqrt{\frac{\Omega}{2}}[\lambda_4\mu e^{-i(\phi+\pi/2)} + \lambda_3\nu^* e^{i\phi}]e^{-i\epsilon t}, \tag{15}$$

$$\epsilon = \Omega - \omega_3 = \omega_4 - \Omega. \tag{16}$$

ϵ is the modulation frequency

Now we define

$$B = g\hat{a}_3(L) + h\hat{a}_4(0), \tag{17}$$

$$\hat{B}^\dagger = g^*\hat{a}_3^\dagger(L) + h^*\hat{a}_4^\dagger(0), \tag{18}$$

then

$$\hat{E}_1 = \hat{B} + \hat{B}^\dagger, \tag{19}$$

where $B^\dagger$ is the adjoint of $\hat{B}$.

4 Higher−order noise moment $< (\Delta\hat{E}_1)^N >$ and higher −order squeezing

By using the Campbell−Baker−Hausdorff formula, we get the Nth−order moment of $\Delta\hat{E}_1$,

$$\begin{aligned} < (\Delta\hat{E}_1)^N > &= <:: (\Delta\hat{E}_1)^N ::> + \frac{N^{(2)}}{1!}(\frac{1}{2}C_0) <:: (\Delta\hat{E}_1)^{N-2} ::> + \frac{N^{(4)}}{2!}(\frac{1}{2}C_0)^2 \\ & <:: (\Delta\hat{E}_1)^{N-4} ::> \\ & + \cdots + (N-1)!!C_0^{N/2}. \qquad \text{(N is even)} \end{aligned} \tag{20}$$

where

$$N^{(r)} = N(N-1)\cdots(N-r+1), \quad C_0 = \frac{1}{2i}[\hat{E}_1, \hat{E}_2] = [\hat{B}, \hat{B}^+], \tag{21}$$

and :: :: denotes normal ordering with respect to $\hat{B}$ and $\hat{B}^+$.

We take the initial quantum state to be $|\alpha>_4 |0>_3$, which is a product of the coherent state $|\alpha>_4$ for $\hat{a}_4(0)$ mode and the vacuum state for $\hat{a}_3(L)$ mode. Since $|\alpha>_4 |0>_3$ is the eigenstate of $\hat{B}$, we get

$$\begin{aligned} <:: (\Delta\hat{E}_1)^N ::> &= <:: (\Delta\hat{B} + \Delta\hat{B}^+)^N ::> \\ &= \sum_{\gamma=0}^{N} \begin{bmatrix} N \\ \gamma \end{bmatrix} {}_3<0|_4<\alpha| :: (\Delta\hat{B}^+)^\gamma (\Delta\hat{B})^{N-\gamma} :: |\alpha>_4 |0>_3 = 0. \end{aligned} \tag{22}$$

Then from (20),

$$< (\Delta\hat{E}_1)^N >= (N-1)!!C_0^{N/2}, \tag{23}$$

$$\begin{aligned} C_0 &= [\hat{B}, \hat{B}^+] = |g|^2 + |h|^2, \\ &= \frac{\Omega}{2}\{(\lambda_3^2 + \lambda_4^2)(|\mu|^2 + |\nu|^2) + 2\lambda_3\lambda_4[\mu^*\nu^* e^{i(2\phi + \frac{\pi}{2})} + \mu\nu e^{-i(2\phi + \frac{\pi}{2})}]\}. \end{aligned} \tag{24}$$

where

$$\lambda_3^2 + \lambda_4^2 = 1, \qquad \lambda_3\lambda_4 = \sqrt{1 - \frac{\epsilon^2}{\Omega^2}}.$$

Substituting eqs. (8), (10), (24) into (23), we get the Nth−order moment of ΔE_1,

$$\begin{aligned} < (\Delta\hat{E}_1)^N > &= (N-1)!!\Omega^{N/2}[sec^2|k|L + tan^2|k|L \\ &- 2\sqrt{1 - \frac{\epsilon^2}{\Omega^2}} sec|k|L tan|k|L cos(2\phi - \theta_1 - \theta_2)]^{N/2}. \end{aligned} \tag{25}$$

If ϕ is chosen to satisfy

$$2\phi - \theta_1 - \theta_2 = 0, \quad \text{or} \quad cos(2\phi - \theta_1 - \theta_2) = 1.$$

then the above eq. (25) leads to the result

$$\begin{aligned} < (\Delta\hat{E}_1)^N > &= (N-1)!!\Omega^{N/2}[sec^2|k|L + tan^2|k|L \\ &- 2\sqrt{1 - \frac{\epsilon^2}{\Omega^2}} sec|k|L tan|k|L]^{N/2}. \end{aligned} \tag{26}$$

When $0 < |k|L < \pi$, the right−hand side is less than $(N-1)!!\Omega^{N/2}$, which is the corresponding Nth−order moment for two−mode coherent states. It follows that the field of the combined mode of the probe wave and the phase conjugate wave in NDFWM exhibits higher−order squeezing to all even orders.

The squeeze parameter q_N for measuring the degree of Nth−order squeezing is

$$q_N = \frac{< (\Delta\hat{E}_1)^N > - < (\Delta\hat{E}_1)^N >_{two-mode\ \ coh.s}}{< (\Delta\hat{E}_1)^N >_{two-mode\ \ coh.s}} \tag{27}$$

$$= [sec^2|k|L + tan^2|k|L - 2\sqrt{1 - \frac{\epsilon^2}{\Omega^2}}sec|k|Ltan|k|L]^{N/2} - 1. \tag{28}$$

We find that q_N is negative, and q_N increases with N. This gives out the conclusion that the degree of higher−order squeezing is greater than that of the second order.

5 Generalized uncertainty relations in NDFWM

$\hat{E}_2$ can be regarded as a special case of $\hat{E}_1$ if ϕ is replaced by $\phi + \pi/2$. Then if ϕ is chosen to satisfy $2\phi - \theta_1 - \theta_2 = 0$, from eq. (25) it follows that

$$< (\Delta\hat{E}_2)^N >= (N-1)!!\Omega^{N/2}[sec^2|k|L + tan^2|k|L + 2\sqrt{1 - \frac{\epsilon^2}{\Omega^2}}sec|k|Ltan|k|L]^{N/2}. \tag{29}$$

when $0 < |k|L < \pi$, the right-hand side is greater than $(N-1)!!\Omega^{N/2}$.

From eqs. (26) and (29), we obtain

$$< (\Delta\hat{E}_1)^N > \cdot < (\Delta\hat{E}_2)^N >= [(N-1)!!]^2\Omega^N[1 + 4\frac{\epsilon^2}{\Omega^2}sec^2|k|Ltan^2|k|L]^{N/2}. \tag{30}$$

Eq. (30) shows that $< (\Delta\hat{E}_1)^N >$ and $< (\Delta\hat{E}_2)^N >$ can not be made arbitrarily small simultaneously. We call eq. (30) the generalized uncertainty relations in NDFWM, and the right−hand side is dependent on ϵ, Ω, N, and $|k|L$.

In the degenerate case $\omega_4 = \omega_2 = \Omega, \epsilon = 0$ from eqs. (26), (28) and (30) we obtain

$$< (\Delta\hat{E}_1)^N > = (N-1)!!\Omega^{N/2}[sec|k|L - tan|k|L]^N, \tag{31}$$

$$q_N = [sec|k|L - tan|k|L]^N - 1, \tag{32}$$

$$< (\Delta\hat{E}_1)^N > \cdot < (\Delta\hat{E}_2)^N >= [(N-1)!!]^2 \cdot \Omega^N. \tag{33}$$

When $N = 2$,

$$< (\Delta\hat{E}_1)^2 > = \Omega[sec|k|L - tan|k|L]^2, \tag{34}$$

$$q_2 = [sec|k|L - tan|k|L]^2 - 1, \tag{35}$$

$$< (\Delta \hat{E}_1)^2 > \cdot < (\Delta \hat{E}_2)^2 > = \Omega^2 \qquad (36)$$

These results are in agreement with the conclusions in the previous relevant references[3][5].

6 Acknowledgements

This research was supported by the National Natural Science Foundation of China, and Tianjin Natural Science Foundation.

References

[1] C.K Hong and L.Mandel, Phys. Rev. Lett. 54, 323 (1985)

[2] C.K.Hong and L.Mandel, Phys. Rev. A32, 974 (1985)

[3] Xi-zeng Li and Ying Shan, Phys. Rev. A40, 7384 (1989)

[4] Xi-zeng Li and Bao-xia Su, in "The Third International Workshop on Squeezed States and Uncertainty Relations". ed. by D.Han *et al.* (NASA Conference Publication 3270, Washington DC, 1994) p.33

[5] H.P.Yuen and J.H.Shapiro. Opt. Lett. 4, 334 (1979)

NEXT
DOCUMENT

THE SQUEEZING OPERATOR AND THE SQUEEZING STATES OF "SUPERSPACE"

Ma Aiqun

Department of Physics, Harbin College, Harbin, 150020

Yan Changzhi

Department of Physics, Harbin Institute of Electrical Technology, Harbin, 150080

Lu Qiquang

Department of Physics, Harbin Teacher's College, Harbin, 150080

Shi Weichun

Department of Physics, Northeast Forestry University, Harbin, 150040

Abstract

In this paper, the unitary squeezing operator of "superspace" is introduced and by making this operator act on the supercoherent state, the squeezing supercoherent states are obtained, then come out the four orthonormalization eigenstates of the square of annihilation operator A of the supersymmetry harmonic oscillator, and their squeezing character is also studied.

1 Introduction

Early in the 1970's, D. Stoler[1] put forward the concept of the squeezing state first. Following him, H. P. Yuen[2] made a detailed study of the quantum characteristic of the squeezing state which was obtained from the squeezing operator acting on the coherent state. This kind of squeezing state they studied is the squeezing coherent state. Having less noise than the coherent state, the squeezing state would be a vast applied vistas in the optical communication and the gravitational force wave probing, etc. The squeezing state has become an attentive problem.

In recent years, a lot of studies about the supersymmetry have been done, P. Salomonson[3] and other persons put forward the supersymmetry harmonic oscillator, and C. Aragone[4], along with other, introduced the supercoherent state. People found that the inner link of different atoms and ions are related to the abstract supersymmetry[5]. Chen Cheng — ming and Xu Donghui[6] acted the displacement operator on one supersymmetry Hamiltonian, and also drew the supercoherent state, moreover, made the discussion on the squeezing state extend into the supercoherent state. The eigenstate of the annihilation operator A of the supersymmetry harmonic oscillator which they introduced — — the supercoherent state can not be introduced by using the displacement operator to affect the supersymmetry harmonic oscillator Hamiltonian. Acting the squeezing operator on the Hamiltonian of the displacement harmonic oscillator, the eigenstate of the new constructed Hamiltonian is the squeezing state[7]. According to this theory, to discuss the problem about supersymmetry requires not only constructing proper annihilation operator of the Hamiltaonian of the supersymmetry harmonic oscillator, but also introducing the displacement operator and squeezing operator of "superspace".

This paper introduces the squeezing operator of "superspace", and acts it on the supercoherent state, so as to get the squeezing supercoherent state. This method is equivalent to acting the squeezing operator of "superspace" on the displacement supersymmetry harmonic oscillator, and then, to get the eigenstate of the new constructed Hamiltonian. In this paper, the annihilation operator A of the supersymmetry harmonic oscillaor has such characters: $[A, H]=\omega A$, $[A, A^+]=1$ and $H=\omega A^+A$, As a result, the obtained squeezing supercoherent state is different from the squeezing state in literature[6]. In this paper, the squeezing character of the eigenstate of A is also discussed.

2 Supercoherent State

The Hamiltonian of the supersymmetry harmonic oscillator is[3]

$$H=\frac{1}{2}P^2+\frac{1}{2}\omega^2X-\frac{1}{2}\omega\sigma_3=\omega\begin{pmatrix}a^+a & 0\\ 0 & aa^+\end{pmatrix} \tag{1}$$

Where, x and p are the coordinate operator and momentum operator in the general space, σ_3 is the third component in Parli matrix; a and a^+ are the annihilation and creation operators of the ordinary harmonic oscillator.

The Harmiltonian of the supersymmetry harmonic oscillator is also written as:

$$H = \omega A^+ A \tag{2a}$$

$$= \frac{1}{2}P^2 + \frac{1}{2}\omega^2 Q^2 - \frac{1}{2}\omega \tag{2b}$$

in it,

$$A = \begin{pmatrix} 0 & \sqrt{aa^+} \\ \dfrac{1}{\sqrt{aa^+}}a^2 & 0 \end{pmatrix} \tag{3}$$

$$Q = \sqrt{\frac{1}{2\omega}}(A^+ + A), P = i\sqrt{\frac{\omega}{2}}(A^+ - A) \tag{4a}$$

$$A = \sqrt{\frac{\omega}{2}}Q + i\sqrt{\frac{1}{2\omega}}P, A^+ = \sqrt{\frac{\omega}{2}}Q - i\sqrt{\frac{\omega}{2}}P \tag{4b}$$

test and verify easily,

$$[A, H] = \omega A \tag{5}$$

$$[A, A^+] = I, [Q, P] = i \tag{6}$$

Because (5) is tenable, A is called the annihilation operator of the supersymmetry harmonic oscillator; A^+ the creation operator of the supersymmetry harmonic oscillator. (2b) is equal to the relevant expression form of the ordinary harmonic oscillator, and Q and P are called the generalized coordinate operator and the generalized momentum operator of "superspace" separately.

We can get the energy eigenvalue of H and the relevant eigenstate from literature[4], they are

$$E_0 = 0, \psi_0 = \begin{pmatrix} |0\rangle \\ 0 \end{pmatrix} \tag{7a}$$

$$E_{n>0} = n\omega, \psi_{n>0} = C_n^+ \psi_n^+ + C_n^- \psi_n^- \tag{7b}$$

$$|C_n^+|^2 + |C_n^-|^2 = 1 \tag{7c}$$

where

$$\psi_{n>0}^+ = \begin{pmatrix} |n\rangle \\ 0 \end{pmatrix}, \psi_{n>0}^- = \begin{pmatrix} 0 \\ |n-1\rangle \end{pmatrix} \tag{7d}$$

The eigenvalue of σ_3 is $+1$ and -1.

It is easy to prove that

$$A\psi_{n>1} = \sqrt{n}\psi_{n-1}, A^+\psi_n = \sqrt{n+1}\psi_{n+1}, A^+A\psi_n = n\psi_n \tag{8}$$

the eigenquation of A is

$$A|\Psi(\alpha)\rangle = \alpha|\Psi(\alpha)\rangle \tag{9}$$

Where, α is the complex parameter, $\alpha = |\alpha|e^{i\theta}$.

The definition of the displacement operator of "superspace" is

$$D(\alpha) = \exp(\alpha A^+ - \alpha^* A) \tag{10}$$

It has the similar character of the ordinary displacement operator $D(\alpha)$:

$$D^+(\alpha) = D(-\alpha) = [D(\alpha)]^{-1} \tag{11a}$$

$$D^+(\alpha)AD(\alpha) = A + \alpha \tag{11b}$$

$$D^+(\alpha)A^+D(\alpha) = A^+ + \alpha^* \tag{11c}$$

The eigenstate of A (double degenerate) is obtained by solving the eigenequation of (9), or by using $D(\alpha)$

$$|\Psi_1(\alpha)\rangle = \exp\left(-\frac{|\alpha|^2}{2}\right)(\mathrm{ch}|\alpha|^2)^{\frac{1}{2}}\begin{pmatrix} |\alpha\rangle_0 \\ \dfrac{\alpha}{\sqrt{aa^+}}|\alpha\rangle_0 \end{pmatrix} \tag{12a}$$

$$|\Psi_2(\alpha)\rangle = \exp\left(-\frac{|\alpha|^2}{2}\right)(\mathrm{sh}|\alpha|^2)^{\frac{1}{2}}\begin{pmatrix} |\alpha\rangle_0 \\ \dfrac{\alpha}{\sqrt{aa^+}}|\alpha\rangle_0 \end{pmatrix} \tag{12b}$$

Where, $|\alpha\rangle_e$ and $|\alpha\rangle_o$ are odd coherent state and even coherent state respectively[8,9]. The two mathematical expression formulas produced by the translation of the orthonormalization eigenstate are

$$|\Psi_1(a)\rangle = D(a)\begin{pmatrix}|0\rangle\\0\end{pmatrix} \tag{13a}$$

$$|\Psi_2(a)\rangle = D(a)\begin{pmatrix}|1\rangle\\0\end{pmatrix} = D(a)\begin{vmatrix}0\\\frac{1}{\sqrt{aa^+}}a|0\rangle\end{vmatrix} \tag{13b}$$

For the eigenstate of A, it is easy to prove that

$$\langle\Delta Q\rangle\langle\Delta P\rangle = \frac{1}{2} \tag{14}$$

Namely, the eigenstate of A is the minimum uncertainty state of Q and P, they are the conjugate Hermitian operators. In this sense, the eigenstate of A is called the supercoherent state.

3 Squeezing Supercoherent State

First, let us introduce the unitary evolutional operator of "superspace" generally:

$$S_k(Z) = \exp[Z_k(A^+)^k - Z_k^* A^k],\ Z_k = Z/K! \tag{15}$$

When $k=1$, it is the displacement operator D (a) $(a=z)$; When $k=2$, $S_{k(z)}$ is called the squeezing operator of complex parameter, written as $S(z)$.

$$S(z) = \exp\left[\frac{1}{2}z(A^+)^2 - \frac{1}{2}z^* A^2\right],\quad z = re^{i\theta} \tag{16}$$

Where r is the squeezing factor, θ the squeezing angle. Since the character of A is the same as a, and also

$$S^*(Z)AS(Z) = Ach r + A^+ shre^{i\theta} \tag{17}$$

And

$$S(Z) = R(-\frac{\theta}{2})S(r)R(\frac{\theta}{2}) \tag{18a}$$

Where, $R(\theta)$ is the revolving operator of the phasespace, S(r) the squeezing operator of the real parameter,

$$R(\theta) = \exp(-i\theta A^+ A) \tag{18b}$$

$$S(r) = \exp\left[\frac{r}{2}(A^{+2} - A^2)\right] \tag{18c}$$

To redefine the quadrature phase amplitude operator of "superspace"

$$X(\varphi) = \frac{1}{2}(Ae^{i\varphi} + A^+ e^{-i\varphi}) \tag{19}$$

Since the eigenstate of H and A all have the double degeneracy, the squeezing states are double. One of the squeezing state of "superspace" can be defined

$$|a,z\rangle_1 = D(a)S(z)\begin{pmatrix}|0\rangle\\0\end{pmatrix} \tag{20}$$

Because of $D^+(\alpha)AD(\alpha)=A+\alpha$, and making use of (17) and (18), the expection value of $X(\varphi)$ in $|\alpha, Z\rangle_1$, can be calculated, that is

$$\langle X(\varphi)\rangle_1 = \frac{1}{2}(ae^{i\varphi} + a^* e^{-i\varphi}) \tag{21}$$

but the expection value of $X^2(\varphi)$ in $|\alpha,Z\rangle_1$ is

$$\langle X^2(\varphi)\rangle_1 = \frac{1}{4}\left[(ae^{i\varphi} + a^* e^{-i\varphi})^2 + |ch r + e^{i(2\varphi+\theta)}sh r|^2\right] \tag{22}$$

thus,

$$\langle\Delta X^2(\varphi)\rangle_1 = \langle X^2(\varphi)\rangle_1 - \langle X(\varphi)\rangle_1^2 = \frac{1}{4}|ch r + e^{i(2\varphi+\theta)}sh r|^2 \tag{23}$$

When $r=0$, the formula above is the fluctuation of the supercoherent state. $\langle\Delta X^2\rangle_1$ is irrelevant to φ. When $r\neq 0$ (supposing $r>0$), if φ satisfies the inequality.

$$\cos(2\varphi + \theta) < -th r \tag{24}$$

then

$$\langle\Delta X^2(\varphi)\rangle_1 < \frac{1}{4} \tag{25}$$

Namely, (24) is the condition that the squeezing of $X(\varphi)$ exists in $|\alpha,z\rangle_1$. $X(\varphi+\pi/2)$ is the phase amplitude operator which is quadrature with $X(\varphi)$. Its squeezing condition is

$$\cos(2\varphi+\theta) > \text{th}r \tag{26}$$

Obviously (24) and (26) can be tenable at the same time. That is, $|\alpha,z\rangle_1$ can not exist the squeezing of $X(\varphi)$ and $X(\varphi+\pi/2)$.

Especially, if

$$\text{th}r \geqslant \cos(2\varphi+\theta) \geqslant -\text{th}r \tag{27}$$

neither of the quadrature phase components has the squeezing.

From (23) we get

$$\langle\Delta X^2(\varphi)\rangle_1\langle\Delta X^2(\varphi+\frac{\pi}{2})\rangle_1 = \frac{1}{16}[1+\text{sh}^2 2r\sin^2(2\varphi+\theta)] \tag{28}$$

When $2\varphi+\theta=0$ or π, the formula above takes the minimum value,

$$\langle\Delta X^2(\varphi)\rangle_1\langle\Delta X^2(\varphi+\frac{\pi}{2})\rangle_1 = \frac{1}{16} \tag{29}$$

the relation of the minimum uncertainty is tenable.

When $2\varphi+\theta=0$, (29) and (26) are satisfied at the same time; when $2\varphi+\theta=\pi$, (29) and (24) too. Similar to the definition of the squeezing coherent state, the squeezing supercoherent state $|\alpha,z\rangle_1$ is named.

Using (17)

$$S^+(z)\,D(a)S(z) = D(\beta) \tag{30a}$$

is solved, that is

$$D(a)S(z) = S(z)\,D(\beta) \tag{30b}$$

Where,

$$\beta = a\text{ch}r - a^*\text{sh}re^{i\theta} \tag{30c}$$

Now make

$$|z,\beta\rangle_1 = S(z)D(\beta)\begin{pmatrix}|0\rangle\\0\end{pmatrix} = S(z)|\Psi_1(\beta)\rangle \tag{31}$$

from (30b), here is

$$|z,\beta\rangle_1 = |a,z\rangle_1 \tag{32}$$

Next another squeezing state of "superspace" will be discussed. Let

$$|z,\beta_2\rangle = S(z)|\Psi_2(\beta)\rangle \tag{33}$$

Using (17), here is

$$\begin{aligned}\langle X(\varphi)\rangle_2 &= \frac{1}{2}\langle\Psi_2(\beta)|[\text{ch}re^{i\varphi}+\text{sh}re^{-i(\varphi+\theta)}]A+[\text{ch}re^{-i\varphi}+\text{sh}re^{i(\varphi+\theta)}]A^+|\Psi_2(\beta)\rangle\\ &= \text{ch}r\,Re(\beta e^{i\varphi})+\text{sh}r\,Re[\beta e^{-i(\varphi+\theta)}]\end{aligned} \tag{34}$$

$$\begin{aligned}\langle X^2(\varphi)\rangle_2 &= \frac{1}{4}\langle A^2e^{2i\varphi}+2A^+A+A^{+2}e^{-2i\varphi}\rangle_2+\frac{1}{4}\\ &= [\text{ch}r\,Re(\beta e^{i\varphi})+\text{sh}r\,Re(\beta e^{-i(\varphi+\theta)})]^2+\frac{1}{4}[\text{ch}^2r+\text{sh}^2r+\text{sh}2r\cos(2\varphi+\theta)]\end{aligned} \tag{35}$$

So,

$$\begin{aligned}\langle\Delta X^2(\varphi)\rangle_2 &= \langle X^2(\varphi)\rangle_2-\langle X(\varphi)\rangle_2^2\\ &= \frac{1}{4}[\text{ch}^2r+\text{sh}^2r+\text{sh}2r\cos(2\varphi+\theta)]\\ &= \frac{1}{4}|\text{ch}r+\text{sh}re^{i(2\varphi+\theta)}|^2\end{aligned} \tag{36}$$

It is clear that $|z,\beta\rangle_2$ and $|z,\beta\rangle_1 = |\alpha,z\rangle_1$ have the same squeezing character, and both are the squeezing supercoherent states.

The eigenstate and of A can be generally written as

$$|\Psi(a)\rangle = C_1|\Psi_1(a)\rangle + C_2|\Psi_2(a)\rangle \tag{37a}$$

$$|C_1|^2 + |C_2|^2 = 1 \tag{37b}$$

To make

$$|z,\beta\rangle = S(z)|\Psi(\beta)\rangle \tag{38}$$

Similarly, $|z,\beta\rangle$ is the squeezing supercoherent state. It includes $|z,\beta\rangle_1$ and $|z,\beta\rangle_1$.

Since

$$S(z)AS^{+}(z)S(z)|\Psi(\beta)\rangle = \beta S(z)|\Psi(\beta)\rangle|$$

that is, $|z,\beta\rangle$ is the eigenstate of the unitary transformation operator $S^{+}(z)AS(z)$ of A. The unitary transformation does not change the eigenvalue of operator. It is still β.

$$S(z)AS^{+}(z)|z,\beta\rangle = \beta|z,\beta\rangle \tag{39}$$

The eigenstate of equation (39) is double degenerate, with the same characher.

4 The Squeezing Characher of The Eigenstate of A^2

As an example, the squeezing character of the eigenstate of A^2 will be discussed. The orthonormalization eigenstates (quartet degenerate state) of A^2 can be obtained easily. They are

$$|\Phi_1(a)\rangle = \begin{pmatrix} |a\rangle_e \\ 0 \end{pmatrix} = |a\rangle_{ee} \tag{40a}$$

$$\Phi_2(a)\rangle = (cth|a|^2)^{\frac{1}{2}}\begin{pmatrix} 0 \\ \dfrac{a}{\sqrt{aa^{+}}}|a\rangle_e \end{pmatrix} = |a\rangle_{0e} \tag{40b}$$

$$|\Phi_3(a)\rangle = \begin{pmatrix} |a\rangle_0 \\ 0 \end{pmatrix} = |a\rangle_{e0} \tag{40c}$$

$$\Phi_4(a)\rangle = (th|a|^2)^{\frac{1}{2}}\begin{pmatrix} 0 \\ \dfrac{a}{\sqrt{aa^{+}}}|a\rangle_0 \end{pmatrix} = |a\rangle_{00} \tag{40d}$$

$$\langle\Phi_i(a)|\Phi_j(a)\rangle = \delta_{ij} \tag{41}$$

$$A^2|\Phi_i(a)\rangle = a^2|\Phi_i(a)\rangle, \quad (i = 1,2,3,4) \tag{42}$$

The eigenstate of A^2 has the character that can be converted by A acting on.

$$\begin{aligned} A|\Phi_1(a)\rangle &= a(th|a|^2)^{\frac{1}{2}}|\Phi_2(a)\rangle \\ A|\Phi_2(a)\rangle &= a(cth|a|^2)^{\frac{1}{2}}|\Phi_1(a)\rangle \\ A|\Phi_3(a)\rangle &= a(cth|a|^2)^{\frac{1}{2}}|\Phi_4(a)\rangle \\ A|\Phi_4(a)\rangle &= a(th|a|^2)^{\frac{1}{2}}|\Phi_3(a)\rangle \end{aligned} \tag{43}$$

According to (41), (42) and (43), the following can be got easily,

$$\langle X(\varphi)\rangle_{ee} = \langle X(\varphi)\rangle_{0e} = \langle X(\varphi)\rangle_{e0} = \langle X(\varphi)\rangle_{00} = 0 \tag{44}$$

thereby

$$\begin{aligned} \langle\Delta X^2(\varphi)\rangle_{ee} &= \langle X^2(\varphi)\rangle_{ee} \\ &= \frac{1}{2}|a|^2[\cos 2(\varphi+\xi) + th|a|^2] + \frac{1}{4} \end{aligned} \tag{45a}$$

$$\begin{aligned} \langle\Delta X^2(\varphi)\rangle_{0e} &= \langle X^2(\varphi)\rangle_{0e} \\ &= \frac{1}{2}|a|^2[\cos 2(\varphi+\xi) + cth|a|^2] + \frac{1}{4} \end{aligned} \tag{45b}$$

$$\begin{aligned} \langle\Delta X^2(\varphi)\rangle_{e0} &= \langle X^2(\varphi)\rangle_{e0} \\ &= \frac{1}{2}|a|^2[\cos 2(\varphi+\xi) + cth|a|^2] + \frac{1}{4} \end{aligned} \tag{45c}$$

$$\begin{aligned} \langle\Delta X^2(\varphi)\rangle_{00} &= \langle X^2(\varphi)\rangle_{00} \\ &= \frac{1}{2}|a|^2[\cos 2(\varphi+\xi) + th|a|^2] + \frac{1}{4} \end{aligned} \tag{45d}$$

Because the minimum value of $\mathrm{cth}|a|^2$ is 1, the squeeze can not exist in $|\Phi_2(a)\rangle$ and $|\Phi_3(a)\rangle$. But the maximum of the $|a|^2$ is 1 and not negative, so if the value of φ can be chosen properly, it can make

$$\cos 2(\varphi+\xi) < -th|a|^2 \tag{46}$$

thus,

$$\langle\Delta X^2(\varphi)\rangle_{ee} = \langle\Delta X^2(\varphi)\rangle_{00} < \frac{1}{4} \tag{47}$$

That is to say, $|\Phi_1(a)\rangle$ and $|\Phi_4(a)\rangle$ both have the squeeze. But

$$\langle\Delta X^2(\varphi)\rangle_{ee}\langle\Delta X^2(\varphi+\frac{\pi}{2})\rangle_{ee} = \langle\Delta X^2(\varphi)\rangle_{00}\langle\Delta X^2(\varphi+\frac{\pi}{2})\rangle_{00} > \frac{1}{16}, \quad (|a|^2 \neq 0) \tag{48}$$

so $|\Phi_3(\alpha)\rangle$ and $|\Phi_4(\alpha)\rangle$ are the generalized squeezing states.

5 Conclusion

As far as $[A, H]=\omega A$, the common expression of the annihilation operator of the supersymmetry harmonic oscillator is

$$A=\begin{pmatrix} \delta a & r \\ \lambda a^{+} & \rho a \end{pmatrix} \tag{49}$$

in it, δ, r, λ and ρ can be either figure C, or the operator function of $a^{+}a$. If A can still satisfy the commutation relation $[A, A^{+}]=I$, then the eigenstate of A can be produced by the displacement operator of "superspace" acting on the two minimum energy state of H.

The annihilation operator of the supersymmetry harmonic oscillator, being discussed in this paper, has the special significance. Besides it satisfies the commutation relation $[A, H]=\omega A$ and $[A, A^{+}]=I$, there is $H=\omega A^{+}A$ also, which is like the general annihilation operator a. So the study in this paper is very resemble in forms to the similar discussion about the ordianry space. But on the other hand, it can make our study in this paper have many particularities because of the double degeneracies of H, A and $S(z)AS^{+}(z)$.

Reference

1. D. Stoler, Phys. Rev., D1, 3217(1970).
2. H. P. Yuen, Phys. Rev., A13, 2226(1976).
3. P. Salomonson, et al., Nucl. Phys., B196, 509(1982).
4. C. Aragone and F. Zypman, L. Phys., A. 19, 2267(1986).
5. V. A. Kostelecky and M. M. Nieto, Phys. Rev. Lett., 53, 2285(1984).
6. Chen Chengming and Xu Donghui, ACTA PHYSICS SINICA 41, 529(1992).
7. S. Chatwvedi, M. S. Sriram and V. Srinivasan, J. Phys. A, 20, L1071(1987).
8. M. Hillery, Phys. Rev. A, 36, 3786(1987).
9. Xia Yunjie and Guo Guang chan, Chinese Journal of Quantum Electronics, 5, 301(1988).

NEXT
DOCUMENT

The Total Gaussian Class of Quasiprobabilities and its Relation to Squeezed-state Excitations

Alfred Wünsche
Arbeitsgruppe "Nichtklassische Strahlung" der Max-Planck-Gesellschaft
Rudower Chaussee 5, 12489 Berlin, Germany

Abstract

The class of quasiprobabilities obtainable from the Wigner quasiprobability by convolutions with the general class of Gaussian functions is investigated. It can be described by a three-dimensional, in general, complex vector parameter with the property of additivity when composing convolutions. The diagonal representation of this class of quasiprobabilities is connected with a generalization of the displaced Fock states in direction of squeezing. The subclass with real vector parameter is considered more in detail. It is related to the most important kinds of boson operator ordering. The properties of a specific set of discrete excitations of squeezed coherent states are given.

1 Introduction

The representation of density operators by quasiprobabilities forms one of the bridges between classical and quantum mechanics. Whereas the classical distribution function is uniquely defined and gives the probability density to find the system at the corresponding point of the phase space, a quantum-mechanical distribution function over the phase space is uniquely defined only in relation to a certain operator ordering and does not possess all properties of a true probability density, for example, positive definiteness or orthonormality of the involved states. The best compromise between classical and quantum mechanics is given by the Wigner quasiprobability $W(\alpha,\alpha^*)$ introduced by Wigner in 1932 [1] and corresponding to symmetrical (Weyl) ordering. However, other quasiprobabilities are in use and sometimes advantageous as the coherent-state quasiprobability $Q(\alpha,\alpha^*)$, the Glauber-Sudarshan quasiprobability $P(\alpha,\alpha^*)$, or the one-parameter class of s-ordered quasiprobabilities ($-1 \leq s \leq +1$) which linearly interpolates between the coherent-state quasiprobability and the Glauber-Sudarshan quasiprobability with the Wigner quasiprobability in its center [2, 3, 4]. The quasiprobabilities are auxiliary functions in analogy to the classical distribution function and are appropriate for the convenient calculation of expectation values of operators being invariant quantities in quantum mechanics. Therefore, each of the quasiprobabilities must carry the complete information of the density operator and a reconstruction of the density operator from the quasiprobability must be possible. We consider here the general three-parameter class of quasiprobabilities obtainable by convolutions of the Wigner quasiprobability with the total class of normalized Gaussian functions of the phase-space variables and call this the total Gaussian class of quasiprobabilities. In particular, it contains the quasiprobabilities related to standard and antistandard ordering of the canonical operators and the linear interpolation between them.

2 The displacement structure of the quasiprobabilities

A strong and important restriction to the form of quasiprobabilities over a phase space with the topology of a plane results from the requirement that displacements of the whole system in the phase plane (Heisenberg-Weyl group) must lead to correspondingly displaced quasiprobabilities in analogy to classical mechanics. If the transition from the density operator ϱ to a normalized quasiprobability $F(\alpha,\alpha^*)$ is written by a transition operator $T(\alpha,\alpha^*)$ as follows

$$F(\alpha,\alpha^*) = \langle \varrho T(\alpha,\alpha^*)\rangle, \quad \int \frac{i}{2} d\alpha \wedge d\alpha^* \, F(\alpha,\alpha^*) = 1,$$
$$\frac{i}{2} d\alpha \wedge d\alpha^* = d\,\mathrm{Re}(\alpha) \wedge d\,\mathrm{Im}(\alpha), \quad \langle \ldots \rangle \equiv \mathrm{Trace}(\ldots), \tag{1}$$

then the requirement regarding displacements implies the following "displacement structure" of the transition operators

$$\begin{aligned} T(\alpha,\alpha^*) &= D(\alpha,\alpha^*) T(0,0) (D(\alpha,\alpha^*))^\dagger, \\ \int \frac{i}{2} d\alpha \wedge d\alpha^* \, T(\alpha,\alpha^*) &= I, \quad \langle T(\alpha,\alpha^*)\rangle = \langle T(0,0)\rangle = \frac{1}{\pi}, \end{aligned} \tag{2}$$

where the displacement operator $D(\alpha,\alpha^*)$ is defined by

$$D(\alpha,\alpha^*) \equiv \exp(\alpha a^\dagger - \alpha^* a), \quad [a, a^\dagger] = I, \tag{3}$$

with a and $a^\dagger$ as the boson annihilation and creation operator and with I as the unity operator. This means that the transition operators $T(\alpha,\alpha^*)$ provide a phase-space decomposition of the unity operator. The given trace of the transition operators is a consequence of the following identity which can be proved for arbitrary operators A [5, 6]

$$\int \frac{i}{2} d\alpha \wedge d\alpha^* \, D(\alpha,\alpha^*) A (D(\alpha,\alpha^*))^\dagger = \pi \langle A \rangle I. \tag{4}$$

The reconstruction of the density operator ϱ from the quasiprobability $F(\alpha,\alpha^*)$ can be made by an operator $\overline{T}(\alpha,\alpha^*)$ in the following way

$$\varrho = \pi \int \frac{i}{2} d\alpha \wedge d\alpha^* \, F(\alpha,\alpha^*) \overline{T}(\alpha,\alpha^*), \tag{5}$$

under the condition

$$\langle \overline{T}(\alpha,\alpha^*) T(\beta,\beta^*) \rangle = \frac{1}{\pi} \delta(\alpha-\beta, \alpha^*-\beta^*). \tag{6}$$

It can be proved that the operator $\overline{T}(\alpha,\alpha^*)$ possesses the same "displacement structure" as the operator $T(\alpha,\alpha^*)$ with all its consequences (phase-space decomposition of the unity operator, trace equal to $1/\pi$, see [6]).

3 The three-parameter Gaussian class of quasiprobabilities

The discussed restrictions from the displacement structure of the quasiprobabilities admit still a rich variety of possible quasiprobabilities. We consider here the three-parameter class of quasiprobabilities $F_{\boldsymbol{r}}(\alpha,\alpha^*)$ with the vector parameter $\boldsymbol{r} \equiv (r_1,r_2,r_3)$ which can be obtained from the Wigner quasiprobability $W(\alpha,\alpha^*) \equiv F_{\boldsymbol{0}}(\alpha,\alpha^*)$, $(\boldsymbol{0} \equiv (0,0,0))$, by the following convolutions

$$\begin{aligned} F_{(r_1,r_2,r_3)}(\alpha,\alpha^*) &= g_{(r_1,r_2,r_3)}(\alpha,\alpha^*) * W(\alpha,\alpha^*) \\ &= \tilde{g}_{(r_1,r_2,r_3)}\left(\frac{2}{i}\frac{\partial}{\partial\alpha^*},\frac{2}{i}\frac{\partial}{\partial\alpha}\right)W(\alpha,\alpha^*), \end{aligned} \tag{7}$$

with the normalized Gaussian functions g or their Fourier transforms $\tilde{g}$

$$\begin{aligned} g_{(r_1,r_2,r_3)}(\alpha,\alpha^*) &\equiv \frac{2}{\sqrt{\boldsymbol{r}^2}\pi}\exp\left\{-\frac{1}{\boldsymbol{r}^2}\left(r_1(\alpha^2-\alpha^{*2})+ir_2(\alpha^2+\alpha^{*2})+r_3 2\alpha\alpha^*\right)\right\}, \\ \tilde{g}_{(r_1,r_2,r_3)}\left(\frac{2}{i}\frac{\partial}{\partial\alpha^*},\frac{2}{i}\frac{\partial}{\partial\alpha}\right) &\equiv \exp\left\{\frac{1}{4}\left(r_1\left(\frac{\partial^2}{\partial\alpha^2}-\frac{\partial^2}{\partial\alpha^{*2}}\right)-ir_2\left(\frac{\partial^2}{\partial\alpha^2}+\frac{\partial^2}{\partial\alpha^{*2}}\right)+r_3 2\frac{\partial^2}{\partial\alpha\partial\alpha*}\right)\right\}, \\ \boldsymbol{r}^2 &\equiv r_1^2+r_2^2+r_3^2. \end{aligned} \tag{8}$$

This total Gaussian class of quasiprobabilities with, in general, complex vector parameters $\boldsymbol{r} \equiv (r_1,r_2,r_3)$ contains the class of s-ordered quasiprobabilities as the special case $F_{(0,0,\,s)}(\alpha,\alpha^*)$ with real $r_3 = -s$. The subclass $F_{(r_1,0,0)}(\alpha,\alpha^*)$ with real r_1 and $-1 \le r_1 \le +1$ is related to the linear interpolation between standard and antistandard ordering of powers of the canonical operators Q and P that is considered more in detail in [6]. The connection between two arbitrary quasiprobabilities with the vector parameters $\boldsymbol{r}$ and $\boldsymbol{s}$ is given by

$$F_{\boldsymbol{r}}(\alpha,\alpha^*) = g_{\boldsymbol{r}-\boldsymbol{s}}(\alpha,\alpha^*)F_{\boldsymbol{s}}(\alpha,\alpha^*), \tag{9}$$

and the reconstruction of the density operator ϱ by

$$\varrho = \pi\int\frac{i}{2}d\alpha\wedge d\alpha^*\,F_{\boldsymbol{r}}(\alpha,\alpha^*)T_{-\boldsymbol{r}}(\alpha,\alpha^*). \tag{10}$$

A interesting subclass of the total Gaussian class of quasiprobabilities is given by the restriction to real vector parameters $\boldsymbol{r} \equiv (r_1,r_2,r_3))$ and $|\boldsymbol{r}^2| \le 1$. The "diagonal representation" of this subclass leads to a generalization of the displaced Fock states in direction of a kind of displaced squeezed Fock states as we now will show.

4 Diagonal representation of the Gaussian class of quasiprobabilities with real vector parameters

From the Fock-state representation of the operator $T(0,0)$ in Eq.(2) in connection with Eq.(1) one obtains the following, in general, nondiagonal representation of the quasiprobabilities in displaced

Fock states $|\alpha, n\rangle$

$$F(\alpha,\alpha^*) = \sum_{m=0}^{\infty}\sum_{n=0}^{\infty}\langle m|T(0,0)|n\rangle\langle\alpha,n|\varrho|\alpha,m\rangle, \quad \sum_{n=0}^{\infty}\langle n|T(0,0)|n\rangle = \frac{1}{\pi},$$

$$|\alpha,n\rangle \equiv D(\alpha,\alpha^*)|n\rangle = \frac{1}{\sqrt{n!}}(a^\dagger - \alpha^* I)^n|\alpha\rangle. \tag{11}$$

The s-ordered class of quasiprobabilities is diagonal in the representation by the displaced Fock states according to ($s = -r_3$)

$$F_{(0,0,r_3)}(\alpha,\alpha^*) = \frac{2}{(1+r_3)\pi}\sum_{n=0}^{\infty}\left(-\frac{1-r_3}{1+r_3}\right)^n\langle\alpha,n|\varrho|\alpha,n\rangle. \tag{12}$$

The more general Gaussian class of quasiprobabilities with real vector parameters $\boldsymbol{r} \equiv (r_1, r_2, r_3)$ can be diagonalized in the following way (proof is given in [6])

$$F_{(r_1,r_2,r_3)}(\alpha,\alpha^*) = \frac{2}{(1+r)}\sum_{n=0}^{\infty}\left(-\frac{1-r}{1+r}\right)^n\left\langle\alpha,n;\frac{r_1-ir_2}{r+r_3}\right|\varrho\left|\alpha,n;-\frac{r_1-ir_2}{r+r_3}\right\rangle,$$

$$r \equiv \sqrt{r_1^2+r_2^2+r_3^2}, \quad 0 \le \frac{r_3}{r} \le 1, \tag{13}$$

where we have introduced a set of discrete excitations of squeezed coherent states $|\alpha, n; \zeta\rangle$ with a complex squeezing parameter ζ in the nonunitary approach as follows

$$|\alpha,n;\zeta\rangle \equiv D(\alpha,\alpha^*)\frac{1}{\sqrt{n!}}\left(\frac{a^\dagger - \zeta^* a}{\sqrt{1+\zeta\zeta^*}}\right)^n|0,0;\zeta\rangle,$$

$$|0,0;\zeta\rangle \equiv (1+\zeta\zeta^*)^{\frac{1}{4}}\exp\left(-\frac{\zeta}{2}a^{\dagger 2}\right)|0\rangle = (1+\zeta\zeta^*)^{\frac{1}{4}}\sum_{m=0}^{\infty}\frac{(-1)^m\sqrt{(2m)!}}{2^m m!}\zeta^m|2m\rangle. \tag{14}$$

The states $|\alpha, m; -\zeta\rangle$ and $|\alpha, n; \zeta\rangle$ with opposite squeezing parameters ζ are mutually orthonormalized and satisfy a completeness relation in the following way

$$\langle\alpha,m;-\zeta|\alpha,n;\zeta\rangle = \delta_{m,n}, \quad \sum_{n=0}^{\infty}|\alpha,n;\zeta\rangle\langle\alpha,n;-\zeta| = I. \tag{15}$$

In case of vanishing squeezing parameter $\zeta = 0$ the states $|\alpha, n; \zeta\rangle$ become identical with the displaced Fock states $|\alpha, n\rangle$

$$|\alpha,n;0\rangle \equiv D(\alpha,\alpha^*)|n\rangle \equiv |\alpha,n\rangle. \tag{16}$$

Consider now the limiting case of maximal squeezing $|\zeta| = 1$ within the states $|\alpha, n; \zeta\rangle$. If one makes the transition to real variables q and p and to the canonical Hermitean operators Q and P according to

$$\alpha = \frac{q+ip}{\sqrt{2\hbar}}, \quad \alpha^* = \frac{q-ip}{\sqrt{2\hbar}}, \quad a = \frac{Q+iP}{\sqrt{2\hbar}}, \quad a^\dagger = \frac{Q-iP}{\sqrt{2\hbar}}, \tag{17}$$

then, in particular, one obtains

$$\begin{aligned}
\left|\frac{q+ip}{\sqrt{2\hbar}}, n; 1\right\rangle &= D(q,p)\frac{(2\hbar\pi)^{\frac{1}{4}}}{\sqrt{n!}}\left(\frac{P}{i\sqrt{\hbar}}\right)^n |q=0\rangle \\
&= \exp\left(i\frac{pq}{2\hbar}\right)\frac{(2\hbar\pi)^{\frac{1}{4}}}{(i\sqrt{\hbar})^n\sqrt{n!}}(P-pI)^n|q\rangle, \\
\left|\frac{q+ip}{\sqrt{2\hbar}}, n; -1\right\rangle &= D(q,p)\frac{(2\hbar\pi)^{\frac{1}{4}}}{\sqrt{n!}}\left(\frac{Q}{\sqrt{\hbar}}\right)^n |p=0\rangle \\
&= \exp\left(-i\frac{pq}{2\hbar}\right)\frac{(2\hbar\pi)^{\frac{1}{4}}}{(\sqrt{\hbar})^n\sqrt{n!}}(Q-qI)^n|p\rangle, \qquad (18)
\end{aligned}$$

where $D(q,p)$ denotes the displacement operator in the representation by the real variables q and p and $|q\rangle$ and $|p\rangle$ are the eigenstates of the operators Q and P, respectively, normalized in the usual way by means of the delta functions with the scalar product $\sqrt{2\hbar\pi}\langle q|p\rangle = \exp\left((ipq)/\hbar\right)$. The states in Eq.(18) represent discrete sets of excitations of the states $|q\rangle$ and $|p\rangle$ in analogy to the displaced Fock states $|\alpha, n\rangle$ as discrete sets of excitations of the coherent states $|\alpha\rangle$.

The states $|\alpha, n; \zeta\rangle$ with $|\zeta| > 1$ are well defined by Eq.(14) but they are not normalizable in the usual sense or by means of the delta function. They are states of certain rigged Hilbert spaces since their scalar products with itself does not exit but it exists the scalar product with states from spaces of sufficiently well-behaved normalizable states that can be used for auxiliary purposes, for example, for the formulation of completeness relations on contours of the complex variable α. In this connection we introduce the following terminology of normalizability of states:

1. normalizable (scalar product of the state with itself exists meaning that they are states of the usual Hilbert space; case $|\zeta| < 1$ in Eq.(14)),

2. weakly nonnormalizable (states can be considered as limiting cases of normalizable states or states of a certain rigged Hilbert space and can often be normalized with "neighbouring" states by means of the delta function; case $|\zeta| = 1$ in Eq.(14)),

3. strongly nonnormalizable (states cannot be considered as limiting cases of normalizable states but they are states of more general rigged Hilbert spaces or spaces of linear functionals; case $|\zeta| > 1$ in Eq.(14)).

If one admits strongly nonnormalizable states in Eq.(13) in a formal way, then one may omit the restriction to nonnegative values of r_3/r. In the case $r_3 = 0$ one has to do with weakly nonnormalizable states corresponding to $|\zeta| = 1$ and both possible signs of the square root in $r = \sqrt{r_1^2 + r_2^2}$ are admissible leading to two possible representations of equal rank.

5 The sphere of the Gaussian class of quasiprobabilities with real vector parameters

As the main class of quasiprobabilities, the Gaussian subclass of quasiprobabilities with real vector parameter $\mathbf{r} \equiv (r_1, r_2, r_3)$ and with $\mathbf{r}^2 \leq 1$ forms the interior plus surface of a three-dimensional

sphere with the Wigner quasiprobability $W(\alpha,\alpha^*)$ in its center, the coherent-state quasiprobability $Q(\alpha,\alpha^*)$ in the North pole, the Glauber-Sudarshan quasiprobability $P(\alpha,\alpha^*)$ in the South pole and the quasiprobabilities $F_{(\cos 2\varphi,\sin 2\varphi,0)}(\alpha,\alpha^*)$ corresponding to standard or antistandard ordering of the rotated canonical operators Q and P about an angle φ around the Equator (see fig.1 in [6]). Whereas at the surface of this sphere the quasiprobabilities are representable as the expectation values of transition operators of the dyadic form $1/\pi|\alpha,0;\zeta\rangle\langle\alpha,0;-\zeta|$ with squeezing parameters $\pm\zeta$ fixed for each diagonal through the center of the sphere (if we admit strongly nonnormalizable states; in the other case this is only true for the upper hemisphere), in the interior one has mixed states of $|\alpha,n;\zeta\rangle\langle\alpha,n;-\zeta|$, $(n=0,\ldots,\infty)$ as transition operators. This is in a certain analogy to the Poincaré sphere of pure and mixed polarization states where the pure polarization states are situated on the surface of this sphere (right-handed and left-handed circular polarization at the North and South pole and the different linear polarizations around the Equator in dependence on the direction of linear polarization, elliptical polarizations on general surface points) and the mixed polarizations in the interior of the sphere with the fully unpolarized state in the center.

6 Some representations of the states $|\beta,n;\zeta\rangle$

It is interesting to consider the properties of the states $|\beta,n;\zeta\rangle$ itself by the calculation of different representations and quasiprobabilities. These states comprise the squeezed coherent states as the special case $|\beta,0;\zeta\rangle$. We introduced these states in Eq.(14) in a nonnormalized form. First, a normalization factor can be calculated from the following scalar product (see [6])

$$\begin{aligned}\langle\beta,n;\zeta|\beta,n;\zeta\rangle &= \langle 0,n;\zeta|0,n;\zeta\rangle \\ &= \left(\frac{1+\zeta\zeta^*}{1-\zeta\zeta^*}\right)^{n+\frac{1}{2}}\sum_{k=0}^{[\frac{n}{2}]}\frac{n!}{k!^2(n-2k)!}\left(\frac{\sqrt{\zeta\zeta^*}}{1+\zeta\zeta^*}\right)^{2k}. \end{aligned} \tag{19}$$

The polynomials at the right-hand side of Eq.(19) do not belong, at least, to well-known polynomials with a fixed abbreviation.

Next, we calculate the Bargmann representation of the nonnormalized states $|\beta,n;\zeta\rangle$ with the following result of an analytic function of α^*

$$\begin{aligned} f(\alpha^*) &\equiv \langle 0|\exp(\alpha^* a)|\beta,n;\zeta\rangle \\ &= \frac{(1+\zeta\zeta^*)^{\frac{1}{4}}}{\sqrt{n!}}\left(\sqrt{\frac{\zeta^*}{2}}\right)^n H_n\left(\sqrt{\frac{1+\zeta\zeta^*}{2\zeta^*}}(\alpha^*-\beta^*)\right)\exp\left\{-\frac{\zeta}{2}(\alpha^*-\beta^*)^2+\alpha^*\beta-\frac{1}{2}\beta\beta^*\right\}. \end{aligned} \tag{20}$$

where $H_n(z)$ denotes the Hermite polynomials in the usual way. For the "position"representation one obtains

$$\begin{aligned} &\langle q|\beta,n;\zeta\rangle \\ &= \frac{1}{\sqrt{2^n n!}}\left(\sqrt{\frac{1+\zeta^*}{1-\zeta}}\right)^n H_n\left(\sqrt{\frac{1+\zeta\zeta^*}{(1-\zeta)(1+\zeta^*)\hbar}}\left(q-\sqrt{\frac{\hbar}{2}}(\beta+\beta^*)\right)\right) \end{aligned}$$

$$\left(\frac{1+\zeta\zeta^*}{\pi\hbar}\right)^{\frac{1}{4}}\frac{1}{\sqrt{1-\zeta}}\exp\left\{-\frac{1+\zeta}{1-\zeta}\frac{1}{2\hbar}\left(q-\sqrt{\frac{\hbar}{2}}(\beta+\beta^*)\right)^2+\frac{(\beta-\beta^*)q}{\sqrt{2\hbar}}-\frac{\beta^2-\beta^{*2}}{4}\right\}. \tag{21}$$

and for the "momentum" representation

$$\begin{aligned}&\langle p|\beta,n;\zeta\rangle\\ =\;&\frac{(-i)^n}{\sqrt{2^n n!}}\left(\sqrt{\frac{1-\zeta^*}{1+\zeta}}\right)^n H_n\left(\sqrt{\frac{1+\zeta\zeta^*}{(1+\zeta)(1-\zeta^*)\hbar}}\left(p+i\sqrt{\frac{\hbar}{2}}(\beta-\beta^*)\right)\right)\\ &\left(\frac{1+\zeta\zeta^*}{\pi\hbar}\right)^{\frac{1}{4}}\frac{1}{\sqrt{1+\zeta}}\exp\left\{-\frac{1-\zeta}{1+\zeta}\frac{1}{2\hbar}\left(p+i\sqrt{\frac{\hbar}{2}}(\beta-\beta^*)\right)^2-i\frac{p(\beta+\beta^*)}{\sqrt{2\hbar}}+\frac{\beta^2-\beta^{*2}}{4}\right\}.\end{aligned} \tag{22}$$

From Eqs.(20) and (19) one finds the coherent-state quasiprobability $Q(\alpha,\alpha^*)$ for the normalized states $|\beta,n;\zeta\rangle_{norm}$. We give it only for the states $|0,n;\zeta\rangle_{norm}$ because the transition to the states $|\beta,n;\zeta\rangle_{norm}$ can be simply made by the substitutions $\alpha\to\alpha-\beta$ and $\alpha^*\to\alpha^*-\beta^*$. The result for $|0,n;\zeta\rangle_{norm}$ is

$$\begin{aligned}Q(\alpha,\alpha^*)\;\equiv\;&\frac{1}{\pi}\frac{\langle\alpha|0,n;\zeta\rangle\langle 0,n;\zeta|\alpha\rangle}{\langle 0,n;\zeta|0,n;\zeta\rangle}\\ =\;&\frac{\frac{1}{n!}\left(\frac{\sqrt{\zeta\zeta^*}}{2}\frac{1-\zeta\zeta^*}{1+\zeta\zeta^*}\right)^n}{\sum_{k=0}^{[\frac{n}{2}]}\frac{n!}{k!^2(n-2k)!}\left(\frac{\sqrt{\zeta\zeta^*}}{1+\zeta\zeta^*}\right)^{2k}}H_n\left(\sqrt{\frac{1+\zeta\zeta^*}{2\zeta}}\alpha\right)H_n\left(\sqrt{\frac{1+\zeta\zeta^*}{2\zeta^*}}\alpha^*\right)\\ &\frac{\sqrt{1-\zeta\zeta^*}}{\pi}\exp\left\{-\left(\alpha\alpha^*+\frac{\zeta^*}{2}\alpha^2+\frac{\zeta}{2}\alpha^{*2}\right)\right\}.\end{aligned} \tag{23}$$

By convolution of $Q(\alpha,\alpha^*)$ with $2/\pi\exp(2\alpha\alpha^*)$ one obtains from Eq.(23) the Wigner quasiprobability for the normalized states $|0,n;\zeta\rangle_{norm}$ with the result

$$\begin{aligned}W(\alpha,\alpha^*)\;=\;&\frac{(-1)^n}{\sum_{k=0}^{[\frac{n}{2}]}\frac{n!}{k!^2(n-2k)!}\left(\frac{\sqrt{\zeta\zeta^*}}{1+\zeta\zeta^*}\right)^{2k}}\\ &\sum_{j=0}^{n}\frac{(-1)^j n!}{j!^2(n-j)!}\left(\frac{\sqrt{\zeta\zeta^*}}{1+\zeta\zeta^*}\right)^j H_j\left(\sqrt{\frac{1+\zeta\zeta^*}{1-\zeta\zeta^*}}\frac{\alpha+\zeta\alpha^*}{\sqrt{\zeta}}\right)H_j\left(\sqrt{\frac{1+\zeta\zeta^*}{1-\zeta\zeta^*}}\frac{\alpha^*+\zeta^*\alpha}{\sqrt{\zeta^*}}\right)\\ &\frac{2}{\pi}\exp\left\{-\frac{2(\alpha+\zeta\alpha^*)(\alpha^*+\zeta^*\alpha)}{1-\zeta\zeta^*}\right\}.\end{aligned} \tag{24}$$

The transition from $|0,n;\zeta\rangle_{norm}$ to $|\beta,n;\zeta\rangle_{norm}$ can be made again in Eq.(24) by the simple substitutions $\alpha\to\alpha-\beta$ and $\alpha^*\to\alpha^*-\beta^*$. In figs.(1-6) we represent the Wigner quasiprobability in its real representation $W(q,p)$ with the normalization $\int dq\wedge dpW(q,p)=1$ for the first 6 states

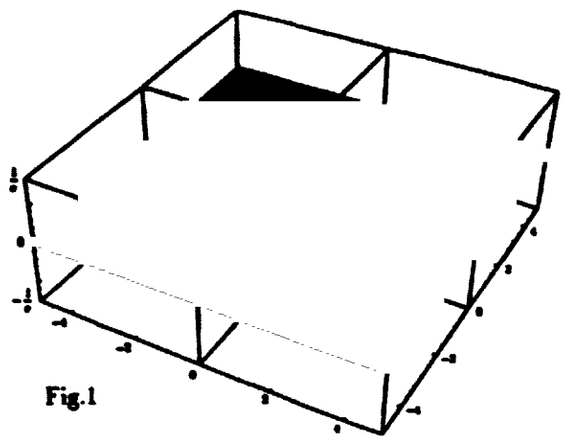

Fig.1

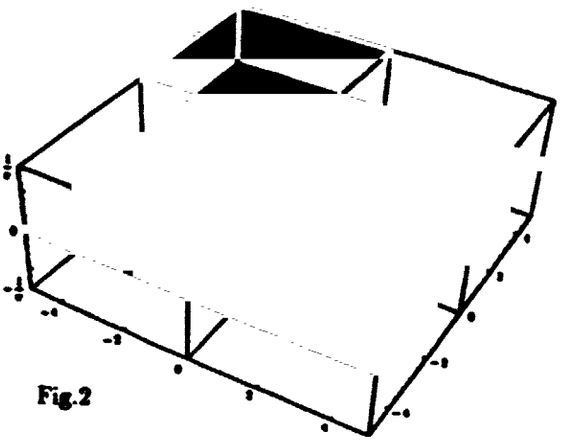

Fig.2

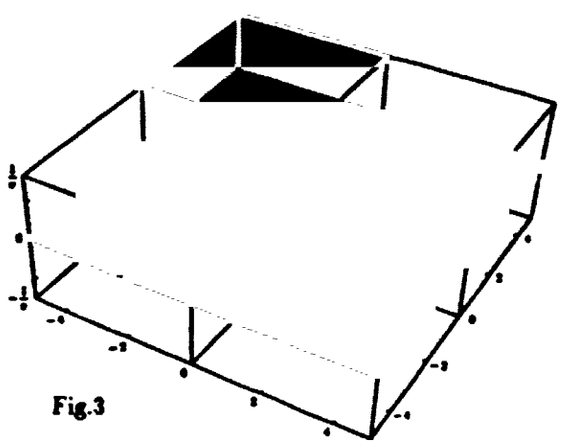

Fig.3

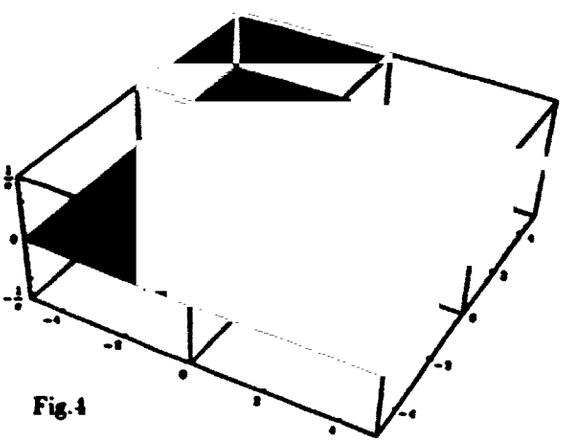

Fig.4

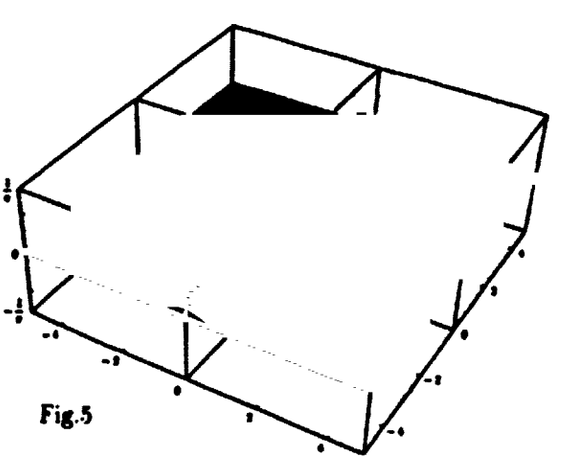

Fig.5

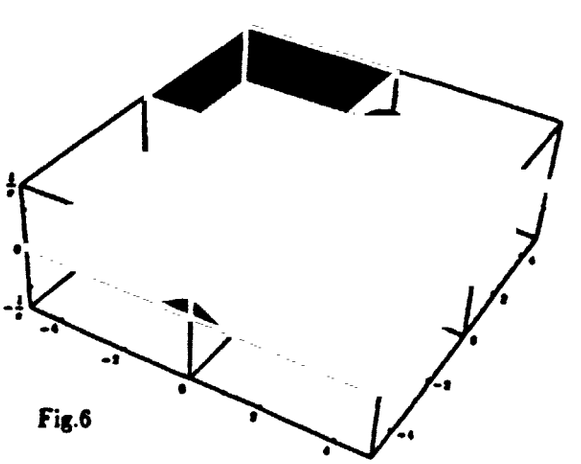

Fig.6

Fig.1-6:

Wigner quasiprobability $W(q,p)$ to states $|0,n;\zeta)_{norm}$ for $n = 0, 1, \ldots, 5$, $\zeta = +0.5$ and $\hbar = 1$.

$|0,n;\zeta)_{norm}$, i.e. for $n = 0, 1, \ldots, 5$, with the squeezing parameter $\zeta = +0.5$ and with $\hbar = 1$. For $\zeta = -0.5$ one obtains the same pictures only rotated about an angle $\pi/2$.

Let us give here additionally the explicit expressions of three partial classes of quasiprobabilities from the total Gaussian class for the normalized squeezed vacuum states $|0,0;\zeta)_{norm}$

$$
\begin{aligned}
F_{(r_1,0,0)}(\alpha,\alpha^*) &= \frac{2}{\pi}\sqrt{\frac{1-\zeta\zeta^*}{(1+r_1^2)(1-\zeta\zeta^*)-2r_1(\zeta-\zeta^*)}} \\
&\quad \exp\left\{-\frac{2(\alpha+\zeta\alpha^*)(\alpha^*+\zeta^*\alpha)+r_1(1-\zeta\zeta^*)(\alpha^2-\alpha^{*2})}{(1+r_1^2)(1-\zeta\zeta^*)-2r_1(\zeta-\zeta^*)}\right\}, \\
F_{(0,r_2,0)}(\alpha,\alpha^*) &= \frac{2}{\pi}\sqrt{\frac{1-\zeta\zeta^*}{(1+r_2^2)(1-\zeta\zeta^*)-i2r_2(\zeta+\zeta^*)}} \\
&\quad \exp\left\{-\frac{2(\alpha+\zeta\alpha^*)(\alpha^*+\zeta^*\alpha)+ir_2(1-\zeta\zeta^*)(\alpha^2+\alpha^{*2})}{(1+r_2^2)(1-\zeta\zeta^*)-i2r_2(\zeta+\zeta^*)}\right\}, \\
F_{(0,0,r_3)}(\alpha,\alpha^*) &= \frac{2}{\pi}\sqrt{\frac{1-\zeta\zeta^*}{(1+r_3^2)(1-\zeta\zeta^*)+2r_3(1+\zeta\zeta^*)}} \\
&\quad \exp\left\{-\frac{2(\alpha+\zeta\alpha^*)(\alpha^*+\zeta^*\alpha)+2r_3(1-\zeta\zeta^*)\alpha\alpha^*}{(1+r_3^2)(1-\zeta\zeta^*)+2r_3(1+\zeta\zeta^*)}\right\}. \qquad (25)
\end{aligned}
$$

The modulus of the complex squeezing parameter ζ determines the amount of squeezing whereas the phase of the squeezing parameter ζ determines the position of the squeezing axes. In particular, the squeezing axes are parallel to the coordinate axes for real $\zeta = \zeta^*$. In this case the class of quasiprobabilities $F_{(r_1,0,0)}(\alpha,\alpha^*)$ simplifies. The squeezing axes are diagonal to the coordinate axes for imaginary $\zeta = -\zeta^*$ and then the class of quasiprobabilities $F_{(0,r_2,0)}(\alpha,\alpha^*)$ simplifies. The usually considered class of quasiprobabilities $F_{(0,0,r_3)}(\alpha,\alpha^*)$ contains the interesting value of the parameter r_3 for which the denominator in the exponential function vanishes and the quasiprobability becomes a singular function. This point depends on the modulus of the squeezing parameter and is given by

$$
r_3^{sing} = -\frac{1-|\zeta|}{1+|\zeta|}, \quad \left(r_3^{'sing} = -\frac{1+|\zeta|}{1-|\zeta|}\right), \qquad (26)
$$

where the second solution given in brackets seems to be not of interest. For parameters r_3 less or equal this singularity point the corresponding quasiprobabilities can be only considered as generalized functions. Recall that the quasiprobabilities for squeezed coherent states $|\beta,0;\zeta)$ can be obtained again from the quasiprobabilities for $|0,0;\zeta)$ by the mentioned argument displacements.

Last, we found for the number representation of the states $|0,n;\zeta)_{norm}$

$$
\begin{aligned}
|0,n;\zeta)_{norm} &= \frac{\left(\sqrt{1-\zeta\zeta^*}\right)^{n+\frac{1}{2}}}{\sqrt{\sum_{k=0}^{[\frac{n}{2}]}\frac{n!}{k!^2(n-2k)!}\left(\frac{\sqrt{\zeta\zeta^*}}{1+\zeta\zeta^*}\right)^{2k}}}\sum_{j=-[\frac{n}{2}]}^{\infty}\frac{(-1)^j}{2^j}\sqrt{\frac{(n+2j)!}{n!}}\zeta^j \\
&\quad \left(\sum_{l=0}^{[\frac{n}{2}]}\frac{n!}{l!(l+j)!(n-2l)!}\left(\frac{\zeta\zeta^*}{4(1+\zeta\zeta^*)}\right)^l\right)|n+2j). \qquad (27)
\end{aligned}
$$

It contains only even or odd number states in dependence on n as an even or odd number. For large modulus of the squeezing parameter ζ the resulting number distribution becomes relatively broad and uniform over even or odd numbers. The transition from the states $|0,n;\zeta\rangle_{norm}$ to the displaced states $|\beta,n;\zeta\rangle_{norm}$ is here more complicated as in the case of the quasiprobabilities. Generally, if an arbitrary state $|\psi\rangle$ has the number representation

$$|\psi\rangle = \sum_{n=0}^{\infty} c_n |n\rangle, \tag{28}$$

then the displaced state $D(\beta,\beta^*)|\psi\rangle$ has the number representation

$$\begin{aligned} D(\beta,\beta^*)|\psi\rangle &= \exp\Big(-\frac{\beta\beta^*}{2}\Big)\sum_{m=0}^{\infty}\Bigg(\sum_{n=0}^{\infty}\frac{c_n}{\sqrt{m!n!}}\sum_{j=0}^{\{m,n\}}\frac{m!n!}{j!(m-j)!(n-j)!}\beta^{m-j}(-\beta^*)^{n-j}\Bigg)|m\rangle \\ &= \exp\Big(-\frac{\beta\beta^*}{2}\Big)\sum_{m=0}^{\infty}\Bigg(\sum_{n=0}^{\infty}\sqrt{\frac{n!}{m!}}\beta^{m-n}L_n^{m-n}(\beta\beta^*)c_n\Bigg)|m\rangle \\ &= \exp\Big(-\frac{\beta\beta^*}{2}\Big)\sum_{m=0}^{\infty}\Bigg(\sum_{n=0}^{\infty}\sqrt{\frac{m!}{n!}}(-\beta^*)^{n-m}L_m^{n-m}(\beta\beta^*)c_n\Bigg)|m\rangle, \end{aligned} \tag{29}$$

where $L_n^{\nu}(z)$ denotes the Laguerre polynomials in the usual way. This is a kind of discrete convolution of the primary number representation.

7 Conclusion

We investigated the total Gaussian class of quasiprobabilities and its diagonal representation in case of real vector parameters. Another interesting special case is given for real r_3 and imaginary r_1 and r_2. It seems that this case may be treated in analogy to the usual s-parametrized class of quasiprobabilities by transition to new boson operators via a Bogolyubov transformation. Some points and proofs are given more in detail in [6] but some are new in the present paper, in particular, all formulae of section 6 for the states $|\beta,n;\zeta\rangle$ are given here for the first time.

References

[1] R.J. Glauber, Phys. Rev. 131, 2766 (1963).

[2] K.E. Cahill and R.J. Glauber, Phys. Rev. 177, 1857 and 1882 (1969).

[3] G.S. Agarwal and E. Wolf, Phys. Rev. D2, 2161 (1970).

[4] M. Hillary, R.F. O'Connell, M.O. Scully and E.P. Wigner, Physics Report 106, 121 (1984).

[5] R.F. Bishop and A. Vourdas, Phys. Rev. A50, 4488 (1994).

[6] A. Wünsche, submitted to Phys. Rev. A (July 1995); this paper contains a more complete list of references to the subject than given here.

NEXT
DOCUMENT

Q(α) Function and Squeezing Effect

Xia Yunjie Kong Xianghe Yan Kezhu Chen Wanping
Department of Physics, Qufu Normal University, Qufu, shandong, China, 273165

Abstract

The relation of squeezing and Q(α) function is discussed in this paper. By means of Q function, the squeezing of field with gaussian Q(α) function or negative P(α) function is also discussed in detail.

1 Introduction

In quantum optics, P(α), Q(α) and W(α) are coammon quasiprobability distribution function [1], but only Q(α) perserve good function (positive and nonregular). Recently, by means of Fokker–Plank equation for Q function, M. S. Kim et. al discussed the fouth–order squeezing[2]. In this paper, we consider the relation between Q function and squeezing, and study the squeezing of field with gaussian Q function or negative P(α) function.

for any field density operator ρ, the Q function is definded as

$$Q(\alpha) = \frac{1}{\pi}\langle \alpha|\rho|\alpha\rangle \tag{1}$$

it satisfies the normalization condition

$$\int d\alpha^2 Q(\alpha) = 1 \tag{2}$$

For antinormally ordered operator $f(a, a^+) = f^{(a)}(a, a^+)$, one can get following equation

$$\langle f(a, a^+)\rangle = \int d^2\alpha Q(\alpha) f^{(a)}(a, a^*) = 1 \tag{3}$$

where a and a^+ are annihilation and creation operators respeotively Ddfining parameter

$$S = \langle :(a + a^+)^2: \rangle - \langle a + a^+\rangle^2 \tag{4}$$

For squeezing, S should be negative

Now, we suppose that Q function can be expanded as following form

$$Q(\alpha) = \frac{1}{\pi} e^{-\beta|\alpha|^2} \sum C_{m,n} a^m a^{*n}, (C_{m,n} = C^*_{n,m}) \tag{5}$$

Using mathmatical identity [3]

$$\int \frac{d^2\alpha}{\pi} e^{-\beta|\alpha|^2+\rho\alpha+\tau\alpha^*} = \frac{1}{\beta} e^{\rho\tau/\beta}, (\beta > 0) \tag{6}$$

one can have

$$\int \frac{d^2\alpha}{\pi} \alpha^m \alpha^{*n} e^{-\beta|\alpha|^2} = \frac{n!\delta_{mn}}{\beta^{m+1}} \tag{7}$$

and the normalization condition is

$$\sum_m C_{m,m} m!/\beta^{m+1} = 1 \tag{8}$$

By means of equations (3) and (7), we have

$$\langle a + a^+ \rangle = \sum_m \frac{2(m+1)! ReC_{m,m+1}}{\beta^{m+2}} \tag{9}$$

$$\langle a^2 + a^{+2} \rangle = \sum_m \frac{2(m+2)! ReC_{m,m+2}}{\beta^{m+3}} \tag{10}$$

$$\langle a^+ a \rangle = \sum_m \frac{(m+1)-\beta}{\beta^{m+2}} m! C_{m,m} \tag{11}$$

and

$$S = \sum_m \frac{2(m+2)! ReC_{m,m+2}}{\beta^{m+3}} + 2\sum_m \frac{m+1-\beta}{\beta^{m+2}} m! C_{m,m} - [\sum_m \frac{2(m+1)! ReC_{m,m+1}}{\beta^{m+2}}]^2 \tag{12}$$

If the field exists squeezing, then

$$\sum_m [\frac{(m+2)! ReC_{m,m+2}}{\beta^{m+3}} + \frac{(m+1-\beta)m! C_{m,m}}{\beta^{m+2}}] < [\sum_m \frac{2(m+1)! ReC_{m,m+1}}{\beta^{m+2}}]^2 \tag{13}$$

2 Squddzing of field with gaussian Q function

We introduce the gaussian Q function as

$$Q(\alpha) = \sqrt{t^2 - 4|A|^2} exp[-t(\alpha^* - \omega^*)(\alpha - \omega) + A^*(\alpha^* - \omega^*)^2 + A(\alpha - \omega)^2] \tag{14}$$

where $t>2|A|$. Using integration formula[3]

$$\int \frac{d^2z}{\pi} e^{-\mu|z|^2+fz^2+gz^{*2}+rz+\sigma z^*} = \frac{1}{\sqrt{\mu^2-4fg}} e^{\frac{\mu r\sigma+r^2g+\sigma^2 f}{\mu^2-4fg}} \tag{15}$$

and equation (3),one can show

$$\langle a + a^+ \rangle = \omega + \omega^* \tag{16}$$

$$\langle a^2 + a^{+2} \rangle = \omega^{*2} + \omega^2 + \frac{2(A + A^*)}{t^2 - 4|A|^2} \tag{17}$$

$$\langle a^+ a \rangle = |\omega|^2 + \frac{t}{t^2 - 4|A|^2} - 1 \tag{18}$$

and easyly obtain

$$S = \frac{2(A + A^* + 4|A|^2 + t - t^2)}{t^2 - 4|A|^2} \tag{19}$$

Thus the condition for the existence of squeezing is

$$A + A^* + 4|A|^2 < t^2 - t \tag{20}$$

If $A=0$,squeezing means $t>1$,if $t<1$ and $A=0$,no squeezing exists in the field. It is worth to point out that the field with $A=0$and $t>1$ has not been found uptill now.

3 Squeezing of field with negative P(α) function

The relation of $P(\alpha)$ and $Q(\alpha)$ is

$$Q(\alpha) = \int \frac{d^2\beta}{\pi} e^{-|\beta-\alpha|^2} P(\beta) \tag{21}$$

for nonclassical field,its $P(\alpha)$ function has two situations [4]: i) $P(\alpha)$ is negative, ii) $P(\alpha)$ is more singular than δ - function. We consider the nonclassical field with negative $P(\alpha)$ function[5]

$$\rho = \int d^2\alpha P(\alpha) |\alpha\rangle\langle\alpha| \tag{22}$$

Suppose $P(\alpha)$ as

$$P(\alpha) = \frac{1}{\pi} e^{-t|\alpha|^2} \sum_{i,j} P_{i,j} \alpha^i \alpha^{*j} \tag{23}$$

Using equations (6)and (21),we obtain

$$Q(\alpha)=\frac{1}{\pi}\sum_{i,j}P_{i,j}e^{\frac{-t}{1+t}|\alpha|^2}\sum_{l=0}^{\min(i,j)}\frac{i!j!\alpha^{i-l}\alpha^{*j-l}}{l!(i-l)!(j-l)!(l+t)^{i+j-l+1}} \tag{24}$$

comparing with equation(5),one can have

$$\beta=\frac{t}{1+t} \tag{25}$$

$$C_{m,n}=\sum_{l}P_{m+l,n+l}\frac{(m+l)!(n+l)!}{l!m!n!(1+t)^{m+n+l+1}} \tag{26}$$

Obviously,the field with negative P function can exihibites squeezing for some situation,but,if $P(\alpha)$ is only the function of $|\alpha|$,i.e, $P(\alpha)$ is sphere symmetry in phase space,then

$$P_{i,j}=0 \qquad (i\neq j) \tag{27}$$

$$C_{m,n}=0 \quad (m\neq n) \tag{28}$$

Form equation (12),one can get

$$S>0 \tag{29}$$

In conclusion ,it is clearly that no suqueezing exists in the field with negative P(α) function which is sphere symmetry in phase space.

References

[1] C. W. Gardiner,Handbook of stochastic methods (springer,Berlin,1983);
W. H. Louisell,Quantum statistical properties of radiation (Wiley,New York,1973)

[2] M. S. Kim,V. Buzek,Min Gyu Kim,Phys. Lett. A186,283,(1994)

[3] Fan Hong—yi and Ruan Tun—nan,Sci. Sim. A27,392(1984);
Fan Hong—yi,H. R. Zaidi and J. R. Klauder,Phys. Rev. D35,183(1987)

[4] M. Hilery,Phys. Lett. A111,409(1985);
Yao Demin and Guo Guangcan,Acta. Sin. 42,463(1988)

[5] G. S. Agarwal and K. Tara,Phys. Rev. A46,485(1992)

NEXT
DOCUMENT

Generalization of the time-energy uncertainty relation of Anandan-Aharonov Type

Minoru HIRAYAMA , Takeshi HAMADA* and Jin CHEN

Department of Physics
Toyama University
Toyama 930, Japan

*Department of Physics
Kanazawa University
Kakuma, Kanazawa 920-11, Japan

Abstract

A new type of time-energy uncertainty relation was proposed recently by Anandan and Aharonov. Their formula to estimate the lower bound of time-integral of the energy-fluctuation in a quantum state is generalized to the one involving a set of quantum states. This is achieved by obtaining an explicit formula for the distance between two finitely separated points in the Grassman manifold.

I. Introduction

We first review briefiy the conventional time-energy uncertainty relation in quantum mechanics. Let A be an ovservable without explicit time-dependence and $|\psi(t)\rangle$ be a normalized quantum state vector obeying the Schrödinger equation with a hermitian Hamiltonian H. If we define ΔA and τ_A by

$$\Delta A = \sqrt{\langle\psi(t)|A^2|\psi(t)\rangle - \langle\psi(t)|A|\psi(t)\rangle^2}\ , \tag{1}$$

$$\tau_A = \left|\frac{d}{dt}\langle\psi(t)|A|\psi(t)\rangle\right|^{-1} \Delta A\ , \tag{2}$$

and take the equation

$$\frac{d}{dt}\langle\psi(t)|A|\psi(t)\rangle = \frac{1}{i\hbar}\langle\psi(t)|\ [A,H]\ |\psi(t)\rangle \tag{3}$$

into account, we are led to the uncertainty relation [1]

$$\tau_A \Delta H \geq \frac{\hbar}{2}\ . \tag{4}$$

The quantity τ_A is interpreted as the time necessary for the distribution of $\langle\psi(t)|A|\psi(t)\rangle$ to be recognized to have clearly changed its shape.

In contrast with the result given above, Anandan and Aharonov [2] have recently succeeded in obtaining quite an interesting inequality. They consider the case that the $|\psi(t)\rangle$ develops in time obeying

$$i\hbar\frac{d}{dt}|\psi(t)\rangle = H(t)|\psi(t)\rangle\ , \tag{5}$$

$$\langle\psi(t)|\psi(t)\rangle = 1\ , \tag{6}$$

where $H(t)$ is an operator which is hermitian and might be time-dependent. They conclude that

$$\int_{t_1}^{t_2} \Delta\mathcal{E}(t)dt \geq \hbar\mathrm{Arccos}(|\langle\psi(t_1)|\psi(t_2)\rangle|)\ , \tag{7}$$

where $\Delta\mathcal{E}(t)$ is given by

$$\Delta\mathcal{E}(t) = \sqrt{\langle\psi(t)|H(t)^2|\psi(t)\rangle - \langle\psi(t)|H(t)|\psi(t)\rangle^2}\ . \tag{8}$$

The inequality (7), which we refer to as the Anandan-Aharonov time-energy uncertainty relation, has been derived through a geometrical investigation of the set of normalized

quantum state vectors. The r.h.s. of (7) can be regarded as the distance between two points in a complex projective space.

Here, we seek the generalized version of (7). We consider a set of N orthonormal vectors $\{|\psi_i(t)\rangle : i = 1, 2, \ldots, N\}$ satisfying

$$\langle\psi_i(t)|\psi_j(t)\rangle = \delta_{ij} \ , \quad i, j = 1, 2, \ldots, N, \tag{9}$$

each of which obeying the Schrödinger equation (5). We define $N \times N$ matrices $A(t_1, t_2)$ and $K(t_1, t_2)$ by

$$A(t_1, t_2) = (a_{ij}(t_1, t_2)) \ , \quad a_{ij}(t_1, t_2) = \langle\psi_i(t_1)|\psi_j(t_2)\rangle \ , \tag{10}$$

$$K(t_1, t_2) = A^\dagger(t_1, t_2)A(t_1, t_2) \tag{11}$$

and $\kappa_i(t_1, t_2), i = 1, 2, \ldots, N$, to be the eigenvalues of $K(t_1, t_2)$. Defining the generalization of (8) by

$$\Delta\mathcal{E}_N(t) = \sqrt{\sum_{i=1}^{N}\langle\psi_i(t)|H(t)^2|\psi_i(t)\rangle - \sum_{i,j=1}^{N}|\langle\psi_i(t)|H(t)|\psi_j(t)\rangle|^2} \ , \tag{12}$$

we find that $\Delta\mathcal{E}_N(t)$ satisfies

$$\int_{t_1}^{t_2}\Delta\mathcal{E}_N(t)dt \geq \hbar\sqrt{\sum_{i=1}^{N}\left\{\mathrm{Arccos}\sqrt{\kappa_i(t_1, t_2)}\right\}^2} \tag{13}$$

The inequality (13) can be written in an operator form as

$$\begin{aligned}\int_{t_1}^{t_2}&\sqrt{\mathrm{Tr}(P(t)[H(t), [H(t), P(t)]])}\mathrm{d}t \\ &\geq \sqrt{2}\hbar\sqrt{\mathrm{Tr}(\{\mathrm{Arccos}\sqrt{P(t_1)P(t_2)}\}^2)} \ ,\end{aligned} \tag{14}$$

where $P(t)$ is defined by

$$P(t) = \sum_{i=1}^{N}|\psi_i(t)\rangle\langle\psi_i(t)|. \tag{15}$$

and Tr denotes the trace in the Hilbert space. The result (13) is obtained through a geometrical investigation of the Grassmann manifold G_N mentioned below.

II. Distance formula for the Grassmann manifold

Given a Hilbert space h,we consider vectors $|\psi_i\rangle, i = 1,2,\ldots,N$,belonging to h and satisfying $\langle\psi_i|\psi_j\rangle = \delta_{ij}$. We call the set

$$\Psi = (|\psi_1\rangle, |\psi_2\rangle, \ldots, |\psi_N\rangle) \tag{16}$$

an N-frame of h and the set

$$[\Psi] = \{\Psi u : u \in U(N)\} \tag{17}$$

an N-plane of h,where Ψu is defined by

$$\Psi u = (\sum_{i=1}^{N} |\psi_i\rangle u_{i1}, \sum_{j=1}^{N} |\psi_j\rangle u_{j2}, \ldots, \sum_{k=1}^{N} |\psi_k\rangle u_{kN}). \tag{18}$$

It is clear that the $[\Psi]$ and the projection operator $P = \sum_{i=1}^{N} |\psi_i\rangle\langle\psi_i|$ are invariant under the replacement $\Psi \rightarrow \Psi u$. We denote the set of all the Ψ's of h by S_N. Then the set G_N defined by

$$G_N = \{[\Psi] : \Psi \in S_N\} \tag{19}$$

is known to constitute a manifold of complex dimension $N(\dim \mathrm{h} - N)$ and is called the Grassmann manifold.

To an N-frame $\Psi(t) = (|\psi_1(t)\rangle, |\psi_2(t)\rangle, \ldots, |\psi_N(t)\rangle) \in S_N, 0 \leq t \leq 1$, there correspond an N-plane $[\Psi(t)] \in G_N$ and a projection operator $P(t) = \sum_{i=1}^{N} |\psi_i(t)\rangle\langle\psi_i(t)|$. Since the eigenvalues of $P(1)$ are equal to those of $P(0)$ including multiplicities,there exists a unitary operator W such that

$$P(1) = W^{\dagger}P(0)W, \quad W = e^{iY}, \quad Y^{\dagger} = Y. \tag{20}$$

We define the distance $d([\Psi(0)],[\Psi(1)])$ between two points $[\Psi(0)]$ and $[\Psi(1)]$ of the Grassmann manifold G_N by

$$d([\Psi(0)],[\Psi(1)]) = \operatorname*{Min}_{Y\in\Sigma} \|Y\|, \tag{21}$$

where Σ is the set of hermitian operators specified by $P(0)$ and $P(1)$ in the following way:

$$\Sigma = \{Y : Y = Y(P(0),P(1)) = -Y(P(1),P(0)) = Y^{\dagger}, e^{-iY}P(0)e^{iY} = P(1)\}. \tag{22}$$

After some manipulations,we find that the distance is given by the formula

$$d([\Psi(0)],[\Psi(1)]) = \sqrt{2\sum_{i=1}^{N}(\mathrm{Arccos}\sqrt{\kappa_i})^2}, \tag{23}$$

where κ_i is defined below (11) and satisfies $0 \leq \kappa_i \leq 1$.

We also find that the above defined distance in G_N satisfies the property of distance:

$$d([\Psi],[\Phi]) = d([\Phi],[\Psi]) \geq 0, \tag{24}$$

$$d([\Psi],[\Phi]) = 0 \iff [\Psi] = [\Phi], \tag{25}$$

$$d([\Psi],[\Phi]) \leq d([\Psi],[\Xi]) + d([\Xi],[\Phi]), \tag{26}$$

for any $[\Psi],[\Phi],[\Xi] \in G_N$.

III. Time-energy uncertainty relation

The projection operator $P(t)$ is defined by (15) and $|\psi_i(t)\rangle, i = 1,2,\ldots,N$, develops in time obeying (5). We then have

$$\begin{aligned} P(t+dt) = P(t) &+ \frac{dt}{i\hbar}[H(t),P(t)] \\ &+ \frac{(dt)^2}{2(i\hbar)^2}\left\{i\hbar[\frac{dH(t)}{dt},P(t)] + [H(t),[H(t),P(t)]]\right\} + \cdots. \end{aligned} \tag{27}$$

When $[\Psi(0)]$ and $[\Psi(1)]$ are close to each other, $\kappa_i, i = 1,2,\ldots,N$, are nearly equal to 1. Noticing that $(\mathrm{Arccos}\sqrt{\kappa})^2 \approx 1-\kappa$ for $\kappa \approx 1$, we see

$$d([\Psi(t)],[\Psi(t+dt)]) \approx \sqrt{2\sum_{i=1}^{N}(1-\kappa_i(t))}, \tag{28}$$

where $\kappa_i(t)$'s are obtained from $P(t)$ and $P(t+dt)$ by similar procedures to those of previous sections. Since, in the above case, we have $\mathrm{Tr}P(t) = N$ and

$$\mathrm{Tr}(P(t)P(t+dt)) = \sum_{i=1}^{N}\kappa_i(t), \tag{29}$$

(28) can be rewritten as

$$d([\Psi(t)],[\Psi(t+dt)]) = \sqrt{2\mathrm{Tr}(P(t)\{P(t)-P(t+dt)\})}. \tag{30}$$

Now we have

$$\begin{aligned} d([\Psi(t)],[\Psi(t+dt)]) &= \frac{|dt|}{\hbar}\sqrt{\mathrm{Tr}(P(t)[H(t),[H(t),P(t)]])} \\ &= \frac{|dt|}{\hbar}\sqrt{\mathrm{Tr}([P(t),H(t)][H(t),P(t)])} \\ &= \left\|\frac{dP(t)}{dt}\right\||dt|. \\ &= \|dP(t)\|. \end{aligned} \tag{31}$$

It can be easily seen that the r.h.s. of (31) is proportional to $\Delta\mathcal{E}_N(t)$ defined by (12). Now we are led to

$$d([\Psi(t)],[\Psi(t+dt)]) = \frac{\sqrt{2}}{\hbar}\Delta\mathcal{E}_N(t)|dt|. \tag{32}$$

For finitely separated $[\Psi(t_1)]$ and $[\Psi(t_2)]$ in G_N, the triangle inequality (26) implies

$$\int_{t_1}^{t_2}\Delta\mathcal{E}_N(t)dt \geq \frac{\hbar}{\sqrt{2}}d([\Psi(t_1)],[\Psi(t_2)]), t_2 \geq t_1. \tag{33}$$

The formula (23) then leads us to (13) or (14). For details , see [3].

References

[1] A.Messiah, *Quantum Mechanics* (North-Holland,Amsterdam, (1961).

[2] J.Anandan and Y. Aharonov, Phys. Rev. Lett. **65**,1697(1990).

[3] M.Hirayama,T.Hamada and J.Chen, Progr. Theor. Phys.**93**,255(1995).

NEXT
DOCUMENT

Study of Nonclassical Fields in Phase-Sensitive Reservoirs

Myung Shik Kim
Department of Physics, Sogang University, Seoul, 121-742, Korea

Nobuyuki Imoto
NTT Basic Research Laboratories,
3-1 Morinosato-Wakamiya, Atsugi-shi, Kanagawa 243-01, Japan

Abstract

We show that the reservoir influence can be modeled by an infinite array of beam splitters. The superposition of the input fields in the beam splitter is discussed with the convolution laws for their quasiprobabilities. We derive the Fokker-Planck equation for the cavity field coupled with a phase-sensitive reservoir using the convolution law. We also analyse the amplification in the phase-sensitive reservoir with use of the modified beam splitter model. We show the similarities and differences between the dissipation and amplification models. We show that a super-Possonian input field cannot become sub-Poissonian by the phase-sensitive amplification.

1 Introduction

A cavity with imperfect mirrors not only lets the cavity field out but also allows the field outside to leak into the cavity so that the reservoir surrounding the cavity gradually influences the cavity field. The mirrors in the cavity can be considered as beam splitters. An arrayx consisting of an infinite number of beam splitters can model a reservoir coupled to the cavity field [1].

It is convenient to utilise quasiprobability distributions such as the Q function to describe states of quantum-mechanical systems in phase space. We briefly show that the fields at the output ports of the beam splitter can be expressed by the convolution of the quasiprobabilities of the input fields. We then use the convolution relation to derive the Fokker-Planck equation for attenuation of the cavity field coupled with the phase-sensitive reservoir.

It is known in quantum mechanics that an amplification process is inevitably accompanied by the increase of the quantum noise in the system. In other words the amplification degrades an optical signal and rapidly destroys quantum features that may have been associated with the signal. The nature of the amplifier affects the physical properties of the amplified states of light. The phase-sensitive amplifier is conceptually based on the establishment of squeezed light and enables a squeezed input to keep the property for a gain larger than the cloning limit [2].

The amplification process can also be modeled by an array of beam splitters, where the beam splitters are somewhat modified from the usual sense. We find the convolution relation for this modified beam splitters and the Fokker-Planck equation is derived from it. We then formaly solve

the Fokker-Planck equation for the phase-sensitive amplifier for an arbitrary input field and study the photon statistics of the amplified field.

2 Phase-Sensitive Attenuation

Consider that two fields at the two input ports of a lossless beam splitter are superposed. For convenience we call one input field the signal and the other the noise (Fig. 1). The input signal mode b with its annihilation operator $\hat{b}$ is superposed on the noise mode a with its annihilation operator $\hat{a}$ by the beam splitter whose amplitude reflectivity is $r = \sin\theta$ and transmittivity $t = \cos\theta$. The two output field annihilation operators $\hat{c}$ and $\hat{d}$ are related to the beam splitter input fields by the transformation using the beam splitter operator $\hat{B}$ [3].

$$\begin{pmatrix} \hat{c} \\ \hat{d} \end{pmatrix} = \hat{B} \begin{pmatrix} \hat{a} \\ \hat{b} \end{pmatrix} \hat{B}^{\dagger} = \begin{pmatrix} t\hat{a} + r\hat{b} \\ t\hat{b} - r\hat{a} \end{pmatrix} ; \quad \hat{B} = \exp\left[\theta\left(\hat{a}\hat{b}^{\dagger} - \hat{a}^{\dagger}\hat{b}\right)\right] . \tag{1}$$

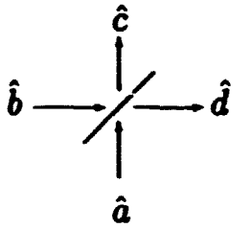

Fig. 1 Beam splitter with the signal input in mode b and the noise field input in mode a.

A field state can be represented in phase space by quasiprobabilities. Let us choose to use the positive P-representation to describe the fields. The density operators $\hat{\rho}_a$ and $\hat{\rho}_b$ for the noise and signal fields are then written with the positive P-representation $P_{a,b}(\alpha,\gamma)$ as

$$\hat{\rho}_i = \int d^2\alpha \, d^2\gamma \frac{P_i(\alpha,\gamma)}{\langle\gamma^*|\alpha\rangle} |\alpha\rangle\langle\gamma^*|, \quad i = a, b \tag{2}$$

The fields $\hat{\rho}_c$ and $\hat{\rho}_d$ at the output ports are calculated by the beam splitter transformation: $\hat{B}\hat{\rho}_a\hat{\rho}_b \longrightarrow \hat{\rho}_c\hat{\rho}_d$. With use of the transformation matrix Eq.(1) we find that the positive P-representation for the field at the port d is found in the form of the convolution relation:

$$P_d(\phi,\psi) = \frac{1}{t^4} \int d^2\alpha \, d^2\gamma \; P_a(\alpha,\gamma) P_b\left(\frac{\phi - r\alpha}{t}, \frac{\psi - r\gamma}{t}\right) , \tag{3}$$

The Q function is another quasiprobability function and is well-defined even for the nonclassical state. The positive P-representation is defined in four-dimensional space. The Q function, which is defined in two-dimensional space, is therefore sometimes easier to treat, so we will extend the

convolution law for the uses of the Q function. The positive P-representation may be defined as the Fourier transform of the characteristic function. The characteristic function $C^{(p)}(\xi)$ is related to the characteristic function $C^{(q)}(\xi)$ for the Q function as $C^{(p)}(\xi) = C^{(q)}(\xi)\exp(|\xi|^2)$. By using the convolution theorem, we can factorise the inverse Fourier transform of the convolution law (3) as

$$C_d^{(p)}(\xi) = C_a^{(p)}(r\xi)C_b^{(p)}(t\xi) \, . \tag{4}$$

Using the relation between the characteristic functions, the convolution relation for the Q function is found as

$$Q_d(\phi) = \frac{1}{t^2}\int d^2\alpha \; Q_a(\alpha)Q_b\left(\frac{\phi - r\alpha}{t}\right) \, . \tag{5}$$

We now derive the Fokker-Planck equation for the phase-sensitive reservoir using the model of an infinite array of beam splitters (Fig.2) [4]. The total duration of time when the field is coupled with the lossy channel is denoted by T, the total number of the beam splitters by $\aleph$, and the interval between the adjacent beam splitters by $\Delta\tau$. The beam splitters are first taken to be discrete components, but their number, $\aleph = T/\Delta\tau$ is later taken to infinity in order to model a continuous attenuating reservoir. Under the assumption that the reflectivity is very small for the beam splitter, Eq. (5) is written as

$$Q(\alpha) \approx (1+R)\int d^2\alpha \; Q_a(\beta)\; Q_b\left(\frac{\alpha - r\beta}{t}\right) \, . \tag{6}$$

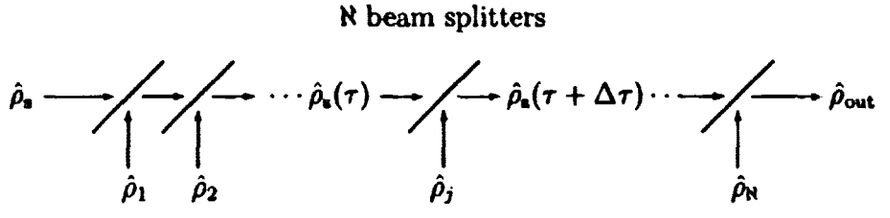

Fig.2 The phase-sensitive reservoir modeled as an array containing an infinite number of beam splitters. The signal is injected from left and the independent squeezed fields (all with the same properties) are injected into the other ports. The transmittivity is considered to be nearly unity.

To calculate the effects of attenuation, we need an expression for the output signal operator in terms of the input operators. To simulate an attenuator, we consider the beam splitters forming a continuous array by taking the limits $\aleph \to \infty$, $\Delta\tau \to 0$, and $R \to 0$. These limits cannot be taken independently: $\aleph\Delta\tau$ should be kept constant. Also, the total energy loss within T is described by $1 - \exp(-\kappa T)$, where κ is the attenuation coefficient, and this loss should be equivalent to the beam splitter loss so that $R \approx \kappa\Delta\tau$.

Let us define $Q(\tau;\alpha)$ as the Q function of the signal field incident on the beam splitter at time τ, $Q_{sq}(\beta)$ as the Q function for the noise added to the signal at the beam splitter, and $Q(\tau+\Delta\tau;\alpha)$ as the Q function for the signal leaving from the beam splitter. The squeezed thermal fields produced by the independent stationary sources act as noise in our model.

From Eq. (6), we obtain the relation

$$Q(\tau+\Delta\tau;\alpha) = (1+R)\int d^2\beta\, Q\left(\tau;\frac{\alpha-r\beta}{t}\right) Q_{sq}(\beta)\,, \tag{7}$$

where $\frac{\alpha-r\beta}{t} \approx \alpha + \frac{R}{2}\,\alpha - \sqrt{R}\,\beta$. With the Taylor expansion for a function having a complex argument:

$$Q\left(\tau;\frac{\alpha-r\beta}{t}\right) = Q + \frac{\partial Q}{\partial\alpha_1}\,\frac{\alpha_1}{2} + R\left(\frac{\partial Q}{\partial\alpha_2}\,\frac{\alpha_2}{2} + \frac{1}{2}\frac{\partial^2 Q}{\partial\alpha_1^2}\beta_1^2 + \frac{1}{2}\frac{\partial^2 Q}{\partial\alpha_2^2}\beta_2^2 + \frac{\partial^2 Q}{\partial\alpha_1\partial\alpha_2}\beta_1\beta_2\right)\,, \tag{8}$$

where the real and imaginary parts of α and β are respectively denoted by α_1, α_2 and β_1, β_2. The function Q is the simplified notation of the function $Q(\tau;\alpha)$. Substituting Eq. (8) into Eq. (7) we obtain

$$\begin{aligned}\frac{dQ(\tau;\alpha)}{d\tau} &= \frac{\kappa}{2}\left[\frac{\partial}{\partial\alpha_1}(\alpha_1 Q) + \frac{\partial}{\partial\alpha_2}(\alpha_2 Q)\right]\int d^2\beta\, Q_{sq}(\beta) \\ &\quad + \frac{\kappa}{2}\left[\frac{\partial^2 Q}{\partial\alpha_1^2}\int d^2\beta\,\beta_1^2 Q_{sq}(\beta) + \frac{\partial^2 Q}{\partial\alpha_2^2}\int d^2\beta\,\beta_2^2 Q_{sq}(\beta)\right]\,.\end{aligned} \tag{9}$$

Taking the squeezed thermal state as noise we substitute the simple Gaussian integration of $Q_{sq}(\beta)$ into Eq. (9) and obtain the Fokker-Planck equation for the field coupled to a phase-sensitive attenuation reservoir:

$$\frac{dQ(\tau,\alpha)}{d\tau} = \frac{\kappa}{2}\left[\frac{\partial}{\partial\alpha_1}\alpha_1 + \frac{\partial}{\partial\alpha_2}\alpha_2 + \frac{1}{2}(1+N+M)\frac{\partial^2}{\partial\alpha_1^2} + \frac{1}{2}(1+N-M)\frac{\partial^2}{\partial\alpha_2^2}\right]Q(\tau,\alpha)\,, \tag{10}$$

where N is the mean photon number for the squeezed thermal field and the phase-dependent term M is zero when the field is not squeezed [4]. The Fokker-Planck equation is relatively simple and observables can be calculated as correlations of the quasiprobability function.

3 Phase-Sensitive Amplification

The amplification process can also be modeled by an array of beam splitters similar to that for dissipation. In their experiment with phase-sensitive amplification, Ou et al. have a nondegenerate parametric amplifier where the signal field is amplified and the idler mode is coupled with the squeezed vacuum [5]. As in their experiment a two-mode parametric optical amplifier is modeled here by an amplification beam splitter matrix. For a two-mode parametric amplifier the signal input $\hat{b}$ is transformed into the amplified output $\hat{d}$ with unavoidable noise $\hat{a}^\dagger$:

$$\begin{pmatrix}\hat{d}\\ \hat{c}^\dagger\end{pmatrix} = \begin{pmatrix}\sqrt{g} & i\sqrt{g-1}\\ -i\sqrt{g-1} & \sqrt{g}\end{pmatrix}\begin{pmatrix}\hat{a}\\ \hat{b}^\dagger\end{pmatrix}\,, \tag{11}$$

where $g > 1$ is the infinitesimal amplification factor. We are going to build a beam-splitter-like relation for amplification, and consecutive application of an infinite number of Eq. (11) will give the final amplification result. The actual gain G by the amplifier will, thus, be proportional to g. The unitary amplification beam splitter operator has been introduced in analogy with the two-mode squeezing operator as $B_1 = \exp[i\theta_1(\hat{a}^\dagger\hat{b}^\dagger + \hat{a}\hat{b})]$ with $\cosh\theta_1 = \sqrt{g}$ and sinh $thetu_1 = \sqrt{g-1}$.

To analyze the beam splitter transformation for the amplifier, let us assume that the input fields are expressed as a weighted sum of diagonal coherent components:

$$\hat{\rho}_{in} = \int d^2\alpha\, d^2\beta\, P_a(\alpha)P_b(\beta)|\alpha\rangle_{aa}\langle\alpha| \otimes |\beta\rangle_{bb}\langle\beta| \,, \tag{12}$$

where P_a and P_b are respectively the Glauber P-representations for modes a and b. Tracing the output field over mode c, we find the output density operator for mode d:

$$\hat{\rho}_d = \int d^2\alpha\, d^2\beta\, P_a(\alpha)P_b(\beta)D_d(\delta)\hat{\rho}_{th}D_d^\dagger(\delta)\,; \qquad \delta = i\sqrt{g-1}\,\alpha^* + \sqrt{g}\,\beta \tag{13}$$

and $\hat{\rho}_{th}$ is the thermal field density operator for the mean photon number $\bar{n} = g - 1$. Even when both the signal and the idler fields are in the vacuum state, i. e., $\alpha = \beta = 0$, the amplifier brings noise into the fields. The density operator for the thermal field can be written with its quasiprobability $P_T(\phi)$ as

$$\hat{\rho}_{th} = \int d^2\phi\, P_T(\phi)|\phi\rangle\langle\phi|\,; \qquad P_T(\phi) = \frac{1/\pi}{g-1}\exp\left(-\frac{|\phi|^2}{g-1}\right) . \tag{14}$$

By using Eq. (14), we find the Glauber P-representation for the output field as convolution of the three P-representations

$$P_d(\zeta) = \frac{1}{g}\int d^2\phi\, d^2\alpha\, P_a(\alpha)P_b\left(\frac{\zeta - \phi - i\alpha^*\sqrt{g-1}}{\sqrt{g}}\right)P_T(\phi) \,. \tag{15}$$

The inverse Fourier transform of the Glauber P-representation gives the characteristic function for the output field in the form of the product of the characteristic functions for the input modes a and b and the thermal field. We can simplify this relation using the relation between the characteristic functions for the various quasiprobabilities. The Fourier transformation of this shows that a modified convolution between Q_b for the signal Q function and P_a for the noise P-representation results in Q_d for the output field:

$$Q_d(\zeta) = \frac{1}{g}\int d^2\lambda\, P_a(\lambda)Q_b\left(\frac{\zeta - i\sqrt{g-1}\,\lambda}{\sqrt{g}}\right) . \tag{16}$$

The convolution relation for amplification differs from that for attenuation (5) because of the unavoidable extra noise due to the thermal field (14).

Consider an array of N beam splitters which satisfy the transformation relation (11). To simulate an amplifier we will take $N \to \infty$ and let the infinitesimal amplification factor for each beam splitter be given by $g = 1 + \epsilon \approx 1$. After a signal passes through the N beam splitters, it is amplified by the factor of $G = e^{\gamma T} = (1+\epsilon)^N$, where γ is the amplification coefficient. By using

the Taylor expansion of Q function (16) to the second-order under the assumption $\epsilon \approx 0$ (we had $r \approx 0$ for attenuation), we obtain the Fokker-Planck equation for amplification:

$$\frac{dQ(\tau,\alpha)}{d\tau} = \frac{\gamma}{2}\left[-\frac{\partial}{\partial\alpha_1}\alpha_1 - \frac{\partial}{\partial\alpha_2}\alpha_2 + \frac{1}{2}(N+M)\frac{\partial^2}{\partial\alpha_1^2} + \frac{1}{2}(N-M)\frac{\partial^2}{\partial\alpha_2^2}\right]Q(\tau,\alpha)\,. \tag{17}$$

The Fokker-Planck equation (17) is solved for an arbitrary signal amplified in the phase-sensitive reservoir. The Q function corresponding to an arbitrary input field can be written as a weighted integral of Gaussian functions:

$$Q_s(\alpha) = \frac{1}{\pi}\int d^2\mu d^2\nu P(\mu,\nu)\exp[-(\alpha_1 - A)^2 - (\alpha_2 - B)^2]\,, \tag{18}$$

where $A = \frac{1}{2}(\mu+\nu)$, $B = \frac{1}{2i}(\mu-\nu)$ and $P(\mu,\nu)$ is the positive P-function for the field. It has been recently shown that if the initial Q function of the quantum system is (complex) Gaussian, then the solution of the Fokker-Planck equation (17) is also Gaussian with time-dependent parameters. The Q function (18) is a weighted integral of complex Gaussian functions, so one can obtain the time evolution of the input state

$$\begin{aligned} Q_{amp}(\alpha,\tau) &= \frac{1/\pi}{\sqrt{(N_1(\tau)+1)^2 - M_1(\tau)^2}}\int d^2\mu d^2\nu P(\mu,\nu) \\ &\quad\times\exp\left\{-\frac{[\alpha_1 - A(\tau)]^2}{1+N_1(\tau)-M_1(\tau)} - \frac{[\alpha_2 - B(\tau)]^2}{1+N_1(\tau)+M_1(\tau)}\right\}\,, \end{aligned} \tag{19}$$

where the time-dependencies of the amplification parameters are

$$A(t) = A\sqrt{G} = Ae^{\gamma\tau}\,,\quad B(t) = B\sqrt{G}\,,\quad N_1(\tau) = (N+1)(G-1)\quad\text{and}\quad M_1(\tau) = M(G-1)\,. \tag{20}$$

The inverse Fourier transformation of the Q function (19) shows that the characteristic function $C^{(q)}_{amp}$ for the Q function of the amplified field is the product of the characteristic function $C^{(p)}_{sq}$ for the P-representation of the squeezed thermal field and that $C^{(q)}_s$ for the Q function of the amplified signal without noise

$$C^{(q)}_{amp}(\zeta) = C^{(p)}_{sq}(i\sqrt{G-1}\,\zeta)C^{(q)}_s(\sqrt{G}\,\zeta)\,. \tag{21}$$

The convolution relation for this relation is then in a form analogous to Eq. (16) for the amplification beam splitter superposition of two input fields.

The antinormally-ordered moments can be calculated from the characteristic function $C^{(q)}$:

$$\begin{aligned} \langle\hat{a}^n(\hat{a}^\dagger)^m\rangle &= \sum_{\ell=0}^{m}\sum_{k=0}^{n}\binom{m}{\ell}\binom{n}{k}(i\sqrt{G-1})^\ell(-i\sqrt{G-1})^k\langle(\hat{a}^\dagger)^\ell\hat{a}^k\rangle_{sq} \\ &\quad\times(\sqrt{G})^{m+n-\ell-k}\langle\hat{a}^{n-k}(\hat{a}^\dagger)^{m-\ell}\rangle_s\,. \end{aligned} \tag{22}$$

We can also consider the phase-sensitive amplifier which can be implemented as a stream of three-level atoms in a ladder configuration with equispaced levels injected into the cavity where the initial state of the field has been prepared. We denote the population in the uppermost state

by ρ_{aa}, the population in the lowest state by ρ_{cc} and the coherences between them by ρ_{ac} and ρ_{ca}. The atomic coherences ρ_{ac} and ρ_{ca} bring about the phase-sensitive effect in the two-photon linear amplifier. The parameters N and M can then be represented by the atomic variables

$$N_1(\tau) = \frac{\rho_{aa}}{\rho_{aa} - \rho_{cc}}(G-1), \qquad M_1(\tau) = \frac{|\rho_{ac}|}{\rho_{aa} - \rho_{cc}}(G-1)\,. \tag{23}$$

The normally-ordered photon number variance, $:(\Delta n)^2:$, where $(\Delta n)^2 = \langle n^2\rangle - \langle n\rangle^2$, measures the deviation of the photon number fluctuations from the Poissonian photon statistics. The Poissonian field has the normally-ordered photon number variance zero, while the quantum mechanical sub-Poissonian field has it less than zero. It is larger than zero for the noisy super-Poissonian field. With use of Eq.(22) we find the normally-ordered photon number variance

$$:(\Delta n)^2_{\rm amp} := G^2 :(\Delta n)^2_{\rm s}: + \zeta, \tag{24}$$

where the additive noise is

$$\zeta = \frac{(G-1)^2}{(\rho_{aa} - \rho_{cc})^2}(\rho_{aa}^2 + |\rho_{ac}|^2) + \frac{G(G-1)}{\rho_{aa} - \rho_{cc}}[2\rho_{aa}\langle a^\dagger a\rangle_{\rm s} - |\rho_{ac}|(\langle a^2\rangle_{\rm s} + \langle (a^\dagger)^2\rangle_{\rm s}]. \tag{25}$$

If the additive noise is negative, the amplified field has less photon number fluctuation than the input field. It is clearly seen that if the atomic coherence, ρ_{ac}, is zero the additive noise is always positive. However as the atomic coherence is nonzero we can have the negative noise to enhance the signal to noise ratio.

If each atom injected into the cavity is in atomic coherences we have the relation $\rho_{aa}\rho_{cc} = |\rho_{ac}|^2$ and the additive noise (25) can be written as

$$\zeta = G(G-1)\frac{c|\rho_{ac}|}{\rho_{aa} - \rho_{cc}} + 2G(G-1)\frac{\rho_{aa} - \rho_{cc}}{\rho_{aa} - |\rho_{ac}|}\langle a^\dagger a\rangle_{\rm in} + (G-1)^2\frac{\rho_{aa}}{(\rho_{aa} - \rho_{cc})^2}, \tag{26}$$

where

$$c = 2\langle a^\dagger a\rangle_{\rm in} - (\langle a^2\rangle_{\rm in} + \langle (a^\dagger)^2\rangle_{\rm in}), \tag{27}$$

which has to be negative to have the additive noise negative. The bosonic operators a and $a^\dagger$ have a simple restriction, $2\langle a^\dagger a\rangle - (\langle a^2\rangle + \langle (a^\dagger)^2\rangle) \geq -1$. It is thus required that

$$-1 \leq c < 0 \tag{28}$$

for the noise reduction in the amplified signal. The noise reduction in the photon number fluctuations seems to be possible if the input field satisfies Eq.(28). However we should not fail to notice that the condition (28) is related to the initial photon number fluctuations. Because the expectation value of an operator times its hermitian conjugate is again positive,

$$c \geq -\frac{:(\Delta n)^2_{\rm in}:}{\langle a^\dagger a\rangle}. \tag{29}$$

It is easily seen from Eqs.(28) and (29) that the input field should be super-Poissonian to have a possibility to reduce the photon number fluctuations by the amplification. If the input field is Poissonian there is no intersection between the two conditions (28) and (29) so that we can say that the Poissonian field does not become sub-Poissonian during the amplification.

Acknowledgments

This work was supported by the NONDIRECTED RESEARCH FUND, Korea Research Foundation and by the Korean Science and Engineering Foundation (project number 951-0205-015-1).

References

[1] M. S. Kim and N. Imoto, Phys. Rev. A **52**, to appear (1995).

[2] R. Loudon and T. I. Shepherd, Optica Acta **31**, 1243 (1984).

[3] R. A. Campos, B. E. A. Saleh, and M. C. Teich, Phys. Rev. A **40**, 1371 (1989).

[4] M. S. Kim and V. Buzek, Phys. Rev. A **47**, 610 (1993).

[5] Z. Y. Ou, S. F. Pereira, and H. J. Kimble, Phys. Rev. Lett. **70** 3239 (1993).

NEXT
DOCUMENT

QUANTUM MECHANICAL NOISE IN A MICHELSON INTERFEROMETER WITH NONCLASSICAL INPUTS — NONPERTURBATIVE TREATMENT

Sun-Kun King
Department of Physics, National Tsing Hua University, Hsinchu, Taiwan 300, ROC

Abstract

The variances of the quantum-mechanical noise in a two-input-port Michelson interferometer within the framework of the Loudon-Ni model were solved exactly in two general cases: (i) one coherent state input and one squeezed state input, and (ii) two photon number states inputs. Low intensity limit, exponential decaying signal and the noise due to mixing were discussed briefly.

1 Introduction

In 1981 the effects of intensity fluctuations in the two light beams and radiation pressure on the mirrors in a Michelson interferometer were modeled in a unified way by Loudon [1]. In 1987, Ni extended the model to include the intrinsic uncertainties of the mirrors and obtained an exact solution of the variance of the quantum mechanical noise for a coherent light source with arbitrary intensity [2]. These results were used recently by Ni in proposing an experimental scheme for controlling a macroscopic quantum state of a mirror by light shining [3].

Quantum-mechanical noise of a Michelson interferometer is an important noise source in gravitational waves detection. Experiments had reached the shot noise limit already. Photon shot noise decreases as the intensity goes up. Roughly speaking, it is propotional to the inverse square root of intensity. But, it was argued [4] that the fluctuation of radiation pressure on the mirrors would increase as the intesity becomes higher so that a minimum would be reached, called the "standard quantum limit" [4]. On the other hand, various works [5] show that such a measurement (without loss) implies no limit while squeezed states were used.

With the knowledge of squeezed states and that semi-classical model of interaction between a macroscopic object and photons, we got chance to probe this problem in detail. Within the framework of the Loudon-Ni model, the method of Ref. [2] was extended to obtain an exact solution for the variance of a two-input-port Michelson interferometer where a squeezed-state light source and a coherent light source (both with arbitrary intensity) were applied on each port respectively. Faithful matrix representations [6] were used in this calculation. The final result is more complicated. Nevertheless, it can be organized in a similar form as in Ref. [2]. Photon number state inputs can be treated in a similar way.

Due to the complicated results we've got, the physical implication is yet under study. However, some features and observation were discussed in the final section.

2 The Model

The usually input port was identified as "a-mode", with an annihilation operator "a" ('^' was omitted for simplicity). The usually unused port was called "b-mode", with an annihilation operator "b" ('^' was omitted, also). Both satisfy the canonical commutation relations, say, $[a, a^\dagger] = 1$ and $[b, b^\dagger] = 1$. Beam splitter played the role of a mixer here. It combined both inputs from a-mode and b-mode then the mixture was sent into two arms as a_1-mode and a_2-mode. Therefore,

$$a = (a_1 + a_2)/\sqrt{2}, \quad b = (a_1 - a_2)/\sqrt{2}. \tag{1}$$

A phase was chosen. Nevertheless, it losts no generality. The reflection coefficient of arm one is

$$\hat{R}_1 = \exp(i \arg r + 2ik\hat{z}_1) \tag{2}$$

where "$\arg r$" is a constant phase (real) and $2\hat{z}_1$ is the optical path length of the first arm. k is wave vector as usual. Since $\hat{z}$ is a hermitian operator, $\hat{R}$ is a unitary operator. The annihilation operator on one of the output ports, which was named "d-mode" as in Ref. [1][2], would be a linear combination of those from both arms. The other output port was called "c-mode". Therefore,

$$d = (\hat{R}_1 a_1 + \hat{R}_2 a_2)/\sqrt{2} \quad \text{and} \quad c = e^{i\Psi_c}(\hat{R}_1 a_1 - \hat{R}_2 a_2)/\sqrt{2} \tag{3}$$

where the phase term $e^{i\Psi_c}$ was kept for generality. Energy conservation was fulfilled.

To treat photon shot noise and the fluctuation or radiation pressure separately was criticized by Marx [7] on the ground that it seems to assume some knowledge of the routes through the interferometer followed by individual photons, which is contrary to our understanding of quantum mechanics today. Loudon proposed a unified calculation [1] by introducing a coupling constant C. Ni pointed out that the position of the mirror itself should be a quantum-mechanical operator [2]. It'll contribute its intrinsic uncertainty to the total quantum uncertainty of the position of mirrors. In the low intensity limit, it was shown that the total uncertainty can be expressed as the sum of all three noise sources. Situation gets complicated at high intensity. The independence and correlation at different intensities among these noise moments provide ways to monitor and control a macroscopic quantum-mechanical object [3].

The Loudon-Ni model can be rephrased as the following:

$$k\hat{z}_1 = k\hat{z}_{1_i} - C_1' a_1{}^\dagger a_1 \qquad \text{and} \qquad k\hat{z}_2 = k\hat{z}_{2_i} - C_2' a_2{}^\dagger a_2 \tag{4}$$

where C_1' is the coupling constant which might be different from each mirror. The prime was to differ our notation from the previous one. There might be a factor of 2 difference. $\hat{z}_{1_i}$ corresponds to the position operator of the first mirror without including the coupling effect. $\hat{z}$ is the mirror position operator we measured finally.

The coupling constant C' can be estimated as below. Suppose the mirror was hanged as a simple pendulum with mass M and length l. Its restoring force would be $\Delta x \cdot Mg/l$ where Δx is a small displacement and g is the gravitational acceleration. Each photon suffers a momentum change $2\hbar k$ after been reflected back from the mirror. On balance we got $C' = 2\hbar k^2 l/(Mg)$

Photon detector usually has its own quantum efficiency, denoted by ξ, which was assumed identical for both c-mode and d-mode. The measured photon intensity would, therefore, differ

from $\langle d^\dagger d\rangle$ and $\langle c^\dagger c\rangle$ by a factor ξ. We've considered two detection schemes as in Ref. [8]. The first is direct detection:

$$\langle m\rangle_{\rm dir} = \langle m_d\rangle = \xi\langle d^\dagger d\rangle. \tag{5}$$

The other is difference detection, which is the difference between the two output ports:

$$\langle m\rangle_{\rm diff} = \langle m_c\rangle - \langle m_d\rangle = \xi(\langle c^\dagger c\rangle - \langle d^\dagger d\rangle). \tag{6}$$

Only the variances of difference detection were presented in this article:

$$\begin{aligned}(\Delta m)^2_{\rm diff} &= \xi^2(\langle c^\dagger c^\dagger c c\rangle + \langle d^\dagger d^\dagger d d\rangle - 2\langle c^\dagger d^\dagger c d\rangle - \langle c^\dagger c\rangle^2 - \langle d^\dagger d\rangle^2 + 2\langle c^\dagger c\rangle\langle d^\dagger d\rangle)\\ &\quad + \xi(\langle c^\dagger c\rangle + \langle d^\dagger d\rangle)\end{aligned} \tag{7}$$

or, equivalently, in its expansion form:

$$\begin{aligned}(\Delta m)^2_{\rm diff} &= \xi^2\big[2\langle a_1^\dagger a_1 a_2^\dagger a_2\rangle - (\langle a_1^\dagger \hat{R}_1^\dagger \hat{R}_2 a_2\rangle + \langle a_2^\dagger \hat{R}_2^\dagger \hat{R}_1 a_1\rangle)^2\\ &\quad + \langle a_1^\dagger \hat{R}_1^\dagger a_1^\dagger \hat{R}_1^\dagger \hat{R}_2 a_2 \hat{R}_2 a_2\rangle + \langle a_2^\dagger \hat{R}_2^\dagger a_2^\dagger \hat{R}_2^\dagger \hat{R}_1 a_1 \hat{R}_1 a_1\rangle\big] + \xi(\langle a_1^\dagger a_1\rangle + \langle a_2^\dagger a_2\rangle).\end{aligned} \tag{8}$$

These are what we want to calculate with our various inputs. It would be more complicated and model-dependent when considering photons with different frequencies.

3 The Solutions

First, a solution for coherent state - squeezed state inputs was solved. We'll have to deal with an expectation value, $\langle \exp[A(a^\dagger a + b^\dagger b) + B(b^\dagger a + a^\dagger b)]\rangle$, where the state vector $|\,\rangle_a$ is in coherent state $|\alpha\rangle$, $|\,\rangle_b$ is in general squeezed state $|\beta,\zeta\rangle$. $\zeta = se^{i\theta}$, where s is squeezing factor and θ is squeezing angle. The coherent parameters α and β are complex numbers with their phases ϕ_α and ϕ_β respectively.

Since coherent states $|\alpha\rangle$ is a's eigenstates, it is reasonable to reorder those operators as

$$\exp[A(a^\dagger a + b^\dagger b) + B(b^\dagger a + a^\dagger b)] = \exp(Ua^\dagger b)\exp(Va^\dagger a)\exp(Yb^\dagger b)\exp(Zb^\dagger a). \tag{9}$$

To get the coefficients U, V, Y, Z, it would be much easier to use faithful matrix representations of those four operators. Suppose $X_{11}, X_{22}, X_{12}, X_{21}$ are their corresponding matrices, which satisfy the same commutators as $a^\dagger a, b^\dagger b, a^\dagger b$ and $b^\dagger a$ do. It is not difficult to find a set of faithful matrices (2×2) which have the same relations. The operators equation becomes a matrix equation after this substitution. Solving this matrix equation we got

$$U = Z = \tanh B. \quad V = A - \ln(\cosh B) \quad \text{and} \quad Y = A + \ln(\cosh B). \tag{10}$$

After reordering, the calculation of the expectation value on a-mode (coherent state input) can be carried out. $\langle\alpha|\exp(Va^\dagger a)|\alpha\rangle$ was given in Ref. [2]. What left would be a calculation on b-mode (squeezed state input), which looks like $\langle\beta,\zeta|\exp(U\alpha^* b)\exp(Yb^\dagger b)\exp(U\alpha b^\dagger)|\beta,\zeta\rangle$. A squeezed state can be expressed as a vacuum state operated by a squeezing operator $S(s,\theta)$ and a displacement operator $D(a,\alpha)$ where

$$D(b,\beta) = \exp(\beta b^\dagger - \beta^* b) \quad \text{and} \quad S(s,\theta) = \exp[(s/2)(e^{-2i\theta}b^2 - e^{2i\theta}b^{\dagger 2})]. \tag{11}$$

Substitute this definition of squeezed state into b-mode, with some algebra, we may express its expectation value as the vacuum expectation value of a product of seperating terms

$$\langle\beta,\zeta|e^{U a^\dagger b}e^{Y b^\dagger b}e^{U a b^\dagger}|\beta,\zeta\rangle = \langle 0|e^{A(b^2/2)}e^{B b^\dagger}e^{C b}e^{Y(b^\dagger b+1/2)}e^{D b^\dagger}e^{E b}e^{F(b^{\dagger 2}/2)}|0\rangle \times (\text{a number}). \quad (12)$$

To solve this, we turned those operators into their normal ordering. Those operators form a Lie algebra. With corresponding commutators and their structure constants it is possible to find a faithful matrix representation [6]. Therefore, the operator equation could be reordered as

$$\begin{aligned} & \langle 0|\exp[A(b^2/2)]\exp[Bb^\dagger]\exp[Cb]\exp[Y(b^\dagger b+1/2)]\exp[Db^\dagger]\exp[Eb]\exp[F(b^{\dagger 2}/2)]|0\rangle \\ = \; & \langle 0|\exp[J(b^{\dagger 2}/2)+Lb^\dagger]\exp[M(b^\dagger b+1/2)]\exp[N(b^2/2)+Pb]\exp[Q]|0\rangle \\ = \; & \exp(M/2)\exp(Q) \end{aligned} \quad (13)$$

and, its corresponding matrix equation can be solved easily. We got

$$e^{-M} = e^{-Y}(1-AFe^{2Y}) \quad (14)$$

$$\begin{aligned} Q = \; & (e^M/2)(2CD+2CEF+2ABD+2ABEF+AB^2e^{-Y} \\ & +E^2Fe^{-Y}+C^2Fe^{Y}+AD^2e^{Y}+2ABCFe^{Y}+2ADEFe^{Y}). \end{aligned} \quad (15)$$

It is now straightforward to evaluate the uncertainty of photon measurements. The expectation value of the photon number of d-mode is

$$\langle d^\dagger d\rangle = (1/2)(\langle n\rangle + |\beta|^2 + |\rho_s|^2) + (E_0|h_0|/2)\langle\cos 2\hat{\phi}'\rangle \quad (16)$$

where $|h_0|$ is roughly proportional to the input intensity and E_0 is an exponential factor which would be discussed later. ρ_s is squeezing related and $\hat{\phi}'$ is essentially the difference in optical path length with additional terms.

$$\hat{\phi}' = (1/2)[H_0 + 2k(\hat{z}_{2i}-\hat{z}_{1i}) - \mathrm{Im}(Q)] \quad (17)$$

$$h_0 = |h_0|e^{iH_0} = \langle n\rangle + \frac{\alpha g' - \alpha^* f' - |\rho_s|^2 e^{Y'}}{\rho_c^2 - |\rho_s|^2 e^{2Y'}} - \frac{f'g'}{(\rho_c^2-|\rho_s|^2e^{2Y'})^2} \quad (18)$$

$$\begin{aligned} E_0 = (\rho_c^2-|\rho_s|^2e^{2Y})^{-\frac{1}{2}}\exp\Big\{\frac{-(1-e^Y)}{1-|\Gamma|^2e^{2Y}}[\langle n\rangle(1+|\Gamma|^2e^Y-|\Gamma|(1+e^Y)\cos(\theta-2\phi_\alpha)) \\ +|\beta|^2(1-|\Gamma|^2e^Y+|\Gamma|(1-e^Y)\cos(\theta-2\phi_\beta))]\Big\} \end{aligned} \quad (19)$$

$$\mathrm{Im}(Q) = \frac{-iUe^Y}{1-|\Gamma|^2e^{2Y}}[(\alpha^*\beta+\alpha\beta^*)(1-|\Gamma|^2e^Y)+(\alpha^*\beta^*\Gamma+\alpha\beta\Gamma^*)(1-e^Y)] \quad (20)$$

$$f' = (\rho_c^2-|\rho_s|^2e^{Y'})\beta + \rho_c\rho_s(1-e^{Y'})\beta^* + |\rho_s|^2e^{2Y'}U'\alpha - \rho_c\rho_s e^{Y'}U'\alpha^* \quad (21)$$

$$g' = (\rho_c^2-|\rho_s|^2e^{Y'})\beta^* + \rho_c\rho_s^*(1-e^{Y'})\beta + |\rho_s|^2e^{2Y'}U'\alpha^* - \rho_c\rho_s^*e^{Y'}U'\alpha \quad (22)$$

$$U' = i\tan\Sigma C', \quad Y' = -i\Delta C' + \ln(\cos\Sigma C') \quad (23)$$

$$U = -i\tan(\Sigma C'), \quad Y = i\Delta C' + \ln(\cos\Sigma C') \quad (24)$$

where $\rho_c = \cosh s$, $\rho_s = e^{i\theta}\sinh s$, $\Gamma = \rho_s/\rho_c$, $\Delta C' = C_2' - C_1'$ and $\Sigma C' = C_2' + C_1'$. Similarly,

$$\langle c^\dagger c - d^\dagger d\rangle = -E_0|h_0|\langle\cos 2\hat{\phi}'\rangle \tag{25}$$

for difference detection. Basically, the Michelson interferometer is a transducer which turns a change of the arm length into a change of light intensity. The measured intensity $\langle m\rangle$ and its variance can be transformed back to the uncertainty of arm length, or more precisely, the difference of the positions of two mirrors. We may write down this uncertainty as

$$(\Delta Z_{total})_{\rm diff} = \sqrt{(\Delta m)^2_{\rm diff}}/(2\xi k E_0|h_0||\langle\sin 2\hat{\phi}'\rangle|) \tag{26}$$

where $(\Delta m)^2_{\rm diff}$ was given by Eq. (7) or, more explicitly, by Eq. (8). This is just the inverse of signal to noise ratio. The final result is

$$\begin{aligned}(\Delta Z_{total})^2_{\rm diff} &= \frac{(\langle n\rangle + |\beta|^2)^2 + 3|\rho_s|^4 + |\rho_s|^2 - 4\langle n\rangle|\beta|^2\cos^2(\phi_\alpha - \phi_\beta)}{8k^2E_0^2|h_0|^2\langle\sin 2\hat{\phi}'\rangle^2} \\ &+ \frac{|\beta|^2[2|\rho_s|^2 - \rho_c|\rho_s|\cos(\theta - 2\phi_\beta)] + \langle n\rangle\rho_c|\rho_s|\cos(\theta - 2\phi_\alpha)}{4k^2E_0^2|h_0|^2\langle\sin 2\hat{\phi}'\rangle^2} \\ &+ \frac{E''|h_2|\langle\cos[4\hat{\phi}' + H_2 - 2H_0 + {\rm Im}(Q'') + 2{\rm Im}(Q)]\rangle}{8k^2E_0^2|h_0|^2\langle\sin 2\hat{\phi}'\rangle^2} \\ &- \frac{\langle\cos 2\hat{\phi}'\rangle^2}{4k^2\langle\sin 2\hat{\phi}'\rangle^2} + \frac{\langle n\rangle + |\beta|^2 + |\rho_s|^2}{4\xi k^2E_0^2|h_0|^2\langle\sin 2\hat{\phi}'\rangle^2}\end{aligned} \tag{27}$$

for difference detection. Where $\langle n\rangle = |\alpha|^2$ is the intensity of the input coherent state on a-mode. h_2 is shorthand notations of complicated modification on intensity square, H_2 is its phase. E'' is another exponential factor which decreases the interference terms in ΔZ_{total}. ${\rm Im}(Q)$ and ${\rm Im}(Q'')$ are imaginary parts of Q and Q'', which came from solving the matrix equation Eq. (13) or its similar version. All of them can be evaluated exactly as follow.

$$\begin{aligned}h_2 = |h_2|e^{iH_2} &= \Big[\langle n\rangle + \frac{\alpha g'' - \alpha^* f'' - 2|\rho_s|^2e^{Y''}}{\rho_c^2 - |\rho_s|^2e^{2Y''}} - \frac{f''g''}{(\rho_c^2 - |\rho_s|^2e^{2Y''})^2}\Big]^2 + \frac{\rho_c^2|\rho_s|^2 - 2|\rho_s|^4e^{2Y''}}{(\rho_c^2 - |\rho_s|^2e^{2Y''})^2} \\ &- \frac{\rho_c\rho_s^*}{\rho_c^2 - |\rho_s|^2e^{2Y''}}(\alpha - \frac{f''}{\rho_c^2 - |\rho_s|^2e^{2Y''}})^2 - \frac{\rho_c\rho_s}{\rho_c^2 - |\rho_s|^2e^{2Y''}}(\alpha^* + \frac{g''}{\rho_c^2 - |\rho_s|^2e^{2Y''}})^2\end{aligned} \tag{28}$$

U'' and Y'' are similar to U' and Y' but with $\Delta C'$ and $\Sigma C'$ replaced by $2\Delta C'$ and $2\Sigma C'$. f'', g'', E'' and ${\rm Im}(Q'')$ are similar to f, g, E_0 and ${\rm Im}(Q)$ except $Y(Y')$ and $U(U')$ were replaced by Y'' and U''. In our calculation, it was assumed that $C_1' = C_2' \equiv C'$.

We now turn to the photon number states input. Photon number state is a quantum state without classical correspondence. Its second order coherence is minimum such that its number variance vanished.

Suppose the input state is $|n_a\rangle_a \otimes |n_b\rangle_b$ with $|n_a\rangle_a = (a^\dagger)^{n_a}/\sqrt{n_a!}|0\rangle$ and $|n_b\rangle_b = (b^\dagger)^{n_b}/\sqrt{n_b!}|0\rangle$ where n_a and n_b are real numbers. With a different reordering from Eq. (9) and the assumption $\Delta C' = 0$, we have

$$\begin{aligned}\langle d^\dagger d\rangle &= \frac{1}{2}(n_a + n_b) + \frac{1}{2}\langle\cos[2k(\hat{z}_{2_i} - \hat{z}_{1_i})]\rangle(\cos 2C')^{n_b - n_a} \\ &\times\{n_a\cos 2C'{}_2F_1(1 + n_b, 1 - n_a, 1; \sin^2 2C') - \frac{n_b}{\cos 2C'}{}_2F_1(n_b, -n_a, 1; \sin^2 2C')\}\end{aligned} \tag{29}$$

where ${}_2F_1(a,b,c;z)$ is hypergeometric function. In perfect detection, that is, $\xi = 1$, the variance of the photon detection becomes

$$\begin{aligned}\langle(\Delta m)^2\rangle = &\frac{1}{8}n_a(n_a+1)+\frac{1}{8}n_b(n_b+1)-\frac{1}{4}\langle\cos[2k(\hat{z}_{2i}-\hat{z}_{1i})]\rangle^2(\cos 2C')^{2(n_b-n_a)}\\ &\times[n_a\cos 2C'\,{}_2F_1(1+n_b,1-n_a,1;\sin^2 2C')-\frac{n_b}{\cos 2C'}\,{}_2F_1(n_b,-n_a,1;\sin^2 2C')]^2\\ &+\frac{1}{8}\langle\cos[4k(\hat{z}_{2i}-\hat{z}_{1i})]\rangle(\cos 4C')^{n_b-n_a}\\ &\times\Big[n_a(n_a-1)\cos^2 4C'\,{}_2F_1(1+n_b,2-n_a,1;\sin^2 4C')\\ &+n_b(n_b-1)\sec^2 4C'\,{}_2F_1(n_b-1,-n_a,1;\sin^2 4C')\\ &-4n_an_b\,{}_2F_1(n_b,1-n_a,1;\sin^2 4C')\\ &-n_an_b(n_a-1)(n_b-1)\sin^2 4C'\,{}_2F_1(1+n_b,2-n_a,3;\sin^2 4C')\Big].\end{aligned}\tag{30}$$

There are relations between a hypergeometric function and its contiguous functions. Further simplification is possible.

4 Discussion

A low intensity limit can be obtained easily [1] while b-mode was in vacuum state. In short, $(\Delta Z_{total})^2 \geq C'/k^2$. We have searched in a limited parameter space and found no violation of this inequality (within error). Though, it is *not* a proof of that limit. At very high intensity, the reflectance $\hat{\mathrm{R}}$ has little effect. The noise behavior can be explained by the mixing of two input states. High order moments are needed to characterize such a superposition. On the other hand, that noise can be eliminated by setting two input states at nearly the same intensity. Nevertheless, there is still an exponential factor E_0 in signal (cf. Eq. (25) and Eq. (26)). It doesn't show up in classical solution and it *always* decreases the signal. We left further discussion to another work.

References

[1] R. Loudon, *Phys. Rev. Lett.* **47**, 815 (1981).

[2] W.-T. Ni, *Phys. Rev.* **D35**, 3002 (1987).

[3] W.-T. Ni, "Controlling a Macroscopic Quantum State by Light Shining" in *Quantum Control and Measurement*. H. Ezawa & Y. Murayama (edit.). Elsevier Science Publishers B. V., 1993.

[4] C. M. Caves, *Phys. Rev. Lett.* **45**, 75 (1980).

[5] See A. F. Pace *et al.*, *Phys. Rev.* **A47**, 3173 (1993) and references therein.

[6] W. M. Zhang, D. H. Feng and R. Gilmore, *Rev. Mod. Phys.* **62**, 867 (1990).

[7] B. Marx, *Nature* **287**, 276 (1980).

[8] C. M. Caves, *Phys. Rev.* **D23**, 1693 (1981).

NEXT
DOCUMENT

VIBRATIONAL SCHROEDINGER CATS

Z. Kis, J.Janszky
Research Laboratory for Crystal Physics
P.O. Box 132, H-1502 Budapest, Hungary

An. V. Vinogradov*, T.Kobayashi†
† *Department of Physics, Faculty of Science, University of Tokyo*
7-3-1 Hongo, Bunkyo-ku, Tokyo 113, Japan
* *P. N. Lebedev Physics Institute, 117924 Moscow, Russia*

Abstract

The optical Schroedinger cat states are simple realizations of quantum states having non-classical features. It is shown that vibrational analogues of such states can be realized in an experiment of double pulse excitation of vibrionic transitions. To track the evolution of the vibrational wave packet we derive a non-unitary time evolution operator so that calculations are made in a quasi Heisenberg picture.

1 Introduction

The analog of the classical harmonic oscillation in the quantum mechanics is the coherent state $|\alpha\rangle$ defined as an eigenstate of the annihilation operator $b|\alpha\rangle = \alpha|\alpha\rangle$. Both in the position and in the momentum representations the absolute square of its wave function has a Gaussian shape. It performs harmonic vibration in time with an amplitude that depends on the initial excitation. The superposition of two coherent states [1]

$$|+\rangle = N_{|+\rangle}(|\alpha\rangle + |-\alpha\rangle), \qquad (1,$$

$$N_{|+\rangle} = \frac{1}{\sqrt{2+2e^{-2\alpha^2}}},$$

situated sufficiently far from each other in the phase-space can be considered as the superposition of two macroscopically distinguishable quasiclassical states called Schroedinger cat state.

Recently great interest has been paid to such superposition states in quantum optics [2-11]. Non-classical features of Schroedinger cat states i.e. squeezing, [4] sub-Poissonian statistics, oscillation in photon statistics, etc. were discussed rather widely. It was shown [5, 7] how the quantum interference between the coherent states involved in the superposition leads to the occurrence of non-classical features. Due to the interference a fringe pattern appears between the Gaussian bells representing the coherent states in the Wigner function picture. This fringe pattern is transformed characteristically when the positions or the number of the coherent states changes. There are several promising schemes to produce nonclassical states of light using the concept of Schroedinger cat states [8, 9].

A wide interest was addressed to wave packet formation and motion during Franck-Condon transitions in both theoretical and experimental points of view [4, 10, 11]. In this paper we shall discuss the possibilities of producing Schroedinger cat like superpositions of the vibrational states during Franck-Condon vibrionic transitions in molecules or in crystals. As we shall see such states can be created by two short pulses separated in time appropriately.

2 The model Hamiltonian

Let us consider a one-vibrational-mode model specified by the adiabatic Hamiltonians

$$\hat{H}_i = \epsilon_i + \frac{\hat{p}^2}{2M} + \frac{M\omega_i^2}{2}(\hat{q} + \gamma_i)^2, \tag{2}$$

$$\hat{H}_e = \epsilon_e + \frac{\hat{p}^2}{2M} + \frac{M\omega_i^2}{2}\hat{q}^2, \tag{3}$$

corresponding to the molecular vibrations in initial (i) and excited (e) electronic states. Here $\epsilon_{i,e}$ are electronic energy levels and $\omega_{i,e}$ vibrational frequencies.

In terms of the annihilation phonon operators b associated with the vibrational potential of the excited states,

$$\hat{q} = \sqrt{\frac{\hbar}{2M\omega_e}}(\hat{b}^\dagger + \hat{b}), \quad \hat{p} = i\sqrt{\frac{\hbar M\omega_e}{2}}(\hat{b}^\dagger - \hat{b}), \tag{4}$$

the Hamiltonians of Eq. (2,3) have the forms

$$\hat{H}_i = \epsilon_i + \frac{M\omega_i^2}{2}q_i^2 + \hbar\omega_i\{\frac{1}{4}(\frac{\omega_i}{\omega_e} + \frac{\omega_e}{\omega_i})(\hat{b}^\dagger\hat{b} + \hat{b}\hat{b}^\dagger) +$$

$$+\frac{1}{4}(\frac{\omega_i}{\omega_e} - \frac{\omega_e}{\omega_i})(\hat{b}^\dagger\hat{b}^\dagger + \hat{b}\hat{b})\} + \frac{\hbar\omega_i^2 q_i}{\omega_e}\sqrt{\frac{M\omega_e}{2\hbar}}(\hat{b}^\dagger + \hat{b}) \tag{5}$$

$$\hat{H}_e = \epsilon_e + \frac{1}{2}\hbar\omega_e(\hat{b}^\dagger\hat{b} + \hat{b}\hat{b}^\dagger). \tag{6}$$

The Hamiltonian of the initial state can be diagonalized by the unitary operator

$$\hat{\Sigma} = e^{-g(\hat{b}^\dagger - \hat{b})}e^{r[\hat{b}^2 - \hat{b}^{\dagger 2}]/2}, \tag{7}$$

$$g = q_i\sqrt{\frac{M\omega_e}{2\hbar}}, \quad r = \frac{1}{2}ln\frac{\omega_i}{\omega_e}.$$

Here g and r are displacement and squeezing parameters correspondingly. The vibrational ground state of the initial electronic level is

$$|\,0\rangle_i = \hat{\Sigma}\,|\,0\rangle_e, \tag{8}$$

where $|\,0\rangle_e$ is the vibrational ground state of the excited electronic level.

The Hamiltonian $\hat{H}'(t)$ describing the interaction with the external field has the form

$$\hat{H}'(t) = \frac{1}{2}d_{ie}E(t)\hat{a}_e^\dagger\hat{a}_i + \frac{1}{2}d_{ie}^* E^*(t)\hat{a}_i^\dagger\hat{a}_e, \tag{9}$$

where

$$E(t) = e(t)exp(-i\Omega_0 t), \tag{10}$$

$\hat{a}_{i(e)}$ is the annihilation operator of the $i(e)$-th electron level, d_{ie} the dipole matrix element of the electronic transition, $\mid e(t) \mid^2$ and Ω_0 are the envelope function and the central frequency of the exciting pulse.

Suppose the electronic transition takes place instantaneously. The emerging vibrational wave packet is described by Eq. (8). The time evolution of the wave packet in the excited level is driven by the unitary operator $\exp[-(i/\hbar)\hat{H}_e t]$. So the evolution of the vibration from $-t_0$ until t is described by the unitary operator

$$\hat{G}(t - t_0) = e^{-\frac{i}{\hbar}\hat{H}_e(t-t_0)}\hat{\Sigma}. \tag{11}$$

Let us assume that initially, at $t = -\infty$ the system is in the ground state $\mid i\rangle \mid 0\rangle_i$. After the exciting pulse has passed according to the first order perturbation theory the electronic-vibrational wave function takes the form:

$$\mid \Psi, t\rangle = \mid i, t\rangle \mid 0\rangle_i - i\frac{E_0 d_{ie}}{2\hbar} \mid e, t\rangle \mid \{E(t)\}\rangle_e. \tag{12}$$

Here $\mid \{E(t)\}\rangle_e$ is unnormalized vibrational wave function of the molecule in the excited electronic state:

$$\mid \{E(t)\}\rangle_e = \int_{-\infty}^{t} d\tau E(\tau)e^{i\Delta\tau}\hat{G}(t - \tau) \mid 0\rangle_e, \tag{13}$$

where $\Delta = \bar{\Omega} + (\omega_e - \omega_i)/2$, $\bar{\Omega} = (\epsilon_e - \epsilon_i)/\hbar$. The timedependent part of $\hat{G}(t)$ is the exponential of $\hat{H}_e$. Assume the pulse duration is short compared with the observation time t. In this case we can put the upper limit of the integration to infinity. This condition means we perform measurements after the excitation pulse has passed. The integration in Eq. (13) can be done explicitly. Separating the operator in Eq. (13) in front of the vacuum the non-unitary time evolution operator is

$$\hat{T}(t) = \exp\left(-\frac{i}{\hbar}\hat{H}_e t\right)\exp\left[-\frac{(\hat{H}_e/\hbar - \delta)^2}{2u^2}\right]\hat{\Sigma}, \tag{14}$$

where $\delta = \Delta - \Omega_0$.

In the following sections we shall investigate the properties of the vibrational wave function of Eq. (13) considering twin exciting laser pulses. For the sake of simplicity we suppose that there is no change of the vibrational frequency due to the electronic transition ($\omega_e = \omega_i = \omega$). In this case the operator $\hat{\Sigma}$ in Eq. (13) simplifies to a displacement operator $\hat{D}$ and the excited vibrational wave function has the form

$$\mid \{E(t)\}\rangle_e = \exp\left(-\frac{i}{\hbar}\omega_e\hat{n}t\right)\exp\left[-\frac{(\omega_e\hat{n} - \delta)^2}{2u^2}\right] \mid g\rangle_{coh}, \tag{15}$$

where $\mid g\rangle_{coh}$ is a coherent state with respect to the phonon operator $\hat{b}$.

3 Double pulse excitation

Let us consider two identical Gaussian shaped pulses following each other by an interval T_1

$$E(t) = \frac{E_0}{2\pi^{\frac{1}{4}}} e^{-\frac{u^2}{2}(t+\frac{T_1}{2})^2 - i\Omega_0(t+\frac{T_1}{2})} + \frac{E_0}{2\pi^{\frac{1}{4}}} e^{-\frac{u^2}{2}(t-\frac{T_1}{2})^2 - i\Omega_0(t-\frac{T_1}{2}) - i\phi}, \tag{17}$$

here ϕ is a possible additional phase difference between the subpulses.

The vibrational state produced by such a twin pulse excitation has the form

$$\mid \{u, T_1, \delta, \phi\}\rangle_e = e^{-i\Omega_0 \frac{T_1}{2}} \mid u, (t + \frac{T_1}{2})\rangle + e^{i\Omega_0 \frac{T_1}{2} - i\phi} \mid u, (t - \frac{T_1}{2})\rangle, \tag{18}$$

$$\mid u, t\rangle = \exp\left(-\frac{i}{\hbar}\omega_e \hat{n} t\right) \exp\left[-\frac{(\omega_e \hat{n} - \delta)^2}{2u^2}\right] \mid g\rangle_{coh} \tag{19}$$

To investigate the quantum properties of the superposition state of Eq. (18) it is convenient to consider its Wigner function

$$W(\alpha) = \frac{1}{\pi^2} \int e^{\eta^* \alpha - \eta \alpha^* - \frac{1}{2}|\eta|^2} {}_e\langle \{u, T, \phi\} \mid e^{\eta b^\dagger} e^{-\eta^* b} \mid \{u, T, \phi\}\rangle_e \, d^2\eta. \tag{20}$$

For extremely short pulses we have coherent superposition states which are the vibrational analog of the so called optical Schroedinger cat states. The Wigner function and the time dependence of the absolute square of the wave function are shown in Fig. 1a and Fig. 1b correspondingly. The Wigner function consists of two bells of the superposed coherent states and an interference fringe between them. If the coherent states are far away the fringe has a lot of well-pronounced peaks. On the contrary, if the coherent states are near enough the fringe has only few peaks. In this case the fringe can partially merge with the bells and, depending on the phase between the component states may decrease the uncertainty of one of the quadratures $\hat{X}_+ = b + b^\dagger$ or $\hat{X}_- = -i(b - b^\dagger)$ below the vacuum level.

4 Discussion

Baumert *et. al.* first excited the Na_2 molecule by a short laser pulse [12]. Applying a second laser pulse they excited the state once more. Depending on the time delay between the two successive pulses they had a molecule on another excited level or dissociated fragments. We suggest a similar experiment with a double pulse primary excitation leading to a Schroedinger vibrational state on the level e (Fig. 2). Applying a third pulse when the two parts of the Schroedinger cat state are furthest from each other one obtains a superposition of a molecule with its fragment.

This chemical cat state can lead us very near to the original paradox of Schroedinger. Let us suppose that this molecular superposition is superposition of the undamaged form of a virus's DNA with a denaturalized variant of the same virus. The resulting 'Schroedinger virus state' would be, in fact, a quantum mechanical superposition of a "living" and a 'dead' virus.

Acknowledgments

This work was supported by the National Research Scientific Fund (OTKA) of Hungary, under Contracts No. T14083, T017386.

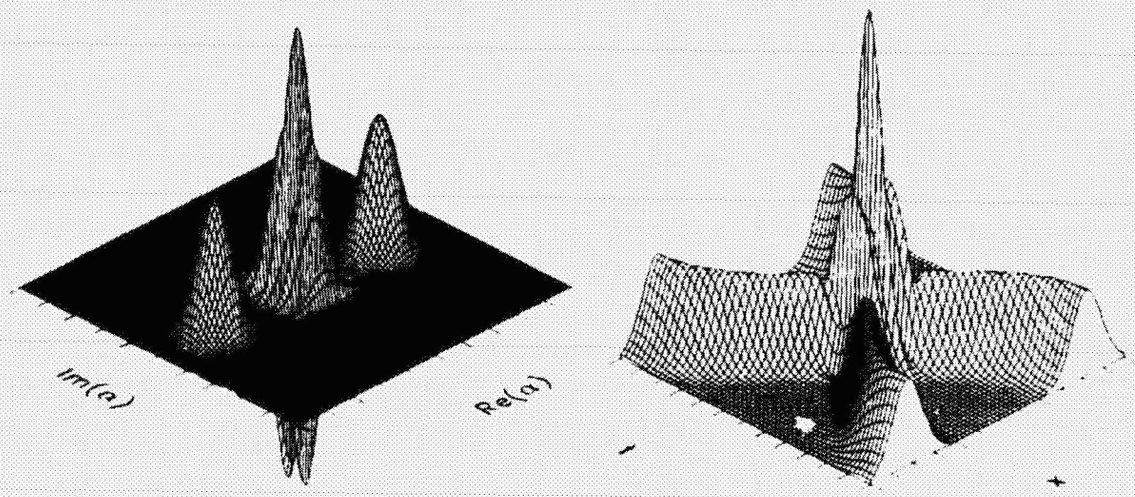

Fig. 1 The Wigner function (Fig. 1a) and the time-dependence of the absolute square of the wave function $|\psi(q)|^2$ (Fig. 1b) of the Schroedinger cats state. The prominent fringe structure between the coherent states' Gaussian bells of the Wigner function is caused by the quantum interference between the two parts of the superposition state. A similar interference fringe of the wave function can be found around $t = \pm\frac{T}{4}$, otherwise in the bigger part of the period $|\psi(q)|^2$ consists of two Gaussians representing the two superposed coherent states.

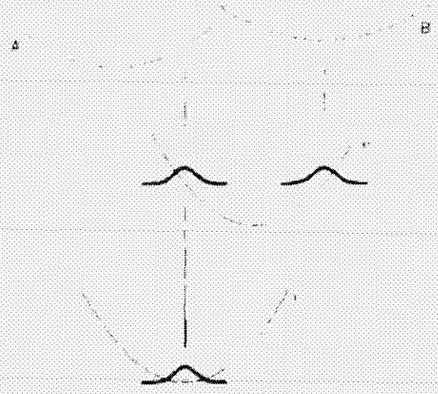

Fig. 2 The schematic terms for creation of a chemical superposition state. First either by double or appropriately chirped single pulse one prepares a vibrational superposition state on level e. At some moment of its separation by some secondary pulse(s) one can transfer the molecule into molecule A represented by the upper left term and simultaneously into molecule B shown as the upper right term, creating this way a chemical "Schroedinger cat" state.

References

[1] V. V. Dodonov, I. A. Malkin, and V. I. Man'ko, Physica **72**, 597 (1974).

[2] B. Yurke and D. Stoler, Phys. Rev. Lett. **57**, 13 (1986).

[3] M. Hillery, Phys.Rev. A **36**, 3796 (1987).

[4] J. Janszky and An. V. Vinogradov, Phys. Rev. Lett. **64**, 2771 (1990).

[5] W. Schleich, M. Pernigo, and Fam Le Kien, Phys. Rev. A **44**, 2172 (1991); V. Buzek and P. L. Knight, Opt.Comm. **81**, 331 (1991); Jinzuo Sun, Jisuo Wang, and Chuankui Wang, Phys. Rev. A **46**, 1700 (1992).

[6] M. S. Kim and V. Buzek, Phys. Rev. **A 46**, 4239 (1992), A **47**, 610 (1993); I. Jex and V. Buzek, J. Mod. Opt. **40**, 771 (1993).

[7] J. Janszky, P. Domokos and P. Adam, Phys. Rev. A **48**, 2213 (1993).

[8] M. Brune, S. Haroche, V. Lefevre, J. M. Raimond, and N. Zagury, Phys. Rev. Lett. **65**, 976 (1990).

[9] T. Ogawa, M. Ueda and N. Imoto, Phys. Rev. Lett. **66**, 1046 (1991); B. Sherman and G. Kurizki, Phys. Rev. A **45**, 7677 (1992).

[10] An. V. Vinogradov and J. Janszky, Sov. Phys. Solid State, **27**, 598 (1985); D. J. Tannor and S. A. Rice, J. Chem. Phys. **83**, 5013 (1985); M. J. Rosker, F. W. Wise and C. L. Tang, Phys. Rev. Lett. **57**, 321 (1986); P. Kowalczyk, C. Radzewicz, J. Mostowski, and I. A. Walmsley, Phys. Rev. A **42**, 5622 (1990); T. J. Dunn, J. N. Sweetser, J A. Walmsley, and C. Radewicz, Phys. Rev. Lett. **70**, 3389 (1993); G. M. Garraway and S. Stenholm, Phys. Rev. **A 46**, 1413 (1992); T. Szakacs, J. Somloi, and A. Lorincz, Chem. Phys. **172**, 1 (1993); I. Averbukh and M. Saphiro, Phys. Rev. **A 47**, 5086 (1993).

[11] J. Janszky, T. Kobayashi, and An. V. Vinogradov, Opt. Commun. **76**, 30 (1990).

[12] T. Baumert, M. Grosser, R. Thalweiser, and G. Gerber, Phys. Rev. Lett. **67**, 3753 (1991).

NEXT
DOCUMENT

CORRELATED LIGHT AND SCHRÖDINGER CATS

V. I. Man'ko
Lebedev Physical Institute
53 Leninsky Prospekt, Moscow 117333, Russia

Abstract

The Schrödinger cat male and female states are discussed. The Wigner and Q-functions of generalized correlated light are given. Linear transformator of photon statistics is reviewed.

1 Introduction

The integral of motion which is quadratic in position and momentum was found for classical oscillator with time-dependent frequency by Ermakov [1]. Two time-dependent integrals of motion which are linear forms in position and momentum for the classical and quantum oscillator with time-dependent frequency were found in [2]; for a charge moving in varying in time uniform magnetic field, this was done in [3]. For the multimode nonstationary oscillatory systems such new integrals of motion, both of Ermakov's type (quadratic in positions and momenta) and linear in position and momenta, generalizing the results of [2] were constructed in [4]. We will consider below the parametric oscillator using the integrals of motion.The Wigner function of multimode squeezed light is studied using such special functions as multivariable Hermite polynomials. The theory of parametric os cillator is appropriate to consider the problem of creation of photons from vacuum in a resonator with moving walls (with moving mirrors) which is the phenomenon based on the existence of Casimir forces (so-called nonstationary Casimir effect). The resonator with moving boundaries (moving mirrors, media with time-dependent refractive index) produces also effect of squeezing in the light quadratures. In the high energy physics very fast particle collisions may produce new types of states of boson fields (pions, for example) which are squeezed and correlated states studied in quantum optics but almost unknown in particle physics, both theoretically and experimentally.

2 Multimode Quadratic Systems

The generic nonstationary linear system has the Hamiltonian

$$H = \frac{1}{2}\mathbf{Q}B(t)\mathbf{Q} + \mathbf{C}(t)\mathbf{Q}, \tag{1}$$

where we use 2N-vectors $\mathbf{Q} = (p_1, p_2, \ldots, p_N, q_1, q_2, \ldots, q_N)$ and $\mathbf{C}(t)$, as well as 2N×2N-matrix $B(t)$, the Planck constant $\hbar = 1$. This system has 2N linear integrals of motion [5], [6] which may be written in vector form

$$\mathbf{Q}_0(t) = \Lambda(t)\mathbf{Q} + \Delta(t). \tag{2}$$

The real symplectic matrix $\Lambda(t)$ is the solution to the system of equations

$$\begin{aligned} \dot{\Lambda}(t) &= \Lambda(t)\Sigma B(t), \\ \Lambda(0) &= 1, \end{aligned} \tag{3}$$

where the real antisymmetrical matrix Σ is 2N-dimensional analog of the Pauli matrix $i\sigma_y$, and the vector $\Delta(t)$ is the solution to the system of equations

$$\begin{aligned} \dot{\Delta}(t) &= \Lambda(t)\Sigma C(t), \\ \Delta(0) &= 0. \end{aligned} \tag{4}$$

If for time $t = 0$, one has the initial Wigner function of the system in the form

$$W(\mathbf{p}, \mathbf{q}, t = 0) = W_0(\mathbf{Q}), \tag{5}$$

the Wigner function of the system at time t is (due to the density operator is the integral of motion)

$$W(\mathbf{p}, \mathbf{q}, t) = W_0[\Lambda(t)\mathbf{Q} + \Delta(t)]. \tag{6}$$

This formula may be interpreted as transformation of input Wigner function into output Wigner function due to symplectic quadrature transform (2). An optical linear transformator of photon distribution function using this output Wigner function i s suggested in [7].

The Hamiltonian (1) may be rewritten in terms of creation and annihilation operators

$$H = \frac{1}{2}\mathbf{A}D(t)\mathbf{A} + \mathbf{E}(t)\mathbf{A}, \tag{7}$$

where we use 2N-vectors $\mathbf{A} = (a_1, a_2, \ldots, a_N, a_1\dagger, a_2\dagger, \ldots, a_N\dagger)$ and $\mathbf{E}(t)$, as well as 2N×2N-matrix $D(t)$. This system has 2N linear integrals of motion [5], [6] which are written in vector form

$$\mathbf{A}_0(t) = M(t)\mathbf{A} + \mathbf{N}(t). \tag{8}$$

The complex matrix $M(t)$ is the solution to the system of equations

$$\begin{aligned} \dot{M}(t) &= M(t)\sigma D(t), \\ M(0) &= 1, \end{aligned} \tag{9}$$

where the imaginary antisymmetric matrix σ is 2N×2N-analog of the Pauli matrix $-\sigma_y$, and the vector $\mathbf{N}(t)$ is th solution to the system of equations

$$\begin{aligned} \dot{\mathbf{N}}(t) &= M(t)\sigma\mathbf{E}(t), \\ \mathbf{N}(0) &= 0. \end{aligned} \tag{10}$$

Analogously to the Wigner function evolution, if for time $t = 0$, one has the initial Q-function of the system in the form

$$Q(\alpha, \alpha^*, t = 0) = Q_0(\mathcal{A}), \qquad \mathcal{A} = (\alpha, \alpha^*), \tag{11}$$

the Q–function of the system at time t is

$$Q(\alpha, \alpha^*, t) = Q_0[M(t)A + \mathbf{N}(t)]. \tag{12}$$

Here $\alpha = (\mathbf{q} + i\mathbf{p})/\sqrt{2}$.

For time-independent Hamiltonian (1), the matrix $\Lambda(t)$ is

$$\Lambda(t) = \exp(\Sigma B t), \tag{13}$$

and the vector $\Delta(t)$ is

$$\Delta(t) = \int_0^t \exp(\Sigma B \tau)\ \Sigma\ \mathbf{C}(\tau)\ d\tau. \tag{14}$$

For time-independent Hamiltonian (7), the matrix $M(t)$ is

$$M(t) = \exp(\sigma D t), \tag{15}$$

and the vector $\mathbf{N}(t)$ is

$$\mathbf{N}(t) = \int_0^t \exp(\sigma D \tau)\ \sigma\ \mathbf{E}(\tau)\ d\tau. \tag{16}$$

For time-dependent linear systems, the Wigner function of generic squeezed and correlated state (generalized correlated state [8]) has Gaussian form and it was calculated in [5].

Thus the evolution of the Wigner function and Q–function for systems with quadratic Hamiltonians for any state is given by the following prescription. Given the Wigner function $W(\mathbf{p}, \mathbf{q}, t = 0)$ for the initial moment of time $t = 0$. Then the Wigner function for time t is obtained by the replacement

$$W(\mathbf{p}, \mathbf{q}, t) = W(\mathbf{p}(t),\ \mathbf{q}(t),\ t = 0),$$

where time-dependent arguments are the linear integrals of motion of the quadratic system found in [5], [4], and [9]. This formula was given as integral with δ–function kernel in [10]. The linear integrals of motion describe initial values of classical trajectories in the phase space of the system. The same ansatz is used for the Q–function. Namely, given the Q–function of the quadratic system $Q(\mathbf{B},\ t = 0)$ for the initial moment of time $t = 0$. Then the Q–function for time t is given by the replacement

$$Q(\mathbf{B},\ t) = Q(\mathbf{B}(t),\ t = 0),$$

where the 2N–vector $\mathbf{B}(t)$ is the integral of motion linear in the annihilation and creation operators. This ansatz follows from the statement that the density operator of the Hamiltonian system is the integral of motion, and its matrix elements in any basis must depend on appropriate integrals of motion.

3 Multimode Mixed Correlated Light

The most general mixed squeezed state of the N–mode light with a Gaussian density operator $\hat{\rho}$ is described by the Wigner function $W(\mathbf{p}, \mathbf{q})$ of the generic Gaussian form,

$$W(\mathbf{p}, \mathbf{q}) = \det \mathbf{M} \exp\left[-\frac{1}{2}(\mathbf{Q} - < \mathbf{Q} >)\mathbf{M}^{-1}(\mathbf{Q} - < \mathbf{Q} >)\right], \tag{17}$$

where 2N parameters $< p_i >$ and $< q_i >$, $i = 1,2,\ldots,N$, combined into vector $< \mathbf{Q} >$, are average values of quadratures,

$$\begin{aligned} < \mathbf{p} > &= \mathrm{Tr}\, \hat{\rho}\hat{\mathbf{p}}, \\ < \mathbf{q} > &= \mathrm{Tr}\, \hat{\rho}\hat{\mathbf{q}}. \end{aligned} \tag{18}$$

A real symmetric dispersion matrix $\mathbf{M}$ consists of $2N^2+N$ variances

$$\mathcal{M}_{\alpha\beta} = \frac{1}{2} < \hat{Q}_\alpha\hat{Q}_\beta + \hat{Q}_\beta\hat{Q}_\alpha > - < \hat{Q}_\alpha >< \hat{Q}_\beta >, \qquad \alpha,\beta = 1,2,\ldots,2N. \tag{19}$$

They obey uncertainty relations constraints [5]. According to previous section the Wigner function of parametric linear system with initial value (17) is

$$W(\mathbf{p},\mathbf{q},t) = \det \mathbf{M} \exp\left[-\frac{1}{2}(\Lambda(t)\mathbf{Q} + \mathbf{\Delta}(t) - < \mathbf{Q} >)\mathbf{M}^{-1}(\Lambda(t)\mathbf{Q} + \mathbf{\Delta}(t) - < \mathbf{Q} >)\right], \tag{20}$$

The photon distribution function of the state (17)

$$\mathcal{P}_\mathbf{n} = \mathrm{Tr}\, \hat{\rho}|\mathbf{n} >< \mathbf{n}|, \qquad \mathbf{n} = (n_1, n_2, \ldots, n_N), \tag{21}$$

where the state $|\mathbf{n} >$ is photon number state, which was calculated in [11], [12] and it is

$$\mathcal{P}_\mathbf{n} = \mathcal{P}_0 \frac{H_\mathbf{nn}^{\{\mathbf{R}\}}(\mathbf{y})}{\mathbf{n}!}. \tag{22}$$

The trace (21) may be calculated using the explicit form of the Wigner function of the operator $|\mathbf{m} >< \mathbf{n}|$ (see, [5]) which is the product of Wigner functions of one-dimensional oscillator expressed in terms of Laguerre polynomials of the form

$$W_{mn}(p,q) = 2^{m-n+1}(-1)^n \sqrt{\frac{n!}{m!}} \left(\frac{q-ip}{\sqrt{2}}\right)^{m-n} e^{-(p^2+q^2)} L_n^{m-n}\left(2(q^2+p^2)\right). \tag{23}$$

The function $H_\mathbf{nn}^{\{\mathbf{R}\}}(\mathbf{y})$ is multidimensional Hermite polynomial. The probability to have no photons is

$$\mathcal{P}_0 = \left[\det\left(\mathbf{M} + \frac{1}{2}\mathbf{I}_{2N}\right)\right]^{-1/2} \exp\left[- < \mathbf{Q} > (2\mathbf{M} + \mathbf{I}_{2N})^{-1} < \mathbf{Q} >\right], \tag{24}$$

where we introduced the matrix

$$\mathbf{R} = 2\mathbf{U}^\dagger(1 + 2\mathbf{M})^{-1}\mathbf{U}^* - \sigma_{Nz}, \tag{25}$$

and the matrix

$$\sigma_{Nz} = \begin{pmatrix} 0 & \mathbf{I}_N \\ \mathbf{I}_N & 0 \end{pmatrix}. \tag{26}$$

The argument of Hermite polynomial is

$$\mathbf{y} = 2\mathbf{U}^t(\mathbf{I}_{2N} - 2\mathbf{M})^{-1} < \mathbf{Q} >, \tag{27}$$

and the 2N-dimensional unitary matrix

$$\mathbf{U} = \frac{1}{\sqrt{2}} \begin{pmatrix} -i\mathbf{I}_N & i\mathbf{I}_N \\ \mathbf{I}_N & \mathbf{I}_N \end{pmatrix} \tag{28}$$

is introduced, in which $\mathbf{I}_N$ is the N×N-identity matrix. Also, we use the notation

$$\mathbf{n}! = n_1! n_2! \cdots n_N!.$$

The mean photon number for j-th mode is expressed in terms of photon quadrature means and dispersions

$$< n_j >= \frac{1}{2}(\sigma_{p_j p_j} + \sigma_{q_j q_j} - 1) + \frac{1}{2}(< p_j >^2 + < q_j >^2). \tag{29}$$

The photon distribution function for transformed state (20) is given by the same formulae (22), (24)–(28) but with changed dispersion matrix

$$\widetilde{\mathbf{M}} = \Lambda^{-1} \mathbf{M} \Lambda^{-1t}, \tag{30}$$

and quadrature means

$$< \widetilde{\mathbf{Q}} >= \Lambda^{-1}(\Delta - < \mathbf{Q} >). \tag{31}$$

Thus we have a linear transformator of photon statistics suggested in [7].

Let us now introduce a complex 2N-vector $\mathbf{B} = (\beta_1, \beta_2, \ldots, \beta_N, \beta_1^*, \beta_2^*, \ldots, \beta_N^*)$. Then the Q-function is the diagonal matrix element of the density operator in coherent state basis $| \beta_1, \beta_2, \ldots, \beta_N >$. This function is the generating function for matrix elements of the density operator in the Fock basis $|\mathbf{n}>$ which has been calculated in [12]. In notations corresponding to the Wigner function (17) the Q-function is

$$Q(\mathbf{B}) = \mathcal{P}_0 \exp\left[-\frac{1}{2}\mathbf{B}(R + \sigma_{Nx})\mathbf{B} + \mathbf{B}R\mathbf{y}\right]. \tag{32}$$

Thus, if the Wigner function (17) is given one has the Q-function. Also, if one has the Q-function (32), i.e., the matrix R and vector $\mathbf{y}$, the Wigner function may be obtained due to relations

$$\begin{aligned} \mathbf{M} &= \mathbf{U}^*(R + \sigma_{Nx})^{-1}\mathbf{U}^\dagger - 1/2, \\ < \mathbf{Q} > &= \mathbf{U}^*[1 - (R + \sigma_{Nx})^{-1}\sigma_{Nx}]\mathbf{y}. \end{aligned} \tag{33}$$

Multivariable Hermite polynomials describe the photon distribution function for the multimode mixed and pure correlated light [11], [13], [14]. The nonclassical state of light may be created due to nonstationary Casimir effect [15], [16] and the multimode oscillator is the model to describe the behaviour of squeezed and correlated photons.

4 Parametric Oscillator

For the parametric oscillator with the Hamiltonian

$$H = -\frac{\partial^2}{2\partial x^2} + \frac{\omega^2(t)x^2}{2}, \tag{34}$$

where we take $\hbar = m = \omega(0) = 1$, there exists the time-dependent integral of motion found in [2]

$$A = \frac{i}{\sqrt{2}}[\varepsilon(t)p - \dot{\varepsilon}(t)x], \tag{35}$$

where

$$\ddot{\varepsilon}(t) + \omega^2(t)\varepsilon(t) = 0, \qquad \varepsilon(0) = 1, \qquad \dot{\varepsilon}(0) = i, \tag{36}$$

satisfying the commutation relation

$$[A,\ A\dagger] = 1. \tag{37}$$

It is easy to show that packet solutions of the Schrödinger equation may be introduced and interpreted as coherent states [2], since they are eigenstates of the operator A (35), of the form

$$\Psi_\alpha(x,t) = \Psi_0(x,t)\exp\left(-\frac{|\alpha|^2}{2} - \frac{\alpha^2\varepsilon^*(t)}{2\varepsilon(t)} + \frac{\sqrt{2}\alpha x}{\varepsilon}\right), \tag{38}$$

where

$$\Psi_0(x,t) = \pi^{-1/4}\varepsilon(t)^{-1/2}\exp\frac{i\dot{\varepsilon}(t)x^2}{2\varepsilon(t)} \tag{39}$$

is analog of the ground state of the oscillator and α is a complex number.

Variances of the position and momentum of the parametric oscillator in the state (38), (39) are

$$\sigma_x = \frac{|\varepsilon(t)|^2}{2}, \qquad \sigma_p = \frac{|\dot{\varepsilon}(t)|^2}{2}, \tag{40}$$

and the correlation coefficient r of the position and momentum has the value corresponding to minimization of the Schrödinger uncertainty relation [17]

$$\sigma_x\sigma_p = \frac{1}{4}\frac{1}{1-r^2}. \tag{41}$$

If $\sigma_x < 1/2$ ($\sigma_p < 1/2$) we have squeezing in photon quadrature components.

The analogs of orthogonal and complete system of states which are excited states of stationary oscillator are obtained by expansion of (38) into power series in α. We have

$$\Psi_m(x,t) = \left(\frac{\varepsilon^*(t)}{2\varepsilon(t)}\right)^{m/2}\frac{1}{\sqrt{m!}}\Psi_0(x,t)H_m\left(\frac{x}{|\varepsilon(t)|}\right), \tag{42}$$

and these squeezed and correlated number states are eigenstates of invariant $A^\dagger A$. In case of periodical dependence of frequency on time the classical solution in stable regime may be taken in Floquet form

$$\varepsilon(t) = e^{i\kappa t}u(t), \tag{43}$$

where $u(t)$ is a periodical function of time. Then the states (42) are quasienergy states realizing the unitary irreducible representation of time translation symmetry group of the Hamiltonian and the parameter κ determines the quasienergy spectrum. Unstable classical solutions give continuous spectrum of quasienergy states.

The partial cases of parametric oscillator are free motion ($\omega(t) = 0$), stationary harmonic oscillator ($\omega^2(t) = 1$), and repulsive oscillator ($\omega^2(t) = -1$). The solutions obtained above are described by the function $\varepsilon(t)$ which is equal to $\varepsilon(t) = 1 + it$, for free particle, $\varepsilon(t) = e^{it}$, for usual oscillator, and $\varepsilon(t) = \cosh t + i \sinh t$, for repulsive oscillator.

Another normalized solution to the Schrödinger equation

$$\Psi_{am}(x,t) = 2N_m \Psi_0(x,t) \exp\left(-\frac{|\alpha|^2}{2} - \frac{\varepsilon^*(t)\alpha^2}{2\varepsilon(t)}\right) \cosh\frac{\sqrt{2}\alpha x}{\varepsilon(t)}, \tag{44}$$

where

$$N_m = \frac{\exp(|\alpha|^2/2)}{2\sqrt{\cosh|\alpha|^2}}, \tag{45}$$

is the even coherent state [18] (the Schrödinger cat male state). The odd coherent state of the parametric oscillator (the Schrödinger cat female state)

$$\Psi_{af}(x,t) = 2N_f \Psi_0(x,t) \exp\left(-\frac{|\alpha|^2}{2} - \frac{\varepsilon^*(t)\alpha^2}{2\varepsilon(t)}\right) \sinh\frac{\sqrt{2}\alpha x}{\varepsilon(t)}, \tag{46}$$

where

$$N_f = \frac{\exp(|\alpha|^2/2)}{2\sqrt{\sinh|\alpha|^2}}, \tag{47}$$

satisfies the Schrödinger equation and is the eigenstate of the integral of motion A^2 (as well as the even coherent state) with the eigenvalue α^2. These states are one-mode examples of squeezed and correlated Schrödinger cat states constructed in [19]. The experimental creation of the Schrödinger cat states is discussed in [20]. These states belo ng to family of nonclassical superposition states studied in [21], [22].

References

[1] P. Ermakov, Univ. Izv. Kiev **20**, N9, 1 (1880).

[2] I. A. Malkin and V. I. Man'ko, Phys. Lett. A **32**, 243 (1970).

[3] I. A. Malkin, V. I. Man'ko, and D. A. Trifonov, Phys. Lett. A **30**, 414 (1969).

[4] I. A. Malkin, V. I. Man'ko, and D. A. Trifonov, J. Math. Phys. **14**, 576 (1973).

[5] V. V. Dodonov and V. I. Man'ko, *Invariants and Evolution of Nonstationary Quantum Systems*, Proceedings of Lebedev Physical Institute **183**, ed. M. A. Markov (Nova Science, Commack, New York, 1989).

[6] I. A. Malkin and V. I. Man'ko. *Dynamical Symmetries and Coherent States of Quantum Systems* (Nauka Publishers, Moscow, 1979) [in Russian].

[7] V. V. Dodonov, O. V. Man'ko, V. I. Man'ko, and P. G. Polynkin, Talk at the International Conference on Coherent and Nonlinear Optics, St.-Petersburg, July 1995 (to be published in SPIE Proceedings).

[8] E. C. G. Sudarshan, Charles B. Chiu, and G. Bhamathi, Phys. Rev. A **52**, 43 (1995).

[9] I. A. Malkin, V. I. Man'ko, and D. A. Trifonov, Phys. Rev. D **2**, 1371 (1970).

[10] V. V. Dodonov, O. V. Man'ko, and V. I. Man'ko, Proceedings of Lebedev Physical Institute **191**, ed. M. A. Markov (Nauka Publishers, Moscow, 1989) p.171 [English translation: J. Russ. Laser Research (Plenum Press, New York) **16**, 1 (1995)].

[11] V. V. Dodonov, O. V. Man'ko, and V. I. Man'ko, Phys. Rev. A **50**, 813 (1994).

[12] V. V. Dodonov, V. I. Man'ko, and V. V. Semjonov, Nuovo Cim. B **83**, 145 (1984).

[13] V. V. Dodonov and V. I. Man'ko, J. Math. Phys. **35**, 4277 (1994).

[14] V. V. Dodonov, J. Math. Phys. A: Math. Gen. **27**, 6191 (1994).

[15] V. I. Man'ko, J. Sov. Laser Research (Plenum Press, New York) **12** N5 (1991).

[16] V. V. Dodonov, A. B. Klimov, and V. I. Man'ko, Phys. Lett. A **49**, 255 (1990).

[17] E. Schrödinger, Ber. Kgl. Akad. Wiss. Berlin, **24**, 296 (1930).

[18] V. V. Dodonov, I. A. Malkin, and V. V. Man'ko, Physica, **72**, 597 (1974).

[19] V. V. Dodonov, V. I. Man'ko, and D. E. Nikonov, Phys. Rev. A **51**, 3328 (1995).

[20] S. Haroche, Nuovo Cim. B **110**, 545 (1995).

[21] M. M. Nieto and D. R. Truax, Phys. Rev. Lett. **71**, 2843 (1993).

[22] J. Janszky, Talk at the IV International Conference on Squeezed States and Uncertainty Relations, Shanxi, China, June 1995.

NEXT
DOCUMENT

Classical Trajectories and Quantum Spectra

Bogdan Mielnik[a,b]
and
Marco A. Reyes[a]

[a] *Departamento de Física*
Centro de Investigación y Estudios Avanzados del IPN
Apdo. Postal 14-740, México D.F. 07000, México

[b] *Department of Physics*
Warsaw University, Warsaw, Poland

Abstract

A classical model of the Schrödinger's wave packet is considered. The problem of finding the energy levels corresponds to a classical manipulation game. It leads to an approximate but non-perturbative method of finding the eigenvalues, exploring the bifurcations of classical trajectories. The role of squeezing turns out decisive in the generation of the discrete spectra.

1 The classical model of quantum systems.

The quantum theory devotes a lot of attention to the classical models of quantum phenomena. Much less attention to the quantum models of classical phenomena. Yet, such models exist. Some classical processes can mimick the quantum laws. One of the most provocative examples was given by Avron and Simon in 1986 by explanaining the structure of the Saturn rings in terms of the band spectrum of the Schrödinger's operator [1](Fig.1). Their work shares some epic qualities of Jonathan Swift [2] (something so enormous imitating something so little!).

The analogy, though, is natural and has some antiquity [3]. Consider the 1-dimensional Schrödinger's equation:

$$-\frac{1}{2}\frac{d^2}{dx^2}\psi(x) + [V(x) - E]\psi(x) = 0 \qquad (1)$$

with $V(x)$, $\psi(x)$ and E real. Suppose, we are interested in the solutions of (1) for arbitrary $E \in \Re$, *not necessarily belonging to the spectrum*. Denote now the variable x by t and call it *time* [3, 4, 5]: put also $q = \psi(t)$, $p = \psi'(t)$. The equation (1) becomes:

$$\frac{dq}{dt} = p, \quad \frac{dp}{dt} = 2[V(t) - E]q \tag{2}$$

Note, that (2) is simply the pair of canonical equations for the classical variables q, p of a classical oscillator with a time dependent ellastic constant. The Hamiltonian reads:

$$H(t) = \frac{p^2}{2} + g(t)\frac{q^2}{2}, \qquad g(t) = 2[E - V(t)] \tag{3}$$

The canonical trajectories of (3):

$$\mathbf{q}(t) = \left\| \begin{matrix} q(t) \\ p(t) \end{matrix} \right\| \qquad (t \in \Re) \tag{4}$$

'portrait' every detail of the Schrödinger's wave packet $\psi(x)$ and its first derivative $\psi'(x)$. This includes the phenomenon of the "classical spectral bands".

Figure 1. Saturn rings, the macroscopic imitation of the spectral bands (An imperfect image of Avron and Simon idea: the spectral bands of a cuasi-periodic potential form a Cantor set).

Indeed, assume $V(t)$ is periodic or quasi-periodic. If E belongs to a spectral band of the Schrödinger's operator, the wave functions (1) are bounded in $x \to \pm\infty$ and so are the trajectories of the classical oscillator (2-3). Thus, the spectral bands of $V(t)$ define the stability bands (trapped motions) of the classical system (2-3). In turn, for E belonging to the resolvent set, the "act of creation" was incomplete on the quantum side: the wave functions (1) have no physical meaning. However, the classical trajectories have: they escape to ∞ either for $t \to +\infty$ or $t \to -\infty$, painting the picture of a parametric resonance. Hence, the resolvent set defines the instability regime (escape motions). This explains why the spectral gaps determine the empty spaces in the Saturn rings (Avron and Simon [1]). A temptating question arises: can there be a similar 'classical portrait' for the discrete spectrum?

2 "Classical point-spectrum".

Consider again the classical system (2-3), with $E < 0$ and with $V(t)$ in form of a limited potential well:

$$V(t) = \begin{cases} \leq 0 & \text{for } a \leq t \leq b \\ = 0 & \text{for } t \leq a \text{ or } t \geq b \end{cases} \tag{5}$$

The corresponding classical Hamiltonian:

$$H(t) = \frac{p^2}{2} + [E - V(t)]q^2 \tag{6}$$

represents a rather simple mechanical system. The classical point is driven by a constant repulsive potential, corrected by an "attractive episode" $-V(t)q^2$ (see Fig.2). The motion trajectory, in general, diverges either for $t \to -\infty$ or $t \to +\infty$ (as the result of a constant repulsive term Eq^2). For some E, however, a very special dynamical phenomenon occurs: the trajectory, departing from $q = 0$ at $t = -\infty$, by a rare dynamical coincidence, returns asimptotically to 0 for $t \to +\infty$. This phenomenon, extremally unstable, as exceptional as an eclipse, is our classical equivalent of a bound state [$\psi(x) \to 0$ for $x \to \pm\infty$] ie., the most stable motion form in quantum mechanics!

The "classical portrait", this time, has no astronomic magnitude: it represents rather a kind of classical sport game. This aspect is specially visible if $V(t)$ is a sum of δ-peaks: $V(t) = -a_1\delta(t-t_1) - \ldots - a_n\delta(t-t_n)$, with $a_j > 0$ ($j = 1, 2, \ldots$). The classical Hamiltonian:

$$H(t) = \frac{p^2}{2} + Eq^2 + \sum_{j=1}^{n} a_j\delta(t-t_j)q^2 \tag{7}$$

then describes a point mass in a constant repulsive field, pertrubed by a sequence of attractive pulses. Consider now a trajectory departing from $q = 0$ at $t = -\infty$. What typically happens when the attractive pulses are over, is that the point must escape either to $q = -\infty$ or $q = +\infty$. Yet, for some exceptional $E < 0$, the kicks will provide to the mass point a momentum exactly sufficient to climb asimptotically to 0, against the repulsive forces. When this happens, E is an eigenvalue of (1). The whole phenomenon resembles a ping-pong game against the repulsive potential. The attractive kicks in (7) are an equivalent of the "ping-pong rocket" and the "goal" of the game is to collocate the point at the very repulsion center!

Note, that the picture permits one to guess the number of the bound states. Thus, e.g., for $n = 1$ (one kick), there is only one way (modulo proportionality) to return the escaping point to zero. Henceforth, the single δ-well has exactly one bound state. For $n = 2$ (2 kicks), the point can be returned in two (qualitatively different) ways corresponding to two different values of E and two different bound states. For more peaks, or for continuous $V(t)$, the game complicates and to predict results, some geometry elements on the classical phase plane $\mathcal{P}$ are necessary.

3 The bifurcations.

We shall assume below, that $V(t)$ is a continuous real function, satisfying (5) [the δ peaks (7) are included as limiting cases].

One of the oldest observations of quantum mechanics is that the eigenvectors of (1) are a kind of "recurrent phenomenon", tending to repeat itself as E grows. This fact can be explained in several ways, but its simplest illustration is obtained in terms of the integral trajectories of (2·3).

Since the evolution equations (2) are linear, the phase point (4) depends linearly on the initial condition:

$$\mathbf{q}(t) = u(t,a)\mathbf{q}(a), \tag{8}$$

where $u(t,a)$ is a real 2×2 simplectic evolution matrix. The canonical equations (2) in terms of (8) read:

$$\frac{du}{dt} = \underbrace{\begin{Vmatrix} 0 & 1 \\ -g(t) & 0 \end{Vmatrix}}_{\Lambda(t)} u(t) \tag{9}$$

For $V(t) \equiv 0$ ($t \leq a$ and $t \geq b$), (2) becomes an equation with constant coefficients which can be explicitely solved:

$$\mathbf{q}(t) = \begin{cases} e^{\Lambda(t-a)}\mathbf{q}(a) & \text{for } t \leq a \\ e^{\Lambda(t-b)}\mathbf{q}(b) & \text{for } t \geq b \end{cases} \tag{10}$$

where Λ is a constant 2×2 matrix:

$$\Lambda = \begin{Vmatrix} 0 & 1 \\ 2\,|\,E\,| & 0 \end{Vmatrix} \tag{11}$$

Note that Λ has a pair of real eigenvalues:

eigenvalues	*eigenvectors*
$\lambda_+ = +\sqrt{2\,\|\,E\,\|}$	$\mathbf{e}_+ = \begin{Vmatrix} 1 \\ +\sqrt{2\,\|\,E\,\|} \end{Vmatrix}$
$\lambda_- = -\sqrt{2\,\|\,E\,\|}$	$\mathbf{e}_- = \begin{Vmatrix} 1 \\ -\sqrt{2\,\|\,E\,\|} \end{Vmatrix}$

(12)

Thus, in absence of $V(t)$ (i.e. for $t \notin [a,b]$), the motion on the phase plane $\mathcal{P}$ amounts to a continuous squeezing: the direction $\mathbf{e}_+$ expands while $\mathbf{e}_-$ exponentially shrinks as $t \to +\infty$ (inversely for $t \to -\infty$). The typical phase trajectory (2) diverges for both $t \to \pm\infty$. However, exceptional cases exist. If $\mathbf{q}(a) = Const \times \mathbf{e}_+$, then $\mathrm{q}(t)$ vanishes for $t \to -\infty$, and if $\mathbf{q}(b) = Const \times \mathbf{e}_-$, then $\mathrm{q}(t)$ vanishes for $t \to +\infty$. The number $E < 0$ is an *eigenvalue* of the Schrödinger's operator, *iff* there exists a canonical trajectory vanishing on both extremes $t \to \pm\infty$. This can happen if and only if the evolution between $t = a$ and $t = b$ brings the direction of $\mathbf{e}_+$ into that of $\mathbf{e}_-$, i.e:

$$u(b,a)\mathbf{e}_+ = Const \times \mathbf{e}_- \tag{13}$$

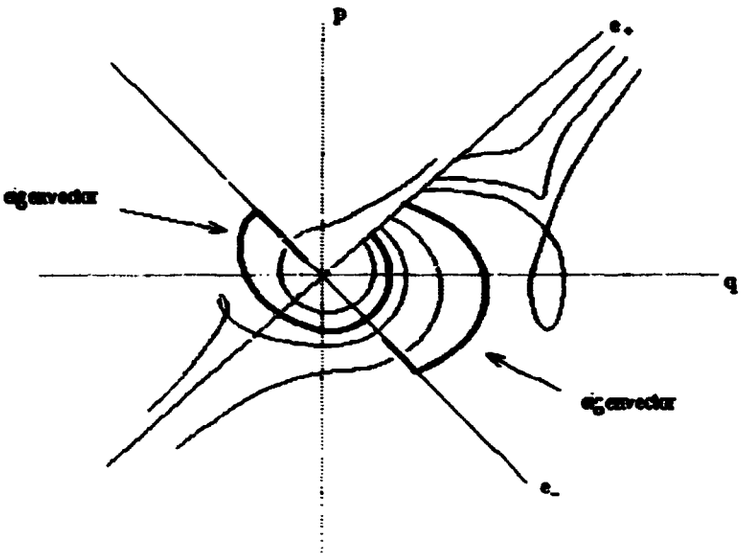

Figure 2 The metamorphosis of the classical trajectory (2–3) for varying E and fixed $V(t)$ (qualitative picture). As E raises to zero from below, the deformation due to the rotating term $-\frac{1}{2}(t)q^2$ expands clockwisely around the phase space origin, crossing several times the "shrinking axis" $\mathbf{e}_-(E)$. At each new intersection a bifurcation occurs, producing a new closed orbit interpretable as an eigenvector of the Schrödinger's equation (1). The trajectory transformations are pictured in the moving frame of the 'squeezing axis' and represent as well the bifurcations which must occur for a fixed $E < 0$ and variable $V(t)$.

To see the 'recurrent nature' of the phenomenon, consider an integral trajectory of (2) with $q(a) = C\mathbf{e}_+$ (i.e., departing from $q(-\infty) = 0$) and observe how does it change for varying $E < 0$. If $V(t) \equiv 0$, the trajectory escapes to infinity along the $\mathbf{e}_+$ direction. If $V(t) < 0$ in (a,b), the escape is corrected by a rotation around the phase space origin (typically generated by the attractive oscillator Hamiltonians). For $t > b$, i.e., when the rotation ceases, the deformation is squeezed back to zero, and the trajectory returns asimptotically to the expanding axis $\mathbf{e}_+$ (see Fig.2). Now, as E grows (approaching zero from below), the repulsion (squeezing) becomes weaker and the deformation caused by $V(t)q^2$ grows, tipically drawing a loop, till $q(b)$ touches the $\mathbf{e}_-$-axis. When this happens, (13) is fulfilled and the trajectory, instead of escaping to infinity, falls to zero, forming a closed orbit (an

eigenvector of (1)). As E still grows (and $\mid E \mid$ decreases) the deformation caused by $-V(t)\mathrm{q}^2$ drives the phase point $\mathbf{q}(b)$ across the $\mathbf{e}_-$-axis and the asimptotic picture suddenly changes: the trajectory escapes to ∞ again, but this time in the direction $-\mathbf{e}_+$ (not $+\mathbf{e}_+$), meaning the bifurcation (discontinuous change of the asimptotic angle by $-\pi$). If E still rises (tending to $E = 0$), the deformation expands clockwisely around the phase space origin, intersecting several times the shrinking axis $\mathbf{e}_-$. Each time this happen, a new bifurcation occurs (a discontinuous change of the asymptotic angle), giving birth to a new closed orbit (next eigenvector) at the exact bifurcation point (Fig.2).

Henceforth, the eigenvalues of (1) are the ***bifurcation values*** of E (i.e. the values for which the trajectories of (2) change their asymptotic type). In order to bifurcate, the trajectories must pass through a sequence of exceptional forms (closed orbits): this is why there exist spectra. Can this help to find the spectral values? The difficulty of finding the ***bifurcation values***, of course, is the same as that of finding the point spectrum (the analytical sciences are empty!). Yet, an advantage of our model (2-3) is, that it turns attention to some new methods till now neglected.

4 The angular Schrödinger equation.

Since the vector norms are irrelevant, our condition (13) can be conveniently written in terms of an ***angular coordinate***. Indeed, define:

$$\mathrm{q} = \rho\cos\alpha, \quad \mathrm{p} = \rho\sin\alpha \tag{14}$$

The canonical equations (2) become:

$$\dot\rho\cos\alpha - \dot\alpha\rho\sin\alpha = \rho\sin\alpha \tag{15}$$

$$\dot\rho\sin\alpha + \dot\alpha\rho\cos\alpha = 2[V(t) - E]\rho\cos\alpha \tag{16}$$

where $\dot\rho$ and $\dot\alpha$ mean the time derivatives. Curiously, the equation for the angular variable separates. In fact, multiplying (15) by $-\sin\alpha$, (16) by $\cos\alpha$ and adding one gets the 1-st order differential equation for α alone:

$$\dot\alpha = 2[V(t) - E]\cos^2\alpha - \sin^2\alpha \tag{17}$$

while permuting the operations, one arrives at:

$$\frac{\dot\rho}{\rho} = [V(t) - E + \frac{1}{2}]\sin 2\alpha \tag{18}$$

The angular equation (17) was found by Drukarev [6] and Franchetti [7] (though without the geometric interpretation) and used to evaluate the phase shifts. Note, that the squeezing directions $\mathbf{e}_\pm$ too can be defined in terms of the angles:

$$\alpha_\pm(E) = \pm\arctan\sqrt{2\mid E\mid} \tag{19}$$

Now, our condition (13) means, that the evolution described by the 1st-order eq.(17) in the time interval $[\,\,]$ should transform the 'expansive direction' $\alpha(a) = \alpha_+(E)$ into the

'shrinking direction' $\alpha(b) = \alpha_-(E) + n\pi$ $(n = 0, 1, 2, \ldots)$. Introducing the *defect angle* $\Gamma(E)$ as a difference between the 'shrinking angle' $\alpha_-(E)$ and the final angle $\alpha(b, E)$ obtained by integrating (17), one can write the spectral condition (13) as:

$$\Gamma(E) = \alpha_-(E) - \alpha(b, E) = n\pi \qquad (n = 0, 1, 2, \ldots) \tag{20}$$

An immediate generalization of (20) is obtained for $V(t)$ constant (though not necessarily vanishing) for $t \notin (a, b)$:

$$V(t) = \begin{cases} V(a) & \text{for } t \leq a \\ V(b) & \text{for } t \geq b \end{cases} \tag{21}$$

The trajectory (2) has then two constant generators $\Lambda(a)$ and $\Lambda(b)$ for $t \leq a$ and $t \geq b$ and the formula (20) holds after substituting $| V(a) - E |$ or $| V(b) - E |$ instead of $| E |$ in the expressions (19) for α_+ and α_- respectively. Two elementary facts make the bifurcation condition (20) specially efficient to determine the eigenvalues:

Observation 1. For a fixed $V(t)$ and $E < 0$, the spectral angle $\Gamma(E)$ is an increasing function of E. (This is an elementary consequence of the Cauchy equation (17); see also [8]). The monotonicity of $\Gamma(E)$ permits one to interpolate easily, helping to find the points where $\Gamma(E)$ intersects the critical values $\Gamma = n\pi$ $(n = 0, 1, 2, \ldots)$.

Observation 2. The function $\Gamma(E)$ is unstable and changes very abruptly when crossing the sequence of critical values $\Gamma = n\pi$ $(n = 1, 2, \ldots)$ (i.e. when E crosses spectral points). Thus, even a little error in E in vecinity of an eigenvalue traduces itself into a visible effect in Γ, improving the accuracy. This instability is caused by the fact that the energy eigenvalues correspond to the orbit bifurcations where the final integration point $\alpha(b, E)$ deflects fast when E crosses a bifurcation value. If the integration could yield $\alpha(+\infty, E)$, $\Gamma(E)$ would be an exact step function (see also the observation in [9, p.274]).

As an example, we have considered the energy levels for the truncated 1-dimensional oscillator potential:

$$V(x) = \begin{cases} \frac{1}{2}\omega^2 x^2 & \text{for } | x | \leq \frac{a}{2} \\ \\ \frac{1}{8}\omega^2 a^2 & \text{for } | x | \geq \frac{a}{2} \end{cases} \tag{22}$$

We have determined the angular function $\Gamma(E)$, $0 < E < V(\frac{a}{2})$, for $w = 1$, $a = 8$ integrating numerically (17) (see Fig.3), and obtaining the 8 energy levels for the oscillator truncated at $a = 4$, all calculated with accuracy up to 10^{-10}. The obtained eigenvalues are very close to the first 8 levels of the exact oscillator, $E_n = n + \frac{1}{2}$ (indeed, even the highest, and last eigenvalue of the truncated potential (22) differs rather little from the orthodox $E_7 = 7.5$).

Note the characteristic shape of $\Gamma(E)$, with sharp steps helping to localize the energy eigenvalues! The same spectral problem would be much more troublesome if approached by the conventional perturbation calculus. (Even compared to Ritz method, our algorithm shows some simplicity as there is no need to invent adequate classes of test functions!). Moreover, the same method can be used without difficulty to find the eigenvalues of arbitrarily deformed wells.

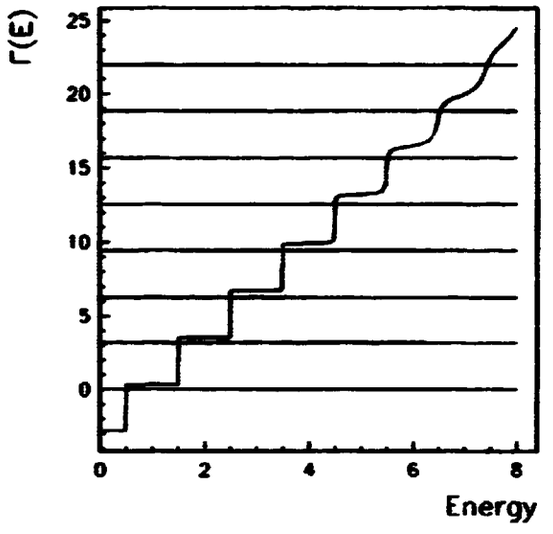

$E_0 = 0.49999999180$
$E_1 = 1.49999970050$
$E_2 = 2.49999476497$
$E_3 = 3.49994158633$
$E_4 = 4.49953028600$
$E_5 = 5.49706782671$
$E_6 = 6.48482891734$
$E_7 = 7.42825181633$

Figure 3. The defect angle $\Gamma(E) = \alpha_+ - \alpha(4, E)$. The intersections of this "stepping" function with the lines $n \times \pi$ give the eigenvalues of the Schrödinger problem.

The method, till now, concerns the limited potential wells. However, the generalization for unlimited and/or singular wells is already reported (it involves the substitution of the constant angles $\alpha_\pm(E)$ by their variable analogue [5, 8]). The (generalized) spectral function $\Gamma(E)$ shows the same "step behaviour" permitting to determine spectra with a high accuracy.

It is interesting to notice that all the structure elements which we have introduced were basically known since long time, though very seldom used. Thus, the idea about the classical model of (1) (with x substituted by t) was considered as far back as 1970 (or even earlier; see the discussion in [3]). The angular equation (17) was found by Drukarev [6] and then by Franchetti [7] (though without geometric pictures) and was used to examine the phase shifts. The idea that the *angles* determine the *discrete spectra* is quite old (see e.g. discussions in [10]) though is usually focused on the *phase of the complex wave function*, and mixed up with the WKB approximation. The implications of the classical angle were known to Calogero (see [11, p.82] and [9, p.274]), though Calogero was not interested in the numerical algorithms! The idea that the eigenvalues are bifurcations is as old (though usually contemplated without paying attention to the geometry of $\mathcal{P}$, and the role of squeezing in producing the bifurcation).

It seems also worth noticing, that the definition of the *bifurcation* does not require the *linearity* of the evolution equations (2). Hence, the definition of the spectrum via *bifurcations* might be a natural answer to the intriguing problem of how to extend the concept of spectrum to non-linear variants of the Schrödinger's operator (see, e.g. discussions in [12]). Some work in this direction is being recently carried [13].

Acknowledgements

The authors are grateful to the Conference organizers for their interest and kind hospitality in Shanxi, China, June 1995. The support of CONACyT, México, is appreciated.

References

[1] J.E.Avron and B.Simon, Phys.Rev.Lett. **46**, 1166 (1981).

[2] J.Swift, "Guliver's travels", Bantan Books Inc., New York (1986).

[3] I.A. Malkin and V.I. Man'ko, Sov.Phys. JETP **31**, 386 (1970).

[4] D.I.G. Sanjines C., "Ecuación unidimensional de Schrödinger como un problema dinámico clásico". Master Thesis, CINVESTAV, México (1990).

[5] M.A. Reyes, "La ecuación angular de Riccati y el problema espectral unidimensional", Master Thesis, CINVESTAV, México (1992).

[6] G.F. Drukarev, J.Eksp.Theor.Phys. **19**, 247 (1949).

[7] S. Franchetti, Nuovo Cim. **6**, 601 (1957).

[8] B. Mielnik and M.A. Reyes, "The Classical Schrödinger's Equation" (preprint, CINVESTAV 1995).

[9] F. Calogero, Nuov.Cim. **27**, 261 (1963).

[10] R.G. Newton, J.Math.Phys. **1**, 319 (1960).

[11] F. Calogero, Commun.Math.Phys. **1**, 80 (1965).

[12] M. Czachor, "Elements of Non-linear Quantum Mechanics" (preprint, 1994).

[13] P. Grochowski, W. Kaniowski and B. Mielnik (in preparation).

NEXT
DOCUMENT

Quantum Zeno effect in the measurement problem[1]

Mikio Namiki
Department of Physics, Waseda University, Tokyo 169, Japan

Saverio Pascazio*
**Department of Physics, University of Bari, I-70126 Bari, Italy*

Abstract

Critically analyzing the so-called quantum Zeno effect in the measurement problem, we show that observation of this effect does not necessarily mean experimental evidence for the naive notion of wave-function collapse by measurement (the simple projection rule). We also examine what kind of limitation the uncertainty relation and others impose on the observation of the quantum Zeno effect.

1 Introduction

The quantum Zeno paradox, named after the famous Greek philosopher Zeno, states that an unstable quantum system becomes stable (i.e. never decays) in the limit of infinitely frequent measurements. However, we cannot observe this limit, practically and in principle, as will be seen later on the basis of the uncertainty relations. Physically, its milder version, i.e. the quantum Zeno effect (QZE) can be observed. On the other hand, one may consider as if observation of this kind only of phenomenon were a clear-cut support for the naive notion of wave-function collapse (WFC) (the simple projection) onto an observed state. The purpose of this paper is to contrast this kind of misunderstanding by analyzing the mechanism of QZE and to discuss the important role of the uncertainty relations in observation of QZE.

A quantum system that is initially prepared in an eigenstate of the unperturbed Hamiltonian undergoes a temporal evolution that can be roughly divided into three steps [1]-[6]: A Gaussian-like behavior at short times, a Breit-Wigner exponential decay at intermediate times, and a power law at long times.

The first idea of the QZE was introduced under the assumption that the Gaussian short-time behavior can be observed in a quantum decay and only the naive WFC takes place in quantum measurements [7] [8]. In this context, the QZE is closely connected to the WFC by measurement, so that we have to examine one of the central measurement problems: What is the wave-function collapse? The authors have formulated a reasonable theory of measurement without resorting to the naive WFC [9][10]. In this paper, however, we shall not discuss this problem (see refs). Rather, we shall explain the QZE along the line of thought of the naive WFC.

Usually, the Gaussian decay is very difficult to observe. For this reason, the QZE was not considered to be easily amenable to experimental test until Cook [11] proposed using atomic

[1]In collaboration with H. Nakazato, G. Badurek and H. Rauch.

transitions in two-level atoms. On the basis of this idea, Itano and his group [12] recently carried out an interesting experiment, claiming that they experimentally justified the naive WFC by observing the QZE. As opposed to this, Prigogine and his group asserted, by theoretically deriving the same result only through a dynamical process without the help of the naive WFC, that this experiment did not necessarily support the naive WFC. This provoked an interesting debate [13].

The present authors and others proposed to use neutron spin-flip, instead of atomic transitions, in order to confirm and simplify (and generalize) Prigogine et al's theory [14]. Similar kind of experiments were proposed and recently performed by making use of photon polarization [15][16].

It is also important to note that Itano et al's experiment did not observe the state every time except the final one, and therefore was not exactly the same as Cook proposed. One of the main interests in this paper is, therefore, to find the reason why their experiment could give the same result as Cook's prediction, which was given by assuming the naive WFC (a simple projection) at every step.

2 Naive formulation of QZE

We first formulate the QZE along the line of thought of the naive WFC, and discuss it as an dynamical process in the next section.

For initial state u_a at $t = 0$ (an eigenstate of unperturbed Hamiltonian $\hat{H}_0$), the wave function dynamically changes as

$$\psi_t = \exp(-iE_a t - \frac{1}{2}F_a t^2)u_a + O(t) \ : \ F_a \equiv (u_a, \hat{H}_I^2 u_a) \tag{1}$$

at very short $t(>0)$, provided that $(u_a, \hat{H}_I u_a) = 0$.

According to the idea of the naive WFC, the system suffers such a sudden change as

$$\psi_t \Longrightarrow \exp(-iE_a t - \frac{1}{2}F_a t^2)u_a \simeq (1 - \frac{1}{2}F_a t^2)u_a e^{-iE_a t} \tag{2}$$

for its wave function, or

$$\rho_t \Longrightarrow \exp(-F_a t^2)\rho_{aa} \simeq (1 - F_a t^2)\rho_{aa} \ : \ \rho_{aa} \equiv |u_a >< u_a| \tag{3}$$

for its density matrix, at very short t.

The probability of finding state u_a at very short $t(>0)$ is given by

$$P_a(t) = (1 - F_a t^2) \ . \tag{4}$$

Therefore, the probability of finding the same state N times by repeated measurements of this kind in time intervals $(0, T/N), \cdots, ((N-1)T/N, T)$ (note that $t = T/N$ for one step) during $(0, T = tN)$ is given by

$$P_a^N(T) = \left[1 - F_a \left(\frac{T}{N}\right)^2\right]^N \overset{N\to\infty}{\longrightarrow} 1 \ . \tag{5}$$

We *propose to distinguish* the QZE from the quantum Zeno paradox in the following way:

Quantum Zeno paradox:

$$\lim_{N\to\infty} P_a^N(T) = 1 \ : \quad \textit{only} \text{ in the infinite } N \text{ limit}, \tag{6}$$

Quantum Zeno effect:

$$P_a^N(T) > P_a^{N'}(T) \ , \ \text{if } N > N' \ : \ \text{for finite } N \text{ and } N'. \tag{7}$$

Remember that we have simply formulated the quantum Zeno paradox and the QZE by making use of the Gaussian decay and the naive WFC.

3 Neutron spin-flip and discussion on QZE

In Cook's case, we observe only the temporal evolution of the type $\cos^2(\omega/2)$, so that we obtain

$$P_a^N(T) = \left(\cos^2\frac{\pi}{2N}\right)^N \tag{8}$$

for the probability of finding the initial state u_a at time T after N-step measurements, if we choose T so as to give $\cos(\omega T/2) = 0$.

In the neutron spin-flip case, we can also formulate the theoretical procedure in a similar way as in Cook's case, if we use a polarized neutron beam along the z-axis and N magnetic fields with strength B along the x-axis as shown in Fig.1 (Case A), where $\omega = \mu B/\hbar$ (μ being the neutron magnetic moment). Therefore, we can describe the one-step measurement as

$$\begin{aligned} \rho(t) \quad &= \quad \rho_{aa}\cos^2\frac{\omega t}{2} + \rho_{bb}\sin^2\frac{\omega t}{2} \\ &\qquad -i\rho_{ab}\cos\frac{\omega t}{2}\sin\frac{\omega t}{2} + \text{h.c.} \\ &\Longrightarrow \quad \rho_{aa}\cos^2\frac{\omega t}{2} \quad \text{(naive WFC projection)} \end{aligned} \tag{9}$$

where $a = \uparrow$, $b = \downarrow$, $t = T/N$ (or $\omega t/2 = \pi/2N$), and then the final density matrix after N-step measurements becomes

$$\rho_A^N(T) = \left(\cos^2\frac{\pi}{2N}\right)^N \rho_{aa} \ . \tag{10}$$

and correspondingly, we can get the probability of finding the upward spin state at time T in the same form as (8) with $a = \uparrow$.

In this case, we can explicitly write down the whole density matrix in the channel representation before the final spin-detection in the following way:

$$\rho_A^N(T) = \begin{pmatrix} c^{2N} & & & 0 \\ & s^2c^{2N-2} & & \\ & & s^2c^{2N-4} & \\ & & & \ddots \\ 0 & & & s^2 \end{pmatrix},$$

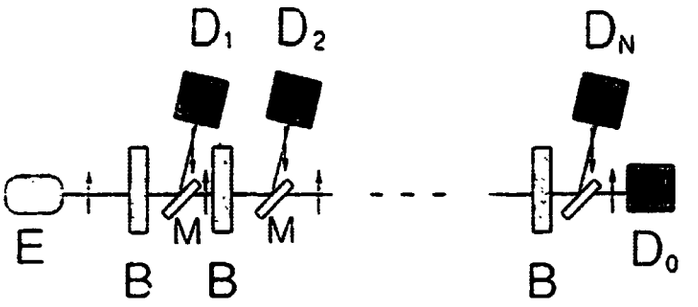

Figure 1: QZE in case A.

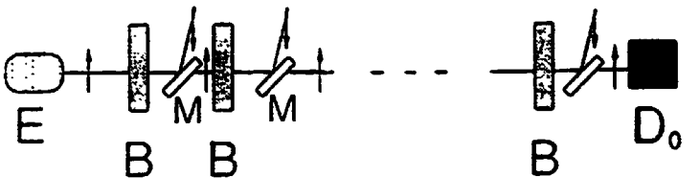

Figure 2: QZE in case B

where $c = \cos(\pi/2N)$ and $s = \sin(\pi/2N)$.

On the other hand, we know that a measurement process can be divided into two steps, the first being the spectral decomposition and the second the detection. Usually, spectral decomposition step is a sort of dynamical process that keeps coherence among the branch waves. In this case, the experimental procedure is illustrated in Fig. 2 (Case B). We can easily show that, through the N-step spectral decompositions, the density matrix of the system will dynamically change as

$$\rho_B^N(T) = \left(\cos^2\frac{\pi}{2N}\right)^N \rho_{aa} + \text{other components} . \tag{11}$$

Therefore, we can explicitly write down the whole density matrix in the same channel representaion before the final spin-detection as follows:

$$\rho_B^N(T) = \begin{pmatrix} c^{2N} & isc^{2N-1} & isc^{2N-2} & \cdots & isc^N \\ -isc^{2N-1} & s^2c^{2N-2} & s^2c^{2N-3} & \cdots & s^2c^{N-1} \\ -isc^{2N-2} & s^2c^{2N-3} & s^2c^{2N-4} & \cdots & s^2c^{N-2} \\ \vdots & \vdots & \vdots & \ddots & \vdots \\ -isc^N & s^2c^{N-1} & s^2c^{N-2} & \cdots & s^2 \end{pmatrix} .$$

Note that both the density matrices $\rho_A^N(T)$ and $\rho_B^N(T)$ have the same aa-component. Correspondingly, we obtain the same formula as (8) (with $a = \uparrow$) for the probability of finding the upward spin-state by the final detector D_0 at time T. This is the answer to the question asked at the end of the preceding section. That is, we cannot conclude that observation of $P^N(T)$ going to unity is an experimental evidence in support of the naive WFC.

4 The uncertainty relation and other situations

Undoubtedly, one of the most important quantities is

$$\phi \equiv \omega t = \frac{\mu B l}{\hbar v} (= \frac{\pi}{2N}), \quad \text{in} \quad P_{\uparrow}^{N}(T) = \left[1 - \left(\frac{\mu B l}{\hbar v}\right)^2\right]^N \tag{12}$$

where l stands for the length of each magnet and v for the neutron speed.

Mathematically, ϕ is of order $O(N^{-1})$, but we cannot take the infinite N limit for the following reasons: (i) In practice, we cannot make the zero limit of the magnetic region, and (ii) in principle, it is impossible to avoid uncertainties Δv and Δx, because

$$\phi \sim \phi_0 \equiv \frac{\mu B l}{\hbar v_0} > \frac{\mu B \Delta x}{\hbar v_0} > \frac{\mu B}{2 m v_0 \Delta v} = \frac{1}{4} \frac{\Delta E_m}{\Delta E_k} \tag{13}$$

where v_0, $\Delta E_m = 2\mu B$ and $\Delta E_k = \Delta(mv^2/2)$ are the mean neutron speed, the magnetic energy gap and the neutron kinetic energy spread, respectively. Consequently, we should have

$$P_{\uparrow}^{N}(T) \simeq \left[1 - \frac{1}{32}\left(\frac{\Delta E_m}{\Delta E_k}\right)^2\right]^N \tag{14}$$

For this reason we can set the following limitation:

$$N_{\max} \sim 10^4 \, .$$

Additionally, we have to take into account the probability of neutron leakage or absorption, $\sigma < 1$, at each step, which should modify the probability of finding the neutron as follows:

$$\tilde{P}_{\uparrow}^{N}(T) = \sigma^N P_{\uparrow}^{N}(T) \, . \tag{15}$$

We cannot take the limit $N \to \infty$ also for this reason, but we can estimate this kind of loss factor, both experimentally or theoretically, in order to get the net effect.

5 Concluding remarks

We have shown that observation of the QZE does not signify any experimental evidence of the naive WFC (the simple projection), and found the reason why Itano et al's experiment got the same result as Cook's one, even though they did not exactly follow Cook's proposal. We have also examined an important limitation arising from the uncertainty relations and other limitations to be imposed on observation of QZE.

Acknowledgments

One of the authors (MN) is indebted for financial supports to the Ministry of Education, Culture and Sciences and the other (SP) to the Japan Society for Promotion of Science and to Italian Consiglio Nazionale delle Ricerche for financial support.

References

[1] E.J. Hellund, Phys. Rev. **89** (1953) 919.

[2] M. Namiki and N. Mugibayashi, Prog. Theor. Phys. **10** (1953) 474.

[3] H. Araki, Y. Munakata, M. Kawaguchi and T. Goto, Prog. Theor. Phys. **17** (1957) 419; J. Schwinger, Ann. of Phys. **9** (1960) 169.

[4] L.A. Khalfin, Zh. Eksp. Teor. Fiz. **33** (1958) 1371 [Sov. Phys. JETP **6** (1958) 1053]; Phys. Lett. **B 112** (1982) 223. And see also: V. Fock and N. Krylov, J. of Phys. **11** (1947) 112.

[5] A. DeGasperis, L. Fonda and G.C. Ghirardi, Nuovo Cimento **A 21** (1974) 471; L. Fonda, G.C. Ghirardi and A. Rimini, Rep. Prog. Phys. **41** (1978) 687.

[6] G.C. Cho, H. Kasari and Y. Yamaguchi, Prog. Theor. Phys. **90** (1993) 803.

[7] L.A. Khalfin, Pis'ma Zh. Eksp. Teor. Fiz. **8** (1968) 106 [Sov. Phys. JETP Lett. **8** (1968) 65].

[8] B. Misra and E.C.G. Sudarshan, J. Math. Phys. **18** (1977) 756; C.B. Chiu, B. Misra and E.C.G. Sudarshan, Phys. Rev. **D 16** (1977) 520; Phys. Lett. **117** (1982) 34.

[9] S. Machida and M. Namiki. Prog. Theor. Phys. **63** (1980) 1457; 1833; M. Namiki, Found. Phys. **18** (1988) 29.

[10] M. Namiki and S. Pascazio, Phys. Rep. **232** (1993) 301; M. Namiki, S. Pascazio and C. Schiller, Phys. Lett. **A 182** (1994) 17.

[11] R.J. Cook, Phys. Scr. **T21** (1988) 49.

[12] W.H. Itano, D.J. Heinzen, J.J. Bollinger and D.J. Wineland, Phys. Rev. **A 41** (1990) 306.

[13] T. Petrosky, S. Tasaki and I. Prigogine, Phys. Lett. **A 151** (1990) 109; Physica **A 170** (1991) 306; A. Peres and A. Ron, Phys. Rev. **A 42** (1990) 5720; L.E. Ballentine, Phys. Rev. **A 43** (1991) 5165; W.H. Itano, D.J. Heinzen, J.J. Bollinger and D.J, Wineland, Phys. Rev. **A 43** (1991) 5168; S. Inagaki, M. Namiki and T. Tajiri, Phys. Lett. **A 166** (1992) 5; D. Home and M.A.B. Whitaker, Phys. Lett. **A 173** (1993) 327.

[14] Inagaki et al's paper in [13]; S. Pascazio, M. Namiki, G. Badurek and H. Rauch, Phys. Lett. **A 179** (1993) 155; S. Pascazio and M. Namiki, Phys. Rev. **A 50** (1994) 4582; H. Nakazato, M. Namiki, S. Pascazio and H. Rauch, Phys. Lett. **A 199** (1995) 27.

[15] A. Peres, Am. J. Phys. **48** (1980) 93.

[16] P. Kwiat, H. Weinfurter, T. Herzog, A. Zeilinger and M. Kasevich, Ann. of the N.Y. Acad. Sci. **755** (1995) 383.

NEXT
DOCUMENT

MULTI-PARTICLE INTERFEROMETRY BASED ON DOUBLE ENTANGLED STATES

Todd B. Pittman, Y.H. Shih, D.V. Strekalov, A.V. Sergienko, M.H. Rubin
Department of Physics, University of Maryland Baltimore County
Baltimore, MD 21228 USA

Abstract

A method for producing a 4-photon entangled state based on the use of two independent pair sources is discussed. Of particular interest is that each of the pair sources produces a two-photon state which is simultaneously entangled in both polarization and space-time variables. Performing certain measurements which exploit this double entanglement provides an opportunity for verifying the recent demonstration of nonlocality by Greenberger, Horne, and Zeilinger.

1 Introduction

The incompatibility of quantum mechanics with some of the intuitive concepts found in the premises of the Einstein-Podolsky-Rosen argument (EPR) [1] has recently been shown through the remarkable demonstration of nonlocality by Greenberger, Horne, and Zeilinger (GHZ) [2]. Whereas traditional Bell-type [3] arguments have been based on the statistical correlations of two entangled particles, the GHZ theorem relies only on the perfect correlations of three or more particles to exhibit a blatant contradiction in the premises of EPR. The beauty and simplicity of this theorem has provided strong motivation for the experimental construction of a multi-particle entangled state.

In this paper we present a method for constructing a 4-photon state entangled in space-time variables. As has been shown in the pioneering work of Yurke and Stoler [4] [5], EPR effects can arise even when the particles do not originate from one central decaying source. Yet rather than basing our system on four independent single particle sources, we will use two independent pair sources.

The use of two independent pair sources in two-photon correlation experiments has been discussed by Zukowski, Zeilinger, Horne, and Ekert [6], and by Pavicic and Summhammer [7]. Here, however, the interesting feature of the pair sources is that they each produce two-photon states which are simultaneously entangled in both polarization *and* space-time variables. This double entanglement is used to overcome a basic problem in 4-photon experiments which is introduced through the simple example of the double Franson-interferometer [8]. Throughout the paper simplified models in which the states evolve along the optical paths are used to highlight the importance of the double entanglement.

2 The Double Franson-Interferometer Example

Perhaps the easiest way to envision constructing a 4-photon space-time entangled state from two pair sources would be to use two standard Franson-interferometer setups, and a 4-fold coincidence counting scheme such as that shown in Figure 1. Here, two type-I down-conversion crystals, X and X', are coherently pumped by the same continuous wave (CW) laser source. The signal and

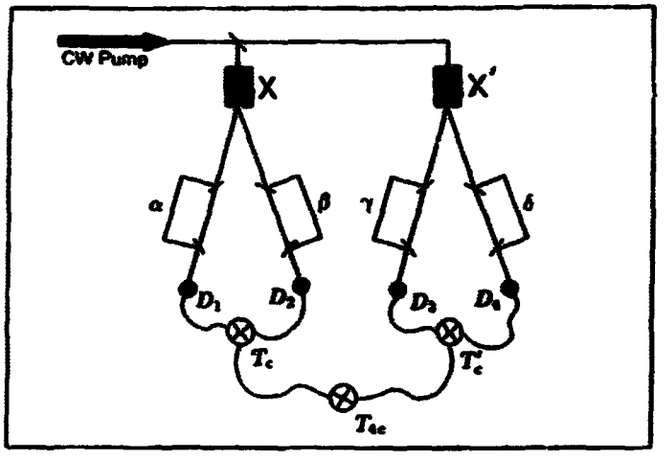

FIG.1. The double Franson-interferometer simply consists of two standard Franson-Interferometer setups coherently pumped by a single laser.

idler photons of each down-converted pair can follow either a long or short path to their respective detectors. For simplicity α, β, γ, and δ, which are the phase delays between the long and short paths in the four arms, can be taken to be equal.

Considering the single Franson-interferometer setup following crystal X, one would first perform the standard procedure of making the two-photon coincidence circuit time window, T_c, much shorter than the time delays associated with α and β. By doing this the two-photon probability amplitudes corresponding to one photon of a down-converted pair taking the short path while the other takes the long path can not contribute to the two-photon coincidence counting rate, and the two-photon space-time entangled state originating from crystal X is: $|\psi_2\rangle \sim |S\rangle_1|S\rangle_2 + e^{i(\alpha+\beta)}|L\rangle_1|L\rangle_2$, where $|S\rangle_1$ denotes the photon taking the short path to detector 1, and so on. By reducing T_c' a similar state is realized in the other two-photon setup : $|\psi_{2'}\rangle \sim |S'\rangle_3|S'\rangle_4 + e^{i(\gamma+\delta)}|L'\rangle_3|L'\rangle_4$, where the primes always indicate origination in crystal X'.

Therefore, the 4-photon quantum state realized by combining the outputs of these two-photon coincidence circuits into a 4-photon coincidence circuit would be the product:

$$
\begin{aligned}
|\psi_4\rangle \;\sim\; & \left(|S\rangle_1|S\rangle_2 + e^{i(\alpha+\beta)}|L\rangle_1|L\rangle_2\right) \otimes \left(|S'\rangle_3|S'\rangle_4 + e^{i(\gamma+\delta)}|L'\rangle_3|L'\rangle_4\right) \\
= \; & |S\rangle_1|S\rangle_2|S'\rangle_3|S'\rangle_4 + e^{i(\gamma+\delta)}|S\rangle_1|S\rangle_2|L'\rangle_3|L'\rangle_4 + \\
& e^{i(\alpha+\beta)}|L\rangle_1|L\rangle_2|S'\rangle_3|S'\rangle_4 + e^{i(\alpha+\beta+\gamma+\delta)}|L\rangle_1|L\rangle_2|L'\rangle_3|L'\rangle_4. \qquad (1)
\end{aligned}
$$

This, however, is not a 4-photon space-time entangled state because of the two middle terms, describing the amplitudes where some photons followed the short paths while others followed the

long paths. What is desired is tne ellimination of these two terms so that the 4-fold coincidence counting rate shows the signature interference due to the two indistinguishable processes in which all 4 photons take their short paths, or all 4 take their long paths.

At first glance, one might be tempted to try and achieve this ellimination by reducing the 4-fold coincidence time window, T_{4c}, (as had been done in each of the two-photon coincidence circuits) to "cut-off" these unwanted terms. However, this will not work, as can be seen through the following simplistic indistinguishability argument: Consider the case when a down conversion pair is "born" in crystal X at some time t and each of the photons follows its long path en route to detectors 1 and 2. Then at some later time $t+\tau$ a pair is born in cyrstal X' but these photons follow their short paths to detectors 3 and 4. Well, in the extremely unfortunate circumstance that τ is exactly equal to the time delay between the short and long paths, all 4 detectors will fire simultaneously. Thus, even though in principle T_{4c} can be made extremely small, the 4-fold coincidence count resulting from this type of $|L\rangle_1|L\rangle_2|S'\rangle_3|S'\rangle_4$ amplitude is indistinguishable from a $|L\rangle_1|L\rangle_2|L'\rangle_3|L'\rangle_4$ or $|S\rangle_1|S\rangle_2|S'\rangle_3|S'\rangle_4$ amplitude when the two pairs were born at exactly the same time. In other words, simple attempts at space-time based projective measurements will not result in a space-time entangled state.

However, these two unwanted middle terms can be elliminated in a similar setup where each of the two-photon states is entangled in both polarization and space-time variables. As will be seen, the final projective measurements can be based on polarization, leaving a 4-photon state entangled in space-time varibles.

3 The Two-Photon Double Entangled State

Since we will solve the above problem by constructing our 4-photon entangled state from two double entangled two-photon states, we will briefly review their interesting features. The two-photon state which is simultaneously entangled with respect to both polarization and space-time variables has been observed [9], and even used to demonstrate two different types of violations of Bell's inequalities in a single experimental setup [10].

One way to construct such a state is shown in the cartoon schematic of Figure 2a. Consider a down-conversion crystal, X, cut at a type-II phase matching angle [11] which produces pairs of orthogonally polarized signal (parallel to the e-ray plane of crystal X) and idler (parallel to the o-ray plane of crystal X) photons that travel collinearly in the same direction as the pump. Ideally, the crystal should be thin enough so that its birefringence does not impart any significant temporal phase lag between the two down-converted photons, although in practice a thick crystal may be used followed by a compensation device [12] [13].

At this point the state can be roughly described by polarization kets: $|\psi\rangle \sim |\mathbf{o}\rangle \otimes |\mathbf{e}\rangle$. After filtering out the pump beam, the down-converted photons pass through a thin birefringent crystal, BC, whose fast and slow axes are aligned at $\pm 45°$ to the signal and idler polarizations (see Figure 2b). Thus, upon encountering BC, the state emerging from the crystal evolves as:

$$|\mathbf{o}\rangle \otimes |\mathbf{e}\rangle \longrightarrow \frac{1}{2}(|\mathbf{F}\rangle + |\mathbf{S}\rangle) \otimes (-|\mathbf{F}\rangle + |\mathbf{S}\rangle) = -\frac{1}{2}(|\mathbf{F}\rangle|\mathbf{F}\rangle - |\mathbf{S}\rangle|\mathbf{S}\rangle) \qquad (2)$$

where $|\mathbf{F}\rangle$ and $|\mathbf{S}\rangle$ describe photons polarized along the fast and slow axes of BC.

In order for a coincidence detection to occur, the photon pair must be split by 50/50 beam splitter BS. In each of the output ports of BS are delay units, which could be variable thickness birefringent material or even Pockel's cells, that are oriented with their fast and slow axes parallel

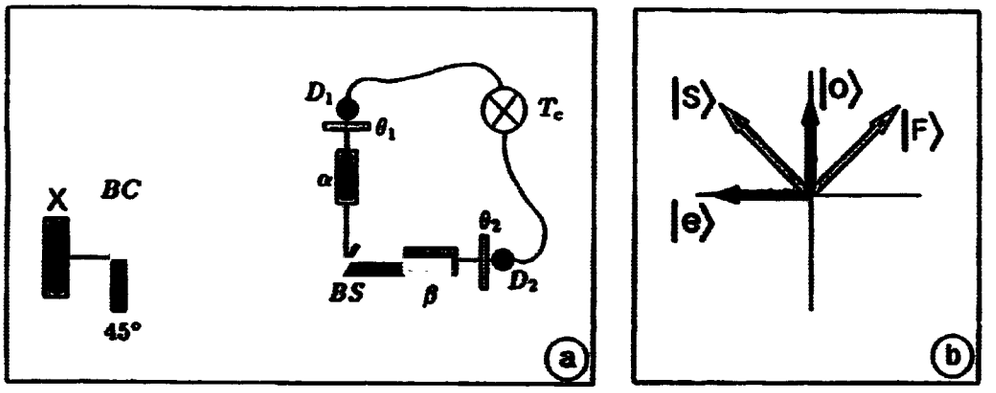

FIG.2. a) A cartoon schematic of the experiment which can realize the two-photon double entangled state. b) The polarization orientations of the signal (e-ray) and idler (o-ray) photons, and the fast and slow axes of BC.

to those of BC. In this way we can impart variable space-time phase delays, α and β, between the fast and slow "paths" leading to each detector. Behind each delay unit is a polarization analyzer (θ_1 and θ_2) and a detector.

It is easy to see that after BS and the delay units,

$$|\psi\rangle \longrightarrow \left(|\mathrm{F}\rangle_1|\mathrm{F}\rangle_2 - e^{i(\alpha+\beta)}|\mathrm{S}\rangle_1|\mathrm{S}\rangle_2\right) \tag{3}$$

State 3 is the double entangled state. Note that as we vary the phase delay $\alpha + \beta$ we see a space-time interference between the two indistinguishable amplitudes in which both photons followed their fast paths and both photons followed their slow paths, in exact analogy to the standard Franson-interferometer. Furthermore, if we go to a space-time coincidence counting rate minimum or maximum (e.g. $\alpha + \beta = 0, \pi$) we may rotate the analyzers θ_1 and θ_2 and see a polarization interference in analogy to that seen in some of the earlier tests of Bell's inequalties. It should be emphasized that there was no need of a short coincidence time window to see this effects.

4 The 4-Photon Space-Time Entangled State

We now proceed to employ two of these double entangled two-photon setups in a manner analogous to the use of two Franson-interferometers in Figure 1. Additionally, we insert an extra 50/50 beam splitter, EBS, so that photons transmitted by BS and BS' can reach either detector 2 or detector 4, as is shown in Figure 3a. Furthermore, we align the fast and slow axes of the elements in the primed system orthogonal to those of the unprimed system (see Figure 3b). As in equation 1, the

4-photon state here is the product of two two-photon entangled states (state 3 and its analog in the primed system), so that taking into account the action of EBS and ignoring the terms which will not contribute to the 4-fold coincidence counting rate, it is not difficult to see that [14]:

$$\begin{aligned}|\psi_4\rangle \sim\ & |F\rangle_1|F'\rangle_3\{|F\rangle_2|F'\rangle_4 - |F'\rangle_2|F\rangle_4\} \\ & -e^{i(\gamma+\delta)}|F\rangle_1|S'\rangle_3\{|F\rangle_2|S'\rangle_4 - |S'\rangle_2|F\rangle_4\} \\ & -e^{i(\alpha+\beta)}|S\rangle_1|F'\rangle_3\{|S\rangle_2|F'\rangle_4 - |F'\rangle_2|S\rangle_4\} \\ & +e^{i(\alpha+\beta+\gamma+\delta)}|S\rangle_1|S'\rangle_3\{|S\rangle_2|S'\rangle_4 - |S'\rangle_2|S\rangle_4\} \end{aligned} \quad (4)$$

Although analagous to equation 1, we see that the inclusion of the extra beam splitter has essentially divided each of the four possible 4-photon amplitudes into two equal phase parts, as indicated by the curly bracketed terms in equation 4. Based on the polarization, it is these equal

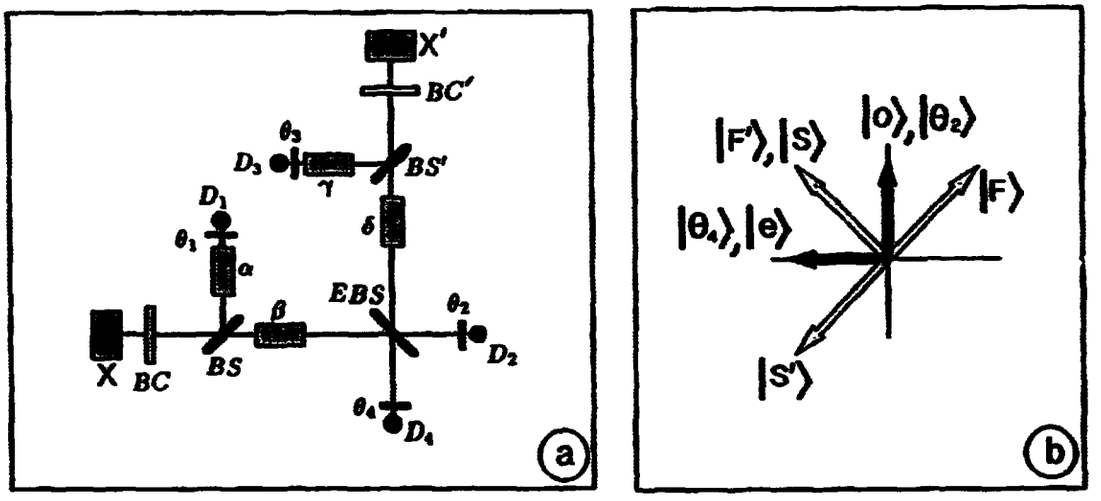

FIG.3. a) The envisioned scheme consists of two coherently pumped "double entangled two-photon state" setups which overlap through the use of an extra beam splitter (EBS). b) The important polarization orientations of the various elements in the scheme. Note that BC' is orthogonal to BC.

phase parts which will constructively or destructively interfere to produce the space-time entangled state.

For example, we consider the projection of the state on to the polarization analyzers and note from Figure 3b that $|F\rangle$ and $|S'\rangle$ are antiparallel. Thus, regardless of the settings of analyzers θ_2 and θ_4 the two equal phase parts in the curly brackets of the second term will subtract and this corresponding 4-photon amplitude will vanish. Likewise, since $|S\rangle$ and $|F'\rangle$ are parallel, the two equal phase parts in the curly brackets of the unwanted third term will also subtract. Furthermore, we note that if we orient θ_2 and θ_4 as shown in Figure 3b, and define the relevant part of the polarizer projection operator as $\mathcal{P} \equiv |\theta_2\rangle|\theta_4\rangle\langle\theta_4|\langle\theta_2|$, then in the curly brackets of the first 4-photon term:

$$\mathcal{P}|F\rangle_2|F'\rangle_4 = -\mathcal{P}|F'\rangle_2|F\rangle_4, \quad (5)$$

and these two equal phase parts *add together*. The same is true inside the curly brackets of the last 4-photon term.

In other words, since the polarizations are associated with space-time paths, the amplitudes in which some photons take the fast paths while others take the slow paths are seen to vanish, while those in which all four photons take the fast paths or all four photons take the slow paths remain!

The remaining 4-photon state is entangled in space-time variables:

$$|\psi_4\rangle = |F\rangle_1|F\rangle_2|F\rangle_3|F\rangle_4 + e^{i(\alpha+\beta+\gamma+\delta)}|S\rangle_1|S\rangle_2|S\rangle_3|S\rangle_4. \quad (6)$$

It is interesting to see that with the above choice of θ_2 and θ_4 settings, there is no dependence on the difference in pair birth times (provided it is within the coherence time of the pump), nor any reliance on any type of ultra-short coincidence time windows provided we can assure at most one pair of photons from each crystal is in the system at any given time.

5 Acknowledgements

This work was supported by the Office of Naval Research Grant No. N00014-J-1430.

References

[1] A. Einstein, B. Podolsky, and N. Rosen, Phys. Rev. **35**, 777 (1935).

[2] D.M. Greenberger, M.A. Horne, A. Shimony, and A. Zeilinger, Am. J. Phys. **58**, 1131 (1990).

[3] J.S. Bell, Physics **1**, 195 (1964).

[4] B. Yurke and D. Stoler, Phys. Rev Lett. **68**, 1251 (1992).

[5] B. Yurke and D. Stoler, Phys. Rev A **46**, 2229 (1992).

[6] M. Zukowski, A. Zeilinger, M.A. Horne,and A.K. Ekert, Phys. Rev Lett. **71**, 4287 (1993).

[7] M. Pavicic and J. Summhammer, Phys. Rev Lett. **73**, 3191 (1994).

[8] J.D. Franson, Phys. Rev Lett. **62**, 2205 (1989).

[9] Y.H. Shih and A.V. Sergienko, Phys. Lett. A. **191**, 201 (1994).

[10] T.B. Pittman, Y.H. Shih, A.V. Sergeinko, and M.H. Rubin, Phys. Rev. A. **51**, 3495 (1995).

[11] D.N. Klyshko, *Photons and Non-linear Optics* (Gordon and Breach Science, New York, 1988).

[12] Y.H. Shih and A.V. Sergeinko, Phys. Lett. A. **186**, 29 (1994).

[13] M.H. Rubin, D.N. Klyshko, Y.H. Shih, and A.V. Sergeinko, Phys. Rev. A. **50**, 5122 (1994).

[14] T.B. Pittman, Phys. Lett. A **204**, 193 (1995).

NEXT
DOCUMENT

QUANTUM MECHANICS OF A TWO PHOTON STATE

Morton H. Rubin
Department of Physics, University of Maryland Baltimore County
Baltimore, MD 21228-5398

Abstract

We review the formalism for describing the two photon state produced in spontaneous parametric down conversion.

1 Introduction

In this discussion we will first outline the general theory of optical spontaneous parametric down-conversion (OPDC). We will then discuss the phase matching conditions. After this we will discuss the classification of OPDC into type-I and type-II. Finally we will present our picture of the two photon state generated by the thory.

The work discussed in this paper is the result of the efforts of the members of the UMBC Quantum Optics Group:

Y. H. Shih
A. V. Sergienko
T. Pittman
D. Strekalov
J. Orzak
D. N. Klyshko (Moscow State University)

2 Optical Parametric Downconversion

Optical Parametric down conversion is modeled (in the interaction picture) by the interaction Hamiltonian [1][2]

$$H_1 = \frac{\epsilon_0}{2}\int d^3r \chi^{(2)}_{pbc} E_p(\mathbf{r},t) E_b(\mathbf{r},t) E_c(\mathbf{r},t) \tag{1}$$

where E_p is the pump electric field and $\chi^{(2)}_{abc}$ is the second order susceptibility, ($\chi = \chi^{(1)} + \chi^{(2)} + \chi^{(3)} + \ldots$). The integral is over the intersection of the birefringent crystal and the pump beam. In writing this it is assumed that the crystal does not have a center of symmetry so $\chi^{(2)}_{abc} \neq 0$ and that wave length of the light is much greater than atomic dimensions so the crystal can be treated in the continuum limit. The pump is be treated classically. For spontaneous optical parametric down conversion the wave function incident on the crystal is assumed to be the vacuum, $|\Psi> = |0>$.

Using first order perturbation theory, we can compute the wave function produced at the output face of the crystal. It is a superposition of the vacuum and a two-photon state. The two photon beams are often referred to as the signal and idler beams. In our case, we choose the orientation of the optic axis of the crystal and the polarization of the pump beam so that the produced photons have orthogonal polarizations corresponding to ordinary (o-rays) and extraordinary (e-rays) rays in the crystal.

$$\begin{aligned} |\Psi> &= |0> - \frac{i}{\hbar}\int_{-\infty}^{\infty} dt H_1 |0> \\ &= |0> + \sum_{\mathbf{k},\mathbf{k}'} F_{\mathbf{k},\mathbf{k}'} a^{\dagger}_{o\mathbf{k}'} a^{\dagger}_{e\mathbf{k}'} |0>, \end{aligned} \tag{2}$$

$$F_{\mathbf{k},\mathbf{k}'} = \Gamma_{\mathbf{k},\mathbf{k}'} \delta(\omega_{o\mathbf{k}} + \omega_{e\mathbf{k}} - \omega_p) L h(L\Delta_{\mathbf{k},\mathbf{k}'}) h_{tr}(\mathbf{k},\mathbf{k}'). \tag{3}$$

In Eq. (3) $\mathrm{Lh}(\mathrm{L}\Delta_{\mathbf{kk}'})$ comes from the integral over the length L of the crystal,

$$h(x) = \frac{1 - e^{-ix}}{ix} \tag{4}$$

$$\Delta_{\mathbf{kk}'} = k_p - k_z - k'_z \tag{5}$$

The integral over the area A of the intersection of the beam cross-section and the crystal gives

$$h_{tr}(\mathbf{k},\mathbf{k}') = \int_A d^2\rho\, e^{i(\mathbf{k}+\mathbf{k}')\cdot\rho}. \tag{6}$$

The time integral gives the 2π times the Dirac delta function which is the *steady-state or frequency phase matching condition.* If we assume that the crystal is very large and the pump beam has a large cross section, then the integrals can be taken to extend over an infinite volume. This leads to the *wave number phase matching condition*

$$\mathbf{k} + \mathbf{k}' = k_p \hat{\mathbf{e}}_z. \tag{7}$$

The assumption of a monochromatic pump beam gives

$$\omega_p = \omega_{o\mathbf{k}} + \omega_{e\mathbf{k}'}. \tag{8}$$

3 The properties of the two photon state

3.1 Terminology

We introduce some terminology for OPDC.

- Collinear k and k' are parallel to $\mathbf{k}_p$
- Degenerate $\omega_1 = \omega_2$
- Type-I Signal and idler have same polarization
- Type-II Signal and idler have orthogonal polarization

We next remind the reader of the definition of an *entangled state* [3]. For two degrees of freedom, we say a state $\Psi(1,2)$ is entangled if it is not a product state, i.e. $\Psi(1,2) \neq \phi(1)\phi(2)$. A simple example of an entangled state is the singlet state of two spin-1/2 particles.

3.2 OPDC two photon state

[4] The state in Eq.(2) is entangled in wave number and frequency or, equivalently, in space and time because $F_{kk'}$ does not factor into a function of k and k'. In general, it is not entangled in polarization.

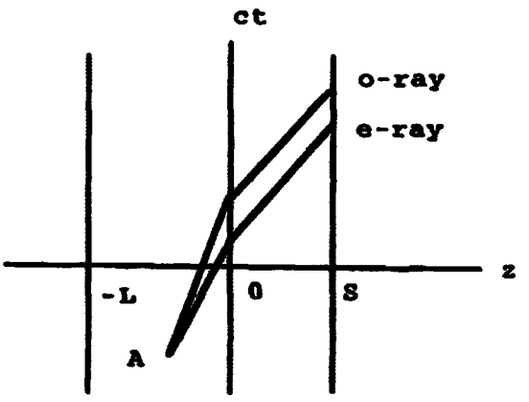

FIG. 1. A Feynman-like diagram showing a pair created at point A inside the crystal. For the case shown the speed of the e-ray is greater than that of the o-ray in the crystal. Since the first photon is always the e-ray, the state is not entangled in polarization.

The simplest experiment to study the two photon state is illustrated below.

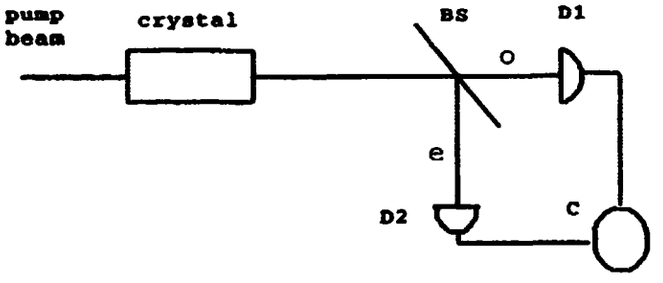

FIG. 2. A collinear, type-II experiment. The beam splitter seperates the polarizations and sends them to the two detectors D1 and D2. A coincident counter, C, detects coincidences.

For this is a collinear, type-II experiment the output is given by the coincident counting rate

$$R_c = \lim_{T\to\infty} \frac{1}{T}\int_0^T dT_1 \int_0^T dT_2 < \Psi | E_1^{(-)} E_2^{(-)} E_2^{(+)} E_1^{(+)} | \Psi > S(T_1 - T_2) \qquad (9)$$

where S(t) is a coincidence time window. The probability of a coincidence is

$$< \Psi | E_1^{(-)} E_2^{(-)} E_2^{(+)} E_1^{(+)} | \Psi >= |A(t_1, t_2)|^2 \tag{10}$$

$$A(t_1, t_2) =< 0 | E_2^{(+)} E_1^{(+)} | \Psi > \tag{11}$$

$$t_j = T_j - z_j/c \tag{12}$$

where T_j is the time at which a photon is detected at detector j which is a distance z_j from the output surface of the crystal. A is called the ***two-photon amplitude*** or ***biphoton***. The two-photon amplitude is of the form

$$A(t_1, t_2) = v(t_1 + t_2) u(t_1 - t_2) \tag{13}$$

$$u(t) = e^{i\omega_d \frac{t}{2}} \Pi(t), \tag{14}$$

$$v(t) = v_0 e^{i\omega_p \frac{t}{2}} \tag{15}$$

$$\omega_d = \Omega_o - \Omega_e. \tag{16}$$

The quantities Ω_o and $\Omega_e, (\Omega_o + \Omega_e = \omega_p)$ are chosen for convenience. For details see [4].

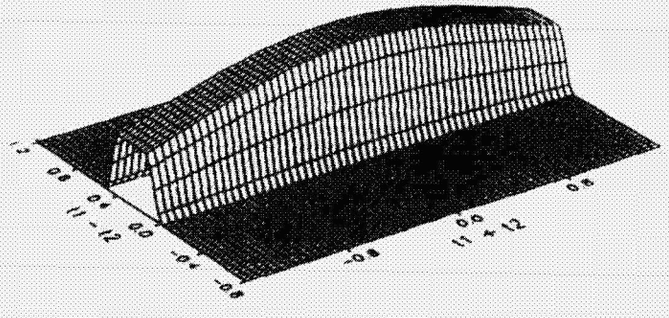

FIG. 3. An illustration of the two-photon amplitude. In most experiments the width in $t_1 - t_2$ is much smaller than the length in $t_1 + t_2$. The latter is determined by the coherence length of the pump.

3.3 Double entanglement

It is possible to entangle the polarization as well as the energy and momentum. The simplest experiment for seeing this is shown in figure 4 below.

A birefringent crystal is placed in the path of the rays to compensate for the different group velocities of the o- and e-rays. If the e-ray emerges from the crystal first, the compensator is

arranged so the e-ray passes along its slow axis. The length of the compensator may be varied so that it introduces a delay τ in the e-ray relative to the o-ray.

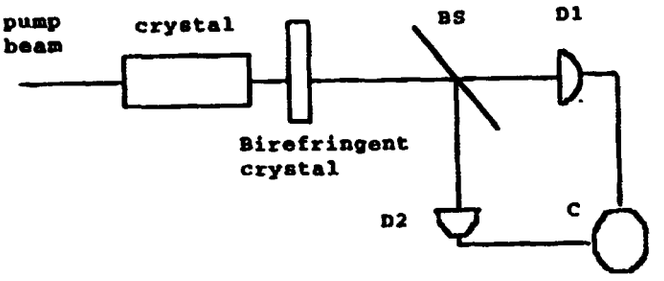

FIG. 4. The use of a birefringent crystal as a compensator.

If the beam splitter is a 50-50 beam splitter, then the two photon amplitude becomes

$$A(t_1, t_2) = \frac{1}{\sqrt{2}} v(t_1 + t_2 - \tau)[u(t_1 - t_2 + \tau) - u(-t_1 + t_2 + \tau)]. \tag{17}$$

The minus sign comes from the reflection off the mirror. The figure below illustrates the form of the bracketed term in Eq.(17). The probability amplitude will show interference between these two terms if τ is chosen so the two terms overlap. The xounting rate is then vee shaped, going to zero for complete overlap. We refer you to Dr. Sergienko's talk for details of the experimental

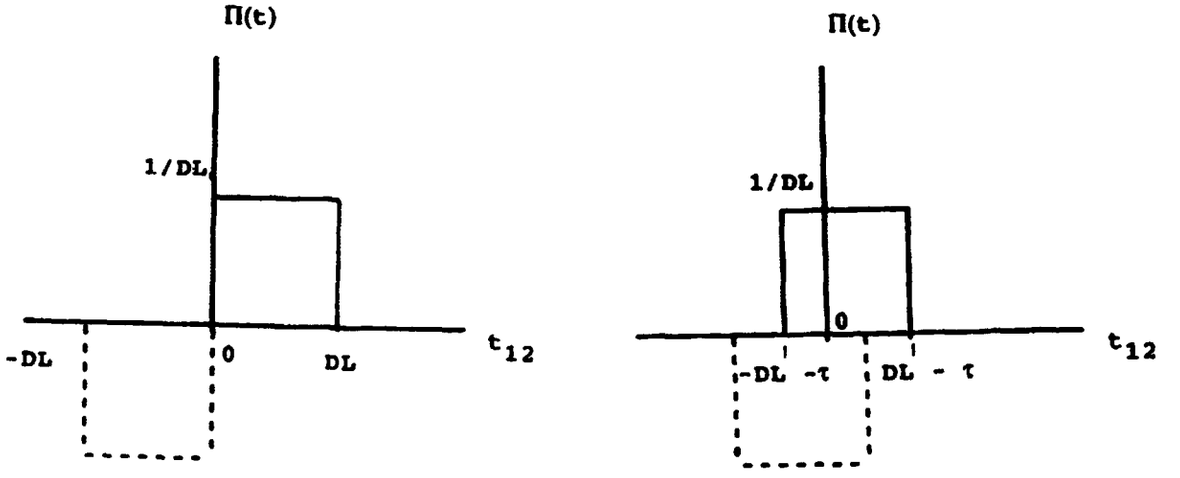

FIG. 5. The form of the amplitude in Eq. (17) is shown for no overlap and partial overlap.

We also illustrate this effect using Feynman-like diagrams for a some typical pairs.

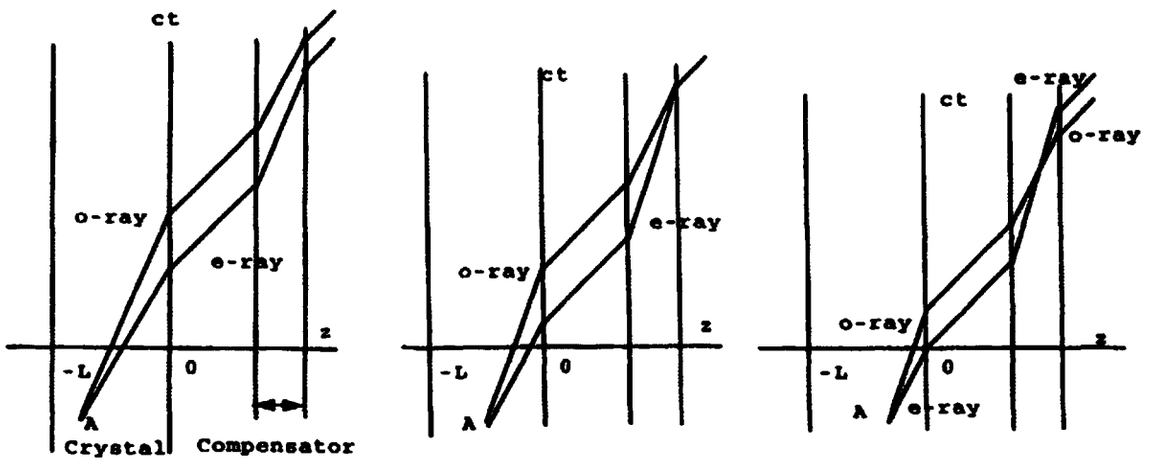

FIG. 6. These diagrams illustrate how the compensator effects pairs that are created at point A near the input, at the center, and near the output of the crystal.

4 Conclusion

We have a good understanding of the structure of the two-photon amplitude both theoretically and experimentally. The experimental results have been reported by other members of our group at this meeting. We have recently completed some work on the transverse correlations of the signal and idler beams.

5 Acknowledgments

This work was supported by the U. S. Office of Naval Research. I also wish to thank the University of Maryland Baltimore County for providing partial support for travel to this workshop.

References

[1] W. H. Louisell, A. Yariv, and A. E. Siegman, Phys Rev. **124**, 1646 (1961).

[2] D. N. Klyshko, *Photons and Nonlinear Optics*, (Gordon and Breach Science Publishers, New York, 1988).

[3] E. Schrödinger, Naturwissenschften **23**, 807, 823, 844 (1935). Translation in J. A. Wheeler and W. H. Zurek, ed. *Quantum Theory of Measurement*.

[4] Morton H. Rubin, David N. Klyshko, Y. H. Shih, and A. V Sergienko, Phys. Rev. A**50**, 5122 (1994).

NEXT
DOCUMENT

A PROPOSAL FOR TESTING LOCAL REALISM WITHOUT USING ASSUMPTIONS RELATED TO HIDDEN VARIABLE STATES

Luiz Carlos Ryff[1]

University of Maryland Baltimore County, Baltimore, Maryland 21228

Abstract

A feasible experiment is discussed which allows us to prove a Bell's theorem for two particles without using an inequality. The experiment could be used to test local realism against quantum mechanics without the introduction of additional assumptions related to hidden variables states. Only assumptions based on direct experimental observation are needed.

The experiment I wish to discuss is represented in Fig.1. It is a variant of Franson's two-photon correlation experiment [1]. However, variants of other experiments could also be considered [2-4]. A source (S) emits pairs of photons (γ_1 and γ_2). The photons are emitted simultaneously [5], but there is uncertainty about the time of emission. H_1 and H_2 are 50%:50% beam splitters. As in an experiment recently discussed [6], H_1', H_2', H_3, and H_4 are not 50%.50% beam splitters, and have real amplitude transmissivities T_1, T_2, T_3, and T_4, and real amplitude reflectivities R_1, R_2, R_3, and R_4. M_1, M_1', M_2, M_2' and M_2'' are mirrors, and ϕ_1, ϕ_2, and ϕ_3 are phase shifters. L_2-S_2=L_1-S_1=$c\Delta T$ is much greater than the coherence lengths of the packets associated with γ_1 and γ_2. This implies that $\Delta\omega_1\Delta T\gg 1$ and $\Delta\omega_2\Delta T\gg 1$, where $\Delta\omega_1$ and $\Delta\omega_2$ are the uncertainties in the angular frequencies of γ_1 and γ_2. However, $\Delta(\omega_1+\omega_2)\Delta T\ll 1$. As is well known [1], in this case the situation in which both photons follow the long paths is indistinguishable from the situation in which both photons follow the short paths. In the present proposal a balanced Mach-Zehnder interferometer for photons γ_2, constituted by H_3, H_2', M_2'', and H_4 has been introduced.

---

[1]Permanent address: Universidade Federal do Rio de Janeiro, Instituto de Física, Caixa Postal 68528, 21945-970 Rio de Janeiro, RJ, Brazil

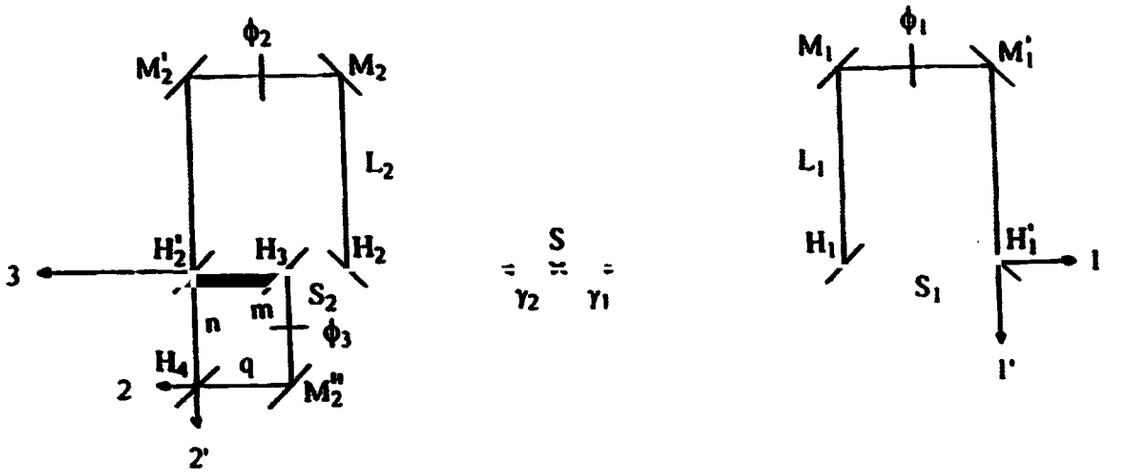

FIG.1. Experiment proposed.

I will consider four different situations: (A) H_2' and H_4 are removed; (B) H_2' is in place and H_4 is removed; (C) H_2' is removed and H_4 is in place; (D) H_2' and H_4 are in place. The detections relevant to our discussion are only the coincident detections occuring at sites 1 and 2, 1 and 2', 1' and 2, and 1' and 2'. Naturally, the probability of coincident detections occuring at sites 1' and 2 in situation A, $P_A^c(1',2)=0$, since in situation A $\gamma_1(\gamma_2)$ has to follow the long(short) path to be detected at 1'(2).

The probability amplitude of coincident detections occuring at sites 1 and 2' in situation B is [6]

$$A_B^c(1,2')= \sum_{\omega_1\omega_2} c_{\omega_1\omega_2} (\alpha_1\alpha_2+\beta_1\beta_2) , \qquad (1)$$

where $c_{\omega_1\omega_2}$ is the probability amplitude of having a photon γ_1 with a frequency ω_1 and a photon γ_2 with frequency ω_2, $\alpha_1= 2^{-1/2} \exp(i\omega_1 t_S)T_1$ is the probability amplitude of having a photon $\gamma_1(\omega_1)$ following the short path, where t_S is the time spent by light to follow the short path, $\alpha_2=2^{-1/2}T_3iR_2\exp[i\omega_2(t_S+t')]$ is the probability amplitude of having a photon $\gamma_2(\omega_2)$ following the short path, where t' is the time spent by light from H_2' to H_4, $\beta_1=i2^{-1/2}\exp(i\phi_1)\exp(i\omega_1 t_L)iR_1$ is the probability amplitude of having a photon $\gamma_1(\omega_1)$ following the long path, where t_L is the time spent by light to follow the long path, and $\beta_2=i2^{-1/2}\exp(i\phi_2)T_2\exp[i\omega_2(t_L+t')]$ is the probability amplitude of having a photon $\gamma_2(\omega_2)$ following the long path. Using (1) and the condition $\Delta(\omega_1+\omega_2)\Delta T\ll 1$ we obtain

$$A_B^c(1,2')=(i/2)\sum_{\omega_1\omega_2} A_{\omega_1\omega_2}(T_1T_3R_2-BR_1T_2)\ , \tag{2}$$

where $A_{\omega_1\omega_2}=c_{\omega_1\omega_2}\exp[i\omega_1 t_S+i\omega_2(t_S+t')]$ and $B=\exp[i(\phi_1+\phi_2)+i(\omega_{10}+\omega_{20})\Delta T]$ where ω_{10} and ω_{20} are the central frequencies of γ_1 and γ_2. Choosing $T_1T_3R_2=R_1T_2$ and using the condition

$$\sum_{\omega_1\omega_2} |c_{\omega_1\omega_2}|^2=1\ , \tag{3}$$

we obtain

$$P_B^c(1,2')=(1/2)(T_1T_3R_2)^2(1-\mathrm{Re}B)\ . \tag{4}$$

In an ideal situation we can have $[P_B^c(1,2')]_{min}=0$ (ReB=1) and $[P_B^c(1,2')]_{max}=(T_1T_3R_2)^2$ (ReB=-1). This follows from quantum mechanical nonlocality. But in a real situation this is not so. Let us then assume that ReB=1-ε (ReB=-1+ε) in the minimum (maximum) case. Then we can introduce the visibility V_B given by

$$V_B=\frac{[P_B^c(1,2')]_{max}-[P_B^c(1,2')]_{min}}{[P_B^c(1,2')]_{max}+[P_B^c(1,2')]_{min}}=1-\varepsilon\ . \tag{5}$$

Thus,

$$[P_B^c(1,2')]_{min}=(1/2)(T_1T_3R_2)^2(1-V_B)\ . \tag{6}$$

Using a similar reasoning, we obtain

$$A_C^c(1,2')=\sum_{\omega_1\omega_2} c_{\omega_1\omega_2}\delta(\rho_1+\rho_2)\ . \tag{7}$$

where $\delta=2^{-1/2}\exp(i\omega_1 t_S)$, $\rho_1=2^{-1/2}T_3iR_2\exp[i\omega_2(t_S+t')]T_4$, and $\rho_2=2^{-1/2}iR_3\exp(i\phi_3)\exp[i\omega_2(t_S+t')]iR_4$, which leads to

$$A_C^c=(1/2)\sum_{\omega_1\omega_2} A_{\omega_1\omega_2}(iT_3R_2T_4-CR_3R_4)\ , \tag{8}$$

where $C=\exp(i\phi_3)$. Thus, choosing $T_3R_2T_4=R_3R_4$ and using (3) we obtain

$$P_C^c(1,2')=(1/2)(T_3R_2T_4)^2(1-\mathrm{Im}C)\ . \tag{9}$$

As in (5) and (6), we can introduce the visibility V_C to obtain

$$[P_C^c(1,2')]_{min}=(1/2)(T_3R_2T_4)(1-V_C) \ . \qquad (10)$$

In an ideal situation we can have $V_C=1$ and $[P_C^c(1,2')]_{min}=0$. This follows from the wave like properties of light.

It is also easy to see that

$$A_D^c(1,2')=\sum_{\omega_1\omega_2} c_{\omega_1\omega_2}[\lambda_1(\sigma_1+\sigma_2)+\lambda_2\sigma_3] \ , \qquad (11)$$

where $\lambda_1=2^{-1/2}\exp(i\omega_1 t_S)T_1$, $\sigma_1=2^{-1/2}T_3iR_2\exp[i\omega_2(t_S+t')]T_4$, $\sigma_2=2^{-1/2}iR_3\exp(i\phi_3)\exp[i\omega_2(t_S+t')]iR_4$, $\lambda_2=i2^{-}\exp(i\phi_1)\exp(i\omega_1 t_L)iR_1$, and $\sigma_3=i2^{-1/2}\exp(i\phi_2)T_2\exp[i\omega_2(t_L+t')]T_4$, which leads to

$$A_D^c=(i/2)T_1T_3R_2T_4\sum_{\omega_1\omega_2}^{\cdot} A_{\omega_1\omega_2}(1-B+iC) \ . \qquad (12)$$

Then, choosing ϕ_1 and ϕ_2 such that $P_B^c(1,2')=[P_B^c(1,2')]_{min}$, and ϕ_3 such that $P_C^c(1,2')=[P_C^c(1,2')]_{min}$, we obtain

$$P_D^c(1,2')=(1/2)(T_1T_3R_2T_4)^2[(3/2)-V_B-V_C+V_BV_C-(1-V_B)^{1/2}(1-V_C)^{1/2}] \ . \qquad (13)$$

To prove a Bell's theorem for two particles without using an inequality we can consider the ideal situation: $V_B=V_C=1$. I will assign the value $i(1)$ for detections that occur at sites 1 and 2' (1' and 2). Thus, assuming there can be hidden variables states (HVS) of the photon pair which mimic quantum mechanics, we can only have: (A) $a_R^c(\lambda)b_R^c(\lambda)=i,-1$; (B) $a_P^c(\lambda)b_R^c(\lambda)=i,1$, from (6); and (C) $a_R^c(\lambda)b_P^c(\lambda)=i,1$, from (10). $a_P^c(\lambda)$ ($b_R^c(\lambda)$) represents the result of a measurement performed at 1,1' (2,2') when H_1' (H_4) is in place (removed), and so on, the superscript c refers to coincident detections, and λ represents the HVS of the photon pair [7]. Assuming locality, that is, that $a_R^c(\lambda)$ is the same in A and C, for example, we see that $a_P^c(\lambda)=i\xrightarrow{B}b_R^c(\lambda)=1\xrightarrow{A}a_R^c(\lambda)=i\xrightarrow{C}b_P^c(\lambda)=1$. That is, $P_D^c(1,2')=0$ (local realism), in disagreement with $P_D^c(1,2')=(1/4)(T_1T_3R_2T_4)^2$ (quantum mechanics), from (13).

Introducing some assumptions which are based on direct experimental observation the above argument can be extended to the case of a real (i.e., non-ideal) experiment. Let us initially consider situation C and select only those events in which detection at 2'

occurs. In this case, whenever a coincident detection at 1 occurs we know that γ_1 and γ_2 have followed the short paths. I will assume that: (A1) if H_1' had been in place (sit.C⟶sit.D) the number of photons *following the short path* that would be coincidentally detected at 1 could not be greater than the number of photons coincidentally detected at 1 when H_1' is removed (I will return to this point). Therefore, the number of coincident detections at 1 and 2' in sit.D *which correspond to the possibility in which* γ_1 *and* γ_2 *follow the short paths* cannot be greater than $N_C^c(1,2')$, the number of coincident detections at 1 and 2' in sit.C.

Let us now consider situation B and select only those events in which detection at 1 occurs. In this case, only the coincident detections at 1 and 2' can correspond to the possibility in which γ_1 and γ_2 follow the long paths. According to (A1), if H_4 had been in place (sit.B⟶sit.D) the number of photons *following path n* that would be coincidentally detected at 2' could not be greater than the number of photons coincidentally detected at 2' when H_4 is removed. Therefore, the number of coincident detections at 1 and 2' in sit.D *which correspond to the possibility in which* γ_1 *and* γ_2 *follow the long paths* cannot be greater than $N_B^c(1,2')$, the number of coincident detections at 1 and 2' in sit.B. Hence, $N_D^c(1,2') \leq N_C^c(1,2') + N_B^c(1,2')$, or, in terms of probabilities,

$$P_D^c(1,2') \leq P_C^c(1,2') + P_B^c(1,2') \ , \qquad (14)$$

since : (A2) coincident detections can only occur when photons of the emitted pair either (a) both follow the long paths, or (b) both follow the short paths.

Let us examine (A1) closer. It was assumed, when changing from situation C(B) to situation D, that the number of detections generated by photons $\gamma_1(\gamma_2)$ following path $S_1(n)$ could not be increased by placing a beam splitter $H_1'(H_4)$ in front of the detectors. Although this may appear to be a nonenhancement assumption [8], this can be directly verified. For example, by blocking path $L_1(q)$ in situation D. Now we are not assuming that for *every* HVS of a photon the probability of it being detected cannot be enhanced by placing a beam splitter in front of the detector. However, it might still be argued that when $H_1'(H_4)$ is in the position represented in Fig.1, in which case photons from two different directions can impinge on it, its properties are modified, in such a way that photons coming via path $S_1(n)$ become more "detectable" after impinging on $H_1'(H_4)$ and being transmitted, whilst photons coming via path $L_1(q)$ become less

"detectable" after impinging on $H_1'(H_4)$ and being reflected [9]. However, this sounds as a much too contrived supposition.

To have a rough estimation of the expected disagreement between the local realistic and the quantum mechanical predictions in a real experiment, we can make $V_B = V_C = V$. Hence, using (6), (10), and (13), we see that in order to have a violation of (14) we must have

$$(T_1T_4)^2[(1/2)-2V+2V^2]/[(T_4^2+T_1^2)(1-V)] > 1. \qquad (15)$$

Then, making $T_1 = T_4 = T, R_1 = R_4 = R$, which leads to $T_3 = R_2, T_2 = R_3 = [-R+(1+3T^2)^{1/2}]/2T$, we obtain

$$(T^2/4)(1-4V+4V^2)/(1-V) > 1 \ . \qquad (16)$$

We see that the minimum visibility we must have in order to violate (16) is given by $V > 0.87$ ($T = 1$). Apparently our best choice would be $T = 1$. However, this corresponds to the situation in which H_1' and H_4 have been removed. In this case the probabilities drop to zero, and we would have to wait an infinite time to get any result. $V = 0.90$, $T = 1/(1.2)^{1/2}$ $\longrightarrow$ l.h.s.(16) > 1.3. To have an idea of the time necessary to perform an experiment using these data we can calculate the ratio between the probability of having a coincident detection in a Franson's experiment in the case of perfect correlations and the probability given by (13) in the ideal case ($V = 1$). We easily see that we need about eleven times more time to have the same statistics as in a Franson's experiment.

REFERENCES

[1] J.D. Franson, Phys. Rev. Lett. **62**, 2205 (1989); Z.Y. Ou, X.Y. Zou, L.J. Wang, and L. Mandel, *ibid* **65**, 321 (1990); P.G. Kwiat, W.A. Vareka, C.K. Hong, H. Nathel, and R.Y. Chiao, Phys. Rev. A **41**, 2910 (1990); J. Brendel, E. Mohler, and W. Martienssen, Europhys. Lett. **20**, 575 (1992); Y.A. Shih, A.V. Sergienko, and M.H. Rubin, Phys. Rev. A **47**, 1288 (1993).

[2] M.A. Horne, A. Shimony, and A. Zeilinger, Phys. Rev. Lett. **62**, 2209(1989); J.G.Rarity and P.R. Tapster, *ibid* **64**, 2495 (1990).

[3] M. Zukowski and J. Pikacz, Phys. Lett. A **127**, 1 (1988).

[4] D.N. Klyshko, Phys. Lett. A **132**, 299 (1988).

[5] D.C. Burnham and D.L. Weinberg, Phys. Rev. Lett. **25**, 84 (1970); S. Friberg, C.K.Hong, and L. Mandel, *ibid* **54**, 2011 (1985).

[6] L.C.B. Ryff, Phys. Rev. A **51**, 79 (1995).

[7] D.M. Greenberger, M.A. Horne, A. Shimony, and A. Zeilinger, Am. J. Phys. **58**, 1131 (1990); L. Hardy, Phys. Rev. Lett. **71**, 1665 (1993).

[8] J.F. Clauser and M.A. Horne, Phys. Rev. D **23**, 526 (1974); J.F. Clauser and A. Shimony, Rep. Prog. Phys. **41**, 1881 (1978); F. Selleri, in *Quantum Mechanics versus Local Realism: the Einstein, Podolsky, and Rosen Paradox*, edited by F. Selleri (Plenum, New York, 1988); E. Santos, Phys. Rev. Lett. **66**, 1388 (1991); *ibid* **68**, 2702 (1992).

[9] L.C.B. Ryff, in *Advances in Fundamental Physics*, edited by M. Barone and F. Selleri (Hadronic Press, Palm Harbor, 1995).

NEXT
DOCUMENT

Two-Photon Entanglement and EPR Experiments Using Type-II Spontaneous Parametric Down Conversion

A.V. Sergienko, Y.H. Shih, T.B. Pittman, and M.H. Rubin
Department of Physics, University of Maryland Baltimore County
Baltimore, MD 21228 USA

Abstract

Simultaneous entanglement in spin and space-time of a two-photon quantum state generated in type-II spontaneous parametric down-conversion is demonstrated by the observation of quantum interference with 98 % visibility in a simple beam-splitter (Hanburry Brown-Twiss) anticorrelation experiment. The nonlocal cancellation of two-photon probability amplitudes as a result of this double entanglement allows us to demonstrate two different types of Bell's inequality violations in one experimental setup.

1 Introduction

Two-particle entangled states play a particularly important role in the study of the Einstein-Podolsky-Rosen (EPR) paradox [1] and in the test of Bell's inequalities [2]. Entangled states are states of two or more particles that can not be written as products of single particle states. [1]. The physical consequences resulting from the EPR states violate classical local realism [3].

In the past, EPR type two-particle entanglement has been demonstrated by two types of experiments: (1) two-particle polarization correlation measurements; most of the historical EPR-Bohm experiments [4] and the measurements testing Bell's inequality exhibited nonlocal two-particle *polarization* correlation [5]. These experiments demonstrated the EPR type two-particle spin-type entanglement. (2) two-particle interference (fourth order interference) experiments; recent two-particle nonclassical interference experiments demonstrated two-particle *space-time* entanglement [6].

Usually two-photon entanglement appears in the form that if one wants to measure the linear polarization of a single photon, one would find that neither of them has a preferred polarization direction. however, whenever a single photon is measured to be polarized in a certain direction the other one must be polarized orthogonal to that direction. A typical EPR type two-photon space-time entangled state, was proposed by Franson recently [7]. In this state one can never predict "which path" for a single photon, however, if one of the photons traveled through the longer (shorter) path the other must have traveled through the longer (shorter) path. The signature of this state is a cosine sum frequency interference fringe pattern of the coincidence counting rate.

The non-local spin or space-time two-particle entanglement phenomena is unusual from the classical theory point of view. The third type of simultaneous two- particle entanglement both in spin and in space-time will be discussed in detail by reporting several experiments. In these experiments, it is interesting to see that the measurement of the spin and space-time observables of either particle determines the value of these observables for the other particle with unit probability.

2 EPR experiments

Spontaneous parametric down-conversion (SPDC) is one of the most effective sources for generating two-photon entangled states. In SPDC a pump beam is incident on a birefringent crystal. The nonlinearity of

the crystal leads to the spontaneous emission of a pair of entangled light quanta which satisfy the phase matching condition [8],

$$\omega_1 + \omega_2 = \omega_p, \quad \vec{k}_1 + \vec{k}_2 = \vec{k}_p \tag{1}$$

where ω_i is the frequency and $\vec{k}_i$ the wave vector, linking pump (p), signal (1), and idler (2). The down-conversion is called type-I or type-II depending on whether the photons in the pair have parallel or orthogonal polarization. The light quanta of the pair that emerges from the nonlinear crystal may propagate in different directions or may propagate collinearly. The frequency and propagation directions are determined by the orientation of the nonlinear crystal and the phase matching relations in (1).

In order to understand the two-photon behavior of SPDC, consider the experiment which is shown in Fig. 1, a simple beam-splitting experiment. Assume that a type-II BBO ($\beta - BaB_2O_4$) crystal is used for the SPDC. The collinear down-conversion beam is split by a beamsplitter. The beamsplitter is assumed to be polarization dependent so that the o-ray is transmitted and the e-ray is reflected. Single photon counting detectors D_1 and D_2 are placed in the transmission and reflection output ports of the beamsplitter for detecting the o-ray and the e-ray, respectively. An introduction of the effective wavefunction $\Psi(t_1, t_2)$ is helpful for understanding the physics of the phenomenon.

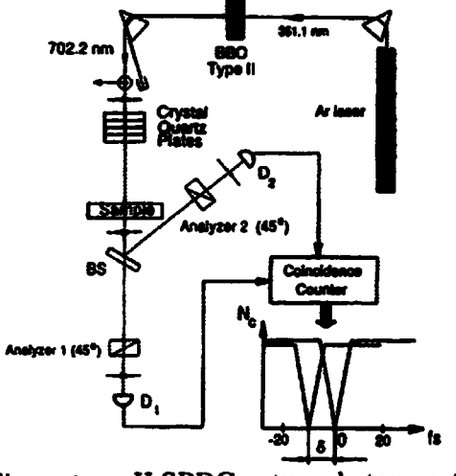

Figure 1. Schematic experiment for study of the type II SPDC biphoton. BS is a beamsplitter. D_1 and D_2 are photon counting detectors. A coincidence circuit is used for recording the coincidence rate.

For collinear type-II SPDC, a two-photon part of the state exiting the crystal may be calculated from the standard theory of SPDC [9].

$$|\Psi\rangle = \sum_{1,2} \delta(\omega_1 + \omega_2 - \omega_p)\psi(k_1 + k_2 - k_p)a_o^\dagger(\omega_1(k_1))a_e^\dagger(\omega_2(k_2))0\rangle \tag{2}$$

The effective wavefunction may be calculated for the system presented in Fig.1 [9]

$$\Psi(t_1, t_2) = \langle 0|E_1^{(+)}E_2^{(+)}|\Psi\rangle. \tag{3}$$

$$\Psi(t_1, t_2) = v(t_1 + t_2)u(t_1 - t_2) \tag{4}$$

$$\begin{aligned} v(t) &= v_0 exp(-i\omega_p t/2) \\ u(t) &= u_0 exp(-i\omega_d t/2)\int_{-\infty}^{\infty} d\nu[1 - exp(-\nu DL)]/(i\nu DL)exp(-i\nu t) \\ &= exp(-i\omega_d t/2)\Pi(t) \end{aligned}$$

$$\Pi(t) = \begin{cases} u_0 & DL > t > 0 \\ 0 \end{cases} \tag{5}$$

where v_0, u_0 are constants (normalization). We have approximated the pump to be a plane wave in the calculation. If the pump beam were taken to be a Gaussian with bandwidth σ_p, it is not difficult to show that the constant v_0 will be replaced by a Gaussian function $v_0 exp(-\sigma_p^2 t^2/8)$.

Equation (4)demonstrates a two dimensional wavepacket, referred to as the two-photon effective wavefunction or for short the ***Biphoton*** [8, 9]. It is clear that the biphoton is entangled in space-time because the wavefunction can not factor into a function of t_1 times a function of t_2.

Fig. 1 illustartes the experimental set up for the verification of Π-shaped biphoton. The beamsplitter is polarization independent, so that both the o-ray and the e-ray could be transmitted or reflected to trigger D_1 or D_2. A Glan Thompson linear polarization analyzer, oriented at 45° relative to the o-ray and e-ray polarization planes of the BBO crystal, is placed in front of each of the detectors. Birefringent material, for example a set of quartz plates, is introduced into the single incident beam for manipulating the optical delay δ between the o-ray and the e-ray. The fast axes of the quartz plates were carefully aligned to match the o-ray or e-ray polarization planes of the BBO crystal. In order to see the ***natural spectral shape*** of the SPDC, no any narrowband spectral filters are used except UV cut off filters to get rid of the pump scattered light [10].

It is interesting to see that when no quartz plates are used the two terms in the effective wavefunction (4) do not show any interference since $\Pi(t_1 - t_2)$ and $\Pi(t_2 - t_1)$ do not overlap. Physically it means that the o-ray and the e-ray photons are well distinguished in space-time. Now consider the case of having a quartz plate in the down-conversion incident beam. If we align the quartz carefully to match its fast axis to the o-ray polarization direction of the BBO, an optical delay, $\delta \cong (n_o - n_e)l/c$, is introduced between the o-ray and the e-ray of BBO, where n_o and n_e are the index of refraction of the quartz plates for the o-ray and the e-ray of BBO, and l is the thickness of the quartz plate. The effective wavefunction becomes (consider the analyzers are set at 45°).

$$\Psi(t_1, t_2) = a_1 a_2 v(t_1 + t_2 - \varphi)[u(t_1 - t_2 + \delta) - u(-t_1 + t_2 + \delta)] \tag{6}$$

It is easy to see from eq.(6) that there is interference now, because the two terms overlap. When $\delta = DL/2$,the two terms completely overlap and therefore cancel each other. This may be considered as a perfect anti-correlation

$$R_c = R_{c0}[1 - \rho(\delta)]$$

$$\rho = \begin{cases} 0 & -\infty < \delta < 0 \\ \kappa\delta & 0 < \delta < DL/2 \\ 1 - \kappa(\delta - DL/2) & DL/2 \leq \delta < DL \\ 0 & DL < \delta < \infty \end{cases} \tag{7}$$

The width and the shape of the biphoton can be evaluated by the width and the shape of R_c.

Fig.2 reports typically observed 'V-shape' coincidence rate measurements as a function of the optical delay δ, which verifies the Π-shape effective wavefunction [10]. Each of the data points corresponds to different numbers of quartz plates remaining in the path of the down-conversion incident beam. It is easy to find that the vertex of the V-shape function has a displacement of $(72 \pm 3)fs$ from zero, which

corresponds to a time delay of $DL/2$ in a $(0.56 \pm 0.05)mm$ BBO crystal.

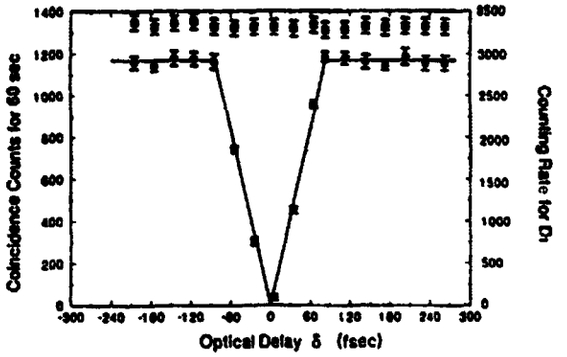

Figure 2. Lower curve: Coincidence counts as a function of optical delay, which corresponds to a certain number of quartz plates. The solid curve is a fitting curve of eq.(7). Upper curve: Single detector counts.

A strong correlation which appears in the form of almost a 100% destructive quantum interference is a clear demonstration of the situation where the Einstein-Podolsky-Rosen argument [1] is directly applicable. The triangular shape of the correlation function is a clear signature of the rectangular shape of original two-photon effective wavefunction. The discussion of the effective wavefunction is important also for the understanding of the two-photon double entanglement.

3 Double Bell's inequality

Taking advantage of the spin and space-time entanglement of the biphoton, another type of two-photon interference phenomena can be demonstrated. With the addition of a Pockel's cells, and a re-orientation of the quartz plates and polarizers, the coincidence counting rate exhibits interference modulation of the pump frequency when manipulating the voltage across the Pockel's cell, regardless of the optical delay by the quartz plates (*which is much greater than the coherence length of the signal and idler down-conversion fields*). This two-photon interference effect is again due to a nonclassical two-photon state which is entangled both in spin and in space-time.

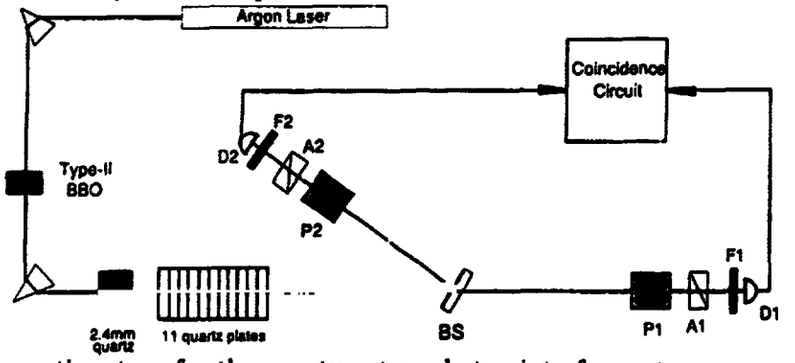

Figure 3. Schematic set up for the new type two-photon interferometer.

The schematic set up of the experiment is illustrated in Fig.3. The type-II SPDC is the same as that in the quantum beats experiment. The collinear down-conversion beam passes through a set of crystal quartz plates before the beamsplitter. The first three quartz plates, which sum to $2.4mm$ in thickness, are oriented in a way to make the two terms of the Π-shape function completely overlap (see the discussion in section 2). 11 more crystal quartz plates follow these three. The fast axes of these 11 quartz plates are aligned carefully to be oriented at 45^o relative to the o- ray and the e-ray polarization planes of the BBO in order to introduce a new basis associated with the fast and slow axecies. Each of these quartz plates is $(1 \pm 0.1)mm$ in thickness, resulting in an optical delay $\Delta l \cong 9\mu m$ between the fast and the slow rays

of the quartz crystal at wavelengths around 700 nm. The optical delay is about $99\mu m$ after 11 quartz plates in comparison with the coherence length of the field which is about 25μm. Therefore, the $|X\rangle$ and the $|Y\rangle$ components of the original o-ray and e-ray of suffer enough optical delay to be non-overlapping, where $|X\rangle$ and $|Y\rangle$ correspond to the fast and the slow axes of the quartz plates. A Pockel's cell with fast and slow axes carefully aligned to match the $|X\rangle$ and the $|Y\rangle$ axes is placed after the quartz plates in each output port of the beamsplitter for fine control of the optical delay between the $|X\rangle$ and the $|Y\rangle$. The spectral filters f_1 and f_2 have Gaussian shape transmission functions centered at $702.2nm$, with bandwidths of $19nm$(full width at half maximum).

The down-conversion $|o\rangle$ and $|e\rangle$ polarized photons both have certain probabilities to be in the $|X\rangle$ or the $|Y\rangle$ state when passing through the crystal quartz plates and the Pockel's cells. The optical delay between the $|X\rangle$ and the $|Y\rangle$ is then introduced by the anisotropic refractive index of the quartz plates and the Pockel's cells. The coincidence time window in this experiment is $1.8nsec$, which is much shorter than the distance between the Pockel's cells. Bell inequality measurements can be performed for both space-time variables and for spin variables in one experiment. For the 45° oriented polarizers, the coincidence counting rate is predicted to be,

$$R_c = R_{c0}\{1 - exp[-\sigma_p^2(\Delta l/2c)^2]\cos(\Omega_1\Delta l_1 + \Omega_2\Delta l_2)/c\} \tag{8}$$

where $\Delta l_i/c$ is the optical delay introduced by the ith Pockel's cell (to simplify the calculation, we assumed the optical delays introduced by the Pockel's cells are the same).

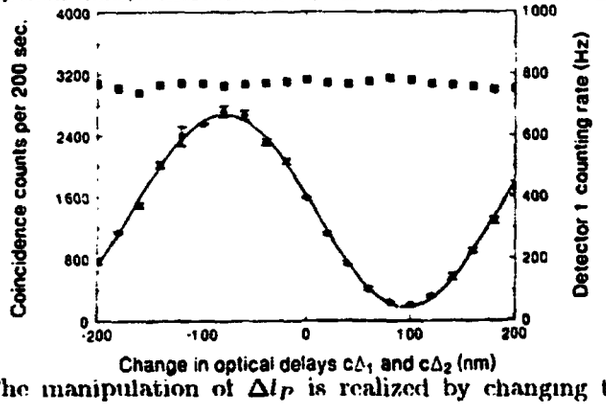

Figure 4. A typical observed sum frequency modulation when the cross voltages of the two Pockel's cells are manipulated (negative values correspond to negative voltages). The interference visibility is (88.2 ± 1.2)%, which violates a Bell inequality for space-time variables by more than 14 standard deviations.[11, 12]

The manipulation of Δl_P is realized by changing the applied voltage of the Pockel's cells. The coincidence counts are direct measurements, with no "accidental" subtractions. It is clear that the modulation period corresponds to the pump wavelength, i.e., $351.1nm$. Contrary to the coincidence counting rate, the single detector counting rate remains constant when Δl_P is manipulated, as is reported in the upper part of Fig. 4.

It is interesting to see that in the same experiment, a test of a spin variable Bell inequality can be made by manipulating the orientation of the polarizers at a totally constructive or destructive space-time interference point. Because of the symmetries present in the measurement, we are able to study one simple form of Bell's inequalities for polarization variables [13],

$$\delta = |[R_c(\pi/8) - R_c(3\pi/8)]/R_0| \leq 1/4 \tag{9}$$

and the measured result is $\delta = 0.309 \pm 0.009$, implying a violation of more than 6 standard deviations.[12]

4 Conclusion

Experiments starting with type-II down-conversion are a very effective mechanism for generating two-photon entangled states (biphoton). The type-II SPDC biphoton is entangled both in space-time and

spin. A two-photon effective wave function produced by Type-II spontaneous parametric down conversion is studied for its natural shape in space-time. The double entanglement of the two-photon state makes it possible to perform EPR type two-photon interference experiments in a simple beam-splitting set up and test Bell's inequalities for space-time variables and spin variables in the same experiment. Two-photon interference visibility as high as $(98 \pm 2)\%$ has been observed. Experimental tests for the space-time variables and spin variables Bell inequalities have been measured with violations of 14 and 5 standard deviations, respectively, in one experimental set up.

5 Acknowledgement

This work was supported by the Office of Naval Research grant no. N00014-91-J-1430.

References

[1] A. Einstein, B. Podolsky and N. Rosen, Phys. Rev. **47**, 777 (1935).

[2] J.S. Bell, Physics, **1**, 195 (1964);D. Bohm, *Quantum Theory*, Prentice Hall, Englewood Cliffs, (1951).

[3] M.A. Horne, A. Shimony, and A. Zeilinger, Phys. Rev. Lett. **62**, 2209(1989).

[4] For a review, see J.F. Clauser and A. Shimony, Rep. Prog. Phys. **41**, 1881 (1976).

[5] A. Aspect, J. Dalibard, G. Roger, Phys. Rev. Lett., **49**, 1804 (1982); Y.H. Shih and C.O. Alley, Phys. Rev. Lett. **61**, 2921 (1988); Z.Y. Ou and L. Mandel, Phys. Rev. Lett. **61**, 50 (1988);T.E. Kiess, Y.H. Shih, A.V. Sergienko, and C.O. Alley, Phys. Rev. Lett., **71**, 3893 (1993).

[6] Z.Y. Ou, X.Y. Zou, L.J. Wang, and L. Mandel,Phys. Lett., **65**, 321 (1990); P.G. Kwiat, A.M. Steinberg, and R.Y. Chiao, Phys. Rev. A, **47**, 2472 (1993); Y.H. Shih, A.V. Sergienko, and M.H. Rubin, Phys. Rev. A **47**, 1288 (1993); P.G. Kwiat, W.A. Vareka, H.Nathel, and R.Y. Chiao, Phys. Rev. A **41**, 2910 (1990); J. Brendel, E Mohler, and W. Martienssen, Phys. Rev. Lett., **66**, 1142 (1991); T.S. Larchuk, R.A. Campos, J.G. Rarity, P.R. Tapster, E. Jakeman, B.E.A. Saleh, and M.C. Teich, Phys. Rev. Lett., **70**, 1603 (1993).

[7] J.D Franson, Phys. Rev. Lett., **62**, 2205 (1989).

[8] D.N. Klyshko, *Photons and Nonlinear Optics*, Gordon and Breach Science Publishers, N.Y., (1988).

[9] For detailed theoretical analysis, see M.H. Rubin, D.N. Klyshko, Y.H. Shih and A.V. Sergienko, Phys. Rev. A, **50**, 5122 (1994). Two-photon wavefunction of single atom cascade decay was first calculated by M.Scully et al. see M.Scully, K. Druhl, Phys. Rev. A **25**, 2208 (1982).

[10] A.V. Sergienko, Y.H. Shih, and M.H. Rubin, J.Opt.Soc.Am. **B** , (1995).

[11] Y.H. Shih and A.V. Sergienko, Phys. Lett. A, **191**, 201 (1994).

[12] T.B. Pittman, Y.H. Shih, A.V. Sergienko, and M.H. Rubin, Phys. Rev. A, **51**, 3495 (1995).

[13] S.J. Freedman, and J.F. Clauser, Phys. Rev. Lett., **28**, 938 (1972).

NEXT
DOCUMENT

The contradiction between the measurement theory of quantum mechanics and the theory that the velocity of any particle can not be larger than the velocity of light

Shen Y.

Department of Physics, East China Normal University, Shanghai, China

Shen Z. J., Shen G. T. and Yang B. C.

Department of Physics, East China Normal University, Shanghai, China

Abstract

By the measurement theory of quantum mechanics and the method of Fourier transform, we proved that the wave function $\psi(x,y,z,t)=\frac{8}{(2\pi\sqrt{2L_\epsilon})^3}\Phi(L_\epsilon,t,x)\Phi(L_\epsilon,t,y)\Phi(L_\epsilon,t,z)$. According to the theory that the velocity of any particle can not be larger than the velocity of light and the Born interpretation, when $|\delta|>(ct+L_\epsilon)$, $\Phi(L_\epsilon,t,\delta)=0$. But according to the calculation, we proved that for some δ, even if $|\delta|>(ct+L_\epsilon)$, $\Phi(L_\epsilon,t,\delta)\neq 0$.

By the measurement theory of quantum mechanics, if someone measures the coordinate of a particle, it will make the particle to the eigenstate of the coordinate. The eigen function (with eigen value zero) of the coordinate of a particle can be assumed as follows:

$$\alpha(x,y,z)=\frac{1}{(\sqrt{2L_\epsilon})^3} \quad \text{when } -L_\epsilon<x<L_\epsilon,\ -L_\epsilon<y<L_\epsilon,\ -L_\epsilon<z<L_\epsilon$$

$$\alpha(x,y,z)=0 \quad \text{otherwise} \tag{1}$$

L_ϵ is an infinitesimally positive real number. Now assume someone measures the coordinate

of a particle at the place $\vec{r}=0$ ($\vec{r}$ represents the coordinate), suppose this particle is measured at the time $t=0$, thus this particle is made to the eigenstate (with eigen value zero) of the coordinate, the wave function $\phi(\vec{r},t)$ of this particle will satisfy the following condition

$$\phi(x,y,z,0)=\alpha(x,y,z) \tag{2}$$

By the Fourier transform and the Schrödinger wave equation, it is not difficult to see

$$\phi(\vec{r},t)=\frac{1}{(2\pi)^{3/2}}\int\varphi(\vec{k})\exp[i(\vec{k}\cdot\vec{r}-\frac{\hbar k^2 t}{2\mu})]d^3\vec{k} \tag{3}$$

Where $\varphi(\vec{k})=\frac{1}{(2\pi)^{3/2}}\int\phi(\vec{r},0)e^{-i\vec{k}\cdot\vec{r}}d^3\vec{r}$

$$=\frac{1}{(2\pi)^{3/2}}\int_{-L}^{L}\int_{-L}^{L}\int_{-L}^{L}\frac{1}{(\sqrt{2L})^3}\exp[-ik_x x-ik_y y-ik_z z]dx\,dy\,dz$$

$$=\frac{1}{(2\pi)^{3/2}}\frac{1}{(\sqrt{2L})^3}\frac{2}{k_x}\sin(k_x L)\frac{2}{k_y}\sin(k_y L)\frac{2}{k_z}\sin(k_z L) \tag{4}$$

Thus $\phi(x,y,z,t)=\frac{1}{(2\pi)^{3/2}}\int\varphi(\vec{k})\exp[i(\vec{k}\cdot\vec{r}-\frac{\hbar k^2 t}{2\mu})]d^3\vec{k}$

$$=\frac{1}{(2\pi)^3}\frac{8}{(\sqrt{2L})^3}\int_{-\infty}^{+\infty}\int_{-\infty}^{+\infty}\int_{-\infty}^{+\infty}\frac{1}{k_x}\sin(k_x L)\frac{1}{k_y}\sin(k_y L)\frac{1}{k_z}\sin(k_z L)$$

$$\exp\{i[k_x x-\frac{\hbar k_x^2 t}{2\mu}+k_y y-\frac{\hbar k_y^2 t}{2\mu}+k_z z-\frac{\hbar k_z^2 t}{2\mu}]\}dk_x\,dk_y\,dk_z$$

$$=\frac{1}{(2\pi)^3}\frac{8}{(\sqrt{2L})^3}\Phi(L,t,x)\Phi(L,t,y)\Phi(L,t,z) \tag{5}$$

Where

$$\Phi(L,t,x)=\int_{-\infty}^{+\infty}\frac{\sin(k_x L)}{k_x}\exp[i(k_x x-\frac{\hbar k_x^2 t}{2\mu})]dk_x \tag{6}$$

$$\Phi(L,t,y)=\int_{-\infty}^{+\infty}\frac{\sin(k_y L)}{k_y}\exp[i(k_y y-\frac{\hbar k_y^2 t}{2\mu})]dk_y \tag{7}$$

$$\Phi(L,t,z)=\int_{-\infty}^{+\infty}\frac{\sin(k_z L)}{k_z}\exp[i(k_z z-\frac{\hbar k_z^2 t}{2\mu})]dk_z \tag{8}$$

Thus $\Phi(0,t,x)=0$ (9)

$$\frac{\partial\Phi(L,t,x)}{\partial L}=\int_{-\infty}^{+\infty}\cos k_x L\exp[i(k_x x-\frac{\hbar k_x^2 t}{2\mu})]dk_x$$

$$=\int_{-\infty}^{+\infty}\frac{\exp(ik_x L)+\exp(-ik_x L)}{2}\exp[i(k_x x-\frac{\hbar k_x^2 t}{2\mu})]dk_x$$

$$=\frac{1}{2}\{\int_{-\infty}^{+\infty}\exp[ik_x(x+L)]\exp[-i\frac{\hbar k_x^2 t}{2\mu}]dk_x$$

$$+\int_{-\infty}^{+\infty}\exp[ik_x(x-L)]\exp[-i\frac{\hbar k_x^2 t}{2\mu}]dk_x\}$$

$$=\frac{1}{2}\{\int_{-\infty}^{+\infty}\exp\{-i[\frac{\hbar k_x^2 t}{2\mu}-k_x(x+L)]\}dk_x$$

$$+\int_{-\infty}^{+\infty}\exp\{-i[\frac{\hbar k_x^2 t}{2\mu}-k_x(x-L)]\}dk_x\}$$

$$=\frac{1}{2}\{\int_{-\infty}^{+\infty}\exp\{-i[(\sqrt{\frac{\hbar t}{2\mu}}k_x-\frac{x+L}{2\sqrt{\frac{\hbar t}{2\mu}}})^2-(\frac{x+L}{2\sqrt{\frac{\hbar t}{2\mu}}})^2]\}dk_x$$

$$+\int_{-\infty}^{+\infty}\exp\{-i[(\sqrt{\frac{\hbar t}{2\mu}}k_x-\frac{x-L}{2\sqrt{\frac{\hbar t}{2\mu}}})^2-(\frac{x-L}{2\sqrt{\frac{\hbar t}{2\mu}}})^2]\}dk_x\}$$

$$=\frac{1}{2}\{\frac{1}{\sqrt{\frac{\hbar t}{2\mu}}}[\sqrt{\frac{\pi}{2}}-i\sqrt{\frac{\pi}{2}}]\exp[i(\frac{x+L}{2\sqrt{\frac{\hbar t}{2\mu}}})^2]+\frac{1}{\sqrt{\frac{\hbar t}{2\mu}}}[\sqrt{\frac{\pi}{2}}-i\sqrt{\frac{\pi}{2}}]\exp[i(\frac{x-L}{2\sqrt{\frac{\hbar t}{2\mu}}})^2]\} \quad (10)$$

By (9),(10)

$$\Phi(L,t,x)=\int_0^L\frac{\partial\Phi(L',t,x)}{\partial L'}dL'+\Phi(0,t,x)=\int_0^L\frac{\partial\Phi(L',t,x)}{\partial L'}dL'$$

$$=\int_0^L\frac{1}{2\sqrt{\frac{\hbar t}{2\mu}}}[\sqrt{\frac{\pi}{2}}-i\sqrt{\frac{\pi}{2}}]\{\exp[i(\frac{x+L'}{2\sqrt{\frac{\hbar t}{2\mu}}})^2]+\exp[i(\frac{x-L'}{2\sqrt{\frac{\hbar t}{2\mu}}})^2]\}dL' \quad (11)$$

$$\frac{\partial\Phi(L,t,x)}{\partial x}=\int_0^L\frac{1}{2\sqrt{\frac{\hbar t}{2\mu}}}\sqrt{\frac{\pi}{2}}(1-i)\{\frac{\partial}{\partial x}\exp[i(\frac{x+L'}{2\sqrt{\frac{\hbar t}{2\mu}}})^2]+\frac{\partial}{\partial x}\exp[i(\frac{x-L'}{2\sqrt{\frac{\hbar t}{2\mu}}})^2]\}dL'$$

$$=\int_0^L\frac{1}{2\sqrt{\frac{\hbar t}{2\mu}}}\sqrt{\frac{\pi}{2}}(1-i)\{\frac{\partial}{\partial L'}\exp[i(\frac{x+L'}{2\sqrt{\frac{\hbar t}{2\mu}}})^2]-\frac{\partial}{\partial L'}\exp[i(\frac{x-L'}{2\sqrt{\frac{\hbar t}{2\mu}}})^2]\}dL'$$

$$=\frac{1}{2\sqrt{\frac{\hbar t}{2\mu}}}\sqrt{\frac{\pi}{2}}(1-i)\{\exp[i(\frac{x+L}{2\sqrt{\frac{\hbar t}{2\mu}}})^2]-\exp[i(\frac{x}{2\sqrt{\frac{\hbar t}{2\mu}}})^2]$$

$$-\exp[i(\frac{x-L}{2\sqrt{\frac{\hbar t}{2\mu}}})^2]+\exp[i(\frac{x}{2\sqrt{\frac{\hbar t}{2\mu}}})^2]\}$$

$$=\frac{1}{2\sqrt{\frac{\hbar t}{2\mu}}}\sqrt{\frac{\pi}{2}}(1-i)\{\exp[i(\frac{x+L}{2\sqrt{\frac{\hbar t}{2\mu}}})^2]-\exp[i(\frac{x-L}{2\sqrt{\frac{\hbar t}{2\mu}}})^2]\} \quad (12)$$

According to the theory that the velocity of any particle can not be larger than the veloc-

ity of light c and the Born interpretation, for any $t(t>0)$, when $|x|>(ct+L.)$, $|y|>(ct+L.)$, $|z|>(ct+L.)$, $\psi(x,y,z,t)$ will be zero. This means if $|\delta|>(ct+L.)$, $\psi(\delta,\delta,\delta,t)$ will be zero. Then by (5), when $|\delta|>(ct+L.)$, $\Phi(L.,t,\delta)$ will be zero. Therefore when $|\delta|>(ct+L.)$, $\frac{\partial\Phi(L.,t,\delta)}{\partial\delta}$ will be zero.

According to (12).

$$\frac{\partial\Phi(L.,t,\delta)}{\partial\delta}=\frac{1}{2\sqrt{\frac{\hbar t}{2\mu}}}\sqrt{\frac{\pi}{2}}(1-i)\{\exp[i(\frac{\delta+L.}{2\sqrt{\frac{\hbar t}{2\mu}}})^2]-\exp[i(\frac{\delta-L.}{2\sqrt{\frac{\hbar t}{2\mu}}})^2]\} \tag{13}$$

Now assume $\frac{\partial\Phi(L.,t,\delta)}{\partial\delta}=0$ (14)

Then it is not difficult to see

$$(\frac{\delta+L.}{2\sqrt{\frac{\hbar t}{2\mu}}})^2=(\frac{\delta-L.}{2\sqrt{\frac{\hbar t}{2\mu}}})^2+2n\pi \tag{15}$$

Where n is an integer

$$\text{Thus } \frac{\delta L.}{\frac{\hbar t}{2\mu}}=2n\pi \tag{16}$$

$$\text{or } \delta=\frac{\hbar t n\pi}{\mu L.} \tag{17}$$

This means when $\frac{\delta\mu L.}{\hbar t\pi}$ is not an integer, even if $|\delta|>(ct+L.)$, $\frac{\partial\Phi(L.,t,\delta)}{\partial\delta}$ will not be zero. This result contradicts that when the velocity of any particle can not be larger than the velocity of light and the Born interpretation is valid, if $|\delta|>(ct+L.)$, $\frac{\partial\Phi(L.,t,\delta)}{\partial\delta}$ will be zero. This contradiction means that there is a contradiction between the measurement theory of quantum mechanics and the theory that the velocity of any particle can not be larger than the velocity of light.

Reference

Eugen Merzbacher, Quantum Mechanics, John Wiley & Sons, New York, 1970, p. 26

NEXT
DOCUMENT

TWO-PHOTON "GHOST" IMAGE AND INTERFERENCE-DIFFRACTION

Y.H. Shih, A.V. Sergienko, T.B. Pittman, D.V. Strekalov, and D.N. Klyshko[1]
Department of Physics, University of Maryland Baltimore County
Baltimore, MD 21228, U.S.A.

1 Introduction

One of the most surprising consequences of quantum mechanics is the entanglement of two or more distant particles. The two-particle entangled state was mathematically formulated by Schrödinger [1]: Consider a pure state for a system composed of two spatially separated subsystems,

$$\rho = |\Psi\rangle\langle\Psi| : \quad |\Psi\rangle = \sum_{a,b} c(a,b)|a\rangle|b\rangle \tag{1}$$

where $|a\rangle$ and $|b\rangle$ are two sets of orthogonal vectors for subsystem 1 and 2. If $c(a,b)$ does not factor into a product of the form $f(a) \times g(b)$, so that the state does not factor into a product state for subsystem 1 and 2 (e.g. $\rho \neq \rho_1 \otimes \rho_2$), the state is defined by Schrödinger as an "entangled state".

The classic example of a two-particle entangled state was suggested by Einstein, Podolsky, and Rosen in their famous 1935 *gedanken experiment* [2]:

$$|\Psi\rangle = \sum_{a,b} \delta(a + b - c_o)|a\rangle|b\rangle \tag{2}$$

where c_o is a constant. What is surprising about the entangled state (2) is the following: *the measured value of an observable for either single subsystem is undeterminate. However, if one of the subsystems is measured to be at a certain value for that observable (the measured value is certainly an eigen value) the other one is 100% determinate.* This point can be easily seen from the delta function in state (2). Based on this unusual quantum behavior, EPR defined their "physical reality" and then asked the question: "Can Quantum-Mechanical Description of Physical Reality Be Considered Complete[3]?" One may not appreciate EPR's criterian of physical reality and insist that "no elementary quantum phenomenon is a phenomenon until it is a recorded phenomenon" [4], however, no one can ignore the unusual nonlocal behavior of state (2), especially considering when the measurements of subsystems 1 and 2 are space-like separated events.

Optical spontaneous parametric down conversion (SPDC) [5] [6] is the most effective mechanism to generate an EPR type entangled two-photon state. In SPDC, an optical beam, called the pump, is incident on a birefringent crystal. The pump is intense enough so that nonlinear effects lead to the conversion of pump photons into pairs of photons, historically called signal and idler.

[1]Permanent address: Department of Physics, Moscow State University, Moscow, Russia

The two-photon state generated from the SPDC crystal may be calculated from the standard theory (first order perturbation theory) to be [6],

$$|\Psi\rangle = \sum_{s,i} \delta(\omega_s + \omega_i - \omega_p)\delta(\mathbf{k}_s + \mathbf{k}_i - \mathbf{k}_p) a_s^\dagger(\omega_s(\mathbf{k}_s))\, a_i^\dagger(\omega_i(\mathbf{k}_i))\,|0\rangle \tag{3}$$

where ω and $\mathbf{k}$ represent the frequency and the wave vector for signal (s), idler (i), and pump (p). The two delta functions in state (3) are usually explicitly written as phase matching conditions:

$$\omega_s + \omega_i = \omega_p\ ,\quad \mathbf{k}_s + \mathbf{k}_i = \mathbf{k}_p \tag{4}$$

Technically, the SPDC is said to be type I or type II, depending on whether the signal and idler beams have parallel or orthogonal polarization. The SPDC conversion efficiency is typically on the order of 10^{-9} to 10^{-11}, depending on the SPDC nonlinear material. The signal and idler intensities are extremely low, only single photon detection devices can register them. It is clear that state (3) is an EPR type two-photon entangled state. The quantum entanglement nature of SPDC has been demonstrated in EPR-Bohm experiments and Bell's inequality measurements [7]. The following two experiments were recently performed in our laboratory, which are more closely related to the original 1935 EPR *gedankenexperiment*.

The first experiment is a two-photon optical imaging type experiment [8], which has been named "ghost image" by the physics community. The *signal* and *idler* beams of SPDC are sent in different directions, so that the detection of the *signal* and *idler* photons can be performed by two distant photon counting detectors. An aperture object (mask) is placed in front of the *signal* photon detector and illuminated by the *signal* beam through a convex lens. Surprisingly, an image of this aperture is observed in the *idler* beam, by scanning the *idler* photon detector in the transverse plane of the *idler* beam, if we are sure that the *idler* photon detector "catches" the "twin brother" of the *signal*, which can be easily performed by a coincidence measurement. This effect is even more striking when we found that the object-lens-image relationship satisfies the *Gaussian thin lens equation*.

The second experiment demonstrates two-photon "ghost" interference-diffraction [9]. The experimental set up is similar to the image experiment, except that rather than a lens and an aperture it is a Young's double-slit (or a single-slit) inserted into the path of the *signal* beam. We could not find any interference (or diffraction) pattern behind the slit. Surprisingly, an interference (or diffraction) pattern is observed when scanning the detector in the *idler* beam, if we are sure that the *idler* photon detector "catches" the "twin brother" of the *signal*.

2 Two-photon "ghost" image experiment

The experimental set-up is shown in fig. 1. The $351.1nm$ line of an Argon Ion laser is used to pump a nonlinear BBO (β-BaB_2O_4) crystal which is cut at a degenerate Type-II phase matching angle to produce pairs of orthogonally polarized signal (e-ray of the BBO) and idler (o-ray of the BBO) photons [5]. The pairs emerge from the crystal near collinearly, with $\omega_s \cong \omega_i \cong \omega_p/2$, where ω_j $(j = s, i, p)$ is the frequency of the signal, idler, and pump, respectively. The pump is then separated from the down conversion beam by a UV grade fused silica dispersion prism and

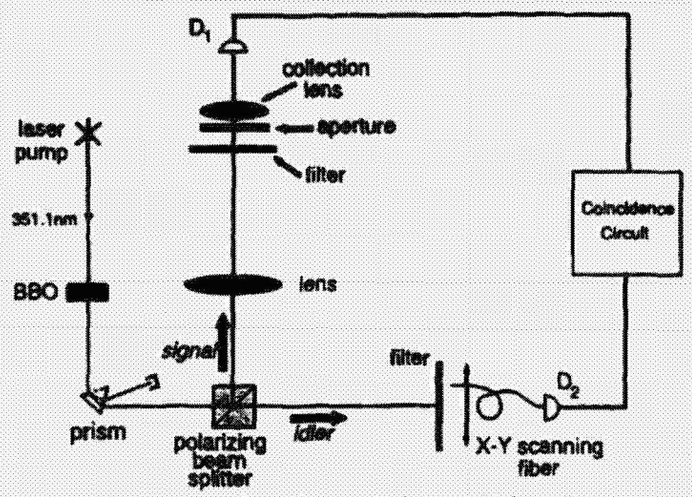

FIG.1. A schematic set-up for the two-photon "ghost" image experiment

the remaining signal and idler beams are sent in different directions by a polarization beam splitting Thompson prism. The signal beam passes through a convex lens with a $400mm$ focal length and illuminates a chosen aperture (mask). As an example, one could choose the letters "UMBC". Behind the aperture is the detector package D_1, which consists of a $25mm$ focal length collection lens in whose focal spot is a $0.8mm$ diameter dry ice cooled avalanche photodiode. The idler beam is met by detector package D_2, which consists of a $0.5mm$ diameter multi-mode fiber whose output is mated with another dry ice cooled avalanche photodiode. The input tip of the fiber is scanned in the transverse plane by two encoder drivers, and the output pulses of each detector, which are operating in the Geiger mode, are sent to a coincidence counting circuit with a $1.8ns$ acceptance window. Both detectors are preceded by $83nm$ bandwidth spectral filters centered at the degenerate wavelength, $702.2nm$.

By recording the coincidence counts as a function of the fiber tips' transverse plane coordinates, we see the image of the chosen aperture (for example "UMBC"), as is reported in fig. 2. It is

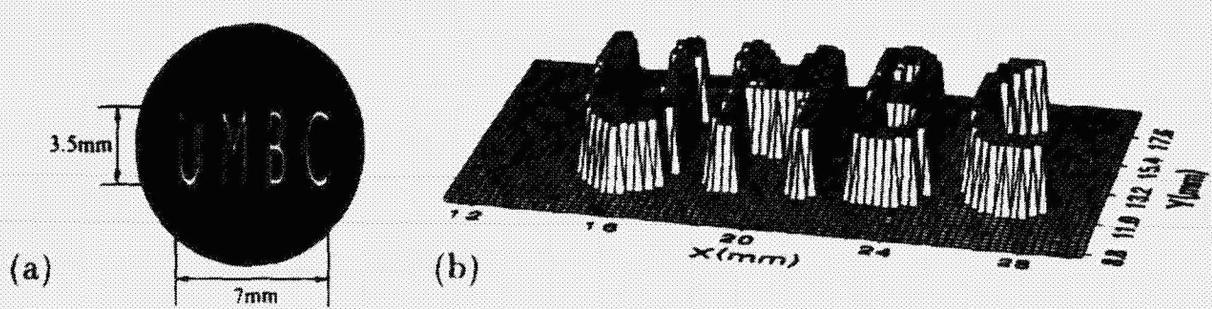

FIG.2. a) A reproduction of the actual aperture "UMBC" placed in the signal beam. Note that the size of the letters is on the order of standard text. b) The image of "UMBC": coincidence counts as a function of the fiber tip's transverse plane coordinates. The scanning step size is 0.25mm. The data shown is a "slice" at the half maximum value, with no image enhancement.

interesting to note that while the size of the "UMBC" aperture inserted in the signal beam is only about $3.5mm$ X $7mm$, the observed image measures $7mm$ X 14mm. We have therefore managed linear magnification by a factor of 2. Despite the completely different physical situation, the remarkable feature here is that *the relationship between the focal length of the lens f, the aperture's optical distance from the lens S, and the image's optical distance from the lens (lens back through beamsplitter to BBO then along the idler beam to the image) S' satisfies the Gaussian thin lens equation*:

$$\frac{1}{S} + \frac{1}{S'} = \frac{1}{f} \tag{5}$$

In this experiment, we chose $S = 600mm$, and the twice magnified clear image was found when the fiber tip was in the plane with $S' = 1200mm$ (see fig.3).

To understand this unusual phenomenon, we examine the quantum nature of the two-photon state produced in SPDC, which is entangled in momentum. The spatial distribution of the photon pairs is the result of the *transverse* components of the wave vector condition in equation (4) and Snell's law upon exiting the crystal:

$$k_s \sin\alpha_s = k_i \sin\alpha_i \longrightarrow \omega_s \sin\beta_s = \omega_i \sin\beta_i \tag{6}$$

where α_s and α_i are the scattering angles inside the crystal and β_s and β_i are the exit angles of the signal and idler photons with respect to the $\mathbf{k}_p$ direction. Therefore, near the degenerate case the photons constituting one pair are emitted at roughly equal, yet opposite, angles relative to the pump. Although the momentum of each photon is indeterminate, if one is measured at a certain value then the other is 100% determined. This then allows for a simple explanation of the experiment in terms of "usual" geometrical optics in the following manner: considering the action of the beamsplitter, we envision the crystal as a "hinge point" and "unfold" the schematic of fig. 1 into that shown in fig. 3. Because of the equal angle requirement of equation (6), we see that

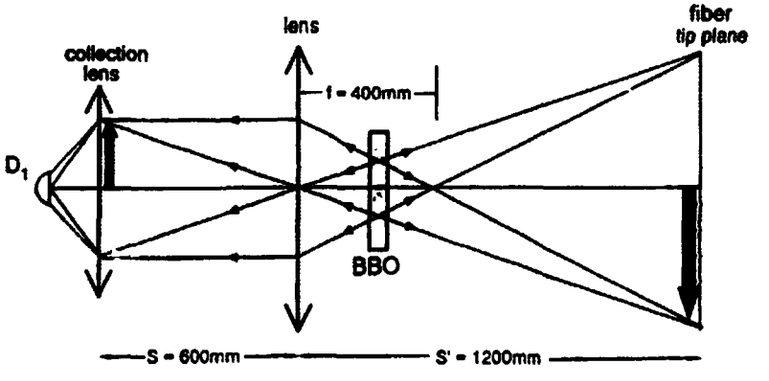

FIG.3. A conceptual "unfolded" version of the schematic shown in fig. 1, which is helpful for understanding the physics. Although the placement of the lens and the detectors obey the Gaussian thin lens equation, it is important to remember that the geometric rays actually represent pairs of SPDC photons which propagate in different directions.

all photon pairs which result in a coincidence detection can be represented by *straight lines* (but keep in mind the different propagation directions) and therefore the image is well produced in coincidences when the aperture, lens, and fiber tip are located according to equation (5). In other words, the image is exactly the same as one would observe on a screen placed at the fiber tip if detector D_1 were replaced by a point-like light source and the BBO crystal by a reflecting mirror [10].

3 "Ghost" interference-diffraction

The schematic experimental set-up is illustrated in fig. 4. It is similar to the first experiment except that after the separation of signal and idler, the signal photon passes through a double-slit (or single-slit) aperture and then travels about $1m$ to meet a point-like photon counting detector D_1 ($0.5mm$ in diameter). The idler photon travels a distance about $1.2m$ from BS to the input tip of the optical fiber. In this experiment only the horizontal transverse coordinate, x_2, of the fiber input tip is scanned by an encoder driver.

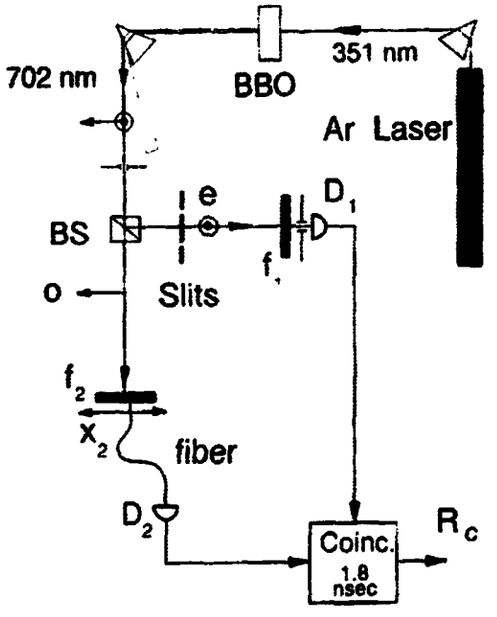

FIG.4. A schematic set-up for the two-photon "ghost" interference-diffraction experiment. The signal (e-ray of BBO) and idler (o ray of BBO) photon pair is generated in nonlinear crystal BBO. The ultra violet pump beam is separated from the down conversion beams by a UV grade fused silica dispersion prism. BS is a beamsplitting Thompson prism for splitting the signal and idler beams to different directions. f_1 and f_2 are spectral filters with $702.2nm$ center wavelength and $10nm$ bandwidth. Both photon counting detectors D_1 and D_2 are dry ice cooled avalanche photodiode operated in Geiger mode.

Fig. 5 reports a typically observed double-slit interference-diffraction pattern. The coincidence counting rate is reported as a function of x_2, which is obtained by scanning the detector D_2 (the fiber tip) in the idler beam, whereas the double-slit is in the signal beam. The Young's double-silt has a slit-width $a = 0.15mm$ and slit-distance $d = 0.47$mm. The interference period is measured to be $2.7 \pm 0.2mm$ and the half-width of the envelope is estimated to be about 8mm.

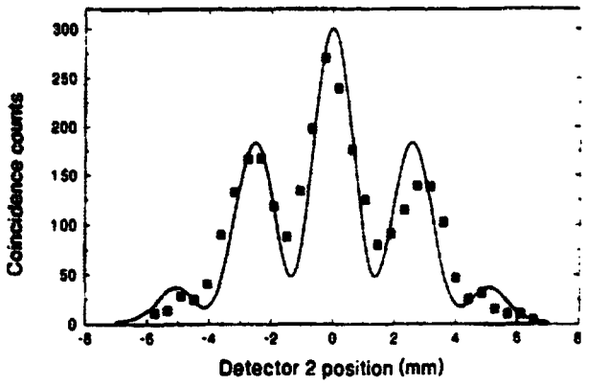

FIG.5. Typically observed interference-diffraction pattern: the dependence of the coincidences (per 400 sec) on the position of optical fiber tip of detector D_2, which counts the idler photons, while the signal photons pass through a double-slit with $a = 0.15mm$ and $d = 0.47$mm. The solid curve is calculated from equation (7).

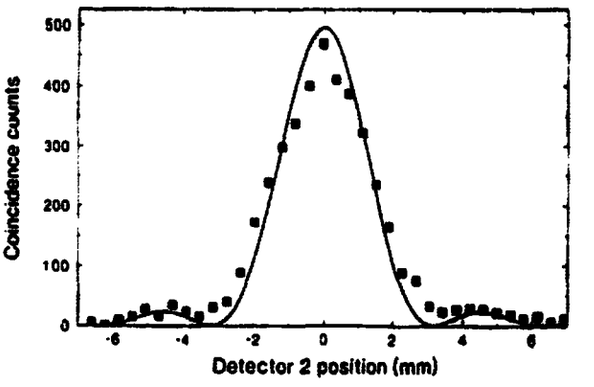

FIG.6. Two-photon diffraction: coincidence counts (per 400 sec) vs. the idler photon counting detector position. A single slit of width $a = 0.4mm$ is in the signal beam. The solid curve is a fit from the theoretical calculations.

By curve fittings, we conclude that the observation is a standard Young's interference-diffraction pattern:

$$R_c(x_2) \propto sinc^2\left(\frac{x_2\pi a}{\lambda z_2}\right)\cos^2\left(\frac{x_2\pi d}{\lambda z_2}\right). \tag{7}$$

The remarkable feature here is that z_2 *is the distance from the slits plane, which is in the signal beam, back through BS to BBO crystal and then along the idler beam to the scanning fiber tip of detector* D_2 (see fig. 4). The calculated interference period and the half-width of the sinc function from equation (7) are $2.67mm$ and $8.4mm$, respectively. Even though the interference-diffraction pattern is observed in coincidences, *the single detector counting rates are both observed to be constant when scanning detector* D_1 *or* D_2. Of course it is reasonable not to have any first order interference-diffraction in the single counting rate of D_2, which is located in the "empty" idler beam. Of interest, however, is that the absence of the first order interference-diffraction structure in the single counting rate of D_1, which is behind the double-slit, is mainly due to the divergence of the SPDC beam ($\gg \lambda/d$). In other words, the "blurring out" of the first order interference fringes is due to the considerably large momentum uncertainty of a single SPDC photon.

Furthermore, if D_1 is moved to an unsymmetrical point, which results in unequal distances to the two slits, the interference-diffraction pattern is observed to be simply shifted from the current symmetrical position to one side of x_2. This is quite mind boggling: *imagine* that there were a first order interference pattern behind the double-slit and D_1 were moved to a completely destructive interference point (i.e. zero intensity at that point) and fixed there. Can we still observe the same interference pattern in the coincidences (same period, shape, and counting rate), except for a phase shift?

Fig. 6 reports a typical single-slit diffraction pattern. The slit-width $a = 0.4mm$. The pattern fits to the standard diffraction sinc function, i.e., the "envelope" of equation (7), within reasonable experimental error. Here again z_2 is the unusual distance described in the above paragraphs.

To explain this unusual phenomenon, we again present a simple quantum model where, similar to the "ghost" image experiment, the momentum of either single photon is undeterminate. However, if one is measured at a certain value the other one is determinate with unit probability. This important peculiarity selects the only possible optical paths in fig. 7, when one photon passes through the double-slit aperture while the other gets to D_2. In the near degenerate case, we can simply treat the crystal as a reflecting mirror.

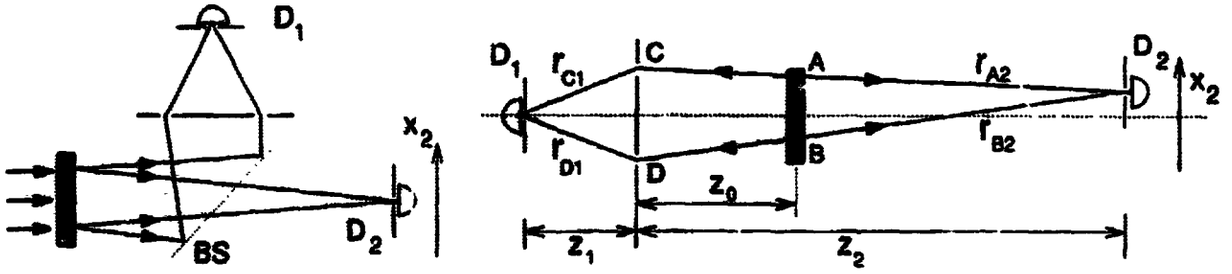

FIG.7: a) Simplified experimental scheme, and b) its "unfolded" version . The overall optical path lengths between D_1 and D_2 along the upper (r_A) and lower (r_B) paths, appearing in equation (11), are defined as: $r_A \equiv r_{A1} + r_{A2} = r_{C1} + r_{C2}$, and $r_B \equiv r_{B1} + r_{B2} = r_{D1} + r_{D2}$, where r_{Ci} and r_{Di} are the optical path lengths from the slits C and D to the ith detector.

The coincidence counting rate R_c is determined by the probability P_{12} of detecting a pair of photons by detectors D_1 and D_2 simultaneously. For SPDC, P_{12} is proportional to the square of the second order correlation function $\langle E_2^{(+)} E_1^{(+)} \rangle$ of the fields at points D_1 and D_2 (it thus plays the role of the two-photon effective wavefunction):

$$P_{12} = \langle E_1^{(-)} E_2^{(-)} E_2^{(+)} E_1^{(+)} \rangle = |\langle E_2^{(+)} E_1^{(+)} \rangle|^2. \tag{8}$$

In equation (8) $\langle \ldots \rangle \equiv \langle \Psi | \ldots | \Psi \rangle$, and $|\Psi\rangle$ is the four-mode state-vector of the SPDC field:

$$|\Psi\rangle = |vac\rangle + \epsilon \left[a_s^\dagger a_i^\dagger e^{i\phi_A} + b_s^\dagger b_i^\dagger e^{i\phi_B} \right] |vac\rangle \tag{9}$$

where $\epsilon \ll 1$ is proportional to the pump field (classical) and the nonlinearity of the crystal, ϕ_A and ϕ_B are the phases of the pump field at A and B, and $a_j^\dagger (b_j^\dagger)$ are the photon creation operators for the upper (lower) mode in fig. 7b (j = s, i). In terms of the Copenhagen interpretation one may say that the interference is due to the uncertainty in the birth-place (A or B in fig. 7) of a photon pair.

In equation (8) the fields at the detectors are given by

$$E_1^{(+)} = a_s e^{ikr_{A1}} + b_s e^{ikr_{B1}} \; ; \quad E_2^{(+)} = a_i e^{ikr_{A2}} + b_i e^{ikr_{B2}} \tag{10}$$

where r_{Ai} (r_{Bi}) are the optical path lengths from region A (B) along the upper (lower) path to the ith detector. Substituting equations (9) and (10) into equation (8),

$$R_c \propto P_{12} = \epsilon^2 |e^{i(kr_A+\phi_A)} + e^{i(kr_B+\phi_B)}|^2 \propto 1 + \cos[k(r_A - r_B)] \tag{11}$$

where we assume $\phi_A = \phi_B$ in the second line of equation (11) (although this is not a necessary condition to see the interference pattern, the transverse coherence of the pump beam at A and B is crucial). In equation (11) we defined the overall optical lengths between the detectors D_1 and D_2 along the upper and lower paths (see fig. 7b): $r_A \equiv r_{A1}+r_{A2} = r_{C1}+r_{C2}$, $r_B \equiv r_{B1}+r_{B2} = r_{D1}+r_{D2}$, where r_{Ci} and r_{Di} are the path lengths from the slits C and D to the ith detector.

If the optical paths from the fixed detector D_1 to the two slits are equal, i.e., $r_{C1} = r_{D1}$, and if $z_2 \gg d^2/\lambda$, then $r_A - r_B = r_{C2} - r_{D2} \cong x_2 d/z_2$ and equation (11) can be written as

$$R_c(x_2) \propto \cos^2\left(\frac{x_2 \pi d}{\lambda z_2}\right). \tag{12}$$

Equation (12) has the form of standard Young's double-slit interference pattern. Here again ***z_2 is the unusual distance from the slits plane, which is in the signal beam, back through BS to the crystal and then along the idler beam to the scanning fiber tip of detector D_2.***

If the optical paths from the fixed detector D_1 to the two slits are unequal, i.e., $r_{C1} \neq r_{D1}$, the interference pattern will be shifted from the symmetrical form of equation (12) according to equation (11). This interesting phenomenon has been observed and reported following the discussion of fig. 5.

To calculate the "ghost" diffraction effect of a single-slit such as shown in fig. 6, we need an integral of the effective two-photon wavefunction over the slit width:

$$R_c(x_2) \propto \left| \int_{\frac{-a}{2}}^{\frac{a}{2}} dx_0 e^{-ikr(x_0,x_2)} \right|^2 \cong sinc^2\left(\frac{x_2 \pi a}{\lambda z_2}\right) \tag{13}$$

where $r(x_0, x_2)$ is the distance between points x_0 and x_2, x_0 belongs to the slit's plane, and the inequality $z_2 \gg a^2/\lambda$ is assumed.

Repeating the above calculations, the combined interference-diffraction coincidence counting rate for the double-slit case is given by

$$R_c(x_2) \propto sinc^2\left(\frac{x_2 \pi a}{\lambda z_2}\right) \cos^2\left(\frac{x_2 \pi d}{\lambda z_2}\right) \tag{14}$$

which is exactly the same as equation (7) obtained from experimental data fittings. If the finite size of the detectors and the divergence of the pump are also taken into account by a convolution, the interference visibility will be reduced. These factors have been taken into account in the theoretical plots in figs. 5 and 6.

4 Acknowledgements

The authors gratefully acknowledge useful discussions with Professors C.O. Alley and M.H. Rubin. This work was supported by the United States Office of Naval Research.

References

[1] E.Schrodinger, Naturwissenschaften **23**, 807, 823, 844(1935); a translation of these papers appears in *Quantum Theory and Measurement*, edited by J.A. Wheeler and W.H. Zurek, Princeton University Press, New York (1983).

[2] A. Einstein, B. Podolsky, and N. Rosen, Phys. Rev. **35**, 777 (1935).

[3] Does a single particle have defined momentum in the following state?

$|\Psi) = \sum_{i,j} \delta(\mathbf{k}_i + \mathbf{k}_j - \mathbf{k}_0)|\mathbf{k}_i)|\mathbf{k}_j)$,

where $\mathbf{k}_0$ is a constant. Quantum mechanics answers: No, "no elementary quantum phenomenon is a phenomenon until it is a recorded phenomenon" [4]. EPR thought: It Should! EPR first suggested the above "perfect entangled" state, i.e., the momentum of either particle is undetermined; however, if one is measured to be $\mathbf{k}_i$ (an eigen value), then the other one is 100% determined to be $\mathbf{k}_0 - \mathbf{k}_i$, and then gave their criteria. Locality: there is no action-at-a-distance; Reality: "if, without in any way disturbing a system, we can predict with certainty the value of a physical quantity, then there exists an element of physical reality corresponding to this quantity". According to EPR's criteria, a single particle in the above state should have defined momentum. After this conclusion, EPR presented their Completeness: "every element of the physical reality must have a counterpart in the complete theory". This led to the question: "Can quantum-mechanical description of physical reality be considered complete?"

[4] W.A. Miller and J.A. Wheeler, *Foundations of Quantum Mechanics in the Light of new Technology*, edited by S. Kamefuchi *et. al.*, Physical Society of Japan, Tokyo, p.110 (1984).

[5] A. Yariv, *Quantum Electronics* John Wiley and Sons, Inc., New York (1989).

[6] D.N. Klyshko, *Photons and Nonlinear Optics*, Gordon and Breach Science Publishers, New York (1988).

[7] See, for example, C.O. Alley and Y.H. Shih, *Foundations of Quantum Mechanics in the Light of New Technology*, edited by M. Namiki *et al.*, Physical Society of Japan, Tokyo, p.47 (1986); C.K. Hong, Z.Y. *Ou*, and L. Mandel, Phys. Rev. Lett. **59**, 2044 (1987); Y.H. Shih and C.O. Alley, Phys. Rev. Lett. **61**, 2921 (1988); Z.Y. *Ou*, and L. Mandel, Phys. Rev. Lett. **61**, 54 (1988).

[8] T.B. Pittman, Y.H. Shih, D.V. Strekalov, and A.V. Sergienko *submitted to Phys. Rev. A. Rapid Communication* (1995).

[9] D.V. Strekalov, A.V. Sergienko, D.N. Klyshko, and Y.H. Shih, Phys. Rev. Lett. **74**, 3600 (1995).

[10] For related theory, see D.N. Klyshko, Phys. Lett. **A 132**, 299 (1988); D.N. Klyshko, Sov. Phys. Usp. **31**, 74 (1988); A.V. Belinskii, and D.N. Klyshko, JETP **78**, 259 (1994).

NEXT
DOCUMENT

SQUEEZED STATES, UNCERTAINTY RELATIONS AND THE PAULI PRINCIPLE IN COMPOSITE AND COSMOLOGICAL MODELS

Hidezumi Terazawa
Institute for Nuclear Study, University of Tokyo
Midori-cho, Tanashi, Tokyo 188 Japan

(Dedicated to Dr. Eugene Paul Wigner, the late Professor)

Abstract

The importance of not only uncertainty relations but also the Pauli exclusion principle is emphasized in discussing various "squeezed states" existing in the universe. The contents include:

I. Introduction

II. Nuclear Physics in the Quark-Shell Model

III. Hadron Physics in the Standard Quark-Gluon Model

IV. Quark-Lepton-Gauge-Boson Physics in Composite Models

V. Astrophysics and Space-Time Physics in Cosmological Models

VI. Conclusion

Also, not only the possible breakdown of (or deviation from) uncertainty relations but also the superficial violation of the Pauli principle at short distances (or high energies) in composite (and string) models is discussed in some detail.

I Introduction

I have been asked by Professor Y.S. Kim, the Principal Organizer for this Conference to present a paper based on my recent research results in the field of squeezed states and uncertainty relations. Since I am a particle theorist, I have not so much to say about "squeezed states" in condensed matter physics (or science). Therefore, what I am going to do is to discuss "squeezed states" in nuclear physics (or science), hadron physics (or science), "quark-lepton-gauge-boson physics (or science)", astrophysics (or astronomy) and "space-time (or cosmic) physics (or science)" (or cosmology). In either one of these discussions, I will try to emphasize the importance of not

only uncertainty relations but also the Pauli exclusion principle. The reason for this is that both the Heisenberg uncertainty principle and the Pauli exclusion principle are the most important principles after the particle-wave idea on which quantum mechanics is based. Also, these two principles are closely related to each other so that they may not be discussed separately. Toward the end of this talk, I will even discuss not only the possible breakdown of (or deviation from) uncertainty relations but also the superficial violation of the Pauli principle at short distances (or high energies) in composite (and string) models.

I would like to dedicate this talk to Dr. Eugene Paul Wigner, the late Professor who has developed the group theory and its application in quantum mechanics of atomic spectrum based on the uncertainty principle and the Pauli principle [1].

II Nuclear Physics in the Quark-Shell Model

In 1975, Arima and Iachello taught me that nuclear physics (or science) [2] yet needs a totally new model, their interacting boson model [3]. In 1979, I proposed another model, the quark-shell model of nuclei in quantum chromodynamics, presented the effective two-body potential between quarks in a nucleus, pointed out violent breakdown of isospin invariance and importance of U-spin invariance in superheavy nuclei and predicted possible creation of "super-hypernuclei" in heavy-ion collisions at high energies.

In this section, let me start with discussing squeezed states in nuclear physics. The nucleon density in an ordinary nucleus with the mass number A and the radius R or in ordinary nuclear matter is $\rho_N \equiv A/V = 3A/4\pi R^3 = 3/4\pi R_o^3 \cong 0.14/(fermi)^3$ where $V = (4\pi/3)R^3$ since $R \cong R_o A^{1/3}$ for $R_o \cong 1.2$ fermi. A much higher nucleon density can be found in an abnormal nuclear matter such as the neutron star or the part of a compound nuclei to be formed in high-energy heavy-ion collisions. The latter of which may be produced in the near future by RHIC, which is now under construction at Brookhaven National Laboratory. It is very intriguing whether the future experiments at RHIC will observe, for the first time, the phase transition of nuclear matter from the ordinary nuclear phase to the abnormal Lee-Wick phase in which "effective" nucleon (or quark) mass inside the nucleus may be much smaller than the normal value [4], which was predicted in 1974, and also the phase transition from the ordinary nuclear phase to the quark-gluon phase in which quarks and gluons may be deconfined or liberated. However, it seems still very difficult to calculate the cross section for producing such abnormal nuclei to a very good accuracy and also to imagine the reliable signals for observing them.

A little later, in 1979, Chin and Kerman, and independently myself predicted another type of abnormal nuclei (called super-hypernuclei or "strange quark matter") consisting of almost equal numbers of up, down and strange quarks, based on the natural expectation that they may enjoy suppression of not only the Fermi energy but also the Coulomb repulsive energy in nuclei [5]. Furthermore, the possible creation of such abnormal matter in bulk (called "quark nuggets") in the early universe or inside the neutron star had been discussed in detail by Witten, and the properties of "strange matter" had been investigated in detail in the Fermi-gas model by Farhi and Jaffe. Recently, Saito et al. found in cosmic rays two abnormal events with the charge of $Z = 14$ and the mass number of $A \cong 370$ and emphasized the possibility that they are super-hypernuclei [6]. In order to determine whether or not these cosmic rays are really super-hypernuclei as claimed by the cosmic-ray experimentalists, I have investigated how the small charge-to-mass-

number ratio of Z/A is determined for super hypernuclei when created and concluded that such a small charge of $3 \sim 30$ may be realized as $Z \leq \sqrt{2/3}A^{1/2}$ ($\cong 15.7$ for $A = 370$) if the nuclei are created spontaneously from bulk strange quark matter due to the Coulomb attraction [7]. The second most likely interpretation of the Saito events is that they are "technibaryonic nuclei" or "technibaryon-nucleus atoms" [8].

In concluding this section, I wish to advocate my proposal for measuring not only the weak mixing angle but also the quark density in nuclei by observing the effect that the electron energy spectrum in nuclear β-decays is affected by the weak neutral current interaction in nuclei to the order of several eV [9]. Also, I wish to advocate my proposal for studying the quark structure of nuclei in inelastic virtual Compton scattering of photons from nuclei for lepton-pair production, $\gamma + A \to \gamma^* + anything$ and $\gamma^* \to e^+ + e^-$ [10].

III Hadron Physics in the Quark-Gluon Model

In this section, let me discuss squeezed states in hadron physics. The quark density in an ordinary hadron with the quark number N_q and the radius R_h or in ordinary hadronic matter is $\rho_q \cong N_q/V_h = 3N_q/4\pi R_h^3 \cong 9/4\pi r_p^3 \cong 1.35 \sim 2.61/(fermi)^3$ where $V_h = (4\pi/3)R_h^3$ and r_p is the proton charge radius of the order of 0.81 fermi or the proton "quark radius" of the order of 0.65 fermi [11]. A much higher quark density can be found in an abnormal hadron or abnormal hadronic matter such as the dense quark-gluon plasma or the part of a compound hadron to be formed in super high-energy hadron collisions. The so-called Centauro events with extremely high multiplicities of produced hadrons ($n_h = 100 \pm 20$) and with unusually high average transverse momenta ($\langle p_T \rangle = 0.35 \pm 0.10$ GeV/c) but without any γ's observed in the cosmic ray experiments by the Brasil-Japan Emulsion Chamber Collaboration in 1977 may be indications of such abnormal hadrons although no candidates for such exotic hadrons have yet been observed in any accelerator experiments [12]. However, my personal prejudice is that such unusual events may not be taken as indications of such exotic hadrons but be explaind either by coherent effects of many nucleons in projectile and target heavy ions or by incoherent effects of individual nucleons since the charged multiplicity in hadron-hadron collisions at very high energies may become much larger than usually expected. In fact, in 1982 I demonstrated that the average charged multiplicity ($\langle n_{ch} \rangle$) and transverse momentum ($\langle p_T \rangle$) of produced particles in hadron-hadron collisions at very high energies ($\sqrt{s}$) have a simple relation of $\langle n_{ch} \rangle^2 \langle p_T \rangle / \sqrt{s} =$ constant ($= 0.70 \pm 0.05$) in the generalized Fermi-Landau statistical and hydrodynamical model. The relation is satisfied remarkably well by the experimantal data up to the SPS p-p Collider energies and will soon be tested by Tevatron Collider experiments. From the relation, I have predicted that the average charged multiplicity will become as large as $\langle n_{ch} \rangle = 47 \pm 2$ at $\sqrt{s} = 1.8$ TeV [13].

I have discussed so far the squeezed states of nuclear matter and hadronic matter which are squeezed by the external force or pressure caused by heavy-ion collisions and hadron-hadron collisions. However, some hadronic matter can be squeezed by itself at low temperatures (or low energies) due to the very strong attractive force between constituents of hadronic matter, the quarks. It may be called "self-squeezing". For example, the very heavy top quark (t) and the antiquark must have a very strong attractive force due to an exchange of the Higgs scalar (H) in the standard model of Glashow-Salam-Weinberg for electroweak interactions. Therefore, suppose

that the vacuum consists of quark-antiquark and lepton-antilepton pairs as in our unified model of the Nambu-Jona-Lasinio type for all elementary-particle forces [14], we can expect that a top quark and an anti-top quark be self-squeezed to form a scalar bound state of $t\bar{t}$ [14]. This is called "top(-antitop) condensation". According to Nambu, this is a kind of "bootstrap", the original form of which was advocated by Chew in hadron physics in the middle of 1960's, since the Higgs scalar is taken as a bound state of $t\bar{t}$ or a condensate of $t\bar{t}$ in our picture. In 1980, I predicted, from the sum rules for quark and lepton masses previously derived in our unified model of 1977 [14], the top-quark and Higgs scalar masses to be $m_t \cong \sqrt{8/3}m_W \cong 131$ GeV and $m_H \cong 2m_t \cong 261$ Gev. Much later, Nambu, Miransky et al. and Bardeen et al. made similar predictions for m_t and m_H in their models of the Nambu-Jona-Lasinio type which are similar to our unified model [14]. In 1990, I derived a similar sum rule for quark and lepton masses in a model-independent way [15].

IV Quark-Lepton-Gauge-Boson Physics in Composite Models

In this section, let me discuss squeezed states in quark-lepton-gauge-boson physics. Since Pati and Salam, and independently ourselves proposed composite models of quarks and leptons in the middle of 1970's [16], hundreds of particle theorists have extensively investigated these models in great detail for the last two decades [17]. For the last decade, thousands of high-energy particle experimentalists have been seriously searching for a possible evidence for the substructure and excited states of not only quarks and leptons but also gauge bosons [18] although they have not yet found any clear evidence [19].

In our unified composite model of quarks and leptons [16], not only quarks and leptons but also gauge bosons as well as Higgs scalars are composite states of subquarks (or preons), the more fundamental and probably most fundamental constituents of matter. All these fundamental particles in quark-lepton-gauge-boson physics may be taken as self-squeezed composite states of the quark-leptonic matter. Since our composite model of quarks and leptons is a simple analogy of the celebrated quark-gluon model of hadrons by Gell-Mann, Zweig and Nambu, it leads us to a lot of easy analogous ideas in quark-lepton-gauge-boson physics. One of the most eminent examples is the principle of "triplicity", which asserts that a certain physical quantity such as the weak current can be taken equally well as a composite operator of hadrons, or of quarks, or of subquarks [20]:

$$\begin{aligned} J_\mu &\cong \bar{\nu}_e\gamma_\mu(1-\gamma_5)e + \bar{\nu}_\mu\gamma_\mu(1-\gamma_5)\mu + \bar{\nu}_\tau\gamma_\mu(1-\gamma_5)\tau \\ &\quad + \frac{G^\beta}{G^\mu}\bar{p}\gamma_\mu(1-\frac{g_A^\beta}{g_V^\beta}\gamma_5)n + \frac{G^\Lambda}{G^\mu}\bar{p}\gamma_\mu(1-\frac{g_A^\Lambda}{g_V^\Lambda}\gamma_5)\Lambda + \cdots \\ &\cong \bar{\nu}_e\gamma_\mu(1-\gamma_5)e + \bar{\nu}_\tau\gamma_\mu(1-\gamma_5)\mu + \bar{\nu}_\tau\gamma_\mu(1-\gamma_5)\tau \\ &\quad + V_{ud}\bar{u}_i\gamma_\mu(1-\gamma_5)d_i + V_{us}\bar{u}_i\gamma_\mu(1-\gamma_5)s_i + \cdots \\ &\cong \bar{w}_1\gamma_\mu(1-\gamma_5)w_2, \end{aligned}$$

where w_1 and w_2 are an iso-doublet of spinor subquarks with charges $\pm 1/2$ (called "wakems").

Another example is scaling mass parameters of hadrons, quarks and subquarks. It asserts that the current mass of light quarks be scaled to those of subquarks which can be as small as 45 GeV and that the "electrostrong" gauge theory for hadrons may appear as an effective theory in QCD as the electroweak gauge theory for quarks with the scaling relations of $m_H/m_W = m_\sigma/m_\rho$, which predicts $m_H \cong 94$ GeV [21].

The principle of triplicity tells us that the Higgs scalars can be taken equally well as composites (or condensates) of subquark-antisubquark pairs or of quark-antiquark (or lepton-antilepton) pairs as in our unified model of the Nambu-Jona-Lasinio type as π's and σ as those of nucleon-antinucleon pairs as in the original form of Nambu-Jona-Lasinio model [14]. In this picture of subquark-antisubquark condensation, we have derived the mass formula for composite quarks and leptons from a partially conserved induced supercurrent hypothesis. In supersymmetric composite models [22], it leads to a simple sum rule for quark and lepton masses of [23]

$$m_e^{1/2} = m_d^{1/2} - m_u^{1/2}$$

if the first generation of quarks and leptons can be taken as almost Nambu-Goldstone fermions [24]. We have found that not only this square-root mass sum rule but also another similar sum rule of $m_\mu^{1/2} - m_e^{1/2} = m_s^{1/2} - m_d^{1/2}$ are satisfied remarkably well by the experimental values. Furthermore, if the first and second generations of quarks and leptons can be taken as almost and quasi Nambu-Goldstone fermions, respectively, we can derive not only a simple relation among lepton masses of $m_\tau \cong (m_\mu^3/m_e)^{1/2}$ [25] but also a simple relation among quark masses $m_t \cong (m_d m_c^3 m_b^2/m_u m_s^3)^{1/2}$ [26]. These relations predict $m_\tau \cong 1520$ MeV and $m_t \cong 177$ GeV, which should be compared to the experimental values of $m_\tau = 1777.1 \pm^{0.4}_{0.5}$ MeV and $m_t = 176 \pm 8 \pm 10$ GeV or $199 \pm^{19}_{21} \pm 22$ GeV [27], respectively.

In 1991, I suggested that the existing mass spectrum of quarks and leptons can be explained by solving a set of sum rules for quark and lepton masses [28]. Today, I am pleased to announce that it can be explained completely by solving a set of not only the previously derived sum rules for quark and lepton masses but also these newly derived relations among quark and lepton masses. As an illustration, given a set of the sum rules and relations of

$$m_e^{1/2} = m_d^{1/2} - m_u^{1/2}, m_\mu^{1/2} - m_e^{1/2} = m_s^{1/2} - m_d^{1/2}, m_e m_\tau^2 = m_\mu^3, m_u m_s^3 m_t^2 = m_d m_c^3 m_b^2,$$

I have obtained the solution of

$$\begin{pmatrix} m_e & m_\mu & m_\tau \\ m_u & m_c & m_t \\ m_d & m_s & m_b \end{pmatrix} = \begin{pmatrix} 0.511 \text{ MeV} & 105.7 \text{ MeV} & 1520 \text{ MeV} \\ (\text{ input }) & (\text{ input }) & (1777.1 \pm^{0.4}_{0.5} \text{ MeV }) \\ 4.5 \pm 1.4 \text{ MeV} & 1350 \pm 50 \text{ MeV} & 183 \pm 78 \text{ GeV} \\ (\text{ input }) & (\text{ input }) & (176 \pm 8 \pm 10 \text{ or } 199 \pm^{19}_{21} \pm 22 \text{ GeV }) \\ 8.0 \pm 1.9 \text{ MeV} & 154 \pm 8 \text{ MeV} & 5.3 \pm 0.1 \text{ GeV} \\ (7.9 \pm 2.4 \text{ MeV }) & (155 \pm 50 \text{ MeV }) & (\text{ input }) \end{pmatrix}$$

where the values indicated in the parentheses denote the experimental, to which my predicted values should be compared. As another illustration, given another set of the sum rules and relations of

$$\sum_{q,l} m_{q,l}^4 / \sum_{q,l} m_{q,l}^2 = \frac{1}{4} m_H^2, \sum_{q,l} m_{q,l}^2 / \sum_{q,l} 1 = \frac{1}{3} m_W^2,$$

$$m_e^{1/2} = m_d^{1/2} - m_u^{1/2}, m_\mu^{1/2} - m_e^{1/2} = m_s^{1/2} - m_d^{1/2}, m_\tau^{1/2} = m_b^{1/2} - m_c^{1/2},$$

$$m_e m_\tau^2 = m_\mu^3, m_u m_s^3 m_t^2 = m_d m_c^3 m_b^2,$$

$$(m_\mu/m_e)^{1/2} = (m_c/m_u)^{1/2} - (m_s/m_d)^{1/2}, (m_\tau/m_\mu)^{1/2} = (m_t/m_c)^{1/2} - (m_b/m_s)^{1/2},$$

I have obtained the other solution of $m_H (\cong \sqrt{32/3} m_W) \cong 261$ GeV and

$$\begin{pmatrix} m_e & m_\mu & m_\tau \\ m_u & m_c & m_t \\ m_d & m_s & m_b \end{pmatrix} = \begin{pmatrix} 0.49 \text{ MeV} & 101 \text{ MeV} & 1454 \text{ MeV} \\ (0.511 \text{ MeV}) & (105.7 \text{ MeV}) & (1777.1 \pm^{0.4}_{0.5} \text{ MeV}) \\ 3.3 \text{ MeV} & 1204 \text{ MeV} & 131 \text{ GeV} \\ (4.5 \pm 1.4 \text{ MeV}) & (1350 \pm 50 \text{ MeV}) & (176 \pm 8 \pm 10 \text{ or } 199 \pm^{19}_{21} \pm 22 \text{ GeV}) \\ 6.3 \text{ MeV} & 140.8 \text{ MeV} & 5.3 \pm 0.1 \text{ GeV} \\ (7.9 \pm 2.4 \text{ MeV}) & (155 \pm 50 \text{ MeV}) & (\text{input}) \end{pmatrix}$$

for $m_W = 80$ GeV.

In 1977, I suggested that the CKM quark mixing matrix (V_{mn}) can be defined by the matrix element between the mth up-like quark (U_m) with charge 2/3 and the nth down-like quark (d_n) with the charge -1/3 as $\langle u_m \mid \bar{w}_1 \gamma_\mu w_2 \mid d_n \rangle = V_{mn} \bar{u}_m \gamma_\mu d_n$ and that the Cabbibo angle (and all the CKM mixing angles) may vary as a function of momentum transfer between quarks [29], which should be observed in the future high energy experiments such as for decays of $b \to c$ at B factories (or $t \to b$) and for scatterings of $\nu + u \to l + s$ and $\nu + u \to l + d$ (or $e + u \to \nu + d$ and $e + u \to \nu + s$ at HERA). In 1981, we predicted that the Cabbibo angle becomes larger as momentum transfer between quarks grows up in a simple subquark model [30]. Furthermore, in 1992, I pointed out that given the us element of the CKM quark mixing matrix (V_{us}), all the other elements can be successfully explained or predicted by using the five relations derived in a composite model of quarks [31]. In fact, given a set of the relations of

$$V_{us} \cong -V_{cd}^*, V_{cb} \cong -V_{ts}^*, \mid V_{ub} \mid \cong (m_s/m_b) \mid V_{us} \mid, \mid V_{ub} \mid \cong (m_c/m_t) \mid V_{us} V_{cb} \mid, \mid V_{td} \mid \cong \mid V_{us} V_{cb} \mid,$$

I have obtained the solution of

$$\begin{pmatrix} V_{ud} & V_{us} & V_{ub} \\ V_{cd} & V_{cs} & V_{cb} \\ V_{td} & V_{ts} & V_{tb} \end{pmatrix} = \begin{pmatrix} 0.975 & 0.218 \sim 0.224 & 0.0017 \\ (0.9747 \sim 0.9759) & (\text{input}) & (0.002 \sim 0.005) \\ 0.218 \sim 0.224 & 0.977 & 0.021 \\ (0.218 \sim 0.224) & (0.9738 \sim 0.9752) & (0.032 \sim 0.048) \\ 0.0046 & 0.021 & 0.9996 \\ (0.001 \sim 0.015) & (0.030 \sim 0.048) & (0.9988 \sim 0.9995) \end{pmatrix}$$

To sum up, I wish to emphasize that not only the mass spectrum of quarks and leptons but also the CKM quark mixing matrix can be explained successfully in the unified composite model of quarks and leptons and that "elementary-particle" physics of quarks and leptons in the last quarter century will no doubt proceed by one step forward to "subphysics", the elementary-particle physics of subquarks.

V Astrophysics and Space-Time Physics in Cosmological Models

In this section, let me discuss squeezed states of matter in the universe. A simplest example of self-squeezed states of matter in the universe is a star. A planetary system, a nebula, a galaxy, a cluster of galaxies and a cluster of the clusters of galaxies are also self-squeezed states in a sense. Since I have no time (or space) to discuss either one of these examples one by one, I only point out the importance of searching for "super-hypernuclear stars", which are self-squeezed states of super-hypernuclei (or strange quark matter) predicted by Chin and Kerman and by myself [5]. It has been especially advocated later by Witten.

More fascinating, however, is to imagine that the universe itself is a self-squeezed state of matter. No question, it was a self-squeezed state of matter right after the big bang. One can imagine that it had also been a self-squeezed state of matter even before the big bang. In order to discuss possible physics before the big bang, if any, we may not be able to use any more Einstein's theory of general relativity on gravitation. Instead, we must adopt "pregeometry", the more fundamental theory, first suggested by Sakharov in 1967 [32] and first demonstrated by us in 1977 [33], in which gravity is taken as a quantum effect of matter fields and in which Einstein's theory of general relativity for gravity appears as an approximate and effective theory at long distances (or low energies). In 1983, we could even suggest the pregeometric origin of the big bang in the following way [31]. Pregeometry has changed the notion of the space-time metric completely since the space-time metric can be taken as a kind of composite object of the fundamental matters. Therefore, we can even imagine that at high temperature the space-time metric would dissociate into its constituents just as ordinary objects do. Then, the metric would vanish although the fundamental matters still remain in the mathematical manifold of the space-time. Namely, the pregeometric phase is the phase of the space-time in which metric $g^{\mu\nu}(g_{\mu\nu})$ vanishes (diverges) and, therefore, the distance of $ds^2 = g_{\mu\nu}dx^\mu dx^\nu$ diverges. There, the space-time still exists as a mathematical manifold for the presence of the fundamental matters. Such an extraordinary phase may be realized in such regions as that beyond the space-time singularity, i.e., before the big bang and that far inside a black hole where the temperature is extremely high (as high as the Planck mass). In a simple model of pregeometry, Akama and I have demonstrated that although the pregeometric phase is stable at very high temperature the geometric phase where the metric is finite and non-vanishing will turn out to be stable as the temperature goes down. This remarkable possibility of phase transitions of the space-time between the geometric and pregeometric phase will exhibit a characteristic feature of pregeometry, if it is found. It seems very attractive to interpret the origin of the big bang of our universe as such a local and spontaneous phase transition of the space-time from the pregeometric phase to the geometric one in the overcooled space-time manifold which had been present in the "pre-big-bang" era for some reason.

This interpretation of the big bang also suggests that there may exist thousands of universes created and expanding in the space-time manifold as our universe. It even predicts that such different universes may collide with each other. Furthermore, even in our universe there may exist "pregeometric holes", the local spots in the pregeometric phase with an extremely high temperature where the space-time metric disappears, liberating enormous latent heat, and/or "space-time discontinuities", the local plains where the metric (and, therefore, the light velocity or the Newtonian gravitational constant) discretely changes due to the phase difference of two

adjacent space-times (or two colliding universes). I have been strongly urging astronomical and cosmological experimentalists to search for these pregeometric holes and space-time discontinuities, which are much more exotic than black holes. It would be fascinating if the recently observed "Great Wall" of galaxies (much older than the Chinese Great Wall) be caused by such space-time discontinuity.

The most fascinating among my suggestions on squeezed states is that in a model of the extended n-dimensional Einstein-Hilbert action for space-time and matter the space-time (or universe), when contracted (or squeezed), may transit into a new one of higher or lower dimensions at the minimum action near the Planck scale [35]. Since I suggested this in 1987, many authors have discussed this "incredible" possibility and concluded that it is possible [36].

In concluding this section, I wish to announce my latest work on squeezed states of matter in the universe entitled, "The Meaning of Dirac's Large Number Hypothesis" [37]. Dirac's large number hypothesis (LNH) [38] states that the Eddington large numbers [39] $N_1(\equiv \alpha/Gm_em_p \cong 10^{39})$, $N_2(\equiv m_e/\alpha H \cong 10^{40})$ and $N_3(\equiv 4\pi\rho/3m_pH^3 \cong 10^{80})$ are not independent but related with each other. By reconsidering the meaning of the LNH, I have shown that not only the "dynamical" LNH relation of $N_3 \sim N_1N_2$ [40] but also the "geometrical" LNH relation of $N_3 \sim (N_2)^2$ holds so that the LNH may not be taken as a hypothesis but become the large number rule (LNR).

VI Conclusion

In the previous sections, I have discussed not only various squeezed states existing in the universe and various squeezed states which might be existing or may be produced in the universe, but also even a squeezed state of the universe (or space-time), itself. In this last section, I have originally planned to emphasize the importance of uncertainty relations and the Pauli principle in discussing these squeezed states in the nature. However, since I have no time (or space) to do that, which seems to be rather trivial, I will instead emphasize how closely these two principles, the Heisembertg uncertainty principle and the Pauli exclusion principle, are related with each other and discuss how they may be violated in the nature.

The close relation between the two principles seems to be self-explained in the following chain diagram:

$$\Delta x \cdot \Delta p \gtrsim \hbar \rightarrow [p,q] = -i\hbar \rightarrow [\varphi(x),\varphi(y)] = i\Delta(x-y) \text{ and } \{\psi(x),\bar{\psi}(y)\} = i(i\not{\partial}_x + m)\Delta(x-y).$$

The possible breakdown of (or deviation from) uncertainty relations at extremely short distances (or high energies) has already been suggested and extensively discussed in superstring models [41] by Amati, Ciafaloni and Veneziano [42]. They have suggested the extended uncertainty relation (EUR or ACV relation) of

$$\Delta x > \frac{\hbar}{\Delta p} + \alpha'\Delta p,$$

where α' is the Regge slope of superstrings which is the order of $(Planckmass)^{-2}$. This realizes not only the old conjecture by Landau and Weiskopf who suggested the existence of natural cutoff at a short distance (or high energy) of the Planck scale but also our hypothesis in the unified composite model for all elementary-particle forces including gravity [43].

Also, the possible simple violation of the Pauli principle has already been investigated not only theoretically but also experimentally [44]. Recently, we have discussed superficial violation of the Pauli principle due to the possible substructure of electrons in composite models of quarks and leptons, and estimated the ratio of the Pauli forbidden atomic transition to the allowed one to be of order $10^{-50} - 10^{-44}$ for heavy atoms if the size of the electron is of order 10^{-17} cm [45]. We have also emphasized that such superficial violation of the Pauli principle must exist, no matter how small it is, if the electron has any substructure at all. It seems even natural since it is a simple extension of the familiar effects at the various levels of atoms, nuclei, and hadrons: For example, the hydrogen atom which consists of the proton and the electron obeys Bose statistics in ordinary situations. However, when two hydrogen atoms overlap each other, the bosonic property of each hydrogen atoms becomes meaningless and, instead, the fermionic property of the constituent protons and electrons becomes effective. Suppose also two helium nuclei are overlapping each other. Then, the genuine bosonic statistics of each helium nucleus is meaningless and only the fermionic statistics of the constituent nucleons is valid. Furthermore, when two protons overlap each other, the fermionic property of protons will be lost and that of constituent quarks will be effective.

A field theoretical formulation of such an effect is unfamiliar. Suppose that the electron consists of a fermion w and a boson C as in the minimal composite model of quarks and leptons [17]. Then, the local field of the composite electron ψ (of mass m and energy E) can be constructed in the Haag-Nishijima-Zimmermann formalism [46] as

$$\psi(x) = \lim_{\substack{\xi^2<0 \\ \xi\to 0}} \frac{w(x+\xi)C(x-\xi)}{[(2\pi)^3(E/m)\langle 0 \mid w(x+\xi)C(x-\xi) \mid \psi\rangle]^{1/2}}.$$

However, in the local limit of $\xi \to 0$ no such effect as a violation of the Pauli principle due to the compositeness of electrons can be expected. To find such an effect, let us consider the bilocal field of a composite electron,

$$\psi(x,\xi) = Nw(x+\xi)C(x-\xi),$$

where ξ represents the finite nonvanishing size of order r_0 [$= (\xi^2)^{1/2}$] and N is an appropriate normalization factor. The anticommutator of the fields, given by

$$N^{-2}\{\psi(x,\xi),\psi(y,\eta)\} = \{w(x+\xi),w(y+\eta)\}C(x-\xi)C(y-\eta)+w(y+\eta)w(x+\xi)[C(y-\eta),C(x-\xi)],$$

clearly indicates the superficial violation of not only the Pauli principle but also causality, since neither $\{w(x+\xi),w(y+\eta)\}$ nor $[C(y-\eta),C(x-\xi)]$ vanishes for $(x-y)^2 < 0$ [although the former vanishes for $(x-y+\xi-\eta)^2 < 0$ while the latter does for $(x-y-\xi+\eta)^2 < 0$].

This demonstration may illustrate what we mean by the superficial violation. Namely, neither the Pauli principle nor causality is violated at the level of constituent fields of w and C since w and C perfectly obey Fermi and Bose statistics, respectively. Also, the anticommutator of w's and the commutator of C's perfectly respect causality. However, due to the possible substructure of electrons, the composite electron field may exhibit the situation in which its statistics looks neither purely fermionic nor purely bosonic when two electrons are located close to and are overlapped with each other at a distance of the order of their size r_0.

The recent experiment of Ejiri et al. [47] using a NaI detector in Osaka University may be able to set an upper bound of order 3×10^{-46} on the ratio for $Z = 53$, which is the atomic number of I. This corresponds to an upper bound of 1×10^{-17} cm on the electron size r_0. If this is the case, it also corresponds to a lower bound of 2 TeV on the inverse size of electrons, $1/r_0$ which is 1 order of magnitude larger than the known lower bounds of order 100 GeV on the compositeness scale of electrons, Λ, obtained by e^+e^- collider experiments [48].

In the rest of my talk, let me talk about the future prospects of these two principles. One possible movement is to take the uncertainty principle not as a fundamental principle but a consequence of a more basic idea. Along this line of thinking, let me remind you of the latest work by Hall, who has shown that the sum of the information gains corresponding to measurements of position and momentum is bounded as

$$I(X \mid \varepsilon) + I(P \mid \varepsilon) \leq log2(\Delta X)_\varepsilon(\Delta P)_\varepsilon/h$$

for a quantum ensemble with position and momentum uncertainties ΔX and ΔP [49]. In any case, we may need to investigate seriously extended uncertainty relations such as the ACV relation in superstring models and generalized nonlocal commutation relations such as ours in composite models discussed in Section V (, and also perhaps quantum group).

Another possible movement is to take the Pauli principle not as a fundamental principle but a consequence of the more basic idea. To this end, we may need to reconsider generalized Bose-Einstein and Fermi-Pauli statistics such as parabose and parafermi statistics (, and also q-bose and q-fermi statistics [50]).

More interesting seems to investigate "prequantum theory (or mechanics)" in which the familiar quantum theory (or mechanics) may appear as an approximate and effective theory. Along this line, we may need to reconsider Bohm's theory with hidden variables and Einstein's argument against Bohr's probability-statistical interpretation in quantum mechanics.

In concluding my talk, I wish to emphasize that both subphysics and pregeometry are at least promising "theories of everything" and working frameworks or machineries for "prephysics", a new line of physics (or philosophy but not metaphysics) in which some basic hypotheses (or principles) taken as sacred ones in ordinary physics such as the four dimensionality of space-time [35], the number of subquarks [51], the invariance under gauge transformation [52], that under general coordinate transformation [53], the microscopic causality, the principle of superposition (or particle-wave idea in more general) and so on are to be reasoned. Therefore, I wish to conclude this talk simply by modifying the original Wheeler's word into the following: Never more than today does one have the incentive to explore prephysics (or "new physics") [54].

Acknowledgements

The author would like to thank Professors Y.S. Kim, V.I. Man'ko, K.C. Peng, E.L. Wang and the other organizers including Professor K. Kakazu for inviting him to the Fourth International Conference on Squeezed States and Uncertainty Relations and for extending him their warm hospitality in Taiyuan, Shanxi from June 5 to 8, 1995. He also wishes to thank Dr. Eugene Paul Wigner, the late Professor to whom this talk has been dedicated, for giving him many invaluable advices during the one year of their overlapping stay at The Rockefeller University in 1971, without which this work would never have been completed.

References

[1] Von Eugen Wigner, Gruppentheorie und ihre Anwendung auf die Quanten-mechanik der Atomspektren (Berlin, 1931).

[2] For a pedagogical review, see for example A. Bohr and B.R. Mottelson, Nuclear Structure (W.A. Benjamin, New York, Amsterdam, 1969) Vol. I and II.

[3] See for example, A. Arima and F. Iachello, Phys. Rev. Lett. 35, 1069 (1975). For a philosophical review, see for example, Y. Nambu, Physica 15D, 147 (1985).

[4] T.D. Lee and G.C. Wick, Phys. Rev. D9, 2291 (1974).

[5] H. Terazawa, INS-Report-338 (INS, Univ. of Tokyo, 1979) Genshikaku Kenkyu (INS, Univ. of Tokyo) Vol. 25, No. 6, 51 (1981); J. Phys. Soc. Jpn. 58, 3555 (1989); 58, 4388 (1989), 59, 1199, (1990); S.A. Chin and A.K. Kerman, Phys. Rev. Lett. 43, 1292 (1979); E. Witten, Phys. Rev. D30, 272 (1984); E. Farhi and R.J. Jaffe, Phys. Rev. D30, 2379 (1984).

[6] T. Saito, Y. Hatano, Y. Fukuda and H. Oda, Phys. Rev. Lett. 65 2094 (1990); For a latest review, see T. Saito, a paper contributed to the 24th International Cosmic Ray Conference, Rome, 1995, to be published in the Proceedings.

[7] H. Terazawa, J. Phys. Soc. Jpn. 60, 1818 (1991).

[8] H. Terazawa, J. Phys. Soc. Jpn. 62, 1115 (1993).

[9] H. Terazawa, J. Phys. Soc. Jpn. 58, 767 (1989).

[10] H. Terazawa, J. Phys. Soc. Jpn. 47, 355 (1979).

[11] J. Pestieau, P. Roy and H. Terazawa, Phys. Rev. Lett. 25, 402 (1970).

[12] Brasil-Japan Emulsion Chamber Collaboration, in Proceedings of the 15th International Cosmic Ray Conference, Plovdiv, 1977, Vol. 7 (1977) p. 208. For an experimental review, see C.M.G. Lattes, Y. Fujimoto and S. Hasegawa, Phys. Rep. C65, 151 (1980) and for a theoretical review, see for example H. Terazawa, in Proceedings of the 21st International Conference on High Energy Physics, Paris, 1982, edited by P. Petiau and M. Porneuf, J. de Phys. C3-191 (1982).

[13] H. Terazawa, J. Phys. Soc. Jpn. 58, 5 (1989).

[14] H. Terazawa, Y. Chikashige and K. Akama, Phys. Rev. D15, 480 (1977); H. Terazawa, Phys. Rev. D22, 2921 (1980); D41, 3541(E) (1990); Y. Nambu, Enrico Fermi Institute Report No. 89-08 (1989), in Proceedings of the 1989 Workshop on Dynamical Symmetry Breaking, Nagoya, 1989, edited by T. Muta and K. Yamawaki (Nagoya University, Nagoya, 1990),p. 1; V.A. Miransky, M. Tanabashi and K. Yamawaki, Mod. Phys. Lett. A4, 1043 (1989); Phys. Lett. B221, 177 (1989); W.A. Bardeen, C.T. Hill and M. Lindner, Phys. Rev. D41, 1647 (1990).

[15] H. Terazawa, Phys. Rev. Lett. 65, 823 (1990).

[16] J.C. Pati and A. Salam, Phys. Rev. D10, 275 (1974); H. Terazawa, Y. Chikashige and K. Akama, Phys. Rev. D15, 480 (1977); H. Terazawa, Phys. Rev. D22, 184 (1980).

[17] For a review, see H. Terazawa, in Proceedings of the 22nd International Conference on High Energy Physics, Leipzig, 1984, edited by A. Meyer and B. Wieczorek (Akademie der Wissenschaften der DDR, Zeuthen, 1984), Vol. I, p. 63.

[18] H. Terazawa, M. Yasuè, K. Akama and M. Hayashi, Phys. Lett. B112, 387 (1982).

[19] For recent experimental searches and theoretical analyses, see for example K. Akama and H. Terazawa, Phys. Lett. B321, 145 (1994); Mod. Phys. Lett. A37, 3423 (1994), and many references therein.

[20] H. Terazawa, Mod. Phys. Lett. A5, 1031 (1990).

[21] H. Terazawa, Mod. Phys. Lett. A6, 1825 (1991).

[22] H. Terazawa, Prog. Theor. Phys. 64, 1763 (1980); W. Buchmüller, R.D. Peccei and T. Yanagida, Phys. Lett. B124, 67 (1983); R. Barbieri, A. Masierro and G. Beneziano, Phys. Lett. B124, 179 (1983); O. Greenberg, R.N. Mohapatra and M. Yasuè, Phys. Lett. B128, 65 (1983); H. Terazawa and M. Yasuè, Phys. Lett. B197, 161 (1987); B206, 669 (1988); H. Terazawa, in Perspectives on Particle Physics, edited by S. Matsuda et al. (World Scientific, Singapore, 1988), p. 4149

[23] H. Terazawa, J. Phys. Soc. Jpn. 55, 4249 (1986).

[24] H. Terazawa and M. Yasuè, Phys. Lett. B206, 669 (1983).

[25] H. Terazawa and M. Yasuè, Phys. Lett. B307, 383 (1993).

[26] H. Terazawa, Mod. Phys. Lett. A10, 199 (1995).

[27] F. Abe et al. (CDF Collaboration), Phys. Rev. Lett. 73, 225 (1994); Phys. Rev. D50, 2966 (1994); Phys. Rev. Lett. 74, 2626 (1995); S. Abachi et al. (DO Collaboration), Phys. Rev. Lett. 72, 2138 (1994), 74, 2422 (1995), 74, 2632 (1995).

[28] H. Terazawa, Mod. Phys. Lett. A7, 1879 (1992); in Proceedings of the 1992 INS Mini-Workshop on Quark and Lepton Mass Matricies, INS, Univ. of Tokyo, 1992, edited by Y. Koide, INS-J-176 (INS, Univ. of Tokyo, 1993), p. 83.

[29] H. Terazawa. Prog. Theor. Phys. 58, 1276 (1977).

[30] H. Terazawa and K. Akama, Phys. Lett. 101B, 190 (1981).

[31] H. Terazawa, Mod. Phys. Lett. A7, 3373 (1992).

[32] A.D. Sakharov, Dokl. Akad. Nauk SSSR 177, 70 (1967) [Sov. Phys. JETP 12, 1040 (1968).] For a recent review, H. Terazawa, in Proceedings of the First International A.D. Sakharov Conference on Physics, Moscow, 1991, edited by L.V. Keldysh and I. Ya. Fainberg (Nova Science, New York, 1992), p. 1013.

[33] K. Akama, Y. Chikashige, T. Matsuki and H. Terazawa, Prog. Theor. Phys. 60, 868 (1977); K. Akama, ibid., 1900 (1978); S.L. Adler, Phys. Rev. Lett. 44, 1567 (1980); A. Zee, Phys. Rev. D23, 858 (1981); D. Amati and G. Veneziano, Phys. Lett. 105 B, 358 (1981).

[34] K. Akama and H. Terazaewa, Gen. Rel. Grav. 15, 20 (1983).

[35] H. Terazawa, in Quantum Field Theory and Quantum Statistics, edited by I.A. Batalin and G. A. Vilkovisky (Adam Hilger, London, 1987), Vol. I, p. 637; in Particles and Nuclei, edited by H. Terazawa (World Scientific, Singapore, 1986), p. 304; in Proceedings of the 5th Seminar on Quantum Gravity, Moscow, 1990, edited by M.A. Markov et al. (World Scientific, Singapore, 1991), p. 643; INS-Report-932 (INS, Univ. of Tokyo, 1992).

[36] J. Godfrey, preprint, "The Cosmological Constant in Weyl's Theory" (Univ. of Notre Dame, 1989); I.V. Volovich, Phys. Lett. B219, 66 (1989); M. Gasperini, Phys. Lett. B224, 49 (1989); D. Hochberg and J. T. Wheeler, preprint, "Spacetime Dimension from a Variational Principle", BA-89-33 (Bartol Research Inst., 1989); M. Gasperini and G. Ummarino, Phys. Lett. B266, 275 (1991).

[37] H. Terazawa, INS-Report-1068 (INS, Univ. of Tokyo, 1994); an invited talk to be presented at The Third Alexander Friedmann International Seminar on Gravitation and Cosmology, St. Petersburg, Russia, July 4-12, 1995, to be published in the Proceedings.

[38] P.A.M. Dirac, Nature 139, 323 (1937); Proc. Roy. Soc. A165, 199 (1938).

[39] A.S. Eddington, in Mathematical Theory of Relativity (Cambridge Univ. Press, New York, 1924).

[40] H. Terazawa, Phys. Lett. 101B, 43 (1981).

[41] For reviews, see for example J. H. Schwarz, Phys. Rev. 89, 223 (1982); M.B. Green, J.H. Schwarz and E. Witten, in Superstring Theory (Cambridge Univ. Press, Cambridge, 1987), p. 1.

[42] D. Amati, M. Ciafaloni and G. Veneziano, Phys. Lett. B216, 41 (1989). For a review see for example G. Veneziano, in Proceedings of the 5th Seminar on Quantum Gravity, Moscow, 1990, edited by M.A. Markov et al. (World Scientific, Singapore, 1991), p. 235.

[43] H. Terazawa, Y. Chikashige, K. Akama and T. Matsuki, Phys. Rev. D15, 1181 (1977); H. Terazawa, ibid, D16 2373 (1977); D22, 1037 (1980); Phys. Lett. 133B, 57 (1983). For recent reviews, see for example, H. Terazawa, in Proceedings of the 19th International Conference on High Energy Physics, Tokyo, 1978, edited by S. Homma et al. (Phys. Soc. Jpn., Tokyo, 1979), p. 617; in Proceedings of the Second Marcel Grossmann Meeting on the Recent

Developments of General Relativity, Miramare-Trieste, 1979, edited by R. Ruffini (North-Holland, Amsterdam, New York, 1982), p. 519; in Proceedings of the Second Seminar "Quantum Gravity", Moscow, 1981, edited by M.A. Markov and P.C. West (Plenum, New York, 1984), p. 47; in Proceedings of the Third Marcel Grossman Meeting on the Recent Developments of General Relativity, Shanghai, 1982, edited by Hu Ning (Science Press and North-Holland, Beijing, 1983), p. 239; in Proceedings of the Third Seminar on Quantum Gravity, Moscow,1984, edited by M.A. Markov et al. (World Scientific, Singapore,1985), p. 236.

[44] For reviews, see O.W. Greenberg and R.N. Mohapatra, Phys. Rev. D39, 2032 (1989) and L.B. Okun, Commun. Nucl. Part. Phys. 19, 99 (1989).

[45] K. Akama, H. Terazawa and M. Yasuè, Phys. Rev. Lett. 68, 1826 (1992).

[46] K. Nishijima, Phys. Rev. 111, 995 (1958); R. Haag, Phys. Rev. 111, 669 (1958); W. Zimmermann, Nuovo Cimento 10, 597 (1958).

[47] H. Ejiri et al., Nucl. Phys. A552, 3050 (1991); in Proceedings of the International Symposium on Nuclear Physics in 1990's in Honor of A. Arima, Santa Fe, 1990 [J. Phys. G (to be published)]; in Proceedings of the Conference on Rare Nuclear Decays and Fundamental Processes, Fourteenth Europhysics Conference on Nuclear Physics, Bratislava, 1990 [Osaka University Report No. OULNS 90-21 (to be published)].

[48] See, for the latest result, OPAL Collaboration, Phys. Lett. B257, 532 (1991).

[49] M.J.W. Hall, Phys. Rev. Lett. 74, 3307 (1995).

[50] For a latest review, see for example, A.I. Solomon and R.J. Mc Dermott, in this Proceedings.

[51] H. Terazawa, Phys. Rev. D22, 184 (1980); in Wandering in the Fields, edited by K. Kawarabayashi and A. Ukawa (World Scientific, Singapore, 1987), p. 388; K. Akama and H. Terazawa, Prog. Theor. Phys. 79, 740 (1988); H. Terazawa, ibid. 86, 337 (1991).

[52] H. Terazawa, Prog. Theor. Phys. 79, 731 (1988).

[53] H. Terazawa, INS-Report-896 (INS, Univ. of Tokyo, 1991).

[54] C.W. Misner, K.S. Thorne and J.A. Wheeler, in Gravitation (W.H. Freeman and Co., San Francisco, 1979).

NEXT
DOCUMENT

DISCRETE PHOTODETECTION AND SUSSKIND-GLOGOWER PHASE OPERATORS

Y. Ben-Aryeh
Department of Physics, Technion-Israel Institute of Technology
Haifa 32000, Israel

Abstract

State reduction processes in different types of photodetection experiments are described by using different kinds of ladder operators. A special model of discrete photodetection is developed by the use of superoperators which are based on the Susskind-Glogower raising and lower operators. The possibility to realize experimentally the discrete photodetection scheme in a micromaser is discussed.

1 Continuous and Discrete Photodetections

Usually, photodetection of the single-mode radiation field is described by the use of the mode annihilation and creations operators $\hat{a}$ and $\hat{a}^\dagger$, which can be written in terms of the Susskind and Glogower (SG) [1,2] operators and the number operator $\hat{n}$

$$\hat{a} = \sqrt{\hat{n}+1}\hat{E}_-, \quad \hat{a}^\dagger = \hat{E}_+\sqrt{\hat{n}+1} \tag{1}$$

where

$$\hat{E}_+ = \sum_{n=0}^{\infty} |n+1><n|, \quad \hat{E}_- = \sum_{n=0}^{\infty} |n><n+1|, \quad \hat{E}_-|0>=0 \tag{2}$$

Here $|n>$ are the number states.

When $\hat{a}$ and $\hat{a}^\dagger$ lower or raise a number state $|n>$, they also generate the weight factor $\sqrt{n}$ or $\sqrt{n+1}$, respectively. The SG operators $\hat{E}_+$ and $\hat{E}_-$ only raise or lower the number states without generating any weight factor. The essential difference between the two types of ladder operators implies differences between two photodetection schemes.

In the model of continuous photodetection [3-6] the density matrix of the field is continuously reduced by the information provided by the photodetector. The instantaneous process of one-photon counting is described by the superoperator J:

$$\hat{\rho}(t^+) = J\hat{\rho}(t) \equiv \frac{\hat{a}\hat{\rho}(t)\hat{a}^\dagger}{Tr[\hat{\rho}(t)\hat{a}^\dagger\hat{a}]} . \tag{3}$$

Here $\hat{\rho}(t)$ and $\hat{\rho}(t^+)$ are the density operators for the radiation field immediately before and after the detection. The superoperator J consists of nonunitary transformation (describing state reduction) and the normalization. The no-count process which occurs for a duration time τ is described by the superoperator S_τ:

$$\hat{\rho}(t+\tau) = S_\tau \hat{\rho}(t) \equiv \frac{\exp(-\frac{1}{2}\lambda \hat{a}^\dagger \hat{a}\tau)\hat{\rho}(t)\exp(-\frac{1}{2}\lambda \hat{a}^\dagger \hat{a}\tau)}{\mathrm{Tr}[\hat{\rho}(t)\exp(-\frac{1}{2}\lambda \hat{a}^\dagger \hat{a}\tau)]} \tag{4}$$

Here λ is a parameter characteristic of the coupling between the detector and the field. In continuous photodetection the strength of the interaction depends on the number of photons.

In the present work another photodetection scheme is described in which two-level Rydberg atoms in the lower state are sent through a cavity and their states are measured at the exit. The experimental scheme is similar to that of a micromaser [7]. According to the theories of the micromaser if one starts with a density operator which is diagonal in the number state representation

$$\hat{\rho} = \sum_{n=0}^{\infty} p(n)|n><n| \tag{5}$$

it remains diagonal after the interaction between the radiation and the two-level atoms [8]. We would like to use the information obtained from the measurement of the atoms outside the cavity in order to describe the time development of the field inside the cavity, for a diagonal density matrix. The idea is that in this photodetection scheme the field reduction is described by the superoprator B_- which includes the SG operators

$$\hat{\rho}_{-1} = B_- \hat{\rho} \equiv \frac{\hat{E}_- \hat{\rho} \hat{E}_+}{1 - <0|\hat{\rho}|0>} \tag{6}$$

where $\hat{\rho}$ and $\hat{\rho}_{-1}$ are the density operators for the radiation field before and after the substraction of a photon. The normalization factor is $Tr(\hat{\rho}\hat{E}_+\hat{E}_-) = 1 - <0|\hat{\rho}|0>$. In order to understand why Eq. (6) is valid, we show in the following discussion the differences between the present model of discrete photodetection and the model of continuous photodetection.

In continuous photodetection the measurement occurs continuously at any time whenever the photodetector is active. In discrete photodetection the measurement occurs only when an atom leaves the cavity, so that the number of measurements is equal to the number of atoms transmitted through the cavity. The only referred measurement is that in which an excited atom is detected. Therefore in this model there is no analog to the no-count process of continuous photodetection. In the present model we are not interested in the properties of the interactions inside the cavity and in the associated probabilities. By getting only the information that one atom is excited we reduce an n-photon state of the radiation into an n-1 photon state. The use of Eq. (6) for the density operator of Eq. (5) has only a statistical meaning, where $p(n)$ is the statistical probability that the state is $|n>$ while in fact only one of the states $|n>$ exists in the cavity. For states with different number of photons it will take different times to excite one atom, but by repeating many times the experiments in which one atom is excited and using only the information that one atom is excited the density operator of Eq. (5) is reduced according to Eq. (6). One should take

into account that the continuous photodetection theory has also only a statistical meaning. The statistics obtained by that model is exploited by averaging the time development of the system over many quantum trajectories [3]. By getting a different information according to our model we obtain a different photodetection theory which we call discrete photodetection.

As the result of state reduction (6), the changes in the photon number distribution of the radiation field can be expressed in the present model in the following form

$$p_{-1}(n) = < n|\hat{\rho}_{-1}|n > = \frac{< n|\hat{E}_-\hat{\rho}\hat{E}_+|n >}{1 - < 0|\hat{\rho}|0 >} = \frac{p(n+1)}{1-p(0)} . \tag{7}$$

For comparison, the continuous photodetection model gives for the one count process

$$p(n,t^+) = < n|\hat{\rho}(t^+)|n > = \frac{< n|\hat{a}\hat{\rho}(t)\hat{a}^\dagger|n >}{< \hat{n} >_t} = \frac{n+1}{< \hat{n} >_t} p(n+1,t) . \tag{8}$$

The mean photon number immediately after the measurement of an excited atom is given according to Eq. (6) by:

$$< \hat{n} >_{-1} = \frac{< \hat{n} >}{1-p(0)} - 1 , \tag{9}$$

while in the continuous photodetection theory the mean photon number immediately after the one count process [6]:

$$< \hat{n} >_{t^+} = < n >_t - 1 + \frac{(\Delta n)_t^2}{< \hat{n}_t >} \tag{10}$$

The difference between the continuous photodetection theory and the model of discrete photodetection can be explained also as the difference between a statistical model of matter-radiation interaction by a detector and a statistical model of nondemolition [9] experiments, respectively. The measurements of atoms excitations outside the cavity in the discrete photodetection model gives information only on the change in the number of photons inside the cavity but does not give information on phase changes of the field. This quantum feature follows from the fundamental principle that it is not possible to produce cloning of all the quantum information. Therefore in the present experimental scheme of the micromaser one can get enough information only for diagonal density matrix in which the information on phases has been eliminated [8].

2 Experimental Realization of Discrete Photodetection

We can generalize our model by sending atoms in the lower state through the cavity till the measurement shows a desired number N of excited atoms. Then the field state is reduced according to

$$\hat{\rho}_{-N} = B_-^N \hat{\rho} \equiv \frac{\hat{E}_-^N \hat{\rho} \hat{E}_+^N}{\mathrm{Tr}(\hat{\rho}\hat{E}_+^N\hat{E}_-^N)} . \tag{11}$$

Our experimental scheme also enables us to add photons to the cavity where in this case we send atoms in the upper state through the cavity and measure their states in the exit till the measurement shows a desired number N of de-excited atoms. Then the field state is reduced according to

$$\hat{\rho}_{+N} = B_+^N \hat{\rho} \equiv \hat{E}_+^N \hat{\rho} \hat{E}_-^N \ . \tag{12}$$

In any real experiment we cannot ignore losses, and the detector of the atoms is not perfect. For imperfect detection we can generalize our model by assuming that the measurement reduces the density operator in the form

$$\hat{\rho}_{\pm N} = \sum_N \alpha_N B_\pm^N \hat{\rho} \ . \tag{13}$$

The detector efficiency distribution α_N must be sufficiently narrow around the true number $\bar{N}$ of excited (or de-excited) atoms in order to realise our mode. The validity of the present model of discrete photodetection theory can be checked by doing the experiments with the micromaser in a very special way. Two-level Rydberg atoms which are in the lower state are transmitted through a cavity which is initially in the vacuum state. In many experiments atoms excitations are measured outside the cavity where each experiment is divided into two stages. In the first stage we wait a time t_1 till a fixed number n of atoms is excited. This time is variable from one experiment to another according to quantum mechanical statistical features [8]. However, in each experiment we rescale the time t_1 to a zero initial time and measure in the second stage the number of atoms excitations during an additional time t which is fixed to be the same, for all the experiments in the second stage. Now, we check the prediction of the usual quantum mechanical statistical theory of the micromaser [8] for a time of interaction t, assuming an initial number state $|n>$. The interesting point here is that we can verify by examining the results of the measurements in the second stage that our initial state obtained from the first stage was the number state $|n>$. Such experiments can be done only if the losses are quite small which means that the criterion of a narrow parameter α_N in Eq. (1) is valid.

REFERENCES

1. L. Susskind and J. Glogower, Physics **1**, 49 (1964).
2. P. Carruthers and M.M. Nieto, Rev. Mod. Phys. **40**, 411 (1968).
3. H. Carmichael, An Open System Approach to Quantum Optics, 1991 (Berlin, Springer).
4. M.D. Srinivas and E.B. Davies, Opt. Acta **28**, 981 (1981).
5. M. Ueda, Quantum Opt. **1**, 131 (1989).
6. M. Ueda, N. Imoto and T. Ogawa, Phys. Rev. **A41**, 3891 (1990).
7. D. Meschede, H. Walther and G. Muller, Phys. Rev. Lett. **54**, 551 (1985),
   G. Rempe, H. Walther and N. Klein, Phys. Rev. Lett. **58**, 353 (1988),
   M. Brune, J.M. Raimond, P. Joy, L. Davidovich and S. Haroche, Phys. Rev. Lett. **59**, 1989 (1987).

8. P. Filipowicz, J. Javanainen and P. Meystre, Phys. Rev. A34, 3077 (1986).

9. K.S. Thorne, P. Drever and C.M. Caves, Phys. Rev. Lett. 40, 667 (1978).

NEXT
DOCUMENT

A new definition to the phase operator and its properties*

Duan Lu-ming and Guo Guang-can
Department of Physics, University of Science and
Techonology of China, Hefei, 230026, P.R.China

By introducing a series of mathematical symbols and the phase quantization condition, we give a new definition of the phase operator, which not only is made directly in infinite state spaces, but also circumvents all difficulties appearing in the traditional approach. Properties of the phase operator and its expressions in some widely-used representations are also given.

PACS: 03.65.Bz, 42.50.-p

I. Introduction

The phase operator is very important in the quantum optics and field theory. But as was clearly pointed out by Susskind and Glogower[2], there are many difficulties in the traditional definition of the phase operator[1,2]. The traditional approach required that the Hermitian number and phase operator were combined in a polar decomposition of the annihilation operator:

$$\hat{a} = \exp\left(i\hat{\theta}\right)\hat{N}^{\frac{1}{2}}, \tag{1}$$

and supposed that they satisfied the following commutator

$$\left[\hat{\theta},\hat{N}\right] = -i. \tag{2}$$

But the commutator(2) gives rise to inconsistency when its matrix elements are calculated in a number-state basis and the uncertainty relation $\Delta N\Delta\theta \geq \frac{1}{2}$ derived from Eq.(2) implies that a number state has infinite phase uncertainty which contradicts to the periodic nature of the phase. Furthermore, the exponential operator $\exp\left(i\hat{\theta}\right)$ in this approach is not unitary so it does not define a Hermitian $\hat{\theta}$. Recently, there appeared many developments on this problem[3-8]. Especially Pegg and Barnett defined a phase operator in a finite-dimensional state space[3,4] and the definition has been widely used. This definition circumvents the difficulties in the traditional approach at the price that it is limited to a finite state space, the dimension of which is allowed to tend to infinity only after physically measurable results, such as expectation values, are calculated. It is now often accepted that a well-behaved Hermitian phase operator does not exist in infinite state spaces[2-4]. In this paper we give a new approach to the definition of the phase operator. We have defined a Hermitian phase operator directly in infinite state spaces. By introducing a series of mathematical symbols and the phase quantization condition, we have overcome the above-mentioned difficulties in the traditional approach. As a result of being defined directly in infinite state spaces, the phase operator here has very succinct expressions in some widely-used representations which make it very convenient for use.

II. Definition of the phase operator

We consider the quantized single-mode boson field. In this system, the dimension of the state space determined by the Hamiltonian $\hat{H}$ is countable-infinite and all the eigenstates of the number operator $\hat{N}$ make a complete basis. So an operator is well defined if its action on an arbitrary eigenstate of the number operator is given. We define the phase operator as the infinitesimal displacement operator of the number basis. So to determine the phase operator, we first give the following definition of an unitary displacement operator $\hat{D}$ of the number basis:

$$\hat{D}|n\rangle = |n-1\rangle \qquad (n \neq 0), \tag{3}$$

$$\hat{D}|0\rangle = |P_\infty - 1\rangle, \tag{4}$$

where $P_\infty = \lim_{n\to\infty} n!$. Some explanation need be added to the definition equation(4). Firstly, one may just suppose $\hat{D}|0\rangle = 0$ But this idea leads to contradiction. It makes $\hat{D}$ not unitary. By intuition, the displacement operator $\hat{D}$ should transform $|0\rangle$ to another eigenstate of $\hat{N}$ Secondly one may let $\hat{D}|0\rangle = |\infty\rangle$. But the state $|\infty\rangle$ is not well defined because ∞ is not a simple number Though $P_\infty - 1$ is also infinity, the states $|P_\infty - 1\rangle$ and $|\infty\rangle$ still have discriminations. The state $|\infty\rangle$ just indicates that the eigenvalue of $\hat{N}$ tends to infinity It does not show the mode of tendency. For example, when $n \to \infty$, the states $|2n\rangle$ and $|2n-1\rangle$ can all be written as $|\infty\rangle$,but these two states are not same because they are orthogonal. Though the discrimination between the states $|P_\infty - 1\rangle$ and $|\infty\rangle$ is not important to the final physical results because the states $|n\rangle$ when $n \to \infty$ have no contribution to actual physical states, it plays a important role in defining a self-consistence Hermitian phase operator because our definition is made directly in infinite state spaces and is not in view of concrete physical states. The mode of tendency to infinity must be determined in this situation. Equation(4) indicates that $\hat{D}$ transforms $|0\rangle$ to an eigenstate of $\hat{N}$ with an eigenvalue tending to infinity and the mode of tendency is given by the sequence $\{n!-1,(n+1)!-1,(n+2)!-1,\cdots\}$. So $\hat{D}$ is completely defined and we will see this definition of $\hat{D}$ makes a good foundation for the definition of a Hermitian phase operator in infinite state spaces.

In the number representation $\hat{D}$ defined by Eqs.(3)(4) has the matrix form

$$\hat{D} = \lim_{n\to\infty} \underbrace{\begin{pmatrix} 0 & 1 & 0 & \cdots & 0 & 0 \\ 0 & 0 & 1 & \cdots & 0 & 0 \\ 0 & 0 & 0 & \cdots & 0 & 0 \\ \cdots & \cdots & \cdots & \cdots & \cdots & \cdots \\ 0 & 0 & 0 & \cdots & 0 & 1 \\ 1 & 0 & 0 & \cdots & 0 & \end{pmatrix}}_{n!} \tag{5}$$

Its eigenvalues have the expression

$$a = e^{i\theta} = e^{i2\pi} \tag{6}$$

When $n \to \infty$, the value of θ is limited to rational numbers and also $e^{i2\pi}$ with any

rational r is the eigenvalue of $\hat{D}$. Writing the eigenstate of $\hat{D}$ with the eigenvalue $e^{i\theta}$ as $|\theta\rangle$, we have

$$\hat{D}|\theta\rangle = e^{i\theta}|\theta\rangle, \tag{7}$$

where θ satisfies the discrete condition

$$\theta = 2\pi r \quad (r \in R), \tag{8}$$

and R is the rational number set. Combining Eq.(7)(8) with Eqs.(3)(4), we get the transition function between the number and the phase representation

$$\langle\theta|n\rangle = Ae^{-in\theta}, \tag{9}$$

where A is a normalization constant.

Before giving the correct normalization of the states $|\theta\rangle$, we make two preparations. Firstly, from the countability of the rational number set, all θ between θ_a and θ_b satisfying the discrete condition (8) can be numbered as $\theta_1, \theta_2, \cdots, \theta_i, \cdots$. We introduce a symbol called discrete integration indicated by $\int d_r\theta$ to represent the mean value of the function $f(\theta)$ over all θ between θ_a and θ_b satisfying the discrete condition, et.al.,

$$\frac{1}{\theta_b - \theta_a}\int_{\theta_a}^{\theta_b} f(\theta)d_r\theta \xlongequal{\text{definition}} \lim_{n\to\infty}\frac{1}{n}\sum_{i=1}^{n} f(\theta_i) = \overline{f(\theta)}. \tag{10}$$

The definition domain of the function $f(\theta)$ can be extended analytically to the real number set (the function after analytical extension is unique and will be still indicated by $f(\theta)$). Because the rational number set is dense in the real number set, it is evident that

$$\frac{1}{\theta_b - \theta_a}\int_{\theta_a}^{\theta_b} f(\theta)d_r\theta = \overline{f(\theta)} = \frac{1}{\theta_b - \theta_a}\int_{\theta_a}^{\theta_b} f(\theta)d\theta \tag{11}$$

So the discrete integration can be expressed by the real integration. Secondly, we introduce a periodic δ – function (indicated by δ_T). The definition of δ_T is

$$\delta_T(\theta) = \delta_T(\theta + 2\pi), \tag{12}$$

$$\delta_T(\theta) = 0 \quad (\theta \neq 2k\pi, k \in Z), \tag{13}$$

$$\int_{-\pi}^{\pi}\delta_T(\theta)d\theta = 1 \tag{14}$$

The symbol Z in Eq.(13) represents the integer set. If the definition domain of the function $\delta_T(\theta)$ is limited to all θ satisfying the discrete condition, it becomes the periodic discrete δ – function and the integration in Eq.(14) should be replaced by the discrete integration.

Having these preparations, we can prove that the states $|\theta\rangle$ satisfy the normalization

$$\langle\theta_1|\theta_2\rangle = \delta_T(\theta_1 - \theta_2) \tag{15}$$

and the complete equation

$$\int_{\theta_0}^{\theta_0 + 2\pi} |\theta\rangle\langle\theta| d_r\theta = \hat{I} \tag{16}$$

when we make the normalization constant

$$A = \frac{1}{\sqrt{2\pi}}. \tag{17}$$

Equation (15) and (16) suggest that the states $|\theta\rangle$ in an arbitrary 2π interval $[\theta_0, \theta_0 + 2\pi]$ satisfying the discrete condition make an orthogonal and normalized complete basis.

With above preparations, the phase operator now can be easily given. $\hat{\theta}$ corresponds to the infinitesimal displacement operator of the number basis and it has the following relation with the displacement operator $\hat{D}$

$$\hat{\theta} = \frac{1}{i} \ln \hat{D}. \tag{18}$$

So from Eq.(7) in the phase representation $\hat{\theta}$ can be expressed as

$$\hat{\theta} = \int_{\theta_0}^{\theta_0 + 2\pi} \theta |\theta\rangle\langle\theta| d_r \theta, \tag{19}$$

where θ_0 is arbitrary. The arbitrary θ_0 is merely the reflection of the periodic nature of the phase

From the definition , we know the eigenvalues of $\hat{\theta}$ cannot be any real number, it must be 2π times a rational number. This confiction can be called phase quantization condition and its explicit form is given here for the first time. This condition suggests that the eigenvalues of $\hat{\theta}$ cannot change continuely though their change can be infinitesimal. This picture is different from that given by the classical phase, but it is natural and necessary. Here the phase operator is defined in a countable-infinite state space, in which the number of independent vectors cannot be beyond countable-infinite, but the eigenvectors of $\hat{\theta}$ with different eigenvalues are orthogonal and independent, so the eigenvalues of $\hat{\theta}$ cannot be continue and at most be countable-infinite. This leads to the phase quantization condition. The condition is very important for a self-consistence definition of the phase operator in infinite state spaces

III. Phase-number commutator and expressions of the phase operator in some widely-used representations

Starting from the phase operator defined in the above section, we can give the expression of the number operator in the phase representation and the phase-number commutator. Firstly we introduce a symbol called discrete differentiation

$$\frac{\partial}{\partial \theta_r} f(\theta_r) \overset{\text{define}}{=\!=} \frac{\partial}{\partial x} f(x)\Big|_{x=\theta_r}, \tag{20}$$

where $f(x)$ is the analytical extension of $f(\theta_r)$ to the real number set . Then the number operator in the phase representation has a succinct form:

$$\hat{N} = \int_{\theta_0}^{\theta_0 + 2\pi} |\theta\rangle i \frac{\partial}{\partial \theta} \langle\theta| d_r \theta. \tag{21}$$

From Eq.(21) , we get the phase-number commutator

$$\left[\hat{N}, \hat{\theta}\right] = i\left[\hat{I} - 2\pi\delta_T\left(\hat{\theta} - \theta_0\right)\right]. \tag{22}$$

If we limit the phase value to $[\theta_0, \theta_0 + 2\pi]$ in the classical case , the commutator given by Eq.(22) just equals $i\hbar$ times the classical Possionian bracket[4]. This fact

shows that the definition here is reasonable. The mean value of Eq.(22) over a physical state $|p\rangle$ gives the result obtained in Ref.[4]

$$\langle p|\left[\hat{N},\hat{\theta}\right]|p\rangle = i\left[1-2\pi P(\theta_0)\right], \tag{23}$$

where $P(\theta_0)=|\langle\theta_0|p\rangle|^2$ is the probability that the phase of the state is θ_0. The phase-number uncertainty relation is

$$\left\langle\left(\Delta\hat{N}\right)^2\right\rangle\left\langle\left(\Delta\hat{\theta}\right)^2\right\rangle \geq \frac{1}{4}\left[1-2\pi P(\theta_0)\right]^2. \tag{24}$$

Further we give direct expressions of the phase operator in the number and coherent representations. They have succinct and useful expressions which benefit from the fact that we have defined the phase operator directly in infinite state spaces.

In the number representation the phase operator have the following expression

$$\hat{\theta}=\sum_n |n\rangle\frac{1}{i}\frac{\partial}{\partial n}\langle n|, \tag{25}$$

where the symbol $\frac{\partial}{\partial n}$ represents the discrete diferentiation defined by Eq.(20). Noticing that $f(n)$ is equivalent to $f(n)e^{i2k\pi n}$ $(k\in Z)$ and $\frac{1}{i}\frac{\partial}{\partial n}f(n)$ is different from $\frac{1}{i}\frac{\partial}{\partial n}\left[f(n)e^{i2k\pi n}\right]$ with a difference $2k\pi$, we know that after $\frac{1}{i}\frac{\partial}{\partial n}$ acts on a function $f(n)$ there may appears a difference $2k\pi$. This fact also results from the periodic nature of the phase and we avoid the arbitary $2k\pi$ by limiting the mean value of $\hat{\theta}$ in Eq.(25) to $[\theta_0,\theta_0+2\pi]$.

Equation(25) is very convenient for use because usual physical states are easy expanded by Fock states and then using Eq.(25) we can analyse phase properties of the states by simple differentiation.

Now we give an approximate form of the phase operator expressed by the annihilation and cretion operators $\hat{a},\hat{a}^+$ when the mean photon number $\langle\hat{N}\rangle>>1$. The result is

$$\hat{\theta}\approx\frac{1}{i}:\ln\hat{a}-\ln\left(\hat{a}^+\hat{a}+1\right):, \tag{26}$$

where the symbol : : represents normal product. Using Eq.(26) we get the approximate expression of the phase operator in the coherent representation when the mean photon number is large.

$$\hat{\theta}=\frac{1}{\pi}\int|\alpha\rangle\frac{1}{i}\left[\ln\alpha-\ln\left(|\alpha|^2+1\right)\right]\langle\alpha|d^2\alpha. \tag{27}$$

* This project is supported by the National Natural Foundation of China

References

[1] P.A.M.Dirac, Proc.R.Soc.London, Sev.A 114,243(1927)
[2] L.Susskind and J.Glogower, Physics 1,49(1964)
[3] S.M.Barnett and D.T.Pegg, J.Mod.Opt.36,7(1989)
[4] D.T.Pegg and S.M.Barnett, Phys.Rev.A 39,1665(1989)
[5] J.H.Shapiro and S.R.Sheparol, Phys.Rev.A 43,3795(1991)
[6] M.Ban, Phys.Lett.A 176,47(1993)
[7] J.W.Noh,A.Fougeres and L.Mandel, Phys.Rev.Lett .71,2579(1993)
[8] A.Luks and V.Perinova Quantum Opt.6,125(1994)

NEXT
DOCUMENT

There aren't Non-standard Solutions for the Braid Group Representations of the QYBE Associated with 10-D Representations of SU(4).

Huang Yijun, Yu Guochen and Sun Hong*
Department of Foundation the First Aeronautical College of Air Force
Xinyang Hennan 464000 P. R. China.

Abstract

In this paper by employing the weight conservation and the diagrammatic techniques we show that the solutions associated with the 10-D representations of SU (4) are standard alone.

1 Introduction

It is well known that the quantum Yang-Baxter equations (QYBE) play an important role in various theoretical and mathematical physics, such as completely integrable system in (1+1)-dimensions, exactly solvable models in statistical mechanics, the quantum inverse scattering method and the conformal field theories in 2-dimensions. Recently, much remarkable progress has been made in constructing the solutions of the QYBE associated with the representations of lie algrebras. It is shown that for some cases except the standard solutions, there also exist new solutions, but the others have not non-standard solutions. In reference 11, we derived the braid group representations associated with the 10-dimensional representation of SU (4) and corresponding trigonometric and rational solutions. In this paper, the classical limit of the braid group representations is checked. Then it is shown that the solutions associated with the 10-dimentional representations are standard alone.

2 Classical Limit

It is well known that in the classical limits as $q \to 1$ the standard solution of QYBE require that[16]

$$S\Big|_{q \to 1} = P\,[\,1 + (q-1)\,r\,] + o[\,(q-1)^2\,] \qquad (2.1)$$

and

$$\Phi_\nu^T r \Phi_\nu = C_V = 2C_R - C_{c_\nu} \qquad (2.2)$$

where P is the permutation operator and Φ_ν stands for the normalized classical eigenvectors, r is the classical r-matrix, C_R and C_{c_ν} are the Casimirs. The eigenvalues are given by

$$\lambda_\nu = (\pm)\, q^{C_\nu} \qquad (2.3)$$

In Ref. (11), We have derived the braid group representations associated with the 10-D

---

* Address: Jinan 250023

representations of SU (4) . The Casimir eigenvalues of S－matrix were given by

$$\lambda_1 = q^3 , \quad \lambda_2 = -q , \quad \lambda_3 = q^3 \qquad (2.4)$$

From the result of Ref . (11) we know that there are some fundamental submatrices , A_1, $A_2^{(1)}$ $A_3^{(1)}$, $A_4^{(2)}$, $A_5^{(3)}$ and $A_6^{(2)}$, and others can be expressed by direct sum of the fumdamental su－bmatrices . So we discuss only the classical limits of this submatrices .

For example, we discuss only $A_3^{(1)}$:

$$A_3^{(1)} = \begin{bmatrix} 0 & 0 & q \\ 0 & q^{-1} & qw \\ q & qw & (1-q^2)\ w \end{bmatrix} \qquad (2.5)$$

$$A_3^{(1)}\Big|_{q \to 1} = \begin{bmatrix} 0 & 0 & q \\ 0 & 2-q & 4\ (1-q) \\ q & 4\ (1-q) & 0 \end{bmatrix} \qquad (2.6)$$

$$r_3^{(1)} = \begin{bmatrix} 1 & -4 & 0 \\ 0 & -1 & 4 \\ 0 & 0 & 1 \end{bmatrix} \qquad (2.7)$$

$$\Phi_1^T = \frac{1}{\sqrt{6}}(1\ \ 2\ \ 1), \quad \Phi_2^T = \frac{1}{\sqrt{2}}(1\ \ 0\ \ -1), \quad \Phi_3^T = \frac{1}{\sqrt{3}}(1\ \ -1\ \ 1) \qquad (2.8)$$

and

$$\Phi_v^T r_3^{(1)} \Phi_v = C_v = \begin{cases} 3 & v=1 \\ 1 & v=2 \\ 3 & v=3 \end{cases} \qquad (2.9)$$

Therefore the solutions of QYBE are standard .

3 About absence of the nonstandard solution

From Ref . (11) we have known that so long as $u_6 = u_2 = u_{-4} = u_{-6}$, there exists the alone solution . In Ref . (11), we have

$$\begin{cases} u_4 q_8^{2(2,4)} + w_{10}^{(4,6)} p_8^{2(2,4)} = w_{10}^{(4,6)} p_6^{2(2,4)} \\ u_6 q_8^{2(2,4)} + w_{10}^{(4,6)} u_4^2 = u_4 w_{10}^{2(2,6)} + w_{10}^{(4,6)} p_{10}^{2(4,6)} \\ u_4^2 = P_{10}^{(4,6)} p_6^{2(4,6)} \end{cases} \qquad (3.1)$$

$$\begin{cases} u_6 p_8^{(2.6)} = p_{10}^{2(\cdot\cdot)} \\ u_2 p_8^{(2.6)} = p_6^{2(\cdot\cdot)} \end{cases} \qquad (3.2)$$

$$\begin{cases} u_{-5}\, q_{-10}^{2(\cdot\cdot)} + w_{-9}^{(-5.-4)} \quad p_{-10}^{2(\cdot\cdot)} = w_{-9}^{(-5.-4)} \quad p_{-11}^{2(\cdot\cdot)} \\ u_{-4} q_{-10}^{2(\cdot\cdot)} + w_{-9}^{(-5.-4)} \quad u_{-5}^{2} = w_{-9}^{2(\cdot\cdot)} \quad u_{-5} + w_{-9}^{(-5.-4)} \cdot p_{-9}^{2(\cdot\cdot)} \\ u_{-5}^{2} = p_{-11}^{(-6.-5)} \quad p_{-9}^{(-5.-4)} \end{cases} \qquad (3.3)$$

$$\begin{cases} u_{-6}\, p_{-10}^{(-6.-4)} = p^{2(-6.-5)}_{-11} \\ u_{-4} p_{-10}^{(-6.-4)} = p_{-9}^{2(\cdot\cdot)} \end{cases} \qquad (3.4)$$

$$\begin{cases} u_0 q_0^{2(\cdot\cdot)} + w_{-6}^{(-6.0)} \quad p_0^{2(\cdot\cdot)} = w_{-6}^{(-6.0)} \quad p_6^{2(\cdot\cdot)} \\ u_5 q_0^{2(\cdot\cdot)} + u_0^{2} w_6^{(0.6)} = u_0 w_6^{2(\cdot\cdot)} + w_6^{(0.6)} \quad p_6^{2(\cdot\cdot)} \\ u_0^{2} = p_6^{(0.6)} \quad p_{-6}^{(-6.0)} \end{cases} \qquad (3.5)$$

$$\begin{cases} u_{-6} p_0^{(-6.6)} = p_{-6}^{2(\cdot\cdot)} \\ u_6 p_0^{(-6.6)} = p_6^{2(\cdot\cdot)} \end{cases} \qquad (3.6)$$

From eq . (3 . 1,, we have

$$u_4 = p_{10}^{(4.6)} \quad ; \quad p_6^{(2.4)} = p_{10} \qquad (3.7)$$

From eq . (3 . 2) + eq . (3 . 6), we have

$$u_2 = u_6 \qquad (3.8)$$

$$u_{-5}=p_{-9}^{(-5.-4)} \quad , \quad p_{-9}^{(-5.-4)}=p_{-11}^{(-6.-5)} \qquad (3.9)$$

$$u_{-4}=u_{-6} \qquad (3.10)$$

$$u_0=p_6^{(0.6)} \quad , \quad p_6^{(0.6)}=p_{-6}^{(-6.0)} \qquad (3.11)$$

$$u_{-6}=u_6 \qquad (3.12)$$

From eq. (3.8), (3.10) and (3.12) we have

$$u_6=u_2=u_{-4}=u_{-6} \qquad (3.13)$$

Therefore the solutions of the QYBE are standard alone.

References

[1] C. N. Yang, Phys. Rev. Lett. 19 (1967) 1312.

[2] R. J. Baxter, Ann. Phys. 70 (1972) 1.

[3] A. B. Zamolodchikov and Al. B. Zamolochikov, Ann. Phys. 120 (1979) 253.

[4] L. D. Faddeev, Sov. Sci. Rev. Math. Phys. c1 (1980) 107.

[5] Molin Ge, Yongshi wu and Kang Xue, ITP-SB-90-02.

[6] Molin Ge, and Kang Xue, ITP-SB-90-20.

[7] Y. Q. Li, Weight Conservation and Braid Group Repersentations. Ph. D. thesis, Lanzhou University (1989).

[8] Molin Ge, Changpu Sun, Luyu Wang and Kang Xue, Weight conservation and Quantum Group Construction of the Braid Group Representation, J, Phys. A.

[9] Molin Ge, Y. Q. Wang and K. Xue, Int. J. Mod. Phys. (1990).

[10] N. Yu, Reshetikhin, LOMI E-4-87, E-14-87 (1988).

[11] Guochen Yu, Xifu Wang and Kang Xue, Commun. Theor. Phys. 18 (1992).

NEXT
DOCUMENT

Solutions of the Quantum Yang－Baxter Equations Assocated with $(1-3/2)^{-}D$ Representations of $SU_q(2)$

Huang Yijun, Yu Guochen and Sun Hong*
Department of Foundation, the First Aeronautical College of Air Force,
Xinyang Henan 464000 P. R. China.

Abstract

The solutions of the spectral independent QYBE associated with $(1-3/2)-D$ representations of $SU_q(2)$ are derived, based on the weight conservation and extended Kauffman diagrammatic technique. It is found that there are nonstandard solutions.

1 Introduction

It is well known that the quantum Yang－Baxter equations (QYBE) play an important role in various theoretical and mathematical physics, such as completely integrable systems in $(1+1)$ dimensions, exactly solvable models in statistical mechanics, the quamtum inverse scatteringmethod and the conformal filed theories in 2－dimensions.[1-7] Recently, much remarkable progress has been made in construction the solutions of the QYBE associated with the representations of Lie algebras.[8-9] In this paper we derive the solutions of the spectral independent QYBE associated with $(1-3/2)-D$ representations of $SU_q(2)$, based on the weight conservation and extended Kauffman diagrammatic technique. It is found that there are nonstandard solutions.

2 Braid relations of $(1-3/2)-D$ representations of $SU_q(2)$

We know that there is the relation for Universal R－matrix:

$$R_{12}^{j_1 j_2} R_{13}^{j_1 j_3} R_{23}^{j_2 j_3} = R_{23}^{j_2 j_3} R_{13}^{j_1 j_3} R_{12}^{j_1 j_2} \qquad (2.1)$$

We define the new R－matrix:

$$\bar{R}^{j_1 j_2} = PR^{j_1 j_2} \qquad (2.2)$$

Where P is the transposition $(P: V^{j_1} \otimes V^{j_2} \rightarrow V^{j_2} \otimes V^{j_1})$

Then the eq. (2－1) can be rewritten ax follows

$$\bar{R}_{12}^{j_1 j_2} \bar{R}_{23}^{j_1 j_3} \bar{R}_{12}^{j_2 j_3} = \bar{R}_{23}^{j_2 j_3} \bar{R}_{12}^{j_1 j_3} \bar{R}_{23}^{j_1 j_2} \qquad (2.3)$$

---

* Adress: Jinan 250023

For the $(1-3/2)-D$ representation of $SU_q(2)$, $(j_1, j_2, j_3) \in (1, 1, 3/2)$, then eq. (2.3) gives the following relations

$$\bar{R}^{11}_{12}\ \bar{R}^{1\,3/2}_{23}\ \bar{R}^{1\,3/2}_{12} = \bar{R}^{1\,3/2}_{23}\ \bar{R}^{1\,3/2}_{12}\ \bar{R}^{11}_{23} \qquad (2.4-1)$$

$$\bar{R}^{3/2\,1}_{12}\ \bar{R}^{11}_{23}\ \bar{R}^{11}_{12} = \bar{R}^{11}_{23}\ \bar{R}^{3/2\,1}_{12}\ \bar{R}^{3/2\,1}_{23} \qquad (2.4-2)$$

$$\bar{R}^{1\,3/2}_{12}\ \bar{R}^{11}_{23}\ \bar{R}^{3/2\,1}_{12} = \bar{R}^{3/2\,1}_{23}\ \bar{R}^{11}_{12}\ \bar{R}^{1\,3/2}_{23} \qquad (2.4-3)$$

These are the braid relations associated $(1-3/2)-D$ representations of $SU_q(2)$. We suppose that the $\bar{R}$ satisfies the $C-P$ invarance, then eq. (2.4-1) is equal to eq. (2.4-2).

3 The weight conservation and the solutions of QYBE

To determine the structure for the solutions, We consider the weight conservation

$$(\bar{R})^{ab}_{cd} = 0 \qquad \text{unless} \quad a+b=c+d \qquad (3.1)$$

where

$$\bar{R} = \bar{R}^{1\,3/2}, \ \bar{R}^{3/2\,1}, \ \bar{R}^{11}$$

$$a, b, c, d \in (\pm 3/2, \pm 1/2, \pm 1, 0)$$

It is well known that $\bar{R}^{11}$ which satisfied the conditions of $c-p$ invarance and eq. (3.1) be written as

$$\bar{R}^{11} = \sum_a u_a E_{aa} \otimes E_{aa} + \sum_{a<b} W^{(a,b)} E_{ab} \otimes E_{ab} + \sum_{a \pm b} P^{(a,b)} E_{ab} \otimes E_{ba}$$

$$+ \sum_{a \leqslant b} q^{(a,c)}_{a+b} (E_{ab} \otimes E_{cd} + E_{cd} \otimes E_{ab}) \qquad (3.2)$$

Where

$$u_0 = 1, \ u_{\pm 1} = q^2, \quad p^{(0,1)} = p^{(1,0)} = 1, \ p^{(+1,+1)} = q^{-2}$$

$$w^{(0,1)} = w = q^2 - q^{-2}, \ w^{(-1,1)} = (1-q^{-2})\, w, \ q_0^{(1,0)} = q_0^{(0,-1)} = q^{-1} w \qquad (3.3)$$

By the weight conservation $\bar{R}^{1\,3/2}$ can be constructed in the form

$$\bar{R}^{13/2} = \sum_{a,b} p^{a,b}_{a+b} \; E_{ab} \otimes E_{ba} + \sum_{\substack{a<d \\ c<d}} q^{a,c}_{a+b} \; E_{ac} \otimes E_{bd} \qquad (3.4)$$

Where

$a, b \in (\pm 1, 0)$; $b, c \in (\pm 3/2, \pm 1/2)$ $P^{(ab)}_{a+b}$ and $q^{(a,c)}_{a+b}$

are the determined parameters.

Substituting eq. (3.2), (3.4) into eq. (2.4-13), We obtain the unknown parameters by extended Karffman diagrammatic technique.

$$P^{(1,3/2)}_{5/2} = q^3 \; P^{(-1,-3/2)}_{-5/2} = P^{(1,3/2)}_{5/2} \quad Q = q^3 Q$$

$$P^{(-1,-1/2)}_{-3/2} = P^{(1,1/2)}_{3/2} \quad Q = qQ \;, \quad P^{(0,b)}_{b} = Q^{1/2} \qquad (3.5-1)$$

$$q^{(0,1/2)}_{3/2} = Q^{-1/2} q^{(-1,-3/2)}_{3/2} = (1-q^{-2})\, q^{3/2} \; ([3]!)^{1/2} \; Q^{1/4}$$

$$q^{(-1,1/2)}_{1/2} = Q^{1/2} \; q^{(0,-3/2)}_{-1/2} = (1-q^{-2})\, q^{-1/2} \; ([3]!)^{1/2} \; Q^{1/4}$$

$$q^{(0,-1/2)}_{1/2} = Q^{-1/2} \; q^{(-1,-1/2)}_{1/2} = (1-q^{-2})\, q^{1/2} \; ([2]!)^{3/2} \; Q^{-1/4}$$

$$q^{(1,-1/2)}_{1/2} = q^{(-1,-3/2)}_{-1/2} = (1-q^{-2})\, q \; ([2]![3]!)^{1/2} Q^{3/4} \qquad (3.5-2)$$

Where

$$[u] \equiv \frac{q^u - q^{-u}}{q - q^{-1}} \;, \quad [u]! \equiv [u]\,[u-1]\ldots[1] \;, \quad [0]! \equiv 1 \qquad (3.5-3)$$

Substituting eq.(3.5) into eq.(2.4), we obtain the solutions $\bar{R}^{1\,3/2}$. And we obtain the solutions $\bar{R}^{3/2\,1}$ by employing the c-p invarance.

We have derived the solutions of the spectral independent QYBE associated with $(1-3/2)$-D representations. It is easy to see that there is a new arbitary parameter, Q, then there are new solutions. In fact when $Q=1$, the solutions is Universal R-matrix of $SU_q(2)$.

$$(\bar{R}^{j_2 j_1})^{m_2 m_1}_{m_1 m_2} = \delta^{m_1'+m_2'}_{m_1+m_2} \frac{[(1-q^{-2})^{m_1'-m_1}]}{[m_1'-m_1]!} \; q^{m_1 m_2' + m_2 m_1' - 1/2\,(m_1'-m_1)(m_1'-m-1)}$$

$$\left| \frac{(j_1+m_1)!\,(j_1-m_1)!\,(j_1-m_2)!\,(j_2+m_2)!}{(j_1-m_1)!\,(j_1+m_1)!\,(j_2+m_2)!\,(j_2-m_2)!} \right|^{1/2} \qquad (3.6)$$

Standard solutions . When $Q \neq 1$, there are new solutions .

Referene

[1] C . N . Yang, phys . Rev . Lett . 19 (1967) 1312: Phys . Rev . 168 (1968) 1920.

[2] R . J . Baxter, Exactly Solved Models in Statistical Mechanics, Academic London (1982) .

[3] A . B . Zamolodchikov and Al . B . Zamolochikov, Am . of Phys . 120 (1979) 253 .

[4] L . D . Faddeev, Integrable Models in (1 + 1) -D Quantum Field Theory . Les Houches Sesio XXXIX . (1982) 536 .

[5] E . X . Skyanin, L . A . Takhtajan and L . D . Faddeev, Math . Phys . 40 (1979) 194 (in Russian)

[6] L . A . Takhtajan and L . D . Faddeev, Uspekhi Mat . Nauk . 24 (1979) 13 .

[7] G . Segal, Comformal field theory, Oxford pereprint 1987 .

[8] M . L . G . and K . Xue, phys . Lett . A146 (1990) 245 .

[9] A . N . Kirillov and N . Yu. Reshetikhin . Lomt . Preprint (1988) .

NEXT
DOCUMENT

QUANTIZATION OF ELECTROMAGNETIC FIELDS IN CAVITIES

Kiyotaka Kakazu and Kazunori Oshiro
Department of Physics, University of the Ryukyus, Okinawa 903-01, Japan

Abstract

A quantization procedure for the electromagnetic field in a rectangular cavity with perfect conductor walls is presented, where a decomposition formula of the field plays an essential role. All vector mode functions are obtained by using the decomposition. After expanding the field in terms of the vector mode functions, we get the quantized electromagnetic Hamiltonian.

1 Introduction

Recently we have carried out the field quantization in several rectangular cavities using the vector mode functions [1]. The vector mode functions have been obtained with the help of an orthogonal matrix. However, the procedure developed there has not been applicable to other cavities in a straightforward manner.

To overcome the above difficulty, we have presented another quantization scheme for the field in a circular cylindrical cavity [2]. All vector mode functions have been obtained by using a decomposition formula derived from Maxwell's equations directly. This method is more general than before, because it is also applicable to rectangular and spherical cavities.

In this paper, we applied the above method to a rectangular cavity with perfect conducting walls. Then spontaneous emission of an atom inside the cavity is calculated.

2 Decomposition of Electromagnetic Fields

In this section, we derive the decomposition formula for the field in the Cartesian coordinates. We shall use this result in performing the field quantization in a rectangular cavity in Sec. 3.

Maxwell's equations for the electric field $\mathbf{E}$ and the magnetic field $\mathbf{B}$ in free space are given by $\nabla \cdot \mathbf{E} = 0$, $\nabla \cdot \mathbf{B} = 0$, and

$$\nabla \times \mathbf{E} + \partial_t \mathbf{B} = 0, \qquad \nabla \times \mathbf{B} - \frac{1}{c^2}\partial_t \mathbf{E} = 0, \tag{1}$$

where c is the velocity of light in free space and $\partial_t = \partial/\partial t$.

The electromagnetic field $\mathbf{E}$ and $\mathbf{B}$ can be written in the Cartesian coordinates (x, y, z) as $\mathbf{E} = \mathbf{E}_T + \mathbf{E}_z$, $\mathbf{B} = \mathbf{B}_T + \mathbf{B}_z$, where $\mathbf{E}_T = \mathbf{e}_x E_x + \mathbf{e}_y E_y$ is the transverse component of the field

and $\mathbf{E}_z = \mathbf{e}_z E_z$. Here $\mathbf{e}_x$, $\mathbf{e}_y$, and $\mathbf{e}_z$ are the unit vectors in the x, y, and z directions, respectively. For simplicity, the derivative with respect to, for example, x is described as $\partial/\partial x = \partial_x$.

Since $\nabla_z \times \mathbf{E}_z = 0$, the first equation in (1) gives

$$\partial_t \mathbf{B}_z = -\nabla_T \times \mathbf{E}_T, \quad \partial_t \mathbf{B}_T = -\nabla_T \times \mathbf{E}_z - \nabla_z \times \mathbf{E}_T. \tag{2}$$

Similarly, the second equation in (1) leads to

$$\frac{1}{c^2}\partial_t \mathbf{E}_z = \nabla_T \times \mathbf{B}_T, \quad \frac{1}{c^2}\partial_t \mathbf{E}_T = \nabla_T \times \mathbf{B}_z + \nabla_z \times \mathbf{B}_T. \tag{3}$$

Equations (2) and (3) give

$$\triangle_T \mathbf{E} = -\nabla \times \nabla \times \mathbf{E}_z + \nabla \times \partial_t \mathbf{B}_z, \quad \triangle_T \mathbf{B} = -\frac{1}{c^2}\nabla \times \partial_t \mathbf{E}_z - \nabla \times \nabla \times \mathbf{B}_z. \tag{4}$$

To rewrite Eq. (4), we must decompose the components E_z and B_z into two parts. Suppose that the field is in a finite region. Let us expand E_z and B_z in terms of a certain complete system of functions with mode s:

$$E_z(\mathbf{r}, t) = \sum_s (E_{zs}(\mathbf{r}, t) + \text{c.c.}), \quad B_z(\mathbf{r}, t) = \sum_s (B_{zs}(\mathbf{r}, t) + \text{c.c.}), \tag{5}$$

where $E_{zs}(\mathbf{r}, t) = \tilde{E}_{zs}(\mathbf{r}) e^{-i\omega_{s1} t}$ and $B_{zs}(\mathbf{r}, t) = \tilde{B}_{zs}(\mathbf{r}) e^{-i\omega_{s2} t}$. Here $\omega_{s\sigma}$ ($\omega_{s\sigma} \geq 0$, $\sigma = 1, 2$) is determined by using given boundary conditions. Since E_z and B_z satisfy the wave equation, the components E_{zs} and B_{zs} satisfy the Helmholts equations:

$$\triangle E_{zs} = -k_{s1}^2 E_{zs}, \quad \triangle B_{zs} = -k_{s2}^2 B_{zs}(\mathbf{r}), \tag{6}$$

where $k_{s\sigma}^2 = \omega_{s\sigma}^2/c^2$. We assume that the components satisfy

$$\partial_z^2 E_{zs} = -h_{s1}^2 E_{zs}, \quad \partial_z^2 B_{zs} = -h_{s2}^2 B_{zs}, \tag{7}$$

where $h_{s\sigma}^2$ is determined by the boundary conditions. Then we have two dimensional Helmholtz equations:

$$\triangle_T E_{zs}(\mathbf{r}) = -g_{s1}^2 E_{zs}(\mathbf{r}), \quad \triangle_T B_{zs}(\mathbf{r}) = -g_{s2}^2 B_{zs}(\mathbf{r}), \tag{8}$$

where $g_{s\sigma}^2 = k_{s\sigma}^2 - h_{s\sigma}^2$.

Here we define two functions F_σ from E_{zs} and B_{zs} with $g_{s\sigma}^2 \neq 0$ as

$$F_\sigma(\mathbf{r}, t) = \sum_{g_{s\sigma}^2 \neq 0} [F_{s\sigma}(\mathbf{r}, t) + \text{c.c.}] = \sum_{g_{s\sigma}^2 \neq 0} [\tilde{F}_{s\sigma}(\mathbf{r}) e^{-i\omega_{s\sigma} t} + \text{c.c.}], \tag{9}$$

where

$$F_{s1} = E_{zs}/g_{s1}^2, \quad F_{s2} = B_{zs}/g_{s2}^2, \qquad (g_{s\sigma}^2 \neq 0). \tag{10}$$

The functions F_σ and their components $F_{s\sigma}$ satisfy the same equations as E_z and E_{zs}, respectively. The component F_σ is a solution of the Poisson equation. On the other hand, if there is a component E_{zs} or B_{zs} with $g_{s\sigma}^2 = 0$, Eq. (8) reduces to two dimensional Laplace equation.

The functions $\triangle_T F_\sigma$ satisfy

$$-\triangle_T F_1 \quad \sum_{g_{s1}^2 \neq 0} g_{s1}^2 F_{s1} \quad \sum_{g_{s1}^2 \neq 0} E_{zs}, \quad -\triangle_T F_2 \quad \sum_{g_{s2}^2 \neq 0} g_{s2}^2 F_{s2} \quad \sum_{g_{s2}^2 \neq 0} B_{zs}. \tag{11}$$

Here define E_{0z} and B_{0z} as

$$E_{0z} \quad E_z + \triangle_T F_1 \quad \sum_{g_{s1}^2 \; 0} E_{zs}, \quad B_{0z} \quad B_z + \triangle_T F_2 \quad \sum_{g_{s2}^2 \; 0} B_{zs}, \tag{12}$$

which satisfy $\triangle_T E_{0z} \quad 0$ and $\triangle_T B_{0z} \quad 0$. Then we have useful formulas for E_z and B_z:

$$E_z \quad -\triangle_T F_1 + E_{0z}, \quad B_z \quad -\triangle_T F_2 + B_{0z}. \tag{13}$$

Using Eq. (13) and defining $\mathbf{F}_\sigma$ as $\mathbf{F}_\sigma \quad \mathbf{e}_z F_\sigma$, we can rewrite Eq. (4) as

$$\triangle_T\Big(\mathbf{E} - \nabla \times \nabla \times \mathbf{F}_1 + \nabla \times \partial_t \mathbf{F}_2\Big) \quad -\nabla \times \nabla \times \mathbf{E}_{0z} + \nabla \times \partial_t \mathbf{B}_{0z}, \tag{14}$$

$$\triangle_T \left(\mathbf{B} - \frac{1}{c^2}\nabla \times \partial_t \mathbf{F}_1 - \nabla \times \nabla \times \mathbf{F}_2\right) \quad -\frac{1}{c^2}\nabla \times \partial_t \mathbf{E}_{0z} - \nabla \times \nabla \times \mathbf{B}_{0z}, \tag{15}$$

where $\mathbf{E}_{0z} \quad \mathbf{e}_z E_{0z}$ and $\mathbf{B}_{0z} \quad \mathbf{e}_z B_{0z}$. Define $\mathbf{E}_0$ and $\mathbf{B}_0$ as the quantities in the parentheses at the left hand side in Eqs. (14) and (15), respectively. The results of this section is summarized in the following theorem.

Theorem 1: If the components E_{zs} and B_{zs} satisfy Eq. (7), the field can be decomposed into three components as follows:

$$\mathbf{E} \quad \nabla \times \nabla \times \mathbf{F}_1 - \nabla \times \partial_t \mathbf{F}_2 + \mathbf{E}_0, \quad \mathbf{B} \quad \frac{1}{c^2}\nabla \times \partial_t \mathbf{F}_1 + \nabla \times \nabla \times \mathbf{F}_2 + \mathbf{B}_0, \tag{16}$$

where $\mathbf{E}_0$ and $\mathbf{B}_0$ satisfy

$$\triangle_T \mathbf{E}_0 \quad -\nabla \times \nabla \times \mathbf{E}_{0z} + \nabla \times \partial_t \mathbf{B}_{0z}, \quad \triangle_T \mathbf{B}_0 \quad -\frac{1}{c^2}\nabla \times \partial_t \mathbf{E}_{0z} \quad \nabla \times \nabla \times \mathbf{B}_{0z}. \tag{17}$$

Theorem 1 plays a central role in performing the field quantization in this paper. It is worth emphasizing that each term in Eq. (16) is a solution to Maxwell's equations.

3 Vector Mode Functions and Field Quantization

The cavity we treat here is enclosed by rectangular walls having sides L_x, L_y, and L_z in the x, y, and z directions, respectively: $0 < x < L_x$, $0 < y < L_y$, and $0 < z < L_z$. We assume that the cavity has perfectly conducting walls. The tangential component of the electric field $\mathbf{E}|_{\tan}$ and the normal component of the magnetic field $\mathbf{B}|_{\text{norm}}$ must accordingly vanish at the boundaries of the cavity.

The above boundary condition reduces to that for the z components

$$E_z \quad 0, \quad \partial_x B_z \quad 0, \qquad (x \quad 0, \ L_x), \tag{18}$$
$$E_z \quad 0, \quad \partial_y B_z \quad 0, \qquad (y \quad 0, \ L_y), \tag{19}$$
$$B_z \quad 0, \quad \partial_z E_z \quad 0, \qquad (z \quad 0, \ L_z). \tag{20}$$

The solution to the Helmholts equation (6) for the components E_{zs} and B_{zs} under the above boundary conditions is given by

$$\begin{aligned} E_{zs}(\mathbf{r},t) \quad & C_{s1}(t)\sin(\ell\pi x/L_x)\sin(m\pi y/L_y)\cos(n\pi z/L_z), \\ B_{zs}(\mathbf{r},t) \quad & C_{s2}(t)\cos(\ell\pi x/L_x)\cos(m\pi z/L_z)\sin(n\pi z/L_z), \end{aligned} \tag{21}$$

where the mode index is $s \quad (\ell,m,n)$ $(\ell,m,n \quad 0,\pm1,\pm2,\cdots)$.

From the solution (21) we have

$$\begin{aligned} g_{s\sigma}^2 &\equiv g_s^2 \quad (\ell\pi/L_x)^2 + (m\pi/L_y)^2, \\ k_{s\sigma}^2 &\equiv k_s^2 \quad (\ell\pi/L_x)^2 + (m\pi/L_y)^2 + (n\pi/L_z)^2. \end{aligned} \tag{22}$$

Consequently, we can use Theorem 1 in the preceding section. Although it follows from Eq. (22) that $g_{s\sigma}^2 \geq 0$, we can prove that $g_{s\sigma}^2 > 0$, which results from the following lemma. We omit its proof.

Lemma: $\mathbf{E}_0, \ \mathbf{B}_0 \quad 0$ and $g_{s\sigma}^2 > 0$. As a result, the term with $\ell \quad m \quad 0$ in Eq. (21) cannot be used.

Let us next obtain the functions F_σ, whose definitions are given in Eqs. (9) and (10). That is, the functions are given by

$$\begin{aligned} F_{s1}(\mathbf{r},t) \quad & \frac{E_{zs}(\mathbf{r},t)}{g_s^2} \equiv i\sqrt{\frac{\hbar\omega_s}{2\varepsilon_0}}a_{s1}(t)\psi_{s1}(\mathbf{r}), \\ F_{s2}(\mathbf{r},t) \quad & \frac{B_{zs}(\mathbf{r},t)}{g_s^2} \equiv i\sqrt{\frac{\hbar\omega_s}{2\varepsilon_0}}a_{s2}(t)\psi_{s2}(\mathbf{r}), \end{aligned} \tag{23}$$

where $\omega_{s\sigma} \equiv \omega_s$ and we have introduced $a_{s\sigma}(t) \quad a_{s\sigma}(0)e^{-i\omega_s t}$ and $\psi_{s\sigma}$ given by

$$\psi_{s1}(\mathbf{r},t) \quad c_{s1}\sin(\ell\pi x/L_x)\sin(m\pi y/L_y)\cos(n\pi z/L_z), \tag{24}$$
$$\psi_{s2}(\mathbf{r},t) \quad c_{s2}\cos(\ell\pi x/L_x)\cos(m\pi y/L_y)\sin(n\pi z/L_z), \tag{25}$$

with $c_{s1} \quad [8/(Vk_s^2g_s^2)]^{1/2}$ and $c_{s2} \quad [8/(V\omega_s^2g_s^2)]^{1/2}$. The functions $\psi_{s\sigma}$ has the orthonormality property

$$\int_c d\mathbf{r}\,\psi_{s\sigma}^*(\mathbf{r})\psi_{s'\sigma}(\mathbf{r}) \quad \frac{1}{8}|c_{s\sigma}|^2V\delta_{ss'}, \tag{26}$$

where $\int_c d\mathbf{r} \quad \int_{\text{cavity}} dxdydz$ and V is the cavity volume. Here the quantity $\cos x$ in Eqs. (24) and (25) must be changed to $1/\sqrt{2}$ when $x \quad 0$.

Substituting the functions F_σ in Eq. (23) into $\mathbf{E}$ in Eq. (16), we find

$$\mathbf{E}(\mathbf{r},t) \quad i\sum_{s\sigma}\sqrt{\frac{\hbar\omega_s}{2\varepsilon_0}}\left[a_{s\sigma}(t)\mathbf{u}_{s\sigma}(\mathbf{r}) - a_{s\sigma}^*(t)\mathbf{u}_{s\sigma}^*(\mathbf{r})\right], \tag{27}$$

where the vector mode functions $\mathbf{u}_{s\sigma}$ are given by

$$\mathbf{u}_{s1} \quad \nabla \times \nabla \times \mathbf{e}_z \psi_{s1}, \quad \mathbf{u}_{s2} \quad i\omega_s \nabla \times \mathbf{e}_z \psi_{s2}. \tag{28}$$

The vector mode functions satisfy $\nabla \cdot \mathbf{u}_{s\sigma} \quad 0$, $(\triangle + k_{s\sigma}^2)\mathbf{u}_{s\sigma} \quad 0$, and at the boundaries $\mathbf{u}_{s\sigma}|_{\tan} \quad 0$, $\nabla \times \mathbf{u}_{s\sigma}|_{\mathrm{norm}} \quad 0$. They also satisfy the orthonormality property needed for quantization:

$$\int_c d\mathbf{r}\, \mathbf{u}_{s\sigma}^*(\mathbf{r}) \cdot \mathbf{u}_{s'\sigma'}(\mathbf{r}) \quad \delta_{ss'}\delta_{\sigma\sigma'}. \tag{29}$$

To get the quantized field, the functions $a_{s\sigma}(t)$ are regarded as annihilation operators satisfying the commutation relation $[a_{s\sigma}(t), a_{s'\sigma'}^\dagger(t)] \quad \delta_{ss'}\delta_{\sigma\sigma'}$. Then we get the following theorem.

Theorem 2: The quantized field and the Hamiltonian are given by

$$\mathbf{E}(\mathbf{r},t) \quad i\sum_{s\sigma}\sqrt{\frac{\hbar\omega_s}{2\varepsilon_0}}\left[a_{s\sigma}(t)\mathbf{u}_{s\sigma}(\mathbf{r}) - a_{s\sigma}^\dagger(t)\mathbf{u}_{s\sigma}^*(\mathbf{r})\right], \tag{30}$$

$$\mathbf{B}(\mathbf{r},t) \quad \sum_{s\sigma}\sqrt{\frac{\hbar}{2\varepsilon_0\omega_s}}\left[a_{s\sigma}(t)\nabla \times \mathbf{u}_{s\sigma}(\mathbf{r}) + a_{s\sigma}^\dagger(t)\nabla \times \mathbf{u}_{s\sigma}^*(\mathbf{r})\right], \tag{31}$$

$$H_R \quad \sum_{s\sigma}\frac{1}{2}\hbar\omega_s\left(a_{s\sigma}^\dagger a_{s\sigma} + a_{s\sigma}a_{s\sigma}^\dagger\right) \quad \sum_{s\sigma}\hbar\omega_s\left(a_{s\sigma}^\dagger a_{s\sigma} + \frac{1}{2}\right). \tag{32}$$

4 Spontaneous Emission

As an application, we consider the transition rates of an atom in the cavity, using the dipole approximation. The Hamiltonian is given by $H \quad H_A + H_R + H_I$, where H_A is the free Hamiltonian for the atom, H_R for the field which is given in Eq. (32), and $H_I \quad -e\mathbf{D}\cdot\mathbf{E}(\mathbf{R})$ ($-e\mathbf{D}$: the total electric dipole moment of the atom; $\mathbf{R} \quad (X,Y,Z)$: the position of the atom).

At $t \quad 0$, the atom is in an energy state $|i_0>$ (with energy E_{i_0}) and the field is in the vacuum. Then the probability per second of finding the atom in a state (with energy E_i) at sufficiently large time t is given by

$$w \quad \frac{e^2\pi}{\varepsilon_0\hbar}\sum_{s\sigma}|\mathbf{u}_{s\sigma}(\mathbf{R})\cdot <i_0|\mathbf{D}|i>|^2\frac{\omega_s\sin(\omega_s-\omega_0)t}{\pi(\omega_s-\omega_0)}, \tag{33}$$

where $\hbar\omega_0 \quad E_{i_0} - E_i$.

Let us take the average of the coordinates Y and Z and take $L_z \to \infty$. The transition rates w_y and w_z vanish (w_i indicates the rate where the dipole moment is along with the i direction). The rate w_x is given by

$$w_x/w_0 \quad \frac{6}{\pi\xi_y}\sum_m(1-m^2/\xi_y^2)^{-1/2}\theta(1-m^2/\xi_y^2), \tag{34}$$

where $\xi_i \quad \omega_0 L_i/c\pi$, $\xi_x \quad 1/2$, $w_0 \quad e^2|<i_0|\mathbf{D}|i>|^2\omega_0^3/(3\pi\hbar\varepsilon_0 c^3)$, $\theta(x) \quad 1$ $(x>0)$, and

$\theta(x)$ 0 ($x < 0$), which is shown in FIG. 1.

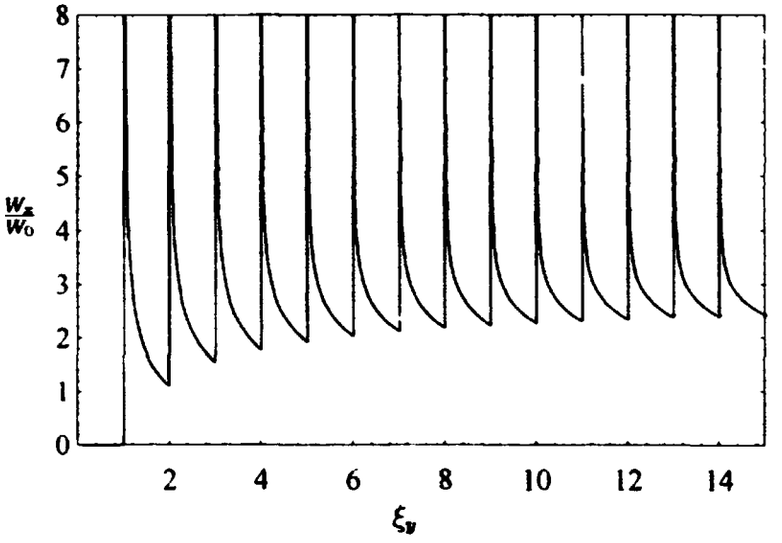

FIG. 1. Transition rate w_x for $L_z \to \infty$, where the dipole moment is along with the x direction.

Setting here ω_0 10^{13} Hz, we have L_x 4.7×10^{-2} mm, so that the cavity is quite narrow. Also, FIG. 1 shows that the transition is forbidden when $\xi_y < 1$, i.e., $L_y < 9.4 \times 10^{-2}$ mm., where the cavity is a thin tube in this case.

5 Conclusions

The quantization for the field in the cavity has been performed as follows: obtain the decomposition formula (16) in the Cartesian coordinates; solve the Helmholts equations (6) for the components E_{zs} and B_{zs} under the boundary conditions; determine the functions F_σ, substitute them into the decomposition formula (16), and obtain the vector mode functions satisfying the orthonormality property (29); then we arrive at the quantized field and Hamiltonian. In the whole process of quantization, the decomposition formula in Theorem 1 plays an important role.

Acknowledgments

We would like to thank Prof. M. Namiki, Prof. S. Matsumoto, Dr. A. Vourdas, and Dr. S. Kudaka for numerous valuable discussions.

References

[1] K. Kakazu and Y. S. Kim, Phys. Rev. A **50**, 1830 (1994).

[2] K. Kakazu and Y. S. Kim, preprint DPUR-84.

NEXT
DOCUMENT

On the stochastic quantization method: characteristics and applications to singular systems

Masahiko KANENAGA and Mikio Namiki
Department of Physics, Waseda University
Tokyo 165, Japan

Abstract

Introducing the generalized Langevin equation, we extend the stochastic quantization method so as to deal with singular dynamical systems beyond the ordinary territory of quantum mechanics. We also show how the uncertainty relation is built up to the quantum-mechanical limit with respect to fictitious time, irrespective of its initial value, within the framework of the usual stochastic quantization method.

1 Basic ideas of stochastic quantization method (SQM)

The Parisi-Wu stochastic quantization method (SQM) [1, 2] was so designed as to give quantum mechanics as the thermal equilibrium limit of a hypothetical stochastic process with respect to a new (fictitious) time other than the ordinary time. The Background idea is that a d-dimensional quantum system is equivalent to a $(d+1)$-dimensional classical system with random noise. We can consider the SQM to be a third method of quantization remarkably different from the conventional theories, i.e., the canonical and path-integral ones. The SQM has the following advantages:

1. We can quantize any dynamical system only on the basis of *equation of motion*, while the canonical method is based on *Hamiltonian* and the path-integral method on *Lagrangian*.

2. We can quantize the gauge field without resorting to the conventional gauge fixing procedure [3].

We deal with the dynamical system described by Euclidean action $S_E[q]$, where $q(x) = \{q_i; i = 1, 2, \cdots\}$ are dynamical variables and x is the ordinary time for particles or 4-dimensional coordinates for fields. As the first step, we show that SQM gives the same result as given by the conventional path-integral method:

$$< G > = C \int \mathcal{D}q G(q) \exp(-S_E[q]/\hbar) , \tag{1}$$

$$\Delta(x, x') = C \int \mathcal{D}q q(x) q(x') \exp(-S_E[q]/\hbar) , \tag{2}$$

where $< G >$ is the quantum-mechanical expectation value of an observable $G(q)$, $\Delta(x, x')$ is the propagator and C the normalization constant. In this paper we also observe how the uncertainty

relation is built up to the quantum-mechanical limit within the framework of the hypothetical stochastic process of SQM.

According to the prescription of SQM, we set up the basic Langevin equation in the following way:

$$\frac{\partial q_i(x,t)}{\partial t} = -\left.\frac{\delta S_E[q]}{\delta q_i(x)}\right|_{q=q(x,t)} + \eta_i(x,t) , \tag{3}$$

$$< \eta_i(x,t) >_\eta = 0 , < \eta_i(x,t)\eta_j(x',t') >_\eta = 2\alpha\delta_{ij}\delta(x-x')\delta(t-t') , \tag{4}$$

where t stands for the fictitious time, η_i for Gaussian white noises and α for the diffusion constant. Using its solution in the thermal equilibrium limit, we get the same expectation value as given by the conventional path-integral method. To show this situation more clearly, we need to use the Fokker-Planck equation corresponding to the Langevin equation.

Defining the probability distribution functional $\Phi[\phi,t]$ by

$$\int \mathcal{D}qG(q)\Phi[q,t] =< G(q_i^\eta(x,t) >_\eta , \tag{5}$$

we can derive the Fokker-Planck equation as

$$\frac{\partial}{\partial t}\Phi[q,t] = \hat{F}\Phi[q,t] , \quad \hat{F} = \alpha\int dx \sum_i \frac{\delta}{\delta q_i(x)}\{\frac{\delta}{\delta q_i(x)} + \frac{1}{\alpha}\frac{\delta S_E[q]}{\delta q_i(x)}\} , \tag{6}$$

where $\hat{F}$ is the Fokker-Planck operator. If the drift force $K_i(q,t) = -(\delta S_E[q]/\delta q_i)_{q=q(x,t)}$ has a damping effect, i.e. $(\delta S_E[q]/\delta q_i)_{q=q(x,t)} > 0$, we get the thermal equilibrium limit ($t \to \infty$) as follows:

$$\Phi_{eq}[q] = C\exp(-\frac{1}{\alpha}S_E[q]) . \tag{7}$$

Putting $\alpha = \hbar$, therefore, we obtain the prescription of SQM:

$$\lim_{t\to\infty} < G(q_i^\eta(x,t) >_\eta = \lim_{t\to\infty}\int \mathcal{D}qG(q)\Phi[q,t]$$
$$= \int \mathcal{D}qG(q)\Phi_{eq}[q] = C\int \mathcal{D}qG(q)\exp(-\frac{1}{\hbar}S_E[q]) =< G > . \tag{8}$$

2 Building-up of the uncertainty relation in the hypothetical stochastic process

Quantizing one-dimensional harmonic oscillator by means of SQM, let us see the dependence of the uncertainty relation on the fictitious time. The Euclidean action of the one-dimensional harmonic oscillator is given by

$$S[q] = \int dx_0 \left[\frac{M}{2}(\frac{dq}{dx_0})^2 + \frac{1}{2}M^2\omega^2q^2\right] . \tag{9}$$

According to the prescription of SQM, we set up the Langevin equation of this harmonic oscillator as follows:

$$\frac{\partial}{\partial t}q(x_0,t) = M^2\left[\frac{\partial}{\partial x_0^2} - \omega^2\right]q(x_0,t) + \eta(x_0,t) , \tag{10}$$

$$< \eta(x_0,t) >_\eta = 0, \quad < \eta(x_0,t)\eta(x_0',t') >_\eta = 2\hbar\delta(x_0-x_0')\delta(t-t') . \tag{11}$$

Solving this, we easily obtain the following dependence of the uncertainty relation on t:

$$(\Delta q(t))^2(\Delta p(t))^2 = \left[\frac{1}{2\pi}\int dk\rho(k)e^{-2M(k^2+\omega^2)t} + \frac{\hbar}{2M\omega}\frac{2}{\sqrt{\pi}}\int_0^{\sqrt{2M\omega^2 t}} e^{-z^2}dz\right] \times \left[\frac{1}{2\pi}\int dkk^2\rho(k)e^{-2M(k^2+\omega^2)t} - \frac{\hbar M\omega}{2}\frac{2}{\sqrt{\pi}}\int_0^{\sqrt{2M\omega^2 t}} e^{-z^2}dz\right] , \quad (12)$$

where $\rho(k) = (\Delta q(k,0))^2$ is the initial value at $t = 0$.

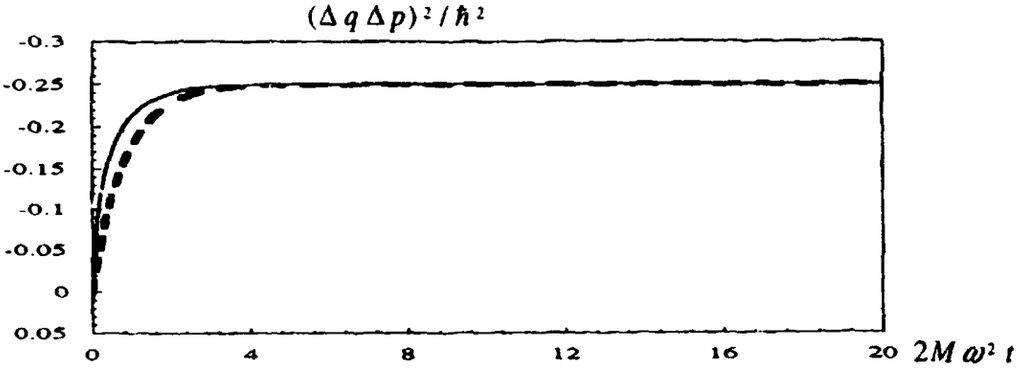

FIG. 1. We show how the uncertainty relation were built up with respect to the fictitious time. The solid line corresponds to the uncertainty relation for $\Delta q(k,0) = 0$, the dotted line to that for $\Delta q(k,0) \neq 0$. Note that the negative sign of $(\Delta q \Delta p)^2$ is due to the Wick rotation ($x_0 \to -ix_0$).

In FIG. 1, we can clearly see that the uncertainty relation in the hypothetical stochastic process approaches to the quantum-mechanical limit, irrespective of its initial values.

3 Generalized stochastic quantization method

We have many basic Langevin equations to give the same quantum mechanics [2]. By making use of this kind of freedom, we can go beyond the ordinary territory of quantum mechanics.

A generalized Langevin equation to give the same quantum mechanics is given by

$$\frac{\partial}{\partial t}\phi(x,t) = -\int d^d x'\ K(x,x';\phi)\frac{\delta S}{\delta\phi(x',t)} + \int d^d x'\frac{\delta K(x,x';\phi)}{\delta\phi(x',t)} + \int d^d x'\ G(x,x';\phi)\ \eta(x',t)\ , \quad (13)$$

$$< \eta(x,t) >= 0\ , \qquad < \eta(x,t)\eta(x',t') >= 2\delta^d(x-x')\delta(t-t')\ . \quad (14)$$

Note that we put $\hbar = 1$ hereafter. As an example, let us discuss the bottomless system described by scalar field $\phi(x)$ with the following action

$$S_E[\phi] = S_{\rm free}[\phi] + S_{\rm int}[\phi]\ , \quad (15)$$

x being d-dimensional Euclidean space-time point. $S_{\rm free}[\phi]$ is the free part of the action and $S_{\rm int}[\phi]$ the bottomless interaction part. We know that we can hardly quantize the bottomless system by means of the conventional quantization method. For

$$K(x,x';\phi) = \delta^d(x-x')K[\phi]\ , \qquad G(x,x';\phi) = \delta^d(x-x')K^{1/2}[\phi]\ , \quad (16)$$

we simplify the above generalized Langevin equation as

$$\frac{\partial}{\partial t}\phi(x,t) = -K[\phi]\frac{\delta S_{\rm E}[\phi]}{\delta\phi(x,t)} + \frac{\delta K[\phi]}{\delta\phi(x,t)} + K^{1/2}[\phi]\ \eta(x,t), \tag{17}$$

i.e.

$$\frac{\partial}{\partial t}\phi(x,t) = -K[\phi]\frac{\delta S_{\rm K}[\phi]}{\delta\phi(x,t)} + K^{1/2}[\phi]\ \eta(x,t), \tag{18}$$

where we have put $S_{\rm K} = S_{\rm E} - \ln K$. Provided that the drift force has a damping effect, that is to say, $S_{\rm K} = S_{\rm E} - \ln K > 0$, this Langevin equation has the thermal equilibrium limit. To satisfy this condition in the bottomless system, we may choose the Kernel as $K[\phi] = \exp\{S_{\rm int}\}$. In this case the generalized Langevin equation becomes

$$\frac{\partial}{\partial t}\phi(x,t) = -K[\phi]\frac{\delta S_{\rm free}[\phi]}{\delta\phi(x,t)} + K^{1/2}[\phi]\ \eta(x,t)\ . \tag{19}$$

Based on this equation, we can perform the numerical simulations of bottomless scalar field models and the bottomless hermitian matrix model.

4 Application to bottomless systems

A simple bottomless example [4] is given by

$$S[\phi] = S_2[\phi] - S_4[\phi]\ ,\quad S_2[\phi] = \frac{1}{2}m^2\phi^2\ ,\quad S_4[\phi] = \frac{\lambda}{4}\phi^4\ ,\quad \lambda > 0\ , \tag{20}$$

where ϕ is a zero-dimensional field. If we put $K[\phi] = \exp(\lambda_K\phi^4)$, the well-posed condition mentioned in the preceding section becomes

$$S_K = S_E - \ln K = \frac{1}{2}m^2\phi^2 + \frac{1}{4}(\lambda_K - \lambda)\phi^4 > 0\ ,\quad \text{i.e.}\quad \lambda_K \geq \lambda\ . \tag{21}$$

If we choose λ_K equal to λ, the Langevin equation reduces to

$$\frac{\partial}{\partial t}\phi(t) = -m^2\exp[-S_4]\phi(t) + \exp[-S_4/2]\eta(t)\ . \tag{22}$$

Based on this Langevin equation, we have numerically simulated the stochastic process of ϕ.

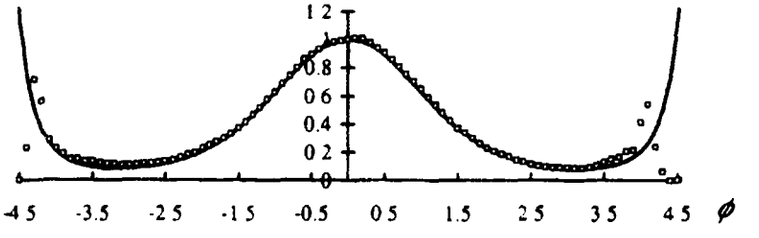

FIG. 2. Distribution of numerical solution of the Langevin equation (22) (open circles) for $\lambda = 0.1, m = 1$. For comparison, we plot the path-integral measure $\exp\{-S\}$ of the bottomless action (20) (solid line) for the same parameters.

FIG. 2 shows that the form of the distribution of numerical solution is consistent with the form of the path-integral measure $\exp\{-S\}$ of the bottomless action (20) in the central region of ϕ. From the prescription of SQM that at the thermal equilibrium limit we get the same expectation value as given by the path-integral method, we conclude that, in the central region of ϕ, the probability distribution of solutions of the generalized Langevin equation (22) is consistent with the path-integral measure $\exp\{-S\}$ even of the bottomless action.

As the next example, let us consider the bottomless hermitian matrix model [5], which is regarded as an important model of two-dimensional quantum gravity [6]. The partition function of $N \times N$ hermitian matrix model is given by

$$Z = \int d\phi \exp\{-S[\phi]\} , \quad d\phi \equiv \prod_{i=1}^{N} d\phi_{ii} \prod_{1 \le i < j \le N} d(\mathrm{Re}\phi_{ij}) d(\mathrm{Im}\phi_{ij}) . \tag{23}$$

Independent variables of the hermitian matrix model are $\mathrm{Re}\phi_{ij}$, $\mathrm{Im}\phi_{ij}$ $(i < j)$ and ϕ_{ii} with $i, j = 1, 2, \cdots N$. The action of the bottomless hermitian matrix model is given by

$$S[\phi] = S_{\mathrm{free}}[\phi] + S_{\mathrm{int}}[\phi] , \quad S_{\mathrm{free}}[\phi] = N\mathrm{tr}[\frac{1}{2}\phi^2] , \quad S_{\mathrm{int}}[\phi] = -N\mathrm{tr}[g\phi^4] \equiv -S_4[\phi] , \quad g > 0 . \tag{24}$$

For kernel $K[\phi] = \exp\{-S_4[\phi]\}$, the generalized Langevin equation becomes

$$\frac{\partial}{\partial t}\phi_{ii}(t) = -Ne^{-S_4}\phi_{ii}(t) + e^{-\frac{1}{2}S_4}\eta_{ii}(t) , \tag{25}$$

$$\frac{\partial}{\partial t}\phi_{ij}^{R,I}(t) = -2Ne^{-S_4}\phi_{ij}^{R,I}(t) + e^{-\frac{1}{2}S_4}\eta_{ij}^{R,I}(t) , \quad (i < j) . \tag{26}$$

The statistical properties of the Gaussian white noises must be subjected to

$$< \eta_{ii}(t) >_\eta = 0 , \quad < \eta_{ii}(t)\eta_{jj}(t') >_\eta = 2\delta_{ij}\delta(t - t') , \tag{27}$$

$$< \eta_{ij}^A(t) >_\eta = 0 , \quad < \eta_{ij}^A(t)\eta_{kl}^B(t') >_\eta = 2\delta^{AB}\delta_{ik}\delta_{jl}\delta(t - t') , \quad (i < j, k < l) , \tag{28}$$

$$< \eta_{ij}^A(t)\eta_{mm}(t') >_\eta = 0 , \quad (i < j) , \quad (A, B = R, I) . \tag{29}$$

One of the most remarkable results is observed in the deviation of $< \mathrm{tr}\phi^2 > /N$ from the planar calculation [6], as shown in FIG. 3.

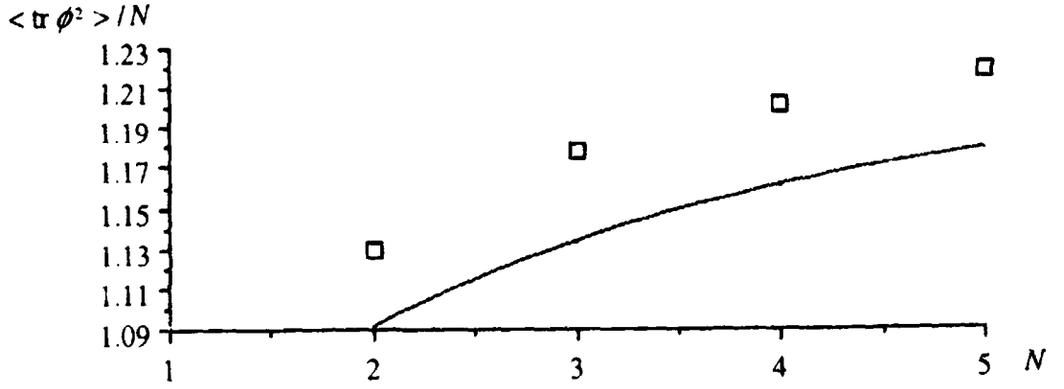

FIG. 3 Expectation values $< \mathrm{tr}\phi^2 > /N$ for various values of N(open squares). The solid line shows the planar result [6]

This deviation has so far been anticipated only from theoretical conjecture.

5 Conclusion

We have observed, within the framework of SQM, that the uncertainty relation will be built up to the quantum-mechanical limit, irrespective of its initial value, in a hypothetical stochastic process with respect to the fictitious time.

Introducing generalized (kernelled) Langevin equations, we have extended SQM so as to deal with singular dynamical systems beyond the ordinary territory of quantum mechanics. We also have attempted to quantize a few singular systems, such as bottomless systems, by means of SQM which is based on the generalized Langevin equations.

Acknowledgments

Applications of the generalized Langevin equation to the above singular system have been done in collaboration with S. Tanaka, I. Ohba, and M. Mizutani. The authors are indebted to all of them and H. Nakazato for stimulated discussions and also to the Ministry of Education, Culture and Sciences for financial supports.

References

[1] G. Parisi and Y. S. Wu, Sci. Sin. **90** (1981), 483.

[2] M. Namiki, *Stochastic Quantization* (Springer, Heidelberg, 1992)

[3] N. Namiki, I. Ohba, K. Okano and Y. Yamanaka, Prog. Ther. Phys. **69** (1983), 1580.

[4] S. Tanaka, M. Namiki, I. Ohba, M. Mizutani, N. Komoike and M. Kanenaga, Phys. Lett. **288B** (1992), 129.

[5] M. Kanenaga, M. Mizutani, M. Namiki, I. Ohba and S. Tanaka, Prog. Ther. Phys. **91** (1994), 599.

[6] F. David, Mod. Phys. Lett. **A5** (1990), 1019; Nucl. Phys. **348** (1991), 507.

NEXT
DOCUMENT

DAMPED OSCILLATOR WITH DELTA-KICKED FREQUENCY

O. V. Man'ko
Lebedev Physical Institute
Leninsky Prospekt, 53, Moscow 117924, Russia

Abstract

Exact solutions of the Schrödinger equation for quantum damped oscillator subject to frequency δ-kick describing squeezed states are obtained. The cases of strong, intermediate, and weak damping are investigated.

1 Introduction

The aim of the paper is to consider parametric excitation of damped quantum oscillator. The parametric excitation is choosen in the form of very short pulse simulated by δ-kick of frequency. The damping is considered in the frame of Caldirola-Kanai model [1], [2]. This model is a partial case of the multidimensional system described by nonstationary Hamiltonian which is a general quadratic form in coordinates and momenta operators considered in [3], [4]. The problem of quantum oscillator with a time-dependent frequency was solved in [3]-[16]. In [3], [4] it was shown that the solutions for systems with quadratic Hamiltonian are expressed in terms of classical trajectory of the system. The case under consideration is interesting due to possibility of finding the classical trajectory in explicit form. The goal of this work is to extend the analysis of [13] to more simple one-oscillator case but taking into account the dissipation and to study the influence of the damping on the squeezing phenomenon for the kicked oscillator. Here the quantum dispersion of coordinate of damped oscillator is obtained in explicit form and the influence on squeezing phenomenon of strong, intermediate, and weak damping is studied.

2 Integrals of Motion

Let us consider the quantum damped parametric oscillator in the frame of Caldirola-Kanai model [1], [2] using the method of integrals of motion [3], [4], [7]. The Hamiltonian of the system is

$$\widehat{H} = \frac{1}{2}me^{2\gamma t}\omega^2(t)\hat{x}^2 + \frac{1}{2m}e^{-2\gamma t}\hat{p}^2, \tag{1}$$

where m is the mass of the oscillator, γ is the damping coefficient, $\hat{x}$ and $\hat{p}$ are the coordinate and momentum operators, and $\omega(t)$ is time-dependent frequency of the oscillator. The equation of motion for the classical coordinate x and momentum p are of the form

$$\dot{x} = pe^{-2\gamma t}, \quad \dot{p} = -\omega^2(t)e^{2\gamma t}x, \quad \ddot{x} + 2\gamma\dot{x} + \omega^2(t)x = 0. \tag{2}$$

The Heisenberg equation of motion for the position and momentum operators have the same form. Let us look in the Schrödinger representation for the integral of motion $\widehat{A}(t)$ which is linear in coordinate and momentum operators and satisfies the equation $[i\hbar\partial/\partial t - \widehat{H}, \widehat{A}] = 0$. At the initial moment of time, this integral of motion is equal to usual boson annihilation operator. Then for the operator $\widehat{A}$, one obtains the expression

$$\widehat{A}(t) = \frac{i}{\sqrt{2}}\left(\frac{\epsilon(t)\hat{p}l}{\hbar} - \frac{\dot{\epsilon}e^{2\gamma t}\hat{x}}{l\Omega(0)}\right), \tag{3}$$

where $\epsilon(t)$ is the solution to the equation of motion

$$\ddot{\epsilon}(t) + 2\gamma\dot{\epsilon}(t) + \omega^2(t)\epsilon(t) = 0, \quad \Omega^2(0) = \omega^2(0) - \gamma^2, \tag{4}$$

with initial conditions $\epsilon(0) = 1$, $\dot{\epsilon}(0) = i\Omega(0)$. In order the operator (3) and its hermitian conjugate satisfy at any time t the boson commutation relation, $\epsilon(t)$ must satisfy the additional condition

$$e^{2\gamma t}(\dot{\epsilon}\epsilon^* - \dot{\epsilon}^*) = 2i\Omega(0). \tag{5}$$

The eigenstates of operator (3) are the complete set of the squeezed correlated states of damped oscillator. Solving the equation $\widehat{A}(t)\Psi_\alpha(x,t) = \alpha\Psi_\alpha(x,t)$, where α is complex number, one can obtain these eigenstates in the explicit form

$$\Psi_\alpha(x,t) = (\pi\epsilon^2 l^2)^{-1/4}\exp\left(\frac{i\dot{\epsilon}e^{2\gamma t}x^2}{2\epsilon l^2\Omega(0)} + \frac{\sqrt{2}\alpha x}{\epsilon l} - \frac{\epsilon^*\alpha^2}{2\epsilon} - \frac{|\alpha|^2}{2}\right). \tag{6}$$

where $l^2 = \hbar/m\Omega(0)$. The wave functions in coordinate representation are gaussian packets with time- dependent coefficients in quadratic form under the exponential function. The density propability has consequently the gaussian form, too and the quantum dispersion of coordinate in the state (6) can be immediately obtained. It is of the form

$$\sigma_{x^2} = \langle\Psi_\alpha \mid \hat{x}^2 \mid \Psi_\alpha\rangle - \langle\Psi_\alpha \mid \hat{x} \mid \Psi_\alpha\rangle^2 = \frac{l^2|\epsilon|^2}{2}. \tag{7}$$

One can obtain for the quantum dispersion of momentum and for the squeezing coefficient,

$$\sigma_{p^2} = \langle\Psi_\alpha \mid \hat{p}^2 \mid \Psi_\alpha\rangle - \langle\Psi_\alpha \mid \hat{p} \mid \Psi_\alpha\rangle^2 = \frac{\hbar^2 e^{4\gamma t}|\dot{\epsilon}|^2}{2l^2\Omega^2(0)}, \quad k = \frac{\sigma_{x^2}(t)}{\sigma_{x^2}(0)} = |\epsilon|^2. \tag{8}$$

If $|\epsilon|^2 < 1$, which means that the disperssion of coordinate at the same moment of time t is less than at the initial one, the squeezing phenomenon appears. Due to this the states (6) are called squeezed correlated states as well as in the case without damping. Then all physical characteristics of the system are expressed through the solution of classical equation of motion $\epsilon(t)$. The only remaining problem is to find explicit expression for $\epsilon(t)$. In the following sections the explicit expressions for classical trajectories will be found for different regimes of damping.

3 The Case of Weak Damping

We consider a quantum damped oscillator with time-dependent frequency which varies in the specific manner of δ-kick

$$\omega^2(t) = \omega_0^2 - 2\kappa\delta(t),$$

where ω_0 is constant part of frequency, δ is Dirac delta-function. For $\varepsilon(t)$, we have the equation

$$\ddot{\varepsilon}(t) + 2\gamma\dot{\varepsilon}(t) + \omega_0^2\varepsilon(t) - 2\kappa\delta(t) = 0. \tag{9}$$

In this section we consider the case of weak damping, when $\omega_0 > \gamma$. Before and after δ-kick of frequency the solution to Eq. (9) is given by

$$\varepsilon_k(t) = A_k e^{-\gamma t + i\Omega t} + B_k e^{-\gamma t - i\Omega t}, \quad k = 0, 1, \tag{10}$$

where in the case of weak damping $\Omega = (\omega_0^2 - \gamma^2)^{1/2}$. Due to continuity conditions,

$$\varepsilon_0(0) = \varepsilon_1(0), \quad \dot{\varepsilon}_1(0) - \dot{\varepsilon}_0(0) = 2\kappa\varepsilon_0(0). \tag{11}$$

The coefficients A_k and B_k must satisfy the relations which can be expressed in matrix form

$$\begin{pmatrix} A_1 \\ B_1 \end{pmatrix} = \begin{pmatrix} 1 - i\kappa/\Omega & -i\kappa/\Omega \\ i\kappa/\Omega & 1 + i\kappa/\Omega \end{pmatrix} \begin{pmatrix} A_0 \\ B_0 \end{pmatrix}. \tag{12}$$

If $\varepsilon(-0) = 1$, $\dot{\varepsilon}(-0) = i\Omega$ at the initial instant, then $A_0 = 1 - i\gamma/2\Omega$, $B_0 = i\gamma/2\Omega$, one has for the classical trajectory after δ-kick,

$$\varepsilon_1(t) = \left[1 - \frac{i(\kappa + \gamma/2)}{\Omega}\right] \exp(-\gamma t + i\Omega t) - \frac{i(\kappa + \gamma/2)}{\Omega} \exp(-\gamma t - i\Omega t). \tag{13}$$

If before the first δ-kick the oscillator was in the state (6) with $\varepsilon(t) = e^{-\gamma t}(e^{i\Omega t} + \frac{\gamma}{\Omega}\sin\Omega t)$, the parametric excitation will transform it into a squeezed correlated state determined by (6) with $\varepsilon(t)$ given by (13). One can calculate the quantum dispersion of coordinate in excited correlated squeezed state, it is

$$\sigma_{x^2}(t) = \frac{\hbar e^{-2\gamma t}}{2m\Omega}\left[1 + \frac{\sin^2\Omega t}{\Omega^2}(2\kappa + \gamma)^2 + (2\kappa + \gamma)\frac{\sin 2\Omega t}{\Omega}\right]. \tag{14}$$

From the above expressions, we see that the maximum and minimum of $\sigma_{x^2}(t)$ and of squeezing coefficient $k^2(t) = \sigma_{x^2}(t)/\sigma_{x^2}(0)$ depend on ratio of the force of δ-kick and damping constant to the frequency of oscillations, while lower limit of squeezing coefficient is

$$\begin{aligned} k^2 &= \left[1 + 2\frac{(\kappa + \gamma/2)^2}{\Omega^2} - 2\frac{(\kappa + \gamma/2)}{\Omega^2}\sqrt{(\kappa + \gamma/2)^2 + \Omega^2}\right] \\ &\cong \exp\left\{\frac{\gamma}{\Omega}\cos^{-1}\left[\frac{\Omega}{\sqrt{(\kappa + \gamma/2)^2 + \Omega^2}}\right] - \frac{\pi\gamma}{\Omega}(2n - 1)\right\}, \end{aligned} \tag{15}$$

$n = 0, 1, \ldots$. From the above formulae, one can see that the squeezing phenomenon can be achieved for all values of damping coefficient. So choosing kicks of frequency (increasing the force of δ–kick) we can squeeze quantum noise in coordinate even in the case of large (but smaller then ω_0) damping coefficient γ.

In the case of zero damping, formula (15) coincides with the result of [5] and [13] (for two-mode system). In the case of zero damping ($\gamma = 0$) for the limit of free particle ($\omega_0 = 0$), one δ–kick of frequency does not produce squeezing [17].

4 The Case of Strong Damping

Let us consider quantum damped oscillator in the regime of strong damping, when $\gamma > \omega_0$. In this case the solution to Eq. (9) before and after δ–kick of frequency is $\varepsilon_k = A_k e^{(\Omega-\gamma)t} + B_k e^{-(\gamma+\Omega)t}$ with frequency $\Omega = (\gamma^2 - \omega_0^2)^{1/2}$. Making the same procedure as in Section 2 one can obtain that after δ–kick, coefficients A_1 and B_1 are connected with the initial ones through the matrix equation

$$\begin{pmatrix} A_1 \\ B_1 \end{pmatrix} = \begin{pmatrix} 1 + \kappa/\Omega & \kappa/\Omega \\ -\kappa/\Omega & 1 - \kappa/\Omega \end{pmatrix} \begin{pmatrix} A_0 \\ B_0 \end{pmatrix}. \tag{16}$$

Taking the initial conditions in the form $\varepsilon(0) = 1$, $\dot{\varepsilon}(0) = i\Omega$ one has $A_0 = \frac{1}{2}(1 + i + \gamma/\Omega)$, $B_0 + \frac{1}{2}(1 - i - \gamma/\Omega)$. The classical trajectory $\varepsilon(t)$ after δ–kick of frequency is

$$\varepsilon(t) = e^{-\gamma t}\left[\cosh \Omega t + \sinh \Omega t \left(i + \frac{\gamma}{\Omega} + \frac{2\kappa}{\Omega}\right)\right]. \tag{17}$$

The dispersion of coordinate after δ–kick of frequency takes the form

$$\sigma_{x^2}(t) = \frac{\hbar e^{-2\gamma t}}{2m\Omega}\left[\cosh 2\Omega t + \left(\frac{2\kappa + \gamma}{\Omega}\right)^2 \frac{\cosh 2\Omega t - 1}{2} + \left(\frac{2\kappa + \gamma}{2}\right)\sqrt{\cosh^2 2\Omega t - 1}\right]. \tag{18}$$

Since $\cosh \alpha \geq 1$, the dispersion cannot be less than $\hbar e^{-2\gamma t}/2m\Omega$, squeezing (by δ- kick of frequency) cannot exist in the system under study in the regime of strong damping.

5 Parametric Excitation of Free Particle Motion

In the last section we consider the case when the constant part of frequency is equal to zero but parametric excitation acts on the free particle motion. The gaussian wave packets for such systems without parametric excitation were considered in [18]– [20]. The equation for classical trajectory in case $\omega_0 = 0$ is

$$\ddot{\varepsilon}(t) + 2\gamma\dot{\varepsilon}(t) - 2\kappa\delta(t) = 0. \tag{19}$$

Before and after δ–kick the solution to this equation is given by expression: $\varepsilon_k = A_k + B_k e^{-2\gamma t}$. Applying the procedure used in Section 2 and continuity conditions one can obtain the relation

$$\begin{pmatrix} A_1 \\ B_1 \end{pmatrix} = \begin{pmatrix} 1+\kappa/\gamma & \kappa/\gamma \\ -\kappa/\gamma & 1-\kappa/\gamma \end{pmatrix} \begin{pmatrix} A_0 \\ B_0 \end{pmatrix}. \tag{20}$$

Taking into account coeficients $A_0 = 1 + i/2$ and $B_0 = -i/2$, which coincide with the initial conditions considered above, the expession for classical trajectory after δ-kick can be obtained

$$\varepsilon(t) = 1 + \frac{\kappa}{\gamma}(1 - e^{-2\gamma t}) + \frac{i}{2}(1 - e^{-2\gamma t}). \tag{21}$$

The excited states are determined by formula (6) with dispersion of coordinate (7), where $\varepsilon(t)$ is given by (21). The squeezing coefficient is

$$k^2 = 1 + \frac{\kappa^2}{\gamma^2}(1 - e^{-2\gamma t})^2 + \frac{2\kappa}{\gamma}(1 - e^{-2\gamma t}). \tag{22}$$

From this expression, one can see that squeezing coefficient $k^2 > 1$ ($e^{-2\gamma t} < 1$), for $t > 0$ and $\gamma > 0$. The squeezing can not be obtained for free damped particle by one δ-kick of frequency.

6 Conclusion

We have considered in the frame of Caldirola-Kanai model the parametric excitation of damped oscillator and discussed the influence of different regims of damping on the possibility of appearing the squeezing phenomenon in this system. It is worthy to note that different aspects of the damped oscillator problem was considered in [7], [18]- [27]. Here the parametric excitation is choosen in the special form (δ-kick of frequency), which permits to obtain explicit expressions for squeezing coefficient and quantum coordinate dispersion for different regimes of damping. It is shown that in the region of small damping the squeezing can be obtained for all $\gamma < \omega_0$ by choosing different force of δ-kick. In the region of strong damping and for damped free particle motion, it is impossible to have squeezing phenomenon by δ kick of frequency.

Acknowledgements

The work was partially supported by Russian Basic Science Foundation (under grant N 94-02-04715). The author would like to thank the Organizers for their kind invitation to participate in the International Conference "Squeezed States and Uncertainty Relations," the University of Maryland for financial support, and Russian Basic Science Foundation for travel support.

References

[1] P. Caldirola, Nuovo Cim. **18**, 393 (1941).

[2] E. Kanai, Progr. Theor. Phys. **3**, 440 (1948).

[3] I. A. Malkin, V. I. Man'ko, and D. A. Trifonov, J. Math. Phys. **14**, 576 (1975).

[4] V. V. Dodonov, I. A. Malkin, and V. I. Man'ko, J. Theor. Phys. **14**, 37 (1975).

[5] V. V. Dodonov, O. V. Man'ko, and V. I. Man'ko, J. Sov. Laser Research (Plenum Press, New York) **13**, 196 (1992).

[6] V. V. Dodonov, O. V. Man'ko, and V. I. Man'ko, Phys. Lett. A **175**, 1 (1993).

[7] V. V. Dodonov and V. I. Man'ko, *Invariants and Evolution of Nonstationary Quantum Systems*, Proceedings of Lebedev Physical Institute, **183** (Nova Science, New York, 1989).

[8] R. J. Glauber, in: *Quantum Measurements in Optics*, eds. P. Tombesi and D. F. Walls (Plenum Press, New York, 1992).

[9] G. S. Agarwal and S. A. Kumar, Phys. Rev. Lett. **67**, 3665 (1991).

[10] L. S. Brown, Phys. Rev. Lett. **66**, 527 (1991).

[11] Y. S. Kim and V. I. Man'ko, Phys. Lett. A **157**, 226 (1991).

[12] C. F. Lo, Phys. Lett. A **162**, 299 (1992).

[13] O. V. Man'ko and Leehwa Yeh, Phys. Lett. A **189**, 268 (1994).

[14] G. Schrade, V. I. Man'ko, W. P. Schleih, and R. J. Glauber, Quantum Semiclass. Opt. **7**, 307 (1994).

[15] I. Averbukh, B. Sherman, and G. Kurizki, Phys. Rev. A **50**, 5301 (1994).

[16] T. Kiss, P. Adam, and J. Janszky, Phys. Lett. A **192**, 311 (1994).

[17] D. J. Fernandez C., B. Mielnik, J. Math. Phys. **35**, 2083 (1994); B. Mielnik, J. Math. Phys. **27**, 2290 (1986).

[18] R. W. Hasse, J. Math. Phys. **16**, 2005 (1975).

[19] L. H. Buch and H. H. Denman, Amer. J. Phys. **42**, 304 (1974).

[20] V. W. Myers, Amer. J. Phys. **27**, 507 (1959).

[21] P. Caldirola and A. Lugiato, Physica A **116**, 248 (1982).

[22] I. R. Svin'in, Teor. Mat. Fiz. **27**, 270 (1976) [in Russian].

[23] A. Jannussis, N. Patargias, and G. Brodimas, J. Phys. Soc. Japan **45**, 336 (1978).

[24] H. Dekker, Phys. Repts. **80**, 1, (1981).

[25] K. H. Yeon, C. I. Um, W. H. Kahng, and T. F. George, Phys. Rev. A **38**, 6224 (1989).

[26] J. Aliaga, J. L. Gruver, A. N. Proto, and N. A. Cerdeira, Phys. Lett. A **185**, 355 (1994).

[27] H. S. Abdalla and R.K.Collegrave, Phys. Lett. A **181**, 311 (1993).

NEXT
DOCUMENT

EXPONENTIAL FORMULAE AND EFFECTIVE OPERATIONS

Bogdan Mielnik
Departamento de Física, CINVESTAV
A.P. 14-740, 07000 México D.F., MEXICO
and
Institute of Theoretical Physics, Warsaw University
Warszawa, ul. Hoża 69, POLAND

David J. Fernández C.
Departamento de Física, CINVESTAV
A.P. 14-740, 07000 México D.F., MEXICO

Abstract

One of standard methods to predict the phenomena of squeezing consists in splitting the unitary evolution operator into the product of simpler operations (Yuen [1], Ma and Rhodes [2]). The technique, while mathematically general, is not so simple in applications and leaves some pragmatic problems open. We report an extended class of exponential formulae, which yield a quicker insight into the laboratory details for a class of squeezing operations, and moreover, can be alternatively used to programme different type of operations, as: 1) the free evolution inversion, 2) the soft simulations of the sharp kicks (so that all abstract results involving the kicks of the oscillator potential, become realistic laboratory prescriptions).

1 The manipulation problem

Below, we shall dissent from the orthodox subject of "squeezed states" and dedicate some attention to a more general problem. Suppose, one has a quantum system whose states are represented by vectors in a Hilbert space $\mathcal{H}$. Now, choose any unitary operator

$$U : \mathcal{H} \to \mathcal{H} \tag{1}$$

Can U be achieved as a realistic evolution operation, performed under the influence of some external fields?

The problem so stated, belongs to the *quantum manipulation theory*, a domain which has progressed quickly in the last decades. The first cases of the dynamical manipulation (for a finite dimensional space of states) achieved wide publicity under the name of the *spin echo* (e.g. [3]).

The general problem of manipulation (control) of quantum states dates from the works of Lamb [4], Lubkin [5] and followers [6, 7, 8, 9, 10]. Quite independently, the subject has been put forward in quantum chemistry where it may soon become crucial [11, 12]. For an infinite dimensional $\mathcal{H} = L^2(\mathbf{R})$ some dynamical operations present a considerable challenge but only one of them has become a "conference subject". We of course refer to the *operation of squeezing*:

$$U = e^{(za^{\dagger 2} - z^* a^2)/2} \qquad \text{(general squeezing)} \qquad z \in \mathbf{C} \tag{2}$$

and/or

$$U = e^{\imath\lambda(qp+pq)/2} \qquad \text{(scale transformation, coordinate squeezing)} \qquad \lambda \in \mathbf{R} \tag{3}$$

Note, that there are several concepts of squeezing in the literature. By choosing (2-3) we ask about the "operatorial squeezing", i.e. the shape transformation which affects all wave packets alike, independently on their initial form. Thus, under the influence of (3) the canonical observables q, p are transformed into

$$\begin{aligned} U^\dagger q U &= e^{-\lambda} q \\ U^\dagger p U &= e^{\lambda} p \end{aligned} \tag{4}$$

and simultaneously all the wave packets $\psi = \{\psi(x)\}$ are deformed as:

$$(U\psi)(x) = \sqrt{k}\, \psi(kx), \quad k = e^{\lambda} \tag{5}$$

As found by Yuen [1], the simplest method of producing such effects in $L^2(\mathbf{R})$ consists in application of variable oscillator potentials with the time dependent Hamiltonians:

$$H(t) = \frac{p^2}{2} + \omega(t)^2 \frac{q^2}{2}; \quad [q, p] = \imath \tag{6}$$

and the most explicit illustrations of this fact can be found in the *exponential formulae*, which express the evolution operator $U(t)$ [generated by (6)] as the product of simpler exponential operations.

The very subject of the exponential identities has already some antiquity, starting from the papers of Zassenhaus, Baker, Campbell and Haussdorff (BCH) [13]. However, the exponential identities of BCH type involve infinite series and do not offer closed solutions. The key to the techniques of squeezing are the following formulae of Yuen [1] and Ma and Rhodes [2], which might be interpreted as *exactly soluble cases* of BCH and Zassenhauss. If no linear terms in $H(t)$ are present, they read:

$$U(t) \equiv e^{B(t)a^{\dagger 2}} e^{\Omega(t)a^\dagger a} e^{E(t)a^2} \qquad \text{(Yuen, 1976)} \tag{7}$$

and

$$U(t) \equiv e^{[z(t)a^{\dagger 2} - z^*(t)a^2]/2} e^{-i\alpha(t)a^\dagger a} \qquad \text{(Ma and Rhodes, 1988)} \qquad (8)$$

where $B(t)$, $\Omega(t)$, $E(t)$, $z(t)$, $\alpha(t)$ are c-number coefficients and $\equiv$ means the proporcionality of the unitary operators ($U \equiv U' \Rightarrow U = e^{i\alpha}U'$, $\alpha \in \mathbf{R}$). These identities precisely provide the proof that the variable oscillator potentials (more generally: quadratic, time dependent Hamiltonians) can produce the effects of squeezing (2) (or the scale transformation (3)). A particularly simple identity for two oscillator Hamiltonians $H_j = p^2/2 + \omega_j^2 q^2/2$ acting during two time lapses τ_1, τ_2, was detected by Grübl [14]. If the time intervals τ_1, τ_2 are in adequate proportion to the frequencies ω_1, ω_2 (e.g., $\omega_1\tau_1 = \pi/2$, $\omega_2\tau_2 = 3\pi/2$), then:

$$e^{i\lambda(qp+pq)/2} \equiv e^{-i\tau_2 H_2} e^{-i\tau_1 H_1}, \qquad (9)$$

where $\lambda = \ln \omega_2/\omega_1$. (Note, that Grübl had no confidence to the operatorial formulae. He has proved (9) implicitely, working with Gaussian packets).

While mathematically complete, (7-8) are not quite easy to apply, due to involved systems of non-linear equations for the c-number coefficients. This explaines a quick development of alternative methods derived from evolution matrices or adiabatic invariants [15, 16]. Yet, the "damped oscillator" of 1940 [17], and the "step-Hamiltonian" of Grübl (9) remain the principal cases solved with all numerical details.

It will be our purpose to show that the trend of the algebraic identities (7- 8) is not at all exhausted! To the contrary, appart of (7-8), it can provide a class of "easy formulae" for the squeezing and for more general control operations.

2 The spin echo without spin

The first "easy formula" (accidentally detected in 1977 [6]) has the form of the "circular identity":

$$\underbrace{e^{-ip^2/2} e^{-iq^2/2} e^{-ip^2/2} \ldots e^{-iq^2/2}}_{\text{12 terms}} \equiv 1 \qquad (10)$$

for the operators q, p in $L^2(\mathbf{R})$, with $[q,p] = i$. Note, that all signs in the exponents are the same: the product (10) is therefore simpler than it could be in the classical case! The formula (10) has an elementary operational sense. Every operator $\exp[-ip^2/2]$ represents the free evolution per unit time of the Schrödinger's particle in $L^2(\mathbf{R})$. Every $\exp[-iq^2/2]$ is the unitary evolution operation caused by infinitely sharp and quick pulse of time dependent oscillator potential (the "δ-like kick" of the ellastic force):

$$e^{-iq^2/2} = \lim_{\epsilon \to 0} e^{-i\epsilon[p^2/2 + \epsilon^{-1}q^2/2]} \qquad (11)$$

The identity (10) describes a dynamical "evolution loop": the wave packet in $L^2(\mathbf{R})$, manipulated by 6 oscillator kicks and 6 free evolution intervals must return to its initial state (no matter what this state was!). This might be illustrated by the following closed diagramme:

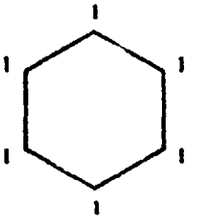

whose sides simbolize the free evolution intervals and vertices the oscillator kicks. An immediate consequence of (10) is:

$$e^{+ip^2/2} = \underbrace{e^{-iq^2/2}e^{-ip^2/2}\ldots e^{-ip^2/2}e^{-iq^2/2}}_{11} \tag{12}$$

The right hand side represesents a sequence of admissible dynamical events (6 kicks and 5 rest intervals), while the left one is the operator inverse to the free evolution. The formula (12) thus tells how to invert the free evolution. Since (12) is an operator identity, the prescription can be applied "in blind": every wave packet in $L^2(\mathbf{R})$, entertained by 11 dynamical events must "go back in time", returning to its past shape, no matter what this shape was [8]. (Compare "Particle Memory" of Brewer and Hahn [18].)

After some consideration, the formula (10) looses a part of mystery: it is just a "discrete imitation" of the oscillator force (the oscillator potential acts only in selected time moments, producing nonetheless a closed dynamical process). Note however the existence of other "circular identities" [8]:

$$\underbrace{e^{-ip^2/2}e^{-i\sqrt{3}q^2/2}e^{-ip^2/2}e^{+i\sqrt{3}q^2/2}\ldots e^{+i\sqrt{3}q^2/2}}_{12} \equiv 1 \tag{13}$$

The left hand side represents a sandwich of the 3 attractive and 3 repulsive pulses interrupted by 6 free evolution intervals. One might expect that the attractive and repulsive shocks will cancel "in average", producing a zig-zag equivalent of the free evolution. However, it is not the case. The whole sequence traps the Schrödinger's packets into a closed dance, with the evolution operator $\equiv 1$ Note furthermore:

$$\left(e^{-ip^2/2}e^{-iq^2}\right)^4 \equiv 1, \quad \text{(4 shocks, 4 free evolutions)} \tag{14}$$

Both formulae (13-14) can be illustrated by graphs:

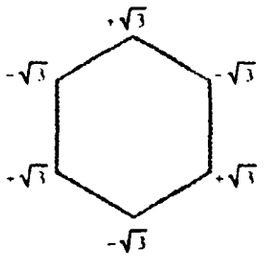

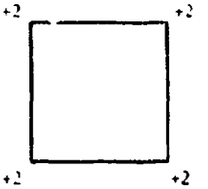

The simplest loop in $L^2(\mathbf{R})$ must involve at least 3 kicks and 3 rest intervals; its general form is:

$$e^{-i\gamma p^2/2}e^{-i\alpha\Gamma q^2/2}e^{-i\beta p^2/2}e^{-i\gamma\Gamma q^2/2}e^{-i\alpha p^2/2}e^{-i\beta\Gamma q^2/2} \equiv 1 \qquad (15)$$

$$\Gamma = \frac{\alpha+\beta+\gamma}{\alpha\beta\gamma}$$

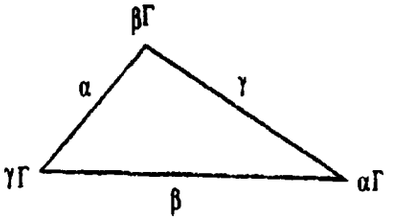

Its "incomplete version":

$$e^{+i\gamma p^2/2} \equiv e^{-i\alpha\Gamma q^2/2}e^{-i\beta p^2/2}e^{-i\gamma\Gamma q^2/2}e^{-i\alpha p^2/2}e^{-i\beta\Gamma q^2/2} \qquad (16)$$

permits one to manipulate the free evolution at will. Thus, for $\alpha, \beta, \gamma > 0$, (16) provides a prescription of how to enforce the Schrödinger's wave packet to "go back in time", whereas for $\gamma < 0$, $\alpha, \beta > 0$ one obtains a "time machine" able to slow or accelerate the free evolution [8, 10].

The loop formulae are the obvious analogue of the spin-echo for non-spin states. As far as we could check, the possibility of the (non-adiabatic) loop effects in $L^2(\mathbf{R})$ was first predicted in 1970 (by reinterpreting the transparency phenomenon of the potential wells; see Malkin and Man'ko [19], p. 388), though the subject was later pursued in a different direction. The first kicked system was considered in 1977 [6] and the manipulation of quantum states by potential pulses systematically studied since 1986 [8, 9, 10].

The exponential identities suggest also how to generate the *scale transformation*. The simplest formula requires again a pair of oscillator pulses of different amplitudes:

$$e^{-i\lambda p^2/2}e^{-i(1+1/\lambda)q^2/2}e^{-ip^2/2}e^{-i(1+\lambda)q^2/2} \equiv e^{i\ln\lambda(qp+pq)/2}\,\mathbf{P} \qquad (17)$$

and produces the scale transformation superposed with parity ($\mathbf{P}$). The repetition of the operator sequence of (17) yields the genuine squeezing (without parity: one of the simplest cases of Brown and Carson algorithm [20]). Some more general scenarios for the squeezing operation (2) (multiple kicks on a background of a constant ellastic force) are recently studied [21].

3 Evolution control in three dimensions

All these techniques concern the Schrödinger's particle in 1 space dimension and are, in fact, only an abstract introduction to physically important problems. It is thus essential to find their analogues in 3 space dimensions. Some results can be already reported.

In the first place, the sequences of sign changing kicks [e.g. (13-14)] can be used to construct sequences of *harmonic pulses* in $\mathbf{R}^3$ generating the loop effect in $L^2(\mathbf{R}^3)$ [8]. This suggests, that the loop effect (state echo) in $\mathbf{R}^3$ might be produced, in principle, by shock waves of *source free external fields*. As the matter of fact, some closed dynamical processes can be induced even *without* any kicks, by a source free, stationary field of an adequately gauged ion trap [9]. A simple scenario of additional potential kicks (electric pulses applied to the trap walls) permits then to generate effects of squeezing upon the charged wave packet retained in the trap interior (see the report by one of us [9]).

What no less important, the effects of positive (attractive) oscillator potentials in $L^2(\mathbf{R})$ traduce themselves immediately into effects of homogeneous magnetic fields in 3 space dimensions. As an example, we have considered a quite simple sequence of identically shaped magnetic pulses in three orthogonal directions: $\mathbf{n}, \mathbf{m}, \mathbf{s}, \mathbf{n}, \mathbf{m}, \mathbf{s} \cdots$. As we have reported on the previous IWSSUR 93, an adequate proportion between time separations and the pulse intensity assures that the sequence must produce the loop effect for the wave packets in $L^2(\mathbf{R}^3)$. Moreover, the same operational scheme, with differently shaped pulses, turns out to work as a "time machine", permitting to accelerate, slow or invert the free evolution operation of the Schrödinger's wave packet [10].

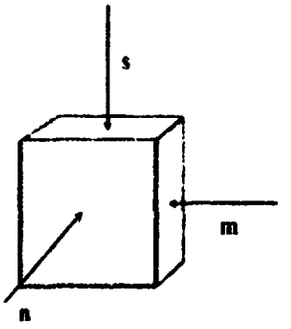

A sequence of homogeneous magnetic pulses from 3 orthogonal directions permits to manipulate the free evolution (see our report in IWSSUR 93).

4 The general manipulation scheme

The most immediate reason why one might be interested in the "evolution loops" is the possibility of controlling the fuzziness (diffraction of the wave packets due to its free evolution), essential for

electronic microscopy, programming the non-demolishing measurements etc. (see also Caves et al. [22], Yuen [23], Royer [24]). Also, the original subject of the transparent wells [19] might still bring some surprises [25]. However, the loop phenomenon seems most crucial for the general manipulation methodology.

The class of the dynamical operations induced by stationary fields is rather narrow (for the Schrödinger's particle they are always of the form $\exp[-tH]$ where the exponent H is at most quadratic in $\mathbf{p}$!).

The situation is more interesting for a microobject trapped in an oscillating field of an evolution loop. As long as the loop fields are mantained, the wave packets perform a "periodic dance". A distinct phenomenon occurs, if the loop fields are perturbed or imperfect. Instead of a closed process, the system will then perform, after every loop period τ, a non trivial unitary operation, interpretable as the *loop precession*.

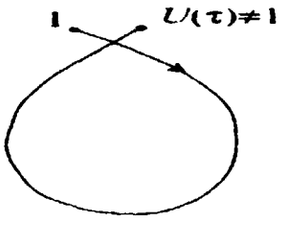

The precession of a distorted loop:
a natural key to the manipulation.

An elementary algebraic argument shows that the precession operations are much more general than the operations stimulated by the stationary fields. In fact, they are the key to solve the manipulation problem: by "adding precessions" an arbitrary unitary operation $U : \mathcal{H} \to \mathcal{H}$ can be approximated [8]. In some cases, already an unsophisticated distortion of the "circular processes" brings interesting results (like e.g. the squeezing or free evolution distortion in "wrong loops"). In principle, every one of the "circular identities" (10.13-15) is a natural starting point for some manipulation procedures solving the inverse evolution problem (1). With one little ammendment, however.

5 The "soft kicks"

The "ellastic kicks", while of undeniable *illustrative* value, are not so easily accessible in laboratories. The difficulty is almost anecdotic if the "δ-like kick" has to be engineered with the help of homogeneous magnetic field acting e.g. inside of a cillindrical solenoid. Since $\omega^2(t)$ of the resulting "magnetic oscillator" is proportional to $B(t)^2$ [10], (where $B(t)$ is the magnetic field intensity), the $B(t)$ in the solenoid would have to model the square root of the Dirac's δ. The request might be promising for the theory of non-linear distributions, but is a nightmare in the laboratory! (Assuming even that the laboratory team would dominate the techniques of approaching $\sqrt{\delta(t)}$, the

radiative corrections would probably spoil the effects of the operation).

What one needs are the *soft analogues* of oscillator kicks (11), and they are not so difficult to programme with the help of exponential formulae. Below, we shall report a quite simple "exponential experiment".

Consider first of all the product of three operators:

$$W = e^{i\lambda(qp+pq)/2} e^{-i\gamma q^2/2} e^{-i\alpha(p^2+q^2)/2} \tag{18}$$

Let's ask the question: can one choose λ, γ, α to be three functions of time in such a way that the product W fulfills a physically interpretable evolution equation

$$\frac{dW}{dt} = -iH(t)W(t) \tag{19}$$

with $H(t)$ having the oscillator form (6)? To simplify the problem, we shall first determine λ and γ as functions of α, $\lambda = \lambda(\alpha)$ and $\gamma = \gamma(\alpha)$, and only afterwards we shall look for $\alpha = \alpha(t)$. Each term in (18) is easily differentiable:

$$i\frac{dW}{d\alpha} = \left(-\dot{\lambda}(\alpha)\frac{qp+pq}{2} + \gamma(\alpha)e^{i\lambda\frac{qp+pq}{2}}\frac{q^2}{2}e^{-i\lambda\frac{qp+pq}{2}} + \right.$$
$$\left. + e^{i\lambda\frac{qp+pq}{2}} e^{-i\gamma\frac{q^2}{2}} H_0 e^{i\gamma\frac{q^2}{2}} e^{-i\lambda\frac{qp+pq}{2}} \right) W(\alpha) \tag{20}$$

where $H_0 = p^2/2 + q^2/2 = a^\dagger a + 1/2$. Due to the transformation rule (4) and:

$$e^{-i\gamma\frac{q^2}{2}} H_0 e^{i\gamma\frac{q^2}{2}} = \frac{(p+\gamma q)^2}{2} + \frac{q^2}{2} \tag{21}$$

one easily finds:

$$i\frac{dW}{d\alpha} = \mathcal{H}(\alpha)W(\alpha) = \left((-\dot{\lambda} + \gamma)\frac{qp+pq}{2} + e^{-2\lambda}\frac{p^2}{2} + (\dot{\gamma} + \gamma^2 + 1)e^{2\lambda}\frac{q^2}{2} \right) W(\alpha) \tag{22}$$

To assure that the term with $(qp + pq)/2$ vanish it suffices to put

$$\gamma(\alpha) = \lambda(\alpha) \tag{23}$$

thus obtaining:

$$\mathcal{H}(\alpha) = e^{-2\lambda}\frac{p^2}{2} + (\dot{\gamma} + \gamma^2 + 1)e^{2\lambda}\frac{q^2}{2} \tag{24}$$

If now $\alpha = \alpha(t)$, the differential equation for W in terms of t reads:

$$\frac{dW}{dt} = \left(\frac{d\alpha}{dt}\right)^{-1} \mathcal{H}(\alpha)W(t). \tag{25}$$

and if in addition $\alpha(t)$ is determined by:

$$\frac{d\alpha}{dt} = e^{2\lambda(\alpha)} \tag{26}$$

then (25) acquires the familiar form:

$$\frac{dW}{dt} = \left[\frac{p^2}{2} + g(t)\frac{q^2}{2}\right] W(t) \tag{27}$$

where $\alpha(t)$ is given by (26) and

$$g(t) = (\gamma + \gamma^2 + 1)e^{4\lambda(\alpha(t))} \tag{28}$$

If now $W(t)$ satisfies (27), then $U(t) = W(t)W(0)^{-1}$ solves the evolution problem (6) with $\omega(t)^2 = g(t)$ and with the initial condition $U(0) = 1$

Adopting $\lambda(\alpha)$ defined in $[0, 2\pi]$ as our arbitrary "manipulation function", we can model at will the desired properties of $W(t)$ [and consistently, of $U(t)$]. Thus, if $\lambda(0) \neq \lambda(2\pi)$ but $\dot{\lambda}(0) = \dot{\lambda}(2\pi)$, U at $\alpha = 2\pi$ becomes the scale operator of form (4) and the function $g(t)$ defined by (28) gives the prescription of how the effect can be generated. If, however, $\lambda(0) = \lambda(2\pi)$ but $\gamma_1 = \dot{\lambda}(2\pi) \neq \dot{\lambda}(0) = 0$, the same product (18) reduces to the single non trivial term

$$W(t) = e^{-i\gamma_1 q^2/2} \tag{29}$$

and henceforth, U imitates the effects of the δ-like kick of the oscillator force. As an example, we report two simple computer simulations where the manipulation function $\lambda(\alpha)$ yields either the "soft imitation" of the oscillator kick or the coordinate squeezing (see below). It seems pertinent to notice, that if an authentic kick were to be applied in the laboratory e.g. by creating a very short and sharp magnetic pulse, then in the first place it could never be exact (nor well approached: the δ-functions are not truly accessible in labs!) In our scenario below, this difficulty is absent:

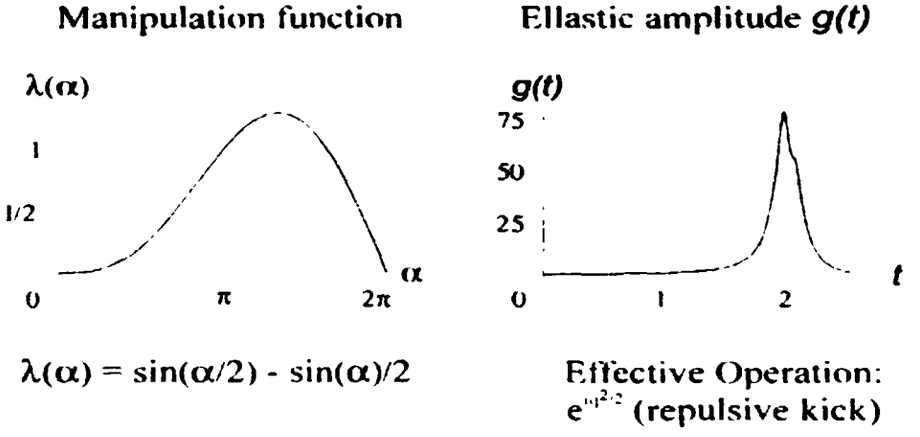

The kick effect can be exact (produced with unlimited accuracy), even if negative, and is achieved by *softly varying fields* awaking little radiative response. By the same, all previous results involving the oscillator kicks [6-9,23] can be interpreted as realistic laboratory prescriptions. Note also the squeezing scenario based on the same formula (18):

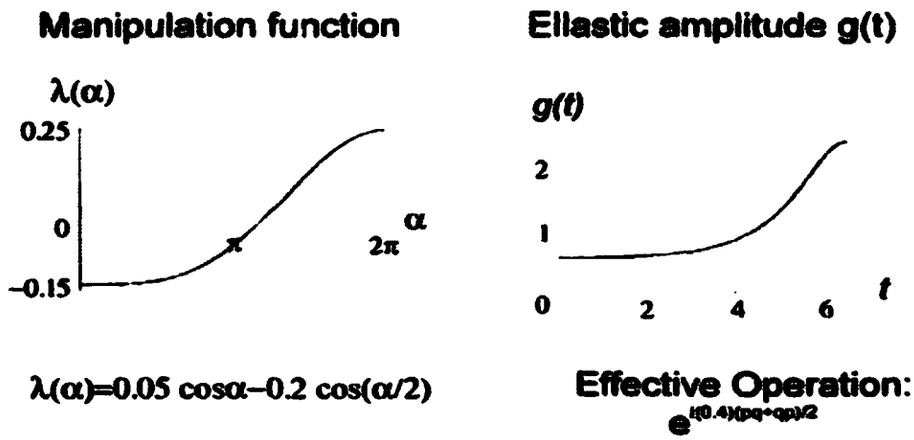

The shape of $g(t)$ agrees with the observation that the squeezing is caused by an increase of the ellastic constant [14, 17].

The story does not end up here; it hardly starts. The method of distorted loops makes possible much more sophisticated manipulations of quantum degrees, which will be probably the daily routine of the experimental physics in a predictable future.

Acknowledgments

The authors are grateful to the conference organizers for their warm hospitality in Shanxi, China, June 1995. The support of CONACYT, México, is acknowledged.

References

[1] H.P. Yuen, Phys. Rev. **A 13**, 2226 (1976).

[2] X. Ma and W. Rhodes, Phys. Rev. **A 39**, 1941 (1988).

[3] E.L. Hahn, Phys. Rev. **80**, 580 (1950).

[4] W.E. Lamb Jr., Phys. Today **22**(4), 23 (1969).

[5] E. Lubkin, J. Math. Phys. **15**, 663 (1974); **15**, 673 (1974).

[6] B. Mielnik, Rep. Math. Phys. **12**, 331 (1977).

[7] J. Waniewski, Commun. Math. Phys. **76**, 27 (1980).

[8] B. Mielnik, J. Math. Phys. **27**, 2290 (1986).

[9] D.J. Fernández C., Nuovo Cim. **107B**, 885 (1992).

[10] D.J. Fernández C. and B. Mielnik, J. Math. Phys. **35**, 2083 (1994); see also Proc. IWSSUR, NASA Conference Publ. 3270 (1994), pp. 173-178.

[11] P. Brumer and M. Shapiro, Annu. Rev. Phys. Chem. **43**, 257 (1992) and the litterature cited there; see also Sci. Am. **272**, 34 (March 1995).

[12] P. Brumer, private letter, June 1994.

[13] J.E. Campbell, Proc. London Math. Soc. **29**, 14 (1898); H.F. Baker, Proc. London Math. Soc. **34**, 347 (1902); F. Hausdorff, Ber. Verhandl. Saechs. Acad. Wiss. Leipzig, Math. Naturwis. Kl. **58**, 19 (1906).

[14] G. Grübl, J. Phys. **A37**, 2985 (1988).

[15] H.R. Lewis and W.B. Riesenfeld, J. Math. Phys. **10**, 1458 (1969).

[16] A. Malkin, V.I. Man'ko and D.A. Trifonov, Phys. Rev. **D2**, 1371 (1970); J. Math. Phys. **14**, 576 (1973).

[17] P. Caldirola, Nuovo Cimento **18**, 393 (1941); **B 77**, 241 (1983); E. Kanai, Prog. Theor. Phys. **3**, 440 (1940).

[18] R.G. Brewer and E.L. Hahn, Sci. Am. **251**(12), 50 (1984).

[19] I.A. Malkin and V.I. Man'ko, Sov. Phys. JETP **31**, 386 (1970).

[20] L.S. Brown and L.J. Carson, Phys. Rev. A **20**, 2486 (1979).

[21] O.V. Man'ko and L. Yeh, Phys. Lett. A **189**, 268 (1994).

[22] C.M. Caves, K.S. Thorne, R.W.P. Drever, V.D. Sandberg and M. Zimmermann, Rev. Mod. Phys. **52**, 341 (1980).

[23] H.P. Yuen, Phys. Rev. Lett. **51**, 719 (1983).

[24] A. Royer, Phys. Rev. A **36**, 2460 (1987).

[25] V.I. Man'ko, private discussion, Gua Shan temple, Shanxi, June 1995.

NEXT
DOCUMENT

THE GENERAL NECESSARY CONDITION FOR THE VALIDITY OF DIRAC'S TRANSITION PERTURBATION THEORY

Nguyen Vinh Quang
Institute of Physics
P.O.Box 429 Boho, Hanoi 10000, Vietnam

Abstract

For the first time, from the natural requirements for the successive approximation the general necessary condition of validity of the Dirac's method is explicitly established. It is proved that the conception of "the transition probability per unit time" is not valid. The "super-platinium rules" for calculating the transition probability are derived for the arbitrarily strong time-independent perturbation case.

1 Introduction

The problem of calculating the probability of a transition caused by a small perturbation was considered by P.A.M.Dirac in 1926 [1] . The validity condition of the Dirac's theory for the case of the constant in time perturbation is that the acting time must be not too large. In an application of the theory the coupling parameter or the interaction constant often plays a role of the perturbation coefficient. Naturally, it is very valuable to clarify the relationship between the perturbation coefficient and the time range, in which the theory is valid.

In this paper the problem is solved: the general necessary condition of validity is established as a explicit function of the perturbation coefficient. By deriving the exact formulae we show that the conception of "the transition probability per unit time" always is not valid.

2 Theory

Let us now analyze the Dirac's method in detail. For calculating the transition probability one has to solve the Schrödinger equation:

$$i\hbar\frac{\partial\Psi(\vec{r},t)}{\partial t} = \hat{H}\,\Psi(\vec{r},t) \tag{1}$$

$$\hat{H} \equiv \hat{H}_0 + \varepsilon\hat{V}(t) \qquad : \quad 0 < \varepsilon < 1$$

with the initial condition:

$$\Psi(\vec{r},t=0) = \varphi_s(\vec{r}) \tag{2}$$

where

$$\hat{H}_0 \varphi_n(\vec{r}) = E_n^{(0)} \varphi_n(\vec{r}) \quad . \tag{3}$$

First, consider the discrete spectrum case [1]. The transition probability W_{if} from state φ_i to φ_f is $| a_f(t) |^2$ where

$$\Psi(\vec{r}, t) = \sum_f a_f(t) \varphi_f(\vec{r}, t) \quad . \tag{4}$$

The equation defining $a_f(t)$ is [2]:

$$i\hbar \dot{a}_f(t) = \varepsilon \sum_k V_{fk}(t) e^{i\omega_{fk}t} a_k(t) \tag{5}$$

or in the integral form is :

$$i\hbar a_f(t) = i\hbar \delta_{if} + \varepsilon \int_0^t dt_1 \sum_k V_{fk}(t_1) e^{i\omega_{fk}t_1} a_k(t_1) \tag{6}$$

where

$$V_{fk}(t) \equiv \int d^3\vec{r} \varphi_f^*(\vec{r}) \hat{V}(t) \varphi_k(\vec{r}) \quad ; \quad \omega_{fk} \equiv \frac{E_f^{(0)} - E_k^{(0)}}{\hbar} \quad . \tag{7}$$

The $a_f(t)$ is expressed in the form [2]:

$$\begin{aligned} a_f(t) &= a_f^{(0)} + \varepsilon a_f^{(1)}(t) + \varepsilon^2 a_f^{(2)}(t) + \ldots \\ a_f^{(0)} &= \delta_{if} \\ a_f^{(1)}(0) &= a_f^{(2)}(0) = \ldots = 0 \quad . \end{aligned} \tag{8}$$

At this stage we have to make the first remark. It is natural that the successive approximation will make sense only if the following question is answered: What ε-order is the contribution of the neglected part less than ? It is evident that $a_f^{(n)}(t)$ takes part in the transition probability:

$$W_{if} = | a_f^{(0)} |^2 + \varepsilon (a_f^{(0)} a_f^{(1)*} + a_f^{(0)*} a_f^{(1)}) + \varepsilon^2 (a_f^{(0)} a_f^{(2)*} + a_f^{(0)*} a_f^{(2)} + | a_f^{(1)} |^2) + \ldots \tag{9}$$

at terms containing ε^p with $p \geq n$. After n steps have been carried out, in order that the contribution of the neglected part is less than $\varepsilon^{(n-1)}$, $| a_f^{(n)}(t) |$ must be of zero-order of ε. Consequently, the numerical value $| F^{(n)}(t) |_N$ of a time-dependent part $F^{(n)}(t)$ of $a_f^{(n)}(t)$ must be less than ε^{-1}. Inserting (8) into (6) one gets:

$$\begin{aligned} &i\hbar (\delta_{mi} + \varepsilon a_m^{(1)}(t) + \varepsilon^2 a_m^{(2)}(t) + \ldots) = \\ &\quad i\hbar \delta_{mi} + \varepsilon \sum_k \int_0^t dt_1 V_{mk}(t_1) e^{i\omega_{mk}t_1} (\delta_{ki} + \varepsilon a_k^{(1)}(t_1) + \varepsilon^2 a_k^{(2)}(t_1) + \ldots) \quad . \end{aligned} \tag{10}$$

Considering $\varepsilon \hat{V}$ as a small quantity of the first order of ε (*i.e* $\hat{V}$ as a zero-order quantity) and " equating terms of the same order " [1], one gets[1]

$$\begin{aligned} i\hbar \varepsilon a_m^{(1)}(t) &= \varepsilon \int_0^t dt_1 V_{mi}(t_1) e^{i\omega_{mi}t_1} \\ i\hbar \varepsilon^p a_m^{(p)}(t) &= \varepsilon^p \sum_k \int_0^t dt_1 V_{mk}(t_1) e^{i\omega_{mk}t_1} a_k^{(p-1)}(t_1) \quad . \end{aligned} \tag{11}$$

[1] From mathematical point of view the group scale $\{ \varepsilon^n \}$ with n being integers is chosen for comparing the terms.

In all of these expressions, the summations are extended over all the eigenfunctions of $\hat{H}_0$.

At this stage we have to make the following remarks: 1.Each side of Eq.(10) has infinite number of terms; the set (11) has infinite number of the equations. 2.Because of the term value is changed in time, the term order may be changed. Therefore "equating terms of the same order " is not always equivalent to " equating terms containing the factor ε of the same order ", in geting (11) one has made actually the latter. 3.For separating (10) into (11) by doing so the following conditions are necessary:

i) The modulus of both sides in every equation of set (11) must be of the same order.

ii) The modulus of the right-hand sides in different equations of set (11) must be of different order, *i.e.* in Eq.(10) the modulus of the terms containing the factor ε of different order must be of different one. Therefore at any time $| F^{(n)}(t) |_N$ must not change their order relation determined by one between their factors $\{ \varepsilon^n \}$. This means that

$$| F^{(n)}(t) |_N < \varepsilon^{-1} \quad \text{for any } n. \tag{12}$$

This condition is in similar but rather deep sence as discussed by Bogoliubov and Mitropolski [3].

Consider now the case when $\hat{V}$ is time-independent. Denoting by I the set of all of the states of energy E_i, *etc*, from Eq.(11) we obtain ($i_\alpha \in I$; $m \notin I$):

$$\begin{aligned}
a_{i_\alpha}^{(1)}(t) &= (-\frac{i}{\hbar}) V_{i_\alpha i} t \\
a_m^{(1)}(t) &= (-\frac{i}{\hbar}) V_{mi} \frac{e^{i\omega_{mi} t} - 1}{i\omega_{mi}} \\
a_{i_\alpha}^{(2)}(t) &= \left(-\frac{i}{\hbar}\right)^2 \left\{ \left(\sum_{i_\beta \in I} V_{i_\alpha i_\beta} V_{i_\beta i} \right) \frac{t^2}{2} + \sum_{n \notin I} V_{i_\alpha n} V_{ni} \left[\frac{t}{i\omega_{ni}} + \frac{(e^{i\omega_{ni} t} - 1)}{\omega_{ni}^2} \right] \right\} \\
a_m^{(2)}(t) &= \left(-\frac{i}{\hbar}\right)^2 \left\{ \sum_{n \notin (M \cup I)} V_{mn} V_{ni} \frac{1}{i\omega_{ni}} \left[\frac{e^{i\omega_{mi} t} - 1}{i\omega_{mi}} - \frac{e^{i\omega_{mn} t} - 1}{i\omega_{mn}} \right] \right. \\
&\quad \left. + \sum_{i_\alpha \in I} V_{mi_\alpha} V_{i_\alpha i} \left[t \frac{e^{i\omega_{mi} t}}{i\omega_{mi}} - \frac{e^{i\omega_{mi} t} - 1}{(i\omega_{mi})^2} \right] + \sum_{m_\beta \in M} V_{mm_\beta} V_{m_\beta i} \frac{1}{i\omega_{mi}} \left[\frac{e^{i\omega_{mi} t} - 1}{i\omega_{mi}} - t \right] \right\}
\end{aligned} \tag{13}$$

It should be noted that in the expression of $a_m^{(3)}$: $m \notin I$ the terms in which the two summation indexes get equal values (*i.e.* the terms with $V_{mk} V_{kk} V_{kj}$, $k \notin J$, $k \; not \in M$) also contain the factor t, *etc*. This means that $a_f^{(n)}(t) with \; n \geq 2$, always contain the secular terms [3].

The general form of $F^{(n)}(t)$ is

$$F^{(n)}(t) = \int_0^t \int_0^{t_1} \cdots \int_0^{t_{n-1}} dt_1 \ldots dt_n \; \exp\{i(\gamma_1 t_1 + \ldots + \gamma_n t_n)\}. \tag{14}$$

where γ_n is real for any n. It is easy to see [4] that

$$| F^{(n)}(t) | \leq \frac{t^n}{n!} \tag{15}$$

The maximal value of $| F^{(n)}(t) |$ corresponds to the transition , in which the final and all of the intermediate states have the same energy as the initial one. Hence the general necessary condition

of validity (Eq.(12)) leads to (τ denotes the numerical value of t)

$$\tau < \tau_l \equiv \min\left\{(n!\varepsilon^{-1})^{\frac{1}{n}}\right\} \qquad n = 1,2,\ldots\infty \ , \tag{16}$$

i.e. the action time of the time-independent perturbation must be less than the limiting value, which is an explicit function of the perturbation coefficient. For example, when $\varepsilon = \frac{1}{137}$ in the system of units with $\hbar = c = 1$ we get $t_l < 2.4 \times 10^{-10} sec$. Hence the time range in which the Dirac's method is valid is ultra-short.

The condition (16) is quite general, purely mathematical and independent of the fact whether the perturbation is turned on suddenly or adiabatically. The time $t = 0$ is namely the moment, from which the perturbation could be considered as constant in time.

In the continuous spectrum case, by repeating the formalism just developed above, it is not difficult to obtain directly the same condition.

This condition is also the necessary one of validity for an arbitrarily time-dependent perturbation case because the time-independent perturbation case is its particular one.

It must be emphasized that when the group scale $\{\varepsilon^n\}$ was chosen it is necessary to use the notions "small of some order of ε", "large of some order of ε^{-1}" *etc.* instead of the uncertain notions as "not too small and not too large", "large enough", "sufficiently small" [1,2,5]. In using the Dirac's results it is necessary to justify the existence of the validity range instead of leaning on such very uncertain statement:" There is no difficulty in satisfying both these conditions simultaneously provided the perturbing energy V is sufficiently small" [1].

Now we prove that the conception of "the transition probability per unit time" is not valid. In the time-independent perturbation case the perturbed Hamiltonian has also certain eigenvalues and the full set of the normalized stationary eigenfunctions

$$\hat{H} \mid q\rangle = E_q \mid q\rangle \ . \tag{17}$$

The initial condition (2) means that at $t = 0$ the system state $\mid t\rangle$ is $\mid i\rangle_0$ where $\langle \vec{r} \mid i\rangle_0 \equiv \varphi_i(\vec{r})$

$$\mid t = 0\rangle = \mid i\rangle_0 = \sum_q \mid q\rangle\langle q \mid i\rangle_0 \tag{18}$$

At time t the system state is:

$$\mid t\rangle = \sum_q \mid q\rangle e^{-iE_q t}\langle q \mid i\rangle_0 \ . \tag{19}$$

The probability W_{if} of a transition to $\mid f\rangle_0$ is:

$$W_{if} \equiv \mid {}_0\langle f \mid t\rangle \mid^2 = \left| \sum_q {}_0\langle f \mid q\rangle e^{-iE_q t}\langle q \mid i\rangle_0 \right|^2 \ . \tag{20}$$

The probability W_i of the transitions to the final states $\mid f'\rangle_0$ in the region Δf_0 [2] is:

$$\begin{aligned} W_i &= \int_{\Delta f_0} df' \left| \sum_q \langle q \mid i\rangle_0 e^{-iE_q t}\, {}_0\langle f' \mid q\rangle \right|^2 \\ &= \sum_{qq'} {}_0\langle i \mid q'\rangle\langle q \mid i\rangle_0 e^{-it(E_q - E_{q'})} \int_{\Delta f_0} df'\, {}_0\langle f' \mid q\rangle\langle q' \mid f'\rangle_0 \end{aligned} \tag{21}$$

It must be emphasized that these results are exact. They show that even when the perturbation is "sufficiently small"and the time t is "not too small and not too large" [1,2,5], the transition probabilities W_{if} and W_i are not proportional to t, *i.e.* it is impossible to define the conception of "the transition probability per unit time". Moreover, when t approachs infinity because of these exact results are always definite, any approximation, in which W_i, W_{if} are proportional to t, *i.e.* approach infinity, is not valid even qualitatively. In fact, this conception and the Fermi's "golden rule" [2,6] are only the consequences of the approximation used by Dirac without justifying the existence of a validity region.

The right way is the following. When Eq.(17) is one of the well-known exactly solved eigenvalue problems in Quantum Mechanics and when by using the dynamical symmetries and the integrals of the motion [7] we can solve exactly the time-dependent Schrödinger equation, the formulae (20) and (21) give the exact results immediately. When it is not so fortunate, it is possible to use the perturbation method for the eigenvalue problem [1,2,5,6] carefully (*i.e.* it is necessary to verify the validity condition at every step) for solving Eq.(17) and then to calculate the transition probability following formula (20) or (21) up to the necessary accuracy. Therefore, it is interesting to call them "the super-platinium rules".

This means that the method of expansion in power of small parameter is possible for the eigenvalue problem but is very bad for solving the time-dependent Schrödinger equation, which is in a similar situation with the one of the analyzed in [3] equations concerned with the secular terms.

The conception of "the transition probability per unit time" is not valid for the particular case and therefore, is not valid for the general case of the time-dependent perturbation either.

Since the nonrelativistic case is a particular one of the relativistic case when the particle velocity is very much less than the light velocity, this conception is not valid in the relativistic case either, consequently, in Quantum field theory,in which there are many self-inconsistences.

Thus, the carelessness of the genius laureates of Nobel prices have the negative influence on the development of the modern physics.

With a honesty and a courage of the scientist we have to see directly to the truth and together reconstruct the current physics without Dirac's conception of "the transition probability per unit time".

The author would like to thank Profs. V.I.Manko, G.C.Ghirardi and E.C.G.Sudarshan for their support.

References

[1] P.A.M.Dirac, *Principles of Quantum Mechanics* (Clarendon Press, Oxford, 1958).

[2] W.Pauli, *The General Principles of Wave Mechanics (Russian translation)* (Gos. Izd., Moscow & Leningrad, 1947).

[3] N.N.Bogoliubov and Iu.A.Mitropolski, *Asymptotic Methods in Theory of Nonlinear Oscillations (in Russian)* (Gos.Izd., Moscow, 1958).

[4] G.Korn and T.Korn, *Mathematical Handbook* (McGraw-Hill B.C., 1968).

[5] L.D.Landau and E.M.Lifshitx. *Quantum Mechanics (in Russian)* (Nauka, Moscow, 1989).

[6] E.Fermi, *Notes on Quantum Mechanics (Russian translation* (Mir, Moscow, 1965).

[7] I.A.Malkin and V.I.Manko, *Dynamical Symmetries and Coherent States of Quantum Systems (in Russian)* (Nauka, Moscow, 1979).

NEXT
DOCUMENT

NONCLASSICAL PROPERTIES OF Q—DEFORMED SUPERPOSITION LIGHT FIELD STATE

Ren Min

South China Construction University, West Campus, Guangzhou 510405

Wang Shenggui

Department of Physics, Jiujiang Teacher's College Jiujiang, 332000

Ma Aiqun

Department of Physics, Harbin College, Harbin, 150020

Jiang zhuohong

Department of Physics, Heilongjiang University, Harbin, 150080

Abstract

In this paper, the squeezing effect, the bunching effect and the anti—bunching effect of the superposition light field state which involving q—deformation vacuum state $|o\rangle_q$ and q—Glauber coherent state $|z\rangle_q$ are studied, the controllable q—parameter of the squeezing effect, the bunching effect and the auti—bunching effect of q—deformed superposition light field state are obtained.

1 Introduction

In recent years people have made progress in the research of some concrete physical problem using quantum groups $SU_q(2)$, Quantum algebra has been realized by using q — oscillator and the parametrized Fock state $|n\rangle_q$ was obtained too. From this q—Glauber coherent state $|n\rangle_q$ was introduced. Hao Sanyu[1] showed that the coherent degree can be controlled by q—deformation parameter. Zhu Chongxu[1] showed that some quantum statistical properties of q—even—odd coherent state can be coutrolled by q—parameter.

We studied the squeezing effect of q—deformed superpostion light field which involving q—deformation vaccuum state $|o\rangle_q$ and q—Glauber Coherent state $|z\rangle_q$. The results showed that the squeezing effect, the bunching effect and the anti—bunching effect can be controlled by q—parameter.

2 Nonclassical properties of q—deformed superposition Light field state.

The q—deformed superpositon Light field state is

$$|\psi\rangle_q = a|o\rangle_q + \beta|z\rangle_q \tag{1}$$

where

$$|z\rangle_q = e_q^{-\frac{1}{2}|z|^2}\sum_{n=0}^{\infty}\frac{Z^n}{\sqrt{[N]!}}|n\rangle_q \tag{2}$$

$$Z = Re^{i\varphi}, a = r_1e^{i\varphi_1}, \beta = r_2e^{i\varphi_2} \tag{3}$$

$$[X] = \frac{q^{\frac{x}{2}} - q^{-\frac{x}{2}}}{q^{\frac{1}{2}} - q^{-\frac{1}{2}}}(q \neq 1) \quad e_q^x = \sum_{n=0}^{\infty}\frac{z^n}{[N]!}, [X]! = [X]\cdot[X-1]\cdots[1] \tag{4}$$

The normalization condtion is

$$r_1^2 + r_2^2 + 2r_1r_2e_q^{-\frac{1}{2}|z|^2}\cos(\theta_1 - \theta_2) = 1 \tag{5}$$

2.1 The squeezing effect of q−deformed superposition light field state

The two orthogonal comcponets of q−deformed electromagnetic field are defined as

$$Y_1 = \frac{1}{2}(a_q^+ + a_q), Y_2 = \frac{1}{2i}(a_q^+ - a_q) \tag{6}$$

where a_q is q−annihilation operator and a_q^+ is q−creaton operator. Becacsse of $[Y_1, Y_2] = \frac{i}{2}[a_q, a_q^+]$,so we have the uncertainty relation.

$$<(\Delta Y_1)^2>_q <(\Delta Y_2)^2>_q \geqslant \frac{1}{4}|<[Y_1, Y_2]>|^2 \tag{7}$$

If the squeezing exists, then we have

$$Fi = <(\Delta Y_i)^2>_q - \frac{1}{4} < 0 \ (i = 1,2) \tag{8}$$

For q−deformed superposition light field state, we have

$$<\psi|a_q a_q^+|\psi>_q = (\alpha^* <0| + \beta^* <Z|)a_q a_q^+(\alpha|0>_q + \beta|Z>_q$$

$$= |\alpha|^2 + \beta^*\alpha e_q^{-\frac{1}{2}|z|^2} + \alpha^*\beta e_q^{-\frac{1}{2}|z|^2} + |\beta|^2 e_q^{-|z|^2}\sum_{n=0}^{\infty}\frac{|Z|^{2n}}{[n]!}[n+1] \tag{9}$$

$$<\psi|a_q^+ a_q|\psi>_q = (\alpha^* <0| + \beta^* <Z|)a_q^+ a_q(\alpha|0>_q + \beta|Z>_q)$$

$$= |\beta|^2|Z|^2 \tag{10}$$

$$<\psi|a_q|\psi>_q = (\alpha^* <0| + \beta^* <Z|)a_q^+(\alpha|0>_q + \beta|Z>_q)$$

$$= Z\alpha^*\beta e_q^{-\frac{1}{2}|z|^2} + |\beta|^2 Z \tag{11}$$

$$<\psi|a_q^+|\psi>_q = (\alpha^* <0| + \beta^* <Z|)a_q^+(\alpha|0>_q + \beta|Z>_q)$$

$$= \beta^*\alpha Z^* e_q^{-\frac{1}{2}|z|^2} + |\beta|^2 Z^* \tag{12}$$

$$<\psi|a_q^{+2}|\psi>_q = (\alpha^* <0| + \beta^* <Z|)a_q^{+2}(\alpha|0>_q + \beta|Z>_q)$$

$$= \beta^*\alpha Z^{*2} e_q^{-\frac{1}{2}|z|^2} + |\beta|^2 Z^{*2} \tag{13}$$

$$<\psi|a_q^2|\psi>_q = (\alpha^* <0| + \beta^* <Z|)a_q^2(\alpha|0>_q + \beta|Z>_q$$

$$= \beta\alpha^* Z^2 e_q^{-\frac{1}{2}|z|^2} + |\beta|^2 Z^2 \tag{14}$$

From (8) − (14),we can have

$$F_1 = \frac{1}{4}\{<a_q^{+2}>+<a_q^2>+<a_q a_q^+>+<a_q^+ a_q>-(<a_q^+>+<a_q>)^2\} - \frac{1}{4}$$

$$= \frac{1}{4}\Big[e_q^{-\frac{1}{2}R^2} r_1 r_2 k^2 2\cos(\theta_2 + 2\varphi - \theta_1) + r_2^2 R^2 \cdot 2\cos 2\varphi + e_q^{-\frac{1}{2}R^2} r_1 r_2\, 2\cos(\theta_2 - \theta_1)$$

$$+ r_2 q^{-R^2}\sum_{n=0}^{\infty}\frac{R^{2n}}{[n]!}[n+1] + r_2^2 R^2 + r_1^2 - (Rr_1r_2e_q^{-\frac{1}{2}R^2}\, 2\cos(\theta_2 + \varphi - \theta_1) + Rr_2^2\, 2\cos\varphi)^2 - 1\Big] \tag{15}$$

$$F_2 = \frac{1}{4}\Big[-<a_q^{+2}>-<a_q^2>+<a_q a_q^+>+<a_q^+ a_q>+(<a_q^+>-<a_q>)^2\Big] - \frac{1}{4}$$

$$= \frac{1}{4}\Big[-e_q^{-\frac{1}{2}R^2} r_1 r_2 R^2 2\cos(\theta_2 - 2\varphi - \theta_1) - r_2^2 R^2 2\cos 2\varphi + e_q^{-\frac{1}{2}R^2} r_1 r_2\, 2\cos(\theta_1 - \theta_2)$$

$$+ r_2^2 e_q^{-R^2}\sum_{n=0}^{\infty}\frac{R^{2n}}{[n]!}[n+1] + r_2^2 R^2 + r_1^2 + (Rr_1r_2e_q^{-\frac{1}{2}R^2}\sin(\theta_2 + \varphi - \theta_1) - Rr_2^2\, 2\sin\varphi)^2 - 1\Big] \tag{16}$$

It is clear F_1 and F_2 are periodic function of φ Numerical valve calculating showed that Y_1 and Y_2 may be more than zero and less than zero accompaning the variation of q. This result shows that the generally squeezing may exist and can be controlled by q

2.2 The bunching effect, the anti—bunching effect of q—deformed superposition light field state

For q—defrmed superposition light field state, we have

$$<\psi|a_q^{+2}a_q^2|\psi>_q = |\beta|^2|Z|^4 \tag{17}$$

$$g_q^{(2)}(0) = \frac{<\psi|a_q^{+2}a_q^2|\psi>_q}{(<\psi|a_q^+a_q|\psi>_q)^2} = \frac{|\beta|^2|Z|^4}{|\beta|^4|Z|^4} = \frac{1}{|\beta|^2} = \frac{1}{r_2^2} \tag{18}$$

When $\cos(\theta_1-\theta_2)\geqslant 0$, from (5) we have

$$r_1^2 + r_2^2 \leqslant 1 \tag{19}$$

From (19), we get $r^2<1$, so that

$$g_q^{(2)}(0) = \frac{1}{r^2} > 1 \tag{20}$$

(18) shows that the bunching effect exists.

When $\cos(\theta_1-\theta_2)<0$, we have $r_1^2+r_2^2>1$, so that r_2^2 may be more than 1 and we have

$$g_q^2(0) = \frac{1}{r^2} < 1 \tag{22}$$

(22)Shows that the anti—bunching effect exist.

3. Conclusion

The results of this paper shows that the squeezing effect, the bunching effect and the anti—bunching effect of q—deformed superposition light field state may exist and can be controlled by q—parmeter.

Reference

[1] Hao Sanyu, ACTA PHYSICA SINICA, 42, 1057 (1993)

[2] Zhu Chongxu etal, ACTA PHYSICA SINICA, 43, 1262(1994).

NEXT
DOCUMENT

CHIRAL BOSONIZATION OF SUPERCONFORMAL GHOSTS

Shi Deheng Shen Yang Liu Jinling
Department of Foundation, The First Aeronautical College of Air Force,
Xinyang, Henan 464000, P. R. China
Xiong Yongjian
Department of Physics, Xinyang Teacher's College,
Xinyang, Henan 464000, P. R. China

Abstract

We explain the difference of the Hilbert space of the superconformal ghosts (β, γ) system from that of its bosonized fields φ and χ. We calculate the chiral correlation functions of φ, χ fields by inserting appropriate projectors.

Recently, many authors have investigated the bosonization of superconformal ghosts β and γ[1,2]. Unlike the fermionic ghosts b and c, the bosonization of (β, γ) system have some problems.

Locally, (β,γ) system is equivalent to two scalar fields φ and χ[3]. Although the chiral correlation functions of β, γ fields have been calculated[1,2], the calculation of the chiral correlation functions of φ, χ fields will be troublesome. Besides the redundant zero-modes of the bosonized fields, the main reason is that φ, χ fields have a large Hilbert space than (β, γ) system. In ref. (4), this enlargement was explained as caused by the freedom of choosing the background ghost charge, the so-called picture, and by introducing projectors which specify the picture of each loop, the Hilbert space of φ, χ fields are restricted to the degrees of freedom of the (β, γ) system. In this paper, we explain this problem from an elementary point of view, and then apply new projector for the calculation of the chiral correlation functions of φ, χ fields.

We consider the (β, γ) system corresponding to superstring theory, i. e. with conformal dimensions $\frac{3}{2}$, $-\frac{1}{2}$ respectively. Locally, (β, γ) system is identified with a scalar field φ and a pair of fermions ζ, η with conformal weights 0, 1 respectively.

$$\beta = \partial\zeta e^{-i\varphi} \qquad \gamma = \eta e^{i\varphi} \tag{1}$$

The φ field is coupled to background charge $Q=2$, and is described by the action

$$S[\varphi] = \frac{1}{2\pi}\int d^2z(-\partial_z\varphi\,\partial_{\bar{z}}\varphi - \frac{i}{2}\sqrt{g}\,R\varphi) \tag{2}$$

where, $g_{z\bar{z}}$ is a Riemann metric and R is the corresponding scalar curvature. We can again bosonizing (ζ, η) system via another scalar field χ

$$\zeta = e^{i\chi} \qquad \eta = e^{-i\chi} \tag{3}$$

The χ field is coupled to background charge $Q=-1$ and is described by the action

$$S[\chi]=\frac{1}{2\pi}\int d^2z(\partial_z\chi\partial_{\bar{z}}\chi+\frac{i}{4}\sqrt{g}R\chi) \tag{4}$$

φ and χ fields are both restricted to taking values on a unit circle $R/2\pi Z$; this compactification results soliton configurations on Riemann surface $\sum_g$ with genus $g>0$, and insures the necessary holomorphic factorization[5].

The classical soliton sectors can be labeled by the winding numbers for the canonical homology basis (a_i, b_j). The soliton solutions of φ, χ fields with winding numbers (n_i, b_j) are given by

$$\begin{aligned}\varphi_{nm}(z)&=\pi(m+\bar{\tau}n)(Im\tau)^{-1}z+c.c.\\ \chi_{nm}(z)&=i\pi(m+\bar{\tau}n)(Im\tau)^{-1}z+c.c.\end{aligned} \tag{5}$$

where τ is the period matrix of $\sum_g$. For simplicity, we have denoted the Jacobi map $\int_{p_0}^{z}\omega$ as z. The corresponding action

$$\begin{aligned}S[\varphi_{nm}]&=\frac{\pi}{2}(m+\bar{\tau}n)(Im\tau)^{-1}(m+\tau n)+2S_b\\ S[\chi_{nm}]&=\frac{\pi}{2}(m+\bar{\tau}n)(Im\tau)^{-1}-S_b\\ S_b&=\pi(m+\bar{\tau}n)(Im\tau)^{-1}\Delta-c.c.\end{aligned} \tag{6}$$

where, Δ is Riemann class.

We consider the following correlation functions

$$A_\delta=\int[d\varphi d\zeta d\eta]_\delta e^{-s(\varphi,\zeta,\eta)}\prod_{a=1}^{n+1}\zeta(\chi_a)\prod_{b=1}^{n}\eta(y_b)\prod_{c=1}^{n}e^{iq_c\varphi(z_c)} \tag{7}$$

where q_c are integer satisfying $\sum q_c=2(g-1)$, and δ is a specific spin structure.

If φ and χ are treated independently, the result will be different from that of the corresponding β, γ fields. We notice that

a) the bosonized fields have redundant zero-modes of ζ and η fields.

and b) the (φ, χ) system has a larger Hilbert space than that of the (β, γ) system, since φ and χ are not independent globally. Thus we must have appropriate constriants, otherwise, some global configurations will be computed repeatly.

The first aspect can be resolved by inserting operators $\delta(\zeta(\chi))$, $\prod_{i=1}^{g}\delta(\eta(r_i))$ to remove zero-modes of ζ, η fields. η has zero-modes at $i=1, \cdots, g$, and ζ has a constant zero-mode, thus χ is an arbitrary point on $\sum_g$. In order to avoid to compute the similar part of global configurations of φ, χ fields, we introduce projector

$$\delta(m_\chi - m_\varphi)\,\delta(n_\chi - n_\varphi) \tag{8}$$

to restrict φ, χ on the same soliton sector at the same time.

Now, according to Riemann-Roch theorem, (7) must be modified as follow

$$A_\delta = \int [d\varphi\, d\zeta d\eta]_\delta e^{-s[\varphi,\zeta,\eta]} \prod_{a=1}^{n}\zeta(x_a) \prod_{b=1}^{n}\eta(y_b) \prod_{c=1}^{n} e^{iq_c\varphi(z_c)} \tag{9}$$

Inserting our projector

$$\delta(\zeta(x)) \prod_{i=1}^{g}\delta(\eta(r_i))\,\delta(m_\varphi - m_\chi)\,\delta(n_\chi - n_\varphi)$$

we have

$$A_\delta = \langle \prod_{a=1}^{n}\zeta(x_a) \prod_{b=1}^{n}\eta(y_b) \prod_{c=1}^{n} e^{iq_c\varphi(z_c)} \cdot \delta(\zeta(x)) \prod_{i=1}^{g}\delta(\eta(r_i))\,\delta(m_\chi - m_\varphi)\,\delta(n_\chi - n_\varphi)\rangle_\delta$$

For the δ-functions with fermion arguments, $\delta(\zeta)=\zeta$, $\delta(\eta)=\eta$, and labelling the arbitrary X as X_{n+1}, we get

$$A_\delta = \langle \prod_{a=1}^{n+1} e^{i\alpha(x_a)} \prod_{b=1}^{n} e^{-i\alpha(y_b)} \prod_{c=1}^{n} e^{iq_c\varphi(z_c)} \prod_{i=1}^{g} e^{-i\alpha(r_i)}\,\delta(m_\chi - m_\varphi)\,\delta(n_\chi - n_\varphi)\rangle_\delta$$

This result can be written as a soliton sum $\Lambda_{sol.\,\delta}$ multiplied the amplitude of zero soliton sector A_{00}

$$A_\delta = \Lambda_{sol.\,\delta} \cdot A_{00} \tag{10}$$

A_{00} is the result of the single-valued part of φ, χ fields. It is trivial that[5]

$$A_{00} = \exp\{2\pi i \mathrm{Im}(\textstyle\sum X_a - \sum Y_b - \sum r_i + \sum q_c z_c - \Delta)(\mathrm{Im}\tau)^{-1}\mathrm{Im}(\sum X_a - \sum Y_b$$

$$- \textstyle\sum r_i + \sum q_c z_c - \Delta)\} \times \left| \frac{\prod_c \sigma(z_c)^{-2q_c}}{\prod_{c_1<c_2} E(z_{c_1}, z_{c_2})^{q_{c_1}q_{c_2}}} \cdot \frac{\prod_b \sigma(y_b)\prod_i \sigma(r_i)}{\prod_a \sigma(x_a)} \right.$$

$$\left. \times \frac{\prod_{a_1<a_2} E(x_{a_1}, x_{a_2}) \prod_{b_1<b_2} E(y_{b_1}, y_{b_2}) \prod_{r_i<r_j} E(r_i, r_j) \prod_{b<r_i} E(y_b, r_i)}{\prod_{a,\,b} E(x_a, y_b) \prod_{a,\,r_i} E(x_a, r_i)} \right|^2 \tag{11}$$

Using Possion summation formula, we get.

$$\Lambda_{\omega l,\delta} = (\det \mathrm{Im}\tau)\exp\{-2\pi \mathrm{Im}(\Sigma x_a - \Sigma y_b + \Sigma q_c z_c - \Sigma r_i - \Delta)(\mathrm{Im}\tau)^{-1}\cdot \mathrm{Im}(\Sigma x_a - \Sigma y_b + \Sigma q_c z_c - \Sigma r_i - \Delta)\}\cdot \left|\sum_{p_\chi} \exp\{\pi i p_\chi \tau p_\chi + 2\pi i p_\chi(\Sigma x_a - \Sigma y_b - \Sigma r_i + \Delta)\}\right.$$

$$\left.\cdot \left|\sum_{p_\varphi} \exp\{-\pi i(p_\varphi + \delta')\tau(p_\varphi + \delta') + 2\pi i(p_\varphi + \delta')(\Sigma q_c z_c - 2\Delta + \delta'')\}\right|^2 \right. \tag{12}$$

Here, $\delta', \delta'' \in (\frac{1}{2}\mathbf{z}/\mathbf{z})^g$, and $\delta = [\begin{smallmatrix}\delta' \\ \delta''\end{smallmatrix}]$

From (11) and (12), holomorphic anomaly factors of A_ω and $\Lambda_{\omega l,\delta}$ can cancell each other. Thus we can have chiral correlation functions

$$A_\delta^{\mathrm{chiral}} = (\det \mathrm{Im}\tau)^{\frac{1}{2}} \frac{\prod_{b_0=1}^{n}\theta[\delta](-y_{b_0} + \Sigma x_a - \Sigma y_b + \Sigma q_c z_c - 2\Delta)}{\prod_{a_0=1}^{n+1}\theta[\delta](-x_{a_0} + \Sigma x_a - \Sigma y_b + \Sigma q_c z_c - 2\Delta)}$$

$$\cdot \frac{\prod_{a_1<a_2} E(x_{a_1}, x_{a_2}) \prod_{b_1<b_2} E(y_{b_1}, y_{b_2})}{\prod_{a,b} E(x_a, y_b) \prod_{c_1,c_2} E(z_{c_1}, z_{c_2})^{q_{c_1} q_{c_2}} \prod_c \sigma(z_c)^{2q_c}} \tag{13}$$

Thus, by inserting appropriate projector to remove the zero-modes of ζ, η fields and restrict φ, χ on the same soliton sector, we get the correct chiral correlation functions of φ, χ fields. As compared with ref. (4), our approach is more comprehensive.

References

[1] E. Verlinde, H.Verlinde, Phys. Lett., B192, 95 (1987)

[2] A. Losev, Phys. Lett., B226, 62 (1989)

[3] D. Friedan, E. Martince, S. H.Shenker, Nucl. Phys., B271, 93 (1986)

[4] U.Carow-Watamura, Z. F. Ezawa, K. Harada, A. Tezuka, S. Watamura, Phys. Lett., B227, 73 (1989)

[5] E.verlinde, H. Verlinde, Nucl. Phys., B288, 357 (1989)

NEXT
DOCUMENT

NUMBER-PHASE UNCERTAINTY RELATIONS FOR OPTICAL FIELDS

Ryszard Tanaś
Nonlinear Optics Division, Institute of Physics, Adam Mickiewicz University, Grunwaldzka 6, 60-780 Poznań, Poland.

Abstract

The Hermitian phase formalism of Pegg and Barnett allows for direct calculations of the phase variance and, consequently, the number-phase uncertainty product. This gives us a unique opportunity, inaccessible before, to study the number-phase uncertainty relations for optical fields in a direct way within a consistent quantum formalism. A few examples of fields generated in nonlinear optical processes are studied from the point of view of their number-phase uncertainty relations.

1 Number-phase uncertainty relations

Pegg and Barnett [1] introduced the Hermitian phase formalism, which is based on the observation that in a finite-dimensional state space the states with well-defined phase exist. Thus they restrict the state space to a finite $(s+1)$-dimensional Hilbert space Ψ spanned by the number states $|0\rangle$, $|1\rangle,\ldots,|s\rangle$. In this space they define a complete orthonormal set of phase states by

$$|\theta_m\rangle = \frac{1}{\sqrt{s+1}} \sum_{n=0}^{s} \exp(in\theta_m)\,|n\rangle, \qquad m = 0,1,\ldots,s, \tag{1}$$

where the values of θ_m are given by

$$\theta_m = \theta_0 + \frac{2\pi m}{s+1}. \tag{2}$$

The value of θ_0 is arbitrary and defines a particular basis set of $(s+1)$ mutually orthogonal phase states.

The Pegg-Barnett Hermitian phase operator is defined as

$$\hat{\Phi}_\theta \equiv \sum_{m=0}^{s} \theta_m\,|\theta_m\rangle\langle\theta_m|. \tag{3}$$

Of course, phase states (1) are eigenstates of the phase operator (3) with the eigenvalues θ_m restricted to lie within a phase window between θ_0 and $\theta_0 + 2\pi s/(s+1)$. The Pegg-Barnett prescription is to evaluate any observable of interest in the finite basis (1) and only after that to take the limit $s \to \infty$.

Since the phase states (1) are orthonormal, $\langle\theta_m|\theta_{m'}\rangle = \delta_{mm'}$, the kth power of the Pegg-Barnett phase operator (3) can be written as

$$\hat{\Phi}_\theta^k = \sum_{m=0}^{s} \theta_m^k |\theta_m\rangle\langle\theta_m|. \tag{4}$$

Substituting eqs. (1) and (2) into eq. (3) and performing summation over m yields the phase operator explicitly in the Fock basis

$$\hat{\Phi}_\theta = \theta_0 + \frac{s\pi}{s+1} + \frac{2\pi}{s+1} \sum_{n\neq n'} \frac{\exp[\mathrm{i}\,(n-n')\theta_0]\,|n\rangle\langle n'|}{\exp[\mathrm{i}\,(n-n')2\pi/(s+1)]-1}. \tag{5}$$

It is well apparent that the Hermitian phase operator $\hat{\Phi}_\theta$ has well defined matrix elements in the number state basis and does not suffer from such problems as the original Dirac phase operator. A detailed analysis of the properties of the Hermitian phase operator was given by Pegg and Barnett [1]. As the Hermitian phase operator is defined, one can calculate the expectation value and variance of this operator for a given state of the field $|f\rangle$.

The Pegg-Barnett phase operator (5), expressed in the Fock basis, readily gives the phase-number commutator [1]:

$$[\hat{\Phi}_\theta, \hat{n}] = -\frac{2\pi}{s+1} \sum_{n\neq n'} \frac{(n-n')\exp[\mathrm{i}(n-n')\theta_0]}{\exp[\mathrm{i}(n-n')2\pi/(s+1)]-1} |n\rangle\langle n'|. \tag{6}$$

Equation (6) looks very different from the famous Dirac postulate of the phase-number commutator.

Having defined the Hermitian operators for the number and phase variables and knowing their commutator, we can easily test the number-phase Heisenberg uncertainty relation for any given field with known number state decomposition.

$$\Delta\hat{\Phi}_\theta \Delta\hat{n} \geq \frac{1}{2}|\langle[\hat{n}, \hat{\Phi}_\theta]\rangle| \tag{7}$$

For physical states the number-phase commutator can be considerably simpified [1], and its expectation value in the physical state $|p\rangle$ can be expressed in terms of the phase distribution function $P(\theta_0)$, which makes calculations of this quantity pretty simple.

$$\langle p|\,[\hat{\Phi}_\theta, \hat{n}]\,|p\rangle = -i[1-(s+1)|\langle p|\,|\theta_0\rangle|^2] \tag{8}$$

$$\to -i[1-2\pi P(\theta_0)] \tag{9}$$

In the next Sections we give a few examples of the number-phase uncertainty relations calculated using the above formulas.

2 Examples

2.1 Anharmonic oscillator model

The anharmonic oscillator model is described by the Hamiltonian

$$\hat{H} = \hbar\omega\hat{a}^\dagger\hat{a} + \frac{1}{2}\hbar\kappa\hat{a}^{\dagger 2}\hat{a}^2, \tag{10}$$

where $\hat{a}$ and $a^\dagger$ are the annihilation and creation operators of the field mode, and κ is the coupling constant, which is real and can be related to the nonlinear susceptibility $\chi^{(3)}$ of the medium if the anharmonic oscillator is used to describe propagation of laser light (with right or left circular polarization) in a nonlinear Kerr medium. If the state of the incoming beam is a coherent state $|\alpha_0\rangle$, the resulting state of the outgoing beam is given by

$$|\psi(\tau)\rangle = \hat{U}(\tau)|\alpha_0\rangle = \exp(-|\alpha_0|^2/2)\sum_{n=0}^{\infty}\frac{\alpha_0^n}{\sqrt{n!}}\exp\left[i\frac{\tau}{2}n(n-1)\right]|n\rangle, \tag{11}$$

where $\tau = -\kappa t$.

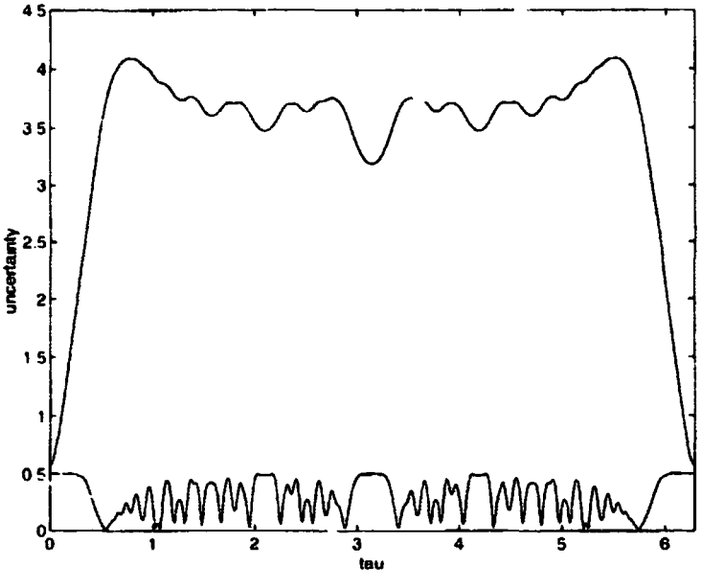

FIG. 1. Evolution of the uncertainty product (lhs of eq. (7) - upper curve) and its lower bound (rhs of eq. (7) - lower curve) for the anharmonic oscillator state with $|\alpha_0|^2 = 4$.

The appearance of the nonlinear phase factor in the state (11) modifies essentially the properties of the field represented by such a state with respect to the initial coherent state $|\alpha_0\rangle$. It was shown by Tanaś [2] that a high degree of squeezing can be obtained in the anharmonic oscillator model. Squeezing in the same process was later considered by Kitagawa and Yamamoto [3] who used the name *crescent squeezing* because of the crescent shape of the quasiprobability distribution contours obtained in the process.

The Pegg-Barnett Hermitian phase formalism has been applied for studying the phase properties of the states (11) by Gerry [4], who discussed the limiting cases of very low and very high light intensities, and by Gantsog and Tanaś [5], who gave a more systematic discussion of the exact results.

In Fig. 1 we show the evolution of the number-phase uncertainty product as given by the lhs of ineq. (7) (upper curve) and its lower bound as given by the rhs of ineq. (7) (lower curve) for

the state (11) of the anharmonic oscillator assuming that the mean number of photons $|\alpha_0|^2 = 4$. It is seen that the number-phase uncertainty product rapidly increases at the early stage of the evolution, which is due to the rapid randomization of the phase, since the photon statistics remain all the time Poissonian with the number of photons variance equal to the mean number of photons $|\alpha_0|^2$. This is a typical behavior for mean numbers of photons greater than unity. It is also seen that the states generated in the anharmonic oscillator model are never the minimum uncertainty or intelligent states. The level of noise is much bigger than its lower bound allowed by quantum mechanics. Since the dynamics is periodic, after time $\tau = 2\pi$ the system returns back to its initial state. It can be shown [5] that for $|\alpha_0|^2 \gg 1$ the number and phase uncertainty product takes the approximate analytical form

$$\langle(\Delta)^2\rangle\hat{\Phi}_\theta\langle(\Delta)^2\rangle\hat{n} \;=\; (\frac{1}{4} + |\alpha_0|^2\tau^2), \tag{12}$$

explicitly showing rapid increase of the uncertainty product from the value 1/4 known for the coherent state.

2.2 Jaynes-Cummings model

The model is described by the Hamiltonian (at exact resonance)

$$\hat{H} \;=\; \hbar\omega(\hat{a}^\dagger\hat{a} + \hat{R}^z) + \hbar g(\hat{R}^\dagger\hat{a} + \hat{R}\hat{a}^\dagger), \tag{13}$$

where $\hat{a}^\dagger$ and $\hat{a}$ are the creation and annihilation operators for the field mode; the two-level atom is described by the raising, $\hat{R}^\dagger$, and lowering, $\hat{R}$, operators and the inversion operator $\hat{R}^z$, and g is the coupling constant.

To study the phase properties of the field mode we have to know the state evolution of the system. After dropping the free evolution terms, which change the phase in a trivial way, and assuming that the atom is initially in its ground state and the field is in a coherent state $|\alpha_0\rangle$, the state of the system is found to be

$$|\psi(t)\rangle \;=\; \sum_{n=0}^{\infty} b_n \exp(in\vartheta_0)\left[\cos(\sqrt{n}\,gt)|n,g\rangle - i\sin(\sqrt{n}\,gt)|n-1,e\rangle\right], \tag{14}$$

where $|g\rangle$ and $|e\rangle$ denote the ground and excited states of the atom, the coefficients b_n are the Poissonian weighting factors of the coherent state α_0) and ϑ_0 is the coherent state phase (phase of α_0). The main oscillations of the uncertainty product reflect the oscillations of the phase variance, which has its extrema for the revival times (in the figure time $T = gt/(2\pi|\alpha_0|)$ is scaled in the revival times). Small oscillations seen on the figure stem from the oscillations of the photon number variance and have only minor effect on the overall behavior. They are associated with the revivals of the rapid Rabi oscillations in the model. However, this is the phase variance that smoothly oscillates in the time scale of the subsequent revivals. In this way, the well known phenomenon of collapses and revivals has obtained clear interpretation in terms of the cavity mode phase [6].

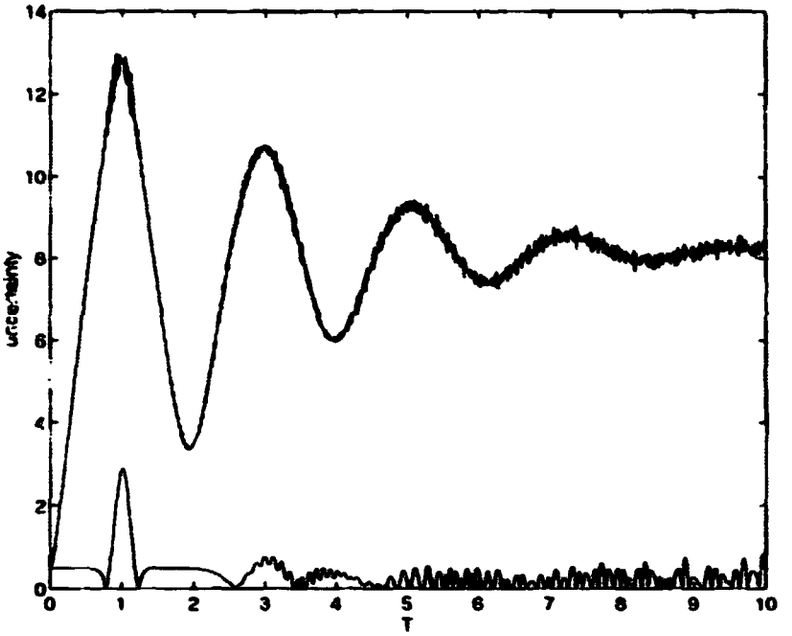

FIG. 2. Same as fig. 1 but for the Jaynes-Cummings model with $|\alpha_0|^2 = 20$.

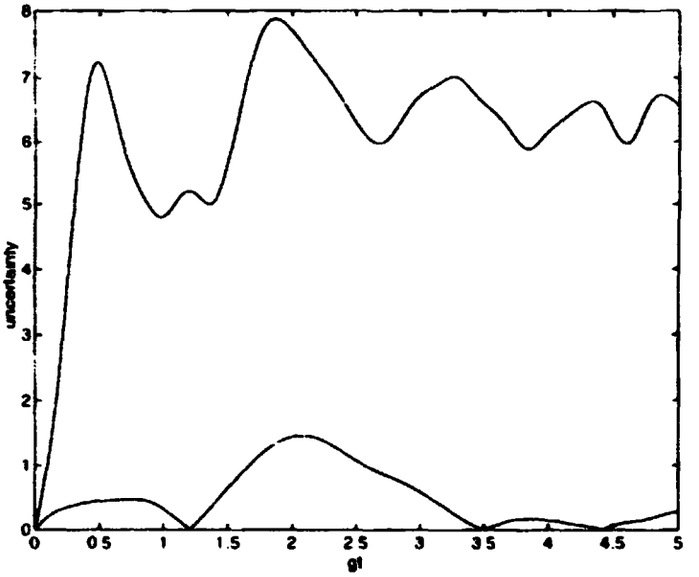

FIG. 3. Same as fig. 1 but for the down conversion with quantum pump with the initial mean number of photons equal to 4.

2.3 Down conversion with quantum pump

The parametric down conversion with quantum pump is governed by the Hamiltonian

$$\hat{H} = \hat{H}_0 + \hat{H}_I = \hbar\omega\hat{a}^\dagger\hat{a} + 2\hbar\omega\hat{b}^\dagger\hat{b} + \hbar g(\hat{b}^\dagger\hat{a}^2 + \hat{b}\hat{a}^{\dagger 2}), \tag{15}$$

where $\hat{a}$ ($\hat{a}^\dagger$) and $\hat{b}$ ($\hat{b}^\dagger$) are the annihilation (creation) operators of the signal mode of frequency ω and the pump mode at frequency 2ω, respectively. The coupling constant g, which is real, describes the coupling between the two modes.

Phase properties of this system have been described by Gantsog et al. [7] and Tanaś and Gantsog [8] and the details of the calculations can be found there. Here, in Fig. 3, we show, as in previous examples, the evolution of the number phase uncertainty product and its lower bound for this process. For finite initial mean number of photons the number-phase uncertainty product remains finite during the evolution contrary to the parametric approximation under which it rapidly explodes to infinity.

3 Conclusions

All above examples, are typical examples of the fields generated in nonlinear optical processes, and they show clearly that nonlinear processes typically evolve to quantum states which are far from being the minimum uncertainty or intelligent states.

Acknowledgments

I thank Drs. Ts. Gantsog and A. Miranowicz for many discussions and cooperation. This work was supported by the Polish Committee for Scientific Research (KBN) under the grant No. 2 P03B 128 8.

References

[1] D. T. Pegg and S. M. Barnett, Phys. Rev. A **39**,1665 (1989).

[2] R. Tanaś, in *Coherence and Quantum Optics V*, L. Mandel and E. Wolf, Eds., (Plenum, New York, 1984), p. 645.

[3] H. Kitagawa and Y. Yamamoto, Phys. Rev. A **34**, 3974 (1986).

[4] C. C. Gerry, Opt. Commun. **75**, 168 (1990).

[5] Ts. Gantsog and R. Tanaś, J. Mod. Opt. **38**, 1021 (1991).

[6] H. T. Dung, R. Tanaś, and A. S.Shumovsky, Opt. Commun. **79**, 462 (1990)

[7] Ts. Gantsog, R. Tanaś, and R. Zawodny, Opt. Commun. **82**, 345 (1991)

[8] R. Tanaś and Ts. Gantsog, Quantum Opt. **4**, 245 (1992); Phys. Rev. A **45**, 5031 (1992)

NEXT
DOCUMENT

THE INTERFERENCE OF THE DYNAMICALLY SQUEEZED VIBRATIONAL WAVE PACKETS

An. V. Vinogradov
P. N. Lebedev Physical Institute, 117924 Moscow, Russia

J. Janszky
Research Laboratory for Crystal Physics, P. O. Box 132, H-1508, Budapest

T. Kobayashi
Department of Physics, Faculty of Sciences, University of Tokyo, Hongo 7-3-1, Bunkyo-ku, Tokyo 113, Japan

An electronic excitation of a molecule by a sequence of two femtosecond phase-locked laser pulses is considered. In this case the interference between the vibrational wave packets induced by each of the subpulses within a single molecule takes plac.. It is shown that due to the dynamical squeezing effect of a molecular vibrational state the interference of the vibrational wave packets allows one to measure the duration of a femtosecond laser pulse. This can be achieved experimentally by measuring the dependence of the integral fluorescence of the excited molecule on the delay time between the subpulses. The interference can lead to a sharp peak (or to a down-fall) in that dependence, the width of which is equal to the duration of the laser pulse. It is shown that finite temperature of the medium is favorable for such an experiment.

Recently a great interest has been shown to the study of spatially localized vibrational wave packets in molecules induced by ultrashort laser pulses. The time evolution of the mean position of such a wave packet corresponds to the nearly classical nuclei motion, and can be observed in the pump and probe spectroscopic optical experiments [1-4]. The idea of controlling the chemical reactions due to the possibility of the nearly classical nuclei motion has been widely discussed and experimentally verified [5-10].

An impo;tant characteristic feature of the vibrational wave packet is its spatial extent. In the case of a harmonic nuclear potential the spatial properties of the wave packet are closely connected with the phonon statistics and can be treated by the methods developed in quantum optics. In a series of previous publications [11-16] we have studied the statistical properties of the vibrational states appearing due to the excitation of Franck-Condon transitions by the transform-limited light pulses of finite duration. The problem was to learn how is it possible, by varying the characteristics of a laser pulse (i.e. its amplitude and phase modulation), to excite the molecular vibrations with the given quantum fluctuations of the conjugated variables. In particular, it was theoretically predicted [11-13] and experimentally verified [17] that, when the spectral width of the exciting pulse is smaller than that of the absorption band, there appears a molecule in a squeezed vibrational state with a reduced quantum uncertainty of the nuclei position. The mechanism of squeezing, which arises here, is of the dynamical nature and can be explained as the result of quantum interference in the phase space of the molecular vibrations [13]. An application of the dynamical squeezing effect to the problem of wave packets optimal shaping for the control of the chemical reactions was considered in [18-21].

Our goal now is to show how this dynamical squeezing effect can be put to use in another way for the duration measurement of a femtosecond laser pulse. Following [22], we shall consider the

excitation of a Franck-Condor transition in a molecule by a sequence of two femtosecond phase-locked Gaussian-shaped pulses:

$$\mathbf{E}(t) = \frac{\mathbf{E}_0}{2\pi^{1/4}}\left\{\exp\left[-\frac{u^2}{2}\left(t+T/2\right)^2\right]+\alpha\exp\left[-\frac{u^2}{2}\left(t-T/2\right)^2\right]\right\}\exp(-i\Omega t)+c.c., \quad (1)$$

separated from each other by the time interval T. Here α is a possible additional complex coefficient between the pulses: $\alpha = |\alpha|\exp(i\varphi)$. As it was demonstrated experimentally in [22] it is possible to change the time interval T, keeping constant the value of phase φ.

We shall assume that due to the electronic transition only a spatial shift of the harmonic nuclear potentials occurs in the molecule. The adiabatic Hamiltonians describing molecular vibrations in the initial (i) and excited (e) electronic states have the form

$$H_i = \varepsilon_i + \frac{\hat{p}^2}{2m} + \frac{m\omega^2}{2}(\hat{q}+q_i)^2, \quad (2)$$

$$H_e = \varepsilon_e + \frac{\hat{p}^2}{2m} + \frac{m\omega^2}{2}\hat{q}^2, \quad (3)$$

where $\varepsilon_{i,e}$ are the electronic energy levels. It is convenient to rewrite Eqs. (2) and (3) expressing $\hat{q}$ and $\hat{p}$ through the phonon creation and annihilation operators:

$$\hat{q} = \sqrt{\frac{\hbar}{2m\omega}}(b^+ + b), \quad \hat{p} = i\sqrt{\frac{\hbar m\omega}{2}}(b^+ - b). \quad (4)$$

Then

$$H_i = \varepsilon_i + \frac{m\omega^2 q_i}{2} + \frac{\hbar\omega}{2}(b^+b + bb^+) + \hbar\omega g(b^+ + b), \quad g = q_i\sqrt{\frac{m\omega}{2\hbar}}, \quad (5)$$

$$H_e = \varepsilon_e + \frac{\hbar\omega}{2}(b^+b + bb^+). \quad (6)$$

A non-dimensional coupling constant g, which appears in Eq. (4), is equal to the ratio of the Franck-Condon shift to the amplitude of zero vibrations. The Hamiltonian (5) can be diagonalized by means of the unitary displacement operator

$$D = \exp[-g(b^+ - b)], \quad (7)$$

$$D^+ H_i D = \varepsilon_i + \frac{\hbar\omega}{2}(b^+b + bb^+). \quad (8)$$

It is easily seen from Eq. (8) that the ground state vibrational wave function of the molecule in the initial electronic state has the form

$$|\Phi_i\rangle = D|0\rangle, \quad (9)$$

where $|0\rangle$ is the phonon vacuum, which coincides with the ground vibration state of the electronically excited molecule. Let us note that the displacement operator acting on the vacuum state gives the coherent state. Then Eq. (9) simply means that the ground state wave function of the harmonic oscillator being placed in the shifted potential is a coherent state.

The case of zero temperature. We shall assume that initially at $t = -\infty$ the molecule was prepared in the state $|i\rangle|\Phi_i\rangle$, where $|i\rangle$ is the electronic wave function of the unexcited molecule. After the resonance interaction with the field (1) the wave function of the molecule will have the form

$$|\Psi, t\rangle = |i, t\rangle|\Phi_i, t\rangle - i\frac{(\mathbf{E}_0\cdot\mathbf{d}_{i,e})}{2\hbar u}|e, t\rangle|V^+, t\rangle, \quad \frac{|(\mathbf{E}_0\cdot\mathbf{d}_{i,e})|}{2\hbar u} << 1. \quad (10)$$

Eq. (10) is derived in the first-order perturbation theory. Here $\mathbf{d}_{e,g}$ is the dipole matrix element of the electronic transition, which is assumed to be independent of the vibrational coordinate in accordance with the Condon approximation, and $|V,t\rangle$, the unnormalized vibrational wave function of the excited molecule. Due to (1) this wave function consists of two terms

$$|V,t\rangle = |V_-,t\rangle + \alpha |V_+,t\rangle. \tag{11}$$

e functions $|V_\pm,t\rangle$ correspond to the vibrational wave packets being excited respectively by each of the subpulses in (1). Generally, the wave functions $|V_-,t\rangle$ and $|V_+,t\rangle$ are not orthogonal and their overlap depends on the delay time T between the subpulses. This opens a possibility to observe the delay time dependent interference effects in the physical processes which are determined by the population of the excited electronic state of the molecule. For the sake of explicitness we shall assume that the measuring quantity is the quantum fluorescence yield of the excited molecule. In the case of the transition in the pure electronic system (without a vibrational degree of freedom) functions $|V_-,t\rangle$ are reduced to numerical amplitudes

$$V_- = 2^{1/2}\pi^{1/4}\exp\left[-\frac{\delta^2}{2u^2} \mp \frac{i\delta T}{2}\right], \tag{12}$$

where $\delta = \varepsilon_e/\hbar - \varepsilon_1/\hbar - \Omega$. The dependence of the excited state population on the delay time between the subpulses in this case is of a trigonometric character:

$$|V|^2 = 2\pi^{1/2}\exp\left(-\frac{\delta^2}{u^2}\right)\left[1 + |\alpha|^2 + 2|\alpha|\cos(\varphi + \delta T)\right]. \tag{13}$$

In the remainder part of the paper we shall consider how the accounting of the molecular vibrations changes Eq. (12). The general expressions for functions $|V_\pm,t\rangle$ are given by

$$|V_\pm,t\rangle = \frac{u}{\pi^{1/4}}\int dt_1 \exp\left[-\frac{u^2}{2}\left(t_1 \pm T/2\right) - i\Omega t_1 + \frac{i}{\hbar}H_e(t_1 - t) + \frac{i}{\hbar}\varepsilon_e t\right] \cdot \exp\left[\frac{i}{\hbar}H_1 t_1\right]|\Phi_i\rangle. \tag{14}$$

Using (7) and (9) it is convenient to transform the wave functions (14) into the form of a distributed coherent state [13]

$$|V_\pm,t\rangle = \frac{u}{\pi^{1/4}}\exp\left(\mp i\delta\frac{T}{2}\right)\int dt_1 \exp\left[-\frac{u^2}{2}t_1^2 + i\delta t_1\right]D\left(t_1 \mp \frac{T}{2} - t\right)|0\rangle. \tag{15}$$

Time dependence of the Heisenberg displacement operator $D(t)$ in (15) is determined by the Hamiltonian (6). To evaluate the time integral in (15) now it is possible to use the well known Fock-space expansion of the coherent state $D|0\rangle$ [23]. As a result we have:

$$|V_\pm,t\rangle = 2^{1/2}\pi^{1/4}\sum_n \frac{(-g)^n}{\sqrt{n!}}\exp\left[-\frac{g^2}{2} - \frac{(\delta + n\omega)^2}{2u^2}\right]\exp\left[\mp\frac{i(\delta + n\omega)T}{2}\right]|n,t\rangle, \tag{16}$$

$$|n,t\rangle = \exp(-in\omega t)|n\rangle,$$

where $|n\rangle$ are the Fock-space eigenfunctions of the harmonic oscillator. Comparing Eqs. (12) and (16) it is easy to see that the coefficients at $|0,t\rangle$ in (16) coincide with the amplitudes V_-. Exact Eq. (16) is convenient for the numerical calculations. Another way to evaluate the integral (15) is based on the replacement of the coherent state $D\left(t_1 \mp T/2 - t\right)|0\rangle = \left|-ge^{i\omega(t_1 \mp T/2 - t)}\right\rangle$ by

$\left|-ge^{i\omega(t-T_2)}(1-i\omega t_1)\right\rangle$, which is possible when $u >> \omega$. In [13,15] it was shown that the integration in (15) in this case can be performed in the operator form, and leads to the result:

$$|V_-,t\rangle \approx W^{1/2}\exp\left(\mp i\frac{\delta T}{2}\right)\tilde{D}\left(t \pm T/2\right)S\left(t \pm T/2\right)|0\rangle. \tag{17}$$

In (17) the normalizing factor W is the absorption spectrum of the electronic-vibrational transition:

$$W = \pi^{1/2}\frac{u}{B_0}\exp\left(-\frac{\Delta^2}{B_0^2}\right), \quad \Delta = \delta + g^2\omega, \quad B_0^2 = u^2 + 2g^2\omega^2. \tag{18}$$

$\tilde{D}$ and S are the unitary displacement and squeezing operators:

$$\tilde{D}(t) = \exp\left\{-g\left(1-\frac{\omega\Delta}{B_0^2}\right)\left[b^+(t)-b(t)\right]\right\},$$

$$b(t) = \exp(-i\omega t)b, \tag{19}$$

$$S(t) = \exp\left\{\frac{1}{2}\ln\left(\frac{B_0}{u}\right)\left[b(t)^2 - b^+(t)^2\right]\right\}.$$

The action on the vacuum state of the operator $\tilde{D}S$ gives an ideal coherent squeezed state in which, generally, the mean position and momentum of the oscillator have nonzero value, the uncertainties of the position and the momentum are not equal to each other and their product has the minimal possible value. In the a-plane of the coherent states each of the vectors $|V_-,t\rangle$ can be considered as an ellipse uniformly moving along the circle with the radius $\tilde{g} = g\left(1-\omega\Delta/B_0^2\right)$, and keeping the orientation of the axes in the rotating frame. At moments t, for which the arguments of the operators in (17) are equal to the integer number of the vibrational periods, the values of the ellipse main axes are equal to the non-dimensional uncertainties of the position and the momentum with the small axis corresponding to the uncertainty of the position:

$$\Delta q = \frac{u}{\sqrt{2}\sqrt{2g^2\omega^2+u^2}}, \qquad \Delta p = \frac{\sqrt{2g^2\omega^2+u^2}}{\sqrt{2}u}. \tag{20}$$

If the coupling constant is large enough ($g>>1$), then the wave functions $|V_-,t\rangle$ are located at a sufficient distance from each other, and are approximately orthogonal except for the case when the time delay between the subpulses appears to be equal to an integer number of the periods. From geometrical considerations it is clear that when the delay time between the subpulses gains an integer number of the vibrational periods, the overlap of the vibrational wave functions $|V_-,t\rangle$ and $|V_+,t\rangle$ can be observed in the a-plane as the approaching of two ellipses along the direction of their big axes. So it is likely to expect the following qualitative effect of the molecular vibrations on the interference picture given by Eq. (13): (i) the dependence of the population of an excited state on the delay time between the subpulses should be more pointed in comparison to the trigonometric dependence in Eq. (13), (ii) while the delay time approaches the integer number of the periods the interference picture should be sensitive to the quantum state of the molecular vibrations, and the squeezing effect can be seen due to the dependence of the interference picture on the subpulse duration.

Let us put $T = \frac{2\pi m}{\omega} + \tau$ in Eqs. (15), (16), where τ, is a small deviation from the integer number of the vibrational periods, and evaluate the population of the excited state. In accordance with Eqs. (15) and (16) one finds

$$\langle V|V\rangle = u\int d\eta \exp\left(i\delta\eta - \frac{u^2}{4}\eta^2\right)\left[\begin{array}{c}\left(1+|\alpha|^2\right)M(\eta)+\\ \alpha e^{i\frac{2\pi m}{\omega}\tau\delta}M(\eta+\tau)+\alpha^* e^{-i\frac{2\pi m}{\omega}\tau\delta}M(\eta-\tau)\end{array}\right], \qquad (21)$$

where $M(\xi) = \langle 0|D^+(0)D(\xi)|0\rangle$, and

$$\langle V|V\rangle = 2\pi^{1/2}\sum_n \frac{g^{2n}}{n!}\exp\left[-g^2 - \frac{(\delta+n\omega)^2}{u^2}\right]\left\{1+|\alpha|^2+2|\alpha|\cos\left[\varphi + 2\pi m\frac{\delta}{\omega} + (\delta+n\omega)\tau\right]\right\}. \qquad (22)$$

While deriving Eq. (21) we have performed the integration over the summary time $\frac{1}{2}\left(t_1 + t_1'\right)$. The remaining integration in (21) is carried out over the difference time $t_1 - t_1' = \eta$. The vacuum average of two displacement operators in (21) frequently arises in the theory of Franck-Condon transitions and can be evaluated, for example, using the coherent states method [23]:

$$M(\xi) = \exp\left[g^2\left(e^{i\omega\xi} - 1\right)\right]. \qquad (23)$$

It is worth noting that Eq. (22) can be received from (21) by expanding in (23) the exponent in the powers of $g^2\exp(i\omega\xi)$. Due to the condition $u >> \omega$ integral in (21) can be evaluated asymptotically (by the steepest descent method [24]). To do that one can expand the index of the exponent in the powers of ξ up to the second order terms:

$$M(\xi) = \exp\left(ig^2\omega\xi - \tfrac{1}{2}g^2\omega^2\xi^2\right). \qquad (24)$$

Substituting (24) into (21) and performing the integration, one obtains

$$\langle V|V\rangle = W\left\{1+|\alpha|^2+2|\alpha|\exp\left[-\frac{1}{4}\left(\frac{\tau}{\gamma_0}\right)^2\right]\cos\left(\varphi + \frac{2\pi m\delta}{\omega} + \frac{\Delta u^2\tau}{B_0^2}\right)\right\}, \qquad (25)$$

$$\gamma_0 = \frac{B_0}{\sqrt{2}g\omega u} = \frac{\sqrt{u^2+2g^2\omega^2}}{\sqrt{2}ug\omega}.$$

Equation (25) describes the interference between the vibrational wave packets within a single molecule. Depending on the experimental conditions, i.e. the values of φ, δ, and m, this interference can lead to a sharp peak (constructive interference), or to a down-fall (destructive interference) in the fluorescence dependence on the delay time between the subpulses. The new and the most constitutive feature of Eq. (25) is the dependence of the interference peak width γ_0 on the reciprocal pulse duration u. Within the range of pulse duration $\omega^2 << u^2 << 2g^2\omega^2$, where, in accordance with Eq. (20), the squeezing effect is the most considerable, the width of the interference peak approximately equals to the subpulse duration $\gamma_0 \approx u^{-1}$. This gives a practical possibility to use this effect for the duration measurement of a femtosecond laser pulse. The fact that the dependence of the interference peak width on the pulse duration is indeed the consequence of the dynamical squeezing effect becomes clear if we note that the second order expansion in Eq. (24) is equivalent to the first order expansion over $t_1 \pm \tau/2$ in Eq. (15). In the limit of extremely short pulses $u^2 >> 2g^2\omega^2$ Eq. (25) coincides with that previously received in [20]. In that limit the

interference peak width does not depend on the pulse duration: $\gamma_0 \approx (\sqrt{2}g\omega)^{-1}$. It should be noted, that the limiting interference peak width is achieved for those laser pulses, during the action of which the initial vibration state of a molecule in the process of electronic excitation has no time to change. The effect of the dynamical squeezing in this limit is absent. The picture of the interference peak as the function of the variables τ and u, numerically evaluated with the help of Eq. (22), can be seen in Fig. 1.

The case of nonzero temperature. In the case of nonzero temperature we shall assume that the initial vibrational state of the molecule is described by the equilibrium density matrix. The population of the excited electronic state in this case can be evaluated in the second order perturbation theory for the density matrix. An expression for the nonequilibrium density matrix of the phonons, arising due to the excitation of a Franck-Condon transition by a single laser pulse was obtained in [11, 14]. In the present paper we need to calculate the trace of an analogous density matrix, appearing due to the action of the field (1). It seems to be evident, that the expression for this trace will have the form of Eq. (21) with the functions $M(\xi)$ replaced by

$$\langle M(\xi)\rangle = Sp\left[\rho_0 D^+(0) D(\xi)\right] = \exp\left\{g^2\left[(\bar{n}+1)e^{i\omega\xi} + \bar{n}e^{-i\omega\xi} - 2\bar{n} - 1\right]\right\}, \tag{26}$$

where ρ_0 is the equilibrium density matrix of phonons, and $\bar{n}$, the thermal equilibrium phonon number. The Fourier expansion of $\langle M(\xi)\rangle$ is given by

$$\langle M(\xi)\rangle = \sum_{n=-\infty}^{+\infty}\left(\frac{\bar{n}+1}{\bar{n}}\right)^{\frac{n}{2}} I_n\left(2g^2\sqrt{\bar{n}(\bar{n}+1)}\right)\exp\left[-g^2(2\bar{n}+1) + in\omega\xi\right], \tag{27}$$

where I_n is the modified Bessel function. A generalization of equation (22) for the case of a nonzero temperature has the form

$$\begin{aligned}\langle V|V\rangle = 2\pi^{1/2}\sum_{n=-\infty}^{+\infty}\left(\frac{\bar{n}+1}{\bar{n}}\right)^{\frac{n}{2}} I_n\left(2g^2\sqrt{\bar{n}(\bar{n}+1)}\right)\exp\left[-g^2(2\bar{n}+1) - \frac{(\delta+n\omega)^2}{u^2}\right]\cdot \\ \left\{1 + |\alpha|^2 + 2|\alpha|\cos\left[\varphi + 2\pi\frac{\delta}{\omega} + (\delta+n\omega)\tau\right]\right\}.\end{aligned} \tag{28}$$

To evaluate the integral in Eqs. (21), in analogue to the case of the zero temperature, we shall expand the index of the exponent in Eq.(26) in the powers of ξ up to the second order terms. In this way we find that the effect of finite temperature in Eqs. (18) and (25) is manifested in the replacing coefficients B_0 and γ_0 by

$$B = \sqrt{u^2 + 2g^2\omega^2(2\bar{n}+1)}, \qquad \gamma = \frac{\sqrt{u^2 + 2g^2\omega^2(2\bar{n}+1)}}{ug\omega\sqrt{2(2\bar{n}+1)}}. \tag{29}$$

From (29) one can see that the temperature growth leads to the extension of the area of linear dependence of the interference peak width on the laser pulse duration. Accordir.g to. Eq. (29), $u_0^{-1} = \left[2g^2\omega^2(2\bar{n}+1)\right]^{-1/2}$ can be considered as the limiting value of pulse duration for the range of this linear dependence. It is interesting to estimate the value of u_0^{-1} for a real physical system. To do this we shall use the data for I_2 molecule from [22]. Taking $g^2 = 6.4$, $2\pi/\omega = 300\,fs$ and $T = 300^0\,K$, we obtain $u_0^{-1} \approx 7\,fs$. The natural upper limit for u_0^{-1} is the inverse vibrational frequency ω^{-1}. In the experiment [22] the laser pulses of about $50\,fs$ duration have been used. In accordance with the given estimate the pulses of such duration belong to the area where $\gamma \approx u^{-1}$.

In conclusion note that the measurements of the interference peak width aimed at determining the duration of a femtosecond laser pulse represents only one of the possibilities to use the intramolecular interference phenomenon of the vibrational wave packets. Another interesting and important possibility is the observation of the wave packet distortions due to the intramolecular propagation. This problem we are planning to consider in our forthcoming paper.

Acknowledgments. This work was supported by Russian Foundation for Fundamental Research - Project No. 93-2-3583 and also by National Research Foundation of Hungary (OTKA) under Contracts Nos. 14083 and F14139.

References:

1. An. V. Vinogradov, J. Janszky, Fiz. Tverd. Tela (Leningrad) **27**, 982 (1985) [Sov. Phys. Solid. State **27**, 598, (1985)].
2. M. J. Rosker, F. V. Wise, C. L. Tang, Phys. Rev. Lett. **57**, 321 (1986).
3. C. L. Tang, F. M. Wise, I. A. Walmsley, J. Mod. Opt. **35**, 939 (1988).
4. H. Metiu, V. Engel, J. Opt. Sos. Am. B. **7**, 1709 (1990).
5. D. J. Tannor, S. A. Rice, J. Chem. Phys. **83**, 5013 (1985).
6. D. J.Tannor, R. Kozloff, S. A. Rice, J. Chem. Phys. **85**, 5805 (1985).
7. M. Grueble, A. Zewail, Physics Today. **43**, 24 (1990).
8. E. D. Potter, J. L. Herek, S. Rederson, Q. Lin, A. H. Zewail, Nature **355**, 66 (1992).
9. B. Garraway, S. Stenholm, K. A. Suominen, Physics World **6**, №4, 46 (1993).
10. M. S. Kurdoglyan, Optika i Spektroskopiya **76**, 832 (1994).
11. An. V. Vinogradov, J. Janszky, Kratk. Soobsh. Fiz. №4, 45 (1989).
12. An. V. Vinogradov, J. Janszky, Acta Phys. Pol. A **78**, 231 (1990).
13. J. Janszky, An. V. Vinogradov, Pys. Rev. Lett. **64**, 2771 (1990).
14. J. Janszky, T. Kobayashi, An. V. Vinogradov, Opt. Commun. **76**, 30 (1990).
15. An. V. Vinogradov, J. Janszky, Zh. Ekks. Teor. Fiz. **100**, 386, (1991) [Sov. Phys. JETP **73**, 2111 (1991)].
16. J. Janszky, An. V. Vinogradov, I. A. Walmsley, J. Mostowski Phys. Rev. A **50**,732 (1994).
17. T. J. Dunn, J. N. Sweetser, I. A. Walmsley, C. Radzevich, Phys. Rev. Lett. **70**, 3388 (1993).
18. J. Janszky, P. Adam, An. V. Vinogradov, T. Kobayashi, Chem. Phys. Lett.**213**, 368 (1993).
19. I. Averbuch, M. Shapiro, Phys. Rev. A **47**, 5086 (1993).
20. Y. -J. Yan, R. E. Gillilan, R. M. Whitnell, K. R. Wilson, S. Mukamel, J. Phys. Chem. **97**, 2320 (1993).
21. S. Szabo, Zs. Kis, J. Janszky, P. Adam, T. Kobayashi, An. V. Vinogradov, Acta Phys. Hung. **74**, 409 (1994).
22. N. F. Scherer, R. J. Carlson, A. Matro, M. Du, A. J. Ruggiero, Romero-Rochin, J. A. Cina, G. R. Fleming, S. A. Rice, J. Chem. Phys. **95**, 1847 (1991).
23. R. J. Glauber, Phys. Rev.**131**, 2766 (1963).
24. An. V. Vinogradov, Fiz. Tverd. Tela (Leningrad) **12**, 3081 (1970) [Sov. Phys. Solid. State **12**, 2493 (1970)].

NEXT
DOCUMENT

Coherent states on Riemann surfaces as m-photon states

A. Vourdas
Department of Electrical Engineering and Electronics,

The University of Liverpool,

Brownlow Hill, P.O. Box 147,

Liverpool, L69 3BX.

Abstract

Coherent states on the the m-sheeted sphere (for the SU(2) group) are used to define analytic representations. The corresponding generators create and annihilate clusters of m photons. Non-linear Hamiltonians that contain these generators are considered and their eigenvectors and eigenvalues are explicitly calculated. The Holstein-Primakoff and Schwinger formalisms in this context are also discussed.

1 Introduction

In recent work [1] we have generalised two-photon states into m-photon states. Previously m-photon states have been considered in [2, 3]. The approach of ref. [2] is related to the Hamiltonian

$$H = \omega a^+ a + \lambda (a^+)^m + \lambda^* a^m \tag{1}$$

and is known to have several difficulties. Our m-photon coherent states are more related to those of ref. [3]. Our approach is heavily based on the theory of analytic representations and it goes far beyond previous work [4-7] in the sense that it uses them in the context of Riemann surfaces.

In refs. [1] we have studied m-photon states in connection with the m-sheeted complex plane (for the Heisenberg-Weyl group) and the m-sheeted unit disc (for the $SU(1,1)$ group). In this paper we extend these results to the $SU(2)$ case. Using our formalism we calculate explicitly the eigenvalues and eigenvectors of the Hamiltonian

$$H = \omega J_z + \lambda J_+^{(m)} + \lambda^* J_-^{(m)} \tag{2}$$

where $J_+^{(m)}$, $J_-^{(m)}$ are $SU(2)$ generators that move an electron up or down by m steps.

From a mathematical point of view the work is a contribution to the study of highly non-linear Hamiltonians. It has been motivated by recent developments in conformal field theory [8], but of course the details are very different here. Only simple cases of m-sheeted Riemann

surfaces have been considered so far. but the final goal is to extend this work to more complex Riemann surfaces and solve very large classes of highly non-linear Hamiltonians. We believe that this can become a major tool in the study of non-linear Hamiltonians.

In the context of condensed matter the Hamiltonians considered here describe m-particle clustering. Pairing of particles plays an important role in superfluidity and superconductivity and the more general m-particle clustering studied here, could be useful in the study of new phases in condensed matter.

2 Analytic representations in the extended complex plane ($SU(2)$ group)

$SU(2)$ coherent states in a finite-dimensional Hilbert space H_{2j+1}, are defined in the extended complex plane (which is the stereographic projection of a sphere) as:

$$\begin{aligned} |z\rangle &= (1+|z|^2)^{-j}\sum \delta(j,n) z^{j+n}|j,n\rangle \\ \delta(j,n) &= [(2j)!]^{\frac{1}{2}}[(j+n)!(j-n)!]^{-\frac{1}{2}} \end{aligned} \tag{3}$$

Let $|f\rangle$ be an arbitrary (normalised) state in H_{2j+1}:

$$|f\rangle = \sum_{n=-j}^{j} f_n|j;n\rangle \quad \sum_{n=-j}^{j}|f_n|^2 = 1 \tag{4}$$

Its Bargmann analytic representation in the extended complex plane is the following polynomial (of order 2j):

$$f(z) = (1+|z|^2)^j(z^*|f\rangle = \sum_{n=-j}^{j}\delta(j,n)f_n z^{j+n} \tag{5}$$

The scalar product of two such functions is defined as:

$$\langle f|g\rangle = \frac{2j+1}{\pi}\int f^*(z)g(z)(1+|z|^2)^{-2j}d\mu_1(z) \tag{6}$$

$$d\mu_1(z) = (1+|z|^2)^{-2}d^2z \tag{7}$$

The $SU(2)$ generators are represented as:

$$J_- = \partial_z, \quad J_z = z\partial_z - j, \quad J_+ = -z^2\partial_z + 2jz \tag{8}$$

$SU(2)$ transformations on $f(z)$ of equ(5) are implemented through the Mobius conformal mappings:

$$w = \frac{az-b^*}{bz+a^*}; \quad |a|^2+|b|^2 = 1 \tag{9}$$

$$f(z) \to f(w)(bz+a^*)^{2j} = \sum_{n=-j}^{j} f_n\delta(j,n)[az-b^*]^{j+n}[bz+a^*]^{j-n} \tag{10}$$

3 Analytic representations in the m-sheeted extended complex plane

The formalism developed in the previous section is generalised here by replacing z by z^m. In order to have one-to-one mappings we introduce appropriate Riemann surfaces: an m-sheeted complex plane and an m-sheeted extended complex plane. The point $z = 0$ is a branch point of order $m - 1$ in all three cases. We also have cuts along the lines

$$\begin{aligned} z &= r\omega^l; \quad l = 0, 1, \ldots (m-1) \\ \omega &= \exp\left[i\frac{2\pi}{m}\right] \end{aligned} \tag{11}$$

We shall call sheet number s(z) of a complex number z the

$$s(z) = \mathrm{IP}\left(\frac{\mathrm{marg}(z)}{2\pi}\right) \tag{12}$$

where IP stands for the integer part of the number. s(z) takes the integer values from 0 to m-1 (modulo m). The Hilbert space is $(2j+1)$-dimensional and we only consider cases where the $2j + 1$ is an integer multiple of m

$$2j + 1 = m(2k + 1) \tag{13}$$

The states $|jn\rangle$ can also be relabeled as:

$$|jn\rangle = |ml; kh\rangle \tag{14}$$

$$h = \mathrm{IP}\left[\frac{j+n}{m}\right] \tag{15}$$

$$i = \mathrm{REM}\left[\frac{j+n}{m}\right] \tag{16}$$

where IP and REM stand for the integer part and remainder of the indicated division, correspondingly. The Hilbert space H_{2j+1} can be decomposed as:

$$H_{2j+1} = \sum_{l=0}^{m-1} H_l \tag{17}$$

$$H_l = \{|ml; kh\rangle; \quad -k \leq h \leq k\} \tag{18}$$

The SU(2) coherent states of equ(3) are generalised into coherent states on an m-sheeted covering of the SU(2) group, defined as follows:

$$|z; m\rangle = (1 + |z|^{2m})^{-k} \sum_{h=-k}^{k} \delta(k, h)(z^m)^{k+h} |m, s(z); k, h\rangle \tag{19}$$

They are SU(2) coherent states within the Hilbert subspace $H_{s(z)}$. A resolution of the identity in terms of these states is written as follows:

$$\frac{2k+1}{\pi} \int_C |z; m\rangle\langle z; m| d\mu_{r_1}(z) = 1 \tag{20}$$

$$d\mu_m(z) = (1+|z|^{2m})^{-2} m^2 |z|^{2(m-1)} d^2 z \tag{21}$$

The metric $a\mu_m(z)$ comes from the metric of equ(7) with z replaced by z^m. Using the states (19) we define the extended Bargmann representation in the m-sheeted extended complex plane of the arbitrary state $|f\rangle$ of equ(4) as:

$$f(z;m) = (1+|z|^{2m})^k (z^*;m|f\rangle = \sum_{h=-k}^{k} \delta(k,h)(z^m)^{k+h} f_{h,s(z)} \tag{22}$$

f(z;m) is a polynomial of order 2km=2j-(m-1) and is analytic at the interior of each sheet. The scalar product is given as

$$\langle f|g\rangle = \frac{2k+1}{\pi} \int_C f^*(z;m) g(z;m) (1+|z|^{2m})^{-2k} d\mu_m(z) \tag{23}$$

Substitution of z by z^m in (8) gives the operators:

$$J_+^{(m)} = -m^{-1} z^{1+m} \partial_z + 2kz^m \tag{24}$$

$$J_-^{(m)} = m^{-1} z^{1-m} \partial_z \tag{25}$$

$$J_z^{(m)} = m^{-1} z \partial_z - k \tag{26}$$

$$\left[J_z^{(m)}, J_+^{(m)}\right] = J_+^{(m)} \tag{27}$$

$$\left[J_z^{(m)}, J_-^{(m)}\right] = -J_-^{(m)} \tag{28}$$

$$\left[J_+^{(m)}, J_-^{(m)}\right] = 2J_z^{(m)} \tag{29}$$

$$J_+^{(m)}|ml;kh\rangle = |k(k+1) - h(h+1)|^{\frac{1}{2}} |m,l;k,h+1\rangle \tag{30}$$

$$J_-^{(m)}|ml;kh\rangle = |k(k+1) - h(h-1)|^{\frac{1}{2}} |m,l;k,h-1\rangle \tag{31}$$

$$J_z^{(m)}|ml;kh\rangle = h|ml;kh\rangle \tag{32}$$

They act as $SU(2)$ generators within H_l and therefore they move the state $|jn\rangle$ upwards or downwards by m steps. SU(2) transformations on the f(z;m) of equ(22) are implemented as generalised Mobius conformal mappings:

$$w = \left[\frac{az^m - b^*}{bz^m + a^*}\right]^{\frac{1}{m}}; \quad |a|^2 + |b|^2 = 1 \tag{33}$$

$$f(z;m) \to f(w;m)(bz^m + a^*)^{2k} \tag{34}$$

4 Applications to m-photon states

We consider the Hamiltonian:

$$H = \omega J_z + \lambda J_+^{(m)} + \lambda^* J_-^{(m)} \tag{35}$$

Its eigenvectors and eigenvalues are:

$$HU_m(\theta,\phi)|ml;kh\rangle = \{|l - \frac{1}{2}(m-1)|\omega + \tau h\} U_m(\theta,\phi)|ml;kh\rangle \tag{36}$$

$$U_m(\theta,\phi) = \exp\left[-\frac{1}{2}\theta e^{-i\phi} J_+^{(m)} + \frac{1}{2}\theta e^{i\phi} J_-^{(m)}\right] \tag{37}$$

$$\tau = [(\omega m)^2 + |\lambda|^2]^{\frac{1}{2}} \tag{38}$$

$$\phi = \arg(\lambda) \tag{39}$$

$$\cos(\theta) = \omega m \sigma^{-1} \tag{40}$$

5 Holstein-Primakoff and Schwinger formalisms

The operators $J_+^{(m)}$, $J_-^{(m)}$, $J_z^{(m)}$ studied in this paper can be connected with the creation and annihilation operators of m-photons $a_m^\dagger$, a_m studied explicitly in [1], through the Holstein-Primakoff and Schwinger formalisms. In the Holstein-Primakoff case:

$$\begin{aligned} J_+^{(m)} &= \left[(2k+1) - a_m^\dagger a_m\right]^{\frac{1}{2}} a_m^\dagger \\ J_-^{(m)} &= a_m \left[(2k+1) - a_m^\dagger a_m\right]^{\frac{1}{2}} \\ J_z^{(m)} &= a_m^\dagger a_m - k \end{aligned} \tag{41}$$

In the Schwinger case the operators $J_+^{(m)}$, $J_-^{(m)}$, $J_z^{(m)}$ are expressed in terms of two modes as:

$$\begin{aligned} J_+^{(m)} &= a_{mA}^\dagger a_B \\ J_-^{(m)} &= a_{mA} a_B^\dagger \\ J_z^{(m)} &= (a_{mA}^\dagger a_{mA} - a_B^\dagger a_B)/2 \end{aligned} \tag{42}$$

$a_{mA}^\dagger$, a_{mA} are m-photon creation and annihilation operators for the mode A; and $a_B^\dagger$, a_B are ordinary creation and annihilation operators for the mode B. Terms like $a_{mA}^\dagger a_B$ describe the conversion of one B-photon into m A-photons. Inserting (41), (42) into the Hamiltonian (35) we get other Hamiltonians whose eigenvalues and eigenvectors we can calculate.

6 Discussion

Previous work on coherent states in the m-sheeted extended complex plane (for the Heisenberg-Weyl group) [1], has been extended to the m-sheeted sphere (for the $SU(2)$). They have been used to define analytic representations and study highly non-linear Hamiltonians that describe m-photon clustering. Further work should be directed to more complicated Riemann surfaces and their possible use in the study of even more general classes of non-linear Hamiltonians.

7 Acknowledgement

Financial support from the Royal Society and the Royal Academy of Engineering in the form of a travel grant is gratefully acknowledged.

8 References

1. A. Vourdas, J. Math. Phys. 34, 1223 (1993), J. Math. Phys. 35, 2687 (1994)
2. R.A. Fisher, M.M. Nieto, V.D. Sandberg, Phys. Rev. D29, 1107, (1984)
   S.L. Braunstein, R.I. McLachlan, Phys. Rev. A35, 1659, (1987)
   M. Hillery, Phys. Rev. A42, 498 (1990)
   P.V. Elyutin, D.N. Klyshko, Phys. Let. A149 (1990) 241
3. J. Katriel, A. I. Solomon, G. D'Ariano, M. Rasetti, Phys. Rev. D34, 2332 (1986)
   J. Katriel, M. Rasetti, A. I. Solomon, Phys. Rev. D35, 1248, (1987)
   G. D'Ariano, S. Morosi, M. Rasetti, J. Katriel, A. I Solomon, Phys. Rev. D36, 2399, (1987).
   G. D'Ariano, Intern. J. Mod. Phys. B6, 1291 (1992).
4. V. Bargmann Commun. Pure Appl. Math. 14, 187 (1961), Rev. Mod. Phys. 34, 829 (1962)
5. F.A. Berezin, Math. USSR Izv. 8, 1109 (1974), 9, 341 (1975), Commun. Math, Phys. 40, 153 (1975)
6. A.M. Perelomov "Generalized Coherent states and their applications" (Springer, Berlin, 1986), Commun. Math, Phys. 26, 222 (1972), Sov. Phys. Uspekhi 20, 703 (1977)
7. T. Paul, J. Math. Phys. 25, 3252, (1984)
   J.R. Klauder, Ann. Phys. 188, 120, (1988)
   A. Vourdas, Phys. Rev. A41, 1653, (1990), Phys. Rev. A45, 1943, (1992), Physica Scripta, T48, 84 (1993)
   J.P. Gazeau, V. Hussin, J. Phys. A25, 1549, (1992)
8. M. Jimbo, T. Miwa, A. Tsuchiya (Editors), "Conformal field theory and solvable lattice models", (Academic, London, 1988)
   P. Goddard, D. Olive (Editors), "Kac-Moody and Virasoro algebras", (World Scientific, Singapore, 1988)
   V.G. Kac (Editor), "Infinite dimensional lie algebras and groups", (World Scientific, London, 1989)

NEXT
DOCUMENT

CONTROLLED QUANTUM PACKETS

Salvatore De Martino
Silvio De Siena
Dipartimento di fisica, Universita' di Salerno,
and INFN, Sezione di Napoli, gruppo collegato di Salerno
84081 Baronissi, Italy

Abstract

We build Quantum wave packets as dynamically controlled systems. It is useful to use, to this aim, Stochastic Mechanics, a probabilistic simulation of Quantum Mechanics.

1 Introduction

We look at time evolution of a physical system from the point of view of dynamical control theory. Normally we solve motion equation with a given external potential and we obtain time evolution. Standard examples are the trajectories in classical mechanics or the wave functions in Quantum Mechanics. In the control theory, we have the configurational variables of a physical system, we choose a velocity field and with a suited strategy we force the physical system to have a well defined evolution. The evolution of the system is the "premium" that the controller receives if he has adopted the right strategy. The strategy is given by well suited laboratory devices. The control mechanisms are in many cases non linear; it necessary, namely, a feedback mechanism to retain in time the selected evolution. Our aim is to introduce a scheme to obtain Quantum wave packets by control theory. The program is to choose the characteristics of a packet, that is, the equation of evolution for its centre and a controlled dispersion, and to give a building scheme from some initial state (for example a solution of stationary Schroedinger equation). It seems natural in this view to use stochastic approach to Quantum Mechanics, that is, Stochastic Mechanics [S.M.] [2] [3]. It is a quantization scheme different from ordinary ones only formally. This approach introduces in quantum theory the whole mathematical apparatus of stochastic control theory. Stochastic Mechanics, in our view, is more intuitive when we want to study all the classical-like problems. We apply our scheme to build two classes of quantum packets both derived generalizing some properties of coherent states [4].

2 Stochastic Mechanics

We give a brief outline of S.M.. A way to introduce S.M. can be the following. We consider a diffusion process with diffusion coefficient $\nu(q,t)$. $q(t)$ is a stochastic dynamical variable. We introduce its associated Ito forward and backward equations

$$dq(t) = v_{(+)}(q(t),t)dt + \nu(q,t)dw(t)\,, \quad dt > 0\,. \tag{1}$$

$$dq(t) = v_{(-)}(q(t),t)dt + \nu(q,t)dw(t)\,, \quad ; dt > 0\,. \tag{2}$$

In the above stochastic differential equations $v_{(+)}$ and $v_{(-)}$ are respectively forward and backward drift fields, and w is the Wiener process. We can equivalently consider forward Fokker Planck equation

$$\partial_t \rho(q,t) = \nu \Delta \rho(q,t) - \nabla v_{(+)} \rho \tag{3}$$

and the correspondent backward one with $v_{(-)}$. For $q(t)$ are also defined the osmotic velocity

$$u(x,t) = \frac{v_{(+)} - v_{(-)}}{2}, \tag{4}$$

and the current velocity

$$v(x,t) = \frac{v_{(+)} + v_{(-)}}{2}. \tag{5}$$

The simple identity holds

$$v_{(+)} = v_{(-)} + \frac{\nu \nabla \rho}{\rho}. \tag{6}$$

The sum of the Fokker-Planck equations, using (5), gives us the continuity equation:

$$\partial_t \rho \; = \; -\nabla(\rho v), \tag{7}$$

thus expressing probability storage. Now if we assign "a priori" $v_{(+)}$ or $v_{(-)}$, the diffusion process so introduced is completely determined. By the integration of Ito equations (equivalently of Fokker Planck equations) we have the complete evolution of the dynamical stochastic system under study. A notable [5] inequality to take in account is the following

$$\Delta q \Delta u \geq \langle \nu(q,t) \rangle. \tag{8}$$

It derives by the nondifferentiability of the process. We remark that diffusion processes are not time reversal invariant. There is, however, a time reversal approach to diffusion processes, thus introducing a very different class of diffusions. In this different way Ito equations become a kinematical condition to complete with a suitable dynamical principle. It comes simple to add as a dynamical condition a variational principle. Namely, choosing the following mean regularized Eulerian action A:

$$A \; = \; \int_{t_a}^{t_b} \left[\frac{m}{2}(v^2 - u^2) - \Phi \right] \rho d^3x, \tag{9}$$

where $\Phi(x,t)$ denotes the external potential, taking smooth variations, with the continuity equation (7) taken as a constraint, after standard calculations we obtain Hamilton-Jacobi-Madelung (H-J-M) equation

$$\partial_t v + (v \cdot \nabla) v - \nu^2 \nabla \Big(\frac{\nabla^2 \sqrt{\rho}}{\sqrt{\rho}} \Big) = -\nabla \Phi. \tag{10}$$

The current velocity is fixed to be a gradient field $v = \nabla S/m$, with $S(x,t)$ a scalar field. This class of diffusion processes have time reversal invariance and is commonly appelled "Stochastic Mechanics". S.M., in fact, presents us as a generalization of classical mechanics in which ordinary classical trajectories become probabilistic. There are many applications of S.M. (biological population segregation, bode law, planetary atmosphere, stochastic neurodynamics); it is then a theory interesting for itself. It is well known that the equations of S.M. show, also, some interesting link with the equations of Quantum Mechanics.

3 Quantum Mechanics and Stochastic Mechanics

Now we introduce an interpretative scheme in which phenomenological previsions of S.M. coincide with that of Quantum Mechanics for all experimentally measurable quantum effects. S.M., in this view, is a quantization scheme different from ordinary ones only formally, but completely equivalent from the point of view of physical interpretation. Stochastic Mechanics can be interpreted as a probabilistic simulation of Quantum Mechanics giving a bridge between Quantum Mechanics and stochastic differential calculus. Defining now the complex function $\Psi = \sqrt{\rho}\exp[iS/\hbar]$, where ρ and S are the same that satisfy the equations of Stochastic Mechanics, and choosing $\nu = \frac{\hbar}{2m}$, we immediately have that the continuity equation (7) together with the dynamical equation (8) are equivalent to the Schrödinger equation. The correspondence between expectations and correlations defined in the stochastic and in the canonic pictures are

$$\langle\hat{q}\rangle = E(q)\,, \qquad \langle\hat{p}\rangle = mE(v)\,,$$
$$\Delta\hat{q} = \Delta q\,, \qquad (\Delta\hat{p})^2 = m^2[(\Delta u)^2 + (\Delta v)^2]\,. \tag{11}$$

The following chain inequality holds:

$$(\Delta\hat{q})^2(\Delta\hat{p})^2 \geq m^2(\Delta q)^2(\Delta u)^2 \geq \frac{\hbar^2}{4}\,. \tag{12}$$

In the above relations $\hat{q}$ and $\hat{p}$ denote the position and momentum observables in the Schrodinger picture, $\langle\cdot\rangle$ denotes the expectation value of the operators in the given state Ψ, $E(\cdot)$ is the expectation value of the stochastic variables associated in the Nelson picture to the state $\{\rho, v\}$, and $\Delta(\cdot)$ denotes the root mean square deviation.

The chain of inequalities (11), i.e. the osmotic uncertainty relation and its equivalence with the momentum-position uncertainty, were proven in Ref. [6].

4 Ehrenfest equation and quantum packets

It is opportune to give a brief outline of the standard arguments about wave packets motion. It is usual to start with the Ehrenfest equation. The argument is the following. In order to have a wave packet following a controlled motion, that is the packet motion may be likened to the motion of classical particle, it is not only necessary that its position and its momentum follow the laws of classical mechanics, but we must control the dimensions of the packet; it must remain small or controlled at any time. In fact (we pose $m = 1, \hbar = 1/2$), if we look at Ehrenfest equations

$$\frac{d}{dt}E(q) = E(v) \tag{13}$$

and

$$\frac{d^2}{dt^2}E(q) = -E(\nabla\Phi), \tag{14}$$

(written directly in the stochastic formalism), it is immediately seen that all the moments of ρ are implicated through the mean values. We can see this in an intuitive manner. Consider the

motion of a particle in an external potential Φ. In order to have a classical-like motion the "right" Ehrenfest equation should be

$$\frac{d^2}{dt^2}E(q) = -\nabla\Phi|_{E(q)}. \tag{15}$$

If we take Taylor expansion of $\nabla\Phi$, all the moments are contained in the Ehrenfest equation as a matter of fact. Now it is necessary to obtain a set of equations that rule the evolution of moments. It is not difficult to see that it is satisfied the following set of equations

$$\frac{1}{n}\frac{d}{dt}E((q-E(q))^n) = E((q-E(q))^{n-1}v) - E((q-E(q))^{n-1})E(v). \tag{16}$$

They are interesting by itself. From these equations it is possible to connect moments and the external potential. This set of equations has in general a very complicated structure, namely, we have infinite coupled equations, and only in some particular case the equations collapse to a finite number (for example when ρ has some gaussian behaviour, as in our examples). The equations express the fact that the positional dispersion is controlled by the whole density. The equation to consider, in general, is the equation for positional Entropy

$$\frac{d}{dt}E(\log\rho) = -E(\nabla v). \tag{17}$$

5 Controlled quantum packets

Now we illustrate the scheme to build controlled quantum systems. We prove that it is theoretically possible, choosing a well suited control device, to have packets with a well defined motion and form. This point of view is not new; namely the coherent states and in particular the parametric oscillator are, in an opportune sense, linearly controlled systems in which the equation for dispersion depend by the coefficients of the external potential. The general scheme of control we introduce is non-linear. Our idea is the following. If we select a particular current velocity, we choose ,in fact, the phase of the wave function and, as a consequence, we choose the caracteristics of the motion of the centre of the packet. Moreover, a choice of current velocity selects a class of solutions of continuity (Fokker-Planck) equation. The(H-J-M) equation becomes in this scheme a constraint to retain time-reversal invariance, giving us the controlling device. Now we build two classes of controlled quantum packets as example. We need some initial condition ρ_0 for probability density; it can be a generic L^1 function and we can choose always that it satisfies a stationary Schrödinger equation with Φ_0 as external potential. In the first example we take the current velocity selected as that of coherent states [7]

$$v = E(v) + \frac{x-E(q)}{\Delta q}\frac{d\Delta q}{dt}. \tag{18}$$

As second example we impose gaussian behaviour simply balancing current and osmotic velocity :

$$v = E(v) - \frac{1}{2}u(x,t)\frac{d}{dt}\Delta q. \tag{19}$$

6 Generalized coherent states

We have already introduced the first example as generalized coherent states [7] [8]. If we insert the current velocity in continuity equation (7) we solve in a very simple way and we obtain:

$$\rho(\xi) = \int \delta(y-\xi)\rho_0(y)dy \ , \ \xi = \frac{x - E(q)}{\Delta q}. \tag{20}$$

Now we can examine the Ehrenfest equation, and then (H-J-M) equation that now is become an identity. It is not difficult to see that

$$\frac{dE(v)}{dt}x + \frac{1}{2}\xi^2\frac{d^2\Delta q}{dt^2} - \frac{\int \Phi_0(y)\rho_0(y)\delta(y-\xi)dy}{\int \rho_(0)\delta(y-\xi)dy} + L(t) = -\Phi. \tag{21}$$

Φ_0 is the external potential in the stationary Schrödinger equation of which ρ_0 is a solution, Φ is the state dependent control device. Inserting now our current velocity (19) in the eq.(17) we see that

$$E(\log \rho(x,t)) = -\log \Delta q. \tag{22}$$

The whole positional entropy come by dispersion and this means that the set of eq.s (16) is close. We can extract from eq.s (18)-(20) one equation for Δq, and all the others depend from this last one. The equation is:

$$\frac{d^2\Delta q}{dt^2} = \frac{a}{\Delta q^3} - E(\xi\nabla\Phi) \tag{23}$$

where a is a number. The Ehrenfest equation becomes for this states

$$\frac{d^2}{dt^2}E(q) = -\nabla\Phi|_{E(q)}. \tag{24}$$

The couple of equations (24), (25) comes from equation (22) taking the first and second order of Taylor expansion. It is, also, significative to write Ito equation for this class of stochastic processes

$$dq(t) = E(v)dt + \nu dw. \tag{25}$$

They are associated, as Glauber states, to Wiener processes with a drift that is solution of the classical Eherenfest equation (25). For more details see [9].

7 Controlled gaussian wave packets

Now we give our second example [10]. If we insert the current velocity (22) into the continuity equation (7) we have the following Fokker-Planck equation

$$\partial_t\rho(x,t) = E(q)\nabla\rho(x,t) + \frac{d}{dt}\Delta q\nabla^2\rho(x,t) \tag{26}$$

whose general solution is

$$\rho(\xi,t) = \frac{1}{\Delta q}\int \rho_0(y)\exp -[(x-\xi)^2]dy. \tag{27}$$

Now, also in this case it is possible to verify that Ehrenfest equation is classical-like; it sufficient to control the first and second moment. The equation for positional entropy is very simple as in the first example, and we have the following control potential:

$$\frac{dE(v)}{dt}x - \log\rho(x,t)\frac{d^2}{dt^2}\Delta q^2 - (1+(\frac{d}{dt}\frac{\Delta q^2}{\nu})^2)[\frac{\int \Phi_0(y)G(y,\xi)dy}{\int G(y,\xi)dy} + \tag{28}$$

$$+\frac{\int u_0(y)^2 G(y,\xi)dy}{\int G(y,\xi)} - [\frac{\int u_0(y)G(y,\xi)}{\int G(y,\xi)dy}]^2 + N(t) = -\Phi$$

where $G(y,\xi) = \rho_0(y)\exp[(y-\xi)^2]$, and $N(t)$ is a generic time function. Also in this case the Ehrenfest equation is classical like. It is not difficult to see that

$$E(\nabla\Phi) - \nabla\Phi|_{E(q)} = F(E(q),\Delta q). \tag{29}$$

Using this identity and expanding (28), by the first and second order one obtain Ehrenfest equation and the coupled equation for dispersion. Note that the Ito equation is now

$$dq(t) = E(v)dt + \nu\frac{d\Delta q}{dt}dw. \tag{30}$$

This wave packets are Gaussian modulation of the initial state. The equations are all implicit if we do not specify the initial condition.

References

[1] J. R. Klauder and B. S. Skagerstam, *Coherent States* (World Scientific, Singapore, 1985); W. M. Zhang, D. H. Feng, and R. Gilmore, Rev. Mod. Phys. **62**, 867 (1990).

[2] E. Nelson, *Dynamical Theories of Brownian Motion* (Princeton University Press, Princeton, 1967); *Quantum Fluctuations* (Princeton University Press, Princeton, 1985).

[3] F. Guerra, Phys. Rep. **77**, 263 (1981); F. Guerra and L. M. Morato, Phys. Rev. D **27**, 1774 (1983).

[4] R. J. Glauber, Phys. Rev. **130**, 2529 (1963); Phys. Rev. **131**, 2766 (1963); J. R. Klauder, J. Math. Phys. **4**, 1058 (1963); E. C. G. Sudarshan, Phys. Rev. Lett. **10**, 227 (1963).

[5] S. De Martino, S. De Siena, F. Illuminati, and G. Vitiello, Mod. Phys. Lett. B **8**, 977 (1994); see also Ref.[7], p. 331.

[6] L. De La Peña and A. M. Cetto, Phys. Lett. A **39**, 65 (1972); D. de Falco, S. De Martino and S. De Siena, Phys. Rev. Lett. **49**, 181 (1982).

[7] S. De Martino, S. De Siena, and F. Illuminati, Mod. Phys. Lett. B **8**, 1823 (1994).

[8] S. De Martino, S. De Siena, and F. Illuminati, *Dynamics of Generalized Coherent States*, Preprint DFPD 94/TH/66, December 1994, to be published.

[9] S.De Martino, S.De Siena, *Operatorial approach to generalized coherent states*, in these proceedings.

[10] S. De Martino, S. De Siena, to appear.

NEXT
DOCUMENT

A secure key distribution system of quantum cryptography based on the coherent state

Guo Guang-can and Zhang Xiao-yu
Physics Department, University of Science and Technology of China, Hefei, Anhui, P.R.China

Abstract

A quantum key distribution based on coherent state is introduced in this paper. Here we discuss the feasibility and security of this scheme.

The cryptographic communication has a lot of important applications, particularly in the magnificent prospects of private communication. As one knows, the security of cryptographic channel depends crucially on the secrecy of the key. The Vernam cipher is the only cipher system which has guaranteed security. In that system the key must be as long as the message and must be used only once. Quantum cryptography is a method whereby key secrecy can be guaranteed by a physical law So it is impossible, even in principle, to eavesdrop on such channels. Quantum cryptography has been developed in recent years. Up to now, many schemes of quantum cryptography have been proposed[1]-[8]. Now one of the main problems in this field is how to increase transmission distance.

In order to use quantum nature of light, up to now proposed schemes all use very dim light pulses. The average photon number is about 0.1. Because of the loss of the optical fiber, it is difficult for the quantum cryptography based on one photon level or on dim light to realize quantum key-distribution over long distance.

Here we introduce a scheme of quantum cryptography based on coherent state. The average photon number per pulse can be increased, so that we can transmit the key over longer distance.

First of all, we consider the quantum theory of the beam splitter (Fig. 1). Alice sends a mode a_1 which is in state $|\alpha_1\rangle$ into the beam splitter. Bob sends a mode b_1 which is in state $|\beta_1\rangle$ into the BS to measure the state sent by Alice. Suppose the output modes are a_2 and b_2, which are in state $|\alpha_2\rangle$ and $|\beta_2\rangle$ respectively.

According to the quantum theory of BS[9], in Heisenberg picture we have following formula:

$$\begin{bmatrix} b_1 \\ b_2 \end{bmatrix} = \begin{bmatrix} B_{11} & B_{12} \\ B_{21} & B_{22} \end{bmatrix} \begin{bmatrix} a_1 \\ a_2 \end{bmatrix} = U \begin{bmatrix} a_1 \\ a_2 \end{bmatrix} U^{+} \tag{1}$$

$$B_{ij} = |B_{ij}| e^{i\phi_{ij}}, \quad \phi_{11} - \phi_{21} = \phi_{12} - \phi_{22} \mp \pi$$

$$|B_{11}|^2 = |B_{22}|^2 = \cos^2\theta, \quad |B_{12}|^2 = |B_{11}|^2 = \sin^2\theta$$

Here U is Unitary Operator of the BS. $\cos^2\theta$ is the reflection rate of the beam splitter.

In Schrödinger picture, if the incoming state is $|\psi_1\rangle = |\alpha_1, \beta_1\rangle$, then the output state $|\psi_2\rangle$ should be

$$|\psi_2\rangle = |\alpha_2, \beta_2\rangle = U^+|\alpha_1, \beta_1\rangle \tag{2}$$

$$U = e^{-iL_3(\phi_r - \phi_p)} e^{-i2\cos^{-1}(r^{1/2})L_2} e^{-iL_3(\phi_r + \phi_p)} \tag{3}$$

$$L_1 = \frac{1}{2}(a_1^\dagger a_2 + a_2^\dagger a_1), \quad L_2 = \frac{1}{2i}(a_1^\dagger a_2 - a_2^\dagger a_1), \quad L_3 = \frac{1}{2}(a_1^\dagger a_1 + a_2^\dagger a_2)$$

$$\phi_r \equiv \frac{1}{2}(\phi_{11} - \phi_{22}), \quad \phi_p \equiv \frac{1}{2}(\phi_{11} - \phi_{22} \mp \pi)$$

Using these formula, we can in principle derive the output state for any incoming state. We are particularly interested in the following situation:

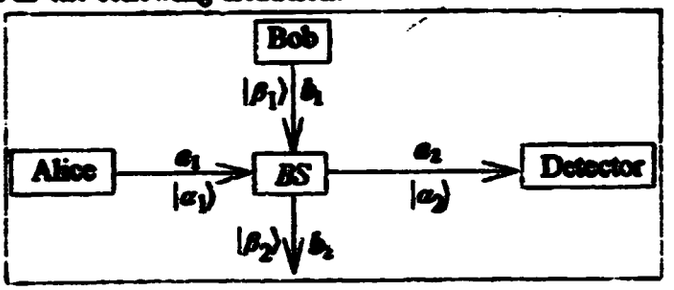

FIG. 1. The basic scheme of quantum cryptography based on coherent states.

Suppose input is a coherent state $|\alpha_1, \beta_1\rangle$. According to above formula, the output state is also a coherent state as following,

$$|\psi_2\rangle = |\alpha_1 \cos\theta - \beta_1 \sin\theta, \beta_1 \cos\theta + \alpha_1 \sin\theta\rangle \equiv |\alpha_2\rangle|\beta_2\rangle \tag{4}$$

$$\alpha_2 = \alpha_1 \cos\theta - \beta_1 \sin\theta, \beta_2 = \beta_1 \cos\theta + \alpha_1 \sin\theta$$

So the output state $|\alpha_2\rangle$ depends on the eigenvalues of incoming coherent states α_1, β_1 and θ. Here $\cos^2\theta$ is the reflection rate of the beam splitter. Now we use a symmetrical beam splitter, $\theta = \frac{\pi}{4}$, and let $\alpha_1 = \alpha$ or $\alpha + \delta\alpha$, $\beta_1 = \alpha$ or $\alpha + \delta\alpha$. In this case, the output state $|\alpha_2\rangle$ is

$$|\alpha_2\rangle = \begin{cases} |0\rangle & \alpha_1 = \beta_1 \\ |\frac{\sqrt{2}}{2}\delta\alpha\rangle & \alpha_1 = \alpha + \delta\alpha, \beta_1 = \alpha \\ |-\frac{\sqrt{2}}{2}\delta\alpha\rangle & \alpha_1 = \alpha, \beta_1 = \alpha + \delta\alpha \end{cases} \tag{5}$$

That means when Alice and Bob send the same coherent state, output state $|\alpha_2\rangle$ is vacuum state $|0\rangle$. When they use different states, $|\alpha_2\rangle$ will be a coherent state and its eigenvalue is proportional to $\pm\frac{\sqrt{2}}{2}\delta\alpha$. Therefore, the probability of detecting photon in state $|\alpha_2\rangle$ is given by this expression,

$$P_n = |\langle n|\alpha_2\rangle|^2 = \begin{cases} 0 & \alpha_1 = \beta_1 \\ e^{-\frac{1}{2}|\delta\alpha|^2} \frac{\delta\alpha/\sqrt{2}}{n!} & \alpha_1 \neq \beta_1 \end{cases} \tag{6}$$

These results tell us when Alice and Bob use the same coherent state, there is no photon to be detected in output state $|\alpha_2\rangle$. Whereas they use different coherent states, the probability of detecting photon is not zero. Now we take the value of $|\delta\alpha|$ is equal to $\sqrt{2\ln 2}$. Then we get

$$\text{when } \alpha_1 = \beta_1, \qquad P_n = 0 \quad (n \geq 1)$$

$$\text{when } \alpha_1 \neq \beta_1, \qquad \begin{cases} P_0 = \frac{1}{2} \\ P = \sum_{n=1}^{\infty} P_n = \frac{1}{2} \end{cases}$$

That means in this case, probability of detecting no photon is 50%, and the other 50% is to detect at least one photon.

Now Alice randomly sends a sequence of coherent states $|\alpha\rangle$ or $|\alpha + \delta\alpha\rangle$, and Bob also randomly use the coherent states $|\alpha\rangle$ or $|\alpha + \delta\alpha\rangle$ to measure the state sent by Alice

Suppose the detecting results after the transmission are shown in Tab.1,

TABLE I. Key distribution using coherent states.

Alice	α	α	$\alpha+\delta\alpha$	α	$\alpha+\delta\alpha$	$\alpha+\delta\alpha$	α	α
Bob	$\alpha+\delta\alpha$	α	α	$\alpha+\delta\alpha$	$\alpha+\delta\alpha$	α	α	$\alpha+\delta\alpha$
detector	Yes	No	Yes	No	No	Yes	No	No
	o	×	o	×	×	o	×	×
Key	1		0			0		

After completing the transmission, Bob announces publicly the cases in which photons are detected, but keeps secret the states he used. Alice and Bob adopt these cases as the key distribution and translate them into a logical 0 or 1 according to their preexitant agreement. For example, Alice's $|\alpha\rangle$ represents a logical 1 and Bob's $|\alpha\rangle$ stands for a logical 0. By far, we have established a shared key distribution between Alice and Bob.

Of course, above results are in the absence of an eavesdropper. Now we consider how to find the eavesdropper in our system if there is. Suppose there is a an eavesdropper named Eve, she wants to split the incoming states $|\alpha_1\rangle$ from Alice and $|\beta_1\rangle$ from Bob into two parts $\{|\alpha_1'\rangle, |\alpha_1''\rangle\}$ and $\{|\beta_1'\rangle, |\beta_1''\rangle\}$ using her beam splitter. Then she sends states $|\alpha_1'\rangle$ and $|\beta_1'\rangle$ to Bob, and keeps states $|\alpha_1''\rangle$ and $|\beta_1''\rangle$ for her own measurement. Repeating above calculation, we can get

$$\alpha_1' = \alpha_1 \cos\varphi, \qquad \alpha_1'' = \alpha_1 \sin\varphi$$

$$\beta_1' = \beta_1 \cos\varphi, \qquad \beta_1'' = \beta_1 \sin\varphi$$

Here $\cos^2\varphi$ is the reflection rate of Eve's beam splitter. We suppose that Bob does the same measurement as before, but in this time he receives the states $|\alpha_1'\rangle$ and $\beta_1'\rangle$ at the beam splitter. When $\alpha_1' \neq \beta_1'$, the probability of detecting photon P' is given by following expression

$$P' = 1 - \exp\{-1/2|\delta\alpha|^2 \cos^2\varphi\} < P \tag{7}$$

Here P is the probability in the absence of an eavesdropper. Now we define a channel disturbance parameter ξ as

$$\xi = \frac{P - P'}{P}$$

In order to check if there is an eavesdropper, they can calculate the channel disturbance parameter ξ after the transmission. If they discover noticeably $\xi > 0$, they can conclude that

there must be an eavesdropper and discard this key distribution. In fact, In order not to been exposed, Eve has to make $\cos\varphi \approx 1$. However, in this case the probability of her detecting photon is

$$P^{\prime\prime} = \frac{1}{2}(1 - e^{-\frac{1}{2}|\delta\alpha|^2 \sin^2\varphi}) \approx \frac{1}{4}|\delta\alpha|^2 \sin^2\varphi \approx 0$$

This means that Eve can hardly get any information of the key between Alice and Bob.

Bibliography

[1] S. Wiesner, SIGACT News 15, 78 (1983).

[2] C. H. Bennett and G. Brassard, in *Proceedings of IEEE International Conference on Computers, Systems, and Signal Processing, Bangalore, India* (IEEE, New York, 1984), p.175.

[3] C. H. Bennett, G. Brassard, and J. M. Robert, SIAM J. Comput. 17, 210 (1988).

[4] C. H. Bennett, F. Bessette, G. Brassard, L. Salvali, and J. Smolin, J. Cryptology 5, 3 (1991).

[5] A. K. Ekert, Phys. Rev. Lett. 67, 557 (1991).

[6] C. H. Bennett, G. Brassard, and N. D. Mermin, Phys. Rev. Lett. 68, 557 (1992).

[7] A. Ekert, J. G. Rarity, P. R. Tapster, and G. M. Palma, Phys. Rev. Lett. 69, 1293 (1992).

[8] C. H. Bennett, Phys. Rev. Lett. 68, 3121 (1992).

[9] B. Huttner and Y. Ben-Aryeh, Phys. Rev. A 38, 204 (1988)

NEXT
DOCUMENT

SOLVABLE QUANTUM MACROSCOPIC MOTIONS and DECOHERENCE MECHANISMS in QUANTUM MECHANICS on NONSTANDARD SPACE

Tsunehiro KOBAYASHI
Institute of Physics, University of Tsukuba, Ibaraki 305, Japan

Abstract

Quantum macroscopic motions are investigated in the scheme consisting of N-number of harmonic oscillators in terms of ultra-power representations of nonstandard analysis. Decoherence is derived from the large internal degrees of freedom of macroscopic matters.

1. Introduction

How to describe motions of macroscopic matters in quantum mechanics is not only a very interesting problem but also a very important problem to develop the present situation of theoretical physics. Before going into the details we shall start from the question "What are macroscopic matters?". One may characterize them in terms of the following three properties:
(1) The number of constituents N is very large and cannot be precisely counted in measurements.
(2) Every measurement of energy E of macroscopic matters is accompanied by experimental margin of uncertainty ΔE and an enormous number of different quantum states are contained within the energy uncertainty.
(3) Macroscopic matters are usually classical objects. This means that the density matrices describing their quantum states have no interference terms (decoherence mechanism exists.).

The first character indicates that we have no way to measure the precise number of the constituents in realistic measurement processes. Furthermore we may say that the precise determination of the quantum states for all the constituents are impossible. This property has a close connection with the second character. In usual measurements the energies of macroscopic matters are not quantum mechanical order ($O(\hbar)$) which disappears in the limit of $\hbar \to 0$ ($lim_{\hbar \to 0} O(\hbar)$). It means that every measurement of the energy of macroscopic objects may contain some uncertainty ΔE which is in the order $O(\hbar)$. How to introduce these features in quantum mechanics is the main theme of this paper.

An interesting possibility is to describe the macroscopic matters on the Hilbert spaces extended by nonstandard analysis,[1] where infinity (∞) like $N \to \infty$ and infinitesimal (≈ 0) like $\hbar \to 0$ are treated rigorously. It should also be pointed out that quantum states of N constituents which may be described by the direct product of the quantum states of the constituents such that $\Psi_N(r_1,..,r_N) = \prod_{i=1}^{N} \phi_{E_i}(r_i)$ become ultra-products in the limit $N \to \infty$. Then we can represent the macroscopic states in terms of ultra-power representation of nonstandard analysis by introducing some equivalence relation based on the ultra-filter on the ultra-products.

From the discussions of quantum mechanics on nonstandard spaces[2,3,4] we know that
(1) there exist new eigenfunctions called as "ultra-eigenfunctions" which are not described by the

superposition of eigenfunctions on usual quantum mechanics on real number space ($\mathcal{R}$), and (II) in the limit $\hbar \to 0$ we can introduce infinitesimal energy uncertainties ΔE which are in the order $O(\hbar)$. It is important that the introduction of such energy uncertainties is expressed by the monad (infinitesimal neighborhoods) of real numbers on nonstandard spaces.

Now we may expect that we can describe macroscopic states in terms of new eigenfunctions (ultra-eigenfunctions) containing the energy uncertainty $\Delta E \sim O(\hbar)$. In this paper I shall present a solvable model to realize the above consideration.

2. Model

Let us investigate a system consisting of N-harmonic oscillators which are bounded around a fixed point X_0. The Hamiltonian is given by $H_N = \frac{1}{2m}\sum_{i=1}^{N} p_i^2 + \frac{k}{2N}\sum_{i=1}^{N}\sum_{j=1}^{N}(x_i - x_j)^2 + \frac{K}{2}\sum_{i=1}^{N}(x_i - X_0)^2$, where m the mass of the constituents, k and K the oscillator constants, p_i and x_i, respectively, stand for the momentum and position operators of i-th constituent. This Hamiltonian describes the bounded N-oscillator system moving in the harmonic oscillator potential of which center is at X_0. Our interest is focused on the relative motion between the fixed point X_0 and the center of mass(CM) of the N-oscillator system, because the motion will become the observable as the motions of the macroscopic system in the macroscopic limit $N \to \infty$. The Hamiltonian is separable in terms of the following choice of coordinates; $R^N = X_G^N - X_0$, $\rho_n^N = [nx_{n+1} - (\sum_{i=1}^{n} x_i)]/\sqrt{n(n+1)}$, for $n = 1, 2, ..., N-1$, where $X_G^N = \frac{1}{N}\sum_{i=1}^{N} x_i$ is the CM(center of mass) coordinate of the N-oscillator system. We can rewrite the Hamiltonian as

$$H^N = \frac{1}{2mN}(P^N)^2 \ . \ \frac{NK}{2}(R^N)^2 + \sum_{n=1}^{N-1} H_n, \tag{1}$$

where $H_n = \frac{1}{2m}p_n^2 + \frac{1}{2}(k+K)\rho_n^2$. The eigenfunctions for (1) are obtained as follows; $H^N\Psi^N = (E_R + \sum_{n=1}^{N-1}\epsilon_n)\Psi^N$, where

$$\Psi^N(R^N, [\rho_n]) = \Phi_R(R^N)\prod_{n=1}^{N-1}\phi_{l_n}(\rho_n) \tag{2}$$

with $[\rho_n] \equiv [\rho_1, \rho_2, \cdots, \rho_{N-1}]$, which satisfy $H_R\Phi_R = E_R\Phi_R$ and $H_n\phi_{l_n} = \epsilon_n\phi_{l_n}$ with $E_R = (n_R + 1/2)\omega_R\hbar$ ($\omega_R = \sqrt{K_N/M_N} = \sqrt{K/m}$) and $\epsilon_n = (l_n + 1/2)\omega\hbar$ ($\omega = \sqrt{(k+K)/m}$). Note that the eigenvalues of H^N and $\sum_n H_n$ are, respectively, given by $E^N = E_R + \epsilon_L^N$ and $\epsilon_L^N \equiv \sum_{n=1}^{N-1}\epsilon_n = (L + \frac{1}{2}(N-1))\omega\hbar$ with $L = \sum_{n=1}^{N-1} l_n$ and all the energies are of the order of $O(\hbar)$, i.e. $E^N \sim E_R \sim \epsilon_L^N \sim O(\hbar)$. We see that E_R and ϵ_L^N are not enough to specify the state given in (2) uniquely. That is, there are many different states having a fixed value of ϵ_L^N, of which multiplicity is evaluated as $W(N,L) = \frac{(L+N-2)!}{L!(N-2)!}$. *In general we should write eigenfunctions specified by* E_N and ϵ_L^N in terms of the suprepositons of those different states such that

$$\Psi_L^N(E^N; R^N, [\rho_n]) = \Phi_{E_R}(R^N)\sum_{l_1=0}^{L}\cdots\sum_{l_{N-1}=0}^{L}\delta_{\sum_{n=1}^{N-1} l_n, L}\, a([l_n])\prod_{n=1}^{N-1}\phi_{l_n}(\rho_n) \tag{3}$$

with $[l_n] \equiv [l_1, l_2, \cdots, l_{N-1}]$, where $a([l_n])$ are the coefficients satisfying the constraint required from the normalization $\sum_{l_1=0}^{L}\cdots\sum_{l_{N-1}=0}^{L}\delta_{\sum_{n=1}^{N-1} l_n, L}\,|a([l_n])|^2 = 1$.

3. Oscillator system in nonstandard spaces

Now let us study the limit represented by $N \to \infty$. The state given in (2) becomes an infinite direct-product

$$\Psi_{E_R,L}(R;[\rho_n]) = \Phi_{E_R}(R) \prod_{n=1}^{\infty} \phi_{l_n}(\rho_n). \tag{4}$$

The Hamiltonian (1) is modified as $\hat{H} = H_R + \sum_{n=1} \hat{H}_n$, where in order to evade the divergence arising from the sum of zero point oscillations $\sum_{n=1}^{N-1} \frac{1}{2}\hbar\omega$ in the limit of $N \to \infty$ $\hat{H}_n$ is taken as $\hat{H}_n = H_n - \frac{1}{2}\hbar\omega$. We have

$$\hat{H}\Psi_{E_R,L}(R,[\rho_n]) = (E_R + \epsilon_L)\Psi_{E_R,L}(R,[\rho_n]), \tag{5}$$

where $H_R\Phi_{E_R}(R) = E_R\Phi_{E_R}(R)$, and $\epsilon_L = L\hbar\omega$ with $L = \sum_{n=1} l_n$. Note that, since $l_n \in \mathcal{N}$ for $\forall n \in \mathcal{N}$, then $L \in \mathcal{N}$.

Following the expression of (3), we can write the most general wave-functions for the macroscopic object characterized by the CM(center of mass) energy eigenvalue E_R as $\Psi(E_R,[C_L([l_n])];R,[\rho_n]) = \Phi_{E_R}(R)\phi([C_L([l_n])];[\rho_n])$, where

$$\phi([C_L([l_n])];[\rho_n]) = \sum_{L=0}^{L_f} \sum_{l_1=0}^{L} \sum_{l_2=0}^{L} \cdots \delta_{\sum_{n=1} l_n,L}\, C_L([l_n]) \prod_{n=1}^{\infty} \phi_{l_n}(\rho_n), \tag{6}$$

L_f is an arbitrary natural number ($L_f \in \mathcal{N}$) and the normalization condition is given by $\sum_{L=0}^{L_f}\sum_{l_1=0}^{L}\sum_{l_2=0}^{L}\cdots\delta_{\sum_{n=1} l_n,L}\,|C_L([l_n])|^2 = 1$. The expectation value of the total energy is obtained as $< E >= E_R + \Delta E([C_L])$, where $\Delta E([C_L]) \equiv \sum_{L=0}^{L_f}\sum_{l_1=0}^{L}\sum_{l_2=0}^{L}\cdots\delta_{\sum_{n=1} l_n,L}\,|C_L([l_n])|^2\,\epsilon_L$.

Now let us consider measurements of the CM energy. When we try to observe it by using a photon as a probe, we have to measure it through the interaction of the photon with the constituents. This means that we cannot measure the CM energy directly and then we have to take account of the internal motions of the macroscopic object. In realistic measurement processes for macroscopic objects, which will be carried out by using a photon flux composed of many photon, we should consider that direct observable is the total energy rather than the CM energy. In those measurements the total of the internal energy $\Delta E([C_L]) \equiv < E > - < E_R >$ may be understood to be the errors for the CM energy. Note that the errors should not be confused with those arising from inefficiencies of detectors. We may conclude that we have always to take account of the existence of these errors in the observed CM energies when we discuss the CM motions of macroscopic objects which are studied in the classical mechanics.

In nonstandard analysis the error must be infinitesimal. Then as we take into account that the center of mass energy E_R and its angular frequency ω_R are observables represented by real numbers, the possibility allowed here is only the following choice; "$n_R \in {}^*\mathcal{N} - \mathcal{N}$, $L \in \mathcal{N}$, $\hbar \approx 0$." ¿From now on we define the macroscopic limit $st_{n\to\infty}$ by taking

$$N^{-1} \approx 0 \quad and \quad \hbar \approx 0. \tag{7}$$

Let us investigate the equivalence relation introduced on the ultra-products. We can explicitly write this equivalence relation for the macroscopic objects by using the ultra-filter in nonstandard analysis as follows; $\phi_L([\rho],) = \prod_{n=1} \phi_{l_n}(\rho)$ with $\epsilon_L = \sum_n l_n\hbar\omega$ and $\phi_{L'}([\rho_{n'}]) = \prod_{n'=1} \phi_{l'_{n'}}(\rho_{n'})$ with

$\epsilon_{L'} = \sum_{n'} l'_{n'} \hbar\omega$ are equivalent ($\longleftrightarrow_{macro}$), if and only if the number of $n \in \mathcal{N}$ satisfying $l_n \neq 0$ and that of $n' \in \mathcal{N}$ satisfying $l_{n'} \neq 0$ are finite numbers. That is, it is represented as

$$\phi_L \longleftrightarrow_{macro} \phi_{L'}, \quad \textit{if and only if the sets of numbers defined by}$$

$$(n \in \mathcal{N}; l_n \neq 0) \textit{ and } (n' \in \mathcal{N}; l_{n'} \neq 0) \textit{ are finite sets of } \mathcal{N}.$$

The physical space for the macroscopic motions is represented by $\mathcal{S}_{macro}({}^*\mathcal{H}) = {}^*\mathcal{H}/\longleftrightarrow_{macro}$.

Let us start from the most general expression of ultra-eigenfunctions satisfying

$$\hat{H}\Psi_c(R, [\rho_n]) \approx_{macro} E\Psi_c(R, [\rho_n]), \tag{8}$$

where $st_{macro}(E) \in \mathcal{R}$ and $\neq 0$, that is, it is observable in the classical limit. In the above equation Ψ_c is factorized with respect to the CM motion and the internal ones as $\Psi_c = \Phi_c(R)\phi([\rho_n])$. Since E have the freedom of the order of $O(\hbar)$, the general expression for the internal motions is given as $\phi([C_L([l_n])]; [\rho]) = \sum_{L=0}^{L_f} \sum_{l_1=0}^{L} \cdots \sum_{l_n=0}^{L} \cdots \delta_{\sum_{n=1} l_n, L}\, C_L([l_n]) \prod_{n=1} \phi_{l_n}(\rho_n)$, of which energy expectation value is obtained as

$$\Delta E([C_L([l_n])]) \equiv \sum_{L=0}^{L_f} \sum_{l_1=0}^{L} \cdots \sum_{l_n=0}^{L} \cdots \delta_{\sum_{n=1} l_n, L}\, |C_L([l_n])|^2 \epsilon_L \sim O(\hbar). \tag{9}$$

We can derive the equation for the CM motions by operating the internal trace operation represented by the partial trace operation for all the internal variables (${}^\forall\rho$), that is,

$$< \phi([C_L([l_n])]; [\rho]), H\Psi_c(R, [\rho]) >_{internal} = (H_R + \Delta E)\Phi_c(R) \approx_{macro} H_R\Phi_c(R). \tag{10}$$

As was shown in Ref.s[3,4], it is required for us to solve the equation only in the classical region satisfying $st_{macro}(E - \Delta E - V(R)) \in \mathcal{R}_+$. In order to obtain stationary states represented by $\Phi_c^{E_R}(R) = \hat{N} e^{iW(R)/\hbar}$, where $\hat{N}$ denotes the normalization constant, we can reduce the Schroedinger equation to that for $W(R)$ as $i\frac{\hbar}{2M}\frac{d^2W}{dR^2} \approx_{macro} \frac{1}{2M}(\frac{dW}{dR})^2 + \frac{1}{2}\hat{K}R^2 - (E - \Delta E)$. This equation has already solved in Ref.s 3 and 4 and is given in the classical region as

$$W(R) \approx W_{cl}^{E,\Delta E}(R) + \frac{1}{2} i\hbar \ln(u_{cl}^{E,\Delta E}(R)), \tag{11}$$

where $W_{cl}^{E,\Delta E}(R) = \int^R \sqrt{2M(E - \Delta E - V(R'))}dR'$, $u_{cl}^{E,\Delta E}(R) = \sqrt{2M(E - \Delta E - V(R))}$ and $V(R) = \frac{1}{2}\hat{K}R^2$. In the non-classical region we may take $\Psi_c = 0$. (In details for the derivation of $\Phi_c^{E_R}$ and their orthogonality, see Ref.s[3,4].) It should be stressed that $\rho_c = |\Phi_c^{E_R}|^2$ in the classical limit gives the exact distribution for the ensemble of the particles moving in the potential $V(R)$, which is expected from classical mechanics.

4. Decoherence mechanism of ultra-eigenfunctions

As was shown in the last section, the most general expression of the ultra-eigenfunctions has the $[C_L([l_n])]$-dependence. Through the observations of classical quantities written only by the CM(center of mass) variables, we can not fix the coefficients $[C_L([l_n])]$ at all. In other words the CM energy is determined only within the error $\Delta E([C_L([l_n])])$, for which only the constraint $st_{macro}(\Delta E([C_L([l_n])])) = 0$ is required. Therefore, we may introduce integration procedures

with respect to the coefficients $[C_L([l_n])]$ in order to take off the apparent dependence on those unobservable parameters in the density matrices. It should be stressed that this integration stands for the average over undetermined energy uncertainties ΔE and then it has well-defined physical meaning and its introduction is not ad hoc. Let us study this situation in the density matrix for the following superposed state of two ultra-eigenfunctions with different energies, $st_{macro}(E-E') \neq 0$, $\Psi^{E,E';\Delta E} = c_E \Psi_c^{E,\Delta E} + c_{E'} \Psi_c^{E',\Delta E}$, where $|c_E|^2 + |c_{E'}|^2 = 1$. The density matrix is given by

$$\rho_c^{E,E';\Delta E} = |c_E|^2 \rho_c^{E,E;\Delta E} + |c_{E'}|^2 \rho_c^{E',E';\Delta E} + (c_E c_{E''}^* \Psi_c^{E,\Delta E} \Psi_c^{E',\Delta E\dagger} + h.c.). \tag{12}$$

In order to obtain the density matrix for the CM motions which is independent of the coefficients, we introduce the integrations with respect to the undetermined complex coefficients $[C_L([l_n])]$. The number of the coefficients is counted as $\hat{W} \equiv \sum_{L=0}^{L_I} W(N,L)$, where $W(N,L)$ is the number of the different combinations for $[l_n]$. The multiplicity $\hat{W}$ is same as that of the equivalent internal wave-functions $\phi_L([l_n])$. Then we can rewrite the internal state $\phi([C_L([l_n])])$ as $\phi(I;[\rho_n]) = \sum_{I=1}^{\hat{W}} C_I \phi_I([\rho_n])$, where $[C_I] \equiv [C_1, C_2, \cdots, C_{\hat{W}}]$ are the new coefficients and $\phi_I([\rho])$ stands for the internal wave-function corresponding to the number I. Of course, they satisfy the relation $< \phi_I, \phi_{I'} >= \delta_{I,I'}$. The energy expectation value is rewritten by $\Delta E([C_I]) = \sum_{I=1}^{\hat{W}} |C_I|^2 \epsilon_I$. Using these coefficients, we can write the integrations with respect to $[C_I]$ as follows;

$$\hat{\rho}_c^{E,E'} \equiv \prod_{I=1}^{\hat{W}} \int d^2 C_I \mathcal{G}(C_I) \rho_c^{E.E';\Delta E}, \tag{13}$$

where $\int d^2 C_I$ stands for the integrals with respect to the real and imaginary parts of C_I and $\mathcal{G}(C_I)$ is the metric function for C_I satisfying the condition $st_{macro}(\prod_{I=1}^{\hat{W}} \int \epsilon^2 \mathcal{G}(C_I) \sum_{I'=1}^{\hat{W}} |C_{I'}|^2) = 1$ so as to derive the normalization condition $st_{macro}\,(Tr(\hat{\rho}_c^{E,E'})) = 1$. Since the metric should not depend on the phases of C_I, we take as $\mathcal{G}(C_I) = \frac{1}{2\pi}\mathcal{G}(|C_I|) > 0$.

In the density matrix the integrations are written down as follows;

$$\prod_I \int d^2 C_L \mathcal{G}(C_I) \sum_{I'} \sum_{I''} C_{I'} C_{I''}^* \frac{\hat{N}^E \hat{N}^{E'*}}{\sqrt{u_{cl}^{E,\Delta E}(R) u_{cl}^{E',\Delta E'}(R)}} \times e^{i\frac{1}{\hbar}(W_{cl}^{E,\Delta E}(R) - W_{cl}^{E',\Delta E'}(R))} \phi_{I'}([\rho]) \phi_{I''}([\rho])^*, \tag{14}$$

where $\Delta E = \sum_{I'} |C_{I'}|^2 \epsilon_{I'}$ and $\Delta E' = \sum_{I''} |C_{I''}|^2 \epsilon_{I''}$. The diagonal term with $E = E'$ is written as

$$\prod_I \frac{1}{2\pi} \int d^2 C_I \mathcal{G}(|C_I|) [\sum_{I'} |C_{I'}|^2 |\phi_{I'}|^2 + \sum_{I'} \sum_{I'' \neq I'} C_{I'} C_{I''}^* \phi_{I'} \phi_{I''}^*] \frac{|\hat{N}_E|^2}{\sqrt{u_{cl}^{E,\Delta E}(R) u_{cl}^{E,\Delta E'}(R)}}. \tag{15}$$

The second term becomes zero because of the integrations with respect to the phases of $C_I = |C_I| e^{i\theta_I}$ from zero to 2π. Then we can evaluate the diagonal term as

$$\hat{\rho}_c^{E,E}(R,[\rho]) = \prod_I \int d|C_I| \mathcal{G}(|C_I|) [\sum_{I'} |C_{I'}|^2 |\phi_{I'}|^2] \frac{N_E^2}{u_c^{E,\Delta E}(R)}. \tag{16}$$

Now let us estimate the interference terms. Taking into account that differences with the order $O(\hbar)$ having no contribution in the st_{macro}- operation are allowed in the expression of $\Phi_c^E(R)$ and also the order of the error ΔE is $O(\hbar)$, we can use the following equivalent expression for $W_{cl}^{E,\Delta E}(R)$

in the classical region $0 < st_{macro}(E-V(R)) \in \mathcal{R}_+$; $W_d^{E,\Delta E}(R) \approx_{macro} \int^R \sqrt{2M(E-V(R'))}dR' - \frac{1}{2}\Delta E(|C_I|)\int^R \sqrt{\frac{2M}{E-V(R')}}dR'$. Then we can write the off-diagonal term as

$$\hat{\rho}_c^{E,E'}(R,|\rho|) \approx_{macro} \prod_I \int d^2C_I \mathcal{G}(C_I) \sum_{I'}\sum_{I''} C_{I'}C_{I''}^* \frac{\hat{N}^E \hat{N}^{E'*}}{\sqrt{u_d^E(R)u_d^{E'}(R)}}$$

$$\times e^{-\frac{1}{2}\sum_{I'} I'|C_{I'}|^2\omega(f(E;R)-f(E';R))} e^{i\frac{1}{\hbar}(W_d^E(R)-W_d^{E'}(R))} \phi_{I'}(|\rho|)\phi_{I''}(|\rho|)^*, \quad (17)$$

where $u_d^E(R) = \sqrt{2M(E-V(R))}$, $W_d^E(R) = \int^R \sqrt{2M(E-V(R'))}$, $f(E;R) = \int^R \sqrt{\frac{2M}{E-V(R')}}dR'$ and $u_d^{E,\Delta E}(R) \approx_{macro} u_d^E(R)$ are used. As same as the second term of the diagonal elements, the terms with $I' \neq I''$ disappear by the integrations over the phases of C_Is. The remaining terms with $I' = I''$ include the following integrals with respect to $|C_I|$s;

$$\prod_{I=1}^{\hat{W}} \int d|C_I|\mathcal{G}(|C_I|)e^{iI a_I|C_I|^2} \sum_{I'} |C_{I'}|^2, \quad (18)$$

where $a_I = -\frac{1}{2}(f(E;R) - f(E';R))\omega \not\approx 0$ in the classical region. The normalization can be rewritten as $\sum_{I'=1}^{\hat{W}}(< |C_{I'}|^2 > \prod_{I\neq I'}^{\hat{W}} < 1 >) = (< 1 >^{\hat{W}-1})(\sum_{I'=1}^{\hat{W}} < |C_{I'}|^2 >) = 1$, where $< A_I > \equiv \int d|C_I|\mathcal{G}(|C_I|)A_I$. Taking into account that this equation must be satisfied for arbitrary number of $\hat{W} \in \mathcal{N}$, it is reasonable to impose the following relations $\sum_{I'=1}^{\hat{W}} < |C_{I'}|^2 >= 1$ and $< 1 >= 1$. We obtain the relations $q_I \equiv | < e^{iI a_I|C_I|^2} > | \quad < \quad < 1 >= 1$ and $|\sum_{I'=1}^{\hat{W}} < |C_{I'}|^2 e^{iI' a_{I'}|C_{I'}|^2} > | \quad < \quad \sum_{I'=1}^{\hat{W}} < |C_{I'}|^2 >= 1$ because of $\mathcal{G}(|C_I|) > 0$ and $\forall a_I \neq 0$ and $\not\approx 0$ for $^\forall I \in \mathcal{N}$ in the classical region. We estimate the integrations as

$$|\sum_{I'=1}^{\hat{W}}(< |C_{I'}|^2 e^{iI' a_{I'}|C_{I'}|^2} > \prod_{I\neq I'}^{\hat{W}} < e^{iI a_I|C_I|^2} >)| \quad < \quad (q_{max})^{\hat{W}-1} \approx_{macro} 0, \quad (19)$$

where q_{max} denotes the maximum number among q_Is and the last equality is derived from the fact that $q_{max} < 1$ and $\hat{W}$ goes to infinity in the macroscopic limit. ¿From the above result we know that the magnitudes of the off-diagonal terms in $\hat{\rho}_c^{E,E'}$ are infinitesimal and the contributions from the off-diagonal terms are always infinitesimal in the evaluation of expectation values for all operators ($\mathcal{O}$) which are written only in terms of the CM variables. (In details, see Ref.5.)

5. Remarks

There is no space enough to explain the coherent states reproducing the classical trajectories of the CM motions.We may conclude that the quatum states of macroscopic objects are well described in terms of the ultra-eigenfunctions of quantum mechanics on nonstandard spaces.[5]

References

[1] A. Robinson, Non Standard Analysis (North-Holland, Amsterdam, 1970).

[2] M. O. Farrukh, J. Math. Phys. 16 (1975)177.

[3] T. Kobayashi, Proceedings of the Symposium on Symmetries in Science VII, eds. B. Gruber et al. (Plenum, New York, 1993)287 and Soryushiron-Kenkyu 89(1994)211 (in Japanese).

[4] T. Kobayashi, IL Nuovo Cim. 110B(1995)61.

[5] T. Kobayashi, preprint of Unversity of Tsukuba, UTHEP-279 (1994).

NEXT
DOCUMENT

ON A RELATION BETWEEN QUANTUM INTERFERENCE AND STANDARD QUANTUM LIMIT

R. Momose, M. Osaki, M. Ban†, M. Sasaki, and O. Hirota
Research Center for Quantum Communications,
Tamagawa University, Tokyo, JAPAN

†*Advanced Reseach Laboratory, Hitachi Ltd., Saitama, JAPAN*

Abstract

This paper discusses a physical meaning of the standard quantum limit (SQL) in quantum decision theory. It will be shown that a necessary condition for overcoming the SQL is quantum interference.

1 Introduction

The problem of finding the best quantum measurement process in order to distinguish quantum states is called quantum decision theory which was devised extensively by Helstrom, Yuen and Holevo as quantum aspect of communication theory. In this theory, the measurement process is treated as a black box, and it is described by a probability operator measure as a simple mathematical generalization of the Born statistical postulate[1]. The discrimination among quantum states is one of the interesting topics in quantum optics and related fields, because they require the control of the quantum measurement process to find better measurement apparatus. So it is interesting to clarify the relation between the abstract description of quantum measurement processes and its physical correspondence.

Recently, Usuda and Hirota[2] pointed out that the performance of the decision error probability for binary pure state signals can be improved by means of received quantum state control consisting of the Kerr medium and the conventional homodyne system. Then Sasaki, Usuda, and Hirota[3] verified that the improvement of the performance is caused by quantum interference effect. Thus, quantum decision theory has predicted a possibility of overcoming the standard quantum limit. However, we have not yet understood what it means in general. We shall clarify in the present paper the physical meaning of the improvement of the decision error probability by control of the quantum measurement process.

2 Quantum interference

According to the quantum mechanics, any state vector represents a realizable physical state. When the state is represented by a linear superposition, we can find the quantum interference between the superposed states as follows:

$$N|\langle x|(|\Psi_1\rangle + |\Psi_2\rangle)|^2$$
$$= N[|\langle x|\Psi_1\rangle|^2 + |\langle x|\Psi_2\rangle|^2 + 2\mathrm{Re}\{\langle x|\Psi_1\rangle\langle x|\Psi_2\rangle^*\}], \tag{1}$$

where N is a normalization constant. The third term represents the quantum interference. This corresponds to the fact that the quantum probability is affected by off-diagonal elements of the density operator of a coherent superposition state. On the other hand, in the quantum measurement process, if the measurement process itself generates the superposition effect from a standard basis $\{|y\rangle\}$,

$$N|(\langle y| + \langle \delta y|)|\Psi\rangle|^2$$
$$= N[|\langle y|\Psi\rangle|^2 + |\langle \delta y|\Psi\rangle|^2 + 2\mathrm{Re}\{\langle y|\Psi\rangle\langle \delta y|\Psi\rangle^*\}], \tag{2}$$

then the resulting interference term represents the macroscopic quantum interference effect by the quantum measurement itself. Here the macroscopic means that the interference term is clearly observed.

3 Decision problem for quantum states

We first give a brief survey of quantum decision theory. The theory is formulated on the basis of the quantum probability describing the quantum measurement processes. According to quantum probability theory, measurement processes can be classified as standard and generalized processes. The standard quantum measurement process is described by the spectral theorem of von Neumann as follows:

$$\begin{cases} \hat{A}|x\rangle = x|x\rangle \\ p(x)\mathrm{d}x = \mathrm{Tr}\hat{\rho}|x\rangle\langle x|\mathrm{d}x\,, \end{cases} \tag{3}$$

where $\hat{\rho}$: density operator, $\hat{A}$: observable in the quantum system.
Any observable $\hat{A}$ and state $\hat{\rho}$ induce a mapping from a quantum state to a classical probability measure. On the other hand, the generalized quantum measurement process is described by the probability operator measure (POM) $\mathrm{d}\hat{\Pi}(x)$ which satisfies to the following conditions[1]:

$$\hat{\mathrm{I}} = \int \mathrm{d}\hat{\Pi}(x) \quad \text{and} \quad \mathrm{d}\hat{\Pi}(x) \geq 0\,. \tag{4}$$

In general, $\mathrm{d}\hat{\Pi}(x)$ is not a projection-valued measure (PVM). Then the measurement probability is given by

$$p(x)\mathrm{d}x = \mathrm{Tr}\hat{\rho}\mathrm{d}\hat{\Pi}(x)\,.$$

Based on the above formulas, one can define the decision operator for decision among the quantum states. Let $\{\hat{\rho}_i\}$ be a set of quantum states representing M signals. The probability of decision is

$$P(j|i) = \mathrm{Tr}\hat{\rho}_i\hat{\Pi}_j \qquad i,j \in M\,, \tag{5}$$

where $\hat{\Pi}_j$ is called the decision operator. This is a probability operator measure (POM) as follows:

$$\hat{\mathrm{I}} = \sum_j \hat{\Pi}_j \quad \text{and} \quad \hat{\Pi}_j \geq 0 . \tag{6}$$

This is the discrete case of the generalized resolution of identity: Eq(4). The optimization in the quantum decision problem is formulated as follows:

$$P_e = \min_{\{\hat{\Pi}_j\}} \left\{ 1 - \sum_j \xi_j \mathrm{Tr}(\hat{\rho}_j \hat{\Pi}_j) \right\} . \tag{7}$$

If the decision operators consist of PVM of the *signal observable* given by a specific basis,

$$\begin{cases} \hat{\Pi}_{j(\mathrm{SQL})} = \int f_j(x_d)|x\rangle\langle x| dx \\ \sum_j \hat{\Pi}_{j(\mathrm{SQL})} = \hat{\mathrm{I}} \quad \text{and} \quad \hat{\Pi}_{j(\mathrm{SQL})} \geq 0 , \end{cases} \tag{8}$$

where $f_j(x_d)$ is a Wald's decision function, then they are called the standard decision operators[4]. In this case, the optimization is only for Wald's decision function, and we do not need quantum decision theory. Decision operator based on different observations of the signal is called "generalized decision operator." In this general case, the role of decision and measurement process is embedded into a decision operator, and we do not separate out an observable. In general, we have PVM or POM. The whole process is treated as a black box, and this is called Helstrom-Holevo formalism[1].

4 Standard quantum limit in decision theory

Here we give the definition of the standard quantum limit. Suppose we fix a single signal observable and generate the M different signals with different quantum state. Basically, modulation scheme will be set as such a way. Minimum error probability based on the standard decision operator of the signal observable will be called the Standard Quantum Limit (SQL)[4]. If the signal observable is a set of non-commuting observables, then the minimum error probability based on the simultaneous measurement for such non-commuting observables is called the SQL. Or it is equivalent to that based on standard decision operator on the Naimark extension space. In this case, the standard decision operator is constructed by PVM of corresponding signal observables on the extended space.

Our definition is convenient to evaluate how new scheme is different from it as conventional one in the measurement process. In this definition, signal quantum state does not play so important role. We emphasize that the SQL is given for each system with various quantum states.

Let us give some examples. For a single observable, the binary PSK with coherent states is a typical example. In this case, the signal observable corresponds to the quadrature amplitude $\hat{X}_c$ or $\hat{X}_s$. The SQL is given by a homodyne receiver corresponding to $|x_c\rangle\langle x_c|$ or $|x_s\rangle\langle x_s|$. However, if we send more than two classical phase information of light wave, for instance, ternary PSK and quarternary PSK, then the SQL is given by a heterodyne receiver or an optical costas-loop system based on homodyne. When the quantum state is squeezed state, the SQL is for the squeezed state. But the measurement process which give the SQL is the same homodyne receiver. So we

say the SQL is for a system with squeezed state. If the state for the fixed modulation scheme is different, we will say it is the SQL for that state. Our problem is that when the signal observable or modulation signal is prepared, by controlling the measurement process we get performance better than expected in classical communication theory. Here we are concerned with the physical meaning of overcoming the SQL. We would prove the next conjecture:
"In order to overcome the SQL, the quantum interference effect by the quantum measurement process is necessary."
The proof is following: The SQL average error probability is

$$P_{e(\mathrm{SQL})} = 1 - \sum_j \xi_j \mathrm{Tr}(\hat{\rho}_j \hat{\Pi}_{j(\mathrm{SQL})}) \,. \tag{9}$$

Here, from Eq(8), the SQL means bounds when quantum fluctuation can be treated as a classical noise and a classical decision theory is applied to them. As a result, a generation of a quantum effect is required by different measurements to get result better than the SQL. To overcome the SQL, for $P_e < P_{e(\mathrm{SQL})}$, one has

$$\sum_j \xi_j \mathrm{Tr}\hat{\rho}_j(\hat{\Pi}_{j(\mathrm{SQL})} - \hat{\Pi}_j) < 0 \,. \tag{10}$$

Since the decision operators can involve a classical effect, we should choose operators representing a quantum effect from the various measurement schemes. From this point, to choose the different schemes from the standard decision process, which give a quantum effect, has a possibility to bring a result better than the SQL. That is, we can say that the quantum effect which does not have classical interpretation is an essential requirement to overcome the SQL. However it is clear that the different measurement schemes from the standard do not mean better measurements. ¿From now on, we discuss what kind of quantum effect is necessary. If $\left[\hat{\Pi}_j, \hat{\Pi}_{j(\mathrm{SQL})}\right] = 0$, then $\hat{\Pi}_j$ can be represented by the same PVM as the signal observable. Since $\hat{\Pi}_{j(\mathrm{SQL})}$ is the optimum among the class of decision operators consisting of the PVM of the signal observable, we require $\left[\hat{\Pi}_j, \hat{\Pi}_{j(\mathrm{SQL})}\right] \neq 0$ to overcome the SQL. The detail logic of the proof was given by Ban[5]. We check physical meaning of the above statement. Let us discuss here only case that the signal observable is a single one and the non-commutativity of standard decision operators and new operators can be described by applying a certain unitary operator as follows:

$$\begin{aligned} \hat{\Pi}_1 &= \hat{U}^\dagger \hat{\Pi}_{1(\mathrm{SQL})} \hat{U} \,, \\ \hat{\Pi}_2 &= \hat{U}^\dagger \hat{\Pi}_{2(\mathrm{SQL})} \hat{U} \,. \end{aligned} \tag{11}$$

Here we require from Ban's result

$$\left[\hat{U}^\dagger \hat{\Pi}_{j(\mathrm{SQL})} \hat{U} \,,\, \hat{\Pi}_{j(\mathrm{SQL})}\right] \neq 0 \,. \tag{12}$$

It means that $\hat{U}$ must be generated by operators which do not commute with the signal observable and also commutation relation of the generator of $\hat{U}$ and $\hat{A}$ is not c-number. The unitary operator is represented from Stone's theorem by

$$\hat{U} = \int \exp[ig(y)]\mathrm{d}\hat{E}(y) = \int K(y)\mathrm{d}\hat{E}(y)\,. \tag{13}$$

Then

$$\begin{aligned}\hat{\Pi}_2 &= \int f_2(x_\mathrm{d})\left\{\int K^*(y)\langle y|x\rangle \mathrm{d}y|y\rangle \int K(y)\langle x|y\rangle\langle y|\mathrm{d}y\right\}\mathrm{d}x \\ &= \int f_2(x_\mathrm{d})\left\{\int K^*(y)h^*(x,y)\mathrm{d}y|y\rangle \int K(y)h(x,y)\langle y|\mathrm{d}y\right\}\mathrm{d}x\,,\end{aligned} \tag{14}$$

where $h(x,y) = \langle x|y\rangle$.
If we want to overcome the SQL, at least each term of error probabilities must satisfy the following inequality:

$$\begin{aligned}\langle\psi_1|\hat{\Pi}_2|\psi_1\rangle &= \langle\psi_1|\hat{U}^\dagger\hat{\Pi}_{2(\mathrm{SQL})}\hat{U}|\psi_1\rangle \\ &= \int f_2(x_\mathrm{d})\left|\int K(y)h(x,y)\langle y|\psi_1\rangle\mathrm{d}y\right|^2\mathrm{d}x \\ &< \int f_2(x_\mathrm{d})\left|\int h(x,y)\langle y|\psi_1\rangle\mathrm{d}y\right|^2\mathrm{d}x \\ &= \int f_2(x_\mathrm{d})|\langle x|\psi_1\rangle|^2\mathrm{d}x\,.\end{aligned} \tag{15}$$

and

$$\begin{aligned}\langle\psi_2|\hat{\Pi}_1|\psi_2\rangle &= \langle\psi_2|\hat{U}^\dagger\hat{\Pi}_{1(\mathrm{SQL})}\hat{U}|\psi_2\rangle \\ &= \int f_1(x_\mathrm{d})\left|\int K(y)h(x,y)\langle y|\psi_2\rangle\mathrm{d}y\right|^2\mathrm{d}x \\ &< \int f_1(x_\mathrm{d})\left|\int h(x,y)\langle y|\psi_2\rangle\mathrm{d}y\right|^2\mathrm{d}x \\ &= \int f_1(x_\mathrm{d})|\langle x|\psi_2\rangle|^2\mathrm{d}x\,.\end{aligned} \tag{16}$$

These inequalities are the requirement for the new decision process to get below the SQL. We can see $\left[\hat{U}^\dagger\hat{\Pi}_{j(\mathrm{SQL})}\hat{U}\,,\ \hat{\Pi}_{j(\mathrm{SQL})}\right] \neq 0$ in order to obtain the error probability below the SQL, because if it is commutative operator, the inequality becomes inverse. Thus the requirement to be the non-commutativity is clear. Furthermore, in order to hold the inequalities, the probability of the overlapped region of the both signals must be reduced. It is possible by only quantum interference effect (see Ref.[6]). The $\int K(y)h(x,y)\langle y|\psi_1\rangle\mathrm{d}y$ in Eq(15) is, in general, regarded as the superposition on the coordinate of y. The superposition has a potential to give a quantum interference, because this corresponds to Eq(2). By the square of the absolute value of the above term, the modified measurement probability of the original probability: $|\langle\psi_1|x\rangle|^2$ based on the quantum interference may be obtained. We can easily understand, however, that even if the decision operator is non-commuting with $\hat{\Pi}_{j(\mathrm{SQL})}$, we cannot always obtain the macroscopic quantum interference. For example, even if $\{x \text{ and } y\}$ are physical quantities with non c-number commutator, it does not always give the macroscopic quantum interference which shows reduction and increase of probability on the standard basis. That is, it sometimes provides only a kind of transformation of function. In this case, we have no hope to overcome the SQL. This means that we must find a decision operator which gives the macroscopic quantum interference from non-commuting decision operators.

5 Conclusions

We have clarified the followings:

1. The physical meaning of the SQL is given.
2. To overcome the SQL is caused by the quantum interference effect in the quantum measurement process.
3. A physical meaning of the POM involves the quantum interference in the quantum measurement process, though it has been regarded as unsharp measurements like the random decision, convolution effect or cross correlation effect with other uncertainty[7, 8].

References

[1] A. S. Holevo, J. of Mult. Anal. **3**, 337 (1973).

[2] T. S. Usuda, and O. Hirota, Proc. of QCM'94, 419, ed by Belavkin, Hirota and Hudson (Plenum Press, 1995).

[3] M. Sasaki, T. S. Usuda, and O. Hirota, Phys. Rev. A **51**, 1702 (1995).

[4] O. Hirota, Annals of New York Academy of Sciences, **755**, 863 (Plenum Press, 1995).

[5] M. Ban, M. Osaki, and O. Hirota, to be appeard in IEEE. Trans. IT.

[6] O. Hirota, Memoirs of the Reserach Institute of Tamagawa University, **1**, 1 (1995).

[7] O. Hirota, *Optical communication theory*, in Japanese (Morikita Pub. Co., Tokyo, 1985).

[8] P. Busch, Proc. of II international Wigner Symposium, 19, ed by Doebner, Scherer and Schroeck (World Scientific Pub. Co., 1993).

NEXT
DOCUMENT

PHYSICAL MEANING OF THE OPTIMUM MEASUREMENT PROCESS IN QUANTUM DETECTION THEORY

Masao Osaki, Haruhisa Kozuka, Osamu Hirota
Research Center for Quantum Communications,
Tamagawa University, Tokyo, JAPAN

Abstract

The optimum measurement processes are represented as the optimum detection operators in the quantum detection theory. The error probability by the optimum detection operators goes beyond the standard quantum limit automatically. However the optimum detection operators are given by pure mathematical descriptions. In order to realize a communication system overcoming the standard quantum limit, we try to give the physical meanings of the optimum detection operators.

1 Introduction

The purpose of the quantum detection theory is to realize a communication system with its performance overcoming the standard quantum limit (SQL). Standard quantum limit is often referred as a detection limit achieved by classical detection theory, so that overcoming the SQL is purely quantum mechanical effect. To go beyond the SQL, the quantum measurement process must be generalized to the probability-operator measure (POM) [1, 2]. The optimization of the POM to minimize an error probability results in "the optimum detection operator" which expresses not only a measurement process but also a decision process. However the optimum detection operator works as a mapping from a signal quantum state to a decision result, so that its physical meaning is not evident. In order to realize a communication system whose detection performance is quantum mechanically optimum, investigations into the physical meanings of the optimum detection operators are indispensable.
Recently we have derived some analytical solutions of the optimum detection operators and our group gave the physical example overcoming the SQL by means of the quantum interference [3, 4, 5]. In this paper we would like to interpret the physical meaning of the optimum detection operators as the quantum interference.

2 Summary of Quantum Detection Theory

The significance of the quantum detection theory is the prediction of a receiver whose signal detection performance is superior to the conventional ones optimized by the classical detection theory. The bound between the quantum and classical detection theories is well-known as "the standard quantum limit: SQL" which is rigorously defined as follows:[6]

Definition.1
Standard quantum limit is defined as the minimum error probability achieved by the quantum measurement based on the orthonormal spectrum measure of the signal observable.

Namely, the SQL can be obtained by quantum mechanical re-description of the conventional measurement processes with the optimum decision rule. To go beyond this limit, signal measurement processes must be generalized quantum mechanically. The generalized measurement process is represented by the probability- operator measure (POM), $\hat{\Pi}_j$, which is a non- negative Hermitian operator satisfying the resolution of identity.

$$\hat{\Pi}_j = \hat{\Pi}_j^\dagger \geq 0, \tag{1}$$

$$\sum_{j=1}^{M} \hat{\Pi}_j = \hat{I}. \tag{2}$$

Because of the resolution of identity, POM can include the meaning of a decision process and such a POM is called "a detection operator." Therefore, the measurement of a signal quantum state, $\hat{\rho}_i$, by a detection operator, $\hat{\Pi}_j$, gives a conditional probability, $P(j|i)$, as follows:

$$P(j|i) = \mathrm{Tr}\hat{\rho}_i\hat{\Pi}_j. \tag{3}$$

This probability represents the signal decision probability to be 'j' while the received signal is 'i'. The error probability is also given by signal quantum states and detection operators.

$$P_e = 1 - \sum_{i=1}^{M} \xi_i P(i|i) = 1 - \sum_{i=1}^{M} \mathrm{Tr}\xi_i\hat{\rho}_i\hat{\Pi}_i, \tag{4}$$

where ξ_i is a prior-probability for i-th signal.

The quantum detection theory is the optimization theory for these detection operators to minimize the above error probability. There are several formulae to find the optimum detection operators. For example, necessary and sufficient condition for the optimum detection operators based on the quantum minimax strategy is as follows [7]:

$$\mathrm{Tr}\hat{\Pi}_i\hat{\rho}_i = \mathrm{Tr}\hat{\Pi}_j\hat{\rho}_j, \forall i, j, \tag{5}$$

$$\hat{\Pi}_j \left[\xi_j\hat{\rho}_j - \xi_i\hat{\rho}_i\right] \hat{\Pi}_i = 0, \forall i, j, \tag{6}$$

$$\hat{\Gamma} - \xi_i\hat{\rho}_i \geq 0, \forall i, \tag{7}$$

where $\hat{\Gamma}$ is called "the Lagrange operator" defined by

$$\hat{\Gamma} = \sum_{i=1}^{M} \xi_i\hat{\rho}_i\hat{\Pi}_i = \sum_{i=1}^{M} \xi_i\hat{\Pi}_i\hat{\rho}_i. \tag{8}$$

A solution of the above formula goes beyond the SQL automatically. The practical derivation of the optimum detection operators has been carried out for some signal sets consisting of linearly independent quantum states [3]. In the derivation process, the following Lemma by Kennedy plays an important role [1, 8].

Lemma
When the signal quantum states are linearly independent, the optimum POM for the error probability is indeed projection-valued.

Therefore in the cases of the quantum signal sets with pure states, the optimum detection operators are orthogonal projectors on the signal space.

$$\hat{\Pi}_j = |\omega_j\rangle\langle\omega_j| \quad \text{and} \quad \langle\omega_i|\omega_j\rangle = \delta_{ij}. \tag{9}$$

where $|\omega_j\rangle$ is called "a measurement state." Since the measurement states are the orthonormal bases in the signal space, signal quantum states, $|\psi_i\rangle$: $(\hat{\rho}_i = |\psi_i\rangle\langle\psi_i|)$, can be represented by measurement states.

$$|\psi_i\rangle = \sum_{j=1}^{M} x_{ji}|\omega_j\rangle, \tag{10}$$

where x_{ji} is a parameter defined by

$$x_{ji} \equiv \langle\omega_j|\psi_i\rangle. \tag{11}$$

Then it is possible to represent the relation between the signal quantum states and the measurement states in the matrix form.

$$\begin{bmatrix} |\psi_1\rangle \\ \vdots \\ |\psi_M\rangle \end{bmatrix} = \begin{bmatrix} x_{11} & \cdots & x_{M1} \\ \vdots & \ddots & \vdots \\ x_{1M} & \cdots & x_{MM} \end{bmatrix} \begin{bmatrix} |\omega_1\rangle \\ \vdots \\ |\omega_M\rangle \end{bmatrix}. \tag{12}$$

Inversely, the measurement states can be represented by signal quantum states.

$$\begin{bmatrix} |\omega_1\rangle \\ \vdots \\ |\omega_M\rangle \end{bmatrix} = [x_{ji}]^{-1} \begin{bmatrix} |\psi_1\rangle \\ \vdots \\ |\psi_M\rangle \end{bmatrix}. \tag{13}$$

Hence the problems for the optimum detection operators, Eqs.(5–7), are turned into the algebraic equations for parameters $\{x_{ji}\}$.

As an example, let us consider the Binary Phase Shift Keyed (BPSK) signal with coherent states. The signal quantum states are given by $|\psi_1\rangle = |\alpha\rangle, |\psi_2\rangle = |-\alpha\rangle$. The optimum detection operators can be obtained as follows [3]:

$$\begin{cases} \hat{\Pi}_1 = \frac{1}{2(1-\kappa^2)} & \left\{\left(1+\sqrt{1-\kappa^2}\right)|\alpha\rangle\langle\alpha| + \left(1-\sqrt{1-\kappa^2}\right)|-\alpha\rangle\langle-\alpha| \right. \\ & \left. -\kappa\left(|\alpha\rangle\langle-\alpha| + |-\alpha\rangle\langle\alpha|\right)\right\}, \\ \hat{\Pi}_2 = \frac{1}{2(1-\kappa^2)} & \left\{\left(1-\sqrt{1-\kappa^2}\right)|\alpha\rangle\langle\alpha| + \left(1+\sqrt{1-\kappa^2}\right)|-\alpha\rangle\langle-\alpha| \right. \\ & \left. -\kappa\left(|\alpha\rangle\langle-\alpha| + |-\alpha\rangle\langle\alpha|\right)\right\}. \end{cases} \tag{14}$$

The measurements by these optimum detection operators show the error probability going far beyond the SQL. These optimum detection operators look like the Schrödinger Cat states [9] consisting of the signal quantum states, $|\alpha\rangle$ and $|-\alpha\rangle$, so that the quantum interference may be occurred there.

In general cases, the optimum detection operator can be also represented by a coherent superposition state with signal quantum states from Eq.(13).

$$\hat{\Pi}_j = |\omega_j\rangle\langle\omega_j| = \sum_{k=1}^{M}\sum_{\ell=1}^{M} t_{jk}t_{j\ell}^{*}|\psi_k\rangle\langle\psi_\ell|, \tag{15}$$

where t_{ji} is an element of a matrix $[t_{ji}]$ representing the inverse matrix $[x_{ji}]^{-1}$. The conditional probability given in Eq.(3) becomes

$$\begin{aligned} P(j|i) &= \mathrm{Tr}\hat{\rho}_i\hat{\Pi}_j \\ &= \mathrm{Tr}\left[|\psi_i\rangle\langle\psi_i|\left(\sum_{k=1}^{M}\sum_{\ell=1}^{M} t_{jk}t_{j\ell}^{*}|\psi_k\rangle\langle\psi_\ell|\right)\right] \\ &= \langle\psi_i|\left(\sum_{k=1}^{M}\sum_{\ell=1}^{M} t_{jk}t_{j\ell}^{*}|\psi_k\rangle\langle\psi_\ell|\right)|\psi_i\rangle. \end{aligned} \tag{16}$$

Here we can see the off-diagonal elements generated from the optimum detection operator. Then there is a question "Can we regard this measurement process as a quantum interference by existence of these off-diagonal elements?" According to the general sense of the quantum interference off- diagonal elements should be generated from a density operator representing a signal quantum state. Hence in the following sections, we verify whether the optimum detection process can be interpreted as a quantum interference.

3 Quantum Interference

To specify what is the quantum interference, we follow the conventional definition [10]

Definition.2
When the quantum probability is affected by the off-diagonal elements of a density operator representation of some coherent superposition state, it is called the quantum interference.

In detail, a coherent superposition state is represented by

$$|\psi\rangle = \sum_n k_n|\phi_n\rangle, \tag{17}$$

where k_n is a normalization constant. Then its density operator representation is as follows:

$$\hat{\rho} = |\psi\rangle\langle\psi| = \sum_m\sum_n k_m k_n^{*}|\phi_m\rangle\langle\phi_n|. \tag{18}$$

The quantum probability obtained by a certain measurement, $\mathrm{d}E(x)$, results in

$$p(x) = \mathrm{Tr}\hat{\rho}\mathrm{d}\hat{E}(x) = \mathrm{Tr}\sum_m\sum_n k_m k_n^{*}|\phi_m\rangle\langle\phi_n|\mathrm{d}\hat{E}(x). \tag{19}$$

When the off-diagonal elements remain in the quantum probability, it is called "a quantum interference," where the off-diagonal elements are given in the form

$$\mathrm{Tr}|\phi_m\rangle\langle\phi_n|\mathrm{d}\hat{E}(x) \quad m \neq n. \tag{20}$$

Therefore the quantum interference can be in sight by existence of the off-diagonal elements from a density operator. In the case of the optimum detection operators, however, the off-diagonal elements are generated from a measurement process as itself. If the notations of density operators and the optimum detection operators can be exchange, then we can interpret that the physical meaning of the optimum detection operator is the quantum interference.

4 Density Operators and the Optimum Detection Operators

The conditions for an operator to be the optimum detection operator are as follows [1]:

1. Non-negative Hermitian operator (condition to be POM).

$$\hat{\Pi} = \hat{\Pi}^\dagger \geq 0. \tag{21}$$

2. Projection on the signal space (after Kennedy's Lemma).

$$\hat{\Pi}^2 = \hat{\Pi}, \quad \text{and} \quad \mathrm{Tr}\hat{\Pi} = 1. \tag{22}$$

On the other hand, the features of density operators are [11]

1. Non-negative Hermitian operator.

$$\hat{\rho} = \hat{\rho}^\dagger \geq 0. \tag{23}$$

2. Trace is equal to unit.

$$\mathrm{Tr}\hat{\rho} = 1. \tag{24}$$

As a result, it is possible to exchange the notations of the optimum detection operators and density operators.

$$\begin{cases} \hat{\rho}_i & \Rightarrow & \tilde{\Pi}_i, \\ \hat{\Pi}_j & \Rightarrow & \tilde{\rho}_j. \end{cases} \tag{25}$$

Applying this operation to the conditional probability in Eq.(16),

$$\begin{aligned} P(j|i) &= \mathrm{Tr}\hat{\rho}_i\hat{\Pi}_j \\ &\Rightarrow \mathrm{Tr}\tilde{\Pi}_i\tilde{\rho}_j \\ &= \mathrm{Tr}\left[|\psi_i\rangle\langle\psi_i|\left(\sum_{k=1}^{M}\sum_{\ell=1}^{M} t_{jk}t_{j\ell}^*|\psi_k\rangle\langle\psi_\ell|\right)\right] \\ &= \langle\psi_i|\left(\sum_{k=1}^{M}\sum_{\ell=1}^{M} t_{jk}t_{j\ell}^*|\psi_k\rangle\langle\psi_\ell|\right)|\psi_i\rangle, \end{aligned} \tag{26}$$

we can say that the above conditional probability contains the off- diagonal elements from the density operator, $\tilde{\rho}_j$. Hence we can say that the optimum detection process generates the quantum interference. In other words, when the error probability by the optimum detection goes beyond the SQL automatically, the quantum interference is also used there automatically. The optimum measurement state plays an equivalent role of the Schrödinger Cat state as itself.

5 Conclusions

The physical interpretation of the optimum detection operator which represents the optimum measurement process has been investigated. It is the quantum interference caused by the optimum detection operator as itself. Because the optimum detection operator is represented by a coherent superposition state consisting of signal quantum states. While this result is derived under the restriction that signal quantum states are linearly independent, we assume that any optimum detection operator generates the quantum interference as itself and uses it as much as possible to reduce the error probability.

Acknowledgments

We would like to represent our acknowledgments to Dr. M. Ban (Advanced Research Lab. Hitachi Ltd.).

References

[1] C. W. Helstrom, *Quantum Detection and Estimation Theory* (Academic Press, NY, 1976).

[2] A. S. Holevo, J. of Mult. Anal. **3**, 337 (1973).

[3] M. Osaki, and O. Hirota, *Proc. of Quantum Communication and Measurement*, 401, (Plenum Publishing, NY, 1995).

[4] T. S. Usuda, and O. Hirota, *Proc. of Quantum Communication and Measurement*, 419, (Plenum Publishing, NY, 1995).

[5] M. Sasaki, T. S. Usuda, and O. Hirota, Phys. Rev. A **51**, 1702 (1995).

[6] O. Hirota, *Annals of New York Academy of Science* **755**, 863, (Plenum Publishing, NY, 1995).

[7] O. Hirota, and S. Ikehara, The Trans. of IECE Japan **E65**, 627 (1982).

[8] R. S. Kenndy, M.I.T. Res. Lab. Electron. Quart. Progr. Rep. **110**, 142 (1973).

[9] B. Yurke, and D. Stoler, Phys. Rev. Lett. **57**, 13 (1986).

[10] K. Blum, *Density Matrix Theory and Applications* (Plenum Publishing, NY, 1981).

[11] W. H. Louisell, *Quantum Statistical Properties of Radiation* (John Wiley & Sons, NY, 1973).

NEXT
DOCUMENT

DECOHERENCE AND EXPONENTIAL LAW. A SOLVABLE MODEL

Saverio Pascazio
Dipartimento di Fisica, Università di Bari
and Istituto Nazionale di Fisica Nucleare, Sezione di Bari
I-70126 Bari, Italy

Mikio Namiki
Department of Physics, Waseda University
Tokyo 169, Japan

Abstract

We analyze a modified version of the "AgBr" Hamiltonian, solve exactly the equations of motion in terms of SU(2) coherent states, and study the weak-coupling, macroscopic limit of the model, obtaining an exponential behavior *at all times*. The asymptotic dominance of the exponential behavior is representative of a purely stochastic evolution and can be derived quantum mechanically in the so-called van Hove's limit (which is a weak-coupling, macroscopic limit). At the same time, a temporal behavior of the exponential type, yielding a "probability dissipation" is closely related to dephasing ("decoherence") effects and one can expect a close connection with a dissipative and irreversible behavior. We stress the central relevance of the problem of dissipation to the quantum measurement theory and to the general topic of decoherence.

1 Introduction

Decoherence and dephasing have become very important concepts in quantum theory. Because 'decoherence' technically means the elimination of the off-diagonal elements of the density matrix, a system described by such a diagonal density matrix should exhibit a purely stochastic behavior and we naturally expect a close connection with a dissipative and irreversible behavior.

On the other hand, the temporal evolution of a quantum mechanical system, initially prepared in an eigenstate of the unperturbed Hamiltonian, is known to be roughly characterized by three distinct regions: A Gaussian behavior at short times, a Breit-Wigner exponential decay at intermediate times, and a power law at long times [1]. It is well known that the asymptotic dominance of the exponential behavior is representative of a purely stochastic evolution and can be derived quantum mechanically in the weak-coupling, macroscopic limit (the so-called van Hove's limit) [2]. One may expect a close connection between dissipation and exponential decay. Such a connection has been recently emphasized by Leggett [3]. The Gaussian short-time behavior is in itself of particular significance due, in particular, to the so-called quantum Zeno effect [4, 5].

In this note, an exponential behavior at all times is derived for a solvable dynamical model [6, 7] in the weak-coupling, macroscopic li:- [8]. We shall emphasize the important role played by van Hove's diagonal singularity in the present model, together with the central relevance of the problem of dissipation to the quantum measurement theory [9] and to the general topic of decoherence [10]. The present derivation of the exponential behavior differs from the one given in Ref. [8], in that no use is made of scaled variables.

A temporal behavior of the exponential type, yielding a "probability dissipation" is closely related to dephasing effects and is a rather common feature of the interaction between microscopic and macroscopic systems. In this context, the present model is very interesting, because the measurement process is often viewed as a dephasing process and "decoherence" is regarded as a consequence of the interaction with (macroscopic) measuring devices, within the framework of quantum mechanics.

2 The 'AgBr' model

We shall base our discussion on the AgBr model [6], that has played an important role in the quantum measurement problem, and its modified version [7], that is able to take into account energy-exchange processes.

The modified AgBr Hamiltonian [7] describes the interaction between an ultrarelativistic particle Q and a 1-dimensional N-spin array (D- system). The array is a caricature of a linear "photographic emulsion" of AgBr molecules, when one identifies the *down* state of the spin with the undivided molecule and the *up* state with the dissociated molecule (Ag and Br atoms). The particle and each molecule interact via a spin-flipping local potential. The total Hamiltonian for the Q+D system reads

$$H = H_0 + H', \qquad H_0 = H_Q + H_D,$$
$$H_Q = c\hat{p}, \quad H_D = \frac{1}{2}\hbar\omega \sum_{n=1}^{N} \left(1 + \sigma_3^{(n)}\right), \quad H' = \sum_{n=1}^{N} V(\hat{x} - x_n) \left[\sigma_+^{(n)} \exp\left(-i\frac{\omega}{c}\hat{x}\right) + \text{h.c.}\right], \quad (1)$$

where H_Q and H_D are the free Hamiltonians of the Q particle and of the "detector" D, respectively, H' is the interaction Hamiltonian, $\hat{p}$ the momentum of the Q particle, $\hat{x}$ its position, V a real potential, x_n $(n = 1, ..., N)$ the positions of the scatterers in the array $(x_n > x_{n-1})$ and $\sigma_{i,\pm}^{(n)}$ the Pauli matrices acting on the nth site. An interesting feature of the above Hamiltonian, as compared to the original one [6], is that we are not neglecting the energy H_D of the array. This enables us to take into account energy-exchange processes between Q and D. The original Hamiltonian [6] is reobtained in the $\omega = 0$ limit.

The evolution operator in the interaction picture can be computed exactly [7] as

$$\begin{aligned} U(t,t') &= e^{iH_0 t/\hbar} e^{-iH(t-t')/\hbar} e^{-iH_0 t'/\hbar} \\ &= \prod_{n=1}^{N} \exp\left(-\frac{i}{\hbar}\int_{t'}^{t} V(\hat{x} + ct'' - x_n)dt'' \left[\sigma_+^{(n)} \exp\left(-i\frac{\omega}{c}\hat{x}\right) + \text{h.c.}\right]\right), \end{aligned} \quad (2)$$

and a straightforward calculation yields the S-matrix

$$S^{[N]} = \lim_{\substack{t\to\infty \\ t'\to-\infty}} U(t,t') = \prod_{n=1}^{N} S_{(n)} = \exp\left(-i\frac{V_0\delta}{\hbar c}\boldsymbol{\sigma}^{(n)} \cdot \boldsymbol{u}\right) \quad (3)$$

where $\boldsymbol{u} = (\cos(\omega x/c), \sin(\omega x/c), 0)$ and $V_0\delta = \int_{-\infty}^{\infty} V(x)dx$. The "spin-flip" probability, i.e. the probability of dissociating one AgBr molecule, reads

$$q = \sin^2\left(\frac{V_0\delta}{\hbar c}\right). \tag{4}$$

If the initial D state is taken to be the ground state $|0\rangle_N$ (N spins down), and the initial Q state is a plane wave, the final state is

$$S^{[N]}|p,0\rangle_N = \sum_{j=0}^{N}\binom{N}{j}^{1/2}(-i\sqrt{q})^j\left(\sqrt{1-q}\right)^{N-j}|p-j\frac{\hbar\omega}{c},j\rangle_N. \tag{5}$$

This enables us to compute several interesting quantities, such as the visibility of the interference pattern obtained by splitting an incoming Q wave function into two branch waves, one of which interacts with D, the energy "stored" in D after the interaction with Q, as well as the fluctuation around the average. The final results are

$$\begin{aligned} \mathcal{V} &= (1-q)^{N/2} \to e^{-\overline{n}/2}, \qquad \langle H_D\rangle_F = qN\hbar\omega \to \overline{n}\hbar\omega, \\ \langle\delta H_D\rangle_F &= \sqrt{\langle(H_D - \langle H_D\rangle_F)^2\rangle_F} = \sqrt{pqN}\hbar\omega \to \sqrt{\overline{n}}\hbar\omega, \end{aligned} \tag{6}$$

where F stands for final state, $p = 1-q$, and the trivial trace over the Q particle states is suppressed. The arrows signify the weak- coupling, macroscopic limit $N \to \infty$, $qN = \overline{n} =$ finite [7]. All results are exact. It is worth stressing that $qN = \overline{n}$ represents the average number of excited molecules, so that interference, energy and relative energy fluctuations "gradually" disappear as $\overline{n}$ increases. Observe also that (5) is a generalized [SU(2)] coherent state and becomes a Glauber coherent state in the $N \to \infty$, $qN =$ finite limit.

Our next (and main) task is to study the behavior of the propagator. We start from Eq. (2), set $t' = 0$ for simplicity, and return to the Schrödinger picture by inverting Eq. (2). The exponential is easily disentangled by making use of SU(2) properties. We get

$$e^{-iHt/\hbar} = e^{-iH_0t/\hbar}\prod_{n=1}^{N}\left(e^{-i\tan(\alpha_n)\sigma_+^{(n)}(\hat{x})}e^{-\ln\cos(\alpha_n)\sigma_3^{(n)}}e^{-i\tan(\alpha_n)\sigma_-^{(n)}(\hat{x})}\right), \tag{7}$$

where $\alpha_n = \alpha_n(\hat{x},t) \equiv \int_0^t V(\hat{x}+ct'-x_n)dt'/\hbar$. Notice that the evolution operators (2) and (7) as well as the S-matrix (3) are expressed in a factorized form: This is a property of a rather general class of similar Hamiltonians [11].

Let the Q particle be initially located at position $x' < x_1$ (x_1 is the position of the first scatterer in the linear array) and be moving towards the array with speed c. The initial D state is again the ground state $|0\rangle_N$ of the free Hamiltonian H_D (all spins down). This choice of the ground state is meaningful from a physical point of view, because the Q particle is initially outside D.

The propagator

$$G(x,x',t) \equiv \langle x|\otimes {}_N\langle 0|e^{-iHt/\hbar}|0\rangle_N \otimes |x'\rangle, \tag{8}$$

can be easily calculated from eq. (7). We place for simplicity the spin array at the far right of the origin ($x_1 > 0$) and consider the case where potential V has a compact support and the Q particle is initially located at the origin $x' = 0$, i.e. well outside the potential region of D. We get

$$G(x,0,t) = \delta(x-ct)\prod_{n=1}^{N}\cos\tilde{\alpha}_n(t), \qquad \tilde{\alpha}_n(t) \equiv \int_0^{ct} V(y-x_n)dy/\hbar c. \tag{9}$$

This result is *exact*. Notice that the "spin-flip" probability (4) is $q = \sin^2 \bar{\alpha}_n(\infty) = \sin^2(V_0\Omega/\hbar c)$. We consider again the weak-coupling, macroscopic limit

$$q \simeq \left(\frac{V_0\Omega}{\hbar c}\right)^2 = O(N^{-1}), \tag{10}$$

and set

$$x_n = x_1 + (n-1)\Delta, \qquad L = x_N - x_1 = (N-1)\Delta. \tag{11}$$

The following derivation is different from the one given in Ref. [8]. We keep L finite and consider the continuous limit $\Delta/L \to 0$ as $N \to \infty$. A summation over n is then replaced by a definite integration

$$q\sum_{n=1}^{N} f(x_n) \to \frac{q}{\Delta}\int_{x_1}^{x_N} f(x)dx \simeq \frac{\overline{n}}{L}\int_{x_1}^{x_N} f(x)dx. \tag{12}$$

For the sake of simplicity, we restrict our attention to the case of δ-shaped potentials, by setting $V(y) = (V_0\Omega)\delta(y)$. We get

$$G \propto \exp\left(\sum_{n=1}^{N} \ln\left\{\cos\int_{-x_n}^{ct-x_n} (V_0\Omega/\hbar c)\delta(y)dy\right\}\right) = \exp\left(\sum_{n=1}^{N} \ln\left\{\cos\left[(V_0\Omega/\hbar c)\theta(ct-x_n)\right]\right\}\right)$$
$$\to \exp\left(-\frac{q}{\Delta}\int_{x_1}^{x_n}\theta(ct-x)dx\right) = \exp\left(-\frac{\overline{n}}{2}\left[\frac{ct-x_1}{L}\theta(x_N-ct)\theta(ct-x_1) + \theta(ct-x_N)\right]\right), \tag{13}$$

where θ is the step function and the arrow denotes the weak- coupling, macroscopic limit (10). This brings about an exponential regime *as soon as the interaction starts*: Indeed, if $x_1 < ct < x_N$,

$$G \propto \exp\left(-\overline{n}\frac{c(t-t_0)}{2L}\right), \tag{14}$$

where $t_0 = x_1/c$ is the time at which the Q particle meets the first potential. Notice that there is *no* Gaussian behavior at short times and *no* power law at long times. Observe that $|G|^2$ is nothing but the probability that Q goes through the spin array *and* leaves it in the ground state.

It is well known [1, 4] that deviations from exponential behavior at short times are a consequence of the finiteness of the mean energy of the initial state. If the position eigenstates in eq. (8) are substituted with wave packets of size a, a detailed calculation shows that the exponential regime is attained a short time after t_0, of the order of a/c, which, in the present model, can be made arbitrarily small. Moreover, a detailed calculation (by H. Nakazato), making use of square potentials of strenght V_0 and width b yields, for $x_1 + \frac{b}{2} < ct < x_N - \frac{b}{2}$,

$$G \propto \exp\left(-\overline{n}\frac{c(t-t_0)}{2L} + \frac{\overline{n}b}{12L}\right). \tag{15}$$

In this case, the exponential regime is attained a short time after t_0, of the order of the width of the potential V. The regions $t \sim t_0 + O(a/c)$ and/or $t \sim t_0 + O(b/c)$ may be viewed as a possible residuum of the short-time Gaussian-like behavior. For this reason, the temporal behavior derived in this Letter is not in contradiction with some general theorems [1, 4].

What causes the occurrence of the exponential behavior displayed by our model ? This is a delicate problem. Our analysis suggests that the exponential behavior is mainly due to the locality

of the potentials V and the factorized form of the evolution operator U. On the other hand, there are also profound links between the limiting procedure considered in this letter and van Hove's "$\lambda^2 T$" limit [2]. Work is in progress in order to clarify different aspects of this issue. Let us briefly discuss them. First of all, the evolution operators (2), (7) and the S-matrix (3) are expressed in a factorized form: This shows that the interactions between Q and adjacent spins of the array are independent, and the evolution "starts anew" at every step. This suggest the presence of a sort of Markovian process, which would justify the purely dissipative behavior (14). At the same time, the role played by the energy gap ω deserves to be clarified: ω plays undoubtedly an important role by guaranteeing the consistency of the physical framework, as discussed in [8]. On the other hand, the connection between the exponential "probability dissipation" (14) and the (practically irreversible) energy-exchange between the particle and the "environment" (our spin system) is a very open problem and should be investigated in detail. Leggett's remark [3], about the central relevance of the problem of dissipation to the quantum measurement theory makes the above topic very interesting: Indeed, in our opinion, the temporal behavior derived in this note is certainly related to dephasing ("decoherence") effects of the same kind of those encountered in quantum measurements.

Second, it is worth discussing the link between the weak-coupling, macroscopic limit $qN = \overline{n} =$ finite considered above and van Hove's "$\lambda^2 T$" limit [2], leading to the master equation. The interaction Hamiltonian H' has nonvanishing matrix elements only between those eigenstates of H_0 whose spin-quantum numbers differ by one. As discussed in [8], this causes van Hove's so-called diagonal singularity, because for each diagonal matrix element of H'^2, there are N intermediate-state contributions: For example

$$\langle 0,\ldots,0|H'^2|0,\ldots,0\rangle = \sum_{j=1}^{N} |\langle 0,\ldots,0|H'|0,\ldots,0,1_{(j)},0,\ldots,0\rangle|^2. \tag{16}$$

On the other hand, at most 2 states can contribute to each off-diagonal matrix element of H'^2. This ensures that only the diagonal matrix elements are kept in the weak-coupling, macroscopic limit, $N \to \infty$ with $qN < \infty$, which is the realization of diagonal singularity in our model. The link with the $\lambda^2 T$ limit is easily evinced from the following reasoning: The free part of the Hamiltonian is $H_Q = c\hat{p}$, so that the particle travels with constant speed c, and interacts with the detector for a time $T = L/c$, where $L \simeq N\Delta$ is the total length of the detector. Since the coupling constant $\lambda \equiv g \propto V_0\Omega$, one gets $\lambda^2 T = g^2 N\Delta/c \propto qN$. Notice that the "lattice spacing" Δ, the inverse of which corresponds to a density in our 1-dimensional model, can be kept finite in the limit. (In such a case, we have to express everything in terms of scaled variables.) As a final remark, we stress that the limit $N \to \infty$ with $qN < \infty$ considered in this note is physically very appealing, in our opinion, because it corresponds to a *finite* energy loss of the Q particle after interacting with the D system.

Acknowledgments

We acknowledge many scientific discussions with Hiromichi Nakazato. SP was partially supported by the Administration Council of the University of Bari (Grant 95/2748).

References

[1] E.J. Hellund, Phys. Rev. **89**, 919 (1953); M. Namiki and N. Mugibayashi, Prog. Theor. Phys. **10**, 474 (1953).

[2] L. van Hove, Physica **21**, 517 (1955). See also E.B. Davies, Commun. Math. Phys. **39**, 91 (1974); G.L. Sewell, *Quantum tueory of collective phenomena*, (Clarendon Press, Oxford, 1986).

[3] A.J. Leggett, Proc. 4th Int. Symp. *Foundations of Quantum Mechanics*, eds. M. Tsukada et al. (Phys. Soc. Japan, Tokyo, 1993) p.10.

[4] L.A. Khalfin, Zh. Eksp. Teor. Fiz. **33**, 1371 (1958) [Sov. Phys. JETP **6**, 1053 (1958)]; A. DeGasperis, L. Fonda and G.C. Ghirardi, Nuovo Cimento **A21**, 471 (1974); B. Misra and E. C. G. Sudarshan, J. Math. Phys. **18**, 756 (1977).

[5] S. Pascazio, M. Namiki, G. Badurek and H. Rauch, Phys. Lett. A **179**, 155 (1993); S. Pascazio and M. Namiki Phys. Rev. A **50**, 4582 (1994); M. Namiki and S. Pascazio, these proceeedings.

[6] K. Hepp, Helv. Phys. Acta **45**, 237 (1972); J.S. Bell, Helv. Phys. Acta **48**, 93 (1975); S. Machida and M. Namiki, Proc. Int. Symp. *Foundations of Quantum Mechanics*, eds. S. Kamefuchi et al. (Phys. Soc. Japan, Tokyo, 1984) p.136; S. Kudaka, S. Matsumoto and K. Kakazu, Prog. Theor. Phys. **82**, 665 (1989). See also other references in [7].

[7] H. Nakazato and S. Pascazio, Phys. Rev. Lett. **70**, 1 (1993); Phys. Rev. **A48**, 1066 (1993); K. Hiyama and S. Takagi, Phys. Rev. **A48**, 2568 (1993).

[8] H. Nakazato, M. Namiki and S. Pascazio, Phys. Rev. Lett. **73**, 1063 (1994).

[9] J. von Neumann, *Die Mathematische Grundlagen der Quantenmechanik* (Springer Verlag, Berlin, 1932); *Quantum Theory and Measurement*, eds. J.A. Wheeler and W.H. Zurek (Princeton University Press, 1983); P. Busch, P.J. Lahti and P. Mittelstaedt, *The quantum theory of measurement* (Springer Verlag, Berlin, 1991).

[10] S. Machida and M. Namiki, Prog. Theor. Phys. **63** 1457 (1980); 1833 (1980). M. Namiki, Found. Phys. **18** 29 (1988); M. Namiki and S. Pascazio, Phys. Rev. A **44**, 39 (1991); Physics Reports **232**, 301 (1993).

[11] C.P. Sun, Phys. Rev. **A48**, 898 (1993).

NEXT
DOCUMENT

PRESELECTED SUB–POISSONIAN CORRELATIONS

Mladen Pavičić

Max-Planck-G. Nichtklassische Strahlung, Rudower Chaussee 5, D-12484 Berlin, Germany;
Atominstitut der Österreichischen Universitäten, Schüttelstraße 115, A-1020 Wien, Austria;
*and University of Zagreb, GF, Kačićeva 26, Pošt. pret. 217, HR-41001 Zagreb, Croatia**

Abstract

The simplest possible photon–number–squeezed states containing only two photons and exhibiting sub–poissonian statistics with the Fano factor approaching 0.5 have been used for a proposal of a loophole–free Bell experiment requiring only 67% of detection efficiency. The states are obtained by the fourth order interference first of two downconverted photons at an asymmetrical beam splitter and thereupon of two photons from two independent singlets at an asymmetrical beam splitter. In the latter set–up the other two photons which nowhere interacted and whose paths never crossed appear entangled in a singlet–like correlated state.

1 Introduction

In 1985 Chubarov and Nikolayev [1] showed that quantum states with sub–poissonian statistics of photons interfering at a beam splitter (in a polarization experiment) violate the Bell inequality. Analyzing their result Ou, Hong, and Mandel [2] showed in 1987 that a pair of downconverted photons interfering in the fourth order at a symmetrical beam splitter should violate the inequality to the same extent although they exhibit poissoinan statistics. In 1988 Ou and Mandel [3] carried out the experiment and gave, together with Hong, its correct theoretical description in Ref.[4]. (The description of Ref. [3] was erroneous.[5, 6]) Pavičić and Summhammer provided in 1994 a theoretical description of two pair spin entanglement at a symmetrical beam splitter which would enable a loophole–free Bell experiment with 83% detection efficiency. On the other hand, in 1989 Campos, Saleh, and Teich [7], in effect, pointed out that not only two (or more) photons incoming to the beam splitter from the same side (as with Chubarov and Nikolayev) but also two photons incoming from the opposite sides (as with Ou and Mandel) and interferening in the fourth order at an *asymmetrical* beam splitter (the simplest photon–number–sqeezed state) exhibit sub–poissonian statistics with the *Fano factor* (the ratio between the variance and the mean of the photocounts) changing from 1 to 0.5 as the ratio between reflection and transmission coefficients changes from 1 to 0. A theoretical description of the interference at an asymmetrical beam splitter was given in 1994 by Pavičić [6]. In Sec. 2 we show how one can use such a beam splitter to devise a loophole–free Bell experiment with a detection efficiency as low as 67%. In 1995 it was pointed out by Pavičić [8] that two pair spin entanglement at an asymmetrical beam splitter enables a preselected loophole–free Bell 67% experiment. In Sec. 3 we present such an experiment.

* Permanent address: Internet: mpavicic@dominis.phy.hr

2 Simple sub–poissonian correlations

To describe the behavior of the photons at a beam splitter in the spin space we follow the results obtained in Pavičić [6, 8]. The signal and idler downconverted photons emerging from a nonlinear crystal of type–I (see Fig. 1) are parallelly polarized [3]. Because of this a 90^0 rotator is introduced. Since the signal and idler photons have random relative phases, we will have no interference of the second order but only of the fourth order which we describe in the second quantization formalism following Reff. [6, 8]. The actions of beam–splitter BS, polarizer Pj, and detector Dj $(j = 1, 2)$ are taken into account by the outgoing electric fields as given in Ref. [8]. For a realistic elaboration by means of wave packets we refer to Reff. [5, 8]. We only stress here that these equations remain unchanged insomuch that all experimental paramaters are absorbed by η and r below.

The probability of joint detection of two ordinary photons by detectors D1 and D2 is

$$P(\theta_1, \theta_2) = \langle \Psi | \hat{E}_2^\dagger \hat{E}_1^\dagger \hat{E}_1 \hat{E}_2 | \Psi \rangle = \eta^2 s^2 (\cos\theta_1 \sin\theta_2 - r \sin\theta_1 \cos\theta_2)^2 , \tag{1}$$

for $z_1 = z_2$ in Fig. 1, where $\hat{E}_j$ $(j = 1, 2)$ are as given in Reff. [5, 8], $s = t_x t_y$, $r = \frac{r_x r_y}{t_x t_y}$, r_x and r_y are reflection coefficients, t_x and t_y are transmission coefficients, and η is detection efficiency. The probability tells us that the photons appear to be in a nonmaximally correlated state whenever they emerge from two different sides of BS. The singles–probability of detecting one photon by, e.g., D1 and the other going through P2 and through either D2 or $D2^\perp$ without necessarily being detected by either of them is

$$P(\theta_1, \infty) = \eta s^2 (\cos^2\theta_1 + r^2 \sin^2\theta_1) . \tag{2}$$

The singles–probability of detecting one photon by D1 and the other going through P1 and D1 (without necessarily being detected by it) is (assuming $t_x = t_y$)

$$P(\theta_1 \times \theta_1) = \frac{\eta s^2 r}{2} \sin^2(2\theta_1) . \tag{3}$$

Let us see the effect of these results on the violations of the Bell inequality $B \leq 0$ where B is defined by

$$\eta s^2 B \equiv P(\theta_1, \theta_2) - P(\theta_1, \theta_2') + P(\theta_1', \theta_2') + P(\theta_1', \theta_2) - P(\theta_1') - P(\theta_2) , \tag{4}$$

where $P(\theta_1') = P(\theta_1', \infty)$ [as given by Eq. (2)] and $P(\theta_2) = P(\infty, \theta_2)$. To be able to use Eq. (4) we have to have a perfect "control" of all photons at BS. If we do not have it, we have to subtract Eqs. (3) (for appropriate angles) from Eq. (4) in order to take into account that detectors cannot tell one from two photons when they both emerge from the same side of BS.

By a computer optimization of angles we obtain $Max[B](r, \eta)$ surfaces as shown in Fig. 2. The values above the $B = 0$ plane mean violations of the Bell inequality. As shown by the lower curve in Fig. 3, for controlled photons, for $r = 1$ $Max[B] = 0$ yields $\eta = 0.828427$ and for $r \to 0$ we get a violation of the Bell inequality for any efficiency greater then 66.75%. The efficiencies for uncontrolled photons are shown as the upper curve in Fig. 3. We see that uncontrolled photons, i.e., the ones that also may emerge from the same sides of BS as well, violate the Bell inequality—starting with 85.8% efficiency—in opposition to the widespread belief that "unless the detector can differentiate one photon from two... no indisputable test of Bell's inequalities is possible." [9]

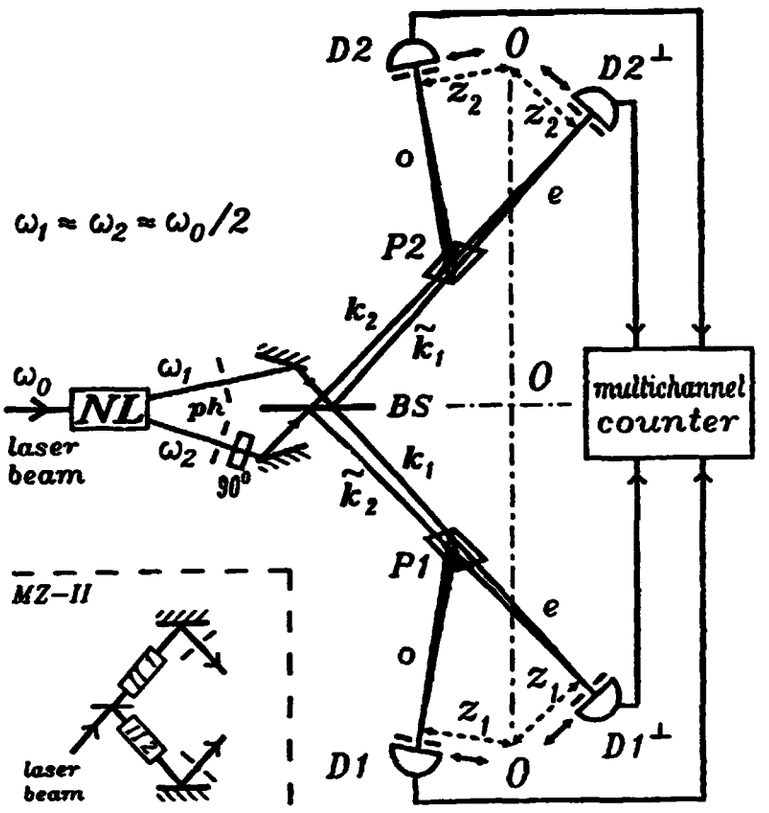

FIG. 1. Beam splitter set-up and MZ-II set-up (when inset MZ-II is put in place of NL; according to Kwiat *et al.* [9]). As birefringent polarizers P1 and P2 may serve Nicol or Wollaston prisms (which at the same time filter out the uv pumping beam in case of MZ-II). Pinholes *ph* determining the frequency ($\omega_0/2$) of signal and idler coming to the beam splitter BS and assuring that only one downconverted pair appears at a time are positioned as far away from the crystal as possible.

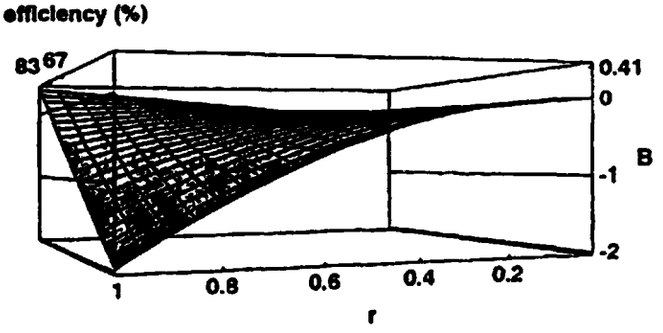

FIG. 2. The surface showing maximal violation of the Bell inequality for the optimal angles of the polarizers. All the values above the $B = 0$ plane violate the Bell inequality $B \leq 0$, where B is given by Eq. (4).

The afore-mentioned "control" of all photons can be achieved best if photons never emerge from the same side of a beam splitter and this is what Kwiat *et al.* [9] aimed at. We obtain their set-up by substituting the nonlinear crystal in Fig. 1 with two type-II crystals (MZ-II inset in Fig. 1) which downconvert two collinear and orthogonally polarized photons of the same average frequencies (half of the pumping beam frequency). The crystals are pumped by a 50:50 split laser beam (filtered out before reaching detectors) whose intensity is accommodated so as to give only one downconversion at a chosen time-window. Since one cannot tell which crystal a downconverted pair is coming from, the state of the photons incoming at the beam splitter must be described by the following superposition

$$|\Psi\rangle = \frac{1}{\sqrt{2}}\left(|1_x\rangle_1|1_y\rangle_1 + f|1_x\rangle_2\,|1_y\rangle_2\right), \tag{5}$$

where $0 \leq f \leq 1$ describes attenuation of the lower incoming beam.

The probability of both photons emerging from the same sides of BS is

$$P(\infty \times \infty) = (t_x t_y \pm f r_x r_y)^2 + (r_x r_y \pm f t_x t_y)^2, \tag{6}$$

where '$-$' stands for $z_1 = z_2$ and '$+$' for $z_2 - z_1 = L/2$ where L is the spacing of the interference fringes.

The probability of both photons emerging from the opposite sides of BS is

$$P(\theta_1, \theta_2) = \eta^2(\cos\theta_1 \sin\theta_2 \mp f \sin\theta_1 \cos\theta_2)^2, \tag{7}$$

where '$+$' stands for $z_1 = z_2$ and '$-$' for $z_2 - z_1 = L/2$. This gives the same η curve as shown in Fig. 3 but, in order to collect data for the probabilities in B in Eq. (4), we must be able to "control" single pairs of photons so as to prevent them to emerge both from the same side of BS. This means that the conditions $r_x r_y = f t_x t_y$ and $t_x t_y = f r_x r_y$ from Eq. (6) should be simultaneously satisfied what is however clearly impossible for $f < 1$. Thus, contrary to the claims of Kwiat *et al.* [9], the only way to make use of $f < 1$ is the crosstalk $t_y = r_x = 0$ for either $z_1 = z_2$ or $z_2 - z_1 = L/2$ and this is apparently difficult to control within a measurement.[9] It therefore turns out that the set-up is ideal for a loophole-free experiment with maximal singlet-like states, i.e., with $f = 1$ and $\eta > 83\%$ but that attenuation ($f < 1$) is not the best candidate for Bell's *event-ready* [10] preselector. We therefore propose another "event-ready set-up" which dispenses with variable f and offers a more fundamental insight into the whole issue.

3 Preselected sub-poissonian correlations

Schematic of the proposed experiment is given in Fig. 4. Two afore-discussed set-ups MZ-II 1 and MZ-II 2, fed by a split laser beam act as two independent sources of two independent singlet pairs. As shown above, for $z_2 - z_1 = L/2$ photons appear only from the opposite sides of the beam splitters of MZ-II 1 and MZ-II 2. Two photons from each pair interfere at the beam splitter of the *event-ready preselector* and as a result the other two photons appear to be in a nonmaximal singlet state although the latter photons are completely independent and nowhere interacted. The state of the four photons immediately after leaving MZ-II 1 and MZ-II 2 is

$$|\Psi\rangle = \frac{1}{\sqrt{2}}\left(|1_x\rangle_{1'}|1_y\rangle_1 - |1_y\rangle_{1'}|1_x\rangle_1\right) \otimes \frac{1}{\sqrt{2}}\left(|1_x\rangle_{2'}|1_y\rangle_2 - |1_y\rangle_{2'}|1_x\rangle_2\right). \tag{8}$$

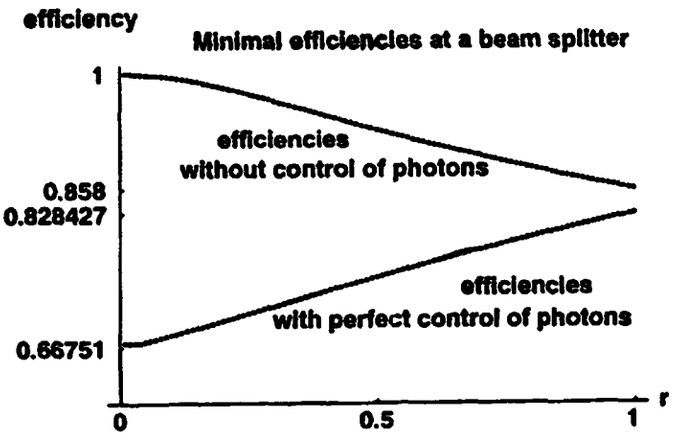

FIG. 3. Minimal efficiencies. Lower plot: η's as obtained for $B = 0$ from Eq. (4). Upper plot: η's as obtained for $B = r[\sin^2(2\theta_1') + \sin^2(2\theta_2)]/2$ from Eqs. (1–4).

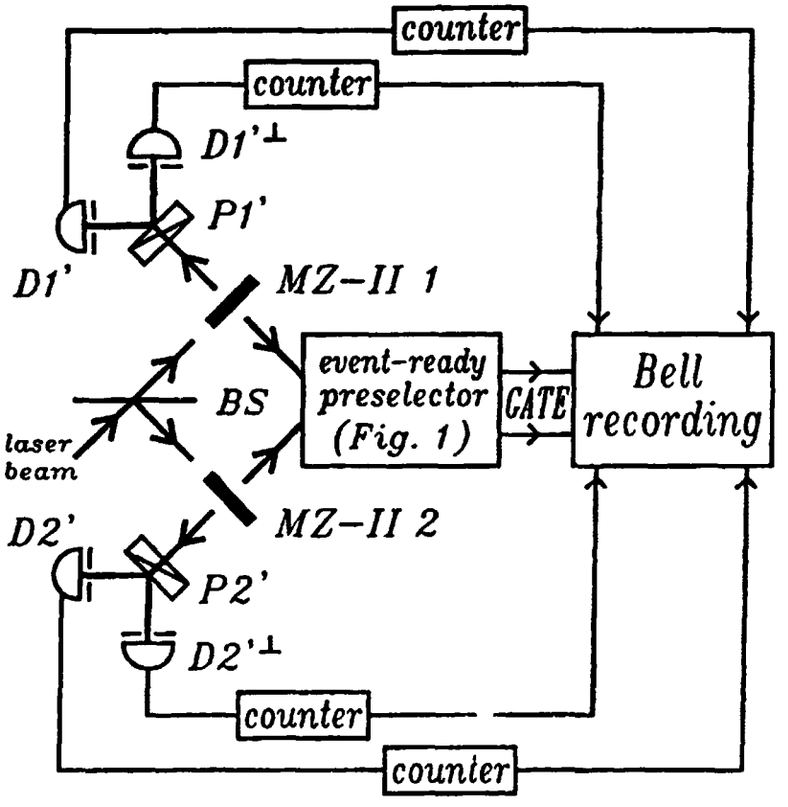

FIG. 4. Proposed experiment. As the event-ready preselector serves a beam splitter with detectors D1, D1$^{\perp}$, D2 and D2$^{\perp}$ as shown in Fig. 1. MZ-II 1 and MZ-II 2 are devices as shown in Fig. 1 with MZ-II from the inset substituted for NL; they serve as sources of singlet pairs. As birefringent polarizers P1' and P2' may serve Wollaston prisms (which at the same time filter out the uv pumping beam).

The probability of detecting all four photons by detectors D1, D2, D1', and D2' is thus

$$P(\theta_{1'},\theta_{2'},\theta_1,\theta_2) = \langle\Psi|\hat{E}_{2'}^{\dagger}\hat{E}_{1'}^{\dagger}\hat{E}_2^{\dagger}\hat{E}_1^{\dagger}\hat{E}_1\hat{E}_2\hat{E}_{1'}\hat{E}_{2'}|\Psi\rangle = \frac{1}{4}(A-B)^2\,, \tag{9}$$

for $z_1 = z_2$ where $\hat{E}_j$ are as given in Reff. [5, 8], $A = Q(t)_{1'1}Q(t)_{2'2}$ and $B = Q(r)_{1'2}Q(r)_{2'1}$; here $Q(q)_{ij} = q_x \sin\theta_i \cos\theta_j - q_y \cos\theta_i \sin\theta_j$.

For $\theta_1 = 90°$ and $\theta_2 = 0°$ Eq. (9) yields (non)maximal singlet-like probability $P(\theta_{1'},\theta_{2'})$ given by Eq. (1) which permits a perfect control of photons 1' and 2' and which is much more appropriate for the whole issue than Eq. (7), because the former reflects total spin conservation and quantum mechanical nonlocality while the latter satisfies the Bell inequality only inasmuch as it belongs to a non-product state [11]. This means that D1 and D2—while detecting coincidences—act as event-ready preselectors [10] and with the help of a gate (see Fig. 4) we can extract those 1' and 2' photons that are in a non-maximal singlet state, take them miles away and carry out a loophole-free Bell experiment by means of P1', D1', D1'$^{\perp}$, P2', D2', and D2'$^{\perp}$ with only 67% efficiency in the limit $r \to 0$. Thus, one might also view the experiment as a realistic device for *teleportation* of Bennett *et al.* [12]

Acknowledgments

I acknowledge supports of the Alexander von Humboldt Foundation, the Technical University of Vienna, and the Ministry of Science of Croatia and I would like to thank my host Prof. H. Paul, AG *Nichtklassische Strahlung*, Humboldt University of Berlin for many stimulating discussions.

References

[1] M. S. Chubarov and E. P. Nikolayev, Phys. Lett. A **110**, 199 (1985);

[2] Z. Y. Ou, C. K. Hong and L. Mandel, Phys. Lett. A **122**, 11 (1987);

[3] Z. Y. Ou and L. Mandel, Phys. Rev. Lett. **61**, 50 (1988);

[4] X. Y. Ou, C. K. Hong, and L. Mandel, Opt. Commun. **67**, 159 (1988).

[5] M. Pavičić and J. Summhammer, Phys. Rev. Lett. **73**, 3191 (1994).

[6] M. Pavičić, Phys. Rev. A **50**, 3486 (1994).

[7] R. A. Campos, B. E. A. Saleh, and M. A. Teich, Phys. Rev. A **40**, 1371 (1989).

[8] M. Pavičić, J. Opt. Soc. Am. B, **12**, 821 (1995).

[9] P. G. Kwiat *et al.*, Phys. Rev. A, **49**, 3209 (1994).

[10] J. F. Clauser and A. Shimony, Rep. Prog. Phys. **41**, 1881 (1978).

[11] N. Gisin, Phys. Lett. A **154**, 201 (1991).

[12] C. H. Bennett *et al.*, Phys. Rev. Lett. **70**, 1895 (1993).

NEXT
DOCUMENT

GENERALIZED ENTROPIC UNCERTAINTY RELATIONS WITH TSALLIS' ENTROPY

M. Portesi and A. Plastino
Departamento de Física, Universidad Nacional de La Plata, C.C. 67, (1900) La Plata, Argentina

Abstract

A generalization of the entropic formulation of the Uncertainty Principle of Quantum Mechanics is considered with the introduction of the q-entropies recently proposed by Tsallis. The concomitant generalized measure is illustrated for the case of phase and number operators in Quantum Optics. Interesting results are obtained when making use of q-entropies as the basis for constructing generalized entropic uncertainty measures.

1 Introduction

The Uncertainty Principle (UP) can be stated quantitatively in the following fashion

$$\mathcal{U}(\hat{A}, \hat{B}; \psi) \geq \mathcal{B}(\hat{A}, \hat{B}) \tag{1.1}$$

where $\mathcal{U}$ is an estimation of the uncertainty in the result of a simultaneous measurement of two incompatible observables $\hat{A}$ and $\hat{B}$, when the system is in a state $|\psi\rangle$. What the UP asserts is that such an estimation is limited by an irreducible lower bound, the infimum $\mathcal{B}$, which merely depends on both operators. $\mathcal{U}$ must attain a fixed minimum value ($\mathcal{U}_{\min} \equiv 0$) if and only if $|\psi\rangle$ is a common eigenstate of $\hat{A}$ and $\hat{B}$, and $\mathcal{B}$ vanishes when the observables share at least one eigenvector.

The extension of Heisenberg's inequality to describe the UP for *arbitrary* pairs of operators (when their commutator is not a c-number) has been criticized because its r.h.s. is not a fixed lower bound [1]. Much effort has been devoted to present quantitative formulations of the UP (see, for example, refs. [1]–[8]). A central idea underlying these works is that the most natural measure of uncertainty is precisely the *missing information* [9] that remains once a measurement is made.

Deutsch first proposed [1] the use of Shannon's information-theory entropy [9] ($S(\{p_i\}) \equiv -\sum_{i=1}^{N} p_i \ln p_i$, for any probability distribution $\{p_i\}$) to measure uncertainty, in the following way

$$\mathcal{U}_1(\hat{A}, \hat{B}; \psi) = S(\hat{A}; \psi) + S(\hat{B}; \psi) \tag{1.2}$$

with the entropies calculated for the distributions $\{p_{\hat{A},i} = |\langle a_i|\psi\rangle|^2\}$ and $\{p_{\hat{B},j} = |\langle b_j|\psi\rangle|^2\}$, which correspond to the projections of $|\psi\rangle$ onto the bases of eigenvectors of $\hat{A}$ and $\hat{B}$, respectively. With reference to an $\hat{A}$-measurement, a system in a state with a probability distribution $\{\delta_{i_0}\}$ has a "minimum lack of information" (or "maximum knowledge"), and then $S(\hat{A}; \psi) = S_{\min} = 0$. On

the other hand, a uniform distribution $\{1/N\}$ characterizes a situation of "maximum ignorance", with $S(\hat{A};\psi) = S_{\max} = \ln N$.

It has been shown [1] that $\mathcal{U}_1$ satisfies

$$\mathcal{U}_1(\hat{A},\hat{B};\psi) \geq 2 \ln \frac{2}{1+c} \tag{1.3}$$

with $c = \sup_{ij} |\langle a_i|b_j\rangle|$. It was conjectured first by Kraus [3] and demonstrated later by Maassen and Uffink [4] that a better bound can be given,

$$\mathcal{U}_1(\hat{A},\hat{B};\psi) \geq 2 \ln \frac{1}{c} \tag{1.4}$$

Kraus specifically considered having two *complementary* observables: exact knowledge of the measured value of one of them implies maximum uncertainty in the other measurement, and consequently $|\langle a_i|b_j\rangle| = 1/\sqrt{N}$, for all $i,j = 1,\ldots,N$.

It seems natural to look for alternative descriptions of the UP expressed in entropic terms. In Section 2, we analyze the quantitative formulation of uncertainty in the spirit of Information Theory, with the aid of the recently introduced Tsallis' entropy [10], which is regarded as information measure [11]. We illustrate with a simple example, namely the phase–number uncertainty measures within the Pegg-Barnett formalism, and outline some conclusions in Section 3.

2 Tsallis' entropy as measure of uncertainty

A quite interesting generalization of the conventional entropy form has been recently advanced by Tsallis [10]. For any normalized probability distribution $\{p_i\}$, Tsallis' entropy reads

$$S_q(\{p_i\}) = \frac{1 - \sum_{i=1}^{N} p_i^q}{q-1} \tag{2.1}$$

where q is any real number, characterizing a particular statistics. (The sum must be carried out over non-zero probabilities.) The $q \to 1$ limit of (2.1) yields the Boltzmann–Shannon's logarithmic expression.

The physics is an extensive one only for $q = 1$ [10, 12]. Tsallis' entropy is related to the more familiar Rényi's entropy by $S_q^R = (\ln[1+(1-q)S_q])/(1-q)$. A crucial difference distinguishes these two *alternative* entropies, however. Tsallis' entropy always possesses a definite concavity, being a concave (convex) function of the probabilities for $q > 0$ ($q < 0$), which is not the case for Rényi's one. It is thus the former the generalized entropy recently employed in several distinct physical contexts. The generalized statistics associated to (2.1) has been shown to satisfy appropriate forms of Ehrenfest theorem [11], Jaynes' information-theory duality relations [11], von Neumann's equation [13], and the fluctuation–dissipation theorem [14, 15], among others. H-theorems and irreversibility have been in this connection also discussed [16, 17], as well as a possible connection with quantum groups [18], for instance. This nonextensive statistics has allowed, within an astrophysical context, to overcome the inability of the conventional, extensive one, to adequately deal (without infinities) with self-gravitating stellar systems, in what constituted the first physical

application of the $q \neq 1$-theory [19]. A second application refers to Lévy flights, relevant for a variety of systems [20].

Some properties of the q-entropies are: i) $S_q \geq 0$ for any q and $\{p_i\}$, with $S_q = 0$ for $p_i = \delta_{ii_0}$ (certainty); ii) S_q reaches the extreme value $(1 - N^{1-q})/(q-1)$ for every q and $p_i = 1/N$ (equiprobability); iii) S_q is a non-increasing function of $q > 0$ for each $\{p_i\}$; iv) For two independent distributions $\{p_i\}$ and $\{p'_j\}$ (such that the joint probability is $p_{ij} = p_i p'_j$), it verifies that $S_q(\{p_{ij}\}) = S_q(\{p_i\}) + S_q(\{p'_j\}) + (1-q) S_q(\{p_i\}) S_q(\{p'_j\})$.

We consider the new entropy as measure of uncertainty. Let us recall first that Heisenberg's relation, as well as the entropic relations given above, refer to *independent* measurements of the observables $\hat{A}$ and $\hat{B}$ on different microsystems in the same state $|\psi\rangle$. The UP states that the probability distributions obtained when $|\psi\rangle$ is projected on the corresponding eigenbases cannot be both arbitrarily peaked, given operators $\hat{A}$ and $\hat{B}$ "sufficiently non-commuting" [3]. The uncertainty measure appearing in eq. (1.2) takes into account the total information entropy associated to two independent probability distributions. Shannon's entropy is additive and $\mathcal{U}_1$ is just $S(\hat{A}) + S(\hat{B})$. We introduce now Tsallis' entropy to measure the amount of uncertainty, in the same spirit. The generalized expression reads

$$\mathcal{U}_q(\hat{A}, \hat{B}; \psi) \equiv S_q(\hat{A}; \psi) + S_q(\hat{B}; \psi) + (1-q) S_q(\hat{A}; \psi) S_q(\hat{B}; \psi) \tag{2.2}$$

where q is a positive parameter and the entropies are given by (2.1) for the probability sets $\{p_{A,i}\}$ and $\{p_{\hat{B},j}\}$. It is immediately seen that $\mathcal{U}_q \geq 0$, with $\mathcal{U}_q = 0$ if and only if $|\psi\rangle$ is a common eigenstate of $\hat{A}$ and $\hat{B}$. Besides this, $\mathcal{U}_q$ never exceeds $(1 - N^{2(1-q)})/(q-1)$. (We mention that these ideas can be extended to deal with pairs of observables with continuous spectra. However, one must be careful when defining the (generalized) information entropy for non-discrete distributions $\{p(x)\}$ [17, 21].)

A (weak) bound can be imposed on (2.2), namely

$$\mathcal{U}_q(\hat{A}, \hat{B}; \psi) \geq \frac{1}{q-1} \left(1 - \left(\frac{2}{1+c} \right)^{2(1-q)} \right) \tag{2.3}$$

which holds for any $q > 0$. By recourse to Riesz' theorem (as used in ref. [4]), it can be demonstrated that a better bound for $\mathcal{U}_q$ exists, at least in the region $1/2 \leq q \leq 1$:

$$\mathcal{U}_q(\hat{A}, \hat{B}; \psi) \geq \frac{1}{q-1} \left(1 - \left(\frac{1}{c} \right)^{2(1-q)} \right) \tag{2.4}$$

3 Example and conclusions

We shall apply our ideas to the phase and number operators in Quantum Optics. The treatment of optical states can be accomplished by recourse to the Pegg-Barnett (PB) formalism [22]. This implies working in a finite but arbitrarily large $(s+1)$-dimensional Hilbert space $\mathcal{H}^{s+1}$ spanned by the number states $|0\rangle_s, |1\rangle_s, \ldots, |s\rangle_s$, and taking the limit $s \to \infty$ at the end. The *Hermitian* phase operator is defined as

$$\hat{\Phi} = \sum_{m=0}^{s} \theta_m |\theta_m\rangle_{s\,s}\langle\theta_m|, \qquad |\theta_m\rangle_s = \frac{1}{\sqrt{s+1}} \sum_{n=0}^{s} e^{in\theta_m} |n\rangle_s \tag{3.1}$$

The corresponding eigenvalues are $\theta_m = \theta_0 + 2\pi m/(s+1)$. (Hereafter, the arbitrary reference phase θ_0 will be set equal to 0.) The phase and number operators, $\hat{\Phi}$ and $\hat{N}$, are mutually complementary, with overlap $c = 1/\sqrt{s+1}$.

It is found that, for a system in a state $|\psi\rangle \in \mathcal{H}^{s+1}$, $\mathcal{U}_1(\hat{\Phi}, \hat{N}; \psi, s) \geq \ln(s+1)$ which diverges when $s \to \infty$. In order to extract some information out of this relation, Abe examined [5] the entropy differences from a certain reference state before going to the infinite-s limit. Number and phase eigenstates (which actually saturate that inequality) were chosen. Within the framework of Tsallis' information entropy, for a given $q > 0$ and a state $|\theta_m\rangle_s$, for instance, the entropies are given by $S_q(\hat{\Phi}; \theta_m, s) = 0$ and $S_q(\hat{N}; \theta_m, s) = (1 - (s+1)^{1-q})/(q-1)$. Consequently,

$$\lim_{s\to\infty} \mathcal{U}_q(\hat{\Phi}, \hat{N}; \theta_m, s) = \begin{cases} \infty, & \text{if } 0 < q \leq 1 \\ \frac{1}{q-1}, & \text{if } q > 1 \end{cases} \tag{3.2}$$

The same obtains for a number eigenstate. We stress that, considering generalized information entropies with $q > 1$, the divergence in the uncertainty for number or phase states is removed.

Let us consider the generalized entropic uncertainty measures for a system prepared in a phase coherent state (PCS). These states, recently found by Kuan and Chen [21], are given by

$$|z\rangle_s = \frac{1}{\sqrt{e_s(|\tilde{z}|^2)}} \sum_{m=0}^{s} \frac{\tilde{z}^m}{\sqrt{m!}} |\theta_m\rangle_s \tag{3.3}$$

where $\tilde{z} \equiv \sqrt{2\pi/(s+1)}\, z$ is a complex number and the normalizing function is given by $e_s(x) = \sum_{n=0}^{s} x^n/n!$. The projections of a PB PCS on phase and number eigenstates are

$$p_m \equiv |{}_s\langle \theta_m | z\rangle_s|^2 = \frac{1}{e_s(|\tilde{z}|^2)} \frac{|\tilde{z}|^{2m}}{m!} \tag{3.4}$$

and

$$p'_n \equiv |{}_s\langle n | z\rangle_s|^2 = \frac{1}{(s+1)\, e_s(|\tilde{z}|^2)} \left| \sum_{k=0}^{s} \frac{\tilde{z}^k e^{-in\theta_k}}{\sqrt{k!}} \right|^2 \tag{3.5}$$

respectively, with $m, n = 0, 1, \ldots, s$.

The $\hat{\Phi} - \hat{N}$ Heisenberg's inequality has been discussed for the $s = 1$ case [21]. We have analyzed the shapes of the phase and number q-entropies, for many different values of s. Within a given statistical frame of index q, the entropies $S_q(\hat{\Phi}; z, s)$ and $S_q(\hat{N}; z, s)$, will depend on both $|z|$ and s. The complementariness of $\hat{\Phi}$ and $\hat{N}$ is clearly seen. The phase entropy vanishes both for $|z| = 0$ (as it should for the vacuum phase state $|\theta_0\rangle$) and for $|z|$ sufficiently large. The number entropy has a minimum in the intermediate region (those PCS for which the entropy approach zero can be interpreted as "number-like" states). Those states are also of relatively low uncertainty. It can be seen that $(1 - (s+1)^{1-q})/(q-1)$ is a lower bound for the generalized uncertainty measure (see eq. (2.4)). This is obtained for arbitrary size of the PB space, s, or statistical parameter, q. Fig. 1 displays the q-entropies and the uncertainty $\mathcal{U}_q(\hat{\Phi}, \hat{N}; z, s)$ as a function of $|z|$, assuming particular values for both q and s.

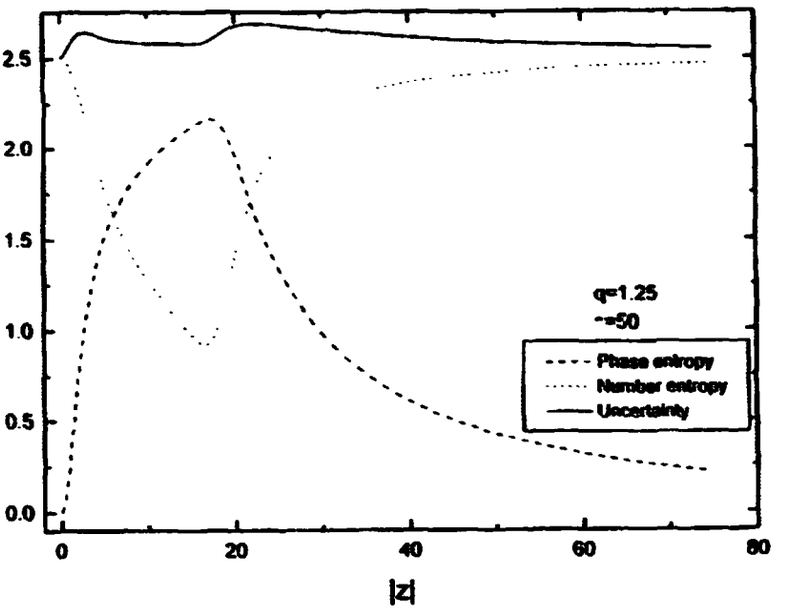

FIG. 1. Phase and number q-entropies and generalized uncertainty measure, for a PB PCS, as a function of coherence.

As a conclusion, generalized entropies recently introduced by Tsallis have been discussed in order to establish general uncertainty relations for the measurement of two quantum incompatible observables. Number and phase operators within the Pegg–Barnett formalism have been investigated in some detail. Interesting results are obtained when making use of q-entropies as the basis for constructing generalized entropic uncertainty measures.

Acknowledgments

The authors acknowledge support from Consejo Nacional de Investigaciones Científicas y Técnicas (CONICET) and Universidad Nacional de La Plata (UNLP), Argentina.

References

[1] D. Deutsch, Phys. Rev. Lett. **50**, 631 (1983).

[2] M. Hossein Partovi, Phys. Rev. Lett. **50**, 1883 (1983).

[3] K. Kraus, Phys. Rev. D **35**, 3070 (1987).

[4] H. Maassen and J.B.M. Uffink, Phys. Rev. Lett. **60**, 1103 (1988).

[5] S. Abe, Phys. Lett. A **166**, 163 (1992).

[6] Jorge Sánchez-Ruiz, Phys. Lett. A **181**, 193 (1993).

[7] A. Katz, *Principles of Statistical Mechanics, The information theory approach* (W.H. Freeman and Co., San Francisco and London, 1967).

[8] C. Tsallis, J. Stat. Phys. **52**, 479 (1988).

[9] A.R. Plastino and A. Plastino, Phys. Lett. A **177**, 177 (1993).

[10] E.M.F. Curado and C. Tsallis, J. Phys. A **24**, L69 (1991); Corrigenda: **24**, 3187 (1991) and **25**, 1019 (1992).

[11] A.R. Plastino and A. Plastino, Physica A **202**, 438 (1994).

[12] A. Chame and E.V.L. de Mello, J. Phys. A **27**, 3663 (1994).

[13] C. Tsallis, in *New trends in magnetism, magnetic materials, and their applications*, ed. by J.L. Morán-López and J.M. Sanchez (Plenum Press, New York, 1994).

[14] Ananias M. Mariz, Phys. Lett. A **165**, 409 (1992).

[15] John D. Ramshaw, Phys. Lett. A **175**, 169 and 171 (1993).

[16] M. Portesi, A. Plastino, and C. Tsallis, *Nonextensive thermostatistics can yield "dark magnetism"*, submitted for publication.

[17] A.R. Plastino and A. Plastino, Phys. Lett. A **174**, 384 (1993).

[18] P.A. Alemany and D.H. Zanette, Phys. Rev. E **49**, R956 (1994).

[19] John D. Ramshaw, Phys. Lett. A **116**, 110 (1986).

[20] D.T. Pegg and S.M. Barnett, Europhys. Lett. **6**, 483 (1988), and Phys. Rev. A **39**, 1665 (1989); S.M. Barnett and D.T. Pegg, J. Mod. Opt. **36**, 7 (1989).

[21] L.-M. Kuan and X. Chen, Phys. Lett. A **186**, 8 (1994).

NEXT
DOCUMENT

QUANTUM LIMITS IN INTERFEROMETRIC GW ANTENNAS

R. Romano, F. Barone, P. Maddalena, S. Solimeno[1] and F. Zaccaria
Dipartimento di Scienze Fisiche,
Universita' di Napoli "Federico II",
Istituto Nazionale di Fisica Nucleare, Sezione di Napoli,
Mostra d'Oltremare, Pad. 20-80125 Napoli, Italy

M. A. Man'ko and V. I. Man'ko
Lebedev Physics Institute,
Leninsky pr.,53, 117924 Moscow, Russia

Abstract

We discuss a model for interferometric GW antennas illuminated by a laser beam and a vacuum squeezed field. The sensitivity of the antenna will depend on the properties of the radiation entering the two ports and on the optical characteristics of the interferometer components, e.g. mirrors, beam-splitter, lenses.

1 Introduction

An important ingredient for improving the sensitivity of Michelson interferometric gravitational wave detectors (GWD) is using appropriate states for the light beams illuminating its two input ports. In interferometric measurements the quantum noise is due to the fluctuations of the number of photons and to the random motion of the mirrors induced by the radiation pressure. The GW signal is extracted from the spectral density of the output.

Purpose of this paper is to discuss the dependence of the sensitivity of an interferometric GW antenna on the photon-noise and radiation pressure noises. In particular we will consider an interferometer driven by a fluctuating laser beam and a squeezed-vacuum field generated by a degenerate OPO driven by the second harmonic of the laser beam. Particular attention will be paid to the influence of phase and amplitude fluctuations of the laser beam.

2 Michelson interferometer

We consider a Michelson interferometer with two mirrors M_1 and M_2 suspended at the ends of two arms. The vertices of M_1 and M_2 are located on the axes y and x passing through the origin O, while the beam splitter is centered on O (see Fig. 1).

In order to account for aberration effects, we will model the interferometer as a multimode device: we consider two groups of beams entering through the ports P_1, P_2 (Fig. 1), described by

[1] also with Istituto Nazionale di Ottica (INO)

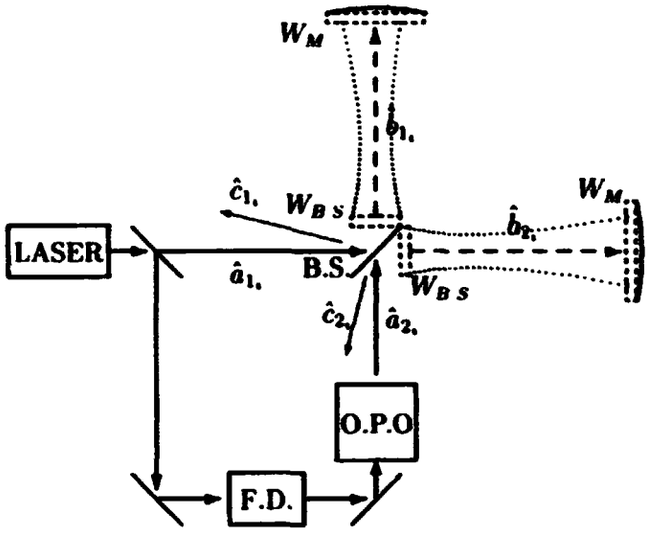

Figure 1: Michelson's interferometer. B.S.= beam-splitter; W_M aberration regions due to the mirrors; $W_{B.S.}$ aberration regions due to the beam-splitter; F.D.= frequency doubler; O.P.O.= Optical Parametric Oscillator; $\hat{a}_{1_0}, \hat{a}_{2_0}$ = in-fields at the port 1,2; $\hat{b}_{1_0}, \hat{b}_{2_0}$ = fields at the mirror 1,2; $\hat{c}_{1_0}, \hat{c}_{2_0}$ = out-fields at the port 1,2.

the operators $(\hat{a}_{j_1}, \hat{a}^\dagger_{j_1}), (\hat{a}_{j_2}, \hat{a}^\dagger_{j_2})$ with $j = 0, 1, \ldots, N-1$, acting on a Hilbert space $\mathcal{H}_a = \mathcal{H}_{a_1} \otimes \mathcal{H}_{a_2}$, with $\mathcal{H}_{a_i} = \mathcal{H}^{(0)}_{a_i} \otimes \ldots \otimes \mathcal{H}^{(N-1)}_{a_i}$, $i = 1, 2$. More specifically, the modes relative to port P_1 consist of Gauss-Hermite beams travelling along the x-axis with waist in O,

$$u_{lm}(y, z; x) \propto e^{-\frac{y^2+z^2}{2q(x)}} H_l\left(\frac{\sqrt{2}y}{w(x)}\right) H_m\left(\frac{\sqrt{2}z}{w(x)}\right)$$

The pair of indices lm will be denoted by i_1. Analogously, for P_2 we consider a similar family of Gauss-Hermite beams propagating along the y-axis with waist in O (see Fig. 2).

Passing through the beam-splitter, the input beams transform in two fields at M_1, M_2 described by $(\hat{b}_{j_1}, \hat{b}^\dagger_{j_1}), (\hat{b}_{j_2}, \hat{b}^\dagger_{j_2})$ with $j = 0, 2, \ldots, N-1$, acting on a Hilbert space $\mathcal{H}_b = \mathcal{H}_{b_1} \otimes \mathcal{H}_{b_2}$, such that $\mathcal{H}_{b_i} = \mathcal{H}^{(0)}_{b_i} \otimes \ldots \otimes \mathcal{H}^{(N-1)}_{b_i}$ and two outgoing beams described at P_1, P_2 by $(\hat{c}_{j_1}, \hat{c}^\dagger_{j_1}), (\hat{c}_{j_2}, \hat{c}^\dagger_{j_2})$ with $j = 0, 1, \ldots, N-1$, acting on a Hilbert space $\mathcal{H}_c = \mathcal{H}_{c_1} \otimes \mathcal{H}_{c_2}$, where, again, $\mathcal{H}_{c_i} = \mathcal{H}^{(0)}_{c_i} \otimes \ldots \otimes \mathcal{H}^{(N-1)}_{c_i}$.

For the sake of notational convenience, we introduce the bold symbols $\hat{\mathbf{a}}_i = \hat{a}_{i_1} \otimes \hat{a}_{i_2} = \begin{pmatrix} \hat{a}_{i_1} \\ \hat{a}_{i_2} \end{pmatrix}$, for indicating the pair of i-th modes relative to P_1 and P_2 respectively. Analogously, we introduce the vector $A \equiv \begin{pmatrix} \hat{a}_0 \\ \vdots \\ \hat{a}_{N-1} \end{pmatrix}$. With the same meaning, we will introduce the vectors **B** and **C** for the operators $\hat{b}_j$ and $\hat{c}_j$, relative respectively to the mirrors and the output ports.

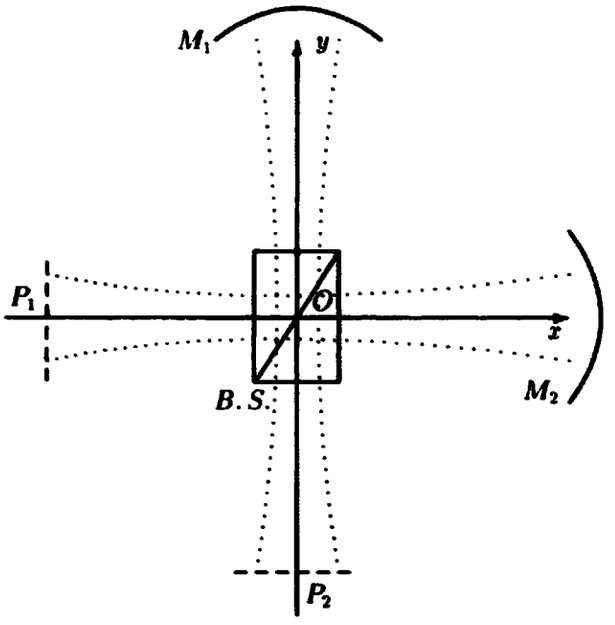

Figure 2: Schematic of Gauss-Hermite beams.

Assuming the fraction of energy lost during the passage through the interferometer be indipendent of the mode considered, **B** and **C** can be redefined as vectors proportional to the actual ones and carrying the same energy of **A**. In view of the energy conservation, the linearity and time invariance of the antenna, the outgoing vector **C** can be related to the ingoing one **A** by the unitary matrix **U**,

$$C = U \cdot A, \tag{1}$$

with

$$U \equiv \begin{pmatrix} U_{0,0} & U_{0,1} & \cdots & U_{0,N-1} \\ U_{1,0} & U_{1,1} & \cdots & U_{1,N-1} \\ \vdots & \vdots & \vdots & \vdots \\ U_{N-1,0} & U_{N-1,1} & \cdots & U_{N-1,N-1} \end{pmatrix}, \tag{2}$$

where each $U_{i,j}$ is a 2×2 matrix. Moreover, to preserve the bosonic commutation relations, U must be a symplectic matrix, that is $U \in Sp(2N, R)$ and $U_{i,j} \in Sp(2, R)$.

From now on we will consider an interferometer illuminated by two TEM_{00} gaussian modes on ports P_1 and P_2 respectively. This amounts to considering an input state vector of the form

$$|\Psi >= |\psi_0 > |0_1 > \ldots |0_N - 1 >, \tag{3}$$

where $|0_i >= |0_{i_1} > |0_{i_2} >$ indicates that the modes i_1, i_2 are unexcited ground state. As a result of the propagation through the imperfect interferometer, the states of all these modes will be mixed up to some extent. So that, a mode initially in the ground state will be partially excited at the output ports.

In view of (3), it is worth splitting $\mathcal{H}_a$ in the product $\mathcal{H}_a = \mathcal{H}_{a_0} \otimes \mathcal{H}_{a_\beta}$, whith $\mathcal{H}_{a_0}$ relative to the fundamental modes entering the two ports, and $\mathcal{H}_{a_\beta}$ relative to the remaining $2N - 2$ modes.

In the same manner we will write $A \equiv \begin{pmatrix} \hat{a}_0 \\ \hat{a}_\beta \end{pmatrix}$, where $\hat{a}_0 = \begin{pmatrix} \hat{a}_{0_1} \\ \hat{a}_{0_2} \end{pmatrix}$, $\hat{a}_\beta = \begin{pmatrix} \hat{a}_1 \\ \vdots \\ \hat{a}_2 \end{pmatrix}$, and so for **B** and **C**.

Analogously to (1), the fields **B** at the mirrors will depend linearly on **A**

$$B = V \cdot A,$$

whith **V** a unitary linear transformation $V \equiv \begin{pmatrix} V_0 & V_{0\beta} \\ V_{\beta 0} & V_\beta \end{pmatrix}$. Physically, **V** describes reflection and transmission at the beam-splitter, followed by propagation through the interferometer arms. Then, it can be expressed as the product

$$V = \Phi \cdot \Phi_{(BS)} \cdot K,$$

where **K** describes the aberration-free beam-splitter, $\Phi_{(BS)}$ is the aberration matrix relative to the beam-splitter itself and Φ is the interferometer arm delay matrix.

Introducing the $N \times N$ matrices $1_{ij} = \delta_{i_1 j_1}\delta_{i_2 j_2}$, $\bar{1}_{ij} = \delta_{i_1 j_2}\delta_{i_2 j_1}$, and the 2×2 matrices k_1, k_2, we can write **K**, whose elements are 2×2 matrices, as

$$K = e^{i\phi}(cos\ \gamma\ \sigma_0 1 + sin\ \gamma\ \sigma_1 \bar{1}). \tag{4}$$

with σ_0, σ_1 Pauli matrices. The aberrations of the beam splitter are modeled by including at the two output faces two transparencies characterized by the aberration eykonals $W_{(BS)}(x, z)$ and $W_{(BS)}(y, z)$ for the faces perpendicular to y- and x-axes respectively. $\Phi_{(BS)}$, representing the aberration eykonal phase factor, is symmetric with respect to the exchange of the pair of indices i_1, i_2 with j_1, j_2,

$$\Phi_{(BS)} = \begin{pmatrix} \Phi_{(BS)0,0} & \Phi_{(BS)0,1} & \cdots & \Phi_{(BS)0,N-1} \\ \Phi_{(BS)1,0} & \Phi_{(BS)1,1} & \cdots & \Phi_{(BS)1,N-1} \\ \vdots & \vdots & \vdots & \vdots \\ \Phi_{(BS)N-1,0} & \Phi_{(BS)N-1,1} & \cdots & \Phi_{(BS)N-1,N-1} \end{pmatrix}, \tag{5}$$

where

$$\Phi_{(BS)ij} = \begin{pmatrix} e^{iW_{(BS)i_1 j_1}} & 0 \\ 0 & e^{iW_{(BS)i_2 j_2}} \end{pmatrix}. \tag{6}$$

The symmetry of the $\Phi_{(BS)}$ matrix is a consequence of the identities $W_{(BS)i_1,j_1} = W_{(BS)j_1,i_1}$ and $W_{(BS)i_2,j_2} = W_{(BS)j_2,i_2}$.

Finally, the time-delay matrix is diagonal

$$\Phi = \begin{pmatrix} \Phi_0 & 0 & \ldots & 0 \\ 0 & \Phi_1 & \ldots & 0 \\ \vdots & \vdots & \vdots & \vdots \\ 0 & 0 & \ldots & \Phi_{N-1} \end{pmatrix} \tag{7}$$

with $\Phi_i = \begin{pmatrix} e^{i\phi_{i_1}} & 0 \\ 0 & e^{i\phi_{i_2}} \end{pmatrix}$, $\phi_{i_{1,2}}$ representing the phase delay of the $i_{1,2}$-th Gauss-Hermite mode hitting $M_{1,2}$. In particular,

$$\phi_{i_{1,2}} = kL_{1,2} - \delta\phi_{i_{1,2}} + \delta\phi_{GW_{1,2}} + \delta\phi_{(sus)_{1,2}} + \delta\phi_{(mir)_{1,2}} + \delta\phi_{(pres)_{1,2}} + \delta\phi_{(rp)_{1,2}} \tag{8}$$

where $\delta\phi_{i_{1,2}}(> 0)$ stands for the delay of the i-th Gauss-Hermite mode with respect the phase delay $kL_{1,2}$ of a plane wave. $\delta\phi_{GW_{1,2}}$ represents the gravitational wave ($\delta\phi_{GW_1} = -\delta\phi_{GW_2}$). The other terms stand for : (i) $\delta\phi_{(susp)}$=noise transmitted to the mirrors through the suspensions, (ii) $\delta\phi_{(mir)}$= noise caused by the vibration modes of the mirrors, (iii) $\delta\phi_{(pres)}$= pressure fluctuations in the partially evacuated pipes of the interferometer arms, and (iv) $\delta\phi_{(rp)}$= radiation pressure noise.

As a result of the reflection on M_1 and M_2, the different modes propagate toward the exit ports, by retracing the same paths followed before. Then,

$$U = -K \cdot \Phi_{(BS)} \cdot \Phi \cdot \Phi_{(M)} \cdot \Phi \cdot \Phi_{(BS)} K \tag{9}$$

where $\Phi_{(M)}$ is the mirror aberration matrix.

3 Interferometer output

The interferometer output is proportional to the expectation value of the difference I between the photocurrents detected at the ports 1 and 2 respectively

$$I = \sum_i (c_{i_1}^\dagger c_{i_1} - c_{i_2}^\dagger c_{i_2}) = C^\dagger \cdot \sigma_3 \cdot C = A^\dagger \cdot S \cdot A \tag{10}$$

where **S** is the unitary self-adjoint operator $S = U^\dagger \cdot \sigma_3 \cdot U$.

Introducing the quantity $K_3 \equiv K^* \cdot \sigma_3 \cdot K = cos(2\gamma)\sigma_3\ 1 - sin(2\gamma)\sigma_2\ \bar{1}$ (see Eq. 4) and assuming an input state of the form (3), it yelds

$$S = K^* \cdot \Phi_{(BS)}^* \cdot \Phi^* \cdot \Phi_{(M)}^* \cdot \Phi^* \cdot \Phi_{(BS)}^* \cdot K_3 \cdot \Phi_{(BS)} \cdot \Phi \cdot \Phi_{(M)} \cdot \Phi \cdot \Phi_{(BS)} \cdot K = S_{(0)} + S_{(ab)} \tag{11}$$

where $S_{(0)} \equiv -sin\ \tilde{\phi}\sigma_1 - cos\ \tilde{\phi}\sigma_3$, with $\tilde{\phi} \equiv 2(\phi_{0_2} - \phi_{0_1})$, is the matrix in absence of aberrations and $\delta\gamma = 0$, while $S_{(ab)} \equiv \alpha_1\sigma_1 + \alpha_2\sigma_2 + \alpha_3\sigma_3$ describes the effects of the aberrations and the deviation from the condition of exact equipartition of the incident intensity between the two B.S. outputs.

Now introducing the quantities $A_1 = a_0^\dagger \cdot \sigma_1 \cdot a_0$, $A_2 = a_0^\dagger \cdot \sigma_2 \cdot a_0$, $A_3 = a_0^\dagger \cdot \sigma_3 \cdot a_0$ and considering an interferometer operating on a dark fringe, we can express the photocurrent I as $I \equiv I_{(d)} + I_N$, that is as the sum of a deterministic part $I_{(d)} =< A_3 > [\delta\phi_{GW} + \alpha_3]$ depending on the GW signal and the aberrations, and a noise depending part

$$\begin{aligned} I_N &\approx A_1(-1 + \alpha_1) + A_2\alpha_2 + < A_3 > \delta\varphi_N + (A_3 - < A_3 >)\alpha_3 \\ &= I_{N_{(pn)}} + I_{N_{(sus)}} + I_{N_{(mir)}} + I_{N_{(pres)}} + I_{N_{(rp)}} + I_{N_{(ab)}} \end{aligned} \tag{12}$$

In particular, as regards to the radiation pressure noise $I_{N_{(rp)}}$, the mirrors M_1 and M_2 can be considered as multiple damped pendula driven by known time dependent pressure forces,

$$y_1(t), x_2(t) = \int_{-\infty}^{t} \left(b_{1,2}^{\dagger}(t') b_{1,2}(t') + \frac{1}{2} \right) \Gamma_M(t - t') dt' \tag{13}$$

with $\Gamma_M(t)$ the impulse response of the mirrors. Accordingly $\delta\phi_{(rp)}(t) = k(y_1(t) - x_2(t)) = \Gamma_M \star (b^{\dagger} \cdot \sigma_3 \cdot b)$, having indicated with $\Gamma_M\star$ the convolution integral (13). So That $I_{N_{(rp)}} = (-1)^{k+1}(\Gamma_M \star A_2) < A_3 >$.

4 Fourier analysis of the interferometer output

In most GW antennas the signal is extracted from the frequency spectrum of the photocurrent $I = I_{(d)} + I_N$. Therefore, the sensitivity of the interferometer depends on the autocorrelation of I,

$$<: I(\tau), I(0) :>=<: I_{(d)}, I_{(d)} :> + <: I_N, I_N :> \tag{14}$$

having considered $I_{(d)}$ and I_N as indipendent.

The limiting sensitivity of the antenna will be obtained by equating the Fourier component $S_{GW}(\omega)$ of $<: I_{(d)}, I_{(d)} :>$ at the frequency of the gravitational wave to the noise component, $S_{GW}(\omega) = S_N(\omega)/ < A_3 >^2$

The noise terms $I_{N_{(sus)}}, I_{N_{(mir)}}, I_{N_{(pres)}}$ are mutually independent, so that

$$\begin{aligned} S_{GW}(\omega) &= S_{(sus)}(\omega) + S_{(mir)}(\omega) + S_{(pres)} + S_{(rp)}(\omega) + \frac{\alpha_1^2 S_1(\omega) + \alpha_2^2 S_2(\omega) + \alpha_3^2 S_3(\omega)}{< A_3 >^2} \\ &+ \frac{S_1(\omega)}{< A_3 >^2} + |H_M(\omega)|^2 S_2(\omega) + \frac{S_{12}(\omega) + S_{21}(\omega)}{< A_3 >} \end{aligned} \tag{15}$$

where S_1, S_2, S_3 are the Fourier transforms of the convolutions $<: A_1, A_1 :>, <: A_2, A_2 :>, <: \delta A_3, \delta A_3 :>$, while S_{12} and S_{21} represent the Fourier transforms of the convolutions $<: A_1, \Gamma_M \star A_2 :>$ and $<: \Gamma_M \star A_2, A_2 :>$ respectively.

The beam $\hat{a}_2$, entering the port 2 of our interferometer, is generated by a degenerate parametric oscillator (OPO) excited by a pump beam $\hat{a}_p$, obtained by duplicating the laser beam $\hat{a}_1$, entering P_1. In the following we will treat $\hat{a}_1(t) = e^{i\phi(t)}\sqrt{n_l(t)}$ as a classical field (semiclassical analysis) whose instantaneous phase $\phi(t)$ and intensity fluctuations $\delta n_l(t) = n_l(t) - < n_l >_l$ will be assumed to be both Gaussian and mutually independent stationary processes, with autocorrelations $< (\phi(\tau) - \phi(0))^2 >= \sigma_\phi^2(|\tau|), < \delta n_l(\tau), \delta n_l(0) >= \sigma_l^2 C_l(|\tau|)$ with $\sigma_l^2 =< (\delta n_l)^2 >$.

The evolution of the the field operator $\hat{a}_2$ has been derived by Collett and Gardiner [13] for a classical coherent pump. We have integrated C.-G. equation of motion of $\hat{a}_2$ by representing the pump as $\hat{a}_p = \eta e^{2i\theta + 2i\phi} n_l$ and applying the WKB method.

The expectation values of the Eq.(14) have been obtained by averaging over the noise entering the OPO and the laser field amplitude and phase.

In particular, as a consequence of the classsical approximation for $\hat{a}_p$ we can write

$$A_1 = \hat{a}^{(1)\dagger}\hat{a}^{(2)} + \hat{a}^{(2)\dagger}\hat{a}^{(1)} \equiv a_l X_{\phi}^{(2)}, \; A_2 = a_l X_{\phi+\pi/2}^{(2)}, \; A_3 = n_l - n^{(2)} \tag{16}$$

with $n^{(2)} = a^{(2)\dagger}a^{(2)}$.

References

[1] *The Detection of Gravitational Waves*, edited by D.G. Blair (Cambridge University Press, Cambridge, England, 1991), and the references therein.

[2] C. M. Caves, Phys. Rev. D **23**, 1693 (1981); Phys. Rev. Lett., **45**, 75 (1980).

[3] C. W. Gardiner, *Handbook of Stochastic Methods* (Springer, Berlin, 1983).

[4] R. J. Glauber, Phys. Rev. Lett. **10**, 84 (1963); Phys. Rev. **131**, 2766 (1963).

[5] A. Luis and L. I. Sanchez-Soto, J. Mod. Opt. **38**, 971 (1991).

[6] R. Loudon, Phys. Rev. Lett., **47**, 815 (1981)

[7] D. Schoemaker, R. Schilling, L. Schnupp, W. Winkler, K. Maischberger and A. Rudiger, Phys. Rev. D **38**, 423 (1988)

[8] A. Rudiger, R. Schilling, L. Schnupp, W. Winkler, H. Billing and K. Maischberger, *Gravitation Wave Detection by Laser Interferometry,* MPQ Report-68 (1983)

[9] A. Brillet, Ann. Phys. Fr. **10**, 219 (1985)

[10] J. Gea-Banacloche and G. Leuchs, J. Opt. Soc. Am. **B4**, 1667 (1987); J. Mod. Opt. **34**, 793 (1987); J. Mod. Opt. **36**, 1277 (1989).

[11] W. G. Unruh, in "Quantum optics experimental gravitation and measurement theory", eds. P. Meystre and M.O. Scully, Plenum Press, N.Y. (1983) p. 647

[12] M. T. Jackel and S. Reynaud, Europhysics Lett. **13**, 301 (1991)

[13] M. J. Collett and C. W. Gardiner, Phys. Rev. A **30**, 1386 (1984).

[14] C. W. Gardiner and C. M. Savage, Opt. Commun. **50**, 173 (1984).

[15] S. Solimeno, F.Barone, C. de Lisio, L. Di Fiore, L. Milano, and G. Russo, Phys. Rev. **A 43**,6227 (1991).

[16] N.A. Ansari, L. Di Fiore, M.A. Man'ko, V.I. Man'ko, S. Solimeno and F. Zaccaria, Phys. Rev. A**49**, 2151 (1994).

[17] Nadeem A. Ansari, L. Di Fiore, M. Man'ko, V. Man'ko, R. Romano, S. Solimeno and F. Zaccaria, in *Technical Digests of EQEC '93*, (Firenze, 1993), Ed. P. De Natale, R. Meucci, and S. Pelli, Vol. 2, 688 (1993); 2nd Workshop on Harmonic Oscillator, Cocoyoc, Mexico, March (1994) (to be published as NASA reports)

[18] J.N. Hollenhorst, Phys. Rev. D **19**, 1669 (1979).

[19] V.V. Dodonov, I.A. Malkin, and V.I. Man'ko, Physica **72**, 597 (1974).

[20] B. Yurke and D. Stoler, Phys. Rev. Lett. **57**, 13 (1986).

[21] C. Fabre, E. Giacobino, A. Heidmann, L. Lugiato, S. Reynaud, M. Vadacchino and Wang Kaige, Quantum Optics **2**, 159 (1990);

[22] A. S. Lane, M. D. Reid, D. F. Walls, Phys. Rev. A **38**, 788 (1988).

[23] J. Mertz, T. Debuisschert, A. Heidmann, C. Fabre, and E. Giacobino, Opt. Lett. **16**, 1234 (1991).

[24] T. Debuisschert, A. Sizmann, E. Giacobino, and C. Fabre, J.O.S.A. **B10**, 1668 (1993).

NEXT
DOCUMENT

CONTINUOUS FEEDBACK AND MACROSCOPIC COHERENCE

Paolo Tombesi and David Vitali
Dipartimento di Matematica e Fisica
Università di Camerino, 62032 Camerino, Italy
and
Istituto Nazionale di Fisica della Materia, Unità di Camerino

Abstract

We show that a model, recently introduced for quantum nondemolition measurements of a quantum observable, can be adapted to obtain a measurement scheme which is able to slow down the destruction of macroscopic coherence due to the measurement apparatus.

1 Introduction

One of the most important limitations in the observation of quantum coherence at macroscopic level is the possibility of generating at least to macroscopic quantum states which show the quantum coherence. Since the seminal work of Yurke and Stoler [1] it becomes clear that a Kerr medium could be used to generate such states at optical level. They showed, indeed, that the unitary evolution of an initial coherent state, interacting with a Kerr medium with a well defined length, will produce a superposition of coherent states. For instance an initial states $|\alpha\rangle$ will generate the superposition

$$|\psi\rangle = \frac{1}{\sqrt{2}}(e^{-i\pi/4}|\alpha\rangle + e^{i\pi/4}|-\alpha\rangle) \tag{1}$$

after an interaction time $t_0 = \pi/(2\Omega)$ where Ω is the strenght of Kerr nonlinearity. At well defined shorter times three or more coherent states could also be generated [1]. This, of course, requires the precise knowledge of the length of the medium (or interaction time). It is also well known, and was shown in great details by Daniel and Milburn [2], that as soon as one takes into account the loss in the Kerr medium the generation of those states is suddenly inhibited. Thus, the best should be to have a Kerr medium with high nonlinearity to loss ratio. Recently [3], quadrature squeezed light was observed in semiconductors at frequencies less than half of band gap, where large ratios of nonlinearity to loss can be obtained [4]. Then, semiconductors could be the best media to generate the superposition of states because of the large ratio of the nonlinear phase shift to the optical losses which in the reported experiment [3] was extimated greater than 100. Furthermore, it has been recently shown [5] that a quasi-superposition of macroscopic states, with interference fringes still present, could be generated in a Kerr medium with the above ratio of 10,

when one uses a squeezed bath to model the loss. In this context it was also shown that a squeezed bath could be realized by a suitable feedback [6]. Moreover, it was also shown [7] that by using a time modulation of the Kerr nonlinearity one could obtain the coherent superposition without the precise knowledge of the length of the medium (or interaction time) by only adjusting the phase of the time modulation. However, even though we could assume that such a macroscopic superposition (or quasi-superposition) has been generated, one should have some experimental apparatus suitable to observe the interference pattern. Yurke and Stoler [1] pointed out that any unavoidable dissipation, introduced by the measurement process, will suddenly destroy the interference fringes which are the signature of the coherent superposition. Kennedy and Walls [8], following a suggestion of Mecozzi and Tombesi [9], showed that a phase-sensitive experimental apparatus, like the one modeled by a squeezed bath, might preserve the macroscopic coherence. In the present paper we will show that such an experimental device could be phisically realized by using an appropriate quantum nondemolition (QND) model, introduced by Alsing, Milburn and Walls [10], when one takes into account the detunings of the coupled modes with respect to the cavity characteristic frequencies.

Maryland 20771, U.S.A.

har@trmm.gsfc.nasa.gov.

2 The Model

We consider a cavity supporting two different modes, with annihilation operators a and b. The two modes are coupled by a nonlinear crystal, so that (in the interaction picture)

$$H_{int} = \hbar\chi X_\xi Y_\varphi \,, \tag{2}$$

where $X_\xi = \left(ae^{i\xi} + a^\dagger e^{-i\xi}\right)/2$ and $Y_\varphi = \left(be^{i\varphi} + b^\dagger e^{-i\varphi}\right)/2$. This interaction could be achieved by, for example, a crystal with a $\chi^{(2)}$ nonlinearity in which two processes driven by classical fields, amplification at the frequency $\omega_s = \omega_a + \omega_b$, and frequency conversion at the frequency $\omega_d = \omega_a - \omega_b$, have equal strengths [10]. Because of the QND condition, when the "meter" mode b is heavily damped at rate k_b, one can monitor the quadrature X_ξ of the signal mode a just by performing a homodyne measurement of a quadrature Y_δ of the mode b. In fact, when $k_b \gg k_a$ (damping rate of the a mode) the homodyne photocurrent $I(t)$ can be directly expressed in terms of the "instantaneous" mean value $\langle X_\xi(t)\rangle_c$, conditioned on the result of the measurement [11, 12], as

$$I(t) = \eta\chi\left[2\sin(\delta-\varphi)\,\langle X_\xi(t)\rangle_c + \sqrt{\frac{2k_b}{\eta\chi^2}}\xi(t)\right] \,, \tag{3}$$

where η is the efficiency of the homodyne detection and $\xi(t)$ is a Gaussian white noise with $\langle\xi(t)\xi(t')\rangle = \delta(t-t')$.

The QND-mediated feedback model of [6, 11] is obtained by taking part of the output homodyne photocurrent $I(t)$ and feeding it back to the cavity so to add a driving term $H_{fb}(t) = \hbar g I(t) X_\theta$ to the a mode Hamiltonian. The constant g represents the gain of the feedback process and $X_\theta = \left(ae^{i\theta} + a^\dagger e^{-i\theta}\right)/2$. If one adiabatically eliminates the meter mode b and applies the Markovian feedback theory recently developed by Wiseman and Milburn [13], the dynamics of the a

mode can be exactly determined, and in [11] we have shown that in the unstable regime the decoherence time of an optical Schrödinger cat can be appreciably increased, so to facilitate its detection.

In the present paper we reconsider this model and we eliminate the electro-optical feedback loop. We simply detune the two modes in the cavity, so that their uncoupled evolution is no more driven by the standard vacuum bath term alone, but by

$$\mathcal{L}_a\rho = k_a\left(2a\rho a^\dagger - a^\dagger a\rho - \rho a^\dagger a\right) - i\left[\delta_a a^\dagger a, \rho\right] \tag{4}$$

and an analogous expression holds for the b mode. The effect of the two nonzero detunings δ_a and δ_b can be intuitively described in terms of an "internal feedback" mechanism, because the detunings mix the two quadratures X_ξ and Y_φ with their respective $\pi/2$ out of phase quadrature, so that any variation of X_ξ is "fed back" to the X_ξ dynamics itself by the joint action of the detunings and the nonlinear coupling. Provided that the adiabatic condition $k_b \gg k_a$ is satisfied, the homodyne measurement of the quadrature Y_δ allows monitoring the a mode quadrature X_ξ also in the presence of nonzero detunings. In fact, when $\delta_b \neq 0$, Eq. (3) generalizes to

$$I(t) = \eta\chi\left\{\left[\frac{2k_b^2}{k_b^2+\delta_b^2}\sin(\delta-\varphi)\right.\right. \tag{5}$$
$$\left.\left. -\frac{2k_b\delta_b}{k_b^2+\delta_b^2}\cos(\delta-\varphi)\right]\langle X_\xi(t)\rangle_c + \sqrt{\frac{2k_b}{\eta\chi^2}}\xi(t)\right\},$$

so that from the homodyne photocurrent it is still possible to reconstruct the marginal probability distribution of the quadrature X_ξ, which is the quantity usually considered for revealing the interference fringes associated to an optical Schrödinger cat. We have therefore the model defined by the following master equation for the density matrix D of the two modes

$$\dot{D} = \mathcal{L}_a D + \mathcal{L}_b D - \frac{i}{\hbar}\left[H_{int}, D\right], \tag{6}$$

where the superoperator $\mathcal{L}_i$ $(i = a, b)$ is given by (4). We shall now see that all the interesting results obtained for the feedback model of [11] (the preservation of macroscopic quantum coherence in particular) can also be obtained with this simpler model.

Eq. (6) can be exactly solved, because the Wigner function of the two modes evolves according to the Fokker-Planck equation for a four-dimensional Ornstein-Uhlenbeck process [14]. Anyway, the analytical expressions in the general case are very cumbersome and therefore we shall explicitely discuss only the adiabatic limit $k_b \gg k_a$, where the meter mode b can be adiabatically eliminated, and which, as we have seen above, is the most interesting case for our purposes. After the adiabatic elimination of the b mode, one gets the following master equation for the a mode reduced density matrix ρ

$$\dot{\rho} = \mathcal{L}_a\rho - \frac{\Gamma}{2}\left[X_\xi, \left[X_\xi, \rho\right]\right] + iF\left[X_\xi, \left\{X_\xi, \rho\right\}\right], \tag{7}$$

where $\Gamma = \chi^2 k_b/2(k_b^2 + \delta_b^2)$, $F = \chi^2\delta_b/4(k_b^2 + \delta_b^2)$.

3 Macroscopic Coherence

We will now focus on the detection of optical Schrödinger cats rather than on their generation, and therefore we shall assume that at $t = 0$ a superposition of coherent states of the a mode has been already prepared, i.e., we consider an initial condition $\rho(0) = \sum_{\alpha,\beta} N_{\alpha,\beta}|\alpha\rangle\langle\beta|$. The exact time evolution from this initial state can be obtained with the same method of [11] and it is better expressed in terms of the normally ordered characteristic function $\chi(\lambda,\lambda^*;t) = \mathrm{Tr}\left\{\rho(t)\exp(\lambda a^\dagger)\exp(-\lambda^* a)\right\}$

$$\chi(\lambda,\lambda^*;t) = \sum_{\alpha,\beta} N_{\alpha,\beta}\langle\beta|\alpha\rangle \exp\left\{B^*(t)\lambda - A(t)\lambda^* - \nu(t)|\lambda|^2 + \frac{\mu(t)}{2}\lambda^{*2} + \frac{\mu(t)^*}{2}\lambda^2\right\}, \tag{8}$$

where

$$\begin{aligned} A(t) &= \left[\frac{\alpha}{2}\frac{2\Delta - iF + 2i\delta_a}{2\Delta} - \beta^*\frac{iFe^{-2i\xi}}{4\Delta}\right]e^{-(k_a+\Delta)t} \\ &+ \left[\frac{\alpha}{2}\frac{2\Delta + iF - 2i\delta_a}{2\Delta} + \beta^*\frac{iFe^{-2i\xi}}{4\Delta}\right]e^{-(k_a-\Delta)t} \end{aligned} \tag{9}$$

$$\begin{aligned} B^*(t) &= \left[\frac{\beta^*}{2}\frac{2\Delta + iF - 2i\delta_a}{2\Delta} + \alpha\frac{iFe^{2i\xi}}{4\Delta}\right]e^{-(k_a+\Delta)t} \\ &+ \left[\frac{\beta^*}{2}\frac{2\Delta - iF + 2i\delta_a}{2\Delta} - \alpha\frac{iFe^{2i\xi}}{4\Delta}\right]e^{-(k_a-\Delta)t} \end{aligned} \tag{10}$$

$$\begin{aligned} \nu(t) = &\frac{F}{16}\left(\frac{\Gamma\delta_a}{\Delta^2} - \frac{2F}{\Delta}\right)\left(\frac{1 - e^{-2(k_a+\Delta)t}}{2(k_a+\Delta)}\right) \\ &-\frac{\Gamma\delta_a(2\delta_a - F)}{8\Delta^2}\left(\frac{1 - e^{-2k_a t}}{2k_a}\right) \\ &+\frac{F}{16}\left(\frac{\Gamma\delta_a}{\Delta^2} + \frac{2F}{\Delta}\right)\left(\frac{1 - e^{-2(k_a-\Delta)t}}{2(k_a-\Delta)}\right) \end{aligned} \tag{11}$$

$$\begin{aligned} \mu(t) = &\frac{F^2 e^{-2i\xi}}{16(2\delta_a - F + 2i\Delta)}\left(\frac{\Gamma\delta_a}{\Delta^2} - \frac{2F}{\Delta}\right)\frac{1 - e^{-2(k_a+\Delta)t}}{2(k_a+\Delta)} \\ &-\frac{F\Gamma e^{-2i\xi}\delta_a}{8\Delta^2}\frac{1 - e^{-2k_a t}}{2k_a} \\ &+\frac{F^2 e^{-2i\xi}}{16(2\delta_a - F - 2i\Delta)}\left(\frac{\Gamma\delta_a}{\Delta^2} + \frac{2F}{\Delta}\right)\frac{1 - e^{-2(k_a-\Delta)t}}{2(k_a-\Delta)} \end{aligned} \tag{12}$$

$$\Delta = \sqrt{\delta_a F - \delta_a^2}\,. \tag{13}$$

We see that the system is stable and reaches a steady state if and only if

$$\Delta < k_a \quad \text{i.e.} \quad \chi^2 \delta_a \delta_b < 4\left(k_b^2 + \delta_b^2\right)\left(k_a^2 + \delta_a^2\right) . \tag{14}$$

In the stable case, the stationary state is described by a Gaussian density operator of the form

$$\rho_{st} = Z^{-1} \exp\left\{-n a^\dagger a - \frac{m}{2} a^{\dagger 2} - \frac{m^*}{2} a^2\right\} , \tag{15}$$

where Z is a normalization constant and the equilibrium parameters m and n can be written as

$$n = \frac{\nu_\infty + 1/2}{\sqrt{(\nu_\infty + 1/2)^2 - |\mu_\infty|^2}} \times \log\left\{\frac{\left[\sqrt{(\nu_\infty + 1/2)^2 - |\mu_\infty|^2} + 1/2\right]^2}{\nu_\infty(\nu_\infty + 1) - |\mu_\infty|^2}\right\} \tag{16}$$

$$m = \frac{\mu_\infty}{\nu_\infty + 1/2} n , \tag{17}$$

where the asymptotic values ν_∞ and μ_∞ are easily obtained from (11) and (12). An interesting aspect of this stationary state is that it can show arbitrary quadrature squeezing. For example, the stationary variance of the quadrature X_ξ is given by

$$\left\langle X_\xi^2 \right\rangle = \frac{1}{2}\left[\frac{1}{2} + \frac{\delta_a(\Gamma\delta_a + 2Fk_a)}{8k_a(k_a^2 - \Delta^2)}\right] \tag{18}$$

and one has squeezing when $\delta_a\delta_b < 0$ and $k_b/k_a < |\delta_b/\delta_a|$. It is easily seen that when $\delta_a = 0$ no squeezing is possible, while for $\delta_a \neq 0$ but $\delta_b = 0$ extra noise is added to the system. The possibility to obtain squeezing with this model is thus only due to the existence of detunings, which give a sort of implicit feedback.

4 Interference Fringes

Let us now focus on the detection of the interference fringes associated to a linear superposition of coherent states. These fringes can generally be seen from the marginal probability distribution of the quadrature X_ξ, $P(x_\xi) = \langle x_\xi|\rho(t)|x_\xi\rangle$, where $|x_\xi\rangle$ is the eigenstate of X_ξ with eigenvalue x_ξ. As we have seen above, this probability distribution can be reconstructed from the homodyne measurement of the meter mode b and its general expression can be easily obtained from the characteristic function (8) [8, 11]

$$P(x_\xi, t) = \sum_{\alpha,\beta} N_{\alpha,\beta} \frac{\langle\beta|\alpha\rangle}{\sqrt{\pi\sigma_x^2(t)}} \exp\left\{-\frac{(x_\xi - \delta_{\alpha,\beta}(t))^2}{\sigma_x^2(t)}\right\} , \tag{19}$$

where

$$\sigma_x^2(t) = \frac{1}{2} + \nu(t) + \mathrm{Re}\left\{\mu(t)e^{2i\xi}\right\}, \tag{20}$$

$$\delta_{\alpha,\beta}(t) = \frac{A(t)e^{i\xi} + B^*(t)e^{-i\xi}}{2}. \tag{21}$$

As a special case we consider the initial superposition trated by Yurke and Stoler [1], produced by the unitary evolution of a coherent state in a Kerr medium

$$\rho(0) = \frac{1}{2}\left(e^{-i\pi/4}|\alpha\rangle + e^{i\pi/4}|-\alpha\rangle\right)\left(e^{i\pi/4}\langle\alpha| + e^{-i\pi/4}\langle-\alpha|\right). \tag{22}$$

With this choice (19) simplifies to

$$P(x_\xi,t) = \frac{1}{2}\left\{p_+^2(x_\xi,t) + p_-^2(x_\xi,t) + 2p_+(x_\xi,t)p_-(x_\xi,t)\sin\left[\Omega(x_\xi,t)\right]|\langle\alpha|-\alpha\rangle|^{\eta(t)}\right\}. \tag{23}$$

The first two terms $p_\pm^2(x_\xi,t)$ describe the two Gaussian peaks corresponding to the two coherent states $|\pm\alpha\rangle$ of the initial superposition and they are explicitely given by

$$p_\pm^2(x_\xi,t) = \frac{1}{\sqrt{\pi\sigma_x^2(t)}}\exp\left\{-\frac{(x_\xi \mp \delta_{++}(t))^2}{\sigma_x^2(t)}\right\}, \tag{24}$$

where

$$\delta_{++}(t) = \mathrm{Re}\left\{\alpha e^{i\xi}r(t)\right\} \tag{25}$$

$$r(t) = e^{-k_a t}\left(\cosh\Delta t - i\frac{\delta_a}{\Delta}\sinh\Delta t\right). \tag{26}$$

The third term in (23) describes the quantum interference between the two coherent states, where the function

$$\Omega(x_\xi,t) = \frac{2x_\xi}{\sigma_x^2(t)}\mathrm{Im}\left\{\alpha e^{i\xi}r(t)\right\} \tag{27}$$

gives the probability oscillations associated with the interference fringes and the factor $|\langle\alpha| - \alpha\rangle|^{\eta(t)} = \exp\{-2|\alpha|^2\eta(t)\}$ describes the suppression of quantum coherence due to dissipation. It is clear that this suppression is practically immediate for macroscopically distinguishable states (i.e., large $|\alpha|$), unless $\eta(t) \simeq 0$. It is therefore important to analyze the behavior of this decoherence function $\eta(t)$, which is equal to

$$\eta(t) = 1 - \frac{|r(t)|^2}{2\sigma_x^2(t)}. \tag{28}$$

To be more specific, if we want to determine the conditions under which the detection of macroscopic quantum coherence is facilitated, we have to compare $\eta(t)$ with the corresponding decoherence function of a standard vacuum bath, which is given by [8]

$$\eta_{vac}(t) = 1 - e^{-2k_a t}. \tag{29}$$

This function shows that in the standard case, after a time $t \simeq 1/(2k_a)$, it is $\eta_{vac}(t) \simeq 1$ and therefore the quantum interference is quickly washed out. On the contrary, in the present model it is possible that $\eta(t)$ assumes much smaller values, so to significantly slow down the destruction of the interference pattern.

5 Conclusions

Differently from a very large part of the literature on optical Schrödinger cats, we have focused on their detection rather than their generation because, as realized since the paper by Yurke and Stoler [1], to detect a linear superposition of macroscopically distinguishable states is more difficult than to create it. To the best of our knowledge, only the paper by Brune *et al.* [15] affords a detailed discussion of both aspects. our opinion, Brune *large number of atoms reconstruction of the probability distribution revealing the contrary shows how to prepare a fully optical detection scheme based on a very simple model. offer a promising way to both measurements and detect a linear superposition of coherent states.*

Acknowledgments

This work has been partially supported by the Istituto Nazionale di Fisica Nucleare. Discussions with Philippe Grangier are greatly acknowledged.

References

[1] B. Yurke and D. Stoler, Phys. Rev. Lett. **57**, *13 (1986);*

[2] D. J. Daniel and G. J. Milburn, Phys. Rev. A **39**, *4628 (1989).*

[3] A.M. Fox, J.J. Baumberg, M. Dabbicco, B. Huttner, and J.F. Ryan, Phys. Rev. Lett. **74**, *1728(1995);*

[4] S.T. Ho, C.E. Soccolich, M.N. Islam, W.S. Hobson, A.F.J. Levi, and R.E. Slusher, Appl. Phys. Lett. **59**, *2558(1991)*

[5] G.M. D'Ariano, M. Fortunato, and P. Tombesi, Quantum Semicl. Opt. (to appear)

[6] P. Tombesi and D. Vitali, Phys. Rev. A **50**, *4253 (1994).*

[7] S. Mancini, and P. Tombesi, Phys. Rev. A (to appear)

[8] T.A.B. Kennedy and D.F. Walls, Phys. Rev. A **37**, *152 (1988).*

[9] A. Mecozzi and P. Tombesi, Phys. Lett. A **121**, *101 (1987); J. Opt. Soc. Am. B* **4**,*1700 (1987).*

[10] P. Alsing, G.J. Milburn, and D.F. Walls, Phys. Rev. A **37**, *2970 (1988).*

[11] P. Tombesi and D. Vitali, Appl. Phys. B **60**, *S69 (1995); Phys. Rev. A* **51**, *4913 (1995).*

[12] H.M. Wiseman, and G.J. Milburn, Phys. Rev. A **47**, *642 (1993).*

[13] H.M. Wiseman, and G.J. Milburn, Phys. Rev. Lett. **70**, *548 (1993); Phys. Rev A* **49**,*1350 (1994); Phys. Rev. A* **49**, *4110 (1994); H.M. Wiseman, Phys. Rev. A* **49**, *2133 (1994).*

[14] H. Risken, The Fokker Planck Equation 2nd ed. (Springer, Berlin 1989).

[15] M. Brune, S. Haroche, J.M. Raimond, L. Davidovich and N. Zagury, Phys. Rev. A **45**, *5193 (1992);*

NEXT
DOCUMENT

CLASSICAL-QUANTUM CORRESPONDENCE BY MEANS OF PROBABILITY DENSITIES

Gabino Torres Vega and J.D. Morales-Guzmán
Departamento de Física, Centro de Investigación y de Estudios Avanzados del IPN
Apdo. Postal 14-740, 07000 México, D.F.

Abstract

Within the frame of the recently introduced phase space representation of non relativistic Quantum Mechanics, we propose a Lagrangian from which the phase space Schrödinger equation can be derived. From that Lagrangian, the associated conservation equations, according to Noether's theorem, are obtained. This shows that one can analyze quantum systems completely in phase space as it is done in coordinate space, without additional complications.

In this paper, we make use of a recently introduced phase space representation of non relativistic Quantum Mechanics[1] which complies with the requirements for a quantum representation. This allows the researcher to investigate quantum dynamics in the same dynamical space in which classical dynamics is commonly studied. Some advantages of this approach is a better comparison between quantum and classical dynamics, a better understanding of quantum effects and the possibility of analizing quantum systems completely in phase space in the same way as it is done in coordinate space, without the complications found in other approaches.[2, 3]

In this approach to non relativistic Quantum Mechanics in phase space, the operators associated to the momentum and coordinate operators are $\hat{F} \leftrightarrow p/2 - i\hbar\partial/\partial q$ and $\hat{Q} \leftrightarrow q/2 + i\hbar\partial/\partial p$, respectively. As expected, these operators do not commute with each other, in fact, $[\hat{Q}, \hat{P}] = i\hbar$. Then, the phase space Schrödinger equation is given by

$$i\hbar\frac{\partial}{\partial t}\langle\Gamma \mid \psi_t\rangle = \left[\frac{1}{2m}\left(\frac{p}{2} - i\hbar\frac{\partial}{\partial q}\right)^2 + V\left(\frac{q}{2} + i\hbar\frac{\partial}{\partial p}\right)\right]\langle\Gamma \mid \psi_t\rangle \qquad (1)$$

where $\Gamma = (p, q)$ denotes a point in phase space and $\langle\Gamma \mid \psi_t\rangle$ denotes the phase space wave function. This is the equation which governs the dynamics of the phase space wave packet and should be solved in order to find eigenfunctions, eigenenergies, etc.

Worth mentioning is the set of phase space eigenfunctions found for the harmonic oscillator, (from here after, we use dimensionless units)

$$\psi_n(\Gamma;\alpha) = \left(\frac{\sqrt{1/4-\alpha^2}}{2^n\pi n!}\right)\exp\left[-\left(\frac{1}{2}+\alpha\right)\frac{q^2}{2} - \left(\frac{1}{2}-\alpha\right)\frac{p^2}{2} - i\alpha pq\right]H_n(\Gamma;\alpha) \quad , \qquad (2)$$

functions which involve the phase space version $H_n(\Gamma;\alpha)$ of Hermite polynomials, with recursion relationship $H_{n+1}(\Gamma;\alpha) = 2u(\Gamma;\alpha)H_n(\Gamma;\alpha) - 4n\alpha H_{n-1}(\Gamma;\alpha)$, where $u(\Gamma;\alpha) = (1/2+\alpha)q - i(1/2-$

$\alpha)p$, and $-1/2 \leq \alpha \leq 1/2$. These polynomials have similar properties as the usual one-variable Hermite polynomials but now in phase space This is in contrast with other sets introduced in previous works.[4]

The wave function in coordinate space $\psi(q)$ can be recovered from the wave function in phase space $\psi(\Gamma;\alpha)$ by means of the projection $\psi(q) = \int_{-\infty}^{+\infty} \exp(ipq/2)\psi(\Gamma;\alpha)dp$, and the wave function in momentum space $\psi(p)$ can be obtained from the wave function in phase space by means of the projection $\psi(p) = \int_{-\infty}^{+\infty} \exp(-ipq/2)\psi(\Gamma;\alpha)dq$

The diagonal matrix element of the quantum probability conservation equation is

$$\frac{\partial}{\partial t}\langle \Gamma \mid \hat{\rho} \mid \Gamma \rangle = -\frac{\partial}{\partial q}\frac{1}{2}\left[\langle \Gamma \mid \hat{P}\hat{\rho} \mid \Gamma \rangle + \langle \Gamma \mid \hat{\rho}\hat{P} \mid \Gamma \rangle\right] + \frac{\partial}{\partial p}\sum_{n=1}^{\infty} V_n \sum_{l=0}^{n-1} \langle \Gamma \mid \hat{Q}^l \hat{\rho} \hat{Q}^{n-l-1} \mid \Gamma \rangle \quad , \tag{3}$$

where $\hat{\rho}$ denotes the density operator, and where we have assumed that the potential function can be written as a power series in its argument, $V(q) = \sum_{n=0}^{\infty} V_n q^n$. Note that Eq. (3) is a combination of the corresponding equations in coordinate

$$\frac{\partial}{\partial t}\langle q \mid \hat{\rho} \mid q \rangle = -\frac{\partial}{\partial q}\frac{1}{2}\left[\langle q \mid \hat{P}\hat{\rho} \mid q \rangle + \langle q \mid \hat{\rho}\hat{P} \mid q \rangle\right] \quad , \tag{4}$$

and momentum

$$\frac{\partial}{\partial t}\langle p \mid \hat{\rho} \mid p \rangle = \frac{\partial}{\partial p}\sum_{n=1}^{\infty} V_n \sum_{l=0}^{n-1} \langle p \mid \hat{Q}^l \hat{\rho} \hat{Q}^{n-l-1} \mid p \rangle \quad , \tag{5}$$

spaces, providing an alternative description of quantum dynamics.

For a density operator of the form $\hat{\rho} = \sum_{\psi,\chi} P(\psi,\chi) \mid \psi \rangle\langle \chi \mid$, we introduce the Lagrangian

$$L = \sum_{\psi,\chi} P(\psi,\chi)\frac{1}{2}\left\{\chi^* \hat{E}\psi + \psi(\hat{E}\chi)^* - \chi^* \hat{V}(\hat{Q})\psi - \psi[\hat{V}(\hat{Q})\chi]^* - \frac{1}{2}\chi^* \hat{P}^2\psi - \frac{1}{2}\psi\left[\hat{P}^2\chi\right]^*\right\} \quad , \tag{6}$$

where ψ and χ are wave functions in phase space. By means of the methods used for continuous systems,[5] this Lagrangian leads to the Euler-Lagrange equations

$$\frac{\hat{c}L}{\partial\psi} + \hat{E}^* \frac{\partial L}{\partial \hat{E}\psi} + \hat{P}^2 \frac{\partial L}{\partial \hat{P}^2\psi} + \hat{V}^*(\hat{Q})\frac{\partial L}{\partial \hat{V}(\hat{Q})\psi} = 0 \quad , \tag{7}$$

and

$$\frac{\partial L}{\partial \chi^*} + \hat{E}^* \frac{\partial L}{\partial (\hat{E}\chi)^*} + \hat{P}^2 \frac{\partial L}{\partial (\hat{P}^2\chi)^*} + \hat{V}^*(\hat{Q})\frac{\partial L}{\partial [\hat{V}(\hat{Q})\chi]^*} = 0 \quad , \tag{8}$$

equations from which the Schrödinger equation and its complex conjugate in phase space are obtained.

In order to obtain the conservation equations derived from this Lagrangian, we make use of Noether's theorem,[5] which leads to

$$\begin{aligned} -\frac{\partial L}{\partial x} &= \sum_{\psi,\chi} P(\psi,\chi)\left\{\frac{\partial}{\partial t}\left(\frac{i}{2}\chi^*\frac{\partial\psi}{\partial x} - \frac{i}{2}\psi\frac{\partial\chi^*}{\partial x}\right)\right. \\ &+ \frac{1}{4}\left[\frac{\partial\psi}{\partial x}(\hat{P}^2\chi)^* - \chi^*\frac{\partial\hat{P}^2\psi}{\partial x} + \frac{\partial\chi^*}{\partial x}\hat{P}^2\psi - \psi\frac{\partial(\hat{P}^2\chi)^*}{\partial x}\right] \\ &+ \left.\frac{1}{2}\left[\frac{\partial\psi}{\partial x}(\hat{V}\chi)^* - \chi^*\frac{\partial\hat{V}\psi}{\partial x} + \frac{\partial\chi^*}{\partial x}\hat{V}\psi - \psi\frac{\partial(\hat{V}\chi)^*}{\partial x}\right]\right\} - \frac{dL}{dx} \quad , \end{aligned} \tag{9}$$

where x is any of the variables t, q or p.

Now, Eq. (9), for $x = t$, leads to

$$\frac{\partial}{\partial t}\Re\langle\Gamma \mid \hat{H}\hat{\rho} \mid \Gamma\rangle + \frac{\partial}{\partial q}\frac{1}{2}\Re\langle\Gamma \mid \hat{P}(\hat{H}\hat{\rho} + \hat{\rho}\hat{H}) \mid \Gamma\rangle$$
$$-\frac{\partial}{\partial p}\sum_{n=1}^{\infty} V_n \sum_{l=0}^{n-1} \Re\langle\Gamma \mid \hat{Q}^l \hat{H}\hat{\rho}\hat{Q}^{n-l-1} \mid \Gamma\rangle = \Re\langle\Gamma \mid \frac{\partial \hat{V}(t)}{\partial t}\hat{\rho} \mid \Gamma\rangle \quad . \tag{10}$$

For $x = q$, Eq. (9) leads to

$$\frac{\partial}{\partial t}\Re\langle\Gamma \mid (\hat{P} - \hat{P}^*)\hat{\rho} \mid \Gamma\rangle + \frac{\partial}{\partial q}\frac{1}{2}\Re\langle\Gamma \mid \hat{P}\left[(\hat{P} - \hat{P}^*)\hat{\rho} + \hat{\rho}(\hat{P} - \hat{P}^*)\right] \mid \Gamma\rangle$$
$$-\frac{\partial}{\partial p}\sum_{n=1}^{\infty} V_n \sum_{l=0}^{n-1} \Re\langle\Gamma \mid \hat{Q}^l(\hat{P} - \hat{P}^*)\hat{\rho}\hat{Q}^{n-l-1} \mid \Gamma\rangle = 2\Re\langle\Gamma \mid \hat{F}(\hat{Q})\hat{\rho} \mid \Gamma\rangle \quad , \tag{11}$$

and, for $x = p$, Eq. (9) leads to

$$\frac{\partial}{\partial t}\Re\langle\Gamma \mid (\hat{Q} - \hat{Q}^*)\hat{\rho} \mid \Gamma\rangle + \frac{\partial}{\partial q}\frac{1}{2}\Re\langle\Gamma \mid \hat{P}\left[(\hat{Q} - \hat{Q}^*)\hat{\rho} + \hat{\rho}(\hat{Q} - \hat{Q}^*)\right] \mid \Gamma\rangle$$
$$-\frac{\partial}{\partial p}\sum_{n=1}^{\infty} V_n \sum_{l=0}^{n-1} \Re\langle\Gamma \mid \hat{Q}^l(\hat{Q} - \hat{Q}^*)\hat{\rho}\hat{Q}^{n-l-1} \mid \Gamma\rangle = 2\Re\langle\Gamma \mid \hat{P}\hat{\rho} \mid \Gamma\rangle \quad . \tag{12}$$

It has been pointed out[1] that the classical analog to the quantum density $\langle\Gamma \mid \hat{\rho} \mid \Gamma\rangle$ is the classical density $\rho(\Gamma; t)$, so, we can ask for the classical analogs to the quantum conservation equations derived previously. These classical analogs are obtained by taking the time derivative of the densities of interest and combining the resulting equation with Hamilton's $\dot{p} = -\partial H/\partial q$, $\dot{q} = \partial H/\partial p$, and Liouville's $\partial\rho/\partial t = -p\partial\rho/\partial q - F(q)\partial\rho/\partial p$, equations. The classical energy conservation equation so obatained is

$$\frac{\partial}{\partial t}H\rho(\Gamma; t) + \frac{\partial}{\partial q}pH\rho(\Gamma; t) + \frac{\partial}{\partial p}F(q)H\rho(\Gamma; t) = \frac{\partial V(q; t)}{\partial t}\rho(\Gamma; t) \quad . \tag{13}$$

Note the close resemblance that the above equation has with Eq. (10), the difference being the symmetrization of the classical products $H\rho(\Gamma; t)$, $pH\rho(\Gamma; t)$, $F(q)H\rho(\Gamma; t)$, with $F(q) = -\sum_{n=1}^{\infty} nV_n q^{n-1}$, and $[\partial V(q, t)/\partial t]\rho(\Gamma; t)$

The conservation equation for the momentum density $p\rho(\Gamma; t)$ is

$$\frac{\partial}{\partial t}p\rho(\Gamma; t) + \frac{\partial}{\partial q}p^2\rho(\Gamma; t) + \frac{\partial}{\partial p}F(q)p\rho(\Gamma; t) = 2F(q)\rho(\Gamma; t) \quad , \tag{14}$$

which is the classical analog to Eq. (11). Note that the quantum density corresponding to $p\rho(\Gamma; t)$ is $\Re\langle\Gamma \mid (\hat{P} - \hat{P}^*)\hat{\rho} \mid \Gamma\rangle$, the quantum density corresponding to $p^2\rho(\Gamma; t)$ is $\Re\langle\Gamma \mid \hat{P}\left[(\hat{P} - \hat{P}^*)\hat{\rho} + \hat{\rho}(\hat{P} - \hat{P}^*)\right] \mid \Gamma\rangle/2$ and $\sum_{n=1}^{\infty} V_n \sum_{l=0}^{n-1} \Re\langle\Gamma \mid \hat{Q}^l(\hat{P} - \hat{P}^*)\hat{\rho}\hat{Q}^{n-l-1} \mid \Gamma\rangle$ is the quantum analog corresponding to $F(q)p\rho(\Gamma; t)$. It would be very difficult to gess the correct quantum densities without the help of a Lagrangian and Noether's theorem.

The conservation equation for $q\rho(\Gamma;t)$ is given by

$$\frac{\partial}{\partial t}q\rho(\Gamma;t)+\frac{\partial}{\partial q}pq\,\rho(\Gamma;t)+\frac{\partial}{\partial p}F(q)q\rho(\Gamma;t)=2p\rho(\Gamma;t)\quad , \tag{15}$$

which is the classical analog to Eq. (12). Note that the quantum density corresponding to $q\rho(\Gamma;t)$ is $\Re\langle\Gamma\mid(\hat{Q}-\hat{Q}^{*})\hat{\rho}\mid\Gamma\rangle$, the quantum density corresponding to $pq\rho(\Gamma;t)$ is $\Re\langle\Gamma\mid\hat{P}\left[(\hat{Q}-\hat{Q}^{*})\hat{\rho}+\hat{\rho}(\hat{Q}-\hat{Q}^{*})\right]\mid\Gamma\rangle/2$ and $\sum_{n=1}^{\infty}V_n\sum_{l=0}^{n-1}\Re\langle\Gamma\mid\hat{Q}^{l}(\hat{Q}-\hat{Q}^{*})\hat{\rho}\hat{Q}^{n-l-1}\mid\Gamma\rangle$ is the quantum analog corresponding to $F(q)q\rho(\Gamma;t)$. It would be very difficult to gess the correct quantum densities without the help of a Lagrangian and Noether's theorem.

With these results, we can see that one can analyze quantum systems completely in phase space and in the same way as it is done in coordinate space, without the need of further complications, increasing our confidence in this representation.

of article) on by sending an on your Subject line. that be its be draftperson. The package to equation numbers. with the equation commands

We acknowledge financial support from CONACyT and SNI, México.

References

[1] Go. Torres-Vega and J.H. Frederick, *J. Chem. Phys.* **93**, 8862 (1990); *Phys Rev Lett.* **67**, 2601 (1991); *J. Chem. Phys.* **98**, 3103 (1993); Go. Torres-Vega, *J. Chem. Phys.* **98**, 7040 (1993); Go. Torres-Vega, *J. Chem. Phys.* **99**, 1824 (1993); Go. Torres-Vega and J.D. Morales-Guzmán, *J. Chem. Phys.* **99**, 1824 (1993). Go. Torres-Vega, *Proceedings of the Third International Workshop on Squeezed States and Uncertainty Relations,* NASA conference publication 3270. D. Han, Y.S. Kim, N.H. Rubin, Y. Shih, W.W. Zachary, Editors. p. 275.

[2] E. Wigner, *Phys. Rev.* **40**. 749 (1932); M. Hillery, R.F. O'Connell, M.O. Scully and E. P. Wigner, *Phys. Rep.* **106**, 121 (1984), and references therein; Wlodarz-JJ, *J. Chem. Phys.* **100**, 7476 (1994).

[3] K. Husimi, *Proc. Phys. Math. Soc. Jpn.* **22**, 264 (1940); *Coherent States*, edited by J.R. Klauder and B.S. Skagerstum (World Scientific, Singapore, 1985).

[4] Dattoli, G., Torres, A. Lorenzutta, S., Maino, G., Chiccoli, C., *Proceedings of the Third International Workshop on Squeezed States and Uncertainty Relations,* NASA conference publication 3270. D. Han, Y.S. Kim, N.H. Rubin, Y. Shih, W.W. Zachary, Editors, p. 257.

[5] H. Goldstein, *Classical Mechanics* (Addison- Wesley, Reading, MA, 1980).

NEXT
DOCUMENT

ON A NEW DETECTION SCHEME FOR M-ARY ORTHOGONAL COHERENT STATE SIGNAL

Kouichi Yamazaki
Dept. of Information & Communication Eng., Tamagawa University
6-1-1, Tamagawagakuen, Machida, Tokyo, 194, Japan

Abstract

We propose a new receiver for M-ary orthogonal coherent-state signal. It is shown that the proposed receiver performs better than a photon counting receiver as to signal detection error probability criterion. It is also shown that the error probability of the proposed receiver is almost minimum for the signal.

1 Introduction

Recent development of technology of the optical communication system brought the error probability of the system almost to the standard quantum limit "SQL", which is the classical error performance limit of an optical communication system. It is well known, however, that ultimate error performance limit of optical communication system is far below the SQL[1,2]. In order to overcome the SQL, quantum phenomena of optical signal, which is one of the most remarkable difference from a communication system using radio frequency carrier, have to be utilized in the detection process. There have been several proposals of detection schemes overcoming the SQL for several signaling schemes[3-12].

Optical M-ary orthogonal signal, especially optical M-ary pulse position modulation (PPM), has a great potential for a very low-energy communication in deep-space data transmission. So far, many authors reported the system performance[14,15]. In these investigations, a photon counting receiver has been employed as a detection scheme. Because, its construction is very simple, and it brings good channel property. The error probability of the receiver for the signal in a coherent-state, however, is much larger than the minimum error probability, which is predicted by the quantum detection theory[13,16]. As far as the author knows, there is no proposal for receiver superior to the photon counting receiver for this signal.

The main purpose of this paper is to propose a new detection scheme for an optical M-ary orthogonal coherent-state signal, which is superior to a photon counting receiver. By comparing its error probability with the minimum error probability, it is shown that it performs quasi-optimally.

2 Proposal of a New Receiver

Pulse position modulation (PPM) signaling is one of the typical orthogonal signals. In a PPM signaling, a symbol of time duration T consists of M time slots of duration $T_s(= T/M)$. Each

symbol has only one pulse, and then information is transmitted by the position of the pulse. If PPM signaling is employed for the optical communication system, a laser is pulsed at the transmitter during the slot having the pulse. Therefore, the pulsed slot is in a coherent state, and the other $m-1$ slots are in vacuum states. Then, a symbol S_i (for i=1, 2, ..., M) is expressed by

$$S_i : |\psi_i> = \prod_{j=1}^{M} |\mu_{ij}>_j \qquad \mu_{ij} = \begin{cases} N_s^{1/2} & j = i \\ 0 & j \neq i \end{cases} \tag{1}$$

where N_s is an average photon number contained in one optical pulse. At the receiver side, a receiver has to decide the position of the pulsed slot among M slots in the symbol. For this purpose, a photon counting receiver has been employed as a detection scheme. In this case, the pulse position is determined by finding the slot with the maximum photocount among them. If the system is under the quantum noise limit, where no external noise exists, photon number fluctuation of an optical pulse may cause a symbol detection error. Because of the Poissonian statistics of photon number of coherent state, photons are never counted during unpulsed slots. However, no photon may be counted during the pulsed slots. This occurs with the probability of e^{-N_s}. In this case, the detector can not determine the pulsed slot. If one of M symbols is selected randomly, an symbol detection error happens with the probability of

$$Pe^{counting} = \frac{(M-1)}{M} e^{-N_s}. \tag{2}$$

On the other hand, the minimum error probability of the M-ary orthogonal coherent-state signal is given by[13,16]

$$\begin{aligned} Pe^{min} &= \frac{M-1}{M^2}\left\{[1+(M-1)e^{-N_s}]^{1/2} - (1-e^{-N_s})^{1/2}\right\}^2 \\ &\approx \frac{M-1}{4}\exp[-2N_s] \qquad \text{for } N_s \gg 1. \end{aligned} \tag{3}$$

By comparing this with the error probability of the photon counting receiver, it is found that the exponent of the former is twice as large as the latter. What causes this difference? As shown in the deviation of Eq.(2), there remained no information about which of M signal has been sent when a photocount of the pulsed slot is zero. That is, the photon counting receiver does not examine whether the incoming signal is $|\psi_i>$ or $|\psi_j>$ $(j \neq i)$, but does whether $|\psi_i>$ or $\prod_{j=1}^{M}|0>_j$. In order to examine whether the incoming signal is $|\psi_i>$ or $|\psi_j>$ $(j \neq i)$, and to make its error probability to approach to the minimum error probability, the information that all the $M-1$ unpulsed slots are in vacuum sates as well as that the pulsed slot is in a coherent state should be used for symbol detection.

For this purpose, we propose a new detection scheme. The block diagram of the proposed receiver is shown in FIG.1. The receiver consists of a local laser, a highly transmissive beam splitter, a photon counter, an optical shutter and its feedback control system. Frequency of the local laser is identical to that of signal field, and its phase is shifted by π [rad.] with respect to the signal of pulsed slot. The intensity of the local field is prepared so that its part reflected by the beam splitter is the same as the transmitted part of the signal. Assuming that the transmission coefficient of the beam splitter is nearly equal to unit, the combination process can be considered as displacement process of coherent component. Let α ($|\alpha|^2 = N_s$) be complex amplitude of the pulsed slot, then the conditional quantum state of the combined field is given in Table I.

TABLE.I Conditional quantum state of combined field.

State of shutter	open	close
Pulsed slot	$\|0>$	$\|\alpha>$
Unpulsed slot	$\|-\alpha>$	$\|0>$

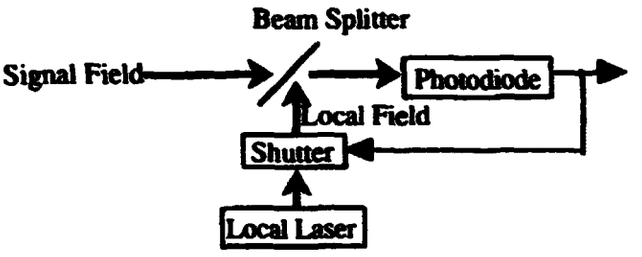

FIG. 1. Block diagram of proposed detection scheme.

Using this construction, the receiver operates in the following way.

1. At the beginning of each symbol, the shutter is *open*.
2. A photon number of combined field is counted during each slot individually.
3. If no photon is counted during a certain, say "ith", slot, the feedback control system switches the shutter into *close* from the next, "$i+1$st", slot till the end of the symbol.

The symbol is decided by the following rules.

i. If the shutter is closed at the ith slot and no other photons are counted after closing the shutter till the end of the symbol, a symbol S_i having an optical pulse at the ith slot, is decided as the transmitted symbol.

2. If some other photons are counted in the ith time-slot after closing the shutter, a symbol S_i is selected.

In the case when S_i is transmitted, if one or more photons are counted during every first i-1 slots, the combined field of the ith slot is in a vacuum state, and then no photons are counted during the slot. Therefore, the shutter is closed from the $i-1$st slot, so that no other photons are detected till the end of the symbol. In this case, S_i is decided as the transmitted symbol by the

decision rule 1, and errors never occur. On the other hand, when a symbol S_i is transmitted, if no photon is counted in a certain, say "jth" ($j < i$), time-slot, and the shutter is closed from the j+1st time slot, no photon is counted during from the j+1st to i-1st slots. However, some photon may be counted during the ith slot, whose combined field is in a coherent state $|-\alpha>$. In this case, S_i is also decided correctly as the transmitted symbol by the decision rule 2. If no photons are counted during the ith slot in the previous case, S_j is decided incorrectly, and which causes a symbol detection error. The symbol detection error from S_i to S_j occurs only for $j < i$ with the probability given by

$$P(S_j|S_i) = e^{-2N_s}\left(1 - e^{-N_s}\right)^{(j-1)} \qquad for\ j < i \tag{4}$$

By summing $P(S_j|S_i)$ with respect to j from 1 to i-1, we obtain conditional symbol detection error probability $Pe(S_i)$ as follows:

$$\begin{aligned} Pe(S_i) &= \sum_{j=1}^{i-1} P(S_j|S_i) \\ &= e^{-Ns}\{1 - (1 - e^{-Ns})^{j-1}\} \end{aligned} \tag{5}$$

This is symbol-dependent. Averaging these symbol-dependent error probabilities with respect to *a priori*-probabilities, we obtain average symbol detection error probability. For equally probable signal, an average error probability is given as follows:

$$Pe_{ave.}^{prop.} = \frac{M-1}{M}e^{-Ns} - \frac{1 - e^{-Ns}}{M}\{1 - (1 - e^{-Ns})^{M-1}\} \tag{6}$$

3 Numerical Results

Symbol detection error probability of the proposed detection scheme is shown as a function of signal energy N_s for symbol lengths M of 64 and 256 in FIGs. 2 (a) and (b), respectively. Those of optimum-quantum receiver, and a photon counting receiver are also shown. It is found in FIG.2 that the proposed scheme is superior to a photon counting receiver on error probability. It is also found that the proposed receiver performs almost optimally. It is easily shown that the error probability of the proposed receiver is approximately only twice as large as the minimum error probability for $N_s \gg 1$. FIG.3 compares the symbol detection error probabilities of the three receivers as a function of block length M for an average photon number N_s of 15. It can be seen from FIG.3 that error probability of the photon counting receiver is almost symbol-length independent, while those of the other two receivers are increasing functions of the length. Though the advantage of the proposed receiver over the photon counting receiver becomes less as the length increases, the proposed receiver is much better than the photon counting receiver for practical use, i.e. $M \leq 1024$. It seems from these results that we can expect the proposed detection scheme to perform ultimately low-energy optical communication.

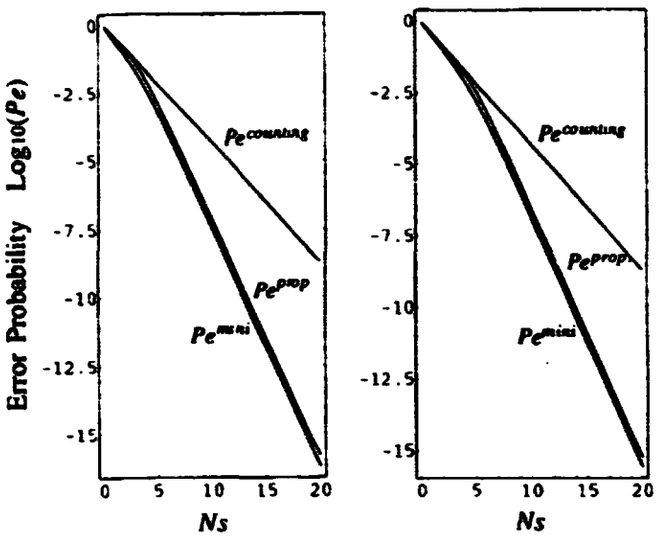

FIG. 2. Symbol detection error probability properties of proposed detection scheme compared with two classical receivers and minimum error probability. (a) is for M=64. (b) is for M=256.

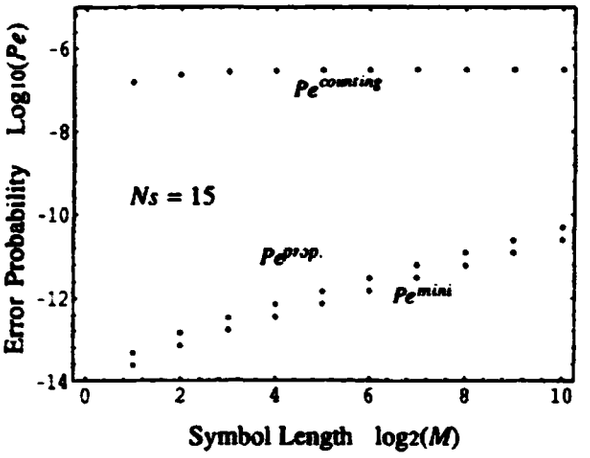

FIG. 3. Error probability dependence on block length M for the case that N_s is 15.

4 Conclusions

In this paper, we proposed a new detection scheme for the M-ary orthogonal coherent-statesignal. The error probability of the scheme was derived. It was shown by comparing its error performance with those of several receivers that the proposed receiver is superior to a photon counting receiver. and it performs almost optimally.

Acknowledgments

The author would like to express his deep appreciation to Prof.O.Hirota, Dr.M.Osaki of Tamagawa university and Dr.T.S.Usuda of Nagoya Inst. Tech. for their variable discussions and comments.

References

[1] O. Hirota, *Optical Communication Theory*, (Morikita Pub. Company, Tokyo, 1985). (*in Japanese*)

[2] C. W. Helstrom, *Quantum Detection and Estimation Theory*, (Academic Press, New York, N.Y, 1976).

[3] S.J. Dolinar Jr. , Quarterly Progress Report No.111, Research Laboratory of Electronics, M.I.T. ,115, (1973) .

[4] R.S. Kennedy, Quarterly Progress Report No.108, Research Laboratory of Electronics, M.I.T., 219, (1973).

[5] R.S. Bondurant, Optics Letters, **18**, 1896, (1993).

[6] K. Yamazaki, Technical Report of IEICE, IT-94-17 (1994). (*in Japanese*)

[7] K. Yamazaki, *Quantum Aspects of Optical Communications*, (eds.) C.Bendjaballah, et.al. (Springer-Verlag LNP-378, 367, 1991).

[8] K. Yamazaki, Tech. Digest of Quantum Communications and Measurement (Nottingham, UK), 86, (1994).

[9] T. Sasaki, and O. Hirota, The Trans. of IEICE Japan, **E75-B**, 514, (1992).

[10] O. Hirota, Technical Report of IEICE Japan, IT-93-531, (1994). (*in Japanese*)

[11] M. Osaki and O. Hirota, Tech. Digest of Quantum Communications and Measurement (Nottingham, UK), 61, (1994).

[12] T.S. Usuda and O. Hirota, Tech. Digest of Quantum Communications and Measurement (Nottingham, UK), 72, (1994).

[13] C.W. Helstrom, IEEE, Proc. IEEE, **62**, 139, (1974).

[14] J.R. Pierce, IEEE Trans. Commun., **COM-26**, 1819, (1978).

[15] O. Hirota, K. Yamazaki, Y. Endo, M. Nakagawa and M. Takahara, Trans. IEICE, **E.70**, 7, (1987).

[16] H.P. Yuen, R.S. Kennedy and M. Lax, IEEE. Proc. IEEE, **58**, 1770, (1970).

NEXT
DOCUMENT

HIGH-RATE STRONG-SIGNAL QUANTUM CRYPTOGRAPHY

Horace P. Yuen
Department of Electrical Engineering and Computer Science
Department of Physics and Astronomy
Northwestern University, Evanston, IL 60208

Abstract

Several quantum cryptosystems utilizing different kinds of nonclassical lights are described which can accommodate high intensity fields and high data rate. However, they are all sensitive to loss and both the high rate and the strong-signal character rapidly disappear. A squeezed light homodyne detection scheme is proposed which, with present-day technology, leads to more than two orders of magnitude data rate improvement over other current experimental systems for moderate loss.

The following is the second half of my talk "Squeezing, vacuum fluctuation, and all that" given at the Fourth International Conference on Squeezed States and Uncertainty Relations held in Taiyuan, China, June 1995. The first half consists of a brief review of sqeezing, a discussion of its coherence properties, the reality of vacuum fluctuation, and a treatment of the photon localization problem. At least two of these topics require a quantum field treatment that I cannot go into here, so I will just concentrate on quantum cryptography.

Quantum cryptography [1] -[7] is a very interesting and novel approach to secure communication with eigenstates of noncommuting observables as carriers of information to assure secrecy. In all the concrete optical realizations of such systems which have been studied theoretically or experimentally so far [2] -[7], either single-photon eigenstates orweak coherent states with less than one average photon per mode are employed to provide security [8]. Such systems not only face serious practical limitations in their detection, they are also inherently data-rate limited, especially after large transmission attenuation in possible applications such as the INTERNET. However, from an abstract point of view, two sets of states having the same linear geometry in the Hilbert space of states have the same security in principle. Thus, it is quite possible to describe *strong-signal* quantum cryptosystems, i.e., systems with quantum states that are *macroscopically distinguishable*, which are as secure as the ones that have been proposed. In the following we will describe several such systems involving nonclassical lights [9]. Unfortunately, such equivalent sets of states behave very differently in loss depending on the field intensity. In all the following systems, one cannot maintain either the strong-signal or the high-rate characteristics in the presence of the usual linear loss. Although a general proof is not yet available, the evidence indicates that there is no strong-signal quantum cryptosystem that would function properly in loss, for the same kind of reasons as the difficulties in generating and observing macroscopic superpositions of quantum states. This feature also leads to serious obstacles in transmitting more than $\frac{1}{2}$ bit per mode securely, although it is not clear what the fundamental rate limit is. As a small compensation, a currently implementable system is proposed which may be of practical importance.

Consider the following standard quantum cryptosystem [2] with a single polarized photon in four different possible polarization states,

$$| 1 >_1 | 0 >_2, \ | 0 >_1 | 1 >_2 \tag{1}$$

$$\frac{1}{\sqrt{2}} (| 1 >_1 | 0 >_2 \pm | 0 >_1 | 1 >_2) \tag{2}$$

where $| 1 >_1$ is the photon number = 1 eigenstate of a vertically polarized light mode, $| 0 >_2$ the vacuum state of the horizontally polarized light mode, so that the two states of (2) are the single photon eigenstates of the corresponding diagonally polarized light modes. A sender, Adam, picks the basis (1) or (2) at random for transmitting a single bit to the legitimate user, Babe, who would choose to measure (1) or (2) also randomly. After comparison in another public channel to match basis, they would succeed in communicating on the average $\frac{1}{2}$ bit per use. An eavesdropper, Eve, cannot duplicate a copy of the transmitted state and wait for the public measurement announcement, because the four possible states in (1) and (2) are nonorthogonal [10]. Similarly, Eve cannot use a quantum measurement to determine without large error which state was transmitted; thus any state she re-sends after measurement would induce large error in the otherwise perfect bit correlations between Adam and Babe, who could therefore detect the eavesdropping via various public forms of comparison. Apart from the practical difficulty of generating and detecting single photons, the data rate of this system is reduced to $\frac{\eta}{2}$ after suffering an energy loss $1 - \eta$ due to transmission attenuation, detection quantum efficiency, and whatever. If the optical system has bandwidth W, i.e., a total number of W adjacent frequency modes per polarization per second, the data rate becomes $\frac{\eta W}{2}$ bits per second assuming perfect detection. In the coherent-state realizations of this scheme with energy $S < 1$, the data rate is further reduced to $\eta SW/2$. Because of the smallness of this rate in practice, especially when the loss is large, it is important to investigate the possibility of rate increase for a single mode.

Clearly, the state vectors

$$| \psi >_1 | \phi >_2, \ | \phi >_1 | \psi >_2 \ ; \ \frac{1}{\sqrt{2}} (| \psi >_1 | \phi >_2 \pm | \phi >_1 | \psi >_2) \tag{3}$$

where $< \psi \mid \phi >= 0$ in each mode 1 and 2 have the same Hilbert space geometry as (1)-(2) in the sense of equal inner products, and hence the same security in principle. A strong-signal scheme can be obtained, say, by using photon number eigenstates $| \psi >= | n >$, $| \phi >= | 0 >$ or more generally $| \psi >= | n_1 >$, $| \phi >= | n_2 >$ with $(n_1 - n_2) >> 1$ for macroscopic distinguishability. Note that $\frac{1}{\sqrt{2}} (| n >_1 | 0 >_2 \pm | 0 > | n >_2)$ are not the number eigenstates of the diagonally polarized light for $n > 1$. In a single pair of modes, one can increase the data rate by utilizing $| \psi_n >= | n + \Delta n >$, $| \phi_n >= | n >$ while keeping $\Delta n >> 1$. If $N >> 1$ is the upper bound on the photon numbers that can be used in a mode, such a scheme would have a data rate of $\frac{W}{2} log_2 (1 + N - \Delta n)$ bits per second. Such high rate can also be obtained for a lossless system via conjugate coding [1], in which the first basis contains N orthogonal states and each state in the second basis is some linear combination of all the N states in the first. While it is possible to suggest concrete optical realizations for certain number state superpositions, it is not clear how the N-state superpositions in conjugate coding may be generated. In any case, all such superpositions degenerate quickly in loss as presently demonstrated.

It is well known [11]-[12] that linear combinations of macroscopically distinguishable coherent states are very sensistive to loss: they degenerate into a mixture of the states very readily. In a way, number states fare even worse. In the present context, this means the cryptosystem would be incapacitated entirely as the second basis degenerates into the first. Let the lossy system be represented by [13]-[14]

$$b = \eta^{\frac{1}{2}} a + (1-\eta)^{\frac{1}{2}} c \tag{4}$$

where c is the photon annihilation operator of a vacuum mode, a and b the input and output mode operators. For a pair of independent modes suffering the same loss $1-\eta$, each would be represented by (4) with different a, b, c . For $|\psi>=|n>$, $|\phi>=|0>$, the difference $\Delta\rho$ between the two density operators resulting from passing the two superposed states of (3) through (4) can be conveniently calculated via eqns (6)-(7) of ref [15], with the result

$$\Delta\rho = \eta^n (|n>_1|0>_2\ {}_1<0|\ {}_2<n| + |0>_1|n>_2\ {}_1<n|\ {}_2<0|) \tag{5}$$

which goes to zero exponentially in η. If $|\psi>=|n_1>$, $|\phi>=|n_2>$ in (3), a similar but more complicated result is obtained with the eigenvalues of $\Delta\rho = \pm 2\eta^{n_1+n_2}$. For the single-mode system

$$|n_1>, |n_2>;\ \frac{1}{\sqrt{2}}(|n_1> \pm |n_2>) \tag{6}$$

the eigenvalues of the superposed state difference $\Delta\rho$ in loss are $\pm\sqrt{\eta}^{n_1+n_2}$. Since two equiprobable states can only be discriminated with probability equal to the positive eigenvalue of $\Delta\rho$ from quantum detection theory [16], such superposed number state schemes are useless with even a tiny amount of loss.

The coherent-state superpositions in the following 4-state scheme

$$|\alpha>, |-\alpha>, \frac{(|\alpha> \pm |-\alpha>)}{\sqrt{2[1 \pm exp(-2|\alpha|^2)]}} \tag{7}$$

can, at least in principle, be obtained from a Kerr medium [17]. For large $|\alpha|$, $<\alpha|-\alpha> = \exp(-2|\alpha|^2)$ is nearly zero and the states (7) would perform in practice like an orthogonal scheme such as (6). For the general coherent-state superpositions in the following scheme

$$|\alpha_1>, |\alpha_2>;\ \mathcal{N}_{\pm}(|\alpha_1> \pm |\alpha_2>) \tag{8}$$

where $\mathcal{N}_{\pm}$ are normalization factors, the resulting density operator difference $\Delta\rho$ in loss is proportional to $<\sqrt{1-\eta}\,\alpha_1|\sqrt{1-\eta}\alpha_2>$ which goes to zero exponentially in $(1-\eta)^{\frac{1}{2}}\ |\alpha_1 - \alpha_2|$. To avoid this sensitivity to loss, $|\alpha_1 - \alpha_2|$ has to be chosen small and the resulting data rate for (7) or (8) would be comparable to coherent-state sysytems such as $\{|\pm\alpha>\}$ or $\{|\pm\alpha>; |\pm i\alpha>\}$, although (7) or (8) may be more secure because of their similarity to the single-photon scheme [7]. If one increases the rate in such systems by displacing the amplitude with $(m \pm in)\alpha_0$ for integers m, n and a real α_0 with $\eta\alpha_0^2 \geq 10$ to assure near orthogonality of the displaced states, which can be readily accomplished experimentally, the resulting rate is increased to $\sim \frac{\alpha^2 W}{2}\log(\eta S)$ for large available energy $S >> \alpha_0^2$. However, Eve can split off a small fraction of the signal and determine m, n fairly closely, thus obtaining many bits of information probabilistically so that such systems do not truly have a high secure rate.

Consider the following 4-state cryptosystem with two 2-state bases given by two-photon coherent states (TCS) [13] or pure squeezed coherent states which can readily be generated over a considerable range of parameters [18],

$$|\mu,\ \nu\ ;\pm\alpha>\ ;\ |\mu,-\nu;\pm i\alpha> \tag{9}$$

where $|\ \mu,\nu;\alpha>$ is the $|\ \beta;\mu,\nu>$ of ref [13] with mean field $\alpha = \mu^*\beta - \nu\beta^*$ and μ,ν,α are all chosen real. In (9), the signal is in the small noise quadrature. As an approximate form of conjugate coding for the two conjugate field quadrature operators whose eigenstates have infinite energy, consider the extension of (9) to the scheme

$$|\mu,\ \nu\ ;\pm m\alpha>\ ;\ |\mu,-\nu\ ;\pm im\alpha>,\ \ m=1,3,5,\cdots \tag{10}$$

From eqn (3.25) of ref [13], $|<\mu,\ \nu;\ \pm\alpha\ |\ \mu,-\nu;\ \pm\beta>|^2 = \exp(-|\alpha-\beta|^2)$ and

$$|<\mu,\ \nu;\ m\alpha\ |\ \mu,-\nu;\ ni\alpha>|^2 = (\mu^2+\nu^2)^{-1}\exp\{-(n^2+m^2)\alpha^2/(\mu^2+\nu^2)\} \tag{11}$$

Thus $(\mu^2+\nu^2)$ cannot be too large from (11), and α also cannot be too large or else Eve can determine the state by a phase insensitive linear amplifier followed with beamsplitting or by heterodyne detection with the following signal-to-noise ratio in the quadrature containing the signal [19]

$$SNR_{het} = \frac{4\eta\alpha^2}{\eta(\mu-\nu)^2+2-\eta} \tag{12}$$

In general, one has to assume that Eve may tap at $\eta = 1$.

When the correct quadrature is detected with homodyne detection, the signal-to-noise ratio is [13],[19]

$$SNR_{hom} = \frac{4\eta\alpha^2}{\eta(\mu-\nu)^2+1-\eta} \tag{13}$$

One must also require that at $\eta = 1$, the homodyne SNR obtained by Eve with a beamsplitter of transmittance ϵ is sufficiently small so that she cannot quite resolve the state even after the measurement announcement with a probability larger than, say, $P_e^E = 0.25$, while the induced reduction in the SNR_{hom} for Babe from (13) to

$$SNR_{hom}^B = \frac{4(1-\epsilon)\eta\alpha^2}{\eta(1-\epsilon)(\mu-\nu)^2+\epsilon\eta+(1-\eta)} \tag{14}$$

is already sufficiently large that Babe can detect the eavesdropping from the increase in her error rate. However, even for small ϵ Eve can locate to within a few states among one basis of (10) quite well, unless α is so small that the data rate is strongly affected. Thus, a large number of secure bits cannot be derived from the use of (10). Nevertheless the potential of homodyne systems can be seen from the following two examples.

Consider (9) with $\alpha^2 = 0.8$, $\nu = 0$, $\eta = 1$. The homodyne detection probability of error [19] is $P_e = erfc(\sqrt{SNR}) \sim 0.037$. If Eve tries to resolve the four states with optimized heterodyne detection, it is readily shown from classsical detection theory that the resulting error probability is ≥ 0.2 which is easily detected by Babe. Amplification and beamsplitting would lower Babe's SNR too much at the present signal level. If Eve taps off just a fraction ~ 0.089 of the field

to wait for measurement announcement so that the resulting optimum quantum receiver [16] for binaray coherent states yields an error probability of 0.25, that would already change Babe's error rate to 0.044 via (10), a 25% increase. With 10^4 transmissions, this means an increase of 3.64 standard deviations of error in an asymptotic standard Gaussian distrubution , which occurs with only a probability $\sim 10^{-4}$. Comparing to the photon detection system [5], [6] with $\alpha^2 \sim 0.1$ and considering the fact that close to an order of magnitude improvement in the photodetector quantum efficiency can be obtained from high efficiency photodiode for homodyme detection, this yields almost two orders of magnitude improvement in the data rate. For the TCS system (10) with $m = \pm 1, \pm 3$, $\alpha^2 = 1$, $(\mu + \nu)^2 = 4$, $\eta = 0.5$, and with the homodyne error probability among the four states in one basis still given by $P_e = erfc(\sqrt{SNR})$, Eve cannot exclude the possibility of any state with $\epsilon = 0.04$ which already induces a 3-standard deviation difference in Babe's err - rate for 10^4 transmissions, and $\epsilon = 0.1$ is required for $P_e^E = 0.25$. The data rate is now increased by a factor of ~ 400. The disadvantage of these schemes is that by raising the signal level, the initial beamsplitter attack puts a limit on the transmittance η below which the eavesdroppping cannot be detected. This can be amended by setting the threshold of the binary decision at a higher level and making no decision below it, which of course reduces the data rate, or by decreasing α which would also lower the data rate. Apart from the sensitivity of homodyne detection versus photon counting technology, part of the above improvement is due to more elaborate signal processing which can also be adopted in photon counting systems. Note that as in the direct detection case, the presence of a small error probability for Babe would reduce the information rate from the original data rate by a small fraction. Also, Eve could obtain some probabilistic information without being detected, which can be eliminated by Babe via "privacy amplification" [5] that would further lower the information rate. However, for sufficiently long keys there is no need to eliminate Eve's probabilistic information. A detailed study of the various possibilities will be given elsewhere.

Acknowledgment

This work was supported by the Office of Naval Research and the Advanced Research Project Agency.

References

[1] S. Wiesner, SIGACT News 15, 78 (1983)

[2] C. H. Bennett, G. Brassard, and A. K. Ekert, Scientific American, Oct. 1992, pp. 50-57.

[3] C. H. Bennett, Phys. Rev. Lett. 68, 3121 (1992).

[4] A. K. Ekert, J. G. Rarity, P. R. Tapster, and G. M. Palma, Phys. Rev. Lett. 69, 1293 (1992).

[5] C. H. Bennett, F. Bessette, G. Brassard, L. Salvail, and J. Smolin, J. Cryptol. 5, 3 (1992).

[6] P. D. Townsend, J. G. Rarity, and P. R. Tapster, Electron. Lett. 29, 1291 (1993).

[7] B. Huttner, N. Imoto, N. Gisin and T. Mor, Phys. Rev. A51, 1863 (1995).

[8] Along with all the other papers in the literature, the fundamental question of security will not be addressed here: What is the robustness level of the system against all possible eavesdropping methods consistent with the laws of physics. Only certain specific eavesdropping approaches will be discussed.

[9] H. P. Yuen, in Photons and Quantum Fluctuations, E. R. Pike and H. Walther, eds., (Hilger, London, 1988), p. 1.

[10] H. P. Yuen, Phys. Lett. 113A, 405 (1986).

[11] A. O. Caldeira and A. J. Leggett, Phys. Rev. A31, 1059 (1985).

[12] D. F. Walls and G. J. Milburn, Phys. Rev. A31, 2403 (1985).

[13] H. P. Yuen, Phys. Rev. A13, 2226 (1976).

[14] H. P. Yuen and J. H. Shapiro, IEEE Trans. Inform. Theory 26, 78 (1980).

[15] H. P. Yuen, Phys. Lett. 113A, 401 (1986).

[16] C. W. Helstrom, Quantum Detection and Estimation Theory, Academic Press, 1976.

[17] B. Yurke and D. Stoler, Phys. Rev. Lett. 57, 13 (1986).

[18] H. J. Kimble, Phys. Repts. 219, 227 (1992)

[19] J. H. Shapiro, H. P. Yuen and J. A. Machado Mata, IEEE Trans. Inform. Theory 25, 179 (1979). Note that eqn(3.49) is too small by a factor of 2, which is not important for large SNR but crucial for our present applications.

NEXT
DOCUMENT

Theoretical Analysis about Quantum Noise Squeezing of Optical Fields from an Intracavity Frequency-Doubled Laser

Kuanshou Zhang Changde Xie Kunchi Peng
Institute of Opto-Electronics, Shanxi University, Taiyuan, P.R.China

Abstract

The dependence of the quantum fluctuation of the output fundamental and second- harmonic waves upon cavity configuration has been numerically calculated for the intracavity frequency-doubled laser. The results might provide a direct reference for the design of squeezing system through the second-harmonic-generation.

PACS numbers: 42.50.Dv, 42.65.Ky

1 Introduction

The SHG is a highly efficient process for producing the squeezed state light. The generation of squeezed light by SHG in a passive cavity has been studied intensively in theory and experiment[1-3]. Some authors have discussed the nonclassical properties of the output fields from an intracavity frequency-doubled laser. Most of them consider an idea laser system[4-5].

For the experimental physicists, it is intersting to analyze the nonclassical properties of the output optical fields from a realistic intracavity frequency-doubled laser system. In this paper, the intensity fluctuations spectra of the fundamental and the SH wave in output fields have been calculated. The dependences of the intensity fluctuations on the configuration of the laser cavity and the losses in the cavity have been discussed. These results will provide a direct reference for the design of squeezer with SHG.

2 Fundamental and SH fluctuations spectra

The system we consider here is a single-ended resonator that contains a laser medium and a $\chi^{(2)}$-nonlinear crystal. The laser is pumped by a coherent laser source and the fundamental frequency mode (ω_1) and SH frequency mode ($\omega_2 = 2\omega_1$) are coupled by a $\chi^{(2)}$-nonlinearity. Based on Lax-Louisell laser theory[6] and in the rotating frame, the semiclassical equations of motion for this system are given by:

$$\dot{\alpha}_1 = (-\gamma_1 - i\Delta_1)\alpha_1 + k\alpha_1\alpha_2 + \frac{g\alpha_1}{1 + b|\alpha_1|^2/g} \tag{1}$$

$$\dot{\alpha}_2 = (-\gamma_2 - i\Delta_2)\alpha_2 - \frac{1}{2}k\alpha_1^2 \tag{2}$$

where α_1, α_2 is the complex amplitude of fundamental and SH wave, $\Delta_1 = \omega_1 - \omega_L$ and $\Delta_2 = \omega_2 - 2\omega_L$ are the detuning between the cavity modes and the lasing transition ω_L, γ_1,γ_2 are the

cavity damping rates, g is the pump parameter, b is the saturation parameter of the laser medium, k is the nonlinear coupling constant

$$k = \frac{2\chi^{(2)}}{n^3}\left(\frac{h\omega^3}{V\epsilon_0}\right)^{\frac{1}{2}}\frac{l}{L} \tag{3}$$

The constant k depends on the nonlinearity of the cystal and the configuration of the cavity. V is the mode volume, l is the nonlinear crystal length, L is the cavity length.

It is useful to introduce the real parameters p_j and q_j to describ the real and imaginary parts of the field α_j respectively.

$$p_j = \frac{1}{2}(\alpha_j + \alpha_j^*) \qquad q_j = \frac{1}{2i}(\alpha_j - \alpha_j^*) \tag{4}$$

In the stationary state, the real variables are the solution of the following equations:

$$\frac{k^2 b}{2\gamma_2 g}p_1^4 + \left(\frac{k^2}{2\gamma_2} + \frac{b\gamma_1}{g}\right)p_1^2 + (\gamma_1 - g) = 0 \tag{5}$$

$$p_2 = -\frac{k}{2\gamma_2}p_1^2 \tag{6}$$

whereas the imaginary parts are taken as zero $q_1 = q_2 = 0$.

When the pump parameter g approaches the critical value[5]

$$g_c = \frac{1}{4}(2\gamma_1 + \gamma_2)\left(1 + \left(1 + \frac{8b\gamma_2^2}{k^2(2\gamma_1 + \gamma_2)}\right)^{\frac{1}{2}}\right) \tag{7}$$

the phase variables q_j become unstable and the system presents self-sustained oscillation. We are interested in the regime below the threshold of the instabilities, in which the equations of motion (1) and (2) can be linearized around the stationary state given by equations (5) and (6).

At the case of resonance ($\Delta_j = 0$), we obtains expressions for the outgoing amplitude squeezing spectra of the fundamental and SH wave at the analytic frequency Ω. When the phase angles equal to zero the optimum squeezing can be obtained. Setting zero as the shot-noise level, we have:

$$S_1(\Omega) = -\frac{1 - R_1}{1 - R_1 + L_1}\frac{8\gamma_{R_1}\left(\frac{k}{2}|\bar{p}_2| - \frac{g}{(1+b|\bar{p}_1|^2/g)^2}\right)(\gamma_2^2 + \Omega^2)}{D} \tag{8}$$

$$S_2(\Omega) = -\frac{1 - R_2}{1 - R_2 + L_2}\frac{8\gamma_{R_2}\left(\frac{k}{2}|\bar{p}_2| - \frac{g}{(1+b|\bar{p}_1|^2/g)^2}\right)k^2|\bar{p}_1|^2}{D} \tag{9}$$

where

$$D = \left(k^2|\bar{p}_1|^2 + \frac{2b\gamma_2|\bar{p}_1|^2}{(1 + b|\bar{p}_1|^2/g)^2} - \Omega^2\right)^2 + \Omega^2\left(\gamma_2 + \frac{2b|\bar{p}_1|^2}{1 + b|\bar{p}_1|^2/g)^2}\right)^2 \tag{10}$$

R_j is the reflectivity of the output coupler at the frequency ω_j. L_j is the rest losses per roundtrip in the resonator that include absoption, scattering and residual transmission through mirrors other than the output coupler. γ_{R_j} is the cavity damping rate which only depends on the output coupler loss $(1 - R_j)$, γ_j is total cavitv damping rate which depends on total losses $(1 - R_j + L_j)$. ¿From the equations, it can been seen that the squeezing increase when the rest losses are decreased.

3 Numerical calculation and discussions

Following numerical calculation was processed according to our realistic experimental setup and parameters. The experimental system is shown in Fig.1

Fig.1

A Nd:YAG laser medium and a nonlinear crystal KTP are contained in a semimonolithic laser cavity. One side of Nd:YAG crystal was coated as the input coupler (M_1). The length of Nd:YAG and KTP both are 5mm. The input coupler is high reflectivity for both fundamental and SH waves and the output coupler (M_2) is high reflectivity for the fundamental wave. Former works [4-5] have indicated that the squeezing increases with pump paramter. Considering $g < g_c$, we chose the pump parameter $g = 10^9 s^{-1}$, that corresponds to the pump power of 2W in our system, to discuss the dependence of the squeezing on the configuration of the cavity and the reflectivity of the output coupler for SH wave (R_2). The saturation parameter b of laser crystal is $0.2 s^{-1}$, the rest losses of fundamental wave is 0.5% and the rest losses of SH wave is 1%.

Fig.2

Fig.2 shows that the squeezing degree of th SH wave at zero analytic frequency as a function of the cavity length and R_2. Here the curvature radius of output coupler is designated as 30mm. It can be seen that for the designated curvature radius we can find an optimum $R_2(R_2 = 88\%)$ and an optimum cavity length ($L = 25mm$) to get the maximum squeezing ($S_2(0) = -0.21$). For a certain R_2 there is a corrspondent optimum cavity length which is a near half-concentric configuration.

Fig.3

In Fig.3 the curvature radius of output coupler is taken as 100mm. In this case $R_2 = 92\%$ $L = 46mm$ should be an optimum option which is a near half -confocal cavity other than above near half-concentric.

Fig.4

Fig.4 is the squeezing spectra of the fundamental wave (1) and the SH wave (2) as a function of analytic frequency Ω at the above-mentioned optimum configurations of the cavity. For Fig.4(a) $\rho = 30mm$, $L = 25mm$ and $R_2 = 88\%$; for Fig.4(b) $\rho = 100mm$, $L = 46mm$ and $R_2 = 92\%$. In this designed system the squeezing of the fundamental wave is much less than SH wave. The squeezing bandwidth in Fig.4(a) is larger than Fig.4(b), so that in the experiment the length of laser cavity should be chosen as short as possible to obtain higher intracavity density of power, larger squeezing bandwidth and more compact configuration.

4 Conclusion

We have calculated the dependence of quantum noise squeezing upon the reflectivity of output coupler and the length of cavity in the intracavity- doubled laser. The results might provide some references for designing squeezer with intracavity SHG.

References

[1] S.F.Pereira, Min Xiao, H.J.Kimble, and J.L.Hall, Phys. Rev. A **38**, 4931 (1988)

[2] P.Kurz, R.Paschotta, K.Fiedler, A.Sizmann, G.Leuchs, and J.Mlynek, Appl. Phys. B **55**, 216 (1992)

[3] A.Sizmann, R.J.Horowicz, G.Wagner, and G.Leuchs, Opt. Comm. **80**, 138 (1992)

[4] A.Sizmann, R.Schack, A.Schenzle, Europhys. Lett. **13**, 109 (1990)

[5] R.Schack, A.Sizmann, A.Schenzle, Phys. Rev. A **43**, 6303 (1991)

[6] W.H.Louisell, *Quantum Statistical Properties of Radiation* (John Wiley, New York, 1973).

Figure Caption

Fig.1 The laser configuration

Fig.2 The dependence of squeezing at $\Omega = 0$ upon the reflctivity R_2 and cavity length with $\rho = 30mm$

Fig.3 The dependence of squeezing at $\Omega = 0$ upon the reflctivity R_2 and cavity length with $\rho = 100mm$

Fig.4 The squeezing spectra for the fundamental wave (1) and SH wave (2). (a) $\rho = 30mm$, (b) $\rho = 100mm$

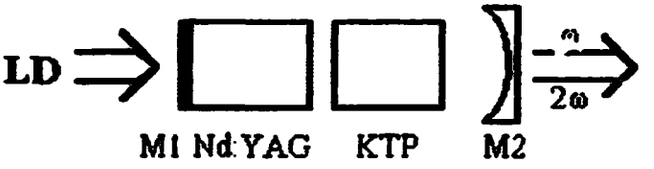

Fig.1 The laser configuration

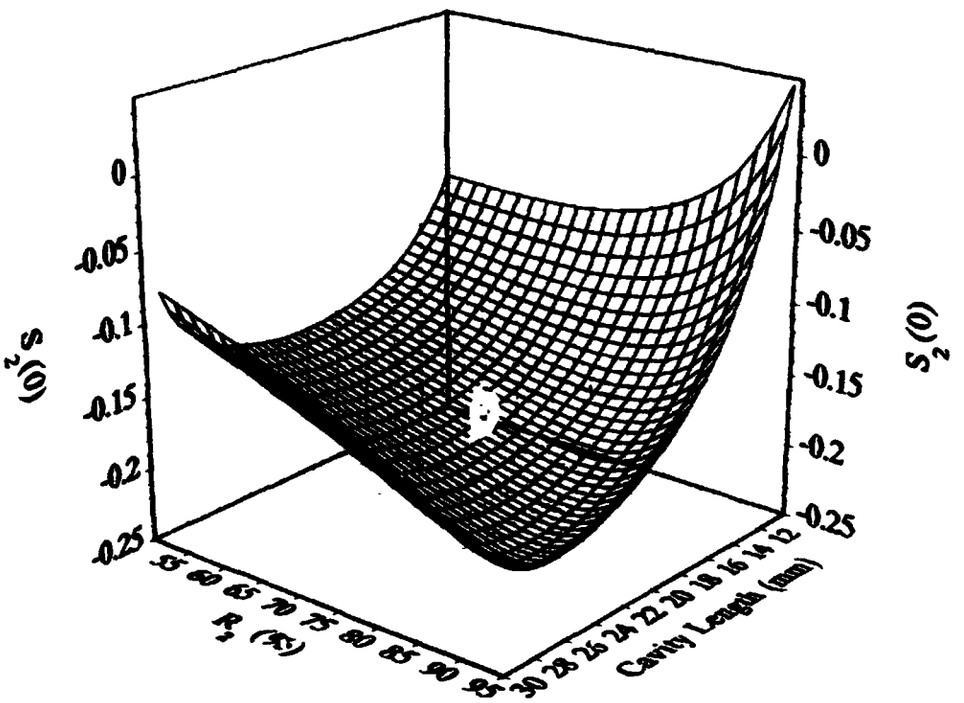

Fig.2 The dependence of squeezing at $\Omega=0$ upon the reflectivity R_2 and cavity length with $\rho=30$mm

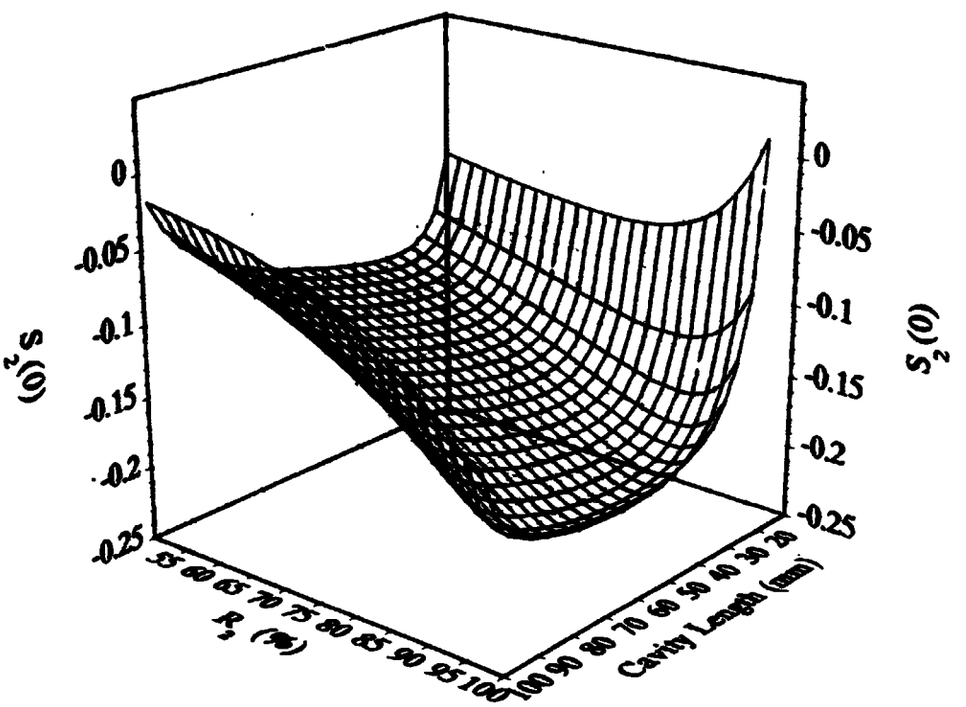

Fig.3 The dependence of squeezing at $\Omega=0$ upon the reflectivity R_2 and cavity length with $\rho=100$mm

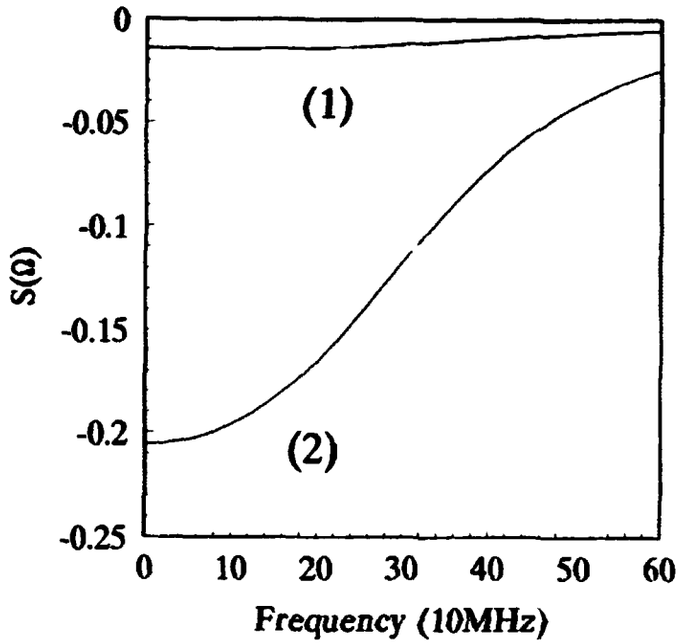

Fig.4(a) The squeezing spectra for the fundamental wave (1) and SH wave (2) (ρ=30mm)

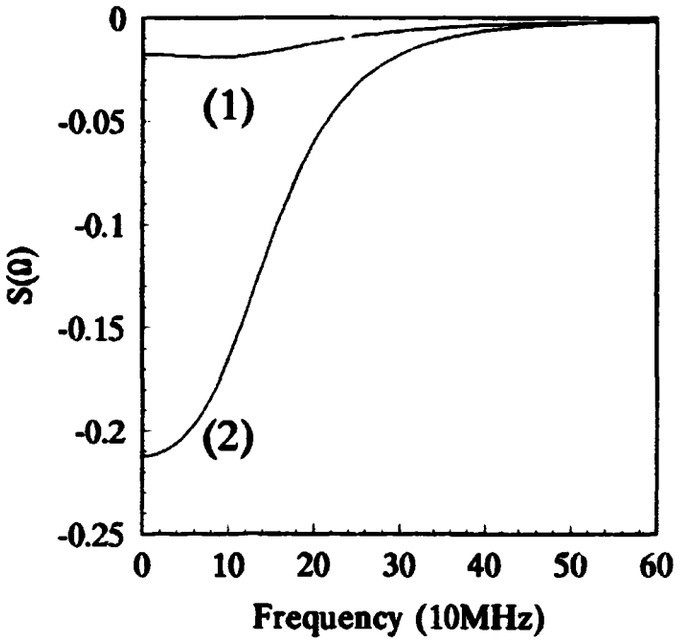

Fig.4(b) The squeezing spactra for the fundamental wave (1) and SH wave (2) (ρ=100mm)

NEXT
DOCUMENT

Experiments with lasers and frequency doublers

H.-A. Bachor, M. Taubman, A. G. White, T. Ralph, D. E. McClelland
Physics Department, The Australian National University, Canberra, ACT, 0200, AUSTRALIA
fax: 61 6 249 0741 email: physics.faculties@anu.edu.au

Abstract

Solid state laser sources, such as diode-pumped Nd:YAG lasers, have given us CW laser light of high power with unprecedented stability and low noise performance. In these lasers most of the technical sources of noise can be eliminated allowing them to be operated close to the theoretical noise limit set by the quantum properties of light. The next step of reducing the noise below the standard limit is known as squeezing. We present experimental progress in generating reliably squeezed light using the process of frequency doubling. We emphasise the long term stability that makes this a truly practical source of squeezed light. Our experimental results match noise spectra calculated with our recently developed models of coupled systems which include the noise generated inside the laser and its interaction with the frequency doubler. We conclude with some observations on evaluating quadrature squeezed states of light.

1 Quantum models of coupled systems

Earlier quantum models considered only one system at a time, one resonator or one laser, and predicted the noise properties of such a system in isolation. Using the ideas developed by Gardiner and Carmichael [1] we have developed algorithms which allow us to describe coupled systems. Examples include a laser pumped by another laser, a laser locked to a passive linear or nonlinear resonator (such as a frequency doubler or optical parametric oscillator), or a laser locked to another laser. This new technique is an extremely powerful tool to evaluate the performance of realistic systems, which usually consist of several coupled components, and it was applied to simulate the experiments described in this paper.

2 Removing excess laser noise

It is possible to actively suppress most of the excess technical noise from the laser, including the intrinsic relaxation oscillation, using electro-optic feedback. Such a circuit, with a suitably designed feedback characteristic, will suppress classical fluctuations in the laser light [2] but cannot suppress quantum noise. In fact there is actually a penalty to be paid for the noise suppression: in spectral regions originally free of excess noise, such as well above the relaxation oscillation, the feedback adds classical noise - particularly when the feedback gain is high [3]. Improvements to direct detection feedback can only be made by replacing the beam splitter with a nonlinear optical component, such as a Kerr medium or a frequency doubler [4].

An alternative technique is to passively suppress the noise at higher frequencies by passing the laser through a narrow bandwidth cavity. This arrangement, typically known as a mode cleaner because the cavity improves the spatial properties of the beam, acts as a low pass filter for the laser noise. The impact of the mode cleaner can be seen in Figure 1a. Trace A shows the amplitude noise spectrum of the laser used in our experiment. Trace B shows the output noise spectrum after a mode cleaner of bandwidth 800 kHz. (The spike is the modulation peak used to lock the mode cleaner). There is a significant improvement, with light reaching the quantum noise limit at 8 MHz, as opposed to beyond 50 MHz.

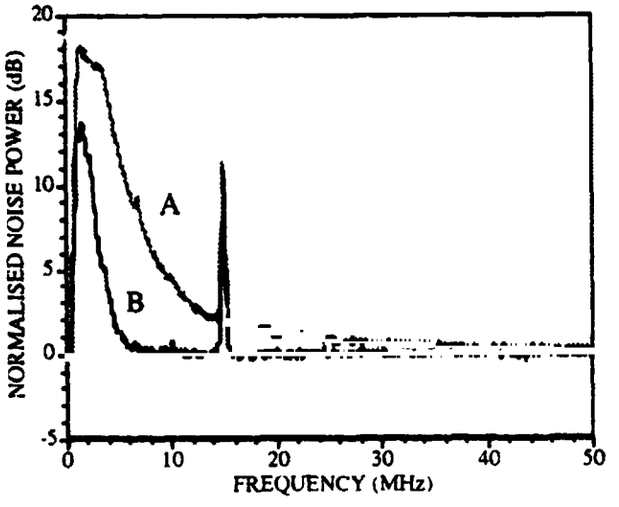

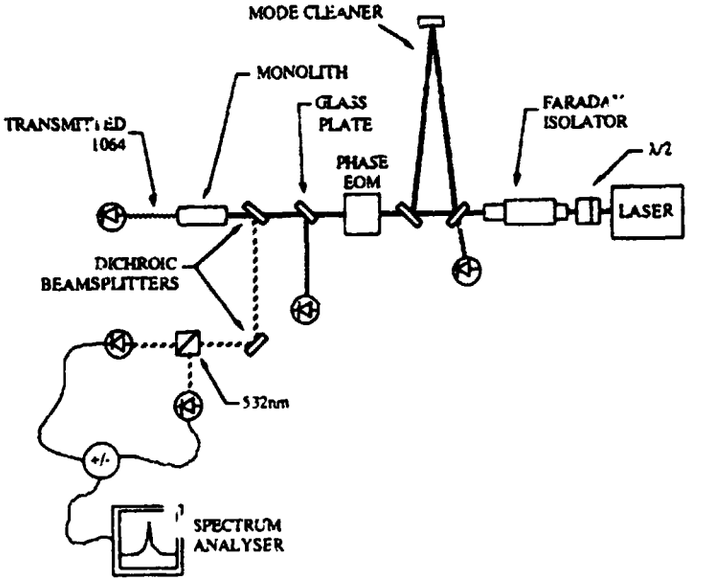

FIG.1a. Intensity noise spectra. A) direct from laser B) after passage through mode cleaner

FIG.1b. Experimental layout for generating squeezed light via frequency doubling

3 Amplitude squeezed light

Having shown that it is possible to remove the technical noise from a practical light source, the question becomes is it possible to produce a practical light source with reduced quantum fluctuations? (In this paper we will concentrate on reduction of amplitude fluctuations.)

This can be done with a diode laser which converts electric current to light with a high quantum efficiency. Currents are a flux of bosons, and thus the Poissonian limit does not apply: standard current regulators generate currents with Poissonian statistics (and thus fluctuations) well below the standard quantum limit. In turn this can be used to drive a laser and generate light with sub Poissonian statistics [5] However to date, such systems have relatively poor spatial properties and are limited to the red region of the spectrum.

An attractive alternative to diode lasers is to use a nonlinear medium to generate bright, amplitude squeezed light directly. Frequency doubling was one of the first processes which was explored for squeezing [6]. A long sequence of technological improvements was required to improve the reliability of these systems. To date, passive monolithic singly resonant cavities have proved

to be by far the most stable systems for noise suppression [7]. In our experiments [8] the doubling material is monolithic $MgO:LiNbO_3$. The end faces are curved, polished and dielectric coated to form high reflectivity cavity mirrors. A diode pumped CW Nd:YAG laser operating at 1064 nm is locked to this resonator and pumps it with $\approx$ 100 mW of power. The doubler has a conversion efficency greater than 50%. The squeezed light, at 532 nm, is picked off with a dichroic mirror and is detected at a balanced pair of detectors (a self-homodyne detector). See Figure 1b.

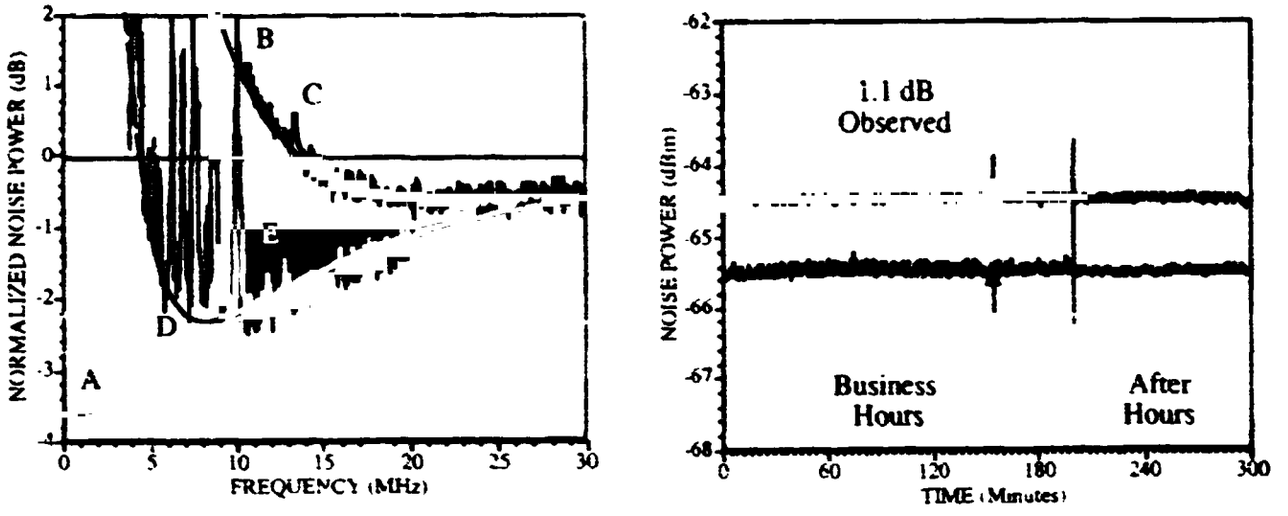

FIG. 2a. Theoretical and experimental noise spectra for doubler.
FIG. 2b. Reliability trace. Degree of squeezing is constant over a 5 hour period.

Figure 2a shows the results of a scan of the detection frequency. Trace A is the predicted squeezing for SHG when illuminated with a coherent state, an example of an unrealistic model based on a single system. It predicts best noise suppression at zero detection frequency. The width of the noise spectrum corresponds to the linewidth of the doubler. Trace B shows the experimental results, after allowing for the nonideal detection efficiency ($\approx$ 65 %). Whilst the agreement at large detection frequencies is reasonable, the prediction of good noise suppression at low frequencies is clearly wrong. The noise properties of the real laser dominate.

Trace C shows the results of a model which simultaneously describes the laser and the doubler: it is in excellent agreement with the measured results. The parameters for the laser model are derived from direct measurement of the laser output, no futher adjustment to the parameters are required when used in the coupled model. To access greater squeezing we placed a mode cleaner between the laser and the doubler and locked it to the laser. The prediction for the coupled system of three cavities (laser, mode cleaner and doubler) is shown in trace D, the corresponding experimental results are shown in trace E (again allowing for nonideal detection efficiency). Both the improvement in squeezing and the agreement between theory and experiment is excellent, apart from the frequency window from 5 to 10 MHz where we see a series of well defined technical noise spikes, most likely due to acoustic resonaces in the doubling crystal. Figure 2b shows the results of the reliability test. Observed squeezing of 1.1 dB (2.2 dB inferred) was measured at 11.16 MHz over a 5 hour period. In all, these results demonstrate the validity of our model for coupled systems and show that bright squeezing greater than 2 dB can be reliably obtained.

4 Evaluating quadrature squeezed states of light

In the previous section we obtained excellent quantitative agreement between theory and experiment. Curiously neither the theoretical model nor the experimental results we used truly quantified the state of the light - information was thrown away. In this section we examine this issue in some detail.

Broadly speaking there are two classes of models, *full* and *linearised*. The starting point for both is the same, the difference arises in the approximations made in the latter to evaluate the effect of the nonlinearity. Either model will give a two dimensional probability or quasiprobability distribution that describes the state of the light. (In the remainder of this discussion we will consider the Q representation and its corresponding Q function.) *Full* models use a full quantum mechanical description, covering both average mean values and fluctuations, to describe the complete state of light. Due to computing and mathematical limitations, these models are mainly used to describe states of low photon number (such as squeezed vacuum). The resulting Q functions may be aysmmetric and may show negative curvature. In *linearised* models, the mean values of the quadratures are evaluated by solving the semiclassical equations. The fluctuations are treated as perturbations, and only terms linear in fluctuations are considered. This allows consideration of high photon states, but limits the model to predicting only symmetrical Q functions. As we will see, the standard measurement taken with a homodyne detector is well matched to the simplified predictions of the linearised theory.

Now consider the experiment. In CW squeezing measurements the experimental signal is the phase dependent noise current from the homodyne detector. This is normally analysed with a spectrum analyser to give the phase and frequency dependent variance of the noise current, $V_{current}(\phi,\omega)$. For an arbitrary state of light no direct and unique mathematical conversion exists between the measured noise variances of the light and the predicted Q function. However, some important features of the Q function can be inferred.

For a coherent state ($\langle\Delta X_1^2\rangle = \langle\Delta X_2^2\rangle$, $\langle\Delta X_1^2\rangle\langle\Delta X_2^2\rangle = 1$) the probability distribution is a symmetric two dimensional Gaussian with a full width half maximum, $\delta X(\phi,\omega) = 1$, centred around the point given by the long term averages $\underline{X1}$, $\underline{X2}$ (where ϕ and ω are the detection angle and frequency respectively). By convention a contour is drawn at the full width half maximum of this probability distribution. For any projection angle the root mean square value of the distribution (i.e. the square root of the variance) is trivially equal to the separation of the contour from the centre of the distribution. The contour is a circle.

Squeezed states are those where the symmetry between X1 and X2 has been broken by some nonlinear process. In other words the fluctuations in X1 and X2 are no longer independent but are correlated. For a mininum uncertainty squeezed state ($\langle\Delta X_1^2\rangle \neq \langle\Delta X_2^2\rangle$, $\langle\Delta X_1^2\rangle\langle\Delta X_2^2\rangle = 1$) the distribution is still a two dimensional Gaussian, but the contour is now an ellipse. Note that such a two dimensional Gaussian function has Gaussian cross section for any angle ϕ. Once an elliptical contour is assumed, which is true for any mininum uncertainty state, measured variance $V_{current}(\phi,\omega)$ and contour $\delta X(\phi,\omega)$ can still be related point by point.

For a squeezed state with excess noise ($\langle\Delta X_1^2\rangle\langle\Delta X_2^2\rangle > 1$) the shape of the Q function can vary significantly from the previous cases. Without specifying the specific squeezing process, no simple assumption about the shape or the symmetry of the contour nor the shape of the various cross sections through the Q function, can be made. The connection between $V_{current}(\phi,\omega)$ and

$\delta X(\phi,\omega)$ is no longer local. The value of $V_{current}(\phi,\omega)$ depends on all parts of the probability distribution. The projection of the entire function, not just one specific cross section at ϕ, must be taken into account when determining the contour points (and thus the Q function shape) from the variance $V_{current}(\phi,\omega)$.

There are three courses in such a situation. To date the most common course has been to simply assume that the Q distribution is Gaussian / the contour is an ellipse. Whilst unsatisfactory, by definition this gives good agreement with the linearised models most often used to describe experiments as they only produce Gaussian distributions / elliptical contours. In fact one can only interpret the variance $V_{current}(\phi,\omega)$ as the limit to the extent of the distribution function in the direction ϕ. The second course then is to obtain a rough idea of the contour for the Q function by taking every value of $V_{current}(\phi,\omega)$ and converting and plotting it as to two tangents with the separation $[V_{current}(\phi,\omega)]^{1/2}$. The actual distribution will lie inside the perimeter bounded by these tangents. The shape and size of the contour can then be estimated from the plot. This can be done easily with typical variance data[9].

The third approach is to measure the Q function directly and was pioneered by the group of Raymer et. al. [10] with pulsed sources of squeezed light. At fixed ϕ, many pulses are recorded and a full histogram of the energy of the pulses is constructed. This gives not only the variance of the fluctuations but the full distribution function at that angle. Using data from various angles the Q function is tomographically reconstructed. Each pulse is a mode of the light and is constructed of a complex mixture of frequencies. In CW squeezing the measured squeezing, and therefore the measured Q function, is highly frequency dependent. (The intracavity squeezing value / probability distribution is for a mode of light - it can be related to the measured extracavity squeezing spectrum of the light field via the input/output formalism of Collett and Gardiner [11]). The analogous experiment is thus to look at only one frequency of the phase dependent noise current from the homodyne detector. This can then be sampled and digitised to build up a histogram of the photocurrent fluctuations. This is repeated for a number of angles and the histograms are then in the tomographical reconstruction. This technique was recently demonstrated successfully to analyse the squeezed vacuum / low photon squeezed light produced by a CW optical parametric amplifer / oscillator [12].

To conclude, mininum uncertainty states are well described by linearised theories, and well evaluated by current measurment techniques. States with excess noise, such as a Kerr squeezed state, cannot be accurately described by a linearised model - interesting (non Gaussian) features are lost. Furthermore, current measurement techniques will also miss these interesting features. New models and experimental techniques are required. Table I summarises the salient points.

TABLE I Summary of Section 4.

	Mininum Uncertainty State	State with excess noise
Theory	Linearised theory / quadratic Hamiltonian gives exact result	Linearised theory is not sufficient. Full quantum theory / higher order higher order Hamiltonian required
Distrib. charac.	$\langle \Delta X_1^2 \rangle \langle \Delta X_2^2 \rangle = 1$	$\langle \Delta X_1^2 \rangle \langle \Delta X_2^2 \rangle > 1$
	Q function is a 2 dimensinal Gaussian. Any cross section is gaussian	Q function has an arbitrary shape
	Contour line is an ellipse	Contour shape is arbitrary
	Contour/Q function defined by the two parameters r and ϕ_0	Definition of cor tour/Q function requires many parameters
	Distance from contour to centre is $\delta X(\phi) = 1/2V(\phi)$	Distance from contour to centre can be greater or smaller than $1/2V(\phi)$
	Conversion of $V(\phi)$ to contour . unique	No unique conversion of $V(\phi)$ to contour
Detect.	Homodyne detector and spectrum analyser gives V_{min} and V_{max} which define contour and Q function uniquely.	Requires tomography to describe Q function. Conditional distribution constructed from homodyne output for a given LO angle. Tomography requires a range of LO anles.
Nonlin. system	Any system with nonlinearity constant across distribution function	System where nonlineariy varies across distribution function (e.g. singularity)

5 Conclusion

Strong squeezing of bright, short wavelength, light has been demonstrated and found to be extremely reliable. We have developed models that describe the behaviour of, and account for the interaction between, the various elements in a realistic system and find excellent agreement with experiment. We conclude that current theory and measurement techniques will need to be extended to properly evaluate the next generation of nonclassical light experiments.

Acknowledgments

The authors wish to thank B. Brown, ANU Canberra, Australia and CSIRO Optical Technology, Sydney, Australia for their technical support. This work was financially supported by the Australian Research Council.

References

[1] C. W. Gardiner, *Phys. Rev. Lett.*, **70**, p.2269, 1993

H. J. Carmichael, *Phys. Rev. Lett.*, **70**, p.2273, 1993

[2] C. C. Harb, M. B. Gray, H.-A. Bachor, R. Schilling, P. Rottengatter, I. Freitag and H. Welling, *IEEE J. Quant. Elec.*, **30**, p.2907, 1994

[3] M. S. Taubman, H. Wiseman, D. E. McClelland and H.-A. Bachor, *JOSA B*, in print 1995

A. V. Masalov, A. A. Putilin, M. V. Vasilyev, *J. Mod. Opt*, **41**, p.1941, 1994

[4] H. M. Wiseman, M. S. Taubman and H.-A. Bachor, *Phys. Rev. A*, June 1995

[5] Y. N. Yamamoto and S. Machida, *Phys. Rev. A*, **35**, p. 5114, 1986

T.-C. Zhang, J.Ph. Poizat, P. Grelu, J.-F. Roch, P. Grangier, F. Marin, A. Bramanti, V. Jost, M. D. Levenson and E. Giacobino, *Quantum and Semiclassical Optics*, in print 1995

[6] A. Sizmann, R. J. Horowicz, G. Wagner and G. Leuchs, *Opt. Comm.*, **80**, p.138, 1990

[7] R. Paschotta, M. Collett, P. Kürz, K. Fiedler, H.-A. Bachor and J. Mlynek, *Phys. Rev. Lett.*, **72**, p. 3807, 1994

R. Bruckmeier, *private communication*, December 1994

[8] T. C. Ralph, M. S. Taubman, A. G. White, D. E. McClelland and H.-A. Bachor, *Optics Letters*, in print, 1995

M. S. Taubman, T. C. Ralph, A. G. White, D. E. McClelland and H.-A. Bachor, *submitted to Europhysics Letters*, 1995

[9] H.-A. Bachor, A. G. White, *in preparation*, 1995

[10] D. T. Smithey, M. Beck, M. G. Raymer and A. Faridani, *Phys. Rev. Lett.*, **70**, p. 1244, 1993

[11] C. W. Gardiner and M. J. Collett, *Phys. Rev. A*, *31*, p. 3761, 1985

[12] G. Breitenbach, S. Mller, S. F. Pereira, S. Schiller, J. Mlynek, *private communication*, March 1995

NEXT
DOCUMENT

Amplitude and transverse quadrature component squeezing of coherent light in high Q cavity by injection of atoms of two-photon transition

Cao Chang−qi
Department of Physics, Peking University, Beijing 100871, China

September 27, 1995

Abstract

The amplitude and transverse quadrature component squeezing of coherent light in high Q cavity by injection of atoms of two-photon transition are studied.

The Golubev-Sokolov master equation and generating function approach are utilized to derive the exact variances of photon number and of transverse quadrature component as function of t. The correlation functions and power spectrums of photon number noise and of output photon current noise are also investigated.

1 Introduction

In this work, the amplitude squeezing as well as the transverse quadrature component squeezing of coherent light in high Q cavity by injection of atoms are investigated. The interaction is assumed to be two-photon transition type and the initial mean photon number N is assumed large.

The interaction interval τ for individual atom is taken the faverable value π/g, where g denotes the effective coupling constant between the atom and the single mode light. This value makes each incoming atom to emit two photons during passing the cavity.

Our approach is based on Golubev-Sokolov master equation[1]. Since this equation was doubted by Benkert and Rzazewski[2] for it may give negative probabilities. We will do some discussion on it first. To our view, even if Golubev-Sokolov equation does not have the meaning as a common differential equation, it is able to give correct mean values, variances and correlation functions of appropriate quantities, when it is utilized along with generating function method. In this work, this approach is not only used to derive photon number variance, the power spectrums of steady photon number noise and of output photon current noise, but also is generalized to study the squeezing of transverse quadrature component.

In the investigation of photon number variance, we find that, in the case that the steady mean value of photon $\overline{n}_s$ is much larger than the initial mean value of photon N, the ratio $\langle \Delta n(t)^2 \rangle / \langle n(t) \rangle$ will first drop to a value which is much smaller than its steady state value 1/2, and then turns up to approach 1/2.

In the investigation of squeezing of transverse quadrature component, we get that its variance square is expressed by $\langle n(t)\rangle/4N$, hence the correspondent steady value $\overline{n}_s/4N$ maybe either smaller on larger thatn the standard value 1/4. It is interesting to note, this steady value is related to the initial parameter N. Furthermore it does not depend on whether the injection is regular or poissonian.

2 Model, Golubev-Sokolov master equation and generating function approach

We assume that the initial state of light in the high-Q cavity is single mode coherent light with mean photon number $N \gg 1$. The injected two level atoms are in upper level, they interact with the cavity field by resonant two-photon transition: $\omega_0 = 2\omega$.

The change of density matrix of photon field due to its interaction with a single atom initially in upper level is described by

$$(\hat{u}\rho)_{mn} = \rho_{mn}\cos(g\tau\sqrt{(m+1)(m+2)})\cos(g\tau\sqrt{(n+1)(n+2)}) + \rho_{m-2,n-2}\sin(g\tau\sqrt{m(m-1)})\sin(g\tau\sqrt{n(n-1)}) - \rho_{mn}. \quad (1)$$

For lage N, m and n for important ρ_{mn} are also large, so that $g\tau\sqrt{(m+1)(m+2)}$ may be approximated[3] by $g\tau(m+\frac{1}{2})$, etc. If we take the value of τ as $\frac{\pi}{g}$ then eq.(1) turns out to be

$$(\hat{u}\rho)_{mn} = (-1)^{m-n}\rho_{m-2,n-2} - \rho_{mn} \quad (2)$$

which means each atom emits two photons during passing the cavity, namely the quantum efficiency of photon production equals one.

We assume that the atoms enter the cavity one by one and at most one atom in the cavity every moment. Therefore after injection of k atoms, ρ will change to $(1+\hat{u})^k\rho$.

If the injection is of poissonian statistics with r as mean injection rate, the average number of injected atom during the interval $t \to t+dt$ will equal $K = r\Delta t$. Thus[1]

$$\rho(t+\Delta t) = \sum e^{-K}\frac{K^k}{k!}(1+\hat{u})^k\rho = e^{r\hat{u}\Delta t}\rho(t), \quad (3)$$

leading to

$$\frac{d\rho(t)}{dt}_{pump} = r\hat{u}\rho. \quad (4)$$

This is just the pumping term in the well known Scully-Lamb master quation.

For regular pumping, k itself is a definite number, $k = r\Delta t$ with r denoting the injection rate.Therefore

$$\rho(t+\Delta t) = (1+\hat{u})^{r\Delta t}\rho(t) = e^{r\Delta t\ln(1+\hat{u})}\rho(t), \quad (5)$$

which leads to[1]

$$\frac{d\rho(t)}{dt}|_{pump} = r[ln(1+\hat{u})]\rho(t) \quad (6)$$

for regular injection. By adding the cavity damping term, Golubev and Sokolov got the equation

$$\frac{d\rho_{mn}(t)}{dt} = r[ln(1+\hat{u})\rho(t)]_{mn} + \Gamma[-\frac{1}{2}(m+n)\rho_{mn}(t) + \sqrt{(m+1)(n+1)}\rho_{m+1,n+1}(t)], \quad (7)$$

in which Γ denote the cavity damping and the thermal photon is assumed negligable.

Benkert and Rzazewski found[2] that this equation gives negative ρ_{nn} when it is solved by letting $\frac{d}{dt}\rho_{nn} = 0$ to derive the steady values of ρ_{nn}. Let us see where this problem might come from. For regular injection $r\Delta t$ equals k therefore must be larger than 1. Thus Δt cannot be taken as arbitrarily small. This in turn means eq.(7) may not be a differential equation of common sense, one ought to avoid by setting $\frac{d\rho}{dt}$ be zero to get the steady value of ρ. Because of stepwise increase of rt, the strickly steady value of ρ may not exist.

In practice, one usually only needs to calculate the expectation values, varicances or correlation functions of some relavant quantities. In this case it is better to evaluate these values directly rather than through evaluating ρ_{nn} first. Generating function aproach is especially good for this purpose. In this work this approach will be used not noly to study the amplitude squeezing (photon number squeezing) but also generalized to study the squeezing of transverse quadrature component.

3 Photon number squeezing[4]

Golubev and Sokolov, as well as some other authors, expanded the logurithm $ln(1+\hat{u})$ and trancated at the second order of $\hat{u}$:

$$log(1+\hat{u}) \cong \hat{u} - \frac{1}{2}\hat{u}^2. \quad (8)$$

W.-h.Tan[5] and the present author[6] has shown independently that for evaluating the variance square $\langle \Delta n^2(t) \rangle$, this treatment is correct. The result so obtained is identical to the exact solution, but it is not so for evaluating $\langle \Delta n(t)^3 \rangle$. In general, for calculating of $\langle \Delta n(t)^l \rangle$, one needs to expand $ln(1+\hat{u})$ to l terms to get the correct value[6].

As did in Ref[1], we introduce the generating function for $\langle \Delta n^2(t) \rangle$ as

$$G(z,t) = \sum_{n=0}^{\infty} \rho_{nn}(t) z^n, \qquad z \leq 1. \quad (9)$$

By utilization of eqs.(7) and (8), we get the equation for $G(z,t)$ as

$$\frac{\partial G(z,t)}{\partial t} = -\frac{r}{2}(3-z^2)(1-z^2)G(z,t) + \Gamma(1-z)\frac{\partial G(z,t)}{\partial z}. \quad (10)$$

This is a partial difference equation of first order, its general solution is expressed by one of its special solution mutiplied by the general solution of equation $\frac{\partial G(z,t)}{\partial t} = \Gamma(1-z)\frac{\partial G(z,t)}{\partial z}$. The latter will be determined by the requirement of initial condition. The desired solution so obtained expressed by

$$G(z,t) = G(y,0)e^{f(z,t)}, \quad (11.1)$$

where

$$y = 1 + (z-1)e^{-\Gamma t}, \tag{11.2}$$

$$f(z,t) = \frac{r}{2\Gamma}[3(z-y) + \frac{3}{2}(z^2-y^2) - \frac{1}{3}(z^3-y^3) - \frac{1}{4}(z^4-y^4)]. \tag{11.3}$$

The values of $\langle n(t)\rangle$ and $\langle \Delta n^2(t)\rangle$ are easily obtained from $G(z,t)$:

$$\langle n(t)\rangle = \frac{\partial G(z,t)}{\partial z}|_{z=1} = \frac{2r}{\Gamma} + \left(N - \frac{2r}{\Gamma}\right)e^{-\Gamma t}, \tag{12.1}$$

$$\langle \Delta n^2(t)\rangle = \frac{\partial^2 G(z,t)}{\partial z^2}|_{z=1} + \frac{\partial G(z,t)}{\partial z}|_{z=1} - \left[\frac{\partial G(z,t)}{\partial z}\right]^2_{z=1}$$

$$= \frac{r}{\Gamma} + \left(N - \frac{2r}{\Gamma}\right)e^{-\Gamma t} + \frac{r}{\Gamma}e^{-2\Gamma t}. \tag{12.2}$$

The steady values of $\langle \Delta n(t)\rangle$ and $\langle \Delta n^2(t)\rangle$ exist.By letting $t = \infty$, one get:

$$\langle n\rangle_s = \frac{2r}{\Gamma}, \quad \langle \Delta n^2(t)\rangle_s = \frac{r}{\Gamma}. \tag{13}$$

If we define $\eta(t)$ as $\langle \Delta n^2(t)\rangle/\langle n(t)\rangle$, then its steady value η_s will be $\frac{1}{2}$, the same as one photon-transition subpoissonian lasers.

Eqs.(12) can be checked in the special case of ideal cavity ($\Gamma = 0$)[3].

The $\eta(t)$ defined above has different behavior for $x(\equiv \overline{n_s}/N) > 1$ or < 1. In the latter case $\eta(t)$ drops from its initial value and monotonically tends to the steady value 1/2. In the former case $\eta(t)$ first drops down to a minimum value η_{min} less than 1/2 and then turns up to approach 1/2. For $x \gg 1$, $\eta_{min} \simeq \sqrt{\frac{2}{x}} \ll 1$, therefore the correspondent state may be closed to the photon number eigen state.

The steady state correlation function $g(t)$ defined as following

$$g(t) = tr\left[\rho_s \hat{a}^\dagger_H(0)\hat{a}^\dagger_H(t)\hat{a}_H(t)\hat{a}_H(0)\right], \quad t > 0 \tag{14}$$

can also be evaluated by a generating function $F(z,t)$. $F(z,t)$ satisfies the same differential equation as eq.(10), but has different initial conditions:

$$F(z,0) = \sum_n (n+1)\rho^{(s)}_{n+1,n+1}z^n. \tag{15}$$

The $g(t)$ so attained is

$$g(t) = \frac{\partial F(z,t)}{\partial z}|_{z=1} = \langle n\rangle^2_s - \frac{1}{2}\langle n\rangle_s e^{-\Gamma t}, \qquad t > 0. \tag{16}$$

The power spectrum of the steady state output photon current noise is related to $g(t)$, in the case that the damping of the cavity field is mainly due to output, its expression will be

$$P_I(\omega) = \Gamma\langle n\rangle_s \frac{\omega^2}{\omega^2 + \Gamma^2}. \tag{17}$$

The correlation function $\langle \Delta n(t_1)\Delta n(t_2)\rangle$ for arbitrary t_1 and t_2 can also be calculated by similar approach[4]. From it we obtain the power spectrum of steady state photonnumber noice as

$$P_n(\omega) = \langle n\rangle_s \frac{\Gamma}{\omega^2 + \Gamma^2}, \tag{18}$$

which mainly lies in low frequency region, in contrast to $P_I(\omega)$ given above.

4 The squeezing of transverse quadrature component.

We are now generalizing the generating function approach to investigate the squeezing of quadrature components of $\hat{a}$.

Let α, the eigen value of $\hat{a}$ for the initial photon state, be real number, then $\hat{a}_1 = \frac{1}{2}(\hat{a} + \hat{a}^\dagger)$, $\hat{a}_2 = \frac{1}{2i}(\hat{a} - \hat{a}^\dagger)$ will be the longitudinal and tranverse quadrature components respectively.

The mean value of longitudinal quadrature component is given by

$$\langle a_1(t)\rangle = \sum_n \sqrt{n+1}\rho_{n,n+1}(t).$$

In our model $(\hat{u}\rho)_{n,n+1} = -\rho_{n-2,n-1} - \rho_{n,n-1}$, which absolute value is not small as compared with $|\rho_{n,n+1}|$. Actually it is almost twice as large as $|\rho_{n,n+1}|$. And the sign of $|(1+\hat{u})^k\rho|_{n,n+1}$ varies alternately between positive and negative as k varies. Because of these features, the evolution of $\langle \hat{a}_1(t)\rangle$ could not be described by differential equations. The situation of transverse quadrature component is different. In our case $\langle a_2(t)\rangle$ remains to be zero. We may generalize the generating function method to investigate its variance square, which is expressed by

$$\langle \Delta a_2(t)^2\rangle = \frac{1}{4} + \frac{1}{2}\sum_n \rho_{nn}(t) - \frac{1}{2}\sum_n \sqrt{(n+1)(n+2)}\rho_{n,n+2}(t). \tag{19}$$

As before, $\sum_n \sqrt{(n+1)(n+2)}\rho_{n,n+2}(t)$ may be approximated by $\sum_n (n+\frac{3}{2})\rho_{n,n+2}(t)$. Define

$$G_2(z,t) = \sum_n \rho_{n,n+2}(t)z^n, \quad z \leq 1, \tag{20}$$

then

$$\sum_n (n+\frac{3}{2})\rho_{n,n+2}(t) = \frac{\partial G_2(z,t)}{\partial z}|_{z=1} + \frac{3}{2}G_2(z,t)|_{z=1}. \tag{21}$$

We see that only first order derivative appears in eq.(21), therefore it is enough[6],[4] to take just one term in the expansion of $ln(1+\hat{u})$. The equation of $G_2(z,t)$ can be derived accordingly, solving it as before, we get $\sum_n (n+\frac{3}{2})\rho_{n,n+2}(t)$, which in turn yields

$$\langle \Delta a_2(t)^2\rangle = \frac{\langle n\rangle_s}{4N} + \frac{1}{4}(1 - \frac{\langle n_s\rangle}{N})e^{-\Gamma t} = \frac{\langle n(t)\rangle}{4N}. \tag{22}$$

This result may also be checked in the special case of ideal cavity. Setting $e^{-\Gamma t} \cong 1 - \Gamma t$ in eq.(22), we get

$$\langle \Delta a_2(t)^2\rangle = \frac{1}{4} + \frac{rt}{2N},$$

which is the same as that given in Ref[3] by a completely different approach.

One may show from eq.(22) that $\langle \Delta a_2(t)^2\rangle - \frac{1}{4}$ may be positive or negative, depending on whether $\langle n_s\rangle/N$ is larger or smaller than one. The steady value of $\langle \Delta a_2(t)^2\rangle$ is given by

$$\langle \Delta a_2(t)^2\rangle_s = \frac{\langle n\rangle_s}{4N}, \tag{23}$$

which may be much larger or much smaller than 1/4. The latter means, in certain sense, deep suppression of phase noise.

It is interesting to note that the stationary value $\langle \Delta a_2(t)^2 \rangle_s$ is still related to the initial parameter N.

It is also interesting to note that $\langle \Delta a_2(t)^2 \rangle$, unlike $\langle \Delta n(t)^2 \rangle$, has no concern with whether the injection is regular or poissonian, since in the above derivation, $ln(1+\hat{u})$ is allowed to be replaced by $\hat{u}$.

This work is part of the project supported by the Chinese Doctoral Program Foundation of the Institution of Higher Education.

References

1. Y.M.Golubev and I.V.Sokolov, Sov.Phys.JETP **60**, 234(1984).

2. C.Benkert and K.Rzazewski, Phys.Rev.A **47**, 1564(1993).

3. Cao Chang-qi and Ding Xiao-hung, Phys, Rev.A **46**, 6042(1992)

4. Cao Chang-qi, to be published in *Quantum and Semiclassical Optics.*

5. W.-h Tan, Phys.Lett.A **190**, 13 (1994).

6. Cao Chang-qi, Pnys.Lett.A **196**, 35(1994)

NEXT
DOCUMENT

ATOMIC DIPOLE SQUEEZING IN THE CORRELATED TWO—MODE TWO—PHOTON JAYNES —CUMMINGS MODEL

Dong Zhengchao and Zhao Yonglin

Shandong Univ. of M and T. at Jinan, 250031, *PR China*

Abstract

In this paper, We study the atomic dipole squeezing in the correlated two—mode two—photon JC model with the field initially in the correlated two—mode SU(1,1) coherent state. The effects of detuning, field intensity and number difference between the two field modes are investigated through numerical calculation.

1 Introduction

The production and nonclassical properties of quantized electromagnetic fields and their interaction with matters have been the topics of fundamental importance in quantum optics, and both saw remarkable development in the past decade. In the first aspect, the correlated two—mode states of radiation fields, such as the two—mode squeezed state[1], the pair coherent state[2] and correlated two—mode SU(1,1) coherent state[3], have received a great deal of attentions among researchers. These states usually display nonclassical properties including field squeezing, antibunching and sub —poissonian photon statistics. In the other aspect, the theoretical model for the interaction of correlated two—mode fields and a two—level atom, better known as the generalized Jaynes—Cummings model[4], was investigated for field squeezing and atomic dynamics[5]. However, little attention has been paid to the atomic dipole squeezing in these systems.

It is well known that the atomic dipole squeezing, in much the same way as the field squeezing, is the reduction of fluctuation of one component of the dipole moment while keeping the uncertainty relations with the other component at the same time. As it is shown[6] that squeezed atom radiates squeezed lights, it is of importance to study the squeezing of the atomic variables. In the present paper, we devote a study to the squeezing of the atomic dipole moment in the correlated two—mode two—photon JC model.

2 The Hamiltonian and State Vector

We consider a system comprising of a two—level atom interacting with the correlated two

—mode, two—photon field. The Hamiltonian for the system in the dipole and the rotating—wave approximation is given by the following expression:

$$H=\omega_0\sigma_3/2+\omega_1(a_1^+a_1+1/2)+\omega_2(a_2^+a_2+1/2)+\lambda(a_1^+a_2^+\sigma_-+\sigma_+a_1a_2),\quad (h=1) \tag{1}$$

where ω_0 is the atomic transition frequency, ω_i is the frequency of the field of mode i; $a_1(a_1^+)$ and $a_2(a_2^+)$ are the field annihilation (creation) operators of the two modes, respectively; σ_3 is the atomic inversion operator and $\sigma_\pm$ are the atomic transition operators; λ is the atom—field coupling constant.

We assume that the atom is initially in the coherent superposition state of the excited state $|e>$ and the ground state $|g>$, and the field in any correlated two—mode state. The initial atom—field state is given by

$$|\Psi(0)>=|A(0)>\otimes|F(0)> \tag{2}$$

where $|A>=\cos\frac{\beta}{2}|e>+e^{i\alpha}\sin\frac{\beta}{2}|g>=A_1|e>+A_2|g>$

and $|F(0)>=\sum_n C_{n,q}|n+q,n>$

At any time $t>0$, the state vector of the system is found from the Hamiltonian (1) to be

$$|\Psi(t)>=A_1\sum_{n=0}^{\infty}\exp\{-i[\omega_1(n+q+1)+\omega_2(n+1)]t\}C_{n,q}G_1|+;n+q,n>-iA_2\sum_{n=0}^{\infty}\exp\{-i[\omega_1(n+q)+\omega_2 n]t\}C_{n,q}H_1|+;n+q-1,n-1>$$

$$+A_2\sum_{n=0}^{\infty}C_{n,q}\exp\{-i[\omega_1(n+q)+\omega_2 n]\}G_2|-;n+q,n>$$

$$-iA_2\sum_{n=0}^{\infty}C_{n,q}\exp\{-i[\omega_1(n+q+1)+\omega_2(n+1)]t\}.H_2|-;n+q+1,n+1> \tag{3}$$

with

$$G_1=\cos At-\frac{i\delta\sin At}{2\ A},\quad G_2=\cos Bt-\frac{i\delta\sin Bt}{2\ B}$$

$$H_1=\alpha_{n-1,q}\frac{\sin Bt}{B},\quad H_2=\alpha_{n,q}\frac{\sin At}{A}$$

$$A=[\delta^2/4+\alpha_{n,q}^2]^{1/2},\quad B=[\delta^2/4+\alpha_{n-1,q}^2]^{1/2}$$

$$\alpha_{n,q}^2=\lambda^2(n+q+1)(n+q),$$

3 Atomic Dipole Squeezing

We define the slowly varying atomic dipole operators as

$$\sigma_1=\frac{1}{2}(\sigma_+\exp(-i\omega_0 t)+\sigma_-\exp(i\omega_0 t)) \qquad (4)$$

$$\sigma_2=\frac{1}{2i}(\sigma_+\exp(-i\omega_0 t)-\sigma_-\exp(i\omega_0 t)) \qquad (5)$$

which correspond to the dispersive and absorptive parts of the dipole moment, respectively.

The atomic state is said to be squeezed if the variance satisfies the condition

$$(\Delta\sigma_i)^2<\frac{1}{4}|<\sigma_3>| \qquad i=1 \text{ or } 2 \qquad (6)$$

This condition can be rewritten as

$$S_i=(\Delta\sigma_i)^2-\frac{1}{4}|<\sigma_3>|<0 \qquad (7)$$

In carrying out the numerical calculations, we assume that the initial field is in the correlated two-mode SU(1,1) coherent state [3]

$$|F(0)>=(1-|\zeta|^2)^{q+1}\sum_{n=0}^{\infty}\left(\frac{(n+q)!}{n!q!}\right)^{1/2}\zeta^n|n+q,n> \qquad (8)$$

where $\zeta=-\tanh(\theta/2)\exp(-i\varphi)$ and where $0<\theta<\infty$ and $0\leqslant\varphi\leqslant 2\pi$. For simplicity, we set $\varphi=0$. Also we focus on the effects of detuning, photon number and the number defference between the two modes on the atomic dipole squeezing.

We assume the atom to be initially in the ground state. In the case of on-resonance excitation, the dispersive part of dipole moment does not squeeze, as is shown by the theoretical expression of the squeezing function S_1. The evolution of S_2 vs reduced time λt for different photon numbers (N_2) and number differences (q) are shown in Figs. 1~3. It is evident from Fig. 1 , where $q=0$, that S_2 exhibits exactly periodic fluctuation behavior, with periodic time $\lambda t=\pi$. Good squeezing for σ_2 is found in the case of weak initial field with $N_2=1$, as shown in Fig. 1a, where σ_2 is squeezed almost all the time except when $\lambda t=k\pi$ $(k=0,1,2\cdots\cdots)$. With the initial field becoming more intensive, both the digree and duration of squeezing grow smaller. (Fig. 1)

When there is number difference between the two modes, the time evolution of S_2 no longer shows periodic behavior (Figs2~3). In weak initial field cases, for example $N_2=1$ (Fig. 2a, Fig. 3a), the fluctuations of S_2 are small and squeezings recur. The first squeezing in the case of $q=1$ lasts longer than that of the case $q=5$, but larger and longer squeezings recover in the case of $q=5$. In both cases the degree and duration fo squeezing get smaller as the initial

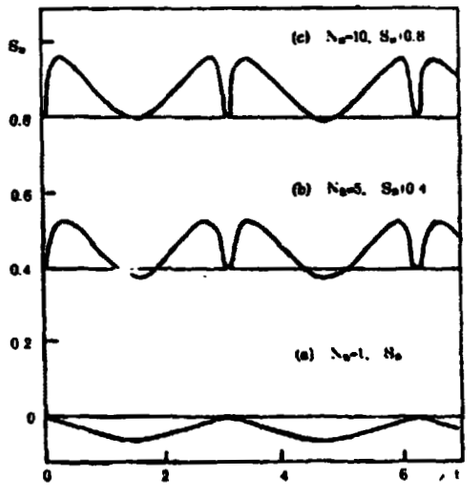

Fig.1 Evolution of S_0 for A_1=0, δ =0, q=0

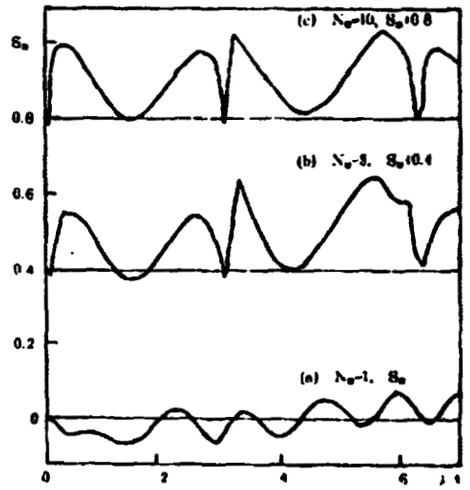

Fig.2 Evolution of S_0 for A_1=0, δ =0, q=1

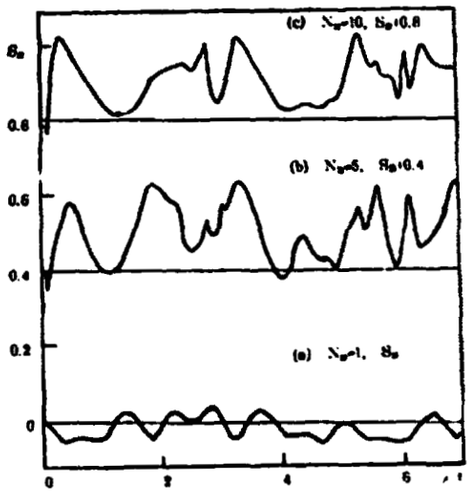

Fig.3 Evolution of S_0 for A_1=0, δ =0, q=5

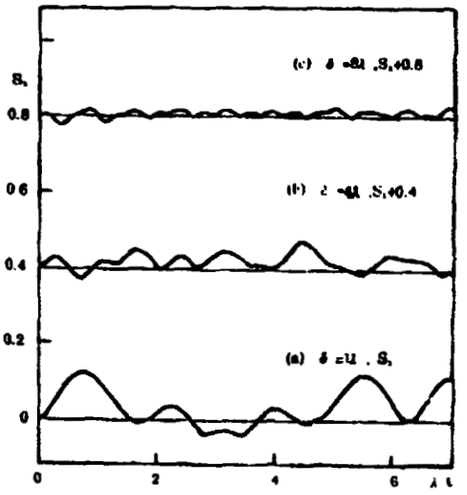

Fig.4 Evolution of S_1 for A_1=0, q=1, N_0=1

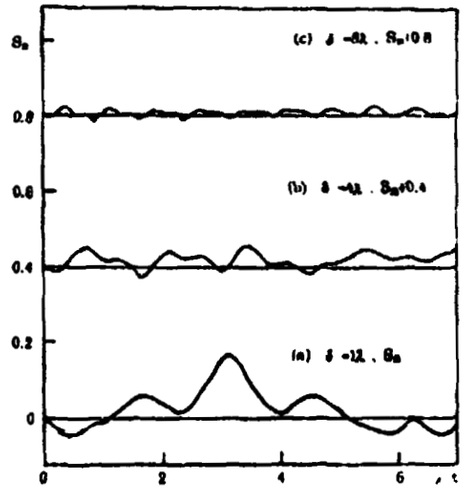

Fig.5 Evolution of S_2 for A_1=0, q=1, N_0=1

field becomes more intensive. As it is observed from Fig. 3b and Fig. 3c, only short and small squeezings occur when $N_2=5$ and 10.

The above results reveal that atomic squeezing is both intensity and phase dependent of the initial field. Two identical field modes ($q=0$), which mean that both modes have identical number and phase distributions, result in periodic fluctuation and squeezing. On the other hand, two different field modes ($q=0$) lead to nonperiodic fluctuation and weaker squeezing effects.

The time evolution of S_1 and S_2 for different off—resonance excitations δ and for $q=1$ and $N_2=1$ are shown in Fig. 4 and Fig. 5 respectively. It is seen that both S_1 and S_2 squeeze recurrently and alternatively. When the detuning is larger, the fluctuation and squeezing become smaller due to weaker coupling between field and atom. We have also studied the cases when q is large and found that squeezing exists only for small detuning (not shown).

4 Conclusion

In summary, we have investigated the atomic dipole squeezing for the correlated two —mode two—photon JC model with the field initially in the correlated two—mode SU(1,1) coherent state. It is shown that in the on—resonance excitation and when the numbers of the two modes are equal, periodic squeezing is found for the absorption part of the dipole . Good squeezing is observed when the atom is initialy in the ground state and the initial field is weak . As the number of photon in mode 2 and the number difference grow larger, the degree and duration of squeezing decrease . In off—resonance excitation, both σ_1 and σ_2 exhibit squeezing effects . Detuning generally displays the effects of reducing fluctuation and squeezing even revokes for large detuning .

References

[1]C. M. Caves, B. L. Schumaker, Phys. Rev. A 31, 3068 (1985)

[2]G. S. Agarwal, J. Opt. Soc. Am. B5, 1940 (1988)

[3]C. C. Gerry, J. Opt. Soc. Am. B8, 685 (1991)

[4]E. T. Jaynes, F. W. Cummings, Proc. IEEE, 51, 89 (1963)

[5]C. C. Gerry, R. F. Welch, J. Opt. Soc. Am, B9, 290 (1992)

[6]M. M. Ashraf, the late M. S. K. Ramzi, J. of Mod. Opt. 39, 2245 (1992), and the references therein.

NEXT
DOCUMENT

OBSERVATION OF TWO-PHOTON EXCITATION FOR THREE-LEVEL ATOMS IN A SQUEEZED VACUUM

K. Edamatsu [1], N. Ph. Georgiades, E. S. Polzik [2], and H. J. Kimble
Norman Bridge Laboratory of Physics 12-33,
California Institute of Technology, Pasadena, CA 91125, U.S.A.

A. S. Parkins [3]
Department of Physics, University of Konstanz, Konstanz, Germany

Abstract

The two-photon transition ($6S_{1/2} \rightarrow 6D_{5/2}$) of atomic Cesium is investigated for excitation with squeezed vacuum generated via nondegenerate parametric down conversion. The two-photon excitation rate (R) is observed to have a non-quadratic dependence of $R = aI^2 + bI$ on the incident photon flux (I), reflecting the nonclassical correlations of the squeezed vacuum field.

1 Introduction

Over the last two decades, there has been great progress in the generation and application of manifestly quantum or nonclassical states of the electromagnetic field. Spectroscopy with such nonclassical light can reveal new optical phenomena associated with the interaction between the nonclassical fields and matter. In this paper, we report the first experimental observation of such a novel field-matter interactions, namely two-photon atomic excitation using squeezed vacuum light.

It is well known that the two-photon excitation rate (R) can often be expressed in terms of the second-order correlation function of the driving field [1]. For classical light, this rate depends quadratically on the incident photon flux (I). In contrast, it is theoretically predicted that the quantum correlations of a squeezed state can enhance this rate so that it depends linearly on I in the limit of small photon flux [2, 3, 4, 5]. More generally, the two-photon excitation rate versus incident photon flux of a squeezed vacuum field is well approximated by the combination of quadratic and linear components, as $R = aI^2 + bI$. As a realization of this theoretical prediction, we have investigated the two-photon transition ($6S_{1/2} \rightarrow 6P_{3/2} \rightarrow 6D_{5/2}$) for trapped atomic Cesium with squeezed vacuum light, and found a non-quadratic dependence of the excitation rate on the incident photon flux.

[1]Department of Applied Physics, Tohoku University, Sendai 980-77, Japan.
[2]Institute of Physics and Astronomy, Aarhus University, Aarhus C, DK-8000, Denmark.
[3]Department of Physics, University of Waikato, Hamilton, New Zealand.

2 Experiment

The squeezed vacuum light is generated from a tunable optical parametric oscillator (OPO) [6] pumped under subthreshold condition. The pump beam is the second harmonic of a Ti:Sapphire laser (λ=883 nm), the frequency of which is locked ($\pm$0.3 MHz) to the two-photon resonance $6S_{1/2}$,F=4 $\rightarrow$ $6D_{5/2}$,F=6 of atomic Cesium. The OPO is tuned to generate two frequencies (λ_1=852 nm and λ_2=917 nm) in resonance with the transitions $6S_{1/2}$,F=4 $\rightarrow$ $6P_{3/2}$,F=5 and $6P_{3/2}$,F=5 $\rightarrow$ $6D_{5/2}$,F=6, respectively. The doubly resonant condition of the OPO cavity (linewidth $\sim$8 MHz) to the two frequencies is identified by monitoring the parametric gain of an auxiliary beam from a diode laser at 852 nm which is locked ($\pm$0.3 MHz) to the $6S_{1/2} \rightarrow 6P_{3/2}$ resonance.

The output from the OPO is focused with a waist of $\sim$10 μm onto Cesium atoms in a magneto-optic trap (MOT) [7], which has a diameter of $\sim$200 μm. The population of the upper excited state ($6D_{5/2}$) is measured by observing the fluorescence at 917 nm ($6D_{5/2} \rightarrow 6P_{3/2}$) with an avalanche photodiode. By chopping the trapping beams of the MOT at 4 kHz, we measure two counting rates R_1 and R_2, the rates with the trapping beams on and off, respectively. Since the trapping beams provide appreciable population of $6P_{3/2}$, R_1 provides a measure of the incident photon flux at 917 nm, while R_2 is proportional to the two-photon excitation rate driven by the squeezed vacuum field at 852 nm and 917 nm.

Since the counting rate R_2 is very small ($\leq 1\ s^{-1}$) in the region of interest, special care has been taken to eliminate and to determine accurately residual backgrounds. We used two different techniques to measure the background for a particular run. First, the magnetic field for the MOT is switched off thus eliminating the trap. Second, an interference filter is placed to block the 852 nm beam thus eliminating the two-photon transition. In both cases, no difference in results is discerned within an accuracy of $\pm$0.1/s, indicating that there are no systematic offsets in the background levels within the precision of our data.

3 Results and Discussion

We have performed several individual runs of the experiment, each of which took up to 10 hours for the actual data acquisition. In Fig. 1 is shown one example of the experimental plot of R_2 vs. R_1, where (a) and (b) are taken with approximate coherent state excitation and squeezed vacuum excitation, respectively [8]. For the coherent state excitation (a), the dependence of R_2 on R_1 is well described by the simple quadratic relation, $R_2 = a'R_1^2$, with the significance level (α) of 0.86. However, for the squeezed vacuum excitation (b), the data tend to depart from the quadratic form in the low intensity region. In fact, the data for (b) are well described by a combination of quadratic and linear components, $R_2 = aR_1^2 + bR_1$, with the significance level of α=0.69, while the simple quadratic fit can be rejected because of the far smaller value of the significance level (α=0.07). In Table I, significance levels calculated for five recent experimental runs are summarized. One can see that the function $R_2 = aR_1^2 + bR_1$ produces the largest significance levels for every experimental run and that it is the only acceptable one. The existence of the linear component is consistent with the theoretical predictions [2, 3, 4, 5], which take account of the quantum correlations between the two fields (λ_1 and λ_2) of the squeezed vacuum.

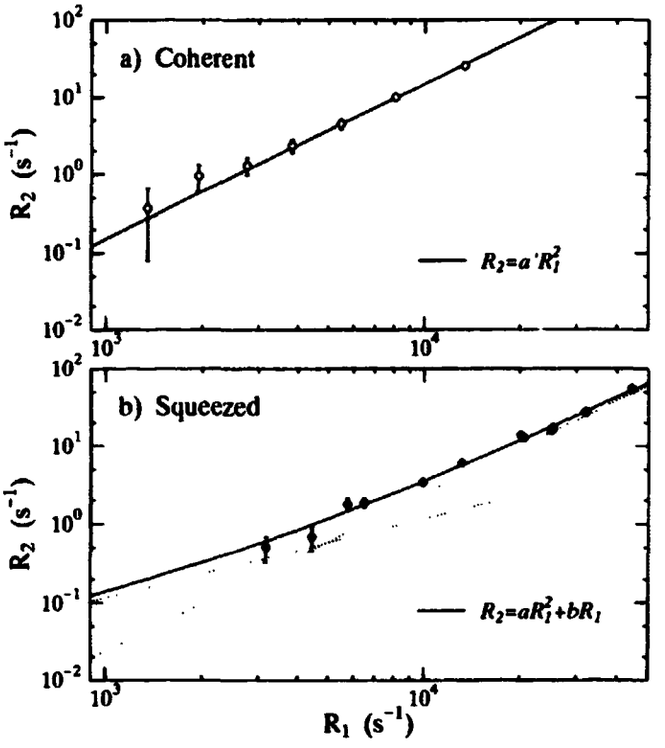

FIG. 1. Two photon excitation rate (R_2) versus excitation intensity (R_1). (a) Excitation with approximately coherent light, and (b) excitation with squeezed vacuum. Solid curves indicate the fitted functions of $R_2 = a'R_1^2$ and $R_2 = aR_1^2 + bR_1$ for (a) and (b), respectively. Dotted curves for (b) are asymptotic linear and quadratic components.

In addition to the measurement of R_1 and R_2, we also record the parametric gain (G) of the OPO at 852 nm. By using the relationship between G and R_1 (or R_2), one can deduct the "knee" position where the linear and quadratic components give equal contributions [9]. The average value of the knee position G_{knee} for five experimental runs is G_{knee}=1.36±0.09, and each value shows reasonable consistency within the statistical error. This value is to be compared with the theoretical expectation G_{knee}=1.7, which is obtained from numerical integration of the Master Equation appropriate to our system [10]. Although the measurements give somewhat smaller values and the reason for that is not clear at present [11], the agreement between the measured and theoretical values of the knee position is not unreasonable. Furthermore, the consistency of the measured values strongly indicates that the observed dependence of R_2 on R_1 is due to the properties of the light emerging from the OPO, and not to some spurious effects.

TABLE I. Significance levels for three trial functions $R_2 = aR_1^2 + bR_1$, $R_2 = a'R_1^2$, and $R_2 = a''R_1^2 + c$. (A) to (E) are the values for particular experimental runs, and (Total) for all the data scaled together as described in the text.

Experiment	$R_2 = aR_1^2 + bR_1$	$R_2 = a'R_1^2$	$R_2 = a''R_1^2 + c$
A	0.001	0.0002	0.002
B	0.69	0.07	0.44
C	0.33	0.0005	0.05
D	0.89	0.32	0.48
E	0.51	0.004	0.11
Total	0.03	2×10^{-10}	0.003

By using the simultaneous measurements of R_1, R_2, and G, one can combine all our experimental data onto a common scale, so that the measured variables (R_1, R_2, and G) fit the theoretical value by means of a least-squares minimization. As shown in Table I (Total), the experimental data thus scaled together can be fit by the function $R_2 = aR_1^2 + bR_1$, with the largest value for the significance level. Meanwhile, the fit with the functions of simple quadratic ($R_2 = a'R_1^2$) and quadratic plus constant ($R_2 = a''R_1^2 + c$) should be rejected because the significance levels for such fits are much smaller. Thus, we conclude that the experimental data do exhibit the predicted linear component of the two-photon excitation rate versus incident photon flux. We believe that the linear dependence is characteristic of the nonclassical nature of the squeezed vacuum excitation, because we can exclude the possibility of a linear dependence for classical fields in several broad cases [12].

In conclusion, we have made the first observation of a nonclassical effect on atomic excitation with a squeezed vacuum field. Our observations reveal a new regime of the field-matter interaction where the nonclassical nature of the field plays a role not heretofore realized.

Acknowledgment

We acknowledge support by the Division of Chemical Sciences, Office of Basic Energy Sciences, Office of Energy Research, U. S. Department of Energy.

References

[1] B. R. Mollow, Phys. Rev. **175**, 1555 (1968).

[2] J. Janszky and Y. Yushin, Phys. Rev. A **36**, 1288 (1987).

[3] J. Gea-Banacloche, Phys. Rev. Lett. **62**, 1603 (1990).

[4] J. Javanainen and P. L. Gould, Phys. Rev. Lett. **41**, 6247 (1991).

[5] Z. Ficek and P. D. Drummond, Phys. Rev. Lett. **43**, 6247 (1992).

[6] E. S. Polzik, J. Carri, and H. J. Kimble, Phys. Rev. Lett. **68**, 3020 (1992), Appl Phys. B **55**, 279 (1992).

[7] N. Ph. Georgiades, E. S. Polzik, and H. J. Kimble, Opt. Lett. **19**, 1474 (1994).

[8] Absolute values of the excitation rate for the squeezed vacuum and those for the coherent light should not be directly compared because of experimental difficulties in reproducing operating conditions from one run to the next.

[9] Another equivalent definition of the "knee" is the position where the slope $d(\log R_2)/d(\log R_1)$ is 1.5.

[10] A. S. Parkins, unpublished (1993-1995).

[11] Small OPO detuning is one suspected reason.

[12] N. Ph. Georgiades, E. S. Polzik, K. Edamatsu, and H. J. Kimble, to be published.

NEXT
DOCUMENT

Effects of the Stark shift on the evolution of the field entropy and entanglement in the two-photon Jaynes- Cummings model

Mao Fa Fang
Department of Physics,Hunan Normal University,
Changsha,Hunan 410081,P.R.China

Abstract

I have investigated the evolution of the field entropy in the two-photon JCM in the presence of the Stark shift and examined the effects of the dynamic Stark shift on the evolution of the field entropy and entanglement between the atom and field.My results have shown that the dynamic Stark shift plays an important role in the evolution of the field entropy in two-photon processes.

1 Introduction

The two-photon Jaynes-Cummings model [1] describing the interaction of a single-mode quantized field with a two-level atom through intermediate state involving the emission or absorption is one of the most intensively studied models in quantum optics . In this model, when the two atomic levels are couple with comparable strength to the intermediate relay level,the Stark shift becomes significant and cannot be ignored [2-5]. Puri and Bullough [3], A.Josh [4], Tahira Nasreen and Razmi [5] studied the influences of the Stark shift terms on the atomic inversion and dipole squeezing . Tahira Nasreen and Razmi [5,8] discussed the effect of the Stark shift on the Atomic emission and cavity field spectra in the two-photon JCM .These works have shown that the dynamic Stark shift plays an important role for the properties of dynamics in two-photon JCM . On the other hand, recently much attention has been focused on the properties of the entanglement between the field and atom in the Jaynes- Cummings model (JCM)[9-15].Phoenix and Knight [9] have shown that the partial entropy is a convenient and sensitive measure of entanglement between the atom and field . The time behavior of the field (atomic) entropy reflects time behavior of the degree of entanglement between the field and atom in JCM . The higher the entropy, the greater the entanglement,the information concerning the field is obtained by measurement performed on atoms .For the two-photon JCM, Phoenix and Knight [11], and Buzek [10] studied the evolution of the field entropy and the entanglement between the field and atom .The author [13] also examined the influence of atomic coherence on the evolution of field entropy in two-photon processes .However,these results are obtained in the case the Stark shift is ignored .In this paper,to make the two-photon JCM closer to the experimental realization,I include the effect of the dynamic Stark shift in studying the evolution of field entropy and entanglement . The results for the entropy evolution and entanglement incorporating the Stark shift are radically different from the results obtained in the absence of the Stark shift.

2 The reduced density operator and the field entropy calculation formalism for two-photon JCM in the presence of the Stark shift

In this paper, the model considered consists of a single-mode cavity field of frequency ω with an effective two-level atom of transition frequency ω_0 through two-photon transitions in a lossless cavity. The excited and ground states of the atom will be designated by $|+\rangle$ and $|-\rangle$, respectively . I assume these states to have identical parity, whereas the intermediate states, labeled $|j\rangle$ (j=3,4,...), are coupled to $|+\rangle$ and $|-\rangle$ by a direct dipole transition and so located as to give rise to a significant Stark shift. The effective Hamiltonian describing such a model has form [3]

$$\widehat{H}_{eff} = \omega\hat{a}^{+}\hat{a} + \omega_0\hat{S}_z + \hat{a}^{+}\hat{a}(\beta_2|+\rangle\langle+| + \beta_1|-\rangle\langle-|) + g(\hat{a}^{+2}\hat{S}_- + \hat{a}^2\hat{S}_+), \tag{1}$$

where I have chosen units such that $\hbar = 1$. $\hat{a}^{+}$and $\hat{a}$ are the creation and annihilation operator of the cavity field; $\hat{S}_z = |+\rangle\langle+| - |-\rangle\langle-|$, $\hat{S}_+ = |+\rangle\langle-|$, and $\hat{S}_- = |-\rangle\langle+|$ are the atomic flopping operators.β_1 and β_2 are the parameters describing the dynamic Stark shift of the two levels due to the virtual transitions to the intermediate relay level,and g is the atom-field coupling constant . For simplicity ,I consider on-resonance interaction ,so that $\omega_0 = 2\omega$. By diagonalizing $\widehat{H}_{eff}$ in the manifold of states $|+,n\rangle$ and $|-,n+2\rangle$, the time-evolution operator in the interaction picture can be obtained [5]

$$\hat{U}_I(t) = \begin{pmatrix} U_{11}(n), & U_{12}(n) \\ U_{21}(n), & U_{22}(n) \end{pmatrix} , \tag{2}$$

where I have written

$$\begin{aligned} U_{11}(n) &= \sin^2(\theta_n)\exp(-i\lambda_n^{+}t) + \cos^2(\theta_n)\exp(-i\lambda_n^{-}t) \\ U_{12}(n) &= \frac{1}{2}\sin(2\theta_n)[\exp(-i\lambda_n^{+}t) - \exp(-i\lambda_n^{-}t)] = U_{21}(n) \\ U_{22}(n) &= \sin^2(\theta_n)\exp(-i\lambda_n^{-}t) + \cos^2(\theta_n)\exp(-i\lambda_n^{+}t), \end{aligned} \tag{3}$$

With

$$\begin{aligned} \sin(\theta_n) &= \frac{1}{\sqrt{2}}(1 + \frac{\xi_n}{\Omega_n})^{1/2} \\ \lambda_n^{\pm} &= g\frac{n(1+r^2)+2r^2}{2r} \pm \Omega_n \\ \Omega_n &= [g^2(n+1)(n+2) + \xi_n^2]^{1/2} \\ \xi_n &= \frac{g}{2r}[n(1-r^2) - 2r^2] \\ r &= (\beta_1/\beta_2)^{1/2}, \end{aligned} \tag{4}$$

I consider the at time t=0 the atom is in a coherent superposition of the excited and ground states

$$|\theta,\varphi\rangle = \cos(\frac{\theta}{2})|+\rangle + \exp(-i\varphi)\sin(\frac{\theta}{2})|-\rangle \quad , \tag{5}$$

and the field is an arbitrary superposition of Fock states,so that at time t=0 the density operator for system

$$\rho(0) = \sum_{n=0}^{\infty}\sum_{m=0}^{\infty} F_{n,m}\{\cos(\frac{\theta}{2}) \mid +,n\rangle + \exp(-i\varphi)\sin(\frac{\theta}{2}) \mid -,n\rangle\}$$
$$\times\{\cos(\frac{\theta}{2})\langle m,+ \mid + \exp(i\varphi)\sin(\frac{\theta}{2})\langle m,- \mid\}. \quad (6)$$

where θ is the degree of excitation, φ is the relative phase of the two atomic levels,$F_{n,m} = F_n F_m^*$ and F_n are coefficients in the Fock- state. At any time $t > 0$ the reduced field density operator for the system is given by

$$\rho_f(t) = Tr_{atom}\{\hat{U}_I(t)\rho(0)\hat{U}_I^{\dagger}(t)\}$$
$$= \cos^2(\frac{1}{2}\theta)\sum_{n=0}^{\infty}\sum_{m=0}^{\infty} F_{n,m}\{U_{11}(n)U_{11}^*(m) \mid n\rangle\langle m \mid + U_{21}(n)U_{21}^*(m) \mid n+2\rangle\langle m+2 \mid\}$$

$$+\frac{1}{2}\sin(\theta)\exp(i\varphi)\sum_{n=0}^{\infty}\sum_{m=0}^{\infty} F_{n,m}\{U_{11}(n)U_{12}^*(m-2) \mid n\rangle\langle m-2 \mid$$
$$+U_{21}(n)U_{22}^*(m-2) \mid n+2\rangle\langle m \mid\}$$

$$+\frac{1}{2}\sin(\theta)\exp(-i\varphi)\sum_{n=0}^{\infty}\sum_{m=0}^{\infty} F_{n,m}\{U_{12}(n-2)U_{11}^*(m) \mid n-2\rangle\langle m \mid$$
$$+U_{22}(n-2)U_{21}^*(m) \mid n\rangle\langle m+2 \mid\}$$

$$+\sin^2(\frac{1}{2}\theta)\sum_{n=0}^{\infty}\sum_{m=0}^{\infty} F_{n,m}\{U_{22}(n-2)U_{22}^*(m-2) \mid n\rangle\langle m \mid$$
$$+U_{21}(n-2)U_{22}^*(m-2) \mid n-2\rangle\langle m-2 \mid\}. \quad (7)$$

The reduced density matrix Equation (7) has included the influences of the Stark shift and atomic coherence .Following the work of Phoenix and Knight [9],the eigenvalues and eigenstates of the reduced field density operator Equation (7) may be obtained

$$\pi_f^{\pm}(t) = \langle U_{11}'^{\dagger}U_{11}'\rangle \pm \exp(\mp\delta) \mid \langle U_{11}'^{\dagger}U_{21}'\rangle \mid$$
$$= \langle U_{21}'^{\dagger}U_{21}'\rangle \pm \exp(\pm\delta) \mid \langle U_{11}'^{\dagger}U_{21}'\rangle \mid, \quad (8)$$

$$\mid \psi_f^{\pm}(t)\rangle = \frac{1}{\sqrt{2\pi_f^{\pm}(t)\cosh(\delta)}}\{\exp[\frac{1}{2}(i\xi \pm \delta)] \mid U_{11}'\rangle \pm \exp[-\frac{1}{2}(i\xi \pm \delta)] \mid U_{21}'\rangle\} \quad . \quad (9)$$

where

$$\mid U_{11}'\rangle = \cos(\frac{1}{2}\theta)\sum_{n=0}^{\infty} F_n U_{11}(n) \mid n\rangle + \sin(\frac{1}{2}\theta)\exp(-i\varphi)\sum_{n=0}^{\infty} F_n U_{12}(n-2) \mid n-2\rangle,$$

$$| U'_{21}\rangle = \cos(\frac{1}{2}\theta)\sum_{n=0}^{\infty} F_n U_{21}(n) \mid n+2\rangle + \sin(\frac{1}{2}\theta)\exp(-i\varphi)\sum_{n=0}^{\infty} F_n U_{22}(n-2) \mid n\rangle.$$

$$\chi = \frac{1}{2 \mid \langle U'^{\dagger}_{11} U'_{21}\rangle \mid}[\langle U'^{\dagger}_{11} U'_{11}\rangle - \langle U'^{\dagger}_{21} U'_{21}\rangle], \tag{10}$$

$$\delta = sinh^{-1}(\chi). \tag{11}$$

I can obtained calculation formalism of the field entropy $S_f(t)$ in terms of the eigenvalue $\pi_f^{\pm}$ of the reduced field density operator

$$S_f(t) = -[\pi_f^+(t) ln \pi_f^+(t) + \pi_f^-(t) ln \pi_f^-(t)]. \tag{12}$$

The field entropy $S_f(t)$ given by Equation (12) shows that the field entropy depends not only on the field statistics parameters $F_{n,m}$,but also on the Stark shift parameter $r = (\beta_1/\beta_2)^{1/2}$ and the initial state of atom. Especially wh $\beta_1 = \beta_2 = 0$,Eq(12) give the results of Refs[11-13] for K=2.

3 Numerical results

I now discuss the numerical results for the field entropy $S_f(t)$ is given by Equation (17) when the initial field state is in the coherent state $| \alpha\rangle$

$$F_{n,m} = \exp(- \mid \alpha \mid^2)\alpha^n \alpha^{*m}/(n!m!)^{1/2}. \tag{13}$$

with $\alpha = \mid \alpha \mid \exp(i\beta)$ and $\mid \alpha \mid^2 = \bar{n}$, where β is the initial phase of the field and $\bar{n}$ is the average number of photons in the coherent state. Here I hope to learn about the roles played by the Stark shift . The numerical results of equation (12) are show in Figs.1-3 for different values of the Stark shift parameter r and different the initial states of the atom with $\bar{n} = 20$.
; **Figure1** Figs.1 Effects of the Stark shift on the evolution of the field entropy. $\theta = 0$,atom initially in excite state,field in the coherent state with mean photon numbers $\bar{n} = 20$,(a),no Stark shift ($\beta_1 = \beta_2 = 0$);(b),$r = 1(\beta_1 = \beta_2)$;(c),$r = 0.5$; (d),$r = 0.3$
; **Figure2** Figs.2 Effects of the Stark shift on the evolution of the field entropy. $\theta = \pi/2$, $\varphi - 2\beta = 0$,atom initially in trapping state, the rest parameters as Figs.1. (a),no Stark shift ($\beta_1 = \beta_2 = 0$); (b),$r = 1(\beta_1 = \beta_2)$;(c),$r = 0.5$;(d),$r = 0.3$; **Figure3** Figs.3 Effects of the Stark shift on the evolution of the field entropy. The same as Figs.2 but $\varphi - 2\beta = \pi/2$. (a),no Stark shift ($\beta_1 = \beta_2 = 0$); (b),$r = 1(\beta_1 = \beta_2)$;(c),$r = 0.5$;(d),$r = 0.3$ **3.1 Atom Initially in the excited state** In Figs.1(a),I have the case $\theta = 0$ (i.e. the atom is in the excited state) and $\beta_1 = \beta_2 = 0$(i.e. in the absence of the Stark shift),corresponding to the evolution of the field entropy in the standard two-photon JCM obtained by Ref[11-13].I note that the field entropy evolves at periods π/g,when $t = n\pi/g, (n = 0, 1, 2, 3...)$, $S_f(t)$ evolves to the zero values and the field is completely disentangled with the atom, while when $t = (n + 1/2)\pi/g$. $S_f(t)$ evolves to the maximum value,and the field is strongly entangled with the atom . The results for the evolution of the field entropy $S_f(t)$ in the presence of the Stark shift are plotted in Figure 1(b)-(d). In Figs.1(b),the Stark shift parameter r is given as 1(namely $\beta_1 = \beta_2$), this correspond to the case the two levels of the atom are equally strongly couple with the intermediate relay level . By making a comparison between Figs.1(a)

and Figs.1(b), I find that the evolution of the entropy is almost similar for both cases. This result corresponds with the fact that in two-photon processes,the Stark shift creates an effective intensity dependent detuning $\Delta_N = \beta_2 - \beta_1$[16].When $r = 1.0$, (namely $\beta_1 = \beta_2$)thus $\Delta_N = 0.0$, the Stark shift does not affect the time evolution of the field entropy . In Figs.1(c),I show the case r=0.5,in which the two levels have the unequal Stark shifts ($\beta_1 < \beta_2$).I note that the Stark shift leads to decreasing the values of maximum field entropy and increasing the values of field minimum entropy .It also results in increasing frequency of the field entropy vibration . As the parameter r further decreased (e.g.,r=0.3,see Figs.1(d)), the values of the maximum field entropy and the degree of entanglement of the field-atom further reduced . **3.2 Atom initially in the superposition states** When $\theta = \pi/2$ and $\varphi - 2\beta = 0$, the atom is initially in trapping state, the evolution of the field entropy are plotted in Figs.2 . Figs.2(a) show the evolution of the field entropy in the absence of the Stark shift while Figs.2(b) show the case that r=1.0 .I can see that under the condition the atom is initially in trapping state,the field entropy obviously reduced with comparison Figs.1 (a),(b) in where the atom is initially in excited state, and the evolution of field entropy in the case r=1.0 is almost same as that in the absence of the Stark shift .Figs.2(c) and Figs.2(d) show the evolution of $S_f(t)$ in two cases that r=0.5 and r=0.3,respectively. As is visible from the figures, the effects of the dynamic Stark shift are more pronounced when r deviates from unity .On the other hand,when atom in initially trapping state,as r decreased,the values of maximum field entropy increased, indicating that the Stark shift leads to increasing the degree of entanglement between the field and atom, which is contrary to the case the atom is initially excited state . The results for the evolution of the field entropy $S_f(t)$ as $\theta = \pi/2$, $\varphi - 2\beta = \pi/2$ and various values of Stark shift parameter r are presented in Figure 3 .In these cases, I note that the maximum field entropy always remains at its maximum values, regardless of the chosen value of r . A possible explanation for above behavior of field entropy evolution can be performed in terms of the Bloch vector in semiclassical theory [17] in the next section .

4 Semiclassical interpretation of the evolution behavior of the field entropy

I can find that the larger the extent of the Bloch vector's motion,the greater the values of the maximum field entropy by examining the evolution of field entropy in semiclassical version . By replacing the field annihilation operator a by the c number $v = \sqrt{\bar{n}}\exp[i(\omega t - \beta)]$ I get semiclassical version of eq.(1)

$$\begin{aligned} H_{eff} &= \bar{n}\omega + \omega_0 S_z + \bar{n}(\beta_2 \mid +\rangle\langle + \mid + \beta_1 \mid -\rangle\langle - \mid) \\ &+ \bar{n}g(S_+ \exp[-i2(\omega t - \beta)] + S_- \exp[i2(\omega t - \beta)]) . \end{aligned} \tag{14}$$

The motion equations of operators $S_\xi(\xi = +, -, z)$can be written

$$\frac{dS_+}{dt} = i\omega_0 S_+ - i2g\bar{n}\exp[i2(\omega t - \beta)]S_z + i\bar{n}\Delta_N S_+ , \tag{15}$$

$$\frac{dS_-}{dt} = -i\omega_0 S_- + i2g\bar{n}\exp[-i2(\omega t - \beta)]S_z - i\bar{n}\Delta_N S_- , \tag{16}$$

$$\frac{dS_z}{dt} = ig\bar{n}(\exp[i2(\omega t - \beta)]S_- - \exp[-i2(\omega t - \beta)]S_+) , \tag{17}$$

where

$$\Delta_N = \beta_2 - \beta_1 = \frac{g(1-r^2)}{r} . \tag{18}$$

is an effective detuning created by the Stark shift . Define the two slowly varying operators which involve the coherence between the two atomic states

$$S_x = \frac{1}{2}\{\exp[-i(\omega_0 t - \Phi)]S_+ + \exp[i(\omega_0 t - \Phi)]S_-\} , \tag{19}$$

$$S_y = \frac{1}{2i}\{\exp[-i(\omega_0 t - \Phi)]S_+ - \exp[i(\omega_0 t - \Phi)]S_-\} . \tag{20}$$

where Φ is a phase angle that may be chosen at will . The atom interacting with the field obeys the optical Bloch equation

$$\frac{d\mathbf{S}(t)}{dt} = \mathbf{\Omega}_s(t) \times \mathbf{S}(t). \tag{21}$$

Where S(t) is the Bloch vector for the atom

$$\mathbf{S}(t) = \{S_x(t), S_y(t), S_z(t)\} . \tag{22}$$

and $\mathbf{\Omega}_s(t)$ is the driving field vector,which can be written by using eqs.(14)-(22)

$$\mathbf{\Omega}_s(t) = \{2g\bar{n}\cos[(2\omega - \omega_0)t - (2\beta - \Phi)], 2g\bar{n}\sin[(2\omega - \omega_0)t - (2\beta - \Phi)], \bar{n}\Delta_N\} . \tag{23}$$

Generally $\mathbf{S}(t)$ precesses in a cone about $\mathbf{\Omega}_s(t)$. The extent of Bloch vector's motion is largest when $\mathbf{S}(t)$ and $\mathbf{\Omega}_s(t)$ are orthogonal and minimum when $\mathbf{S}(t)$ and $\mathbf{\Omega}_s(t)$ are parallel or antiparallel.Thus the time evolution of the Bloch vector is quite different for different initial preparations. If the atom is initially coherent superposition state given by eq(5), the Bloch vector at time t=0 can be expressed [17]

$$\mathbf{S}(0) = \{\frac{1}{2}\sin(\theta)\cos(\Phi - \varphi), \frac{1}{2}\sin(\theta)\sin(\Phi - \varphi), \frac{1}{2}\cos(\theta)\} , \tag{24}$$

$$\mathbf{\Omega}_s(0) = \{2g\bar{n}\cos(\Phi - 2\beta), 2g\bar{n}\sin(\Phi - 2\beta), \bar{n}\Delta_N\} . \tag{25}$$

For simplicity,I let $\Phi = \varphi$,the initial Bloch vector in this case is on the x-z plane. When the atom is initially in excite state ($\theta = 0$),the initial Bloch vector $\mathbf{S}(0) = \{0, 0, \frac{1}{2}\}$ and the vector $\mathbf{\Omega}_s(0) = \{2g\bar{n}, 0, \bar{n}\Delta_N\}$. Under this condition,the extent of Bloach vector's motion is dependent of the effective detuning Δ_N created by the Stark shift . When $\beta_1 = \beta_2 = 0$ (in the absence of the Stark shift) or $r = 1.0(\beta_1 = \beta_2)$, $\Delta_N = 0$, the vector S(0) and $\mathbf{\Omega}_s(0)$ are orthogonal and the extent of Bloach vector is the maximum for these two cases so that the maximum field entropy always remains at its maximum value and the degree of the entanglement of atom-field is the largest (see Figs.1(a) and (b)). With r reduced,Δ_N increased,S(0) and $\mathbf{\Omega}_s(0)$ are no longer orthogonal and the extent of Bloach vector's motion is reduced .This leads to the values of the maximum field entropy and the degree of entanglement of atom-field decreased as the Stark shift parameter r reduced under the condition the atom is initially in excite state . When the atom is initially trapping state (namely $\theta = \frac{\pi}{2}, \varphi - 2\beta = 0$),Bloach vector $\mathbf{S}(0) = \{\frac{1}{2}, 0, 0\}, \mathbf{\Omega}_s(0) = \{2g\bar{n}, 0, \bar{n}\Delta_N\}$.The motion extent of $\mathbf{S}(t)$ is also dependent of the effective detuning Δ_N . When

$\beta_1 = \beta_2 = 0$ (in the absence of the Stark shift) or $r = 1.0(\beta_1 = \beta_2)$, $\Delta_N = 0.0$ and the vector **S(0)** is parallel to $\Omega_s(0)$,the motion extent of the $S(t)$ tends to zero,and the values of the maximum field entropy obviously reduced (see Figs.2(a),(b). With parameter r decreased,Δ_N increased and the vector **S(0)** and $\Omega_s(0)$ are no longer parallel . The greater the effective detuning Δ_N (the smaller the parameter r), the larger the extent of the $S(t)$,this leads to the values of maximum field entropy and the degree of entanglement of the atom-field increased as parameter r decreased (see Figs.2(c),(d)) under the atom is initially in trapping state . Furthermore,when $\theta = \pi/2$,relative phase $\varphi - 2\beta = \pi/2$ is chosen,$S(0) = \{\frac{1}{2}, 0, 0\}, \Omega_s(0) = \{0, 2g\bar{n}, \bar{n}\Delta_N\}$ are completely orthogonal irrespective of values of Δ_N . Therefore,at this case,the extent of $S's$ motion and the values of maximum field entropy are independent of the influences of the Stark shift, and are maximum at all(see Figs.3(a)-(d)).

Acknowledgments

The author thanks the Natural Science Foundation of China for support .

References

[1] C.V.Sukumar and B.Buck,Phys.Lett.A **83**,211 (1981).

[2] Alsingh,P.,and M.S.Zubairy,J.Opt.Soc.Am.B **4**,177 (1987).

[3] Puri,R.R.,and R.K.Bullough,J.Opt.Am.B **5**,2021 (1088).

[4] A.Josh and R.R.Puri,J.Mod.Opt **36**,215 (1989).

[5] Tahira Nasreen and M.S.K.Razmi,J.Opt.Soc.Am.B **8**,2303 (1991). Phys.Rev.A **46**,4161 (1992).

[6] I.Ashraf and M.S.Zubairy,Opt.Commun **77**,85 (1990).

[7] S.-C.Gou,Phys.Lett.A **147**,218(1990).

[8] Tahira Nasreen and M.S.K.Razmi,J.Opt.Soc.Am.B **10**,1292 (1993), **11**,386 (1994).

[9] S.J.D.Phoenix and P.L.Knight,Ann.Phys.(N.Y),**186**,381 (1988). Phys.Rev.A **44**,6023 (1991).

[10] V.Buzek,H.Moya-Cessa,and P.L.Knight,Phys.Rev.A **45**,8190 (1992).

[11] S.J.Phoenix and P.L.Knight,J.Opt.Soc.Am.B **7**,116 (1990).

[12] P.L.Knight and B.W.Shore,Phys.Rev.A **48**,642 (1993),V.Buzek and B.Hladky,J.Mod.Opt **40**,1309 (1993).

[13] M.F. Fang,and G.H.Zhou,Phys.Lett.A **184**,397 (1994).

[14] M.F. Fang,J.Mod.Opt 41(1994)1319,Acta Physica Sinica **43**,1776 (1994),**13**,799 (1994).

[15] M.F. Fang, and P.Zhou,Acta Physica Sinica,**43**,570 (1994), Acta Optica Sinica **13**,799 (1993),**14**,475(1994).

[16] H.I.Yoo and J.H.Eberly,Phys.Rep.**118**,241 (1985).

[17] D.Grischkowsky, and M.M.T.Loy,Phys.Rev.A **12**,2514 (1975). P.Zhou,Z.L.Hu and J.S.Peng,J.Mod.Opt.**39**,49 (1992).

The figure captions

Figs.1 Effects of the Stark shift on the evolution of the field entropy. $\theta = 0$,atom initially in excite state,field in the coherent state with mean photon numbers $\bar{n} = 20$,(a) no Stark shift ($\beta_1 = \beta_2 = 0$);(b),$r = 1(\beta_1 = \beta_2)$;(c),$r = 0.5$;(d),$r = 0.3$

Figs.2 Effects of the Stark shift on the evolution of the field entropy. $\theta = \pi/2$, $\varphi - 2\beta = 0$,atom initially in trapping state, the rest parameters as Figs.1. (a),no Stark shift ($\beta_1 = \beta_2 = 0$); (b),$r = 1(\beta_1 = \beta_2)$;(c),$r = 0.5$;(d),$r = 0.3$

Figs.3 Effects of the Stark shift on the evolution of the field entropy. The same as Figs.2 but $\varphi - 2\beta = \pi/2$. (a),no Stark shift ($\beta_1 = \beta_2 = 0$); (b),$r = 1(\beta_1 = \beta_2)$;(c),$r = 0.5$;(d),$r = 0.3$

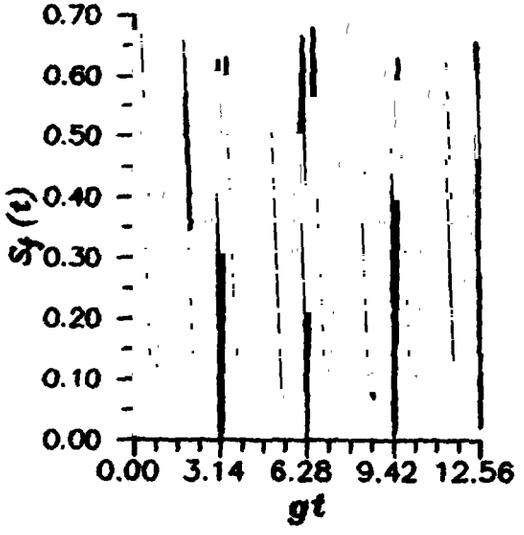
0.70
0.60
0.50
0.40
0.30
0.20
0.10
0.00
Sf (t)
0.00 3.14 6.28 9.42 12.56
gt

(a)

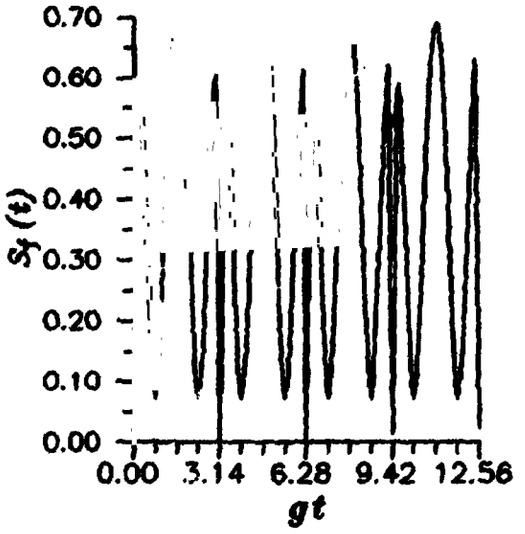
0.70
0.60
0.50
0.40
0.30
0.20
0.10
0.00
Sf (t)
0.00 3.14 6.28 9.42 12.56
gt

(b)

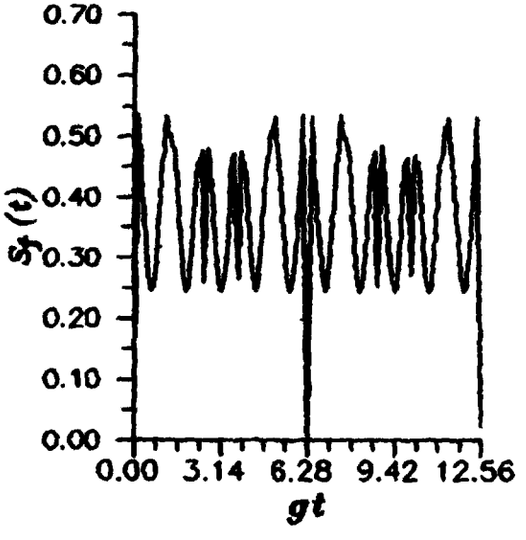
0.70
0.60
0.50
0.40
0.30
0.20
0.10
0.00
Sf (t)
0.00 3.14 6.28 9.42 12.56
gt

(c)

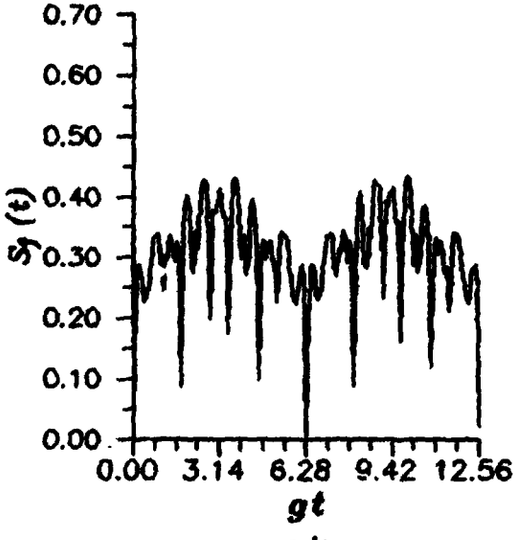
0.70
0.60
0.50
0.40
0.30
0.20
0.10
0.00
Sf (t)
0.00 3.14 6.28 9.42 12.56
gt

(d)

Figs. 1

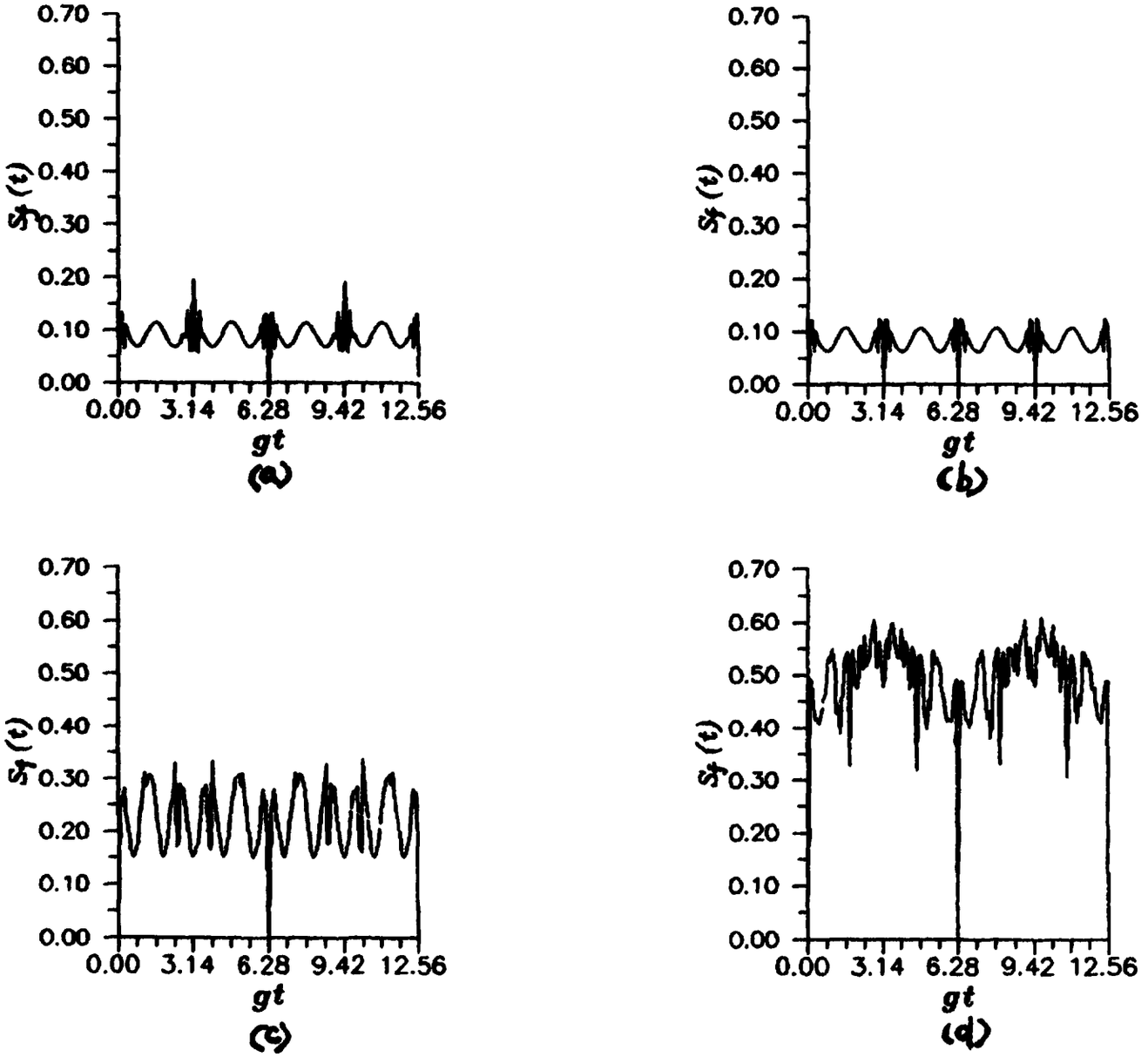

Figs. 2

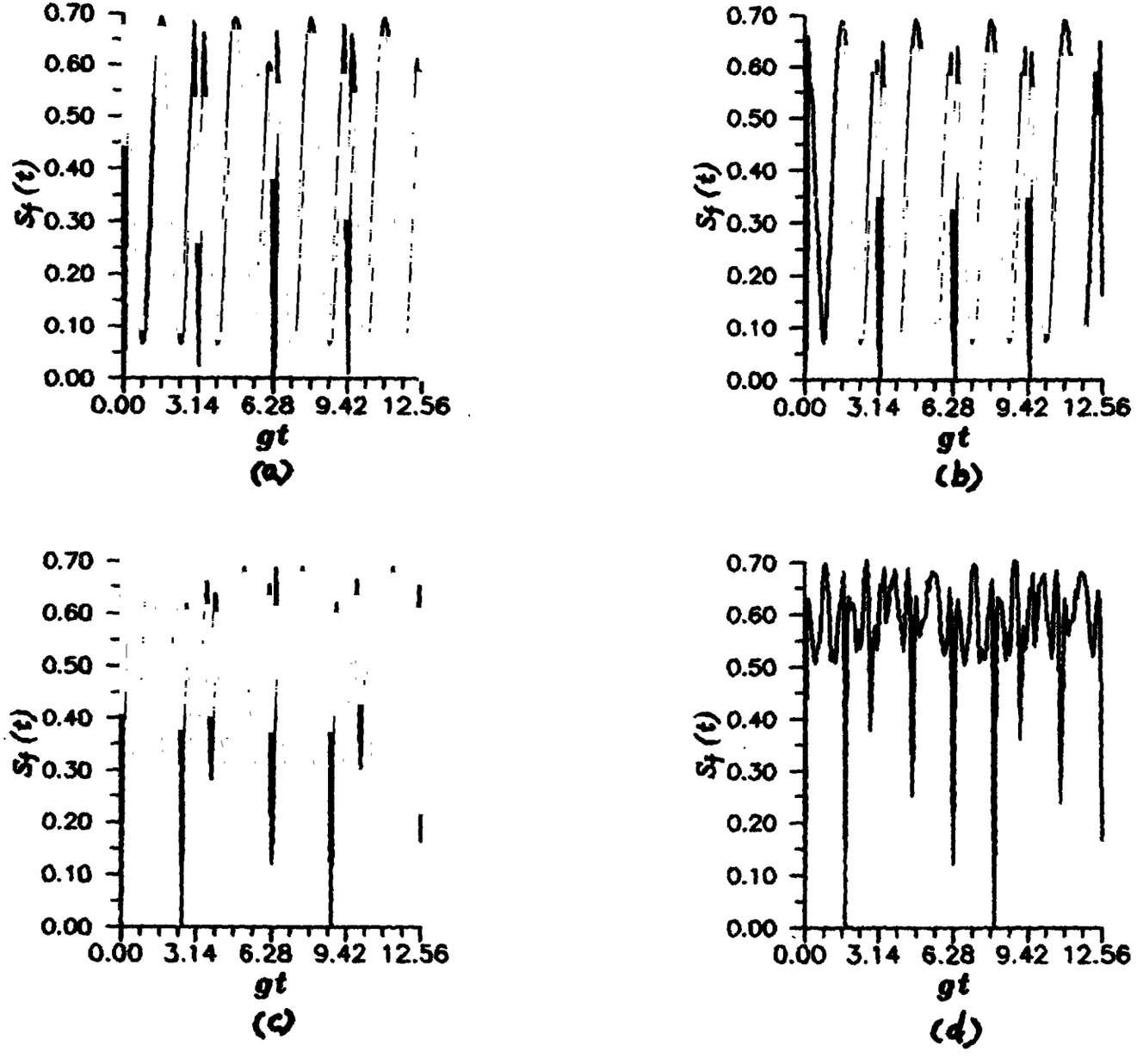

Figs.3

NEXT
DOCUMENT

Experimental Observation of Thermal Self- Modulation in OPO

Jiangrui Gao Hai Wang Changde Xie Kunchi Peng
Institute of Opto-Electronics, Shanxi University, Taiyuan, P.R.China

Abstract

The thermal self-modulation has been observed experimentally via SHG in OPO. the threshold pump power for the thermal self- modulation is much smaller than that of the nonlinear self-pulsing. The thermal effect prevent from realizing the theoretical prediction for the self-pulsing.

PACS numbers: 42.65.Ky

1 Introduction

In recent years the interest in the continuous optical parametric oscillators (OPO's) has been renewed because of their ability to generate nonclassical states of light efficiently[1,2]. The bright amplitude squeezed light have been produced from the single and double resonant OPO's through second-harmonic generation (SHG)[3,4]. Due to technical problem, especially thermal instibility, the double resonance system was not stable[4]. Therefor it is necessary to study the thermal effects in OPO's

In 1978 K.J.McNell et. al. predicted the self-pulsing behaviour in the intensity of the second harmonic mode for sufficient strong coherent input to the fundamental mode[5]. Plenty of theoretical papers in this subject has been published but so far there is no experimental result to be presented to our knowledge. We designed a ring OPO tc realize self-pulsing experimental. Although a similar intensity modulation phenomenon between the second harmonic mode and the fundamental mode has been observed the oscillation period was totally different with that pr ted by McNell et. al.. The theoretical analyses showed that the intensity modulation record . . us derived from the thermal effect in the nonlinear crystal. We named it thermal self-mc .ation. The thermal self-modulation effect n be explained by means of the phase mis-matching of SHG during the crystal temperature rising due to the absorption. O ur experimer points out that the threshold of the thermal self-modulation is much lower than that of the self-pulsing giving in ref.[5] for the crystals with the large absorption to the second harmonic wave such as $LiNbO_3$. The thermal effect prevents from demonstrating experimentally to the nonlinear self-pulsing predictions. This might be the reason of that why the experimental observation has not been finished untill now. In this paper we shall present the experimental results of the thermal self-modulation and compare the threshold power of the thermal self-modulation with that of the nonlinear self- pulsing.

2 Experimental set-up and result

We designed a ring OPO cavity to prevent the laser source from being desturbed by the feedback light. The pump source is a frequency- stablized cw ring $Nd:YAG$ laser. The output power of $1.06\mu m$ wavelength up to $3W$ can be available. The experimental scheme is showen in Fig.1.

Fig.1

The OPO consists of four mirrors: M_1 and M_2 are the input and output couplers respectively with the curvature radiis of $20mm$ and $50mm$, M_3 and M_4 are the plane mirror with high reflectivty for both fundamental and second harmonic waves. The total length of ring cavity is $15cm$. The transmissivity of input coupler M_1 for the fundamental wave is $T_{1.06} = 4\%$ and it is highly reflective for harmonic wave. The output coupler M_2 is highly reflective for both waves. A $MgO:LiNbO_3$ of size $5 \times 5 \times 25cm$ was used as the nonlinear crystal for SHG. The crystal was placed on the common curvature centre of M_1 and M_2. A half wave plate HP placed front M_1 was used to align the polarization of the input pump light for optimum phase-matching. A beam splitter S following M_2 separated the leakage light from M_2 to two parts of $1.06\mu m$ and $0.53\mu m$ wavelengths. The detectors D_1 and D_2 respectively received the second harmonc wave ($0.53\mu m$) and the fundamental wave ($1.06\mu m$), then their power were analysed with the oscillascope (OS). The experimentally measured finesses of the OPO are 103 for $1.06\mu m$ wave and 136 for $0.53\mu m$ SH.

When the pump power were lower than $2.4W$ the increases of pump power results in the increase of SH power as usual. Once the pump power were over $2.4W$ the transmission curve of pump power presented the M-type (see Fig. 2).

Fig.2

The peak of SH wave was corresponding with the dip of M-type curve for the fundamental wave. Raising the pump power continuously when input power is over $2.7W$ the intensity modulation phenomena between the second harmonic mode and the fundamental mode were observed. The Fig. 3 (a) and (b) are the recorded experimental modulation curves at the pump power of $2.7W$ and $3W$. The period of modulation is about the order of millisecond. During recording this curves the cavity of OPO was locked in the pump frequency. By controlling the temperature of the crystal the cavity operated in near double resonant situation.

Fig.3

3 Discussion to the experimental results

The period of modulation (mS) in above experimental curve is 3 orders longer than that predicted by K.J.McNell et. al. (μS)[5]. Therefor they are totally different phenomena. Usually the thermal response time is at the order of millisecond. We consider that the observed intensity modulation derived from thermal effect. The absorptivity of the crystal used in our experiments for SH wave is $\alpha^{ab}_{0.53} = 0.012/cm$ which is much higher than that for the fundamental wave, so that the absorption

for $1.06\mu m$ wave can be neglected, i.e. the crystal is heated up only through the absorption to SH wave. Due to that the refractive indexes n_o and n_e of crystal are the function of temperature, the heating up of crystal must result in the phase mis-match then the intensity of SH wave decreases and that of the fundamental wave increases. During the reduction of SH intensity the temperature of crystal drops down. When the temperature return to the phase matching point, the intensity of SH wave restores to the maximum. The temperature change between phase mis-matching and matching point results in the thermal self-modulation.

Based on experiment observation we calculated the critical temperature rising ΔT_{crit} and the phase mis-matching (Δk) for the thermal self-modulation. The nonlinear equation of motion for the slowly varying amplitudes α_1 and α_2 of the fundamental and the second harmonic waves in OPO are written as follows:

$$\dot{\alpha}_1 = -\gamma_1\alpha_1 + G_0\alpha_1\alpha_2 + E \tag{1}$$

$$\dot{\alpha}_2 = -\gamma_2\alpha_2 - \frac{1}{2}G_0\alpha_1^2 \tag{2}$$

where γ_1, γ_2 are the cavity damping rates for α_1 and α_2 modes. E is the pump parameter corresponding to the power of the coherent driving field. G_0 is the coupling coefficient at perfect phase matching. For our system $\gamma_1 = 7 \times 10^7$, $\gamma_2 = 4 \times 10^7$ and $G_0 = 57.15$. Substituting above parameters into eqs. (1) and (2) and taking $2.7W$ as the critical pump power we get the intracavity intensity of SH wave with which the thermal self- modulation starts. If the absorbed power of SH wave per unit volume is q the temperature rising at the radius r in the *Gaussian* beam due to the absorption is expressed as:

$$\Delta T_r = \frac{q\omega_0^2}{4k_c}\exp\left(\frac{-r^2}{\omega_0^2}\right) \tag{3}$$

k_c is the thermal conducttivity of crystal, ω_0 is the spot size of the SH beam in crystal. Integreting ΔT_r through the beam spot we obtain the average temperature rising $\overline{\Delta T}$:

$$\overline{\Delta T} = \frac{1}{\pi\omega_0^2}\int_0^{\omega_0} \Delta T_r 2\pi r\, dr = 0.63\Delta T_0 \tag{4}$$

ΔT_0 is the temperature rising at the centre of beam ($r = 0$). The phase mis-matching (Δk) resulting from the temperature rising is equal to:

$$\Delta k = \frac{4\pi}{\lambda}\Delta T_r\left(\frac{dn_\omega^e}{dT} - \frac{dn_{2\omega}^o}{dT}\right) \tag{5}$$

here λ is the wavelength of fundamental wave, $\frac{dn^o}{dT}$ and $\frac{dn^e}{dT}$ are the temperature coefficients of refractive indexes respectivly for the fundamental wave with ordinary polarization and the SH wave with extraordinary polarization. For $LiNbO_3$ crystal we have [8]

$$\frac{dn_\omega^o}{dT} - \frac{dn_{2\omega}^e}{dT} = -5.9 \times 10^{-5}$$

$$k_c = 5.6W/mK$$

In our experimental system $\omega_0 = 48\mu m$, we obtain the critical temperature rising:

$$\overline{\Delta T_{crit}} = 0.03℃ \tag{6}$$

and corresponding phase mis-matching:

$$\Delta k_{crit} = 21 \tag{7}$$

Obviously the thermal effect is very sensitive.

¿From ref.[5] the nonlinear self-pulsing read:

$$| E |^2 = \frac{(2\gamma_1 + \gamma_2)^2[2\gamma_2(\gamma_1 + \gamma_2)]}{G_0^2} \tag{8}$$

$$P_{th} = \frac{\hbar\omega\Delta t}{T_{1.06}} | E |^2 \tag{9}$$

Where Δt is the round trip time in the cavity. Using above given parameters we have:

$$P_{th} = 238W \tag{10}$$

Clearly P_{th} is much large than the critical pump power for the thermal self-modulation.

4 Conclusion

The phase matching condition for SHG in OPO may be disturbed by the thermal effect. When the absorption of crystal for SH wave is large the threshold pump power for the thermal self-modulation is much lower than that for the nonlinear self-pulsing predicted in ref.[5]. For realizing experimentally the nonlinear self-pulsing the crystal with quite low absorption for both fundamental and SH waves has to be chosen. Of course the crystal must also have high nonlinear coefficient. This might be the reseaon of that the nonlinear self-pulsing has not been observed experimentally so far.

References

[1] S.F.Pereira, Min Xiao, H.J.Kimble, and J.L.Hall, Phys. Rev. A **38**, 4931 (1988).

[2] A.Heidmann, R.J.Horowicz, S.Reynaud, E.Giacobino, and C.Fabre, Phys. Rev. Lett **59**, 2555 (1987).

[3] P.Kurz, R.Paschotta, K.Fiedler, and J.Mlynek, Europhys. Lett. **24**, 449 (1993).

[4] R.Paschotta, M.Cllett, P.Kurz, K.Fiedler, H.A.Bachor and J.Mlynek, Phys. Rev. Lett. **72**, 3807 (1994).

[5] K.J.McNell, P.D.Drommond, and D.F.Walls Optics Commun. **27**, 292 (1978).

[6] M.Okada, S.Ieiri IEEE J. QE-7,469 (1971).

[7] A.Yariv, Quantum Electronics, John Wiley & Sons Inc., Second Edition (1975).

[8] M.J.Weber, CRC Handbook of Laser Sci. and Tec. CRC press Inc. (1973).

Figure Caption

Fig.1 The experimental set-up

Fig.2 The output curves of OPO at pump power $P = 2.4W$

Fig.3 The output curves of OPO at pump power (a) $P = 2.7W$, (b) $P = 3W$

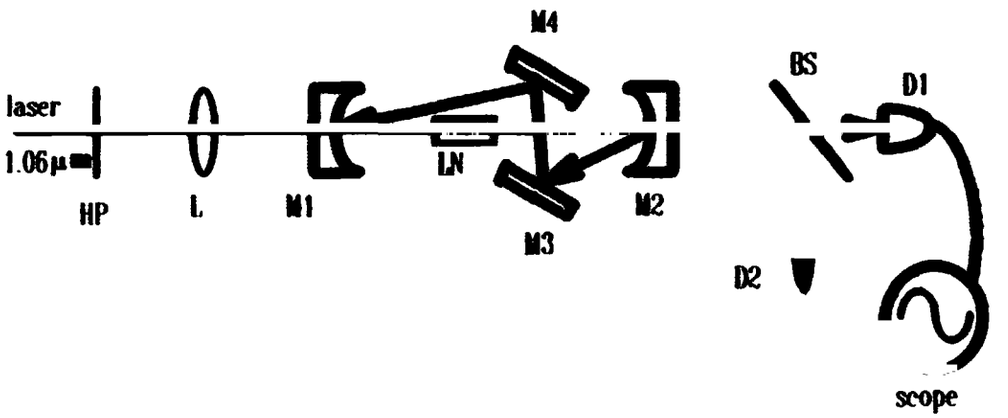

Fig. 1 Experimental Set-up

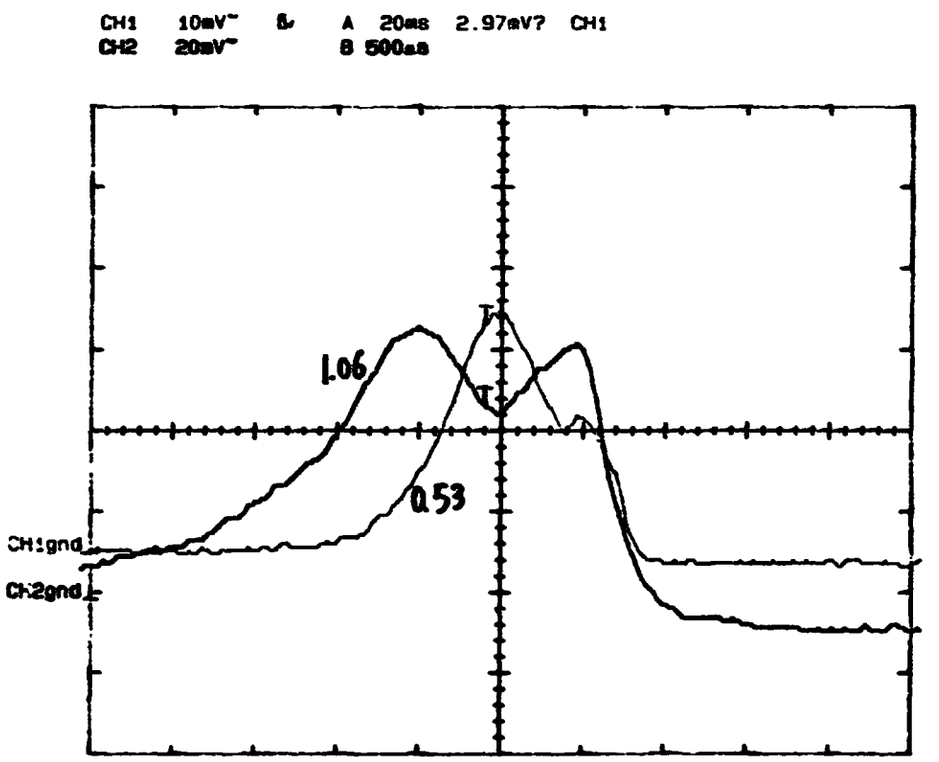
CH1 10mV~ &
CH2 20mV~
A 20ms 2.97mV?
B 500ns
CH1
1.06
0.53
CH1gnd
CH2gnd

Fig. 2

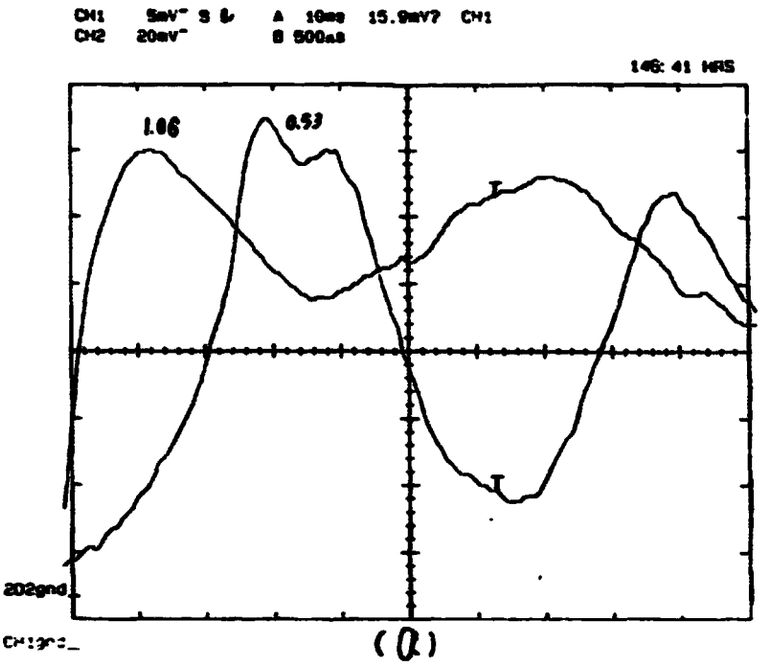
CH1 5mV⁻ S 8
CH2 20mV⁻
A 10ms 15.9mV? CH1
B 500uS
146: 41 HRS
1.06
0.53
202gnd
(a)

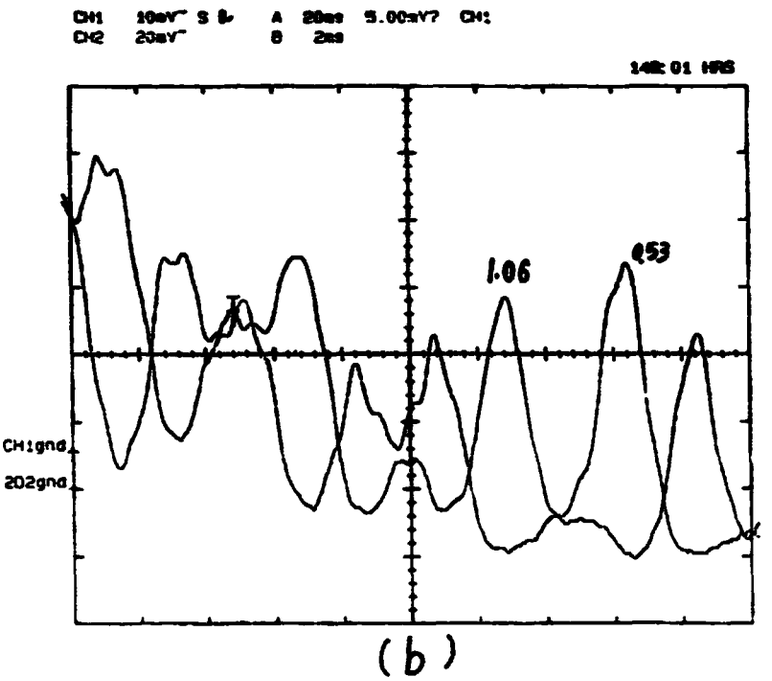
CH1 10mV⁻ S 8
CH2 20mV⁻
A 20ms 5.00mV? CH1
B 2ms
148: 01 HRS
1.06
0.53
CH1gnd
202gnd
(b)

Fig. 3

NEXT
DOCUMENT

OPTIMAL SIGNAL FILTRATION IN OPTICAL SENSORS WITH NATURAL SQUEEZING OF VACUUM NOISES

A. V. Gusev, V. V. Kulagin
Sternberg Astronomical Institute, Moscow State University
Universitetsky prospect 13, 119899, Moscow, Russia

Abstract

The structure of optimal receiver is discussed for optical sensor measuring a small displacement of probe mass. Due to nonlinear interaction of the field and the mirror a reflected wave is in squeezed state (natural squeezing) two quadratures of which are correlated and therefore one can increase signal-to-noise ratio and overcome the SQL. A measurement procedure realizing such correlation processing of two quadratures is clarified. The required combination of quadratures can be produced via mixing of pump field reflected from the mirror with local oscillator phase modulated field in dual-detector homodyne scheme. Such measurement procedure could be useful not only for resonant bar gravitational detector but for laser longbase interferometric detectors as well.

Measurement of small gravitational force acting on high quality mechanical oscillator is of great importance in modern physics. However in usual measurement scheme there is a Standard Quantum Limit (SQL) on force resolution [1] :

$$F_0 \geq F_Q = (2/\hat{\tau})(M\hbar\omega_\mu)^{1/2}, \tag{1}$$

where F_0 is force amplitude and we suppose that gravitational signal has the following form

$$F_s(t) = F_0 \sin\omega_0 t, 0 \leq t \leq \hat{\tau}, \tag{2}$$

ω_μ and M are resonant frequency and mass of probe oscillator ($\omega_\mu \approx \omega_0$) .

There are measurement procedures which allow to achieve the sensitivity larger than SQL [1, 2, 3] . For example in scheme with external squeezing of vacuum noises [2, 3] one can achieve the sensitivity

$$F_0 \geq g^{-1}F_Q,$$

where g is squeezing coefficient. In this contribution a scheme with internal (natural) squeezing is proposed for optical sensor.

Optical sensor in the most simple modification is a mirror attached to mechanical resonator and illuminated with coherent pump field. Usual schemes measuring the phase of reflected pump field (i.e. one quadrature component) have the limit of resolution of force acting on mechanical system according to (1). On the other hand reflected wave is in squeezed state (natural squeezing) due to nonlinear interaction of the field and the mirror and a coefficient of squeezing could be large

[4] . For such system two quadratures of reflected wave are correlated. One quadrature consists of the signal (gravitational displacement of mechanical oscillator) and the noise and the other only of the noise. Using correlation of noises in two quadratures one can increase signal-to-noise ratio and overcome the SQL. A photodetector in this scheme must measure linear combination of quadratures of reflected wave with weight functions rather than the phase of reflected wave. Such combination of quadratures can be produced via mixing of reflected wave with phase modulated local oscillator field.

The similar scheme was analized earlier in [5, 6] . However the modulation of local oscillator does not depend there on gravitational signal form therefore the optimal filtration procedure cannot be realized.

Let the reflection coefficient of the mirror be $r \approx 1$. The incident and reflected fields one can take in the following form:

$$\begin{aligned} E_1(x,t) &= Re(A(x,t)\exp\{j(\omega_0 t - kx)\}) \\ E_2(x,t) &= Re(B(x,t)\exp\{j(\omega_0 t + kx)\}) \end{aligned} \tag{3}$$

where $A(x,t)$ and $B(x,t)$ are complex amplitude operators of the fields ($k = (\omega_0/c)$. Let for simplicity

$$A(0,t) = A_0 + a(t) - jb(t) \tag{4}$$

where $A_0 = (2P_0 z_0/S)^{1/2}$ - amplitude of the pump with power P_0, $z_0 = 120\pi$ [ohm] - resistance of free space, S - cross section of pump beam, $a(t)$ and $b(t)$ - operators of field quadrature components with correlation matrix (we assume this field in the vacuum state)

$$\begin{aligned} &< a(t)a(t+\tau) > = < b(t)b(t+\tau) >= N_0\delta(\tau), \\ &< a(t)b(t+\tau) > = 0 \\ &N_0 = \hbar\omega_0 z_0/(2S) \end{aligned} \tag{5}$$

In linear approximation ($| kx | \ll 1$,$| a(t), b(t) | \ll A_0$) one can obtain (constant term is omitted)

$$\tilde{B}(0,t) = \tilde{B}_1(t) + j\tilde{B}_2(t) \tag{6}$$

$$\tilde{B}_1(t) = -a(t)$$

$$\tilde{B}_2(t) = b(t) + 2A_0 kG(p)(F + \lambda a) \tag{7}$$

where $G(p) = [\, M(p^2 + 2\alpha p + \omega_\mu^2)\,]^{-1}$ - mechanical oscillator transfer function, $p = d/(dt), 2\alpha = H/M, \omega_\mu^2 = K/M; \lambda = SA_0/(z_0 c), M, K$ and H are dynamical parameters of mechanical oscillator. Force $F(t)$ acting on mechanical oscillator have the following form

$$F(t) = F_s(t) + F_\mu(t), \tag{8}$$

where $F_s(t)$ is signal force and $F_\mu(t)$ is zero mean white Gaussian process with covariance function

$$< F_\mu(t)F_\mu(t+\tau) >= N_\mu\delta(\tau), \tag{9}$$

The process $F_\mu(t)$ corresponds to zero temperature thermal noise of mechanical oscillator or any other white noise.

Using eqs. (6,7) one can obtain spectral density matrix for quadrature components $\tilde{B}_1$ and $\tilde{B}_2$:

$$\begin{aligned} W_{11}(\omega) &= N_0, \qquad W_{22}(\omega) = N_0 + (2A_0k)^2(|\,G(j\omega)\,|)^2(N_\mu + \lambda^2 N_0) \\ W_{12}(j\omega) &= -N_0(2A_0k)\lambda G(j\omega), \qquad W_{12}(j\omega) = W_{21}^*(j\omega) \end{aligned} \tag{10}$$

From eq. (10) one can see that the noises in two quadrature components $\tilde{B}_1$ и $\tilde{B}_2$ have nonzero correlation $W_{12}(j\omega)$.

Optimal receiver on the base of the vector output signal $[\tilde{B}_1(t), \tilde{B}_2(t)]^T$ must construct a following functional [7] (time of observation $0 < t < T$)

$$Z = C_0\int_0^T [\,\tilde{B}_1(t)\rho_1(t) + \tilde{B}_2(t)\rho_2(t)\,]\,dt \tag{11}$$

where C_0 is arbitrary scale coefficient, $\rho_1(t)$ and $\rho_2(t)$ are the reference signals defined by the following system of integral equations

$$\begin{aligned} \int_0^T [\,K_{11}(t-\tau)\rho_1(\tau) + K_{12}(t-\tau)\rho_2(\tau)\,]\,d\tau &= 0 \\ \int_0^T [\,K_{21}(t-\tau)\rho_1(\tau) + K_{22}(t-\tau)\rho_2(\tau)\,]\,d\tau &= < \tilde{B}_2(t) >, \end{aligned} \tag{12}$$

where $K_{mn}(t-\tau) = < \tilde{B}_m(t)\tilde{B}_n(\tau) >|_{F_\mu=0}$ - are correlation matrix elements of time stationary noises in quadrature components $\tilde{B}_1$ and $\tilde{B}_2, m, n = 1, 2$.

Using a transformation of variables in eq. (11)

$$\rho_1(t) = Q(t)\cos\varphi(t), \qquad \rho_2(t) = Q(t)\sin\varphi(t) \tag{13}$$

one can obtain

$$Z = C_0\int_0^T Q(t)\Theta_0(t)dt = C_0\int_0^T \Theta(t)dt \tag{14}$$

where

$$\Theta_0(t) = [\,\tilde{B}_1(t)\cos\varphi(t) + \tilde{B}_2(t)\sin\varphi(t)\,], \qquad \Theta(t) = Q(t)\Theta_0(t) \tag{15}$$

Let a field of local oscillator be $E(t) = E_0(t)\cos(\omega_0 t + \varphi_0(t))$. Then for a photocurrent $I_{ph}(t)$ in dual detector scheme one can obtain for $\varphi_0(t) = \varphi(t)$ [8]

$$I_{ph}(t) \propto Re\,[\,\tilde{B}(0,t)E^*(t)\,] = E_0(t)\Theta_0(t) \tag{16}$$

This photocurrent acts on an input of the optimal receiver.

From eqs. (14)-(16) one can consider that for local oscillator field without amplitude modulation $E_0(t) = const$ the optimal receiver can be realized either in the form of correlation receiver with reference signal $\propto Q(t)$ or in the form of concordant filter with transfer function [7]

$$G_{opt}(t) = K_0 Q(t - t_0),$$

where K_0 is arbitrary scale coefficient, t_0 is time of observation.

For local oscillator field with amplitude modulation $E_0(t) \propto Q(t)$ the optimal receiver can be realized in the form of ideal integrator (cf. (14)-(16)).

The calculation of reference signals $\rho_1(t)$ and $\rho_2(t)$ considerably simplifies in the assumption of unlimited time of observation. For $T \to \infty$ one can obtain from eq. (12) the reference signals $\rho_{i\omega}(j\omega), i = 1, 2$:

$$\begin{aligned} \rho_{1\omega}(j\omega) &= -[W_{12}(j\omega)/\Delta(\omega)]Y_\omega(j\omega) \\ \rho_{2\omega}(j\omega) &= [W_{11}(\omega)/\Delta(\omega)]Y_\omega(j\omega), \end{aligned} \tag{17}$$

where

$$\begin{aligned} \Delta(\omega) &= W_{11}(\omega)W_{22}(\omega) - |W_{12}(j\omega)|^2 \\ Y_\omega(j\omega) &= 2A_0 kG(j\omega)F_{s\omega}(j\omega) \end{aligned} \tag{18}$$

and $W_{mm}(j\omega)$ is the spectral density matrix corresponding to $K_{mm}(\tau)$ (cf. (10), (12)),$F_{s\omega}(j\omega)$ is the spectrum of the signal $F_s(t)$.

Taking into account eqs. (13), (17) one can obtain optimal modulation functions for the scheme

$$\begin{aligned} Q(t) &= [\rho_1^2(t) + \rho_2^2(t)]^{1/2} \qquad \varphi(t) = arctg[\rho_2(t)/\rho_1(t)] \\ \rho_1(t) &= -(2\pi)^{-1}\int_{-\infty}^{\infty} W_{12}(j\omega)Y_\omega(j\omega)\exp\{j\omega t\}d\omega/\Delta(\omega) \\ \rho_2(t) &= (2\pi)^{-1}\int_{-\infty}^{\infty} W_{11}(\omega)Y_\omega(j\omega)\exp\{j\omega t\}d\omega/\Delta(\omega) \end{aligned} \tag{19}$$

and $\rho_1(t), \rho_2(t)$ depend on the signal form according to eq. (19).

The signal-to-noise ratio [7] for the measurement of Z (cf. eq. (14)) in the assumption of unlimited time of observation one can obtain from eqs. (17), (18)

$$\begin{aligned} S/N &= (2\pi)^{-1}\int_{-\infty}^{\infty} |Y_\omega(j\omega)|^2 W_1(\omega)d\omega/\Delta(\omega) \\ &= (2\pi)^{-1}\int_{-\infty}^{\infty} |F_{s\omega}(j\omega)|^2 \left[N_\mu + \kappa|G(j\omega)|^{-2}\right]^{-1} d\omega \end{aligned} \tag{20}$$

where $\kappa = N_0(2A_0k)^{-2} \propto 1/P_0$. When the pump power increases the influence of the noises due to vacuum fluctuations decreases and the sensitivity (20) approachs the limit which depends only on the dissipation in mechanical system.

It is worth mentioning that this scheme is useful not only for resonant mechanical oscillator but for longbase laser interferometric detector as well. In this case the transfer function $G(p)$ in eq. (6) must be specified for free masses gravitational antenna and the noise $F_\mu(t)$ in eqs. (7), (8) will be a thermal noise of free masses suspension.

References

[1] C. M. Caves, K. S. Thorne, R. W. P. Drever, V. D. Sandberg and M. Zimmerman, Rev. Mod. Phys., **52**, 341 (1980).

[2] V. V. Kulagin and V. N. Rudenko, Sov. Phys. JETP, **67**, 677 (1988).

[3] V. V. Kulagin and V. N. Rudenko. Nuovo Cimento C, **10C**, 601 (1987).

[4] C. Fabre, M. Pinard, S. Bourzeix, A. Heidmann, E. Giacobino and S. Reynaud, Phys. Rev. A **49**, 1337 (1994).

[5] S. P. Vyatchanin, E. A. Zubova and A. B. Matsko, Optics Communications, **109**, 492 (1994).

[6] S. P. Vyatchanin and E. A. Zubova, Optics Communications, **111**, 303 (1994).

[7] H. Van Treece, *Detection, Estimation and Modulation Theory* (Plenum Press, N.Y.-L., 1968).

[8] J. H. Shapiro, IEEE J. Quantum Electronics, **QE-21**, 237 (1985).

NEXT
DOCUMENT

REGULAR AND CHAOTIC QUANTUM DYNAMICS OF TWO-LEVEL ATOMS IN A SELFCONSISTENT RADIATION FIELD

L.E.Kon'kov and S.V.Prants
Pacific Oceanological Institute
Russian Academy of Sciences
690041 Vladivostok, Russia

Abstract

Dynamics of two-level atoms interacting with their own radiation field in a single-mode high-quality resonator is considered. The dynamical system consists of two second-order differental equations, one for the atomic $SU(2)$ dynamical-group parameter and another for the field strength. With the help of the maximal Lyapunov exponent for this set we investigate numerically transitions from regularity to deterministic quantum chaos in such a simple model. Increasing the collective coupling constant $b \equiv 8\pi N_0 d^2/\hbar\omega$ we observed for initially unexcited atoms usual sharp transition to chaos at $b_c \simeq 1$. If we take the dimensionless individual Rabi frequency $a = \Omega/2\omega$ as a control parameter, then a sequence of order-to-chaos transitions has been observed starting with the critical value $a_c \simeq 0.25$ at the same initial conditions.

1 Introduction

When studying field-matter interactions it is usually of interest to consider the possibility of controlling the temporal behavior of the field and/or the atomic subsystems. Say, in resonator quantum electrodynamics, it is important to drive the interaction between atoms, moving through a cavity, and a quantizied field mode in such a way to attain specified states of the electromagnetic field (Fock, coherent, squeezed, and so on) in the cavity and/or desirable states of atoms leaving the cavity. It is inexplicitely supposed that we are able, in principle, to attain any desirable state (which is accessible, of course, in quantum mechanics) under an appropriate control.

However, it has been shown in resent years [1] that beyond the rotating-wave approximation even the simple model, consisting of N two-level atoms interacting with their own radiation field, may demonstrate impredictable temporal behavior in the sense of deterministic chaos. Our previous results [2] have shown that even slight modification in a model, describing this interaction, could create dramatic artifacts. The purpose of this work is to treat the routes to deterministic chaos in the framework of the dynamical-symmetry approach which has been proved to be useful in investigating regular dynamics of a variety of quantum models [3],[4].

2 Dynamical $SU(2)$ model

We consider an ensemble of N identical two-level atoms placed in a single- mode high-quality resonator with the volume V. Each two-level system is described by the $SU(2)$ Hamiltonian

$$H = \hbar\omega R_0 - \hbar\Omega\epsilon(t)(R_+ + R_-), \tag{1}$$

in which the operators satisfy the usual commutation relations

$$[R_0, R_\pm] = \pm R_\pm, \; [R_+, R_-] = 2R_0, \tag{2}$$

and ω is the atomic transition frequency that coincides with the resonator frequency. The individual Rabi frequency Ω is given by

$$\Omega = \frac{dE_0}{\hbar}, \tag{3}$$

where d is the dipole moment of the atomic transition. Atoms interact self-consistently by dipole interaction with an electric field, whose strength is written in the form

$$E(t) = E_0\epsilon(t), \tag{4}$$

where E_0 is the constant amplitude and $\epsilon(t)$ the dimensionless variable, $0 \leq \epsilon \leq 1$.

We treat the field *ab initio* semiclassically, assuming that it satisfies the usual Maxwell equation

$$\frac{d^2E}{dt^2} + \omega^2 E = 4\pi\omega^2\mathcal{P}, \tag{5}$$

where $\mathcal{P} = N_0 d < R_+ + R_- >$ is the polarisation created by atoms, $N_0 = N/V$ is the density of atoms in the resonator. Substituting $\tau = \omega t$, we can write the eq.5 in the dimensionless form with the derivative with respect to τ

$$\ddot{\epsilon} + \epsilon = \frac{b\omega}{\Omega} < R_+ + R_- > . \tag{6}$$

We have introduced following to [1] the dimensionless constant

$$b = \frac{8\pi N_0 d^2}{\hbar\omega}, \tag{7}$$

characterizing the energy exchange between the atomic ensemble and the field.

In addition another dimensionless constant

$$a = \frac{\Omega}{2\omega} \tag{8}$$

will be used to investigate transitions from order to chaos in our model. The expression (8) is simply the dimensionless individual Rabi frequency.

In the dynamical-symmetry approach, each two-level atom is governed by the following single equation for the $SU(2)$ complex-valued group parameter [5]

$$\ddot{g} - \left(\frac{\dot{\epsilon}}{\epsilon} + i\right)\dot{g} + (2a\epsilon)^2 g = 0, \; g(0) = 1, \; \dot{g}(0) = 0. \tag{9}$$

The derivatives in (10) are also defined with respect to τ.

Thus we have two coupled oscilators (9) and (6) describing the self-consistent interaction between two-level atoms and a single-mode classical field. Rewriting (9) and (6) in the equivalent first-order form, we obtain the following nonlinear dynamical system

$$\begin{aligned} \dot{x}_1 &= 2a\varepsilon y_2, \\ \dot{x}_2 &= -2a\varepsilon y_1, \\ \dot{y}_1 &= -y_2 + 2a\varepsilon x_2, \\ \dot{y}_2 &= y_1 - 2a\varepsilon x_1, \\ \dot{\varepsilon} &= -\mathcal{P} \\ \dot{\mathcal{P}} &= \varepsilon \mp \tfrac{b}{2a}(x_1 y_1 + x_2 y_2). \end{aligned} \tag{10}$$

Signs $-$ and $+$ in the last equation of (10) refer to the initially unexcited and excited atoms, respectively.

The atom-field system (10) obeys two conservation laws

$$x_1^2 + x_2^2 + y_1^2 + y_2^2 = 1, \tag{11}$$

$$\pm \frac{b}{4a^2}(x_1^2 + x_2^2 - y_1^2 - y_2^2) - (\varepsilon^2 + \mathcal{P}^2) \pm \frac{b}{a}\varepsilon(x_1 y_1 + x_2 y_2) = const. \tag{12}$$

It should be noted that the variables $x_1 \equiv Re\, g$ and $x_2 \equiv Im\, g$ are not independent [5]. Therefore we have three independent real variables, that is the minimum required for chaos [6].

For two-level atoms the dynamical system (10) is equivalent to the usually adopted Maxwell-Bloch equations. Let us introduce the components of the Bloch vector

$$\begin{aligned} u(t) &= c_1^* c_2 + c_1 c_2^*, \\ v(t) &= i(c_1^* c_2 - c_1 c_2^*), \\ w(t) &= |c_2|^2 - |c_1|^2, \end{aligned} \tag{13}$$

where c_1 and c_2 are the probability amplitudes of lower and upper states respectively. On the other hand these components can be expressed in terms of the variables x and y as follows

$$\begin{aligned} u &= 2(x_1 y_1 + x_2 y_2), \\ v &= 2(x_1 y_2 - x_2 y_1), \\ w &= y_1^2 + y_2^2 - x_1^2 - x_2^2. \end{aligned} \tag{14}$$

Thus we can rewrite (10) in the standard Maxwell-Bloch form

$$\begin{aligned} \dot{u} &= -v, \\ \dot{v} &= u + 4a\varepsilon w, \\ \dot{w} &= -4a\varepsilon v, \\ \dot{\varepsilon} &= -\mathcal{P}, \\ \dot{\mathcal{P}} &= \varepsilon - \tfrac{b}{4a}u. \end{aligned} \tag{15}$$

3 Numerical results

Our model possesses two control parameters a and b. We will numerically treat here transitions from order to chaos varying one of them in a certain range and keeping another constant. Chaos will be diagnosed with the help of the maximal Lyapunov exponent λ, which is a quantitative characteristic of deterministic chaos describing the mean exponental rate of divergence of two initially adjacent trajectories in a phase space [6]. The sign of λ gives up a reliable criterion to distinguish between regular and chaotic dynamics of a system in question. When it is neglibly small the motion is said to be regular. If λ becomes positive for a certain range of values of a control parameter a system is chaotic for this range. Chaos may also be confirmed by continuous power spectra

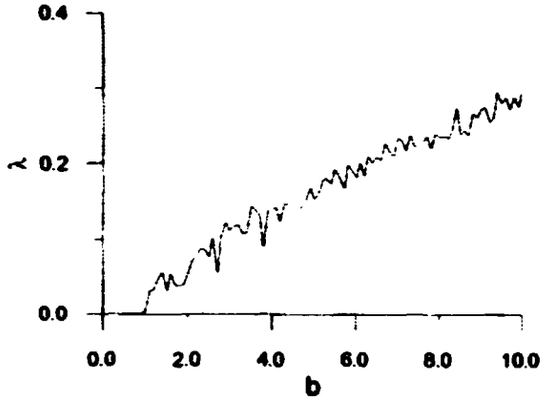

Fig.1 The maximal Lyapunov exponent as a function of the control parameter b for initially unexcited atoms, $a=0.25 \cdot 10^{-6}$.

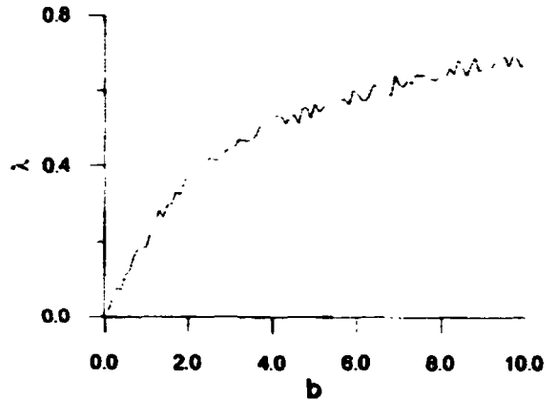

Fig.2 The maximal Lyapunov exponent as a function of the control parameter b for initially excited atoms, $a=0.25 \cdot 10^{-6}$

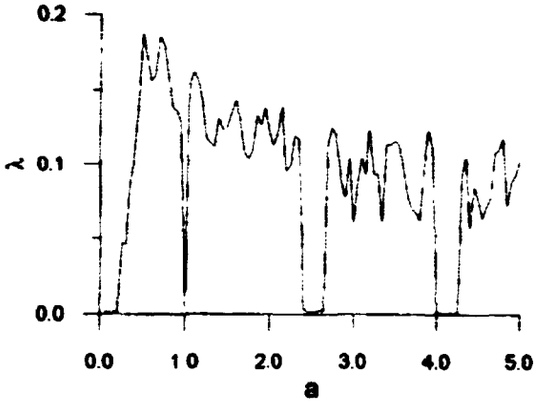

Fig.3 The maximal Lyapunov exponent as a function of the control parameter a for initially unexcited atoms, b=1

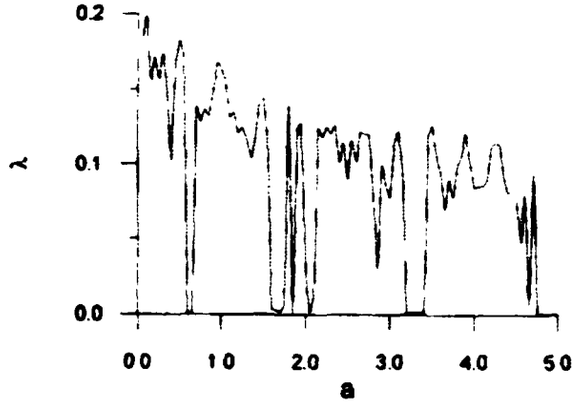

Fig.4 The maximal Lyapunov exponent as a function of the control parameter a for initially excited atoms, b=1

By varying the collective coupling parameter b we, in fact, change the density of atoms N_0 in a cavity. Numerical integration shows that the maximal Lyapunov exponent λ becomes positive when b exceeds a critical value b_c. Its magnitude depends essentially on initial conditions. It is seen from Fig.1 that $b_c \simeq 1$ for initially unexcited atoms. For initially excited atoms (Fig.2) the maximal Lyapunov exponent becomes positive for much smaller critical value of b.

We have observed a quite different transition to chaos with chaotic regimes alternating among regular regimes when varying the individual dimensionless Rabi frequency a and fixing the parameter b. Fig.3 and Fig.4 demonstrate such a behavior for initially unexcited and excited atoms, respectively.

4 Outlooks

We have demonstrated two possible routes to chaos in the interaction of two-level atoms with their own radiation field. From a more general points of view, we have observed numerically order-to-chaos transitions in the system of two coupled nonlinear oscillators (6) and (9). At last, from an abstract point of view, we have treated such transitions in a system consisting of the "driven" $SU(2)$ group treated as a nonlinear dynamical system. Thus, the results, obtained in this work, are applicable in a more general context. They may be applied with slight modifications to any driven physical (chemical, biological, ecological, etc) system with the underlying $SU(2)$ dynamical symmetry.

Acknowledgments

This research was made possible by Grant NZ7000 from the International Science Foundation and by Grant NZ7300 from the International Science Foundation and Russian Government.

Authors thank the corporation "Russki Sakhar" and express their deep gratitude to A.P.Ilushin for support.

References

[1] P.I.Belobrov, G M.Zaslavskii and G.Kh. Tartakovskii, Zh. Eksp. Theor. Fiz., **71**, 1799-1812 (1976).

[2] L.E.Kon'kov, S.V.Prants, to appear in Proc.SPIE on 15th International Conference on Coherent and Nonlinear Optics, Washington (1995).

[3] I.A.Malkin and V.I.Man'ko, *Dynamical Symmetries and Coherent States of Quantum Systems* (Nauka, Moskow, 1979).

[4] S.V.Prants, J. Sov. Laser Research, **2**, 165 (1991).

[5] S.V.Prants, Izv. Rus. Acad. Sci. (Ser.fiz.), **58**, 30-35 (1994).

[6] A.J.Lichtenberg and M.A.Lieberman, *Regular and Stochastic Motion* (Springer-Verlag, New York, 1983).

NEXT
DOCUMENT

Motion of Cesium Atoms in the One-Dimensional Magneto-Optical Trap*

Li Yimin *Chen Xuzong* *Wang Qingji* *Wang Yiqiu*

Department of Radio-Electronics, Peking University
Beijing 100871, P.R.China

Abstract

We calculated the force to which Cs atoms are subjected in the one-dimensional magneto-optical trap (1D-MOT) and properties of this force are also discussed. Several methods to increase the number of Cs atoms in the 1D-MOT are presented on the basis of the analysis of the capture and escape of Cs atoms in the 1D-MOT.

PACs. 3280P; 3270N; 4250

1. INTRODUCTION

Laser cooling and trapping of neutral atoms is one of the most active research fields in physics in this decade . Several kinds of neutral atom traps have been achieved experimentally [1] ,one of which is the magneto-optical trap(MOT) whose basic principles were discussed in detail in Refs.[2] and [3]. The MOT is formed in the intersection of three orthogonal pairs of counter propagating laser beams with opposite circular polarization A pair of anti-Helmholtz coils is used to generate an inhomogeneous magnetic field. whose zero point coincides with the center of the intersection region where a stable potential well is formed Atoms confined in this volume will experience a damping force and a restoring force. MOT has become almost a standard technique for obtaining large number of cold atoms due to its large depth, large trap size and long trap lifetime. A lot of theoretical and experimental work has been carried out since Raab et al.[2] first achieved MOT in 1987. In 1990, Wieman et al [4] built a MOT into which for the first time Cs atoms were loaded directly from low pressure Cs vapor in a quartz cell and this greatly promoted the research on MOT At present about 10^{10} atoms can be trapped in MOT with a density of 10^{11} atoms/cm^3 [5] and temperatures below the Doppler limit [6] . In recent years, the research of MOT has been concentrated on two aspects: (1)investigating the properties of MOT with the aim of increasing the number and density of trapped atoms and lowering the temperature so as to optimize the performance of MOT as a source of cold atoms, (2)using MOT to carry out some fundamental or applied research work such as atomic fountain[7] , cold atoms collision[8] , atomic interferometry[9] and Bose-Einstein condensation, etc.

A simple case of a fictitious atom with a $J_g = 0 \rightarrow J_e = 1$ transition in the 1D-MOT

*project supported by National Natural Science Foundation of China.

In this paper we use a simple method to deal with this problem and have got some valuable results.

In section 2 we calculate the force as well as the capture and escape of Cs atoms in 1D-MOT ; in section 3 we continue by analyzing the features of the force and we present several measures to increase the number of Cs atoms in MOT; finally in section 4 we give a conclusion and some comments on our future work.

2. CALCULATION OF THE FORCE AND THE MOTION OF Cs ATOMS

A. Calculation of the force

The force that an atom experiences in a laser field is[10]

$$F = -\langle \frac{dV}{dx} \rangle \qquad (1)$$

where < > represents the mean value, $V = \vec{D} \cdot \vec{E}$ is given by the interaction Hamiltonian between the induced electric dipole $\vec{D}$ of the atom and the electric field vector $\vec{E}$ of the laser. The authors of Ref.[10] analyzed the force of a fictitious atom with $J_g = 1 \rightarrow J_e = 2$ transition under $\sigma^- - \sigma^-$ configuration. The transition used for cooling and trapping of Cs atoms is $6S_{1/2}, F_g = 4 \rightarrow 6P_{3/2}, F_e = 5$ and the schematic diagram of the corresponding energy levels is shown in Fig. 1[11].

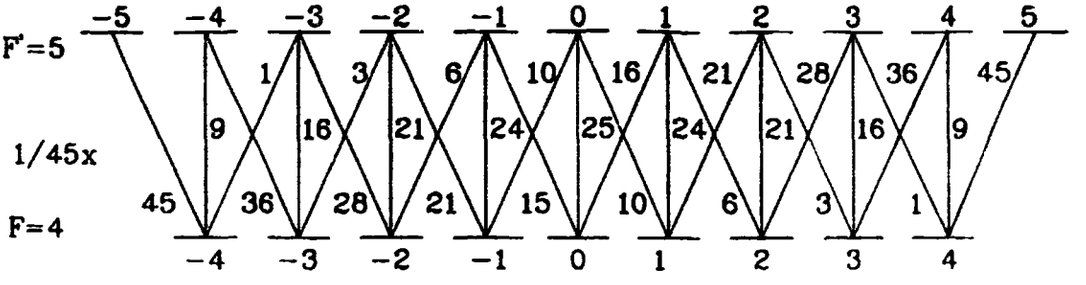

Fig 1 Energy levels of Cs $6S_{1/2}, F_g = 4 \rightarrow 6P_{3/2}, F_e = 5$

There are several kinds of mechanisms which contribute to the total force exerted on Cs atoms in the case of complicated energy level structure . The most important two are , namely , the scattering force and the polarization gradient force[1] By extending the result of Ref.[10] to the case $F_g \to F_e = F_g + 1$ (the contribution of the excited-state population is taken into account in the calculation) , we have

$$f = f_{scatter} + f_{grad} \tag{2}$$

$$f_{scatter} = \frac{\hbar k \Gamma}{2} \sum_{m=-F_g}^{F_g} [(\rho_m^{(g)} - \rho_{m+1}^{(e)}) S_{m,m+1} (C_m^{m+1})^2$$

$$-(\rho_m^{(g)} - \rho_{m-1}^{(e)}) S_{m,m-1} (C_m^{m-1})^2] \tag{3}$$

$$f_{grad} = \frac{\hbar k \Gamma}{2} \sum_{m=0}^{F_g} C_m^{m-1} C_{m-2}^{m-1} [(S_{m-2,m-1} - S_{m,m-1}) \mathrm{Re}(\tilde{\rho}_{m,m-2})$$

$$-\frac{2}{\Gamma}(\delta_{m-2,m-1} S_{m-2,m-1} + \delta_{m,m-1} S_{m,m-1}) \mathrm{Im}(\tilde{\rho}_{m,m-2}) \tag{4}$$

where $\rho_m^{(g)} = < F_g, m_g | \rho | F_g, m_g >$, $\rho_m^{(e)} = < F_e, m_e | \rho | F_e, m_e >$ are diagonal elements of the density matrix, $S_{m,m\pm1} = \dfrac{\Omega^2 / 2}{\delta_{m,m\pm1}^2 + \Gamma^2 / 4}$ is the saturation factor, $\Omega = 2 d E \hbar^{-1}$ is the Rabbi frequency, $(C_{m_g}^{m_e})^2$ is corresponding normalized transition probabilities shown in Fig 2, $_{m,m\pm1} = \delta \mp kV + [m g_g - (m \pm 1) g_e] \mu_B X \dfrac{dB}{dx}$ is the relative frequency detaining, is the frequency detaining, k is the optical wave vector, v is the atomic velocity, μ_B is the Bohr magneton, g_g and g_e are the g factors of the ground state and the excited state, respectively , and $\tilde{\rho}_{m,m-2} = \langle F_g, m | \rho | F_g, m-2 \rangle \exp(-2ikVt)$ represents the coherence between sublevels of the ground state.

In formula (3) , $\dfrac{\Gamma}{2} \sum_{m=-F_g}^{F_g} (\rho_m^{(g)} - \rho_{m+1}^{(e)}) S_{m,m+1} (C_m^{m+1})^2$ represents the scattering rate for σ^+ photons by spontaneous emission and $\dfrac{\Gamma}{2} \sum_{m=-F_g}^{F_g} (\rho_m^{(g)} - \rho_{m-1}^{(e)}) S_{m,m-1} (C_m^{m-1})^2$ is that for σ^- photons The atom will obtain a momentum $\hbar k$ or $-\hbar k$ if it scatters a σ^+ photon or a σ^- photon , respectively The net effect is that the atom will experience a scattering force $f_{scatter}$

From formula (4) , we know that f_{grad} is due to the off-diagonal element $\rho_{m,m-2}$, that is , the coherence between sublevels of the ground state Fig 2 shows the stimulated

absorption-stimulated emission process which contributes to the coherence under σ^+ -σ^- configuration.

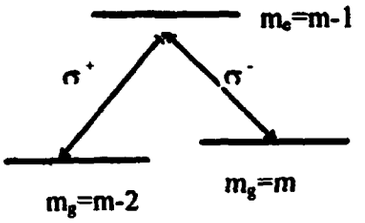

Fig.2 Stimulated absorption-stimulated emission process between sublevels of the ground state of Cs under σ^+-σ^- configuration.

The authors of Ref.[10] also pointed out that f_{grad} would contribute dominantly to the force experienced by an atom only when the condition $(\delta_{m_g,m_e\pm1} - \delta) < \Gamma'$ (Γ' refers to the optical pumping rate. The condition can also be written as $\Delta V=\Gamma'/k$, $\Delta X=\hbar\Gamma'(g_e \mu_B dB/dx)^{-1}$) is satisfied. We may neglect the effect of f_{grad} , if this condition is not fulfilled. Taking the Cs atom for example, with $\Gamma'<0.5$MHz under the condition δ= -10 MHz , I = 4mW/cm^2 , dB/dx = 1mT/cm , g_g ($6S_{1/2}$, F = 4) = 0.25 , g_e ($6P_{3/2}$, F' = 5) = 0.4 , the velocity range is $\Delta V<0.45$m/s and the spatial range is $\Delta X<1$mm. Such a small interaction range makes f_{grad} negligible and we can keep only the term of $f_{scatter}$ when discussing the process of capture and escape of Cs atoms.

It can be seen from formula (3) that $f_{scatter}$ only relates to the diagonal elements of density matrix so we can use rate equations to calculate it. Taking into account the effect of spontaneous emission, stimulated emission and stimulated absorption, we have the following rate equations[11]

$$\dot{\rho}_m^{(g)} = -\frac{\Gamma}{2}[S_{m,m+1}(C_m^{m+1})^2(\rho_m^{(g)} - \rho_{m+1}^{(e)}) +$$

$$S_{m,m-1}(C_m^{m-1})^2(\rho_m^{(g)} - \rho_{m-1}^{(e)})] + \Gamma\sum_{q=-1}^{1}(C_m^{m+q})^2\rho_{m+q}^{(e)} \qquad (5)$$

$$\dot{\rho}_m^{(e)} = \frac{\Gamma}{2}[S_{m-1,m}(C_{m-1}^{m})^2(\rho_{m-1}^{(g)} - \rho_m^{(e)}) +$$

$$S_{m+1,m}(C_{m+1}^{m})^2(\rho_{m+1}^{(g)} - \rho_m^{(e)})] - \Gamma\rho_m^{(e)} \qquad (6)$$

and the normalization condition

$$\sum_{m_e}\rho_{m_e}^{(e)} + \sum_{m_g}\rho_{m_g}^{(g)} = 1 \qquad (7)$$

After obtaining the steady solutions $\rho_m^{(e)}$ and $\rho_m^{(g)}$ to the above equations we can calculate the scattering force exerted on a Cs atom under different physical conditions. Fig.(a) shows the influence of light intensity;Fig.3(b) is the variation of force with different laser detuning;Fig.3(c) shows the forces as a function of the magnetic field gradient at a fixed point in space In these figures, the X-axis represents velocity in m/s and the Y-axis is the force in units of $\hbar k\Gamma$ (it equals to 4×10^{-21} N for the transition Cs $6S_{1/2} \rightarrow 6P_{3/2}$).

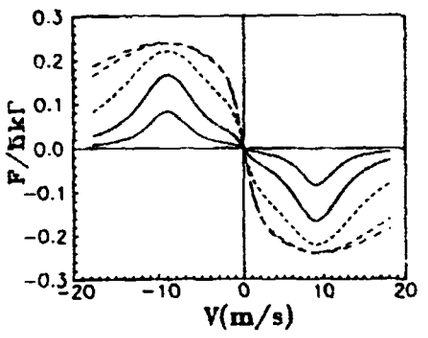

(a) For curves in the direction of the arrow, from lower to upper, I=0 27, 1 1 , 4.4 , 18 , 27 mW/cm ^{2}, at Δ = - 10.6 MHz, B=0T

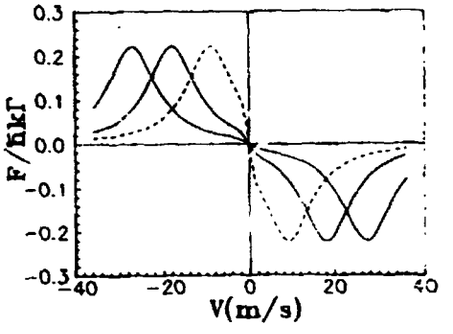

(b) For curves in the direction of the arrow, from right to left, Δ = - 10.6, -21.2 , -42 4 MHz, at I=4.4mW/cm^2, B=0T

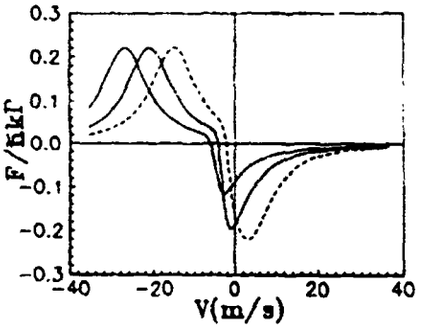

(c) For curves in the direction of the arrow, from right to left , dB/dx=0 5 , 1 , 1.5 mT/cm , at I = 4 4 mW/cm^2 , and Δ = -10 6 MHz. The distance to the center of the trap is 1cm

Fig 3 The force experienced by a Cs atom under different conditions

Fig 4 shows the position dependence of the scattering force on a Cs atom with different velocities The X-axis is the position and the Y-axis represents the force as in Fig 3

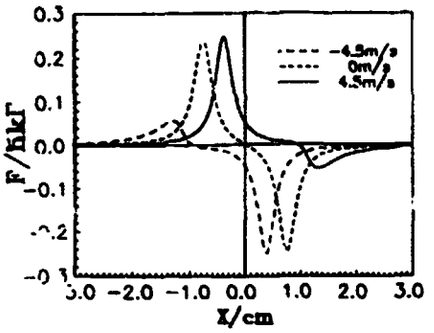

Fig.4 The scattering force of a Cs atom with different velocities . For curves in the direction of the arrow , from left to right V= -4.5, 0,4.5 m/s, at I= 1.1mW/cm^2 , Δ = -10.6MHz , dB/dx=1mT/cm

From Fig . 3(a) it can be seen if an atom is stopped at the center of the MOT and has a small velocity , we can obtain

$$f_{scatter} = -\alpha V \qquad (8)$$

From Fig 4 , we derive that if an atom has zero velocity and is near the trap center, then

$$f_{scatter} = -kX \qquad (9)$$

Therefore when both X and V are relatively small, we may rewrite $f_{scatter}$ approximately as

$$f_{scatter} = -kX - \alpha V \qquad (10)$$

where K and α are the string constant and damping coefficient respectively This is the typical form of force in a potential well with damping

B Calculation of the capture and escape of Cs atoms

Before the calculation , we would like to explain several related concepts and introduce two important parameters . In practice the MOT is three dimensional and is formed at the intersection of six laser beams The size of the MOT is determined by the radius of the laser beams We will then also use the radius of laser beam as the spatial range of 1D-MOT The atom is considered to be trapped if it finally stops at the trap center The maximum velocity of atoms captured at the edge of the MOT is defined as the capture velocity V_c . Mainly due to collisions with fast background atoms , trapped atoms at the center of the MOT may obtain enough initial velocity to be knocked out of the trap The minimum initial velocity is defined as the escape velocity V_e

For the calculation of the parameters of motion the Cs atom is treated as classical particle Its dynamical behavior obeys the Newton's second law . The force is obtained by the approach discussed above After integrating the equations of motion by the Runge-Kutta algorithm we obtain curves showing variation of the velocity and position of a Cs atom in the process of capture and escape Fig 5(a) shows the variation of the position in the capture process The motion of Cs atoms with different initial velocities is given where the atoms' initial position is supposed to be at the edge of the trap . Fig .5(b) shows the variation of the velocity in the same process . Finally Fig 6 presents the same curves in the escape process Here the atoms' initial position is assumed to be at the trap's center

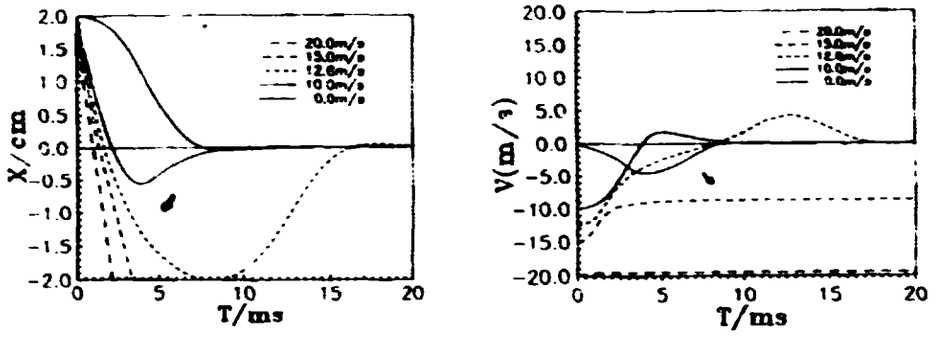

(a) Variation of position (b) Variation of velocity

Fig 5 The variation of position and velocity in the process of capture For curves in the direction of the arrow , from upper to lower , the initial velocity is V_i = 0 , 10 , 12 58 , 15 , 20 m/s , the radius of the laser beam is 2cm , I = 4.4 mW/cm^2 , Δ = - 10 6 MHz , dB/dx = 1mT/cm From these curves , we obtain V_c = 12 58 m/s .

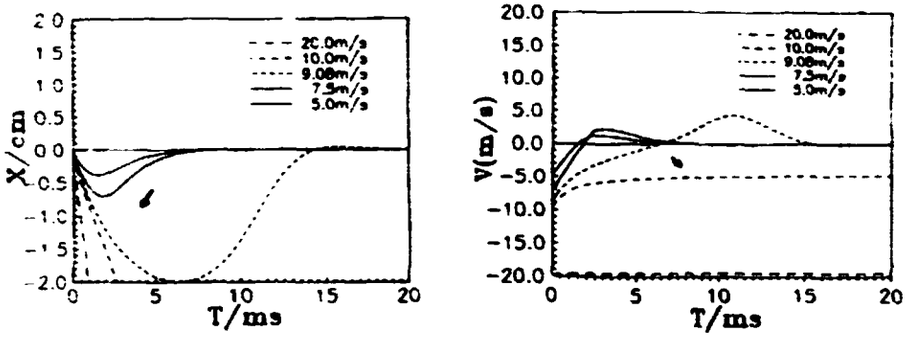

(a) Variation of position (b) Variation of velocity

Fig 6 The variation of position and velocity in the process of escape For curves in the direction of the arrow , from upper to lower , V_i = 5 ,7 5,9 08 ,10, 20 m/s The parameters of laser are the same as those in Fig 5. From these curves we see that the escape velocity evaluates to be V_e = 9 08 m/s

V_i and V_e are determined respectively in the following way first , we set the velocity range to be [0m/s, 20m/s] , which , according to our calculation , cover the value of V_c

and V_s ; then , the velocity range is step by step decreased by the dichotomy ; finally , we get the approximate values of V_c and V_e for a velocity range smaller than 0.01m/s The magnitude of V_c and V_e is related closely to the number of trapped atoms

$$N_{tr} = \frac{r^2}{\sigma} \cdot \left(\frac{V_c}{\mu} \right)^4 \qquad [5] \qquad (11)$$

where r is the radius of the laser beam , μ is the average velocity and σ is the cross section for a trapped atom to be knocked out of the trap by a background atom.Obviously , σ decreases with V_c . From (11) , we know that for a large number of trapped atoms it is beneficial to increase V_c and V_e by changing the trap parameters

3 DISCUSSION

A The properties of the force in MOT

A Cs atom experiences three kinds of forces in MOT . These are the gravitational force the magnetostatic force and the optical force . The magnetostatic force is caused by the inhomogeneous magnetic field When dB/dx = 2 mT/cm , a cs atom in the $F_g = 4, m_g = 4$ sublevel obtains an acceleration of about g (gravitational acceleration) The optical force is due to the interaction between the light and the atom . For Δ = - 10.6 MHz and I = 4mW/cm^2 , the acceleration caused by this force is about 103 g , which is much greater than that by the gravitational force and the magnetostatic force Therefore , we could neglect the gravitational and the magnetostatic force .

As discussed above,both $f_{scatter}$ and f_{grad} contribute to the optical force in the 1D-MOT The capture and escape of atoms are mainly determined by the former due to its large interaction range of velocity and space . Even though f_{grad} has a smaller interaction range than that of $f_{scatter}$ but it acts in this very small range much stronger on the atom [10] When atoms in MOT reach a steady state , they concentrate at the trap center with very small velocity amplitudes In this situation , the temperature and density of atomic cloud are determined by f_{grad}

B Contribution of Zeeman effect and Doppler effect

In MOT the origin of $f_{scatter}$ is due to the different relative detuning for σ^- and σ^+ photons This imbalance between the absorbed photons from opposite directions results in the net scattering force But an atom in the MOT can not tell whether the relative detuning is caused by the Zeeman effect or by the Doppler effect , because there is certain equivalence between these two effects on their contribution to the net force When Zeeman splitting between $\Delta m = 2$ sublevels of a Cs atom excited state in compensated by Doppler shift , i e

$$\hbar^{-1} g_e \mu_B \frac{dB}{dx} X = kV \qquad (12)$$

then the relative detuning for σ^+ light is the same as that for σ^- , Therefore the scattering rate of photons is equal in both directions , under which circumstance the atom experiences no force ,

$$f = 0 \tag{13}$$

By substituting (12), (13) into (10) , we obtain

$$K = g_e \mu_B (\hbar k)^{-1} \frac{dB}{dx} \cdot \alpha \tag{14}$$

which indicates the equivalence between the Zeeman effect and the Doppler effect , i.e. K is proportional to α It also shows that they both are dependent on the parameters of the laser field (detuning and intensity) However they are different in that K is proportional to dB/dx whereas α is independent of dB/dx , which indicates that the scattering force originates in the inhomogeneous magnetic field . Under the condition of small V and X the calculation is simplified and we have obtained the approximate formula for α and K (see appendix for detail)

$$\alpha \approx -0.9644 \frac{\hbar k^2 \delta S_0 \Gamma}{(1+S_0)(\delta^2 + \Gamma^2/4)} \tag{15}$$

$$K \approx -0.9644 \frac{g_e \mu_B k \delta S_0 \Gamma}{(1+S_0)(\delta^2 + \Gamma^2/4)} \cdot \frac{dB}{dx} \tag{16}$$

C The relation of the force on the parameters of MOT

We will concentrate our discussion on the effect of the laser intensity I , the frequency detuning Δ , the radius r of the laser beam and the gradient of the magnetic field dB/dx on the scattering force in MOT

From Fig.3(a) we know that for small intensities the force increases sharply with the laser intensity When $I > I_0 \delta^2 \Gamma^{-2} = 4.4 mW/cm^2$ (i e. $S_0 = 1$ The saturated intensity for the cycling transition $F_g = 4, m_g = 4 \rightarrow F_e = 5, m_e = 5$ is $I_0 = 1.1 mW/cm^2$) , the intensity has only a small influence on the force $S_{m,m\pm1}$ increases with the laser intensity but the population difference $\rho_m^{(g)} - \rho_{m\pm1}^{(e)}$ will become small due to the saturation effect . Therefore the influence of laser intensity is diminished due to the compensation of these two effects with each other Fig 3(b) shows that the capture range of velocity increases with laser detuning Since the volume of the MOT is determined by the radius r of the laser beam , increasing r may increase the volume efficiently , Fig 3(c) shows the effect of the magnetic field gradient At a point far from the trap center , atoms will be cooled to

non-zero velocity . The curve of the force is asymmetric about its zero point , which is caused by the difference of g-factor between the upper and the lower state . (Upper state $6P_{3/2}, F = 5, g_e = 0.4$; lower state $6S_{1/2}, F = 4, g_g = 0.25$) . From Fig.3(c) we know that increasing the gradient dB/dx tends to decrease the damping force, whereas the string constant K increases with dB/dx(See [16]). This situation sets a certain limit on the value of dB/dx.

D. Several measures to increase the number of trapped atoms

We have known that increasing light intensity will not increase the number of trapped atoms if $I > I_0 \delta^2 \Gamma^{-2}$. Under the condition of $I \approx I_0 \delta^2 \Gamma^{-2}$, enlarging r (the radius of the laser beam) may increase the volume of MOT and increasing δ (laser detuning) may increase the velocity capture range. After r and δ being determined, we use the condition $\delta_{m,m-1} \leq 0$ as the limit on the value of dB/dx. Among all the relative detunings , $\delta_{-4,-5}(V = 0 , X = r) = \delta + \hbar^{-1} r\mu_B$ dB/dx is the biggest one. If it is negative, i.e., (note that $\delta < 0$) , the condition will be satisfied

All in all, we think that the following methods may increase the number of trapped atoms: (1) increasing the detuning; (2) enlarging the radius of the laser beam as possible as to keep $I \approx I_0 \delta^2 \Gamma^{-2}$; (3) $dB/dx = -\hbar \delta(\mu_B r)^{-1}$ when r and δ are determined

4. CONCLUSION

The properties of MOT have been studied profoundly for years. On the basis of these studies, we used a simple method to calculate the force and motion of Cs atoms in 1D-MOT. The approximate formulas for α and K are given in the case of small velocity and volume and the characteristics of the force and the contribution of Zeeman effect and Doppler effect are also discussed The condition to increase V_c and V_e upon which we may build an efficient MOT are given

However in this paper we don't discuss the problems about the atomic density and equilibrium temperature in MOT, because the approximate method we used does not include f_{grad} and atomic momentum diffusion. Thus it cannot be applied to calculate the atomic density and temperature. Furthermore the theory of density and temperature in MOT is quite complicated because it requires the consideration of various effects, which are not easy to evaluate Anyway the related work is in proceeding.

The authors are gratefully indebt to Prof. Wu Jike of Department of Mechanics, Peking University and Dr Zhang Wenqing of Institute of Physics, Academia Science Sinica for their instruction and help with the computer program

APPENDIX

At first, we give the cited definition of the saturation factor

$$S_0 = \frac{\Omega^2 / 2}{\delta^2 + \Gamma^2 / 4} \qquad \text{(a.1)}$$

and the relative detuning when X is small can be rewritten as follows

$$\delta_{m_g, m_g \pm 1} = \delta \mp kV \qquad \text{(a.2)}$$

Finally the approximate population difference between the upper and the lower state is

$$\rho_{m_g}^{(g)} - \rho_{m_g \pm 1}^{(e)} \approx \frac{1}{1 + S_0} \rho_{m_g}^{(0)} \qquad \text{(a 3)}$$

where $\rho_{m_g}^{(0)}$ is the population of sublevels of the ground state in the case of very weak light intensity under σ^+-σ^- configuration and the calculated results are presented below

$$\rho_4^{(0)} = \rho_{-4}^{(0)} = 0.3864 \quad , \qquad \rho_3^{(0)} = \rho_{-3}^{(0)} = 0.0498$$

$$\rho_2^{(0)} = \rho_{-2}^{(0)} = 0.0336 \quad , \qquad \rho_1^{(0)} = \rho_{-1}^{(0)} = 0.0188$$

$$\rho_0^{(0)} = 0.0172$$

After combining (3), (a 2) and (a 3), we have

$$f_{scatter} = \frac{\hbar k \Gamma}{2(1 + S_0)} \cdot \left[\frac{\Omega^2 / 2}{(\delta - kV)^2 + \Gamma^2 / 4} \sum_{m_g} \rho_{m_g}^{(0)} (C_{m_g}^{m_g - 1})^2 - \right.$$

$$\left. \frac{\Omega^2 / 2}{(\delta + kV)^2 + \Gamma^2 / 4} \sum_{m_g} \rho_{m_g}^{(0)} (C_{m_g}^{m_g - 1})^2 \right] \qquad \text{(a 4)}$$

By substituting the values of $\rho_{m_g}^{(0)}$ and corresponding C-G coefficients

$$\sum_{m_g} \rho_{m_g}^{(0)} (C_{m_g}^{m_g - 1})^2 = \sum_{m_g} \rho_{m_g}^{(0)} (C_{m_g}^{m_g + 1})^2 = 0.4822 \qquad \text{(a 5)}$$

and using the approximate condition δ-kV $\approx \delta$+kV $\approx \delta$ for very small V as well as formula (a 1), finally we obtain

$$f_{scatter} \approx \frac{0.9644 \hbar k^2 \delta S_0 \Gamma}{(1 + S_0)(\delta^2 + \Gamma^2 / 4)} \cdot V \qquad \text{(a 6)}$$

$$\alpha \approx -0.9644 \frac{\hbar k^2 \delta S_0 \Gamma}{(1+S_0)(\delta^2+\Gamma^2/4)} \qquad (a.7)$$

REFERENCE

[1] Wang Yiqiu, Wuli(Physics) 19(1990), 389(in Chinese).
[2] E L Raab , M . Prentise , A Cable , S . Chu , D E. Pritchard , Phys Rev Lett.,9(1987), 2631
[3] H Metcalf, J.Opt. Soc Am B, 6(1989), 2206
[4] C Monroe, W. Swann, H. Robinson, C. Wieman, Phys Rev. Lett , 65(1990), 1571.
[5] K E. Gibble, S. Kasapi, S. Chu, Opt. Lett , 17(1992), 526.
[6] A M. Steane, C J. Foot, Europhys Lett., 14(1991), 231
[7] M. A Kasevich, E Riis, S Chu, Phys. Rev Lett , 63(1989), 612; A Clairon, C Salomon, S. Guellati , W D. Phillips, Europhys Lett., 16(1991), 165
[8] J Wiener, J. Opt. Soc Am B, 6(1989), 2270
[9] M Kasevich, S. Chu, Phys Rev Lett. , 67(1991) , 181.
[10] J Dalibard, C Cohen-Tannoudji, J Opt. Soc Am. B , 6(1989), 2023
[11] Wang Yiqiu, Wang Qingji, Fu Jishi, Dong Taiqian, Principle of Quantum Frequency Standard , Science Press, Beijing, 1986.

NEXT
DOCUMENT

The Multiphoton Interaction of "Λ" Model Atom and Two-Mode Fields

Tang-Kun Liu
Department of Physics, Hubei Normal College,Huangshi,435002,P.R.China

Abstract

Starting from the C.T.Lee's criterion on non-classical effects in two-mode fields,the author of this paper have studied the system of two-mode fields interacting with atom by means of multiphotons, discussed the non-classical statistic quality of two-mode fields with interaction. Through mathematical calculation, we've come to realize some new rules of non-classical effects of two-mode fields which evolue with time.

1 Introduction

The non-classical effects of field is very interesting topic in quantum optics,and for a long time the interaction of atom with field,and its quantum statistic quality have been paid extensive attention to.Since E.T.Jaynes and F.W.Cummings put forward an ideal model of interaction of two-level atom and one-mode field[1] strictly resolved by pure quantum methods, people have done lots of research on J-C Model in quantum optics these years, for example,interactions of two-level atom with one photon[2],two- photons[3] and multiphotons[4-8],etc. Because one atom may often have multiple levels,and plenty of experiments require the consideration of a third level, people have naturally proceeded the J-C Model to the third level and discussed the interaction of three-level atom with one field.(These are called broad J-C Model),one photon process and multiphoton process,and as a result discovered many non-classical phenomena with different quanlities,for instance,those of revival-collapse as well as squeezing of field and antibunching,etc.[9-11]

The significance of studying J-C Model and broad J-C Model exist in the realization of the respective quantum dynamics qualities of atom and field when they interact. Though people have done a great deal of research on J-C Model, their research is restricted to the resonance and non-resonance of one or two-photon, not covering the function of $K(>2)$ photons. We have already discussed the quantum statistic quality of multiphoton process[12].By adopting the broad J-C Model and using density operator, we have obtained the mean-photon number value in this paper,and then discussed the quantum statistic quality of interaction of three-level atom with two-mode fields according to the criterion on non-classical effects put forward by C.T.Lee and consequent found some new evolution rules.

2 Theoretical model

Let's think about the system of the interaction of "Λ" atom with two-mode fields,$|\ a>$ is given as common upper level,$|\ b>$ and $|\ c>$ are given as lower levels, the state vector of atom are taken from

$$|\ a>=\begin{pmatrix}1\\0\\0\end{pmatrix}\ |\ b>=\begin{pmatrix}0\\1\\0\end{pmatrix}\ |\ c>=\begin{pmatrix}0\\0\\1\end{pmatrix}$$

$|\ a>$ and $|\ b>$, $|\ a>$ and $|\ c>$ is related with mode 1 and mode 2, between the $|\ b>$ and $|\ c>$ is forbiddenness of a transition. On condition of resonance $(\omega_a-\omega_b=k_1\Omega_1,\omega_a-\omega_c=k_2\Omega_2)$ and RWA, the Hamiltonian of the system is expressed as

$$H=\hbar(H_0+H_{int}) \tag{1}$$

the free part of which is

$$H_0=\omega_a s_{11}+\omega_b s_{22}+\omega_c s_{33}+\sum_{i=1}^{2}\Omega_i a_i^{+}a_i \tag{2}$$

and the interacting part is

$$H_{int}=\sum_{i=1}^{2}\lambda_i(s_{1,i+1}a_i^{k_i})+h.c \tag{3}$$

where,$s_{1,i+1}$ are the transition operators of atom,s_{ii} (i=1,2,3) is the level projection oprators of atom,a_i, a_i^{+} and Ω_i(i=1,2) are the annihilation and creation operators, and angle frequencies of the mode i field, λ_i is the coupling constant of atom and field,ω_a,ω_b and ω_c are the correspondence frequencies of $|\ a>$,$|\ b>$ and $|\ c>$,k_1 and k_2 are the photon number of absorption or emission in transition process of atom between $|\ a>$ and $|\ b>$,$|\ a>$ and $|\ c>$.
Because H_0 and H_{int} are the motion constant, then

$$[H_0,H_{int}]=[H_0,H]=[H_{int},H]=0 \tag{4}$$

so,in the interacting picture, there exists

$$H_{int}^{I}=e^{iH_0t}H_{int}e^{-iH_0t}=H_{int} \tag{5}$$

evolution operator of time in interacting picture is

$$U(t)=exp(-iH_{int}^{I}t) \tag{6}$$

where the factors of density matrix $\rho(0)$ of the initial system of atom and field is given, the average value of physical quantities of the system can be obtained from

$$< Q >= T_r[\rho(t)Q] = T_r[U(t)\rho(0)U^+(t)Q] \tag{7}$$

If t=0,the atom is in the common upper state $| a >$, the two-mode fields are in coherent states $| \alpha_1 >$ and $| \alpha_2 >$, and possese their respective mean photon numbers $\overline{n_1} =| \alpha_1 |^2$ and $\overline{n_2} =| \alpha_2 |^2$, the initial density matrix of atom and fields of the system can be shown as

$$\rho(0) = \begin{pmatrix} \rho_f(0) & 0 & 0 \\ 0 & 0 & 0 \\ 0 & 0 & 0 \end{pmatrix} \tag{8}$$

where the initial density operator of field

$$\rho_f(0) = \sum_{m_1,m_1'} \frac{\alpha_1^{m_1}\alpha_2^{m_2}\alpha_1^{m_1'}\alpha_2^{m_2'}}{(m_1!m_2!m_1'!m_2'!)^{1/2}} exp[-\overline{n}_1 - \overline{n}_2] \mid m_1, m_2 >< m_1', m_2' \mid \tag{9}$$

the mean photon numbers of two-mode fields can be gained from(6)-(9)

$$< n_1 >= \overline{n}_1 + \sum_{n_1,n_2} \lambda_1^2 k_1 \frac{(n_1+k_1)!}{n_1!} \frac{sin^2 ut}{u^2} p(n_1,n_2) \tag{10}$$

$$< n_2 >= \overline{n}_2 + \sum_{n_1,n_2} \lambda_2^2 k_2 \frac{(n_2+k_2)!}{n_2!} \frac{sin^2 ut}{u^2} p(n_1,n_2) \tag{11}$$

and

$$< n_1^2 >= \overline{n}_1(\overline{n}_1+1) + \sum_{n_1,n_2} \lambda_1^2(2n_1+k_1)k_1 \frac{(n_1+k_1)!}{n_1!} \frac{sin^2 ut}{u^2} p(n_1,n_2) \tag{12}$$

$$< n_2^2 >= \overline{n}_2(\overline{n}_2+1) + \sum_{n_1,n_2} \lambda_2^2(2n_2+k_2)k_2 \frac{(n_2+k_2)!}{n_2!} \frac{sin^2 ut}{u^2} p(n_1,n_2) \tag{13}$$

$$< n_1 n_2 >= \overline{n}_1\overline{n}_2 + \sum_{n_1,n_2} \left[\lambda_1^2 k_1 n_2 \frac{(n_1+k_1)!}{n_1!} + \lambda_2^2 k_2 n_1 \frac{(n_2+k_2)!}{n_2!} \right] \frac{sin^2 ut}{u^2} p(n_1,n_2) \tag{14}$$

where

$$u = \left[\lambda_1^2 \frac{(n_1+k_1)!}{n_1!} + \lambda_2^2 \frac{(n_2+k_2)!}{n_2!} \right]^{1/2}$$

$$p(n_1,n_2)=\frac{\overline{n}_1^{n_1}\overline{n}_2^{n_2}}{n_1!n_2!}exp(-\overline{n}_1-\overline{n}_2)$$

3 The Statistic quality of field

In general,the non-classical effects of field include squeezing state,antibunching and sub-Poisson distribution,which have been experimented. In 1990,C.T.Lee put forward the definition of second-order correlation function at zero time in identical and different modes in the two-mode field theory.The definition goes as:

$$c_i^{(2)}(0)=<n_i^{(2)}>-<n_i>^2\ (i=1,2) \tag{15}$$

$$c_{12}^{(2)}(0)=<n_1n_2>-<n_1><n_2> \tag{16}$$

where $<n^{(2)}>$ is the second factorial moment of the photon number.Therefore we have $C_i^{(2)}(0)=0$ for a coherent radiation, since it has a Poisson distribution of photon numbers, when $C_i^{(2)}(0)>0$, we call it intramode photon bunching, which is always true for classical radiation; and, in contrast,we have intramode photon antibunching when $C_i^{(2)}(0)<0$,which is possible only for non-classical fields.In analogy to Epn.(15), we call it intermode photon bunching, if we have $C_{12}^{(2)}>0$,or intermode photon antibunching if $C_{12}^{(2)}(0)<0$. C.T.Lee also put forward the criterion of second order non-classical effects about two-mode radiation fields,the criterion is:

$$D_{12}^{(2)}=<n_1^{(2)}>+<n_2^{(2)}>-2<n_1n_2><0 \tag{17}$$

the smaller the $D_{12}^{(2)}$, the deeper the non-classical degree of two-mode radiation fields.
Now let's discuss the evolution rules of $C_1^{(2)}(0), C_2^{(2)}(0), C_{12}^{(2)}(0)$ and $D_{12}^{(2)}$ in case of given initial mean photon numbers $\overline{n}_1$ and $\overline{n}_2$, transition photon numbers k_1 and k_2. Let $\lambda_1=\lambda_2=\lambda, \varphi_1=\varphi_2=0$,we can see:
(a) When initial strength of two-mode fields is weak,$\overline{n}_1=\overline{n}_2=1$.the transition photon number $k_1=k_2=1$ or 10, the evolution curves of $C_1^{(2)}(0)$ and $C_2^{(2)}(0)$ are the same. In $k_1=k_2=1$ process, there is cyclic fluctuation of intramode photon antibunching and bunching, and there is always intermode photon antibunching, and begin $D_{12}^{(2)}>0$, then there are non-classical effects, which become deeper and deeper as time increases,whth fluctuation being weak, getting close to oblique line to the right below. In $k_1=k_2=10$ process, there is not intramode photon antibunching, but there is intermode photon antibunching for $C_{12}^{(2)}(0)$, and there is $D_{12}^{(2)}<0$ from beginning to end, the evolution curves are irregular.
(b) When initial strength of the field increases,$\overline{n}_1=\overline{n}_2=10$, and $k_1=k_2=1$, there are alway intramode photon antibunching, the revival- collapse phenomena of the evolution curves are obvious, there is intermode photon antibunching for $C_{12}^{(2)}(0)$,and $D_{12}^{(2)}<0$,the evolution curves are steeper compared with(a). When $k_1=k_2=10, C_1^{(2)}(0)$ and $C_2^{(2)}(0)$ are both bigger than zero,but there is intermode photon antibunching for $C_{12}^{(2)}(0)$,and $D_{12}^{(2)}<0$, the evolution curves fluctuate

faster, compared with the above.
(c)When initial strength of the field $\overline{n}_1$ and $\overline{n}_2$ are constant, and the transition photon numbers is changed. If $\overline{n}_1 = \overline{n}_2 = 1, k_1 = 1, k_2 = 10$, there is alway intramode photon antibunching for $C_1^{(2)}(0)$, but not for $C_2^{(2)}(0)$, there is alway intermode photon antibunching for $C_{12}^{(2)}(0)$, there is $D_{12}^{(2)} < 0$ from start to finish, all amplitudes of evolution curves increase. If $k_1 = 10, k_2 = 1$,the evolution curves of $C_1^{(2)}(0)$ are pictured as $C_2^{(2)}(0)$, curves of $C_2^{(2)}(0)$ as $C_1^{(2)}(0)$, curves of $C_{12}^{(2)}(0)$ and $D_{12}^{(0)}$ are as the above. When the transition photon number is given, the initial strength of the field is changed, if $k_1 = k_2 = 1, \overline{n}_1 = 0.1, \overline{n}_2 = 1$, the evolution curves of $C_1^{(2)}(0)$ are pictured as $C_1^{(2)}(0)$ in (a)($\overline{n}_1 = \overline{n}_2 = k_1 = k_2 = 1$),but the wavy curves are parallelly shifted down, and the amplitudes increase a little, and $C_2^{(2)}(0)$ are pictured as $C_1^{(2)}(0)$ in (a). If $\overline{n}_1 = 1, \overline{n}_2 = 0.1$,the evolution curves of $C_1^{(2)}(0)$ and $C_2^{(2)}(0)$ are reversed compared with the above. There are anti-bunching for $C_{12}^{(2)}(0)$ and non-classical effects for $D_{12}^{(2)}$.

4 conclusion

The result of the paper continues to show that the non-classical effects of two-mode fields interacting with "Λ" atom by means of multiphotons are not only related to the initial strength of two-mode fields,but also absorption or emission the number of photons in the transition process between atomic levels.In the same time an interesting phenomenon of mode-competition exists,under identical conditions, two modes have identical status in the mode-competition, and $C_1^{(2)}(0)$ and $C_2^{(2)}(0)$ reveal identical evolution rules. Different conditions ,namely identical number of photons transition between atomic levels but different initial strengths of two-mode fields,or different number of photons transition between atomic levels but identical initial strength of two-mode fields will all lead to the generation of the phenomenon of mode- competition. On the other hand, the more the transition photons. the more disadvantageous they are to register where fields enter non-classical effects.

References

[1] E.T.Jaynes,F.W.Cummings,Proc.IEEE.**51**,89(1963).

[2] P.Meyster and M.S.Zubairy,Phys.lett.**89A**,390(1982)

[3] G.Compagnc,Peng Jinsheng and F.Persico, Opt.commun.**57** 415(1986).

[4] A.S.shumovsky,Kien Famle and E.I.Aliskenderov,Phys.lett. **124A**,351(1987).

[5] P.Zhou and J.S.Peng,Optics Acta.**10(9)**,837(1990).

[6] H.Li and T.K.Liu,Quantum Electronics, Supplementary.**9**,19(1992).

[7] G.X.Luo and G.C.Guo,Chinese Laser.**17(2)**,99(1990).

[8] P.Zhou,Optics.Acta.**12(7)**,583(1992).

[9] X.S.Li,Z.D.Liu and C.D.Gong,Phys.Acta.**36(12)**18(1988).

[10] Y.N.Peng,Z.D.Liu and X.S.Li,Optics Acta.**9(1)**,18(1988)

[11] Z.D.Liu,Phys.Acta.**36(12)**,1641(1987).

[12] T.K.Liu,H.Li and Z.D.Liu,Quantum Electronics.**9(2)**,136(1992).

[13] C.T.Lee,Phys.Rev. **A42(3)**,1608(1990). Phys.Rev.**A41(3)**,1569(1990)

NEXT
DOCUMENT

Generation of squeezed light using photorefractive degenerate two-wave mixing

Yajun Lü Meijuan Wu Ling-An Wu* Zheng Tang and Shiqun Li

Dept. of Modern Applied Physics, Tsinghua Univ., Beijing 100084, China
*Institute of Physics, Academia Sinica, Beijing 100080, China

Abstract

We present a quantum nonlinear model of two-wave mixing in a lossless photorefractive medium. A set of equations describing the quantum nonlinear coupling for the field operators is obtained. It is found that, to the second power term, the commutation relationship is maintained. The expectation values for the photon number concur with those of the classical electromagnetic theory when the initial intensities of the two beams are strong. We also calculate the quantum fluctuations of the two beams initially in the coherent state. With an appropriate choice of phase, quadrature squzzing or number state squeezing can be produced.

PACS numbers 42.654 Hw, 42.50.Dv, 42.50 Lc

1 Introduction

The photorefractive effect in electro-optic crystals, a phenomenon in which the local index of refraction is changed by the spatial variation of light intensity [1], has been studied extensively for its potential in many applications. The fundamental process may be described as follows. When the crystal is illuminated with a spatially modulated intensity pattern, free carriers (for example, electrons) are nonunifromly generated due to the photoionization of impurities (generally, which may be doped). The impurities that can be ionized and provide free carriers are called donors. Once these donors are ionized they can serve as trap sites which capture electrons. The electrons can be transported by diffusion or drift and become trapped at these sites. The trapped electrons can then be re-excited except for those in the dark region. Thus a space-charge separation is created, which leads to a space-charge field. Such a field induces a change in index of refraction via the Pockels effect (linear electro-optic effect), creating an index grating. The presence of such an index grating will in turen affect the propagation of these beams. Crystals such as $LiNbO_3$, $BaTiO_3$, SBN, BSO, $GaAs$ and InP, are efficient media for the generation of the photorefractive effect with relatively low intensity level (eg., $1W/cm^2$).

Many different nonlinear optical phenomena in photorefractive media have been studied. These include wave mixing, phase conjugation, self-oscillation, photorefractive resonance, etc. The fundamental photorefractive process is two-wave mixing (TWM), in which two beams intersect inside a photorefractive midia. A stationary index grating is formed which is sptaially

shifted $\pi/2$ relative to the intensity pattern. Such a spatial phase shift leads to nonreciprocal energy transfer when these two beams propagate through the medium. The basic classical electromagnetic theory explaining the nonlinear interaction involved is already well established. Much attention has been focused on its applications including photorefractive resonatore, nonreciprocal transmission windows, self-pumped phase conjugators, laser beam clean-up, optical interconnection, etc. Although a number oi cases of TWM have been analysed, a quantum theory is not available and photorefractive non-classical effects have not been discussed. In this paper we present, to our knowledge for the first time, a quantum treatment of two-wave coupling in a lossless photorefractive medium.

2 Quantum model of photorefractive TWM

A typical geometry for studying two-wave mixing is shown in Fig.1. Under certain circumstances, two beams of light can interact in a photorefractive crystal in such a manner that energy is transferred from one beam to the other. This process is also known as two-beam coupling. The signal and pump waves, of amplitudes A_s and A_p respectively, interfere to form a nonuniform intensity distribution within the crystal. Due to the nonlinear response of the crystal, this nonuniform intensity distribution produces a refractive index grating within the material. However, this grating is displaced from the intensity distribution in the direction of the positive (or effective electrooptic coefficient) crystalline c axis. As a result of this phase shift, the light scattered from A_p into A_s interferes constructively with A_s, whereas the light scattered from A_s into A_p interferes destructively with A_p, and consequently the signal wave is amplified whereas the pump wave is attenuated.

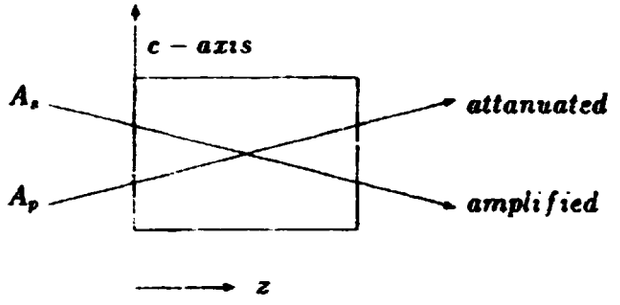

Fig.1. Typical geometry for studying two-beam coupling in a photorefractive crystal

An ideal quantum model for degenerate two-wave mixing may be constructed as follows. Consider the effective interaction Hamiltonian

$$H_{eff} = \hbar\chi' A^\dagger (A^\dagger B + B^\dagger A) B + h.c. \qquad (1)$$

where χ' is the effective interaction coefficient for the nonlinear process, A and B are the Boson operators for two modes with frequency $\omega_a = \omega_b$. Factor $(A^\dagger B + B^\dagger A)$ represents the interference of two modes [2]. The TWM can be understood from the following physical picture. Mode A is generated accompanied by the annihilation of mode B, due to scattering from the grating induced by the interference. In other words, mode B is "scattered" by the grating in the direction of beam A, to yield mode A, which is responsible for the energy coupling. The Heisengerg equations

of motion for the field operators A and B may be easilly obtained from H_{eff}. Making the conversion $z = vt$ for propagation along the z-axis at a velocity v, we can write the equations as

$$\frac{dA}{dz} = -2i\chi A^\dagger B^2 - i(\chi + \chi^*)AB^\dagger B \tag{2}$$

$$\frac{dB}{dz} = -2i\chi^* B^\dagger A^2 - i(\chi + \chi^*)BA^\dagger A \tag{3}$$

where $\chi = \chi'/v$. We find the field operators satisfy the Boson commutation rules. From the equations of motion for the photon number operatore N_a and N_b

$$\frac{dN_a}{dz} = -2i\chi A^{\dagger 2}B^2 + 2i\chi^* A^2 B^{\dagger 2} \tag{4}$$

$$\frac{dN_b}{dz} = 2i\chi A^{\dagger 2}B^2 - 2i\chi^* A^2 B^{\dagger 2} \tag{5}$$

we can show that the total photon number is constant throught the process. In the short path approximation, the solutions of Eqs.(2) and (3) for the field operators with expansion up to the quadratic $(\chi z)^2$ term is

$$\begin{aligned} A(z) = \; & a - 2i(\chi z)a^\dagger b^2 - iz(\chi + \chi^*)ab^\dagger b \\ & - |\chi z|^2 [(4a^\dagger a^2 + a)b^\dagger b - (2a^\dagger - a)b^{\dagger 2}b^2 + (a^{\dagger 2}b^2 + b^{\dagger 2}a^2)a + 2a^\dagger a^2] \\ & - z^2[\chi^2(a^{\dagger 2}ab^2 + b^{\dagger 2}b^2 a/2 + b^\dagger ba/2) + \chi^{*2}(a^3 b^{\dagger 2} + ab^{\dagger 2}b^2/2 + ab^\dagger b/2)] \end{aligned} \tag{6}$$

$$\begin{aligned} B(z) = \; & b - 2i(\chi^* z)b^\dagger a^2 - iz(\chi + \chi^*)ba^\dagger a \\ & - |\chi z|^2 [(4b^\dagger b^2 + b)a^\dagger a - (2b^\dagger - b)a^{\dagger 2}a^2 + (b^{\dagger 2}a^2 + a^{\dagger 2}b^2)b + 2b^\dagger b^2] \\ & - z^2[\chi^{*2}(b^{\dagger 2}ba^2 + a^{\dagger 2}a^2 b/2 + a^\dagger ab/2) + \chi^2(b^3 a^{\dagger 2} + ba^{\dagger 2}a^2/2 + ba^\dagger a/2)] \end{aligned} \tag{7}$$

where a and b are the input field operators, respectively. It may be seen that, to the quadratic term, the field operators still satisfy the commutation relation

$$[A(z), A^\dagger(z)] = 1, \qquad [B(z), B^\dagger(z)] = 1 \tag{8}$$

In order to test our quantum model for photorefractive TWM, we may derive the expectation values for the photon number in each beam and verify if the result of the quantum calculation concur with those of the classical electromagnetic theory. When the two beams are initially in the coherent state $|\alpha\rangle$ and $|\beta\rangle$ with

$$\alpha = |\alpha| exp(i\delta_a/2) \tag{9}$$

$$\beta = |\beta| exp(i\delta_b/2) \tag{10}$$

$$\chi = |\chi| exp(i\phi) \tag{11}$$

we obtain

$$\begin{aligned} \langle N_a \rangle = \; & |\alpha|^2 + 4sin(\phi + \delta_b - \delta_a)|\chi z||\alpha\beta|^2 + 4|\chi z|^2(|\beta|^4 - |\alpha|^4) \\ & + 8|\chi z|^2|\alpha\beta|^2(|\beta|^2 - |\alpha|^2)[1 + cos\phi cos(\phi + \delta_b - \delta_a)] \end{aligned} \tag{12}$$

$$\langle N_b \rangle = |\alpha|^2 + |\beta|^2 - \langle N_a \rangle \tag{13}$$

where ϕ, δ_b and δ_a are phase angles, depending on the initial condition. We take $\delta_b - \delta_a = \pi$ and write $I_a = |\alpha|^2$, $I_b = |\beta|^2$, then obtain

$$\langle N_a \rangle = I_a - 4sin\phi\,|\chi z|\,I_a I_b + 4|\chi z|^2 (I_b^2 - I_a^2) \tag{14}$$

$$\langle N_b \rangle = I_a + I_b - \langle N_a \rangle \tag{15}$$

According to the classical electromagnetic theory, the coupled equations for photorefractive TWM can be written as [3]

$$\frac{dI_1}{dz} = -\gamma \frac{I_1 I_2}{I_1 + I_2} \tag{16}$$

$$\frac{dI_2}{dz} = \gamma \frac{I_1 I_2}{I_1 + I_2} \tag{17}$$

where I_1 and I_2 are the intensities of beams 1 and 2, respectively, and γ is the coupling constant with

$$\gamma = \frac{2\pi n_1}{\lambda cos\theta} sin\phi \tag{18}$$

Here n_1 is the depth of index modulation related to the electro-optic coefficient, 2θ is the angle between the two beams inside the medium and ϕ is the phase that indicates the degree to which the index grating is shifted spatially with respect to the light interference pattern.

By examining the coupled equations, we note that I_2 is an increasing function of z, provided γ is positive. This indicates that the energy is flowing from beam 1 to beam 2. The direction of energy flow is determined by the sign of γ, which depends on the orientation of the crystal axis. The solution for the intensities $I_1(z)$ and $I_2(z)$ are

$$I_1(z) = I_1(0) \frac{I_1(0) + I_2(0) exp(\gamma z)}{I_0} \tag{19}$$

$$I_2(z) = I_2(0) exp(\gamma z) \frac{I_1(0) + I_2(0) exp(\gamma z)}{I_0} \tag{20}$$

where $I_1(0)$ and $I_2(0)$ are the input intensities of beam 1 and beam 2, respectively, and I_0 is the sum intensity with $I_0 = I_1(0) + I_2(0)$. In the short path approximation, the solutions can be expanded to the quadratic $(\gamma z)^2$ term as

$$I_1(z) = I_1(0) - \gamma z \frac{I_1(0) I_2(0)}{I_0} + (\gamma z)^2 \frac{I_1(0) I_2(0)}{2 I_0^2} [I_2(0) - I_1(0)] \tag{21}$$

$$I_2(z) = I_0 - I_1(z) \tag{22}$$

Comparing Eqs.(14) and (15) with Eqs.(21) and (22), we find that the results of the quantum theory are consistent with those of the classical theory, so long as $I_1(0) = I_a$, $I_2(0) = I_b$, $\gamma = 4|\chi| sin\phi I_0$ and $I_a >> 1$, $I_b >> 1$. When the input intensities of the two beams are strong, the effective Hamiltonian H_{eff} can give and accurate description of the energy exchange phenomenon in photorefractive two-wave mixing, as shown in Fig.2. We can

thus conclude that our quantum model for photorefractive TWM is reasonable and successful.

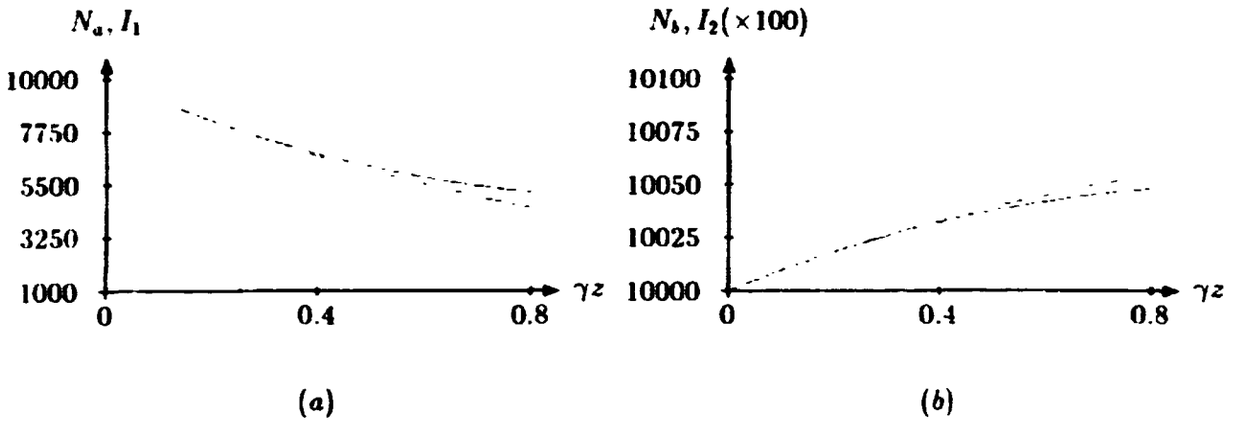

Fig.2. The intensities of two beams versus the effective interaction length (γz). Dashed curve the intensities of the classical electromagnetic theory I_1 and I_2, from Eqs.(19) and (20). Solid curve: the quantum average photon number N_a and N_b. The initial intensities $I_1 = 10^4$, $I_2 = 10^6$, respectively.

3 Quantum statistic of photorefractive TWM

To discuss the photon number fluctuations of the quantized field we consider the variance $\langle \Delta N_j^2(z) \rangle$ or the Fano factor

$$F_j(z) = \frac{\langle \Delta N_j^2(z) \rangle}{\langle \Delta N_j(z) \rangle} \tag{23}$$

where $\langle \Delta N_j^2(z) \rangle = \langle N_j^2(z) \rangle - \langle N_j(z) \rangle^2$ and $j = a, b$. To obtain the above expression we need to find the expectation values for $\langle \Delta N_a^2(z) \rangle$ and $\langle \Delta N_b^2(z) \rangle$. When the input fields are in the coherent state $|\alpha\rangle$ and $|\beta\rangle$, after some tedious calculation we may obtain the expectation values

$$\langle \Delta N_a^2(z) \rangle = I_a - 8 sin\phi \mid \chi z \mid I_a I_b + 8 \mid \chi z \mid^2 I_a [2 I_a^2 I_b cos(2\phi) + 2 I_a I_b^2 (1 - sin^2\phi) - I_b^2 - I_a^2] \tag{24}$$

$$\langle \Delta N_b^2(z) \rangle = I_b + 8 sin\phi \mid \chi z \mid I_a I_b + 8 \mid \chi z \mid^2 I_b [2 I_b^2 I_b cos(2\phi) + 2 I_b I_a^2 (1 - sin^2\phi) - I_a^2 - I_b^2] \tag{25}$$

where we have taken $\delta_b - \delta_a = \pi$. Here $\phi = \pm\frac{\pi}{2}$ corresponds to the maximum energy coupling between the two beams. Eqs.(14) and (15) show that the energy flows from beam A to beam B when $\phi \in [0, \pi]$. This indicates that A is the pump beam and B the signal beam. Let $\phi = \frac{\pi}{2}$, we rewrite Eqs.(24) and (25) as

$$\langle \Delta N_a^2(z) \rangle = I_a - 8 \mid \chi z \mid I_a I_b + 8 \mid \chi z \mid^2 I_a [-2 I_a^2 I_b + 4 I_a I_b^2 - I_b^2 - I_a^2] \tag{26}$$

$$\langle \Delta N_b^2(z) \rangle = I_b + 8 \mid \chi z \mid I_a I_b + 8 \mid \chi z \mid^2 I_b [-2 I_b^2 I_a + 4 I_b I_a^2 - I_a^2 - I_b^2] \tag{27}$$

The Fano factor plotted against the effective interaction length γz is shown in Fig.3, where $\gamma = 4 \mid \chi \mid sin\phi I_0$. We see that the pump mode A can be in a squeezed number state, whereas the signal mode B becomes super-Poissonion at the some time.

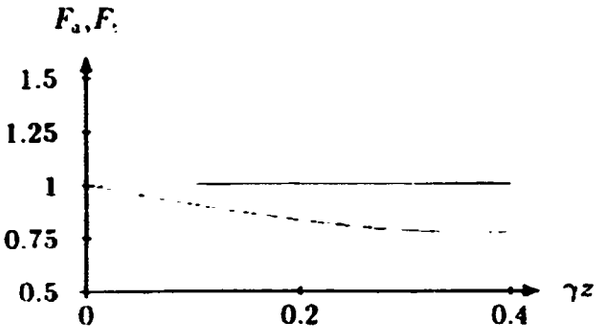

Fig.3. Fano factors of beams A and B versus effective interaction length γz for coherent state inputs. Dashed curve. F_a. solid curve: F_b. The initial intensity ratio $m = \frac{I_a(0)}{I_b(0)} = \frac{1}{100}$ F_a shows the sub-Poissoinan statistical feature

Moreover, the signal mode can never becomes squeezed(at least for our solution expanded to the second order). The degree of squeezing in the pump mode depends on the initial intensity ratio m (here we define $m = \frac{I_a(0)}{I_b(0)}$). If m is large (for example, 100), then the degree of squeezing will be very small (in the short path approximation). This is reasonable as the energy coupling has little effect on the intensity of the pump modes, so the quantum fluctuations will not be reduced greatly.

The quadrature phase amplitudes of the two beams are defined as

$$X_a = \frac{A(z)+A^\dagger(z)}{2} \qquad Y_a = \frac{A(z)-A^\dagger(z)}{2i} \tag{28}$$

$$X_b = \frac{B(z)+B^\dagger(z)}{2} \qquad Y_b = \frac{B(z)-B^\dagger(z)}{2i} \tag{29}$$

When the input field are in the coherent state, the field variances may be determined explicitly to be

$$\langle \Delta X_a^2(z) \rangle = \tfrac{1}{4} + |\chi z| I_b sin(\phi+\delta_b) + 2|\chi z|^2 I_b[I_b + I_a cos^2\phi - I_a cos\delta_a(1+cos^2\phi) - (2I_a + I_b)cos\phi cos(\phi+\delta_b)] \tag{30}$$

$$\langle \Delta Y_a^2(z) \rangle = \tfrac{1}{4} - |\chi z| I_b sin(\phi+\delta_b) + 2|\chi z|^2 I_b[I_b + I_a cos^2\phi + I_a cos\delta_a(1+cos^2\phi) + (2I_a + I_b)cos\phi cos(\phi+\delta_b)] \tag{31}$$

$$\langle \Delta X_b^2(z) \rangle = \tfrac{1}{4} + |\chi z| I_a sin(\delta_a-\phi) + 2|\chi z|^2 I_a[I_a + I_b cos^2\phi - I_b cos\delta_b(1+cos^2\phi) - (2I_b + I_a)cos\phi cos(\delta_a-\phi)] \tag{32}$$

$$\langle \Delta Y_b^2(z) \rangle = \tfrac{1}{4} - |\chi z| I_a sin(\delta_a-\phi) + 2|\chi z|^2 I_a[I_a + I_b cos^2\phi + I_b cos\delta_b(1+cos^2\phi) + (2I_b + I_a)cos\phi cos(\delta_a-\phi)] \tag{33}$$

With an appropriate choice of phase, both modes can produce quadrature squeezing. For example, when$\phi = \pi/2$, $\delta_b = \pi$ and $\delta_a = 0$, it is obvious that $\langle \Delta X_a^2(z) \rangle$ and $\langle \Delta X_b^2(z) \rangle$ may be less than $\frac{1}{4}$ in the short path approximation. The variances plotted against the effective interaction γz are shown in Fig.4. We see that both modes can be in the squeezed state. Furthermore, there is strong dependence on which of the input modes is strong. The degree of squeezing in the pump mode is great when the initial intensity ratio m is small, as shown in Fig.4. In the reverse case,

if the pump mode A is strong, then the degree of squeezing in the signal mode B will be great.

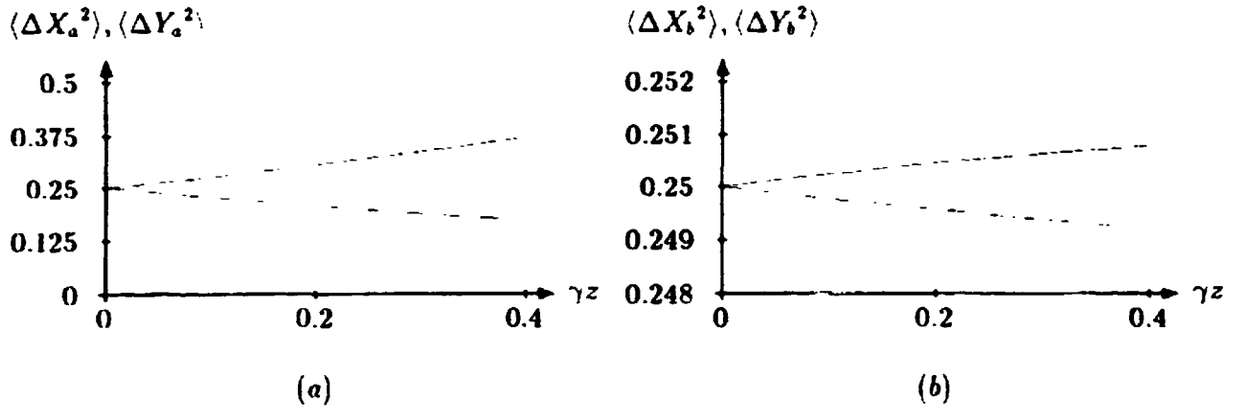

Fig.4 The variances $\langle \Delta X_a^2 \rangle$, $\langle \Delta Y_a^2 \rangle$, $\langle \Delta X_b^2 \rangle$, and $\langle \Delta Y_b^2 \rangle$ when both input field are initially in the coherent state, with $m = \frac{1}{100}$. Dashed curves: the variances of X component, which show quadrature squeezing. Solid curves: the variances of Y component.

4 Conclusion

In conclusion, we have presented a quantum model of photorefractive TWM, which can well describe the energy exchange phenomenon in TWM. A set of coupled mode equations is obtained and solved in the short path approximation We have also calculated the quantum fluctuations of the two modes and find that when both modes are initially in the coherent state, the pump beam can become sup-Poissonian, due to the photon flux in the energy transfer. The same qualitative result was also obtained in our previous approach from a set of simplified field equations [4]. With an appropriate choice of phase relationship, quadrature squeezing can be produced.

References

[1] P. Yeh, *Introduction to Photorefractive Nonlinear Optics* (Wiley, New York, 1993).

[2] J. Perina, *Quantum Statistic of Linear and Nonlinear Optical Phonomena* (Kluwer Academic publishers, 1991).

[3] P. Yeh, *IEEE* J. Quantum Electron, **3**, 484 (1989).

[4] Tang Zheng, Lü Yajun, Wu Meijuan, Li Shiqun and Wu Ling-An, 6th National Conf. on Quantum Optics, Jiangxi, China, Oct, 1994 (in chinese).

NEXT
DOCUMENT

STEADY-STATE SQEEZING IN THE MICROMASER CAVITY FIELD

N. Nayak

Satyendra Nath Bose National Centre for Basic Sciences, DB-17,

Sector-I, Salt Lake City, Calcutta-700064, India

E-Mail: nayak@bose.ernet.in

The micromaser has been extensively studied as a source of radiation fields having various nonclassical properties. One such propety is the sub-Poissonian nature of the radiation field which has been experimentally demonstrated in this dynamics [1].This device involves a microwave cavity of high quality factor Q and cooled down to sub-Kelvin temperature. In the conventional micromaser, two-level Rydberg atoms in their upper states are pumped into the cavity at such a rate that at most one atom at a time is allowed to interact with the cavity field. The very first atom encounters the field at thermal equilibrium. After the interaction, the field evolves under the influence of its own reservoir until the next atom enters the cavity. The process repeats itself with a repeatation time $t_c = \tau + t_{cav}$ where τ is the atom-field interaction time and t_{cav} is the duration between successive atoms. τ is fixed whereas t_{cav} is random following a Poissonian pump with an average $\bar{t}_c = 1/R$ where R is the number of atoms entering the cavity per second. We find that the cavity field is coupled to the atom during τ only whereas it is coupled to its reservoir during the entire duration t_c. Hence, the nonclassical nature of the field would be very sensitive to the cavity field damping.

The theory of micromaser proposed in Ref.[2] is capable of

including the effect of reservoir-induced interactions even during the short duration τ on the evolution of the cavity field. Its influence on the normalized variance $v = [(\langle n^2\rangle - \langle n\rangle^2)/\langle n\rangle]^{1/2}$ ($v < 1$ for sub-Poissonian fields) is clearly evident in the Fig.(1). The spontaneous emission constant between the two masing levels γ= 4400 Hz (dotted), 4.4 Hz (dashed), and 0.0 (full). The dash-dot-dot curve represents the results for the ideal situation during τ i.e no damping whatsever.

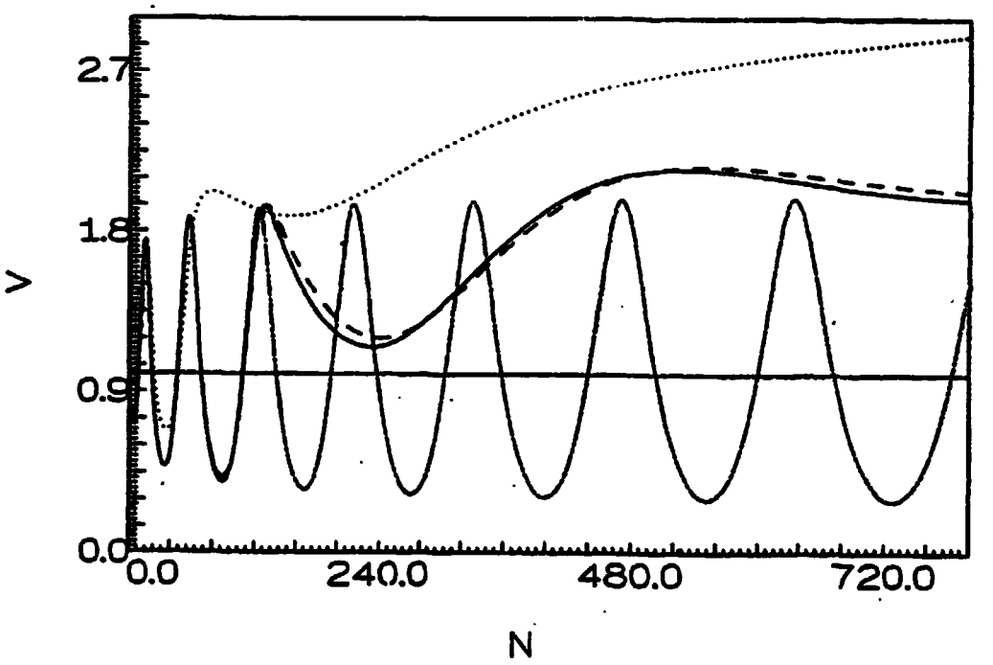

Fig.1. Variation of v with N, the number of atoms streamed through the cavity during photon lifetime for the experimental setup in Ref.[1]. τ=35 μsec., and cavity temperature T=0.5 K.

The above description is for the atoms being in their upper states at the time of entering the cavity. In stead, if the atoms are in a coherent superposition of two masing levels at the beginning of interaction, it can induce a phase information to

the cavity field. This may result in the squeezing of a quadrature of the radiation field.

The two-level Rydberg atoms, at the time of entering the cavity, are in a coherent superposition

$$|\psi\rangle = \alpha|a\rangle + \beta|b\rangle \qquad (1)$$

of their upper ($|a\rangle$) and lower ($|b\rangle$) states. We assume through out this paper that α and β are real. The transition frequency between the levels is in resonance with the single eigenmode of the cavity at frequency ω. We represent the atom by the Pauli pseudo-spin operators obeying the commutation relation $[s^+,s^-] = 2s^z$. The cavity field is represnted by the annihilation (creation) operator a ($a^\dagger$) which satisfy the commutation ralation $[a,a^\dagger] = 1$. The atom-field iteraction is then given by the well-known Jaynes-Cummings Hamiltonian [3]

$$H = g(s^+a + s^-a^\dagger) \qquad (2)$$

where g is is the coupling constant.

In a frame rotating at ω the equation of motion for the composite atom-field system can be taken to be

$$\dot{\rho} = -i[H,\rho] - \varkappa((1+\bar{n}_{th})(a^\dagger a\rho - 2a\rho a^\dagger + \rho a^\dagger a) + \bar{n}_{th}(aa^\dagger\rho - 2a^\dagger\rho a + \rho aa^\dagger)). \qquad (3)$$

The effect of the heat-bath at the temperature T > 0 is introduced through the terms in the Planck function $\bar{n}_{th}$. $\varkappa = \omega/2Q$ is half the bandwidth of the eigenmode. The effect of atomic reservoir is not included here as it has been seen in Ref.(2b) that the significant influence comes from the cavity damping.

We follow the procedure in Ref.(2) to get an expression for time derivative of the density operator for the field only in photon number representation i.e. $\rho_{n,m} = \langle n|\rho|m\rangle$. The resulting expression gives, in the steady-state, the continued fractions

for $W_{n,m}=\rho_{n,m}/\rho_{n-1,m-1}$ for all n and m which is

$$W_{n,m} = Z^{-}_{n,m}/[Z_{n,m}+Z^{+}_{n,m} W_{n+1,m+1}] \qquad (4)$$

where z, $z^{\pm}$ are all functions of system parameters. We need $\rho_{n,n}$, $\rho_{n,n+1}$ and $\rho_{n,n+2}$ to obtain variances X and Y in the two quadratures defined by $a_x=(a+a^{\dagger})/2$ and $a_y=(a-a^{\dagger})/2i$ respectively. X or Y <0 indicates squeezing in that quadrature.

Our numerical study of X and Y as a function of $g\tau$, pump rate N and other parameters reveals interesting results for $g\tau=\pi$ which we display in Fig. (2) for a cavity with $\kappa/g=0.81\times10^{-5}$. The experiment in Ref. [1] had the same value of κ/g but the cavity

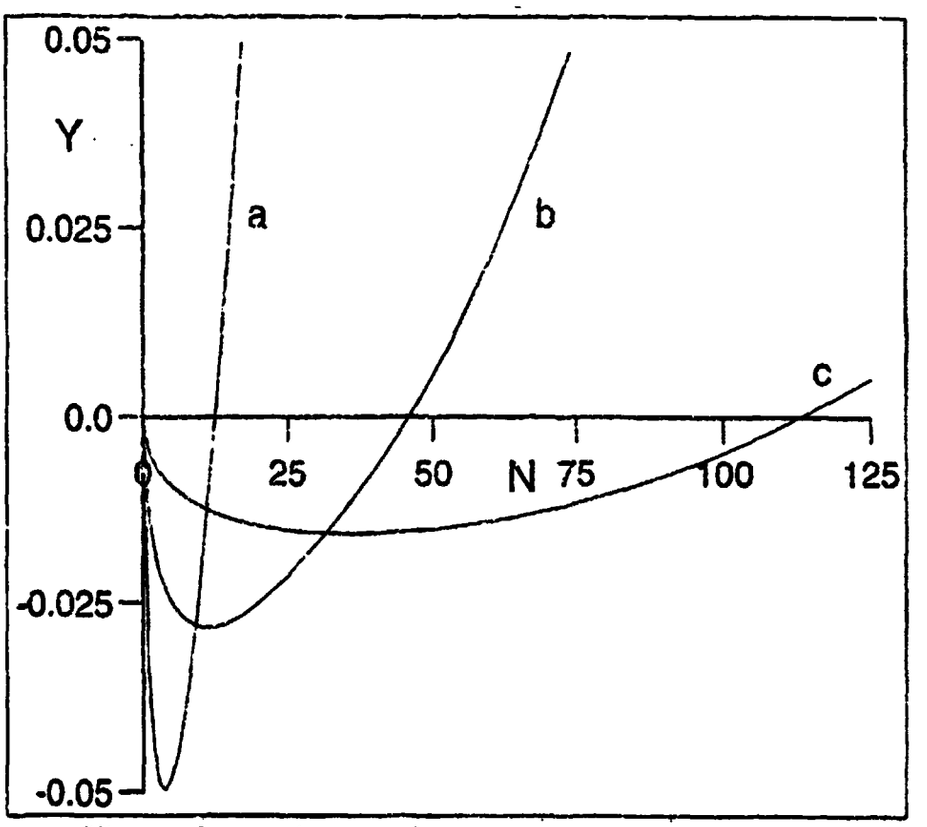

Fig.2. Squeezing Y as a function of dimensionless pump rate $N=R/2\kappa$. The curves are for the atom-field interaction set by $g\tau=\pi$. $|\beta|^2=0.1$.

temperature was at T=0.5 K. Figure 2 indicates that T needs to be further reduced to observe squeezing in the cavity field.The curves a, b and c in the Fig. (2) are for T=0.22[illegible] K, 0.15 K and 0.11 K respectively. The corresponding thermal photons at the cavity mode frequency [1] are $\bar{n}_{th}$=0.01, 0.001 and 0.0001. Fig. (2) shows that the squeezing in a_y quadrature persists for higher pump rate N for lower temperature.

The photon distribution of the cavity field is, in general, peaked at various n at temperatures such as in Fig. (2). These states $|n\rangle$, are known as trapped states [4].These can be easily analysed for an ideal cavity (Q=∞) which reveal that,in the case of polarized atoms, a trapped vacuum state $|0\rangle$ of the cavity field results for $gT=\pi$ and for T $\simeq$ 0.1 K. With cavity dissipation included, it is difficult to notice directly the trapped states of the cavity field in Eq. (4). However, from our numerical study, we notice in the case of Fig.(2c), for lower pump rate N, the cavity field is *almost* in the trapped vacuum state and the uncertainty product of its two quadratures a_x and a_y is close to that for a minimum uncertainty state.

In conclusion, we have shown that the radiation field in the micromaser cavity presently in operation [1] may be squeezed if pumped with polarized atoms. With both α and β considered real, we show squeezing in the a_y quadrature. In Refs. [5], the a_x quadrature has been shown squeezed as α and β are out of phase by $\pi/2$.However, it is difficult to make a quantitative comparison with the results in Ref. [5] as the squeezing there has been studied in various types of fields which are assumed to be present in an ideal cavity, that is Q=∞ during the entire repeatation time t_c. In the present paper, the squeezing is in the steady-state field evolved from the action, same as in

conventional micromaser, with the effect of cavity dissipation included during the entire $t_c = \tau + t_{cav}$. The atoms at the time of entering the cavity is prepared, instead of being in the upper state, in a polarized state such that $\beta \ll \alpha$.

References:

[1] G. Rempe, F. Schmidt-Kaler, and H. Walther, Phys.Rev.Lett. 64, 2783(1990).

[2] (a) N. Nayak and D. Das, Phys.Rev.A 48, 2475 (1993); (b) N. Nayak, Opt.Commun.118, 114 (1995).

[3] E. T. Jaynes and F. W. Cummings, Proc. IEEE 51, 89(1963).

[4] (a)P. Meystre, G. Rempe, and H. Walther, Opt.Lett.13, 1078, (1988);(b) F. W. Cummings and A. K. Rajagopal, Phys.Rev.A 39, 3414(1989).

[5] S. Qamar, K. Zaheer, and M. S. Zubairy, Opt.Commun. 78, 341 (1990); P. Meystre, J. Slosser, and M. Wilkens, Phys.Rev.A 43, 4959 (1991)

NEXT
DOCUMENT

Cooperative effects in a one photon Micromaser .

Miguel Orszag
Facultad de Fisica, Pontificia Universidad Catolica de Chile
Casilla 306, Santiago, Chile

August 7, 1995.

Abstract

For small photon numbers, trapping states are difficult to detect due to the influence of the collective effects. We find that if the atoms are injected with atomic polarization, the micromaser becomes more insensitive to these effects. In particular, the squeezing properties of the cotangent states are basically unchanged.

Recent work studied the effects of having two simultaneous and fully inverted atoms in the one photon micromaser cavity, and found that the trapping states were strongly disrupted by these effects for a low photon number[2, 3].

Here we will describe the cooperative effects of polarized atoms on the trapping states and squeezing properties of the cotangent states[4][1].

The Hamiltonian of the two atom field system, in the Dipole and Rotating wave approximations is:

$$V_I = \hbar g \left\{ \left(a\sigma_1^\dagger + a^\dagger \sigma_1 \right) \otimes 1_2 + \left(a\sigma_2^\dagger + a^\dagger \sigma_2 \right) \otimes 1_1 \right\}. \qquad (1)$$

where g is the one atom- field coupling constant and σ_1 and σ_2 the atomic Pauli spin operators for atom one and two respectively. Here we assume

exact resonance between the field and the atoms.

Let us denote by $|e\rangle_i$ and $|g\rangle_i$, $i = 1, 2$ the excited and ground state of the i-th atom.

The system can be described by the basis:

$$\{|e\rangle_1|e\rangle_2, |e\rangle_1|g\rangle_2, |g\rangle_1|e\rangle_2, |g\rangle_1|g\rangle_2\}$$

The time evolution operator of the system can be calculated in a simple way. It is:

$$U_2(\Delta\tau) = \begin{pmatrix} A & -iaS & -iaS & B \\ -iSa^\dagger & D & E & -iSa \\ -iSa^\dagger & E & D & -iSa \\ B^\dagger & -ia^\dagger S & -ia^\dagger S & \tilde{A} \end{pmatrix} \tag{2}$$

where

$$A = 1 + \frac{a(C-1)a^\dagger}{\Lambda} \qquad B = \frac{a(C-1)a}{\Lambda} \qquad D = \frac{1}{2}(1+C) \tag{3}$$

$$E = -\frac{1}{2}(1-C) \qquad C = \cos(\sqrt{2}g\Delta\tau\sqrt{2n+1}) \qquad \Lambda = 2n+1 \tag{4}$$

$$S = \sin(\sqrt{2}g\Delta\tau\sqrt{2n+1})/\sqrt{4n+2}, \qquad \tilde{A} = 1 + a^\dagger(C-1)a/\Lambda, \tag{5}$$

where $\Delta\tau$ is the interaction time during which the 2 atoms are present in the cavity.

We assume that at $t = 0$ a first atom enters the cavity and a second one Δt seconds later.

The state of the system at the instant just before the first atom leaves the cavity is given by:

$$\rho(\Delta t + \Delta\tau) = U_2(\Delta\tau)\rho_{af}(\Delta t)U_2^{\dagger}(\Delta t)$$

$$\rho_{af}(\Delta t) = U_1(\Delta t)\rho_f(0) \otimes \rho_a(0)U_1^{\dagger}(\Delta t) \tag{6}$$

where $U_1(\Delta t)$ is the time evolution operator of the Jaynes-Cummings Model and ρ_a is given by:

$$\rho_a = \begin{pmatrix} |\alpha|^2 & \alpha^*\beta \\ \alpha\beta^* & |\beta|^2 \end{pmatrix}, \tag{7}$$

that describes the initial state of the atom. Next, we trace over the first atom and get the atom 2 -field density matrix. The evolution of the present system is governed by the Jaynes-Cummings model. Two possibilities arise. One is that the atom 2 leaves before a new atom enters the cavity or a new atom enters before atom 2 leaves.

We may define various sequences as described by Figure 1. Sequence (a) (010) corresponds to no atom-one atom-no atom sequence. Similarly, we may have a sequence (01210) (Figure 1-b) or (0121210) corresponding to Figure 1-c. We discard events containing three or more simultaneous atoms.

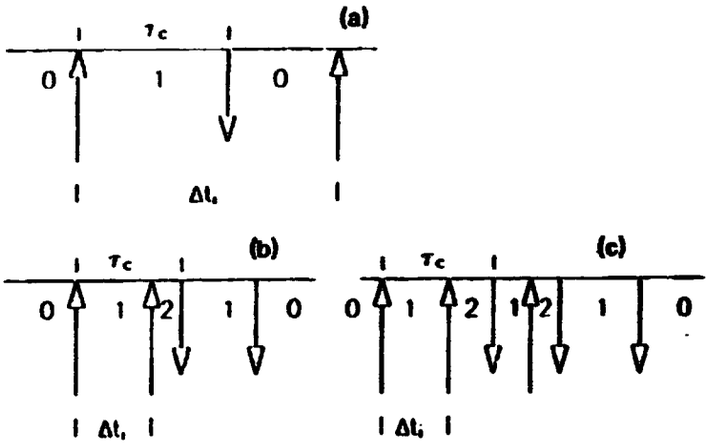

Figure1.Poissonian injection of atoms. The arrow pointing upwards indicates an atom entering the cavity and a downwards arrow means that it leaves. (a)$\Delta t_i \succ \tau_c$and we have either zero or one atom inside the cavity. (b)$\Delta t_i \prec \tau_c$ and $\Delta t_{i+1} \succ \tau_c$.(c)$\Delta t_i \prec \tau_c, \Delta t_{i+1} \prec \tau_c and \Delta t_{i+2} \succ \tau_c$.

For each of these sequences, it is possible, through a tedious but straightforward procedure, to write the field density matrix elements in terms of the relevant parameters of this system.

In order to numerically simulate the process described above in a realistic fashion,we consider that the atomic arrival obeys a Poisson distributic... We characteriz- the atomic flux by a parameter $p = \langle \Delta\tau \rangle / \tau_c$, where $\langle \Delta\tau \rangle$ is the average time between consecutive atoms and τ_c the atomic flight time through the cavity. We also define the usual one photon trapping condition $\sqrt{N_u + 1} g\tau_c = q\pi$, q being an integer number.

Next, we describe some numerical results. The parameters used are $p = 15.6$, $N_u = 10$, $|\alpha|^2 = 0.9$.

In Figure 2-a we show the field density matrix elements after 1000 atoms crossed the cavity, and one can already see a small hill between n= 12 and 18, clearly indicating that a the trap had already : small leak. This effect is of course more dramatic, as one increases the atomic numbers to 2500 (Figure 2-b) and $N_{atom} = 5000$ (Figure 2-c). This set of three Figures clearly

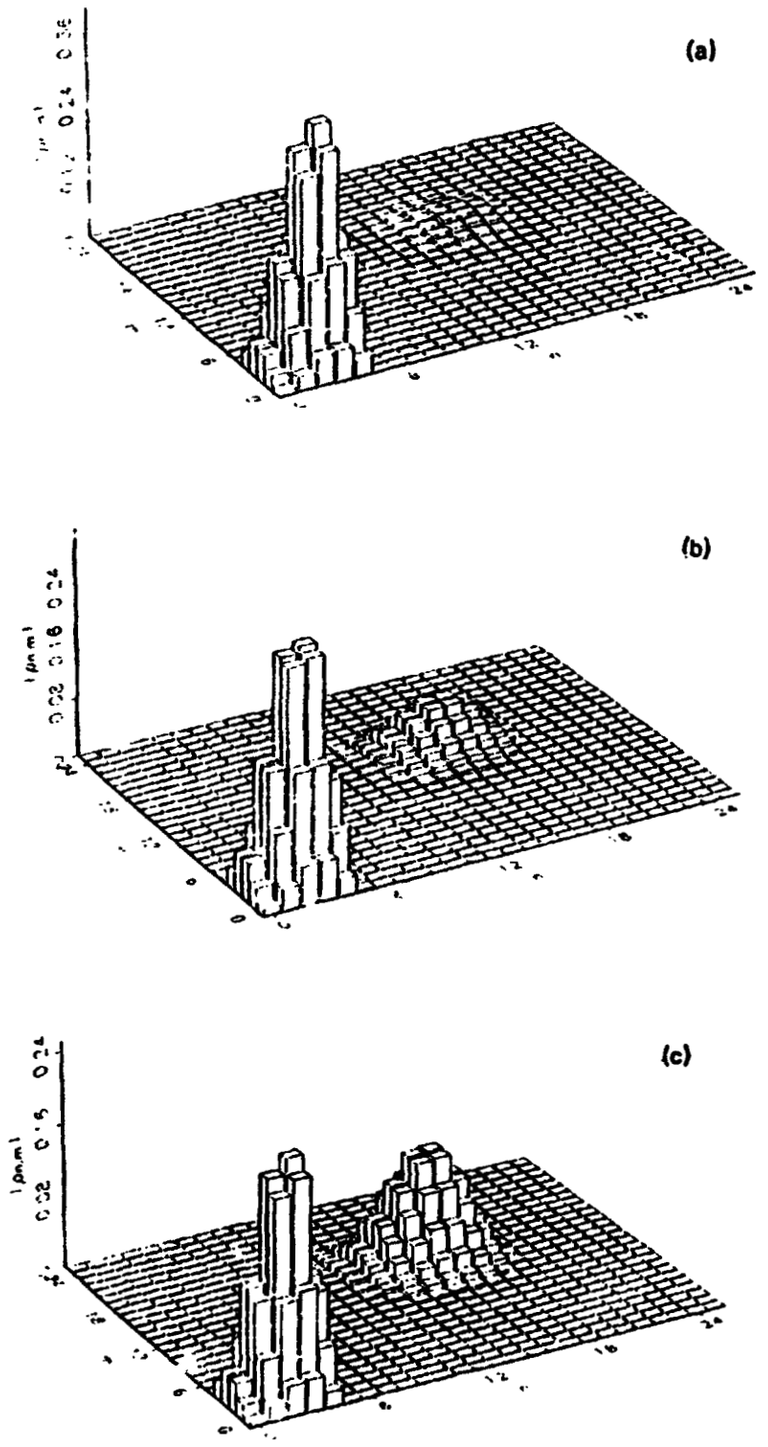

Fig. 2. Reduced field density matrix for $p = 15.6$, $N_u = 4$ and $|\alpha|^2 = .9$. (a) $N_{atom} = 1000$. (b) $N_{atom} = 2500$. (c) $N_{atom} = 5000$.

display the probability diffusion in phase space.

The most important result in this work is shown in Figure3, where the Y-quadrature variance is shown versus atomic Number. The dotted line corresponds to the squeezing of the cotangent states[4], and the full line to the present case. We observe that even for a relatively large atomic flux ($p = 15.6$), *the squeezing property of the cotangent states are extremely robust to the cooperative effects, that otherwise seem to be very destructive.*

In a future work, we would like to explore how the atomic measurement at the outside of the cavity affects all the properties of the field discussed here.

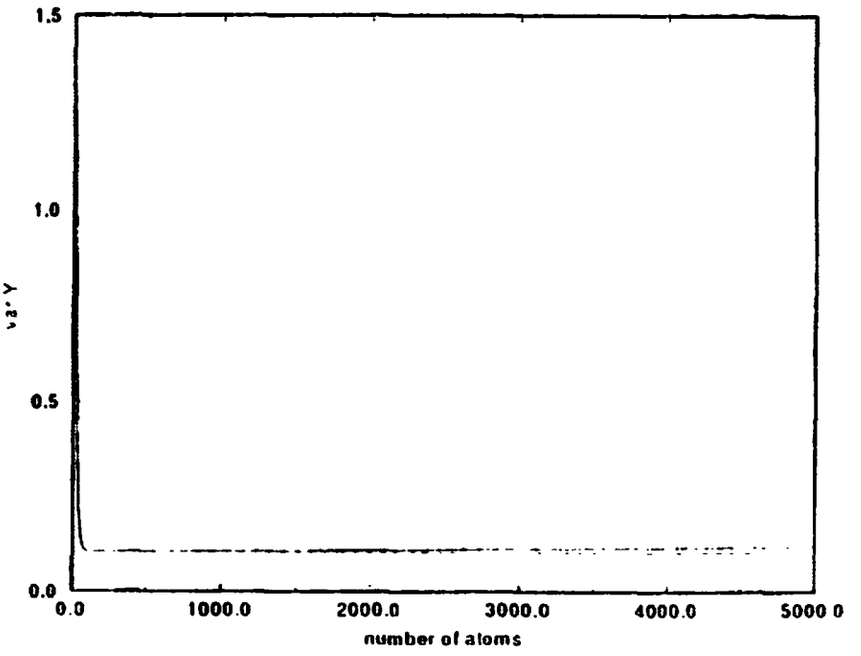

Figure3.Variance of the field quadrature Y versus the number of atoms of the cotangent state(dotted line) and the present case(full line). The parameters are the same as in Figure 2, except N_u=10.

References

[1] L.Ladron de Guevara, M.Orszag, R.Ramirez, L.Roa(to be published)

[2] M.Orszag, R.Ramirez, J.C.Retamal, C Saavedra, Phys. Rev., **A49**, 2933, (1994)

[3] E.Wehner, R.Seno, N.Serpi, B.G.Englert, H.Walther, Opt Comm., **110**, 655 (1994)

[4] J.Slosser, P.Meystre. Phys.Rev.A**41**,3867(1990).

NEXT
DOCUMENT

QUANTUM PROBABILITY CANCELLATION DUE TO A SINGLE-PHOTON STATE

Z. Y. OU
Department of Physics
Indiana University-Purdue University at Indianapolis
Indianapolis, IN 46202, USA
zou@indyvax.iupui.edu

Abstract

When an N-photon state enters a lossless symmetric beamsplitter from one input port, the photon distribution for the two output ports has the form of Bernouli Binormial, with highest probability at equal partition ($N/2$ at one outport and $N/2$ at the other). However, injection of a single photon state at the other input port can dramatically change the photon distribution at the outputs, resulting in zero probability at equal partition. Such a strong deviation from classical particle theory stems from quantum probability amplitude cancellation. The effect persists even if the N-photon state is replaced by an arbitrary state of light. A special case is the coherent state which corresponds to homodyne detection of a single photon state and can lead to the measurement of the wave function of a single photon state.

1 Introduction

Interference effect of light has played an important role in the conceptual development of quantum theory. Richard Feynmann once wrote[1] that the Young's double slit experiment "has in it the heart of quantum mechanics". But the phenomena of interference do not simply stop at Young's double slit experiment and its variations. Much richer phenomena occur in higher-order interference[2-6] when there are more than one particle involved in the process. For example, Greenberger et al.[7] recently proposed new demonstration of locality violation by quantum theory with superposition state of three or more particles.

In the meantime, along a quite different line, Ou and Mandel[8] have investigated a startling quantum interference effect where a strong field interferes with a considerably weak field. It was shown[3] and demonstrated[8] that for certain nonclassical fields, the interference fringe visibility does not change even though the ratio of the intensities of the two interfering fields is much greater than 1, in conflict with the intuitive picture from classical wave theory for interference. In this case, the seemingly insignaficant weak field plays an essential role for the interference effect even though its intensity is negligibly small. Therefore, the presence of the weak field can dramatically change the outcome of the result.

In this paper, we will present another example of how existence of a weak field can make a significant difference. It deals with $N + 1$ photons with N being a positive integer. We will consider a situation when an N-photon state interferes with a single photon state with the help

of a symmetric lossless beamsplitter (see Fig.1). A special case of $N = 1$ has been experimentally investigated as an example of fourth-order interference.[9] However, quite different from the two-photon coincidence measurement technique used in fourth-order interference, we will exam photon probability distribution at two output ports of the beamsplitter. Although no interference pattern exists, the phenomenon discussed here attributes to quantum interference of multi-particle ($N + 1$ particles). We will also extend the discussion to an arbitrary state input in replacement of the N-photon state.

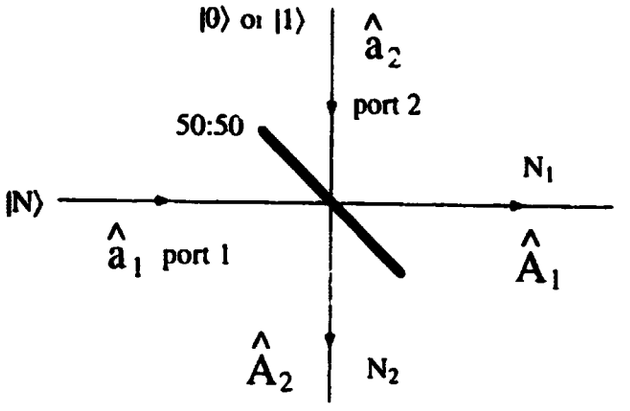

FIG. 1. Layout for the interference between N-photon state and a single photon state via a beamsplitter.

2 Photon Probability Distribution for a Symmetric Lossless Beamsplitter

It is well-known that when a number of particles, say N, enter a 50:50 lossless beamsplitter from one input port, the particles are randomly sent to the two output ports with equal probability, resulting in the simple Bernoulli binormial distribution as

$$P_0(N_1, N_2) = \frac{N!}{2^N N_1! N_2!}\, \delta_{N_1+N_2,N}. \tag{1}$$

N_1 is the number of particles exiting from output port 1 while N_2 is for port 2. In the case of photon, the above result suggests that each photon acts independently as a classical particle. The wave behavior of light does not show up here because of the absence of superposition. This distribution has its maximum when $N_1 = N_2 = N/2$ (equal partition). So it is most likely to find equal number of photons on each side of the beamsplitter. For large N and $|N_1 - N_2| << N$, Eq.(1) becomes

$$P_0(N_1, N_2) = \frac{2}{\sqrt{2N\pi}}\, e^{-(N_1-N_2)^2/2N}\, \delta_{N_1+N_2,N} \tag{2}$$

which is a Gaussian. The extra factor of 2 is because $P_0(N_1, N_2) = 0$ for every other value of $N_1 - N_2$.

Next, we let a single photon state enter the input port 2 of the beamsplitter. We will look for the probability $P_1(N_1, N_2)$ that N_1 photons exit at output port 1 while the other N_2 photons

at port 2 with $N_1 + N_2 = N + 1$. Let us for a brief moment consider the outcome from classical particle theory. As a classical particle, the input single photon will have 50% of probability going out at either ports. Because the single photon is independent of the other N photons, we simply add the probabilities to obtain the final result:

$$P_1^{cl}(N_1, N_2) = \frac{1}{2}\frac{N!}{2^N(N_1-1)!N_2!} + \frac{1}{2}\frac{N!}{2^N(N_2-1)!N_1!} = \frac{(N+1)!}{2^{N+1}N_1!N_2!}, \tag{3}$$

which is in the exactly same form as that in Eq.(1). Therefore the existence of the single photon at the other port does not influence the photon probability distribution at all. The single photon from port 1 acts as if it were part of the N photons from the port 1. This is because classical particles are independent of each other and it doesn't matter which port it enters.

On the other hand, the outcome is totally different if we treat the photons as quantum particles. We cannot simply add the probabilities. The principle of quantum mechanics requires that the probability amplitudes be added. For simplicity, let us first consider the case when N is an odd integer and $N_1 = N_2 = (N+1)/2$. The probability amplitude has two contributions as shown in Fig.2: (a) the single photon input at port 2 goes directly to output port 2 while $N_1 - 1 = (N-1)/2$ of the N photons input at port 1 are reflected and go to output port 2 and $N_2 = (N+1)/2$ photons to port 1, or (b) the single photon is reflected and goes to output port 1 while $N_2 - 1 = (N-1)/2$ photons go to output port 1 and $N_2 = (N+1)/2$ photons are reflected to port 2. From Eq.(1), we find that these two possibilities have equal probability thus their probability amplitudes have equal absolute value. For their phases, however, because there is a $\pi/2$ phase shift for the reflected field and no phase shift for the transmitted one at a symmetric beam splitter, the total phase shift of the $N+1$ photons at the output ports will be different for the two possibilities. Referring to Fig.1, we find that the total phase shift for the first possibility mentioned above is $\varphi_a = (N_2 - 1)\pi/2 = (N-1)\pi/4$ while for the second possibility, $\varphi_b = \pi/2 + N_2\pi/2 = (N+3)\pi/4$. The phase difference between the two possibilities is thus $\varphi_b - \varphi_a = \pi$. Therefore, the two probability amplitudes will cancel each other, resulting zero probability for $N_1 = N_2 = (N+1)/2$. This result is completely different from that of a classical particle theory in Eq.(3). As seen above, the probability cancellation at $N_1 = N_2$ results from the quantum interference of $N+1$ particles.

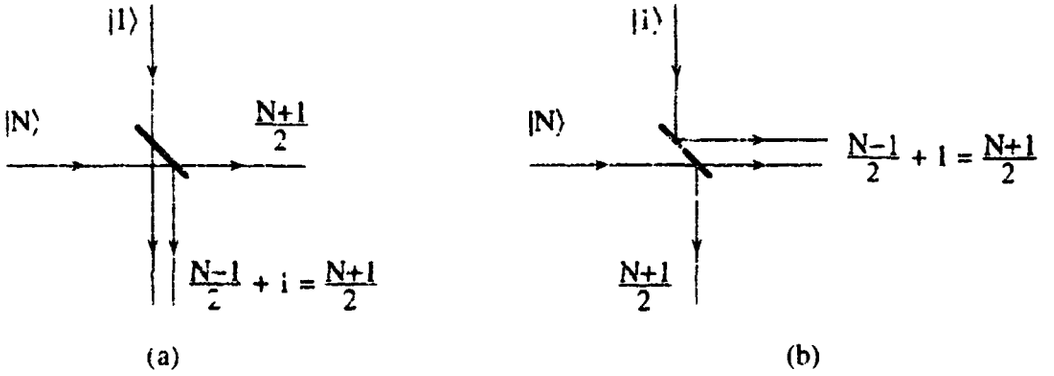

FIG. 2. Two contributions to the output photon distribution.

For the other cases when $N_1 \neq N_2$, we cannot use the simple argument as above. But we may derive the output state along the line of Ref.10 and find the probability distribution $P_1(N_1, N_2)$. Or we can use the formula

$$P_1(N_1, N_2) = \langle : \frac{(\hat{A}_1^\dagger \hat{A}_1)^{N_1}}{N_1!} e^{-\hat{A}_1^\dagger \hat{A}_1} \frac{(\hat{A}_2^\dagger \hat{A}_2)^{N_2}}{N_2!} e^{-\hat{A}_2^\dagger \hat{A}_2} : \rangle. \tag{4}$$

where

$$\hat{A}_1 = (\hat{a}_1 + i\,\hat{a}_2)/\sqrt{2}, \quad \hat{A}_2 = (\hat{a}_2 + i\,\hat{a}_1)/\sqrt{2}$$

are the annihilation operators for the output modes for a symmetric lossless beamsplitter. The input modes represented by $\hat{a}_1, \hat{a}_2$ are in the state of $|\Phi\rangle = |N\rangle_1|1\rangle_2$. After some lengthy calculation, we have

$$P_1(N_1, N_2) = \frac{N!}{2^{N+1} N_1! N_2!} (N_1 - N_2)^2 \delta_{N_1+N_2, N+1}. \tag{5}$$

The above expression can also be derived from the general formula given by Campos, Saleh and Teich in Ref.11 for arbitrary numbers $\{n_1, n_2\}$ of input photons at the two input ports, with the setting of $\tau = 1/2, n_1 = N, n_2 = 1$. When $N, N_1, N_2 >> 1$, Eq.(5) can be approximated by

$$P_1(N_1, N_2) \approx \frac{(N_1 - N_2)^2}{N} \frac{2}{\sqrt{2N\pi}} e^{-(N_1-N_2)^2/2N} \delta_{N_1+N_2, N+1}. \tag{6}$$

Notice that when N is an odd integer, $P_1(N_1, N_2) = 0$ for $N_1 = N_2 = (N+1)/2$, exactly as predicted from the simple argument of probability superposition given in the previous paragraph. When N is an even integer, $P_1(N/2+1, N/2) = N!/2^{N+1}(N/2+1)!(N/2)! \neq 0$, but because $P_1(N/2+1, N/2)/P_0(N/2+1, N/2) = 1/(N+1) << 1$ for $N >> 1$, or the probability with a single photon input is much smaller than that with vacuum state input, the probabilities for $N_1 \approx N_2$ are quite different in the two cases with or without the single photon state at port 2. Actually, the whole probability distribution in Eq.(5) is different from the probability distribution in Eq.(1), as seen in Fig.3. The maximum probability for $P_1(N_1, N_2)$ occurs at $|N_1 - N_2| \approx \sqrt{N}$ or $N_1 \approx (N \pm \sqrt{N})/2$ while for $P_0(N_1, N_2)$ it occurs at $N_1 = N_2 \approx N/2$. The existence of a single photon dramatically changes the pattern of the output photon distribution.

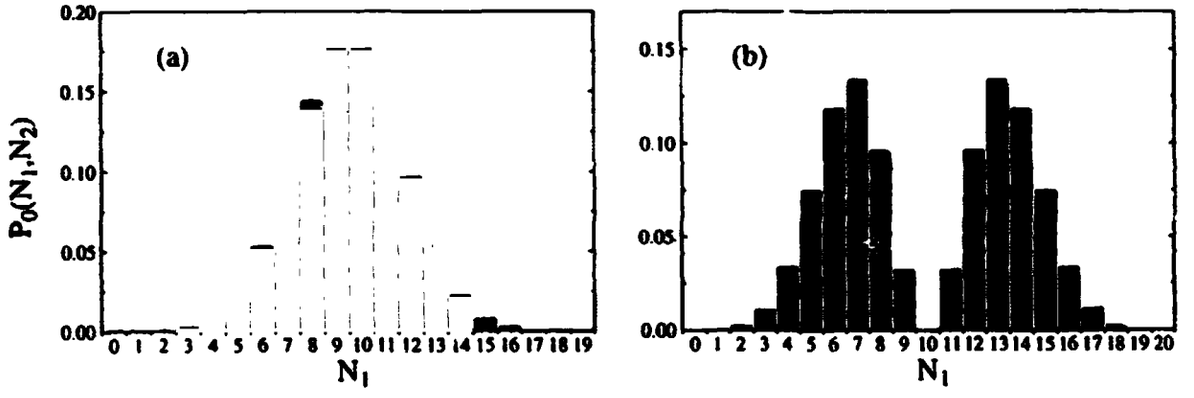

FIG. 3. Output photon distribution for N-photon state input at port 1 with (a) vacuum state or (b) single photon state at port 2 (N=19).

3 Interference of a Single-Photon State with Arbitrary State

The above quantum probability cancellation effect due to a single photon state is not stricted to N-photon state as input state. Let us consider an arbitrary state of light input at port 1. Its state is generally described by the Glauber P-distribution $P_{in}(\alpha)$. But before going into lengthy calculation, we may take a guess about the photon distribution of the output fields by the following argument: since the vacuum state and the single photon state are completely incoherent in the sense that they have a totally random phase distribution, the output fields due to interference of one of these states with any other state will not have any coherence information of the input state. Therefore, the output photon distribution of the beamsplitter will lose all the coherence information of the input state and will depend simply on the photon statistics P_n^{in} of the input state at port 1. So combining this fact with Eqs.(1,5), we come up with the output photon distributions in the form of

$$P_0(N_1, N_2) = \frac{(N_1 + N_2)!}{2^{N_1+N_2} N_1! N_2!} P^{in}_{N_1+N_2} \tag{7a}$$

for vacuum input at port 2 and

$$P_1(N_1, N_2) = \frac{(N_1 + N_2 - 1)!}{2^{N_1+N_2} N_1! N_2!} (N_1 - N_2)^2 P^{in}_{N_1+N_2-1} \tag{7b}$$

for single photon state input at port 2. Of course, we may rigorously derive the output photon distribution by following the procedure described in Ref.10 to first find the state of the output fields of the beamsplitter in terms of the P-distribution. The photon distribution for the output fields can then be calculated through Eq.(4). It can be shown that Eq.(7) is indeed the correct form for the output photon distribution.

By comparing Eqs.(7a) and (7b), we easily find that $P_1(N_1 = N_2) = 0$ for single photon state input at port 2 while

$$P_0(N_1 = N_2) = \sum_{N_1=0}^{\infty} \frac{(2N_1)!}{2^{2N_1}(N_1!)^2} P^{in}_{2N_1} \neq 0$$

for vacuum input. Therefore, the existence of the single photon state at port 2 does make a difference in the output photon distribution even for arbitrary input state at port 1, and the probability for $N_1 = N_2$ is exactly equal to zero. The cancellation of the probability for $N_1 = N_2$ is because of the destructive interference between the N photons and the single photon as we discussed above.

In an actual experiment, however, it is difficult to measure the complete distribution $P(N_1, N_2)$, but the distribution $P(N_1 - N_2 = M)$ can be measured by balanced homodyne detection.[12,13] From Eqs.(7a,b) we find that

$$\begin{aligned} P_0(N_1 - N_2 = M) &= \sum_{N_1=M}^{\infty} \frac{(2N_1 - M)!}{2^{2N_1-M} N_1!(N_1 - M)!} P^{in}_{2N_1-M} \\ P_1(N_1 - N_2 = M) &= M^2 \sum_{N_1=M}^{\infty} \frac{(2N_1 - M - 1)!}{2^{2N_1-M} N_1!(N_1 - M)!} P^{in}_{2N_1-M-1} \end{aligned} \tag{8}$$

for $M \geq 0$. For $M < 0$, the symmetry between N_1, N_2 in Eq.(7) leads to $P(M) = P(-M)$.

Next, we will evaluate $P_0(M), P_1(M)$ for some special states. For N-photon state input with $N >> 1$, we have $P_n^{in} = \delta_{n,N}$, and Eq.(8) gives results similar to Eqs(1,5):

$$\begin{aligned} P_0(M) &= \frac{N!}{2^N(N/2+M/2)!(N/2-M/2)!} \\ &\approx \frac{2}{\sqrt{2N\pi}}\, e^{-M^2/2N} \qquad \text{for } N >> 1 \end{aligned} \tag{9}$$

$$\begin{aligned} P_1(M) &= \frac{M^2 N!}{2^{N+1}(N/2+M/2+1/2)!(N/2-M/2+1/2)!} \\ &\approx \frac{2}{\sqrt{2N\pi}}\frac{M^2}{N}\, e^{-M^2/2N} \quad \text{for } N >> 1. \end{aligned}$$

For coherent state input, $P_{in}^n = \bar{n}^n e^{-\bar{n}}/n!$ with $\bar{n}$ being the average photon number. Therefore, we have

$$\begin{aligned} P_0(M) &= \sum_{N_2=0}^{\infty} \frac{(2N_1+M)!}{2^{2N_1+M}N_2!(N_1+M)!}\frac{\bar{n}^{2N_2+M}e^{-\bar{n}}}{(2N_2+M)!} = e^{-\bar{n}}I_M(\bar{n}) \\ P_1(M) &= \sum_{N_2=0}^{\infty} \frac{M^2(2N_1+M-1)!}{2^{2N_1+M}N_2!(N_1+M)!}\frac{\bar{n}^{2N_2+M-1}e^{-\bar{n}}}{(2N_2+M-1)!} = \frac{M^2}{\bar{n}}e^{-\bar{n}}I_M(\bar{n}), \end{aligned} \tag{10}$$

where $I_M(\bar{n})$ is the Bessel function with purely imaginary argument and has the form of

$$I_M(\bar{n}) \equiv \int_{-\pi}^{\pi} d\varphi e^{-iM\varphi}e^{\bar{n}\cos\varphi} \approx \frac{1}{\sqrt{2\bar{n}\pi}}\, e^{\bar{n}-M^2/2\bar{n}} \quad \text{when } \bar{n} >> 1. \tag{11}$$

Therefore, for large $\bar{n}$,

$$\begin{aligned} P_0(M) &\approx \frac{1}{\sqrt{2\bar{n}\pi}}\, e^{-M^2/2\bar{n}} \\ P_1(M) &\approx \frac{1}{\sqrt{2\bar{n}\pi}}\frac{M^2}{\bar{n}}\, e^{-M^2/2\bar{n}}. \end{aligned} \tag{12}$$

Eq.(12) has the same form as Eq.(9) for large N besides the factor of 2 which is explained earlier right after Eq.(2). This is not surprising if we consider the fact that when the photon number is large, the interference scheme discussed above becomes homodyne detection scheme. Since both vacuum state and single photon state have random phase distribution, homodyne detections with N-photon state ($N >> 1$) and coherent state as local oscillators are equivalent. As a matter of fact, the output photon distributions will always have the form of Eq.(12) for any state as local oscillator, provided that the average photon number is large and photon number fluctuation is much less than average photon number ($\sqrt{\langle \Delta n^2 \rangle} << \bar{n}$). We can see this point from Eq.(8): when $\sqrt{\langle \Delta n^2 \rangle} << \bar{n}$, P_{in}^n has a narrow peak around $\bar{n}$ and is a fast changing function as compared with

other terms in the summation, therefore the contribution to the summation is only from the few terms around $\bar{n}$, so that we can pull all other terms out of the sum, that is,

$$P_0(M) \approx \frac{\bar{n}!}{2^{\bar{n}}(n/2-M)!(\bar{n}/2+M)!}\sum_n P_{in}^n/2 \approx \frac{1}{\sqrt{2\bar{n}\pi}}\ e^{-M^2/2\bar{n}} \quad \text{when } \bar{n} >> 1, \tag{13a}$$

and similarly

$$P_1(M) \approx \frac{1}{\sqrt{2\bar{n}\pi}}\frac{M^2}{\bar{n}}\ e^{-M^2/2\bar{n}} \quad \text{when } \bar{n} >> 1. \tag{13b}$$

We can also understand this result from the fact that any fluctuation in local oscillator is cancelled in balanced homodyne detection scheme.[12]

Furthermore, if we set $\bar{n} \to \infty$, we can replace the discrete variable M with a continuous one defined by $x = M/\sqrt{\bar{n}}$ and the probability distributions in Eqs.(13a,b) lead to probability densities of continuous variable x as

$$P_0(x) = \frac{1}{\sqrt{2\pi}}\ e^{-x^2/2}, \quad P_1(x) = \frac{x^2}{\sqrt{2\pi}}\ e^{-x^2/2} \tag{14}$$

which correspond to the square of the absolute value of the wavefunction for the ground state and single photon state, respectively. Thus by measuring $P(M)$ in homodyne detection, we can deduce the wavefunction of the input state at port 2. This is exactly the technique of optical tomography used by Smithey et al.[13] But here we applied it to a single photon state (input at port 2) and proved that the outcome does not depend on the state of the local oscillator (input field at port 1) as long as the average photon number is large and the fluctuation is not very large for the local oscillator (i.e., the condition for the approximation in Eqs.(13a,b)).

However, there is an exception to the above. It is well-known that for thermal light, we have

$$\langle \Delta n^2 \rangle = \bar{n}(\bar{n}+1)$$

so that $\sqrt{\langle \Delta n^2 \rangle} \approx \bar{n}$ and we cannot use the approximation in Eqs.(13a,b). For thermal light, $P_{in}^n = \bar{n}^n/(\bar{n}+1)^{n+1}$, so from Eq.(8), we have

$$\begin{aligned} P_0(M) &= \sum_{N_2=0}^{\infty} \frac{(2N_2+M)!}{2^{2N_2+M}(N_2+M)!N_2!}\frac{\bar{n}^{2N_2+M}}{(\bar{n}+1)^{2N_2+M+1}} \\ &= \frac{x^M}{\bar{n}+1}\mathcal{F}\left(\frac{M+1}{2}, \frac{M}{2}+1, M+1; 4x^2\right) \\ P_1(M) &= M^2\sum_{N_2=0}^{\infty} \frac{(2N_2+M-1)!}{2^{2N_2+M}(N_2+M)!N_2!}\frac{\bar{n}^{2N_2+M-1}}{(\bar{n}+1)^{2N_2+M}} \\ &= \frac{Mx^M}{\bar{n}}\mathcal{F}\left(\frac{M+1}{2}, \frac{M}{2}, M+1; 4x^2\right) \end{aligned} \tag{15}$$

where $x = \bar{n}/2(\bar{n}+1)$ and $\mathcal{F}(\alpha, \beta, \gamma; z)$ is the hypergeometric function. With some re-arrangement, we can prove that Eq.(15) have a simpler form as

$$P_0(M) = \frac{1}{\sqrt{2\bar{n}+1}}\, q^M$$

$$(M \geq 0) \qquad (16)$$

$$P_1(M) = \frac{M}{\bar{n}}\, q^M$$

with $q = 1 + 1/\bar{n} - \sqrt{2\bar{n}+1}/\bar{n}$. For large $\bar{n}$, q^M becomes $e^{-M/\sqrt{\bar{n}/2}}$ so that Eq.(15) is changed to

$$P_0(M) = \frac{1}{\sqrt{2\bar{n}+1}}\, e^{-M/\sqrt{\bar{n}/2}}$$

$$(M \geq 0) \qquad (17)$$

$$P_1(M) = \frac{M}{\bar{n}}\, e^{-M/\sqrt{\bar{n}/2}}.$$

Therefore, The output photon distribution for thermal light input is different from that of coherent state input. But the general trend in the change of the shape from $P_0(M)$ to $P_1(M)$ is similar in both states (Fig.4). The quantum interference effect due to single photon is the same.

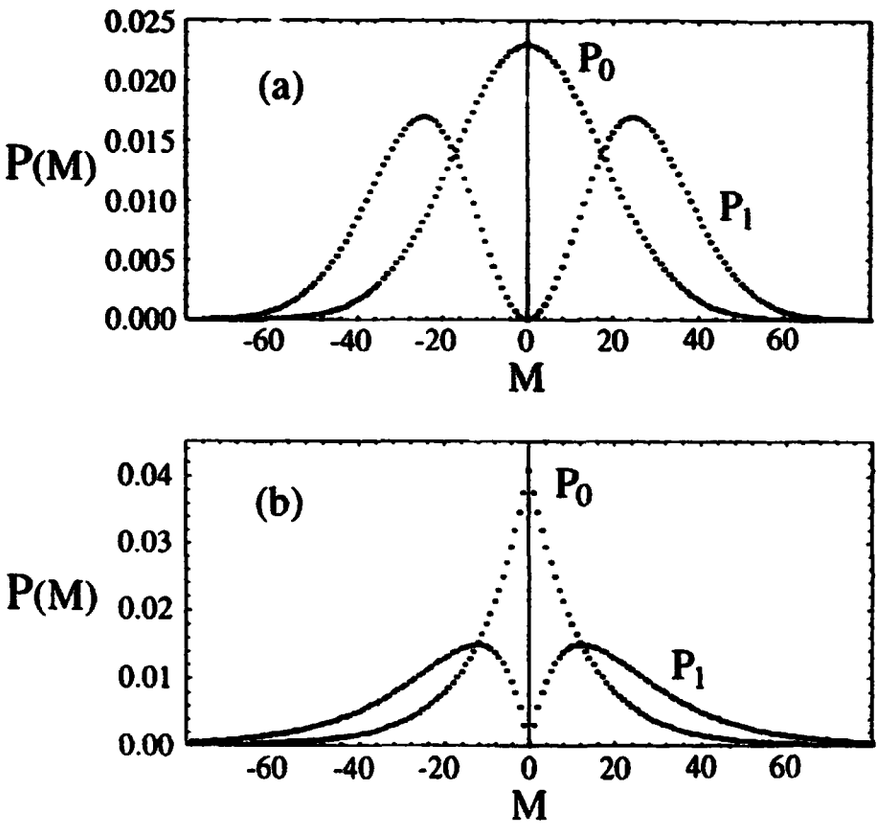

FIG. 4. Probability distribution $P_{0,1}(M)$ for the balanced homodyne detection of vacuum state and single photon state with (a) coherent state or (b) thermal state as local oscillator. $\bar{n} = 300$.

It is interesting to note that the weak nonclassical state (single photon state) plays an important role in the interference with a *strong classical* field (coherent state or thermal state) in contrast to the case discussed in Ref.3 where the nonclassical interference occurs between a *strong nonclassical* field and a weak classical field. Even though the nonclassical field is weak here, the result is very nonclassical in the sense that the probability of detecting equal intensities in the two outputs is zero ($P_1(M = 0) = 0$). It can be proved that in the similar situation (one field is weak and the other is strong), classical wave theory predicts that the probability is largest for equal intensity output at the two ports.

So far we have only discussed the single mode situations. In practice, we always have wide spectrum. Since two different sources of light are involved in the interference, the observation of the probability cancellation effect requires the overlap of both spatial and temporal mode structure of the two fields as well as near unit quantum efficiency of the detectors.

Acknowledgments

This work was supported by the Office of Naval Research and the Purdue Research Foundation.

References

[1] R. P. Feynman, in *The Feynman Lectures on Physics*, Vol.III, Addison-Wesley, Reading, Mass. (1963).

[2] R. Ghosh and L. Mandel, Phys. Rev. Lett. **59**, 1903 (1987).

[3] Z. Y. Ou, Phys. Rev. A**37**, 1607 (1988).

[4] J. G. Rarity and P. R. Tapster, Phys. Rev. Lett. **64**, 2495 (1990).

[5] A. M. Steinberg, P. G. Kwiat, R. Y. Chiao, Phys. Rev. Lett. **68**, 2421 (1992).

[6] T. E. Kiess et al. Phys. Rev. Lett. **71**, 3893 (1993).

[7] D. M. Greenberger, M. A. Horne, and A. Zeilinger, in *Bell's Theorem, Quantum Theory, and Conceptions of the Universe*, M. Katafos, ed., Kluwer Academic, Dordrecht, The Netherlands (1989).

[8] Z. Y. Ou and L. Mandel, Phys. Rev. Lett. **62**, 2941 (1989).

[9] C. K. Hong, Z. Y. Ou, and L. Mandel, Phys. Rev. Lett. **59**, 2044 (1987).

[10] Z. Y. Ou, C. K. Hong, and L. Mandel, Opt. Comm. **63**, 118 (1987).

[11] R. A. Campos, B. E. A. Saleh, and M. C. Teich, Phys. Rev. A**40**, 1371 (1990).

[12] H. P. Yuen and V. W. S. Chan, Opt. Lett. **8**, 177 (1983).

[13] D. T. Smithey, M. Beck, M. G. Raymer, and A. Faridari, Phys. Rev. Lett. **70**, 1244 (1990).

NEXT
DOCUMENT

Reflection spectrum of two level atoms by an evanescent laser wave *

Tan Weihan and Li Qingning
Department of Physics, Shanghai University,
Shanghai Institute of Optics and Fine Mechanics, Academia Scinica
(P.O.Box.800-211,Shanghai 201800,China)

Abstract

An exact solution and numerical caculation of the reflection of two level atoms by atomic mirror are presented. The curve of reflection coefficient against Rabi frequency caculated shows some new features, and the physical machanism underlying is analysed.

PACS number(s): 42.50.Vk, 32.80.Pj

1 INTRODUCTION

One of the fundamental problems in atomic optics is the reflection and diffraction of two level atoms by an evanescent laser wave—atomic mirror[1~5]. Via an adiabatic dressed-state approximation the problem was studied by Deutschmann , Ertmer and Wallis[6] . In this paper an exact solution is presented by using the method given in one of the authors previous paper [7]. The curve of reflection coefficient against the Rabi frequency shows some new features, the physical machanism involved is analysed.

*Project supported by the National Natural Science Foundation of China and Joint Laboratory of Quantum Optics(Shanghai Institute of Optics and Fine Mechanics, Academia Sinica/East China Normal University

2 The Schrödinger equation, Wave Function, Normalization , and Solution

A schematic diagram for an atomic mirror is shown in Fig.1. An atomic beam incident upon the surface of a dielectric interacting with the evanescent wave in the x-y plane. The total Hamitonian H reads

$$H = H_a + \frac{1}{2m}(p_x^2 + p_y^2) - \vec{\mu}\cdot\vec{\varepsilon} \tag{1}$$

Where H_a , depending on the coordinate $\vec{q}$, is the internal energy, $\frac{1}{2m}(p_x^2 + p_y^2)$ represents the translation energy of atom as a whole, and $-\vec{\mu}\cdot\vec{\varepsilon}$ denotes the atom-laser coupling energy. The Schrödinger equation of the atom reads

$$i\hbar\frac{\partial\psi}{\partial t} = -\frac{\hbar^2}{2m}(\frac{\partial^2}{\partial x^2} + \frac{\partial^2}{\partial y^2})\psi + H_a(\vec{q})\psi - \vec{\mu}\cdot\vec{\varepsilon}\psi \tag{2}$$

The solution of Eq.(2) has the form

$$\begin{aligned}\psi &= u_e(x,y)\phi_e(\vec{q})\exp(-i\frac{E_e+E_g}{2\hbar}t - i\frac{\omega t}{2} - \frac{iEt}{\hbar}) \\ &+ u_g(x,y)\phi_g(\vec{q})\exp(-i\frac{E_e+E_g}{2\hbar}t + i\frac{\omega t}{2} - \frac{iEt}{\hbar})\end{aligned} \tag{3}$$

Substituting Eq.(3) into Eq.(1), we obtain

$$\begin{aligned}Eu_e &= (-\frac{\hbar^2}{2m}\frac{d^2}{dy^2} + \frac{p_e^2}{2m} - \frac{\hbar\Delta}{2})u_e - \mu\varepsilon e^{-\eta y}u_g, \qquad \Delta = \omega - \frac{E_e - E_g}{\hbar} \\ Eu_g &= (-\frac{\hbar^2}{2m}\frac{d^2}{dy^2} + \frac{p_g^2}{2m} + \frac{\hbar\Delta}{2})u_g - \mu\varepsilon e^{-\eta y}u_e, \qquad \eta = k_0\sqrt{n^2\sin^2\theta - 1}\end{aligned} \tag{4}$$

Now we introduce the Rabi frequency $\Omega = \frac{2\mu\varepsilon}{\hbar}$, the normalization frequency $\Omega_0 = \hbar\eta^2/m$, and adopt the normalization

$$\begin{aligned}\frac{T_{ey}}{\hbar\Omega_0/2} &= \frac{E + \hbar\Delta/2 - p_e^2/2m}{\hbar\Omega_0/2} = \gamma_1 \\ \frac{T_{gy}}{\hbar\Omega_0/2} &= \frac{E - \hbar\Delta/2 - p_g^2/2m}{\hbar\Omega_0/2} = \gamma_2 \\ \frac{\hbar^2/2m}{\hbar\Omega_0/2}\frac{d^2}{dy^2} &= \frac{1}{\eta^2}\frac{d^2}{dy^2} \Rightarrow \frac{d^2}{dy^2}, \qquad \frac{\Omega}{\Omega_0} \Rightarrow \Omega\end{aligned} \tag{5}$$

$$\gamma_1 - \gamma_2 = \frac{\hbar\Delta - (\hbar\xi)^2/2m - p_g\hbar\xi/m}{\hbar\Omega_0/2}, \qquad \xi = k_0 n \sin\theta$$

After nomalization, Eq.(4) assumes the forms

$$\frac{d^2}{dy^2}u = -\bar{\gamma}u + Me^{-y}u \tag{6}$$

where

$$u = \begin{pmatrix} u_e \\ u_g \end{pmatrix}, \qquad \bar{\gamma} = \begin{pmatrix} \gamma_1 & \\ & \gamma_2 \end{pmatrix}, \qquad M = \begin{pmatrix} & -\Omega \\ -\Omega & \end{pmatrix}$$

Now we rewrite Eq.(6) in the form of first order differential Eqs.

$$\frac{du}{dy} = v, \qquad \frac{dv}{dy} = -\bar{\gamma}u + Me^{-y}u \tag{7}$$

or briefly

$$\frac{dw}{dy} = -\Gamma w + Ne^{-y}w \tag{8}$$

where

$$w = \begin{pmatrix} u \\ v \end{pmatrix}, \quad \Gamma = \begin{pmatrix} & -1 \\ \bar{\gamma} & \end{pmatrix}, \quad N = \begin{pmatrix} & \\ M & \end{pmatrix} \tag{9}$$

The Laplace transformation of $w(y)$ can be written as

$$\tilde{w}(s) = \int_0^\infty e^{-sy}w(y)dy \tag{10}$$

which leads to

$$\begin{aligned}\tilde{w}(s) = \frac{w(0)}{s+\Gamma} + \frac{1}{s+\Gamma}N\tilde{w}(s+1) = \Big(&\frac{1}{s+\Gamma} \\ &+ \frac{1}{s+\Gamma}N\frac{1}{s+1+\Gamma} + \frac{1}{s+\Gamma}N\frac{1}{s+\Gamma+1}N\frac{1}{s+\Gamma+2} + \cdots\Big)w(0)\end{aligned} \tag{11}$$

When the inverse transformation of Eq.(11) is evaluated, the solutions $u(y)$, $v(y)$ can be derived immediately

$$\begin{pmatrix} u_e \\ u_g \\ v_e \\ v_g \end{pmatrix} = \begin{pmatrix} I_1 & I_2 & I_3 & I_4 \\ \tilde{I}_2 & \tilde{I}_1 & \tilde{I}_4 & \tilde{I}_3 \\ \frac{dI_1}{dy} & \frac{dI_2}{dy} & \frac{dI_3}{dy} & \frac{I_4}{dy} \\ \frac{d\tilde{I}_2}{dy} & \frac{d\tilde{I}_1}{dy} & \frac{d\tilde{I}_4}{dy} & \frac{d\tilde{I}_3}{dy} \end{pmatrix} \begin{pmatrix} u_e(0) \\ u_g(0) \\ v_e(0) \\ v_g(0) \end{pmatrix} \tag{12}$$

where $u_e(0)$, $u_g(0)$, $v_e(0)$, $v_g(0)$ is the boundary values of $u_e(y)$, $u_g(y)$, $v_e(y)$, $v_g(y)$ at the target surface $y = 0$.

3 The boundary conditions and the reflection coefficient for atomic wave

3.1 Spontaneous emission

The spontaneous transition of excited atoms to the ground state for large y_m yeilds the condition for excited state wave function

$$\begin{aligned} & u_e(y_m) \simeq 0, \quad v_e(y_m) \simeq 0 \\ y_m \gg 1, \quad & \frac{p_{ey}}{m} T_1 \times k_0 \sqrt{n^2 \sin^2\theta - 1} \end{aligned} \tag{13}$$

where 1 is the thickness of evanescent laser wave, T_1 is the life time of atom and p_e/m the velocity departure from the target. The typical datas are, $\lambda \simeq 0.5\mu$, $T_1 = 10^{-8} sec, p_{ey}/m \simeq 0.5m/sec$, $p_{ey}/m\, T_1 \times k_0\sqrt{n^2\sin^2\theta - 1} \simeq 1.73$, setting $y_m \simeq 7$, the inequality Eq.(13) is satisfied well. Using Eq.(13) to eliminate u_{e0}, v_{e0} in Eq.(12), we obtain

$$u_g = u_{g1} u_{g0} + u_{g2} v_{g0} \tag{14}$$

3.2 Perfect adsorption of the atoms transmitted the target surface, non recoil

This implies that, near the target surface, the ground state atoms have the travelling wave structure for small y

$$u_g(y) = u_{g0} e^{i\sqrt{\gamma_2} y} = (\cos(\sqrt{\gamma_2} y) + i \sin(\sqrt{\gamma_2} y)) u_{g0} \tag{15}$$

Comparison with the analytical solution u_g for small y

$$u_g(y) = \cos(\sqrt{\gamma_2} y) u_{g0} + \frac{\sin(\sqrt{\gamma_2} y)}{\sqrt{\gamma_2}} v_{g0} \tag{16}$$

gives

$$v_{g0} = i\sqrt{\gamma_2} u_{g0} \tag{17}$$

Substituting this relation (17) into Eq.(12), we have

$$\begin{aligned} & u_g(y) = (u_{g1}(y) + i\sqrt{\gamma_2} u_{g2}) u_{g0} = u_{g0} \rho_g e^{i\theta_g} \\ & \rho_g = \sqrt{u_{g1}^2 + \gamma_2 u_{g2}^2}, \quad \theta_g = tan^{-1} \frac{\sqrt{\gamma_2} u_{g2}}{u_{g1}} \end{aligned} \tag{18}$$

3.3 In the region of $y_m \gg 1$

The wave structure of $u_g(y)$ may be also considered as the supperposition of incoming wave $|A|e^{i(\sqrt{\gamma_2}y+\varphi)}$ and the reflected wave $|B|e^{-i(\sqrt{\gamma_2}y+\varphi)}$, i.e.

$$u_g(y) = |A|e^{i(\sqrt{\gamma_2}y+\varphi)} + |B|e^{-i(\sqrt{\gamma_2}y+\varphi)} = \rho_{AB}e^{i\varphi_{AB}} = u_{g0}\rho_g e^{i\theta_g}$$

$$\rho_{AB} = \sqrt{|A|^2 + |B|^2 + 2|AB|\cos 2(\sqrt{\gamma_2}y + \varphi)} = |u_{g0}|\rho_g \tag{19}$$

which gives $\rho_{ABmax} = |A| + |B| = |u_{g0}|\rho_{max}$ at $\sqrt{\gamma_2}y + \varphi = n\pi$, and $\rho_{ABmin} = |A| - |B| = |u_{g0}|\rho_{min}$ at $\sqrt{\gamma_2}y + \varphi = (n + 1/2)\pi$. Thus, the reflection coefficent R can be written as

$$R = \frac{|B|}{|A|} = \frac{\rho_{ABmax} - \rho_{ABmin}}{\rho_{ABmax} + \rho_{ABmin}} = \frac{\rho_{max} - \rho_{min}}{\rho_{max} + \rho_{min}} \tag{20}$$

4 Numerical calculation and discussion

4.1 Parameters

Refering to Eq. (5), the normalized parameters used in the calculation are

$$\gamma_1, \gamma_2 = \begin{cases} 1.96,\ 12.6 & \textit{negative detuning} \\ 12.6,\ 1.96 & \textit{positive detuning} \end{cases} \tag{21}$$
$$y_m = 7.0, \qquad \Omega = 25.0$$

4.2 Reflection coefficient caculated from Fig.2(a), (b)

$R = \dfrac{253.89 - 1.09}{253.89 + 1.09} = 0.991$ for positive detuning

$R = \dfrac{5.156 - 0.928}{5.156 + 0.928} = 0.695$ for negative detuning.

4.3 Reflection coefficient R agaist Rabi frequency Ω Fig. 3

1. The Rabi frequency Ω very small, the reflection cofficients R approaches to zero in the cases of either positive or nagative detuning
2. The reflection coefficient R for positive detuning is much higher than that for negative detuning.
3. The R curve for negative detuning displays some oscillating features with it's maxima at $\Omega \simeq 12.5, 25, 37.5, 50\cdots$, and the interval between successive maxima is $\Delta\Omega \simeq 12.5$.

4.4 The physical machenism

We introduce a relative phase shift δ_l between the real and imaginary part of wave function u_g in Eq.(15), during the atoms are departing from the target surface

$$
\begin{aligned}
u_g(y) &= u_{g0}[\cos(\sqrt{\gamma_2}y - \delta_l) + i\sin(\sqrt{\gamma_2}y + \delta_l)] \\
&\bullet \\
\rho_g &\propto \sqrt{\cos^2(\sqrt{\gamma_2}y - \delta_l) + \sin^2(\sqrt{\gamma_2}y + \delta_l)} \\
&= \sqrt{1 + \sin(2\sqrt{\gamma_2}y)\sin(2\delta_l)}
\end{aligned}
\tag{22}
$$

$$
R = \frac{\sqrt{1+|\sin(2\delta_l)|} - \sqrt{1-|\sin(2\delta_l)|}}{\sqrt{1+|\sin(2\delta_l)|} + \sqrt{1-|\sin(2\delta_l)|}}
$$

The maxima of R occur at $\delta_l \simeq (n + 1/2)\pi/2$, $n = 0, 1, \cdots$. The interval between the successive maxima δ_l is $\Delta\delta_l \simeq \pi/2$. The comprison of $\Delta\delta_l$ with the observed interval $\Delta\Omega \simeq 12.5$ reminds us that the phase shifts δ_l induced are proportional to the Rabi frequency Ω, after $\delta_l = \pi/4$. In the inital stage, $\Delta\Omega = 0 \sim 12.5$, the phase shifts induced, $\Delta\delta_l = 0 \sim \pi/4$, is relatively small in comparision with $\Delta\delta_l = \pi/2$ after $\delta_l = \pi/4$.

In conclusion, the reflection coefficient R of two level atoms by evanescent laser wave is studied through analytical solution and numerical caculation. The curve R versus Ω shows that $R < 0.1$ when $\Omega < 2.5$ and $R > 0.7$ when $\Omega > 37.0$. Especially, in the case of negative detuning, an oscillatory feature with a period $\Delta\Omega = 12.5$ appears.

References

[1] A.Ashkin, Phys.Rev.Lett. 24(1970) 156; 25(1970) 1321.

[2] T.W.Hänsch and A.L.Schawlow, Opt.Comm. 13(1975) 68.

[3] D.Wineland and H.Dehmelt, Bull. Am.Phys.Soc. 20(1975) 637.

[4] V.I.Balykin, Y.S.Letokhov, Yu.B.Ovchinnikov and A.I.Sidorov, Phys. Rev. Lett. 60(1988) 2137.

[5] R.J.Cook and R.K.Hill, Opt.Commu.43(1982) 250.

[6] R.Deutschmann, W.Ertmer and H.Wallis, Phys. Rev. A 47(1993) 2169.

[7] Tan Weisi, Tan Weihan, Zao Dongsheng and Liu Renhong, J.O.S.A.B, 10 (1993) 1610.

Figure Captions

Fig.1. Schematic diagram for an atomic mirror.

Fig.2. The variation of ρ_y versus y

(a) for positive detuning, $\gamma_1 = 12.6, \gamma_2 = 1.96, \eta = 1, \Omega = 25.0$

(b) for negative detuning, $\gamma_1 = 1.96, \gamma_2 = 12.6, \eta = 1, \Omega = 25.0$

Fig.3. The variation of reflection coefficients R versus Rabi frequency Ω

(a) for positive detuning, $\gamma_1 = 12.6, \gamma_2 = 1.96, \eta = 1$

(b) for negative detuning, $\gamma_1 = 1.96, \gamma_2 = 12.6, \eta = 1$

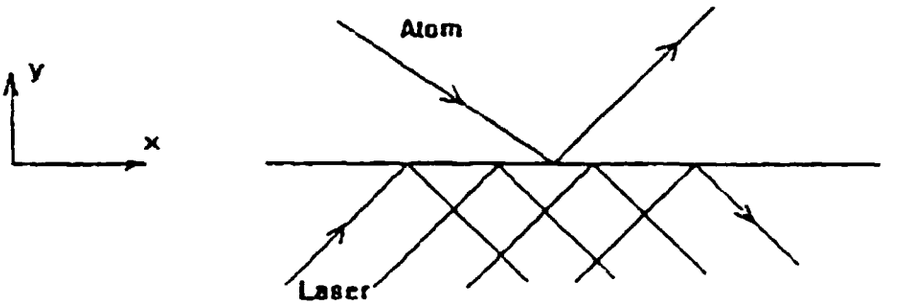

Fig. 1

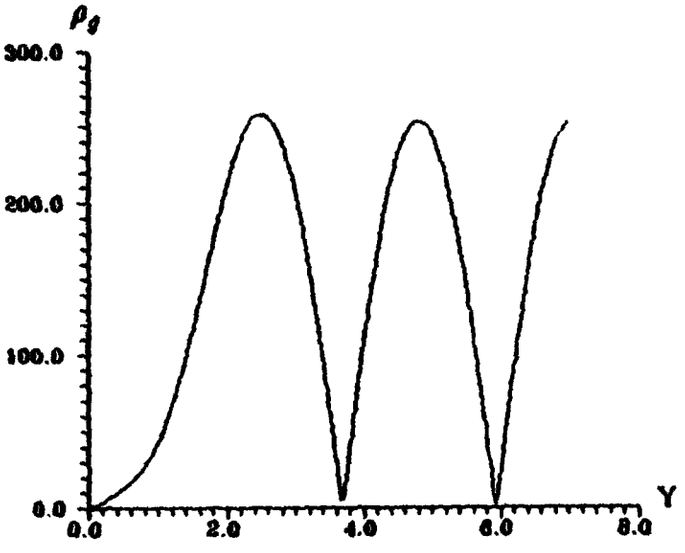
ρ_g
300.0
200.0
100.0
0.0
0.0
2.0
4.0
6.0
8.0
Y

Fig.2(a)

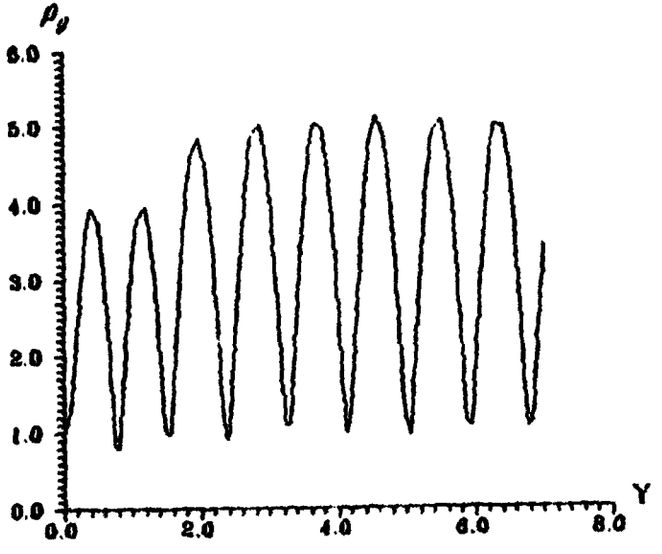
ρ_g
6.0
5.0
4.0
3.0
2.0
1.0
0.0
0.0
2.0
4.0
6.0
8.0
Y

Fig.2(b)

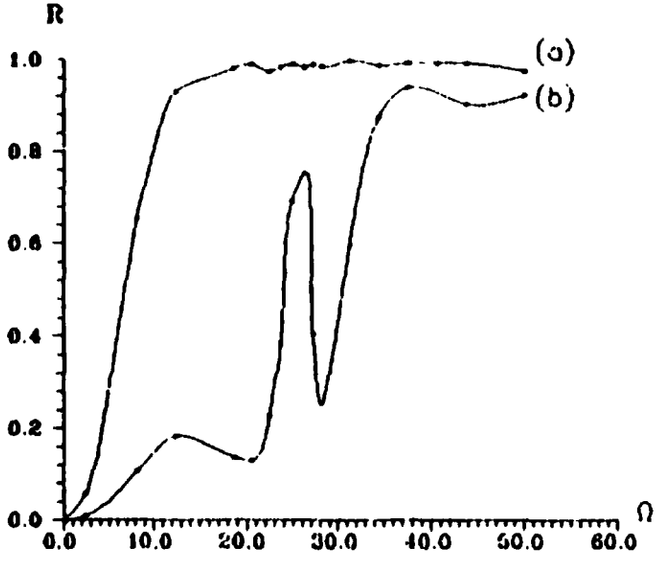

Fig.3

NEXT
DOCUMENT

QUANTUM INTERFERENCE EFFECTS IN MOLECULAR Y- AND RHOMB-TYPE SYSTEMS

Hui-Rong Xia, Cen-Yun Ye, Jian-We Xu, Liang-En Ding
Laboratory for Quantum Optics, National Education Commision
Department of Physics, East China Normal University
Shanghai 200062, China

Abstract

In this paper we report the first observation of molecular population trapping in four-level systems. Constructive and destructive quantum interferences between two sum-frequncy two-photon transitions in Y- and rhomb-type four-level systems, respectively, im sodium molecules have been experimentally achieved by using only one laser source. Their energy-level schemes are featured by the extremely near-rsonant enhancement of the equal-frequency two-photon transitions, sharing both the initial and the intermediate levels for the Y-type, and sharing both the initial and the final levels for the rhomb-type systems. Their novel spectral effects are to show seriously restrained Doppler-free UV peak at the nominal location of the induced two-photon transition with visible fluorescence in rhomb-type schems, and to show a strong extra UV peak but null visible fluorescence in the middle between the two dipole allowed two-photon transitions.

1 Introduction

In last three decades many physical phenomena have been discovered for a multi-level quantum system drived by coherent light field. Among them, coherent population trapping (CPT) in a Λ -type and V- type three-level system has been an interesting topic in the field of quantum optics for many years [1]-[8]. The significance of the topic, in addition to be interested by basic research for laser-matter interactions, deals with the recently interested topics such as laser without inversion [9]-[12], quantum interference and new phenomena [13]-[14]. However, so far all of the experimental demonstrations for CPT are for a V-type three-level system in atomic samples [3]-[8] by using two sets of lasers.

In this paper we report the first observation of molecular population trapping in four-level systems. We use molecules as the sample for taking the advantages of their abundant selectable gradual changing energy-level schems. Constructive and destructive quantum interferences between two sum-frequncy two-photon transitions in Y- and rhomb-type four-level systems, respectively, in sodium molecules have been experimentally achieved by using only one laser source. Their energy-level schemes are featured by the extremely near-rsonant enhancement of the equal-frequency two-photon transitions, sharing both the initial and the intermediate levels for the Y-type, and sharing both the initial and the final levels for the rhomb-type systems. Their novel spectral effects are to show seriously restrained Doppler-free UV peak at the nominal location of

the induced two-photon transition with visible fluorescence in rhomb-type schems, and to show a strong extra UV peak but null visible fluorescence in the middle between the two dipole allowed two-photon transitions.

2 Theory

The schems available in sodium dimers for our study is attributing to the existence of the spin-orbital perturbation between the rotational levels with same J in the singlet and triplet states, located in available dye laser regions. Such a mutual perturbation can form a pair of levels, not only close each other but also with their wavefunctions sharing. So that, once they have proper frequency location as the final level or as the intermediate levels for near-resonantly enhanced two-photon transition for the so called Y-type or rhomb-type four-level systems, respectively, they will show their characteristic quantum interference effects in their observable lineshape patterns. Indeed, we have found a series schemes with gradually changing parameters in Na_2 for study each of the models.

In the calculation with density matrix equations, we use the form of the interacting Hamiltonian

$$H_Y^I = \begin{bmatrix} 0 & -\mu_{ab}E & 0 & 0 \\ -\mu_{ba}E & 0 & \mu_{bc}E & \mu_{bd}E \\ 0 & -\mu_{cb}E & 0 & 0 \\ 0 & -\mu_{db}E & 0 & 0 \end{bmatrix}$$

for the Y-type four-level system, where c and d are the perturbation coupled levels in the molecular high-lying states. Similarly, we use the interacting Hamiltonian of

$$H_R^I = \begin{bmatrix} 0 & -\mu_{ab}E & -\mu_{ac}E & 0 \\ -\mu_{ba}E & 0 & 0 & -\mu_{bd}E \\ -\mu_{ca}E & 0 & 0 & -\mu_{cd}E \\ 0 & -\mu_{db}E & -\mu_{dc}E & 0 \end{bmatrix}$$

for the rhomb-type four-level system, where b and c are the perturbation coupled levels in the molecular intermediate states. Substituting these forms, instead of the known form as

$$H_1^I = \begin{bmatrix} 0 & -\mu_{ab}E & 0 \\ -\mu_{ba}E & 0 & \mu_{bd}E \\ 0 & -\mu_{db}E & 0 \end{bmatrix} + \begin{bmatrix} 0 & -\mu_{ac}E & 0 \\ -\mu_{ca}E & 0 & \mu_{cd}E \\ 0 & -\mu_{dc}E & 0 \end{bmatrix}$$

for two independent two-photon transitions individually enhanced by the middle level b and c in two three-level systems, or the form as

$$H_2^I = \begin{bmatrix} 0 & -\mu_{ab}E & 0 \\ -\mu_{ba}E & 0 & \mu_{bc}E \\ 0 & -\mu_{cb}E & 0 \end{bmatrix} + \begin{bmatrix} 0 & -\mu_{ab}E & 0 \\ -\mu_{ba}E & 0 & \mu_{bd}E \\ 0 & -\mu_{db}E & 0 \end{bmatrix}$$

for two independent two-phton transitions reaching separated upper levels in two three-level systems, we get different results.

The calculation with H_V^I for the steady state solution of the density matrix equations reveals the existing constructive quantum interference as showing an extra UV peak, origining from the non zero and non diagonal element ($\rho_{cd} \neq 0$), and predicts its maximum location right in the middle between the two usual lines, according to H_1^I. The dependence of the term on the perturbation coupling coefficients is also obtained.

The calculations with H_R^I for the steady state solution of the density matrix equations reveals that the destructive quantum interference can completely cancel each other for their enhancement for the two-photon transition from a to d, origining from the non zero and non diagonal element ($\rho_{bc} \neq 0$). The dependence of the phenomenon on the relative detunings and the signs between the two enhancements are obtained.

3 Experimental Demonstrations

The experiments are performed by using an Argon ion laser pumped single mode scannable dye laser at R6G and DCM dye regions and with a four-arm stainless steel oven containing sodium. For study both constructive and destructive quantum interferences mentioned above we search to find two serierses of the coupled levels consisting of paired spin-orbital perturbation levels with small separations from tens MHz to few GHz [15]-[18].

We observed the constructive quantum interference characterized by showing a strong extra fluorescence peak with null visible emission in the middle between the dipole allowed signals of the sum-frequency two-phton transitions, as predicted by the calculations. The relative intensity of the extra signal to the dipole allowed signals is determined by the degree of the wavefunction coupling as shown by the upper traces in Fig.1 for two distinct cases : The left trace is for 20% wavefunction sharing, whereas the right for 40%. The observed serious pressure influnce on the signal intensity revealed the disparity pressure-shift among these levels.

The destructive quantum interference was characterized by showing varying location of the Doppler-free peak on its Doppler-broadened peddestal, accompanied by the varying reduction (until complete null !) from the sharp UV peak, in a series of the observed near-resonantly enhanced two-photon absorption lines. The spectral patterns reveal that destructive quantum interference is dominated by the magnitudes as well as the relative signs of the detunings of the intermediate levels from two-phton resonance. The lower traces in Fig.1 present the degree different of the destructive interference for two distinct cases : The left trace is resulted by disparity detunings, whereas the right is with comparable magnitudes but opposit signs of the intermediate detunings.

In conclusion, molecular population trapping in intermidiate and in high-lying Rydberg states can be sufficiently achieved, especially via the mechanism of quantum interference between extremely near-esonantly enhanced two-photon absorptions, in comparison with that in atomic two-photon transitions.

References

[1] E. Arimondo, G. Orriols, Nuovo Cimento Lett. **17**,333 (1976)

[2] C. Cohen-Tannoudji, S. Reynaud, J.Phys. **B10**, 2311 (1977)

[3] H. R. Gray, R. M. Whithey, C. R. Stroud,Jr., Opt. Lett. **3**, 218 (1978)

[4] N. Kaivola, P. Thorsen, O. Poulsen, Phys. Rev.**A32**, 207 (1985)

[5] A. Aspect, E. Arimondo, R. Kaiser, N. Vansteenkiste, C. Cohen-Tannoudji, Phys. Rev. Lett. **61**, 826 (1988)

[6] D. Kosachiov et al., Opt. Commun. **85**, 209 (1991)

[7] S. Adachi, H. Niki, Y. Izawa, S. Nakai, C. Yamanaka, Opt. Commun. **81**, 364 (1991)

[8] A. M. Akulshin, A. A. Celikov, V. L. Velichansky, Opt. Commun. **84**, 139 (1991)

[9] S. E. Harris, Phys. Rev. Lett. **62**, 1033 (1989)

[10] O. A. Kocharovskaya, P. Mandel, Phys. Rev. **A42**, 523 (1990)

[11] J. Gao et al., Opt. Commun. **93**, 323 (1992)

[12] A. Nottelmann, C. Peter, W. Lange, Phys. Rev. Lett. **70**, 1783 (1993)

[13] M. O. Scully, Phys. Rev. Lett. **67**, 1855 (1991)

[14] M. O. Scully, S. Y. Zhu, Opt. Commun. **87**, 134 (1992)

[15] H. R. Xia, G. Y. Yan, A. L. Schawlow, Opt. Commun. **39**, 153 (1981)

[16] G. P. Morgan, H. R. Xia, A. L. Schawlow, J. Opt. Soc. Am. **72**, 315 (1982)

[17] H. R. Xia, J. W. Xu, I. S. Cheng, in *Laser Materials and Laser Spectroscopy* (World Scientific88)

[18] Z. G. Wang, H. R. Xia, *Molecular and Laser Spectroscopy* (Springer91)

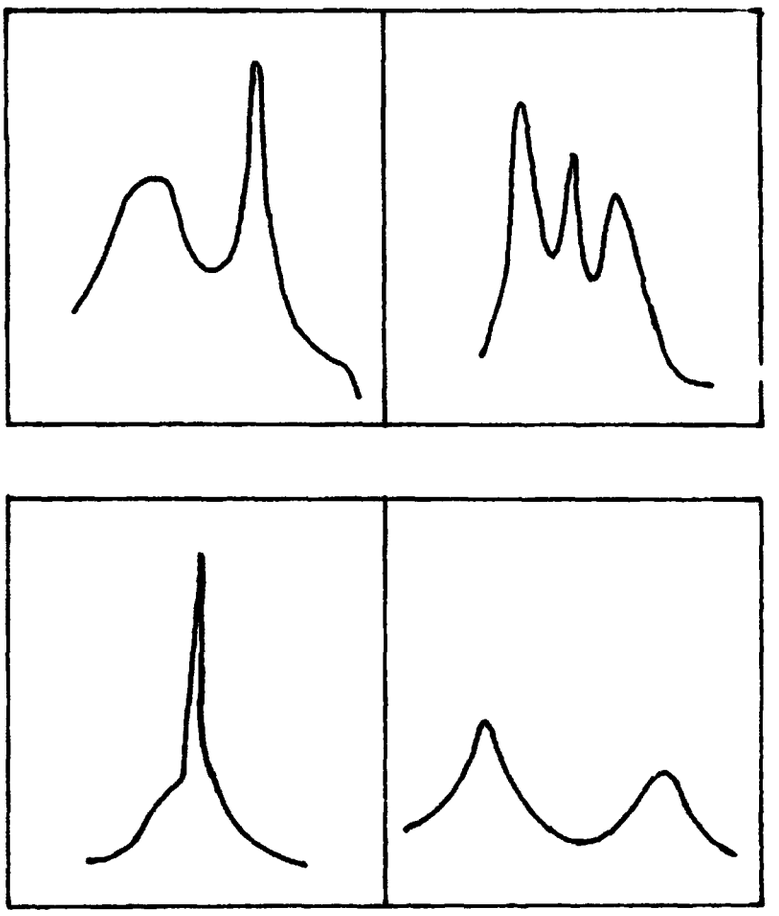

NEXT
DOCUMENT

Application of Twin Beams in Mach-Zehnder Interferometer

J.X.Zhang
Shanxi Fenyang Medical College, Fenyang, Shanxi, 032200, PRC
C.D.Xie, K.C.Peng
Institute of Opto-Electronics, Shanxi University, Taiyuan, Shanxi, 030006, PRC

Abstract

Using the twin beams generated from parametric amplifer to drive the two port of a Mach-Zehnder interferometer, it is shown that the minimum detectable optical phase shift can be largly reduced to the Heisenberg limit($1/n$) which is far below the Shot Noise Limit($1/\sqrt{n}$) in the large gain limit. The dependence of the minimum detectable phase shift on parametric gain and the inefficient photodetectors has been discussed.
PACS numberes: 42.50.Dv, 42.50.Lx, 07.60.Ly

1 Introduction

As well known, the output signal of the Mach-Zehnder interferometer is sensitive to the relative phase shift between two fields travelling down separated paths. The interferometers can be used in the precision measurements such as optical gravitational wave and gyroscopy detector[1 – 2]. The sensitivity of interferometers relies on the ability to resolve extremely small relative shifts in the two path lengths. The smallest detectable phase shift in principle is determined by the quantum properties of the illuminating field.

Usually the coherent state light is injected into one port of the standard intereferometer and the other one left unused. In this case the vacuum noise must enter the interferometer and the effect of zero-point fluctuations in the vacuum is amplified by the mean intensity of the laser[3 – 4], so that the minimum detectable phase shift is limited by the shot noise limit, i.e. ($\theta_{SNL} = 1/\sqrt{n}$) rad, here n is photon numbers of the input coherent state during the measurment interval. Therefore increasing the strength of the input laser light can increase the resolution of the interferometer, which requires the huge and expensive laser sources and sometimes it is not available. One possible device for enhancing the sensitivity is to replace the vacumm state with squeezed light in interferometer. In the experiment with squeezed vacua performed by Min Xiao et. al[5], an improvement in the signal-to-noise ratio of 3.0dB ralative to the SNL has been achieved. M.J.Holland and K.Burnett show that the Heisenberg limit of sensitivity can be realized by driving the interferometer with two Fock state lights[6].

A research group of Kastler-Brossel lab in France has successfully generated the twin beams with optical parametric osclillator above thresheld and a perfect quantum noise suppression on the difference between the intensities of the two generated beams has been demonstrated[7]. We suggest a device in which twin beams with same polarization orientation are respectively injecetd

into the two ports of Mach-Zhender interferometer instead of the usual coherent and vacuum states, therefore the sensitivity of the interferometer is improved to approach the Heisenberg limit of $1/n$.

2 Interferometer with twin-beams

The arrangment of the system is illustrated in Fig.1, the signal and idler mode of twin beams are injected into on the first beam splitter (B_1) of M-Z interferometer through the two ports. M is a phase shift medium set in one of the paths. A half-wave plate($\lambda/2$) is used to align the polarization. The intensities of output fields are detected by D_1 and D_2, at last the fluctuation spectrum of different photocurrent is analysed by spectrum analyzer.

the ralationship between the input and output field operators of the interferometer is:

$$c = e^{(\frac{i\theta}{2})}[\cos(\frac{\theta}{2})a_1^{out} + i\sin(\frac{\theta}{2})a_2^{out}] \tag{1}$$

$$d = e^{(\frac{i\theta}{2})}[\cos(\frac{\theta}{2})a_2^{out} + i\sin(\frac{\theta}{2})a_1^{out}] \tag{2}$$

Where θ is the measured phase shift, a_1^{out} and a_2^{out} are the mode operators of twin beams generated by the optical parametric amplifer with same polarization orientation . The output operators of amplifer is ralated to the input operators by the following formula:

$$a_1^{out} = \sqrt{G}a_1^{in} + \sqrt{G-1}a_2^{+in} \tag{3}$$

$$a_2^{out} = \sqrt{G}a_2^{in} + \sqrt{G-1}a_1^{+in} \tag{4}$$

G is thc power gain of amplifer.

The intensity difference measured is proportional to:

$$I_- = c^+c - d^+d$$

$$= \cos\theta(a_1^{+out}a_1^{out} - a_2^{+out}a_2^{out}) - i\sin\theta(a_2^{+out}a_1^{out} - a_1^{+out}a_2^{out}) \tag{5}$$

Taking $\alpha_1^{in} = \alpha_2^{in} = \alpha$ we obtain:

$$< I_- >= 2|\alpha|^2\sin\theta[\sqrt{G(G-1)}\sin 2\phi + (2G-1)\sin\phi] \tag{6}$$

$$V < I_- >=< (I_-)^2 > - < (I_-) >^2$$

$$= 2(\cos\theta)^2|\alpha|^2 + \sin\theta\cos\theta|\alpha|^2B + (\sin\theta)^2[|\alpha|^4C - |\alpha|^4A + |\alpha|^2E + D] \tag{7}$$

Where

$$D = 4G(G-1)$$

$$B = 4\sqrt{G(G-1)}\sin 2\phi$$

$$A = 4[\sqrt{G(G-1)}\sin 2\phi + (2G-1)\sin\phi]^2$$

$$C = 2[G^2 + (G-1)^2 + 3G(G-1)] - 2G(G-1)\cos 4\phi$$
$$+4[G\sqrt{G(G-1)} + (G-1)\sqrt{G(G-1)}]\cos\phi - 2[G^2 + (G-1)^2]\cos 2\phi$$
$$-2[2G\sqrt{G(G-1)} + 2(G-1)\sqrt{G(G-1)}]\cos 3\phi$$
$$E = 8[G\sqrt{G(G-1)} + (G-1)\sqrt{G(G-1)}\cos\phi + 2[G^2 + (G-1)^2 + 6G(G-1)]$$

The Signal-to-Noise Ratio(SNR) is defined by

$$SNR = \frac{< I_- >}{\sqrt{V(I_-)}} \geq 1 \tag{8}$$

Therefore

$$|\alpha|^4 A(\sin\theta)^2 \geq 2|\alpha|^2(\cos\theta)^2 + |\alpha|^2 B\sin\theta\cos\theta$$
$$+ [|\alpha|^4 C - |\alpha|^4 A + |\alpha|^2 E + D](\sin\theta)^2 \tag{9}$$

We get

$$|\alpha|^4 A \geq 2|\alpha|^2(\frac{\cos\theta}{\sin\theta})^2 + |\alpha|^2 B\frac{\cos\theta}{\sin\theta} + [|\alpha|^4 C - |\alpha|^4 A + |\alpha|^2 E + D| \tag{10}$$

We set $\sin\theta \sim \theta, \cos\theta \sim 1$ for the small θ, $|\alpha|^2$ is the average photon numbers (n) of the incident fields for parametric amplifier.

Then we have

$$[2n^2 A - n^2 C - nE - D]\theta^2 - nB\theta - 2n \geq 0 \tag{11}$$

Because of $2n^2 A - n^2 C - nE - D > 0$, the solution of equation is

$$\theta \geq \frac{B + \sqrt{B^2 + 8[(2A-C)n - E - \frac{D}{n}}}{2(2A-C)n - E - \frac{D}{n}} \tag{12}$$

According to the equation (12) the minimum detectable phase shift (θ_{min}) as a function of n is illustrated in Fig.2. The solid line is the Heisenberg limit, the dashed line and dot-dashed line illustrate the minimum detectable phase shift calculated with $G = 2.3 \times 10^7$ and $G = 2.0 \times 10^7$. We can see that for $G = 2.3 \times 10^7$ and small photon numbers n, the minimum detectable phase shift is gratually approach to the Heisenberg limit. The larger the G is, the smaller the minimum detectable phase shift is. Bright twin beams of wavelength $1.06\mu m$ with power of 3mw has been experimently obtained. With the twin beams of 3mw the minimum detectable phase shift of $10^{-16} rad$ can be easily realized in the interferometer suggested by us, but if using the coherent state the incident power of 1000kw must be demanded.

3 Inefficient photodetection

A detector with quantum efficiency η is equivalent to a beamsplitter which mixes the input mode(a) with a vacuum mode(v), then the output mode from beamsplitter is detected by a perfectly efficient detector[8].

For brevity, setting that the quantum efficiencies of the photodetectors D_1 and D_2 are equal, i.e $\eta_1 = \eta_2 = \eta$, then the anihilation operators for detected modes by D_1 and D_2 are given by:

$$j = \eta^{1/2}c + (1-\eta)^{1/2}v \tag{13}$$

$$k = \eta^{1/2}d + (1-\eta)^{1/2}v \tag{14}$$

j and k are the anihilation operators for the inefficient detector with η.

The analyzed photocurrent and its variance are:

$$< j^+j - k^+k >= \eta < c^+c - d^+d > \tag{15}$$

$$|\Delta(j^+j - k^+k)|^2 = \eta^2 < (c^+c - d^+d)^2 > -\eta^2 < c^+c - d^+d >^2 + \eta(1-\eta)|< c^+c > + < d^+d >| \tag{16}$$

The SNR is

$$SNR = \frac{< j^+j - k^+k >}{\sqrt{|\Delta(j^+j - k^+k)|^2}} \geq 1 \tag{17}$$

$$|\Delta(j^+j - k^+k)|^2 = \eta^2 n^2 (C - A)(\sin\theta)^2 + \eta^2 nB\sin\theta\cos\theta + 2\eta^2 n(\cos\theta)^2 + \eta^2 nE(\sin\theta)^2 + \eta^2 D(\sin\theta)^2 + \eta(1-\eta)nF\sin\theta + \eta(1-\eta)nM + \eta(1-\eta)H \tag{18}$$

Where

$$F = 2|(2G-1)\sin\phi + \sqrt{G(G-1)}\sin 2\phi|$$

$$M = 4|(2G-1) + 2\sqrt{G(G-1)}\cos\phi|$$

$$H = 4(G-1)$$

From eq. (17) (18) we get the inequality:

$$A\prime\theta^2 - B\prime\theta - C\prime \geq 0 \tag{19}$$

where $A\prime = (2A - C)n - E - D/n$

$B\prime = B + \frac{\eta(1-\eta)}{\eta^2}F$

$C\prime = \frac{\eta(1-\eta)}{\eta^2}M + 2 + \frac{\eta(1-\eta)}{\eta^2}\frac{H}{n}$

The solution of eq.(19) is:

$$\theta \geq \frac{B\prime^2 + \sqrt{B\prime^2 + 4A\prime C\prime}}{2A\prime} \tag{20}$$

Fig.3 shows the dependence of the minimum detectable phase shift θ_{min} on the power gain respectively for detector with $\eta = 1$ and detector with $\eta = 0.99$. When the gain(G) increase, the θ_{min} decrease, i.e. the sensitivity of interferometer is raised. The effect of inefficiency is very severe. The physical origin of above results is that the quantum correlation degree between the twin beams a_1^{out} and a_2^{out} depends positively on G and η. Therefore the quantum correlation between twin beams is the key to realize high sensitivity detection.

4 Conclusion

We have shown that the Heisenberg limit can be met in the detection of phase shift by using twin beams as the input fields of the interferometer. The dependence of the minimum detectable phase shift on the gain of parametric amplifier which produces the twin beams and the quantum efficiency of detectors has been presented. The sensitivity of the suggested device is always higher than SNL and can tend to the Heisenberg limit for appropriate parameters.

Reference

[1] K.Thorne, Rev.Mod.Lett., 52, 285 (1980).
[2] W.W.Chou, Rev.Mod.Phys., 57, 61 (1985).
[3] C.M.Caves, Phys.Rev.D, 23, 1693 (1981).
[4] R.S.Bondurant and J.H.Shapiro, Phys.Rev.D, 30, 2548 (1984).
[5] Min Xiao, Ling-An Wu, and H.J.Kimble, Phys.Rev.Lett, 59, 278 (1987).
[6] M.J.Holland and K.Burnett, Phy.Rev.Lett., 71, 1355 (1993).
[7] J.Mertz, T.Debuisschert, A.Heidmann, C.Fabre and E.Giacobino, Opt.Lett., 16, 1234(1991).
[8] H.P.Yuen, V.M.S.Chan, Opt.lett., 2(2), 177 (1983).

Figure captions

Fig.1 The diagram of interferometer with twin beams
Fig.2 The minimum detectable phase shift vs the numbers of incident photons
Solid line corresponds to Heisenberg limit
Dashed line for $G = 2.3 \times 10^7$
Dot-dashed for $G = 2.0 \times 10^7$
Fig.3 The minimum detectable phase shift vs the power gain of amplifer with $n = 2 \times 10^{16}$
Solid line for $\eta = 1$
Dotted line for $\eta = 0.99$

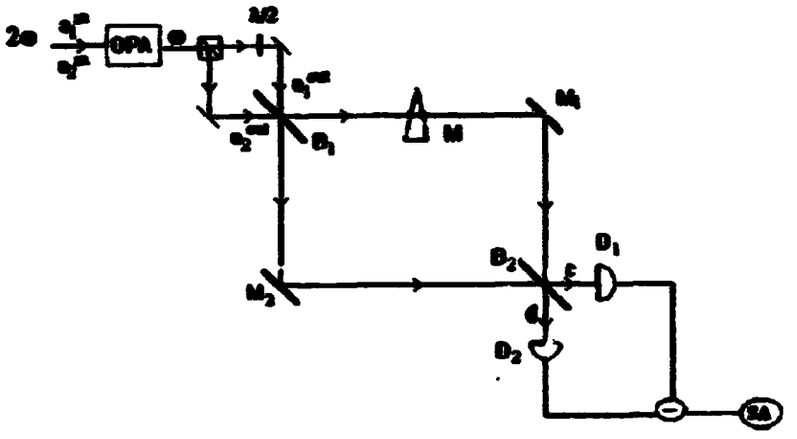

Fig.1 The diagram of interferometer with twin beams

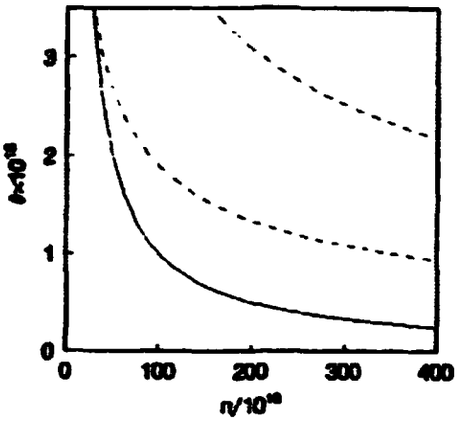

Fig.2 The minimum detectable phase shift vs the numbers of incident photons
Solid line corresponds to Heisenberg limit
Dashed line for $G = 2.3 \times 10^7$
Dot-dashed for $G = 2.0 \times 10^7$

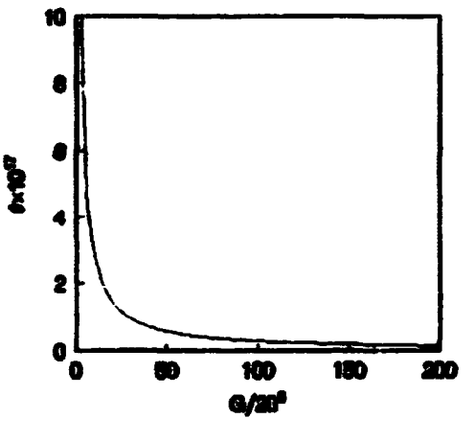

Fig.3 The minimum detectable phase shift vs the power gain of amplifer with $n = 2 \times 10^{16}$
Solid line for $\eta = 1$
Dotted line for $\eta = 0.99$

NEXT
DOCUMENT

Transient Sub-Poissonian Distribution for Single-Mode Lasers

J. Y. Zhang, Q. Gu, L. K. Tian

(Department of Physics, Northwest University, Xian, 710069, P. R. China)

Abstract In this paper, the transient photon statistics for single-mode lasers is investigated by making use of the theory of quantum electrodynamics. By taking into account of the transitive time τ, we obtain the master equation for Jaynes-Cummings model. The relation between the Mandel factor and the time is obtained by directly solving the master equation. The result shows that a transient phenomenon from the transient super-Poissonian distribution to the transient sub-Poissonian distribution occurs for single-mode lasers.

In addition, the influences of the thermal light field and the cavity loss on the transient sub-Poissonian distribution are also studied.

Key words: single-mode laser; Jaynes-Cummings model; Transient sub-Poissonian photon statistics.

1 Introduction

As is well known, sub-Poissonian light field is a typical nonclassical light field. And it has widely applications to the ultraweak signal detection and to the optical communication etc.[1] According to the usual theory, there is no sub-Poisonian distribution for single-mode lasers.

In this paper, the transient photon statistics for single-mode lasers is investigated by making use of the theory of quantum electrodynamics. by taking

into account of the transitive time τ. the master equation for Jaynes-Cummings model and its solution are obtained.

2 Master equation

First of all, the interaction of one atom with the light field is taking into account. According to the theory of the quantum electrodynamics. for the Jaynes-Cummings model the Hamiltonion has the following form[2-4](with $\frac{h}{2\pi}=1$)

$$H=\omega a^{+}a+\frac{1}{2}\omega_0\sigma_z+_{\omega}(a\sigma^{+}+a^{+}\sigma^{-}), \tag{1}$$

where a and a^{+} are annihilation and creation operators of photon; σ^{+} and σ^{-} are raising and lowering operators of the atom; ω and ω_0 are the mode frequency and the transition frequency, respectively; σ_z is the inversion papurition of the atom; g is the coupling constant between the atom and the field mode.

The eignequation of the expcession (1) is given by

$$H|\Phi>=E|\Phi>, \tag{2}$$

where

$$E_n^{\pm}=[\omega(n+\frac{1}{2})\pm\Omega_n] \tag{3}$$

$$Eg=-\frac{1}{2}\omega_0 \tag{4}$$

and

$$\Omega_n=[(\frac{\triangle}{2})^2+g^2(n+1)]^{\frac{1}{2}} \tag{5}$$

$$\triangle=\omega-\omega_0 \tag{6}$$

The eignstates corresponding to expressions (3) and (4) are given by

$$|\Phi_n^{\pm}>=\begin{vmatrix}\sin\theta_n\\ \cos\theta_n\end{vmatrix}|n,a>\pm\begin{vmatrix}\cos\theta_n\\ \sin\theta_n\end{vmatrix}|n+1,b> \tag{7}$$

$$|\Phi g>=|0,b> \tag{8}$$

here

$$\theta_n=\tan^{-1}\left(\frac{g\sqrt{n+1}}{\frac{\Delta}{2}+\Omega_n}\right) \tag{9}$$

where n denoting the photon number; a and b denoting the upper and lower atomic levels.

All nonzero matrix elements of the evolving operator

$$U(\tau)=\exp(-iH\tau) \tag{10}$$

in the state $|n, \alpha\rangle=|n\rangle|\alpha\rangle$ ($\alpha=a, b$) are given by

$$a_n=\langle n+1,b|U(\tau)|n+1,b\rangle=\cos^2\theta_n e^{-iE_n^+\tau}+\sin^2\theta_n e^{-iE_n^-\tau} \tag{11}$$

$$b_n=\langle n+1,b|U(\tau)|n,a\rangle=\sin\theta_n\cos\theta_n(e^{-iE_n^+\tau}-e^{-iE_n^-\tau}) \tag{12}$$

$$C_n=\langle n,a|U(\tau)|n,a\rangle=\sin^2\theta_n e^{-iE_n^+\tau}+\cos^2\theta_n e^{-iE_n^-\tau} \tag{13}$$

and

$$B_n(\tau)=|b_n(\tau)|^2=\frac{g^2(n+1)}{\frac{\Delta}{2}+g^2(n+1)}\sin^2\left(\sqrt{(\frac{\Delta}{2})^2+g^2(n+1)}\tau\right), \tag{14}$$

Assuming at the initial time t there is no correlation between the atom and the fidd, thus we have

$$\rho_s(t)=\rho_a(t)\otimes\rho(t). \tag{15}$$

This means that the matrix elements of $\rho_s(t)$ is the combination state $|n, \alpha\rangle$ and can be written as

$$\langle n, \alpha|\rho_s(t)|n', \alpha'\rangle=\langle n|\rho(t)|n'\rangle\langle\alpha|\rho_a(t)|\alpha'\rangle. \tag{16}$$

After τ, the expression (15) becomes

$$\rho_s(t+\tau)=U(\tau)\rho_s(t)U^{-1}(\tau) \tag{17}$$

and

$$\rho(t+\tau)=\sum_\alpha\langle\alpha|\rho_s(t+\tau)|\alpha\rangle \tag{18}$$

In the photon number representation, the matrix elements of equation (18) may be given by

$$\rho_{n,m}(t+\tau)=\sum_k\sum_{k'}\langle n, m|G(\tau)|k,k'\rangle\langle k|\rho(t)|k'\rangle, \tag{19}$$

where

$$\langle n, m|G(\tau)|k, k'\rangle = \sum_{\alpha}\sum_{\alpha'}\sum_{\alpha''}\langle n, \alpha''|U(\tau)|k, \alpha\rangle\langle k', \alpha'|U^{-1}(\tau)|m, \alpha'\rangle P_{\alpha\alpha'}, \tag{20}$$

where $|m\rangle$ and $|k\rangle$ denotes the photon-number states, and

$$P_{\alpha\alpha'} = \langle\alpha|\rho_a(t)|\alpha'\rangle. \tag{21}$$

For the arbitrary initial state of the atom and the light field, using expressions (11)—(13), (20) and (21), we obtain

$$\begin{aligned}\rho_{n,m}(t+\tau) = {} & P_{aa}[a_n a_m^* \rho_{n,m}(t) + b_{n-1} b_{m-1}^* \rho_{n-1,m-1}(t)] \\ & + P_{ab}[b_n a_m^* \rho_{n+1,m}(t) + C_{n-1} b_{m-1}^* \rho_{n,m-1}(t)] \\ & P_{ba}[a_n b_m^* \rho_{n,m+1}(t) + b_{n-1} C_{m-1}^* \rho_{n-1,m}(t)] \\ & P_{bb}[b_n b_m^* \rho_{n+1,m+1}(t) + C_{n-1} C_{m-1}^* \rho_{n,m}(t)]\end{aligned} \tag{22}$$

Expression (22) is a generol form. For the laser system under considern-tion, we have

$$P_{ab} = P_{ba} = 0 \tag{23}$$

By taking into account equation (14) and the following expression

$$|a_n|^2 + |b_n|^2 = |C_n|^2 + |b_n|^2 = 1 \tag{24}$$

then equation (22) can be deduced to the following form:

$$\begin{aligned}\rho_{n,m}(t+\tau) = {} & P_{aa}\{\sqrt{[1-B_n(\tau)][1-B_m(\tau)]}\rho_{n,m}(t) \\ & + \sqrt{B_{n-1}(\tau)B_{m-1}(\tau)}\rho_{n-1,m-1}(t)\} + P_{bb}\{\sqrt{B_n(t)B_m(t)} \\ & \cdot \rho_{n+1,m+1}(t) + \sqrt{[1-B_{n-1}(t)][1-B_{m-1}(t)]}\rho_{n,m}(t)\}.\end{aligned} \tag{25}$$

Under the coarse grain approximation, equation of motion for the density matrix elements are given by

$$\dot{\rho}_{n,m}(t) = \nu\int_0^{\infty} d\tau' P(\tau')[\rho_{n,m}(t+\tau') - \rho_{n,m}(t)] + L\rho_{n,m}(t), \tag{26}$$

where

$$p(\tau') = Ne^{-\nu\tau'} \tag{27}$$

denotes the distribution function of the interaction duration τ between atom and field; N is a normalization constant; ν stands for the atomic decay rate.

Form the norwalization condition

$$\int_0^\tau P(\tau')d\tau' = 1 \tag{28}$$

we get

$$N = \frac{v}{1-e^{-T}} \tag{29}$$

where

$$T = v\tau \tag{30}$$

By substituting expression (25) into (26) and making use of Ref. [5], we finally obtain

$$\begin{aligned}
\dot{\rho}_{n,m} = & -v_a\rho_{n,m}(t)\{1-\int_0^\tau d\tau' P(\tau')\sqrt{[1-B_n(\tau')][1-B_m(\tau')]}\} \\
& + v_a\rho_{n-1,m-1}(t)\int_0^\tau d\tau' P(\tau')\sqrt{B_n(\tau')B_{m-1}(\tau')} \\
& - v_b\rho_{n,m}(t)\{1-\int_0^\tau d\tau' P(\tau')\sqrt{[1-B_{n-1}(\tau')][1-B_{m-1}(\tau')]}\} \\
& + v_b\rho_{n+1,m+1}(t)\int_0^\tau d\tau' P(\tau')\sqrt{B_n(\tau')B_m(\tau')} \\
& - \frac{c}{2}n_b[(n+1+m+1)\rho_{n,m}(t) - 2\sqrt{nm}\rho_{n-1,m-1}(t)] \\
& + \frac{c}{2}n_b[2\sqrt{(n+1)(m+1)}\rho_{n+1,m+1}(t) - (n+m)\rho_{n,m}(t)]
\end{aligned} \tag{31}$$

where n_b is the average photon number of the thermal light field; C is the cavity loss.

Expression (31) is the master equation for the single-mode lasers.

3 Numerical calculation

In the case of resonance, master equation (31) can be reduced to the following form:

$$\dot{\rho}_{n,m}(t) = -v_a[1-(A^-_{n,m}+A^+_{n,m})]\rho_{n,m}(t)$$

$$+ v_0[(A^-_{n-1,m-1} - A^+_{n-1,m-1}]\rho_{n-1,m-1}(t)$$
$$- v_0[1 - (A^-_{n-1,m-1} + A^+_{n-1,m-1})]\rho_{n,m}(t)$$
$$+ v_0[A^-_{n,m} - A^+_{n,m}]\rho_{n+1,m+1}(t)$$
$$- \frac{c}{2}n_0[(n+1+m+1)\rho_{n,m}(t) - 2\sqrt{nm}\,\rho_{n-1,m-1}(t)]$$
$$+ \frac{c}{2}n_0[2\sqrt{(n+1)(m+1)}\rho_{n+1,m+1}(t) - (n+m)\rho_{n,m}(t) \quad (32)$$

where

$$A^{\pm}_{n,m} = \frac{1}{2}\int_0^{\tau} d\tau' P(\tau')\{\sqrt{[1 - B_n(\tau')][1 - B_m(\tau')]} \mp \sqrt{B_n(\tau')B_m(\tau')}\} = \frac{1}{2(1-e^{-\tau})} \cdot$$
$$\frac{1 + e^{-\tau}\{A(\sqrt{n+1} \pm \sqrt{m+1})\sin[A(\sqrt{n+1} \pm \sqrt{m+1})\tau] - \cos[A(\sqrt{n+1} \pm \sqrt{m+1})\tau]\}}{1 + [A(\sqrt{n+1} \pm \sqrt{m+1})]^2} \quad (33)$$

In particulnr, for the diagonal matrix elements[5] expression (32) may be further reduced to the following form:

$$\dot{P}_n(\sigma) = \dot{\rho}_{n,n}(\sigma) = -(\frac{1}{2} + \frac{\mu}{2} + \frac{(2n+1)n_0 + n}{R} - A^+_n - \mu A^+_{n-1})\rho_{n,n}(\sigma)$$
$$+ (\frac{1}{2} - A^+_{n-1} + \frac{n - n_0}{R}\rho_{n-1,n-1}(\sigma) + (\frac{\mu}{2} - \mu A^+_n + \frac{(n+1)(n_0+1)}{R})\rho_{n+1,n+1}$$
$$(\sigma) \quad (34)$$

where

$$A^+_n = \frac{1}{2(1-e^{-\tau})} \frac{1 + e^{-\tau}\{\frac{2\chi}{\sqrt{2R}}\sqrt{n+1}\sin[\frac{2\chi t}{\sqrt{2}R}\sqrt{n+1}] - \cos[\frac{2\chi t}{\sqrt{2R}}\sqrt{n+1}]\}}{1 + [\frac{2\chi}{\sqrt{2R}}\sqrt{n+1}]^2}$$

(35)

here
$$R = \frac{v_0}{C},$$
$$\mu = \frac{A_b}{A},$$
$$\chi = \sqrt{\frac{A}{C}},$$
$$\sigma = v_0 t;$$

and

$$A = 2\bar{n}_0(\frac{g}{\gamma})^2, \tag{37}$$

$$A_0 = 2\bar{n}_0(\frac{g}{\gamma})^2.$$

The photon statistical properties of the lingt field can be expressed by Mandel factor Q:

$$Q = \frac{<n^2>-<n>^2-<n>}{<n>}, \tag{38}$$

where

$$<n>=\sum_{n=0}^{\infty} nP_n,$$

$$<n^2>=\sum_{n=0}^{\infty} n^2P_n, \tag{39}$$

During the trnnsient processes, Mandel factor $Q>0$, $Q=0$ or $Q<0$ correspond to transient super-Poissonian distribution, Poissonian distribuition or sub-Poissonian distribution, respectively.

Time evolution of the Mandel factor may be obtained by making use of the expressions (34), (35) ,(38) and (39). The numerical results are shown in Figures 1-5.

Figure 1 shows that the transient photon statistical property passes from super-Poissonian distribution through Poissonian distribution into sub-Poissoninn distribution with the increase of σ.

Figure 2 shows that the maximum value of the Q drift apart from the right and decrease. At the same time, the velocity toward the trnnsient sub-Poissonian distribution is also quickened.

Figure 3 indicates that the influence of the loss μ on the Mandel factor is marked and the transient sub-Poissonian distribution will disappear when the χ increase to some certain value.

Figure 4 indicates that the thermal light photon number not only deerease

sub-Poissonian distribution but also diminish the velocity for toward sub-Poissoniar distribution.

4 Brief discussion

In the present paper, we have studied the transient sub-Poissonian distribution for single-mode lasers. The result shows that for single-mode lasers the sub-Poissonian distribution may occur not only in the case of stotionary state[5] but also in the case of transient state.

As is well known, transient sub-Poissonian photon statistics is a character for the quantum light field. And its appearance would deepen our knowledge of the light field essence.

References

[1] Q. Gu, Science 41, 35 (1989).

[2] Q. Gu, Acta Physica Sinica (china) 37, 75, (1988).

[3] Q. Gu, China lasers 15, 484(1988).

[4] Q. Gu, J.Y.Zhang, Acta Optica sinica (china) 9, 478(1989).

[5] Q. Gu. Science in China A 33, 1460(1990).

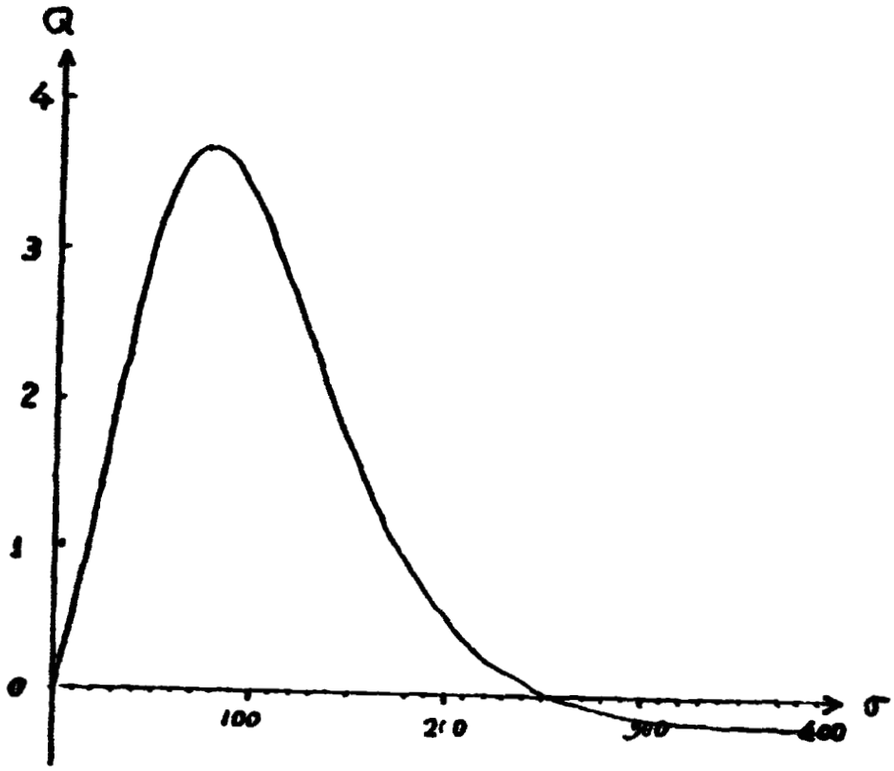

Fig. 1.

Caption of Fig. 1. Time evolution of the mandel factor for $T = 1.1$; $R = 100$; $\mu = n_b = 0$, $\chi = 6$

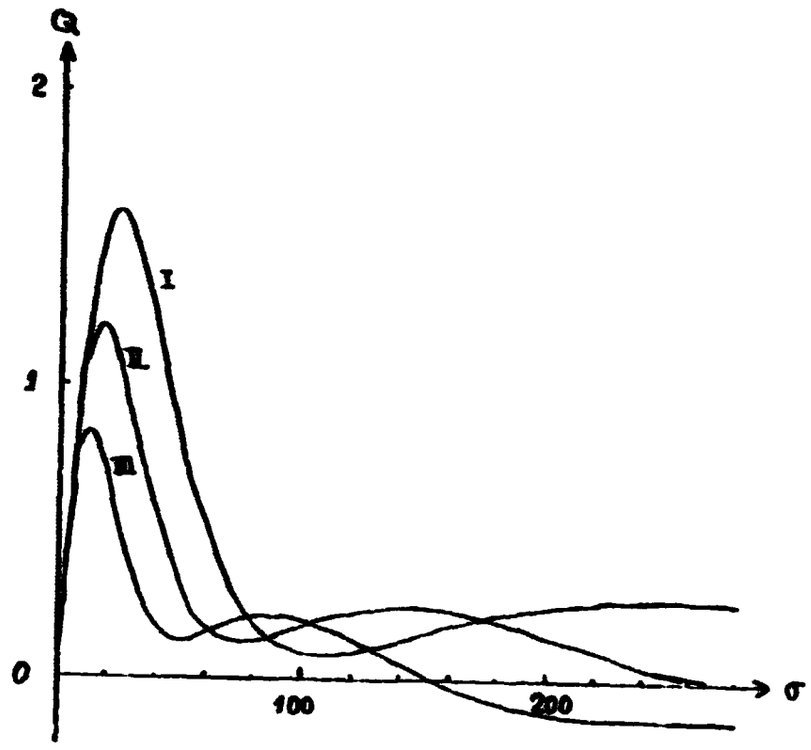

Fig. 2.

Caption of Fig. 2. Time evolution of the mandel factor for $T=1.1$; $R=100$; $\mu=n_0=0$, (I) $\chi=9.5$; (II) $\chi=10.8$; (III) $\chi=12.5$

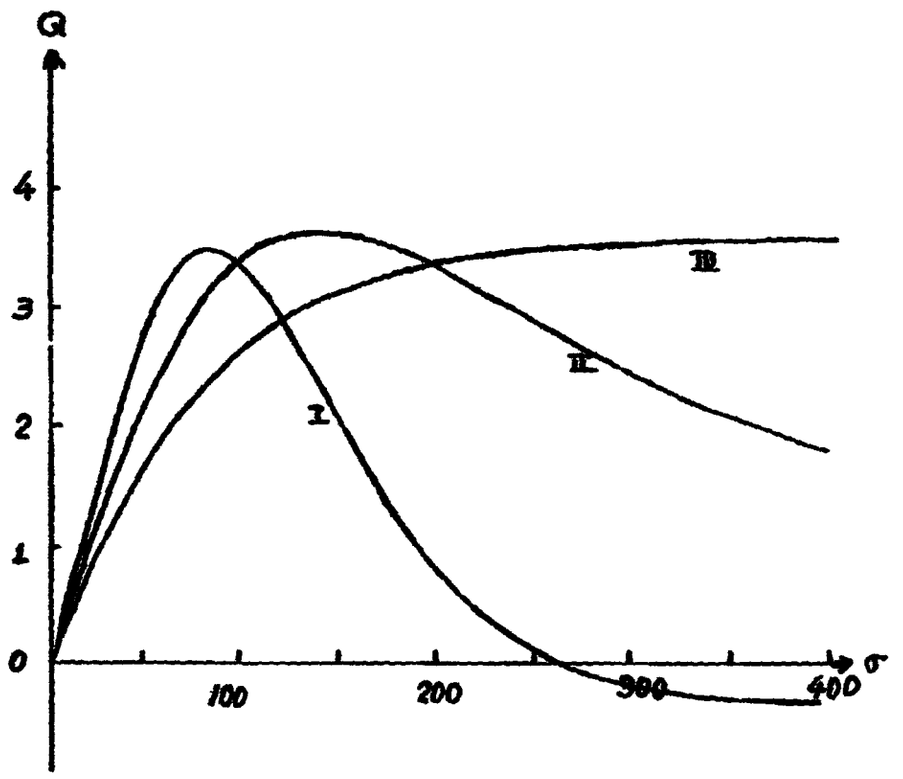

Fig. 3.

Caption of Fig. 3. Time evolution of the mandel factor for T = 1. 1; R = 100; $n_b = 0$; $\chi = 6$; (I) $\mu = 0.1$; (II) $\mu = 0.5$; (III) $\mu = 0.8$

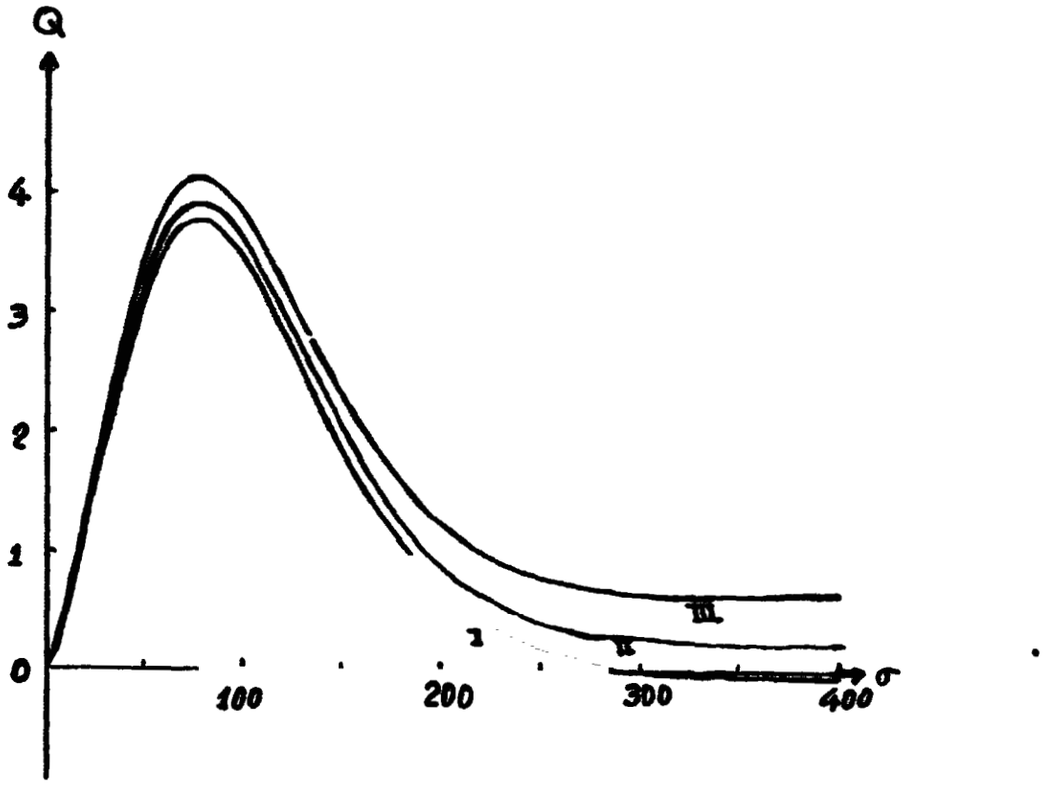

Fig. 4.

Caption of Fig. 4. Time evolution of the Mandel factor for $T=1.1$; $\chi=6$; $R=100$; $\mu=0$; (I) $n_b=0.2$; (II) $n_b=0.5$ (III) $n_b=1$

NEXT
DOCUMENT

Phase Noise Reduction of Laser Diode

T.C.Zhang
Institute of Opto-Electronics, Shanxi University, Taiyuan, Shanxi 030006, PRC
J.-Ph.Poizat, P.Grelu, J.-F.Roch, P.Grangier
Institut d'Optique, B.P.147, F91403 Orsay Cedex-France
F.Marin, A.Bramati, V.Jost, M.D.Levenson, and E.Giacobino
Laboratoire Kastler Brossel, Universite Pierre et Marie Curie, F75252 Paris Cedex 05-France

Abstract

Phase noise of single mode laser diodes, either free-running or using line narrowing technique at room temperature, namely injection-locking, has been investigated. It is shown that free-running diodes exhibit very large excess phase noise, typically more than 80 dB above shot-noise at 10 MHz, which can be significantly reduced by the above- mentionned technique.

PACS numbers: 42.50.Px, 42.50.Dv, 42.62.Fi

1 Introduction

Quantum intensity noise reduction of laser diode based on pump noise suppression has been extensively studied since 1984 [1]. Intensity squeezing of constant-current- driven laser diodes was observed for the first time by Machida et al in 1987 [2], and further improved to 8.3 dB in 1991 [3]. This last result was obtained at 66 K. In 1993, it was shown by Steel and his group[4] that line narrowing techniques (see [5] and references therein) greatly helped in the noise reduction. Intensity squeezing of 1.8 dB (2.0 dB corrected) at room temperature was obtained by injection-locking the laser [6] or by feedback from an external grating [4]. However, all the experiments realized so far were limited to measurement of intensity noise. How about the phase noise? In fact, in the early time in 1980's, Yamomoto et al [7] and Spano et al [8] studied the phase noise in laser diode, but they did not measure the phase noise with a reference to the standard quantum limit.

It is well known that in injection scheme the slave laser locks its frequency, and therefore its phase to the master laser. To our knowledge, the effect of injection locking on quantum phase-noise of laser diodes has not yet been reported experimentally. In reference [9], it is mentioned that injection-locking of a regularly pumped slave laser could lock the phase of the slave laser to the master laser, reducing thereby the excess phase-noise leading to a minimum uncertainty state(true squeezed state), if the master laser has a shot-noise- limited phase noise.

In this paper, we investigated the phase noise of laser diode, using injection-locking with a Ti:Sapphire laser. We have shown that the large excess phase noise of semiconductor lasers can be reduced by this technique.

2 Experimental Set-up and General Features

The laser diodes we have used are index-guided quantum well GaAlAs laser diodes (model SDL 5422-H1 and SDL 5411-G1), operating at 850 and 810 nm. The rear facet reflection coefficient is 95%, the front facet is AR coated with a reflection coefficient of about 4%. The laser diodes are temperature stabilized and carefully electromagnetically shielded.

The free-running laser diodes have a rather low threshold of 18 mA and a differential quantum efficiency (slope above threshold) of 66%. The operating current in the experiments described below is typically 5 to 7 times larger than the threshold current.

The injection-locking scheme is depicted in Fig.1. The master laser is a Ti:Sapphire laser which is frequency stabilized (linewidth of 500 kHz) and both intensity and phase are shot-noise limited. It is injected into the slave laser by means of an optical isolator. The master beam enters through the escape port of the polarizer placed after the Faraday rotator. Locking is observed on a rather broad power range[1] of the master laser, from 1 to 4 mW. The direction of the master laser must be carefully adjusted for optimum phase noise reduction.

3 Phase Noise Detection Scheme

The investigation of the phase noise of a laser beam requires a phase-to-amplitude converter, i.e. a device whose complex transmission T depends on the frequency ω. In this work, we use for this purpose the reflection off an empty detuned Fabry-Pérot cavity as shown in Fig.2. When the rear mirror is highly reflecting, this system has the advantage over a Mach-Zehnder interferometer that the mean field transmission $|T(\omega=0)|$ does not depend on the cavity detuning and is always equal to unity. This makes shot-noise reference level independent of the analysed quadrature. Phase noise analysis is then carried out conveniently for frequencies in the range of the cavity bandwidth.

Explicit expressions of the quadrature rotation after reflection off a detuned Fabry-Pérot cavity are given in reference [10]. A simple way to understand this effect is to have in mind that in Fourier space, the quadrature component $X(\omega)$ can be written as

$$X(\omega) = (a(\omega) + a^{\dagger}(\omega))/\sqrt{2} = (a(\omega) + [a(-\omega)]^{\dagger})/\sqrt{2}.$$

The key point which yields a quadrature rotation is that the various frequency components at 0 (mean field), ω and $-\omega$ do not undergo the same phase shift when the laser is scanned across the resonance peak of the cavity. The quadrature rotation is zero in two cases : when the laser is tuned exactly on resonance, where the phase shifts for both frequency components $\pm\omega$ cancel out, and when it is tuned far outside the peak, where all frequency components undergo the same phase shift of 0 or π.

In our set-up the Fabry-Pérot cavity has a half-width at half-maximum (HWHM) of 8 MHz and a finesse of $\mathcal{F} = 125$. The rear mirror is highly reflecting, but its small leaks nevertheless allow us to monitor the intracavity intensity to adjust the mode matching. One of the mirrors is mounted on a piezo-electrical transducer, so that the length of the cavity can be scanned.

[1] It should be mentionned that only a small fraction (a few %) of this injected power is actually coupled to the lasing mode of the diode due to the imperfect mode overlap.

4 Experimental Results

We have measured the quadrature noise of a free-running and injection-locked laser diode. These results are presented in Fig.3. The phase noise (quadrature angle $\pi/2$ with respect to the mean field) is inferred from the experimental curves by fitting them with a simple model (see reference [10]). This model has a single adjustable parameter which is the excess phase noise.

This value has then to be corrected for various losses : propagation from the output of the laser to the detectors (3 dB), scattering losses inside the analyzing cavity (3 dB on resonance), imperfect mode-matching to the cavity (1 dB).

The phase noise inferred at the laser output for the free-running diode and the injection- locked scheme are respectively of 82 dB, and 46 dB above the shot-noise level.

Let us compare these experimental results with the prediction given by the Schawlow- Townes model [11]. Within this model, the phase noise normalized to the shot-noise level at a noise angular frequency $\omega = 2\pi f$ is

$$V_\Phi(\omega) = 1 + \frac{8DI_o}{\omega^2}(1+\alpha^2) = 1 + \frac{2\kappa^2(1+\alpha^2)}{\omega^2} \tag{1}$$

where I_o is the flow of photon outside of the laser (photons/sec), κ is the cavity decay rate for intensity, α is the line enhancement factor[12] (also called phase-amplitude coupling coefficient), and D is the Schawlow-Townes phase diffusion coefficient defined as:

$$D \doteq \frac{\kappa^2}{4I_o} \tag{2}$$

The first term is the contribution of the vacuum fluctuation (shot-noise) and the second term is due to the phase diffusion assuming a random walk of the phase in the laser.

Using the value of κ deduced from the experiment[2], one can calculate a theoretical estimation of the phase noise if the factor $(1+\alpha^2)$ is known. Conversely, by using the experimental value of the phase noise, one can deduce a value of $(1+\alpha^2) = 10$, which is in agreement with other measurements. However, the linewidth of the laser diode was also measured directly by sending the light through a Fabry-Pérot cavity with a linewidth (HWHM) of 2 MHz. We obtained $D(1+\alpha^2)/(2\pi) = 2$ MHz (HWHM linewidth). Using the value $I_o = 2.5 \times 10^{17}$ phot/sec corresponding to 60 mW laser output, the above model predicts $D(1+\alpha^2)/(2\pi) = \kappa^2(1+\alpha^2)/(8\pi I_o) = 50$ kHz, which is significantly smaller than the measured value. This discrepancy could be attributed to jitter of the laser frequency due to power supply noise and thermal fluctuations.

In the injection locking case, the phase noise reduction mechanism relies on the fact that the slave laser locks its phase to the one of the master laser [13]. The phase noise of this master laser is therefore of great importance. In this experiment we have used a frequency-stabilized Ti:Sapphire laser, which has a linewidth of 500 kHz and is both phase and intensity shot-noise limited at 10 MHz. We have observed a very significant phase noise reduction, from 82 dB to 46 dB for an injected power of 2 mW (see Fig.3(b)).

[2]The quantity $1/\kappa$ is the lifetime of the photon in the laser diode cavity, calculated from the measured free spectral range of $\Delta\lambda = 0.12$ nm, and from the transmission coefficient of the output mirrors ($R_1 = 95\%$ and $R_2 = 4\%$). This yields $\kappa = (c\Delta\lambda/\lambda^2)\ln(1/(R_1R_2)) = 1.8 \times 10^{11}$ s^{-1}.

Finally, let us emphasize that the quadrature noise detection scheme that we used is expected to work well only for a true single-mode laser. This is not the case for so-called "single mode" laser diode, for which weak longitudinal side-modes are very noisy and can play therefore an important role in the overall noise behaviour [14]. As long as the intensity noise power in the main mode is small with respect to the total phase noise power, which is generally the case in the results described above, these effects can be neglected. However, one has to be cautious in some cases. For instance, it can be noticed that the experimental trace of Fig.3(b) exhibits a slight asymmetry around its basis. This effect can be modelled simply, using an input covariance matrix such that the main axis of the noise ellipse is not exactly the phase axis (quadrature angle $\pi/2$) but is slightly tilted. In our experiments, this small rotation effect has been observed for the injection-locked laser, decreases as the driving current increases, and the dip on the right-hand side was always above shot-noise [15]. It is likely that a detailed analysis of this effect should include the contributions of the small modes, since intensity-phase correlations are essential in this process.

The intensity noise in this process was also measured and intensity squeezing was obtained and we have another paper to discuss these effects in details (See E.Giacobino's paper in this issue).

5 Conclusion

In this paper we have reported on a detailed experimental analysis of phase noise of commercial laser diodes at room temperature. We have studied the free-running diode and the injection-locking diode. The main result is that laser diodes exhibit a very large excess phase noise (up to 80 dB above shot-noise) and in the injection-locking scheme, the phase noise reduction mechanism involves the master laser, and using a shot-noise limited frequency stabilized Ti:Sapphire laser, we observed a reduction of the phase noise from 82 dB to 46 dB above shot-noise.

We believe that these results have important practical implications for spectroscopy and quantum optics experiments involving laser diodes. This results have also demonstrated that there is still a long way to realize the squeezed minimum uncertainty states with laser diodes.

6 Acknowledgments

This research was carried out in the frameworks of the ESPRIT Basic Research Project 6934 QUINTEC, and of the HCM network "Non-Classical Light" (ERB CHRX CT93 0114). Two of us had fellowships : TCZ was supported by a Programme International de Coopération scientifique (PICS) sponsored by the CNRS. and AB was supported by the HCM program from the European Community (ERB CHBG CT93 0437).

References

1. Yu.M. Golubev, I.V. Sokolov, Zh. Eksp. Teor. Phys, 87, 804, (1984) (Sov. Phys. JETP, 60, 234 (1984)).
2. S. Machida, Y. Yamamoto, and Y Itaya, Phys. Rev. Lett., 58, 1000 (1987);
3. W.H. Richardson, S. Machida, and Y. Yamamoto, Phys. Rev. Lett., 66, 2867 (1991).
4. M.J. Freeman, H. Wang, D.G. Steel, R. Craig, and D.R. Scifres, Opt. Lett., 18, 2141 (1993).

5. C.E. Wieman and L. Hollberg, Rev. Sci. Instrum., 62, 1 (1991).
6. H. Wang, M.J. Freeman, and D.G. Steel,Phys. Rev. Lett., 71, 3951 (1993).
7. S.Saito, Y.Yamamoto, Electronics Letters, 17, 327 (1981).
8. B.Daino, P.Spano, M.Tamburrini and S.Piazzolla, IEEE, Journal of Quantum Electronics,QE-19, 266 (1983).
9. H.M.Wiseman and G.J.Milburn, Phys.Rev.Lett., 70, 548 (1993).
10. T.C.Zhang, J-Ph.Poizat, P.Grelu, J-F.Roch, P.Grangier, F.Marin, A.Bramati, V.Jost, M.D.Levenson and E.Giacobino, Quantum and Semiclassical Optics, 7, (1995)to be published.
11. A.L. Schawlow and C.H. Townes, Phys. Rev., 112,1940 (1958).
12. C.H. Henry, IEEE J. Quantum Electron., 18, 259 (1982).
13. P. Spano, S. Piazzolla, and M. Tamburrini,Opt. Lett.,10, 556 (1985); IEEE J. Quantum Electronics, 22, 427 (1986).
14. F. Marin, A. Bramati, E. Giacobino, T.-C. Zhang, J.-Ph. Poizat, J.-F. Roch, and P. Grangier, submitted to Phys. Rev. Lett.
15. A. Karlsson and G. Björk, Phys. Rev. A, 44, 7669 (1991).

FIGURES

Fig.1. Injection-locking scheme. The Faraday rotator rotates the linear polarization by 45°. PBS is a polarizing beam splitter. The master laser is a frequency stabilized Ti:Sapph laser.

Fig.2. Phase noise detection set-up. Great care has been given in order to avoid any feedback from the analysing cavity to the laser, and optical isolation (OI) of about 80 dB has been used. The rear mirror is a high reflector and its position is controlled by a piezo electrical transducer (PZT).

Fig.3. Raw noise power at 10 MHz as the laser diode is scanned across the peak of the analysing Fabry-Perot cavity. (a) for the free-running laser diode, (b) for the Ti:Sapph injection-locked laser diode. The laser diode driving current is 80 mA The reference level 0 dB is the shot-noise level. The resolution bandwidth is 1 MHz with a video filter of 10 kHz. On each graph the thin line is the best fit using the theoritical expression. The small peaks on the sides are due to an imperfect mode-matching.

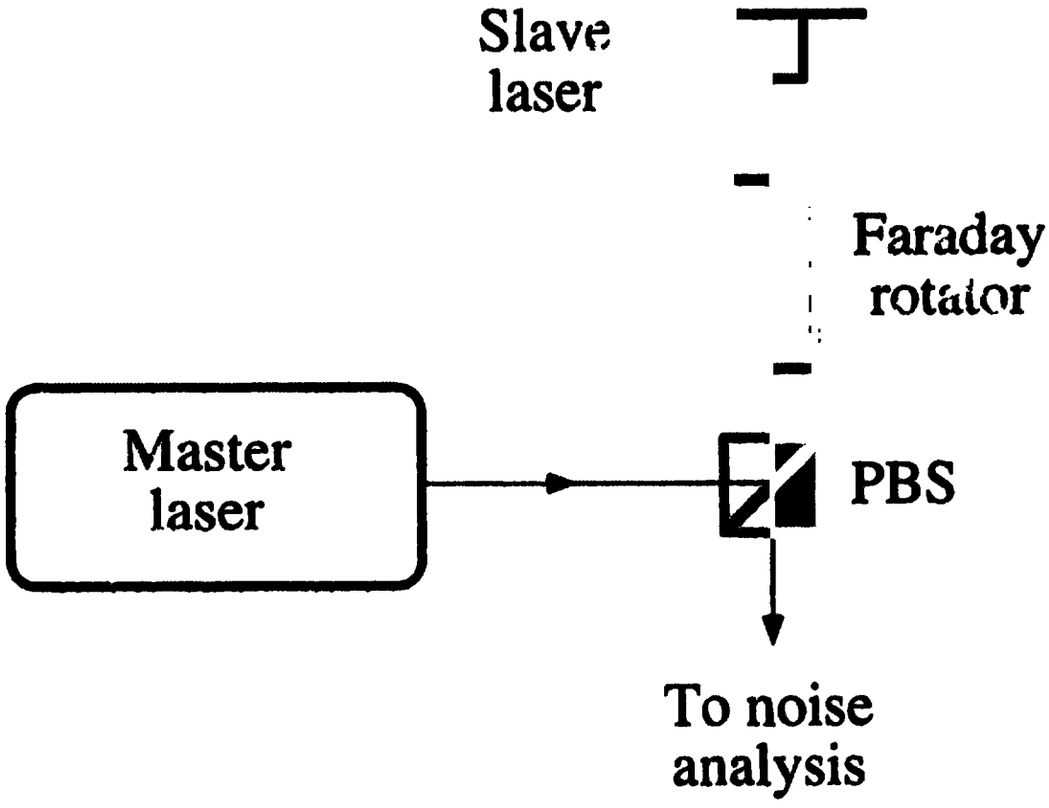
Slave
laser
Faraday
rotator
Master
laser
PBS
To noise
analysis

Fig.1

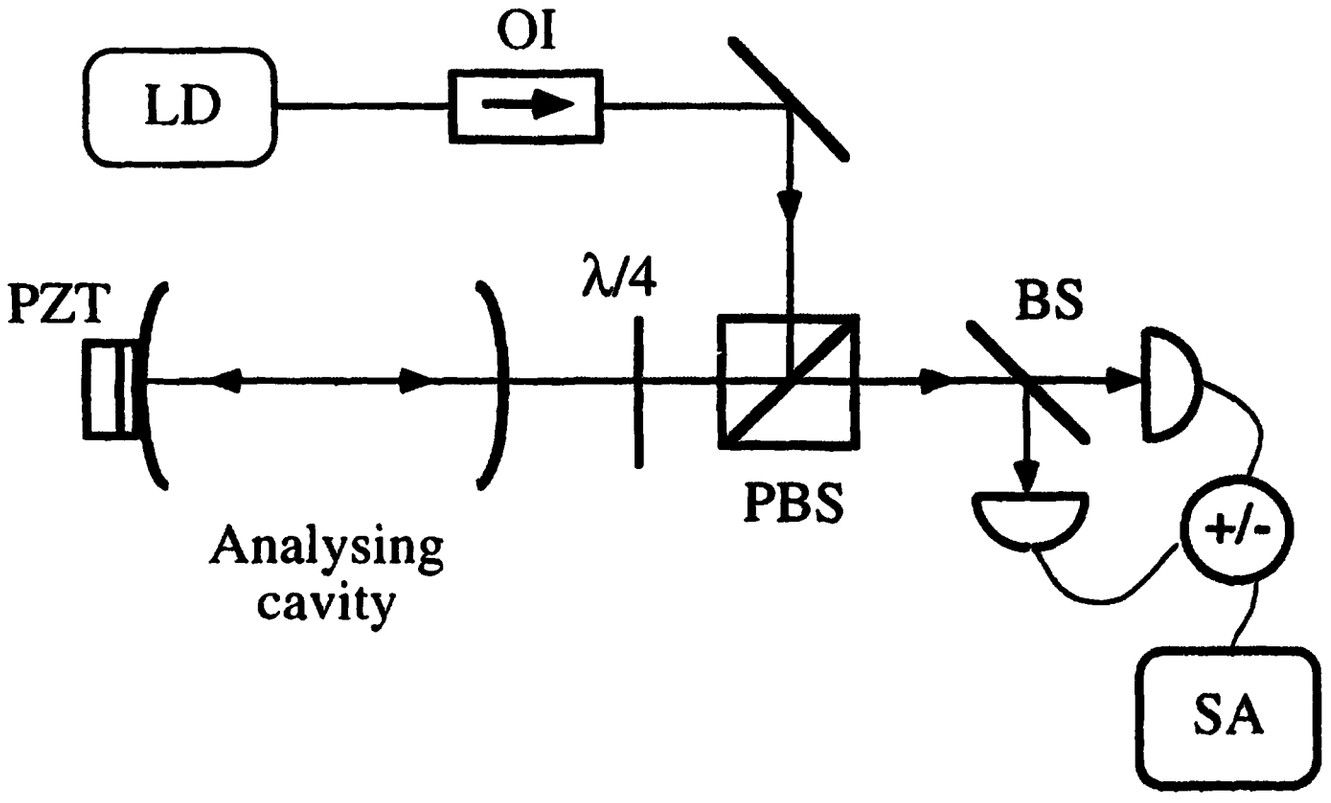

Fig.2

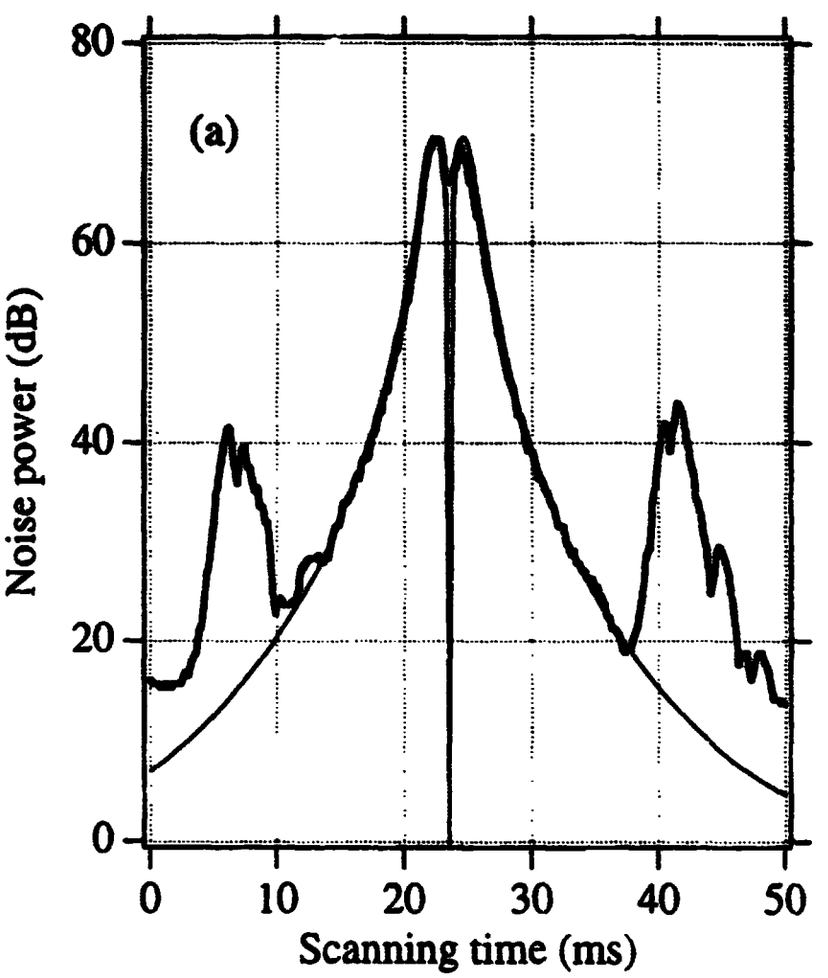

Fig.3(a)

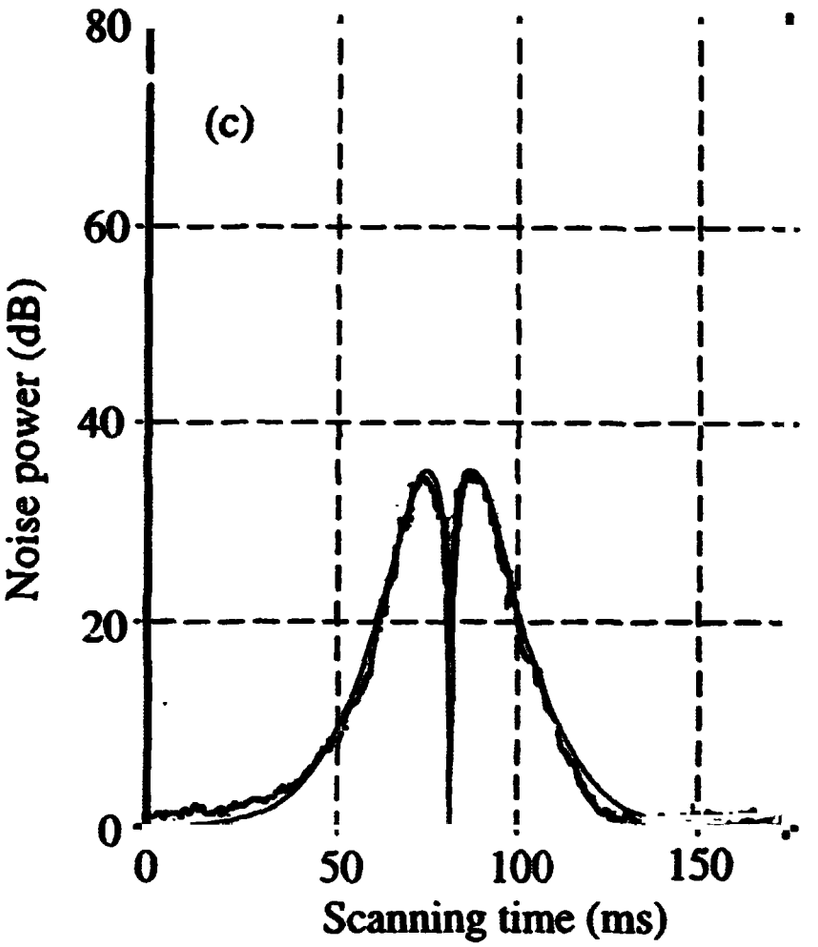

Fig.3(b)

NEXT
DOCUMENT

The Amplitude Nth-Power Squeezing of Radiation Fields in the Degenerate Raman Process

Zhi-Ming Zhang
Department of Physics, Xi'an Jiaotong University, Xi'an, Shaanxi 710049, PRC
Jin-Fang Pan
Department of Physics, Shanxi Normal University, Linfen, Shanxi 041004, PRC
Lei Xu
Institute of Nuclear Research, Academia Sinica, Shanghai 201800, PRC

Abstract

In this paper we study the amplitude Nth-power squeezing of radiation fields in the degenerate Raman process by using the modified effective Hamiltonian approach recently suggested by us. We found that if the field is initially in a coherent state it will not get squeezing for any Nth-power; if the field is initially in a squeezed vacuum, it may get Nth-power squeezing. The time evolution of the field fluctuation was discussed. Its dependences on power-order N, mean photon number $\bar{n}$, and squeezing angle ξ are analyzed.

1 Introduction

Squeezed states of radiation fields have been studied considerably in recent years. Besides the normal squeezing[1] it is also possible to define higher-order squeezing. Hong and Mandel[2] defined the 2Nth-order squeezing, and Hillery[3] introduced the amplitude squared squeezing. More recently, Zhang et al[4] suggested the amplitude Nth-power squeezing(ANPS), which includes the normal squeezing and the ampliuide-squared squeezing as special cases. All these higher-order squeezing have been shown to be independent nonclassical features of radiation fields[5]. ANPS of radiation fields has been studied in many quantum optics systems[4-12].

On the other hand, the degenerate Raman process(DRP) is one of the most interesting two-photon interactions between atoms and radiation fields, and has been studied intensively[13-16]. Usually, this process was studied by the full microscopic Hamiltonian approach(FMHA)[13-14], and the effective Hamiltonian approach(EHA)[15]. Generally speaking, FMHA gives exact solution, but it may be too complicated to be used in some situations. Although EHA is simpler than FMHA, it loses a phase factor, it can not be used to deal with the quantities involving the off-diagonal elements of the density matrix. To overcome these shortages we have suggested a modified effective Hamiltonian approach(MEHA)[16].

In this paper we use MEHA to study ANPS of radiation fields in DRP.

2 The Degenerate Raman Process(DRP)

The DRP refers to the interaction between a Λ-type three level atoms and a single mode of a radiation field(Fig.1).

The modified effective Hamiltonian for DRP is [17]

$$H_{MEH} = H_{EH} + h_S \tag{1}$$

$$H_{EH} = \lambda a^+ a(|e><g| + |g><e|) \tag{2}$$

is the effective Hamiltonian(when the detuning is very large, one can eliminate the upper level adiabatically and obtain it) and

$$H_S = -a^+ a(\beta_1|g><g| + \beta_2|e><e|) \tag{3}$$

is the part representing the ac Stark shift of atomic levels. β_1 and β_2 are the Stark parameters for levels $|g>$ and $|e>$, respectively.

If the initial state for the atom-field system is

$$|\Psi(0)\rangle = \sum_{n=0}^{\infty} q_n |C_g(0)|g,n\rangle + C_e(0)|e,n\rangle| \tag{4}$$

we can express the state for a later time as

$$|\Psi(t)\rangle = \sum_{n=0}^{\infty} q_n |C_g^n(t)|g,n\rangle + C_e^n(t)|e,n\rangle| \tag{5}$$

¿From the time-dependent Schrödinger equation we can obtain $C_g^n(t)$ and $C_e^n(t)$.

The reduced density matrix for the field can be expressed as

$$\rho(t) = \sum_{n,n'=0}^{\infty} \rho_{nn'}(t)|n\rangle\langle n'| \tag{6}$$

$$\rho_{nn'}(t) = q_n q_{n'}^* |C_g^n(t) C_g^{n'*}(t) + C_e^n(t) C_e^{n'*}(t)| \tag{7}$$

Supposing initially the atom is in the state $|g\rangle$, i.e. $C_g(0) = 1$, and $C_e(0) = 0$, and let $g_1 = g_2 = g$ for simplisity, we get

$$\rho_{nn'}(T) = q_n q_{n'}^* exp|-i(n-n')T| cos(n-n')T \tag{8}$$

in which $T = \lambda t$. We see that the diagonal elements ρ_{nn} are independent of time and just the photon distribution function of initial field.

3 The Amplitude Nth-Power Squeezing(ANPS)

The amplitude Nth-power squeezing of a radiation field is defined in terms of the following quantities[4]

$$Z_1(N) = \frac{1}{2}(a^N + a^{+N}), \qquad Z_2(N) = \frac{1}{2i}(a^N - a^{+N}) \tag{9}$$

$Z_1(N)$ and $Z_2(N)$ satisfy the commutation relation and the uncertainty relation

$$|Z_1(N), Z_2(N)| = \frac{i}{2}|a^N, a^{+N}| \tag{10}$$

$$\langle(\Delta Z_1(N))^2\rangle\langle(\Delta Z_2(N))^2\rangle \geq \frac{1}{16}|\langle|a^N, a^{+N}|\rangle|^2 \tag{11}$$

The field is said to be Nth-power squeezed if

$$\langle(\Delta Z_i(N))^2\rangle < \frac{1}{4}\langle|a^N, a^{+N}|\rangle \qquad (i = 1,2) \tag{12}$$

Here we introduce a parameter named squeezed degree $S_i(N)$

$$S_i(N) = \frac{D_i(N)}{C(N)} \qquad (i = 1,2) \tag{13}$$

where $C(N)$ and $D_i(N)$ are defined as

$$C(N) = \langle|a^N, a^{+N}|\rangle, \qquad D_i(N) = 4\langle(\Delta Z_i(N))^2\rangle - \langle|a^N, a^{+N}|\rangle \tag{14}$$

Then the field is Nth-power squeezed if $D_i(N) < 0$, ($S_i(N) < 0$). $S_i(N) = -1$ corresponds to 100% squeezing. In the following section we will study ANPS in DRP. We will consider several kinds of initial field states.

4 ANPS in DRP

4.1. For an Initial Coherent State

$$|\alpha\rangle = \sum_{n=0}^{\infty} q_n^c |n\rangle, \qquad \alpha = \bar{n}^{\frac{1}{2}} e^{i\xi_c}$$

$$q_n^c = Q_n^c e^{in\xi_c}, \qquad Q_n^c = (e^{-\bar{n}} \frac{\bar{n}^n}{n!})^{\frac{1}{2}} \tag{15}$$

then we have

$$\rho_{nn'}^c(T) = Q_n^c Q_{n'}^c exp[-i(n-n')(T-\xi_c)] cos(n-n')T \tag{16}$$

We can find

$$D_1(N) = 4\bar{n}^N sin^2(NT) sin^2[N(T-\xi_c)]$$

$$D_2(N) = 4\bar{n}^N sin^2(NT) cos^2[N(T-\xi_c)] \tag{17}$$

We see that in a degenerate Raman process the field will not get Nth-power squeezing if it is initially in a coherent state.

4.2. For an Initial Squeezed Vacuum

$$|0_{sq}\rangle = \sum_{n=0}^{\infty} q_{2n} |2n\rangle, \qquad q_{2n} = Q_{2n} e^{in\xi}$$

$$Q_{2n} = (\frac{1}{\bar{n}+1})^{\frac{1}{4}} [-\frac{1}{2}(\frac{\bar{n}}{\bar{n}+1})^{\frac{1}{2}}]^n \frac{[(2n)!]^{\frac{1}{2}}}{n!} \tag{18}$$

where $\bar{n}$ is the mean photon number and ξ is the squeezing angle of the initial field. Then we have

$$\rho_{2n,2n'}(T) = Q_{2n} Q_{2n'} exp[-i(n-n')(2T-\xi)] cos(n-n')2T \tag{19}$$

We see that only even-photon-number states can be found in a squeezed vacuum. The photon-number distribution function is

$$P_{2n} = \rho_{2n,2n} = Q_{2n} Q_{2n} \tag{20}$$

For $N = odd = 2M-1 (M = 1, 2, 3, ...)$ we can find

$$C(1) = 1$$

$$D_1(1) = 2\{\bar{n} - [\bar{n}(\bar{n}+1)]^{\frac{1}{2}} cos(2T-\xi) cos(2T)\}$$

$$D_2(1) = 2\{\bar{n} + [\bar{n}(\bar{n}+1)]^{\frac{1}{2}} cos(2T-\xi) cos(2T)\} \tag{21}$$

$$C(3) = 3(9\bar{n}^2 + 9\bar{n} + 2)$$

$$D_1(3) = 6\{\bar{n}^2(5\bar{n}+3) - 5[\bar{n}(\bar{n}+1)]^{\frac{1}{2}} cos(6T-3\xi) cos(6T)\}$$

$$D_2(3) = 6\{\bar{n}^2(5\bar{n}+3) + 5[\bar{n}(\bar{n}+1)]^{\frac{1}{2}} cos(6T-3\xi) cos(6T)\} \tag{22}$$

We can show that $[D_2(2M-1)]_{\xi=\pi} = [D_1(2M-1)]_{\xi=0}$ can be smaller than zero, but $[D_1(2M-1)]_{\xi=\pi} = [D_2(2M-1)]_{\xi=0}$ can not be smaller than zero. This shows that we can have squeezing in $Z_1(2M-1)$ components for $\xi = 0$ and in $Z_2(2M-1)$ components for $\xi = \pi$, but we have not squeezing in $Z_1(2M-1)$ components for $\xi = \pi$ and in $Z_2(2M-1)$ components for $\xi = 0$.

For $N = even = 2M (M = 1, 2, 3, ...)$ we have

$$C(2) = 2(2\bar{n}+1)$$

$$D_1(2) = 2\bar{n}\{(3\bar{n}+1) + (\bar{n}+1)[3cos(4T-2\xi)cos(4T) - 2cos^2(2T-\xi)cos^2(2T)]\}$$
$$D_2(2) = 2\bar{n}\{(3\bar{n}+1) - (\bar{n}+1)[3cos(4T-2\xi)cos(4T) + 2sin^2(2T-\xi)cos^2(2T)]\} \quad (23)$$
$$C(4) = 24(10\bar{n}^3 + 15\bar{n}^2 + 7\bar{n} + 1)$$
$$D_1(4) = 6\bar{n}^2\{(35\bar{n}^2+30\bar{n}+3) + (\bar{n}+1)^2[35cos(8T-4\xi) - 6cos^2(4T-2\xi)cos^2(4T)]\}$$
$$D_2(4) = 6\bar{n}^2\{(35\bar{n}^2+30\bar{n}+3) - (\bar{n}+1)^2[35cos(8T-4\xi) + 6sin^2(4T-2\xi)cos^2(4T)]\} \quad (24)$$

We can show that $[D_2(2M)]_{\xi=\pi} = [D_2(2M)]_{\xi=0}$ can be smaller than zero, but $[D_1(2M)]_{\xi=\pi} = [D_1(2M)]_{\xi=0}$ can not be smaller than zero. This shows that we can have squeezing in $Z_2(2M)$ components for both $\xi = 0$ and $\xi = \pi$, but we can not get squeezing in $Z_1(2M)$ components for $\xi = 0$ and $\xi = \pi$.

We are also interested in the optimal squeezing.

$$[S(1)]_{min} = 2\{\bar{n} - [\bar{n}(\bar{n}+1)]^{\frac{1}{2}}\}$$
$$[S(2)]_{min} = -\frac{2\bar{n}}{2\bar{n}+1}$$
$$[S(3)]_{min} = \frac{2\{\bar{n}^2(5\bar{n}+3) - 5[\bar{n}(\bar{n}+1)]^{\frac{3}{2}}\}}{9\bar{n}(\bar{n}+1)+2}$$
$$[S(4)]_{min} = -\frac{2\bar{n}^2(5\bar{n}+4)}{10\bar{n}^3+15\bar{n}^2+7\bar{n}+1} \quad (25)$$

We see that $[S(N)]_{min} \to 0$ when $\bar{n} \ll 1$, and $[S(N)]_{min} \to -1$ (100% squeezing) when $\bar{n} \gg 1$.

To see the features of the field fluctuation more clearly, we have done numerical calculation and drawn some figures(Fig.2-10). From these figures we see the follows:

1. Generally, the field fluctuation oscillates periodically, and the oscillation frequency is proportional to N(Fig.2-9).

2. For a given $\bar{n}$, the oscillation amplitude decreases as N increase (Fig.2-5).

3. For a given N, the oscillation amplitude increases as $\bar{n}$ increases, but $[S(N)]_{min}$ changes smaller as $\bar{n}$ increases (Fig.6-9). $S_{min} \to -1$ when $\bar{n} \gg 1$(Fig.10).

5 Conclusion

In this paper we have studied ANPS of radiation fields in DRP by using MEHA. We found that if the field is initially in a coherent state it will not get squeezing in any Nth-power; if the field is initially in a squeezed vacuum, it may get Nth-power squeezing. The relations between the time evolution of the field fluctuation with N, $\bar{n}$, and ξ are discussed.

References

1. R.Loudon and P.L.Knight,J.Mod.Opt.,34,709(1987)
2. C.K.Hong and L.Mandel,Phys.Rev.Lett.,54,323(1985); Phys.Rev.,32,974(1985)
3. M.Hillery, Opt.Commun.,62,135(1987); Phy.Rev.A,36,3796(1987)
4. Z.M.Zhang et al.,Phy.Lett.A,150,27(1990)
5. S.D.Du and C.D.Gong,Phys.Lett.A,168,296(1992); Phys.Rev.A,48,2198(1993)
6. Y.Zhan,Phys.Rev.A,46,686(1992)
7. J.Sun et al.,Phys.Rev.A,46,1700(1992)
8. A.Q.Ma et al.,Chin.J.Lasers B,2,257(1993)
9. H.H.Jiang and L.S.He,Acta Physica Sinica,42,1223(1993)
10. X.L.Wu,Acta Physica Sinica.43,1433(1994)
11. J.Wang et al.,Acta Optica Sinica,14,819(1994)

12.T.Song et al.,Chin.J.Quant.Electr.,11,46(1994)
13.J.C.Retamal et al.,Phys.Rev.A,45,1876(1992)
14.S.Y.Zhu et al.,Z.Phys.D,22,483(1992)
15.P.L.Knight,Phys.Scr.T,12,51(1986)
16.S.D.J.Phoenix, and P.L.Knight,J.Opt.Soc.Am.B,7,116(1990)
17.L.Xu and Z.M.Zhang,Z.Phys.B,95,507(1994)

Figiure Captions

Fig.1 Schematic diagram of the degenerate Λ-type three-level atom interaction with a single-mode field. ω: frequency of field; δ: atom field detuning.
Fig.2 S_1 vs T. $\bar{n}$=0.1 a: N=1; b: N=3
Fig.3 S_1 vs T. $\bar{n}$=1.0 a: N=1; b: N=3
Fig.4 S_2 vs T. $\bar{n}$=0.1 a: N=2; b: N=4
Fig.5 S_2 vs T. $\bar{n}$=1.0 a: N=2; b: N=4
Fig.6 $S_1(1)$ vs T. a: $\bar{n}$=0.1; b: $\bar{n}$ = 1.0; c: $\bar{n}$ = 5.0
Fig.7 $S_2(2)$ vs T. a: $\bar{n}$=0.1; b: $\bar{n}$ = 1.0; c: $\bar{n}$ = 5.0
Fig.8 $S_1(3)$ vs T. a: $\bar{n}$=0.1; b: $\bar{n}$ = 1.0; c: $\bar{n}$ = 5.0
Fig.9 $S_2(4)$ vs T. a: $\bar{n}$=0.1; b: $\bar{n}$ = 1.0; c: $\bar{n}$ = 5.0
Fig.10 $[S(N)]_{min}$ vs $\bar{n}$. a,b,c,d correspond to N=1,2,3,4 espectively.

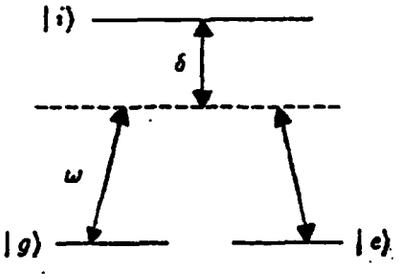

Fig.1

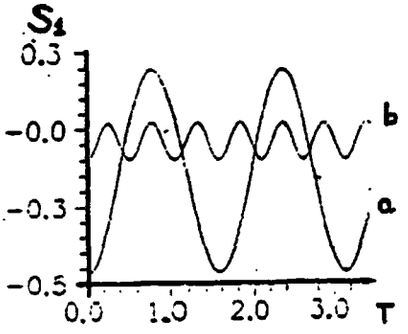

Fig.2

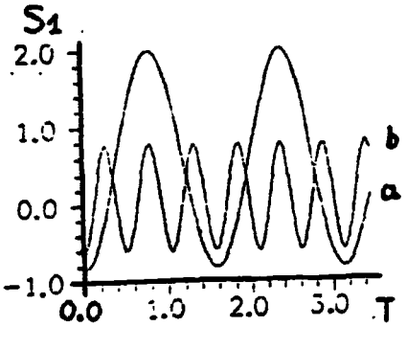

Fig.3

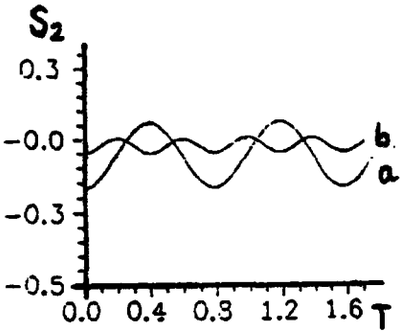

Fig.4

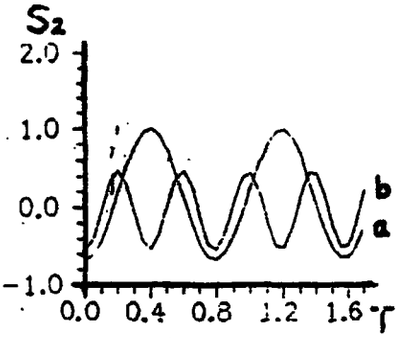

Fig.5

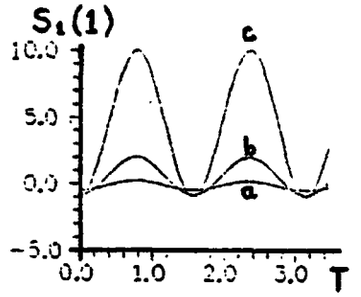

Fig.6

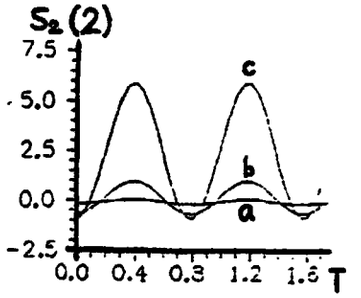

Fig.7

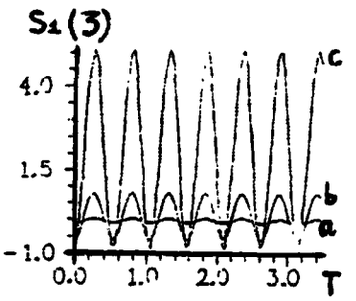

Fig.8

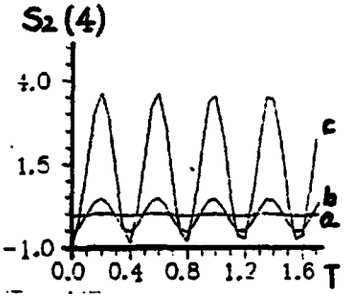

Fig.9

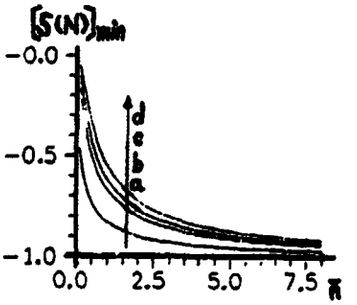

Fig.10

NEXT
DOCUMENT

ON THE THEORY OF HIGH-POWER ULTRASHORT PULSE PROPAGATION IN RAMAN-ACTIVE MEDIA

M. Belenov (deceased), V. A. Isakov, A. P. Kanavin, and I. V. Smetanin
P. N. Lebedev Physical Institute, Russian Academy of Sciences,
Leninskii Prosp. 53, Moscow 117924, Russia

Abstract

The propagation of an intense femtosecond pulse in a Raman-active medium is analyzed. An analytic solution which describes in explisit form the evolution of the light pulse is derived. The field of an intense light wave undergoes a substantial transformation as the wave propagates through the medium. The nature of this transformation can change over time scales comparable to the period of the optical oscillations. As a result, the pulse of sufficiently high energy divides into stretched and compressed domains where the field decreases and increases respectively.

1 Introduction

The physics of interaction of intense ultrashort light pulses with nonlinear media has attracted interest because of progress in subpicosecond-range laser technology and the attainment of laser-beam power levels of terrawatt range (see, for example, [1]). The light pulse dynamics and the medium evolution in an intense field differ qualitatively from the usual picture drawn by standard nonlinear-optics perturbation theory. A fundamental distinctive feature of ultrashort pulses is that their duration is shorter than the time scale of the response of the medium, so the interaction definitely occurs in a coherent regime. The standard approximation of a slowly varying amplitude and a slowly varying phase of the field becomes ineffective. A description of the interaction based on the actual (instantaneous) field values is appropriate [2].

The Raman-active media can be effectively excited by a single femtosecond pulse because its wide spectrum initially contains intense Stokes and anti-Stokes components of the field [3, 2]. The qualitatively new interaction regime, so-called self-scattering, occurs for light intensities much lower than the threshold ones for ordinary stimulated Raman scattering developing from spontaneous noise [4]. The estimations testify to the fact that the effective excitation of high vibrational levels and even the dissociation of molecules in the field of an ultrashort electromagnetic pulse can be observed using modern femtosecond lasers [5].

On the other hand, the shape and spectrum of femtosecond pulse should undergo a substantial transformation as it propagates through the Raman-active medium. The description of pulse evolution should take into account a substantial redistribution of the medium level populations during the pulse duration that results in different interaction regimes for different pulse fractions: either absorption due to Stokes scattering or amplification due to anti-Stokes component generation become predominant. The simplest model which is widely used in the theory of stimulated

Raman scattering and includes the effect of medium saturation is the model of two-level nonlinear oscillator. Within the framework of this model we succeeded to describe in explicit form the evolution of high-power femtosecond pulse in Raman-active medium.

2 Solution of Wave Equation

We shall describe the dynamics of a Raman-active medium in the field of an ultrashort pulse by a two-level model of a nonlinear oscillator [6]:

$$\frac{\partial^2 Q}{\partial t^2} + \frac{1}{T_2}\frac{\partial Q}{\partial t} + \Omega^2 Q = -\frac{1}{2M}\left(\frac{\partial \alpha}{\partial Q}\right) E^2 \rho, \quad \frac{\partial \rho}{\partial t} + \frac{\rho - \rho_0}{T_1} = \frac{1}{\hbar\Omega}\left(\frac{\partial \alpha}{\partial Q}\right) E^2 \frac{\partial Q}{\partial t}. \quad (1)$$

Here Q is a normal coordinate, M is the reduced mass, Ω is the eigenfrequency of the equivalent nonlinear oscillator (the Stokes shift), T_1 and T_2 are relaxation times, the coefficient $\partial\alpha/\partial Q$ is the derivative of the polarizability at the equilibrium value $Q = Q_0$, and ρ is the difference between the populations of the upper and lower levels (the value $\rho_0 = \rho(t = -\infty)$ corresponds to the state of the system before the beginning of the interaction with the field).

Equations (1) are to be solved jointly with the wave equation. In the case at hand, in which the interaction of the carrier pulse with only the scattered wave propagating in the same direction is taken into account, the wave equation can be written

$$\frac{\partial E}{\partial z} + \frac{1}{c}\frac{\partial E}{\partial t} = -\frac{4\pi}{c}\frac{\partial P}{\partial t} \quad (2)$$

with macroscopic nonlinear polarization of the medium $P = N\left(\frac{\partial \alpha}{\partial Q}\right) EQ$ induced by the field $E(z,t)$, where N is the density of the medium. We stress that the quantity $E = E(z,t)$ in (1) is the instantaneous value of the pulse field strength, not its envelope. The reduced form of the wave equation (2) is provided by the fact that the stimulated Raman backward scattering is very weak owing to the short interaction length of pulses moving in different directions [6].

We restrict the analysis to the case of the coherent interaction, in which the pulse duration does not exceed the time scales of the response and relaxation of the medium $\tau_p \ll \Omega^{-1}, T_1, T_2$.[1]

Material equations (1) can then be integrated for an arbitrary time dependence of the field $E(z,t)$ and the solution looks like rotation of material variables

$$\rho(z,t) = \rho_0 \cos\Psi(z,t), \quad \frac{\partial Q}{\partial t} = -\rho_0\left(\frac{\hbar\Omega}{2M}\right)^{-1/2} \operatorname{sign}\left(\frac{\partial \alpha}{\partial Q}\right) \sin\Psi(z,t). \quad (3)$$

The phase $\Psi(z,t)$ of the material variable rotation is directly proportional to the energy of the pulse fraction which has passed through the given space point z up to the given time t

$$\Psi(z,t) = \left|\frac{\partial \alpha}{\partial Q}\right| (2\hbar\Omega M)^{-1/2} \int_{-\infty}^{t} E^2(z,t')\,dt' \quad (4)$$

[1]Strictly speaking the coherent regime of interaction is provided by the condition $\Omega_0 = \frac{1}{2}\left|\frac{\partial \alpha}{\partial Q}\right|(2\hbar\Omega M)^{-1/2} E_0^2 \gg \Omega, T_1^{-1}, T_2^{-1}$, i.e., the analog of Rabi frequency of the two-level oscillator is the highest frequency of the problem. For high-energy femtosecond pulses this condition as well as inequality $\tau_p \ll \Omega^{-1}, T_1, T_2$ leads to the solution (3), (4).

From (3) it follows a strong nonlinear dependence of polarization on the pulse field and the wave equation of the form

$$\frac{\partial E}{\partial z} + \frac{1}{c}\frac{\partial E}{\partial t}\left[1 + \beta c \int_{-\infty}^{t} \sin \Psi(z,t')\,dt'\right] = -\beta E \sin \Psi, \tag{5}$$

where $\beta = \frac{\pi}{2} N \mid \partial\alpha/\partial Q \mid (\hbar\Omega/2Mc^2)^{1/2}$ is the inverse length of induced Raman self-scattering.

The nonlinear equation (5) allows an analytic solution describing in explicit form the evolution of the pulse shape and spectrum [7].

Multiplying (5) by E and integrating it with respect to time one can easely obtain the equation for phase $\Psi(z,t)$ (i.e., for current pulse energy)

$$\frac{\partial \Psi}{\partial z} + \frac{1}{c}\frac{\partial \Psi}{\partial t}\left[1 + \beta c \int_{-\infty}^{t} \sin \Psi(z,t')\,dt'\right] = \beta(\cos \Psi - 1). \tag{6}$$

Let us regard the pulse field $E(z,t)$ as a function of the spacial variable z and the phase $\Psi(z,t)$, i.e., $E(z,t) = \tilde{E}(z,\Psi)$. Taking into account that $\frac{\partial E}{\partial z} = \frac{\partial \tilde{E}}{\partial z} + \frac{\partial \tilde{E}}{\partial \Psi}\frac{\partial \Psi}{\partial z}$, $\frac{\partial E}{\partial t} = \frac{\partial \tilde{E}}{\partial \Psi}\frac{\partial \Psi}{\partial t}$, we can finaly rewrite Eq. (5) in the following form:

$$\frac{\partial \tilde{E}}{\partial z} + \beta(\cos \Psi - 1)\frac{\partial \tilde{E}}{\partial \Psi} = -\beta \tilde{E} \sin \Psi. \tag{7}$$

This partial differential equation can be easily solved by integrating along characteristics on which

$$\tan \frac{\Psi(z,t)}{2} = \frac{\tan \dfrac{\Psi_0(\eta)}{2}}{1 + \beta z \tan \dfrac{\Psi_0(\eta)}{2}}, \tag{8}$$

$$E(z,t) = \frac{E_0(\eta)}{1 + \beta z\left[\sin \Psi_0(\eta) + \dfrac{\beta z}{2}(1 - \cos \Psi_0(\eta))\right]}, \tag{9}$$

where $\Psi_0(\eta)$ is the given phase at the boundary of the medium (i.e., the energy of the pulse fraction which has entered the medium) which is connected with the field strength at the boundary by the relation $\Psi_0(\eta) = \left|\frac{\partial \alpha}{\partial Q}\right| (2\hbar\Omega M)^{-1/2} \int_{-\infty}^{\eta} E_0^2(\eta')\,d\eta'$. According to (8) the pulse fraction which energy corresponds to the phase $\Psi_0 = 2\pi n$, $n = 1, 2, \ldots$ moves through the Raman-active medium under conditions of self-indused transparency, when the energy of the leading part of 2π-pulse absorbed due to Stokes scattering completely returns to the trailing part of the pulse due to anti-Stokes scattering. In this case the spectrum of the leading part of the pulse becomes enriched by long-wavelength components of the field and the spectrum of the trailing part - by the short-wavelength components. This analysis generalizes the results found on the basis of numerical calculations [2].

The characteristics themselves are given implicitly by the expressions

$$\eta + \Phi(z,\eta) = t - z/c, \quad \Phi(z,\eta) = \beta z \int_{-\infty}^{\eta} d\eta' \left[\sin \Psi_0 + \frac{\beta z}{2}(1 - \cos \Psi_0)\right]. \tag{10}$$

where $\Phi(z,\eta)$ is the nonlinear delay of the individual parts of the pulse as it moves away from the boundary.

It is convenient to describe the evolution of the pulse shape by an effective frequency $\omega(z,t)$ of the pulse field oscillations. The value $\omega(z,t)$ characterizes the density of field oscillations for different parts of the pulse and its variation as the pulse propagates through the medium. It follows from (10) that if we fix a small fraction of the pulse its duration $\Delta\tau$ at the space point z is connected with that one $\Delta\tau_0$ at the boundary by the relation $\Delta\tau = \Delta\tau_0(1 + \partial\Phi/\partial\eta)$. The value $\Delta\tau$ determines the field oscillation period at the given space point z, hence the effective frequency of the field oscillations transforms in accordance with

$$\omega(z,t) = \frac{\omega_0(\eta)}{1 + \beta z\left[\sin\Psi_0 + \frac{\beta z}{2}(1 - \cos\Psi_0)\right]}. \tag{11}$$

3 Femtosecond Pulse Evolution in Raman-active Medium

It can be seen from Eqs. (9) and (11) that the changes in the field $E(z,t)$ and the characteristic frequency $\omega(z,t)$ over space occur identically. At the beginning of the pulse, when the phase of the two-level oscillator satisfies $\Psi_0 \ll 1$ (i.e., when the energy of the pulse fraction which has entered the medium is small), there are decreases in the field strength and the oscillation frequency: $E(z,t) = E_0(\eta)(1 + \beta z\Psi_0/2)^{-2}$, $\omega(z,t) = \omega_0(\eta)(1 + \beta z\Psi_0/2)^{-2}$. This case corresponds to Stocks scaterring. Later, when the phase becomes greater than π and reaches the value $\arctan(-2/\beta z)$, the field and its frequency increase. The generation of anti-Stokes components of the field thus becomes predominant. At $\Psi_0 = \pi$, the nature of the pulse transformation changes again. At a given point in space at different times, corresponding to different characteristics (10), we thus observe oscillations of regimes of compression and stretching of the field oscillation periods. The sequence of regimes of stretching and compression of the pulse with increasing value of the incident energy reverses when we switch from an originally absorbing medium to an originally inverted one.

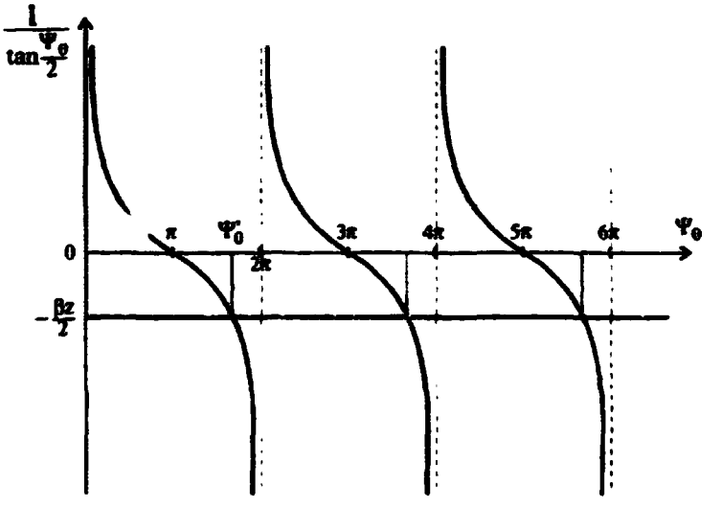

FIG. 1.

A descriptive way to analyze the pulse evolution is provided by Fig. 1. It is seen from (9) and (11) that the nature of pulse transformation is determined by the sign of the expression in brackets of the denominator $\sin\Psi_0 + \frac{\beta z}{2}(1-\cos\Psi_0) = 2\sin^2\frac{\Psi_0}{2}\left[\left(\tan\frac{\Psi_0}{2}\right)^{-1} + \frac{\beta z}{2}\right]$. If $\Psi_0 < \pi$, we have $\left(\tan\frac{\Psi_0}{2}\right)^{-1} > -\frac{\beta z}{2}$ for any distance z from the medium boundary. It means that the energy of such pulses can be only absorbed and the absorption is accompanied by the increase of the field oscillation periods for any pulse fraction (and as a result, by the increase of pulse duration) and by the shift of the pulse spectrum into the low-frequency region due to Stokes scattering.

If $\pi < \Psi_0 < 2\pi$, there are two different regimes of pulse transformation. The leading pulse fraction $0 < \Psi_0 < < \Psi_0' = \arctan(-2/\beta z)$ undergoes energy absorption and stretching of the field oscillation periods and its spectrum becomes enriched with low-frequency components of the field. The field in the trailing pulse fraction amplifies during the pulse propagation, the oscillation periods decrease (that results in the compression of this pulse fraction) and the spectrum is enriched with high-frequency components. For 2π-pulse all the energy concentrates in the trailing edge which is compressed as the pulse propagates through the medium. The same picture takes place for pulse fractions $2\pi n < \Psi_0 < 2\pi(n+1)$.

Figure 2 shows an example of pulse evolution described by the solution (8)-(11) for $\Psi_0 = 4\pi$. The input pulse represents a two-period fraction of a sine-shaped signal. Figure illustrates the time dependence of the pulse field at different distances from the medium boundary. Thus, the high-energy pulse is devided into the set of compressed powerfull 2π-subpulses the maximum field strength and inverse width of which at large distances increase $\sim(\beta z)^2$ according to (8)-(10).

Acknowledgments

This study had financial support from the International Science Foundation (Grant N9T000) and the Russian Basic Research Foundation (Project 93-02-14271).

References

[1] *CLEO/IQEC'94, Technical Digest* (Anaheim, CA, 1994).

[2] É. M. Belenov, A. V. Nazarkin, and I. P. Prokopovich, JETP Lett. **55**, 218 (1992); É. M. Belenov, P. G. Kryukov, A. V. Nazarkin, and I. P. Prokopovich, JETP **78**, 15 (1994).

[3] Y. X. Yan, E. B. Gamble, and K. A. Nelson, J. Chem. Phys. **83**, 5391 (1985).

[4] A. B. Grudinin, E. M. Dianov, D. V. Korobkin, et al., JETP Lett., **45**, 211 (1987).

[5] É. M. Belenov, V. A. Isakov, and A. V. Nazarkin, in: *Third International Workshop on Squeezed States and Uncertainty Relations*, D. Han, Y. S. Kim, N. H. Rubin, Y.Shih, and W. W. Zachary (eds.), NASA Conference Publication 3270 (1994), p. 515.

[6] Y. R. Shen. *The Principles of Nonlinear Optics*, (John Wiley & Sons, Inc., 1984).

[7] É. M. Belenov, V. A. Isakov, A. P. Kanavin, and I. V. Smetanin, JETP Lett. **60**, 770 (1994).

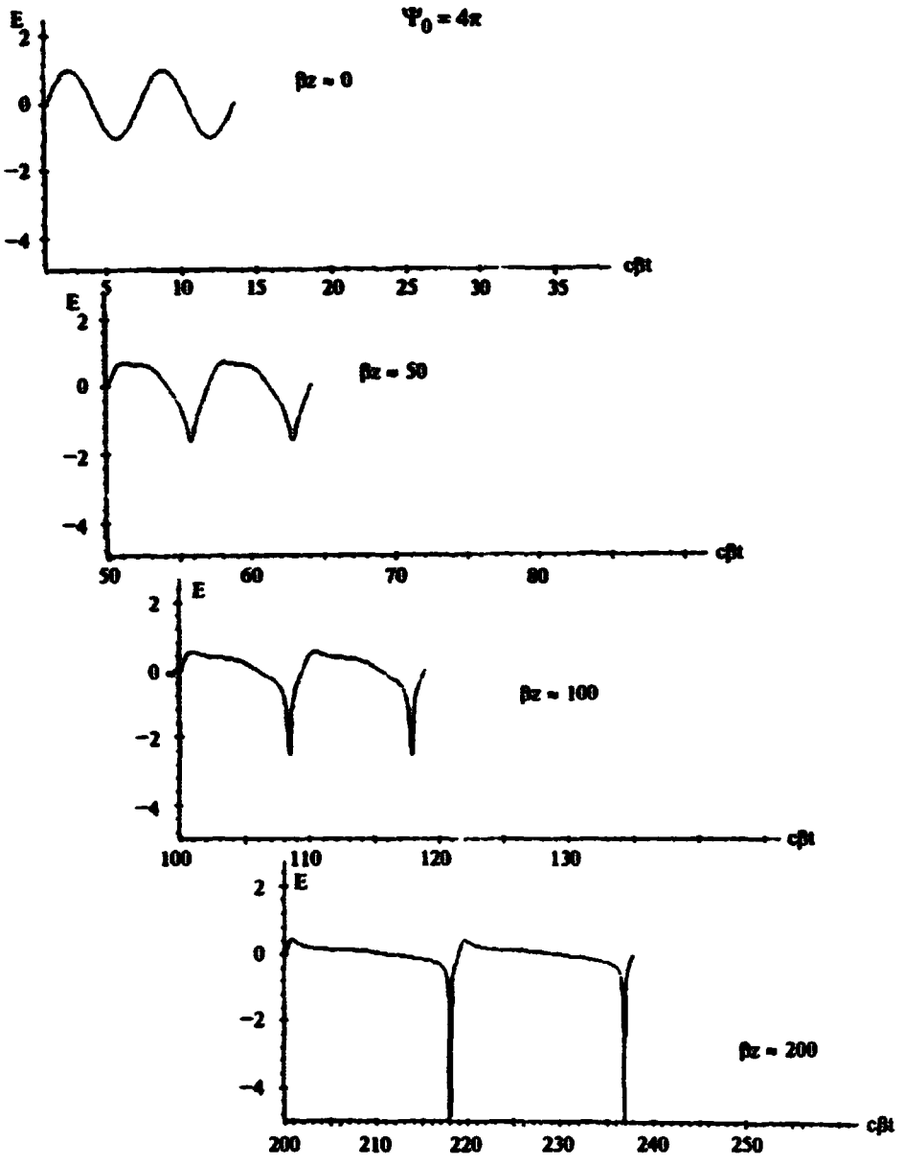

FIG. 2.

NEXT
DOCUMENT

Modification of Einstein A coefficient in dissipative gas medium

Cao Chang-qi
Department of Physics, Peking University, Beijing 100871

Cao Hui (H.Cao)
Edward L. Ginzton Laboratory, Stanford University,
Stanford,CA 94305,USA

Qin Ke-cheng
Department of Physics, Peking University, Beijing 100871.

Abstract

Spontaneous radiation in dissipative gas medium such as plasmas is investigated by Langevin equations and the modified Weisskopf-Wigner approximation. Since the refractive index of gas medium is expected to be nearly unity, we shall first neglect the medium polarization effect. We show that absorption in plasmas may in certain case modify the Einstein A coefficient significantly and cause a pit in the A coefficient-density curves for relatively low temperature plasmas and also a pit in the A coefficient-temperature curves.

In the next, the effect of medium polarization is taken into account in addition. To our surprise, its effect in certain case is quite significant. The dispersive curves show different behavious in different region of parameters.

1 Introduction

This work is motivated by an effect called by the original authors[1] as "quenching of Einstein A coefficient": the ratio of two line intensities I(5805$\AA$) and I(312$\AA$) from a common upper level of C_{IV} is reduced by an order of magnitude when the eletron density N_e changes from $10^{18}/cm^3$ to $10^{19}/cm^3$. But there is some dispute about the interpretation of their experiments. Our work is to see whether this effect is possible theoretically.

Physically, spontaneous emission is resulted from atom (ion) with "vacuum" electromagnetic field, therefore Einstrein A coefficient is a characteristic parameter of the total atom-field system, not just of atom itself. Its value may be different for different enviroment, such as cavity, or, in our case, the dissipative medium.

Our approach is based on Langevin equations[2]. We don't use Fermi golden rule to calculate the emission rate as did by Barnett et al[3], because the radiating ion and radiated field do not

make up a closed system, their states both before and after the emission process are not stationary states.

¿From Langevin equations an emission rate operator is defined, and a part of it, the spontaneous emission rate operator may be separated out.

Since the refractive index $n(\omega)$ of gas medium is expected to be nearly 1, we shall first, in Sec II, neglect the effect of medium polarization, which will be taken into consideration in Sec III.

2 The effect of medium absorption on Einstein A coefficient

Since in this section we take $n(\omega) = 1$, both the frequencies and wave functions of light modes are the same as in vacuum. The reduction of Einstein A coefficient is therefore not by the alteration of modes of e.m. field but is caused by alteration of dynamics: the relevant operators now do not obey the Heisenberg equations but obey Langevin equations instead. We shall see that the frequency dependence of photon decay parameter will play an importance role in the present case.

We have argued[4] that the three-level ion problem may be reduced to two-level ion problem, the only exception is the calculation of population numbers among the levels, in which all the levels involved must be taken into account.

In considering the emission of a particular ion, the whole plasmas other than the radiating ion will be regarded as a reservior, its effects are described by the damping and fluctuation terms in the Langevin equations:

$$\frac{d}{dt}\hat{a}_{\mathbf{k}j}(t) = -\kappa(\omega)\hat{a}^{\dagger}_{\mathbf{k}j}(t) + ig_{\mathbf{k}j}\hat{S}_{+}(t)e^{-i(\omega-\omega_0)t} + \hat{F}^{\dagger}_{\mathbf{k}j}(t), \tag{1.1}$$

$$\frac{d}{dt}\hat{S}_{+}(t) = -\frac{\Gamma}{2}\hat{S}_{+}(t) - 2i\sum_{\mathbf{k}j}\hat{S}_3(t)\hat{a}^{\dagger}_{\mathbf{k}j}(t)e^{-i(\omega-\omega_0)t} + \hat{\Sigma}_{+}(t), \tag{1.2}$$

$$\frac{d}{dt}\hat{S}_3(t) = -\Gamma_3[\hat{S}_3(t) - S_{30}] + \sum_{\mathbf{k}j}[ig^{*}_{\mathbf{k}j}\hat{a}^{\dagger}_{\mathbf{k}j}(t)\hat{S}_{-}(t)e^{-i(\omega-\omega_0)t} + h.c.] + \hat{\Sigma}_3(t). \tag{1.3}$$

where $\hat{S}_{\pm}$ are usual atom level-changing operators, $\hat{S}_3$ is the half of population difference operator: $\hat{S}_3 = \frac{1}{2}(\hat{P}_2 - \hat{P}_1)$, $\hat{a}_{\mathbf{k}j}$ is the photon absorption operator of mode $(\mathbf{k}, j)$, j is photon polarization index. The free-varying phase factors have been separated out from the photon operators and atom level-changing oprators.

We have defined[2] an emission rate operator $\hat{I}(t)$ as that part of $-\frac{d\hat{P}_2(t)}{dt}$ which is caused by the interaction with photons, with the result

$$\hat{I}(t) = \sum_{\mathbf{k}j} ig^{*}_{\mathbf{k}j}\hat{a}^{\dagger}_{\mathbf{k}j}(t)\hat{S}_{-}(t)e^{-i(\omega-\omega_0)t} + h.c.. \tag{2}$$

Solving eq.(1.1) to get $\hat{a}^{\dagger}_{\mathbf{k}j}(t)$ and substituting it into eq.(2), one may separate out the spontaneous emission rate operator $\hat{I}_{sp}(t)$ from $\hat{I}(t)$:

$$\hat{I}_{sp}(t) = \sum_{\mathbf{k}j}|g_{\mathbf{k}j}|^2\int_0^t \hat{S}_{+}(t')\hat{S}_{-}(t)e^{-i(\omega-\omega_0)(t-t')-\kappa(\omega)(t-t')}dt' + h.c. \tag{3}$$

The Weisskopf-Wigner approximation now takes the modified form[2]

$$\sum_{kj} |g_{kj}|^2 e^{-i(\omega-\omega_0)(t-t')-\kappa(\omega)(t-t')} = (\tilde{\gamma} + 2i\delta\tilde{\omega})\delta(t-t'), \ for\ t-t' \geq 0. \tag{4}$$

Substituting it into eq.(3), we get immediataly

$$\hat{I}_{sp} = \tilde{\gamma}\hat{S}_+(t)\hat{S}_-(t) = \tilde{\gamma}\hat{P}_2(t). \tag{5}$$

Eq.(5), after taking the expecting value, is just the Einstein formula for spontaneous emission with $\tilde{\gamma}$ as the new A coefficient.

Taking real part of eq.(4) and integrating it over t' from $-\infty$ to t, we get[2]

$$\tilde{\gamma}/\gamma = \frac{1}{\pi\omega_0}\int_{\omega_p}^{\omega_{max}} \frac{\omega\kappa(\omega)}{(\omega-\omega_0)^2+\kappa^2(\omega)}d\omega \tag{6}$$

where γ is the usual Einstein A coefficient in vacuum, ω_p is the plasma frequency and ω_{max} denotes a cut-off frequency representing the limit of dipole approximation.

We see that $\tilde{\gamma}/\gamma$ is determined solely by photon decay parameter $\kappa(\omega)$, with no direct reference to atomic parameter. This is contrary to the conjectur of Aumayr et al[5].

When κ is small and independent of ω, the right hand side of eq.(6) will reduce to 1.

Actually, in plasmas, κ is contributed by the inverse Bremstrahlung of free electrons and selfabsorption of ions of the same kind as the radiator. Both are ω dependent, but only the latter is important unless at very high plasma electron density ($\sim 10^{21}/cm^3$). So we shall only consider the latter, which will be denoted by $\kappa_I(\omega)$, in the following.

$\kappa_I(\omega)$ is expressed by

$$\kappa_I(\omega) = \frac{\pi c^3 N_I \gamma(P_1-P_2)}{4\omega_0^2}\frac{\Gamma_T}{(\omega-\omega_0)^2+\frac{1}{4}\Gamma_T^2} \tag{7}$$

where N_I represents the ion density, Γ_T is the total width of the spectral line, P_1 and P_2 are the average populations of the lower and upper levels. We have approximated the line profile by a Lorentzian shape in eq.(7), actually the profile is convolution of a homogeneous broadening (Stark broadening) and an inhomogeneous broadening (Doppler broadening).

The frequency behavior of $\kappa_I(\omega)$ is characterized by a peak at $\omega = \omega_0$. It is this behavior which may cause significant reduction of $\tilde{\gamma}/\gamma$.

To explain this, we simulate the variation of κ_I with ω by a simple stepwise function

$$\kappa_I(\omega) = \begin{cases} \kappa_0 & \omega_0 < \omega_c \\ \kappa_0' & \omega > \omega_c \end{cases} \tag{8}$$

with $\kappa_0 > \kappa_0'$.

If in the whole range $\kappa_I(\omega)$ either equals κ_0 or equals κ_0', the integral in the eq.(6) will amount to $\pi\omega_0$. The curve $\frac{\kappa_0'}{(\omega-\omega_0)^2+\kappa_0'^2}$ has a larger height but a smaller width as compared with that of $\frac{\kappa_0}{(\omega-\omega_0)^2+\kappa_0^2}$, so both gives the same integral value when substituted in eq.(6). But the situation of stepwise function eq.(8) is different, comparing it with the above mentioned constant cases, it is not difficult to understand why the stepwise function will reduce the integral value.

One may use $\kappa(\omega_0) \simeq \kappa_I(\omega_0)$ to scale the integration interval of important contribution in eq.(6). If $\kappa_I(\omega)$ drops down rapidly in this region, then the reduction will be large. Since $\Gamma_T/2$ scales the interval of significant variation of $\kappa_I(\omega)$, it follows that tha ratio of these two scales $\Gamma_T/2\kappa_I(\omega_0)$ determines the amount of reduction of $\tilde{\gamma}/\gamma$. The smaller the value of $\Gamma_T/2\kappa_I(\omega_0)$, the heavier will be the reduction.

In this way, we see that the atomic parameters do affect the value of Einstein A coefficient, but in an indirect way.

The numerical results are as follows. For line $\lambda = 5805\mathring{A}$, $\tilde{\gamma}/\gamma$ is almost kept to be nearly 1 in the whole range from $N_e = 10^{15}/cm^3$ to $N_e = 10^{20}/cm^3$, because $\Gamma_T/2\kappa_I(\omega_0)$ is large, since the factor $P_1 - P_2$ in eq.(7) is very small in this case. The result for line $\lambda = 312\mathring{A}$ is shown in Fig 1. In low density region, Γ_T is mainly contributed by Dopper broadening so that it is independent of N_e, and this in turn makes $\kappa_I(\omega_0)$ proportional to N_e. Therefore when N_e increases, $\Gamma_T/2\kappa_I(\omega_0)$ becomes smaller, leading to the drop of $\tilde{\gamma}/\gamma$. But when N_e goes beyond a value about $1.5 \times 10^{18}/cm^3$, $\tilde{\gamma}/\gamma$ turns up, because Γ_T is gradually dominated by Stark broadening, so that it is proportional to N_e, which in turn leads to N_e-independence of $\kappa_I(\omega_0)$. As the result, there is a pit or hollow in the curve $\tilde{\gamma}/\gamma$–N_e.

The dependence of $\tilde{\gamma}/\gamma$ on temperature is also interesting. By a similar analysis, we have argued[4] that there will be also a pit or hollow in the curve $\tilde{\gamma}/\gamma$–T.

3 Einstein A coefficient with index of refraction taken into account

We begin our discussion by deriving the plasmas' refractive index from microscopic equations. First we omit the contribution of free electrons which is less important.

There are numerous ions in the plasmas, the effective coupling constant for ion l and e.m. field has a position-dependent factor $e^{i\mathbf{k}\cdot\mathbf{x}^{(l)}}$.

In gas, the orientation of atomic dipole $\langle \mathrm{d} \rangle_{21}$ is random, yielding $|g_{kj}|^2$ independent of j,

$$|g_{kj}|^2 = G_k^2, \quad G_k^2 = \frac{\pi c^3 \gamma}{2\omega_0^3 V}, \tag{9}$$

where

$$\omega_k = kc.$$

We define a collective atomic operator as usual

$$\hat{S}_{+,kj}(t) = \sum_l e^{i\mathbf{k}\cdot\mathbf{x}^{(l)}} \hat{s}_+^{(l)}(t), \tag{10}$$

the equation for $\hat{a}_{kj}^\dagger(t)$ will be of the form

$$\frac{d}{dt}\hat{a}_{kj}^\dagger(t) = i\omega_k \hat{a}_{kj}^\dagger(t) + iG_k \hat{S}_{+,kj}(t). \tag{11}$$

In the case of steady-state plasmas, we may approximate the $\hat{S}_3^{(l)}$ in the equation of $\hat{S}_{+,kj}$ by its average value $\frac{1}{2}(P_2 - P_1)$ plus a fluctuation term. This leads to

$$\frac{d}{dt}\hat{S}_{+,kj}(t) = (i\omega_0 - \frac{1}{2}\Gamma)\hat{S}_{+,kj}(t) + iG_k N_l V (P_1 - P_2)\hat{a}_{kj}^\dagger(t) + \textit{ fluctuation term.} \tag{12}$$

We see from eqs.(11) and (12) that $\hat{a}^{\dagger}_{kj}$ and $\hat{S}_{+,kj}$ turn into each other.

To derive the expression for index of refraction n, we may assume, as usually does in classical electrodynamics, that $\hat{S}_{+,kj}$ will do forced vibration following $\hat{a}^{\dagger}_{kj}$ except a fluctuation term[8]. By this, we get an expression for $\hat{S}_{+,kj}$ from eq.(12). Substituting it into eq.(11), yields

$$\frac{d}{dt}\hat{a}^{\dagger}_{kj} \cong i\left[\omega_k + \frac{\pi c^3 \gamma N_I (P_1 - P_2)}{2\omega_0^2(\omega - \omega_0 - \frac{1}{2}i\Gamma)}\right]\hat{a}^{\dagger}_{kj} + \hat{F}^{\dagger}_{kj}(t) \tag{13}$$

where ω denotes the actual frequency of $\hat{a}^{\dagger}_{kj}$.

According to the definition, the real part of what inside the square brackets is just equal to ω. Thus we get an equation for ω:

$$\omega = \omega_k + \frac{\pi c^3 \gamma}{2\omega_0^2}\frac{N_I(P_1 - P_2)}{(\omega - \omega_0)^2 + \frac{1}{4}\Gamma^2}(\omega - \omega_0). \tag{14}$$

The expression of index of refraction follows immediately,

$$n \equiv \frac{\omega}{\omega_k} \cong 1 + \frac{\pi c^3 \gamma}{2\omega_0^3}\frac{N_I(P_1 - P_2)}{(\omega - \omega_0)^2 + \frac{1}{4}\Gamma^2}(\omega - \omega_0). \tag{15}$$

The imaginary part of what inside the square bracket will be $\kappa_I(\omega)$. The expression so obtained for $\kappa_I(\omega)$ is the same as eq.(7), except Γ_T is replaced by Γ. The difference lies in that Γ_T in eq.(7) already contains the contribution of Doppler broadening.

We may generalize the above result by including the contribution of plasma free eletrons. Besides, since in the present case the wave number k is real , the operator $\hat{a}^{\dagger}_{kj}$ decays with time, $\hat{S}_{+,kj}$ must also do damped vibration accordingly. This means that ω in eq.(14) must be analytically contiued to complex value which will be denoted by Ω:

$$\Omega = \omega_k + \frac{\pi c^3 \gamma}{2\omega_0^2}\frac{N_I(P_1 - P_2)}{(\Omega - \omega_0 - \frac{1}{2}i\Gamma_T)} + \frac{\omega_p^2}{2(\Omega - if)} \tag{16}$$

in which Γ is also replaced by Γ_T as in eq.(7).

This is a third order equation for Ω, it allows us to derive $\Omega \equiv \omega + i\kappa$ for every given real value of $\omega_k(\omega_k = kc)$. We will choose the root whose real part is nearest to ω_k for photon. In the case of $\lambda = 5805\mathring{A}$, no problem appears. The so obtained curve ω–ω_k is like the usual dispersion curve of gas. In this case the affection of medium polarization on $\tilde{\gamma}$ is indeed very small.

In the case of $\lambda = 312\mathring{A}$, the situation is different. For certain range of N_e, the dispersion curve for photon and for collective atomic dipole ($\hat{S}_{+,kj}$) are totally mixed in the resonance region. This means the quantum of the polarization field has coupled to photon to form polaritons as in solids[6,7]. In this case, the affection of medium polarization is significant.

The occurence of such situation depends on the relative strength of coupling and damping. To show explicitly, let us examine the simpler case without contribution of free electrons. Now Ω satisfies a second order equation. The two roots at $\omega_k = \omega_0$ are

$$\Omega = \omega_0 + \frac{i}{4}\Gamma_T \pm \sqrt{\alpha - \frac{1}{16}\Gamma_T^2}, \tag{17}$$

where

$$\alpha = \frac{\pi c^3 \gamma}{2\omega_0^2} N_I (P_1 - P_2), \tag{18}$$

just the product of the two couple constants between $\hat{a}^{\dagger}_{kj}$ and $\hat{S}_{+,kj}$ in eqs.(11) and (12).

When $\alpha < \frac{1}{16}\Gamma_T^2$ (weak coupling), the real part of the two roots given by eq.(17) equal each other, corresponding to the usual case as $\lambda = 5805\mathring{A}$. On the other hand when $\alpha > \frac{1}{16}\Gamma_T^2$ (strong coupling), the real parts of the two roots are different, corresponding to the situation of polariton formation. It is interesting to note that

$$\frac{\Gamma_T^2}{2\alpha} = \frac{\Gamma_T}{\kappa_I(\omega_0)},$$

therefore the two conditions $\frac{\Gamma_T}{2\kappa_I(\omega_0)} \ll 1$ and $\alpha \gg \frac{1}{16}\Gamma_T^2$ almost correspond to each other. Namely the region of polariton formation will cover the region of the pit discussed in last section.

This work is a part of project supported by National Natural Science Foundation of China.

References

1. Y. Chung, P. Lemaire and S. Suckewer, Phy. Rev. Lett. **60** 1122 (1988),
   Y. Chung, H. Hirose and S. Suckewer, Phy. Rev. A **40** 7142 (1989).

2. Cao Chang-qi and Cao Hui (H. Cao), SPIE **1726**, 124 (1992),
   J. Phys. B, **26**, 3959 (1993).

3. S. M. Barnett, H. Huttner and R. Loudon, Phys. Rev. Lett. **68**, 3698 (1992).

4. H. Cao (Cao Hui) and Cao Chang-qi, J. Phys. B, **28**, 979 (1995).

5. F. Aumayr, J. Hung and S. Suckewer, Phy. Rev. Lett. **63**, 1215 (1989).

6. J. J. Hopfield, Phys. Rev. **112**, 1555 (1958).

7. B. Huttner, J. J. Baumberg and S. M. Barnett, Europhys. Lett. **16**, 1991 (1991).

8. M. Sargent III, M.O.Scully and W.E. Lamb, Jr. *Laser Physics*,
   Addision-Wesley, Reading, MA.1974. Ch.20.

Figure Caption

1. Dependence of $\tilde{\gamma}/\gamma$ on x for line $312\mathring{A}$ of ion C_{IV}. $x = N_e/10^{19}cm^{-3}$, $T = 5ev$.

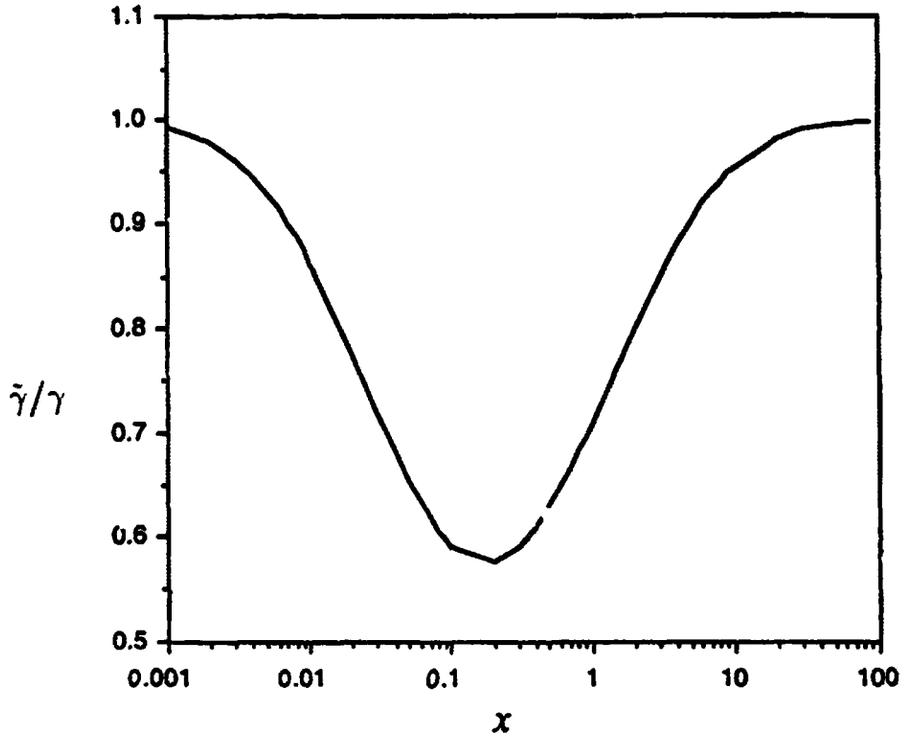

Fig. 1

NEXT
DOCUMENT

Multilevel atomic coherent states and atomic holomorphic representation

Cao Chang–qi
Department of Physics, Peking University, Beijing 100871, China.
Fritz Haake
Fachbereich Physik, Universität-GH Essen,45117 Essen, Germany.

October 4, 1995

Abstract

The notion of atomic coherent states is extended to the case of multilevel atom collective. Based on atomic coherent states, a holomorphic representation for atom collective states and operators is defined. An example is given to illustrate its application.

1 Introduction

Atomic coherent states have been introduced in quantum optics for more than twenty years[1–3]. They are the analogue of boson coherent states and exhibit approximate classical behavior when the mean atom numbers on the relevant levels are large. But until now such states are only available for collective of two-level atoms. We have extended this formulation to multilevel case[4]. Since many optical processes involve atoms of three or more levels, it is expected that this extension will play a role in the theory of such processes as cascade superfluorescence and superradiant lasing. In addition, like the photonic counterparts[5], the atomic coherent states may also be used to define a holomorphic representation. In some cases, it is convenient to use this representation to treat the collective interaction of atoms with the light field.

We shall give a brief introduction of our work in the following.

2 Multilevel atomic coherent states

For concreteness let us consider the fully symmetrical states of N three-level atoms. In Fock representation, such states are denoted by $|n_3, n_2, n_1\rangle$, where n_3, n_2, n_1 are numbers of atoms in the upper, middle and lower level respectively. The observables of l-th atom may be expressed by the generators $\hat{s}_{jk}^{(l)}$ of the group $SU(3)$, where $\hat{s}_{jk}$ are level-change operators for $j \neq k$, and are population operators for $j = k$. The collective atomic operators $\hat{S}_{jk}$ is defined as

$$\hat{S}_{jk} = \sum_{l=1}^{N} \hat{s}_{jk}^{(l)} \tag{1}$$

Each atomic coherent state in this subspace is characterized by two complex parameters α and β:

$$|\alpha,\beta\rangle = \frac{1}{[1+|\alpha|^2(1+|\beta|^2)]^{N/2}} e^{\beta\hat{S}_{12}} e^{\alpha\hat{S}_{23}} |N,0,0\rangle. \tag{2}$$

We might as well define atomic coherent state by $e^{\alpha\hat{S}_{21}}$ and subsequently by $e^{\alpha\hat{S}_{32}}$ operating on $|0,0,N\rangle$. This latter definition is somewhat more close to that of photon coherent state.

The meaning of parameters α and β can be seen from the expectation values of $\langle n_1\rangle$, $\langle n_2\rangle$, $\langle n_3\rangle$ and $\langle S_{jk}\rangle$ for $j \neq k$:

$$\langle n_3\rangle : \langle n_2\rangle : \langle n_1\rangle = 1 : |\alpha|^2 : |\alpha\beta|^2, \tag{3}$$

and the phase of α and β are just those of $\langle S_{32}\rangle$ and $\langle S_{21}\rangle$ respectively.

If both $|\alpha|$ and $|\beta|$ are of order 1, namely all $\langle n_3\rangle$, $\langle n_2\rangle$ and $\langle n_1\rangle$ are of order N. then all $\frac{\delta n_j}{\langle n_j\rangle}$ and $\frac{\sqrt{\langle \hat{S}_{ij}\hat{S}_{ji}\rangle - |\langle \hat{S}_{ij}\rangle|^2}}{|\langle \hat{S}_{ij}\rangle|}$ are of order $\frac{1}{\sqrt{N}}$. This results confirm that atomic coherent states tend to display classical behavior when $\langle n_j\rangle$'s grow large.

The states with different α, β are not orthogonal to each other. But they form an overcomplete set in the discussed subspace. We have found the weight function

$$\xi(|\alpha|,|\beta|) = \frac{(N+1)(N+2)}{\pi^2} \frac{|\alpha|^2}{[1+|\alpha|^2(1+|\beta|^2)]}, \tag{4}$$

such that

$$\int d^2\alpha d^2\beta\, \xi(|\alpha|,|\beta|) |\alpha,\beta\rangle\langle\alpha\beta| = 1. \tag{5}$$

The above dicussion can be extended to other subspaces. It is also easy to be extended to atoms with more levels[4].

3 Atomic holomorphic representation

Like bosonic case, one can define an atomic holomorphic representation based on atomic coherent states. We shall illustrate this interesting concept in the simplest case, a collective of two level atoms, and consider the fully symmetrical subspace.

A holomorphic representation employs a holomorphic function $f(\alpha^*)$ which is analytic in the whole α^* plane to represent every state in the discussed subspace.

Actually, $f(\alpha^*)$ is a polynomial of order N, a rather well behaved function. Accordingly, each atomic operator will be represented by a holomorphic function of two complex variables α^* and β. We shall do some explanation in the following.

The completness of the two-level atomic coherent states in the discussed subspace is expressed by

$$1 = \frac{N+1}{\pi} \int \frac{d^2\alpha}{(1+|\alpha|^2)^2} |\alpha\rangle\langle\alpha|. \tag{6}$$

By this, we get

$$\begin{aligned} |f\rangle &= \frac{N+1}{\pi} \int \frac{d^2\alpha}{(1+|\alpha|^2)^2} |\alpha\rangle\langle\alpha|f\rangle \\ &= \frac{N+1}{\pi} \int \frac{d^2\alpha}{(1+|\alpha|^2)^{N/2+2}} f(\alpha^*)|\alpha\rangle, \end{aligned} \tag{7}$$

in which

$$f(\alpha^*) = (1+|\alpha|^2)^{N/2}\langle\alpha|f\rangle = (1+|\alpha|^2)^{N/2}\sum_{n=0}^{N}\langle\alpha|N-n,n\rangle\langle N-n,n|f\rangle, \tag{8}$$

where $|N-n,n\rangle$ denotes the Fock state in the fully symmetric subspace.

Invoking the well known value of $\langle\alpha|N-n,n\rangle$, we get

$$f(\alpha^*) = \sum_{n=0}^{N} f_n(\alpha^*)^n \tag{9}$$

with

$$f_n = \binom{N}{n}^{\frac{1}{2}}\langle N-n,n|f\rangle. \tag{10}$$

Similarly, we can expand any atomic operator $\hat{T}$ by $|\alpha\rangle\langle\beta|$ as

$$\hat{T} = \frac{N+1}{\pi}\int\frac{d^2\alpha}{(1+|\alpha|^2)^{N/2+2}}\frac{d^2\beta}{(1+|\beta|^2)^{N/2+2}}T(\alpha^*,\beta)|\alpha\rangle\langle\beta|, \tag{11.1}$$

$$T(\alpha^*,\beta) = \sum_{m,n=1}^{N} T_{mn}(\alpha^*)^m\beta^n \tag{11.2}$$

where

$$T_{mn} = \langle N-m|\hat{T}|N-n,n\rangle\binom{N}{m}^{\frac{1}{2}}\binom{N}{n}^{\frac{1}{2}}. \tag{12}$$

The operation of $\hat{T}$ on a state $|f\rangle$ is described as follows. Let

$$|g\rangle = \hat{T}|f\rangle$$

then the holomorphic representation $g(\alpha^*)$ is given by

$$g(\alpha^*) = \frac{N+1}{\pi}\int\frac{d^2\beta}{(1+|\beta|^2)^{N+2}}T(\alpha^*,\beta)f(\beta^*). \tag{13}$$

Futhermore we have shown[4] that in holomorphic representation the collective atomic operators $\hat{S}_+$, $\hat{S}_-$, $\hat{S}_3$ may be also represented by differential operators as $\frac{\partial}{\partial\alpha^*}$, $(N\alpha^* - \alpha^{*2}\frac{\partial}{\partial\alpha^*})$, $(\frac{N}{2} - \alpha^*\frac{\partial}{\partial\alpha^*})$ when operating from left, and as $(N\beta - \beta^2\frac{\partial}{\partial\beta})$, $\frac{\partial}{\partial\beta}$, $(\frac{N}{2} - \beta\frac{\partial}{\partial\beta})$ when operating from right.

To our knowledge, there is only one problem which have been solved analytically for arbitrary value of N, namely a collective of two-level atoms in an external field[6],[7]. This problem can be solved in a comparatively easier way by our formulation. Let us see the simpler case of no detuning.

The atomic density operator $\hat{\rho}$ now obeys the master equation.

$$\frac{\partial\hat{\rho}}{\partial t} = -i\Omega[\hat{S}_+ + \hat{S}_-,\rho] + \gamma[2\hat{S}_-\hat{\rho}\hat{S}_+ - \rho\hat{S}_+\hat{S}_- - \hat{S}_+\hat{S}_-\hat{\rho}]. \tag{14}$$

In our holomorphic representation, this equation may be taken as

$$\frac{\partial\rho(\alpha^*,\beta,t)}{\partial t} = (N\alpha^* - \alpha^{*2}\frac{\partial}{\partial\alpha^*} - \frac{\partial}{\partial\beta})[-i\Omega + \gamma(N\beta - \beta^2\frac{\partial}{\partial\beta})]\rho(\alpha^*,\beta,t) + (c.c.\ with\ \alpha \leftrightarrow \beta). \tag{15}$$

For the steady-state solution, we expand $\rho(\alpha^*,\beta)$ according to eq.(11.2):

$$\rho(\alpha^*,\beta) = \sum_{m,n=0}^{N} \rho_{mn}(\alpha^*)^m\beta^n. \tag{16}$$

Substituting this expansion into eq.(15) and setting the right-hand side be zero, we obtain a recurtion relation for ρ_{mn}, which can be solved analytically to give

$$\rho_{mn} = \frac{(N!)^2 i^{m-n}}{(N-n)!(N-m)!(\Omega/\gamma)^{m+n}}\rho_{00}. \tag{17}$$

The value of ρ_{00} is determined by normalization.

The density operator $\hat{\rho}$ is then given by

$$\hat{\rho} = \sum_{m,n}\rho_{mn}\left(\begin{array}{c}N\\m\end{array}\right)^{-\frac{1}{2}}\left(\begin{array}{c}N\\n\end{array}\right)^{-\frac{1}{2}}|m\rangle\langle n|. \tag{18}$$

The extension of holomorphic representation to three or more level atoms is obvious.

This work of one of us (C. C-q) is supported by the Chinese Doctoral Program Foundation of the Institution of Higher Education.

References

1. F.T.Arecchi, E.Courtens, R.Gilmore and H. Thomas, Phy.Rev A **6**, 2211(1972).
2. L.M.Narducci, C.A. Coulter and C.M. Bowden, Phy.Rev. A **8**, 829(1974).
3. R.Glauber and F.Haake, Phy.Rev. A **13**, 357(1976).
4. Cao Chang-qi and F.Haake, Phy.Rev. A **51**, 4203(1995).
5. R.J.Glauber,Phys.Rev. **131**, 2766(1963).
6. R. R. Puri and S.V.Lawande,Phys.Lett. **72**, 200(1979).
7. R. R. Puri, S.V.Lawande and S.S.Hassan, Opt.Comm. **35**, 179(1980).

NEXT
DOCUMENT

GENERATION OF ANTIBUNCHED LIGHT BY EXCITED MOLECULES IN A MICROCAVITY TRAP

F. De Martini, G. Di Giuseppe and M. Marrocco (*)
Dipartimento di Fisica and Istituto Nazionale di Fisica Nucleare
Universita' di Roma "La Sapienza", 00185 Italy

Abstract

The active microcavity is adopted as an efficient source of non-classical light. By this device, excited by a mode-locked laser at a rate of 100 MHz, single-photons are generated over a *single* field mode with a nonclassical sub-poissonian distribution. The process of adiabatic recycling within a multi-step Franck-Condon molecular optical-pumping mechanism, characterized in our case by a quantum efficiency very close to one, implies a pump self-regularization process leading to a striking n-squeezing effect. By a replication of the basic single-atom excitation process a beam of quantum photon $|n\rangle$-states (Fock states) can be created. The new process represents a significant advance in the modern fields of basic quantum-mechanical investigation, quantum communication and quantum cryptography

1 Introduction

The generation of non-classical light is an important topic of modern physics since it provides the basic tools for the investigation of fundamental processes involving the quantum interferometry of particles. Furthermore, on a more technological perspective, the realization of a reliable source of this kind of radiation is today considered to be an essential feature of any realistic advanced program involving quantum cryptographic communication and, possibly in the future, quantum computation [1,2]. For this purpose the method of pump self-regularization has been adopted in the past within a few dynamical processes to provide the sub-poissonian character of the generated light [3]. These essentially are: the electron-charge induced antibunching process acting within the excitation of a semiconductor laser [4] and the Rabi dynamics in resonant-fluorescence with excitation of single atoms in a beam, in a trap or in a solid host [5,6,7]. The use of the latter process is very difficult in practice because of the delicate high-resolution spectroscopic techniques needed for the *resonant* excitation of confined single atoms in space, of the hard problem of discriminating a very weak beam in the presence of a strong one at the *same* wavelength and, most important, of the inefficiency of the process since the weak resonant scattering occurs in *all* spatial directions. In this letter we demonstrate that these problems can indeed be overcome by a novel, efficient single-molecule

pump self-regularization scheme and by making use of a smart combination of optical techniques partially based on the peculiar properties of the microcavity in the context of atomic spontaneous emission (SpE) [8]. The result is a new, efficient generator of a non-classical single-photon state that can be transformed into a quantum Fock $|n>$-state generator.

2 Experimental setup

Let us outline our method by referring to the single-molecule condition. A single Oxazine 720 molecule absorbing and emitting radiation at $\lambda_p = 2\pi c/\omega_p$ and $\lambda = 2\pi c/\omega$ respectively, was excited within a single longitudinal-mode microcavity, with relevant dimension $d = m\lambda/2$, $m=1$, finesse $f=1600$, and terminated by two parallel, plane Bragg-reflectors (or mirrors, $i=1,2$) highly reflecting at λ ($R_i \equiv |r_i|^2 \approx 1$) and transparent at $\lambda_p < \lambda$. Because of this last property, the excitation of the molecule could indeed be localized within a small volume $V = d \cdot s_p$ about equal to λ^3 at the intersection of the cavity active layer with the focal region of a 3 cm f-l lens collecting the excitation from a pulsed laser beam operating at λ_p. In the best configuration the device was excited by a collision-pulse-mode-locked (CPM) laser emitting at $\lambda_p = 615$ nm a sequence of equal pulses, referred to as "δt-pulses", with duration $\delta t = 0.1$ps, energy $\epsilon = 0.12$ nJ, rate $\nu = (1/\Delta t) = 100$ Mhz. The experiment was also carried out, successfully but with far more critical requirements for the parameters δt, ϵ, at $\lambda_p = 532$ nm, with a $\delta t = 5$ nsec, $\nu = 20$ Hz, pulsed beam SHG by a Nd-Yag Q-switched laser. The selected active system was a molecular solution in ethilene-glycol, a very viscous solvent at T=300°K , with concentration in the range $\rho = 10^{12} \div 10^{18}$ cm^{-3}, absorption cross-section $\sigma_p(\lambda_p) = 2.10^{16}$ cm^2 and free-space SpE time $(T_1)_0 \equiv 1/\Gamma_0 \approx 4$ nsec at the emission $\lambda = 702$ nm at which the microcavity is tuned. Furthermore, very important,the selected molecule had a singlet four-level optical pumping quantum efficiency η very close to one [9]. With a calibrated ρ and well stirred and highly filtered solution, to avoid any molecular clustering, the search for the single-molecule excitation condition was accomplished by transversal displacements of the lens focus in the microcavity active plane. Once found, this condition kept fairly stable in time at T=300°K albeit a long term stability was obtained by cooling the system at 10°K by a closed-cycle Joule-Thomson cryostat. According to a useful property of the microcavity with m=1 and to its actual geometry, the light emission took place over two counter-propagating plane-wave modes with vectors k and $k' = -k$ orthogonal to the mirrors [9]. As far as the basic dynamics is concerned, since the quantum-efficiency of the molecular absorption-emission cycle is $\eta \approx 1$, we may say that virtually *every* pump photon extracted from the laser beam, i.e., with poissonian statistics, at λ_p is re-emitted at a *different* λ over k or k', with an antibunched character because of pump-regularization, and then detected. Precisely, the overall pump-regularization arises from the synergy of several processes: the *short-pulse* excitation of a *single* molecule and the "cycle self-regularization" due to the finite time

taken by the excitation to cycle adiabatically through a 4-level system before restoring de-excitation, as we shall see. The latter process may be somewhat related to the laser squeezing model proposed by Ritsch et al. [10]. The statistical character of the output beam was assessed by a Hanbury-Brown Twiss (HBT) apparatus shown in Fig.1 while detection was provided by two cooled (RCA31034-A) phototubes, $PM_{1,2}$, with quantum efficiencies $\xi_1 \approx \xi_2 \approx 0.12$, average noise rate $\approx$100 Hz. The data analysis was carried out with a gated SR400 photon-counter or, when necessary, by charge integration at the PM anodes. In addition to this experiment, an equivalent Hanbury Brown-Twiss test was also carried out by adopting an active microcavity with $R_1=R_2$, with no use of any external beam-splitter, the two arms of the HBT interferometer being simply provided by the two output modes k, k', as shown by Fig. 1.

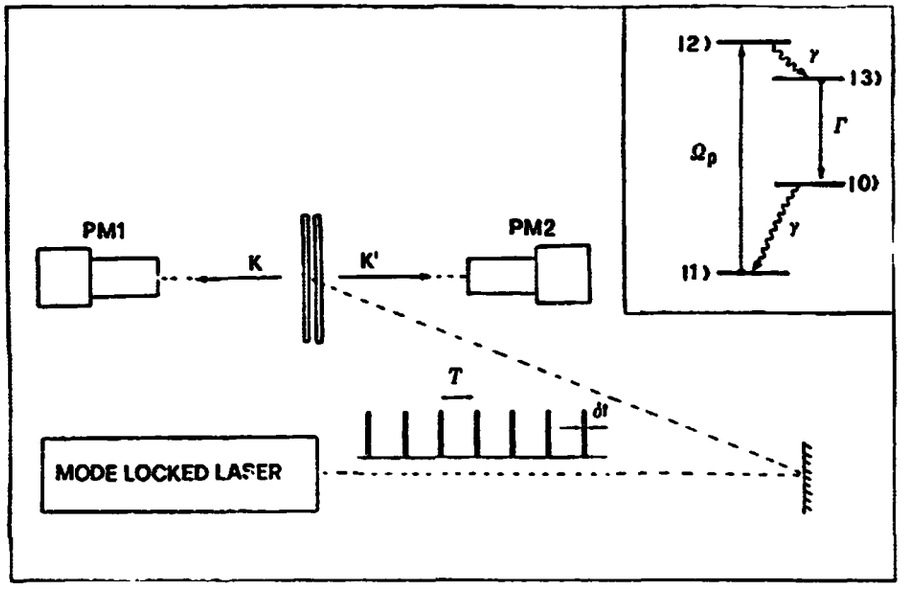

Fig. 1. Collision-Pulse-Mode-Locked laser-excited microcavity and Hanbury Brown-Twiss apparatus.

These ones may be interpreted as corresponding to the two pure momentum-states that form the basis of the quantum superposition representing any single-photon cavity excitation. This novel experimental configuration appears conceptually interesting as it suggests to interpret the microcavity as a new kind of *active beam-splitter.*

3 Quantum description of the antibunching process

Let's look more closely at the coupling process, by assuming a symmetrical cavity, m=1 and a momentum-state superposition of the *polarized* emitted photon over the modes k, k' with corresponding mutually commuting operators: $\hat{a} \equiv \hat{a}_k$, $\hat{a}' \equiv \hat{a}_{k'}$ [11].

The normal-ordered Hamiltonian of the system is:

$$\hat{H} = \hbar\omega_p \hat{o}^\dagger \hat{o} + \hbar\omega\{\hat{a}^\dagger \hat{a} + \hat{a}'^\dagger \hat{a}'\} + \sum_j \hbar\omega_j \hat{\pi}_{jj} - i\hbar K_p \hat{o}^\dagger (\hat{\pi}')^- - i\hbar K (\hat{a}^\dagger + \hat{a}'^\dagger)\hat{\pi}^- + \text{h.c.} \qquad (1)$$

being $\hat{o}$ the single-mode pump field operator, K_p, $K \propto \sqrt{\eta}$ appropriate coupling parameters proportional to corresponding Rabi frequencies Ω_p, Ω, $\eta \approx 3$ the microcavity field-enhancing factor, $\hat{\pi}_{ij} \equiv |i\rangle\langle j|$ (i,j = 0 to 3) the transition operators relative to the 4 -level system modelling the relevant features of the Franck-Condon dynamics of the single molecule. The system evolution is simplified by analyzing it separately in the two 2-dimensional Hilbert subspaces spanned by states ($|1\rangle, |2\rangle$), ($|0\rangle, |3\rangle$) since their respective dynamics are only connected by a roto-vibrational fast relaxation process via a single coupling parameter: $\gamma \equiv 1/T_2 \approx 5.10^{12}$ sec^{-1} [12]. The transition operators are: $\hat{\pi}^- \equiv |0\rangle\langle 3|$, $(\hat{\pi}')^- \equiv |1\rangle\langle 2|$ in the subspaces where the usual spin commutation relations hold for primed and unprimed operators. This allows a detailed study of the main features of the evolution of the absorption-emission cycle responsible for the self-regularization dynamics [3]. In particular, the SpE from level-3 is characterized by a cavity-enhanced, quasi-exponential decay parameter: $\Gamma = 2i|\Omega|^2[\zeta(\Delta\omega) - \zeta^*(\Delta\omega)]$ where $\zeta(\Delta\omega)$ is the complex Heitler's function [13]: for our system: $\gamma >> \Gamma$. By assuming that at the initial time of any (square) δt-pulse, t =0, the molecular excitation is in the ground state, $\langle \hat{\pi}_{11} \rangle = 1$, the dynamics is analyzed by a Torrey type formulation leading to the relevant statistical averages involving the field emitted and detected at the retarded time t'=(t+z/c) by a detector placed at a distance z from the center of the cavity, on its axis [14]. For instance, the intensity $\langle : \hat{I}(t') : \rangle$ radiated after excitation by a sequence of equal δt-pulses, with $\delta t << \Gamma^{-1}$ and time interval $\Delta t \equiv \nu^{-1}$:

$$\langle \hat{E}^-(z, t')\, \hat{E}^+(z, t') \rangle = K \quad \text{rep}_T \langle \hat{\pi}^+(t)\hat{\pi}^-(t) \rangle, \quad \text{rep}_T\, u(t) \equiv \sum_{-\infty}^{+\infty}{}_n\, u(t - n\Delta t) \text{ [15]}. \qquad (2)$$

For $t > \delta t$ is found:

$$\langle \hat{\pi}^+(t)\hat{\pi}^-(t) \rangle = A\{1 - \exp(-3\gamma\delta t/2)\cos(\lambda\,\delta t) + B\exp(-3\gamma\delta t/2)\sin(\lambda\,\delta t)\}\exp(-\Gamma t), \qquad (3)$$

with: $\lambda = [|\Omega_p|^2 - (\gamma/2)^2]^{1/2}$, $A \approx -(3/2)[\gamma|\Omega_p|/(|\Omega_p|^2 + 2\gamma^2)]^2$, $B \approx (|\Omega_p|^2 - 5\gamma^2/2)/(3\gamma\lambda)$ for $\Gamma << \gamma$. Note that with the parameters corresponding to the CPM excitation in our experiment, each laser δt-pulse is a π-pulse for the overall dynamics, since: $\Omega_p \bullet T_2 \approx [6\,\sigma_p \in/(\gamma\,\delta t\, s_p\, \hbar\omega_p)]^{1/2} > 1$, $\Omega_p \bullet \delta t \approx \pi$.

δt-pulse is a π-pulse for the overall dynamics, since: $\Omega_p \bullet T_2 \approx [6\,\sigma_p \in /(\gamma\,\delta t\, s_p\, \hbar\omega_p)]^{1/2} > 1$, $\Omega_p \bullet \delta t \approx \pi$. Then, if a single molecule interacts with that pulse, the excitation does not have time to cycle more than once within the 4-level system, leading to the emission of no more than one photon for each δt-pulse. This is precisely the origin of the mechanism of self-regularization and determines the *antibunched* character of the emitted radiation [16]. With the excitation provided by longer pulses $\delta t \approx 1/\Gamma$, the π-pulse condition becomes very critically dependent on all parameters and there is the possibility of multiple cycles within δt with a Poisson-type multiple emission [9]. The above analysis is completed by the evaluation of the degree of second-order coherence:

$$g^{(2)}(\tau) = <:\hat{I}(t')\hat{I}(t'+\tau):>/[<:\hat{I}(t'):>]^2. \qquad (4)$$

This relevant quantity is evaluated, as usual, by first expressing the emission intensity average $<\hat{\pi}^+(t+\tau)\hat{\pi}^-(t+\tau)>$ as a linear superposition of molecular raising-lowering operator averages evaluated at time t . Then, the second-order correlation function appearing at the numerator of $g^{(2)}(\tau)$ is evaluated with the help of the *quantum regression* theorem [16,17]. In view of the spontaneous emission dynamics involving the states $|3>$, $|0>$, we may write the intensity average in the simple form:

$$<\hat{\pi}^+(t+\tau)\hat{\pi}^-(t+\tau)> = \beta_1(\tau) + \beta_2(\tau) \bullet <\hat{\pi}^+(t)\hat{\pi}^-(t)>, \qquad (5)$$

where $\beta_1(\tau)$, $\beta_2(\tau)$ are evaluated by solving the master equation accounting for the emission process. This leads to a straightforward evaluation of $g^{(2)}(\tau)$. This quantity is given here for a 4-level molecule, for $\tau < \Delta t$ and for two extreme δt-pulse excitation conditions, $\delta t << 1/\Gamma$:

(a) excitation by a single δt-puise: $g^{(2)}(\tau) = [\beta_1(\tau)/\beta_1(\infty)] = [1 - \exp(-\Gamma\tau)]$

(b) excitation by a sequence of δt-pulses, rate Δt^{-1} : $g^{(2)}(\tau) = \Gamma\Delta t \cdot [1 - \exp(-\Gamma\tau)]/[1 - \exp(-\Gamma\Delta t)]$;

$\Gamma\Delta t > 1$. We see that in both cases is $g^{(2)}(0) = 0$, as expected. In order to account formally for the experimental parameters involved in the HBT test, an equivalent quantum photodetection theory may be conveniently expressed in terms of the *coincidence parameter* α introduced by Grangier et al. [18]. Within the context of our work, this parameter is defined in terms of the probabilities of registering, by two detection channels 1, 2 relative to the output ports of the HBT beam-splitter, coincidence- and single-signals for each δt-pulse and within a gate interval Δt_g starting at t:

$$\alpha(t, \Delta t_g) = \frac{\langle p_c(t, \Delta t_g)\rangle}{\langle p_1(t, \Delta t_g)\rangle \cdot \langle p_2(t, \Delta t_g)\rangle} \qquad (6)$$

For single mode excitation of the beam splitter, $\Delta t_g << T_1$, we obtain by quantum theory [3]:

$$\alpha(\bar{n}) \equiv \alpha\left(0, \Delta t_g\right) = \frac{\mathrm{Tr}\left\{\hat{\rho}\hat{N}\left[1-\exp\left(-\xi_1 \hat{a}_1^{\dagger}\hat{a}_1\right)\right]\left[1-\exp\left(-\xi_2 \hat{a}_2^{\dagger}\hat{a}_2\right)\right]\right\}}{\mathrm{Tr}\left\{\hat{\rho}\hat{N}\left[1-\exp\left(-\xi_1 \hat{a}_1^{\dagger}\hat{a}_1\right)\right]\right\} \bullet \mathrm{Tr}\left\{\hat{\rho}\hat{N}\left[1-\exp\left(-\xi_2 \hat{a}_2^{\dagger}\hat{a}_2\right)\right]\right\}} \tag{7}$$

where $\hat{\rho}$ represents the properties of the source field and $\hat{N}$ is the normal-ordering operator. By the n-state expansion: $\hat{\rho}=\sum_n P_n |n\rangle\langle n|$, α is finally obtained for some relevant photon distributions:

1) *Chaotic*: $P_n = \bar{n}^n / (1+\bar{n})^{1+n}$ $\alpha = [2+\xi_1 T' \bar{n}+\xi_2 R' \bar{n}]/[1+\xi_1 T' \bar{n}+\xi_2 R' \bar{n}]$

2) *Coherent*: $P_n = \frac{\bar{n}^n}{n!}\exp(-\bar{n})$ $\alpha = 1$

3) *Antibunched*: $P_n = \delta_{n,\bar{n}}$ $\alpha = [1+(1-\xi_1 T'-\xi_2 R')^{\bar{n}}-(1-\xi_1 T')^{\bar{n}}-(1-\xi_2 R')^{\bar{n}}] \bullet$
$\bullet\{[1-(1-\xi_1 T')^{\bar{n}}][1-(1-\xi_2 R')^{\bar{n}}\}^{-1}$

being $R'=|r|^2$, $T'=|t|^2$ the optical parameters of the (loss-less) beam splitter and $\bar{n}$ the average number of photons emitted after each excitation δt-pulse. By a first order expansion of α, the second-order correlation function may be expressed in the form: $g^{(2)}(0) = [\alpha - B(\bar{n})] \bullet [A(\bar{n})]^{-1}$, where:

$$A(\bar{n}) = \frac{\mathrm{Tr}\left[\hat{\rho}\hat{a}_1^{\dagger}\hat{a}_1\right] \bullet \mathrm{Tr}\left[\hat{\rho}\hat{a}_2^{\dagger}\hat{a}_2\right]}{\mathrm{Tr}\left\{\hat{\rho}\hat{N}\left[1-\exp\left(-\xi_1 \hat{a}_1^{\dagger}\hat{a}_1\right)\right]\right\} \bullet \mathrm{Tr}\left\{\hat{\rho}\hat{N}\left[1-\exp\left(-\xi_2 \hat{a}_2^{\dagger}\hat{a}_2\right)\right]\right\}} \tag{8}$$

and,

$$B(\bar{n}) = \frac{\mathrm{Tr}\left\{\hat{\rho}\hat{N}\left[1-\exp\left(-\xi_1 \hat{a}_1^{\dagger}\hat{a}_1\right)\right]\left[1-\exp\left(-\xi_2 \hat{a}_2^{\dagger}\hat{a}_2\right)\right]-\hat{a}_1^{\dagger}\hat{a}_1\hat{a}_2^{\dagger}\hat{a}_2\right\}}{\mathrm{Tr}\left\{\hat{\rho}\hat{N}\left[1-\exp\left(-\xi_1 \hat{a}_1^{\dagger}\hat{a}_1\right)\right]\right\} \bullet \mathrm{Tr}\left\{\hat{\rho}\hat{N}\left[1-\exp\left(-\xi_2 \hat{a}_2^{\dagger}\hat{a}_2\right)\right]\right\}} \tag{9}$$

According to the theory, for n=1 is: $g^{(2)}(0) = \alpha = 0$.

4 Experimental result

The parameter α is plotted in Fig. 2 for the three cases Vs. $\bar{n}$ and the molecular $\rho \propto \bar{n}$, for our experimental conditions.

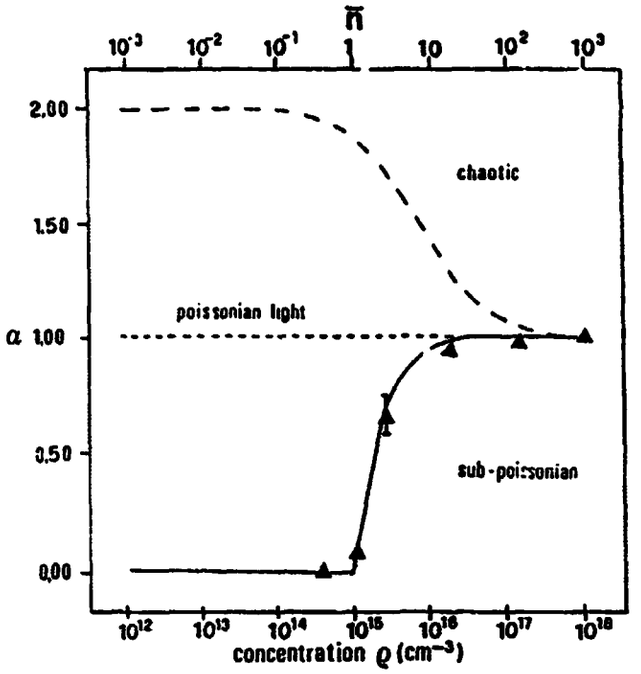

Fig. 2. Coincidence parameter α ($\bar{n}$) as function of the number of photons emitted after each exitation pulse and of the molecular concentration. The time-gate of the TCSPC apparatus was: Δt_g = 1 nsec.

Note in Fig. 2 the good experimental verification for $\bar{n}>1$ of the theoretical curve expressing α ($\bar{n}$) in the sub-poissonian condition, viz., implying the pure n-state distribution: $P_n = \delta_{n,\bar{n}}$. These results of the HBT experiment show that an increasing sub-Poisson character of the output radiation is gradually established for ρ varying over two-order of magnitude, leading for $\rho \approx 7 \bullet 10^{14}$ cm^{-3} to the striking figure $\alpha = g^{(2)}(0) = 0$ for $n=\bar{n}=1$. This last result has been obtained at T=300°K with a 50%-50% beam-splitter within a run involving a number of counts equal to $1.5 \bullet 10^{4}$ by each detection channel. Within this run no coincidences were detected. The other experimental points in Fig. 2 were determined approximately by the same number of counts.

5 Conclusion

All this provides the first demonstration that, under appropriate conditions, it is possible to conceive a macroscopic quantum device that emits, over a *single* output radiation mode a single-photon per pulse, with a quasi *deterministic* generation of a quantum radiation state, at repetition rates as high as 100 Mhz and with a quantum efficiency close to one. This result leads to a still more important consequence. The single-molecule excitation process could be straigthforwardly

reproduced n-times within the same device by multiple focusing within the macroscopic transverse-extension l_t of the *same* field mode [19]. Since within that mode the SpE dynamics of the n excited molecules are strongly coupled by relativistically-causal, superradiant interactions acting with a retardation time τ_t *shorter* than the coherence-time τ_c of the field emitted by the microcavity (with $f>>1$): $\tau_t=l_t/c\approx 2(\lambda/c)\sqrt{f}<<\tau_c\approx(\lambda/c)f$, then the indistinguishable emitted n single-photons do belong to the *same* space-time extension of the output field-mode, i.e., they form a quantum $|n>$-state [20]. The experimental realization of these conditions would certainly determine a new exciting endeavour within the quantum optics community. The preliminary results of our investigation in this direction are quite encouraging. We acknowledge useful discussions with P. Milonni, J. Franson and Y. Shih ■

References

(*) Present address: Max-Planck Institut fur Quantenoptik, Garching D-85748, Germany.

[1] C. H. Bennett, F. Bessette, G. Brassard, L. Salvail and J. Smolin, Journal of Cryptology, 5, 3 (1992), A. K. Ekert, J. G. Rarity and P. R. Tapster, Phys. Rev. Lett. **69**, 1293 (1992)

[2] D. Deutsch, Proc. R. Soc. of London, **A400**, 97 (1985) and 425, 73 (1989).

[3] D. F. Walls and G. J. Milburn, *Quantum Optics* (Springer-Verlag, Berlin, 1994); M. Teich, B. Saleh and J. Perina, J. Opt. Soc. Am. **B1**, 366 (1984)

[4] Y. Yamamoto, Phys. Rev. Lett. **66**, 2867 (1991)

[5] H. J. Kimble, M. Dagenais and L. Mandel, Phys. Rev. Lett. **39**, 691 (1977)

[6] F. Dietrich and H. Walther, Phys. Rev. Lett. **58**, 203 (1987)

[7] T. Basche', W. E. Moerner, M. Orrit and H. Talon, Phys. Rev. Lett. **69**, 1516 (1992)

[8] F. De Martini, G. Innocenti, G. Jacobovitz and P. Mataloni, Phys. Rev. Lett. **59**, 2955 (1987); F. De Martini, M. Marrocco, P. Mataloni, L. Crescentini and R. Loudon, Phys.Rev. **A43**, 2480 (1991).

[9] The system's quantum efficiency is conveniently expressed by: $\eta = (1+ k_{ST}T_1)^{-1} \approx 1$, where $k_{ST}\approx 10^7$ s^{-1} is the typical decay rate of the Oxazine 720 excited molecule to the dissipative triplet-state by inter- system crossing: cfr: O. Svelto, *Principles of Lasers* (Plenum Press, New York, 1989), Ch. 6. In order to test the condition of single-photon emission, a microcavity with axis z, made of two equal, several centimeter thick, plane glass mirrors with lateral cylindrical paraboloidal shape has been conceived. The geometric foci of the two truncated paraboloids, each of which is limited by two parallel, circular, plane transverse surfaces orthogonal to z, are made to overlap and to coincide with the center of the microcavity active plane (diameter: 6 mm.). Then *every* photon

generated at that active center is directed, with estimated *efficiency* ϕ >96% , over either one of the two output modes **k**, **k'** in spite of the limited optical confinement provided by the Bragg reflectors at large emission angles respect to **z**, viz. to the direction of **k** (Fig.1). When needed, the use of one totally reflecting microcavity mirror, R=100% allowed the excitation of *only one* external mode, **k**. Under the given experimental conditions justifying, for $\Omega_p \bullet T_2 > 1$, the adoption of a quantum Rabi dynamics, and the efficiencies $\eta \approx 1$, $\phi \approx 1$, it is assumed that the result $\alpha = g^{(2)}(0) = 0$ implies a single-molecule excitation in the active region. For a very preliminary account of the present work, involving long excitation pulses, $\delta t \approx 5 \bullet 10^{-9}$ s. cfr: M. Marrocco and F. De Martini, in: *Quantum Interferometry*, ed. by F. De Martini, G. Denardo and A. Zeilinger (World Scientific, London, 1994).

[10] H. Ritsch, P. Zoller, C. W. Gardiner and D. F. Walls, Phys.Rev..A44, 3361 (1991).

[11] It is found that, under short-pulse excitation, the beam emitted by an Oxazine 720 active microlaser keeps the same polarization of the pump beam for a time determined by the molecular reorientational diffusion (A.Aiello, F.De Martini and P.Mataloni, subm. for publ.): this may be a lucky discovery indeed. In facts, the possibility of controlling the polarization of the emitted photon may represent a further important property of the adopted molecular system within the present new method.

[12] F. P. Shafer, *Dye Lasers* (Springer, Berlin, 1973); C. V. Shank, E. P. Ippen and O. Teschke, Chem. Phys. Lett. 45,291 (1977).

[13] W. Heitler, *The Quantum Theory of Radiation* (Clarendon, Oxford, 1960) Ch.8

[14] H..C. Torrey, Phys. Rev. 76, 1059 (1949).

[15] P. M. Woodward, *Probability and Information Theory* (McGraw Hill, New York, 1953)

[16] C. W. Gardiner, *Quantum Noise* (Springer, Berlin, 1991) Ch. 8; R. Loudon, *The Quantum Theory of Light*, (Clarendon, Oxford, 1983) Ch. 5, 7.

[17] M. Lax, Phys. Rev. 172, 350 (1968); B. R. Mollow, Phys. Rev. 188, 1969 (1969)

[18] P. Grangier, G. Roger and A. Aspect, Europhys. Lett. 1, 173 (1986)

[19] F. De Martini, M. Marrocco and M. Murra, Phys. Rev. Lett. 65, 1853 (1990)

[20] F. De Martini and M. Giangrasso, App. Phys. B60,S-49 (1995). Note that the strength of the interactions can be spatially modulated being dependent on the intermolecular distances.

NEXT
DOCUMENT

MACROSCOPIC VIOLATION OF THREE CAUCHY-SCHWARZ INEQUALITIES USING CORRELATED LIGHT BEAMS FROM AN INFRA-RED EMITTING SEMICONDUCTOR DIODE ARRAY

P. J. Edwards and X. Huang
Advanced Telecommunications Engineering Centre, Faculty of Information Sciences and Engineering, University of Canberra, PO Box1, Belconnen, ACT 2616, Australia

Y. Q. Li
Department of Physics, University of Arkansas, Fayetteville, AR 72701, USA

Y.Z. Wang
Joint Laboratory for Quantum Optics, Shanghai Institute of Optics and Fine Mechanics, Academica Sinica, PO Box 800-211, Shanghai 201800, PRC

Abstract

We briefly review quantum mechanical and semi-classical descriptions of experiments which demonstrate the macroscopic violation of the three Cauchy-Schwarz inequalities: $g_{11}^{(2)}(0) \geq 1$; $g_{11}^{(2)}(0) \geq g_{11}^{(2)}(t)$, $(t \to \infty)$; $|g_{12}^{(2)}(0)|^2 \leq g_{11}^{(2)}(0)\, g_{22}^{(2)}(0)$.

Our measurements demonstrate the violation, at macroscopic intensities, of each of these inequalities. We show that their violation, although weak, can be demonstrated through photodetector current covariance measurements on correlated sub-Poissonian Poissonian, and super Poissonian light beams. Such beams are readily generated by a tandem array of infrared-emitting semiconductor junction diodes. Our measurements utilise an electrically coupled array of one or more infrared-emitting diodes, optically coupled to a detector array. The emitting array is operated in such a way as to generate highly correlated beams of variable photon Fano Factor. Because the measurements are made on time scales long compared with the first order coherence time and with detector areas large compared with the corresponding coherence areas, first order interference effects are negligible.

The first and second inequalities are violated, as expected, when a sub-Poissonian light beam is split and the intensity fluctuations of the two split beams are measured by two photodetectors and subsequently cross-correlated.

The third inequality is violated by bunched (as well as antibunched) beams of equal intensity provided the measured cross correlation coefficient exceeds $(F-1)/F$, where F is the measured Fano Factor of each beam. We also investigate the violation for the case of unequal beams.

1 Theory of The Macroscopic Violation

The first inequality addresses the correlation between the intensity fluctuations in the two beams emerging from a 50/50 optical beam splitter. Loudon[1] gives the standard quantum result for a

single mode beam with mean photon number, $< n >$:

$$g_{11}^{(2)}(0) =< n(n-1) > / < n >^2 \tag{1}$$

and Paul[2] obtains the same result by treating the photon beam as a beam of classical distinguishable particles, subject to Bernoulli partition. In the absence of interference noise, that is for a broadband, multimode, incoherent source on time scales long compared with the coherence time and with detector areas large compared with the coherence area (Teich[3]), this treatment is justified (as it is also for a single mode situation). It is evident from expansion of equation (1) that g_{11} may be written:

$$g_{11}^{(2)}(0) = 1 + \frac{(F-1)}{< n >} \tag{2}$$

This form shows that any violation, (a value less than unity) requires sub-Poissonian variance ($F < 1$) and must be weak in the macroscopic limit ($n > > 1$). Nevertheless macroscopic violation can be readily demonstrated in a Hanbury Brown type experiment using a single light emitting diode driven from a high impedance source (Edwards[4]). The same configuration serves to show violation of the second inequality. Both these violations can be deduced from the measured covariance between the macroscopic photocurrents i_1, i_2 for the split beams.

As pointed out by Loudon[1], violation of this inequality is a fundamental quantum result resulting from the photoelectric detection of either the transmitted or the reflected photon. As we shall see however, Loudon's assertion that "non-classical effects tend to be most marked for beams with small well defined numbers of photons" is (rather surprisingly) apparently not true for the third inequality:

$$|g_{12}^{(2)}(0)|^2 \leq g_{11}^{(2)}(0) g_{22}^{(2)}(0) \tag{3}$$

which is violated at macroscopic intensities for bunched and unbunched beams as well as for the antibunched beams for which the first inequality is weakly violated at macroscopic intensities.

It is well known that the Cauchy-Schwarz inequality with time delay t between the two beams is [2],[5],[6]

$$|g_{12}^{(2)}(t)|^2 \leq g_{11}^{(2)}(0) g_{22}^{(2)}(0), \tag{4}$$

where $g_{ij}^{(2)}$ is the second-order coherence function. For $t = 0$, we have the following inequality if we use a " classical particle" description[2]:

$$\frac{< n_1 n_2 >^2}{(< n_1 >< n_2 >)^2} \leq \frac{< n_1(n_1-1) >}{< n_1 >^2} \frac{< n_2(n_2-1) >}{< n_2 >^2}. \tag{5}$$

That is

$$< n_1 n_2 >^2 \leq (< n_1^2 > - < n_1 >)(< n_2^2 > - < n_2 >). \tag{6}$$

In order to violate the Cauchy-Schwarz inequality, we should have

$$< n_1 n_2 >^2 > (< n_1^2 > - < n_1 >)(< n_2^2 > - < n_2 >). \tag{7}$$

So that we have

$$F_1 F_2(r^2-1) + < n > [2r\sqrt{F_1 F_2} + 2 - (F_1 + F_2)] + (F_1 + F_2) - 1 > 0 \tag{8}$$

where r is the cross correlation coefficient and F_1 and F_2 are the Fano Factors for each beam. For macroscopic violation (large $< n >$):

$$[2r\sqrt{F_1F_2} + 2 - (F_1 + F_2] > 0 \tag{9}$$

If $F_1 = F_2 = F_o$, the measured Fano Factor, we may obtain the following result from inequality (8):

$$(rF_o - F_o + 1) > 0, \tag{10}$$

hence

$$r > \frac{F_0 - 1}{F_0}. \tag{11}$$

We therefore have the following violation conditions:

1. For $F_o = 1$ (Poission), all positive correlations, i.e. $r > 0$;
2. For $F_o < 1$ (Anti-bunched), all positive correlations, i.e. $r > 0$;
3. For $F_o > 1$ (Bunched), $r > |(F_o - 1)/F_o|$.

This case is shown in Figure 1.

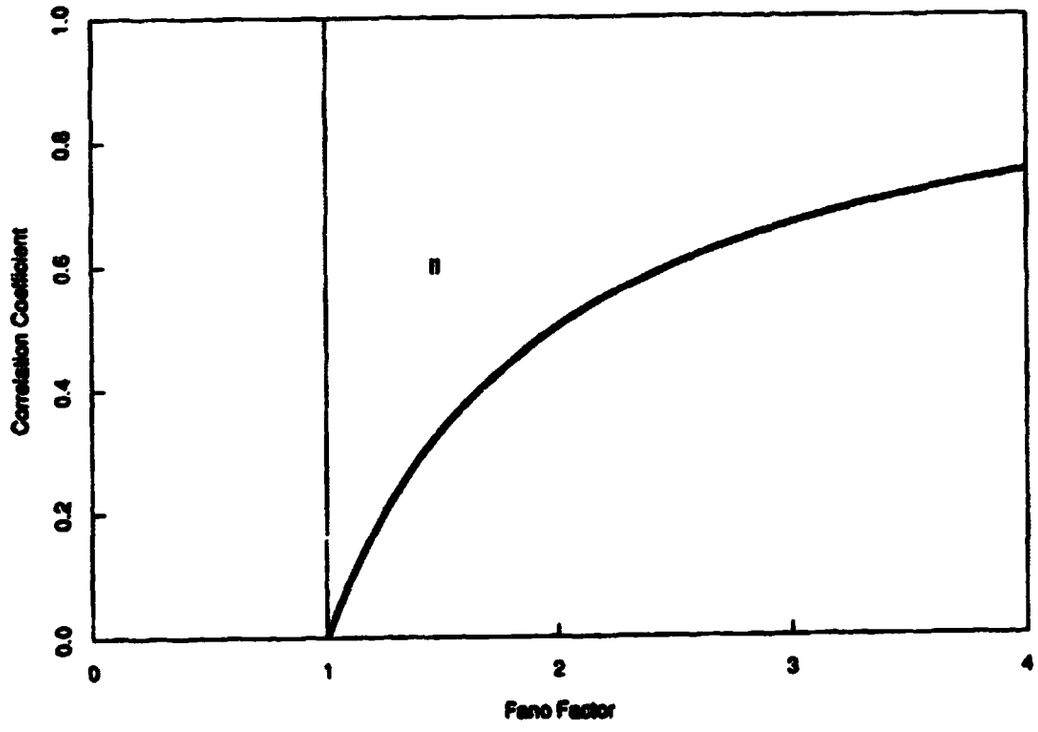

Figure 1: Two different violation regions, I ($F_o < 1$) and II ($F_o > 1$).

2 Violation For Twin Beams Generated by Coupled LED's

Figure 2 shows the arrangement adapted by Edwards[4,7] to generate quantum correlated twin beams.

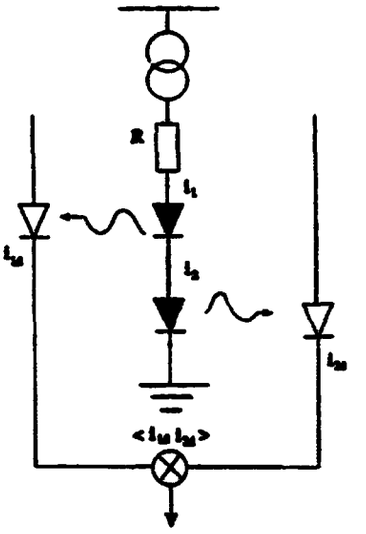

Figure 2: Series-connected infrared emitting diodes (L2656) configured to generate positively correlated intensity fluctuations.

From Figure 2, we have $i_1 = i_2$ and $\eta_1 = \eta_2$, so $i_{1d} = i_{2d}$ and $< i_{1d}^2 > = < i_{2d}^2 >$. The correlation coefficient is given by

$$r_{12} \equiv \frac{< i_{1d} i_{2d} >}{\sqrt{< i_{1d}^2 >< i_{2d}^2 >}}, \tag{12}$$

This can be easily shown to be

$$r_{12} = \frac{\eta F_i}{F_o}. \tag{13}$$

Here F_i is the Fano Factor at the source and

$$F_o = 1 + \eta(F_i - 1) \tag{14}$$

is the Fano Factor measured at the detectors with quantum efficiency, η.
Recall that the macroscopic violation for $F_1 = F_2 = F_o$ was given by

$$r_{12} > \frac{F_o - 1}{F_o}, \tag{15}$$

that is

$$\eta \frac{F_i}{F_o} > \frac{F_o - 1}{F_o} = \frac{\eta(F_i - 1)}{F_o} \tag{16}$$

A violation parameter, Δ can therefore be written as

$$\begin{aligned}\Delta &= r_{12} - \frac{F_o - 1}{F_o} \\ &= \frac{\eta}{F_o} \quad (F_o > \frac{1}{2}) \\ &= 1 + r_{12} \quad (0 < F_o < \frac{1}{2})\end{aligned} \tag{17}$$

3 Experimental Results

Referring to Figure 3, these measurements were performed at room temperature using two series connected Hamamatsu type L2656 infrared emitting diodes. The Fano factors were measured as shown with a swept frequency spectrum analyser. Correlations were measured digitally.

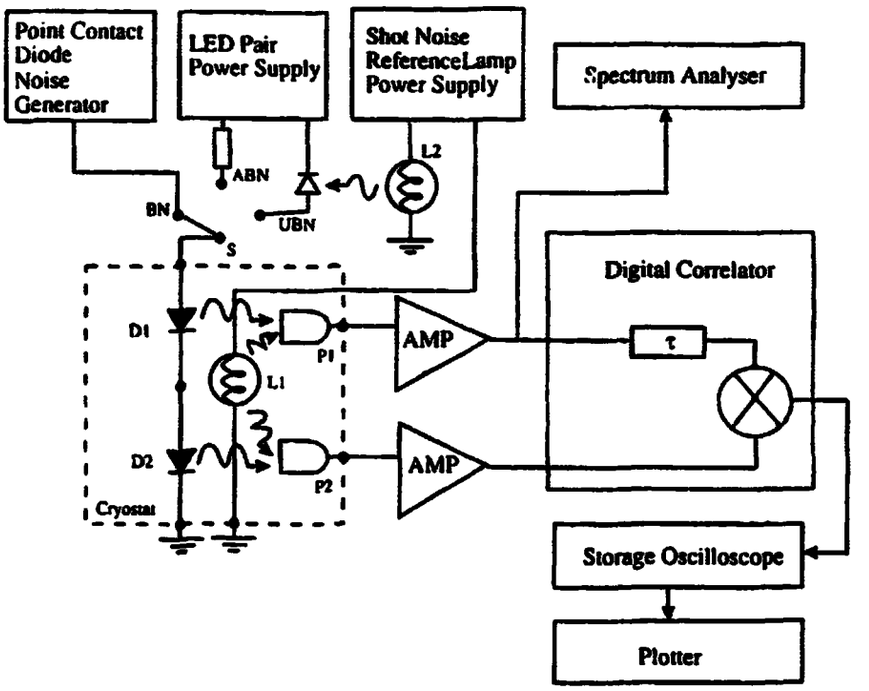

Figure 3: The correlated twin beams are generated by light emitting diodes, D1,D2. Tungsten lamps, L1, L2, provide shot noise reference currents in the pin diode detectors P1,P2, and light emitting diodes, respectively. Switch, S provides unbunched (UBN), bunched (BN) and anti-bunched (ABN) twin beams with detected Fano factors measured by the spectrum analyser. The quantum efficiencies are determined directly from the measured DC currents.

Typical results are shown in Figure 4, together with a curve showing the expected values of the violation parameter for a quantum efficiency of 10%, as employed for all measurements with the exception of the left hand point (12%). These results are in good agreement with the theory.

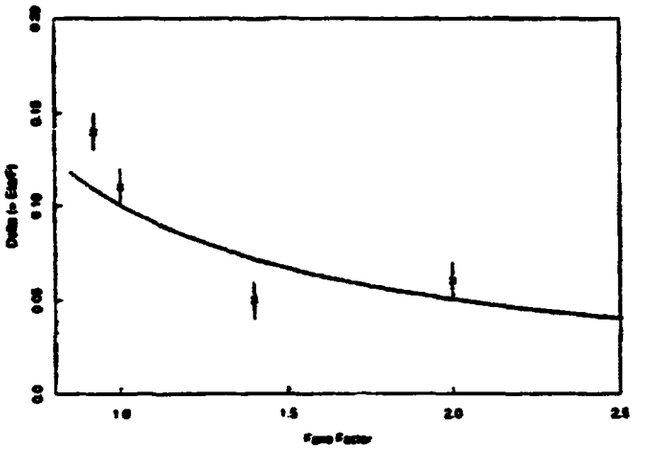

Figure 4: Experimental violation of the Cauchy-Schwarz Inequalities.

4 Conclusions

We have extended theories concerning violation of the Cauchy-Schwarz inequalities (CSI). We have derived a simple condition for the macroscopic violation of a CSI for twin incoherent light beams using a "classical particle" model. We have shown that this CSI is violated for positively correlated, bunched, incoherent twin beams.

References

[1] R. Loudon, Rep. Prog. Phys. 43, 58 (1980).

[2] H. Paul, Reviews of Modern Physics, 54, 1061 (1982).

[3] M. C. Teich and B. E. A. Saleh, *Progress In Optics*, XXVIII, Edited by E. Wolf, North-Holland (1988).

[4] P. J. Edwards, Australian Conference on Optics, Lasers and Spectroscopy, (ACOLS'91), Australian National University, 150 (1991).

[5] M. D. Reid and D. F. Walls, Phys. Rev. A., 34, 1260 (1986).

[6] Y. Q. Li, J. P. Yin and Y. Z. Wang, in IQEC'92 Technical Digest, Proceedings of the Eighteenth International Conference on Quantum Electronics, Vienna, Austria, MoG7 (1992).

[7] P.J. Edwards and G.H. Pollard, Phys. Rev. Lett. 69, 2867 (1992).

NEXT
DOCUMENT

Photon number-phase uncertainty relation in the evolution of the field in a Kerr-like medium

Fan An-fu
Department of Opto-electronics Science and Technology,
Sichuan University, Chengdu 610064, China
and
China Center of Advanced Science and Technology(World Laboratory),
P.O.Box 8730, Beijing 100080, China

Sun Nian-Chun
Southwest Institute of Technical Physics Chengdu, 610041, China

Abstract

A model of a single-mode field, initially prepared in a coherent state, coupled to a two-level atom surrounded by a nonlinear Kerr-like medium contained inside a very good quality cavity is considered. We derive the photon number-phase uncertainty relation in the evolution of the field for a weak and strong nonlinear coupling respectively, within the Hermitian phase operator formalism of Pegg and Barnett, and discuss the effects of nonlinear coupling of thr Kerr-like medium on photon number-phase uncertainty relation of the field.

1 Introduction

Recently, Agarwal et al[1] have considered the propagation of a single-mode resonant field through a nonlinear Kerr-medium. Bužek et al[2] have dealed with a combination of two models: the Jaynes–Cummings model (JCM) describing the interaction of a single-mode cavity field with a single two-level atom, and a nonlinear Kerr-like medium inside a cavity which may be modelled by an anharmonic oscillator[1,3]. Particularly, they have showed that with increasing nonlinear coupling the period between the revivals of the atomic inversion is shortened and its time evolution becomes more regular. Besides, they also described the squeezing of the cavity mode and the time evolution of the photon-number distribution.

As is well-known, the phase properties of light field is very important in quantum optics. Lately, Pegg and Barnett[4-6] have shown that an Hermitian phase operator of radiation field exists. It can be constructed from the phase states. This new phase operator formalism makes it possible to describe the quantum properties of optical phase in a fully quantum mechanics. Gerry[7] has studied the phase fluctuations of coherent light interacting with the anharmonic oscillator using the Hermitian phase operator. Gantsog et al[8,9] have studied the phase properties of self-squeezed states generated by the anharmonic oscillator, elliptically polarized light propagating through a Kerr medium and a damped anharmonic oscillator using the Hermitian phase operator.

In this paper we consider a generalized JCM with an additional Kerr-like medium, namely, a combined model that comprises the JCM and the anharmonic oscillator model (AOM) used to describe a Kerr medium. We deal with not only the field-Kerr medium interaction, but also the field-atom interaction. We derive the photon number-phase uncertainty relation in the evolution of the field for a weak and strong nonlinear coupling respectively, within the Hermitian phase operator formalism of Pegg and Barnett, and discuss the effects of nonlinear coupling of the Kerr medium on the number-phase uncertainty relation of the field.

2 The model

We consider a model which consists of a single two-level atom surrounded by a nonlinear Kerr-like medium contained in a high-Q single-mode cavity. The cavity mode is coupled to the Kerr-like medium as well as to the two-level atom. The Kerr-like medium can be modelled as an anharmonic oscillator [1,3]. In the adiabatic limit, the effective Hamiltonian of the system involving only the photon and atomic operators in rotating-wave approximation, is[1,2]

$$H_{eff} = \hbar\omega(a^+a + \frac{1}{2}) + \hbar\omega_0 S^z + \hbar\chi a^{+2}a^2 + \hbar g(S^+a + a^+S^-), \tag{2.1}$$

where a and a^+ are the annihilation and creation opreators of the field mode, $S^{\pm}$ and S^z are the spin-flip and inversion operators of the atom respectively, g is the field-atom coupling constant and χ describes the strength of the quadratic nonlinearity modelling the Kerr medium, ω_0 is the frequency of the atomic transition, the frequency ω is

$$\omega = \omega_f - \lambda^2/(\omega_k - \omega_f), \tag{2.2}$$

Where ω_f and ω_k are the frequency of the field mode and the anharmonic oscillator modelling the Kerr medium respectively, and λ is the field-Kerr medium coupling constant.

To isolate the effects of the nonlinear coupling of the Kerr medium from that of the finite detuning, we restrict in the case of the resonance ($i.e., \omega_0 = \omega$). Let us assume that the atom is initially in the excited state $|e>$ and the field mode is prepared in a coherent state $|\alpha>$. The initial state vector $|\psi(0)>$ of the system is

$$|\psi(0)>= |\alpha> \otimes |e>= \sum_{n=0}^{\infty} b_n e^{in\beta}|n, e>, \tag{2.3}$$

where

$$b_n = \exp(-\bar{n}/2)(\bar{n}^n/n!)^{1/2}. \tag{2.4}$$

In the interaction picture, the state vector of the system at a later time t is found from the Hamiltonian (2.1) to be

$$|\psi(t)>= \sum_{n=0}^{\infty} b_n e^{in\beta} e^{-i\chi n^2 t}.\{[\cos(\frac{1}{2}\Omega_{n\chi}t) + i\frac{2\chi n}{\Omega_{n\chi}}\sin(\frac{1}{2}\Omega_{n\chi}t)]|n, e>$$

$$-i\frac{2g\sqrt{n+1}}{\Omega_{n\chi}}\sin(\frac{1}{2}\Omega_{n\chi}t)|n+1, g>\}, \tag{2.5}$$

where $|g>$ is the ground state of the atom, $\Omega_{n\chi}$ is the generalized Rabi frequency defined by

$$\Omega_{n\chi} = [4g^2(n+1) + 4\chi^2 n^2]^{1/2}, \tag{2.6}$$

It is obvious that, for $\chi = 0$, the state vector $|\psi(t)>$ given by Eq.(2.5) describes the dynamics of the ordinary JCM.

3 The phase variance of the cavity field

Based on the Hermitian phase formalism of Pegg and Barnett[4-6], The complete set of $s+1$ orthonormal phase state is defined by

$$|\theta_m>= \frac{1}{\sqrt{s+1}} \sum_{n=0}^{s} \exp(in\theta_m)|n>, \tag{3.1}$$

where $\theta_m = \theta_0 + 2\pi m/(s+1), m = 0, 1, 2, \cdots, s$, and θ_m is an arbitrary real number. The Hermitian phase operator is given by

$$\hat{\Phi}_\theta = \sum_{m=0}^{s} \theta_m |\theta_m><\theta_m|, \tag{3.2}$$

Clearly, phase state $|\theta_m>$ are eigenstates of $\hat{\Phi}_\theta$ with the eigenvalues θ_m. The eigenvalues θ_m are restricted to lie within a phase window between θ_0 and $(\theta_0 + 2\pi)$. It has to be noted That, after all expectation values of the phase variables associated with the phase properties of the field have been calculated in the finite $(s+1)$−dimensional space, s is allowed to tend to infinity. The phase distribution of the state given by Eq.(2.5) is

$$p(\theta_m, t) = |<\theta_m|\psi(t)>|^2, \tag{3.3}$$

with the expectation value and the variance

$$<\hat{\Phi}_\theta>= \sum_m \theta_m P(\theta_m, t), \tag{3.4}$$

$$<\Delta\hat{\Phi}_\theta^2>= \sum_m (\theta_m - <\hat{\Phi}_\theta>)^2 P(\theta_m, t). \tag{3.5}$$

We choose the reference phase $\theta_0 = \beta - \pi s/(s+1)$, and introduce a new phase label $\mu = m - s/2$, which goes in integer steps from $(-s/2)$ to $(s/2)$. Then the phase distribution becomes symmetric in μ. In the limit as s tends to infinity, the continuous phase variable can be introduced replacing $\mu 2\pi/(s+1)$ by θ and $2\pi/(s+1)$ by $d\theta$. Then we can find a continuous phase distribution

$$P(\theta, t) = \frac{1}{2\pi}\{1 + 2\sum_{n>n'} b_n b_{n'} [A_{nn'} \cos[(n-n')\theta + (n^2 - n'^2)\chi t]$$
$$+ B_{nn'} \sin[(n-n')\theta + (n^2 - n^2)\chi t]]\}, \tag{3.6}$$

where

$$A_{nn'} = \cos(\frac{1}{2}\Omega_{n\chi} t)\cos(\frac{1}{2}\Omega_{n'\chi} t) + \frac{4g^2\sqrt{(n+1)(n'+1)} + 4\chi^2 nn'}{\Omega_{n\chi}\Omega_{n'\chi}} \sin(\frac{1}{2}\Omega_{n\chi} t)\sin(\frac{1}{2}\Omega_{n'\chi} t)$$

$$B_{nn'} = (2\chi n/\Omega_{n\chi})\sin(\frac{1}{2}\Omega_{n\chi}t)\cos(\frac{1}{2}\Omega_{n'\chi}t) - (2\chi n'/\Omega_{n'\chi})\cos(\frac{1}{2}\Omega_{n\chi}t)\sin(\frac{1}{2}\Omega_{n'\chi}t). \tag{3.7}$$

The function $P(\theta,t)$ is normalized so that

$$\int_{-\pi}^{\pi} P(\theta,t)d\theta = 1. \tag{3.8}$$

If the mean photon number in the field is large, $\bar{n} >> 1$, the coefficient b_n in Eq.(2.4) can be well approximated by a continuous Gaussian distribution

$$b_n = (2\pi\bar{n})^{-1/4}\exp[-(\bar{n}-n)^2/4\bar{n}]. \tag{3.9}$$

If Eq.(3,9) is substituted into Eq.(3.6) and the summation in Eq.(3.6) is replaced by an appropriate integral over the variable n, one can approximately work the phase distribution.

We will consider two limit cases:

(1)The weak nonlinear coupling which is defined by the condition $g^2\bar{n} >> \chi^2\bar{n}^2$, with $\bar{n} >> 1$. In this case the generalized Rabi frequency can be approximated as

$$\Omega_{n\chi} \approx g[(\bar{n})^{1/2} + n(\bar{n})^{-1/2}](1 + \frac{1}{2}\epsilon_\chi^2), \tag{3.10}$$

where

$$\epsilon_\chi = (\chi^2\bar{n}^2/g^2\bar{n})^{1/2}. \tag{3.11}$$

Then using Eqs.(3,9) and (3.10) and replacing the summation in Eq.(3.6) by an appropriate integral over n , we obtain

$$P(\theta,t) = \frac{1}{2\pi}(\frac{2\pi\bar{n}}{1+16\bar{n}^2\chi^2t^2})^2 \cdot \{(1+\epsilon_\chi)\exp[-\frac{2\bar{n}}{1+16\bar{n}^2\chi^2t^2}[2\bar{n}\chi t + (\theta - \frac{gt}{2\sqrt{\bar{n}}})^2]]$$

$$+(1-\epsilon_\chi)\exp[-\frac{2\bar{n}}{1+16\bar{n}^2\chi^2t^2}[2\bar{n}\chi t + (\theta + \frac{gt}{2\sqrt{\bar{n}}})^2]]\}. \tag{3.12}$$

According to Eqs.(3.4) and (3.5), using Eq.(3.12), and taking into account $\theta_m = \theta + \beta$, we can directly find an expectation value of the phase operator and its variance

$$< \hat{\Phi}_\theta >= \beta + \epsilon_\chi\frac{gt}{2\sqrt{\bar{n}}}(1 - 4\bar{n}\epsilon_\chi), \tag{3.13}$$

$$< \Delta\hat{\Phi}_\theta^2 >= \frac{1}{4\bar{n}} + \frac{(gt)^2}{4\bar{n}}(1 + 16\bar{n}\epsilon_\chi^2). \tag{3.14}$$

(2)The strong nonlinear coupling which is defined by the condition $g^2\bar{n} << \chi^2\bar{n}^2$, with $\bar{n} >> 1$. In this case the generalized Rabi frequency can be approximated as

$$\Omega_{nx} \approx 2\chi\bar{n}(1 + \frac{1}{2}\epsilon_g^2), \tag{3.15}$$

where

$$\epsilon_g = (g^2\bar{n}/\chi^2\bar{n}^2)^{1/2}. \tag{3.16}$$

Then, we find

$$P(\theta,t)=\frac{(8\pi\bar{n})^{1/2}}{2\pi}(1+16\bar{n}^2\chi^2t^2)^{-1/2}\exp[-\frac{2\bar{n}}{1+16\bar{n}^2\chi^2t^2}(\theta+2\bar{n}\chi t)^2] \tag{3.17}$$

$$<\hat{\Phi}_\theta>=\beta-2\bar{n}\chi t, \tag{3.18}$$

$$<\Delta\hat{\Phi}_\theta^2>=\frac{1}{4\bar{n}}+4\bar{n}(\chi t)^2. \tag{3.19}$$

We see that the average value of the phase is not equal to the initial quantity β, and the phase variance is always enhanced. For the weak nonlinear coupling, the enhancement of the phase variance is proportional to $(gt)^2/4\bar{n}$, this is similar to that of the resonance field in coherent state JCM[10]. For the strong nonlinear coupling, the enhancement of the phase variance is proportional to $4\bar{n}(\chi t)^2$. Obviously, the enhancement of the phase variance in the strong nonlinear coupling case is larger than that in the weak nonlinear coupling case.

4 The number-phase uncertainty relation

It is not difficult to calculate the variance of the photon-number for the state given by Eq.(2.5). Using $\hat{n}=a^+a$, for the weak nonlinear coupling we obtain

$$<(\Delta\hat{n})^2>=<\hat{n}^2>-<\hat{n}>^2\approx\bar{n}+\sqrt{\bar{n}}gt\exp[-(gt)^2/2]\sin(2\sqrt{\bar{n}}gt). \tag{4.1}$$

¿From Eqs.(3.14) and (4.1), we find that the number-phase uncertainty relation is

$$<(\Delta\hat{n})^2><\Delta\hat{\Phi}_\theta^2>\approx\frac{1}{4}+\frac{1}{4}(gt)^2\{1+16\bar{n}\epsilon_\chi^2+16\sqrt{\bar{n}}gt\epsilon_\chi^2\exp[-(gt)^2/2]\sin(2\sqrt{\bar{n}}gt)\}. \tag{4.2}$$

For the strong nonlinear coupling, we find

$$<(\Delta\hat{n})^2>\approx\bar{n}+2\bar{n}\chi t\epsilon_g^2\exp[-2\bar{n}(\chi t)^2]\sin(2\bar{n}\chi t), \tag{4.3}$$

$$<(\Delta\hat{n})^2><\Delta\hat{\Phi}_\theta^2>\approx\frac{1}{4}+4\bar{n}^2(\chi t)^2\{1+2\chi t\epsilon_g^2\exp[-2\bar{n}(\chi t)^2]\sin(2\bar{n}\chi t)\}. \tag{4.4}$$

We see that, the uncertainty product during the evolution is expanded. The expansion of the uncertainty product is fast in strong nonlinear coupling case. This is similar to that of the self-squeezed state generated by the anharmonic oscillator[8]. This occurs because both the field-atom interaction[11] and the field-Kerr medium interaction are nonlinear, moreover the nonlinear interaction strength of the latter is larger than that of the former.

5 Summary

In the present paper we consider a generalized JCM in the presence an additional Kerr-like medium. we have derived the photon number-phase uncertainty relation in the evolution of a resonant field for a weak and strong nonlinear coupling, within the Hermitian phase operator

formalism of Pegg and Barnett. We have shown that the nonlinear coupling of the cavity mode to Kerr-like medium leads to the enhancement of the phase variance of the field and the expansion of the uncertainty product. Particularly, the expansion of the uncertainty product is fast in strong nonlinear coupling case. We have indicated that this is similar to that of the self-squeezed state generated by the anharmonic oscillator. We have also indicated that the nonlinear interaction strength of the field-Kerr medium is larger than that of the field-atom.

Acknowledgments

This work is supported by the National Natural Science Foundation of China.

References

[1] G.S.Agarwal and R.R.Puri, Phys.Rev.A39, 2969(1989).

[2] V.Bužek and I.Jex, Optics Comm.78, 125(1990).

[3] B.Yurke and D.Stoler, Phys.Rev.Lett.57, 13(1986).

[4] D.T.Pegg and S.M.Barnett, Europhys Lett.6, 483(1988).

[5] S.M.Barnett and D.T.Pegg, J.Mod.Opt.36, 7(1989).

[6] D.T.Pegg and S.M.Barnett, Phys.Rev.A39, 1965(1989).

[7] C.C.Gerry, Optics Comm.75, 168(1990).

[8] Ts.Gantsog and R. Tanaś, J.Mod. Opt.38, 1021(1991);ibid,38, 1537(1991).

[9] Ts.Gantsog and Tanaś, Phys.Rev.A44, 2086(1991).

[10] A.F.Fan, Optics Comm.98, 340(1993).

[11] A.F.Fan, Z.W.Wang and N.C.Sun, Acta Phys.Sin.44, 536(1995).

NEXT
DOCUMENT

The quantum phase-dynamical properties of the squeezed vacuum state intensity-couple interacting with the atom

Fan An-fu
Department of Opto-electronics Science and Technology,
Sichuan University, Chengdu 610064, China
and
China Center of Advanced Science and Technology(World Laboratory),
P.O.Box 8730, Beijing 100080, China

Sun Nian-chun
Southwest Institute of Technical Physics, Chengdu 610041, China

Zhou Xin
Dept. of Opto-electronics Science and Technology, Sichuan University, Chengdu 610064, China

Abstract

The Phase-dynamical properties of the squeezed vacuum state intensity-couple interacting with the two-level atom in an ideal cavity are studied using the Hermitian phase operator formalism. Exact general expressions for the phase distribution and the associated expectation value and variance of the phase operator have been derived. we have also obtained the analytic results of the phase variance for two special cases–weakly and strongly squeezed vacuum. The results calculated numerically show that squeezing has a significant effect on the phase properties of squeezed vacuum.

1 Introduction

The squeezed state exhibits phase sensitive noise properties. Therefore, it is important to examine the phase properties of squeezed state of light. Recently, Sanders et al[1], and Yao[2], and Fan et al[3] have studied phase properties of the ideal squeezed state using Susskind and Glogower phase-operator formalism[4]. Vaccaro et al[5] have re-examined the phase properties of the squeezed vacuum state, particularly, the weakly squeezed vacuum state using the phase-operator formalism of Pegg and Barnett[6-8]. However, they have not considered the field-atom interaction. Dung et al[9] and Fan et al[10-11] have studied the phase properties of a coherent light interacting with a two-level atom. Bužek[12] has studied the time evolution of the squeezing and the atomic population inversion in the Jaynes- Cummings model(JCM) with intensity-dependent coupling with the squeezed vacuum state.

In the present paper, we will study phase properties in the JCM with intensity-dependent coupling with a light field initially prepared in the squeezed vacuum state using Pegg-Barnett phase-operator formalism. The results calculated numerically show that in such a model how the squeezing have an effect on phase properties.

2 The model

The model Hamiltonian for the JCM with the intensity-dependent coupling in the rotating-wave approximation is [13]

$$H = \hbar\omega_0 S^z + \hbar\omega N + \hbar g(S^+ R + S^- R^+), \tag{2.1}$$

where $N = a^+a, R = a\sqrt{N}, R^+ = \sqrt{N}a^+$; a^+ and a is the creation and annihilation operators of the field mode of frequency ω, S^z and $S^\pm$ are the pseudospin operators for the two-level atom of frequency ω_0, g is the atom-field coupling constant. The commutation relations for N, R and R^+ are

$$[R, R^+] = 2N + 1, [R, N] = R, [R^+, N] = -R^+. \tag{2.2}$$

We assume the initial state of the light field to be the squeezed vacuum state $|0, \xi> = S(\xi)|0>$, where $S(\xi)$ is the squeeze operator and ξ is complex squeeze parameter:

$$S(\xi) = \exp[\frac{1}{2}(\xi^* a^2 - \xi a^{+2})]. \tag{2.3}$$

$$\xi = |\xi|e^{i\theta}, r = |\xi|, \beta = 2\eta,$$
$$0 \le r < \infty, 0 \le \beta \le 2\pi. \tag{2.4}$$

We can find the $|n>$ state representation of the state $|0, \xi>$ [14] :

$$|0, \xi> = \sum_{n=0}^{\infty} Q_n |2n>, \tag{2.5}$$

$$Q_n = (\mathrm{sech} r)^{1/2} \frac{[(2n)!]^{1/2}}{n!}(-\frac{1}{2}e^{2i\eta}\tanh r)^n. \tag{2.6}$$

If the atom is supposed to be in the excited state $|e>$ at the initial time, then the initial state $|\Psi(0)>$ of the system is

$$|\Psi(0)> = |0, \xi> \otimes |e> = \sum_{n=0}^{\infty} Q_n |e, 2n>, \tag{2.7}$$

In the resonant case, the exact solution for an initial state $|\Psi(0)>$ given by Eq.(2.7), is

$$|\Psi(t)> = \sum_{n=0}^{\infty} \exp[-i(E_e + 2n\hbar\omega)t] \cdot Q_n[\cos[(2n+1)gt]|e, 2n> - i\sin[(2n+1)gt]|g, 2n+1>], \tag{2.8}$$

where E_e is the energy of excited state of the atom.

3 The phase properties

Accooding to Pegg and Barnett[6-8], the Hermitian phase operator operates on a $(s+1)$ - dimensional subspace spanned by $(s+1)$ number states. The value of s can be made arbitrary large. A complete set of $(s+1)$ orthonormal phase states is defined by

$$|\theta_m> = (s+1)^{1/2} \sum_{n=0}^{s} \exp(in\theta_m)|n>, \tag{3.1}$$

where phase $\theta_m = \theta_0 + 2\pi m/(s+1), m = 0, 1, 2, \cdots, s$. The Hermitian phase operator is

$$\hat{\Phi}_\theta = \sum_{m=0}^{s} \theta_m |\theta_m><\theta_m|, no(3.2)$$

The phase states $|\theta_m>$ are eigenstates of $\hat{\Phi}_\theta$ with the eigenvalues θ_m. We see that the eigenvalues θ_m are restricted to lie within a phase window θ_0 and $\theta_0 + 2\pi$, where θ_0 is an arbitrary real number. It has to be noted that after all expectation values of phase variables of light field have been calculated in the finit $(s+1)$ dimensional space, s is allowed to tend to infinity. The phase distribution of the state given by Eq.(2.8), is

$$P(\theta_m, t) = |<\theta_m|\Psi(t)>|^2, \tag{3.3}$$

with the expectation value and the variance

$$<\hat{\Phi}_\theta> = \sum_m \theta_m P(\theta_m, t), \tag{3.4}$$

$$<\Delta\Phi_\theta^2> = \sum_m (\theta_m - <\hat{\Phi}_\theta>)^2 P(\theta_m, t). \tag{3.5}$$

Now we choose the reference phase $\theta_0 = \eta - \pi s/(s+1)$, and introduced a new phase label $\mu = m - s/2$, which ranges in integer steps from $-s/2$ and $s/2$. When s tends to infinity we replace $\mu 2\pi/(s+1)$ by $d\theta$ and $2\pi/(s+1)$ by θ. Then we find a continuous phase distribution

$$P(\theta, \tau) = \frac{1}{2\pi}\{1 + 2\mathrm{sech}r \sum_{n,n',n>n'} \frac{[(2n)!(2n')!]^{1/2}}{n!n'!}(-\frac{1}{2}\tanh r)^{n+n'} \cos[2(n-n')\theta]\cos[2(n-n')\tau]\}, \tag{3.6}$$

where $\tau = gt$, $P(\theta_m, \tau)$ is normalized according to

$$\int_{-\pi}^{\pi} P(\theta, \tau) d\theta = 1, \tag{3.7}$$

The numerical calculation results of formula (3.6) are shown in Fig.1. In Fig.1, the phase distributions are plotted against θ in the polar coordinate system. It is seen from Fig.1, that as $\tau = 0$, the phase distribution has always circle shape for any values of τ. As τ is not equal to zero, the bifurcation of the phase distribution appears. At $\tau = 0$, as τ is increased, the circle shape splits into two separate leaves (Fig.1(a)). As the interaction is turned on, this circle shape splits into four separate leaves which rotate and change its shape (Fig.1(b) and (c)). The larger the squeezing parameter is, the more obvious the phase distribution splits. At $\tau = \pi/2$, the four satellite distributions become again two satellite distributions and rotate by $\pi/2$ from the state of $\tau = 0$(Fig.1(d)). At $\tau = \pi$, the shape of $P(\theta, \tau)$ is the same as that at $\tau = 0$ (Fig.1(a)), and so on.

Using Eq.(3.6), and replacing the summation in Eqs.(3.4) and (3.5) by an approrite integral for the variable θ, over the range $-\pi$ to π, and taking into accout $\theta_m = \theta + \eta$, in the limit as s tends to infinity, we obtain

$$<\hat{\Phi}_\theta> = \eta = \beta/2, \tag{3.8}$$

$$<\Delta\Phi_\theta^2> = \frac{\pi^2}{3} + \mathrm{sech}r \sum_{n>n'} \frac{[(2n)!(2n')!]^{1/2}}{n!n'!} \cdot (-\frac{1}{2}\tanh r)^{n+n'} \frac{1}{(n-n')^2} \cos[(2(n-n')\tau], \tag{3.9}$$

The numerical calculation results of the variance of phase given by formula (3.9) are illustrated in Fig.2(a). As $r = 0$, the phase variance of vacuum state is equal to $\pi^2/3$. which reflects random phase character. As $r \neq 0$, the phase variance shows periodic oscilation around $\pi^2/3$. The larger the squeezing parameter is, the larger the oscillational amplitude of phase variance is. The phase variance is calculated numerically as a function of r and plotted in Fig.3 for different values of τ. We see that the variance is departure from $\pi^2/3$ as r is increased.

In the limits of small r (weakly squeezed vacuum) and larger r (strongly squeezed vacuum), from Eq.(3.9), we can find respectively

$$< \Delta\Phi_\theta^2 >= (1/3)\pi^2 - 2^{-1/2} r\cos(2\tau) + 1/4(3/8)^{1/2} r^2 \cos(4\tau) + O(r^3), \tag{3.10}$$

$$< \Delta\Phi_\theta^2 >= \frac{1}{3}\pi^2 - A_1\cos(2\tau) + \frac{1}{4}A_2\cos(4\tau) - \frac{1}{9}A_3\cos(6\tau) + \frac{1}{16}A_4\cos(8\tau) + \cdots, \tag{3.11}$$

where

$$A_1 = \tanh r(1 - \frac{1}{2}\frac{\cosh r}{\sinh^2 r} + \frac{1}{2}\frac{1}{\sinh^2 r}), \tag{3.12}$$

$$A_2 = \tanh^2 r(1 - \frac{5}{12}\frac{\cosh^3 r}{\sinh^4 r} - \frac{3}{8}\frac{\cosh r}{\sinh^2 r} + \frac{5}{12}\frac{\cosh^2 r}{\sinh^4 r} + \frac{7}{12}\frac{1}{\sinh^2 r}), \tag{3.13}$$

$$A_3 = \tanh^3 r(1 - \frac{3}{8}\frac{\cosh^5 r}{\sinh^6 r} - \frac{5}{16}\frac{\cosh^3 r}{\sinh^4 r} - \frac{21}{64}\frac{\cosh r}{\sinh^2 r} + \frac{3}{8}\frac{\cosh^4 r}{\sinh^6 r} + \frac{1}{2}\frac{\cosh^2 r}{\sinh^4 r} + \frac{5}{8}\frac{1}{\sinh^2 r}, \tag{3.14}$$

$$A_4 = \tanh^4 r(1 - \frac{39}{112}\frac{\cosh^7 r}{\sinh^8 r} - \frac{63}{224}\frac{\cosh^5 r}{\sinh^6 r} - \frac{245}{896}\frac{\cosh^3 r}{\sinh^4 r} - \frac{539}{1792}\frac{\cosh r}{\sinh^2 r}$$
$$+ \frac{39}{112}\frac{\cosh^6 r}{\sinh^8 r} + \frac{51}{112}\frac{\cosh^4 r}{\sinh^6 r} + \frac{61}{112}\frac{\cosh^2 r}{\sinh^4 r} + \frac{73}{112}\frac{1}{\sinh^2 r}). \tag{3.15}$$

The numerical calculation results of the variance of phase given by formulas (3.10) and (3.11) are illustrated in Fig.2(b). We see that Fig.2(b) coincides well with Fig.2(a) plotted by exact formula (3.9).

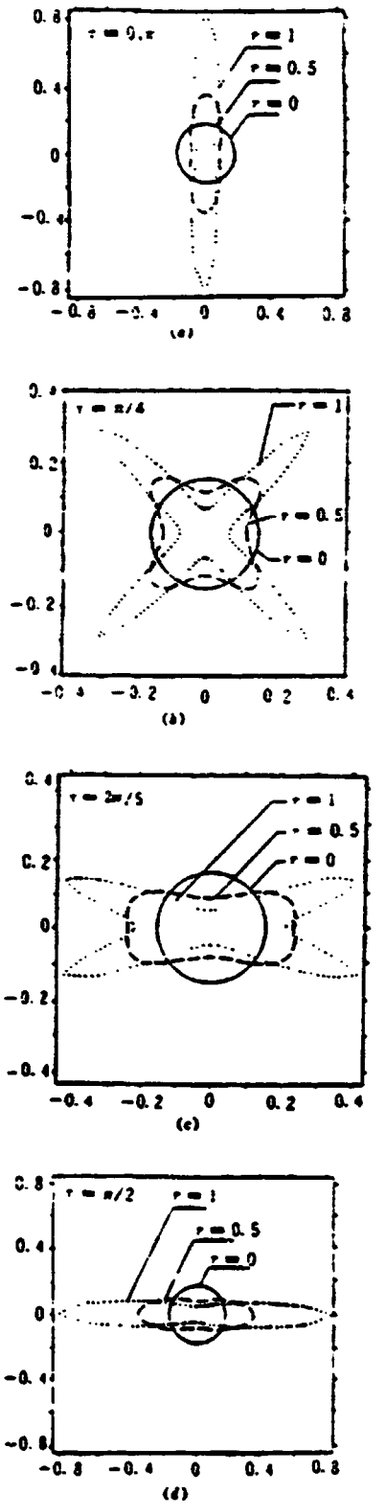

Fig.1. The phase distribution $P(\theta,\tau)$ plotted against θ in the polar coordinate system for various values of τ and different values of r.

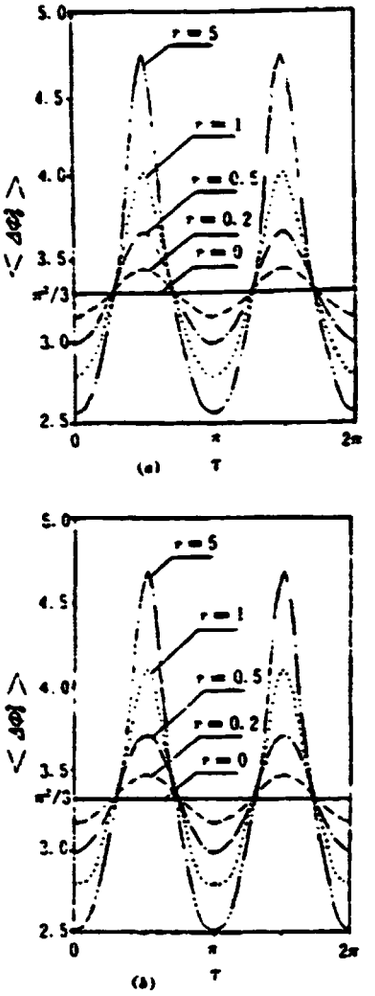

Fig.2. Plot of the phase variance $< \Delta\Phi_\theta^2 >$ as a function of τ for different values of r. (a) according to exact formula (3.9), (b) according to approximate formula (3.10) for $r = 0.2, 0.5$ and (3.11) for $r = 1, 5$.

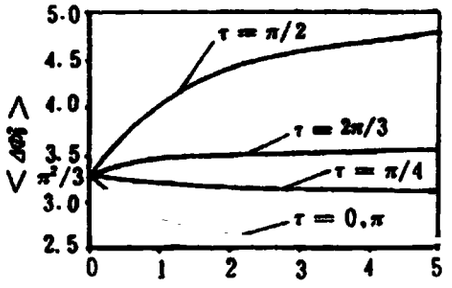

Fig.3. Plot of the phase variance $< \Delta\Phi_\theta^2 >$ as a function of r for different values of τ.

4 Conclusion

Using the Hermitian phase-operator formalism, the phase propeties of the squeezed vacuum intensity-couple interacting with an atom have been obtained. We have found that the bifurcation of the phase distribution appears as squeezing parameter is not equal to zero. At the initial time the phase distribution splits into two symmetric distributions, that is, two satellite leaves in a polar representation. As the interaction is turned on, the phase distribution splits into four symmetric distribution, that is, four satellite leaves which rotate and change its shape in a polar representation. At the scaled time $\tau = gt = \pi/2$, the four satellite leaves become again two satellite leaves and rotate by $\pi/2$ from the state of $\tau = 0$. We have also found that the phase variance shows periodic oscilation around $\pi^2/3$ as squeezing parameter is not equal to zero. This reflects the fact that the squeezed vacuum has the non-random phase character because of the squeezing.

Acknowledgments

This work is supported by the National Natural Science Foundation of China.

References

[1] B.C.Sanders, S.M.Barnett and P.L.Knight, Optics Comm.58,290 (1986)

[2] D.M.Yao, Phys.Lett.A122,77 (1987)

[3] H.Y.Fan and H.R.Zaidi, Optics Comm.68,143 (1988)

[4] L.Susskind and J.Glogower, Physics 1,49 (1964)

[5] J.A.Vaccaro and D.T.Pegg, Optics Comm.70,529 (1989)

[6] D.T.Pegg and S.M.Barnett, Europhysics Lett.6,483 (1988)

[7] S.M.Barnett and D.T.Pegg, J.Mod.Opt.36,7 (1989)

[8] D.T.Pegg and Barnett, Phys.Rev.A39,1965 (1989)

[9] H.T.Dung, R.Tanaś and A.S.Shumovsky, Optics Comm.79,462 (1990); J.Mod.Opt.38,2069 (1991)

[10] A.F.Fan, Optics Comm.98,340 (1993)

[11] A.F.Fan and Z.W.Wang, Phys.Rev.A 49,1509 (1994)

[12] V.Bužek, Phys.Lett.A 139,231 (1989)

[13] B.Buck and C.V.Sukumar, Phys.Lett. A 81,132 (1981)

[14] J.N.Hollenhorst, Phys.Rev. D 19,1669 (1979)

NEXT
DOCUMENT

QUANTUM NOISE IN LASER DIODES

E. Giacobino, F. Marin, A. Bramati, V. Jost
Laboratoire Kastler Brossel, Université Pierre et Marie Curie, F-75252 Paris Cedex 05 - France

J.-Ph. Poizat, J.-F. Roch, P. Grangier
Institut d'Optique, B.P. 147, F-91403 Orsay Cedex - France

T.-C. Zhang
Institute of Optoelectronics, Shanxi University, Taiyuan 030006, China

Abstract

We have investigated the intensity noise of single mode laser diodes, either free-running or using different types of line narrowing techniques at room temperature. We have measured an intensity squeezing of 1.2 dB with grating-extended cavity lasers, and 1.4 dB with injection locked lasers (respectively 1.6 dB and 2.3 dB inferred at the laser output). We have observed that the intensity noise of a free-running nominally single mode laser diode results from a cancellation effect between large anticorrelated fluctuations of the main mode and of weak longitudinal side modes. Reducing the side modes by line narrowing techniques results in intensity squeezing.

1 Introduction

Quantum noise in the intensity of a light beam can be viewed as the result of the random distribution of photons in the beam. It can be fully suppressed if the field is in a particular state where the number of photons is known perfectly, a photon number state. The reduction of the intensity noise below the standard quantum noise is then done at the expense of increased fluctuations in the phase, which is completely undetermined for a number state. Photon number states containing more than one photon have never been produced. However, specific non classical states of the light in which the intensity fluctuations are reduced have been generated using several kinds of methods. One of them relies on the fact that part of the quantum noise in the laser emission comes from the random character of the pumping process, which can be suppressed in some cases.

Quantum noise reduction in laser emission based on pump noise suppression was first predicted in 1984 [1]. Semiconductor lasers are particularly well suited for the implementation of this idea [2]. Furthermore, laser diodes are widely used and are considered as powerful and convenient tools in the field of telecommunications [3] and spectroscopy [4]. Their main advantages are compactness,

energy efficiency, tunability, and low intensity noise. It is the latter property that can be brought into the quantum domain by driving the laser with a current whose noise is well below shot-noise.

Since the noise in an electrical current is limited by thermal noise, it is easy to have a noise in the driving current that is well below shot noise. If the quantum efficiency of the carrier to photon conversion is high enough, the electron statistics of the pumping can be transferred to the light emission, yielding sub-poissonian operation of the laser. Quantum noise in the intensity of constant-current-driven laser diodes was observed for the first time by Machida *et al* in 1987 [5], and further improved to 8.3 dB in 1991 [6]. But the very mechanisms capable of explaining why some laser diodes and not others generate sub-shot-noise light remained unclear.

Actually, other factors than the constant current supply can be important for the noise reduction. In 1993, intensity squeezing was observed with so-called "single mode" commercial laser diodes by Steel and his group [7, 8]. It was shown that line narrowing techniques greatly helped in the noise reduction by further suppressing the weak but very noisy longitudinal side modes. We have investigated intensity noise of laser diodes, using various methods for line narrowing, including injection-locking with another diode laser and feedback from an external grating. The best intensity squeezing at room temperature was 1.4 dB (2.3 dB when corrected from the detection efficiency), and was obtained with injection-locking.

In order to explore the role of the line narrowing processes in squeezing more precisely, we have investigated the noise properties of the individual side modes. The arguments given in refs [7, 8] tended to suggest that the less powerful these side modes are, the less they will contribute to the total intensity noise. However, this argument ignores possible correlations between the modes, which were demonstrated for instance by Inoue *et al* [9] for multimode semiconductor lasers. We have shown that the noise of the free-running diode lasers results from a cancellation effect between very large anticorrelated fluctuations of the main mode on one hand, and of many weak longitudinal side modes on the other hand. When line-narrowing techniques are used, the total intensity noise goes below the shot-noise level [7, 8, 10], but we show that, in some cases, the sub-Poissonian character of the light can be due to a cancellation effect between large anticorrelated noises of the various modes. Thus sub-shot-noise operation of these lasers does not always correspond to single mode squeezing.

2 Experimental set-up

The laser diodes we have used are index-guided quantum well GaAlAs laser diodes (model SDL 5422-H1 and SDL 5411-G1). Appropriate electrical filtering is used on the power supply in order to stabilize the current. The free-running laser diodes have a low threshold of 18 mA and a differential quantum efficiency (slope above threshold) of 66%. The operating current in the experiments described below is typically 5 to 7 times larger than the threshold current, and the resulting high overall quantum efficiency is at the origin of squeezing. No squeezing was found in similar experiments performed on laser diodes with higher threshold (80 mA), which operate only twice above their threshold.

The quantum noise in the intensity is measured in the standard way with a balanced detection [11]. The beam going out of the laser is split in two equal parts by a beamsplitter. Each output of the beamsplitter is sent into a high efficiency (90%) photodiode. The amplified AC signals, proportional to the noise signals, are either subtracted or added by a RF +/- power combiner to

measure the shot-noise (in the difference position) and the intensity noise (in the sum position). We have then sent the laser beam through a high resolution monochromator (Jobin-Yvon HR1000) which allowed us to clearly separate the different modes. We have measured the noise both before and after the spectrometer.

3 Intensity squeezing

Intensity squeezing in the laser diodes was obtained by using constant current supply and line-narrowing techniques. either cavity extension with an external grating. or injection-locking with another laser.

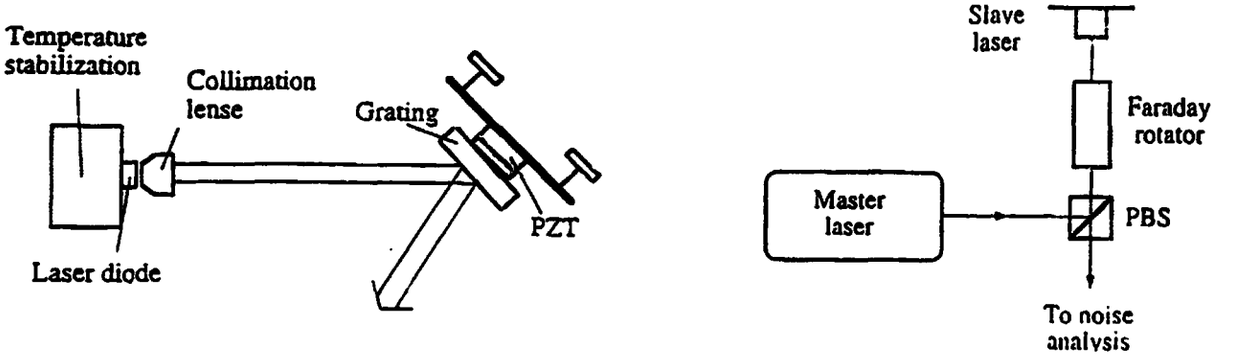

Figure 1: (a) external grating stabilization scheme; (b) injection locking scheme

The extended-cavity laser diode is shown in Fig. 1. The beam going out of the laser diode is collimated with a $f = 8$ mm objective placed in front of the output facet of the diode. The cavity is extended to 10 cm with a reflection holographic grating reflecting the first order into the cavity, while the 0 order goes out of the cavity (Littrow configuration). The efficiency of the grating is 60% in the 0 order (output coupling) and 24% in the first order (feedback to the laser). with 16% losses. The alignment of the grating is critical. When it is achieved. the threshold of the laser is lowered from 18 to 13 mA and the DC power of the side modes goes down to -60 dB below the DC power of the main mode. while the total intensity noise is decreased below the shot-noise level.

The injection-locking scheme is depicted in Fig. 1(b). The master laser is either an external-grating diode laser or a Ti:Sapphire laser. It is injected into the slave laser by means of an optical isolator. The master beam enters through the escape port of the polarizer placed after the Faraday rotator. Locking is observed on a rather broad power range of the master laser. from 1 to 4 mW.

We have investigated intensity squeezing in the two cases described above. Noise spectra were recorded for various supply currents. Squeezing was observed for currents higher than 50 mA ($I/I_{th} = 2.8$) for the injected laser and 30 mA ($I/I_{th} = 2.4$) for the extended cavity laser. at noise frequencies from 1 to 30 MHz (limited by our detection bandwidth). The noise. measured with a resolution bandwidth of 1 MHz. was nearly constant from 7 MHz to 30 MHz.

The optimum squeezing was observed in the injection-locking scheme. At 7 MHz. with a driving current of 130 mA. we obtained a noise reduction of 27%. i.e. 1.4 dB. Taking into account the total detection quantum efficiency of 65% from the laser output power to the photodiode current (through the optical isolator). we infer a value of 2.3 dB at the output of the laser diode.

The best squeezing obtained with the grating-extended cavity is 25% (1.2 dB) at 30 MHz and 110 mA. from which we infer a 1.6 dB noise reduction at the output of the grating. The fact that the squeezing is better with the injection-locking scheme can be attributed to the large losses due to the grating.

These numbers are similar to those of refs. [7, 8]. They are below the theoretical maxima expected from the quantum efficiency of the laser. which are respectively of 58% (3.8 dB) at 130 mA for the injected laser and 42% (2.4 dB) at 110 mA for the grating-extended cavity. Actually, the ratio between the intensity squeezing and the current-to-current efficiency goes towards a maximum asymptotical value of 0.75. instead of the expected unity value. The authors quoted above obtained comparable values for this ratio. This non-unity value can be attributed to additional noise sources in the semiconductor devices which are not included in the simple theoretical prediction mentionned above.

4 Intermode correlat .on

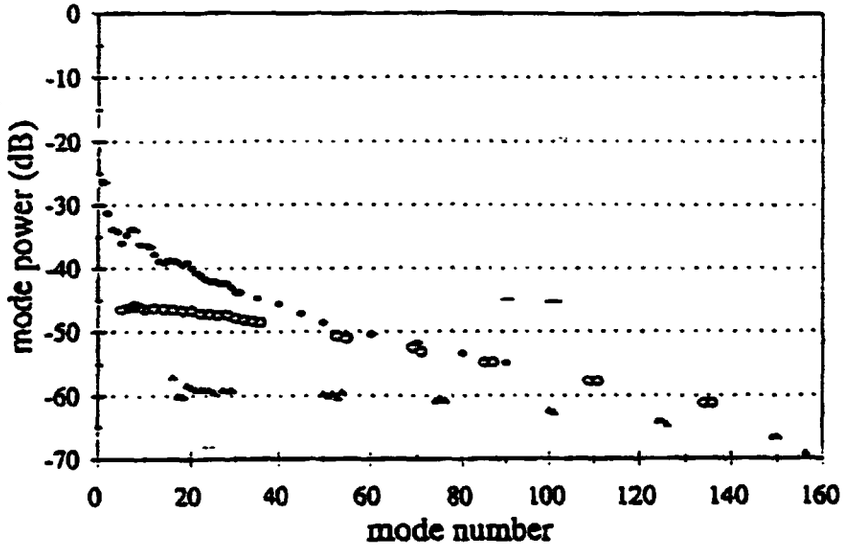

Figure 2: Power of individual longitudinal modes for a driving current of 80 mA. On the x-axis each mode is labelled by a number. the number 0 corresponding to the main mode. (• : free-running laser. o : injection-locked laser. ▲ : extended cavity laser).

The free-running laser diodes apparently operates on a single mode. However. the longitudinal side modes have a non negligible power. the closest ones being only -10 to -25 dB below the main mode (Fig. 2). For the free-running laser. the power of one of the first side modes is typically -25

dB lower than the one of the main mode (see Fig. 2), and the total power in the side modes is about -18 dB below the main mode.

As far as the noise of the individual modes is concerned, we have observed that the intensity noise of the main mode alone is much higher than the total intensity noise. For example, for a driving current of 80 mA the main mode exhibits an excess noise of + 39 dB, while the total intensity noise is only 2 dB above SNL. The intensity noise of the sidemodes is then expected to be comparable to the intensity noise of the main mode despite their much weaker power. To check this assumption, we compared the noise of the main mode alone to the noise of the main mode plus two side modes, four side modes, etc. For this measurement, the output slit of the spectrometer was kept centered on the main mode, and was progressively opened. Figure 3 shows that the intensity noise decreases, with steps corresponding to the point where symmetrical side modes enter the detector. This clearly demonstrates that the observed total intensity fluctuations results from a cancellation effect between the very large anticorrelated fluctuations of the main mode and of the side modes. In fact, all of the 160 side modes displayed in Fig. 2 contribute to some extent to this cancellation effect.

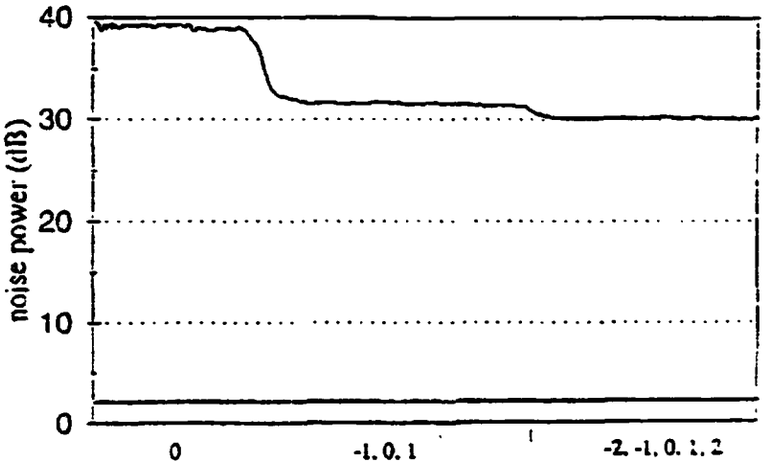

Figure 3: Intensity noise of the free-running laser diode, referred to the shot noise, as the output slit is opened. In the first section, only the main mode is detected, while the two steps correspond to the entrance of the two couples of side modes (-1,1) and (-2,2). The straight line at 2 dB shows the total intensity noise level (measured before the spectrometer).

As can be seen from Fig. 2, the power of the first side modes of the injection-locked laser is reduced down to less than -45 dB below the main mode, while the total power in the side modes is -30 dB below the main mode. The total intensity noise referred at the laser output is now squeezed by -2.3 dB below SNL (see [10]), while the intensity noise of the main mode alone is still well above the quantum limit. The total intensity noise of the injection-locked laser again results from a cancellation effect among anticorrelated fluctuations of the main and side modes. In this case the sub-Poissonian intensity noise is not single mode squeezing.

For the laser in the extended cavity configuration, the side modes are suppressed further, to about -55 dB below the main mode (see Fig. 2), which corresponds to a total side mode power of

-35 dB below the main mode. In that case, we have noticed virtually no difference between the total intensity noise and the noise of the main mode alone. In this case, and only in this case, it can be concluded that the side modes are actually negligible, and that true single-mode squeezing is generated.

Acknowlegments. This research was carried out in the framework of the ESPRIT Basic Research Project 6934 QUINTEC, and of the HCM network "Non-Classical Light" (ERB CHRX CT93 0114). Two of us aknowledge the support of fellowships : A.B. was supported by the HCM program from the European Community (ERB CHBG CT93 0437), and T.C.Z. was supported by a Programme International de Coopération scientifique (PICS) sponsored by the CNRS.

References

[1] Yu. M. Golubev, I.V. Sokolov, Zh. Eksp. Teor. Phys, **87**, 804, (1984) (Sov. Phys. JETP **60**, 234 (1984)).

[2] Y. Yamamoto, S. Machida, and O. Nilsson, Phys. Rev. A **34**, 4025 (1986).

[3] See for example, J.-C. Bouley and G. Destefanis, IEEE Comm. Magazine **32**, 54 (1994).

[4] C.E. Wieman and L. Hollberg, Rev. Sci. Instrum. **62**, 1 (1991).

[5] S. Machida, Y. Yamamoto, and Y Itaya, Phys. Rev. Lett. **58**, 1000 (1987).

[6] W.H. Richardson, S. Machida, and Y. Yamamoto, Phys. Rev. Lett. **66**, 2867 (1991).

[7] M.J. Freeman, H. Wang, D.G. Steel, R. Craig, and D. R. Scifres, Opt. Lett. **18**, 2141 (1993).

[8] H. Wang, M.J. Freeman, and D.G. Steel, Phys. Rev. Lett. **71**, 3951 (1993).

[9] S. Inoue, H. Ohzu, S. Machida, and Y Yamamoto, Phys. Rev. A **46** 2757 (1992).

[10] T.-C. Zhang, J.-Ph. Poizat, P. Grelu, J.-F. Roch, P. Grangier, F. Marin, A. Bramati, V. Jost, M.D. Levenson and E. Giacobino, Quantum Semiclass. Opt., **7**, 601 (1995).

[11] H.P. Yuen and V.W.S. Chan, Opt. Lett. **8**, 177 (1983)

NEXT
DOCUMENT

Competition effect in atomic-molecular system*

Jia Suotang, Qin Lijuan, Qian Zuliang,Wang Zugeng
Department of Physics,East China Normal University,Shanghai 200062

Wang Gang,Zhou Guosheng
Department of Electronics Information Technology,
Shanxi University,Taiyuan 030006

Abstract

The competition effects among the processes of atomic ionization, optical pumped stimulated radiation(OPSR),four-wave frequency mixing (FWFM) and molecular stimulated diffuse band radiation at the atomic two-photon resonance of $3S \rightarrow 4D$ in $Na_2 - Na$ mixture were observed. The dip at the two-photon resonance in the excitation spectrum for the diffuse-band radiation was interpreted as suppression of population in $4D$ state.

1 Introduction

The generating and utilizing of molecular diffuse-band radiation is an important subject for studying excimer lasers and atomic-molecular physics. The various mechanisms of producing molecular diffuse-band stimulated radiaton were developed, for example, in atomic-molecular system the stimulated radiation from high-lying triple state to low triple state could be obtained by two-photon resonantly exciting atoms then following collision between atoms in high-lying excited state and molecules in the ground state[1-2]. This is an efficient process of producing diffuse-band stimulated radiaton. However there are others processes accompanying process of two-photon resonantly exciting atoms: The photo-ionization process following two-photon resonance,the stimulated radiation starting from high-lying excited state of atoms,four-wave frequency mixing process. The competition effect occuring in above processes resulted in decreasing molecular diffuse- band stimulated radiation. In this paper,we not only finded optimum condition of producing molecular diffuse-band stimulated radiation but also understand clearly the interaction among nonlinear processes through studying the competition effect.

2 Experiment

The laser beam from a Nd:YAG pumped dye laser(Quanta Ray DCR-3D,PDL-2) was focused into the center of the crossed heat-pipe oven by an optical system. Using RD590 dye, the output energy

*Project Supported by the National Natural Science Fundation of China
and the Natural Science Fundation of Shanxi Province of China

of the tunable dye laser was about 40 mJ at the wavelength region from 565 nm to 591 nm with line width about 0.1 cm^{-1} and pulse width of 8ns. The mixture vapor of atomic and molecular sodium was produced by the heat-pipe oven containing pure sodium sample, the densities of atomic and molecular sodium were determained by the temperature of the oven center. An ionization detector was installed in the heat-pipe oven to measure photo-ionization signal when optical signal being detected. The buffer gas was not filled in the oven. The radiation from the forward direction of the oven was received after passing the monochromater, then photo- electric signal was fed into channel B of the BOXCAR. At the same time the ionization signal produced from two-photon resonance three-photon ionization was introduced by a resistance of 10KΩ and sent to channel A of the BOXCAR. The optical and the ionization signals were monitored by oscilloscope 1 and 2 respectively. The BOXCAR and the two oscilloscopes were trigged by a photo-electric detector as receiving a small pulse signal of the laser. Because of the different time decay behavior for optical and ionization signals, the different time delay and gate widths of two gates were chosen to get the higher signal- noise rate of the average value of the signals. All measurements were performed under the condition that the laser energy was stabilized, which was guaranteed through monitored laser energy in the experiment. The error, which is brought about by the fluctuation of the sample temperature, could be reduced with the help of high accuracy of the temperature controller.

3 Results and discussion

The part of energy-level diagram of atomic and molecular sodium is shown in Fig.1. After atomic sodium transition from the ground state $3S$ to $4D$ state produced by two- photon excitation corresponding to laser wavelength of 578.7 nm,there are some possible processes:
(1) The two-photon resonance three-photon ionization through the atoms in the $4D$ state absorbing one more photon.

$$Na(4D) + h\nu \xrightarrow{\text{ionization}} Na^+ + e^- \tag{1}$$

(2) The optical pumped stimulated radiation owing to population inversion between $4D$ and $3P$ states, $4D$ and $4P$ states.

$$Na(4D) \xrightarrow{\text{radiation}} Na(4P) + h\nu(2.33\mu m) \tag{2}$$

$$Na(4D) \xrightarrow{\text{radiation}} Na(3P) + h\nu(568.6nm, 568.8nm) \tag{3}$$

(3) The four-wave frequency mixing by nonliear interaction between pumping wave and optical stimulated radiation wave in the sodium vapor:

$$h\nu_{uv} = 2h\nu_L - h\nu_{IR} \tag{4}$$

where, $\nu_L, \nu_{IR}, \nu_{uv}$ are the frequencies of pumping optical wave,optical pumped stimulated radiation wave and coherent radiation wave respectively
(4) The diffuse-band stimulated radiation generated by transition from high-lying triplet state populated through collision between atoms in $4D$ state and molecules in the ground state.

$$Na(4D) + Na_2(X^1\Sigma_g^+) \xrightarrow{\text{collision}} Na_2(^1\Lambda_g, 2^3\Pi_g) + Na(3S) \tag{5}$$

$$Na_2(^1\Lambda_g) \xrightarrow{\text{collision}} Na_2(2^3\Pi_g) \quad (6)$$

$$Na_2(2^3\Pi_g) \xrightarrow{\text{radiation}} Na_2(a^3\Sigma_u^+) + h\nu(around436.0nm) \quad (7)$$

To understand the competition among the reaction processes above under different temperature, the four kinds of signal were measured respectively. The change of excitation spectrum measured with temperature for producing the diffuse-band stimulated radiation of molecular sodium are shown in Fig.2. For the ionization signals,optical pumped stimulated radiation signal, measurements which is similar to Fig.2.were also done and the changes of those signals at different temperatures were also obtained.The result showed clealy:the optimum temperature was different for producing the above signals. For example, the diffuse-band signal gradually approached zero at low temperature.But with increasing of the temperature, it not only increased at the two-photon resonance exciting of $3S \rightarrow 4D$, but also could be observed in the certain wavelength region corresponding to offset of $3S \rightarrow 4D$.When oven temperature arrived 380°C, the diffuse-band radiation signal reached maximum. As the temperature continusly increases (350 – 370°), the diffuse-band signal at the position of atomic resonant excitation weakened. However, it rose on two sides of resonant excitation of atoms. As the temperature was above $410°C$, the peak of atomic resonant excitation disappeared.At $450°C$,the "dip" appeared at the position of atomic resonant excitation. Such a phenomenon has been observed in our provious work about molecular potassium[3–4].
The changes of various signals generated by two- photon resonant excitation of atoms($3S \rightarrow 4D$) with temperature were shown in Fig.3. Within the temperature below $310°C$, there were two processes of atomic ionization and molecular diffuse-band radiation but OPSR and FWFM signals weakened, the ionization signal started to increase at 150°. It reached the maximum at the $250°C$, but diffuse-band signal decreased; When the temperature was above $250C$, the ionization signal started to decreas, but the diffuse-band signal increased.When the ionization vanished at $340°C$, the diffuse-band signal reached the maximum. Apparently, there was the competition between two-photon resonance three- photon ionization and the collisional population from excited state atoms to molecules.
In the range of 340 – 500°, the ionization signal weakened but OPSR and FWFM signals started to increase,at 390° both of them reached the maximum value, the diffuse-band signals started to fall from the maximum value. When the temperature continused to increase, OPSR and FWFM signals reduced. This fact shown that in the temperature of 340° to $500°C$, there were apparent competitions among the processes described in eq.(1) to eq.(4b). The presence of OPSR and FWFM depopulated atoms in $4D$ state. This led to decrease the population in high-lying states of molecule. The transmission spectrum of laser light passing the sodium vapor is shown in Fig.4. There was a intense absorption at the two-photon resonance excitation of atom but the diffuse-band radiation was still small. This could also indicated that the population in $4D$ state was suppresed by other reaction processes.

We should notice that with rising of temperature, the density of molecular sodium increased too. So the diffuse-band radiation by two-photon exciting Na_2 in wider rage of pumping wavelength could be produced. This have been proved in our previous paper[5]. In the present experiment, the diffuse-band stimulated radiation could be detected in the excitation wavelength range of 577-580 nm. It increased with temperature as shown apparently in Fig.2. At low temperatures, the diffuse-band radiation signal were composed of the intense signal got by two-photon

excitation of Na and the weaken signal got by two-photon excitation of Na_2; with increasing of temperature, the signal of Na_2 also increased. At high tempwerature, the diffuse- band signal produced by two-photon excitation of Na_2 was large. At the position of two-photon resonant absorption of atoms,the possible reason for the appearence of "dip" can be as follows: (1) The two-photon absorption of atomic sodium decreased the excitation of Na_2.(2) After atomic sodium being populated in $4D$ state, the collisional transfer from atoms to molecules was decreased.

4 Conclusion

The competition among the processes in producing diffuse-band by the collisional transfer of energy from atoms to molecules, four-wave frequency mixing and three-photon ionization were studied in experiment. At lower temperatures, there was mainly the competition between diffuse-band stimulated radiation and two-photon resonance three- photon ionization of atoms;At high temperatures, there was the interaction among the diffuse-band stimulated radiation, optical pumped stimulated radiation and four-wave frequency mixing; At further higher temperatures, the "dip" at the position of two-photon excitation of atoms for excitation spectrum of producing diffuse-band radiation resulted from the coherent process of optical pumped stimulated radiation and four-wave frequency mixing supressing the non coherent process of collisional transfer energy from atoms to molecules.

References

[1] Z.G.Wang, L.S.Ma, H.R.Xia, K.C.Zhang, I.S.Cheng,Opt.Commun.,58(1986),315.

[2] C.Y.Robert Wu,J.K.Chen,D.L.Judege,C.C.Kim,Opt.Commun.,48(1983),28.

[3] S.T.Jia,Y.Wang,G.Wang,S.L.Deng,L.J.Qin,G.S.Zhou,Z.G.Wang,Optica Acta Sinica,13(1993),865.

[4] S.T.Jia,L.J.Qin,Y.Wang,G.S.Zhou,Z.G.Wang,Chinese Journal of Lasers,B2(1993),527

[5] Z.G.Wang,K.C.Zhang,X.L.Tang,I.S.Cheng,Optica Acta Sinica,6(1986),1081.

Captions of Figure

Fig.1. The part of energy-level diagram of Na_2 and Na.

Fig.2. The excitation spectra for generating diffuse band radiation from transition of $2^3\Pi_g \rightarrow a^3\Sigma_u^+$.

Fig.3. The dependence of four kinds of signal on temperature for two-photon transition $3S \rightarrow 4D$.

Fig.4. Transmission spectrum in sodium vapor at $450°C$.

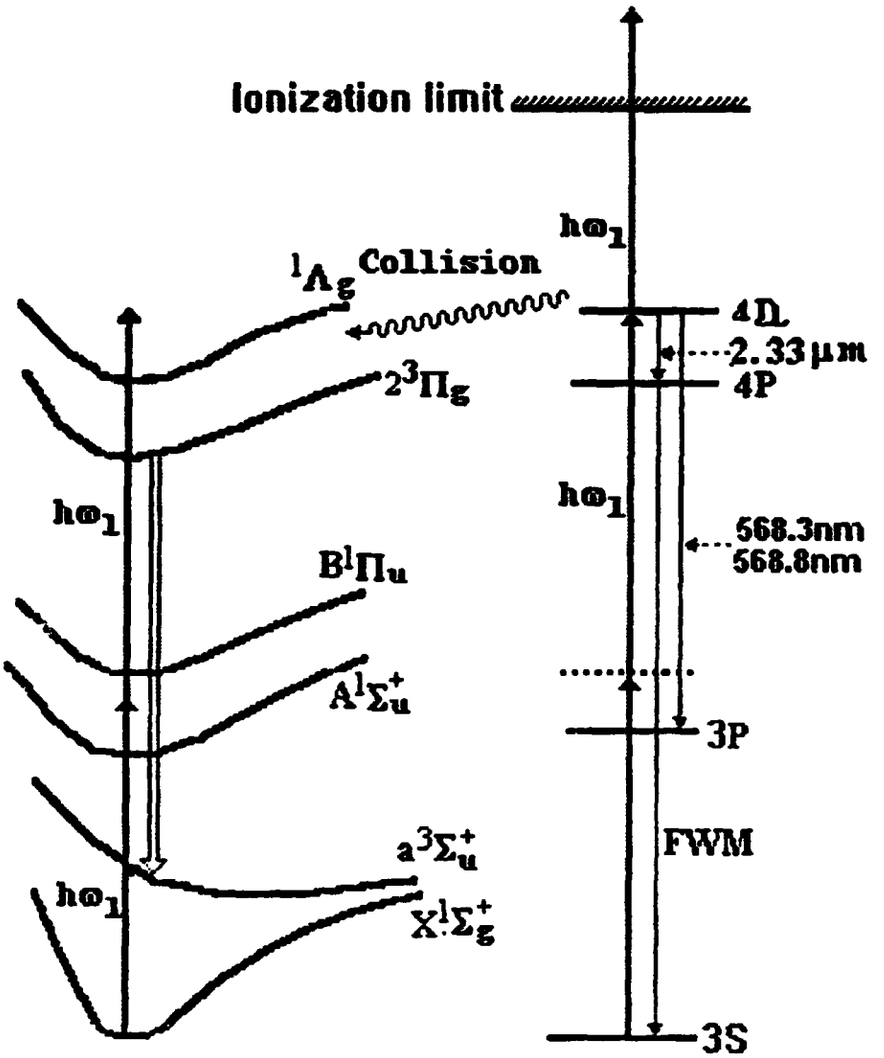
Ionization limit
hω1
1Ag
Collision
4D
2.33 μm
4P
2³Πg
hω1
hω1
568.3nm
568.8nm
B¹Πu
A¹Σu+
3P
a³Σu+
FWM
hω1
X¹Σg+
3S

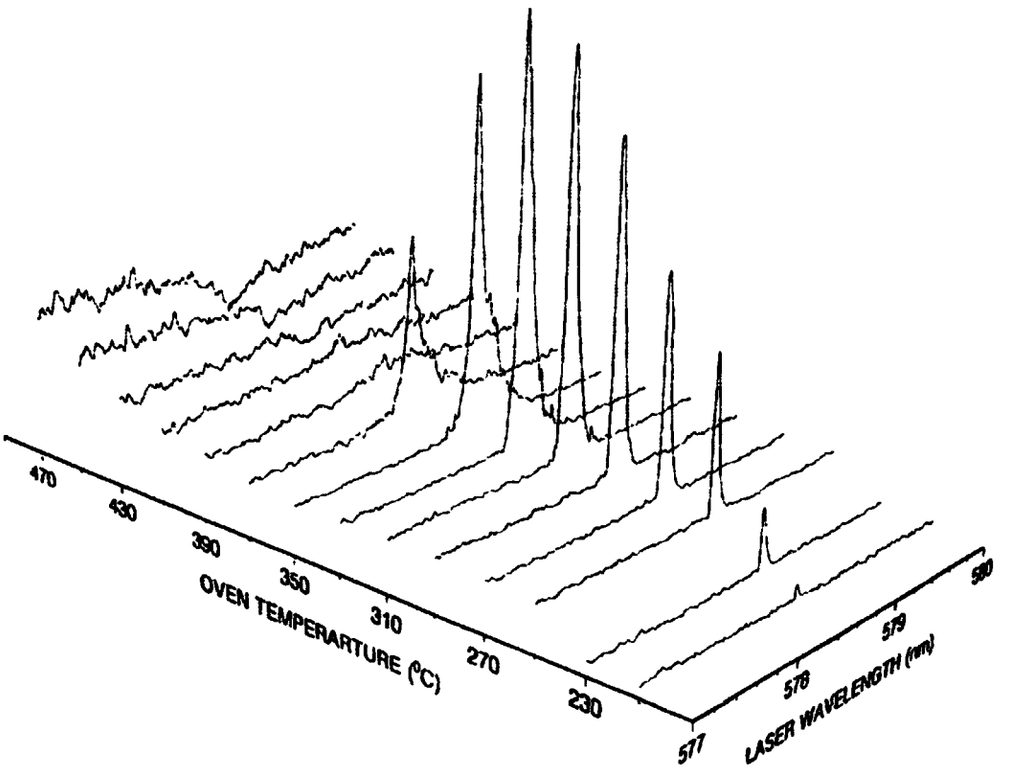
470
430
390
350
310
270
230
OVEN TEMPERARTURE (°C)
577
578
579
580
LASER WAVELENGTH (nm)

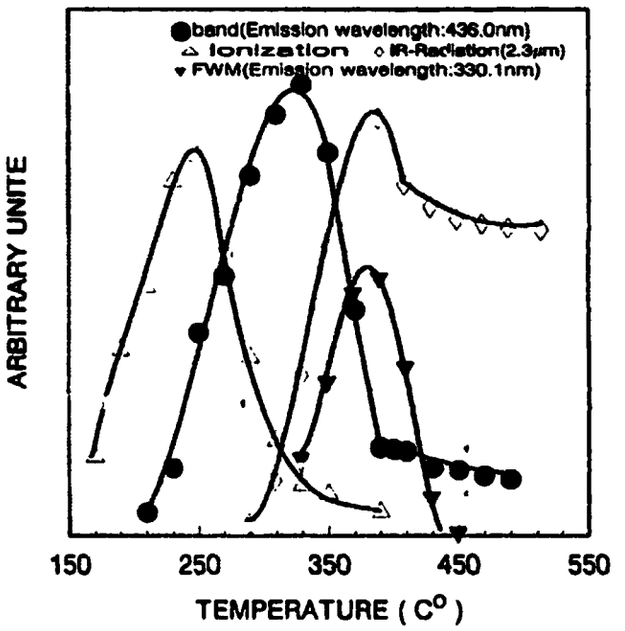
band(Emission wavelength:436.0nm)
Ionization
IR-Radiation(2.3μm)
FWM(Emission wavelength:330.1nm)
ARBITRARY UNITE
150
250
350
450
550
TEMPERATURE (C°)

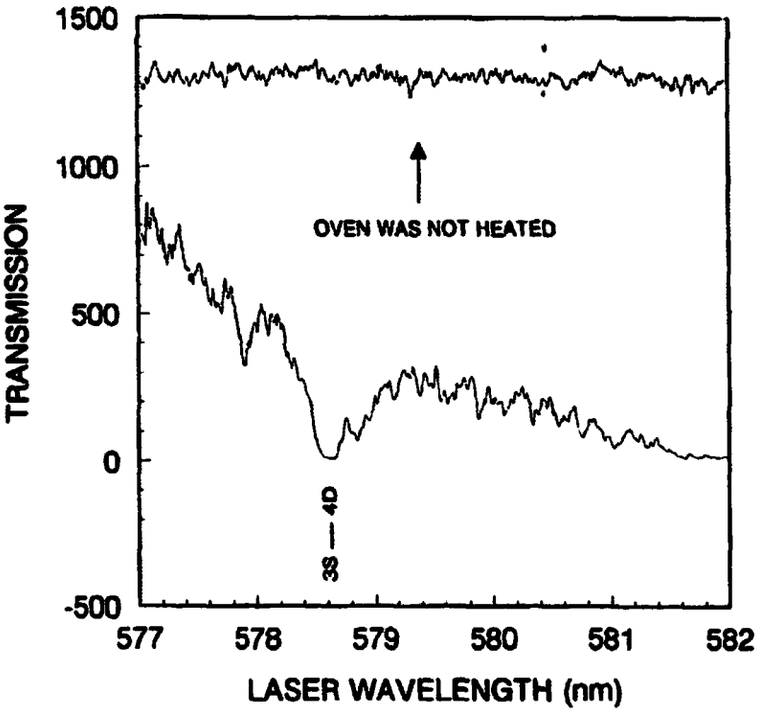
1500
1000
500
0
-500
TRANSMISSION
OVEN WAS NOT HEATED
3S — 4D
577
578
579
580
581
582
LASER WAVELENGTH (nm)

NEXT
DOCUMENT

FOCK STATE GENERATION FROM THE NONLINEAR KERR MEDIUM

W. Leoński and R. Tanaś
Nonlinear Optics Division, Institute of Physics, Adam Mickiewicz University, Grunwaldzka 6, 60-780 Poznań, Poland.

Abstract

We discuss a system comprising a nonlinear Kerr medium in a cavity driven by an external coherent field directly or through the parametric process. We assume that the system is initially in the vacuum state, and we show that under appropriate conditions, i.e., properly chosen detuning and intensity of the driving field, the one or two-photon Fock states of the electromagnetic field can be achieved.

1 One-photon state generation

The model discussed here contains a nonlinear Kerr medium, described as an anharmonic oscillator, placed in a lossless cavity driven by an external coherent field. The coupling of the cavity field with the external field is governed by the following Hamiltonian in the interaction picture (we use units of $\hbar = 1$):

$$\hat{H}_{ext.} = \epsilon \left(\hat{a} + \hat{a}^{\dagger} \right) \ , \tag{1}$$

where ϵ denotes the strength of the coupling, whereas $\hat{a}$ and $\hat{a}^{\dagger}$ are the annihilation and creation operators of the cavity field, respectively. The Hamiltonian corresponding to the dynamics of the nonlinear Kerr medium in the cavity can be written as follows :

$$\hat{H}_{Kerr} = \frac{\lambda}{2} \hat{n} \left(\hat{n} - 1 \right) \ , \tag{2}$$

where λ is proportional to the third-order nonlinear susceptibility of the medium and $\hat{n}$ is the photon number operator. Our aim here is to determine the time evolution of the system. We assume that the system is initially in the vacuum state $|0\rangle$. Moreover, we assume that the external field driving the cavity according to (1) is weak, i.e. $\epsilon \ll \lambda$. In consequence, we can treat the problem perturbatively with respect to the small parameter ϵ.

Let us express the state of the system in a Fock basis:

$$|\Psi(t)\rangle = \sum_{j=0}^{\infty} a_j(t) \, |j\rangle \ . \tag{3}$$

This state vecto. obeys the Schrödinger equation with the Hamiltonians expressed by eqs. (1,2):

$$i \frac{d}{dt} |\Psi(t)\rangle = \left(H_{Kerr} + H_{ext.} \right) |\Psi(t)\rangle \ . \tag{4}$$

Applying the standard procedure to the state vector (3) and the Hamiltonians (1,2), we obtain a set of equations for the probability amplitudes a_j. Although this set of equations is infinite, it can be shown [1] that due to the degeneracy of the Hamiltonian (2) and the weakness of the driving field the system dynamics is restricted to the subspace of the degenerate states. In consequence, the evolution of the systems starts from the vacuum $|0\rangle$ and the only state that can be essentially populated with the driving field, according to (1), is the one photon state $|1\rangle$. The crucial point of our considerations is the fact that the unperturbed Hamiltonian for the Kerr process (2) produces degenerate states $|0\rangle$ and $|1\rangle$. In practice, we deal here with a situation analogous to that discussed in the paper [2] and we can write the following equations of motion for the probability amplitudes:

$$\begin{aligned} i\frac{d}{dt}a_0(t) &= \epsilon a_1 \ , \\ i\frac{d}{dt}a_1(t) &= \epsilon a_0 \ . \end{aligned} \tag{5}$$

Assuming $a_0(t=0)=1$ and $a_1(t=0)=0$ we get the following solution for the probability amplitudes

$$\begin{aligned} a_0 &= i\cos(\epsilon t) \ , \\ a_1 &= \sin(\epsilon t) \ . \end{aligned} \tag{6}$$

We treat eq.(6) as the zero-order solution. For this order the amplitude $a_2 = 0$. To obtain the formula for a_2 we need higher order solutions. We write the first-order formula for a_2:

$$a_2 = -\frac{\epsilon\sqrt{2}}{\lambda}\sin(\epsilon t) + O(\epsilon^2) \ , \tag{7}$$

where we have removed all terms proportional to ϵ^2. Obviously, we are in a position to perform this perturbative procedure due to the fact that the coupling (1) is weak, i.e. ($\epsilon \ll \lambda$). Moreover, since we are interested in finding the time evolution of the probabilities rather than the amplitudes a_j, we neglect the influence of the dynamics of the state $|2\rangle$ on the system as being proportional to ϵ^2.

To verify these results we shall now perform a numerical experiment and compare its results with those based on formulas (6). This will be done similarly as in the paper [3].

The history of our system is governed by the unitary evolution operator $\hat{U}(t)$ defined as follows:

$$\hat{U}(t) = \exp(-i\hat{H}t) \ . \tag{8}$$

Hence, the state vector $|\Psi(t)\rangle$ for arbitrary time t can be expressed as:

$$|\Psi(t)\rangle = \hat{U}(t)\,|0\rangle \, . \tag{9}$$

For numerical calculations we use the number state basis, which is truncated as to obtain sufficient numerical accuracy.

Fig.1 shows the probabilities of finding the system in the vacuum $|0\rangle$ and one-photon states $|1\rangle$. We assume that for the time $t = 0$ the field was in the vacuum state

($a_0(t=0)=1$), and that the coupling (1) is weak, i.e., $\epsilon = \pi/50 \ll \lambda$ (in units of $\lambda = 1$).

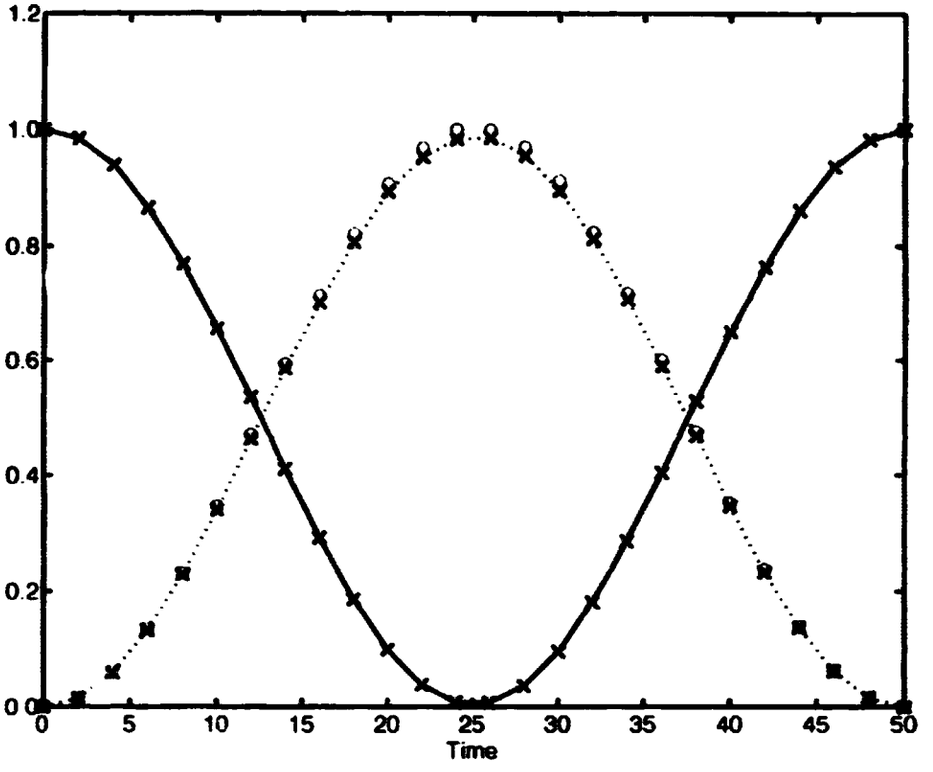

FIG.1 Analytical solutions for the probabilities of the vacuum (solid line) and one-photon (dotted line) states, and the mean number of photons (circle marks) obtained from the numerical experiment. The parameter $\epsilon = \pi/50$ (all parameters are measured in units of $\lambda = 1$). X-marks correspond to the probabilities found in the numerical experiment.

We see that our analytical results (solid and dashed lines) agree perfectly with those generated in the numerical experiment (star marks). The system starts to evolve from the vacuum and after the time $t = 25$ the probability $|a_1|^2 = 1$. This means that at this moment of time the field is in the pure one-photon state. For longer times the system returns to its initial state and starts to evolve in the same way as from $t = 0$. Moreover, we have plotted in Fig.1 the time dependence for the mean number of photons $n(t)$ (dotted line)

$$n(t) = \langle \Psi(t=0)| \hat{U}^{\dagger}\hat{a}^{\dagger}\hat{a}\hat{U} |\Psi(t=0)\rangle \tag{10}$$

found in our numerical experiment. It is seen that the behavior of $n(t)$ reflects the evolution of the probabilities and oscillates between 0 ad 1. One should keep in mind, however, that if we increase the strength of the external coupling the picture changes drastically. For this situation the perturbation procedure breaks down. In consequence, as it is visible from the numerical

experiment, higher n-photon Fock states start to play a significant role. Fig.2 shows the probability amplitudes for $\epsilon = \pi/15$. We see that the influence of the amplitude corresponding to the two-photon state becomes visible and perturbs the dynamics of the vacuum and one-photon states significantly. Of course, results of the numerical experiment become different from those obtained analytically under assumption of week coupling.

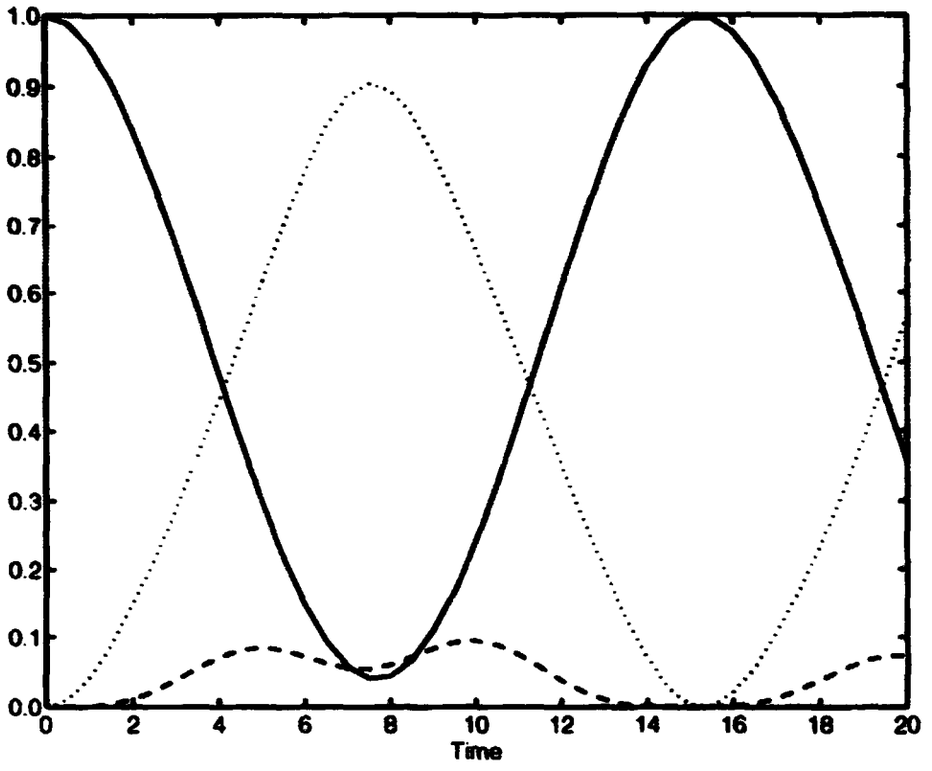

FIG. 2. The probability amplitudes corresponding to the vacuum (solid line), one-photon (dotted line) and two-photon (dashed line) states. The strength $\epsilon = \pi/15$ and the remaining parameters are the same as in Fig.1.

2 Two-photon state generation

Now, we consider a system containing the nonlinear Kerr medium which is parametrically excited by the electromagnetic field. The parametric excitation seems to be more suitable for the experimental realization of the model than the previous one. In this case the system is governed by the following Hamiltonian:

$$H = \frac{\chi}{2} n(n-2) + \epsilon \left(\left(a^{\dagger}\right)^2 + (a)^2 \right) , \tag{11}$$

where the $\hat{n}(\hat{n}-1)$ is replaced by $\hat{n}(\hat{n}-2)$. This replacement can be justified by the appropriate choice of the detuning. With such a choice of the detuning the states $|0\rangle$ and $|2\rangle$ are degenerate,

and the parametric process, second term in (11), couples resonantly the two states This suggests that the dynamics of the system will be restricted to the two states if the coupling is sufficiently weak. Except for a special choice of the detuning, the system discussed here resembles that discussed by Milburn [4], and Milburn and Holmes [5]. However, their model involved series of ultra-short excitations, whereas in this paper we assume continuous excitation.

Applying the same procedure as that for the one-photon state generation case we get the following equations for the probability amplitudes:

$$\begin{aligned} i\frac{d}{dt}a_0(t) &= \epsilon\sqrt{2}a_2 \ , \\ i\frac{d}{dt}a_2(t) &= \epsilon\sqrt{2}a_0 \ . \end{aligned} \tag{12}$$

We again assume that $a_0(t=0)=1$. In consequence the solutions for the amplitudes a_0 and a_2, to which the dynamics is restricted, are of the following form:

$$\begin{aligned} a_0 &= i\cos\left(\epsilon\sqrt{2}t\right) \ , \\ a_2 &= \sin\left(\epsilon\sqrt{2}t\right) \ . \end{aligned} \tag{13}$$

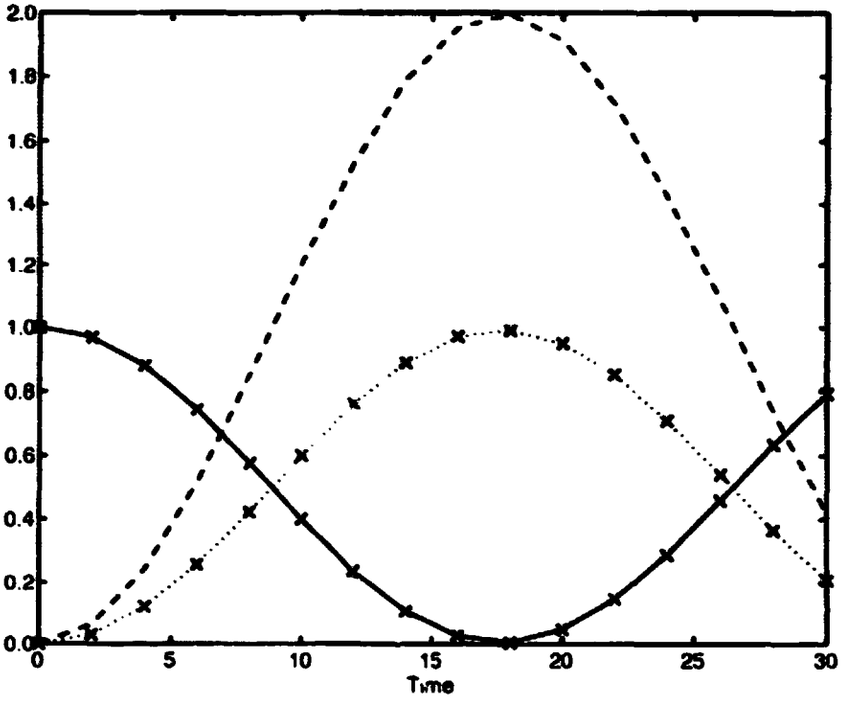

FIG. 3. Analytical solutions for the probabilities of the vacuum (solid line) and two-photon (dotted line) states, and the numerically found mean number of photons (dashed line). The parameters $\epsilon = \pi/50$, $\lambda = 1$. Marks correspond to the numerical experiment results.

Obviously, formulas (13) are the zero-order solutions analogously as for the one-photon state (eq.(6)). Moreover, we shall perform numerical experiment and compare its results with those of eq.(13) again. For this case the unitary evolution operator $\hat{U}$ is constructed on the basis of the Hamiltonian defined in (11). Fig.3 depicts the probability amplitudes for the vacuum $|0\rangle$ and two-photon states $|2\rangle$ obtained from the eq.(13) and from the numerical experiment. We see very good agreement between the perturbative analytical results and those obtained from the experiment again. The system starts its evolution from the vacuum state and after the time $t = \pi/\left(2\sqrt{2}\epsilon\right) \simeq 17.7$ the two-photon Fock state is reached. Moreover, the numerical results show that the probability for the four-photon $|4\rangle$ state is proportional to $\epsilon^2 \simeq 3 \cdot 10^{-3}$ and can be neglected for the case discussed here.

3 Conclusions

We have shown here that it is possible to generate the one-photon and two photon Fock states by the use of nonlinear Kerr media placed in a lossless cavity driven by a week external field. This generation is associated with resonant transitions between two Fock states and can be described analytically using standard perturbative procedure. Moreover, we have performed numerical experiments that show very good agreement with the analytical solutions. Of course, our considerations are based on a very simple model, and one should realize that many difficulties, for instance damping processes, can obscure the model and make it difficult to realize in practical experiments. Although it was not the aim of this paper to investigate the influence of such obstacles, one should keep in mind the fact of their existence. A short discussion of these problems was given in [3].

Acknowledgments

This work was supported by the Polish Committee for Scientific Research (KBN) under the grant No. 2 P03B 128 8.

References

[1] W. Leoński, S. Dyrting, and R. Tanaś, Coherence and Quantum Optics VII, Rochester, 1995, and in preparation

[2] W. Leoński, Acta.Phys.Slov. **45**, 383 (1995).

[3] W. Leoński and R. Tanaś, Phys.Rev. A **49**, R20 (1994).

[4] G. J. Milburn, Phys.Rev. A **41**, 6567 (1990).

[5] G. J. Milburn and C. A.R. Holmes, Phys.Rev. A **44**, 4704 (1991).

NEXT
DOCUMENT

The dissipation in lasers and in coherent state

Tan Weihan Xu Wencang
Department of Physics, Shanghai University
Joint Laboratory of Quantum Optics,
Shanghai Institute of Optics and fine Mechanics, Academia Scinica
(P.O.Box.800-211, Shanghai 201800, China)

I. The general process in laser

The general process in lasers is defined in the photon number representation[3].

$$\frac{d\rho_n}{dt} = \mu_0(u - \mu_1 u^2 + \mu_2 u^3 + \mu_3 u^3 - \cdots)\rho_n \tag{1}$$

where u is the matrix change operation[2] $u\rho_n = \rho_{n-1} - \rho_n$, and μ_1, μ_2, $\cdots$ are the coefficients. In the same way as previous paper[1], we deduced the generating function $G_0(z,t)$ for eq.(1)

$$G_0(z,t) = \sum z^n \rho_n(t) = \exp\left\{\int_0^t (\mu_0(z-1) - \mu_2(z-1)^2 + \cdots)dt\right\} \tag{2}$$

With the aid of generating function $G_0(z,t)$ the mean photon number $< n >_0$ and variance of photon number $< (\Delta n)^2 >_0$ can be evaluated

$$\begin{aligned} < n >_0 &= \int \mu_0(t)dt \\ < (\Delta n)^2 >_0 &= (1 - 2\mu_1) < n >_0 \end{aligned} \tag{3}$$

Now we include the cavity dumping in the treatment, the equation (1) reads

$$\frac{d\rho_n}{dt} = \mu_0(u - \mu_1 u^2 + \cdots) + c(-n\rho_n + (n+1)\rho_{n+1}) \tag{4}$$

After some tedious caculation, finally we arrive at

$$< (\Delta n)^2 >= (1 - \mu_1) < n >_0 \tag{5}$$

Eq.5 shows that when the cavity dissipation is introduced, the variance $< (\Delta n)^2 >$ turns out to be smaller by a factor $(1-\mu_1)$ than it would be for a Poisson distribution. However, when the cavity dissipation be moved, the factor should be $(1-2\mu_1)$ according to eq. (3).

We note that in view of the noise reduction the only coefficient evolved is μ_1 in expansion. Three dominant sources of noise contributing to the laser output are pump fluctuations, spontaneous emission, and vaccum fluctuation entering the cavity through the mirror. We may evaluate the fraction $\mu(z)$ by treating the interaction between atoms and field a closed system first , then take the vaccum fluctuation into account by introducing cavity damping c.

For the atom–field system, if there is any variation in atoms excited $\Delta m = m - < m >$, this must reflect on the photons created $\Delta n = n - < n >$, so that we have

$$\Delta m = \Delta n, \qquad < (\Delta n)^2 > = < (\Delta m)^2 > \tag{6}$$

For example, the three–level system shown in Fig.1(a), $N_3 \ll N_1, N_2$, the excitation probability p and de–excitation probability q of one atom satisfy the relations of stationary solution

$$p = \frac{N_2}{N_1 + N_2}, \qquad q = \frac{N_1}{N_1 + N_2} \tag{7}$$

The probability of $n = N_1 + N_2$ atoms, m in excited state, $(n-m)$ in the ground state, obeys the binomial distribution

$$p_n(m) = \frac{n!}{m!(n-m)!} p^m q^{n-m} \tag{8}$$

This yields the factorial moment of atoms

$$< (\Delta m)^2 > = < m > (1-p) \tag{9}$$

below the threshold, $N_2 \ll (N_1 + N_2), \mu_1 \ll 1$, Poisson

above the threshold, $N_2 \geq N_1$, $\mu_1 = p/2 \geq 1/4$, sub–Poisson

We have a photon noise reduction factor $1/2 < 1 - \mu_1 \leq 3/4$ (with cavity damping). Similarly for a four–level system (Fig.1(b)) $N_4 \simeq 0, p = N_2/(N_1 + N_2) \ll 1, q = N_1/(N_1 + N_2) \simeq 1$, this is essentially a Poisson distribution.

II. The dissipative cohrent state and quantum interference

The coherent state is defined as the eigenstate of annihiration operator a for a harmonic oscillator, what is the eigenstate of annihiration operator a for the harmonic oscillator with

dissipation? If we use the classical solution $a = ae^{-\nu t - i\Omega t}$ for the annihiration operator, evidently the commutation relation $[a, a^\dagger] = 1$ is violated.

$$\frac{da}{dt} = (-i\Omega - \frac{\nu}{2})a + F \tag{1}$$

$$\begin{aligned} a &= a_0 e^{(i\Omega t - \nu/2)t} + \int_0^t F(t') e^{(i\Omega - \nu/2)(t-t')} dt' = a_0 e^{(i\Omega/2 - \nu/2)t} + \beta \\ a^\dagger &= a_0^\dagger e^{(-i\Omega t - \nu/2)t} + \int_0^t F^\dagger(t') e^{(-i\Omega - \nu/2)(t-t')} dt' = a_0^\dagger e^{(-i\Omega/2 - \nu/2)t} + \beta^\dagger \end{aligned} \tag{2}$$

The dissipative coherent state $|\alpha>_d$ corresponding to the dissipative harmonic oscillator may be defined as

$$\begin{aligned} a|\alpha>_d &= (\alpha + \beta)|\alpha>_d \\ {}_d<\alpha|a^\dagger &= (\alpha^* + \beta^\dagger)_d<\alpha| \end{aligned} \tag{3}$$

The states $|\alpha>_d$, ${}_d<\alpha|$ satisfying the definition can be expresed as

$$\begin{aligned} |\alpha>_d &= e^{\beta a^\dagger} e^{-\beta^\dagger a}|\alpha> \\ {}_d<\alpha| &= <\alpha| e^{\beta^\dagger a} e^{-\beta a^\dagger} \end{aligned} \tag{4}$$

Here a, $a^\dagger$, $|\alpha>$, $<\alpha|$ are the usual operators and coherent stats of harmonic oscillator without dissipation, the operators β, $\beta^\dagger$ act on the heat bath only but nothing to do with $|\alpha>$, $<\alpha|$.

$${}_d<\alpha|O(a, a^\dagger)|\alpha>_d = O(\alpha^* + \beta^*, \alpha + \beta) \tag{5}$$

The "quantum interference between two wave packets" studied here we mean that there are two wave packets ψ_1, ψ_2 with it's centers initially located at $x = \pm x_0$, the temporal evolution of ψ_1, ψ_2 assumes[5~7]

$$\begin{aligned} \psi_1(x,t) &= \sqrt{\frac{\alpha}{\pi}} \exp[-\frac{1}{2}(x - x_0\cos\Omega t)^2 - i(\frac{\Omega}{2}t + xx_0\sin\Omega t - \frac{x_0^2}{4}\sin 2\Omega t)] \\ \psi_2(x,t) &= \sqrt{\frac{\alpha}{\pi}} \exp[-\frac{1}{2}(x + x_0\cos\Omega t)^2 - i(\frac{\Omega}{2}t - xx_0\sin\Omega t - \frac{x_0^2}{4}\sin 2\Omega t)] \end{aligned} \tag{6}$$

The superposition of ψ_1, ψ_2 gives

$$\psi(x,t) = \frac{1}{\sqrt{2}}[\psi_1(x,t) + \psi_2(x,t)] \tag{7}$$

and the probability density $I(x,t)$ is

$$I(x,t) = |\psi(x,t)|^2 = I_1 + I_2 + 2\sqrt{I_1 I_2}\cos\theta \tag{8}$$

where

$$I_1 = \frac{\alpha}{2\pi}\exp[-(x - x_0\cos\Omega t)^2]$$

$$I_2 = \frac{\alpha}{2\pi}\exp[-(x + x_0\cos\Omega t)^2] \tag{9}$$

$$\theta = 2xx_0\sin\Omega t$$

The density distribution $I(x,t)$ is depicted in Fig.2.

Now we consider the influence on quantum interference when the damping ν is taken into account. In the weak damping limit, i.e. $\nu t \ll 1$, the classical solution $a = a_0 e^{-\nu t/2 - i\Omega t}$ may be use to evaluate the probability $I_c(x,t)$, because the violation of commutation relation $[a, a^\dagger] = 1$ is not seriously.

$$I_c(c,t) = I_{1c} + I_{2c} + 2\sqrt{I_{1c}I_{2c}}\cos\theta_c \tag{10}$$

where

$$I_{1c} = \frac{\alpha}{2\pi}\exp[-(x - x_0 e^{-\nu t/2}\cos\Omega t)^2]$$

$$I_{2c} = \frac{\alpha}{2\pi}\exp[-(x + x_0 e^{-\nu t/2}\cos\Omega t)^2] \tag{11}$$

$$\theta_c = 2xx_0\exp(-\nu t/2)\sin\Omega t$$

If we use the quantum Langevin squation's solution (2) and rewrite a, $a^\dagger$ as

$$\begin{aligned} a &= (a_0 + \tilde{\beta})\exp(-i\Omega t - \nu t/2), \quad \tilde{\beta} = \int_0^t \exp[(i\Omega + \nu/2)t']F(t')dt' \\ a^\dagger &= (a_0^\dagger + \tilde{\beta}^\dagger)\exp(i\Omega t - \nu t/2), \quad \tilde{\beta}^\dagger = \int_0^t \exp[(-i\Omega + \nu/2)t']F^\dagger(t')dt' \end{aligned} \tag{12}$$

From eq. (12), setting $y_0 = 0$, we derive

$$\begin{aligned} x &= x_0 e^{-\nu t/2}\cos\Omega t + \Delta_1 e^{-\nu t/2}\cos\Omega t + \Delta_2 e^{-\nu t/2}\sin\Omega t \\ y &= x_0 e^{-\nu t/2}\sin\Omega t + \Delta_1 e^{-\nu t/2}\sin\Omega t + \Delta_2 e^{-\nu t/2}\cos\Omega t \end{aligned} \tag{13}$$

where

$$x = \frac{a + a^\dagger}{2}, \qquad y = \frac{a - a^\dagger}{-2i}$$

$$\Delta_1 = \frac{\tilde{\beta} + \tilde{\beta}^\dagger}{2}, \qquad \Delta_2 = \frac{\tilde{\beta} - \tilde{\beta}^\dagger}{-2i}$$

Refering to (11), (13), naturally leads to the following formula for quantum Langevin equation's solution.

$$
\begin{aligned}
I_q &= I_{1q} + I_{2q} + 2\sqrt{I_{1q} I_{2q}} \cos\theta_q \\
I_{1q} &= \frac{\alpha}{2\pi} \exp[-(x-\bar{x})^2] \\
I_{2q} &= \frac{\alpha}{2\pi} \exp[-(x+\bar{x})^2] \\
\theta_q &= 2x\bar{y}
\end{aligned}
\tag{14}
$$

The mean amplitude and variance of vacuum fluctuation $\Delta_1 e^{-\nu t/2}$, $\Delta_2 e^{-\nu t/2}$ can be find out

$$
\begin{aligned}
< \Delta_1 e^{-\nu t/2} > &= < \Delta_2 e^{-\nu t/2} >= 0 \\
< (\Delta_1 e^{-\nu t/2})^2 > &= \frac{e^{-\nu t}}{4} < (\int_0^t F(t') e^{(i\Omega+\nu/2)t'} dt' + \int_0^t F^\dagger(t') e^{(-i\Omega+\nu t/2)t'} dt')^2 > \\
&= \frac{1}{2}(n_\omega + \frac{1}{2})(1 - e^{-\nu t}) \\
< (\Delta_2 e^{-\nu t/2})^2 > &= \frac{1}{2}(n_\omega + \frac{1}{2})(1 - e^{-\nu t})
\end{aligned}
\tag{15}
$$

From equ. (15) we write out immediately the distribution functions $f(\Delta_1 e^{-\nu t/2})$, $f(\Delta_2 e^{-\nu t/2})$ as

$$
\begin{aligned}
f(\Delta_1 e^{-\nu t/2}) &= \frac{1}{\sqrt{\pi(n_\omega + \frac{1}{2})(1 - e^{-\nu t})}} \exp\left[-\frac{(\Delta_1 e^{-\nu t/2})^2}{(n_\omega + \frac{1}{2})(1 - e^{-\nu t})}\right] \\
f(\Delta_2 e^{-\nu t/2}) &= \frac{1}{\sqrt{\pi(n_\omega + \frac{1}{2})(1 - e^{-\nu t})}} \exp\left[-\frac{(\Delta_2 e^{-\nu t/2})^2}{(n_\omega + \frac{1}{2})(1 - e^{-\nu t})}\right]
\end{aligned}
\tag{16}
$$

Via $f(\Delta_1 e^{-\nu t/2})$, $f(\Delta_2 e^{-\nu t/2})$ and (14) the expectation value of density operator $< I_q(x,t) >$ can be find out

$$
\begin{aligned}
< I_q(x,t) > &= \int\int f(\Delta_1 e^{-\nu t/2}) f(\Delta_2 e^{-\nu t/2}) I_q(x,t) d\Delta_1 e^{-\nu t/2} d\Delta_2 e^{-\nu t/2} \\
&= I_1(x,t) + I_2(x,t) + I_3(x,t)
\end{aligned}
\tag{17}
$$

where

$$I_1(x,t) = \frac{\alpha}{2\pi\sqrt{1+(n_\omega+1/2)(1-e^{-\nu t})}} \exp\left[-\frac{(x-x_0e^{-\nu t/2}\cos\Omega t)^2}{1+(n_\omega+1/2)(1-e^{-\nu t})}\right]$$

$$I_2(x,t) = \frac{\alpha}{2\pi\sqrt{1+(n_\omega+1/2)(1-e^{-\nu t})}} \exp\left[-\frac{(x+x_0e^{-\nu t/2}\cos\Omega t)^2}{1+(n_\omega+1/2)(1-e^{-\nu t})}\right] \tag{18}$$

$$I_3(x,t) = \frac{\alpha}{\pi\sqrt{1+(n_\omega+1/2)(1-e^{-\nu t})}} \exp\left\{-[1+(n_\omega+\frac{1}{2})(1-e^{-\nu t})]x^2\right\}$$

$$\times \exp\left[-\frac{x_0^2e^{-\nu t}\cos^2\Omega t}{1+(n_\omega+\frac{1}{2})(1-e^{-\nu t})}\right]\cos(2xx_0e^{-\nu t/2}\sin\Omega t)$$

If the vaccum is squeezed to a degree of $\ln\mu$,the variance of $\Delta_1e^{-\nu t/2}$, $\Delta_2e^{-\nu t/2}$ reads as

$$<(\Delta_1e^{-\nu t/2})^2> = \frac{\mu}{2}(n_\omega+\frac{1}{2})(1-e^{-\nu t})$$

$$<(\Delta_2e^{-\nu t/2})^2> = \frac{1}{2\mu}(n_\omega+\frac{1}{2})(1-e^{-\nu t}) \tag{19}$$

The expectation value for squeezed vaccum fluctuation $< I_s(x,t) >$ assumes a similar formula as (17)

$$< I_s(x,t) = I_{1s}(x,t) + I_{2s}(x,t) + I_{3s}(x,t) \tag{20}$$

where

$$I_{1s}(x,t) = \frac{\alpha\sqrt{\mu}}{2\pi\sqrt{(n_\omega+\frac{1}{2})(1-e^{-\nu t})(\sin^2\Omega t+\mu^2\cos^2\Omega t)+\mu}}$$

$$\times \exp\left[-\frac{\mu(x-x_0e^{-\nu t/2}\cos\Omega t)^2}{(n_\omega+\frac{1}{2})(1-e^{-\nu t})(\sin^2\Omega t+\mu^2\cos^2\Omega t)+\mu}\right] \tag{21a}$$

$$I_{2s}(x,t) = \frac{\alpha\sqrt{\mu}}{2\pi\sqrt{(n_\omega+\frac{1}{2})(1-e^{-\nu t})(\sin^2\Omega t+\mu^2\cos^2\Omega t)+\mu}}$$

$$\times \exp\left[-\frac{\mu(x+x_0e^{-\nu t/2}\cos\Omega t)^2}{(n_\omega+\frac{1}{2})(1-e^{-\nu t})(\sin^2\Omega t+\mu^2\cos^2\Omega t)+\mu}\right]$$

$$
\begin{aligned}
I_{ss}(x,t) &= \frac{\alpha\sqrt{\mu}}{\pi\sqrt{(n_\omega+\frac{1}{2})(1-e^{-\nu t})(\sin^2\Omega t+\mu^2\cos^2\Omega t)+\mu}} \\
&\times \exp\left\{-\frac{x^2\mu[1+(n_\omega+\frac{1}{2})^2(1-e^{-\nu t})^2]}{(n_\omega+\frac{1}{2})(1-e^{-\nu t})(\sin^2\Omega t+\mu^2\cos^2\Omega t)+\mu}\right\} \\
&\times \exp\left\{-\frac{x^2(n_\omega+\frac{1}{2})(1-e^{-\nu t})(\mu^2+\sin^2\Omega t+\mu^4\cos^2\Omega t)}{(\sin^2\Omega t+\mu^2\cos^2\Omega t)[(n_\omega+\frac{1}{2})(1-e^{-\nu t})(\sin^2\Omega t+\mu^2\cos^2\Omega t)+\mu]}\right\} \\
&\times \exp\left[-\frac{\mu x_0^2 e^{-\nu t}\cos^2\Omega t}{(n_\omega+\frac{1}{2})(1-e^{-\nu t})(\sin^2\Omega t+\mu^2\cos^2\Omega t)+\mu}\right] \\
&\times \cos\left\{\frac{[(n_\omega+\frac{1}{2})(1-e^{-\nu t})+\mu]2xx_0e^{-\nu t/2}\sin\Omega t}{(n_\omega+\frac{1}{2})(1-e^{-\nu t})(\sin^2\Omega t+\mu^2\cos^2\Omega t)+\mu}\right\}
\end{aligned}
\tag{21b}
$$

The calculation results for $I_s(x,t)$ are shown in Fig.3 and a comparison between I_s and I_q, I_c shown in Fig.4.

References

[1] Weihan Tan, Phys. Lett. A. 190 (1994), 13.

[2] Yu.M.Golubev and I.V.Sokolov, Zh. Eksp. Teor. Fiz. 87, 408(1984) [Sov. Phys -JETP 60, 234(1984)].

[3] Tan Weihan, The General Process in Lasers. to be published in Opt. Comm.

[4] Tan Weihan, Wang Xue-Wen, Xie Cheng-gong, Zhang Guan-Mei, Acta Physica Sinica 31(1982), 1569.

[5] L.I.Schiff, Quantum Mechanics, Third Edition (1955), MeGrAW-Hill Book Company. New York.

[6] A.O.Caldeira, A.J.Leggett, Phys. Rev. A, 31 (1985), 1059.

[7] D.F.Wall, G.J.Milburn, Phys. Rev. A, 31 (1985), 2405.

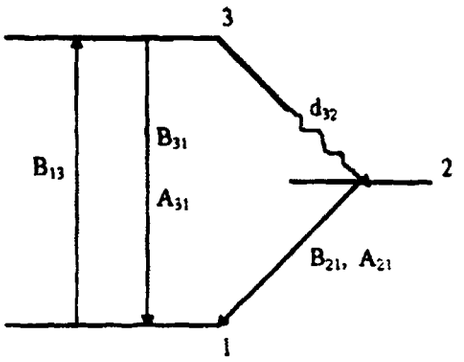

Fig.1(a) Three - Level System

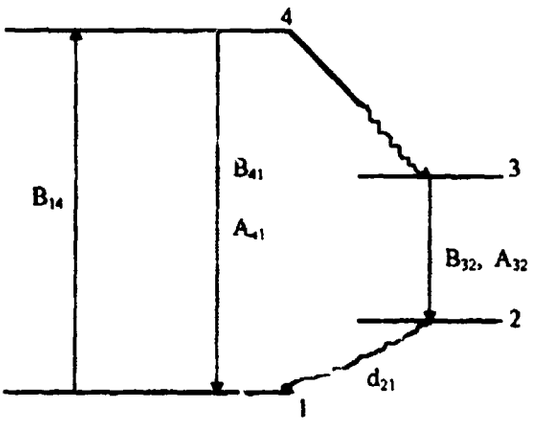

Fig.1(b) Four - Level System

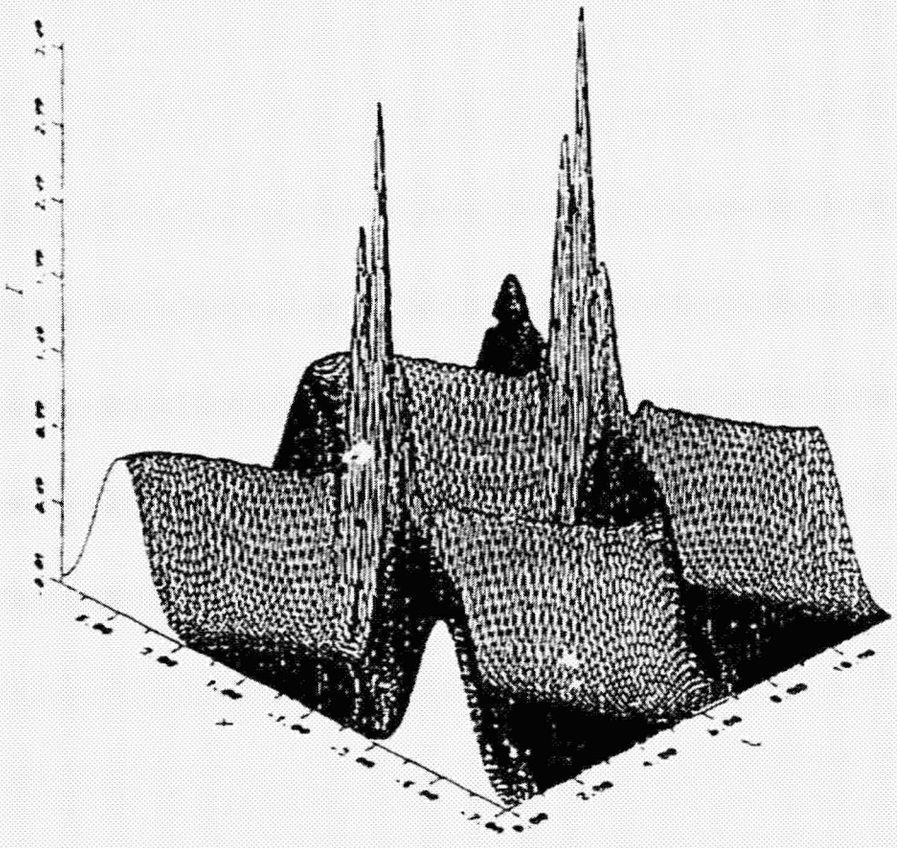

Fig.2 $I(x, t)$, no damping.
$x_0 = 5.0,\ \Omega = 0.5$

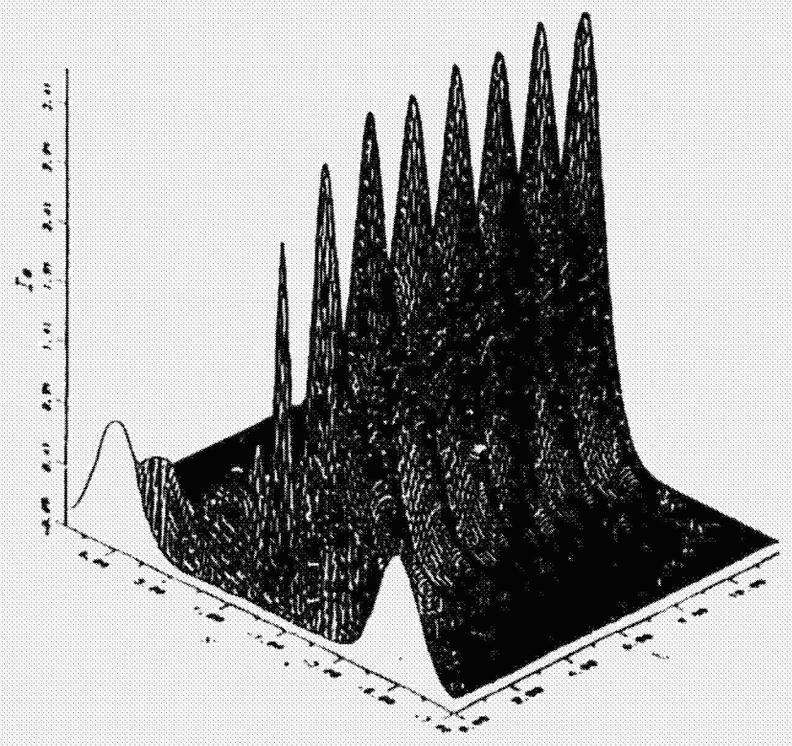

Fig.3 Quantum solution with the vaccum squeezed.
$r_0 = 5.0,\ \Omega = 2.0,\ \nu = 1.0,\ \mu = 4.0$

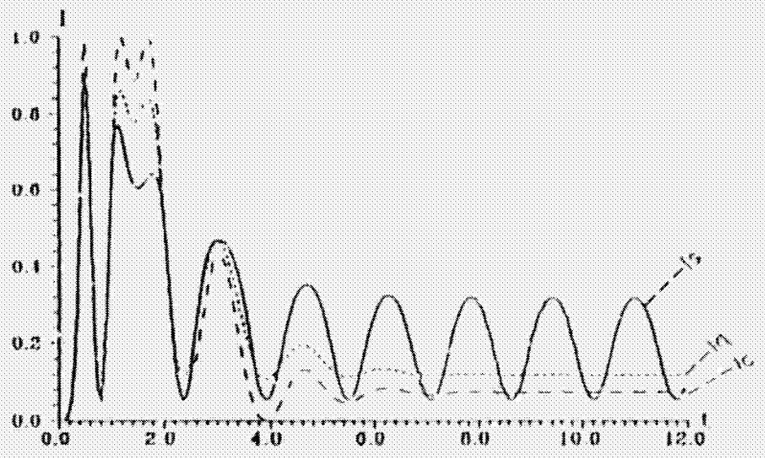

Fig.4 A comparison between I_c, I_t and I_n.
$r_0 = 5.0,\ \Omega = 2.0,\ \nu = 1.0,\ \mu = 4.0,\ x = 2.0$

NEXT
DOCUMENT

MOBILITY OF ELECTRON IN DNA CRYSTALS BY LASER RADIATION

Zhang Kaixi Zhao Qingxun Cui Zhiyun
Department of Physics. Hebei University. Baoding. 071002 P.R.China

Zhang Ping Dong Lifang
Institute of Physics . Academia Sinica . Beijing.100080 P.R.China

Abstract

The mobility of electrons in laser radiated DNA is closed to the energy transfer and energy migration of a biological molecule. Arrhenius [1] has studied the conductivity of the electrons in a biological molecule. But his result is far from the experimental result and meanwhile the relation between some parameters in his theory and the micro-quantities in DNA is not very clear. In this paper, we propose a new phonon model of electron mobility in DNA and use Lippman-Schwinger equation and S-matrix theory to study the mobility of electrons in DNA crystal. The result is relatively close to the experiment result and some parameters in Arrhenius theory are explained in our work.

1 Introduction

Using paramagnetic resonance method, Gordy has studied DNA and found that DNA has the property of semiconductor. Then Duchene[2] measured the energy gap of DNA in 273-313 K and found the energy gap is less than 2ev. Based on above experiment results, Arrhenius deduced the equation of electron conductivity in biological molecule. But his result is not close to the experimental result. We find that the basic reason of this difference is that his explanation of electron transfer is not right. We think that Pullmam's consideration of the DNA molecule being a kind of DNA crystal is good[3]. We think that with electrons being excited to the low energy level in the conduction band, the electrons will act strongly with optic frequency branch of DNA oscillation. Potential trough will form in the area where the electrons are. So these electrons will pass the DNA crystal with the phonon cloud and electron and associated phonon cloud is so called polaron. This is our phonon model of electron mobility in DNA. Using Lippman - Schwinger equation , we get the electron mobility and our result is more close to the experiment result than Arrhenius'.

2 Mobility of Electron in DNA

By means of S -matrix in quantum field theory and Lippman-Schwinger equation[4][5] the polaron-phonon scattering has been discussed and the scattering amplitude expressed by use of matrix elements of initial and find eigen states of hamiltonian. Then we calculate the mobility of electron

in DNA crystals in terms of Lee's hamiltonian and Gurari's polaron wave function[6] . Lee's hamiltonian[7] for electron-phonon interaction is as follows:

$$H = \sum_{\mathbf{k}} a_{\mathbf{k}}^{+} a_{\mathbf{k}} \omega + \sum_{\mathbf{k}} \{V_{\mathbf{k}} a_{\mathbf{k}} e^{i\mathbf{k}\cdot\mathbf{r}} + V_{\mathbf{k}} a_{\mathbf{k}}^{+} e^{-i\mathbf{k}\cdot\mathbf{r}}\} - \frac{\nabla^2}{2m} \tag{1}$$

$$V_{\mathbf{k}} = -i\frac{\omega}{k}(\frac{1}{2m\omega})^{\frac{1}{4}}(\frac{4\pi\alpha}{V})^{\frac{1}{2}} \tag{2}$$

$$\alpha = (\frac{me^4}{2\omega})^{\frac{1}{2}}(\frac{1}{n^2} - \frac{1}{\epsilon_0}) \tag{3}$$

where $a_{\mathbf{k}}^{+}$ and $a_{\mathbf{k}}$ -creation and annihlation operators for free phonons,ω -the branch frequency of the phonon for DNA crystal vibration, V -the volume of DNA crystal, n coefficients of refraction,ϵ_0- static dielectric constant,$\mathbf{k}$ wave vector of the phonon,$\mathbf{r}$ and ∇ -coordinates and impulse operator of the electron respectively.

Gurari's wave function for polaron with impulse $\mathbf{p_0}$ and energy $p_0^2/2m^*$ may be written

$$\psi(\mathbf{p_0}) = V^{\frac{-1}{2}} exp\{i(\mathbf{p} - \sum_{\mathbf{k}} a_{\mathbf{k}}^{+} a_{\mathbf{k}} \mathbf{k}) \cdot \mathbf{r}\} v(\mathbf{p_0}) \phi_0 \tag{4}$$

$$a_{\mathbf{k}} \phi_0 = 0 \tag{5}$$

$$< \phi_0 | \phi_0 >= 1 \tag{6}$$

$$v = \prod_{\mathbf{k}} (1 + V^{-1}|f_{\mathbf{k}}|^2)^{\frac{-1}{2}} (1 + V^{\frac{-1}{2}} f_{\mathbf{k}} a_{\mathbf{k}}^{+}) \tag{7}$$

$$f_{\mathbf{k}} = -i(4\pi\alpha)^{\frac{1}{2}}/k(1 + k^2 - 2\mathbf{k}\cdot\mathbf{p}) \tag{8}$$

Finally with the aid of Lippman-Schwinger equation the expression for mobility μ of the electron is derived which is the function of matrix elements relating to initial and final states of scattering particles and eigen state of hamiltonian as well

$$\mu = \frac{1}{2\alpha\omega}(\frac{e}{m})(\frac{m}{m^*})^3 f(\alpha) e^{\frac{\omega}{\chi T}} \tag{9}$$

where χ -Boltzmann constant, T -absolute temperature,m^*—effective mass of polaron and

$$f(\alpha) = \frac{x_r}{(1 + x_r^2)^2} - \frac{x_r^6}{(1 + x_r^2)}(\frac{\partial G_1(x)}{\partial x})_{x=x_r} \tag{10}$$

$$G_1(x) = \alpha\pi x\{2[\frac{1}{1 + x^2 + |1 - x^2|}]^2 - \frac{1}{2}\theta(1 - x)\} - \alpha\{\frac{1}{x^2(1 + x^2)} - \frac{1}{2x^3} tg^{-1}\frac{2x}{x^2 - 1}\} \tag{11}$$

in which x_r is the root of the following equation

$$x^2 = \frac{1}{1 - G_1(x)} \tag{12}$$

Even if it is difficult to accurately measure the m and m^*, we still show that the result given in this paper is better than that given by Arrhenius.

3 Conclusion

In our electron mobility equation (9) f(α) is a slow-variation function , α is coupling constant of electron-phonon , ω is optical frequency of DNA oscillation and m is DNA lattice mass. Using visible light , Szent could not find the electron mobility but when he used the light of 3000$\mathring{A}$, he found the phenomenon. Now we can use laser beam (wavelength ¡3000$\mathring{A}$) to observe the move. This is the result induced by multiphoton process. Our result explain some parameters in Arrhenius' result. The radiation of laser on DNA will not only cause the change of electron mobility in DNA but also cause Onsager nonlinear transfer induced by the temperature variation and result in the change in the co-transport system of DNA. This changed DNA may bring about the abnormal development of cells and cause the occurrence of cancer.

References

[1] J. B. Birks. Excited States of Biological Molecules. John Wiley & Sons Ltd. 1976

[2] R. F. Steiner. *Excited States of Proteins and Nucleic Acids.* (Plennum Press.New York. 1971)

[3] R. R. Birge. Biochem. Biophys. Acta 293 1016 (1990)

[4] R. P. Feynman. Phys. Rev. 97. 660 (1955)

[5] F. E. Low. and D. Pines . Phys. Rev. 98. 414(1955)

[6] M. Gurari. Phil. Mag. 44. 229(1953)

[7] T. D. Lee. F. E. Low. and D. Pines. Phys. Rev. 90. 297(1953)

[8] B. R. Sigh. Photochem. Photobiol. 52. 249(1990)

[9] Zhang Ping. and Zhang Kaixi. Chinese Journal of Quantum Electronics, 11.23(1994)

NEXT
DOCUMENT

MULTIPHOTON PROCESS AND ANOMALOUS POTENTIAL OF CELL MEMBRANE BY LASER RADIATION

Zhang Kaixi, Zhao Qingxun , Cui Zhiyun
Department of Physics, Hebei University, Baoding, 071002,China

Zhai Ping, Dong Li'ang
Institute of Physics, Academia Sinica, Beijing, 100080,China

Abstract

In this paper, by the use of quantum biology and quantum optics, the laser induced potential variation of cell membrane has been studied. Theoretically , we have found a method of calculating the monophoton and multiphoton processes in the formation of the anomalous potential of cell membrane. In contrast with the experimental results , our numerical result is in the same order. Therefore , we have found the possibility of cancer caused by the laser induced anomalous cell potential.

1 Introduction

The ions of Na^+, K^+, Ca^{++}, Cl^- and electrons exist outside and inside a cell membrane. The distributions of these ions are different between the two sides[1]. Therefore the membrane potential is related to the unsymmetrical ion distribution. The electric field caused by the ion distribution will impose a force on the charged particles passing through the membrane. The balance of ion concentration gradient, potential gradient , Na-pump and Ca-pump is the key condition of forming a normal co-transport system. Under this balance, the free radicals, DNA, RNA and ATP can normally transport[2][3]. Our study is to find the laser induced variation of cell membrane potential. The result shows that the anomalous potential variation will do harm to the normal co-transport system and may promote the occurrence of an abnormal cell or a cancer cell.

2 Multiphoton Process and Anomalous Potential of Cell Membrane

By means of quantum optics and quantum biology, it is a new approach to study the occurrence of cancer induced by the anomalous membrane potential of laser radiated cells. Smith[4] and Bloch[5] have proposed a method for calculating the density of two-photon photoelectric current which is too local to explain the multiphoton photoelectric current of biological cell membrane.

In the present paper the steps adopted for solving this problem are 1) the forced oscillation is induced by the interaction of laser radiation field-electrons in the cell; 2) due to the fact that exists the surface potential of cell membrane, the electron in forced oscillation absorbs photon and

transition occurs. On the cell membrane exists a potential $\omega_A(z > 0)$, at the same time laser radiation propagates along axis z and the vector potential of electromagnetic field is

$$A_x = a\cos(kz - \omega t) \tag{1}$$

$$A_y = A_z = 0 \tag{2}$$

Schrödinger equation may be derived

$$i\frac{\partial\phi(\mathbf{r},t)}{\partial t} = [\frac{1}{2\mu}(\mathbf{p} + \frac{e}{c}\mathbf{A})^2 - \omega_a]\phi(\mathbf{r},t) \tag{3}$$

On account of that energy distribution of electrons in a cell at the ordinary temperature is not different far from that at the absolute zero, Fermi energy ω_f is about several electron-volts and the velocity of electrons would be much smaller than that of light, we have the solution of the equation

$$\phi(\mathbf{r},t) = exp[i\mathbf{p}\cdot\mathbf{r} - i(\epsilon_p + \frac{e^2a^2}{4\mu c^2})t]exp[\frac{iB}{2\sqrt{A}}\sin u - \frac{iD}{4\sqrt{A}}\sin 2u] \tag{4}$$

where

$$\epsilon_p = (p^2/2\mu) - \omega_a \quad u = kz - \omega t$$

$$A = (p_z k/\mu - \omega)^2/4(k^2/2\mu)^2$$

$$B = (ea/\mu c)p_z/(k^2/2\mu)$$

$$D = (e^2a^2/4\mu c^2)/(k^2/2\mu)$$

The wave function illustrates that the electron in laser radiation field has a translation motion and forced oscillation. Its transition Hamiltonian under the action of the second quantization electromagnetic field is as follows:

$$H = \frac{e}{\mu c}\sum_{\mathbf{k}}\sqrt{\frac{2\pi c}{k}}[a\cdot pe^{-i\omega_{\mathbf{k}}t + i\mathbf{k}\cdot\mathbf{r}} + a^+\cdot pe^{i\omega_{\mathbf{k}}t - i\mathbf{k}\cdot\mathbf{r}}] \tag{5}$$

where a^+, a —operators for the creation and annihilation respectively, $\omega_{\mathbf{k}}$—photon frequency characterized by wave vector. Finally we obtain the density of photoelectric current for monophoton process (n=1)

$$j_1 = N(\omega)\frac{e^3\mu^2\omega c}{4}\int_{0,\sqrt{\chi-n}}^{\sqrt{\phi}} R(\xi)(\phi - \xi^2)d\xi \tag{6}$$

and for multiphoton process ($n = 2, 3, 4, \cdots$)

$$j_n = (\frac{n-1}{4n})(\frac{1}{2^{n-1}(n-1)!})^4(2n-3)!N(\omega)e^3\mu^2c(\frac{ea}{\omega})^{2n-2}\int_{0,\sqrt{\chi-n}}^{\sqrt{\phi}} R(\xi)(\phi - \xi^2)^n d\xi \tag{7}$$

where

$$R_n(\xi) = \frac{\xi^2(\chi - \xi^2)^{3/2}}{[\delta\chi(\chi - \xi^2)^{1/2}][\eta(n\eta - \chi + \xi^2/\delta - n\eta/2 + \chi - \xi^2)/2]} \tag{8}$$

$$\lambda_0 = 1\mu c, \quad \xi = \lambda_0 p_z, \quad \chi = 2\lambda_0\omega_a/c$$

$$\delta = \ell/\lambda_0, \quad \phi = 2\lambda_0\omega_f/c, \quad \eta = 2\lambda_0\omega/c$$

As for the integral limit we take zero if $(\chi - n\eta) < 0$ otherwise should take $\sqrt{\chi - \eta}$. ℓ the effective thickness for cell membrane, $N(\omega) = [a^2\omega\Delta\tau\Delta\sigma]/8\pi c$ --the photon number passing through area $\Delta\sigma$ within time interval $\Delta\tau$.

3 Conclusions

Using our theory of monophoton and multiphonton process , we calculate the membrane potential of an Ehrilich cell[3]. The conditions are: the power of laser is 50mw; the energy of photon is 1.48ev and the focus area is $10^{-3}cm^2$. The theoretical result of the anomalous potential is 10mv. In comparison with the normal potential of an Ehrlich cell(40mv), which is measured by a micro-probe, the difference of these two potentials is obvious. This change of membrane potential may cause about 8 percent change in the Na^+ distribution. This change will seriously disorder the normal cell transport system and result in the abnormality of a cell. Above process will cause diffusions and result in the changes of material transport in the cell. This passive transport has been studied [6] and the influence of the passive transport and co-transport will be studied further.

References

[1] B D. Gomperts, The plasma membrane: Mode for structure and function, Academic Press Inc. London, (1977)

[2] A. W. Giotti. Photochem. Photobiol. 51, 497 (1990)

[3] R. Baserga. The cell cycle and cancer, Marcel Dekker Inc. New York, (1971)

[4] R. L. Smith. Phys.Rev. 128, 2225(1962)

[5] P. Bloch. J.Appl.Phys. 35, 2052(1964)

[6] Zhang Ping, Zhang Kaixi, and Fu Guangsheng, Chinese Journal of Quantum Electronics, 11, 23 (1994)

NEXT
DOCUMENT

QUANTUM COHESION OSCILLATION OF ELECTRON GROUND STATE IN LOW TEMPERATURE LASER PLASMA

Zhao Qingxun
Department of Physics, Hebei University, Baoding, 071002 China

Zhang Ping
Institute of Physics , Academia Sinica , Beijing 100080 China

Dong Lifang, Zhang Kaixi
Department of Physics, Hebei University, Baoding, 071002 China

Abstract

The development of radically new technological and economically efficient methods for obtaining chemical products and for producing new materials with specific properties requires the study of physical and chemical processes proceeding at temperature of 10^3 to 10^4K, temperature range of low temperature plasma. In our paper, by means of Wigner matrix o quantum statistical theory, a formula is derived for the energy of quantum coherent oscillatio of electron ground state in laser plasma at low temperature. The collective behavior wo ld be important in ion and ion-molecule reactions.

1 Introduction

The low temperature plasma is characterized by a partial or complete ionization of atoms and molecules, naturally such a plasma is quasi-neutral. Great opportunities for obtaining such a plasma, which from a chemist's viewpoint is temperature range, have arisen as a result for studies in the field of laser[1]. Because of the development of laser techniques, the problem of chemical reactions in a plasma was found to be realizable at a substantially new technological level than was possible many years ago when the first rather timid and technically imperfect attempts were undertaken in this field. At present, the low temperature plasma affords the possibility of conducting chemical processes at temperature up to 10^4K, at pressures ranging from 10^{-4} to 10^4atm. under both equilibrium and nonequilibrium conditions. The character of chemical conversions that occur at temperature of the order of several thousand degrees is largely determined by thermodynamic properties of substances which take part in a reaction at one or another of its stage. Given reliable thermodynamic constants, it should be possible to determine, in most cases, optimal temperature conditions for reactions, values of product yields expected, and energy indices of the process. At the same time, the course of reaction depends, as a rule, not only on the thermodynamic properties of a reacting system. Prior to converting to equilibrium state, determined by the thermodynamics of reaction, the system experiences a series of intermediate stages. The rate at which the system goes through these stages is determined by the kinetics of the process. That is,

the rate of achieving equilibrium energy distribution according to degrees of freedom is determined by physical kinetics and the rate of achieving equilibrium chemical composition is determined by chemical kinetics[2]. In this case, the plasma chemical reactions are characterized by the strong mutual effects of the factors of the physical and chemical kinetics. The terminal rate of setting up equilibrium energy distribution according to different degree of freedom in some cases limits the possibility of using the classical or quantum methods of chemical kinetics based on assumption about energy distribution in the reacting system. In this paper, the energy of coherent oscillation of electron ground state in laser plasma is derived in the presence of neutralizing background. Laser field and collective cohesion behavior in laser plasma would be important in above physical and chemical kinetics.

2 Quantum Cohesion Oscillation of Electron Ground State

We shall study assemblies of charged particle in conditions such that the laws of classical mechanics are no longer an adequate approximation and quantum effects become important or even dominant. The long range Coulomb interaction retain, of course, their main properties, which have been investigated in detail However, the manifestation of these properties will in general be different because the Coulomb effects are combined with and corrected by quantum mechanical effects. The most convenient method for doing this is the method of second quantization. In this paper a formula is derived for the energy of quantum coherent oscillation of electron ground state in laser plasma at low temperature by means of Wigner matrix of quantum statistical theory. It shows the change of structure of the ground state in the presence of long range Coulomb interactions. We consider the model of a gas of charged particles in the presence of a continuous neutralizing background. The hamiltonian of this system is :

$$H = \sum_{\mathbf{k}} \epsilon_{\mathbf{k}} \hat{a}^{+}(\hbar\mathbf{k})\hat{a}(\hbar\mathbf{k}) + \frac{1}{2}e^{2}\sum_{\mathbf{k}}\sum_{\mathbf{l}}\sum_{\mathbf{p}}\sum_{\mathbf{q}} < \mathbf{kl}|V|\mathbf{pq} > \delta_{\mathbf{k+l-p-q}}\hat{a}^{+}(\hbar\mathbf{k})\hat{a}^{+}(\hbar\mathbf{l})\hat{a}(\hbar\mathbf{p})\hat{a}(\hbar\mathbf{q}) \tag{1}$$

where $\mathbf{k}\cdots\mathbf{q}$ are wave vectors. $\hat{a}^{+}(\hbar\mathbf{k})$ and $\hat{a}(\hbar\mathbf{k})$ are respectively creation and destruction operators of the particle with momentum $\hbar\mathbf{k}$. the normalized one particle wave function is

$$|\mathbf{k}><\mathbf{k}\,\mathbf{x}>=\Omega^{\frac{-1}{2}}e^{i\mathbf{k}\,\mathbf{x}}|\mathbf{k}> \tag{2}$$

where Ω is volume. Therefore the matrix is

$$< \mathbf{k}|\sum_{\mathbf{k}} \epsilon_{\mathbf{k}}\hat{a}^{+}(\hbar\mathbf{k})a(\hbar\mathbf{k})|\mathbf{k}>=\hbar^{2}\mathbf{k}^{2}/2m \tag{3}$$

where m is the mass of the particle.

$$< \mathbf{kl}|V|\mathbf{pq} > \delta_{\mathbf{k+l-p-q}} = (8\pi^{3}/\Omega)[V_{|\mathbf{k-q}} - \theta V_{|\mathbf{k-p}}]\delta_{\mathbf{k+l-p-q}} \tag{4}$$

$V_{\mathbf{k}}$ is the Fourier transform of the long range potential. Using Wigner matrix[3] and Weyl rule[4] the collective part of correlation energy E of particles becomes:

$$E = (\hbar/8\pi^{3}c)(1/4)\int_{0}^{e^{2}} d\eta\eta^{-1}(\quad\eta)\int_{k<k_{c}} d\mathbf{k}\int_{0}^{\infty} d\omega[\delta(\omega+\omega_{p}) + \delta(\omega-\omega_{p})] \tag{5}$$

where $\mathbf{k}_c$ is a critical value of $\mathbf{k}$, e is the absolute value of electron charge , ω_p is quantized oscillator frequency. Hence the final result is

$$E = \frac{1}{n}\int_{k<k_c}(\frac{1}{2}\hbar\omega_p)(\frac{d\mathbf{k}}{8\pi^3}) \tag{6}$$

where n is average number density.

3 Conclusions

This result has a extremely suggestive form. It shows that the collective contribution to the ground state energy is precisely the energy of a collection of quantized oscillators of frequency ω_p. It confirms quantitatively the remark, showing how deep is the change of structure of the ground state in the presence of long range interaction. The latter organize the motion of the particle in such a way that a significant part of the ground state energy comes from large groups of particle oscillating in phase[5][6]. This cohesion is perhaps the most characteristic feature of the collective behavior of charged particle. The rate of ionization at a sufficiently high electron concentration is determined by that of Kinetic energy transfer to electron in elastic collisions. In the case of plasma produced by ionizing irradiation of a cold gas, ionization will be ensured by a group of fast electrons with an energy imparted by emission, where as collisions of electrons with heavy particles will decrease the kinetic energy of electron to those inducing no ionization.

References

[1] F.Thomas. J. Chem. Phys. 70, 1187 (1979)

[2] Zhang Ping, Zhang Kaixi and Fu Guangsheng, Chinese Journal of Quantum Electronics, 11, 23 (1994)

[3] D Bohm and D Pines, Phys. Rev. 92 , 609 (1953)

[4] S. Fujita and R. Hirota, Phys. Rev. 118, 6 (1960)

[5] Zhang kaixi and L E. Philipsom, Mat. Sci. Res. 12, 725 (1986)

[6] Zhang Kaixi, Zhang Ping and Zhao Qingxun, The 19th Intern. Conf. Statistical Phys. Xiamen, July, 1995

NEXT
DOCUMENT

ARE THERE OPTICAL SOLITARY WAVE SOLUTIONS IN LINEAR MEDIA WITH GROUP VELOCITY DISPERSION ?

Zhonghao Li
Department of Electronic and Information Technology,
Shanxi University, Taiyuan, Shanxi, 030006, P.R. China

Guosheng Zhou
Department of Electronic and Information Technology,
Shanxi University, Taiyuan, Shanxi, 030006, P.R. China

Abstract

A generalized exact optical bright solitary wave solution in a three dimensional dispersive linear medium is presented. The most interesting property of the solution is that it can exist in the normal group-velocity- dispersion (GVD) region. In addition, another peculiar feature is that it may achieve a condition of "zero-dispersion" to the media so that a solitary wave of arbitrarily small amplitude may be propagated with no dependence on its pulse width.

1 Introduction

It is well known that there exist undistorted travelling wave solutions with arbitrarily shape in bulk linear media in the absence of dispersion effects. We can call such a travelling wave solitary wave or soliton on the analogy of its definition in nonlinear science. In the presence of GVD, it has been proved that transmission of solitary wave or soliton can be achieved in cubic nonlinear media [1,2]. This research for optical solitons has attracted considerable attention because of not only the properties of preserving their shape and energy during propagation through a medium but their potential applications in ultra-high bit-rate optical communication and ultrafast signal-routing systems [3]. Mathematically, these optical solitons are a particular solution of the (1+1)-dimensional nonlinear Schrödinger equation (NLSE) or the equations, which can be transformed into (1+1)- dimensional NLSE. As is well-known, there exist two kinds of solitons in the (1+1)-dimensional NLSE: bright and dark solitons [1]. In physics, optical solitons can be classified as temporal and spatial solitons. In the case of temporal solitons, the GVD is balanced by self- phase modulation. In the spatial domain, a spatial soliton is better known as a "self-trapped beam", in which the self-focusing effect counteracts the diffraction [4]. In fact, the space-time analogy between dispersion pulse compression in time and optical-beam focusing in space has been pointed out early in 1969 [5-6]. When only diffraction or dispersion effects are considered, their governing equations are of the same structure under appropriate conditions. Now the four kinds of solitons (i.e. temporal bright, spatial bright, temporal dark,

spatial dark solitons) have been observed experimentally in optical fibers or in waveguides [2,7-13]. Besides the (1+1)-dimensional NLSE, it is necessary to deal with the higher-dimensional wave equation when a pulse propagate in optical media under the combined effect of diffraction and dispersion. In this case, one would expect that there exist the so-called light-bullets (i.e. stable, nondiffracting and nondispersing optical pulses) under certain conditions [14]. However, in contrast to (1+1)-dimensional NLSE, such a spatio-temporal solitonic solution has not yet been found even in theory due to the mathematical complexity of the higher- dimensional wave equations. On the other hand, the attempts of searching for multidimensional solitonic solutions in other kinds of optical media, such as exponential and quadratic media, have also been made [15-17]. Recently, we have proved, for the first time to our knowledge, that an envelope solitary wave solution mar exist in a two dimensional dispersive linear medium under certain appropriate conditions by taking into account the transverse effect and dispersion effect simultaneously [18]. In this paper, we will generalize the results in a three dimensional dispersive linear medium. It is proved that undistorted transmission of optical pulses in the above mentioned media may be realized even in the presence of GVD under appropriate conditions. Unlike the conventional bright solitary wave in cubic nonlinear media, the present bright solitary wave solution can be obtained in the normal (positive) GVD region. In addition, a peculiar feature of the solution is that it may achieve a condition of "zero-dispersion" to the media so that a solitary wave of arbitrarily small amplitude may be propagated with no dependence on its pulse width.

2 Governing Wave Equation

In the development that follows, we consider the propagation of pulses which are narrowly centered about a given frequency ω_0, and assume that the refractive index $n(\omega)$ is a slowly varying function of ω in the vicinity of ω_0 (which is generally true in situations of practical interest). It is convenient to represent the electric field intensity $\vec{E}(\vec{r},t)$ by a product of an envelope and a rapidly oscillating terms:

$$\vec{E}(\vec{r},t) = \hat{e}A(\vec{r},t)e^{i(qz-\omega_0 t)} \tag{1}$$

where $\hat{e}$ is the polarization unit vector assumed to remain unchanged during pulse propagation, q the reference constant of propagation along z direction and ω_0 the carrier center frequency. Here we have restricted the development to be a scalar complex envelope function $A(\vec{r},t)$.
Now let us consider the propagation of an optical pulse described by Eq.(1) in bulk dispersive homogeneous linear media. After removing the terms describing inhomogeneity and nonlinearity of media in Ref. [15], we can obtain the governing equation for the complex envelope function $A(\vec{r},t)$. This three spatial and one temporal dimensions (3+1) linear wave equation with the GVD term included can be written in the form

$$\left[\nabla^2 - (k_0'^2 + k_0 k_0'')\frac{\partial^2}{\partial t^2} + 2i(q\frac{\partial}{\partial z} + k_0 k_0'\frac{\partial}{\partial t}) + k_0^2 - q^2\right] A(\vec{r},t) = 0, \tag{2}$$

where $k = \omega n(\omega)/c$ is the wave number, the primes indicate the derivatives with respect to ω, and the subscript 0 indicates evaluation at the carrier center frequency ω_0. Here, as is well

known (see, e.g., [1]), k^2 is expanded around ω_0 in Taylor series and only terms up to second order are kept under the weak dispersion approximation (i.e., the refractive index is a slowly varying function of ω_0).
It is well-known that in the absence of GVD ($k_0'' = 0$), there are "complete" solitary wave solutions in Eq.(2). If the GVD does exist ($k_0'' \neq 0$), there will be no "complete" solitary wave solutions in Eq.(2). It is generally believed that the pulse shape will be distorted during its propagation. However, one will see in the following analysis that there may exist steady-state envelope solitary wave solutions in Eq.(2) under the combined action of transverse and dispersion effects.

3 A solitary wave solution and its property

In order to obtain a optical envelope solitary wave solution, let's introduce an ansatz with a hyperbolic secant function profile

$$A(\vec{r},t) = A_0 Sech(\frac{t-\vec{\alpha}\cdot\vec{r}}{\tau})e^{i(\vec{\beta}\vec{r}+\Delta\omega t)}, \tag{3}$$

where A_0 is the maximum amplitude of the optical envelope solitary wave solution. The parameter $\vec{\alpha}$ is the inverse of the group velocity, $\vec{\beta}$ describes the change of the wave vector, and $\Delta\omega$ is the frequency shift.
After substituting the ansatz (3) into Eq.(2), we can obtain three equations for the parameters $\vec{\alpha}$, $\vec{\beta}'$, and $\Delta\omega$:

$$\vec{\alpha}\cdot\vec{\alpha} = k_0'^2 + k_0 k_0'', \tag{4}$$

$$\vec{\alpha}\cdot\vec{\beta}' = (k_0'^2 + k_0 k_0'')\Delta\omega - k_0 k_0', \tag{5}$$

$$\vec{\beta}'\cdot\vec{\beta}' = (k_0'^2 + k_0 k_0'')\Delta\omega^2 - 2k_0 k_0'\Delta\omega + k_0^2 \tag{6}$$

where the parameter $\vec{\beta} = \{\beta_1, \beta_2, \beta_3\}$ has been replaced by $\vec{\beta}' = \{\beta_1, \beta_2, \beta_3 + q\}$.
If all of the parameters are reasonably chosen, we can expect to obtain the optical solitary wave solutions described by Eq.(3). Fortunately, one can prove that all of the parameters may physically choose reasonable value. Therefore, an optical envelope solitary wave solution can exist in Eq.(2).
According to the vector relation $|\vec{\alpha}||\vec{\beta}'| \geq \vec{\alpha}\cdot\vec{\beta}'$, substituting Eq.(4)-(6) into the relation, after tedious algebra calculation, we can obtain the condition:

$$k_0'' \geq 0. \tag{7}$$

This means that it is only in the normal (positive) dispersion region that there may exist optical envelope solitary wave solutions in a dispersive linear medium. This property is contrary to that of (1+1)-dimensional NLSE, in which the sech-like solitary wave solutions exist only in the anomalous (negative) GVD region. The existence of present solitary wave solutions indicates that the physical effects of transverse confinement seems to counteract the effect of normal GVD.
From Eq.(4)-(6) one can see that the parameters A_0 and τ are not included in them. This

implies that the maximum amplitude A_0 is independent of pulse half-width τ. Therefore, the optical envelope solitary wave solution (3) may propagate through a medium with an arbitrarily small amplitude. This means, such a solitary wave has no limitation of threshold.
Additionaly, in normal case, there is always dispersion in a practical medium, that means $k_0'' \neq 0$, this will lead to that the relation $\mid \vec{\alpha} \mid\mid \vec{\beta}' \mid \neq \vec{\alpha} \cdot \vec{\beta}'$ is always satisfied. This implies that the propagating direction of envelope amplitude does not coincide with that of wavefront. Therefore, the optical envelope solitary wave solution (3) represents an inhomogeneous wave. The angle θ of the two directions between envelope amplitude and phase can be written by:

$$\theta = arccos\left(\frac{\vec{\alpha} \cdot \vec{\beta}'}{\mid \vec{\alpha} \mid\mid \vec{\beta}' \mid}\right) \tag{8}$$

Comparing with the nonlinear method of utilizing the nonlinear dependence of refractive on pulse intensity suggested by Hasegawa and Tappert, the present one has three features as follows: For the first, the optical bright solitary wave can be achieved in the normal (positive) GVD region. This feature can greatly extend the range of optical wavelength for realizing transmission of the bright solitary-wave. It is unnecessary to search for special light source, of which the wavelength lies in the range of anomalous GVD for optical guide materials. For the second, it may achieve a condition of "zero-dispersion", in which a solitary wave of arbitrarily small amplitude may propagate with no dependence on its pulse width. While the pulse amplitude A_0 is proportional to the inverse of pulse half-width τ for the nonlinear refractive index case. This implies that the pulse intensity will increases rapidly with the decrease of pulse half-width (to the second order). Therefore, in realizing ultra-high bit-rate optical soliton communications, it will finally meet the limit set by the damage threshold of optical guide materials and other nonlinear effects. This difficulty may be overcome easily in our case as one may achieve ultra-high bit-rate transmission of pulses in optical soliton communication systems, in which the pulse half-width is narrow enough while the intensity still keeps at a low level. Besides above mentioned, it may conveniently utilize all of the advantages of linear techniques (e.g. wavelength division multiplex)in the future optical soliton communication systems. However, it should be noted that this solitary wave is homogeneous. What influence on the optical communication is it? It should be considered in the next work.

4 Conclusion

In conclusion, We have obtained an optical envelope optical solitary wave solution in (3+1)-dimensional dispersive linear wave equation. It is of the following features:
1) It is only in the normal (positive) dispersion range that there exists the solitary wave solution described by (3) in a dispersive linear medium.
2) The optical envelope solitary wave solution represents an inhomogeneous wave.
3) It may achieve a condition of "zero-dispersion", in which a solitary wave of arbitrarily small amplitude may be propagated with no dependence on its pulse width.

Acknowledgments

This research was supported by the National Natural Science Foundation of P.R. China and the Provincial Natural Science Foundation of Shanxi.

References

[1] A. Hasegawa and F. Tappert, Appl. Phys. Lett. **23**, 142 (1973); **23**, 171 (1973).

[2] L.F. Mollenauer, R.H. Stolen, and G.P. Gordon, Phys. Rev. Lett. **45**, 1095 (1980).

[3] A. Hasegawa, *optical Solitons in Fibers* (Springer-Verlag, Berlin, 1989).

[4] R.Y. Chiao, E. Garmire, and C.H. Townes, Phys. Rev. Lett. **13**, 479(1964).

[5] E.B. Treacy, IEEE J. Quantum Electron. **5**, 454 (1969).

[6] S.A. Akhmanov, A.P. Sukhorukov and A.S. Chirkin, Sov. Phys. JETP **28**,748 (1969).

[7] P. Emplit, J.P. Hamaide, F. Reynaud, C. Froehly, and A. Barthelemy, Opt. Commun. **62**, 374 (1987).

[8] A.M. Weiner, J.P. Heritage, R.J. Hawkins, R.N. Thurston, E.M. Kirschner, D.E. Leaird, and W.J. Tomlinson, Phys. Rev. Lett. **61**, 2445 (1988).

[9] S. Maneuf and F. Reynaud, Opt. Commun. **66**, 325 (1988).

[10] J.S. Aitchison, A.M. Weiner, Y. Silberberg, M.K. Oliver, J.L. Jackel, D.E. Leaird, E.M. Vogel, and P.W.E. Smith, Opt. Lett. **15**, 471 (1990).

[11] D.R. Andersen, D.E. Hooton, G.A. Swartzlander, Jr., and A.E. Kaplan, Opt. Lett. **15**, 783 (1990).

[12] G.A. Swartzlander, Jr., D.R. Andersen, J.J. Regan, H. Yin, and A.E.Kaplan, Phys. Rev. Lett. **66**, 1583 (1991).

[13] G.R. Alan, S.K. Skinner, D.R. Andersen, and A.L. Smirl, Opt. Lett. **16**, 156 (1991).

[14] Y. Silberberg, Opt. Lett. **15**, 1282 (1990).

[15] M. Jain and N. Tzoar, J. Appl. Phys. **49**, 4649 (1978).

[16] E.W. Laedke and K.H. Spatschek, Phys. Rev. Lett. **52**, 279 (1984).

[17] K. Hayata and M. Koshiba, Phys. Rev. Lett. **71**, 3275 (1993); 72, 178(E) (1994).

[18] Z.H. Li and G.S. Zhou, Chinese Science Bulletin **40**, 119 (1995).

REPORT DOCUMENTATION PAGE

Form Approved
OMB No. 0704-0188

1. AGENCY USE ONLY *(Leave blank)*	2. REPORT DATE	3. REPORT TYPE AND DATES COVERED
	January 1996	Conference Publication

4. TITLE AND SUBTITLE

Fourth International Conference on Squeezed States and Uncertainty Relations

5. FUNDING NUMBERS

Code 910.1

6. AUTHOR(S)

D. Han, Kunchi Peng, Y. S. Kim, and V. I. Man'ko, Editors

7. PERFORMING ORGANIZATION NAME(S) AND ADDRESS (ES)

Goddard Space Flight Center
Greenbelt, Maryland 20771

8. PEFORMING ORGANIZATION REPORT NUMBER

96B00032

9. SPONSORING / MONITORING AGENCY NAME(S) AND ADDRESS (ES)

National Aeronautics and Space Administration
Washington, DC 20546-0001

10. SPONSORING / MONITORING AGENCY REPORT NUMBER

NASA CP-3322

11. SUPPLEMENTARY NOTES

Han: Goddard Space Flight Center, Greenbelt, Maryland; Peng: Shanxi University, Shanxi, China; Kim: University of Maryland, College Park, Maryland; Man'ko: Lebedev Institute, Moscow, Russia

12a. DISTRIBUTION / AVAILABILITY STATEMENT

Unclassified - Unlimited
Subject Category 74

Availability: NASA CASI (301) 621-0390.

12b. DISTRIBUTION CODE

13. ABSTRACT *(Maximum 200 words)*

The fourth International Conference on Squeezed States and Uncertainty Relations was held at Shanxi University, Taiyuan, Shanxi, China, on June 5 - 8, 1995. This conference was jointly organized by Shanxi University, the University of Maryland (U.S.A.), and the Lebedev Physical Institute (Russia). The first meeting of this series was called the Workshop on Squeezed States and Uncertainty Relations, and was held in 1991 at College Park, Maryland. The second and third meetings in this series were hosted in 1992 by the Lebedev Institute in Moscow, and in 1993 by the University of Maryland Baltimore County, respectively.

The scientific purpose of this series was initially to discuss squeezed states of light, but in recent years, the scope is becoming broad enough to include studies of uncertainty relations and squeeze transformations in all branches of physics, including, of course, quantum optics and foundations of quantum mechanics. Quantum optics will continue playing the pivotal role in the future, but the future meetings will include all branches of physics where squeeze transformations are basic transformation. This transition took place at the fourth meeting of this series held at Shanxi University in 1995.

The fifth meeting in this series will be held in Budapest (Hungary) in 1997, and the principal organizer will be Jozsef Janszky of the Laboratory of Crystal Physics, P.O. Box 132, H-1052. Budapest, Hungary.

14. SUBJECT TERMS

Squeezed States, Quantum Optics, Uncertainty Relations, Group Theory, Information Theory

15. NUMBER OF PAGES

675

16. PRICE CODE

17. SECURITY CLASSIFICATION OF REPORT	18. SECURITY CLASSIFICATION OF THIS PAGE	19. SECURITY CLASSIFICATION OF ABSTRACT	20. LIMITATION OF ABSTRACT
Unclassified	Unclassified	Unclassified	UL

National Aeronautics and
Space Administration

Goddard Space Flight Center
Greenbelt, Maryland 20771